Fundamentals of Rail-Wheel Interaction: Adhesion and Rolling Contact Fatigue

Andrew David Arnall

A thesis submitted in partial fulfilment of the requirements for the degree of Doctor of Philosophy

University of Sheffield
Faculty of Engineering
Department of Mechanical Engineering

24th May 2019

Abstract

How do rolling contact fatigue cracks within the rail interact?

Formed by the wheel-rail contact, rolling contact fatigue cracks within the rail tend to occur as a series of closely spaced cracks. These do not occur as a row of identically sized or spaced cracks, as is commonly modelled. Within this thesis investigations are conducted on how the relative size and separation between these cracks affects the stress intensity factor found at the crack tip. Through improvement in the understanding of how cracks of similar sizes interact, the crack size and separation combinations that are more likely to lead to rail failure from rolling contact fatigue can be better identified. This will permit a more condition based approach for determining maintenance schedules, with cracks more likely to lead to rail failure prioritised.

The two dimensional and three dimensional boundary element approaches used within this thesis demonstrate that the greatest shielding effect is found when the cracks are of similar sizes, with the least shielded case being a large crack surrounded by cracks many times smaller. The overlying crack is found to have a greater influence on the shielding effect experienced by the central crack than the underlying crack. As expected the shielding effect decreased as the crack spacing increased.

In addition the locations of rolling contact fatigue sites that are not generated by cornering forces are compared to the locations of low adhesion events and underbridges. Particular correlation is found with underbridge locations. Further investigations found that abrupt support stiffness changes leads to an increased degree of whole rail bending, which would be expected to lead to increased damage within the rail. However, the increased degree of whole rail bending is not found for gradual support stiffness transitions.

Acknowledgements

Thanks go to David Fletcher and Roger Lewis for their supervision and guidance throughout the course of my studies. These thanks are extended for co-authorship of the journal paper entitled "Geospatial and Temporal Data Mining to Combine Railway Low Adhesion and Rail Defect Data", which was published in the ICE Transport journal in June 2018 [1], and for permission to present the findings within this thesis. The funding for the research within this thesis was provided by Network Rail and the EPSRC.

Additional thanks go to Adam Beagles and David Fletcher for co-authorship of "Interaction of Multiple Cracks in Railheads", which was submitted and presented at the 10th International Conference on Contact Mechanics, 2015 [2]. Thanks are extended to Adam Beagles for permission to enhance the Euler-Bernoulli beam method that he developed for the co-authored conference paper within this thesis.

Thanks also go to Omnicom Ltd (now part of Balfour Beatty) for provision of access to Rail-View software, Michael Jacks at Virgin Trains for provision of the train based data, Brain Whitney at Network Rail for provision of the track based data. Along with Andrew Cornish at Network Rail for assistance with the Track-Ex software and Sharon Mellings at BEASY for support with the boundary element modelling software.

A very special thanks go to my parents, Frances and Raymond, parents-in-law, Rob and Gerry, and to my wife Claire. Without their support and encouragement throughout my studies this would not have been possible. Gerry, an extra big thanks for the final proof read! Final thanks go to Martin Evans, Ben White and Michael Watson for their help with technical problems and provision of the office entertainment (mainly climbing or biking related), Yorkshire tea and the gaming support group (Mark and Pete), for when it all got a bit too much.

Contents

Nomenclature

BE / BEA	Boundary Element / Boundary Element Analysis
BOEF	Beam On Elastic Foundation
ELR	Engineer Line Reference
EPFM	Elastic-Plastic Fracture Mechanics
FE / FEA	Finite Element / Finite Element Analysis
GIS	Geographic Information System
GPS	Global Positioning System
LEFM	Linear Elastic Fracture Mechanics
MGT	Million Gross Tonnes
NR	Network Rail
RCF	Rolling Contact Fatigue
RDMS	Rail Defect Management System
RSSB	Rail Standards and Safety Board
SIF	Stress Intensity Factor
SQL	Structured Query Language
TMS	Train Management System
UK	United Kingdom
WCML	West Coast Main Line
WLRM	Whole Life Rail Model
WSP	Wheel Slide Protection

Chapter 1

Introduction

The UK rail network consists of 10,000 miles of track and was used by 1.7 billion passengers in 2018 [3]. Damage to the rails is a key area for inspection and maintenance to prevent failures such as broken rails, with the possibility of a consequent derailment, from affecting passenger service. To ensure continued safe running of the railway, Network Rail employs preventive maintenance techniques including rail grinding. Reactive measures including rail replacement is conducted for defects that have grown to a size that may compromise rail integrity. Defects that are found to have the potential to compromise rail integrity also affect the operational railway, with temporary speed restrictions employed to mitigate against the potential for a train to cause rail breaks. These continued safety measures have an associated cost; in 2015 Network Rail spent £1bn on track maintenance [4], a sixth of their overall running costs. Rolling Contact Fatigue (RCF) is one of the two main reasons behind rail replacements in the UK, with rail wear being the other.

To be more proactive in maintenance activities such as rail replacement a better understanding of the factors that affect rail RCF propagation is required. Through utilisation of big data and fracture mechanics modelling the work in this thesis provides a better understanding as to whether the occurrence of low adhesion locationally correlates with RCF sites that have not been predicted and why chains of multiple similar (but not identical) RCF cracks develop within rails.

The ability to demonstrate correlation between track damage and transient events such as wheel slides has previously been almost impossible due to the lack of available, consistent data. With recent improvements in the collection of data Chapter 3 explores the possibility of locational correlation between underbridges, low adhesion and fatigue damage in the rail. Locational correlation is sought between RCF cracks and low adhesion or underbridge locations to investigate why RCF is present where it is not predicted. A geospatial analysis of low adhesion events is undertaken and a statistical analysis is used to investigate correlation with track features, such as track gradient.

Chapter 4 furthers the investigation of locational correlation between underbridges and RCF damage in the rail through the use of a quasi-static approach to better understand the factors that affect the transition into crack growth highly likely to lead to a broken rail (phase II growth). This Chapter investigates the effect of sudden support stiffness changes on bending moment experienced by the rail using a quasi-static approach. A discrete support approach originally developed by Beagles [2] is improved to remove the consideration of relative distance between the wheel load and the supports. The findings show that a gradual transition of 6m is sufficient to remove the increased rail loads induced by an abrupt change in support stiffness.

From examining rails over distances of metres rather than 10s to 1000s of metres examined in the first two Chapters it is found that RCF cracks tend to appear as a series of similarly sized and spaced cracks within the railhead. To investigate the local interaction effects between such cracks this thesis considers both two dimensional and three dimensional approaches. The development of the methods is described in Chapter 5 before a detailed analysis of the effect of crack size and spacing on the stress intensity factors at the crack tip is given to reveal the interaction between RCF cracks in Chapter 6. The suitability of two dimensional and three dimensional approaches when undertaking such a detailed investigation is also discussed.

The results and methods presented in this thesis build an understanding as to the manner in which RCF cracks develop within rails. The results demonstrate how the growth of a crack is affected depending on the size and proximity of nearby cracks. This has provided new insight into which grouping of cracks is most likely to lead to crack propagation and rail breaks when multiple, closely separated, cracks develop in the rail. The outcomes of the thesis are concluded and suggestions for further work are given in Chapter 7.

Chapter 2

Literature Review

2.1 Introduction

This Chapter reviews the key areas of the literature that are relevant to this thesis. Discussion focuses on wheel-rail contact mechanics, fatigue crack growth within the rail and track support stiffness. Adhesion at the wheel rail interface is also discussed for the applicability for the use of big data analysis to further understanding in this area. Robust methods to use when analysing such data are demonstrated.

The growth of RCF cracks in rails from initiation through to rail failure is discussed. The different mechanisms that are involved in RCF growth have been studied to varying levels of detail in previous studies. The current understanding of the impact of track support stiffness on crack growth is also reviewed. The review highlighted that much of the previous work on track stiffness was not focused on its influence over crack growth. Factors that exacerbate crack growth are discussed here in more detail and gaps have been identified where the research conducted for this thesis expands upon current understanding.

2.2 Wheel-Rail Contact Mechanics

Within the railway system one of the critical interfaces is that between the wheel and the rail. Here train wheels are in contact with the rail, providing the ability for trains to accelerate and brake. The contact area (commonly referred to as the contact patch) is determined by wheel and rail profiles, track geometry and bogie design. As a result the contact area constantly fluctuates as a train travels along track due to track and wheel geometry changes (Section 2.2.2). However it is typically considered to be around $1cm^2$ in size [5].

When two bodies are in contact the force applied by one body is transmitted to the second body over the contact area. Due to the small nature of the contact patch high contact stresses are generated at the wheel-rail interface. Areas of track where the geometry of the rail or wheel cause the contact patch to reduce in size are prone to increased damage due to the higher contact pressures that are generated. This can lead to either fatigue cracking or excessive wear of the rail and wheel, which is discussed in detail in Sections 2.3.4 and 2.3.5.

Research on the contact patch has been directed towards determining its size and shape and hence the magnitude of the contact stresses. From this the mechanisms that lead to damage in the wheel and rail can be better understood. The simplest solution to the contact problem was first proposed by Hertz [6] (Section 2.2.4.1). This theory has been explored for its applicability to wheel-rail contact by many authors since [7–13]. Johnson's work [8,10,14,15] was at the forefront in the understanding of contact mechanics. In his review Johnson [8] found that understanding of dry elastic contacts in steady rolling is reasonably well understood, but suggested that further study of transient problems is required.

As discussed in greater depth in the following Sections, more recently, numerical [16,17] and Finite Element (FE) methods [18] have been used to gain a more accurate picture of the actual contact patch shape and size. An experimental approach was also proposed by Marshall et al [19] using ultrasonic techniques.

2.2.1 Rail Material Properties

The most widely used rail material is pearlitic steel. This is because it is a material that is cost effective to manufacture and has acceptable wear and fatigue properties. However it is still viewed as a consumable item, with stresses in the rail above fatigue threshold levels. Its elastic nature leads to a progressive work-hardening/microstructural alteration generated by the compressive, rolling-sliding contact applied by the wheel. Pearlitic steels also have the appropriate mechanical properties that are required for a structural beam between sleepers.

In the United Kingdom (UK) the rail grade most commonly used has a minimum hardness of 260HV. However in specific sections of line prone to heavy wear, such as tight radius curves and switches and crossings, head hardened rail (hardness typically 350HV) is used to improve rail wear resistance.

Current research is investigating the application of cladding layers onto the railhead to further improve the rail's resistance to wear and RCF. These apply a high alloy, tool steel coating with hardnesses in the region of 350-500HV onto the railhead [20–23]. However, this is an expensive process and therefore its application is limited to switches and crossings that are particularly prone to heavy damage.

2.2.2 Wheel and Rail Geometry

The size and shape of the contact patch is strongly influenced by the geometry of the wheel and the rail. Subtle changes in the shape of either the rail or the wheel can have a big effect on the contact stresses experienced in the wheel and rail [24] (Section 2.2.4.3). The contact patch shape is particularly dependant on the wheel's lateral position on the railhead due to the varying lateral cross-section of the wheel and rail profiles (Appendix A.1). With the differing profiles between the two surfaces the contact patch is very small relative to the size of the bulk material. This leads to high forces acting over a very small area and induces stresses that may lead to material fatigue, e.g. RCF cracks. Longitudinal stresses induced by traction and braking of the wheel on the rail can lead to sliding between the two surfaces, resulting in friction induced wear [25], wheel slides and thermally initiated defects such as studs underneath white etching layers [26].

Railway wheels in the 1800's had a nominally conical cross-section. By the 1960's the P8 profile was developed in response to derailments as train speeds increased. The P8 profile is intended to maintain the same geometry as the wheel wears. More recently, the P12 profile has been developed which is intended to be more resistant to RCF. However, P8 profiles are still used on a large proportion of rolling stock and is used in this thesis (Figure A.1). Modern railway wheels typically have a tread diameter ranging between 0.73-1m [27–29] and convex cross-sectional radius of 0.33m at the centreline.

Modern UK rail is predominantly of 60E1 type (Figure A.2), with the rails inclined towards each other at an angle of 1 in 20 [5] to direct the normal force from wheel through rail web (Figure 2.1). The railhead has a domed profile with approximately a 0.30m radius at the centre of the head where the wheel-rail contact is most commonly located. Under normal running the combination of modern wheel and rail profiles leads to a near conforming contact, spreading the load of the wheel over a wider area. This reduces the forces in the contact patch in comparison to earlier wheel and rail designs, and somewhat compensates for the heavier axle loads experienced on the rail network today.

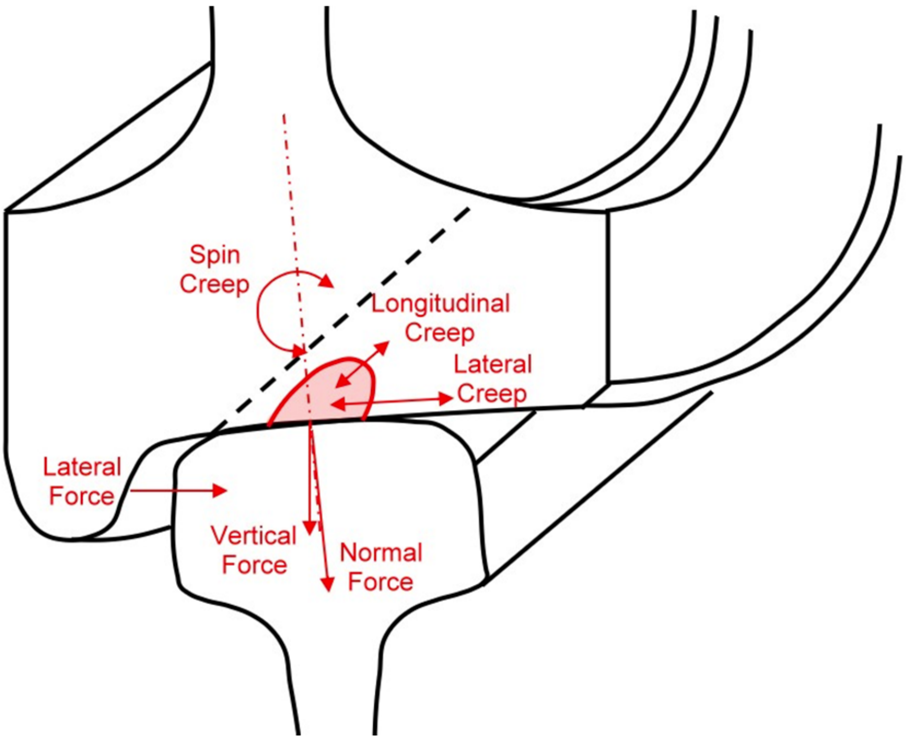

Figure 2.1: Wheel on a rail, showing the contact patch, associated forces and terminology for creep

Passenger rolling stock within the UK is generally configured with two bogies, each with two axles, upon which there are two wheels per axle. An axle is normally assembled with two wheels using a press fit technique upon manufacture and considered as a single entity during use, commonly referred to as a wheelset. When in motion the rolling radius difference inherent in the conical shape of the wheel tread acts to steer the wheelset on curved track (Figure 2.2). The bogies are positioned at either end of the car to provide stability, whilst rotation of the bogies relative to the car body aids cornering capability by reducing the angle of attack of the wheel on the rail and hence reducing associated lateral forces (Figure 2.3).

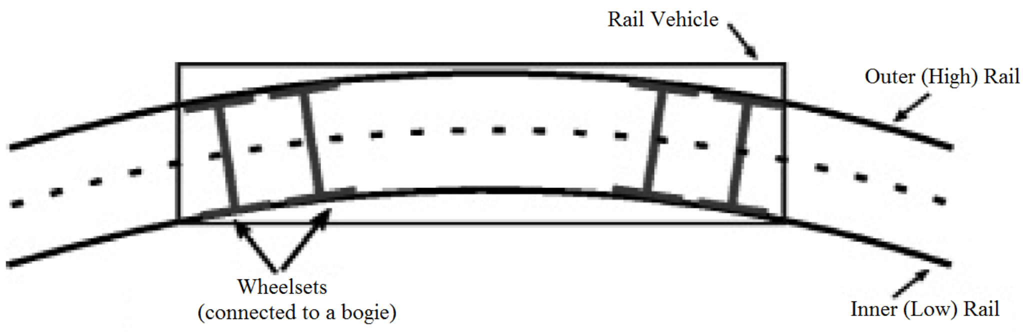

Figure 2.2: Typical arrangement of wheelsets on passenger rolling stock

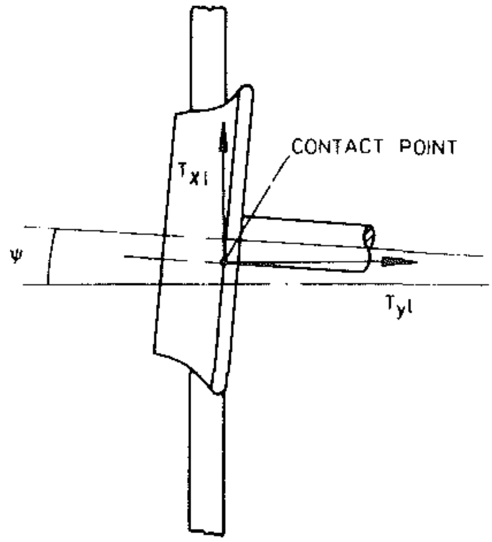

Figure 2.3: Angle of attack of the wheel relative to the rail (plan view). Figure taken from Elkins et al. [30]

The potential areas of contact between the wheel and the rail are shown in Figure 2.4. Under normal running the contact is in Region A, with the wheel-rail in contact as shown in Figure 2.5(a). However during cornering the wheel shifts laterally across the rail (Figure 2.5(b)) and the contact on the high (outer) rail moves to Region B in Figure 2.4, the "gauge corner" of the rail. Due to the change in profile shapes (convex wheel radius reducing from 0.1m to 0.013m; concave rail radius reducing from 0.08m to 0.013m as contact approaches wheel flange) the contact patch size in the gauge corner decreases, increasing stresses in both the wheel and the rail.

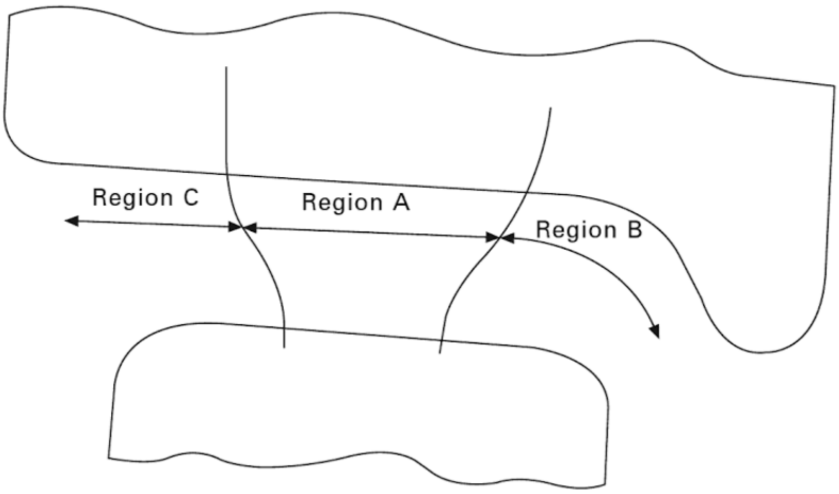

Figure 2.4: Potential areas of contact between the wheel and rail. Figure taken from Tournay [31]

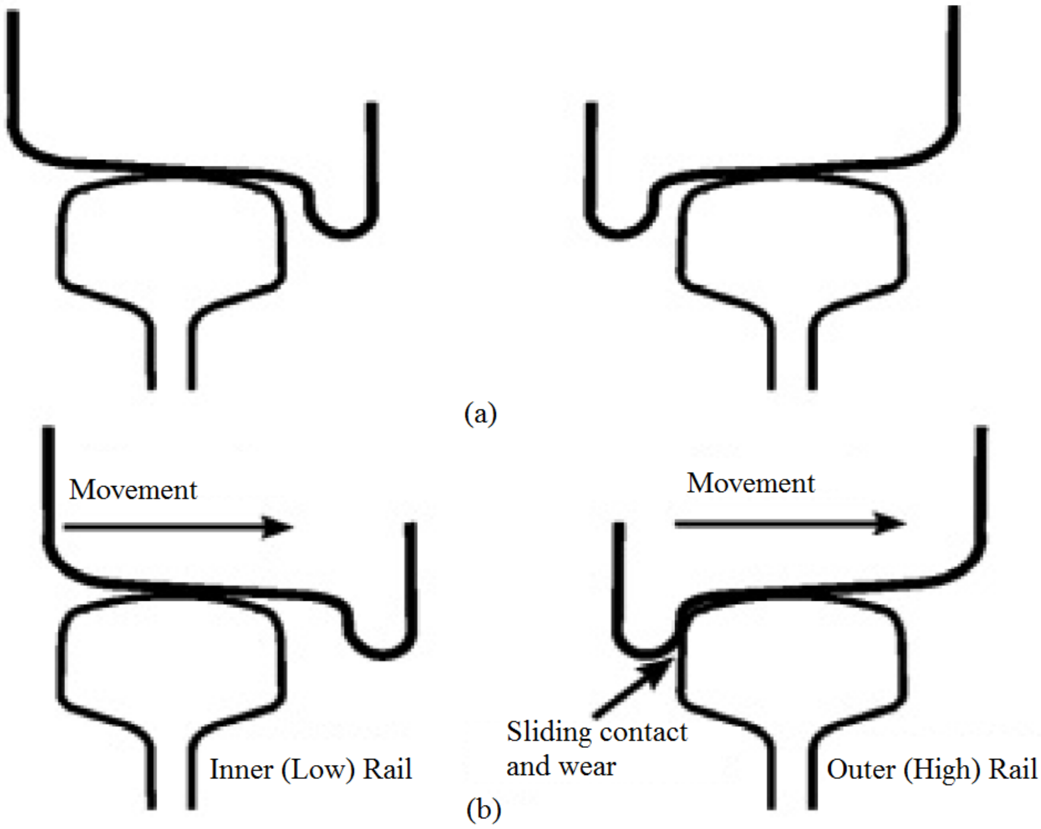

Figure 2.5: Lateral shift of the wheel on the rail on straight track, (a), and curved track, (b). Figure taken from [32]

2.2.3 Adhesion at the Wheel-Rail Interface

The friction force is the resistance parallel to the direction of motion encountered by one body moving over another for both sliding and rolling bodies. For a driven train wheel under acceleration the rotational velocity at the wheel's surface is greater than the longitudinal velocity. This difference is known as longitudinal creep (Figure 2.1). Lateral creep arises through the differing rolling radii of the wheels on the wheelset as the wheel attempts to centralise on the rail and is greatest on curved track. Spin creep is due to yaw angle velocity and conicity of the wheelset. Creep was first discussed by Carter [33], who presented a two dimensional solution for longitudinal creep. Johnson [10] generalised Carter's theory into three dimensions assuming that the wheel and rail were rigid bodies. Kalker [34, 35] then developed the complete theory, creating the programme CONTACT. Kalker's programme can be used for all contact problems that can be described by half-spaces [11].

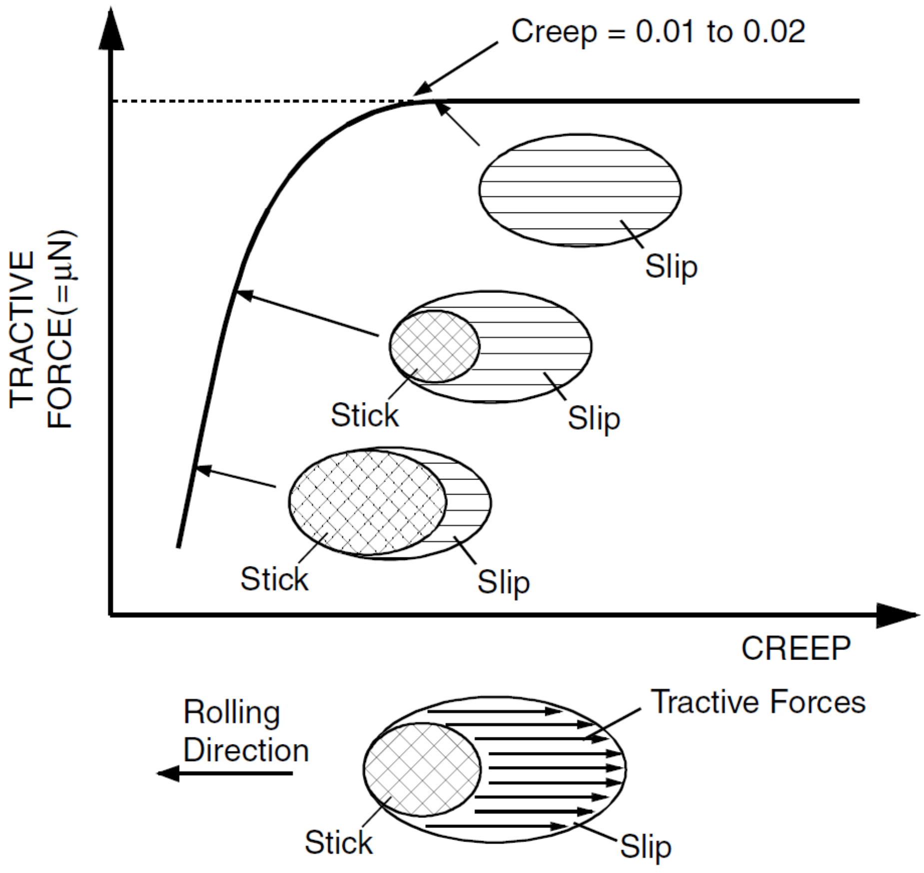

Figure 2.6: Relationship between traction and creep in the wheel-rail contact. Figure taken from WRI handbook [36]

The relationship between longitudinal creep and tractive force, known as the creep curve, is shown in Figure 2.6. For the hypothetical case of “free-rolling” at zero creep no tractive force is transmitted through the contact (full stick contact). However in reality, micro-elastic deformation of the contact patch leads to creep in the contact. As creep increases slip develops at the trailing edge of the contact patch. In this way the contact patch in the wheel-rail contact consists of regions of stick and slip resulting in the combined rolling-sliding contact.

At low levels of tractive force, the contact patch has a large stick region, as the tractive force increases the amount of slip in the contact patch increases. The available adhesion at the contact and thus the available tractive force is limited by the coefficient of friction (μ). Once the limit of adhesion is reached the tractive force reaches saturation and the contact enters full slip/pure sliding. Under full slip conditions further tractive demand will only lead to higher creep forces and an associated increase in sliding damage to the wheel and rail [37].

Numerous authors have studied the creep curves that are generated under different conditions experimentally using tests such as twin disc [11,38,39]. They provide a good insight into the amount of traction the contact patch can transmit under different conditions. Investigating conditions that lead to low adhesion in the contact is of particular interest for the geospatial analysis in Chapter 3.

Table 2.1 lists the adhesion coefficient typically found under certain conditions as found by Moore [40]. Moisture and wet leaves are two major factors that reduce the adhesion coefficient at the wheel-rail interface. Conditions that lead to the lack of adhesion at the railhead are a major concern for the rail network. This is expanded in Section 2.2.3.1.

Condition of the rail Surface	Adhesion Coefficient
Dry rail (clean)	0.25-0.30
Dry rail (with sand)	0.25-0.33
Wet rail (clean)	0.18-0.20
Wet rail (with sand)	0.22-0.25
Greasy rail	0.15-0.18
Moisture on rail	0.09-0.15
Light snow on rail	0.10
Light snow on rail (with sand)	0.15
Wet leaves on rail	0.07

Table 2.1: Examples of wheel-rail adhesion coefficients. Table taken from Moore [40]

2.2.3.1 The Problem of Low Adhesion

Low adhesion between the wheel and rail is a long term challenge for the rail network. Reliable levels of adhesion at the wheel-rail interface are imperative for safe, efficient reliable train operation. A reduced level of wheel-rail adhesion leads to an increased risk of wheel slip or spin which affects a train's ability to brake or accelerate [41]. This is especially evident during the autumn period when the build-up of leaf layers can significantly reduce the available adhesion [42, 43], leading to substantial train delays as defensive driving techniques are adopted [44]. It has been noted from the literature that, although all leaf types have similar chemical composition [42,45], some leaf types, for example sycamore, are more likely to create railhead contamination due to the size and quantity of leaves deposited [46].

Leaf layers are not, however, the sole cause of low adhesion events. Other contaminants such as water [47,48], oil [49], oxide layers [50] and wear debris [51] have also been found to reduce the adhesion coefficient within the wheel-rail contact. In previous research these contaminants, acting alone or in combination, have been shown to reduce the traction coefficient when applied in small scale laboratory testing [52–57]. It has been shown that, of the commonly found contaminants on the rail-head (excluding leaf film), water gives the greatest reduction on the level of adhesion [58] and that, other than leaf contamination, only water would be present in great enough quantity to reduce the adhesion coefficient over a long section of track [59].

Laboratory testing [52] and track trials [58] have demonstrated that the transition period between a wet and dry rail will further reduce the adhesion to a particularly low level. It has been suggested that track-side features such as cuttings shade the track leading to lower railhead temperatures [60] and higher humidity conditions [59] which can reduce the level of adhesion along that section of track. The amount of water on the track will be influenced by the climatic conditions and water (rain or condensation as temperature falls below the dew point) has the potential to reduce the level of adhesion at any time of year.

The mitigation methods used by the rail industry to counter low adhesion are generally only used during the autumn period (1st October to 13th December) and focus primarily on eliminating leaf layers. The rail-head treatment trains used during this period [61] remove the leaf layers from the rail but can introduce other problems onto the rail, such as water induced low adhesion or railhead cracking [62]. During the autumn period, Network Rail reimburse train operating companies for any delay minutes that have been caused by low adhesion on the rail.

For this reason, the majority of train operating companies only collect data for low adhesion incidents during this period, and only if it causes delay or is safety critical, e.g. a station was overrun or a signal was passed at danger. It is therefore often only recorded that a section of track is prone to experiencing low adhesion if it falls within a braking area. This severely limits the available data for analysis of the effect that transient events, such as rainfall, humidity or time of day, have on train performance; as shown in Rail Standards and Safety Board's (RSSB) T1042 report [48] and White et al. [63]. The limited data means that it is difficult to assess the impact track-side features such as tunnels, cuttings or bridges have on the likelihood of a section of track being prone to low adhesion events.

In recent years trains have been fitted with Wheel Slide Protection (WSP) systems, which include the use of applying sand into the contact to improve the level of adhesion. Data from one of these systems has been used in the geospatial analysis in Chapter 3.3.2.

2.2.4 Calculating the Size and Shape of the Contact Patch

To analyse stresses generated within the rail from the wheel contact the size and shape of contact patch must first be identified. In this Section various methods for calculating the size and shape of the contact patch are discussed.

2.2.4.1 Hertzian Contact Theory

The first method for calculating pressure distributions in wheel-rail contacts was by Hertz [6] (Figure 2.7). The theory is applicable to normally loaded frictionless contacts, but has been used on a wide variety of wheel-rail contact conditions. It has several key assumptions. The contact components are assumed to be smooth, consist of linear elastic material and have constant radii of curvature within the area of contact. The contact is assumed to be frictionless and small relative to the overall size of the contacting components. Hertzian contact theory has repeatedly been shown to provide a good approximation of the contact pressure distribution for wheel-rail contact except for gauge corner contact [5].

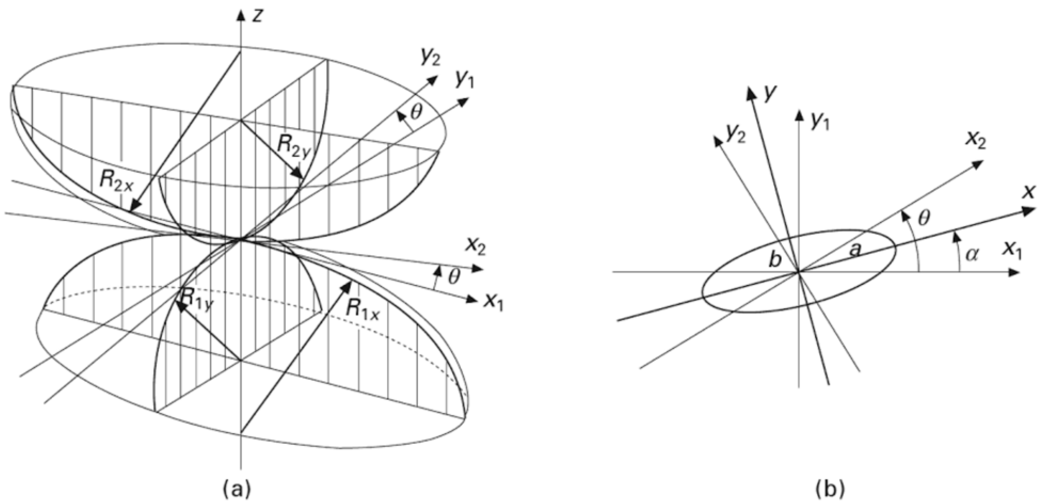

Figure 2.7: Hertzian contact between two solids, (a) contacting bodies, (b) contact area. Figure taken from wheel-rail interface handbook [5]

The Hertz theory defines the pressure distribution of the loaded contact around the initial single point of contact (origin). In Figure 2.7 the geometry of bodies 1 and 2 is described by principal radii, R_{1x}, R_{1y}, R_{2x}, R_{2y}.

For the wheel-rail contact, at an angle of $\theta = 0$ in Figure 2.7, the Hertzian theory is applicable to the wheel profile's concave cross sectional radius within the centre section of the tread (Figure A.1). The concave radius is specified with a negative sign. This gives a more accurate picture of the pressure distribution in the contact patch than the conical wheel profile assumption. Using Equations 2.1-2.5 the contact pressure distribution can be calculated.

The equivalent principal contact radii R_x and R_y are given by:

$$\frac{1}{R_x} = \frac{1}{R_{1x}} + \frac{1}{R_{2x}} \tag{2.1}$$

$$\frac{1}{R_y} = \frac{1}{R_{1y}} + \frac{1}{R_{2y}} \tag{2.2}$$

Giving equivalent contact radius R:

$$R = (R_x R_y)^{1/2} \tag{2.3}$$

The maximum contact pressure (p_0) is given by:

$$p_0 = \left(\frac{6PE*^2}{\pi^3 R^2}\right)^{1/3} \frac{1}{F_1^2(\xi)} \tag{2.4}$$

where P is the normal force and $\frac{1}{E*} = \frac{1-\nu_1^2}{E_1} + \frac{1-\nu_2^2}{E_2}$. $F_1^2(\xi)$ is determined from Figure A.3.

The pressure distribution at any position within the contact patch ($p\,(x, y)$) is given by:

$$p(x, y) = p_0\sqrt{1 - \left(\frac{x}{a}\right)^2 - \left(\frac{y}{b}\right)^2} \tag{2.5}$$

where the major semi-axis, a, and minor semi-axis, b, (Figure 2.7(b)) are given by:

$$a = \begin{cases} \frac{c}{F_3(\xi)} & R_x \geq R_y \\ cF_3\,(\xi) & R_x < R_y \end{cases} \tag{2.6}$$

$$b = \begin{cases} cF_3\,(\xi) & R_x \geq R_y \\ \frac{c}{F_3(\xi)} & R_x < R_y \end{cases} \tag{2.7}$$

and determined from the elliptical integrals in Figure A.3.

2.2.4.2 Approximation of the Hertzian Contact Solution

An exact solution to the Hertz problem is presented by Cooper [9]. However, recently there has been work to approximate the exact solution. This removes the need to work with the tables and diagrams, specifically with respect to the involvement of elliptical integrals to calculate the maximum contact pressure in Equation 2.4.

In the work by Fischer and Wiest [64] which followed on from Tanaka [65] a series of simple equations is presented. These need no evaluation of integrals or rather complicated functions such as elliptical integrals. Their results concur with the exact solution by Cooper [9] within technical accuracy. This approach has been used here in Chapter 5 to generate the Hertzian pressure profile. Below are the key equations used, where P is wheel load, E is Young's modulus and ν is the Poisson's ratio of the wheel and rail.

$$a = P^{1/3}\left(\frac{3}{4}\right)^{1/3}\left(\frac{1-\nu^2}{E}\right)^{1/3}\left(\frac{B}{A}\right)^{\varepsilon_2/(3\beta)}\left(\frac{1}{B^{1/3}}\right) \tag{2.8}$$

$$b = P^{1/3}\left(\frac{3}{4}\right)^{1/3}\left(\frac{1-\nu^2}{E}\right)^{1/3}\left(\frac{B}{A}\right)^{\varepsilon_2/(3\beta)-1/\beta}\left(\frac{1}{B^{1/3}}\right) \tag{2.9}$$

where $A = 1/2R_{1x}$ ($R_{1x} = R/cos(\varepsilon)$, ε being the angle between the tangent and the horizontal direction, and R is the rolling radius of the wheel), $B = \left(1/R_{1y} + 1/R_{2y}\right)/2$, $\beta = 1.550$ and $\varepsilon_2 = 2.100$

$$p_0 = \frac{3P}{2}\left(\frac{1}{ab\pi}\right) \tag{2.10}$$

2.2.4.3 Numerical and Experimental Methods to Calculate Contact Stress Distributions

Numerical solvers have been used by various authors to provide a more accurate solution to the wheel-rail contact area and pressure distribution. Liu et al. [66] published an extensive survey of contact models that specifically investigated contact between rough surfaces.

Several numerical models to calculate the contact stress distribution have been proposed by Kalker, both using a Hertzian approach (FASTSIM) [67] as well as a non-Herztian approach (CONTACT) [68]. In Kalker's method CONTACT [68] the contact surfaces are meshed into rectangular elements with constant normal and tangential stresses in each rectangular element. In 1990 Kalker [69] also reviewed several contact modelling approaches and found that a Hertzian contact approach is sufficient for RCF analysis.

FE analysis has become a more common method for analysing the wheel-rail contact as computing power has increased over recent decades. Telliskivi and Olofsson [18] demonstrated it's ability to model the wheel-rail contact problem and this method has been used by many authors since [13, 70, 71]. In Chapter 5 preliminary investigations are conducted on generating an exact pressure distribution using the boundary element approach, which offers an alternative to FE.

As an alternative to modelling approaches, an experimental approach to the wheel-rail contact problem was proposed by Marshall et al. [19] using an ultrasonic method. They found that the wheel-rail contact area measured for unused specimens showed good agreement with a numerical models.

Studies investigating defects within the rail require a method of rapidly calculating the contact stress distribution at the wheel-rail interface. The size and shape of the contact patch is influenced by the overall vehicle dynamics, global contact forces as well as material properties, such as surface roughness. A comparison between different simulation packages for calculating the area of contact was conducted by Shackleton and Iwnicki [72]. The rolling-sliding nature of the wheel-rail contact means that the stress problem involves tangential loads as well as the normal loads from the vehicle mass. Numerical methods, such as FE or Boundary Element (BE) modelling, can represent the complex geometric shapes but are demanding in computer power and therefore time. For this reason they are rarely used in iterative solutions where the size, shape and pressure in the contact patch needs to be repeatedly calculated. As a result the Hertzian method is widely used due to its simple, closed-form, evaluation.

As highlighted in Fischer et al. [73] it is critical to include the effect of tangential load when modelling the contact pressure distribution. This is because any representation of the wheel which ignores the translational motion of the wheel leads to very different residual stress distributions near the rail surface. It was noted by Fischer [73] that this is especially critical in the case of wheel-rail contact.

The tangential pressure distribution was derived for partial slip conditions by Carter [33]. Figure 2.8 shows the predicted tangential pressure distribution ($q\left(x\right)$) in a rolling-sliding contact. In the slip region the tangential pressure distribution is straightforward to calculate, being proportional to the normal pressure. In the stick region the pressure distribution from pure slip is modified by superimposing an additional traction force ($q''\left(x\right)$) to give the resultant tangential pressure distribution (solid line).

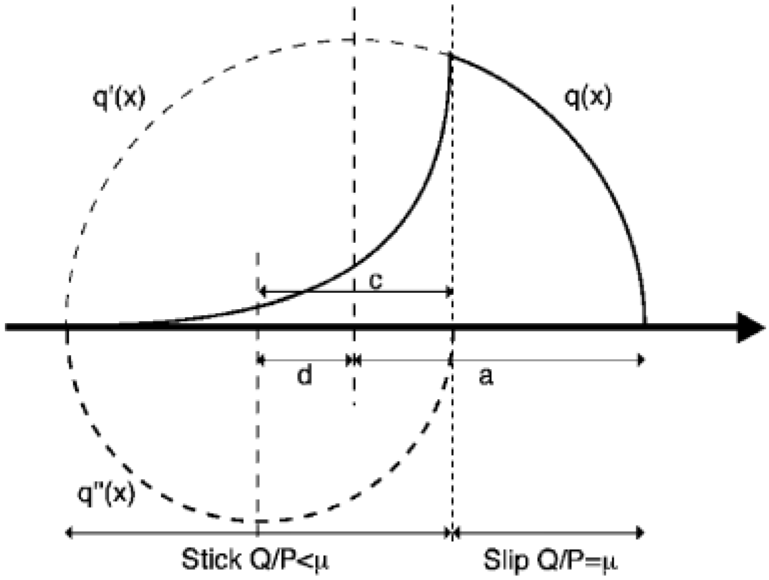

Figure 2.8: Tangential force distribution in a rolling-sliding contact. Figure taken from Johnson [10]

In the rolling-sliding contact the size of the stick and slip regions are constantly changing as the wheel moves along the track. It is therefore difficult to determine the relative sizes of these regions as the tractive force changes (Figure 2.6). In addition any modelling approach applying partial slip contact conditions would be required to recalculate the tangential pressure distribution at each iteration to take into account the changing contact patch size, shape and differing amounts of slip in the contact. This is expensive in terms of computing power.

Numerous authors [74–77] have studied the additional effect of the tangential pressure distribution as well as the normal pressure distribution by assuming full slip conditions. For full slip conditions the adhesion coefficient equals the friction coefficient (Figure 2.6), allowing the tangential pressure distribution within the contact to be calculated using Equation 2.11. This approach has been used in this thesis.

$$\mu = \frac{Q}{P} \tag{2.11}$$

Where Q is tangential load, P is normal load and μ is the friction coefficient.

2.2.5 Ratcheting and Shakedown Limits

Repeated compressive loading of a material usually leads to one of the four responses detailed in Figure 2.9. If the cyclic stress is less than the elastic limit (σ_y) of the material (region (a) in Figure 2.9), the material's behaviour is purely elastic, leading to high cycle fatigue failure. If the cyclic stress is greater than the elastic limit then plastic flow in the material occurs. This leads to the formation of residual stress (region (b) in Figure 2.9). Here the material resumes elastic behaviour after a few cycles. If the cyclic stress is less than the elastic shakedown limit (σ_{EL}), the material enters elastic shakedown. This leads to high cycle fatigue failure. If the cyclic stress is greater than the elastic shakedown limit then the material plastically deforms with each cycle (region (c) in Figure 2.9). Here, after a few cycles, the net change in plastic strain per cycle reduces to zero, forming a closed cycle. As long as the cyclic stress is less than the plastic shakedown limit (σ_{PL}) the material fails from low cycle fatigue due to cyclic plasticity. If the cyclic stress is greater than the plastic shakedown limit (region (d) in Figure 2.9) the material's response to the cyclic loading is a net change in plastic strain each cycle. This open cycle of plastic strain is what is commonly referred to as ratcheting.

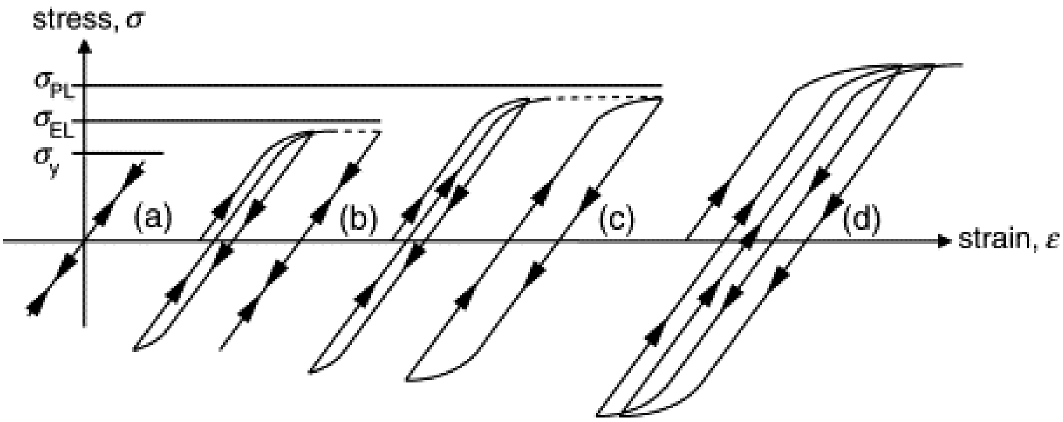

Figure 2.9: Material response to cyclic loading: (a) perfectly elastic, (b) elastic shakedown, (c) plastic shakedown, and (d) ratcheting. σ_y is the yield stress, σ_{EL} is the elastic shakedown limit and σ_{PL} is the plastic shakedown limit of the material. Figure taken from Ringsberg et al. [21]

The behaviour of materials under repeated loading above the elastic limit was originally analysed by shakedown theory in the 1960s [8, 14, 15, 78, 79]. This pioneering work by Johnson and others was followed by further studies in the 1980s [80–82]. More recent studies by various authors have also been undertaken for standard and cladded track [21, 23, 83].

Bower and Johnson [82] found that the shakedown limit varies depending on the contact conditions. Therefore different shakedown limits would need to be used depending on the contact conditions present. This will dictate whether cyclic plastic loading will result in continued cumulative plastic deformation or whether the material will 'shake down' to an elastic state. Evans and Burstow [83] found that steering forces on curved track leads to contact stresses that tend to exceed the shakedown limit.

Ringsberg et al. [21] also validated shakedown theory for two-material rails for cladded rail applications. They successfully demonstrated that a two-material rail system can be designed against RCF and wear resistance.

2.3 Crack Growth in Rails: Rail Rolling Contact Fatigue

RCF crack propagation was first observed by Way [84]. The accumulation of plastic strain from repeated contact loads above the shakedown limit of the rail exhausts ductility of the rail's surface material. Further research in this area was undertaken in the 1970's and 80's by British Rail Research, in particular by Allery and Clayton [85–87]. They found that an increase in the axle loads and train speeds around that time was leading to excessive plastic deformation within the railhead. Their work greatly improved our understanding of the nature of rail surfaces.

Cracks initiate in the surface material of the rail and their propagation leads to failure of the rail by RCF. The life of surface breaking RCF cracks are defined by the three distinct Phases described below [88]. The crack growth rate and an image analysis of the three Phases are shown in Figures 2.10 and 2.11. These three Phases are discussed in detail in Sections 2.3.1-2.3.3.

- Phase I: development of defects in plastically deformed layers - 100s of microns size for normal grade (260) steel.
- Phase II: crack growth at shallow angle to rail surface - up to 10s of millimetres, driven by contact stress.
- Phase III: rapid crack growth into railhead, driven by rail bending.

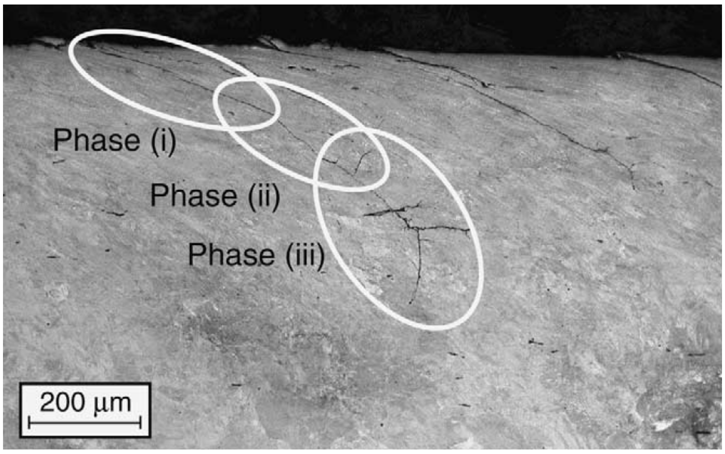

Figure 2.10: Growth stages of a typical rolling contact fatigue crack. Image taken from Ringsberg [89]

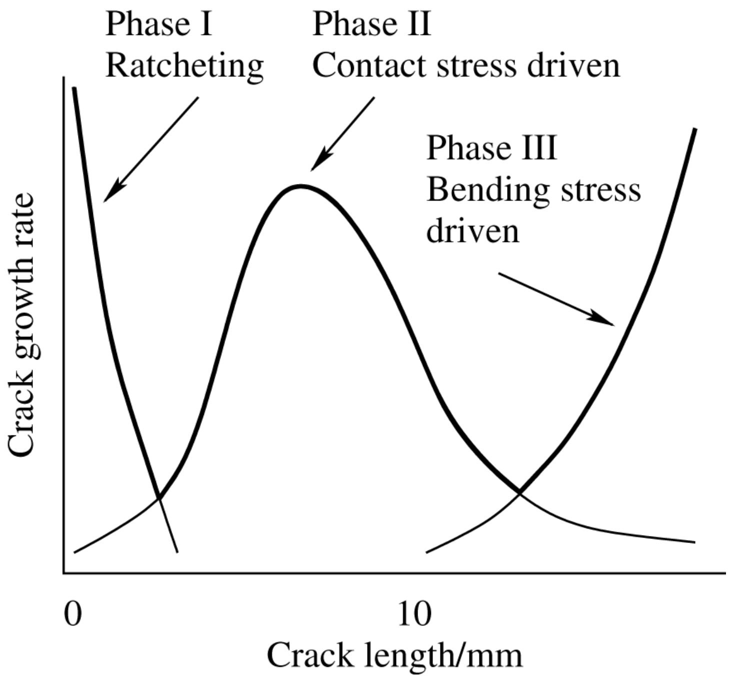

Figure 2.11: Crack growth rate verses crack length curves showing the different phases of crack growth within the rail. Figure taken from Kapoor et al. [88]

Crack initiation and Phase I crack growth (Section 2.3.1) is driven by the ratcheting process. Kapoor [90] demonstrated that the rail deforms through the ratcheting process when the contact pressure exceeds the shakedown limit. Tyfour et al. [91] found that material resistance to RCF deteriorated if the ratcheting level exceeded a certain amount. The degree of ratcheting was found to be governed by the contact pressure, material properties and friction coefficient.

Phase II crack propagation (Section 2.3.2) is driven by contact stresses, which are dominated by the mode I and mode II Stress Intensity Factor (SIF) at the crack tip. Cracks in the rail with the dominant growth method of Phase II crack propagation are commonly found as a series of closely spaced cracks growing down into rail at shallow angle (approx 30° [24]).

Phase III crack growth (Section 2.3.3) is driven by bulk bending stresses in the rail. During Phase III cracks grow rapidly down into the railhead, warranting immediate rail replacement due to the high risk of a rail break. Therefore it is important to understand when this transition from Phase II into Phase III crack growth will occur.

2.3.1 Crack Initiation and Initial Propagation: Phase I

Theoretical [70, 92] and experimental [93] studies have shown that, for conventional normal grade rail (260), there is a very strong plastification of material near the rail surface during use due to the flattening of the asperities that takes place. The shear loading from a train's wheels drives plastic deformation (ratcheting) of the rail until its ductility is exhausted. Cracks initiate in these regions as the surface material fails. The development of these regions of failed material into shallow angle cracks is driven by the subsurface stress and strain fields [82, 94–96].

Cracks are shear strain driven until a depth of around 100μm [70, 73], with initial crack propagation best described by parameters based on an energy formulation of the stress and strain fields in the surface of the material. Miller [97] discussed the inability of Linear Elastic Fracture Mechanics (LEFM) to quantify the behaviour of short cracks found in Phase I development. He demonstrated the importance of understanding the behaviour of short cracks, which require an Elastic-Plastic Fracture Mechanics (EPFM) approach to quantify their behaviour. An EPFM approach by Ringsberg [98] was shown to accurately model these short defects.

2.3.1.1 Known Mechanisms Leading to Rolling Contact Fatigue on the UK Railway

Increased lateral forces generated at the wheel-rail contact on curved track is a well known mechanism for RCF generation and has been investigated by numerous authors.

The study by Evans and Burstow [83] made particular note that large rolling radius differences between the two wheels on the same axle increases wheel-rail forces, leading to the generation of RCF.

Not only can this be caused by curved track, it can also be caused by a number of other mechanisms including wheel-rail profile or lateral track irregularities. Severe lateral track irregularities that are shorter than the kinematic wavelength of the wheelset lead to large steering forces, even on the straight track. In Chapter 3 these known mechanisms are removed from the analysis to focus on alternate crack initiation causes.

2.3.2 Crack Propagation: Phase II

The localized plastic shear strain that drives initiation and Phase I crack growth reduces away from the rail surface. At this point the rail material has shaken down to a quasi-elastic state and the growth mechanism changes to one dominated by the subsurface stress fields generated by the surface contact conditions [83]. The contact conditions continue to propagate cracks below the level of plastic damage within the rail. Cracks now appear as a series of closely spaced cracks on the railhead surface (Figure 2.12). Once cracks reach this stage LEFM can be applied [99] and crack growth can be calculated from the SIF at the crack tip (Section 2.3.2.2).

Figure 2.12: Surface gauge corner rolling contact fatigue cracks. Figure taken from Cannon et al. [100]

The role of crack face friction has been shown to be a critical factor in Phase II crack growth as it dictates the amount of shear between the crack faces. Particularly severe crack growth has been found for crack face friction under 0.2 using modelling methods

[94,95,101,102]. However it is very difficult to measure the actual crack face friction [103] due to it being impossible to instrument a crack.

Using LEFM the SIF at the crack tip can be calculated for the three modes of failure (Figure 2.13). Mode I, crack opening, and Mode II, crack shearing, are the two main failure modes. A crack in the railhead will grow according to the combination of SIFs for these failure modes (Section 2.3.2.2). The combined SIFs for the different failure modes can then converted to the crack growth rate through crack growth law (Section 2.3.2.3). LEFM assumes that the crack growth rate is the same for similar cracks in the same material when they have the same SIF, even if the loading conditions or the geometry differs [104, 105].

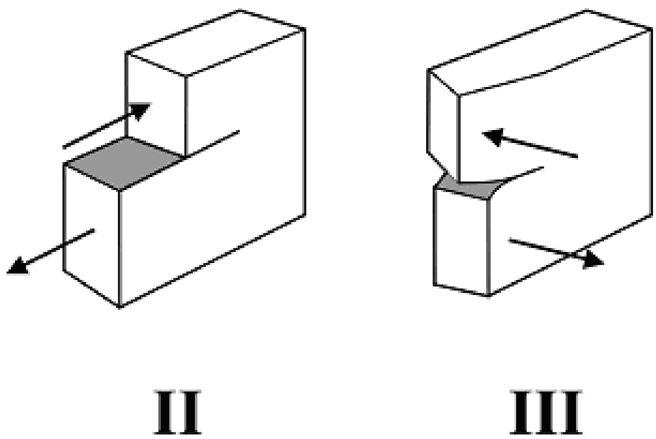

Figure 2.13: Fracture Mechanics Mode I (opening), Mode II (shearing), Mode III (tearing). Figure adapted from Irwin [106]

2.3.2.1 The Importance of Crack Face Friction

Figure 2.14 shows the primary mechanisms for Phase II crack propagation that act in a compressive stress regime:

(a) Shear driven.

(b) Fluid hydraulic pressure transmission.

(c) Fluid entrapment.

(d) Fluid squeeze film.

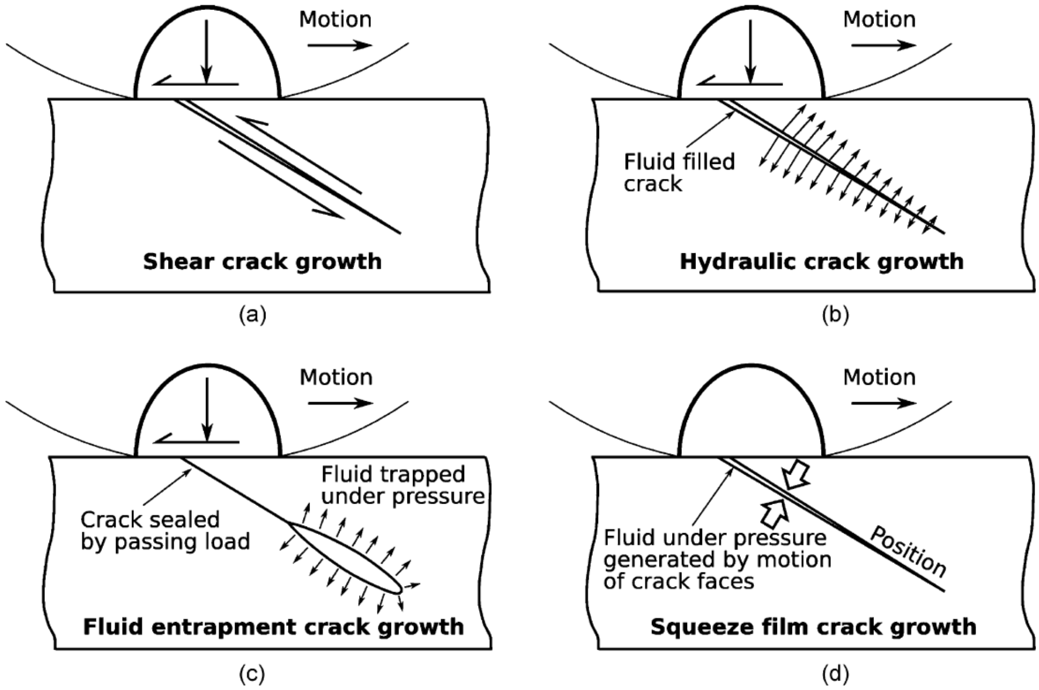

Figure 2.14: Primary mechanisms for Phase II crack propagation within the rail. Figure taken from Fletcher et al. [62]

Bower [94] modelled cyclic shear stress driven growth from the wheel load, demonstrating results consistent with experiments for crack face friction values below 0.2. Crack face friction is the coefficient of friction between the crack faces when they are in contact under compressive loading. The lower this value of friction the greater the mode II SIF at the crack tip as it is easier for the crack faces to slide across each other. A key factor determining this level of crack face friction is the amount of fluid within the crack.

Furthermore Bold [95] demonstrated that co-planer shear driven growth occurred for sequential mixed mode loading in the railhead. Stupnicki et al. [103] observed shear of crack faces from micro-slip occurring at the crack faces, although this was difficult under controlled conditions.

More recently a three dimensional boundary element approach was developed by Fletcher et al. [102] which predicted crack growth rates for a range of crack face friction conditions. The crack growth rates were shown to rise with reduced internal crack face friction at all crack sizes.

Squeeze film fluid action was originally developed to describe the high pressures generated when a lubricant was squeezed out of a small gap in rolling bearings and human joints [107, 108]. This mechanism has been observed by various authors [109–111] to generate high pressures within a fluid filled crack under rolling-sliding conditions such as the wheel-rail contact. As the wheel crosses the crack, high pressures are generated in the fluid filled crack, even if it has not entrapped the fluid by being fully sealed. It is important that this growth mechanism applies even when the crack is not sealed as surface breaking cracks continue to grow when too large to be sealed by passing wheels.

Other crack growth mechanisms have previously been proposed but are unlikely due to their dependence on fully sealing the crack. Hydraulic pressure transmission, where the contact pressure is hydraulically transmitted to the crack faces [94]. Fluid entrapment, where fluid is sealed and compressed in the crack by the passing load [94, 96, 112].

2.3.2.2 Calculating Stress Intensity Factor

The stress intensity factor takes into account the applied stress, the external shape of the body that is cracked and the shape of the crack itself. In this thesis the boundary element method that is used calculates the SIF using the J-integral method. The dimensionless SIF used in Chapters 5 and 6 has been calculated from this. In this Section a high level overview of different methods that have been used to calculate SIF is given to provide some context.

The body force method was developed by Kaneta and Murakami [101, 113] for semi-elliptical cracks. They found that fluid in the cracks acts as a transmitter of the contact pressure. Goshima [114] applied the body force method to fluid filled cracks with additional thermal input. He found that for cracks with fluid present the mode I mechanism dominates, with limited thermal or frictional effects. Without fluid the mode II mechanism dominates, with larger thermal or frictional effects. Solutions for simple configurations are presented in the stress intensity factor handbook [115].

The SIF (K_I and K_{II}) are given by:

$$K_I = F_I \sigma \sqrt{\pi a} \tag{2.12}$$

$$K_{II} = F_{II} \sigma \sqrt{\pi a} \tag{2.13}$$

Where F_I and F_{II} are the dimensionless stress intensity factor at the crack tip, σ is applied stress, a is crack length.

Fletcher and Beynon [116,117] developed a simple method for calculating SIF for cracks at specific angles using crack line Green's functions. This only required numerical integration to calculate crack tip SIF with no further stress analysis required. Their approach had good agreement with the body force method for cracks at an angle of 45°, especially for larger cracks and for mode II SIF.

The J-integral method is used in this thesis to calculate the SIF at the crack tip. The method, proposed by Rice [118], made use of the property that a line integral has the same value for all paths surrounding the tip of a notch in the two-dimensional strain field of an elastic or deformation-type elastic-plastic material. The integral can be related to the near tip deformations. This method of calculating SIF at the crack tip is in-built into many FE and BE packages.

Semi-infinite half-space models are commonly used to model RCF defects (for example, in [94, 116, 117, 119, 120]) to calculate SIF at the crack tip. This is a good assumption for small cracks as the remote railhead geometry has minimal influence over the stress intensity factor at the crack tip. In this work the half-space approach is used for rapid simulation of small cracks (Chapter 6), with larger cracks simulated using a full rail cross section (Chapter 5).

FE and dislocation methods have been used for calculating SIF of cracks in various situations. Among others Bower [94] used FE to calculated the stress intensity factors for subsurface cracks. The mixed mode SIF that are generated during rolling-sliding contact were investigated by Bogdanski [110, 121], who also used a 3D approach. He found that fatigue cracks may branch to a Mode I direction when the residual stress, crack inclination and braking force create favourable conditions. Ringsberg [76, 89, 122] investigated crack initiation and early propagation using a cycle by cycle modelling of ratcheting approach. He proposed a damage summation rule to calculate damage, caused by both low-cycle fatigue and ratcheting and showed that linear elastic fracture mechanics (LEFM) only applies to RCF defects once the material has shaken-down.

The BE approach is particularly well suited to examining cracks in rails. It is capable of modelling the high stress gradient ahead of a crack without very fine mesh (as is required by FE) [123]. This is due to the method of calculation; integration of the applied stress across the boundary surface of the body as opposed to through its volume. The BE approach therefore avoids the very high internal stress gradient ahead of the crack tip. It has been used by various authors to investigate RCF type defects in the rail [124–126]. However both FE and BE model generation is time consuming.

Murakami [115] demonstrated that a geometry factor ratio of 0.59 applied to infinitely wide planar cracks (two dimensional) will give comparable results to semicircular cracks (three dimensional) of the same depth. This relationship was for cracks running normal (90°) to the surface of a semi-infinite specimen, both in uniaxial tension and pure bending conditions. This factor was shown by Fletcher et al. [116, 117] to be valid for a single crack under wheel load, for cracks at 45° to the rail surface.

Kapoor and Fletcher [127] have also developed a 2.5D approach to represent wheel loads offset from the centre-line of the crack. This approach was found to give a rapid method for calculating the SIF of the crack when the contact and crack centre-lines were offset as long as the contact still crossed the crack. This method was also used for cracks at an angle to the contact by Garnham et al. [128].

2.3.2.3 Calculating Crack Growth Rate

Fatigue the crack growth rate $\left(\frac{da}{dN}\right)$ is a more useful quantity than the SIF for analysing the failure rate of materials. To convert the SIF to a crack growth rate, the SIFs for each of the different modes of crack growth are combined through the use of the crack growth law. Using the biaxial specimen (Figure 2.15) Bold et al. [95] extensively tested rail specimens. They proposed an equivalent SIF (ΔK_{eq}), combining mode I mode II SIF (Equation 2.14), which can be used to convert the SIF found at the crack tip to a crack growth rate (Equation 2.15).

$$\Delta K_{eq} = \sqrt{\Delta K_I^2 + (\frac{614}{507}\Delta K_{II}^{3.21})^{\frac{2}{3.74}}} \tag{2.14}$$

$$\frac{da}{dN} = 0.000507(\Delta K_{eq}^{3.74} - \Delta K_{th}^{3.74}) \tag{2.15}$$

Where ΔK_{th} is the threshold SIF range. The threshold SIF (ΔK_{th}) for crack propagation in rail steels is approximately 4MPa$\sqrt{}$m [95] below which the crack growth rate is taken to be zero.

The assumption underlying the application of this laboratory derived law to actual rails is the same as for all application of LEFM. That is; that the crack growth rate remains the same for similar cracks in the same material when they have the same SIF, even though the loading conditions and geometry differ [104, 105]. The mode I stress intensity range for such surface cracks is in the order of the threshold values of steels, which governs the minimum mode I SIF. The mode II stress intensity range is larger than the mode II threshold and depends on the contact loading, crack face friction, residual stresses and crack length.

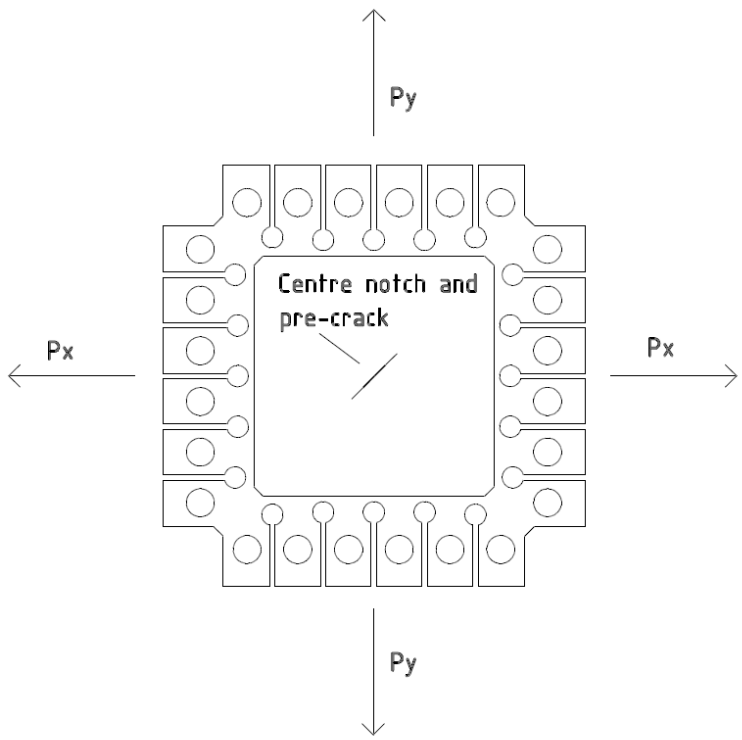

Figure 2.15: Biaxial Specimen used by Bold et al. [95]

2.3.3 Crack Propagation: Phase III

The final Phase of crack propagation, Phase III, (Figure 2.11) is dominated by whole rail bending, which is dependent on the track support stiffness (Section 2.4). Cracks that have a surface length greater than 20mm are categorised as heavy or severe by Network Rail [24] and have been identified as susceptible to turning down into rail under the bending moment in rail from wheel loads, and therefore represent a significant rail break risk. Monitoring and removal of rails with this size of defect is an ongoing problem for Network Rail, with track maintenance costing £1.0bn per year in 2015 [4].

Issues around detecting down-turning cracks within a series of cracks are shown by Cannon et al. [100] (Figure 2.16). This means that the size of the crack would not be able to be determined and the rail would have to be removed on safety grounds at this stage. Garnham et al. [128] found that longer cracks have complex shape, with the deepest part not being below the surface breaking crack. Franklin et al. [129] demonstrated the use of a three dimensional generated mesh to study crack pathways, showing the potential for long cracks to develop in different rail steel microstructures.

Determining the size at which cracks enters this growth phase is important as it is the stage by which cracks develop into highly dangerous rail breaks. Factors that are thought to affect this are investigated in Chapter 4.

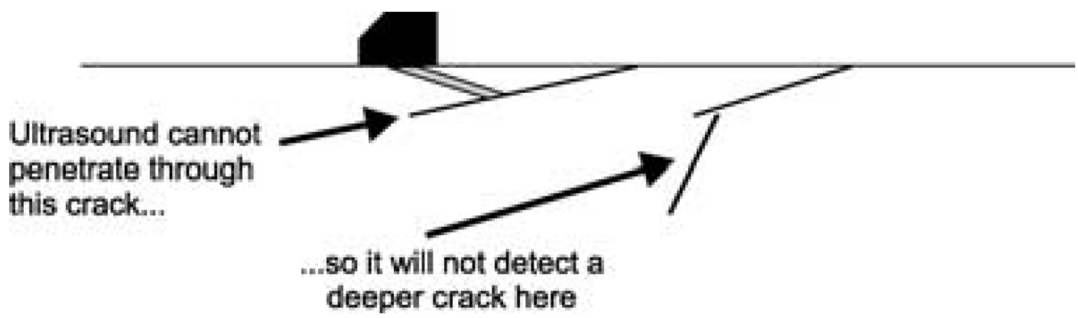

Figure 2.16: Shadowing of ultrasonic sound by head checks and squats. Figure taken from Cannon et al. [100]

2.3.4 Factors that Affect Rail Rolling Contact Fatigue Crack Growth

As summarised above there have been numerous studies investigating rail RCF to understand how the stresses at the contact patch contribute to the initiation and propagation of cracks. With the development of harder rail steels the forces present at the wheel-rail interface during normal operation generate much less extensive plastic flow than in conventional steel grades thus restricting crack initiation. It would be expected that this would delay the development of RCF unless some other factor is present to increase rail-wheel forces.

It is well known that residual stresses [127] or the lateral forces generated during cornering [130] help drive RCF, yet a definitive picture of influences over crack initiation and growth has not yet been established. There has been anecdotal suggestions [131] that locations of RCF cracks are, in part, influenced by the occurrence of low adhesion and this is investigated further in Chapter 3 to establish the impact (if any) of low adhesion over RCF formation.

Establishing the importance of their contribution to crack formation and growth is intended to focus future modelling of RCF crack growth. The following Sections address these points.

2.3.4.1 Importance of Fracture Mechanics Material Parameters: Effect of Loading and Material Strength

The effect of loading has been investigated by Kapoor et al. [132] and Franklin et al. [133]. The effect of material strength has been investigated by Yu et al. [134], Pippan [135] and Girsch et al. [136,137]. The results from these investigations have been the subject of a previously published review by Fischer et al. [73]. It was demonstrated that the loading condition of the rail and the strength of the material determines which mechanism is more important: wear or fatigue crack propagation. They that if the wear rate is larger than the crack propagation rate, then fatigue can be neglected. For fatigue lifetime, the load cycles for crack extension from the first 100µm to a few mm are the most important ones [73].

2.3.4.2 TGamma and the Whole Life Rail Model

This relationship between wear and fatigue was quantified by Burstow and Evans [83] using the Whole Life Rail Model (WLRM) to predict where RCF would occur on the network (Section 2.3.7.1). The relationship is shown in Figure 2.17. They gave an overview of the contact patch energy (Tγ) approach. In this approach T is the tractive force and γ is slip. Tγ is therefore the product of the shear forces and creepages in the contact patch, equating to the energy expended at the contact patch (per unit roll of the wheel). This energy term has previously been related to the observed wear of material in the contact patch.

Burstow and Evans observed that the mechanisms of wear and RCF formation can be very similar. The accumulated plastic strain can lead to either, a loss of material from the rail surface as wear debris or accumulation of failed layers below the surface to form crack-like defects. As shown in Figure 2.17 the contact patch energy (Tγ) determines the degree to which RCF damage occurs and therefore to which of these two outcomes the accumulated plastic strain leads. At high-energy the mechanism driving the wear process changes to an abrasive one (wear zone). At regions of mild wear the material deforms, leading to RCF crack initiation (RCF zone).

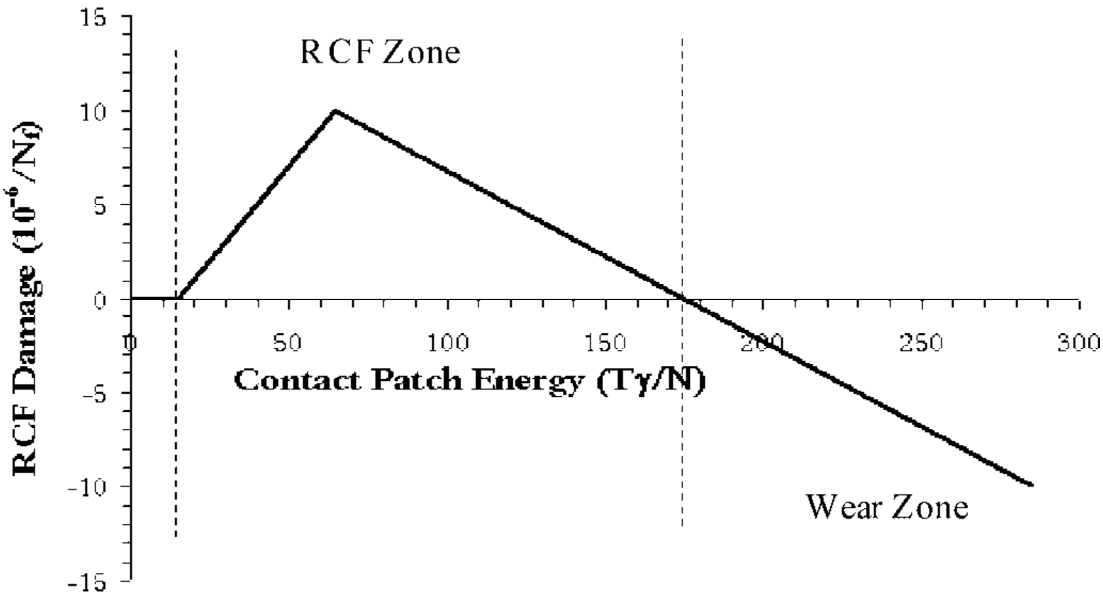

Figure 2.17: Rolling contact fatigue and damage relationship. Figure take from Evans and Burstow [83]

Burstow [130] further demonstrated the WLRM use when investigating head hardened rail. Through the installation of head hardened rails at several trial sites on the UK rail network he demonstrated that it is not always beneficial to install harder rail as this may lead to an increase in RCF crack propagation as rail wear is reduced. He concluded that infrastructure managers must select the most appropriate grade of material for a particular curve geometry and traffic mix. In addition the added cost of head hardened rails means that, in practice, they are used only at sites which experience heavy wear using normal grade rail steel.

The fracture toughness determines the upper limit of the crack length for fatigue propagation which controls the final failure scenario. It has been noted by Girsch et al. [136, 137] that the generation of cracks should be more difficult in the new high-strength steel rails. This is due to the reduction of the plasticity near the rail surface, meaning that propagation in the early stage should be significantly slower.

2.3.4.3 The Effect of Multiple Cracks: Interaction Between Nearby Cracks

The interaction of multiple cracks is complex with the stress fields of cracks influencing each other. As such, there is a need to balance the speed of simulations against the degree of approximation and suitability to consider the real stress fields with the modelling approach.

A two dimensional study by Tillberg et al. [138] demonstrated that for identically sized cracks the peak SIF decreases as the distance between cracks decreases. They attributed this to an effect known as shielding. They showed that the behaviour of five cracks adequately captured the interaction between all cracks. Other two dimensional studies of two cracks of differing sizes captured the interaction effects for specific crack size and spacing combinations [115, 139, 140]. Chapter 6 in this thesis builds on these works with a much more comprehensive study of the interaction effects of three cracks with different size and spacing combinations.

A 3D method was developed by Fletcher et al. [125] using a boundary element approach. They found that, for 10mm radius cracks separated by 5mm, the mode I and II SIF reduced to 40-55% of the single crack value. This leads to a 27% reduction in crack growth rate when compared to single crack models assuming Equations 2.14 and 2.15

apply. They proposed that if this reduction translated to other crack sizes and separations it is large enough to have significant effect on predictions of integrated rail wear and crack growth models.

Using a specific SIF (Section 2.3.2.2) to calculate the interaction between nearby cracks is limited to the individual spacings and crack sizes investigated. However, by using the non-dimensional SIF, this can be expanded to specific size and spacing ratios. This vastly increases the available data, allowing the interaction between multiple cracks to be more thoroughly investigated.

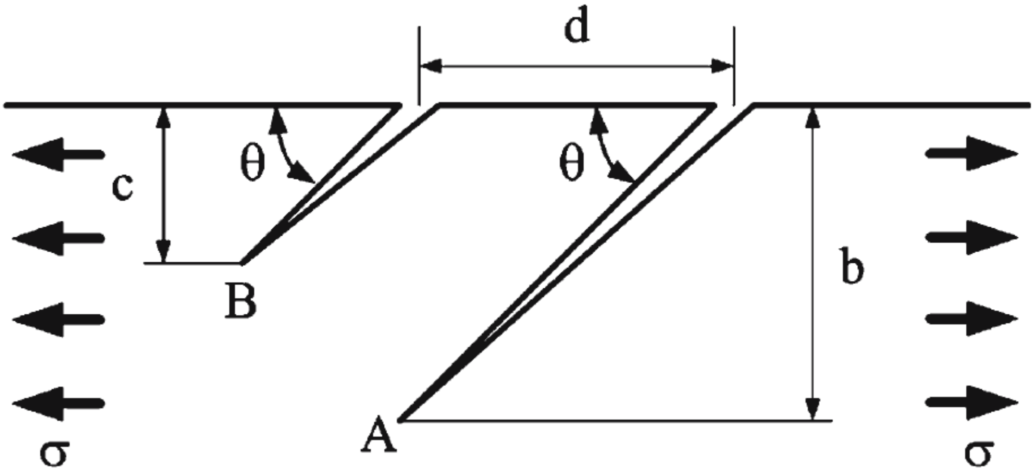

Figure 2.18: Two cracks in a half space. Figure taken from Jin et al. [140]

The non-dimensional SIF removes physical crack sizes from the equation and instead looks at relative dimensions between cracks. This method has been used previously by Murakami and others [115, 139–141] to great effect. From Figure 2.18 the dimensional SIF of cracks A and B can be calculated for any given ratio of b, c, d and θ. This gives one SIF value for that specific crack size and spacing ratio, removing the need for SIF calculation at different crack sizes for the same size and spacing ratio. This work is used to validate the models used in Chapter 6.

2.3.4.4 Residual Stress within the Rail

The effect of residual stress on crack propagation had been investigated by various authors [142–144] prior to the Hatfield accident [145] but its impact on RCF propagation was not properly understood in the UK. After the Hatfield accident a series of detailed studies by Fletcher et al. [127, 146–150] greatly improved our understanding in this area. Key findings were that minor differences between residual stress profiles can dramatically alter crack growth rate predictions; for shallow angle cracks the vertical residual stress is paramount in controlling change in crack growth rate prediction; and that residual stress promotes downward branching of shallow cracks.

Although residual stress has been shown to be a driver of RCF crack growth it has not been incorporated into the modelling in this thesis. Therefore the effect of residual stress is not covered in detail in this literature review. However, the model has been designed to allow future work to incorporate residual stress into the analysis.

2.3.5 Interaction between Wear and Crack Growth Rate

Although rail wear is not the subject of this thesis its interaction with RCF warrants a review here. Contact stresses drive wear as well as RCF and it is not always disadvantageous as it can remove cracked material (Figure 2.19). The removal of material from solid surfaces occurs by mechanical action with loss of material from the contact. Mechanisms include abrasion, adhesion etc, see Engineering Tribology [151].

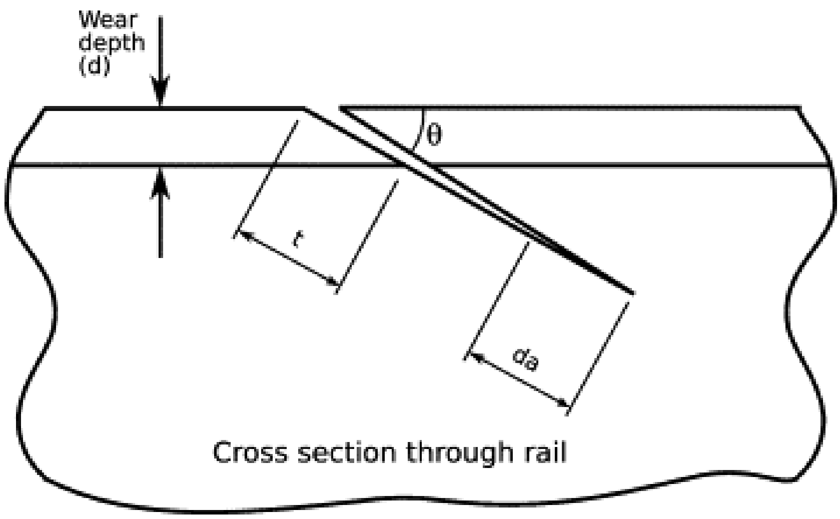

Figure 2.19: Wear-crack growth interaction during Phase II growth. Figure taken from Fletcher et al. [62]

Some wear is beneficial; removing small cracks and slowing the net crack growth rate of longer cracks. The wear rate influences the net crack propagation rate by the relationship shown in Equation 2.16.

$$net\, crack\, growth\, rate = da - t \tag{2.16}$$

Where da is the crack growth rate and t is the truncation rate from Figure 2.19.

Several studies have investigated the interaction between crack growth and wear for very small cracks. Kapoor et al. [132] proposed a mechanism of metallic wear in which laminar wear debris is generated by the process of plastic ratcheting. They found that the wear rate was approximately proportional to the square root of the applied load and an increasing function of a single non-dimensional parameter ψ_s, the plasticity index for repeated sliding.

Franklin et al. [133] discussed how the wear rate fluctuated with the variation of the material properties. However, this was found to not differ significantly from the wear rate with non-varying (i.e. average) material properties.

A ratcheting based computer simulation by Fletcher et al. [152] was developed to allow the simultaneous investigation of wear, crack initiation and early crack propagation. The model, based on the division of the half-space beneath a contact into an array of bricks which defined the material, gave promising results relative to the plastic flow and hardening in the twin disc tests.

2.3.6 Network Rail's understanding of Rolling Contact Fatigue from in Service Rails

Network Rail's (then Railtrack) guidance on RCF type defects has been published [24] on their appearance as well as the relationship between crack surface length and depth. In the field these cracks have been typically found to propagate in the centre of the running band. Small cracks are closely spaced, normally 2-3mm apart, which increases to 10-20mm for longer cracks. The relationship between the visible crack length and depth is shown in Figure 2.20 and is based on historical inspection of rail failures [24].

RCF categorised as light or moderate in Figure 2.20 propagates to a depth of approximately 5mm into the rail head (Phase II). Cracks of this size are often nearly straight and are associated with 10-20mm surface length depending on the angle of the crack to the rail surface (15-30°). Once the crack depth is greater than 5mm RCF is categorised as heavy or severe, with bending being the dominant growth mechanism (Phase III). Cracks of this size are likely to down-turn into the rail and branch, as shown by the increase in crack depth for heavy or severe RCF in Figure 2.20. Cracks will either branch upwards, leading to spalling of the rail surface, or downwards, leading to the potential for rail breaks. The crack depth of 5mm is shown here to be the threshold depth for the down-turning of RCF defects and is therefore used in the 3D modelling work in this thesis.

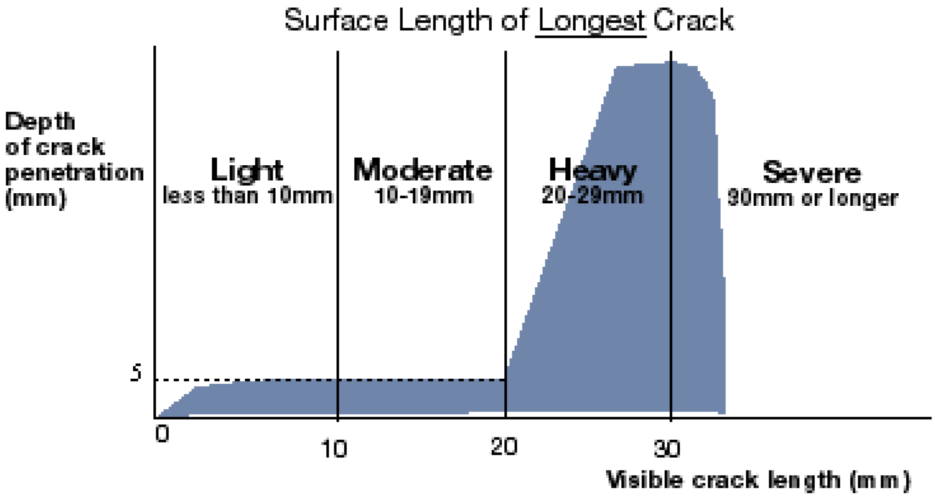

Figure 2.20: Light to severe rolling contact fatigue defects. Relationship between crack surface length and depth. Figure taken from [24]

The exact nature of RCF cracks in rails has been found from destructive testing of cracked rails by grinding and mapping cracks at various depths. Metallography of rail sections can reveal the two dimensional nature of defects (Figure 2.10). The actual crack shape is complex, with the shape during Phase I crack growth determined by the microstructural properties of the rail and by the applied stress during Phase II crack growth. Simplification of the crack shape to straight planar cracks (two dimensional) and semi-elliptical cracks (three dimensional) has been used by numerous authors, a few of which are referenced as examples [94, 101, 102, 122]. An added complexity is that multiple drivers will drive the crack growth within the rail. A common assumption when modelling is to consider the fastest individual driver and assume this dominates, ignoring the other drivers [153]. The boundary element approach developed in Chapter 5 has been designed with the different drivers in mind (residual stress, contact, bending) so that future work can investigate the combination effects.

2.3.7 Network Rail's Current Prediction and Mitigation Methods

2.3.7.1 Network Level Prediction of Rolling Contact Fatigue Locations

The Track-Ex package [154] is a tool used by Network Rail to predict the severity of RCF that will occur. It is based on the WLRM (Figure 2.17) and utilizes the Tγ approach to predict areas of the track that are susceptible to RCF formation based on levels of lateral force inputs. It is a comprehensive tool that combines track and vehicle data to provide value added information, e.g. damage indexes, that are directly used for system management. Track-Ex is a key tool for Network Rail; predicting the network level of RCF that is expected for a given track geometry being used by a specific mix of rolling stock. Track-Ex calculates the damage generated from one wheel pass, which is then extrapolated to the number of wheel passes over the time duration specified for analysis.

2.3.7.2 Mitigation of Rolling Contact Fatigue

The main mitigation method currently used in the UK against RCF is rail grinding [155]. This is conducted in fixed cycles depending on the traffic. For curves grinding is undertaken every 20MGT (Million Gross Tonnes) and on straight track every 50MGT [37,156]. The grinding process removes or reduces the size of cracks in the railhead along with mitigating future crack development by re-profiling the rail head to reposition and reduce contact stresses [24]. In areas prone to high damage (either wear or RCF) different grade steels are used to reduce the maintenance required. The steel grade chosen is based on the estimated Tγ within the area (Section 2.3.4.1).

Remedial grinding is required for sites with RCF damage classed as moderate (Figure 2.20) where the visible length of cracks is in the range 10-15mm. Once cracks reach this size the intention is to modify the cant profile to laterally offset the contact patch away from the cracks to reduce their growth rate. Once cracks are visible it is generally too late to remove them completely and economically by grinding. RCF becomes Heavy or Severe when the crack surface length is greater than 20mm (Section 2.3.3). At this size cracks are likely to branch downward and represent a significant rail break risk. Sites with Heavy or Severe RCF undergo regular ultrasonic and visual inspections whilst plans are put in place for re-railing the site. As a general rule plans for re-railing are made for sites with crack surface lengths greater than 15mm [24].

Grassie [37] suggested that the future trends for maintaining the rail will involve optimisation of the wheel-rail interface, designed for that specific railway system. This would distribute wear more evenly and improve curving behaviour. Grassie et al. [157] demonstrated the effectiveness of this type of maintenance strategy for Sweden's iron ore railway.

2.4 Track Support Stiffness

The rail support structure is shown in Figure 2.21. The rail is connected to sleepers with the fastening system (consisting of railclips and railpads) and supported by the trackbed (ballast and underlying subgrade). Maintaining the rail support structure is critical in ensuring good track geometry, with failures of individual sleepers (unsupportive sleepers) shown to induce high loading on the rail [158, 159]. This leads to further damage from the increased loading. Track with a softer support structure has been correlated with greater rates of track deterioration and increased maintenance [160, 161]. Furthermore transition zones have been highlighted by many authors as an area particularly prone to increasing rail loads [162–164].

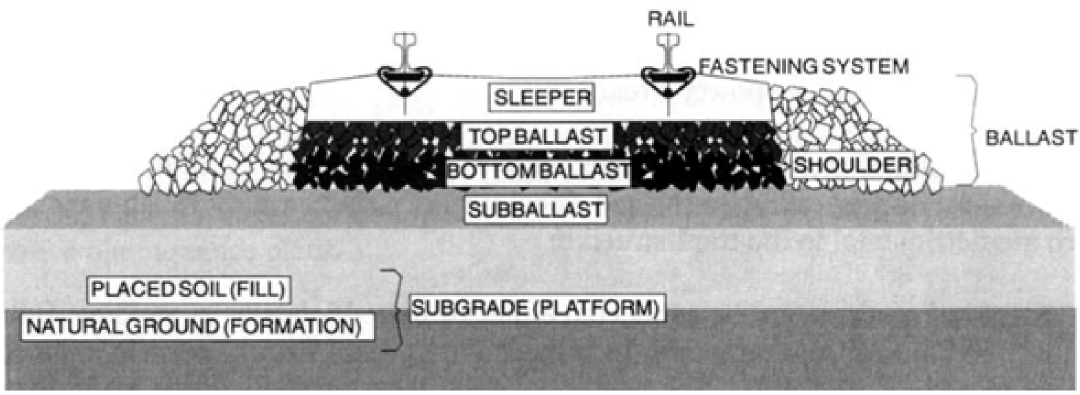

Figure 2.21: Track support structure. Figure taken from Selig and Waters [165]

Several studies have measured the track deflection to calculate track support stiffness. This has either been done via onboard measurements [166, 167] or through the use of accelerometers attached to the track structure [163, 168–170].

The method presented by El-Sibaie et al. [166] gave a notable ability to identify locations of increased risk of derailments, with 3 of the 4 derailments that had occurred in the previous 10 months in locations predicted by the system. Berggren et al. [167] developed a track deflection/stiffness measurement device that can be mounted on a track recording car. This means that measurements with the new method are undertaken at normal speeds and at very little extra cost compared with a dedicated vehicle. Their method found single failures, stiffness transition problems, as well as loose sleepers. It was also used to make better predictions about the degradation rate of single failures using the large amount of data collected during their study.

Coelho et al. [163] conducted a detailed site investigation on a poorly performing transition zone on the Dutch railway system. Their observations of sleeper displacements found that the transition slab does not behave as intended and amplifies track displacements. This is thought to be a result of unsupported or hanging sleepers on the approach slab. Priest and Powrie [169] used geophones attached to sleepers to record the velocity of a limited number of individual sleepers during normal operations. They used the track measurements to validate their rapid Beam On Elastic Foundation (BOEF) approach (Section 2.4.2.1).

2.4.1 Support Stiffness for UK Track

Typical track properties for UK ballasted track is given in Table 2.2. On ballasted track the stiffness of the sleeper is in the region of 10^3 times [171] the trackbed (combined ballast and subgrade) stiffness. Therefore, when applying a quasi-static approach, the sleeper's overall effect on the support stiffness is negligible (support stiffness including sleeper stiffness = 0.999 times support stiffness ignoring sleeper support stiffness). As a result the sleeper can be assumed to act as a rigid body [172] and its stiffness contribution to the foundation ignored [173] (Equation 2.18). For quasi-static analysis it does not matter that trackbed and the railpad are physically separated by the rigid sleeper. This approach is used in this thesis in Chapter 6.

Railpad Stiffness. Taken from Grassie et al. [174]	250MN/m
Trackbed Stiffness per sleeper end. Taken from Grassie et al. [174]	50MN/m
Sleeper spacing [175]	0.6m
Using Equations 2.19, 2.21. Track support stiffness (k)	69MN/m/m
Rail Young's Modulus	210GPa
Moment of inertia (x-x axis) for each rail [176]	30.383x10^{-6}m^{4}

Table 2.2: Typical track properties for UK track, rail specifications are for the 60E1 rail profile

The stiffness at each support calculation including sleeper stiffness is given by:

$$\frac{1}{K_{support}} = \frac{1}{K_{pad}} + \frac{1}{K_{sleeper}} + \frac{1}{K_{trackbed}} \tag{2.17}$$

The stiffness at each support calculation ignoring sleeper stiffness is given by:

$$\frac{1}{K_{support}} = \frac{1}{K_{pad}} + \frac{1}{K_{trackbed}} \tag{2.18}$$

When calculating the support stiffness of each support, two methods have been used by previous authors, either the axle load or the wheel load of the train has been used. In studies using the axle load, for example Priest et al. [169], the support stiffness of the whole track has been taken into account, i.e. the moment of inertia of both rails, stiffness of both railpads and the whole trackbed stiffness. Alternatively, in studies applying a wheel load, for example Dukkipati et al. [172], the support stiffness of half of the track has been taken into account, i.e. the moment of inertia of one rail, stiffness of a single railpad and the trackbed stiffness per sleeper end. This is because in studies considering a wheel load only half of the train's mass is considered.

Both methods yield the same deflection result, but, for the axle load method, the resulting bending moment accounts for both rails and is therefore double that of the wheel load result. In this thesis the wheel load method has been chosen due to the main focus being how the bending moment within the rail is impacted by gradual and abrupt sleeper stiffness changes.

By rearranging Equation 2.18 the support stiffness (K) at each support is given by:

$$K_{support} = \frac{K_{pad}K_{trackbed}}{K_{pad} + K_{trackbed}} \tag{2.19}$$

2.4.2 Modelling of Whole Rail Bending

Many studies have investigated wheel induced rail deflection (Figure 2.22) but the focus has been on problems such as corrugation [177, 178] or vehicle dynamics [172]. How the upwards deflection opens cracks in the railhead either side of the wheel driving crack growth through whole rail bending has received little consideration until recently [148]. Whole rail bending drives phase III crack growth (Section 2.3.3). To model crack growth the rail can be approximated as a beam in pure bending.

A detailed study by Hobbs [179] found that to model whole rail bending a significant length of rail is required in the model to obtain the correct level of constraint for the rail as positioning a loading point close to the end of the rail model resulted in higher bending stresses and deflections. Hobbs found that the highest positive bending stress in the rail head occurred when the wheel loads were equidistant from the location of the crack, under usual wheel loads and sleeper stiffness. He demonstrated that the stiffness of the sleeper supports had a significant effect on the bending stresses within the rail. Softer supports increased the stress while firmer supports reduced the stress (Figure 2.23). Under the bending stresses alone, the tendency was for cracks to turn down into the head of the rail, for all crack depths and angles analysed by Hobbs [179]. A high negative Mode I SIF occurred for cracks in the rail head when the load was directly over the crack. Meaning that the wheel load acts to close the crack when it is directly above the crack.

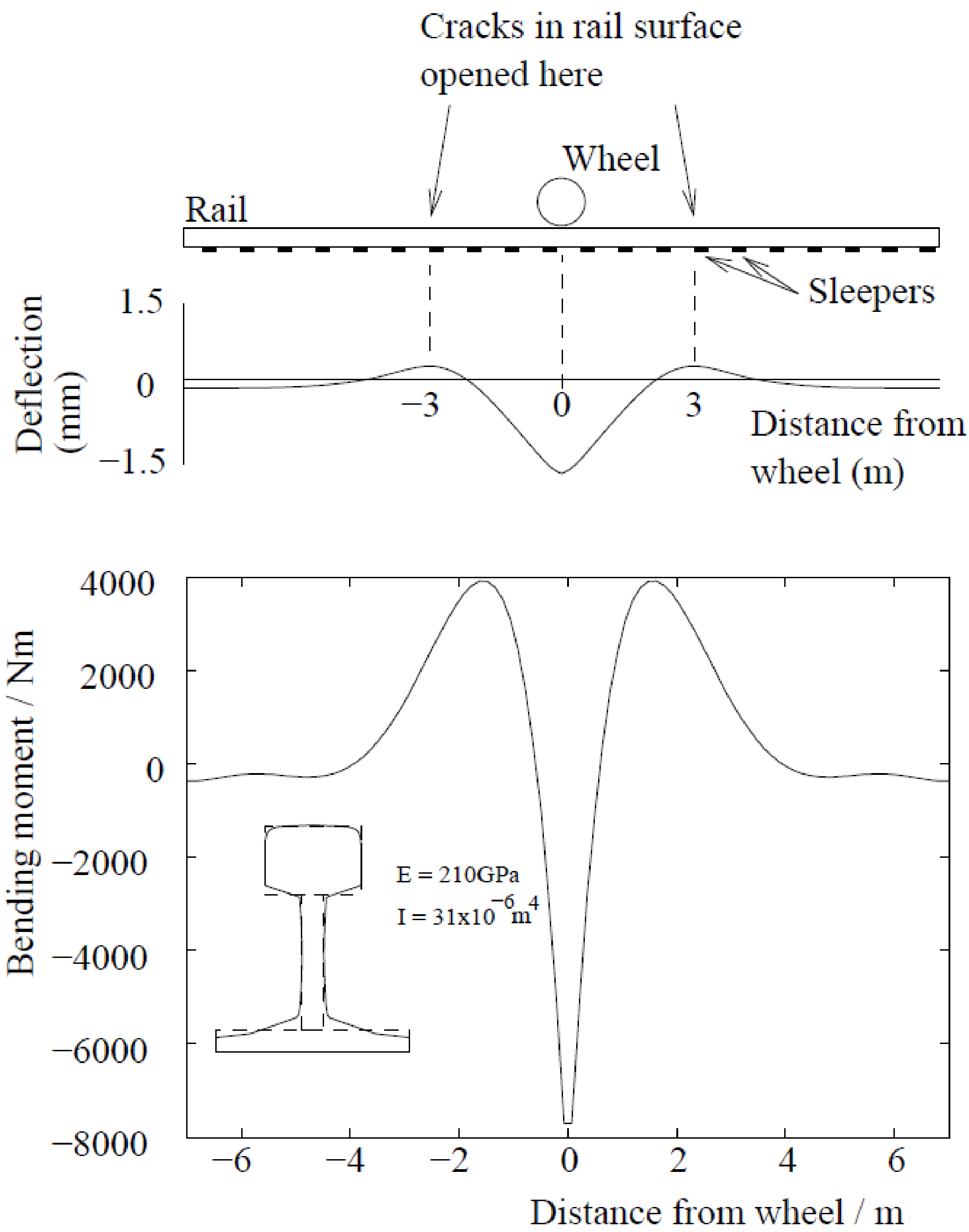

Figure 2.22: A rail loaded by a wheel, showing the rail deflection and bending moment within the rail. Figure taken from Kapoor and Fletcher [148]

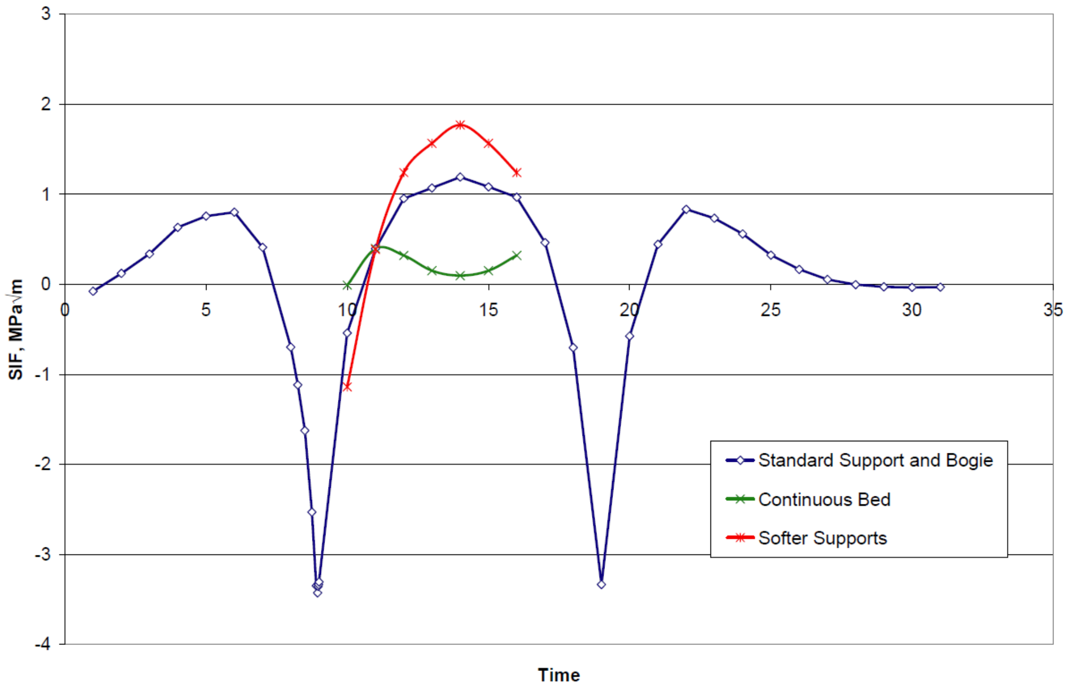

Figure 2.23: Effect of changing rail support stiffness. Figure taken from Hobbs [179]

Fletcher and Kapoor [146] found that for cracks shorter than 35-40mm (i.e. 18-20mm depth assuming 30° crack angle), the bending stress element of the stress intensity factor cycle was much lower in magnitude than the contact stress component. Assuming applicability of Hourlier and Pineau's criterion [153] they deduced that the crack growth rate for smaller cracks is not greatly influenced by rail bending. For larger cracks with lengths over 40mm they found that the bending stresses became increasingly important in determining the SIF cycle during each wheel passage. However, it is worth noting that a crack of this size should not be in the rail anyway. They also found that bending stresses may subject a crack to three or four stress cycles per wheel pass, leading to accelerated growth of cracks in contrast to assuming one stress cycle per wheel pass.

Fletcher and Kapoor's findings that cracks will not be susceptible to bending driven Phase III crack propagation (Section 2.3.3) until crack lengths are over 40mm are inconsistent with Network Rail's experience with RCF type defects (Section 2.3.6) within in service rails. Network Rail's experience is that cracks begin to branch or turn down into the rail when the crack depth exceeds 5mm. This crack branching or down-turning tends to be driven by the Mode II failure mode without the accompanying Mode I cycle (Figure 2.13). Once cracks begin to branch or down-turn, bending driven Phase III crack propagation becomes the dominant growth mode at shorter crack lengths than estimated by Fletcher and Kapoor [146].

2.4.2.1 Modelling Methods: Beam on Elastic Foundation Techniques

For track stiffness problems a quasi-static analysis using the BOEF modelling technique has been applied by many authors. This type of approach was originally developed by Winkler [180]. He represented the foundation as an infinite number of closely spaced springs that were uniformly distributed along the beam (Figure 2.24).

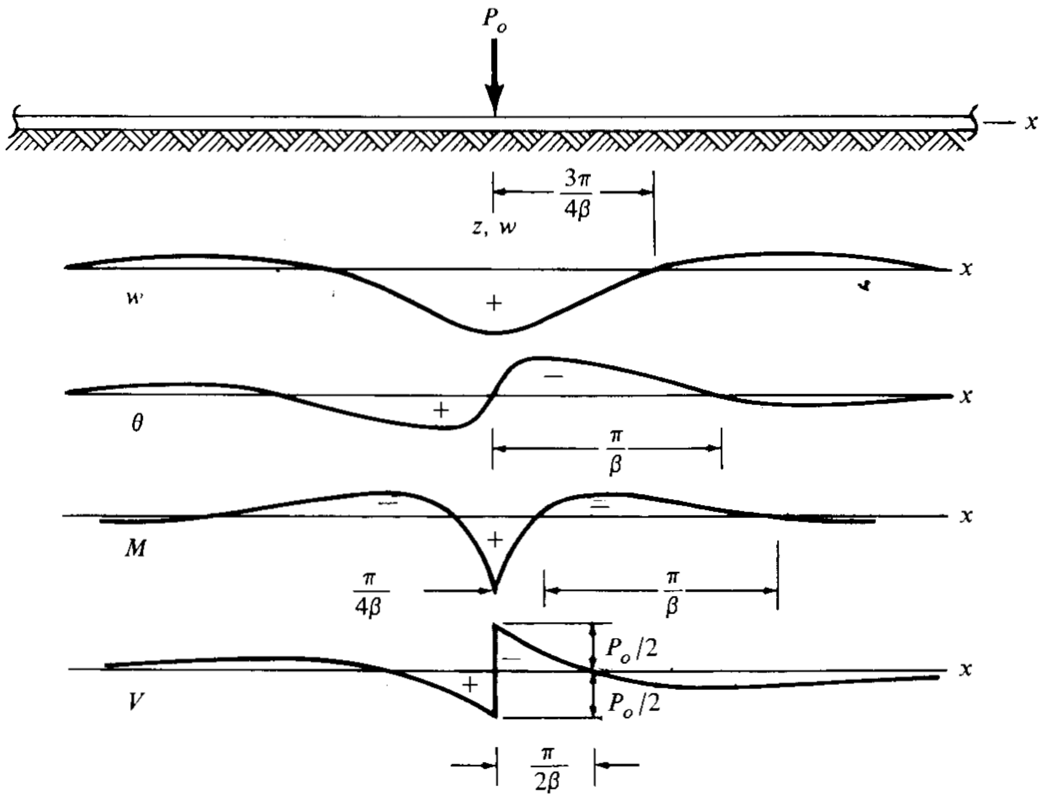

Figure 2.24: Infinite beam under a point load with a Winkler support showing the key parameters for comparison

For the rail scenario it is considered an appropriate approach for determining the response of the rail to the vertical loads applied by a train without the need for complex FEA analysis. The equations behind this approach are given in full in Appendix F and are outlined here.

The governing equation for a semi-infinite beam on a uniform Winkler foundation is given by:

$$0 = kw + EI\frac{d^4w}{dx^4} \tag{2.20}$$

The term k in Equation 2.20 describes the support stiffness of the Winkler foundation (s is the sleeper spacing) and is given by:

$$k = \frac{K_{support}}{s} \tag{2.21}$$

By solving Equation 2.20 then the deflection (w), angle (θ), moment (M) and shear (V) of the beam at any point is given by:

$$w = \frac{\beta P_0}{2k}A_{\beta x} \tag{2.22}$$

$$\theta = \frac{dw}{dx} = -\frac{\beta^2 P_0}{k}B_{\beta x} \tag{2.23}$$

$$M = -EI\frac{d^2w}{dx^2} = -\frac{P_0}{4\beta}C_{\beta x} \tag{2.24}$$

$$V = -EI\frac{d^3w}{dx^3} = -\frac{P_0}{2}D_{\beta x} \tag{2.25}$$

Where β is a parameter defined by Equation F.3.

Together Equations 2.22-2.25 describe the reaction of an infinite beam supported by a Winkler foundation under the point load P_0. The response of an infinite beam is shown diagrammatically in Figure 2.24. The points of zero deflection, slope, bending and shear are defined. The Winkler approach is used in the initial part of the investigation in Chapter 4.

The Winkler approach has been shown to be a good approximation of the track support structure [173, 174]. In Figure 2.25, Priest et al. [169] compared the BOEF approach to measured readings. They found that although the maximum displacements were similar, the dynamic response of the ground was markedly different from the theoretical static response. Within the region between the axles the actual sleeper displacement did not respond instantaneously to the unloading of the sleeper. This agreed with findings from Ishihara [181] who suggested that during dynamic loading, the ground behaves to some extent as a visco-elastic material rather than purely elastically as assumed in the BOEF analysis.

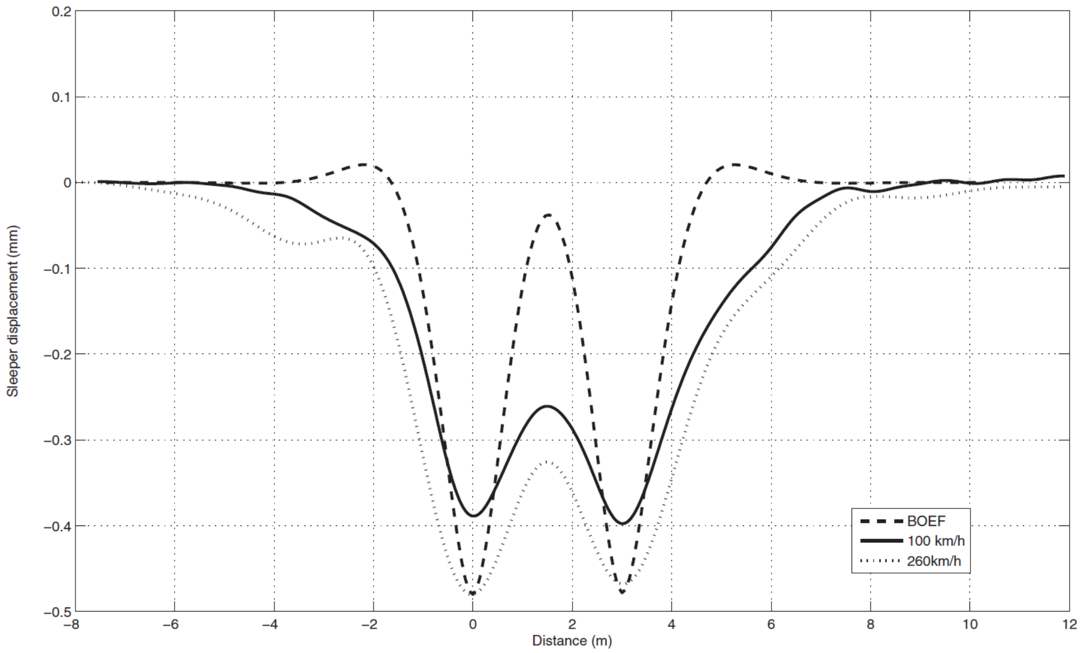

Figure 2.25: Comparison between sleeper displacement measurements and those calculated from beam on elastic foundation theory. Figure taken from Priest et al. [169]

When the foundation stiffness varies along the beam there is no exact solution for Equation 2.20 and therefore a numerical method is required. Eisenberger et al. [182–184] presented several papers on the stiffness formulation for the solution of beams on a variable Winkler foundation. They stated that the accuracy of their approach was dependent only on computer precision.

2.4.2.2 Dynamic Load Factors for Beam on Elastic Foundation Techniques

The dynamic load factor is the factor by which static load is increased due to the dynamic effects of the wheel-rail interaction.

The dynamic wheel load (P_d) is given by:

$$P_d = \phi P_s \tag{2.26}$$

Where ϕ is the dynamic load factor and P_s is the static wheel load.

Doyle [185] and Van Dyk et al. [186] both review several methods for determining dynamic load factors that are used by several countries around the world including America, France, Germany and the UK. As well as incorporating the effects of velocity, analyses of this type can also include the effect of irregularities and non-uniformities in the track and the wheel and rail profile such as rail joints. The most-comprehensive dynamic load factor was developed by Birmann [187], which incorporates the track geometry, vehicle suspension, vehicle speed, vehicle centre of gravity, age of track, curve radius, super-elevation, and cant deficiency, and is valid for train speeds up to 125mph.

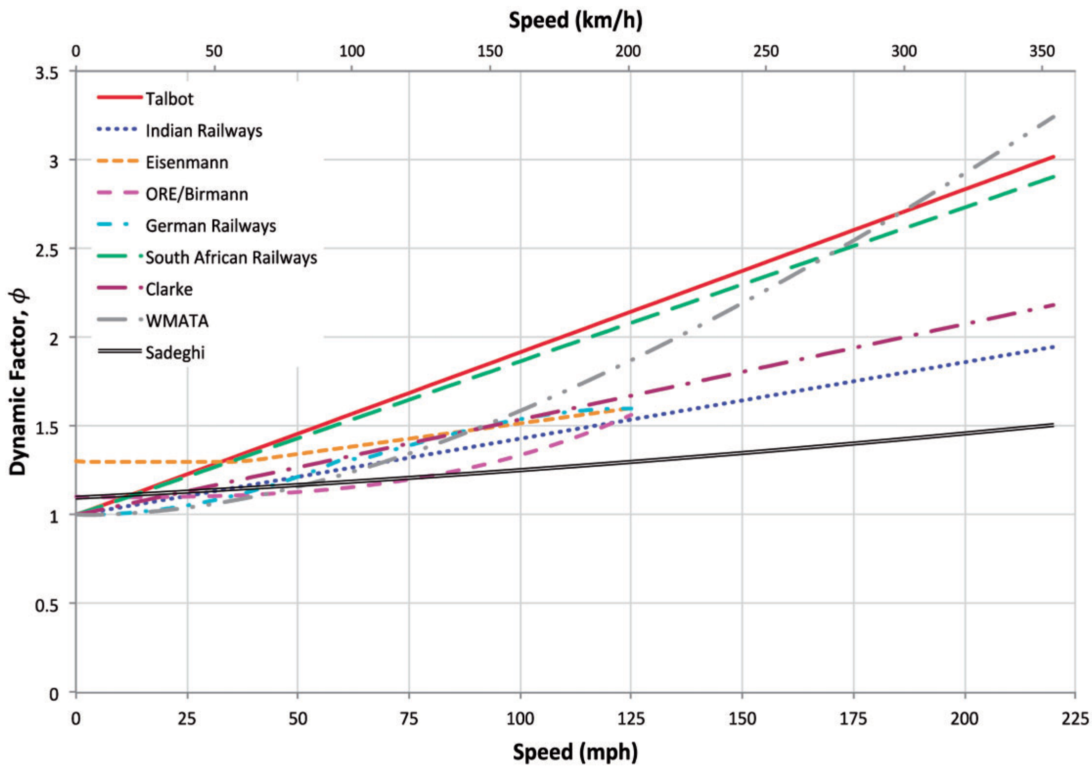

Figure 2.26: Dynamic load factors calculated using different approaches. Figure taken from VanDyk et al. [186]

In the review by VanDyk (Figure 2.26) it can be seen that the dynamic wheel load varies from 1.3 times to 2.2 times the static wheel load at 125mph depending on which approach is used. The effect of this load increase on the rail deflection and bending moment in the rail is investigated in Section 4.2.6 of this thesis.

2.4.2.3 Modelling Methods: Finite Element Analysis

Although finite element models of track stiffness are not the subject of this thesis they are included here for completeness as FEA techniques are commonly used as an alternative to the BOEF approach. Kouroussis et al. [188] found that the dynamic response of track was primarily affected by the soil foundation suggesting that, for continuous subgrade, the Winkler foundation is sufficient. Therefore finite element approaches are best used when considering non-linear factors and some examples of papers using a FE approach are discussed.

Dong et al. [189] used the FE approach to consider non-linear factors such as the loss of wheel-rail contact, rail lift-off from the tie and tie lift-off from the ballast. Their results indicated that the system response was periodic and the dominant wavelength was equal to the tie-spacing, with the position of the peak wheel-rail contact force in the second half of each tie-spacing. They also found that the dynamic deflection of track in a steady-state response was asymmetric and that the wheel centreline was slightly ahead of the maximum rail displacement.

A dynamic stress analysis of a ballasted railway by Yang et al. [190] found that the dynamic effects on the stresses imposed on the soil were noticeable above 10% of the critical velocity (wave propagation velocity of the supporting track-ground system). At 50% of the critical velocity the static loading was found to underestimate the stresses by 30%, with train speeds above the critical velocity inducing a dramatic increase in stresses and displacements within the rail. Furthermore they found that the presence of an unsupported sleeper significantly increased the stresses below the neighbouring sleepers in the sub-ballast. This would lead to an increased rate of deterioration of the track structure.

Grabe and Clayton [191] indicated that a static analysis might be acceptable for speeds up to 240km/h on a firm subgrade. This exceeds the maximum UK rail mainline speeds, therefore a static approach has been used in Chapter 4. However, it is worth noting that in softer subgrades the critical velocity will be lower and therefore the dynamic effects have a larger impact on the stresses imposed on the soil.

2.4.3 Transition Zones

Track structures such as underbridges (i.e. a bridge spanning an opening underneath the railway – ranging from large bridge structures to small culverts) are much stiffer than the surrounding track. To avoid abrupt changes in track stiffness transition zones are used to artificially increase the support structure of the track surrounding the underbridge to provide a gradual stiffness change (usually intended to be linear). The approach often used is sub-ballast approach slabs as shown in Figure 2.27. However, despite this modification, these areas of track still deteriorate at a greater rate than standard track.

An assessment of transition zone performance was undertaken by Coelho et al. [163]. They found that the transition slabs were not behaving as intended and could actually amplify the track displacements. The dynamic vertical movements on approach slabs were found to be four times greater than on free track and over eight times greater than on the culvert. This was shown to result in unsupported sleepers on the approach slab. The study identified that this was driven by the ongoing settling of subsoil, which caused approach slabs to rotate into the subgrade.

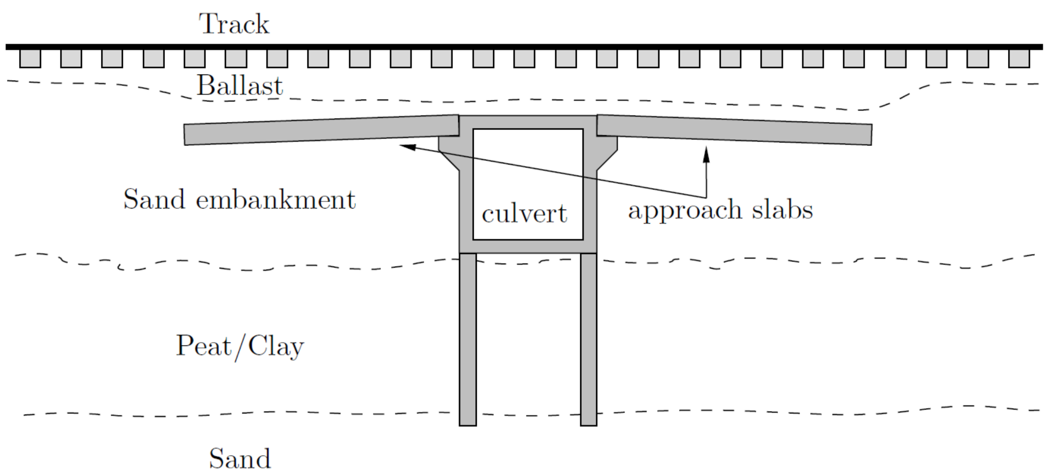

Figure 2.27: Longitudinal view of the track passing over a culvert using approach slabs. Figure taken from Varandas [192]

Li et al. [193] found that a change in track stiffness due to change in track structure led to uneven track deflections under moving traffic loading. This was found to have an adverse effect on the dynamic vehicle/track interaction, with increased forces in track causing or accelerating the uneven rate of settlement. The uneven rate of settlement leads to problems such as hanging sleepers. Lundqvist et al. [159] found that one hanging sleeper with a 1mm gap between the sleeper and the ballast increased the sleeper-ballast contact force by 70% and the displacement by 40% for the adjacent sleeper. This led to rapid deterioration of the track structure. Chapter 4 investigates how altering the track support stiffness at sleeper level affects the bending moment within the rail.

2.5 Conclusions

In this Chapter the literature relevant to this thesis has been reviewed. Current understanding of wheel-rail contact mechanics has been shown to be extensive and it was found that there is a good level of understanding of crack growth in rails for an individual crack. Track support stiffness has been investigated for issues such as noise and vibration but its effect on crack growth has not been the focus of these studies to the same extent.

The review of wheel-rail contact mechanics highlighted that the understanding of the causal factors behind low adhesion could be enhanced. With recent improvements in the collection and collation of big data, our understanding of locations at which low adhesion regularly occurs can be improved. Furthermore, the possibility of locational correlation between low adhesion and fatigue damage in the rail can now be subject to a much more in-depth study. No previous studies were identified that have investigated locational correlation between these two issues.

The review of track support stiffness showed that recent studies have increased our understanding of rail bending induced crack growth. This has been studied in particular depth for transition zones, which have been highlighted as a particular problem area in terms of rapid deterioration in track quality. There is scope for rapid approaches to investigate the effect of rail support stiffness changes on the bending stresses within the rail.

The review of crack growth in rails showed that numerous studies have been undertaken into RCF crack growth using single, or occasionally, two crack models. It was noted that the studies that investigated more than two cracks did so for cracks of identical size and spacing. Therefore, there is scope for an approach which investigates the effect of different sized and spaced cracks and how the presence of these affect the stress intensity factors of the neighbouring cracks.

These gaps in the literature are addressed in the following Chapters.

Chapter 3

Geospatial and Temporal Distribution of Adhesion and Rail Rolling Contact Fatigue

3.1 Introduction

The ability to demonstrate correlation between track damage and intermittent events such as wheel slides has previously been impossible due to the lack of available, consistent data. With recent improvements in the collection of big data our understanding of locations at which low adhesion regularly occurs can now be improved. Furthermore, the possibility of locational correlation between low adhesion and fatigue damage in the rail can now be subject to much more in-depth study. This Chapter aims to improve our understanding within this area by establishing:

- Where does RCF occur locationally with respect to underbridges and low adhesion?
- Does low adhesion only occur during the autumn period?

Using the structure as shown in Figure 3.1. Initial findings were published at the Contact Mechanics 2015 conference by Arnall et al. [194], with the full results later published in the ICE Transport Journal [1] (Appendix B).

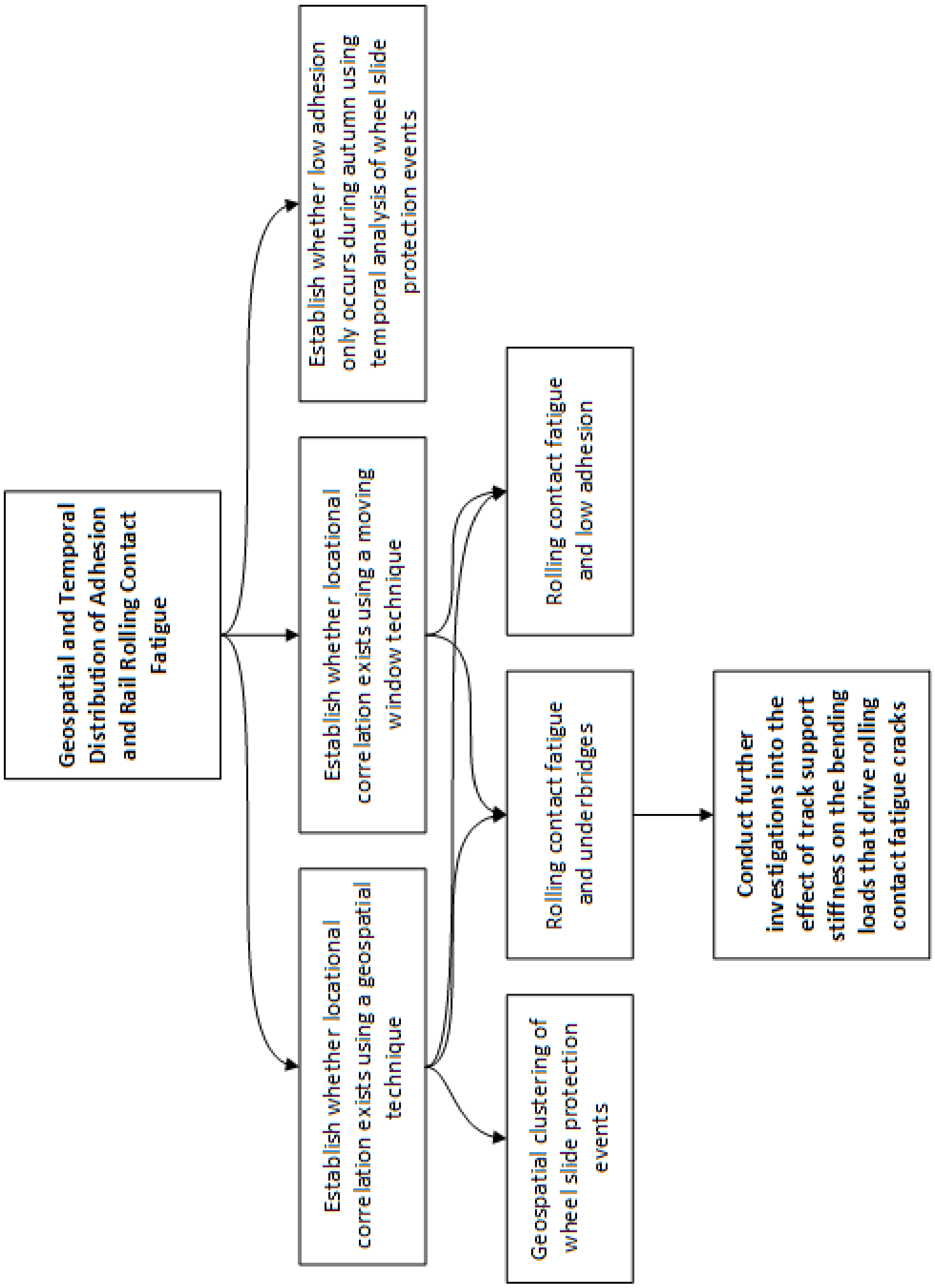

Figure 3.1: Chapter overview

Here a deeper analysis into the methodology, which is similar to that employed in the RSSB T1042 report [48] and White et al. [63], is given. The geospatial approach permitted easy visualisation of the data, providing good insight into locations where low adhesion events were clustered. As a result, the effect that track characteristics, for example track gradient, has on the risk of a train experiencing a low adhesion event could be examined. A further distribution analysis was then undertaken using both geospatial and moving window techniques to establish the impact low adhesion or bridge proximity (if any) has over RCF formation.

Outside of the autumn period there is no policy for the rail industry to collect performance data relating to wheel slides caused by low adhesion. The result of this is that the majority of train operating companies do not store this data throughout the year. The effect that low adhesion has on train delay within the network outside of autumn is therefore unknown. This is of major concern with the increasing demand to increase network capacity whilst maintaining safe train running. Virgin Trains is one of the few train operating companies to collect and store this data on a year round basis. In this Chapter clustering of severe wheel slide events collected from class 390 rolling stock over a five year period along specific sections of track are examined for their statistical significance. This highlights areas where the risk of a train experiencing a wheel slide increases. A temporal analysis of wheel slide events throughout the day and year was examined to demonstrate the highest risk periods for trains to aid driver awareness.

To ensure that the findings from the geospatial analysis were significant, statistical analysis using the Chi squared test [195] was undertaken. Comparison of the actual distribution of wheel slide events to the normal distribution provided confidence that the results obtained using the geospatial method were statistically significant. The normal distribution assumed that the track characteristics had no effect on the number of wheel slide events.

In this Chapter the Track-Ex package [154] has been used, utilizing the contact patch energy ($T\gamma$) approach, to remove locations of RCF that can be predicted with this method, i.e. during cornering. The purpose of filtering the RDMS data was to remove RCF sites that have known causes e.g. generated from lateral forces during cornering calculated in route fleet analysis. This isolates RCF sites with unknown causes so that the impact of the factors discussed below on RCF formation can be assessed.

Comparison of the prediction with Rail Defect Management System (RDMS) data highlighted RCF sites that had not been predicted and therefore highlighted an alternative initiation process to previous literature. Track-Ex utilizes the 80/20 concept of retaining 80% of the accuracy when compared to very high precision models but only consuming 20% of the development costs. It uses several key assumptions with regard to dynamic factors, where only lateral forces are considered. A key area where vertical forces are increased is around underbridges [83]. Their influence on RCF cannot be predicted within Track-Ex, but by removal of RCF sites that were predicted allowed the work in this Chapter to focus on these areas.

A moving window filtering technique and a geospatial approach were used on a section of the rail network. These correlated locations in which RCF occurs with the locations of factors that are known to increase the forces at the wheel-rail contact:

(i) Wheel slides; during which there can be a high level of heat generated at the contact patch and material damage such as transformation of pearlite to brittle martensite, which may subsequently lead to defects in the rail [131, 196–198].

(ii) Underbridges; where the higher support stiffness over the bridge means that the rail deforms less under the lateral and vertical loads, leading to track mis-alignment [83].

Figure 3.2 shows how the two RCF initiation scenarios above can overlap in a complex systems such as the railway. Also shown is RCF formed by cornering forces, which is a well known issue. By using Track-Ex to rule out locations of RCF that were formed by lateral forces during cornering, areas A, D, E and F of Figure 3.2 is removed from the analysis. Therefore locational correlation was established between RCF sites and track mis-alignment around underbridges (B, moving window filtering technique), the presence of low adhesion (C, onboard data) or a combination (G).

Within the analysis two scenarios, Figure 3.3, were considered. Correlation between RCF and wheel slide locations would be a result of either scenario 1(a) or scenario 1(b) occurring. The data are unable to reveal directly whether wheel slides preceded later formation of RCF type defects, or whether wheelset dynamics when crossing an RCF type defect triggers a slide. Correlation between RCF and underbridge locations would demonstrate that alignment issues influence RCF formation (Scenario 2).

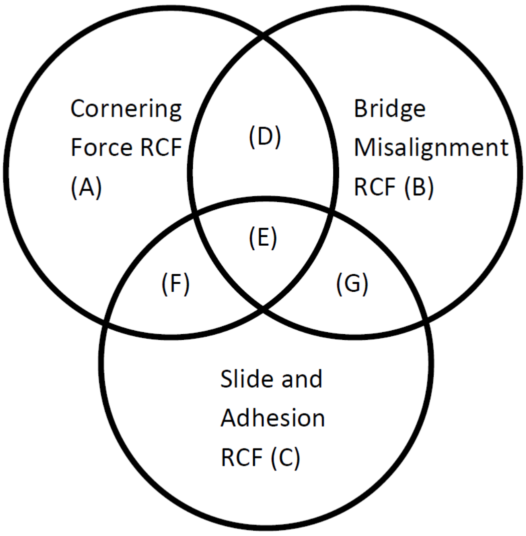

Figure 3.2: Diagram of potential rolling contact fatigue initiation scenarios, highlighting the potential for combination of factors influencing rolling contact fatigue formation

Two types of wheel slides were considered as they were thought to have different causes and therefore different effects on the rail. Momentary sliding is associated with traction peaks during low adhesion and its recovery under traction or braking. Long sliding is associated with low adhesion over a large section of track and predominantly occurs under braking. The location based analysis that has been undertaken identified whether these factors correlated with recorded RCF. It should be noted that these slides are not caused by train faults, but are a consequence of variations in rail-wheel adhesion and reaction of the train systems to this.

The temporal analysis revealed that, although usually associated with autumn problems such as rail head leaf film [42, 43, 46, 55], low adhesion does occur outside the autumn period and therefore cannot be solely attributed to leaf fall. It also showed that the time period where low adhesion is most prevalent falls within the busy morning period, but that this is not the time period when an individual train is most likely to experience a slide.

Through the moving window filtering and geospatial approaches it was identified that there was a statistically significant increase in RCF close to underbridges. Strong correlation between momentary slides and underbridge locations was found. Furthermore strong correlation between the location of RCF and momentary slides was also found. However no correlation was apparent between RCF and long slides. “Momentary” and “long” are defined in Section 3.3.1.1.

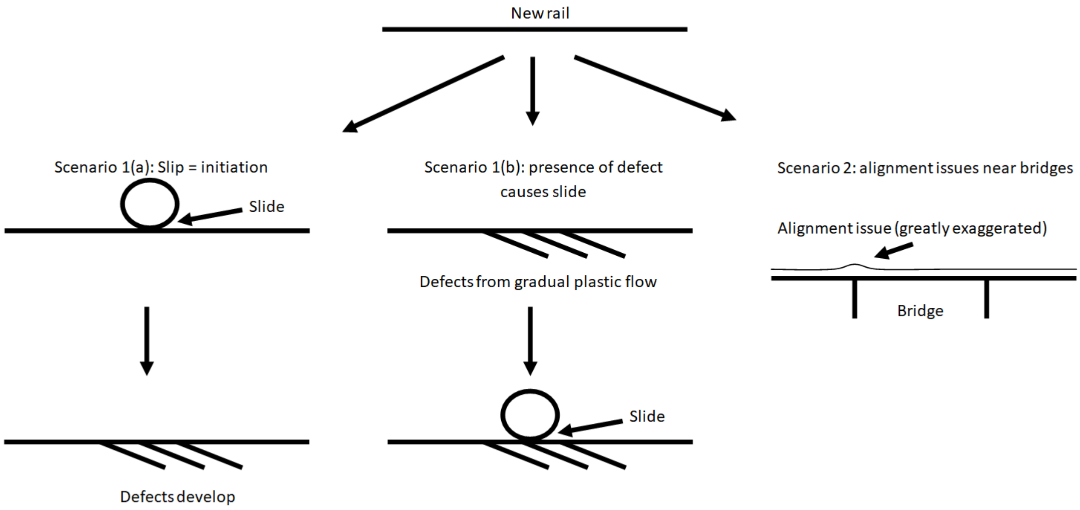

Figure 3.3: Diagram of slide-crack initiation scenarios 1(a): Slip = initiation, 1(b): presence of defect causes slide, 2: alignment issues near bridges. Alignment fault shown is exaggerated

3.2 Analysing Large Data With Geospatial Aspect

3.2.1 Geospatial Technique

The geospatial analysis approach to interrogating data involves the gathering, displaying and manipulation of data with a geographical aspect. Using the geospatial tool ArcGIS [199] permitted a comprehensive analysis through the application of geographic data (maps) in combination with train based technical data. It is commonly used in geographic studies. The advantage of the Geographic Information System (GIS) technique is that it is designed to handle large data-sets. Specific features can be highlighted and manipulated separately through Structured Query Language (SQL) queries and presented over a common base-map. This isolated the more prolonged wheel slide events from very short periods of low adhesion, which allowed for a more focused geospatial study.

3.2.2 Chi-Squared Method for Assessing Statistical Significance

The chi-squared test (χ^2 test), Equation 3.1, is a statistical hypothesis test where the sampling distribution of the test statistic is a chi-squared distribution when the null hypothesis is true [195]. The chi-squared test is used to determine whether there is a significant difference between the expected frequencies and the observed frequencies in one or more categories.

$$\chi^2 = \frac{(observed - expected)^2}{expected} \tag{3.1}$$

Where:

$$expected = total_A \left(\frac{total_1}{total_{total}} \right) \tag{3.2}$$

As an example see Table 3.1. The expected total of area 1 with attribute A is calculated using Equation 3.2, which gives an expected total of 4.125. This value is compared to the observed value of 5 using Equation 3.1, giving a $\chi^2 = 0.186$. This is then compared to the expected value for χ^2 depending on the degrees of freedom, Equation 3.3. If the test statistic is improbably large according to that chi-squared distribution, then one rejects the null hypothesis of independence. This test is used here to assess the statistical significance of the data in relation to geographic features.

$$Degrees\,of\,freedom = (N_{rows} - 1)(N_{columns} - 1) \tag{3.3}$$

	A	B	C	total
1	5	10	15	30
2	6	3	1	10
total	11	13	16	80

Table 3.1: Observed values for Chi-squared test example

3.2.3 Moving Window Filtering Technique

The principle behind the moving window filtering technique, Figure 3.4, is straightforward. Points are arranged along the line at equidistant intervals and the analysis window considered data from a subset of these points on each iteration. As the analysis window slides along the data, the model adapts as it iterates to include data from the newest point and discard data from the oldest point [200,201]. Through this method the changes in the variables over distance are smoothed, permitting an improved analysis in determining proximity relationships between variables. With the gradual introduction of new points and removal of old points, thorough locational relationships can be established. Furthermore, unlike if the analysis window considered new points on each iteration, no locational similarities are missed by some of the nearby events being in the previous analysis window and therefore not counted.

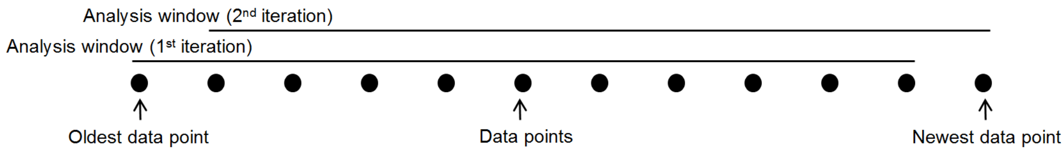

Figure 3.4: A diagram representation of the moving window filtering technique

3.3 Methodology

3.3.1 Data

Rail surface damage data for RCF, together with locations, was collected over a two year period (2013-2015) through the RDMS for the down fast line (trains travelling away from London) of the West Coast Main Line (WCML) [202] in the UK. Locations were defined by the Engineer Line Reference (ELR) and track mileage. Here, the track mileage has been converted into a Global Positioning System (GPS) reference using Rail-View [203] for mapping purposes.

Data on bridge locations focused on underbridges, i.e. any bridge where the railway goes over another feature. At these locations the support structure of the track changes over a small distance. This leads to an abrupt change in track support stiffness and a high likelihood of dynamically generated forces as a train (and its suspension) crosses and reacts to the stiffness change. Minor alignment problems are also common near bridges since lateral as well as vertical stiffness changes with the transition of rail support onto and off the underbridge structure. The combination of these factors has been thought to increase rail damage in these areas. The underbridges considered within the analysis ranged from small culverts up to large underbridges, e.g. viaducts and motorway crossings.

In addition to infrastructure data WSP data was collected over a five year period (2009-2013) from class 390 passenger rolling stock that operates along the WCML. For the results where comparison between WSP events and RCF sites was undertaken only wheel slide events that occurred on the down fast line (the same line as the data for the RCF) were considered. The WSP system on this rolling stock records a wheel slide event when the rotational speed of the free rolling leading axle differs from that of one of the three remaining braked axles on the leading car, i.e. if the rotational speed of the braked axle is less than free rolling axle it is experiencing a slide. The majority of the data used within this Chapter therefore represents an individual axle undergoing sliding and not the whole train experiencing a slide. The number of wheel slides found within this data is representative of any high speed rolling stock operating within the UK, i.e. it is part of normal operation and not caused by a rolling stock fault.

During the period of data collection there have been no major upgrades to the WCML [204] with only routine maintenance being undertaken. Nor have the types of rolling stock and the line speed changed significantly during the study period. These two factors mean that locations that have a high density of RCF type defects would not be expected to change. However it has not been recorded whether the proportion of the different types of rolling stock that operate along the WCML remained consistent throughout the time period studied.

The WSP event data required some preparation to be useable. The full details of the preparation method used on the WSP data for geospatial analysis has been summarised in Appendix C. An example set of the data is shown in Figure 3.5 for ease of reference. In summary, data from the on-board Train Management System (TMS) and lineside balises was used to assign each wheel slide event with a GPS location (TMS data) and a line direction (balise data).

Results | Messages

	MeasuredTime	Unit	Vehicle	Temperature	OHLV	GpsLocation
1	30/07/2012 17:00:03	390053	3	20	25640	N51.57333 W0.31000
2	30/07/2012 17:05:39	390053	8	21	25550	N51.53433 W0.20133
3	30/07/2012 17:05:41	390053	1	21	25530	N51.53467 W0.20033
4	30/07/2012 17:07:01	390053	6	21	25610	N51.54150 W0.17233
5	30/07/2012 17:11:22	390053	1	21	25290	N51.52917 W0.13383
6	30/07/2012 17:12:20	390053	8	21	25450	N51.52917 W0.13383
7	30/07/2012 17:24:05	390053	1	21	25340	N51.52917 W0.13383
8	30/07/2012 17:27:40	390053	8	21	25730	N51.52917 W0.13383
9	30/07/2012 17:50:02	390053	8	22	25600	N51.52917 W0.13383
10	30/07/2012 17:50:07	390053	1	22	25860	N51.52917 W0.13383
11	30/07/2012 17:50:07	390053	8	22	25910	N51.52917 W0.13383
12	30/07/2012 17:50:08	390053	8	22	25900	N51.52917 W0.13383
13	30/07/2012 17:50:19	390053	8	22	25780	N51.52917 W0.13383
14	30/07/2012 17:56:46	390053	1	22	25620	N51.52917 W0.13383
15	30/07/2012 17:58:19	390053	1	20	25680	N51.53283 W0.14133
16	30/07/2012 18:00:00	390053	3	20	25720	N51.54217 W0.15283
17	30/07/2012 18:00:00	390053	1	20	25650	N51.54217 W0.15300
18	30/07/2012 18:00:02	390053	6	20	25730	N51.54233 W0.15333
19	30/07/2012 18:00:04	390053	8	20	25710	N51.54250 W0.15367

Figure 3.5: Sample of data from the train management system table showing the GPS coordinate assigned to each timestamp. Combination of data from this and the wheel slide protection table permitted geospatial analysis of the wheel slide data

When using the TMS supplementary data, only 10% of WSP events occurred at the exact time the TMS had data. Therefore, to include a larger proportion of WSP events within the analysis, several time intervals were considered (Table 3.2). The accuracy of the WSP event locations within each time interval was calculated assuming a train speed of 200kph (125mph). Based on the maximum UK line speed this gave the maximum possible distance between the WSP event and the location given by the GPS coordinates.

The ±5 seconds time interval was applied to the data extraction method. This was because it increased the percentage of WSP events that were captured by 40% over the ±0 seconds time interval whilst introducing the smallest reduction in location accuracy. The ±10 seconds and ±20 seconds time intervals reduced the location accuracy by a further 50% whilst only capturing a further 10% of WSP events. It is also of note that the inaccuracy that would be introduced by applying a ±10 seconds or ±20 seconds time interval is significant compared to the overall slide length being considered in the analysis, which is discussed in Section 3.3.1.1.

Time Interval (seconds)	±0	±5	±10	±20
Percentage of WSP events in the results (%)	10	50	61	75
Accuracy of results (metres) based on train speed of 200kph (125mph)	±15 [205]	±275	±550	±1100

Table 3.2: Percentages of wheel slide protection events captured in results and the accuracy of those results for each time interval

3.3.1.1 Filtering Wheel Slide Data

Long slides and momentary slides were considered separately since they were expected to produce different degrees of track damage. When considering the impact of wheel slides on RCF the main point of consideration was the length of track that the slide occurred along. Therefore the severity criteria for long slides and momentary slides were defined in accordance with whether the associated damage was concentrated locally or over a prolonged section of track.

Two categories of long slides were defined by the following severity criteria:

- Category LD (Long slide, Distance): Slide distance of greater than 800m (0.5 miles).
- Category LT (Long slide, Time): Slide time of greater than 15 seconds.

The time criterion is based on the 800m slide distance for a train with a speed of 200kph (125mph; maximum UK line speed). The severity criteria highlight severe events where the adhesion level available is insufficient over a prolonged distance or time.

Two categories of momentary slides were defined by the following severity criteria:

- Category MD (Momentary slide, Distance): Distance of less than 4.8m (0.003 miles).
- Category MT (Momentary slide, Time): Slide time of less than 0.1 seconds.

The momentary slide time criterion was based on the shortest time that it would be reasonable for the wheel slide protection system to detect and record ‘an event’, i.e. a wheel-set slide. The distance criterion is based on the 0.1 second slide time for a train speed of 200kph (125mph).

For the geospatial distribution analysis (Section 3.4.2.1) an additional speed constraint was added to the long slide category to highlight where the level of adhesion that was available was insufficient to slow down the train.

Two categories of severe slides were defined by the following severity criteria:

- Category SD (Severe slide, Distance): Slide distance of greater than 800m (0.5 miles) with a speed change of less than 24kph (15mph).
- Category ST (Severe slide, Time): Slide time of greater than 15 seconds with a speed change of less than 24kph (15mph).

The speed change aspect of the severity criteria aims to highlight severe events where the adhesion level available is insufficient to slow the train. Under normal conditions the braking standards demand an acceleration rate of at least 0.87m/s^2 for multiple units that operate up to 200kph (125mph) [206]. The analysis undertaken in this study focuses on events where a braking rate of half the required rate, i.e. less than 0.44m/s^2, has been achieved under braking. The data that is presented here for severe slides shows that the train failed to achieve this lower braking rate (and therefore suffered low adhesion) over a prolonged distance/time.

3.3.1.2 Filtering Rolling Contact Fatigue Data

A Track-Ex route fleet analysis, explained in Section 2.3.7.1, was completed for the down line (trains travelling away from London) in ELR's LEC1, LEC2, LEC4 and CGJ1-7. This covered approximately 300 miles of track between London and Carlisle. LEC3 and LEC5 are within station areas only and were therefore not considered. The route fleet analysis predicted the level of RCF that would be present along this line after a 52 week period. The purpose of filtering the RDMS data was to remove RCF sites that have known causes e.g. generated from lateral forces during cornering calculated in route fleet analysis. This isolates RCF sites with unknown causes so that the impact of the factors discussed in Section 3.1 on RCF formation can be assessed.

From the RDMS data it was unknown how long a period of time the RCF site formed. This is likely to be different across the data due to different rail replacement periods. Therefore two levels of aggressiveness were applied to the filtering of the data.

In the less aggressive method RCF sites where the mode predicted level of RCF was greater than zero were removed from further analysis. This means that sites are only removed from the analysis if the Track-Ex route fleet analysis had predicted RCF to occur over the majority of the site in the RDMS data. In the mode filtering method the assumption is that for an RCF site to be driven by cornering forces the majority of that site must be predicted by the route fleet analysis. If this is not true then there must be other influencing factors, warranting the inclusion of these sites.

In the more aggressive method RCF sites where the maximum predicted level of RCF was greater than zero were removed from further analysis. This means that sites are removed from the analysis if the Track-Ex route fleet analysis had predicted any RCF to occur within the site in the RDMS data. The maximum filtering method takes into consideration that it is not known how long the RCF site in the RDMS data has been in the rail. If the RCF site has formed over a longer period than 52 weeks the route fleet analysis will clearly under predict the level of RCF present in the rail. If any RCF is predicted in this area by the route fleet analysis this filtering method assumes that this will expand to cover the whole site within the RDMS data. Therefore only sites where the predicted level of RCF from the route fleet analysis is zero could have other influencing factors and are therefore included.

An example section of line is shown in Figure 3.6 to demonstrate the effect of the two levels of filtering. Here, the RDMS site found at mileage 169.0726 to 169.0960 occurs at a point where RCF has been predicted by the route fleet analysis over the majority of the site. Therefore this section of track was removed from the analysis for both filtering methods. However in the RDMS site found at mileage 170.0072 to 170.0121 the route fleet analysis has predicted a brief instance of RCF. Therefore this section of track was removed from the analysis for the maximum filtering method only. The effect of removing these sites from the analysis is investigated in Section 3.4.1.1. Whilst not the focus of this thesis it is of interest to note that Figure 3.6 implies that, as well as RCF being present where not predicted (which is the focus of this Chapter), at some locations along the line, RCF is predicted but not present.

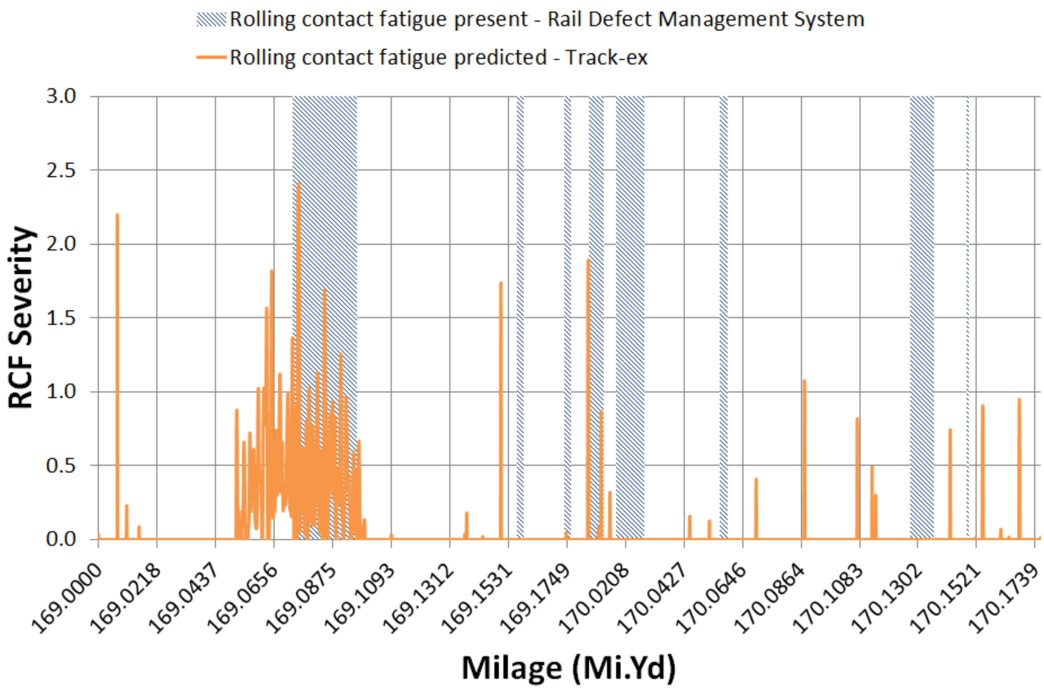

Figure 3.6: Diagram showing the predicted rolling contact fatigue level through Track-Ex output against actual rolling contact fatigue sites from rail defect management system data, demonstrates which rolling contact fatigue sites will be removed from the analysis

3.3.2 Moving Window Filtering Technique

A moving window filtering technique was used to ascertain if correlation existed between the occurrence of underbridges, low adhesion and RCF sites along the WCML between London and Carlisle. The principle behind the technique is explained in Section 3.2.3. Points were arranged along the line at 8m intervals with the analysis window considering data from eleven of these points at any one time (80m of track).

The 80m (0.05 miles) analysis window length allowed for an approximation of curved track to straight track. With this approximation the 80m analysis window would effectively be the chord length across the circular arc that the track would follow. On the tightest curve radius along the WCML of 500m [131] the arc length is 80.09m, leading to a maximum difference between the analysis window length and the actual track length of 0.09m. Therefore minimal inaccuracy has been introduced using an analysis window length of 80m.

Within each analysis window the number of underbridges, RCF and low adhesion events were counted. A baseline value of the likelihood that a factor would occur in any given analysis window and the average number that occurred per analysis window was obtained by consideration of the whole line. A comparison has then been drawn between the baseline value and the value when both factors were present.

For example: when considering the likelihood of locational correlation between RCF sites and underbridges, the proportion of analysis windows that contained both RCF sites and underbridges was compared to the baseline proportion of analysis windows that contained RCF sites. From this a relative likelihood ratio of the occurrence of RCF sites nearby underbridges has been obtained and the amount of locational correlation was ascertained.

3.3.3 Geospatial Distribution

3.3.3.1 Distribution of Low Adhesion

The geospatial analysis approach to interrogating data is outlined in Section 3.2.1 and permitted a comprehensive analysis through the application of geographic data (maps) in combination with train based technical data. Through implementation of a technique designed to handle large data-sets specific characteristics can be isolated and presented over a common base-map. This was used to isolate the wheel slide events of interest, which allowed for a more focused geospatial study and increased the clarity of the results.

This technique improves on the current standard in the UK rail industry of collecting low adhesion data through driver reports. Previously little was known on whether wheel slides occur outside of the most significant braking areas or outside of autumn as driver reports are only collected during the autumn period and if delay occurred due to a station overrun or signal passed at danger.

This data, taken directly from a wheel slide protection system, permits the inclusion of these previously unquantified regions of the network. As a result a complete picture is established when considering the statistical significance of the occurrence of wheel slide events at specific locations.

In mapping the location of low adhesion incidents, the severity criteria outlined in Section 3.3.1.1 are used to define an ‘event’ which then becomes a single data point.

Although this inherently means a loss of data in terms of the duration or severity of low adhesion it does limit the data sufficiently for analysis. It is important to note that, due to GPS accuracy of ±15m [205], some WSP event locations are positioned to one side of the actual line location.

3.3.3.2 Distribution of Rolling Contact Fatigue sites

To ascertain whether any locational correlations found with the moving window technique outlined in Section 3.3.2 occurred at any specific locations along the line the geospatial distribution of RCF sites that occurred within ±40m of underbridges or wheel slides was examined. The choice of distance was guided by research looking at track damage associated with the approaches to underbridges [207].

Other track misalignments, for example at welds or rail joints would excite the suspension of the passing trains, leading to peak rail loads some distance further along the line from the cause of excitation [208]. The exact distances to the point of peak force or maximum damage will vary, for example depending on speed and whether surface contact pressure generated damage is of interest, or rail interior or foot damage.

3.3.4 Adhesion Temporal Analysis

In line with a methodology used in the RSSB T1042 report [48] an analysis was undertaken on how the frequency of wheel slides varied throughout the year and throughout the day. This highlighted the time periods for which large wheel slide events were more prevalent and whether the trends observed remained consistent (within the uncertainty of the data) throughout the five year period studied.

The aim of this was to investigate whether there is a statistically significant rise in wheel slide events during the autumn period when there are leaf layers present [43], or whether they are distributed more evenly throughout the year, indicating that other factors are a significant cause of wheel slide. Similar analysis was undertaken on the hourly wheel slide events to highlight whether there were periods during the day where wheel slide events were more likely to occur. A comparison was drawn between the years to ascertain whether the pattern of wheel slide events remained consistent throughout the five year period studied.

3.4 Results

3.4.1 Moving Window Filtering Technique

3.4.1.1 Effect of Aggressive Filtering on the Rolling Contact Fatigue Data

Here the effect of increasing the aggressiveness of the filtering is examined. In Figures 3.7 and 3.8 the effect of the aggressiveness of the filtering on RCF sites (Section 3.3.1.2) within ±40m of an underbridge or wheel slide can be seen. One important point to note is that the maximum filter has removed any RCF sites near multiple bridges, the reasoning behind this is discussed in Section 3.4.1.2.

Figure 3.7a suggests that the maximum filter is too aggressive. With the likelihood of RCF within ±40m of an underbridge decreasing to 0.8 times the unfiltered value after initially increasing to 1.3 times the unfiltered value for the less aggressive mode filter. However Figure 3.7 shows greater locational correlation between RCF sites and underbridges for the maximum filtering method.

Figure 3.8a shows consistent results between the different filtering approaches when assessing wheel slide events within ±40m of an rolling contact fatigue site. This is explained further in Section 3.4.1.3. However Figure 3.8b shows that locational correlation between wheel slide events and RCF increases by 1.3 then 1.7 times the unfiltered value as the level of aggressiveness of the filtering is increased. Therefore it was decided that the maximum filter was not so aggressive that too much data was lost and would be used for this work.

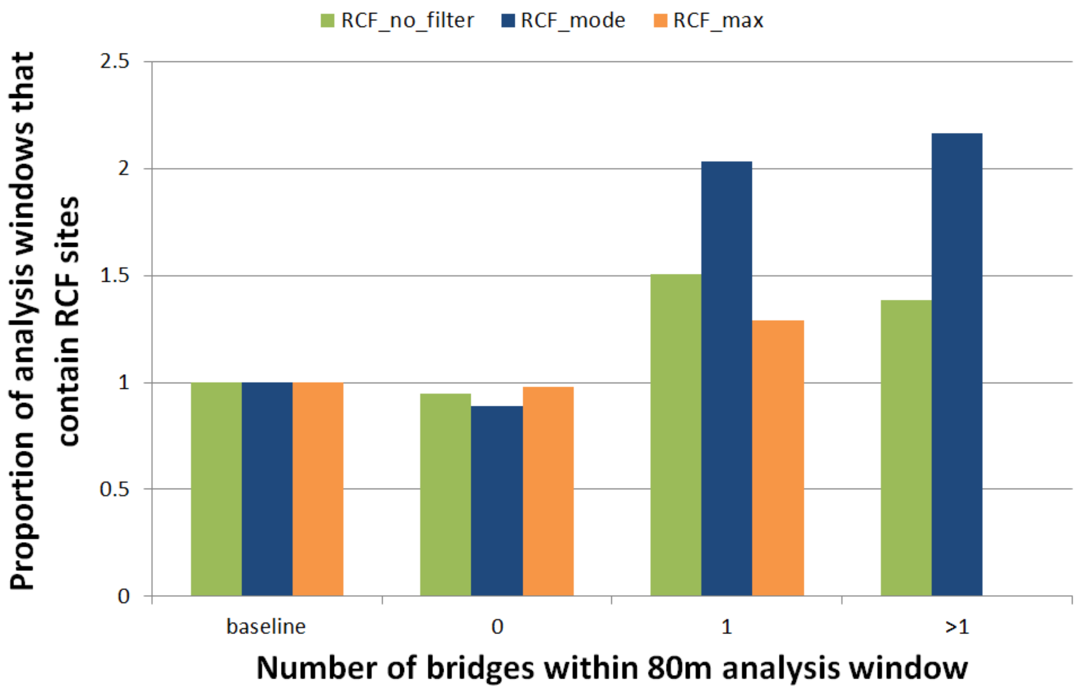

(a)

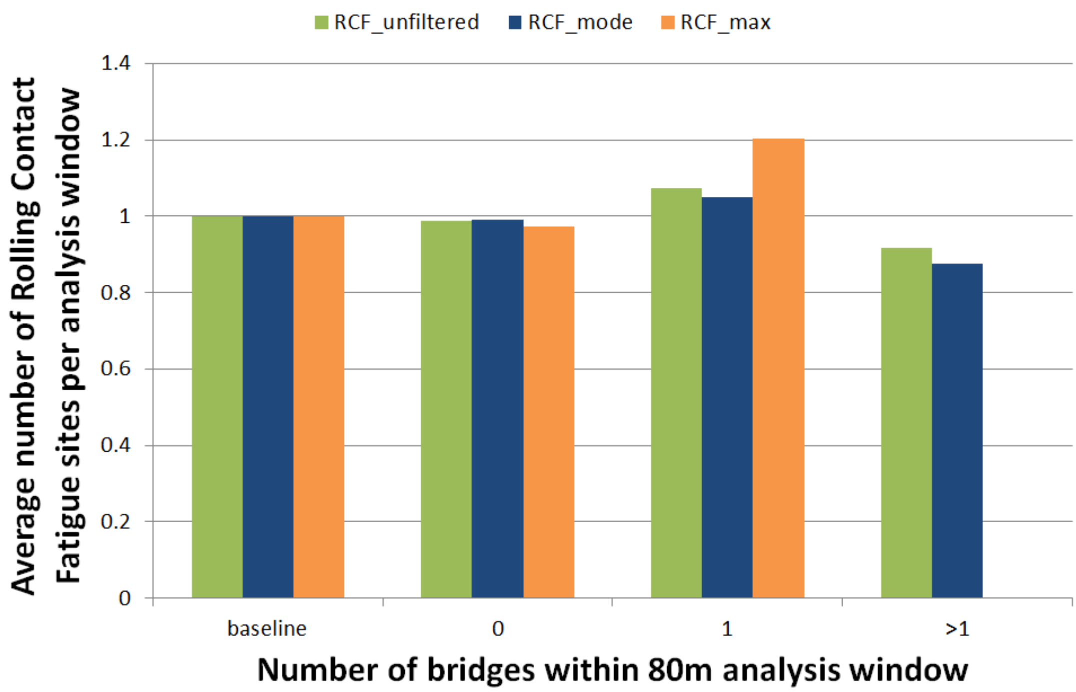

(b)

Figure 3.7: Comparison between the different filtering approaches for the rolling contact fatigue data. Unfiltered rail defect management system data is compared to maximum or most common filtered data. Rolling contact fatigue sites within ±40m of an underbridge, (a) likelihood of rolling contact fatigue occurrence, (b) number of rolling contact fatigue sites that occurred per analysis window

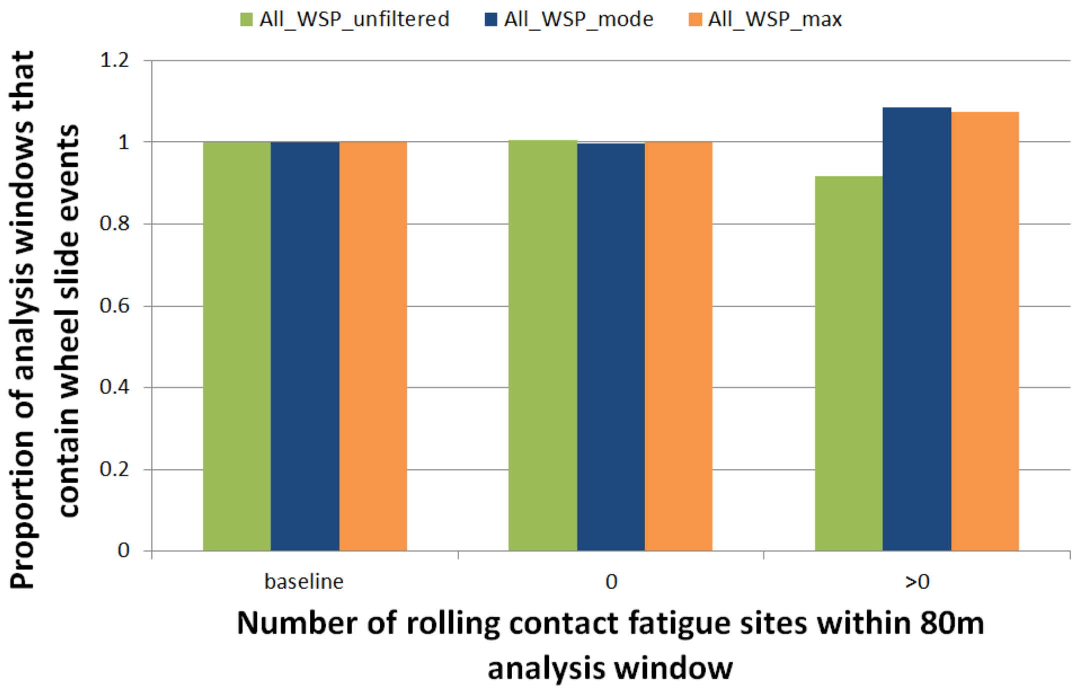

(a)

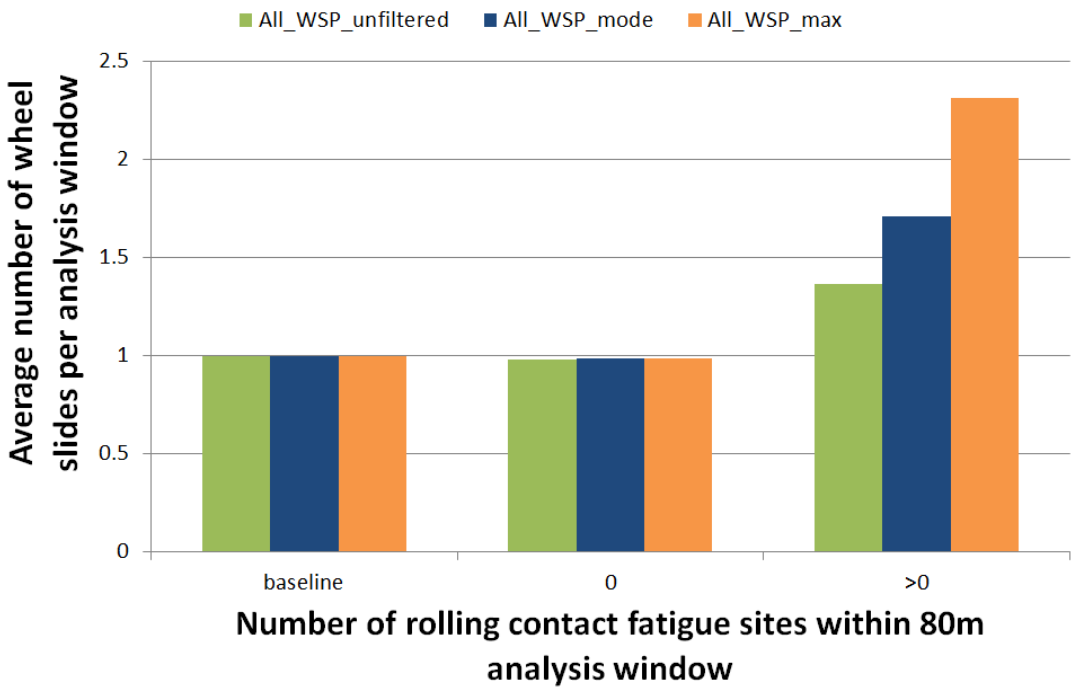

(b)

Figure 3.8: Comparison between the different filtering approaches for the rolling contact fatigue data. Unfiltered Rail Defect Management System data is compared to maximum or most common filtered data. Wheel slide events within ±40m of an rolling contact fatigue site, (a) likelihood of wheel slide occurrence, (b) number of wheel slides that occurred per analysis window

3.4.1.2 Underbridges and Rolling Contact Fatigue

Figure 3.9 shows the proportion of analysis windows that contained RCF and low adhesion events (split into the MD, MT, LD and LT categories discussed in Section 3.3.1.1) within 80m of an underbridge relative to the baseline. The baseline case of 1 demonstrates the proportion of analysis windows that contained each type of event when considering the whole line where the Track-Ex prediction was undertaken, whether or not the analysis window included an underbridge. Analysis windows with underbridges present made up 10% of the total line length considered.

As shown in Figure 3.9 when there were no underbridges in the analysis window the occurrence of RCF and the likelihood of momentary slides occurring was almost identical to the baseline. When the analysis window had a single underbridge within it then the occurrence likelihood of RCF and momentary slide events increased to 1.3 times the baseline. When there were multiple underbridges within the analysis window the percentage of cases that also contained a momentary slide event increased to 1.9 times the baseline. When both categories of long slides were considered together, the likelihood of their occurrence remained almost identical to the baseline. When the severity criteria were not applied to the WSP events the likelihood of their occurrence also remained almost identical to the baseline.

Figure 3.10 shows the average number of RCF or low adhesion events that occurred per analysis window. All results are relative to the baseline, the average number of events that occurred when considering the whole line. As can be seen the average number of RCF sites that occurred increased to 1.2 times the baseline when an underbridge was present. Between the two categories of momentary slide, the average number of events that occurred increased to 1.3 times the baseline in the same analysis window as a single underbridge. This further increased to 1.4 times the baseline when there was more than one underbridge. The average number of long slides that occur increases by 1.1 times the baseline in the same analysis window as a single underbridge, but then decreases to 0.7 times the baseline when there was more than one underbridge. When the severity criteria were not applied to the WSP events the average number that occurred in the same analysis window as a single underbridge increased to 1.2 times the baseline, further increasing to 1.6 times the baseline when there was more than one underbridge.

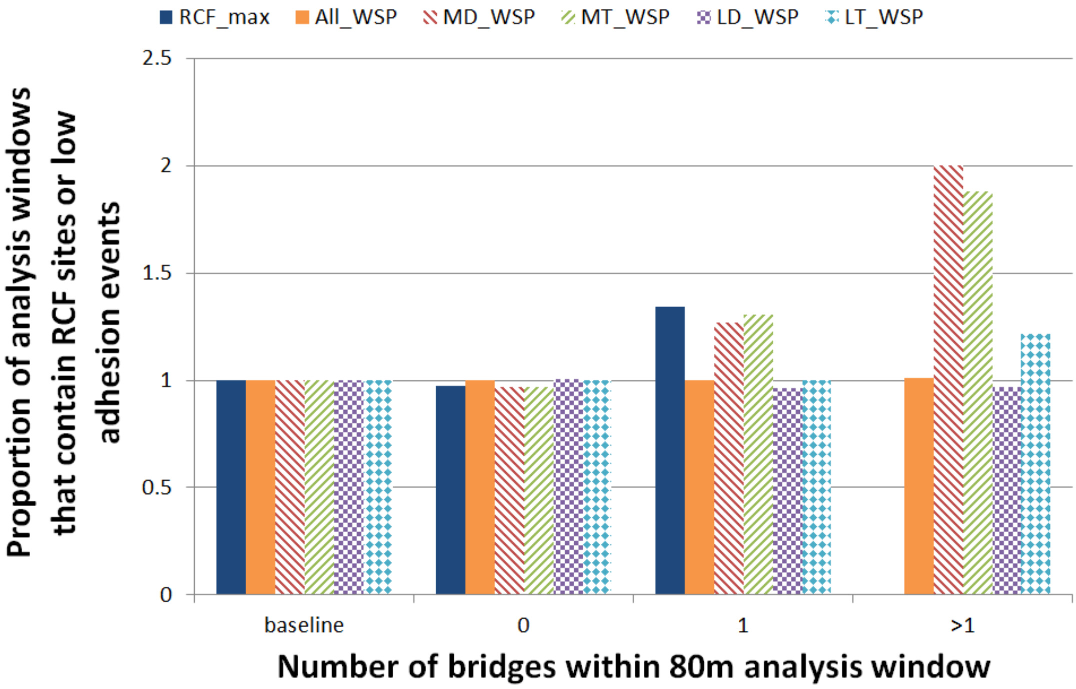

Figure 3.9: Comparison between the proportion of analysis windows that contain RCF sites or low adhesion events within 80m of bridges against the baseline

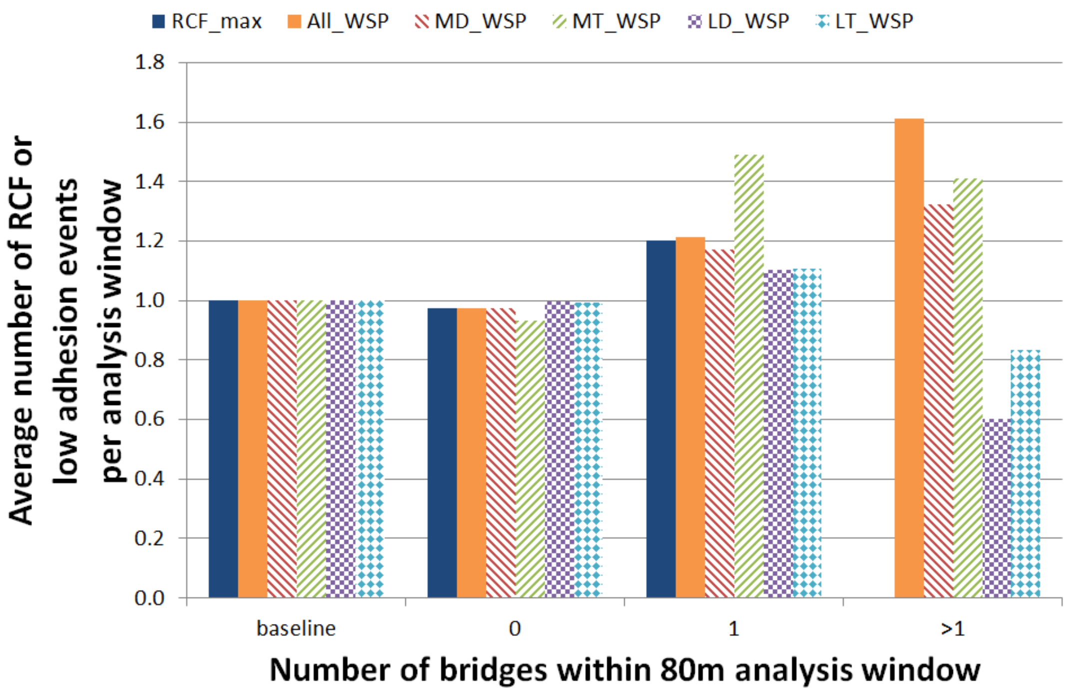

Figure 3.10: Comparison between the number of RCF sites or low adhesion events within 80m of bridges against the baseline

Out of all the analysis windows that contained underbridges, 8% have multiple underbridges within them. This is 8% of the 10% total line length that contained at least one underbridge stated earlier in Section 3.4.1.2. Therefore, the limited number of analysis windows (0.8%) that match this condition has meant that no RCF sites have met this criterion. However the increase in both RCF site likelihood and average number of sites per analysis window with a single underbridge demonstrates the influence that an underbridge has on increasing RCF type defects. Without the application of the severity criteria the number of analysis windows that contained WSP events was 85% of the total number. This meant that when considering the likelihood of the occurrence of WSP events the analysis window was already highly likely to contain WSP events, leading to only small changes in the likelihood results. The increase of the average number of WSP events even though the likelihood of their occurrence remained constant demonstrates clustering of WSP events around underbridges.

When considering the two categories of momentary slides or long slides the number of analysis windows that contained these types of events reduced to 12% and 29% of the total number respectively. This permitted the likelihood analysis to demonstrate clustering of these events. The large increase in momentary slide likelihood and average number of events per analysis window when multiple underbridges are in the same analysis window demonstrates the effect that numerous stiffness changes and increased instances of track misalignment within a short section of line has on momentary slide events, with the wheelset not able to accommodate the sudden changes in track alignment.

No correlation was found between the likelihood of long slides occurring and underbridge locations. This was expected as the stiffness changes associated with underbridges were not expected to affect the adhesion level over 800m of track. The underlying cause of negative correlation in the number of long slides that occurred in the same analysis window as multiple underbridge cannot be confirmed with the available data but an observation that was made is that a key influence behind this correlation could be the proportion of underbridges within heavy braking areas such as on the approach to stations or signals. It is also of interest to note the different responses to the presence of an underbridge that the two different categories of WSP have, supporting the hypothesis that they have different causes.

3.4.1.3 Low Adhesion and Rolling Contact Fatigue

Locational correlation between RCF sites and WSP events is shown in Figure 3.11. When the severity criteria were not applied to the WSP events the likelihood of their occurrence in the same analysis window as an RCF site increased to 1.1 times the baseline. The likelihood of momentary slides occurring within the same analysis window as an RCF site was 2.4 times the baseline average between the two categories. The likelihood of long slides occurring within the same analysis window as an RCF site was 1.5 times the baseline average between the two categories.

Figure 3.12 shows how the average number of WSP events is affected by the presence of an RCF site. When the severity criteria were not applied to the WSP events the average number that occurred in the same analysis window as an RCF site increased to 2.3 times the baseline. The average number of momentary slide events that occurred within the same analysis window as an RCF site was 1.3 times the baseline average between the two categories. The average number of long slides that occurred within the same analysis window as an RCF site was 0.7 times the baseline average between the two categories.

As stated in Section 3.4.1.2, without the application of the severity criteria the number of analysis windows that contained WSP events was 85% of the total number, leading to only small changes in the likelihood results. The increase of the average number of WSP events that occurred per analysis window gives a better understanding of the locational correlation between low adhesion and RCF sites, showing the locational correlation between WSP events in general and RCF sites.

The increase in both the likelihood and the average number of momentary slide events per analysis window in the same analysis window as an RCF site supports the hypothesis that locational correlation exists between momentary slides and RCF sites (but is not a causal link). There was negative correlation between the average number of long slides that occurred and RCF sites whilst positive correlation between the likelihood of long slides occurring and RCF sites. Overall this is inconclusive and therefore no locational correlation between long slides and RCF sites was found. It is important to note that although a single RCF crack would be classed as 'heavy' if having a visible surface crack length over 20mm, and 'severe' if over 30mm [24] (very small relative to the distance of sliding) these cracks do not occur in isolation, but would have to occur in significant quantity to influence the adhesion level over a prolonged section of track.

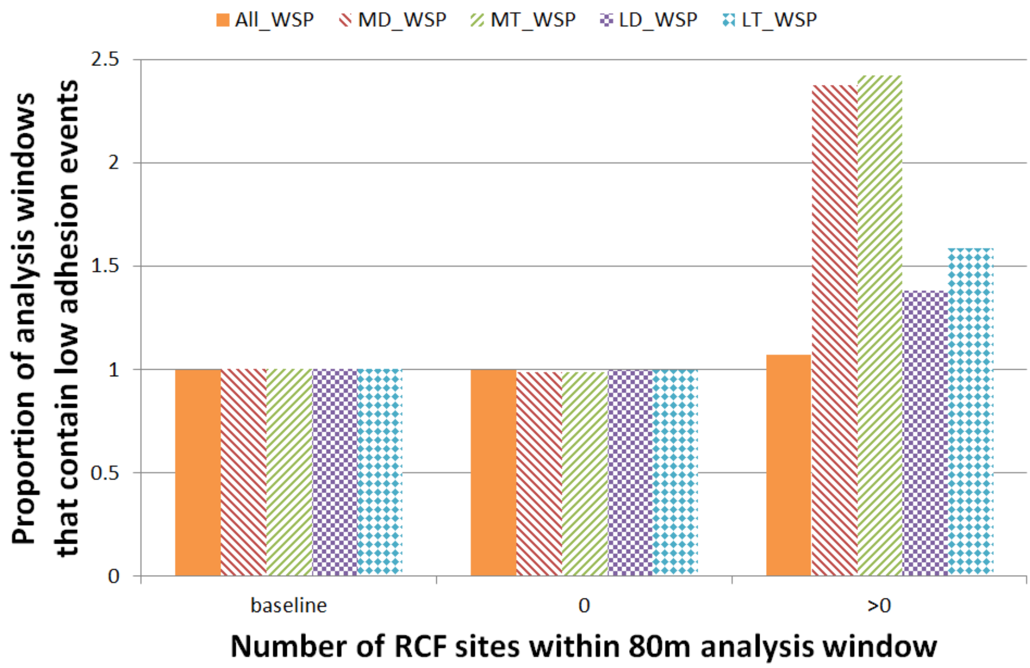

Figure 3.11: Comparison between the proportion of analysis windows that contain low adhesion events within 80m of an RCF sites against the baseline

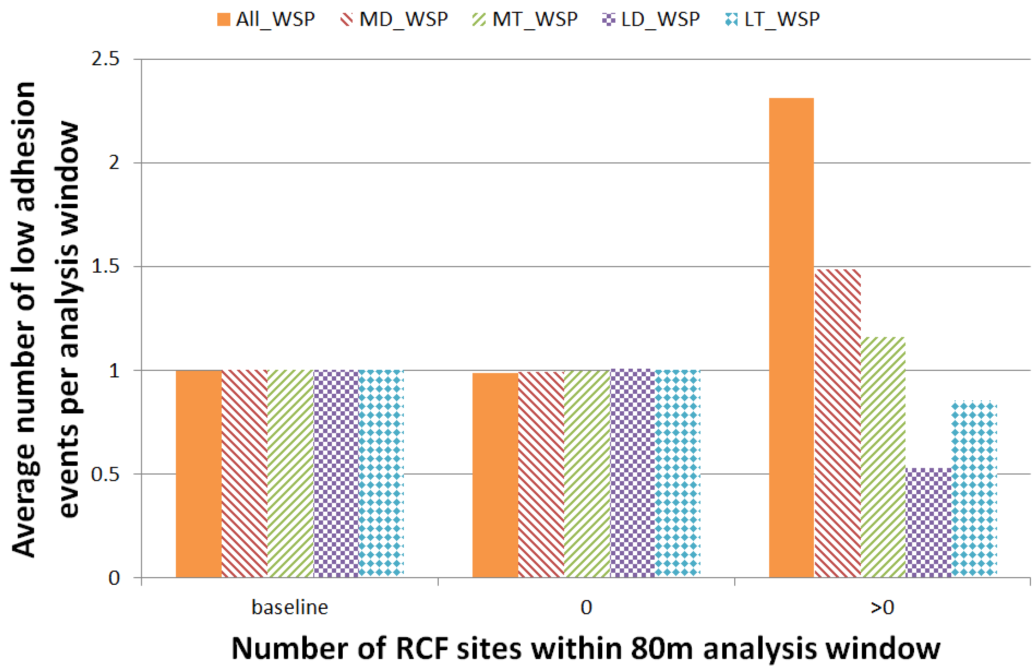

Figure 3.12: Comparison between the average number of low adhesion events within 80m of RCF sites against the baseline

3.4.2 Geospatial Distribution

3.4.2.1 Low Adhesion

An initial review of the data using the geospatial technique [194] demonstrated that wheel slide events tend to occur in clusters that remain consistent in their location across the five year period studied. The low adhesion cluster locations are often different between the up line (southbound, toward London), and the down line (northbound, away from London). Travel direction and the severity category the event matched are shown in the different colours highlighted in Table 3.3 where the arrow direction shows the travel direction. All figures are orientated so that north is vertically up the page.

Line Direction	Travel Direction	Arrow Direction	Colour	
			Severe slide, Distance	Severe slide, Time
Up	Southbound	Downwards	Pink	Purple
Down	Northbound	Upwards	Green	Orange

Table 3.3: Colour categorisation used for the low adhesion events

The analysis considered a selection of locations (labelled areas A-D) where 100+ severe category slides were clustered to highlight features (if any) that correlated with an increased risk of low adhesion. Several reasons were proposed and examined for their effect on the clustering of low adhesion events:

- Different braking areas between the lines. Speed change requirements are communicated to the train from track-side transponders, known as balises, to help the train to pinpoint where braking should be applied.
- Gradient of the line.
- Differing levels of shade, and hence differences in humidity or railhead temperature. This may influence the presence of dew condensing, but also lineside vegetation and bacterial activity at the rail surface [63].
- Nearby roads.
- Other effects not yet identified.

Figure 3.13 shows the wheel slide events that occurred in Area A along the up line. The line has a gradient of 1:-535 in the direction of travel. The satellite image shows significant areas of trees to both the East and to the West of the line and that the cluster occurs before a tunnel; highlighted by the bold blue line to the South. There is a cutting before the tunnel entry; however the event cluster occurs before a train on the Up line (Southbound) has reached this feature. A major motorway crosses the line at the point where the cluster occurs. The balise located within this cluster is demanding a speed decrease from 125mph to 110mph in preparation for the junction four miles ahead.

Figure 3.13: Area A, scale 1:15,000, left satellite image, right topographical map

In comparison, the opposing approach to the junction on the Down line is within a cutting and lined with trees and urban areas (but with no major roads) with a track gradient of 1:2050 in the direction of travel. There are one quarter the number of low adhesion events recorded in the Down line cluster relative to those on the Up line in

Area A. The track characteristics that are different between these two locations are track gradient and a major road crossing the line in Area A.

Figure 3.14 shows wheel slide events in Area B, with two clusters on opposing lines which occur on the approach to a station (outlined with a solid red circle). The station serves the ‘slow’ line only, and class 390 services would not stop here, however a speed restriction also affects the ‘fast’ through lines. The southern cluster is located on the Down line which is ascending with a gradient of 1:529 in the direction of travel. The northern cluster is located on the Up line where the track is beginning to ascend with a gradient of 1:306 in the direction of travel after a descent with a gradient of 1:-115.

The satellite image highlights that there is woodland to the south of the line but that the track has no adjacent woodland and does not follow a cutting at either location. The balises at these locations are demanding a line speed reduction from 125mph to $\simeq$100mph.

Both locations are close to a major road as shown by the topographical map but the southern cluster is within an urban area. The clusters contain a similar number of incidents with the southern cluster containing 2% higher number of events. The track characteristic that is different between these two locations is the presence of an urban area in the southern cluster.

Figure 3.15 shows wheel slide events in Area C, this cluster occurs over an extended section of track along the Up line approaching a junction. The line is descending with a steepening gradient from 1:-686 to 1:-520 in the direction of travel.

The satellite image highlights a significant wooded area to the north of the railway, which borders the line, but the line is not within a cutting and the topographical map shows that a major road crosses the line at the start of this cluster. The balise located within this cluster is demanding an unspecified speed decrease, expected to be for the junction in three miles.

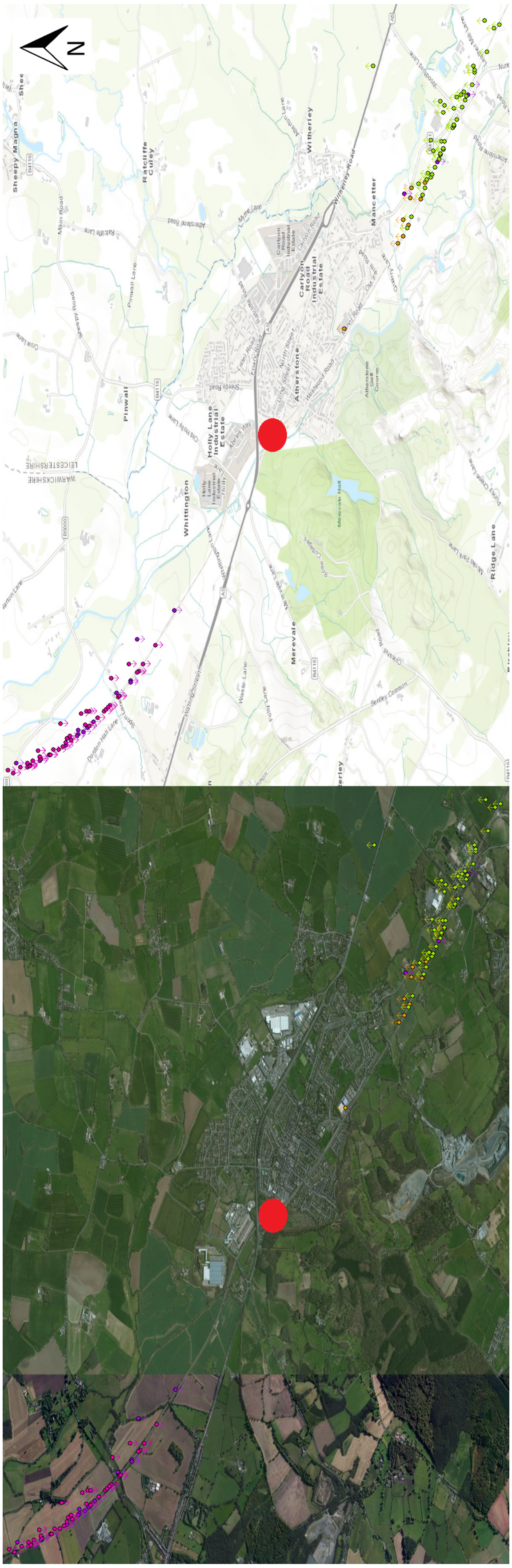

Figure 3.14: Area B, scale 1:30,000, left satellite image, right topographical map

Figure 3.15: Area C, scale 1:20,000, left satellite image, right topographical map

Unlike in Area A and Area B, where the clusters of wheel slide events are more concentrated, the events in Area C are spread over a four mile section of track. The cluster of low adhesion incidents at the opposing approach to the junction occurs on track with a gradient of 1:520 in the direction of travel, has no woodland nearby and occurs next to the crossing of a major road. However it contains one seventh the number of incidents that are present in the Up line cluster in Area C. The track characteristics that are different between these two locations are track gradient and nearby woodland in Area C.

Figure 3.16 shows wheel slide events along the Up line in Area D. The line has a gradient of 1:-257 in the direction of travel. The satellite image highlights that there are no woodland areas in the vicinity of the railway and a series of small cuttings along this section of track where several minor roads (shown more clearly in the topographical map) cross the line. The small number of houses to the East of the line is a holiday park and therefore cannot be considered to be an urban area. The balise located within this cluster is demanding an unspecified speed decrease, expected to be for the station in three miles.

Figure 3.16: Area D, scale 1:20,000, left satellite image, right topographical map

Similar to Area C, the events at this location are spread along three miles of track. There is no notable cluster on the opposing approach to the station, with one thirtieth the number of events occurring along that section. Here the line has a gradient of 1:355 in the direction of travel, has no nearby woodland or cuttings and a major road crosses the line. The track characteristics that are different between these two locations are track gradient and lack of major roads crossing the line in Area D.

As expected severe category wheel slides occurred within areas of heavy breaking, with the analysis highlighting that this often occurred when braking from high speed. However not all areas of heavy breaking had clusters of severe category wheel slide events within them. From the analysis it can be seen that several key factors influence the occurrence of severe category wheel slide events.

Recurring factors at these sites demonstrate the effect that track gradient, road, urban area or woodland proximity have on the likelihood that a train will experience low adhesion at a particular location. Further investigation on the effect of woodland, roads or urban areas could not be undertaken without repeated site visits, which were beyond the scope of this work. However statistical analysis of the full wheel slide event data does provide some additional information on the influence of track gradient on severe category wheel slide events.

The total number of wheel slide events that occurred near each balise was compared with the balise function and the track gradient at the balise location. From this the influence of track gradient on wheel slide events in general and the severe category wheel slide events was ascertained. The balise function was split into three main categories, junction, speed decrease and other (balises with roles unrelated to potential speed changes). The number of events that occurred at each balise was split into five quantity ranges, which allowed for a more structured comparison of event numbers with track features.

The Chi squared test was applied to the full wheel slide data in Figure 3.17. It demonstrated 99% confidence levels that track gradient and 99.9% confidence levels that balise function are correlated with the number of wheel slides that are experienced. The results are presented in Figure 3.18, where each wheel slide event number range category has been expressed as a percentage of the total number of balises within it to normalise the number of balises within each category.

As can be seen in Figure 3.18a balises demanding a speed decrease have a higher number of wheel slide events, across all track gradients. However on descending line balises with other functions also had high numbers of wheel slide events. This demonstrates the influence of track gradient on the general number of wheel slides that occur.

The same trend was also present when considering only wheel slides that met the severity criteria for severe wheel slides, Figure 3.18b, which shows that balises with the highest numbers of wheel slides were on descending lines, with the majority of those within braking areas. This corresponded with the findings of the geospatial analysis in showing that higher numbers wheel slide events occurred at balises within braking areas and on descending track.

Crosstabulation

			Event Number Range					Total
			0-10	10-100	100-1000	1000-10000	10000+	
Track Gradient Direction	Descending	Count	20	39	106	154	13	332
		Expected Count	19.0	50.3	118.8	132.9	10.9	332.0
	Level	Count	4	6	30	20	3	63
		Expected Count	3.6	9.6	22.5	25.2	2.1	63.0
	Ascending	Count	18	66	126	119	8	337
		Expected Count	19.3	51.1	120.6	134.9	11.0	337.0
Total		Count	42	111	262	293	24	732
		Expected Count	42.0	111.0	262.0	293.0	24.0	732.0

Chi-Square Tests

	Value	df	Asymp. Sig. (2-sided)
Pearson Chi-Square	20.469[a]	8	.009
Likelihood Ratio	20.346	8	.009
N of Valid Cases	732		

a. 2 cells (13.3%) have expected count less than 5. The minimum expected count is 2.07.

(a)

Crosstabulation

			Event Number Range					Total
			0-10	10-100	100-1000	1000-10000	10000+	
Balise Function	balise type other	Count	21	67	131	105	5	329
		Expected Count	18.9	49.9	117.8	131.7	10.8	329.0
	junction	Count	15	39	104	62	1	221
		Expected Count	12.7	33.5	79.1	88.5	7.2	221.0
	speed decrease	Count	6	5	27	126	18	182
		Expected Count	10.4	27.6	65.1	72.8	6.0	182.0
Total		Count	42	111	262	293	24	732
		Expected Count	42.0	111.0	262.0	293.0	24.0	732.0

Chi-Square Tests

	Value	df	Asymp. Sig. (2-sided)
Pearson Chi-Square	144.339[a]	8	.000
Likelihood Ratio	148.941	8	.000
N of Valid Cases	732		

a. 0 cells (0.0%) have expected count less than 5. The minimum expected count is 5.97.

(b)

Figure 3.17: Results from the Chi Squared test on the data

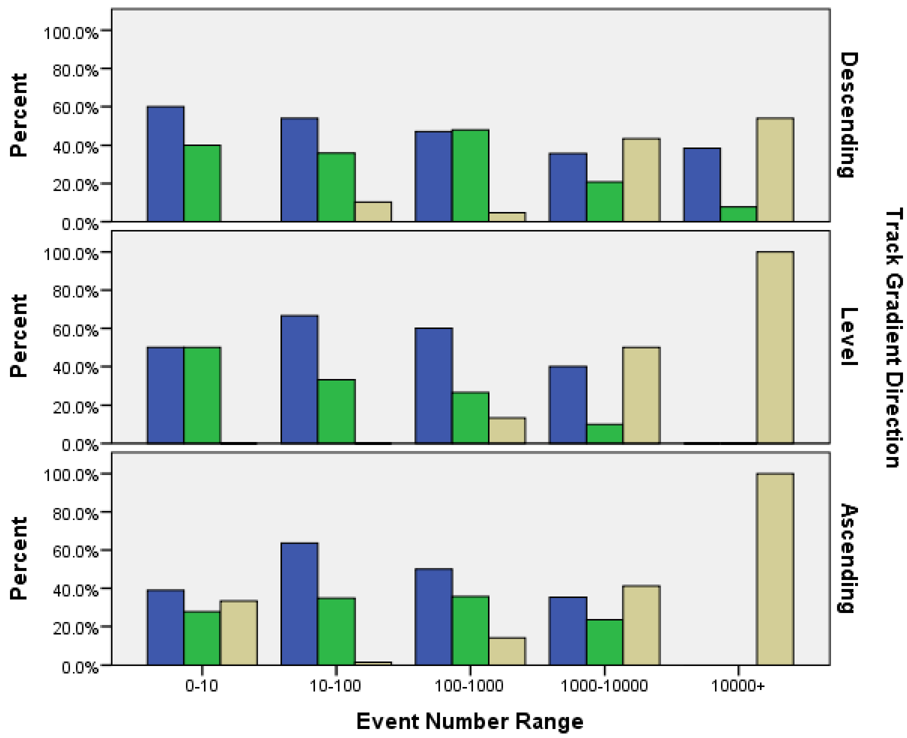

(a)

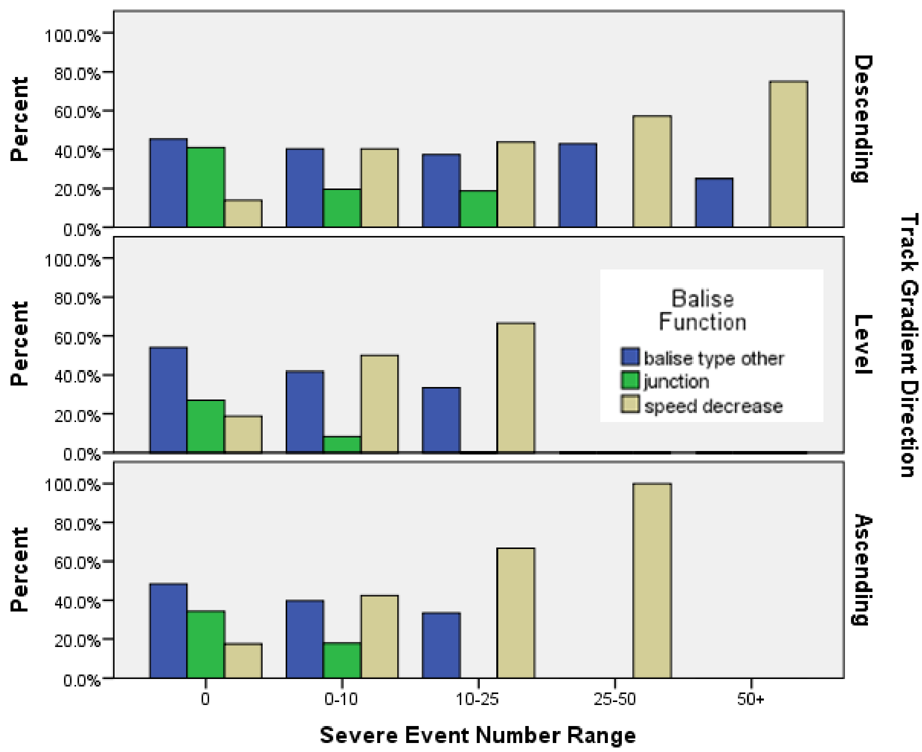

(b)

Figure 3.18: The number of wheel slide events that occurred near balises with different functions compared to track gradient, (a) full wheel slide event data, (b) wheel slide event data that met severity criteria

3.4.2.2 Low Adhesion and Rolling Contact Fatigue

In this Section and Section 3.4.2.3 the geospatial distribution of RCF sites on the down fast line (filtered using the maximum filter method in Section 3.3.1.2) is examined. 67% of the RCF sites occurred within the boxed area highlighted with a 10 times zoom along the section of line between Crewe and Runcorn.

This suggests that characteristics of this section of line have led to an increased number of RCF sites occurring that have not been predicted by Track-Ex. In this work the geospatial distributions of RCF sites and the factors discussed in Section 3.1 are compared to ascertain if correlations exist in the geospatial distributions.

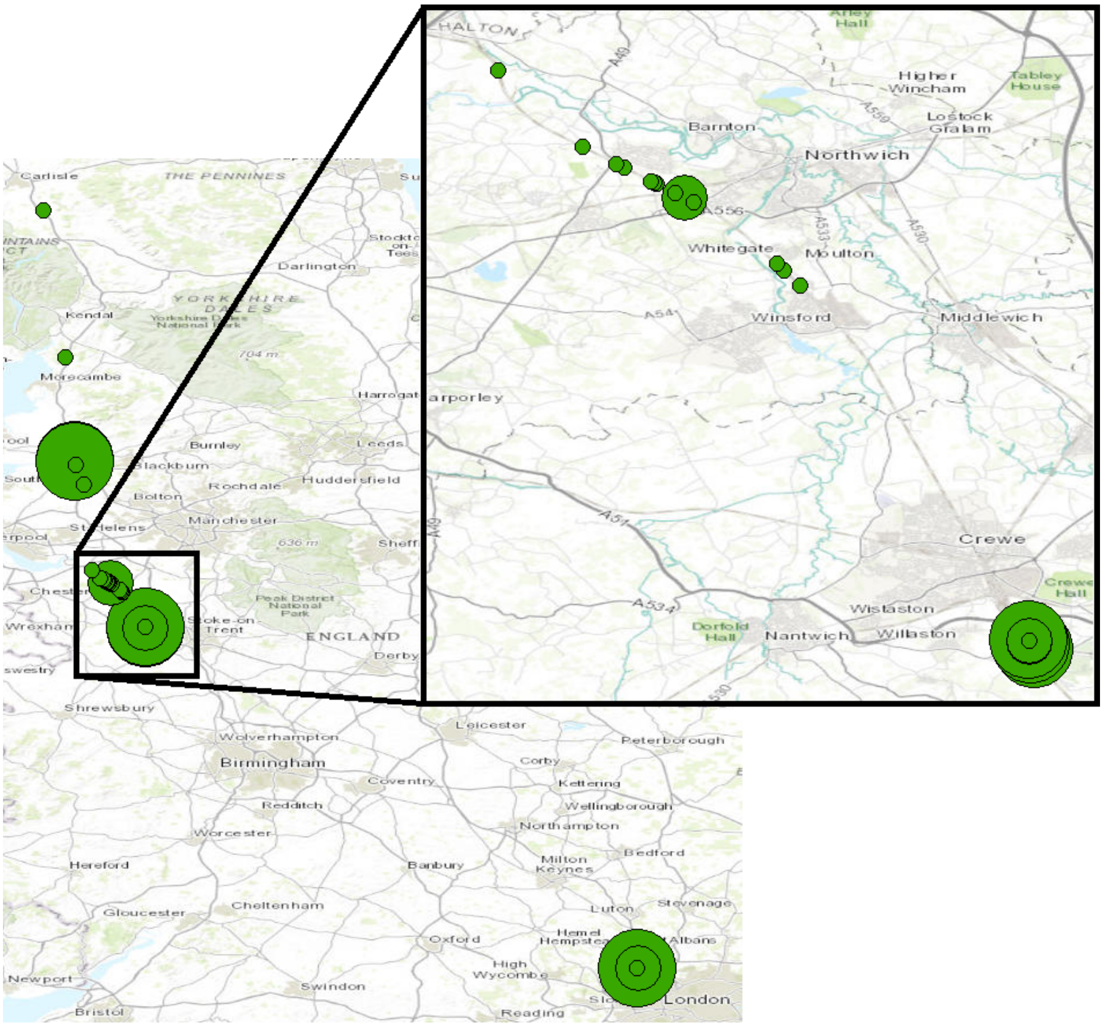

Figure 3.19: Distribution of RCF sites. Dot size indicates momentary slides within ±40m of RCF site: small 0, medium 1-2, large 3+. Boxed area (10 times zoom) highlights section of line where 67% of RCF sites occurred

Within Figure 3.19 RCF sites where momentary slides occurred within ±40m are highlighted with a larger circle. Using this approach it was found that at 37% of the RCF sites momentary slides occurred within ±40m. 55% of these occurred within the boxed area. Momentary slides occurred within ±40m at 30% of the RCF sites in the boxed area. This suggests locational correlation between these two factors.

Within Figure 3.20 RCF sites where a long slide occurred within ±40m are highlighted with a larger circle. Using this approach it was found that at 47% of the RCF sites long slides occurred within ±40m. 78% of these occurred within the boxed area. Long slides occurred within ±40m at 55% of the RCF sites in the boxed area. This suggests locational correlation between these two factors.

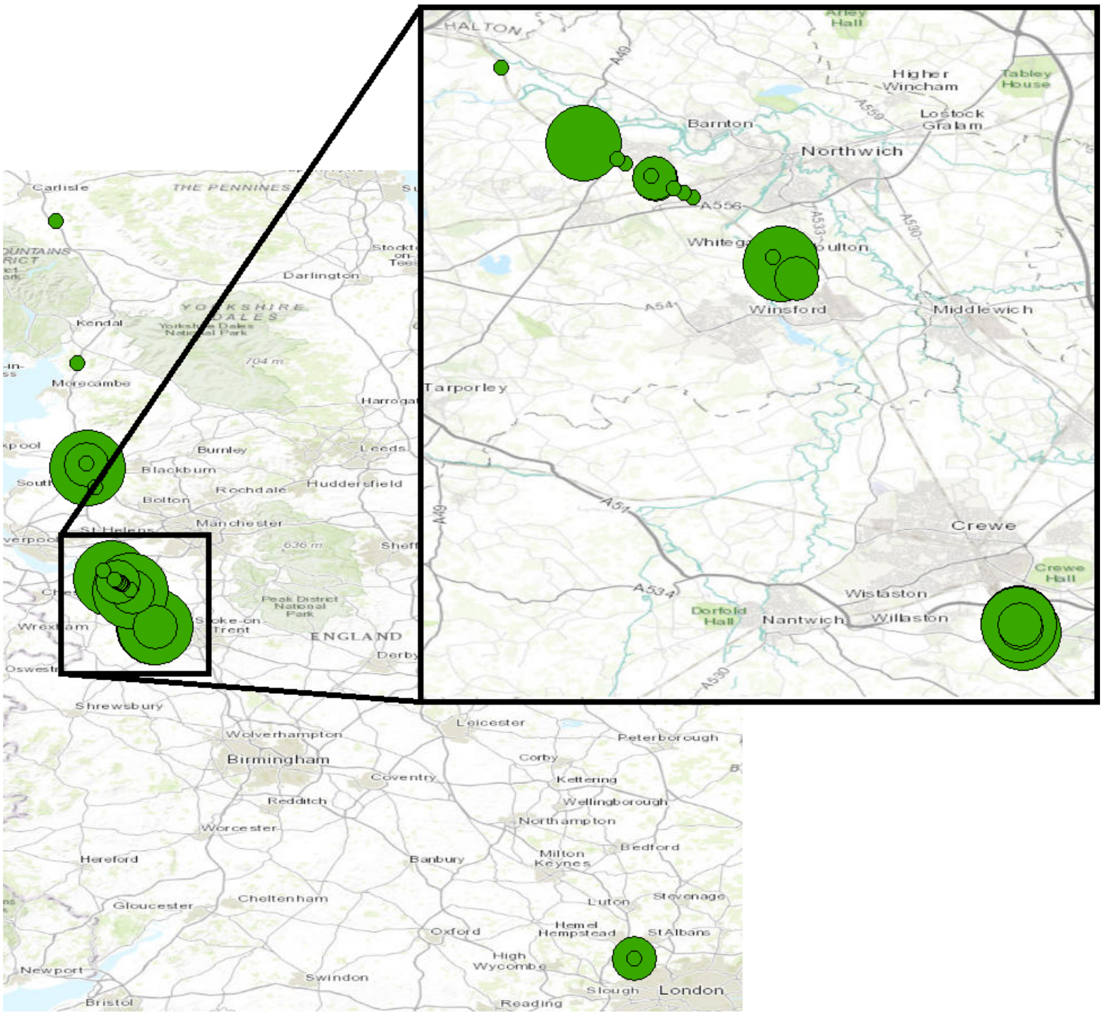

Figure 3.20: Distribution of RCF sites. Dot size indicates long slides within ±40m of RCF site: small 0, medium 1-2, large 3+. Boxed area (10 times zoom) highlights section of line where 67% of RCF sites occurred

3.4.2.3 Underbridges and Rolling Contact Fatigue

RCF sites where an underbridge was present within ±40m are highlighted with a larger circle in Figure 3.21. Using this approach it was found that 23% of the RCF sites had an underbridge within ±40m. These sites are distributed throughout the study area therefore the geospatial distribution did not highlight specific locations at which these sites were more prevalent.

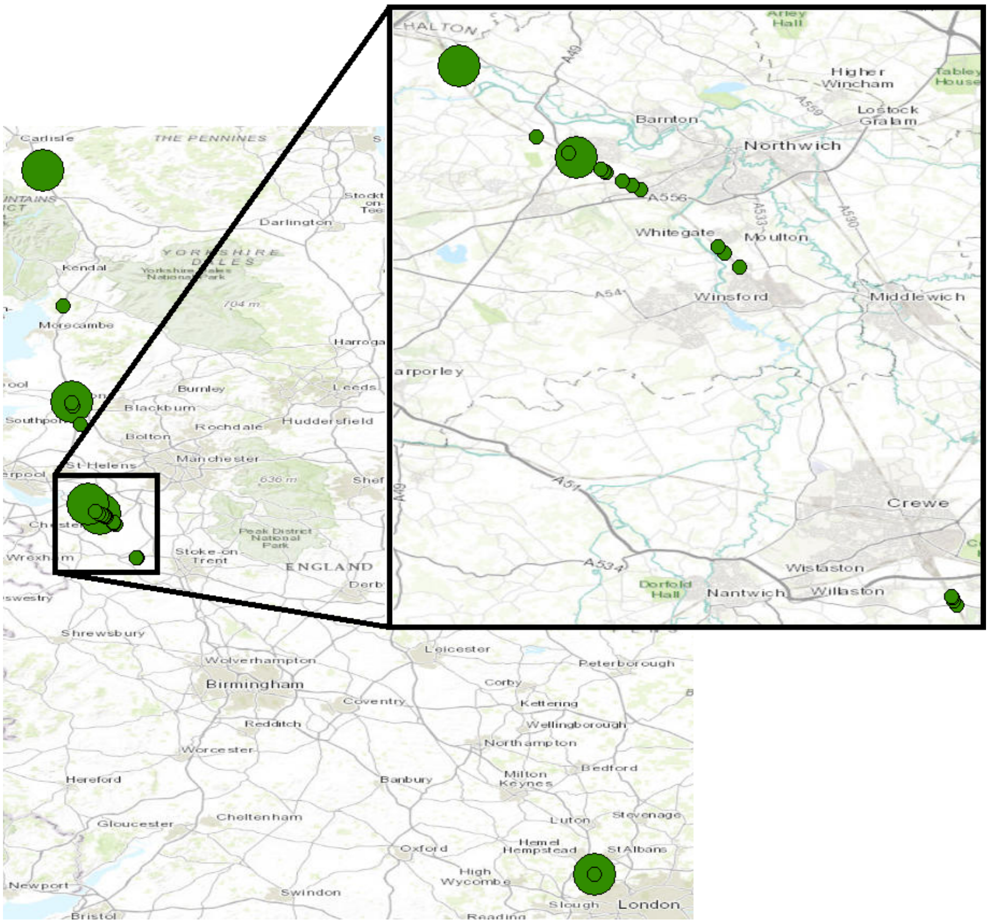

Figure 3.21: Distribution of RCF sites. Dot size indicates underbridge within ±40m of RCF site: small 0, large 1. Boxed area (10 times zoom) highlights section of line where 67% of RCF sites occurred

3.4.3 Temporal Analysis

Temporal analysis aimed to find both long term and daily patterns in the low adhesion events. The monthly temporal analysis, shown in Figure 3.22, highlighted the time of year that wheel slide events occurred as a proportion of the total for the year. It was found that the three month autumn period (October to December) contained the greatest proportion of the yearly total of low adhesion events (40-45%), and this is in line with the general understanding for the UK that low adhesion is a problem during autumn. However Figure 3.22 also shows that 55-60% of wheel slide events are distributed throughout the remaining nine months of the year. Therefore, although fewer events happen per month, a greater number of events in total occur outside the autumn period.

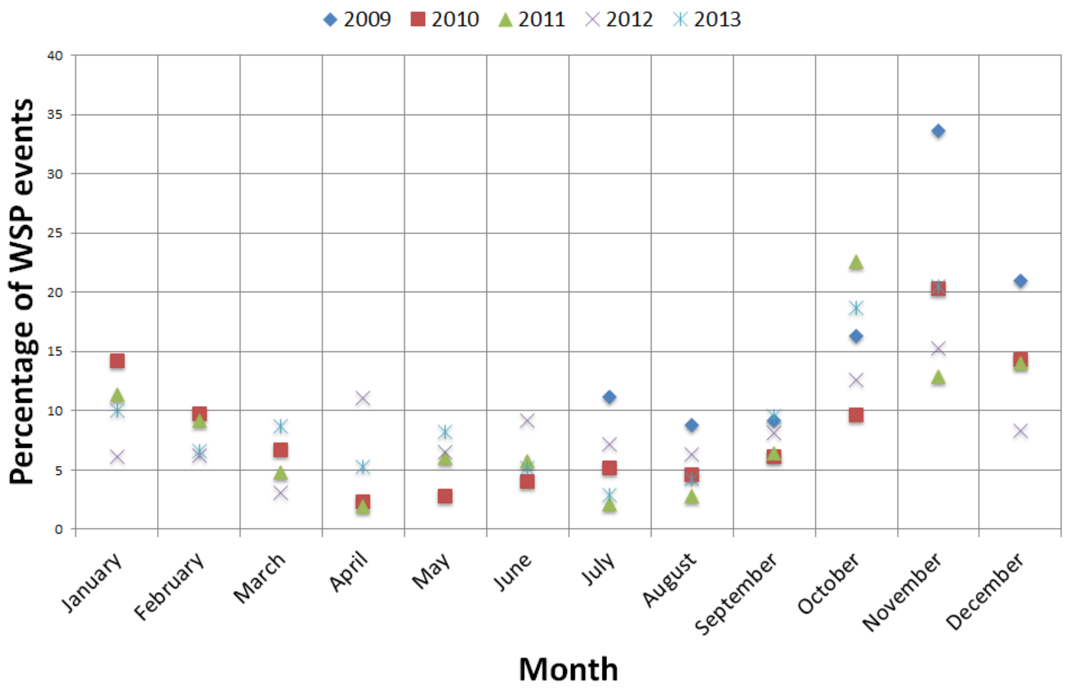

Figure 3.22: Number of wheel slide events that occurred per month as a percentage of the total number of events per year

In addition to the through year analysis an hourly temporal analysis was undertaken using two methods. In method A, Figure 3.23, the data were presented as the total number of wheel slide events per hour summed across the year as a percentage of the total number of wheel slide events for each year. In method B, Figure 3.24, the data were presented as the number of wheel slide events per hour summed across the year normalised by the total number of station stops attempted per hour, which was taken to be representative of the traffic density during each hour. The data used to generate Figure 3.23 is analysed in conjunction with weather data in White et al [63].

Method A highlighted that the highest number of wheel slide events occurred between 06:00 and 10:00AM. This is the morning 'rush hour' period where the consequences of delay is most severe. There is a small evening peak in adhesion events, however it is much smaller than the morning peak, i.e. the number of wheel slides is related to other factors in addition to traffic density.

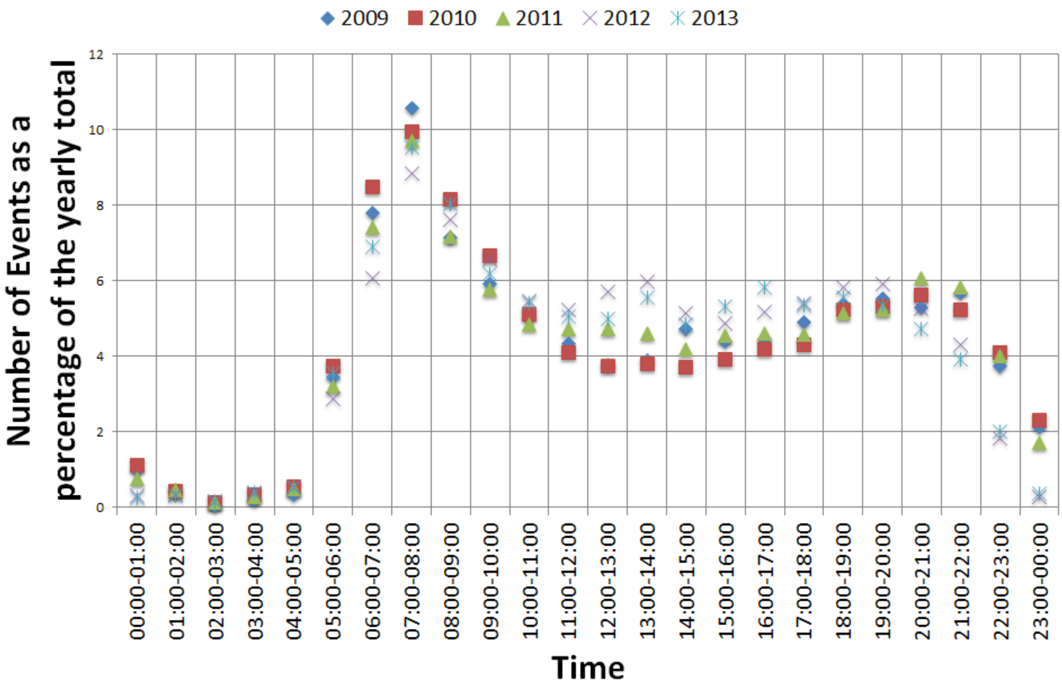

Figure 3.23: Number of wheel slide events that occurred per hour as a percentage of the total number of events per year, Method A (no normalisation)

The normalisation in method B (aiming to remove traffic density from consideration) shows that the time period in which an individual train had the highest chance of experiencing a wheel slide problem was between 03:00 and 04:00AM. The total number of wheel slide events is lower during this time since there are fewer trains moving but each train has a higher chance of experiencing a problem.

This is still a safety concern as wheel slides which cause over-runs beyond the desired stopping point could still be as safety critical as the same event occurring during peak times. The results also showed that the distribution of wheel slide events throughout the day and year remains consistent throughout the five year period. For example, although the data was not identical for each year as there were too few data points the peak rate in Figure 3.24 remained in the early morning.

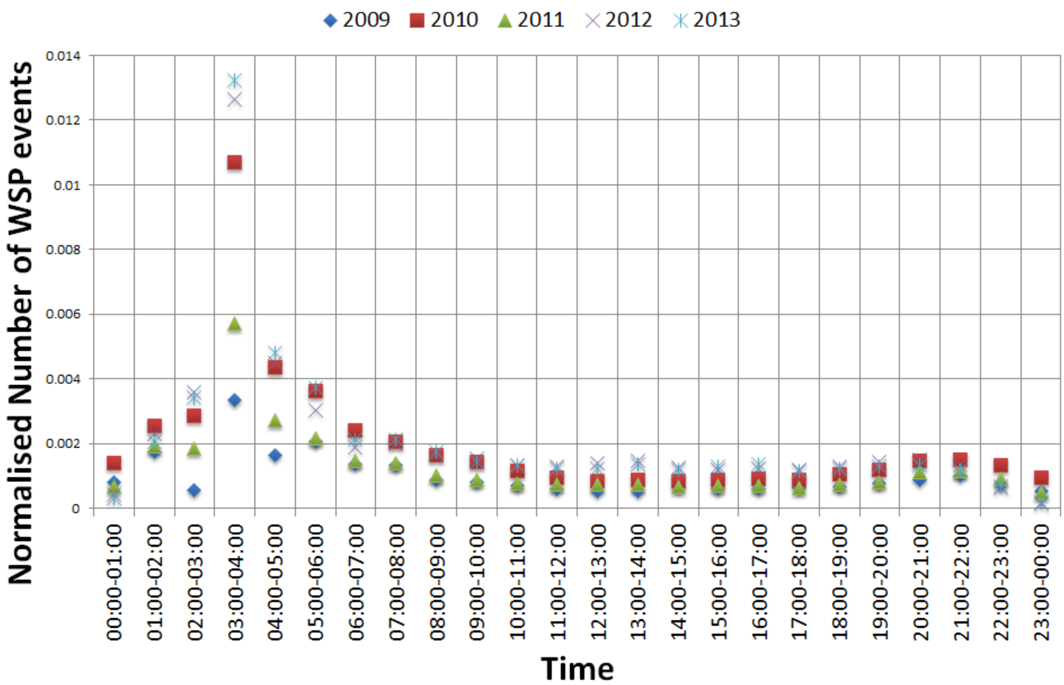

Figure 3.24: Number of wheel slide events that occurred per hour as a percentage of the total number of events per year, Method B (normalised by number of station stops per hour)

3.5 Conclusions

The moving window filtering technique showed that there was a statistically significant increase in RCF in the same analysis window as an underbridge, with an increase in RCF likelihood to 1.3 times the baseline and an increase in the average number of RCF sites to 1.2 times the baseline in the same analysis window as an underbridge. There was a strong correlation between momentary slides and underbridge locations with an increase in the likelihood of momentary slides to 1.9 times the baseline and an increase in the average number of momentary slide events that occurred per analysis window to 1.4 times the baseline in the same analysis window as multiple underbridges. The data showed no correlation between the likelihood of long slides and underbridge location with the likelihood of long slides remaining almost identical to the baseline and the average number events occurring per analysis window decreasing to 0.7 times the baseline in the same analysis window as multiple bridges.

The increase in both the likelihood (2.4 times the baseline) and the average number (1.3 times the baseline) of momentary slide events per analysis window in the same analysis window as an RCF site supports the hypothesis that locational correlation exists between momentary slides and RCF sites (but is not a causal link). This has been backed up by the geospatial distribution findings. The overall impact of negative correlation between the average number (0.7 times the baseline) of long slides that occurred and RCF sites whilst at the same time the positive correlation between the likelihood (1.5 times the baseline) of long slides occurring and RCF sites did not support the locational correlation hypothesis. However the geospatial distribution did highlight locational correlation between long slides and RCF sites. Overall the analysis of locational correlation between long slides and RCF sites was therefore inconclusive, although further work in this area would clarify this. The geospatial approach highlighted a concentration of RCF sites along a short section of track between Crewe and Runcorn but further work (beyond the scope of this thesis due to the need for site visits etc.) would be required to establish the root causes of this.

The geospatial analysis has highlighted factors which affect the adhesion levels experienced along the UK West Coast Main Line. It has been shown that the main geographical factor in common between the locations is the track gradient, with braking on a descending track more likely to result in severe wheel slides, as might be expected with a component of the train's weight acting down the slope, leading to a higher brake force requirement. Nearby woodland, cuttings and roads have also been highlighted as factors that correlated with low adhesion, although the mechanistic link (humidity, leaf-fall, shade, bacteria or differences in vegetation) requires further study.

The temporal analysis highlighted that low adhesion occurred outside the autumn period and therefore cannot be solely attributed to leaf fall. With 55-60% of the yearly total of WSP events occurring outside of autumn this analysis therefore highlighted that low adhesion is still an aspect that would affect train performance throughout the rest of the year. However, the reduction in performance cannot be quantified in this thesis. When analysed by number of incidents it also showed that the time period where low adhesion is most prevalent falls within the busy morning period where the consequences of delays on passengers are most severe. However, the highest risk period for an individual train is the very early morning (3-4AM).

From the research undertaken to date a number of factors appear to be correlated to RCF formation, and the current focus is to determine the root cause of these correlations. In the following Chapter the effect of stiffness transitions on the bending moment generated by the wheel loads is investigated. The effect that this has on the SIF at the crack tip is then shown.

Chapter 4

The Effect of Track Support Stiffness on the Bending Loads that Drive Rolling Contact Fatigue Cracks

4.1 Introduction

The track support stiffness is not consistent throughout the rail network. As discussed in Section 2.4 the support stiffness of the track is dictated by the support structure; whether it is slab or ballasted track, or how hard the underlying ground is. Variation in the track support stiffness often occurs gradually, however in some cases, such as the transition from ballasted track to an underbridge support structure, this change can be sudden. The geospatial analysis in Chapter 3 found locational correlation between RCF sites and underbridge locations, suggesting that the likelihood of RCF being found within the rail increased at support stiffness changes at underbridge support structures.

The track support structure dictates the degree to which the rail is subject to the whole rail bending that drives the final failure mode of RCF cracks (Section 2.3.3). The stiffness of the support structure affects when this phase starts to dominate crack growth. It is critical to understand when this phase starts to dominate crack growth to establish rail life and the risk of safety critical failures, such as rail breaks, increases. This Chapter aims to improve our understanding within this area by establishing:

- The effect multiple wheels in close proximity have on the bending moment within the rail.
- How the bending moment within the rail is impacted by gradual and abrupt sleeper stiffness changes.

Using the structure as shown in Figure 4.1.

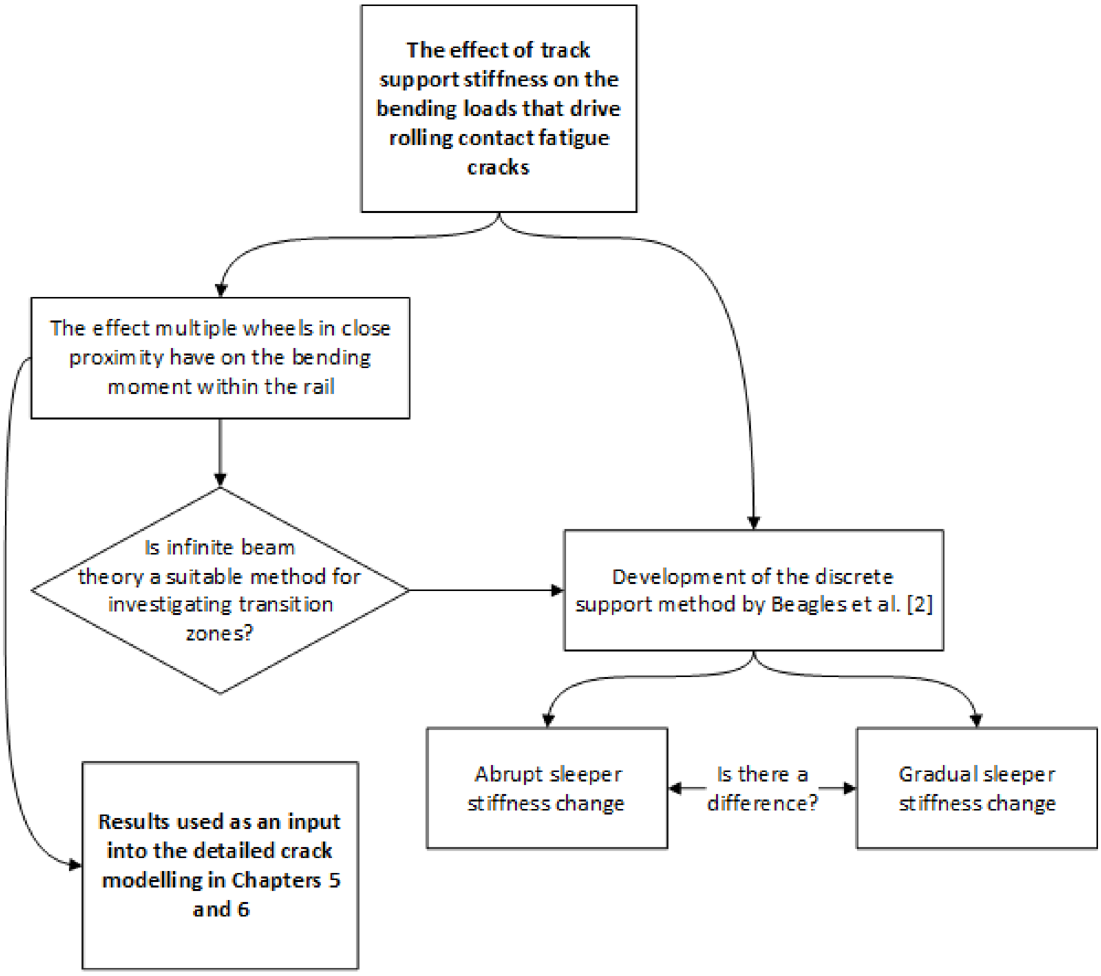

Figure 4.1: Chapter overview

The BOEF theory has been applied using the well established Winkler foundation approach (Section 2.4.2.1) to define the support stiffness of the rail. The continuous Winkler foundation approach provides a rapid, accurate method for determining the whole rail bending. This was used to predict the bending moment within the rail generated by the loading of a train. Multiple wheels in close proximity (as is the case for the bogie configuration) was shown to increase the severity of the bending cycles that occur during the passage of a train in comparison to a single wheel load. The limitations of the continuous foundation assumption used by the Winkler approach are also discussed.

A discrete support method that was originally developed by Beagles, Arnall and Fletcher [2, 209] is further developed here. Improvements included the removal of the need to consider the relative distance between the support and wheel positions in the model. This method was shown to give good results in comparison to the well established Winkler approach.

The discrete support method has then been used to investigate the bending moment within the rail at transition zones. Both abrupt and gradual stiffness changes were investigated.

4.2 Determining the Rail's Response to Vertical Loads Applied by a Train

4.2.1 Rail Vehicle Properties

The rail vehicle chosen for use in this thesis is the class 390 [210]. This was for two main reasons. It is an electrical multiple unit, so its weight is approximately evenly distributed throughout the different cars within the set. This is opposed to a locomotive and carriage configuration such as the Intercity classes (Intercity 125 and 225 [211,212]), which have an uneven weight distribution throughout the set. The class 390 also represents a significant proportion, 40% [204], of the traffic along the west coast main line meaning that it is a good case study vehicle to follow the analysis in Chapter 3.

The track and vehicle specification used within this work is outlined in Table 4.1. This thesis has used the two leading cars within the set of a class 390 because they are the heaviest two car combination within the set [213]. The values and locations of the peak bending moments will be different for different classes of rail vehicle, but this is not the main focus here and therefore only one configuration of a major class type is considered.

Mass class 390 car 1	55600kg
Mass class 390 car 2	52000kg
Car Length	23.9m
Bogie Separation (between centre-points)	17m
Axle Separation	2.7m

Table 4.1: Vehicle properties used in the Winkler beam model, specifications from class 390 car 1 and 2. Specifications taken from [213]

4.2.2 Validating the Response of the Infinite Beam Supported by a Winkler Foundation

As discussed in Section 2.4.2.1 the behaviour of an infinite beam supported by a Winkler foundation under the point load P_0 is described by Equations 2.22-2.25. Figure 4.2 shows the response of the beam supported by a Winkler foundation that has been used in this thesis. The vertical black lines show where the points of zero deflection, slope, bending and shear should occur (Figure 2.24). As can be seen the beam responds correctly for each case, validating that the Winkler foundation is being implemented correctly in this thesis.

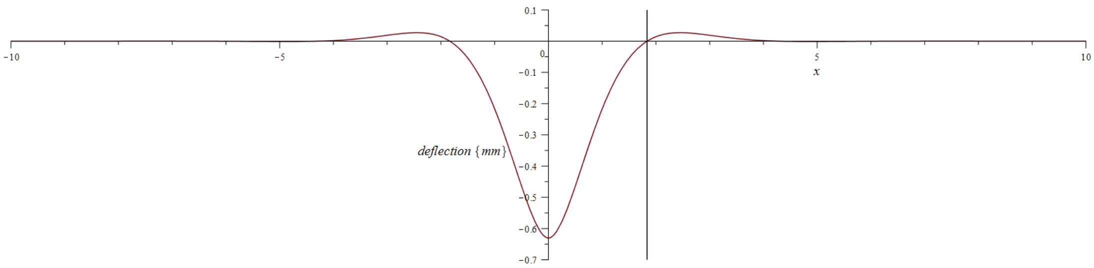

(a)

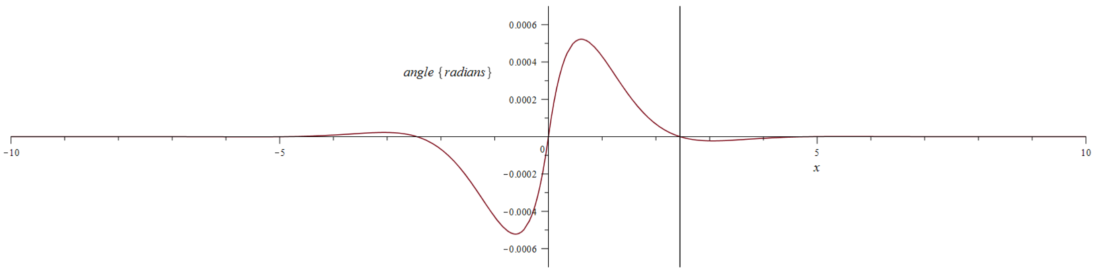

(b)

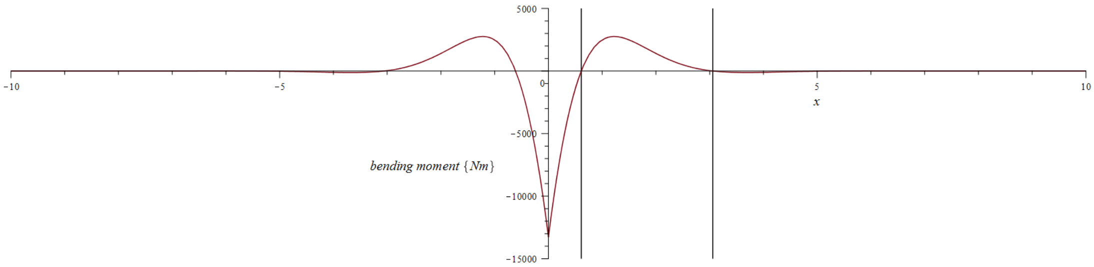

(c)

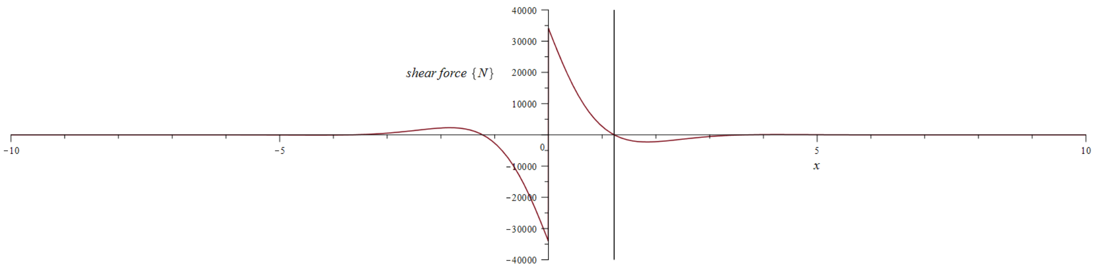

(d)

Figure 4.2: Curves for deflection, (a), angle, (b), bending moment, (c), shear force, (d), for an infinite beam supported by a Winkler foundation. Critical distances along the beam from Figure 2.24 are highlighted with vertical black lines for each case

4.2.3 Effect of Railpad Stiffness on Overall Track Support Stiffness

When applying a BOEF approach to model the track support stiffness the railpad stiffness needs to be considered. Figure 4.3 shows the effect of pad stiffness on overall track support stiffness with increasing trackbed stiffness. As can be seen inclusion of the railpad stiffness progressively reduces the overall track stiffness as the trackbed stiffness increases. For the trackbed stiffness that is typical in the UK (Table 2.2) the effect of the railpad is such that the overall track stiffness is 0.8 times what it would be without the railpad.

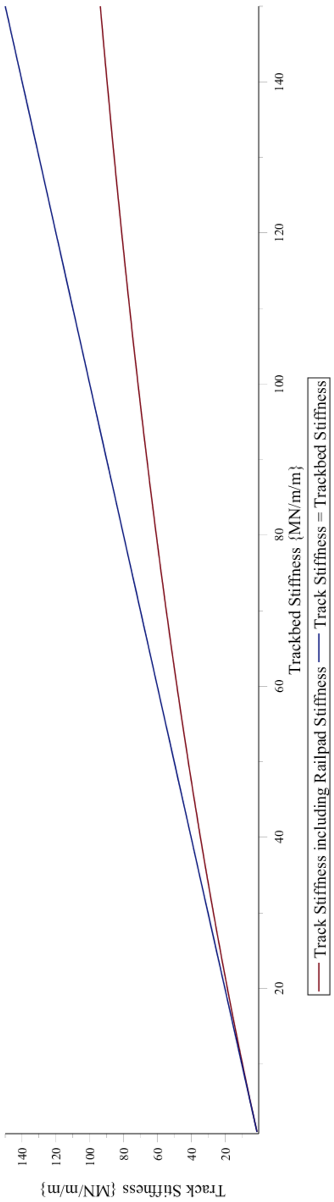

Figure 4.3: Effect of pad stiffness on the overall track stiffness (railpad stiffness = 250MN/m)

4.2.4 Effect of Track Support Stiffness on Rail Deflection

The effect that the track support stiffness has on rail deflection is shown in Figures 4.4 and 4.5. As the track support stiffness decreases the maximum rail deflection increases. The response of the beam to the load is also spread over a longer section of the beam. This is expected as the reduced track support stiffness increases the length of rail that is subject to bending. The increased deflections of the reduced track support stiffness leads to increased stresses in components of the support system such as sleepers and fastenings. Therefore a low track support stiffness is generally associated with a poor track system performance and an increased maintenance requirement [214–216].

The deflection for a given track stiffness under a 10 tonne wheel load for the BOEF model used in this thesis is shown in Figure 4.5. By comparison to previous work by Powrie et al. [161] (Figure 4.4) it can be seen to accurately predict the track deflection for a given track stiffness.

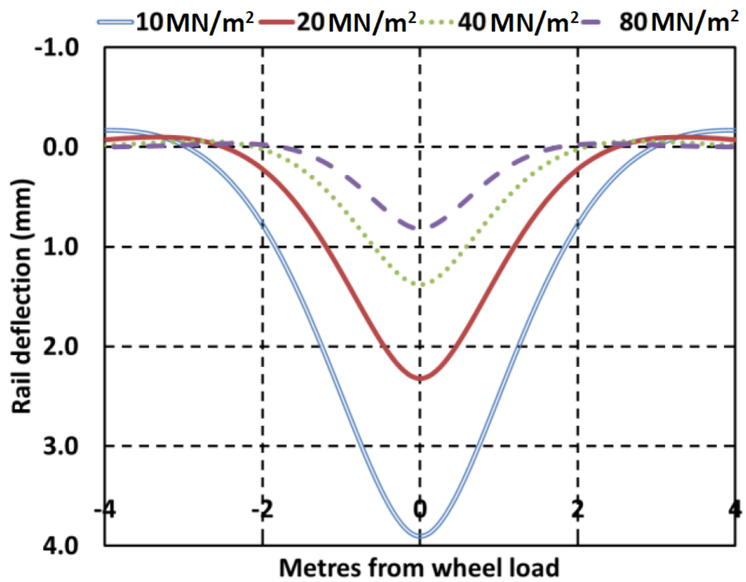

Figure 4.4: Effect of track support stiffness on rail deflection for a wheel load of 10tonnes. Previous work by Powrie et al. Taken from [161]

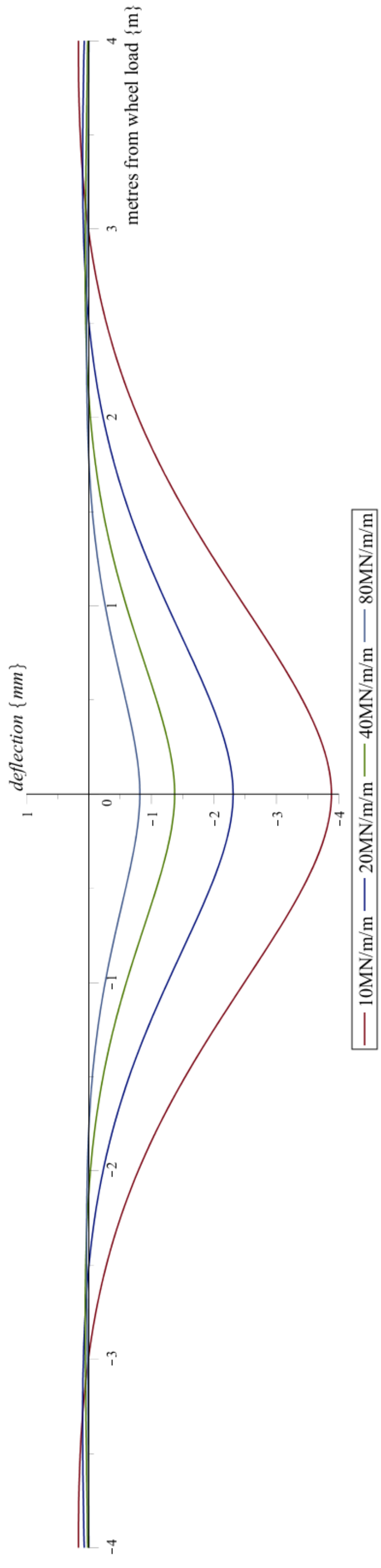

Figure 4.5: Effect of track support stiffness on rail deflection for a wheel load of 10tonnes. Beam on elastic foundation model used in this thesis

4.2.5 Addition of Multiple Loads using Superposition

Point loads in close proximity on a Winkler foundation can be analysed using the superposition method. This method involves the summation of the effects of each point load in isolation to give a net effect on the beam. In this Section the effect of the addition of a second point load by superposition is investigated.

In Figure 4.6 two loads of the same magnitude of the load used in Section 4.2.2 are spaced 2.7m apart (wheelset separation on a CL623 bogie used on class 390 [27]). The individual reactions of the beam to the point loads are shown in Figures 4.6a and 4.6c. The superimposed reaction of the beam is shown in Figures 4.6b and 4.6d.

As can be seen in Figure 4.6b the peak deflection reduces slightly to 0.96 times the single load value. This is because the contribution to overall deflection of the beam from the second point load is positive at the position of the first point load (Figure 4.6a).

Figure 4.6c shows that, at the load separation distance of 2.7m, the peak bending moments for the two individual point loads occur at the same position on the rail. Therefore, for this configuration, the peak positive bending moment within the rail (Figure 4.6d) has doubled to its theoretical worst value in comparison to a single wheel load. Although the bending moment would not occur at all track stiffness or bogie configurations, consideration of the wheel loads in close proximity demonstrates that the peak positive bending moment within the rail can be more severe than predicted from a single wheel load.

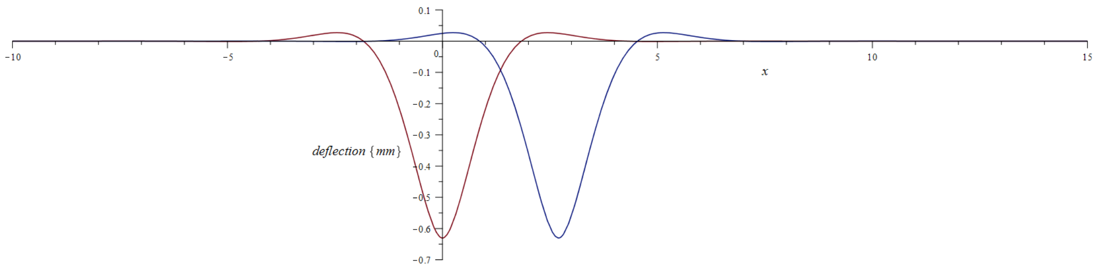

(a)

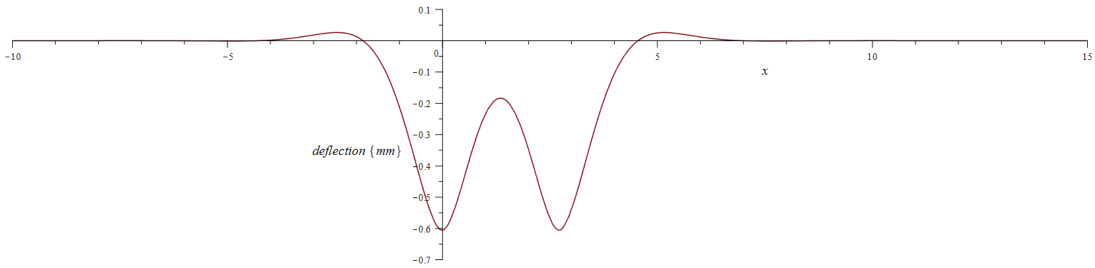

(b)

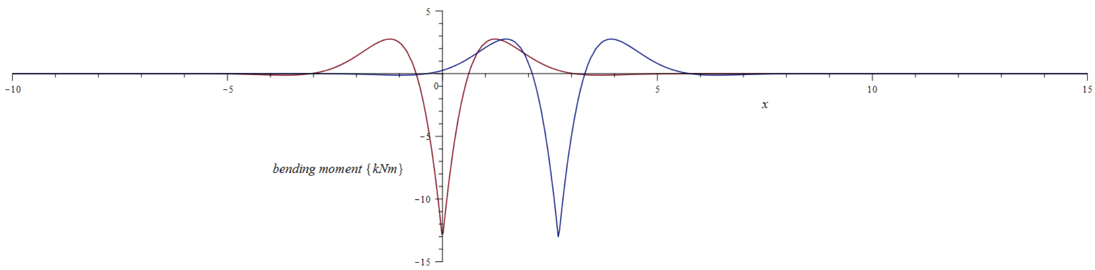

(c)

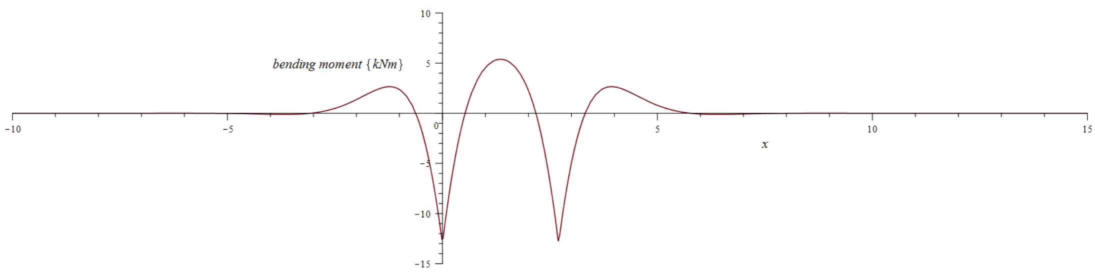

(d)

Figure 4.6: Diagram showing the superposition of two point loads on a Winkler foundation to calculate the net deflection and bending moment of the beam under both loads, (a) deflection separate loads, (b) deflection superimposed loads, (c) bending moment separate loads, (d) bending moment superimposed loads

4.2.6 Effect of Dynamic Load Factors on Rail Deflection and Bending Moment within the Rail

As discussed in Section 2.4.2.2 in previous studies the static wheel load was increased by a dynamic load factor to approximate the dynamic wheel load on the rail. The dynamic load factor suggested by the literature gave dynamic wheel loads that ranged between 1.3 times and 2.2 times the static wheel load at 125mph.

How the implementation of the dynamic load factor affected the results from the BOEF analysis is shown in Table 4.2. The elastic nature of the analysis meant that the percentage increase in the load (by the dynamic load factor) is reflected in the rail deflection and bending moment results. Whilst this method of analysis is linear for varying load, it is not linear for other factors, for example doubling the support stiffness (4.5) does not reduce rail deflection by a factor of 2.

Table 4.2 demonstrates that this analysis could have been undertaken for any load (say 1N) which would give a normalised result that could be scaled up for any case of interest. This would be one way to treat the analysis, however, to make the output moments and deflections easier to interpret, the static wheel load has been used within this thesis.

dynamic load factor (ϕ)	rail deflection (mm)	percentage increase from static rail deflection (%)	peak positive bending moment (Nm)	percentage increase from static bending moment (%)
1	0.61	N/A	5400	N/A
1.25	0.76	25	6700	25
1.5	0.91	50	8100	50
1.75	1.1	75	9400	75
2	1.2	100	11000	100
2.25	1.4	125	12000	125
2.5	1.5	150	13000	150

Table 4.2: Increase in rail deflection and bending moment due to dynamic load factor

4.3 Displacement and Bending Moment of the Rail from a Rail Vehicle

4.3.1 Single Vehicle

Here, the superposition method described in Section 4.2.5 has been used to simulate the multiple wheelsets of a single car of a class 390 train on a Winkler foundation (vehicle and track properties are shown in Tables 2.2 and 4.1). Figure 4.7 shows the rail's response to the car 1 of a class 390 (Table 4.1). The results shown in Figure 4.7 demonstrate that the separation between bogies is sufficient for the rail to respond independently to each bogie, settling back to the neutral position in between. Therefore it is not necessary to include the full car for analysis. One bogie is sufficient to capture the rail bending from the train's static mass. For this configuration of applied load and axle separation the peak positive bending moment is between the axles on the same bogie and is 2 times that from a single wheel load. The peak positive bending moments are displayed in text in Figure 4.7 for ease of reference.

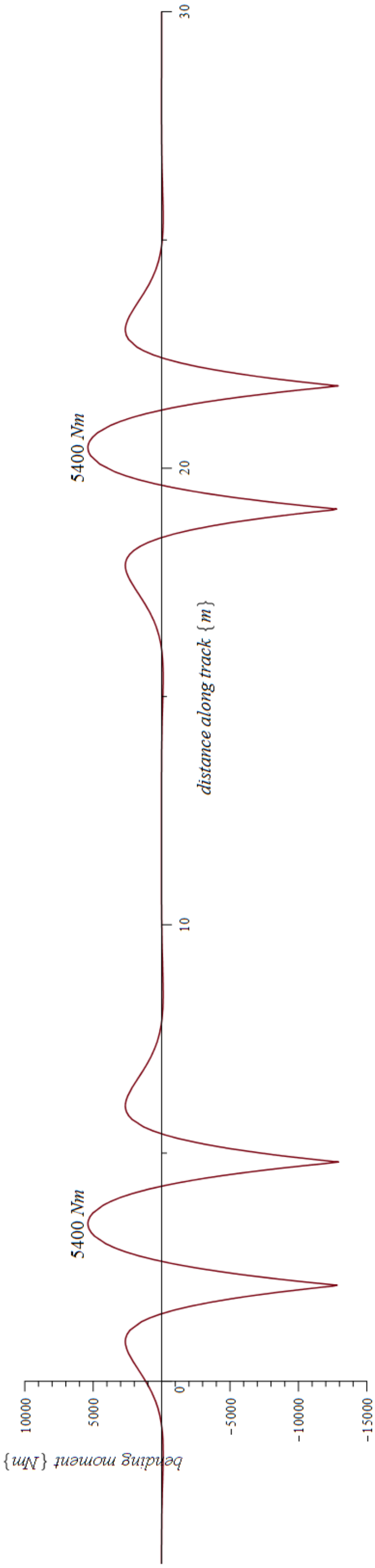

Figure 4.7: Diagram showing the net bending moment of the rail under the load of a singular class 390 vehicle

4.3.2 Multiple Vehicles

Although wheels from each end of a single vehicle act independently those on adjacent vehicles are close enough to interact (4.2m in the case of the class 390). In this Section multiple vehicles are considered to capture the rail's response to the vertical load of a train between vehicles. Bogies on the same vehicle are still included here so the effect of the second vehicle can be more easily seen. However, to reduce modelling times, further models will focus on the trailing and leading bogies of adjacent cars.

Car 2 has a lower mass than car 1 (Table 4.1). This is reflected by the reduced peak rail deflections for the 3rd and 4th bogies with increasing distance along track in Figure 4.8a. The net deflection on the rail can be seen to be influenced by the nearby axles at the interface between the two cars. This is shown through comparison of the isolated bogies (1st and 4th with increasing distance along track) with those that interact with the opposing car (2nd and 3rd with increasing distance along track).

Figure 4.8b shows that the peak positive bending moment is still between axles on the same bogie. However the peak positive bending moment between the cars is clearly influenced by the proximity of the 2nd and 4th bogies. The peak bending moment here is greater than at the extremities for the other bogies. It is easy to see that, for different vehicle configurations where the distance between end axles on a car is different, the location of peak positive bending moment may change. This demonstrates that all wheels within close proximity for a particular train configuration need to be included in rail bending analysis. This reinforces the point made in Section 4.2.5 about the location of the peak positive bending moment.

During the passage of two cars the rail experiences eleven bending cycles, four of which are twice as severe as that predicted from a single wheel load. This means for a nine car class 390 the rail undergoes forty-six bending cycles, twenty-six fewer than if you assumed that the rail underwent two bending cycles per wheel (single wheel case). However eighteen of these bending cycles are twice as severe as that predicted from a single wheel load. The effect that the increased bending moment generated by multiple axles in close proximity has on the crack growth within the rail is investigated in Section 4.3.3.

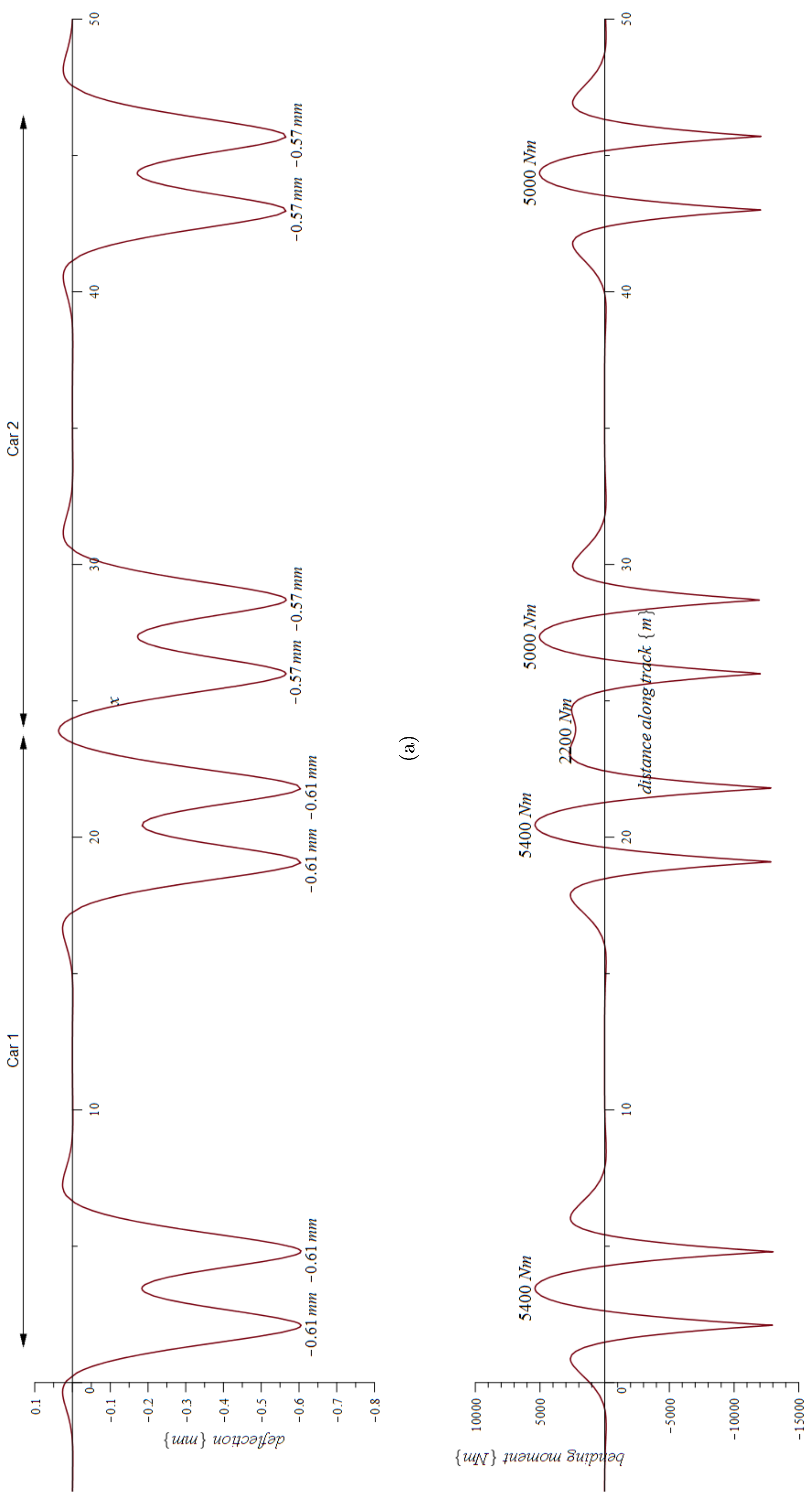

Figure 4.8: Diagram showing the net deflection and bending moment of the rail under the load of two class 390 vehicles, (a) deflection, (b) bending moment

4.3.3 Effect of Multiple Wheel Loads in Close Proximity on Stress Intensity Factor along the Crack Front

Multiple wheel loads in close proximity (as is the case for the bogie configuration on rail vehicles) have been shown to increase the peak positive bending moment within the rail in Section 4.3.2. In this Section the effect that this increased positive bending moment has on the SIF along the crack front of a surface breaking RCF crack is compared to the single wheel load case. Note that the results presented here use a dynamic load factor of 2.5.

The maximum bending moment found for the multiple wheel load case (13kNm) is compared with that from the single wheel load case (6kNm). The SIFs generated by these bending moments are found using the three dimensional crack model that is developed and validated in Chapter 5. These bending moments are applied to The SIF results for the central crack for an increasing number of cracks in series are presented in Figure 4.9. The 3D cracks are semi-elliptical in nature, centrally positioned in the railhead, inclined at 30° to the rail surface and are equally sized with a 10mm radius.

As can be seen in Figure 4.9a the mode I SIF for the central crack in the series doubled when multiple wheel loads are considered in comparison to the single wheel load case. This occurred consistently for all the crack configurations considered. Figure 4.9b shows that the mode II SIF for the central crack in the series also increases by a factor of two for the multiple wheel load case.

For the case where cracks are of the same size and equally spaced all the cracks within the series are open during the positive bending phase of the load cycle. Therefore the proportionality that was found between the results was expected due to the elastic nature of the modelling.

It is of note that, when considering multiple cracks, the mode I and mode II SIF under multiple wheel loads increases to approximately equal to that of a single crack under a single wheel load. Therefore, for the crack opening phase, the presence of multiple wheels in close proximity negates the shielding effect found when multiple cracks of the same size are in close proximity. This means that previous studies that have only included a single crack within the study retain some credibility. However, further work is required to determine the extent to which the level of shielding affects the SIF under the compressive phase of crack growth.

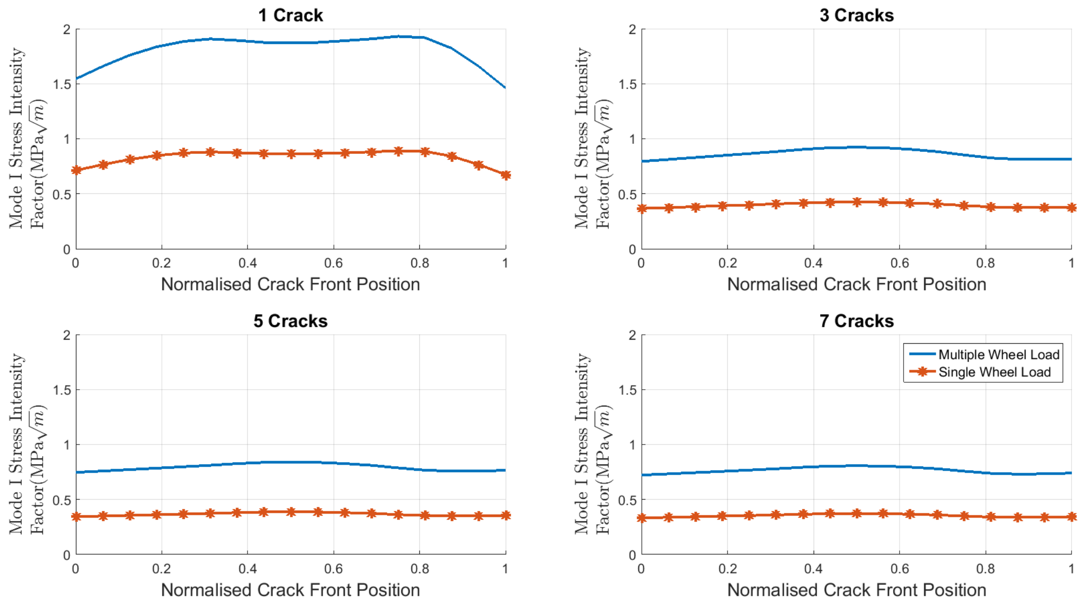

(a)

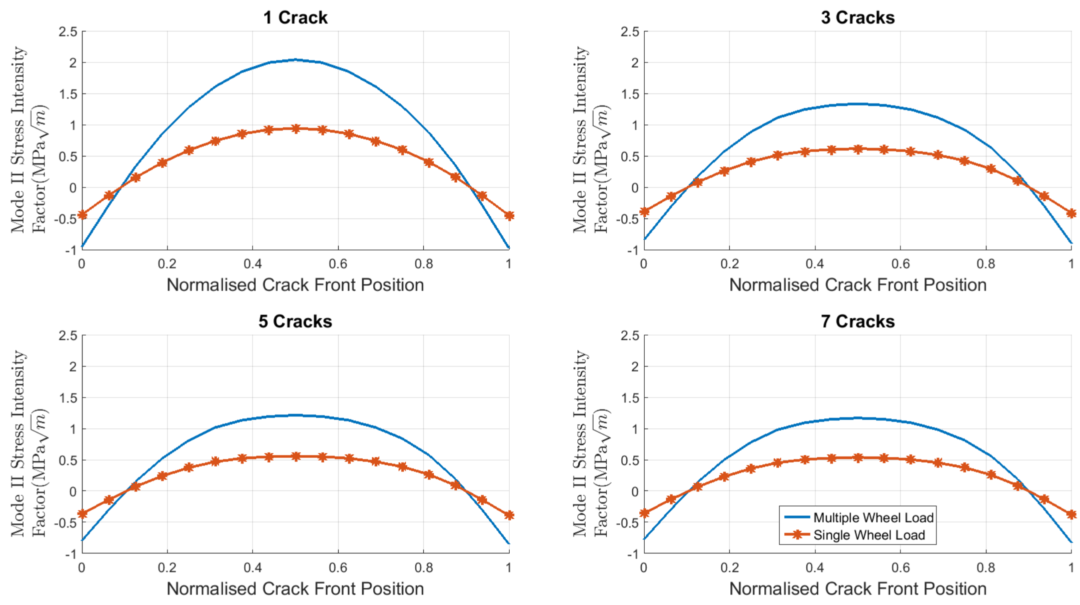

(b)

Figure 4.9: Comparison between Mode I, (a), and Mode II, (b), Stress Intensity Factors of the central crack of 1, 3, 5 and 7 cracks at 30° to the rail surface under the positive bending moment generated from a single wheel load and multiple wheel loads of a class 390. Effect of the number of cracks on the stress intensity factor across the crack front of the central crack

From the crack growth equations defined in Section 2.3.2.3 (using the results in Section 4.3.4 to give ΔK for mode I and mode II), for a single crack the inclusion of multiple wheel loads increases ΔK_{eq} by 20%. By taking the threshold SIF (ΔK_{th}) for crack propagation in a non-corrosive environment as 4MPa√m [95] (below which the crack growth rate is taken to be zero) the crack growth rate $\left(\frac{da}{dN}\right)$ for a single crack driven by rail bending under multiple wheel loads increases by three times that under a single wheel load. For multiple cracks the ΔK_{eq} predicted under a single wheel load is approximately equal to the threshold SIF. Under the bending moment from multiple wheel loads this increases by 12%, leading to a doubling in predicted crack growth rate driven by whole rail bending.

The results in this Section have shown that consideration of multiple wheel loads has a significant effect on the predicted crack growth rate during the open phase of the crack. The increase in predicted crack growth rate under whole rail bending shows that cracks may enter phase III crack growth earlier then has been previously suggested by studies that have considered a single wheel load.

4.3.4 Estimation of the Stress Intensity Factor Close to the Contact – Preliminary Results

Figure 4.10 shows the mode I and mode II SIF found at the crack tip (crack face friction = 0.3) under the peak negative bending moment (using a dynamic load factor of 2.5) found at the wheel positions ($-30kNm$). This is found using the three dimensional crack model that is developed and validated in Chapter 5. The bending moment at the wheel position remained almost identical between the single and multiple wheel load cases (Figure 4.6). The SIF generated from this bending moment is that from the whole rail bending and therefore the contact pressure and associated stresses are not taken into account. This is equivalent to the wheel-crack configuration shown in Figure 4.11a where the contact patch is near, but not over, the crack.

A comparison is made between the mode II SIF result at the 0.5 normalised crack front position in Figure 4.10 (highlighted with the black vertical line) and the peak negative mode II SIF in Figure 4.11b (contact position of 20mm). This comparison demonstrates that the mode II SIF from the current method (using the peak negative bending moment) at the normalised crack front position of 0.5 is very similar to that found in Smith [32]. The results are most comparable for the 0.3 surface friction results in Figure 4.11b.

This therefore suggests that the simple rail bending approach is sufficient to find the peak negative mode II SIF used to calculate ΔK_{II} in the crack growth equations (Section 2.3.2.3). The contact model would therefore only be required to find the peak positive mode II SIF to calculate ΔK_{II} when calculating the crack growth rate. This means that, as well as a faster approach to find the peak negative mode II SIF, approximately half the number of runs would be required in contact model (from inspection of Figure 4.11b) to find the peak positive mode II SIF. This gives significant time savings when finding ΔK_{II} when calculating the crack growth rate. However further work is required to provide further certainty to this conclusion for different crack sizes. Especially for the case of smaller cracks which are more driven by the contact stresses.

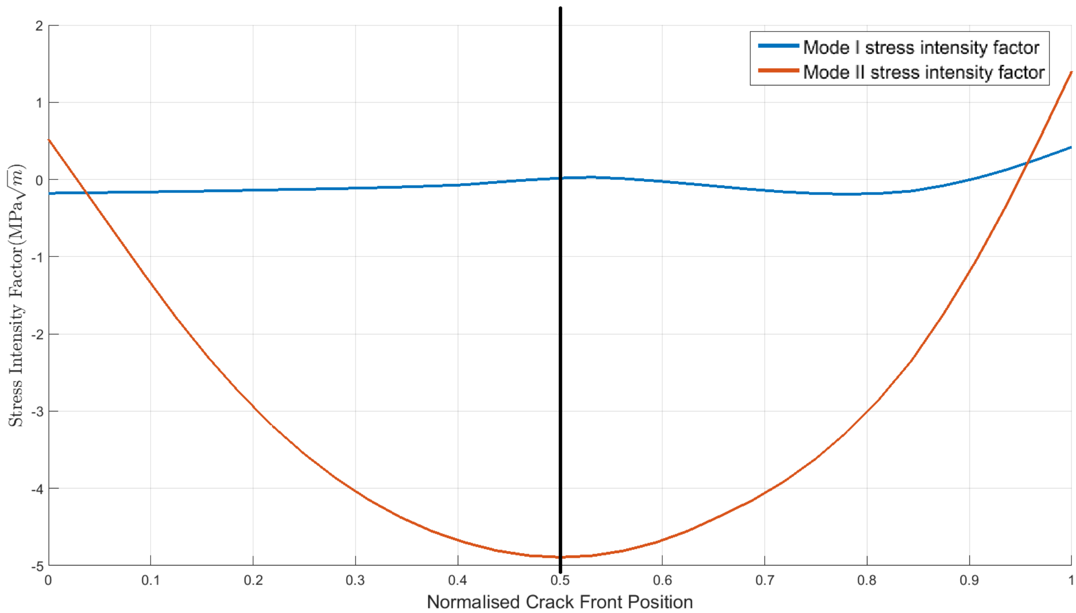

Figure 4.10: Stress intensity factor across the crack front for a single crack under the peak negative whole rail bending moment

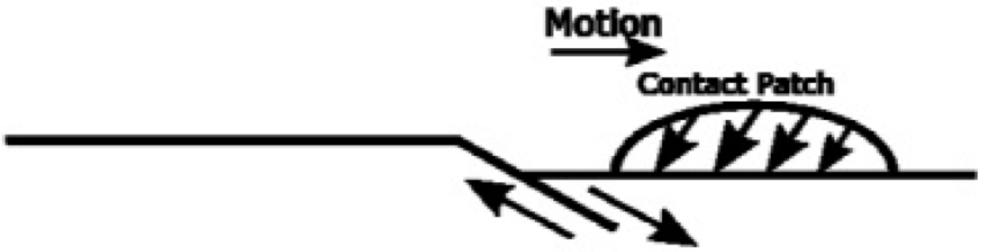

(a)

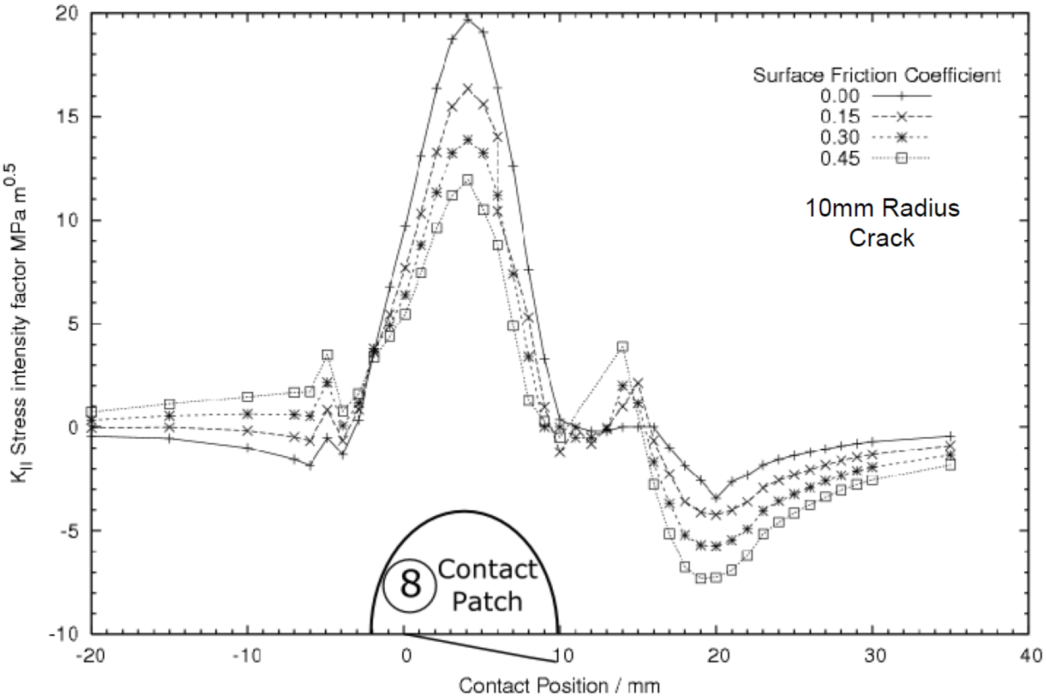

(b)

Figure 4.11: Diagram of, (a), the contact patch and crack face movement direction, (b), mode II stress intensity factor results as the contact moves across the crack. The crack is semi-circular and is 10mm radius at an angle of 30° below the surface (shown schematically). The elliptical contact patch is a=5.92mm in the longitudinal direction and b=3.94mm in lateral direction. Crack face friction coefficient is 0.30 and p =1750MPa. Both Figures taken from Smith [32]

4.4 The Euler-Bernoulli Beam on Discrete Supports

Initial findings using the Euler-Bernoulli beam on discrete supports method has been published at the Contact Mechanics 2015 conference [2], some findings were also presented in a report on the sustainable freight railway [209]. This method was further developed in the work presented in this Chapter. The advantage of using the discrete support approach over the Winkler approach is that the stiffness at each support can be altered independently. This allowed for the investigation to consider the effect of stiffness transitions, which are found at underbridge locations (shown to locationally correlate with RCF in Chapter 3), on rail bending.

The fundamental equations behind the discrete support approach are given in Appendix G. It is based on the Macaulay's method [217] for determining the deflection of Euler-Bernoulli beams. A schematic for the approach is shown in Figure 4.12 (note that the values stated in this figure are examples only and differ from those elsewhere in this thesis), with each support modelled as a vertical and rotational stiffness.

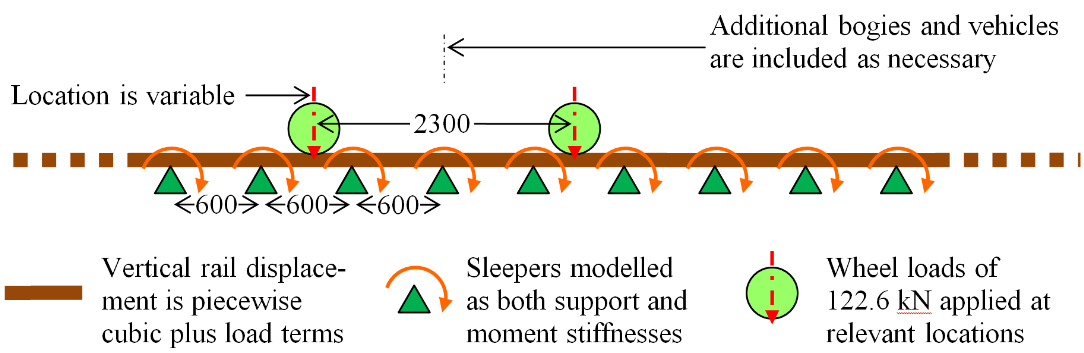

Figure 4.12: Diagram of the Euler-Bernoulli Beam Model on Discrete Supports. Figure taken from Beagles et al. [209]

The deflection of the beam is given by:

$$y(x) = \frac{1}{EI}\left(\sum_{k=1}^{N_R} R_k \cdot f(x, r_k, t_k + 2) - \sum_{k=1}^{N_P} P_k \cdot f(x, p_k, 3) + y_0 + y_0' \cdot x\right) \quad (4.1)$$

The first derivative is the slope of the beam and is given by:

$$y'(x) \equiv \frac{dy(x)}{dx} = \frac{1}{EI}\left(\sum_{k=1}^{N_R} R_k \cdot f(x, r_k, t_k + 1) - \sum_{k=1}^{N_P} P_k \cdot f(x, p_k, 2) + y'_0\right) \tag{4.2}$$

The second derivative multiplied by EI is the bending moment and is given by:

$$BM(x) \equiv EI\frac{d^2y(x)}{dx^2} = \sum_{k=1}^{N_R} R_k \cdot f(x, r_k, t_k) - \sum_{k=1}^{N_P} P_k \cdot f(x, p_k, 1) \tag{4.3}$$

The third derivative multiplied by EI is the shear force and is given by:

$$V(x) \equiv EI\frac{d^3y(x)}{dx^3} = \sum_{k=1}^{N_R} R_k \cdot f(x, r_k, t_k - 1) - \sum_{k=1}^{N_P} P_k \cdot f(x, p_k, 0) \tag{4.4}$$

Where the number of reactions (N_R) is the number of supports within the analysis. Each support has a vertical and rotational stiffness (R_k), at distances along the beam (r_k). Each reaction has a type (t_k), which is zero for a moment constraint or unity for a displacement constraint. The number of point loads (N_P) within the analysis are defined with a magnitude (P_k), at distances along the beam (p_k).

The 'Macaulay function' is:

$$f(x, y, m) = \begin{cases} \frac{(x-y)^m}{m!} & m \geq 0 \, and \, x > y \\ 0 & m < 0 \\ 0 & m > 0 \, and \, x \leq y \\ 1 & m = 0 \, and \, x = y \end{cases} \tag{4.5}$$

Continuity of the beam is achieved because the displacement (Equation 4.1) is defined in terms of the Macaulay functions (Equation 4.5). Derivatives when $m > 0$ are always continuous. For the displacement and slope of the beam the smallest $'m'$ at each support is two and one respectively when t_k is zero (indicating a moment constraint). Therefore the displacement and slope of the beam are both continuous. For the bending moment and shear force of the beam the smallest $'m'$ at each support is zero and minus one respectively when t_k is zero. Therefore, the bending moment and shear force are both discontinuous.

The vertical (R_{ver}) and rotational (R_{rot}) stiffness of the i^{th} support is given by:

$$\begin{aligned} K_{i_{ver}} \cdot y\left(r_i\right) &= -R_{i_{ver}} \\ K_{i_{rot}} \cdot y'\left(r_i\right) &= R_{i_{rot}} \end{aligned} \tag{4.6}$$

The vertical stiffness is the same as the support stiffness ($K_{support}$) found in Equation 2.19. From Figure 4.13 it can be seen that the force required to rotate the sleeper is given by:

$$F = \frac{K_{ver} \cdot xdy}{h} \tag{4.7}$$

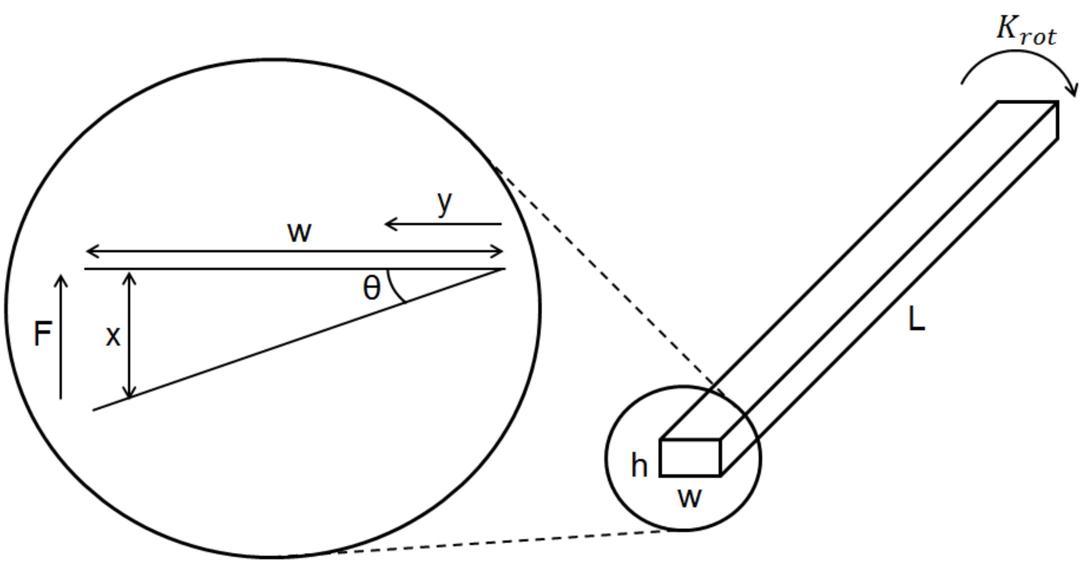

Figure 4.13: Free body diagram of the rotational stiffness of a sleeper with dimensions w, h and L

The torque required to rotate the sleeper is therefore:

$$T = \frac{K_{ver} \cdot xydy}{h} \tag{4.8}$$

For small θ, $x = y \sin\theta \approx y\theta$, therefore Equation 4.8 becomes:

$$T = \frac{K_{ver}\theta}{h} \int y^2 dy \tag{4.9}$$

By integrating with respect to y the rotational stiffness (T/θ) is given by:

$$K_{rot} = \frac{T}{\theta} = \frac{K_{ver} \cdot y^3}{3h} \tag{4.10}$$

In this work the dimension of the sleepers was taken to be $L = 2.5m$, $w = 0.2m$ and $h = 0.2m$. These dimensions are consistent with a G44 type sleeper [171], which is commonly used across the UK network.

4.4.1 Validation of the Discrete Support Approach

The Winkler foundation approach is known to give a good approximation of the rail support stiffness for sleeper spacings that are typically found on a mainline railway (0.6m). In this Section the discrete support method is validated against the Winkler approach.

Figure 4.14a shows that the displacement of the beam for the discrete support method was almost identical to the Winkler foundation. The peak negative bending moment for both approaches were almost identical and the peak positive bending moment of the Winker foundation (Figure 4.14b) was 0.95 times that of the discrete support. This demonstrates the good accuracy of the discrete support model for sleeper spacings that are typical on mainline railway of 0.6m.

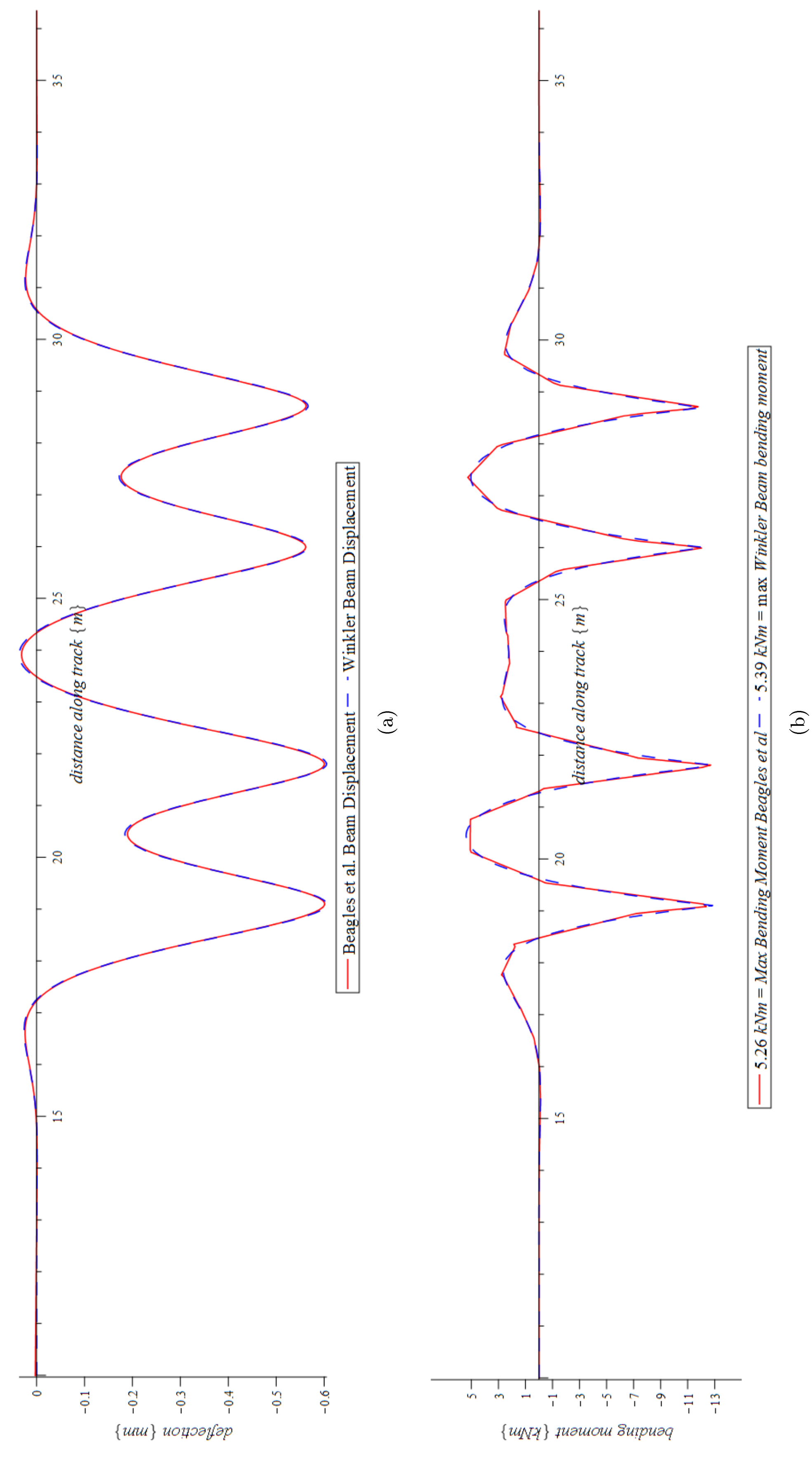

Figure 4.14: Comparison to the Winkler Foundation approach to the Euler-Bernoulli beam with discrete supports for sleeper separation = 0.6m, (a) deflection, (b) bending moment

4.4.2 Variation in Peak Bending Moment Found using the Discrete Support Method

Each element of the discrete support model reacts according to standard beam theory for a beam under point loading (Figure 4.15). The bending moment is therefore defined at the sleeper supports or at load application points, and is linear in between.

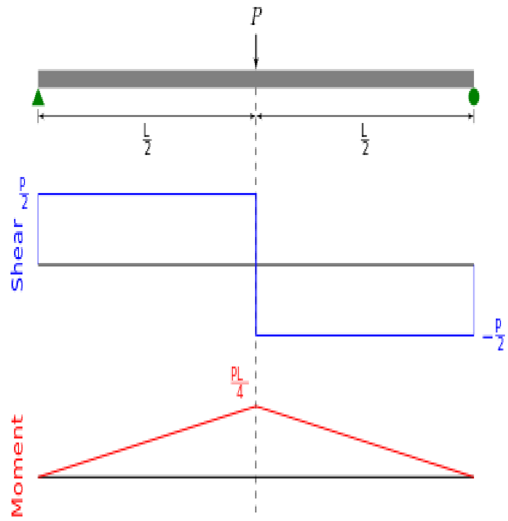

Figure 4.15: Reaction of a simply supported beam under a point load, showing the shear load and bending moment. Figure taken from [218]

This leads to an issue that is demonstrated in the results from the model in Figure 4.16. As shown the bending moment is defined at the the sleeper positions (black dashed vertical lines) and the wheel positions. This method therefore successfully captures the peak negative bending moment at the wheel position. However, the peak positive bending moment found in this case can be seen to differ between the two bogies. The centreline between the axle positions for both bogies and between the cars is shown by the green vertical lines in Figure 4.16. As can be seen for bogie 2 the centreline between the axles falls on a sleeper position, but for bogie 1 it does not. The Winkler foundation approach shows that the peak positive bending moment is found at the centreline between the axle positions, this peak is missed for bogie 1.

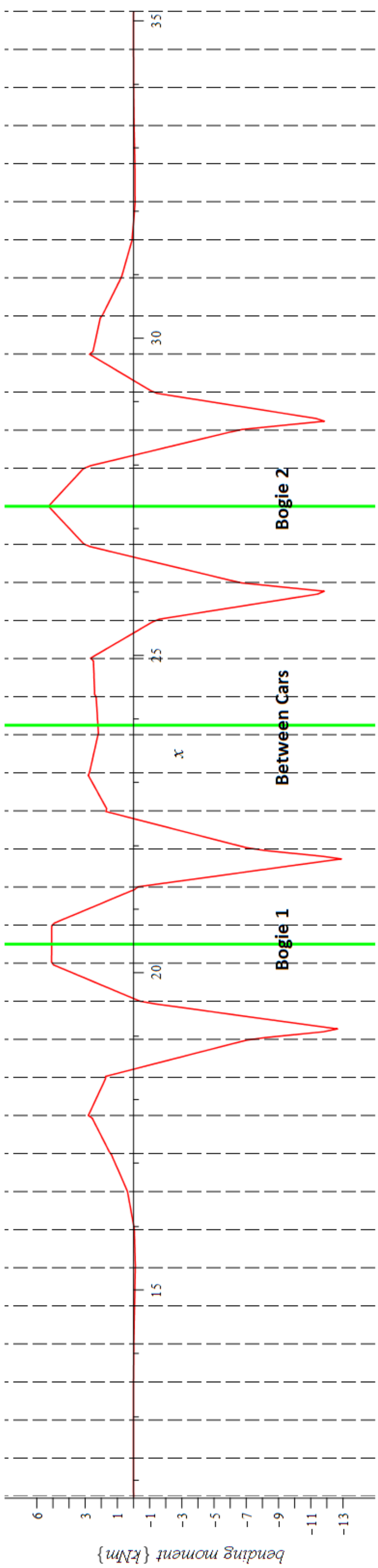

Figure 4.16: Example result from the Euler–Bernoulli Beam Model on Discrete Supports. Dashed black vertical lines represent sleeper positions. Green vertical lines represent centreline between axle positions

The resultant peak positive bending moments found from this approach are therefore dependant on the bogie positioning relative to the sleeper supports. With maximum bending moments only found within the rail when the support position coincides with the centreline between the axles. However the peak negative bending moments that occur at the wheel position are always successfully captured.

4.4.3 Improvement of the Discrete Support Method

To solve the problem of the position of the wheel loads on the discrete support dictating the peak bending moment experienced, an iterative solution was developed. The methods are outlined in Figure 4.17.

(a)

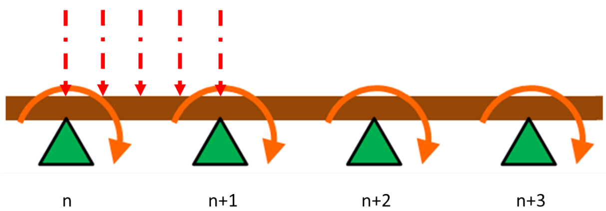

(b)

Figure 4.17: Schematic of the two sleeper-wheel load configurations used to remove the need to consider the relative distance between the applied load and sleeper position within the discrete support model. In Method A, (a), the wheel position is fixed, with the sleeper positions moved relative to wheel load. In Method B, (b), the sleeper positions is fixed, with the wheel position incremented between supports. The wheel positions are defined with the red arrows and the sleeper positions with green triangles. Figure adapted from Beagles et al. [2]

In Method A (Figure 4.17a) the wheel position is fixed, with the sleeper positions moved relative to wheel load. By combining the solutions from each iteration the overall bending stress generated within the track by the wheel load is found. This removes the poorly defined peak in bending stress due to variation in the relative distance between the support and the wheel position.

The result of this method is shown in Figure 4.18. Method A is compared to the Winkler foundation deflection (Figure 4.18a) and bending moment (Figure 4.18b). Through use of method A the discrete support approach shows the full load history of the rail, which can be seen to align well with the Winkler approach for sleeper spacings of 0.6m. The location of the peak positive bending moments can now be seen to agree with the Winkler foundation at all points along the rail.

However, when investigating the range of bending moments experienced by an individual sleeper, Method B (Figure 4.17b), is of more use. In Method B the sleeper positions are fixed, with the wheel position incremented between supports. For example, as the wheel position moves between sleeper n to sleeper $n+1$, the reaction of the sleepers is given at the same point along the rail. Therefore, when combining the solutions from each iteration, the range of bending moments experienced by an individual sleeper as the wheel traverses between sleepers can easily be found by inspection.

This is shown in Figure 4.19. The deflection of the rail using Method B (Figure 4.19a) is shown to be almost identical at all wheel positions. This is the expected result as a typical mainline track support structure is designed to prevent excessive deflections between supports. The bending moment of the rail using Method B is shown in Figure 4.19b. From inspection of the bending moment of the sleeper positioned at 20.3m ($n+2$ sleeper) can be seen to vary between 2kNm and 5.4kNm as the wheel position moves between sleeper n to sleeper $n+1$. The peak negative bending moment can also be seen to increase in magnitude from -11kNm to -13kNm when the wheel load is positioned between the supports.

In this Section the discrete support approach has been improved, removing the variable of the relative distance between the sleeper support and the wheel positions through the use of two different methods. Method A found the full load history of the rail. This method has been shown to give better agreement to the Winkler foundation approach than the basic discrete support model. Method B gave the load history of the sleepers as the wheel traversed between them. The choice to use either approach is dependant on the area the user wishes to investigate.

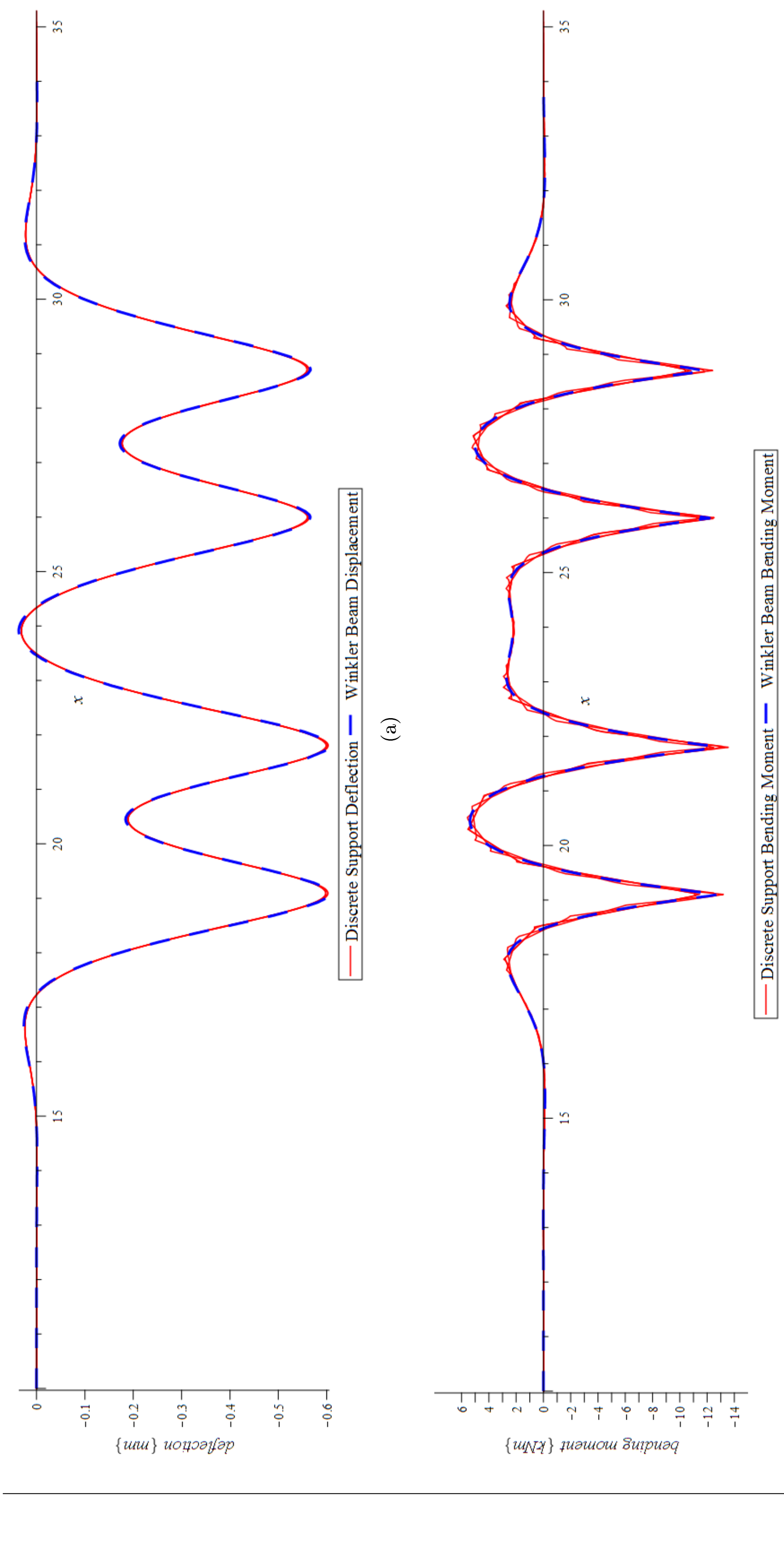

Figure 4.18: Comparison between the Winkler foundation approach and the combined curves from each iteration of the discrete support approach Method A. Deflection, (a), and bending moment, (b)

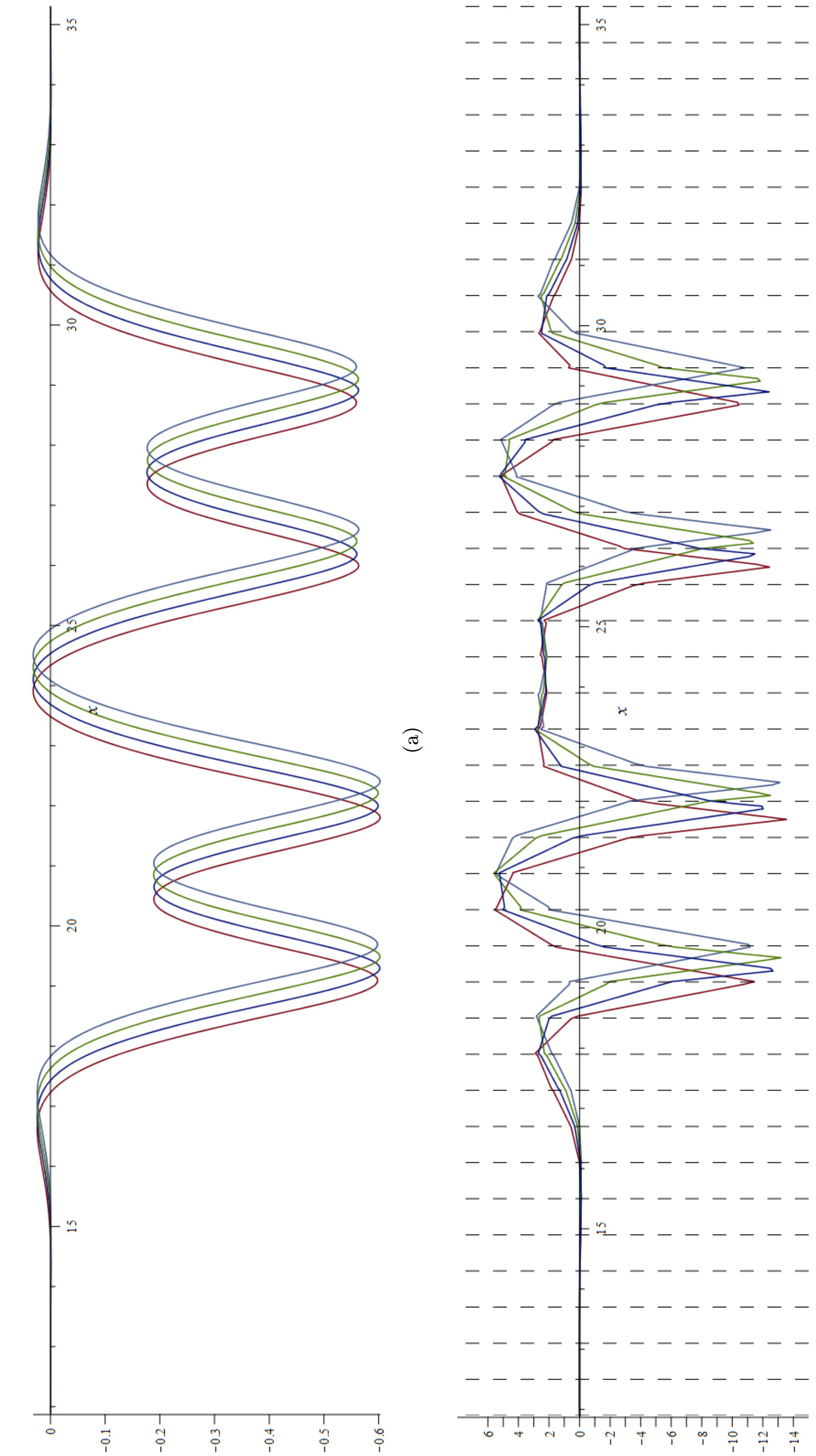

Figure 4.19: Discrete support approach Method B. Deflection, (a), and bending moment, (b)

4.5 Bending Moment of the Rail as a Train Traverses a Stiffness Change

In this Section the effect that support stiffness changes have on rail bending is investigated using Method B (Figure 4.17b). An abrupt stiffness change is investigated where a portion of the supports of the discrete support method are changed to a support structure that is ten times as stiff as the ballasted track structure within the UK (Table 2.2). This stiffness is equivalent to pinned track on a rigid bridge structure. The effect of graduating this stiffness change over ten sleepers (6m) is then investigated.

The effect of the stiffness change on the whole rail bending is investigated for both cases as the wheel loads traverse onto the stiff foundation using the technique developed in Section 4.4.3. The results are compared to the bending moment generated within the rail by the passage of a class 390 with standard track support with sleeper separation distance of 0.6m (Figure 4.19b).

4.5.1 Abrupt Stiffness Change

In Figure 4.20 the effect of the 1st wheel load approaching the stiff foundation on the bending moment within the rail is shown. As the 1st wheel approaches the sleeper at the end of the stiff structure (highlighted with orange dashed line) the peak positive bending moment generated to the right of the wheel load has doubled in magnitude in comparison to standard track. The effect of the abrupt stiffness change is greatest when the wheel load closest to the abrupt stiffness change is on the sleeper next to the abrupt stiffness change. This can be seen in Figure 4.20a when the wheel load is on sleeper $n+17$ and in Figure 4.20b when the wheel load is on sleeper $n+16$.

For these cases the peak positive bending moment generated by the wheel loads is now at this sleeper, and has increased to 1.2 times the magnitude of the peak bending moment found between the axles in evenly supported ballasted track. Therefore, not only has the stiff structure introduced an additional severe bending cycle (i.e. greater in magnitude than that predicted by a single wheel load), but the position of the peak positive bending moment found has moved to the sleeper at the end of the stiff structure.

In Figure 4.21 the effect of the 2nd wheel load approaching the stiff foundation can be seen. The bending moment when the stiffness change is at sleeper $n+14$ (Figure 4.21a) and sleeper $n+13$ (Figure 4.21b) are shown. The peak positive bending moment is at the sleeper at the end of the stiff structure and has increased to 1.2 times that found in evenly supported ballasted track when the wheel load is midway between the 2nd and 1st sleeper from the end of the abrupt stiffness transition, i.e. midway between sleepers $n+12$ and $n+13$ in Figure 4.21a and midway between sleepers $n+11$ and $n+12$ in Figure 4.21b.

The resultant bending moment curve reduces in gradient between the 1st and 2nd wheel loads. The contribution of the 1st wheel load (which is already on the stiff foundation) on the peak positive bending moment between the 1st and 2nd wheel loads is reduced. As a result the peak positive bending moment within the rail as the 2nd wheel approaches the stiff foundation is similar to the 1st.

In Figure 4.22 the effect of the 3rd wheel load approaching the stiff foundation can be seen. The peak positive bending moment when the support stiffness change is at sleeper $n+7$ (Figure 4.22a) and increases to 1.2 times that found in evenly supported ballasted track. When the support stiffness change is at sleeper $n+6$ (Figure 4.22b) the peak positive bending moment increases further to 1.3 times that found in evenly supported ballasted track. This further increase is due to the additional weight of car 1 (Table 4.1).

The wider spacing between the 2nd and 3rd wheel load (i.e. the wheel spacing between the rail vehicles is larger than that between wheels on the same bogie) leads to the resultant bending moment curve equal to zero between the 2nd and 3rd wheel loads when the stiff support is at sleeper $n+2$ (Figure 4.22b). Therefore the rail has independent reactions from the two bogies when they are approaching/on the stiff structure.

In Figure 4.23 the effect of the 4th wheel load approaching the stiff foundation can be seen. Similar to the 3rd wheel, the peak positive bending moment when the support stiffness change is at sleeper $n+3$ (Figure 4.23a) increases to 1.2 times that found in evenly supported ballasted track. When the support stiffness change is at sleeper $n+2$ (Figure 4.23b) the peak positive bending moment increases further to 1.3 times that found in evenly supported ballasted track.

The resultant curve reduces in gradient between the 3rd and 4th wheel loads. The contribution of the 3rd wheel (which is already on the stiff foundation) on the peak bending moment is therefore reduced. As a result the increase in peak positive bending moment within the rail on the approach of the 4th wheel onto the stiff foundation is the same as the 3rd.

In Figure 4.24 all of the wheel loads are on the stiff foundation. Here the peak bending moment has reduced to 0.4 times that found in evenly supported ballasted track. The overall reaction of the rail is shown in Figure 4.24b. The following observations can be made for a train on a structure ten times the stiffness of typical track support stiffness:

a) The resultant bending moment curve can be seen to be much reduced in magnitude relative to that for ballasted track (peak bending moment of (5kNm vs 13kNm for ballasted track).

b) The two wheel loads on the same bogie generate smaller superpositional effects on the overall bending moment within the rail. This can be seen by the plateauing of the bending moment curve between wheel loads on the same bogie.

c) The two vehicles generate independent reactions from the rail. This can be seen by the bending moment being equal to zero between wheel loads two and three.

d) As a result all the peaks are approximately equivalent to that generated from a single wheel load (5kNm).

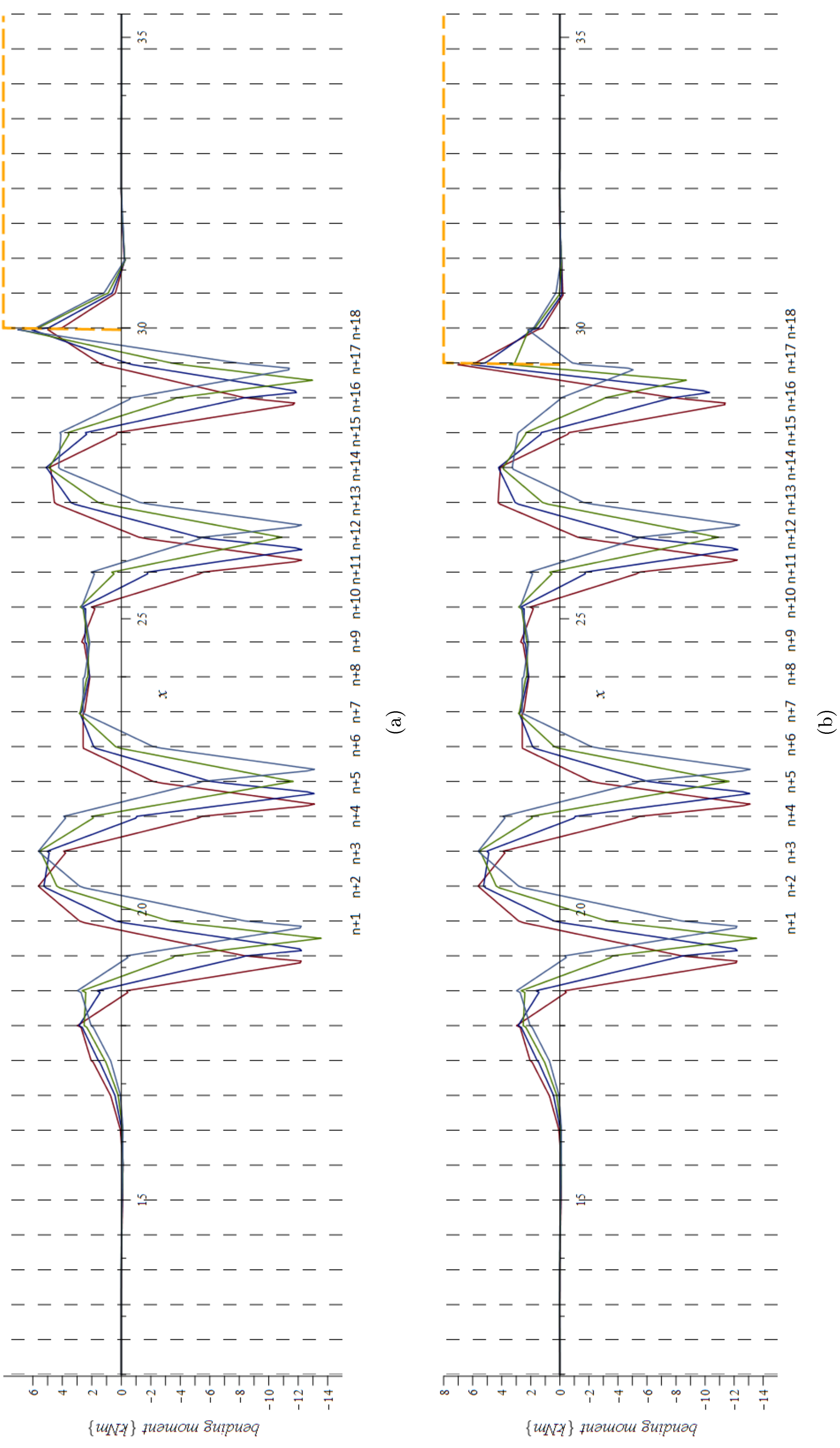

Figure 4.20: Bending moment of the rail as the 1st wheel approaches stiff structure (highlighted with orange dashed line), (a), sleeper at stiffness change is sleeper $n + 18$, (b), sleeper at stiffness change is sleeper $n + 17$

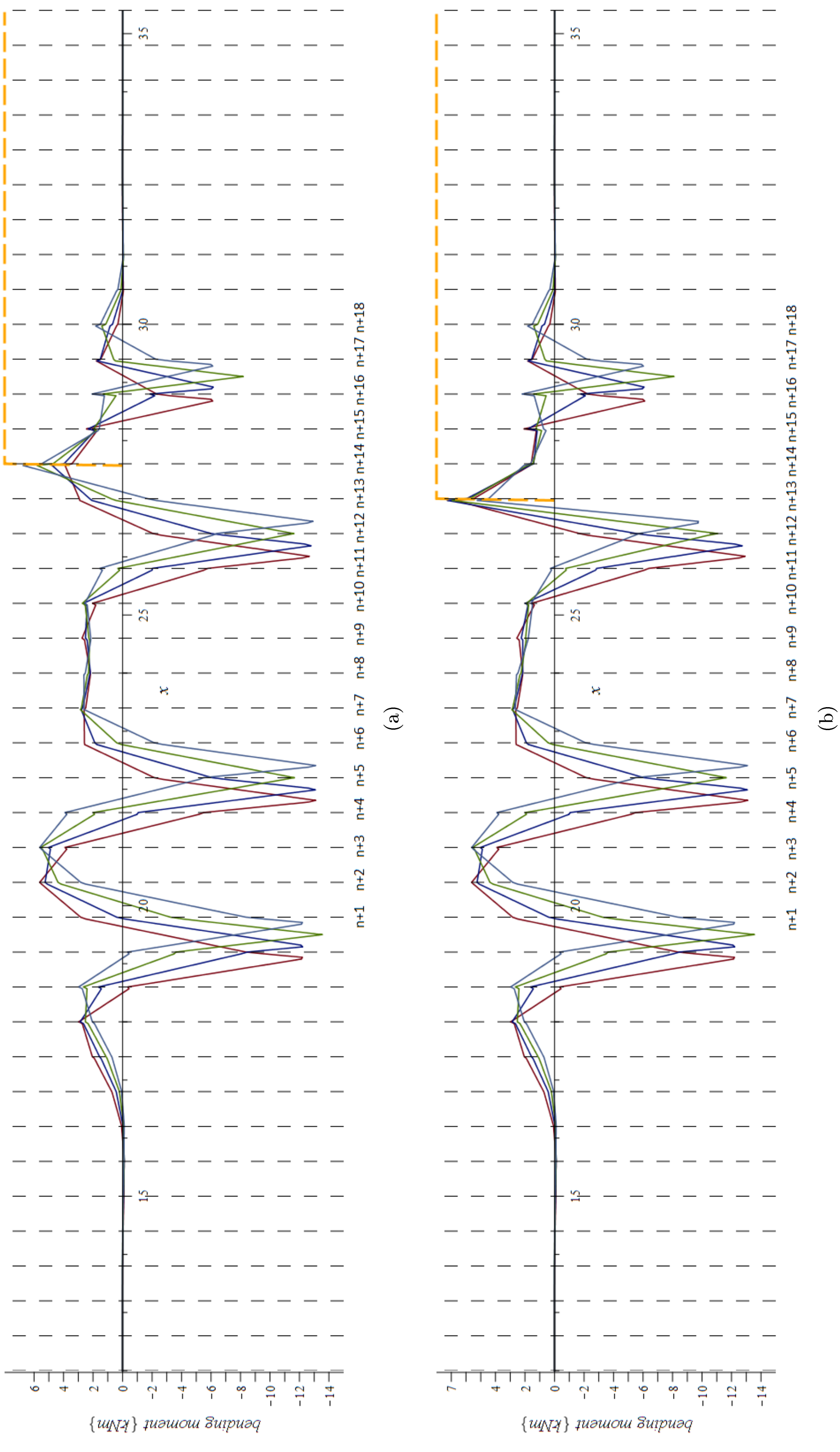

Figure 4.21: Bending moment of the rail as the 2nd wheel approaches stiff structure (highlighted with orange dashed line), (a), sleeper at stiffness change is sleeper $n+14$, (b), sleeper at stiffness change is sleeper $n+13$

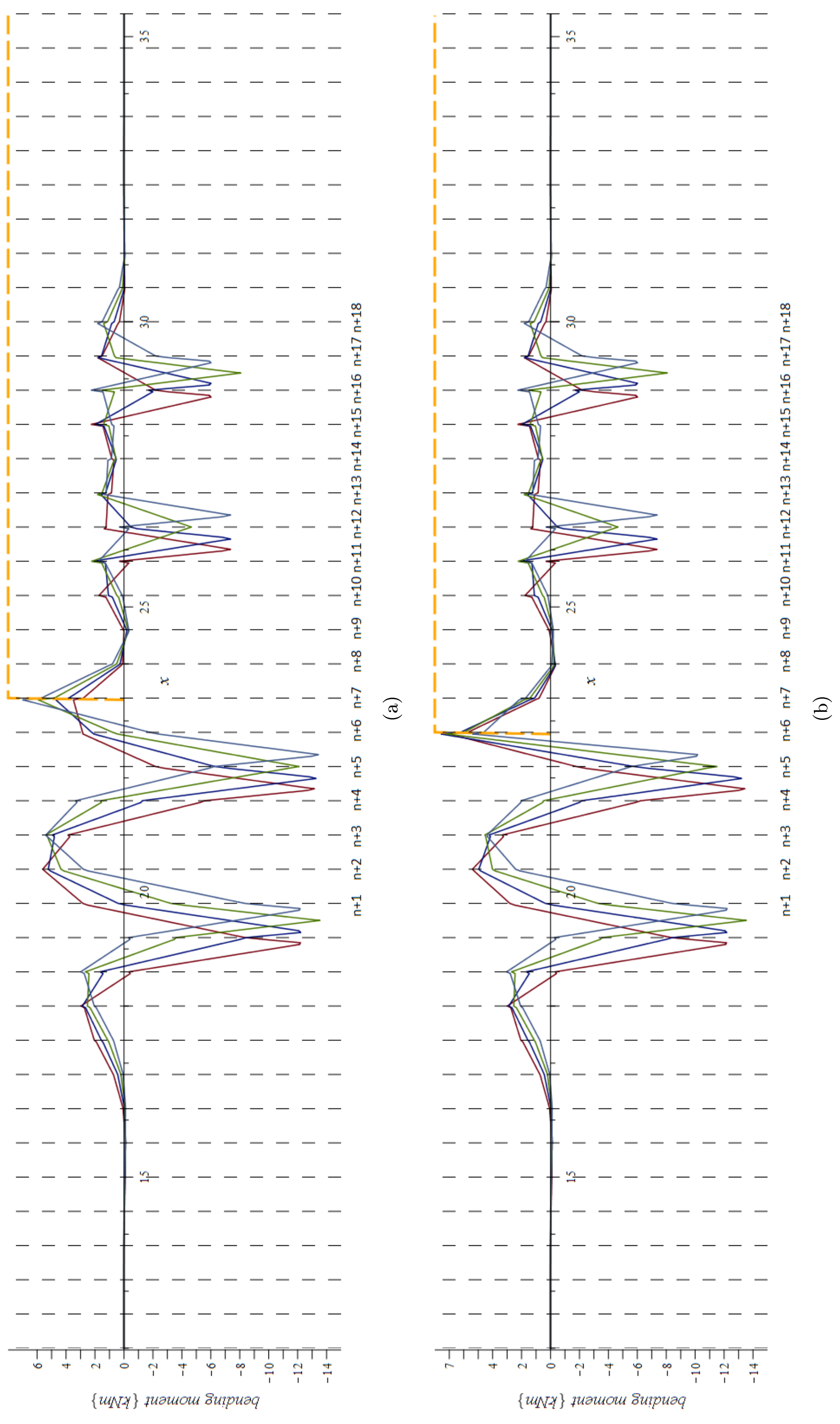

Figure 4.22: Bending moment of the rail as the 3rd wheel approaches stiff structure (highlighted with orange dashed line), (a), sleeper at stiffness change is sleeper $n+7$, (b), sleeper at stiffness change is sleeper $n+6$

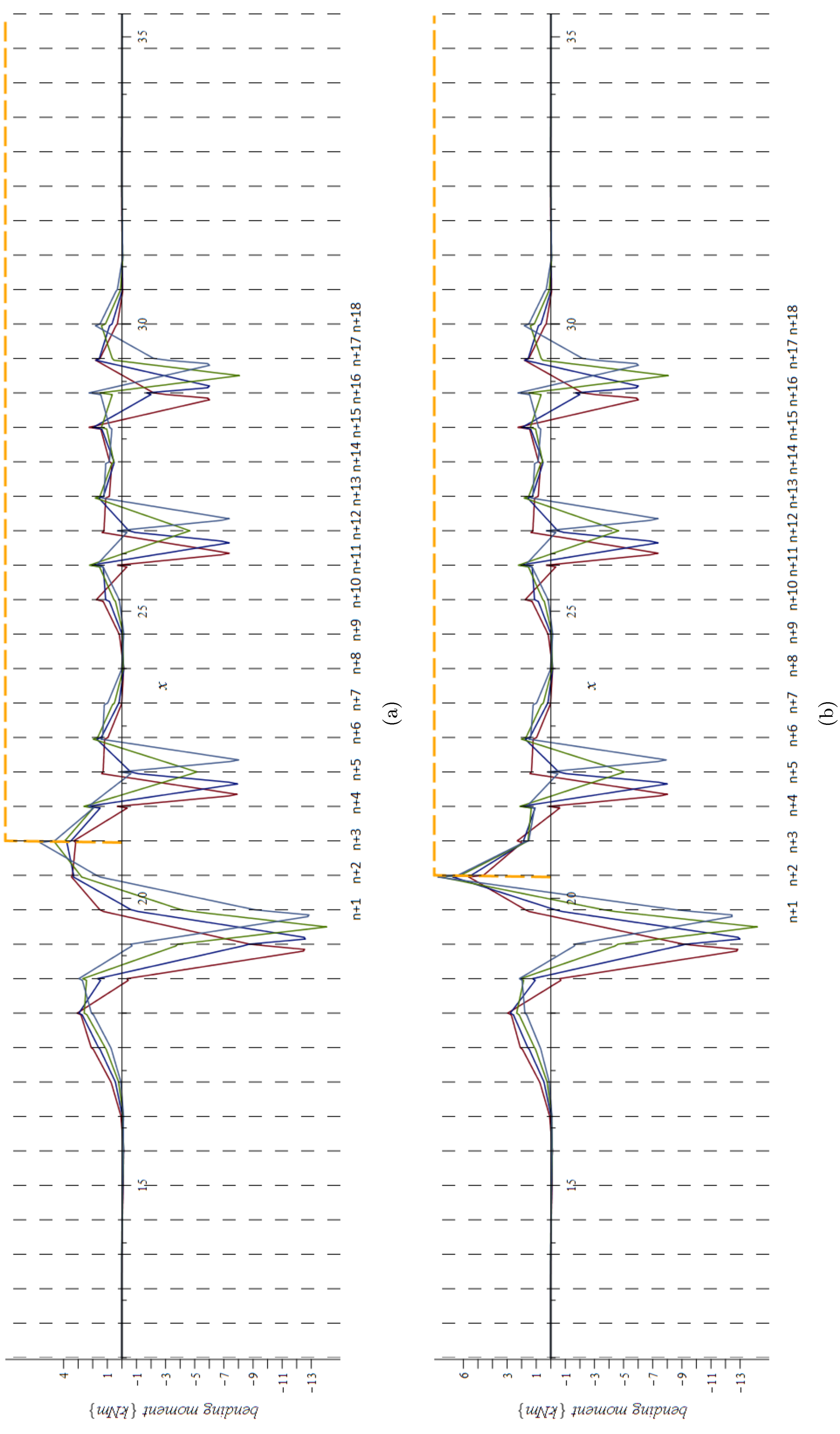

Figure 4.23: Bending moment of the rail as the 4th wheel approaches stiff structure (highlighted with orange dashed line), (a), sleeper at stiffness change is sleeper $n+3$, (b), sleeper at stiffness change is sleeper $n+2$

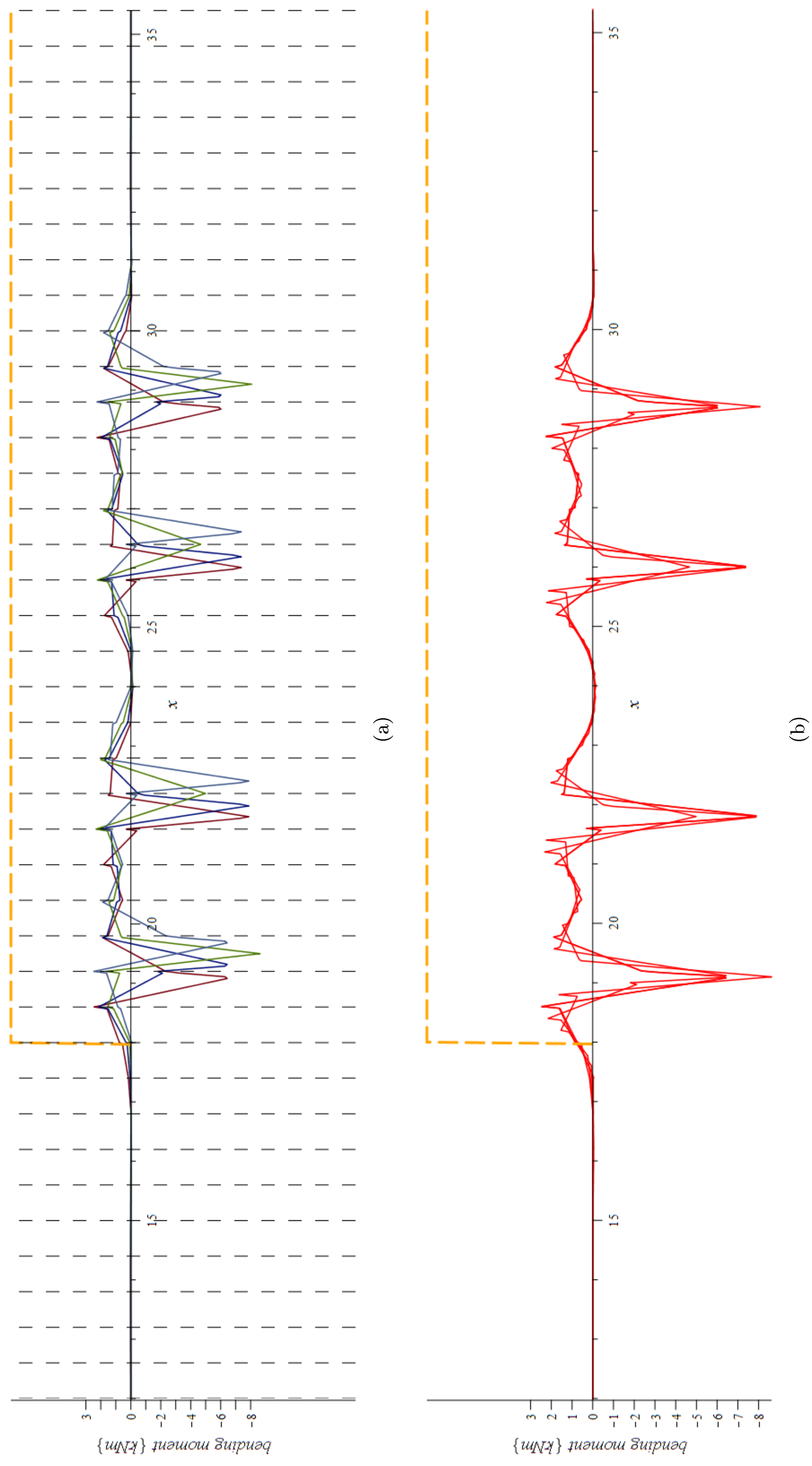

Figure 4.24: Bending moment of the rail when the train is supported by a structure ten times as stiff as typical track support stiffness (highlighted with orange dashed line). (a), fixed sleeper position (Method B), (b), fixed wheel position (Method A)

To summarise, the results show that the abrupt stiffness changes within the track leads to peak bending moments of 1.3 times that found within ballasted track. The location of the peak bending moment also changes from between the wheelsets on the bogie to the point of support stiffness change. This section of track is therefore subject to repeated rail bending of increased severity as a train passes.

The approach of each wheelset towards the stiffness transition generates this peak bending moment of increased severity, resulting in a larger number of bending cycles that have increased severity. For a nine car class 390 this means that the number of bending cycles of increased severity has increased from twenty-six out of forty-six bending cycles to thirty-six out of forty-six bending cycles. This is a significant rise which would be expected to lead to a greater level of crack propagation within the rail. Once on the stiffer structure the peak bending moment and the interaction between wheelsets decreases considerably, as expected.

4.5.2 Gradual Stiffness Transition

In this Section a linear increase in stiffness over ten sleepers (6m) between the ballasted track structure and a support structure that is ten times as stiff is investigated. A comparison is done between the gradual and abrupt transitions to assess the effect of even very short transition zones. The results are shown in Figures 4.25-4.28 with the stiffness change being represented by the orange dashed line.

As can be seen in Figure 4.25 the peak bending moment as the 1st wheel approaches the transition to the stiff structure at sleepers $n+18$ and $n+17$ remains at that found for ballasted track (Figure 4.19b). This is in contrast to the abrupt stiffness change where an increase in the peak bending moment was found at sleepers $n+18$ and $n+17$ (Figure 4.20). This effect can also be seen in Figures 4.26-4.28 where the peak bending moment remains consistent with that found on ballasted track as the 2nd (Figure 4.26, sleepers $n+14$ and $n+13$), 3rd (Figure 4.27, sleepers $n+7$ and $n+6$) and 4th (Figure 4.28, sleepers $n+3$ and $n+2$) wheelsets.

The inclusion of a transition zone has led to a significant reduction of the whole rail bending by 20% in comparison to an abrupt stiffness change, i.e. rail bending was equivalent to evenly supported ballasted track. Therefore the inclusion of a transition zone has been shown to successfully negate the additional severe bending cycles that were induced by the abrupt stiffness change. Therefore the main issue regarding transition zones remains their maintainability. Adjustment of the track support stiffness at sleeper level could prove to be a more maintainable solution to transition zone problems then the sub-ballast concrete ramps used currently that, as discussed in Section 2.4.3, deteriorate over time.

The discrete support method has successfully demonstrated the difference between different types of transitions using a simple quasi-static approach. In future studies this approach could be used in various applications including investigating whether different sleeper spacings would be an effective method to gradually change the track support stiffness.

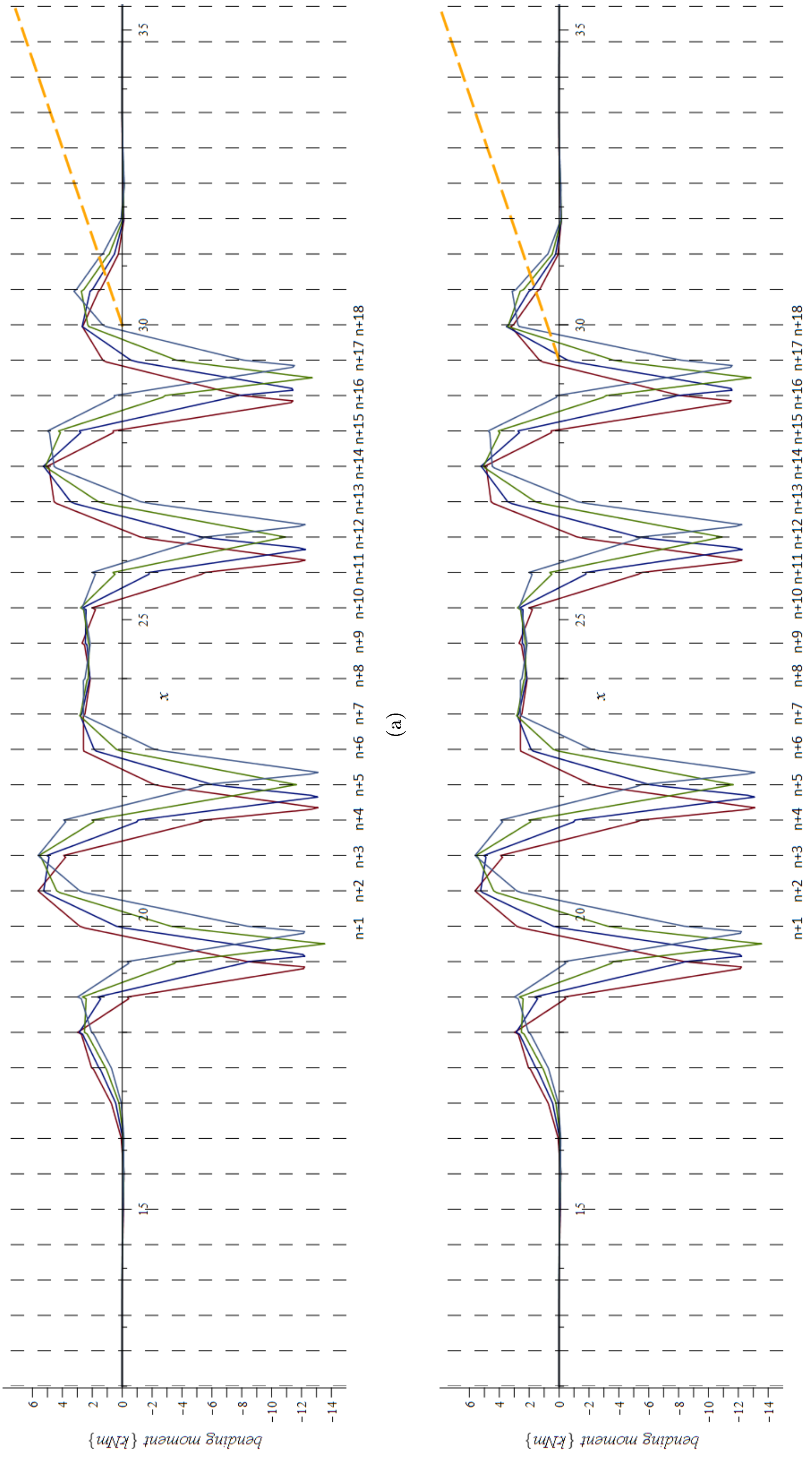

Figure 4.25: Bending moment of the rail as the 1st wheel approaches the transition to the stiff structure (highlighted with orange dashed line), (a), sleeper at start of stiffness transition is sleeper $n + 18$, (b), sleeper at start of stiffness transition is sleeper $n + 17$

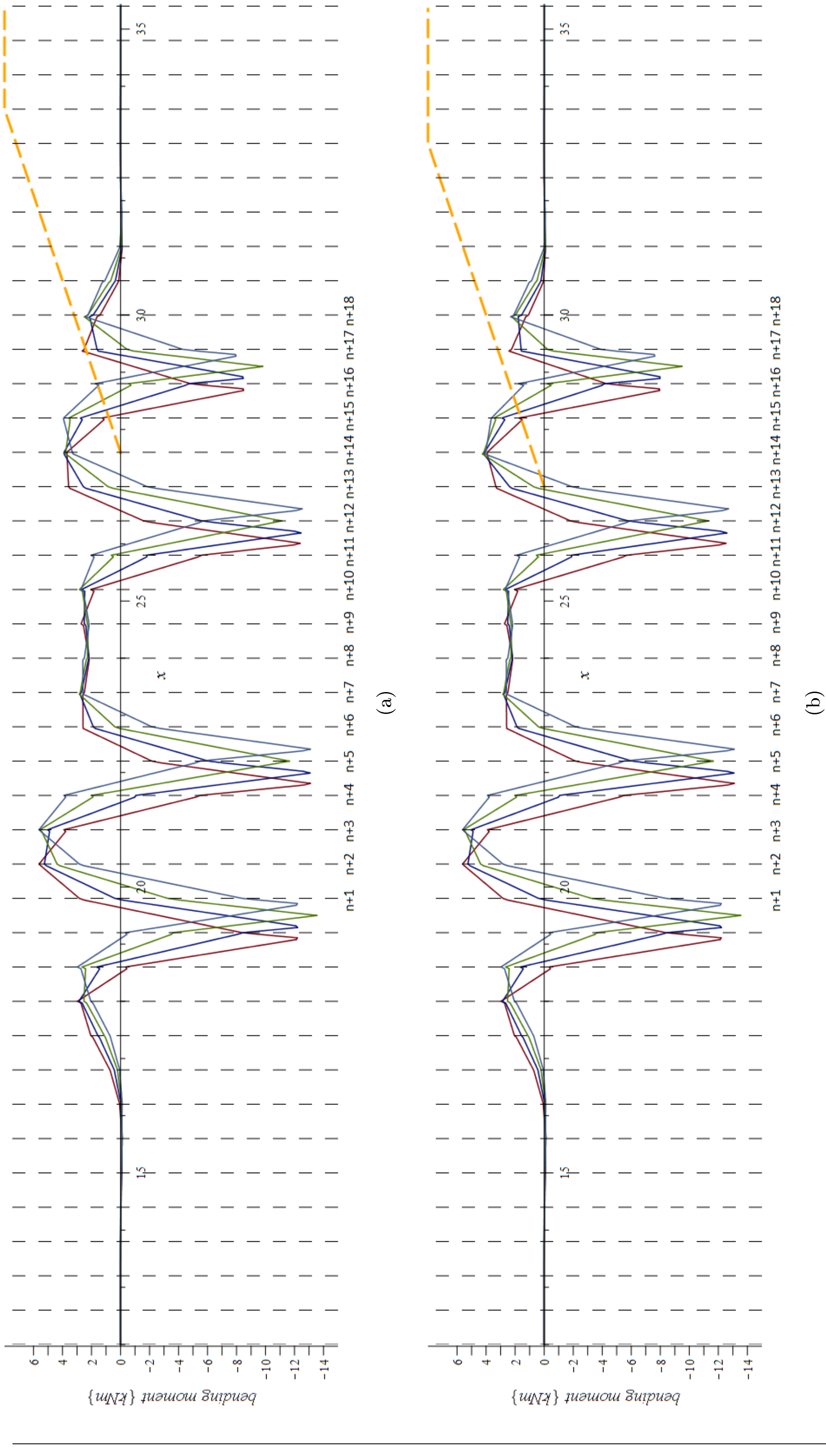

Figure 4.26: Bending moment of the rail as the 2nd wheel approaches the transition to the stiff structure (highlighted with orange dashed line), (a), sleeper at start of stiffness transition is sleeper $n+14$, (b), sleeper at start of stiffness transition is sleeper $n+13$

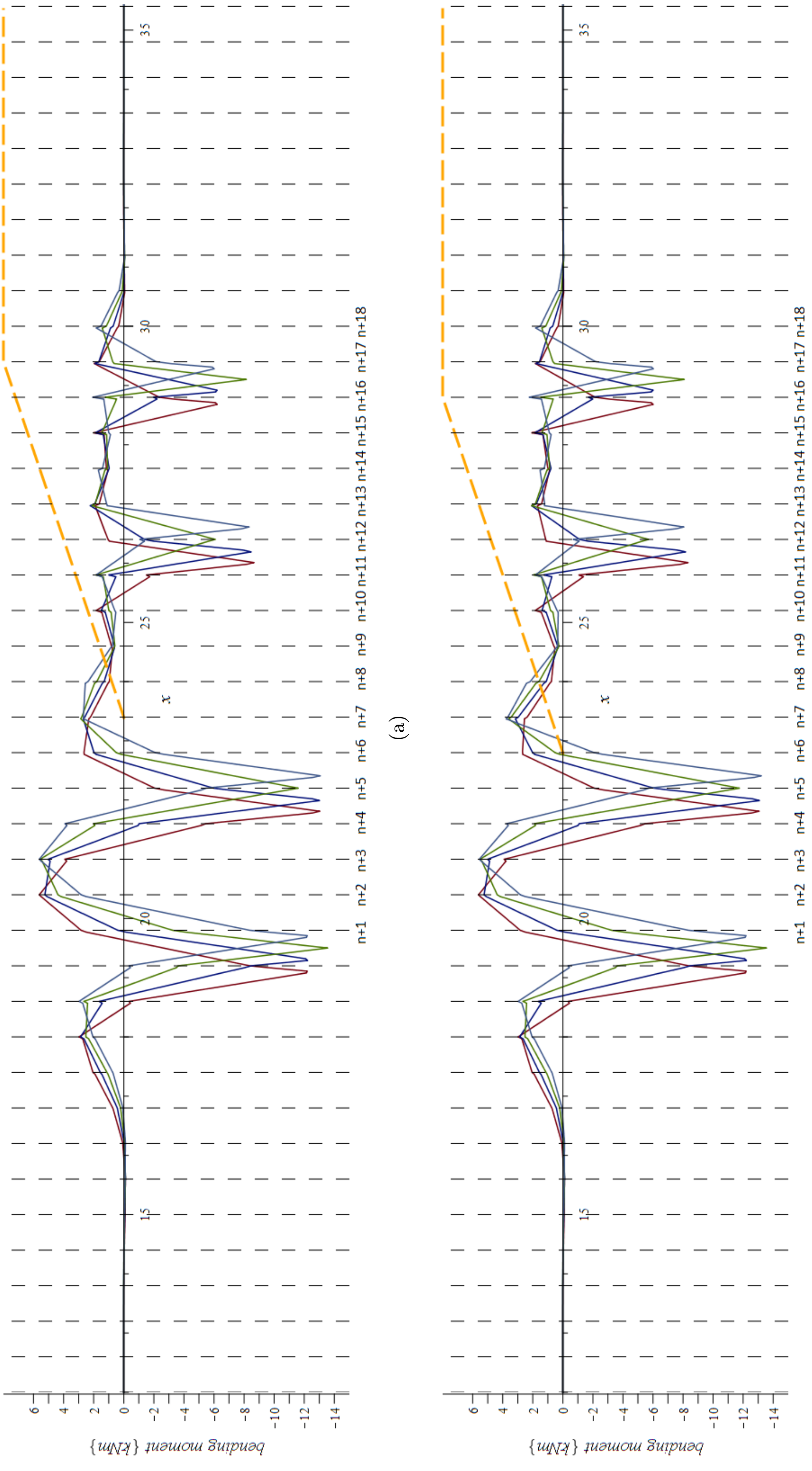

Figure 4.27: Bending moment of the rail as the 3rd wheel approaches the transition to the stiff structure (highlighted with orange dashed line), (a), sleeper at start of stiffness transition is sleeper $n+7$, (b), sleeper at start of stiffness transition is sleeper $n+6$

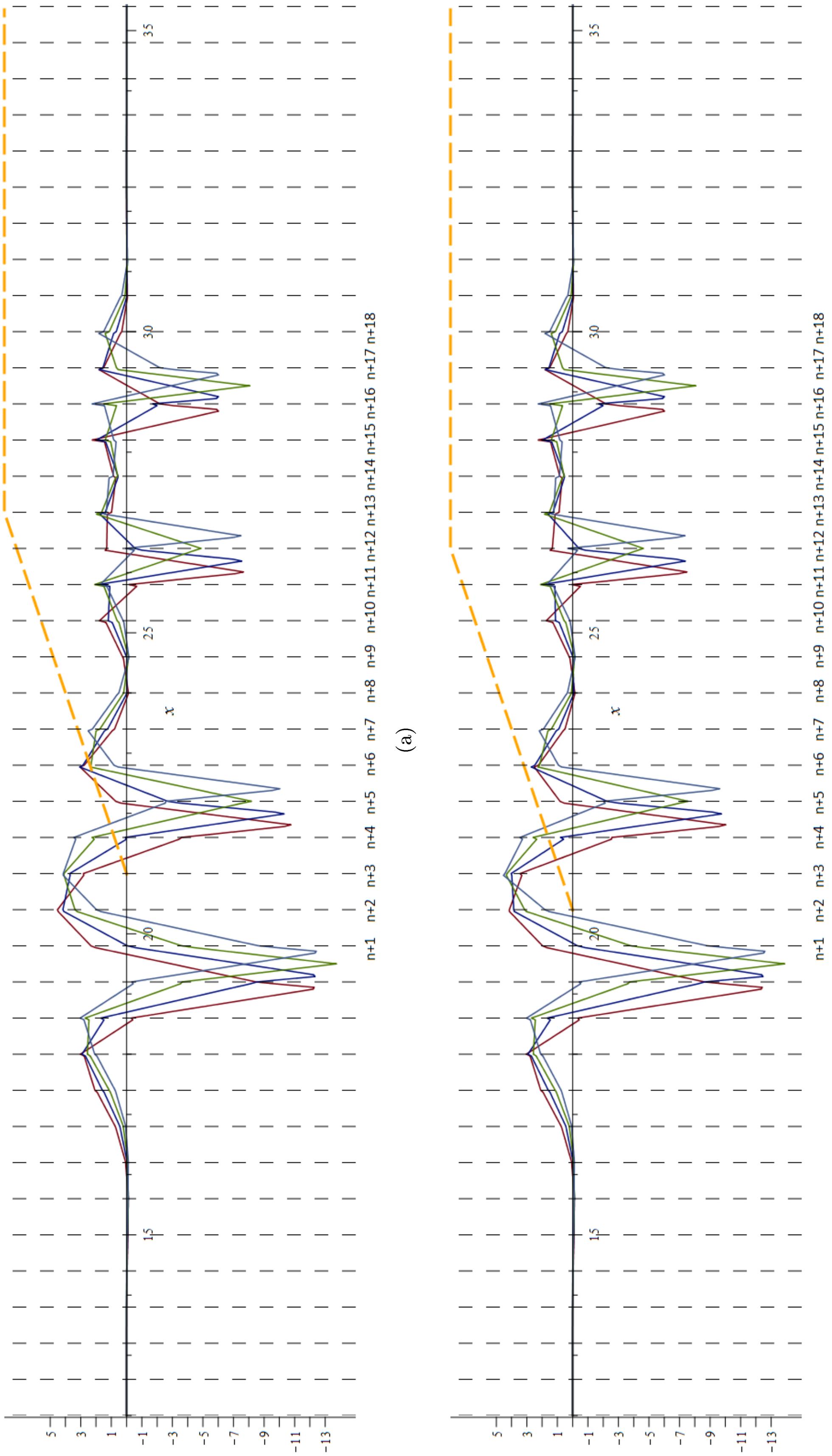

Figure 4.28: Bending moment of the rail as the 4th wheel approaches the transition to the stiff structure (highlighted with orange dashed line), (a), sleeper at start of stiffness transition is sleeper $n+3$, (b), sleeper at start of stiffness transition is sleeper $n+2$

4.6 Conclusions

In this Chapter the BOEF method using a continuous Winkler foundation was successfully implemented to predict the bending moment within the rail generated by the loading of a class 390. The bending moment was found to increase by a factor of two in comparison to a single wheel load when a secondary nearby wheel load was considered. The passage of a nine car class 390 would therefore generate forty-six bending cycles, twenty-six fewer than if you assumed that the rail underwent two bending cycles per wheel (single wheel case). However, twenty-six of these bending cycles are twice as severe as that predicted from a single wheel load, demonstrating the importance of considering multiple wheel loads in a rail application of the Winkler foundation approach.

Improvements to the discrete support method developed by Beagles et al. [2] led to a removal of the need to consider the relative distance between the support and wheel positions. Through use of Method A the full load history of the rail can be found. It has been shown to give better agreement then the basic discrete support model to the Winkler foundation approach. Use of Method B gives the load history of the sleepers. The choice to use either approach is dependant on the area the user wishes to investigate.

Abrupt stiffness changes within the track led to peak bending moments of 1.3 times that found within ballasted track. The abrupt stiffness change was also found to dictate the location of the peak bending moment, with the peak bending moment being found as each wheelset approached the abrupt stiffness change. This resulted in a larger number of bending cycles that have increased severity and means that this section of track is subject to repeated rail bending of increased severity as a train passes (Section 2.4.3).

For a nine car class 390 this means that the number of bending cycles of increased severity has increased from eighteen out of forty-six bending cycles to thirty-six out of forty-six bending cycles. This is a significant rise which would be expected to lead to a greater level of crack propagation within the rail.

The inclusion of a transition zone over a ten sleeper distance led to a significant reduction of the whole rail bending by 20% in comparison to an abrupt stiffness change, i.e. rail bending was equivalent to evenly supported ballasted track. The additional severe bending cycles that were induced by the abrupt stiffness change are also avoided through the inclusion of a transition zone.

Once on the stiffer structure the peak bending moment and the interaction between wheelsets decreases significantly, as expected. The following observations were made for a train on a structure ten times the stiffness of typical track support stiffness:

a) The resultant bending moment curve is much reduced in magnitude relative to that for ballasted track (peak bending moment of 2kNm vs 5.4kNm for ballasted track).

b) The two wheel loads on the same bogie generate smaller superpositional effects on the overall bending moment within the rail. This can be seen by the plateauing of the bending moment curve between wheel loads on the same bogie.

c) The two vehicles generate independent reactions from the rail. This can be seen by the bending moment being equal to zero between wheel loads two and three.

d) As a result all the peaks are approximately equivalent to that generated from a single wheel load (2kNm).

The peak positive bending moment within the rail under multiple wheel loads has been used in the three dimensional boundary element approach (developed in Chapter 5). For multiple cracks within the rail (of 10mm radius and at 30° to the rail surface) this increased the crack growth rate driven by whole rail bending to above threshold levels. It is therefore a critical factor that must be considered when investigating crack growth to ensure that the effect of rail bending on crack growth is captured or that cracks are maintained to avoid transition into the rapid phase III growth (Section 2.3.3).

The peak negative rail bending moment was used within the three dimensional boundary element approach to investigate the mode II SIF of the crack near (but not directly underneath) the contact. The results suggested that use of this simple rail bending approach is sufficient to find an approximation of the peak negative mode II SIF used to calculate ΔK_{II} in the crack growth equations. Therefore, a contact model is only required to find the peak positive mode II SIF to calculate the crack growth rate. This gives significant modelling time savings when calculating the crack growth rate. However further work was identified to provide further certainty to this conclusion for different crack sizes. Especially for the case of smaller cracks which are more driven by the contact stresses.

This analysis has been conducted using static train loads as an input. It was demonstrated that the elastic nature of the analysis meant that the percentage increase in the load (by the dynamic load factor) was reflected in the rail deflection and bending moment results. Whilst this method of analysis is linear for varying load, it is not linear for other factors, for example the support stiffness.. In future work the method developed here is computationally rapid enough to be used to investigate whether adjustment of the input loads would be a valid method of taking into account dynamic factors, such as train speed, without using a complex dynamic model.

In the following chapters a boundary element approach is used to investigate the interaction effects between multiple cracks within the railhead in detail.

Chapter 5

Development of an Improved Boundary Element Approach for Investigating Rolling Contact Fatigue and Preliminary Modelling

5.1 Introduction

In the previous Chapter abrupt sleeper support stiffness changes were shown to increase the bending moment within the rail significantly. The effect of this on RCF type defects within the railhead is investigated in this Chapter. This Chapter aims to:

- Develop a boundary element method to investigate multiple cracks within the rail.
- Conduct preliminary investigations on a crack within the rail directly under the wheel-rail contact.

Using the structure as shown in Figure 5.1.

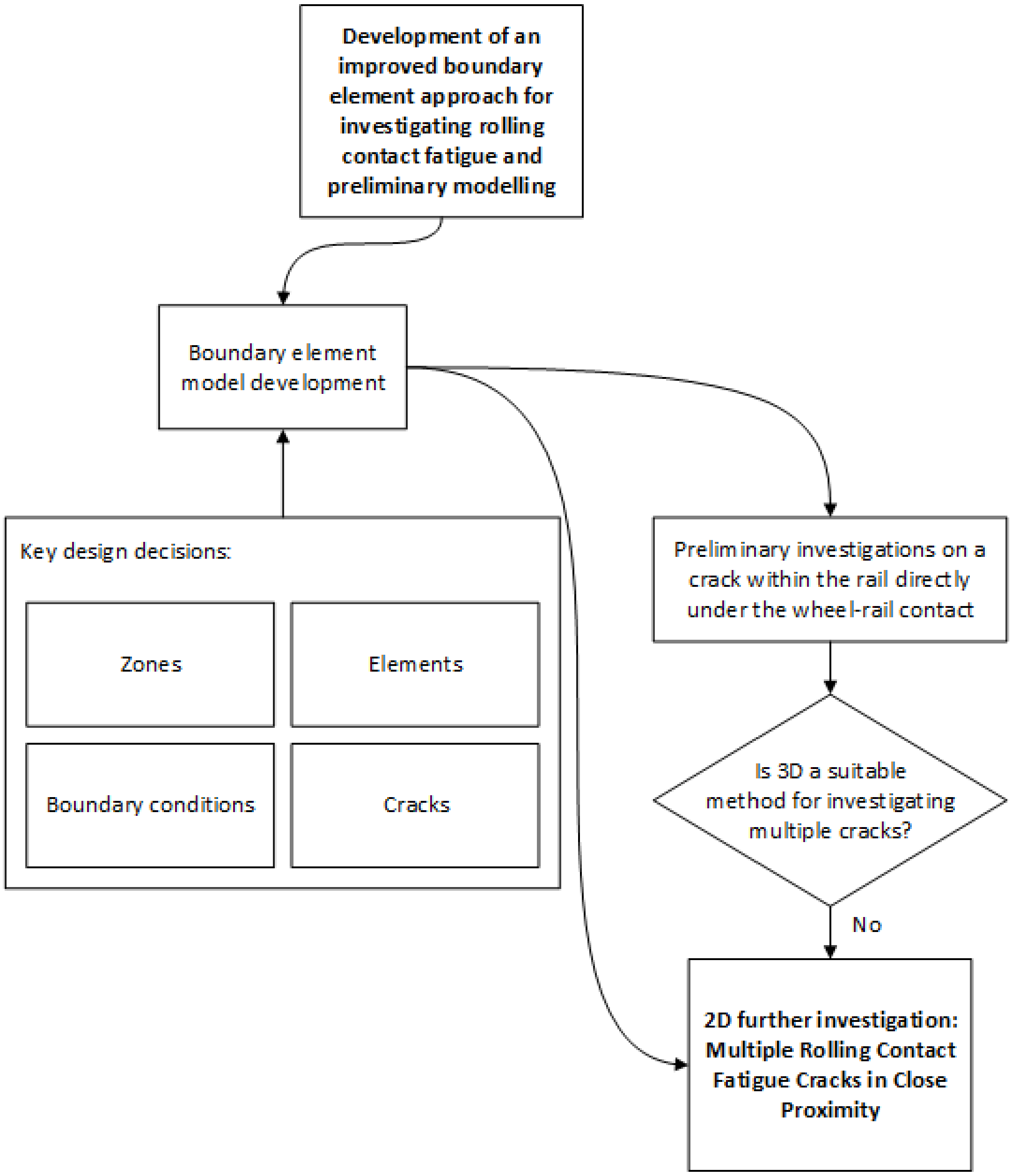

Figure 5.1: Chapter overview

The rail model (Figure 5.2a) considers a 200mm section of rail of with a 60E1 profile consistent with mainline rail used within the UK (BS EN 13674-1:2011 [176]). Grade 260 rail (the standard hardness of rail grade used within the UK [176]) is simulated using the following material properties: Youngs modulus of 210GPa and Poissons ratio 0.3. These material properties are typical values for rail steel [73, 98, 113]. This is an elastic model so more complex parameters describing plasticity are not required.

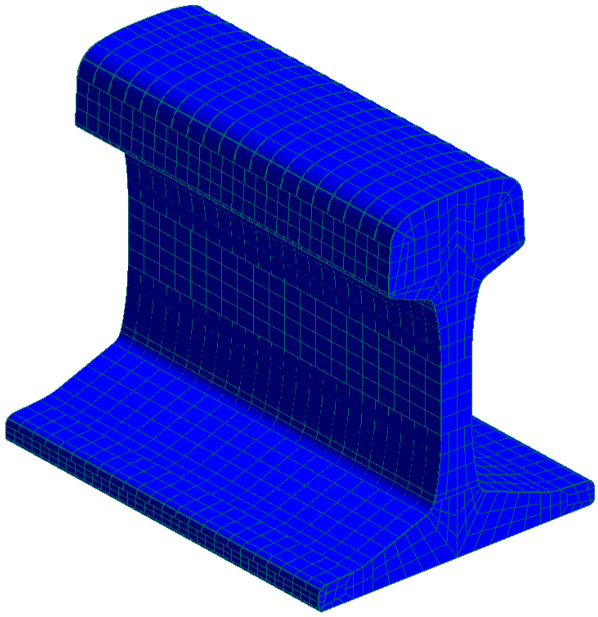

(a)

Figure 5.2: Diagram of the three dimensional model developed in this work

The BE method has been used in this Chapter (three dimensional) and in Chapter 6 (two dimensional). The model design requirements remain similar for both the two dimensional and three dimensional approaches. Therefore, for conciseness, the model design requirements are only discussed with regards to a three dimensional approach. The first part of this Chapter discusses the key design requirements of the BE method to demonstrate that the model developed as part of this thesis was capable of accurate bending stress application and crack growth prediction. The model is then validated prior to further application.

The differences between the three dimensional and two dimensional approaches for investigating RCF cracks within the rail are also discussed. A comparison has been drawn between the two dimensional approach and the three dimensional approach for a case where the two dimensional approach was predicting crack closure of the central crack.

Preliminary investigations were conducted on the application of the loading from the wheel-rail contact to the three dimensional approach. The difficulties found in this area due to the complexity of the contacting surfaces is explained, providing a good basis for potential future work.

5.2 Boundary Element or Finite Element

Both FE methods and BE methods were considered when deciding the most suitable method for the work in this thesis. Both methods have been used successfully by previous authors to model RCF crack growth within the rail (Section 2.3). Each method has advantages and disadvantages that make it more suitable for different engineering applications. Both methods utilise an element mesh to represent the geometry of the component, containing multiple nodes per element. The number of nodes is determined by the element type (Section 5.3.2). Boundary conditions and degrees of freedom of the model are defined on the nodes. A system of differential equations form the matrices that describe the relationship of stress to strain in the model which can then be solved.

With FE methods the solution is found over the entire domain, whereas for BE methods the solution is found over the model boundary, assuming elastic behaviour within the material. For the same mesh density FE methods have a shorter solution time; however FE methods require a much finer mesh than BE methods to accurately model high stress gradients, such as at a crack tip. The element mesh for FE methods also has to be continuous, which constrains the mesh grading (size of an element compared to its neighbours). On the other hand BE methods permit the use of a discontinuous mesh providing neighbouring elements adhere to size ratio constraints (Section 5.3.2). BE methods permit a greater degree of flexibility in the mesh generation stage and generally permit a coarser mesh, resulting in lower solution times in models where high stress gradients are present.

Fatigue crack growth typically occurs to or from the surface of the rail and at the crack tip high stress gradients occur. Therefore BE methods are more suitable for applications where a solution is required on the boundary of the geometry and when modelling high stress gradients. As a result a BE method has been chosen for this thesis using the modelling program BEASY [219]. In the following Sections the key aspects of BE modelling that need to be considered with respect to the specific application used in this thesis are discussed. Full details of the BE method are available within the BEASY manual documentation [219].

5.3 Development of the Boundary Element Model

The Process of developing a BE model is outlined in Figure 5.1. The design decisions that were made in this thesis are explained in Sections 5.3.1-5.3.5.

5.3.1 Zones

BE models are split into zones (Figure 5.3) to improve the aspect ratio of each section of the component being modelled and to reduce modelling times. Each zone can be treated mathematically separately, reducing the dimensions of the array describing their behaviour. As the aspect ratio of zones tends towards long and thin geometry the BE results begin to deteriorate in quality. For this reason it is recommended that the zone aspect ratio does not exceed 7:1. If the geometry of the model will exceed this aspect ratio splitting it into multiple zones will reduce the aspect ratio of each zone, increasing the quality of the results.

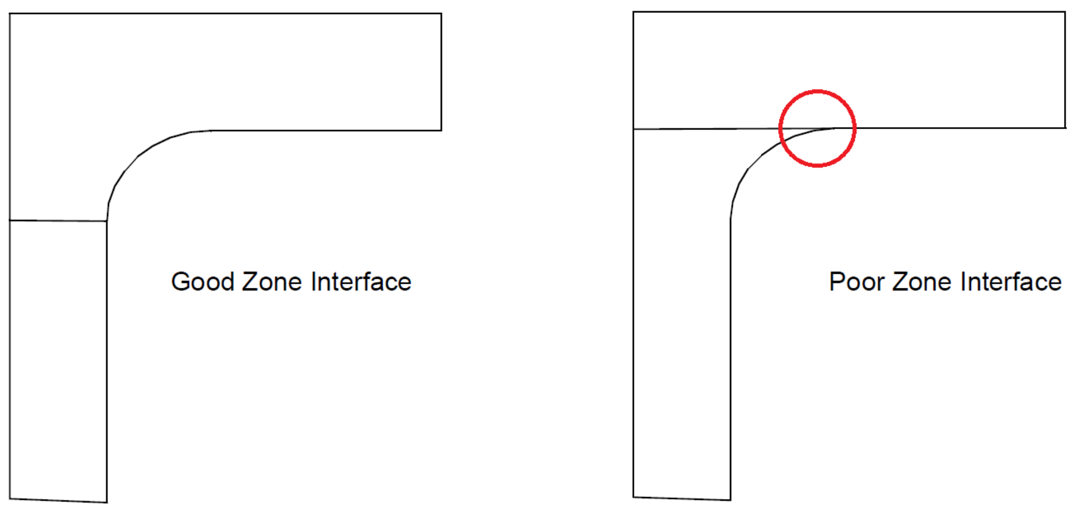

Figure 5.3: Diagram of good zone interface vs poor zone interface. Figure taken from BEASY manuals [219]

To maintain zone aspect ratio it is also undesirable to have elements back to back within the same zone where they are only separated by a thin section of material. This is not only for the model boundary but also for zone interfaces. From Figure 5.3 it can be seen that a poor zone interface location would result in back to back elements within the same zone (highlighted by the red circle). This would lead to, at least, local inaccuracies around this region with the worst case a solution failure due to the inability to solve the integration step (which calculates the influence of each node on each other node in the zone) that occurs between elements of the same zone with the BE method.

Especially for three dimensional applications, zoning is important due to the reduction in CPU time taken to analyse a problem along with significantly cutting disc storage requirements. BE matrices are formed zone by zone, resulting in a set of equations between every pair of elements within a zone that calculates the influence that each element has on the others and describes the behaviour of the zone assuming that it is isolated from the other zones. This means that the number of computer operations required for element matrix integrations for a zone is proportional to the square of the number of elements within the zone.

For example, consider a single zone model containing ten elements. The CPU time to perform the integrations for this zone is therefore one hundred units. Now, split the model into two zones, adding one interface element per zone, each zone now consists of six elements. For each zone, the CPU time is now thirty six units, making a total of seventy two units of CPU time to perform both the integrations for the two zone model, leading to a time saving of 28%.

Important aspects of the model including some boundary conditions and material properties are defined on a zone by zone basis. Boundary conditions such as body loads are defined relative to the zone upon which they act. Body loads have been used in this thesis in the form of load points, which are discussed in Section 5.3.3.2.2. Other body loads include temperature considerations. This has been used in previous work by Fletcher et al. [220] to simulate residual stress within the rail head and is therefore worth considering here to aid potential future work using the model in this thesis.

In the BEASY implementation the first zone within a BE model is required to be restrained against rigid body motion. For three dimensional stress analysis the model must be restrained against rigid movement in the x, y and z directions. The different types of restraints are discussed in more detail in Section 5.3.3.1. For this reason the first zone within the model must be positioned away from the area of interest as nearby restraints would affect the results from the model. For the research reported here the first zone has been positioned on the foot of the rail away from the position of any railhead cracks.

Figure 5.4 shows how zoning has been used along the rail section, with a zone interface between the head and web of the rail. The 200mm length of rail that has been considered here has been split into four 50mm sections. This results in an aspect ratio of 5:1 at the narrowest edge along the foot of the rail in the y direction. Across the rail section in the x direction the model has been split into two zones to keep the aspect ratio in this direction at 7:1. Vertically for the rail section in the z direction four zones have been used to ensure that the aspect ratio of the cross section remains below the 7:1 limit, with the maximum aspect ratio of 6:1 occurring in the rail web.

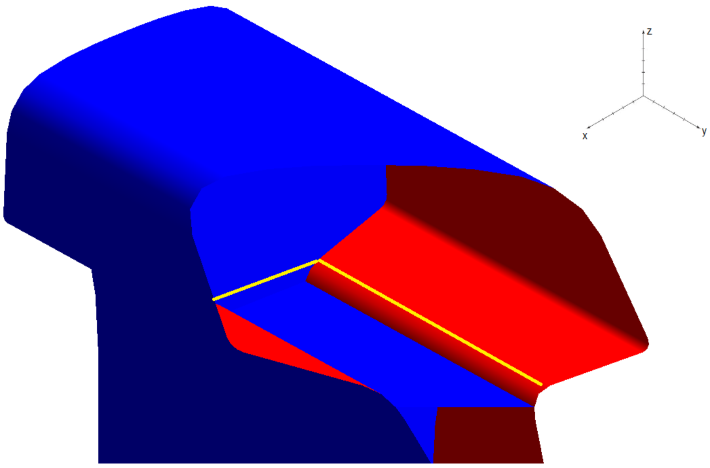

Figure 5.4: Diagram of a cutaway section from Figure 5.2a showing how zoning has been used to remove severe aspect ratios in the geometry. The blue area across the rail web shows the actual zone interface position, the yellow lines highlight the plane where a poor zone interface would have been positioned

If the zone interface in Figure 5.4 had been made along the plane of the yellow lines it would have resulted in a poor zone interface within the rail section, resulting in close back to back elements in the same zone. It can be seen in Figure 5.4 that the positioning of the zone interface within the rail section follows the guidelines for good zone interfacing.

5.3.2 Elements

For the BE method, elements are applied to the model boundary only. For two dimensional problems, elements are applied to the lines that make up the model edges. For three dimensional problems, elements are applied to surfaces (also known as patches).

The elements define the position and curvature of the surface and represent the stress behaviour of that small section of the model.

5.3.2.1 Element Type and Shape

The two element types used in this thesis were quadratic and reduced quadratic (three dimensional models only). Linear and constant elements also exist within BEASY but they are not relevant to this thesis. The element type used determines the number of nodes each element has (black dots in Figure 5.5). The number of nodes within an element dictates the stress gradient that the element can accurately model, which determines the density of the mesh required. Therefore high stress gradient areas require a quadratic mesh. Reduced quadratic elements offer the same accuracy as quadratic elements in lower stress gradient areas and have fewer nodes, reducing solution times. Here quadratic elements were used on the crack faces and reduced quadratic elements were used for the remaining parts of the three dimensional model.

Different element shapes are used to accurately create a mesh across the three dimensional model geometry. Elements can be either quadrilateral or triangular as shown in Figure 5.5. The element shape used is dependent on the best fit to the model geometry and can be either manually or automatically assigned.

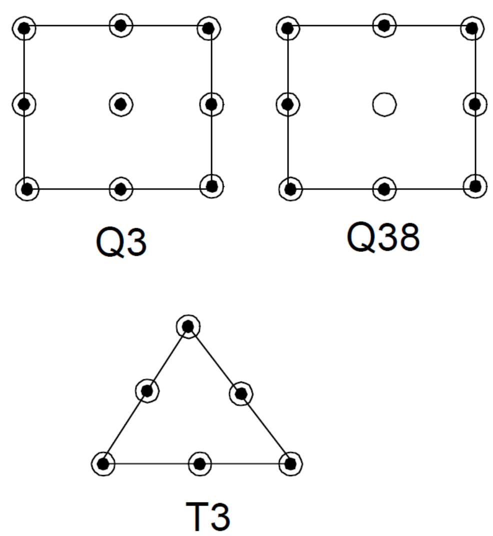

Figure 5.5: Number of nodes per element for quadratic and reduced quadratic elements for the two element shapes (quadrilateral (Q) and triangular (T)) used in the three dimensional model. Q3 & T3 - Quadratic, Q38 - reduced quadratic. Figure adapted from BEASY manuals [219]

5.3.2.2 Element Aspect Ratio

Like finite elements, the accuracy and efficiency of boundary elements decreases as their aspect ratio increases. All elements used here have an aspect ratio of less than 5:1, which was reduced to between 1:1 and 2:1 in areas of high stress gradients. Adjacent elements may differ in size but the sizing cannot be excessively different. This ensures a gradual grading of element size from small to large. For the three dimensional model developed here, the longer side of an element was no more than five times the size of the shortest side of any elements that touched it.

It is important to consider the distortion that an element will undergo under the required loading to ensure that its shape will not cause the element to have reduced accuracy. Two key factors that need to be considered are the curvature of the surface at the position of the element and the skewness of the element corners (i.e. for an irregular quadrilateral element shape). In the case of curvature it is best practice to ensure that the angle of surface curvature that the element covers does not exceed 45°. For skewness it is best practice to keep all internal angles between 45° and 135°. These guidelines were adhered to in the model developed here.

5.3.2.3 Continuous and Discontinuous Nodes

Whether nodes are continuous or discontinuous also needs consideration due to the extent to which it dictates the amount of computer resource required to solve a model. Continuous nodes are shared between neighbouring elements and therefore enforce continuity of stress and strain. Using continuous nodes results in a major reduction in the computer resource required, especially for three dimensional models.

Discontinuous nodes are useful however, especially in applications where there is discontinuity in the component such as a crack within a rail. In these cases a model containing continuous nodes would not be able to accurately simulate the highly discontinuous stress behaviour present at the crack tip. Another advantage is to aid the mesh refinement stage of mesh generation. In a continuous model, as the mesh is graded all the nodes would have to line up with the nodes in adjacent elements. This would restrict the amount of grading possible and increase the time required to generate the mesh. Discontinuous nodes make this task considerably easier as nodes are not shared between adjacent elements, removing the need for the corners to line up exactly. This allows for greater flexibility in mesh grading and saves time for the mesh generation stage.

In the model developed here continuous nodes are used where practical but are not used to dictate the mesh at key locations such as the crack faces and zone interfaces. At these locations a continuous mesh would have restricted the amount of grading possible, increasing the time required to generate the mesh and solution times.

5.3.2.4 Mesh Refinement

Mesh refinement was most critical around the cracks. Figure 5.6 shows a fine and coarse mesh on the crack face. As part of the mesh refinement process different mesh densities were used. A validation of solution independence was done to ensure that the solution was independent of the mesh density. In the final model, to keep modelling times to a minimum, the mesh density varied throughout the model, with higher density used around the cracks in the rail head and lower density used in the rail web and foot.

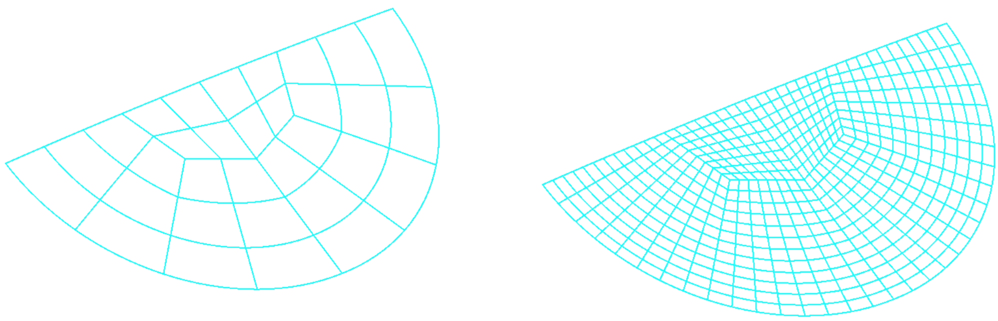

(a) (b)

Figure 5.6: Diagram of the crack mesh, (a), coarse, (b), fine

5.3.3 Boundary Conditions

5.3.3.1 Model Restraint

To prevent rigid body motion of the model the first zone was restrained so that it was not free to move in any direction. For stress analysis this can be done using either or a mixture of displacement or spring boundary conditions. A zero displacement boundary condition was used in this thesis as it provides the best restraint; however it tends to generate localised high stresses around the restraint so care was taken to ensure that this was positioned away from the area of interest (i.e. positioned on the rail foot). It is important to ensure that the model is not over-restrained as this may affect the results in the area of interest (i.e. the railhead).

5.3.3.2 Load Application

In this Section the two methods to apply loading to the model, patch loading (Figure 5.7a) and load points (Figure 5.7b), are discussed with the advantages and disadvantages of each method. Both these methods are normally manually applied to the model. However, for the work in this thesis, the load was required to be easily and rapidly altered to explore a range of loading conditions. Therefore, a technique was developed to automatically apply either load application method to the model, the full details of which can be found in Appendix D. This greatly accelerated the modelling process.

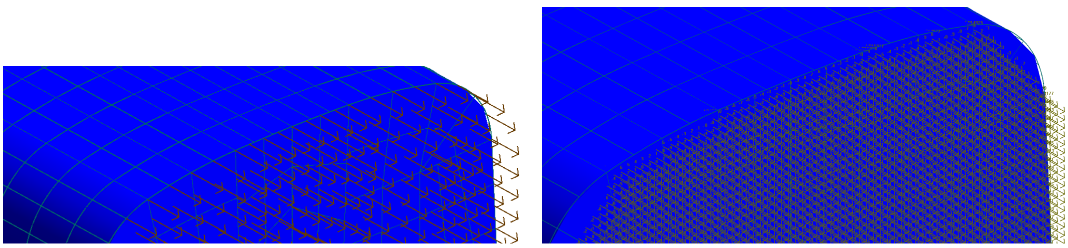

(a) (b)

Figure 5.7: Diagram showing the two types of load application methods within BEASY, (a), patch loading, (b), load points

Where application of a rail bending moment was required, the shear stress distribution that the bending moment would generate was calculated. For the case of patch loading this was then directly applied to the rail cross-section. For the load point case, the force required at each point was calculated from the stress distribution assuming each point acted over a small square area of the cross-section (Figure 5.7b).

In the initial work for this thesis the load point application method was used due to the ease of automating its application to the model. However, it was found, and it is useful to note for further work, that the load point application method took longer to solve and was incompatible with the body loads within BEASY. Therefore, the patch loading application method was implemented in later models in this thesis.

5.3.3.2.1 Patch Loading

Patch loading (Figure 5.7a) is the more straightforward of the two methods to apply manually, with the loading being applied as a stress directly to each node on the element. A constant, linearly varying or spline approach can be used to generate the desired loading. However, considerable difficulty was encountered when developing the script to automatically apply the loading (Appendix D.1), due to the way that BEASY assigns the loading to each element. The order of load application is defined in the same order as the nodes within the element. Nodes are defined anticlockwise round the element, but the start point is not the same for each element and not all elements have the same number of nodes. This means that, in order to calculate the stress at each node, the x, y, z position of each node had to be found, which required significant back calculation from the model data file.

5.3.3.2.2 Load Points

For load points (Figure 5.7b) entering all of the data manually would be extremely time consuming and repetitive. However, the development of the script to automatically apply load points was straight forward in comparison to patch loading (Appendix D.2). An x, y, z position of each load point was iteratively defined at the desired positions. The force applied at each point was calculated from the stress required at that position over the area the point is assumed to act, as defined by the spacing of the load points.

For example, for the spacing of 1mm in Table 5.1 the first row of load points was defined at a height of 0.5mm from the base of the rail model, with each subsequent row 1mm above the previous one. Load points on the same row were also spaced 1mm apart, with the position of the first and last point within a row calculated from the model's width at that row's height (easily found within the data file). For the 1mm spacing this would be approximately 0.5mm from the edge of the model. This results in each load point being located at the centre of a 1mm area where the force applied to a specific load point will generate the required stress over a 1mm^2 area of the model.

Load point spacing (mm)	Area applied force acts upon (mm^2)	Load points required	Reduction in desired stress at crack position (%)	Ratio between stress at load points and stress at crack position
8	64	236	12	11.6
4	16	952	1	3.8
2	4	3684	3	1.6
1	1	15040	3	1.4
0.5	0.25	60584	3	1.4

Table 5.1: Number of Load Points required depending on spacing

When the extremity of the model is curved the area that the force is applied to is no longer equivalent to the assumed 1mm^2 area. Therefore, care was taken to avoid introducing inaccuracy from the loading on the model, primarily by using a larger number of more closely spaced load points (Table 5.1).

The position of a load point cannot be the same as an element node. Therefore, to avoid the incompatibility between node and load point positions, all load points were offset from the surface and positioned 1mm inside the material. This also applied to zone interfaces.

Several load point spacings were considered. As shown in Table 5.1 a load point spacing of 8mm or 4mm was too coarse, generating inaccuracies at the model extremities. For the 8mm spacing case the coarse load point spacing also resulted in a reduced stress at the crack location when compared to the desired stress. Therefore, the maximum load point spacing that maintains accuracy within the model is 2mm. Increasing the number of load points did not increase the solution time of the model therefore a load point spacing of 1mm was applied in the model as locally increased stresses induced by the load points were reduced in comparison to the 2mm spacing and the overall accuracy was the same. The 0.5mm spacing offered no benefits over 1mm spacing in terms of increasing model accuracy but took eight times as long to generate the load point locations and applied forces.

5.3.4 Modelling Contacting Components

BEASY supports modelling either conforming or non-conforming contact. In conforming contact the two contacting objects have very similar profiles over the contact area.

Further details about how the two contact methods are implemented to model contact can be found in the BEASY manuals [219]. Non-conforming contact involves two contacting objects that have different profiles over the contact area and touch over a small region. This is applicable in scenarios such as a wheel on rail contact. The level of friction can be altered depending upon the surfaces in contact. For the case of the wheel-rail contact in this work the contact pair is shown in Figure 5.8.

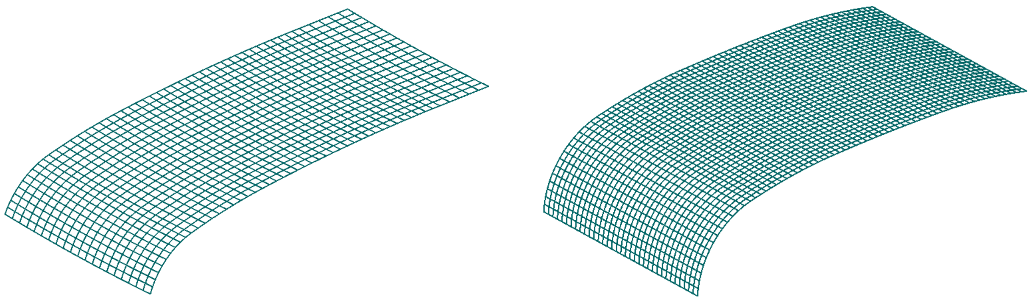

(a) (b)

Figure 5.8: Diagram showing the elements in the wheel and rail contact pair, (a), wheel contact elements, (b), rail contact elements

5.3.5 Inserting Cracks into the Boundary Element Model

Within BEASY cracks are normally added using the standard tool [219]. Using this tool the crack simulation data is defined. Before the solution phase this is integrated into the model. However, for the rail geometry, it was found that this method did not produce a suitable mesh once the crack angle was less than 35° to the rail surface (Figure 5.9). This was due to poor mesh generation at the crack-free surface interface. Further testing demonstrated that this technique did work for crack angles of less than 35° to the surface in two dimensions and in three dimensions for simple geometries. However, for the complex rail geometry the standard tool was unable to produce an accurate mesh. This was problematic as RCF type defects tend to occur at an angle of less than 30° to the rail surface. An alternative method for adding shallow angle cracks into the model was therefore developed (Section 5.3.5.1).

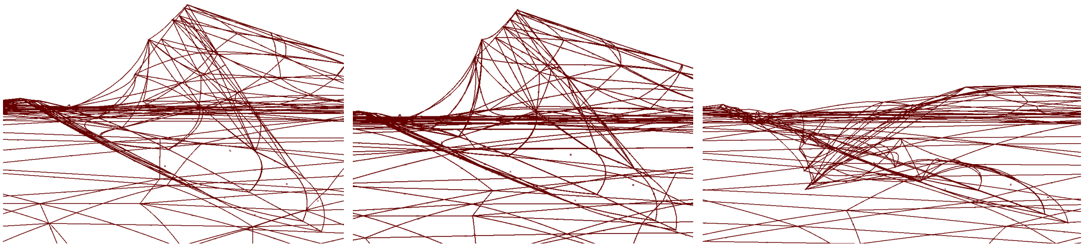

(a) (b) (c)

Figure 5.9: Diagram of the deformed shape of the crack-base model interface, scale 1:5000, crack angle to the rail surface, (a), 40°, (b), 35°, (c), 30°

5.3.5.1 Development of a Method to Explicitly Model the Crack

Manual addition of cracks to the model was an alternative method for adding shallow angle cracks into the model. As the mesh was defined explicitly on the crack and model surfaces it overcame the issues of poor mesh generation inherent in the standard tool. Results reported in this thesis used this method to create a single layer of elements to define the crack surfaces within the model. The crack surfaces can either be added directly into the model or generated separately and then imported into the model (Appendix E).

Difficulties were found when the explicitly defined crack faces experienced crack closure. The default crack type is “load free”, which means that contact isn’t simulated between the crack faces. This is a valid assumption when the crack is in tension and simplifies the modelling process. However, cracks in rails are frequently closed and to incorporate contact between the crack faces, the data file required manual alteration (Appendix E).

The explicit modelling method is less flexible than the standard tool as the mesh for each size and angle of crack studied had to be developed individually. Once the crack mesh had been successfully integrated with the normal boundary mesh the properties of each crack were then defined individually within the model. This limited the different number of cracks that could be studied as this process had to be repeated for each crack in the study. Using this method an accurate mesh at the crack-base model interface for cracks at an angle of 30° to the surface was developed. A comparison between this approach and conventional crack modelling techniques has been shown in Section 5.4.

5.3.5.2 Consideration of Crack Face Friction

For cracks where the main method of growth is mode I, it is not essential to model crack face interaction or crack closure as modelling a load free crack reduces complexity. However, this is an unrealistic condition for actual cracks under compressive load. Therefore, as the wheel contact on the rail induces compressive stresses on the crack faces, the crack face friction has to be considered. As shown in the literature review (Section 2.3.2) the actual value of crack face friction is difficult to determine. Therefore, in line with previous work, it was decided to keep crack face friction consistent with surface friction. A value of crack face friction of 0.3 was chosen for this work based on previous studies (Section 2.3.2.1).

5.4 Three Dimensional Model Validation

5.4.1 Comparison of Load Application Methods Against Previous Work

The three dimensional BE model was validated against previous work by Fletcher et al. [125]. The comparison runs were undertaken for a single crack at various angles (Figure 5.10) and for multiple cracks at 30° to the rail surface (Figure 5.11). Variance between the patch load method (Section 5.3.3.2.1) and the load point method (Section 5.3.3.2.2) is shown. Load points were spaced at 1mm with the force applied to each load point assumed to act over a square area defined by the load point spacing, as discussed in Section 5.3.3.2.2. The applied bending moment was 4000Nm to allow for a direct comparison to the previous study by Fletcher et al. [125].

As shown in Figures 5.10 and 5.11 the current approach compares well with the previous approach with no significant difference in the stress intensity factor along the crack front between the current approach and previous work, particularly for 3 cracks. No significant difference was found between the load application methods used in the current approach.

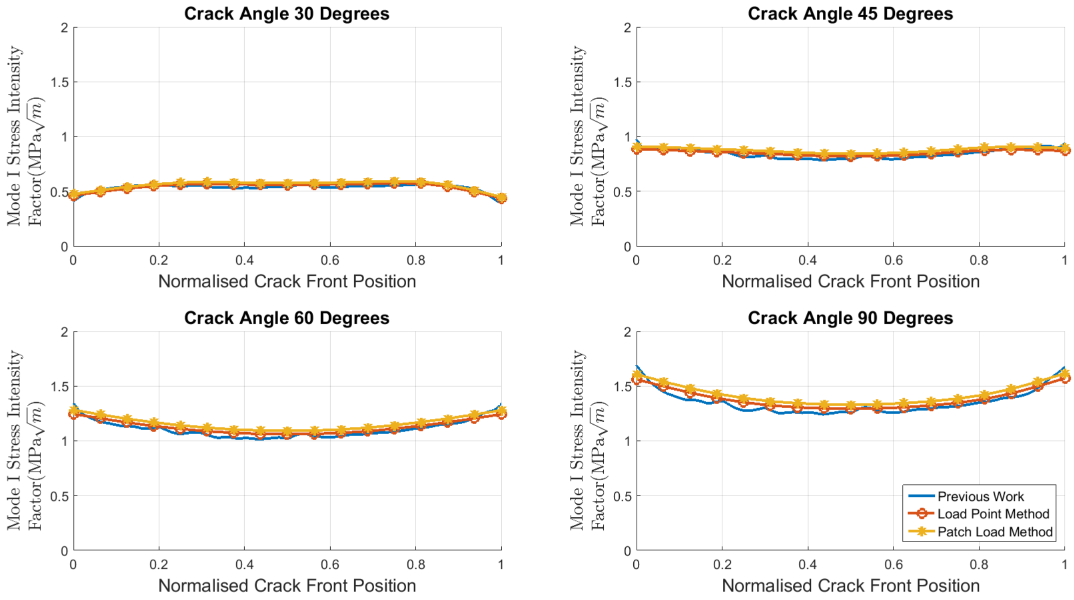

(a)

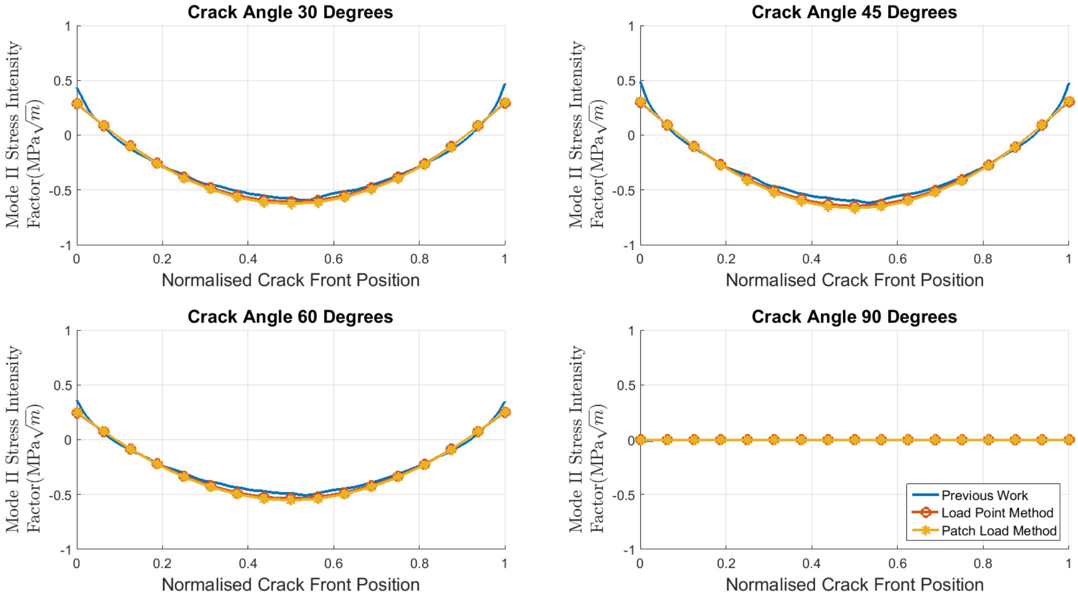

(b)

Figure 5.10: Stress intensity factor results of a single 10mm semi-elliptical crack at different angles to the rail surface. Comparison of previous work by Fletcher et al. [125] and the current method using the two different load application techniques. (a), mode I, (b), mode II

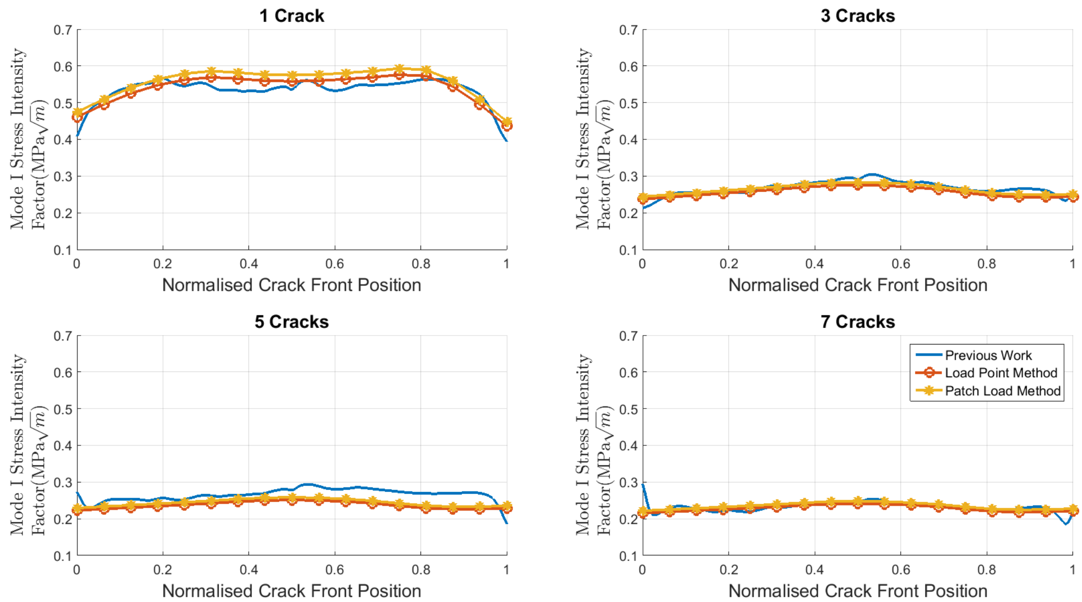

(a)

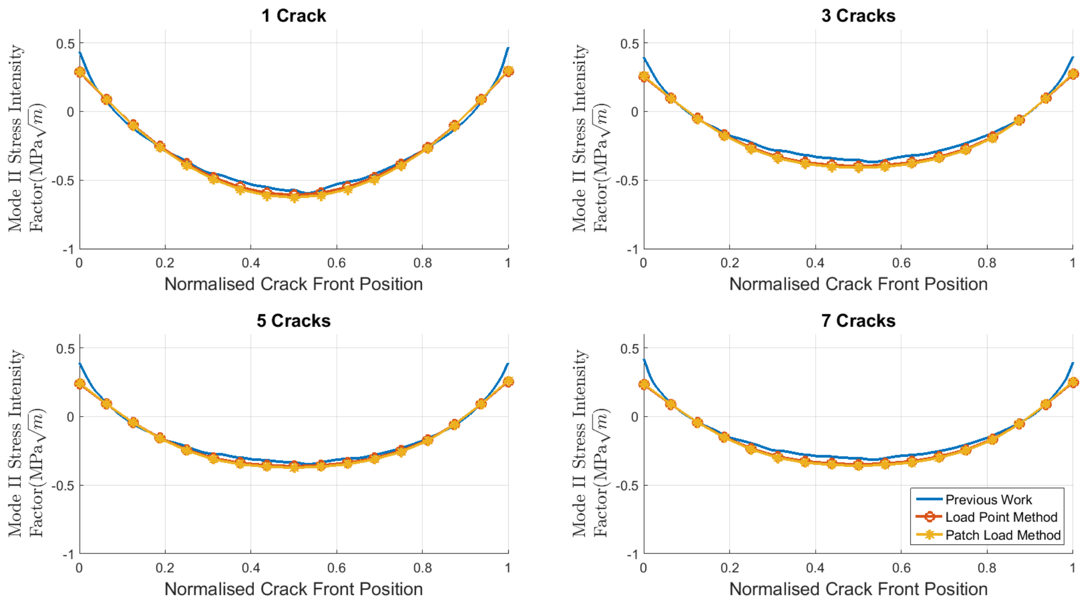

(b)

Figure 5.11: Stress intensity factor results from the central crack of 10mm semi-elliptical cracks at 30° to the rail surface. Comparison of previous work by Fletcher et al. [125] and the current method using the two different load application techniques. (a), mode I, (b), mode II

Lower variance was found across the crack face with the current approach for all crack angles and numbers, demonstrating improved model stability. The maximum difference seen was for the mode I stress intensity factor for the five crack configuration where, at the normalised crack front position of 0.5 a small peak in the stress intensity value was observed in the previous study. For this case a 10% difference between the previous study by Fletcher et al. [125] and the model developed in this thesis was observed. However, for the majority of the crack front the difference is much smaller. Therefore both the patch load and load point load application methods used in the current work are shown to be valid when modelling multiple cracks in close proximity at a variety of angles. Increasing the number of cracks within the rail from one to three identical cracks was found to reduce the SIF found at the crack front of the central crack by 50%.

5.4.2 Comparison Between Loading the Rail in Tension or Bending

Within the approach developed in Chapter 6 near rail surface stress due to bending may be approximated by application of a tensile stress. In this Section the SIF for 10mm semi-elliptical cracks at 30° to the rail surface under the tensile loading and bending moment loading methods are compared. As can be seen in Figure 5.12 both the mode I and mode II SIF at the crack tip of 10mm semi-elliptical cracks under both loading methods are almost identical for all numbers of cracks considered. The loading method has no effect on the results for 10mm semi-elliptical cracks.

This means that the effects of a bending moment can be approximated using tensile loading condition for cracks that have propagated to a depth of 5mm into the railhead (borderline between moderate and severe RCF (defined in Section 2.3)). Assuming this applies in both two dimensional and three dimensional models, the two dimensional results in Chapter 6 can therefore be directly compared with those from the three dimensional approach that used a bending moment loading method.

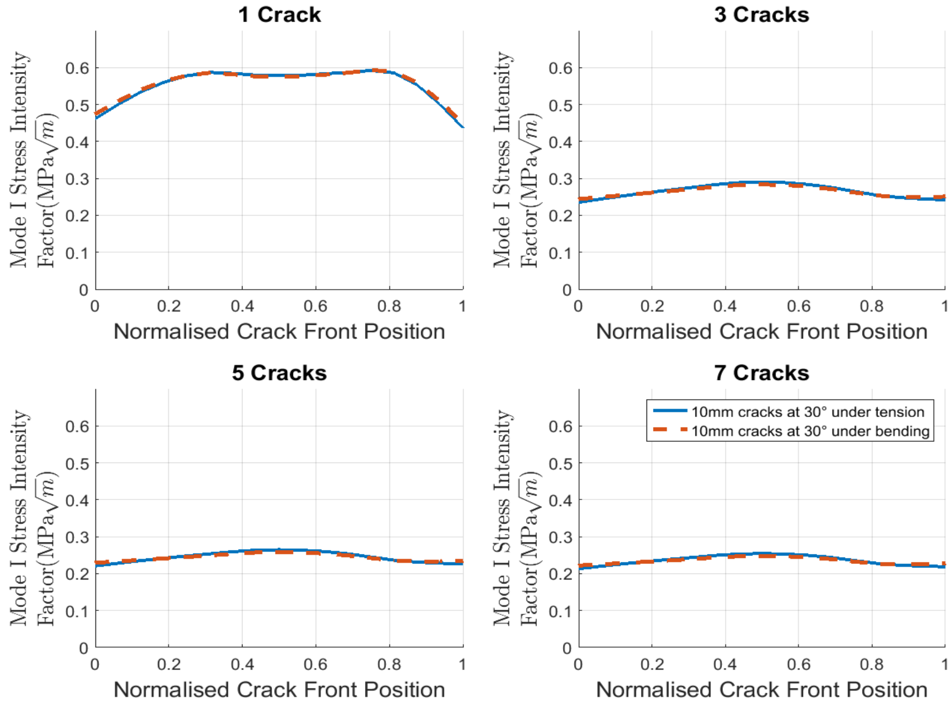

(a)

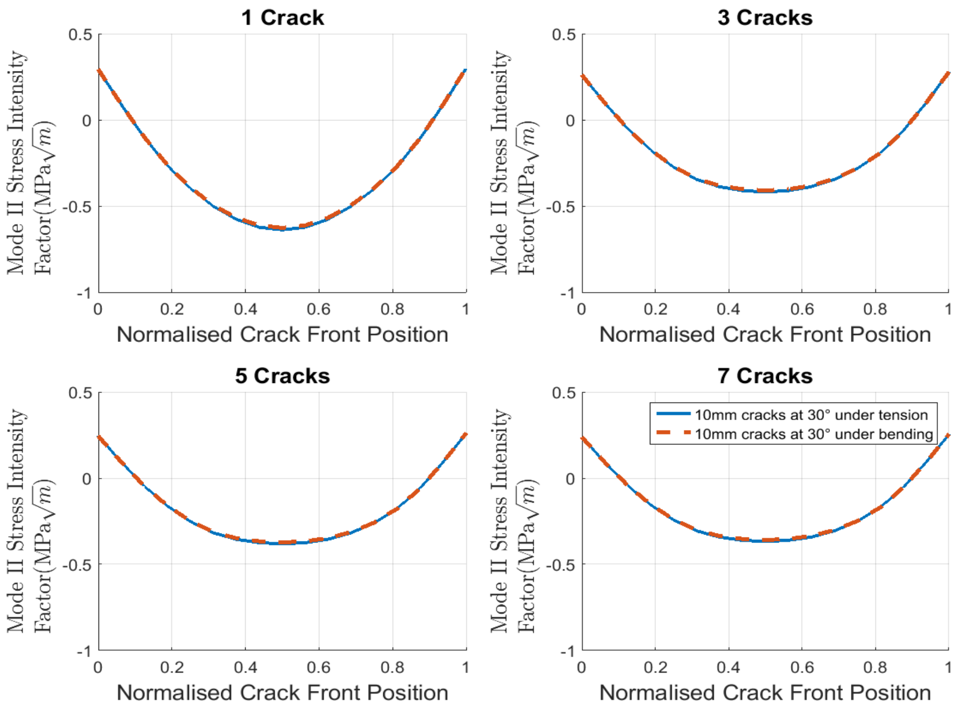

(b)

Figure 5.12: Stress intensity factor of the central crack of 10mm semi-elliptical cracks at 30° to the rail surface under a bending moment and the equivalent tensile stress as calculated from the bending moment at the railhead surface. (a), mode I, (b), mode II

5.5 Representing Wheel-Rail Contact Loads

The next phase in the development of the three dimensional model was to investigate the sensitivity of the results to the accuracy of the pressure distribution representing the wheel-rail contact.

5.5.1 Pressure Distribution of the Wheel-Rail Contact

The BE method is efficient at modelling contacting components. By using a three dimensional approach it was planned to make use of this efficiency, investigating the contact pressures generated from the vertical wheel load at various wheel positions across the railhead. The tractive effort from the wheel could not be considered directly within this approach as the model had to be restrained against rigid body motion. The tractive effort was therefore to be applied to the generated pressure distribution, assuming full slip conditions with a friction coefficient of 0.3 (Section 2.2.4.3). The contact model (Figure 5.13a) used the common P8 wheel profile and a 60E1 rail profile. The wheel load is that from a class 390 high speed passenger train (properties defined in Table 4.1).

The complex nature of modelling the non-conforming contact (Section 5.3.4) in three dimensions became apparent during this research. The contact model proved to take too long to solve, in part due to its large size. As a result the solution process took an excessive amount of time to run. To overcome this, the model was reduced in size (Figure 5.13b) to reduce solution times. In the reduced size contact model (Figure 5.13b) all but the contacting zones from the model were removed. This greatly reduced the size of the model and the solution time. Figure 5.13c shows the pressure distribution found with the reduced model approach. However, even with the reduced model, the solution times were still excessive. The above model was without a crack within the rail; the inclusion of a crack would have further increased the complexity in the model and hence solution times. It was therefore decided not to pursue this method of crack loading and to investigate whether the Hertzian profile approximation of the contact patch was valid in this scenario. This assumes that the contact pressure distribution is independent of the presence of a crack, which is investigated in Section 5.5.2.

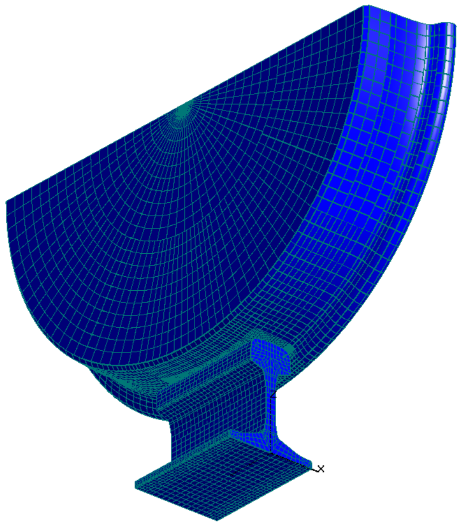

(a)

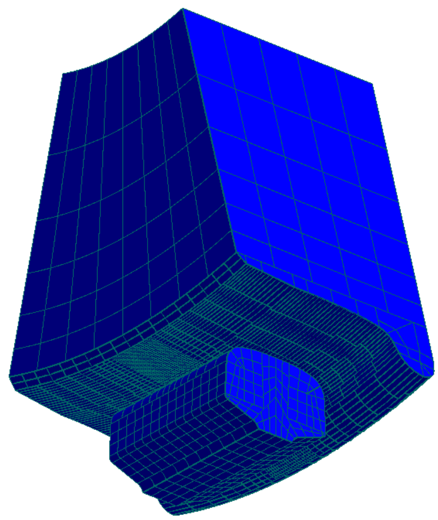

(b)

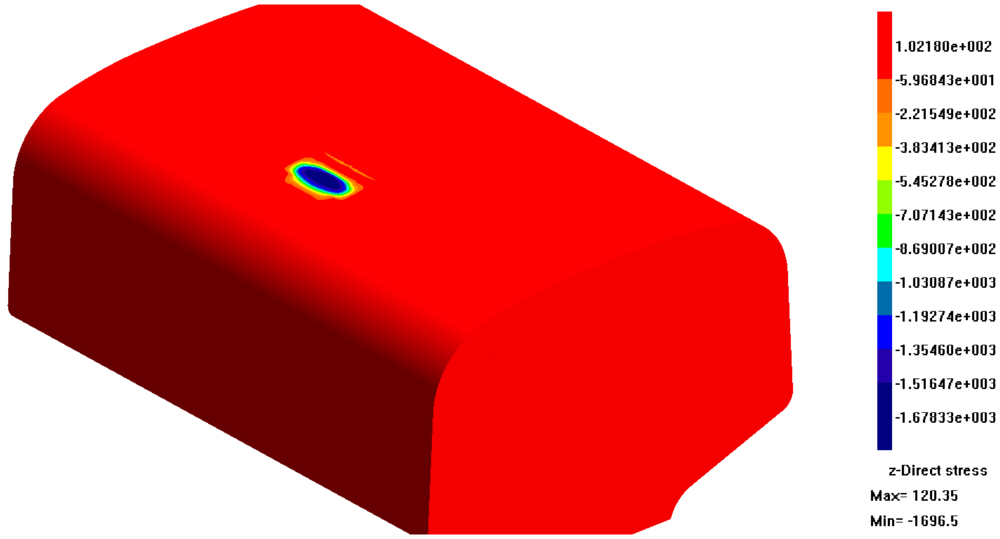

(c)

Figure 5.13: Diagram of the wheel on rail contact model used to generate an actual pressure distribution between a wheel with a P8 profile and a rail with a 60E1 profile. (a), Full model, (b), reduced model, (c), pressure distribution found using reduced model

5.5.2 Wheel-Rail Contact Pressure Distribution over a Crack within the Rail

Given the excessive solution time of three dimensional models, a simple two dimensional wheel-rail contact model (Figure 5.14) was used to explore how the contact pressure exerted by the wheel is affected by a crack within the rail directly beneath the centre of the contact (crack position at 20mm in Figure 5.15a). The wheel-rail contact model consisted of a 500mm radius wheel under a typical wheel load of 4.5 tonnes. A crack at 30° to the rail surface was inserted with the crack lengths shown in Table 5.2.

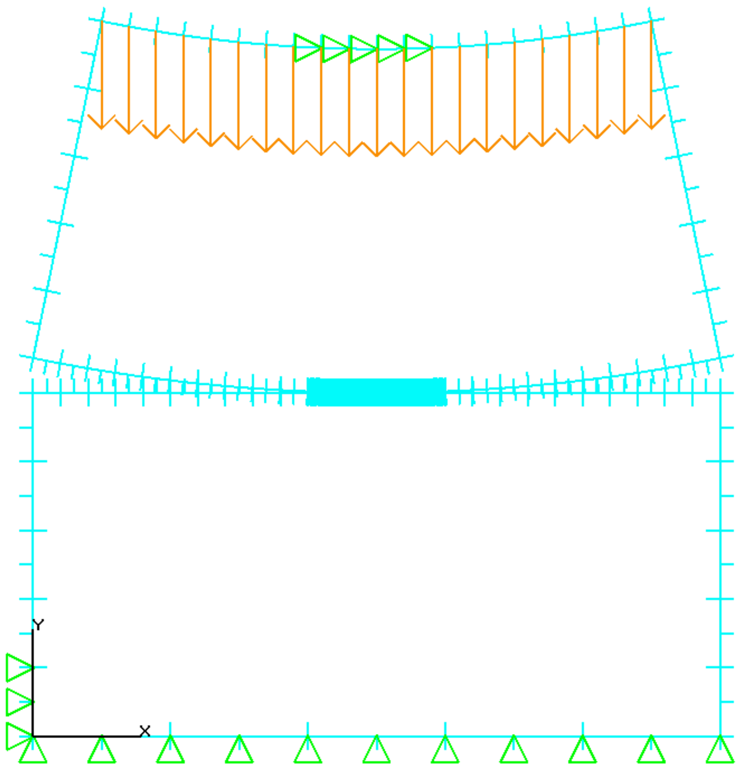

Figure 5.14: Diagram of the simple 2D contact model used to explore how the contact pressure exerted by the wheel is affected by a crack within the rail directly beneath the centre of the contact

The results in Figure 5.15a show that the presence of a crack within the rail has a small local effect on the pressure profile exerted by the wheel upon the rail, but that this is not significant. As an example, for the worst case investigated of a wheel-rail contact over a 10mm crack the maximum percentage difference of the pressure profile from the un-cracked wheel-rail contact solution (equivalent to the Hertzian solution) was 3.2%. However, this is only over a small area, with the majority of the 10mm crack solution equal to the un-cracked solution. This is illustrated in Figure 5.15a and zoomed in view in Figure 5.15b. This validated the assumption that the contact pressure distribution is independent of the presence of a crack and demonstrates that the Hertzian profile is still a good approximation to the exact pressure profile over a cracked rail.

Crack Length (mm)	2	4	6	8	10
Maximum difference in the pressure profile between the un-cracked and cracked rail (%)	0.6	1.0	1.9	2.4	3.2

Table 5.2: Crack lengths considered and the maximum percentage difference in the pressure profile between the un-cracked and cracked rail

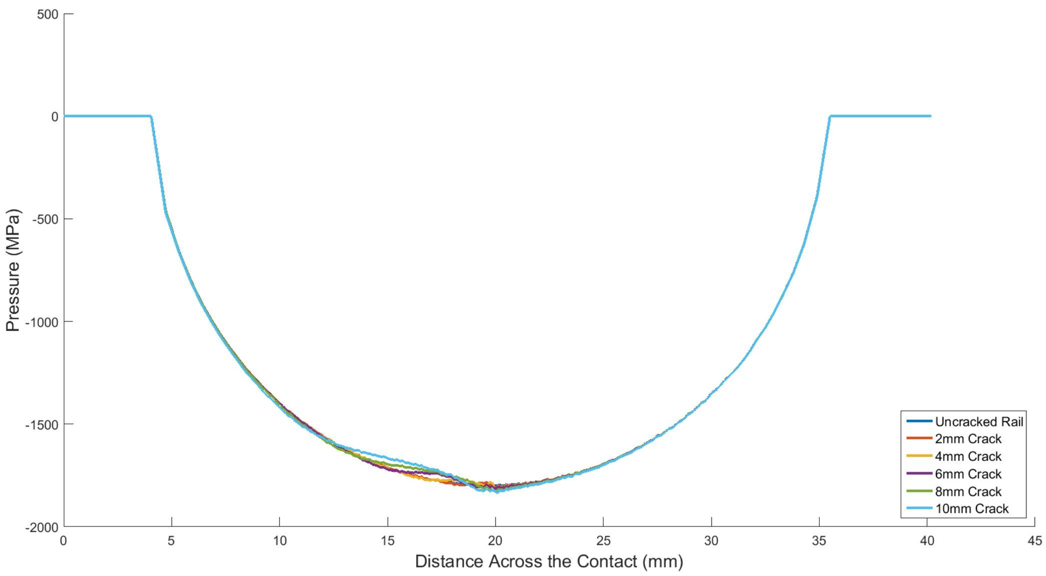

(a)

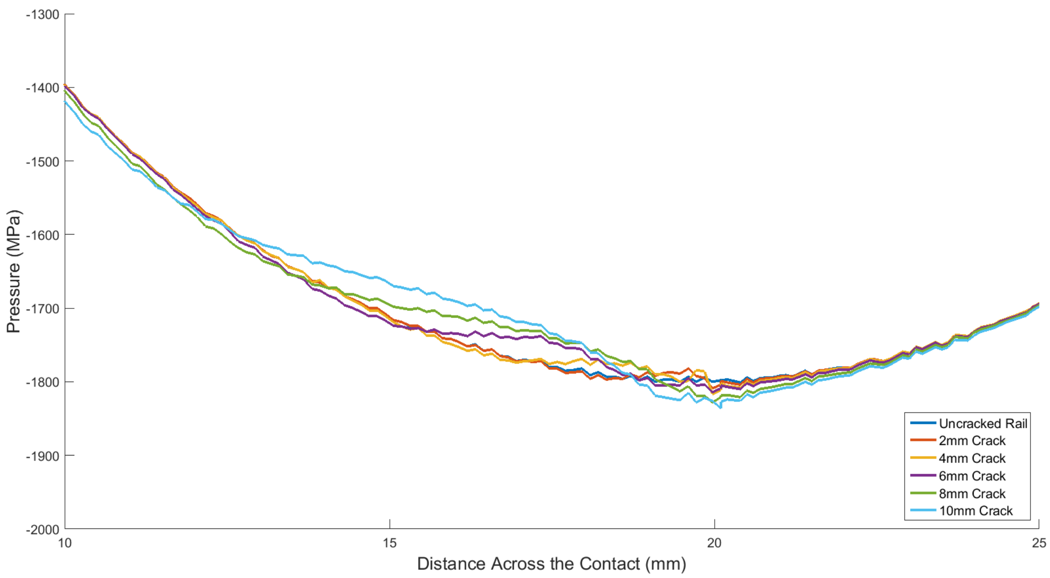

(b)

Figure 5.15: Effect of a crack in the rail on the wheel-rail contact pressure profile solution. (a), the full pressure profile results, (b), zoomed in results

5.5.3 Approximating the Wheel-Rail Contact using a Three Dimensional Hertzian Pressure Distribution

The ability to approximate the wheel contact with a Hertzian pressure profile over a cracked rail removed the need to model the complex non-conforming contact loading. As a result large time savings in modelling time were made and the issues encountered in Section 5.5.1 were avoided. The vertical loading to achieve the required contact pressure was calculated from Fischer et al. [64]. The tractive effort from the wheel was considered assuming full slip conditions with a friction coefficient of 0.3. The calculation method to apply the tractive effort under full slip conditions is explained in Section 2.2.4.3. The Hertzian pressure distributions found here are used in Section 5.5.4 to apply the approximate wheel-rail contact pressure to the three dimensional RCF crack model.

The contact load was calculated from Table 4.1. The rolling radius of the wheel (R_{11}) of the class 390 used in this work is 460mm and the radius of the rail in the longitudinal direction (R_{21}) was assumed to be infinite. The remaining radii are shown in Table 5.3 and were calculated using the initial contact positions from Yan et al. [12] shown in Figure 5.16. These radii were then used to calculate the Hertzian pressure profile at contact positions $a - c$. With the flange contact at contact position d, previous research has shown that the Hertzian assumption reduces in validity [5]. This contact position would only occur at severe track curvatures where severe wear would be expected. Rolling contact fatigue more commonly occurs on mild track curvatures with less wear and therefore only contact positions $a - c$ are relevant to the current work and contact position d is not considered.

Contact position	R_{12}(mm)	R_{22}(mm)
a	-330	300
b	-330	80
c	-100	80
d	-13	13

Table 5.3: Radii of the wheel and rail at the contact positions in Figure 5.16

The Hertzian pressure profiles at the three contact positions considered ($a - c$) are shown in Figure 5.17. The maximum contact pressure at contact position a is the lowest because the pressure is spread over the largest contact area. This is because of the near conformal contact generated by the similar radii of the surfaces at contact position a. The greatest contact pressure is experienced at contact position b. At this contact position the tread of the wheel contacts with the rail shoulder, leading to the least conforming contact and therefore the smallest contact area. At contact position c the wheel profile has an increased radius of curvature to aid cornering. Therefore the contact area at position c is increased in comparison to contact position b, leading to reduced peak contact pressure. The pressure profile that has been found at contact position b has been used to represent the wheel load as it is the most severe case and represents mild curves most relevant for RCF.

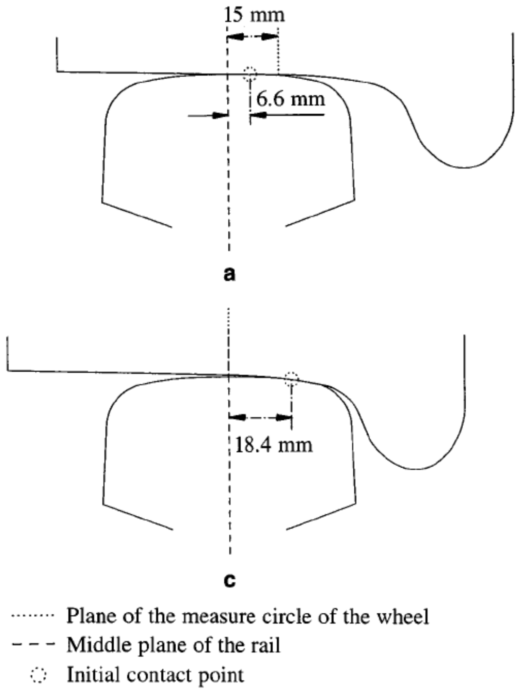

Figure 5.16: Diagram of the wheel-rail contact showing the initial contact position between the wheel and rail at across the rail head. Figure taken from Yan et al. [12]

5.5.4 A Single Crack under a Hertzian Pressure Distribution Approximated Wheel Load – Preliminary Results

The wheel load was applied to the crack model using the process outlined in Appendix D. The alterations that were made to the manually added crack to account for loading on the crack faces are outlined in Appendix E. In this Section the results from the passage of a wheel across the crack from the current method are compared to previous work.

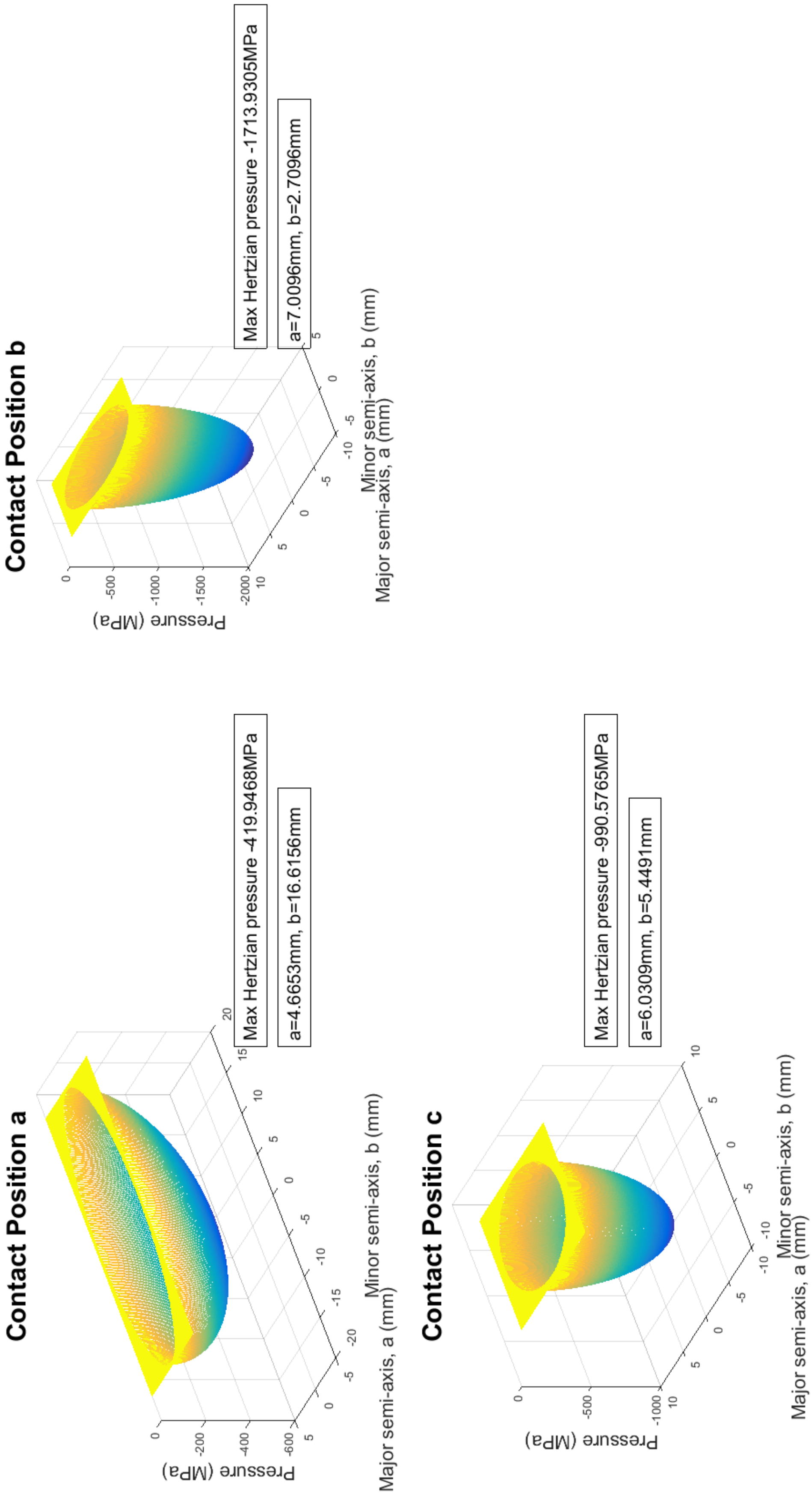

Figure 5.17: Hertzian pressure profiles at the contact positions a, b, and c

In Figure 5.18 it can be seen that the mode I SIF predicted by the current method has a similar peak to the previous work but does not fully agree in wheel position (Figure 5.19a). In the current method a slightly lower mode I SIF is predicted than found previously, with the peak at the contact position -6mm and not at -3mm. The reasons behind this difference are not understood at this point. It is thought to be most likely due to surface contact within the crack when using manually added cracks.

The mode II SIF that drives most of the crack growth for RCF cracks is in good agreement with previous work (0.3 surface friction curve in Figure 5.19b). The shape of the curve is similar although the current method is predicting a lower peak SIF of 11MPa$\sqrt{}$m in comparison to the 14MPa$\sqrt{}$m found in previous work. Agreement for mode II SIF is the most important factor for good predictions of crack growth rate within the rail. This is clearly shown here as the lower peak mode II SIF using the current method of 3MPa$\sqrt{}$m leads to a crack growth rate prediction of half that found in previous work. Further work is required to improve the current approach as these results demonstrate that there are as yet unresolved issues with the current method.

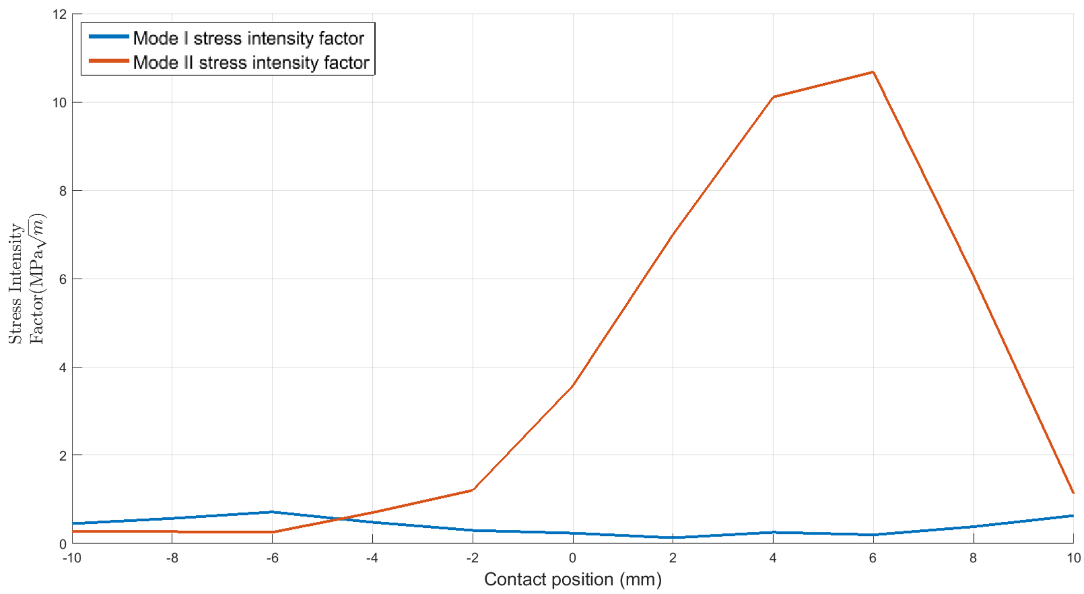

Figure 5.18: The current method under a Hertzian pressure distribution, using surface friction coefficient of 0.3. The elliptical contact patch is the same as used in Smith [32] with: a=5.92mm, b=3.94mm, crack face friction=0.3 and P_0=1750MPa to allow direct comparison to the previous work (Figure 5.19)

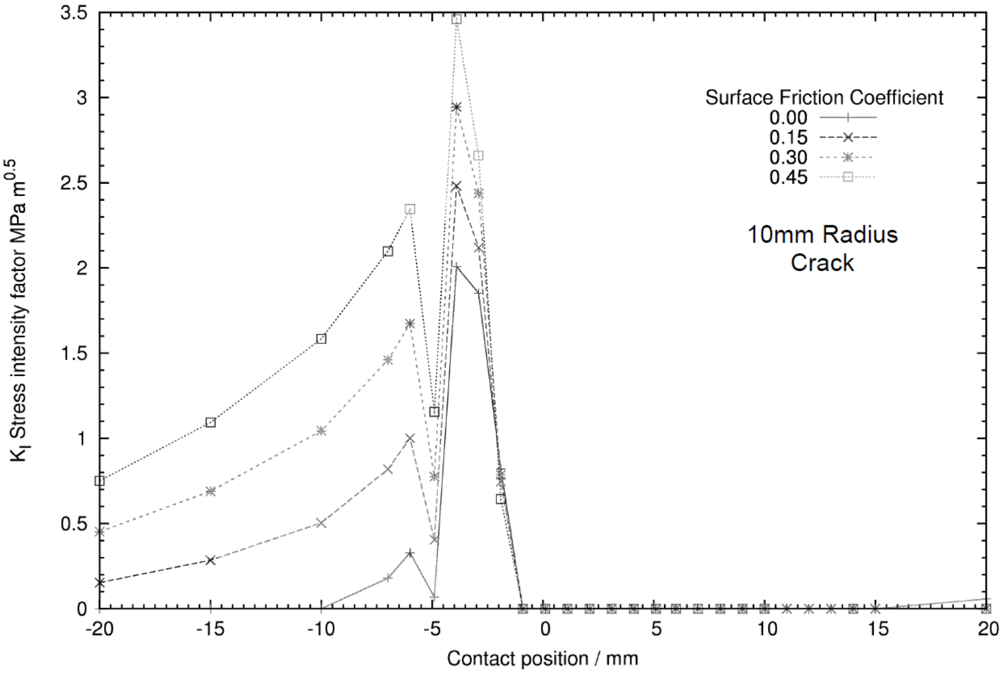

(a)

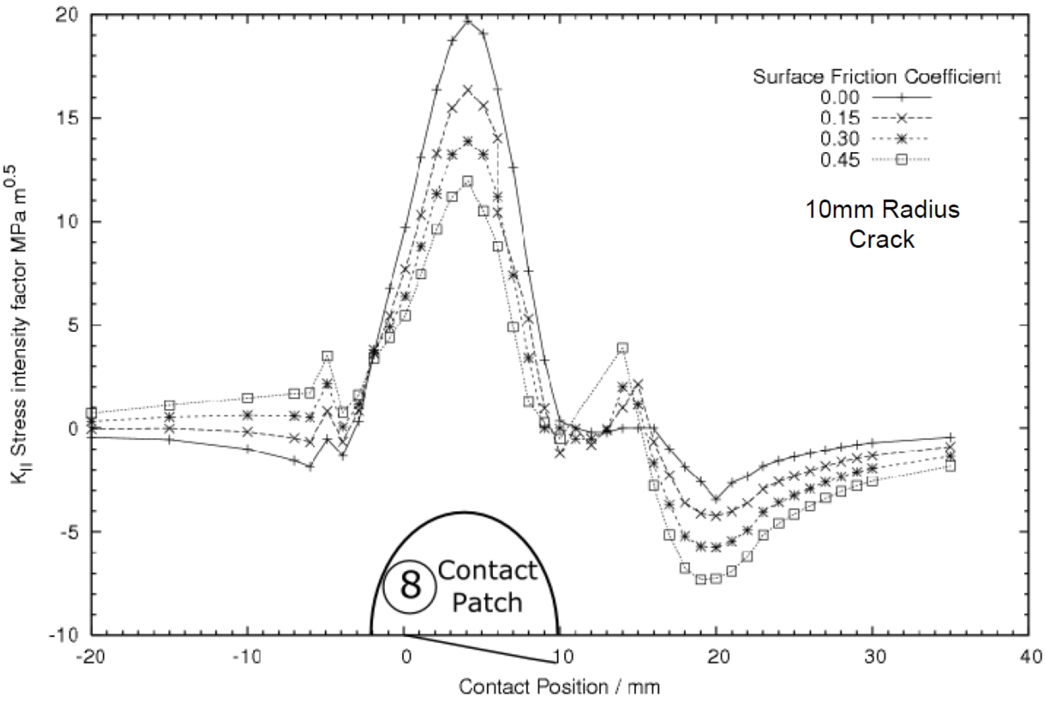

(b)

Figure 5.19: Previous work by Smith [32] for comparison between the mode I and mode II stress intensity factor of a single crack under a wheel load with Figure 5.18

5.6 Conclusions

In this Chapter the work undertaken to develop the three dimensional BE method has been discussed. The method was validated against previous work and shown to be independent of the mesh density used. The development of scripts as part of this work accelerated model creation through automated load application. No significant difference was found between the two load application methods (patch loading and load points) used in this thesis. However, it is useful to note for further work that the load point application method was incompatible with the body load functionality within BEASY.

Some difficulties were encountered with the integration of the crack into the model for shallow angle cracks, with inaccuracies found. This was overcome by developing a method of explicitly defining the crack. However, this is a very manual process, especially under compressive loading, limiting the cases investigated in this work. The results from the limited cases presented here demonstrated that the application of the bending moment could be used as an approximation of the tensile stress for cracks as large as 10mm semi-elliptical cracks.

The effect of the presence of the crack on the wheel-rail contact pressure distribution was then investigated. Modelling of the wheel-rail contact was found to be extremely computationally expensive and other options were explored to reduce this burden. The Herztian pressure profile was found to be a suitable approximation to the wheel-rail contact when over an RCF crack. Preliminary results were obtained using this approach however it was still computationally expensive.

To study multiple cracks adds further complexity and, whilst the three dimensional method was suitable for identically sized cracks, it proved too computationally expensive to investigate different configurations of multiple cracks. It was decided to focus instead on a two dimensional representation of the wheel-rail system to investigate different configurations of multiple cracks, with the results presented in the following Chapter.

Chapter 6

Multiple Rolling Contact Fatigue Cracks in Close Proximity: The Effect of Shielding on Cracks of Different Sizes and Separations

6.1 Introduction

How do rolling contact fatigue cracks within the rail influence one another's growth or "communicate"? Rail RCF cracks appear in sequences and are of similar but not identical sizes or separations, Figure 2.12. Previous research has shown that shielding exists between closely spaced cracks of equal size. In particular the studies by Murakami [115] and Jin and Keer [140] have shown that, for two cracks of unequal sizes under tension in an elastic half-space at 90° and 45° to the surface, it is possible for the smaller crack to be closed by the larger crack. However accurate results for the crack closure cases were not established in these previous studies due to the modelling approach used being unable to simulate loading on the crack faces.

This Chapter is structured in the form of two studies as shown in Figure 6.1 and aims to determine:

- How adjacent cracks of differing size and separation interact to influence outcomes of crack propagation and potential rail breaks.
- The point of crack closure under the peak positive bending moment generated by the wheel load with multiple cracks of differing size.

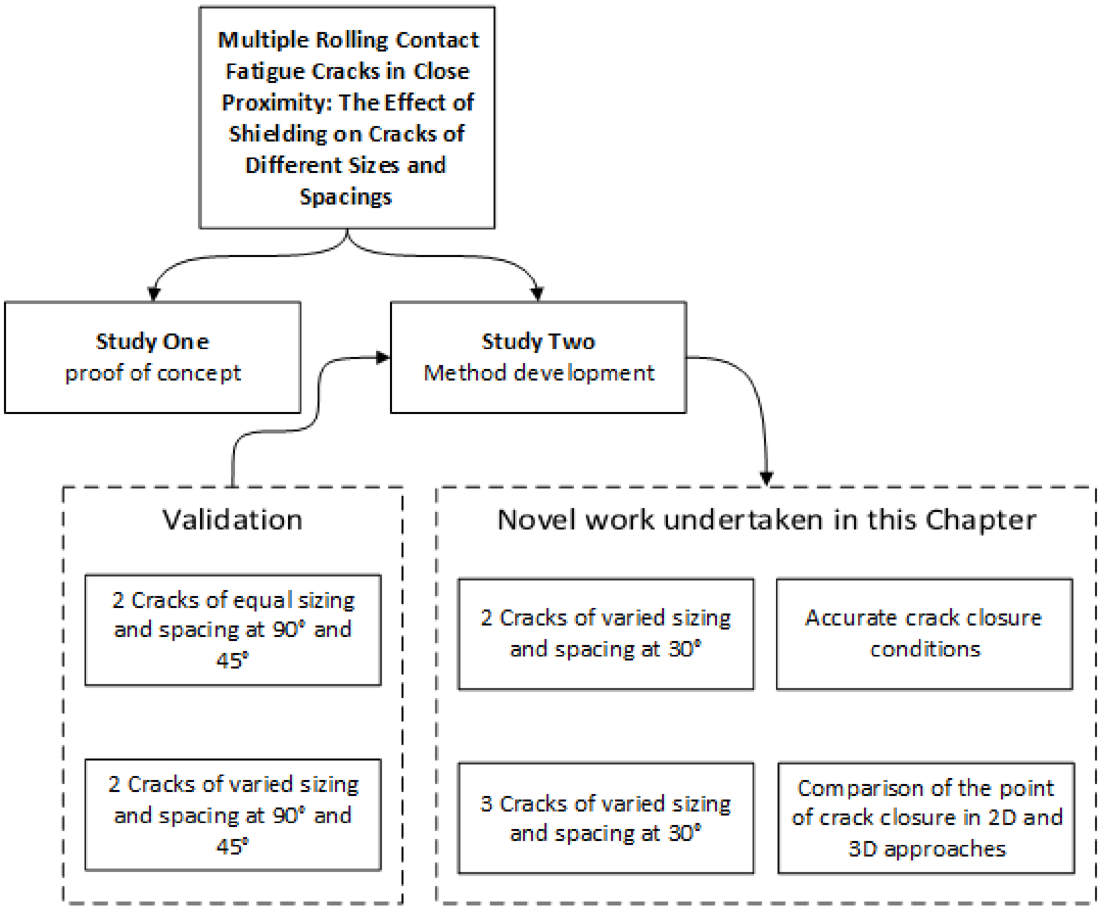

Figure 6.1: Chapter overview

Two studies are presented. Study One is a preliminary investigation that demonstrated the validity of the boundary element approach to investigate multiple cracks in close proximity [2]. It was presented at the 10th International Conference on Contact Mechanics and Wear of Rail Wheel Systems, Colorado Springs, 2015.

Study Two extends the methodology used in Study One. The developments are validated against previous work [115,140] before the method is used to increase understanding of crack behaviour within the railhead. Study Two improves the methodology for the investigation of multiple cracks, particularly for those of unequal sizes. Previous work [115, 140] had only investigated this for a very limited number of crack sizes at 45°. The methodology used in Study Two is not specific to a particular crack size or separation, but utilises relative sizes and separations to consider a wider range of multiple crack configurations. It improves upon the previous work through simulation of angles more typical of those found in RCF type defects, crack closure conditions and consideration of crack face friction.

Study Two's detailed two crack investigation for cracks at 30° to the surface showed that the two cracks reacted differently depending on the relative size of its neighbour, i.e. simulation of two cracks is insufficient to be representative of RCF defects where many cracks are within close proximity. Therefore Study Two was expanded to three cracks, which had been shown in Study One to be representative of an RCF crack within a long series of cracks. The results from the centre crack are presented in this Chapter because it is the most representative of the behaviour found in a long sequence of multiple cracks. The results are compared to the three dimensional approach in Chapter 5 to assess the differences between two dimensional and three dimensional approaches.

The results and methods presented in this Chapter develop an understanding of why chains of multiple similar (but not identical) cracks develop within rails. The results demonstrate how the growth of the central crack is affected depending on the size and proximity of nearby cracks. This has provided new insight into which grouping of cracks is most likely to lead to crack propagation and rail breaks when multiple, closely separated, cracks develop in the rail.

6.2 Study One: Using the Boundary Element Approach to Investigate Multiple Cracks Within the Railhead

Study One [2] demonstrates that the boundary element modelling technique is a suitable approach for considering multiple cracks at typical spacings for RCF type defects. By demonstrating the shielding effect that one crack has on its neighbour the boundary element approach was shown to be suitable for considering multiple cracks in close proximity. The key principles behind the boundary element approach for three dimensional applications are outlined in Chapter 5. They are principally the same for two dimensional applications so will not be further described here.

The two dimensional approach is a simplification of RCF type defects which occur in the complex three dimensional geometry of a rail. However it has been shown in Section 2.3.2.2 to give good results in comparison to three dimensional approaches through the use of a conversion factor for single crack cases. Two dimensional approaches also have much shorter computation times when compared to three dimensional approaches which allows for many more combinations of conditions to be investigated.

Study One was undertaken for a single 5mm crack at angles between 90° and 30° to the surface (the plots show the angle to normal). Multiple 5mm cracks (at an angle of 30° to the surface) were analysed at the spacings outlined in Table 6.1. The model dimensions, together with the crack configurations that were considered, are shown in Figure 6.2. The 51mm model height is equivalent to the railhead height of 60E1 rail (Appendix A.1). A tensile stress of 11.66MPa was applied which is equivalent to the stress generated at the surface of the rail head from a bending moment of 4KNm (which would be produced by a single wheel load [125]). This simple configuration focuses on the rail head surface and is not intended to represent the full stress state within the rail head.

Number of Cracks	Crack Spacing (mm)							
	5	10	15	20	25	30	40	50
2	x	x	x	x	x	x	x	x
3	x	x	x	x	x	x	x	x
5	x							
7	x							
9	x							
11	x							

Table 6.1: Crack spacings used in the two dimensional model, all cracks were 5mm in length and at 30° to the surface

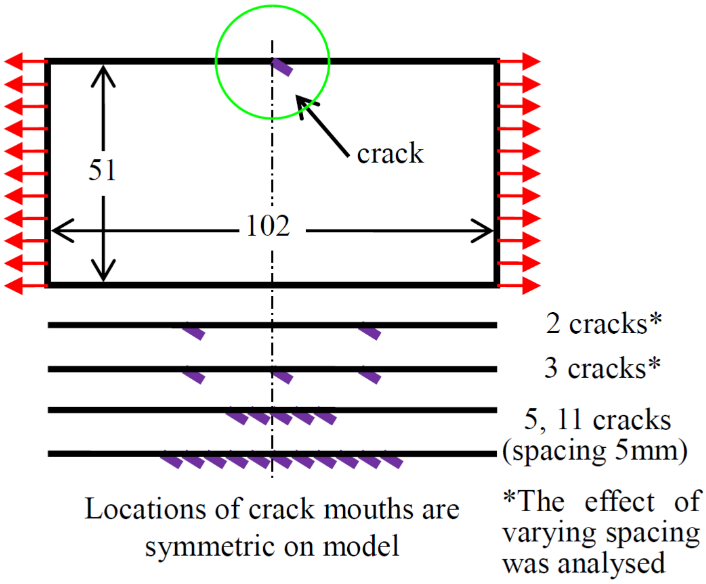

(a)

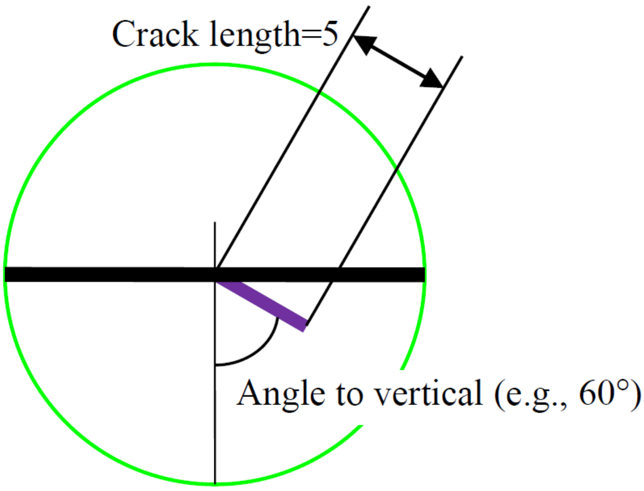

(b)

Figure 6.2: Diagram of the preliminary crack model, (a) showing the crack numbers and spacings considered, (b) showing the crack angle. Figure taken from Beagles et al. [2]

As demonstrated in Section 5.4.2 a uniform tensile stress is appropriate for shallow cracks remote from wheel-rail contact. In contrast to the base of the railhead, which only experiences about 44% of the maximum bending stress seen at the top of the rail (section height 172mm, neutral axis height 81mm) the relevant material (up to twice the crack depth of a 5mm crack at 30° to the surface) experiences only a 5% variation in stress by using a uniform instead of a varying stress.

Figure 6.3 shows the effect that crack angle has on the SIF for a crack of 5mm in length. As expected for a two dimensional model that effectively has a crack across the whole rail-head width the K_I values are larger than, but similar to, the largest three dimensional values which were calculated with a crack that had a limited lateral extent. The SIF reduced by a factor of 3.5 between angles of 90° and 30° to the surface. This is in part because a 5mm long crack at 30° to the surface is half the depth of the same crack at 90° to the surface.

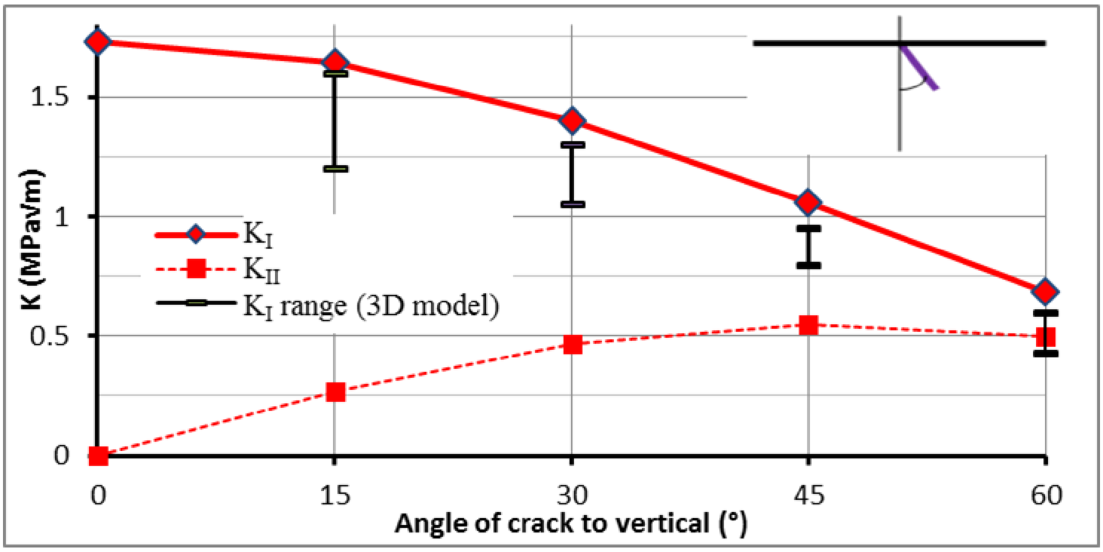

Figure 6.3: Stress intensity factors for single cracks at different angles due to bulk rail stress. Results compared to previous work by Fletcher et al. [125] (vertical bars). Figure taken from Beagles et al. [2]

The effect of changing the spacing between cracks is shown in Figure 6.4. It can be seen that the SIF's are generally reduced when there are multiple identical cracks compared to a single crack. The closer cracks are to each other, the smaller the SIF, with the smallest SIF being almost half that obtained for one crack and occurring for the middle crack in a group. This has also been shown in previous work by several authors [115,125,140,141]. Therefore Study One showed that crack growth models that consider isolated cracks in bending will tend to overestimate the growth of identical RCF cracks that occur in closely spaced groups by about a factor of two. However in the real world, although cracks maybe similar in size, they are rarely genuinely identical.

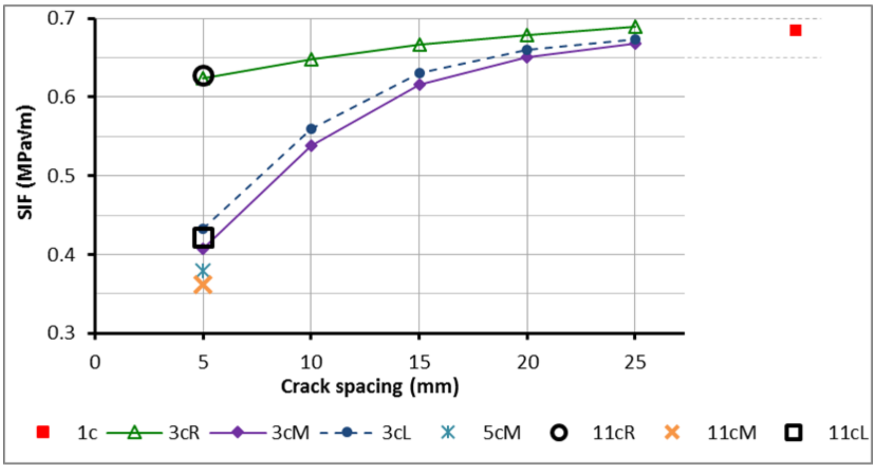

(a)

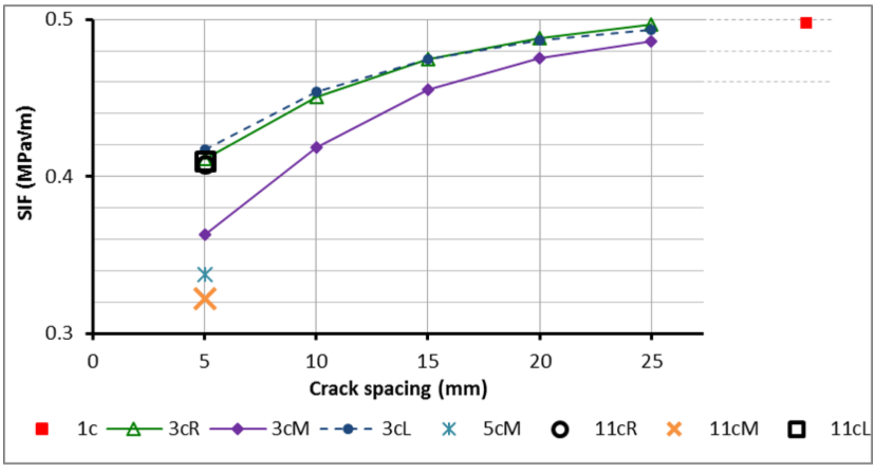

(b)

Figure 6.4: Stress intensity factors, (a) K_I, and, (b) K_{II}, for varying spacing and crack numbers (key: NcA where N is the number of cracks and A is R, M, or L for Right, Middle or Left crack in a group of cracks). Cracks are at 30° to the surface. Figure taken from Beagles et al. [2]

It can be seen in Figure 6.4 that the SIF values for either the left-most (cL) or right-most (cR) crack are almost independent of the number of cracks (with less than 10% variation in cL and cR between two and eleven cracks with a 5mm crack spacing). The middle cracks are of most interest because, for multi-crack RCF, each crack is effectively a middle crack. The variation of SIF with the number of cracks is shown in Figure 6.5. An approximate extrapolation suggests that for a long run of identical cracks the K_I would become about 0.35MPa$\sqrt{m}$ and K_{II} about 0.31MPa$\sqrt{m}$ relative to 0.68MPa$\sqrt{m}$ and 0.5MPa$\sqrt{m}$ for a single crack. As expected the SIF is sub-threshold (Section 2.3.2.3) as cracks of 5mm length would not be expected to grow from whole rail bending. However the fact that the cracks interact is clearly demonstrated.

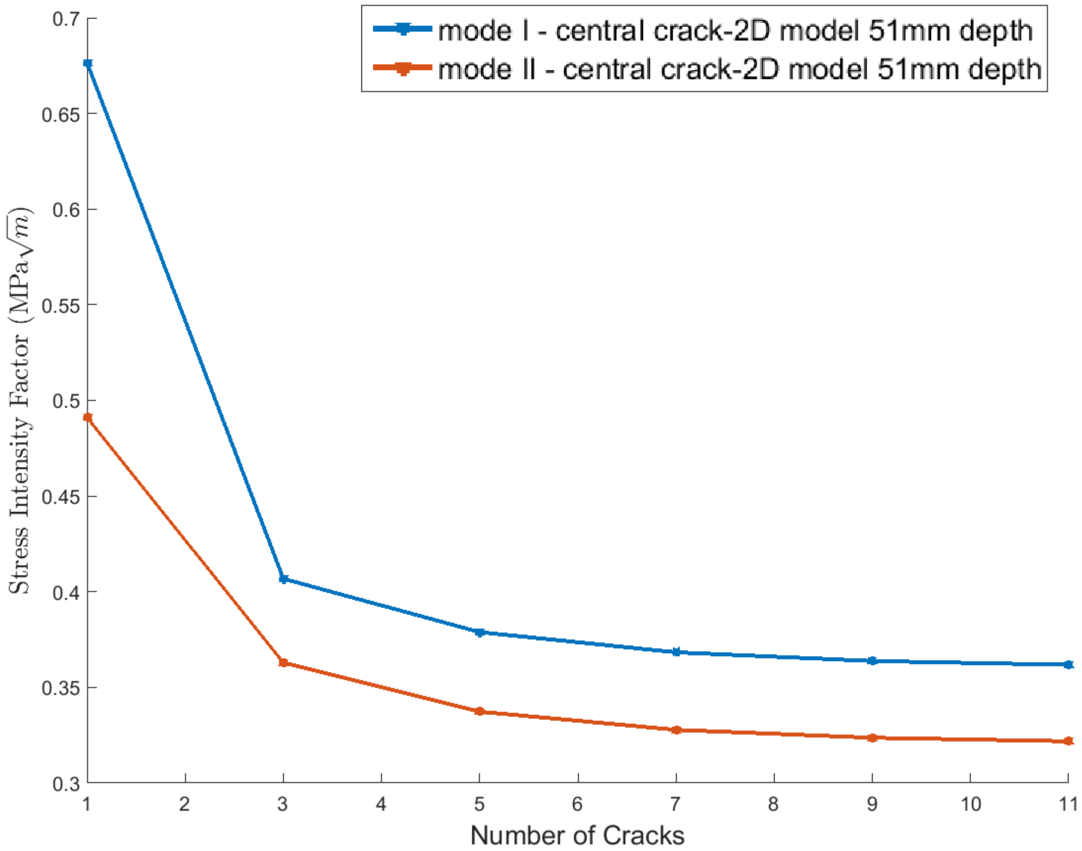

Figure 6.5: Variation of stress intensity factor of the central crack with the number of cracks, for 30° cracks at 5mm spacing

The SIF for the central crack of eleven cracks as a percentage of the central crack of one, three, five, seven and nine cracks is shown in Table 6.2. The difference found here between the SIF for the central crack of eleven cracks and that of a single crack is similar to the difference found in a study by Jin and Keer [140] for the central crack of one hundred cracks and a single crack. This demonstrates that modelling eleven evenly spaced cracks is representative of hundreds of evenly spaced cracks. The results demonstrate that including just three or more cracks within the modelling is a good enough approximation to the numerous cracks that would be present in reality whilst minimising computational resources. From the results presented here it can be seen that Study One has successfully demonstrated that the BE approach can model multiple cracks in close proximity. The following Sections discuss the improvements made to this approach.

Centre crack of	1	3	5	7	9	11
Stress Intensity factor of 11cM (%)	53	89	95	98	99	100

Table 6.2: The stress intensity factor for the central crack of eleven cracks as a percentage of the central crack of one, three, five, seven and nine cracks

6.3 Study Two Method Development and Initial Validation

Study Two develops the method used in Study One to improve the accuracy of the approach. It is validated against previous work [115, 140]. The improvement of the method allows for a detailed study into the interaction of cracks of different sizes and separations. Study Two utilises dimensionless SIF (Equations 6.1 and 6.2 [115]) to give results for a given "relative" crack size and separation. This removes the need to calculate the SIF at the crack tip for every physical crack size, which would be impractical due to the myriad number of possible size and separation combinations that exist.

The dimensionless SIF (F_I and F_{II}) are given by:

$$F_I = \frac{K_I}{\sigma\sqrt{\pi a}} \tag{6.1}$$

$$F_{II} = \frac{K_{II}}{\sigma\sqrt{\pi a}} \tag{6.2}$$

Where K_I and K_{II} are the SIF at the crack tip, σ is applied stress, a is crack length.

For RCF cracks in the rail the critical criterion is crack depth (Section 2.3.6), for cracks not normal to the surface Equations 6.1 and 6.2 become [115]:

$$F_I = \frac{K_I}{\sigma\sqrt{\pi b\frac{1}{\sin\theta}}} \tag{6.3}$$

$$F_{II} = \frac{K_{II}}{\sigma\sqrt{\pi b\frac{1}{\sin\theta}}} \tag{6.4}$$

The dimensionless SIF approach is valid within an elastic half-space, where the crack cannot approach the material boundary. In a finite material the behaviour is non-linear and the dimensionless SIF relationships in Equations 6.3 and 6.4 cannot be applied. In Study Two the infinite nature of an elastic half-space is approximated by defining a model of sufficient size relative to the cracks investigated. This approach is validated in Section 6.3.1.

6.3.1 Ensuring a good Representation of a Half-Space

As an example of non-linear behaviour Figure 6.6 shows a case in which the proximity of the model boundaries within Study One have affected the dimensionless SIF results, with the dimensionless SIF tending towards a value above that of a single crack. Study Two was adapted to better approximate an elastic half-space by increasing the model height to 510mm. This means that the critical dimension, material depth, is one hundred times greater than the deepest cracks that were considered (5mm depth).

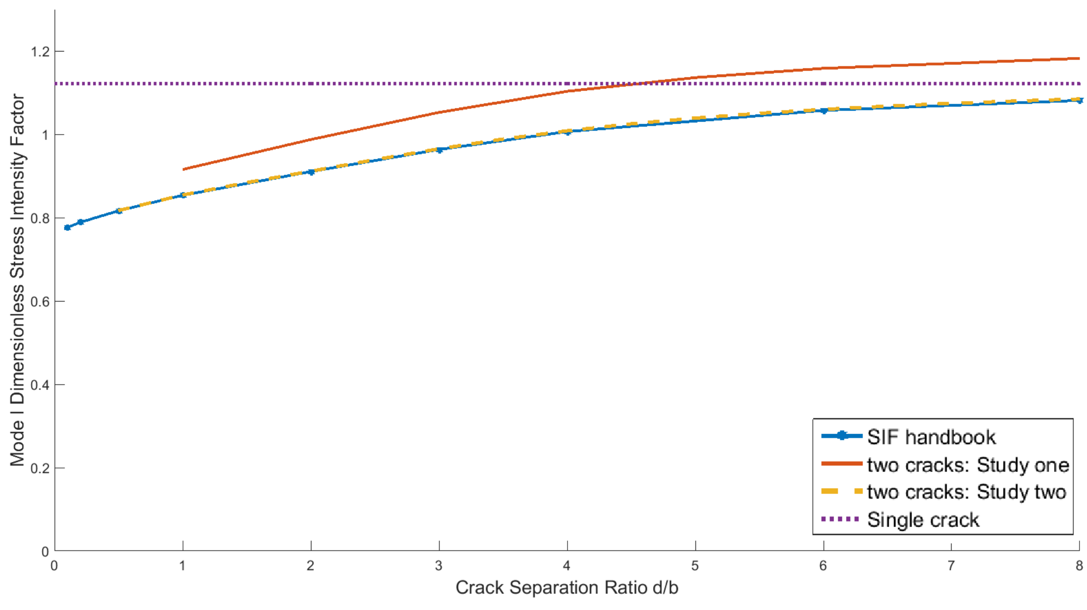

Figure 6.6: Example plot showing the effect of model boundaries on the dimensionless stress intensity factor at the crack tip

The dimensionless SIF is independent to crack size, therefore Study Two was validated across five crack depths between 1mm and 5mm at each crack separation ratio in Figure

6.6. A variation of less than 1% was seen between the specific SIF at the crack tip for each of the five crack depths considered, validating this approach. The average of these five specific SIFs has been used as the dimensionless SIF for the results presented in this thesis.

6.3.2 Single Crack at Various Angles

The dimensionless SIF results from Study Two for a single crack were compared to a half-space approach used in Murikami [115] (Figure 6.7). The crack angles considered ranged between 90° and 30° to the surface. As can be seen, the mode I dimensionless SIF differs from the half-space result by 0.3% for a 5mm crack at 90° to the surface. RCF type cracks typically occur at an angle of 30° to the surface (Section 2.3). At 30° to the surface the difference in the dimensionless SIF results between the half-space and Study Two is 0.9%, demonstrating that Study Two is an accurate approximation to an elastic half-space over a range of crack angles.

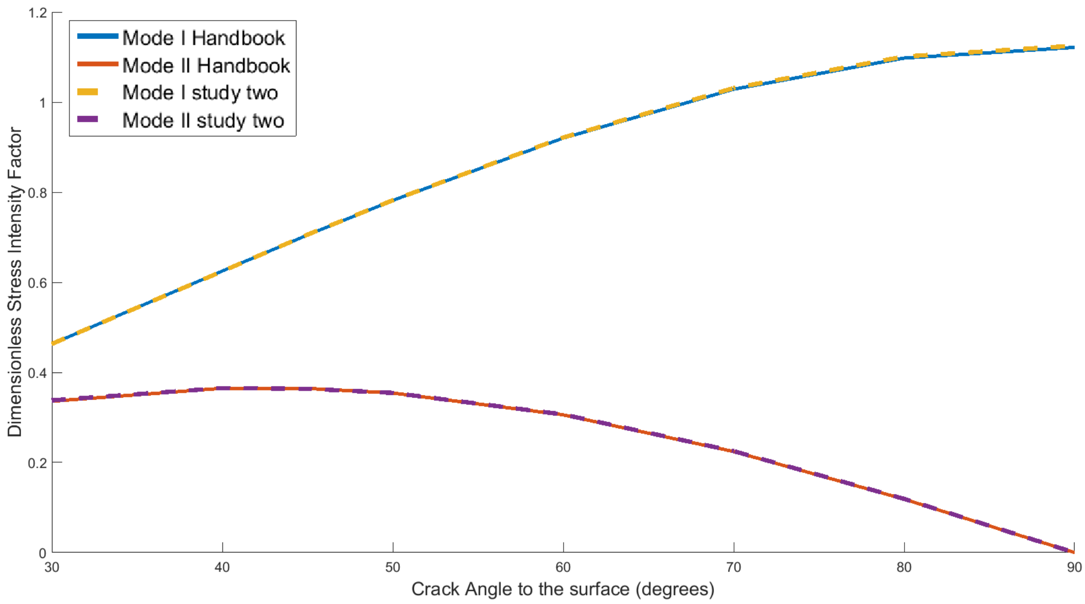

Figure 6.7: Effect of crack angle on dimensionless Stress Intensity Factor for a single crack under tension

6.3.3 Multiple Equally Sized Cracks

This Section investigates the effect that crack separation has on the dimensionless SIF when compared to a single crack. The results from Study Two are compared to the elastic half-space approach for cracks at both 90° and 45° to the surface.

In Figure 6.8a the results for crack angles of 90° to the surface are shown. The half-space case tends towards the value for a single crack as the crack separation increases (shown by the horizontal line). This is expected because, in a half-space, as the crack separation increases the cracks have less influence on each other, reducing the degree of shielding between cracks. There is no material edge to take into account, therefore the cracks tend towards the behaviour of a single crack.

It can be seen in Figure 6.8a that, for cracks at 90° to the surface, Study Two is a very good approximation to a half-space with the results no more than 0.3% different. At a crack separation ratio of 0.5, the dimensionless SIF is reduced by 27% when compared to a single crack. Previous work by Jin et al. [140] only considered a few specific crack separations for cracks at 45° to the surface, but from the data available the trends can also be seen to correspond. The results are shown in Figure 6.8b.

Unlike cracks at 90° to the surface, the dimensionless SIF for the overlying (left hand side crack in Figure 6.9a) and underlying (right hand side crack in Figure 6.9a) cracks is different for cracks at 45° to the surface. The effect of shielding that neighbouring cracks have on each other is different due to the angle of the cracks to the surface. The underlying crack experiences a greater degree of shielding (dimensionless SIF reduced by 33.2%) than the overlying crack (dimensionless SIF reduced by 10.8%). As for cracks at 90°, the effect of shielding decreases as the crack separation ratio increases.

The underlying crack experiences a greater degree of shielding relative to the equivalent separation at 90° to the surface. The overlying crack is more exposed relative to the equivalent separation at 90° to the surface. This effect was also shown in Study One for cracks at 30° to the surface (Figure 6.4). The comparisons drawn here show that Study Two accurately captures the trends with increased crack separation when cracks are equally sized.

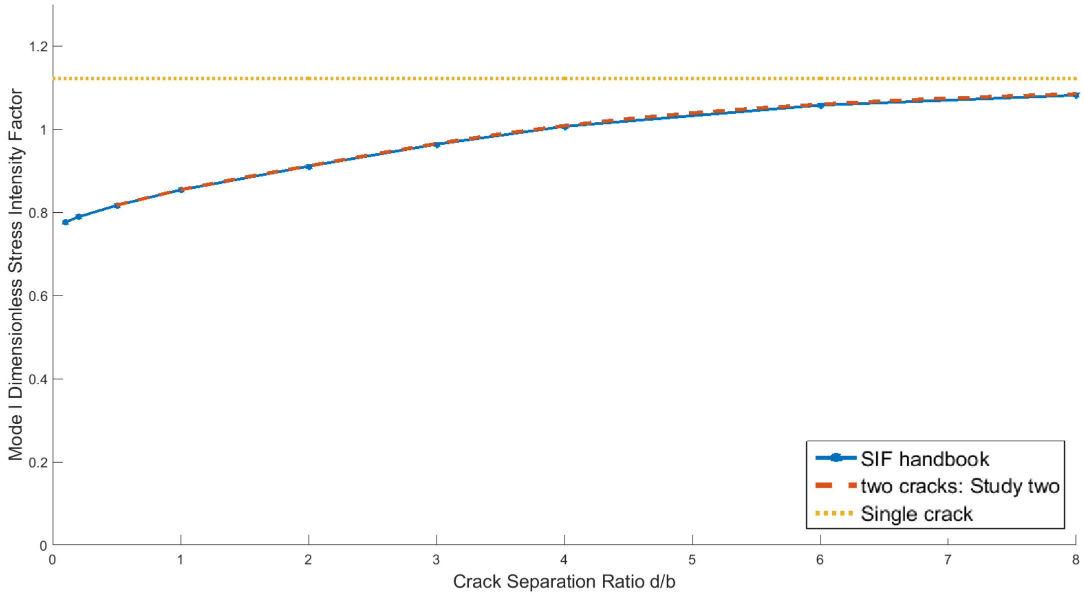

(a)

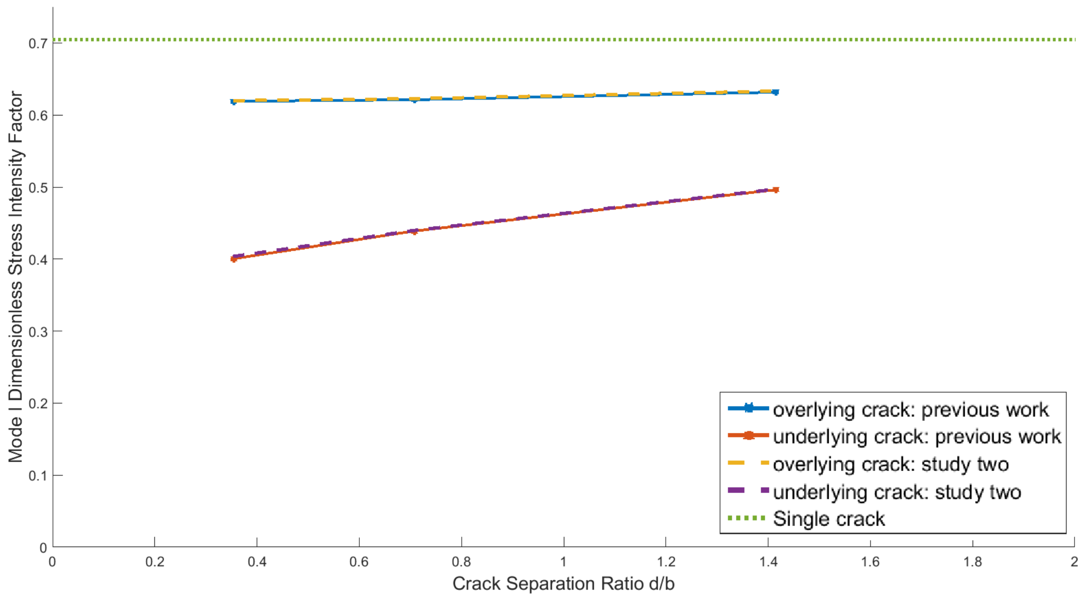

(b)

Figure 6.8: Effect of crack separation for two equally sized cracks at, (a) 90° to the surface, and, (b) 45° to the surface. Comparison to previous work, 90° case Murakami [115], 45° case Jin et al. [140]

6.3.3.1 The Effect of the Number of Equally Sized Cracks

The question arises whether two cracks would be able to accurately simulate the effect of shielding that would be present for hundreds of cracks. This would reduce the required modelling in comparison to investigating three cracks. The extra modelling requirements for three cracks with additional variants such as crack sizing and separation is discussed in Section 6.5. Section 6.3.3 has shown that the effect of shielding has a greater effect on the underlying crack, with the overlying crack being less shielded. Here, a comparison was undertaken between the central crack of three cracks and the underlying crack of two cracks (highlighted with the red circles in Figure 6.9a).

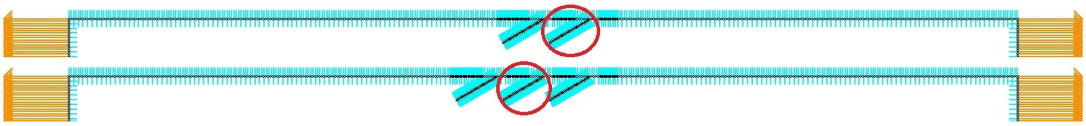

(a)

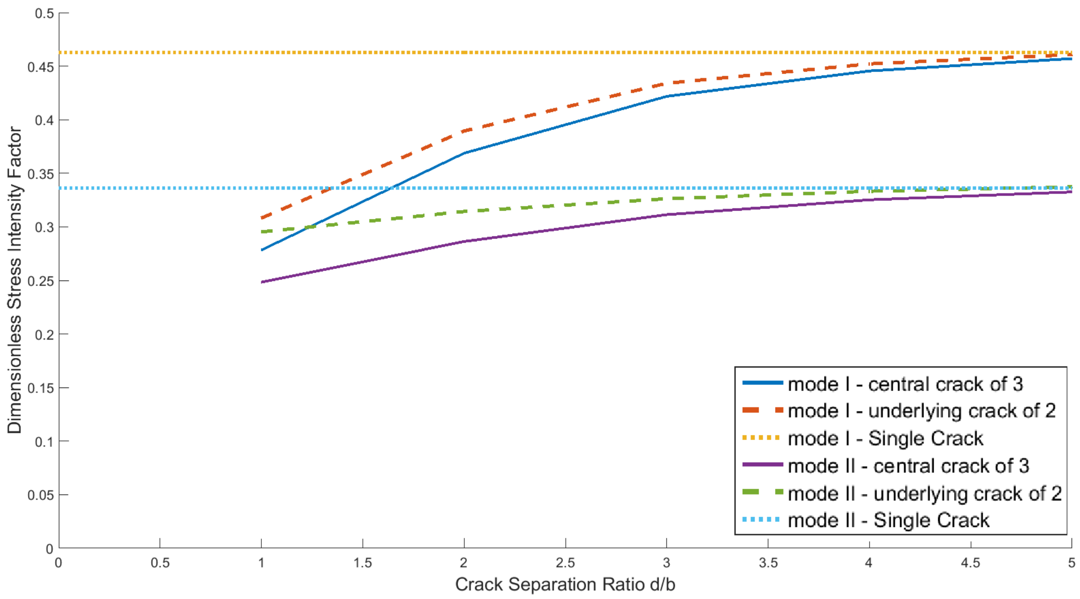

(b)

Figure 6.9: Comparison between the Dimensionless Stress Intensity Factor of Central Crack of three cracks and the underlying crack of two cracks as the crack separation increases, cracks at 30° to the surface. (a), Diagram of cracks compared, (b), results

The results are shown in Figure 6.9b. There is a significant drop in both mode I and II SIF when two cracks are considered in comparison to the single crack case. A further increase in the degree of shielding is found for the central crack of three when compared to the underlying crack of two cracks. The mode I SIF and mode II reduce by a further 10% and 16% respectively for the central crack of three in comparison to the underlying crack of two cracks at the crack separation ratio (d/b) of 1. This difference reduces as the crack separation ratio increases. The results highlight the necessity to have at least three cracks when simulating multiple crack configurations, with both outer cracks shown to contribute to the amount of shielding that the central crack experiences.

The model developed here has been shown to give accurate results for the dimensionless SIF at the crack tip for cracks of the same size over a range of crack separations. In the next Section the effect of different sized cracks is investigated.

6.3.4 Comparison of Stress Intensity Factors between Semi-Elliptical and Planar Cracks

The two dimensional planar crack approach used in this Chapter (Figure 6.10a) is often used in RCF type defect analysis due to the short run times of the method. However, the three dimensional approach used in Chapter 5 (Figure 6.10b) is a more realistic representation of RCF cracks within the railhead. In previous works such as that by Kaneta et al. [113] a conversion ratio of 0.59 has been shown to give comparable SIF results between a single planar crack and the deepest point of a semi-elliptical crack (Section 2.3.2.2). This Section investigates whether this conversion factor holds true for multiple cracks in close proximity.

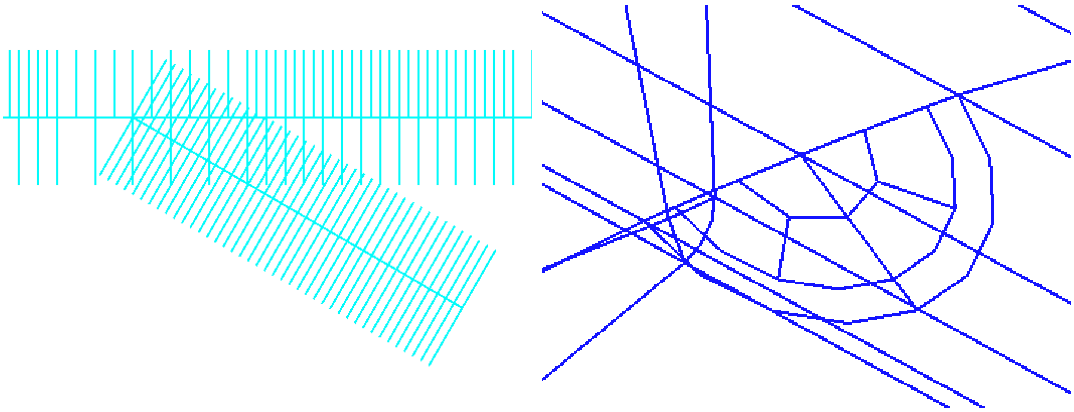

(a) (b)

Figure 6.10: Diagram showing, (a), the 2D planar crack, (b), the 3D semi-elliptical crack

Here results from the three dimensional approach using the full rail profile containing one, three, five and seven 10mm semi-elliptical cracks at 30° to the rail surface with a spacing of 5mm are compared to the two dimensional approach. Figure 6.11 shows the comparison results. The mode I SIF, Figure 6.11a, is almost identical for both approaches for all numbers of cracks studied. The mode II SIF, Figure 6.11b, varies across the crack front of the semi-elliptical crack, being positive at the surface and negative at the deepest point. This would suggest different rates of crack growth across the crack front, over time leading to a change of shape away from the idealised semi-elliptical shape.

With application of the 0.59 conversion factor from Kaneta et al. [113], the results for the mode I SIF are comparable between the two approaches. However, the results for the mode II SIF, show that the application of the 0.59 conversion factor from Kaneta et al. [113] to the planar crack resulted in a SIF of 0.59 times the SIF for the semi-elliptical crack. This was thought to be due to the two dimensional model used in this thesis having a defined thickness of 1mm and not being infinitely thick as assumed by Kaneta et al. [113].

Therefore, for this thesis, which uses a thin two dimensional model, the mode II SIFs from the two approaches are taken to be directly comparable and the conversion factor of 0.59 has been applied to the mode I SIF results only. The need for a conversion factor of 0.59 between planar and semi-elliptical cracks was shown to remain valid for mode I SIFs as the number of cracks increased.

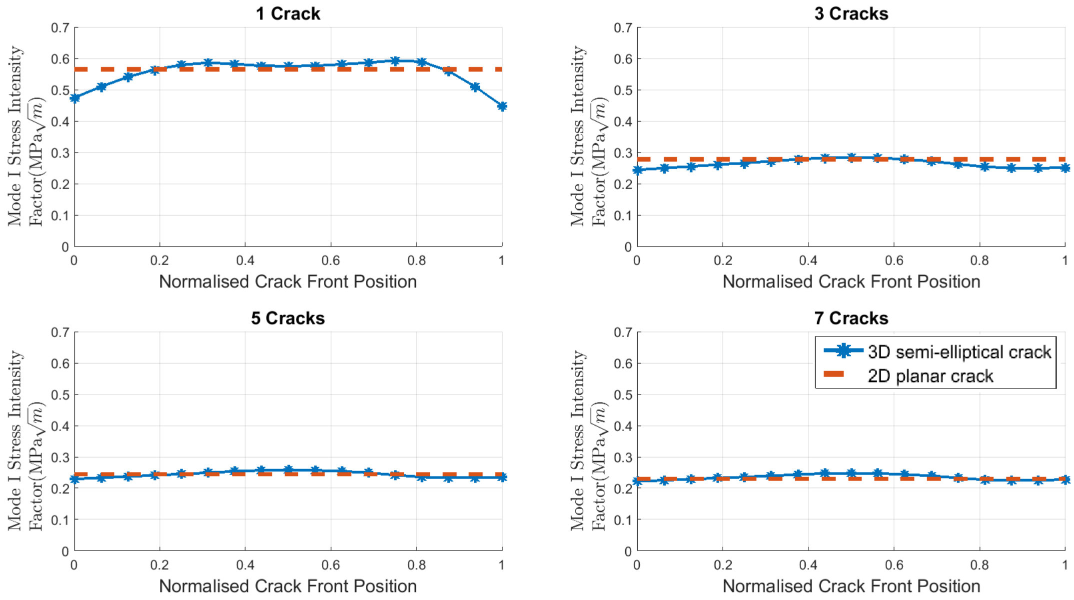

(a)

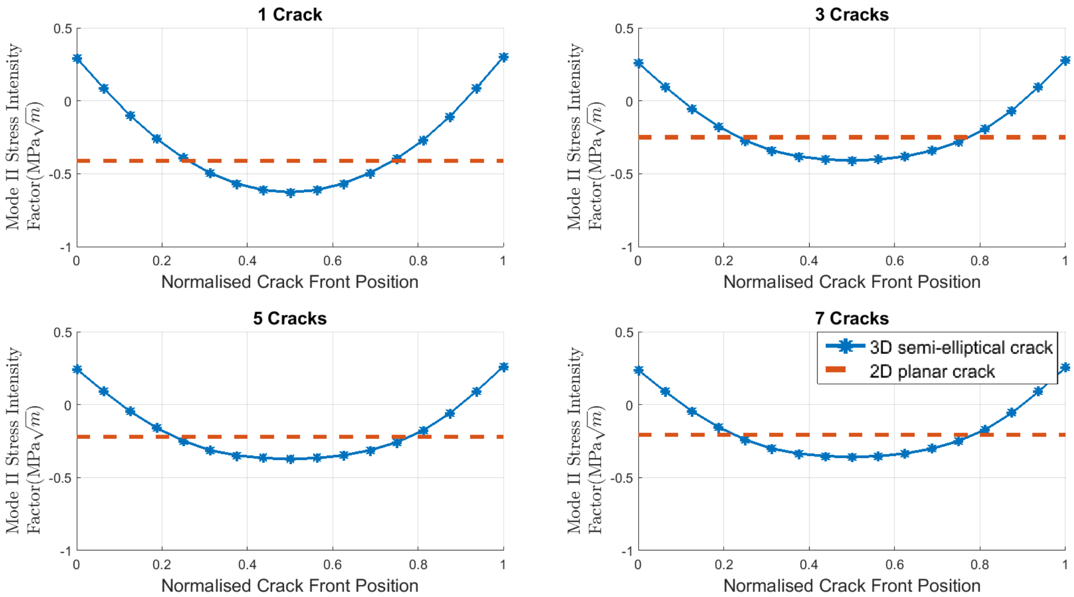

(b)

Figure 6.11: Comparison between stress intensity factors of the central crack of one, three, five and seven semi-elliptical (three dimensional) and planar cracks (two dimensional) with length 10mm and spacing of 5mm at 30° to the surface with the 0.59 conversion factor from Kaneta et al. [113] applied, (a), mode I, (b), mode II

6.4 The Effect of Size and Separation Ratios for Two Cracks at Different Angles to the Surface

In the following Sections the SIF at the crack tip of two cracks of unequal size and separation ratios is investigated (Figure 2.18). The crack size and separation ratios are taken relative to crack A (Figure 2.18), meaning that crack size ratio is defined as c/b, and separation ratio is defined as d/b. Study Two is compared with previous work for cracks at angles of 90° (Section 6.4.1.1) and 45° (Section 6.4.1.2) to the surface. Cracks at 90° to the surface are compared with work by Murakami [115]. Cracks at 45° to the surface are compared with work by Jin et al [140]. The dimensionless SIF is given for crack A (F1A and F2A) and crack B (F1B and F2B).

A shortcoming of the previous studies is the inability of their method to accommodate for crack closure that occurs when the crack size ratio (c/b), and separation ratio (d/b), is small. This is demonstrated in the comparative results to previous work in Sections 6.4.1.1 and 6.4.1.2 where the previous studies predict negative dimensionless mode I SIF for the small crack. This non-physical result occurred because the method used in the previous studies could not account for the interaction between the crack faces for crack closure conditions. The boundary element method that has been developed here can accurately simulate crack closure conditions. When applying the crack closure condition a coefficient of friction between the contacting crack faces of 0.3 was chosen as this is a representative friction coefficient where the effect of lubricated crack faces is not considered.

6.4.1 Study Two Further Validation

6.4.1.1 Two Cracks at 90° to the Surface

Figure 6.12a shows the comparison between the previous method by Murakami [115] and Study Two for two cracks of different sizes at 90° to the surface. The two methods show good correlation; with Study Two almost identical to the previous method for almost all the cases (the exception being when modelling crack closure conditions).

As expected the dimensionless SIF of crack B (F1B) decreases as the size of crack B shrinks relative to crack A due to the increased shielding effect. The dimensionless SIF of crack A (F1A) increases to the single crack value as the size of crack B shrinks relative to crack A. This is due to closure of crack B as its size shrunk relative to crack A, leading to crack A behaving as a single crack. As expected the shielding effect declines with greater crack separation ratios, with the results tending towards the single crack result for all cases with greater crack separation ratios.

Figure 6.12b shows the comparison between the previous method by Murakami [115] and interpolated curves from Study Two for two cracks of different size ratios at 90° to the surface. Exact solutions using Study Two were found for separation ratios given in Table 6.3 and from the relative crack sizes presented here, interpolation was used to give solutions for the intermediate crack separation ratios.

Crack size ratio (c/b)	crack separation ratio (d/b)		
	min d/b	step	max d/b
0.10	0.5	0.5	8
0.20	0.5	0.5	8
0.30	0.5	0.5	8
0.40	0.5	0.5	8
0.50	0.5	0.5	8
0.60	0.5	0.5	8
0.70	0.5	0.5	8
0.80	0.5	0.5	8
0.90	0.5	0.5	8
1.00	0.5	0.5	8
1.11	0.5	0.5	8
1.25	0.5	0.5	8
1.43	0.5	0.5	8
1.67	0.5	0.5	8
2.00	0.5	0.5	8
2.50	0.5	0.5	8
3.33	0.5	0.5	8
5.00	0.5	0.5	8
10.00	0.5	0.5	8

Table 6.3: Crack size ratios (c/b) and separation ratios (d/b) considered at the crack angles of 90° and 30°.

As shown in Figure 6.12b this still gives good correlation, with the previous method giving almost identical results except for crack closure cases (c=0.25b for d<=0.5b). When crack B is closed for both of the cases that are used interpolation, the interpolated results still give good accuracy. However, due to the non-linear behaviour of the smaller crack at the transition between open and closed, the interpolated approximation introduces inaccuracy. By choosing a suitably small interval between exact solutions in Study Two (increments of crack size ratios of 0.1 and crack separation ratios of 0.5) the error in the results to one decimal place was insignificant.

The good correlation found between the interpolated results from Study Two and previous work demonstrates that it is not necessary to give an explicit solution for every combination of crack separation and sizing ratios. A good approximation of the dimensionless SIF was found for any crack size and separation ratio within the range of cases considered. This remains true for the transition between open and closed cracks providing that the intervals between the exact solutions are small.

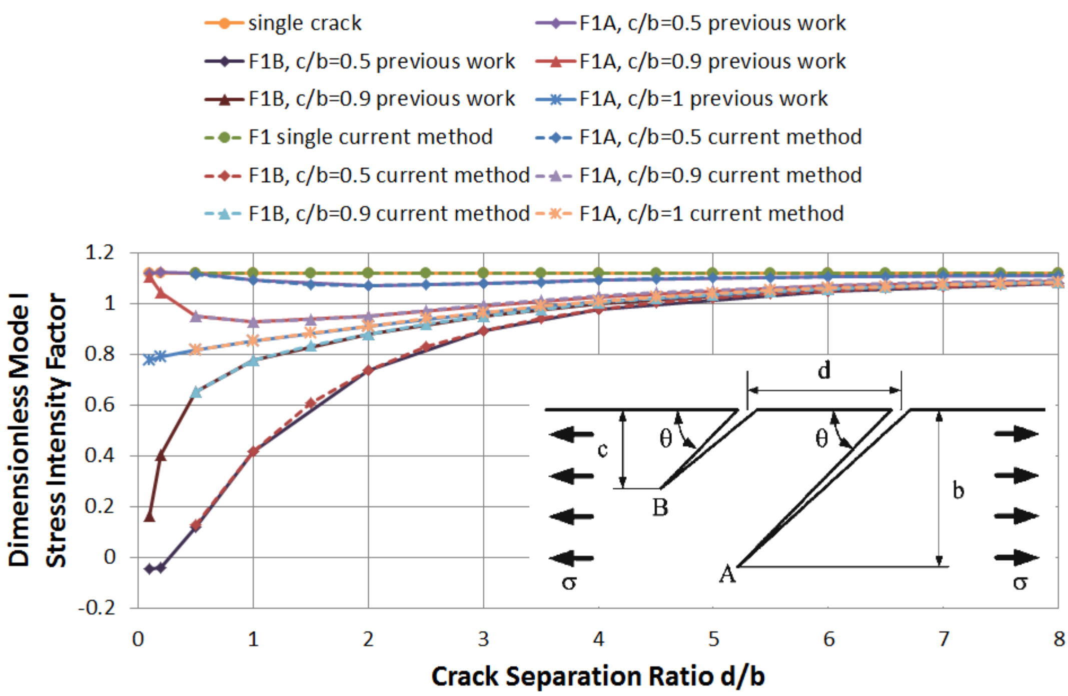

(a)

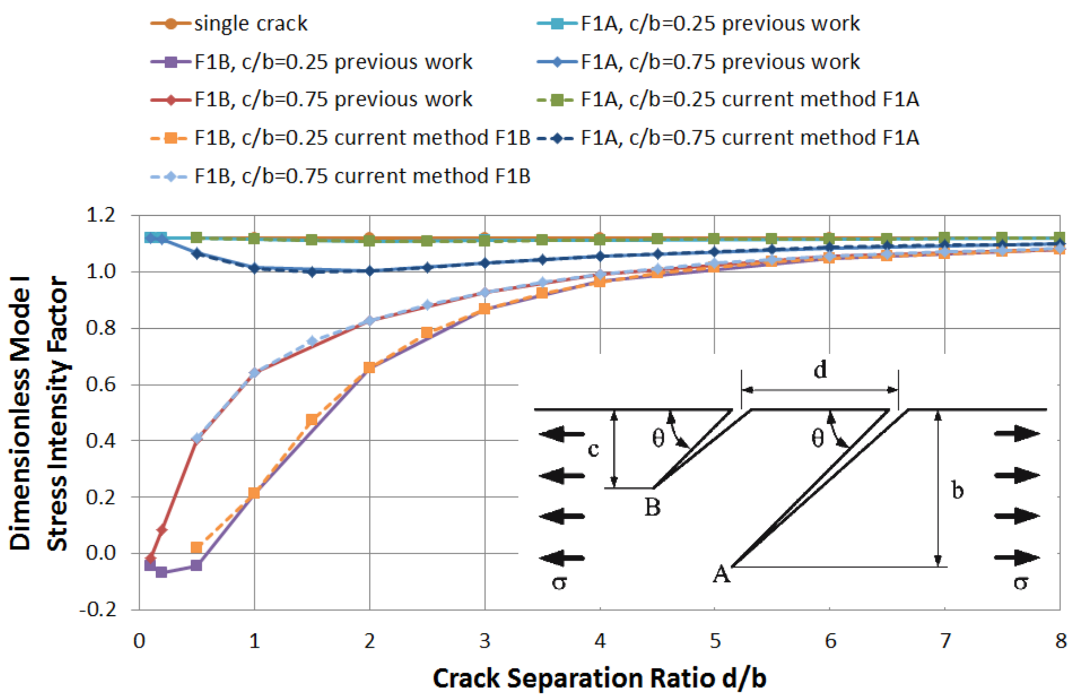

(b)

Figure 6.12: Comparison of mode I dimensionless stress intensity factor between current method and previous work by Murakami [115], two cracks of different sizes at 90° to surface. (a), results at crack separation ratios solved using Study Two, (b), results interpolated between separation ratios directly solved using Study Two

6.4.1.2 Two Cracks at 45° to the Surface

Figure 6.13 shows the comparison between Study Two and the previous method by Jin et al. [140] for two cracks of different sizes at 45° to the surface. Both mode I and mode II dimensionless SIF results are presented. The results from the previous method by Jin et al. [140] are limited to a few specific cases of crack separation ratios for the crack size ratio of c=0.5b. For these cases good correlation between Study Two and the previous method by Jin et al. [140] was found.

In Figure 6.13a the mode I SIF for crack B (underlying crack with depth half that of the overlying crack A) is shown to be slightly different for the crack separation ratio of 0.5. This is because for this case crack B is closed and the previous method by Jin et al. [140] gave a non-physical negative SIF. As the crack separation ratio increases the agreement improves due to crack B being open for these cases.

Figure 6.13b shows limited differences in mode II dimensionless SIF for either crack, even when the crack is closed. This is because as long as crack face friction is low, shear movement between the faces of the cracks will occur regardless of whether the crack is open or closed. Overall, the results from Study Two showed good agreement with previous work by Jin et al. [140] for all cases considered.

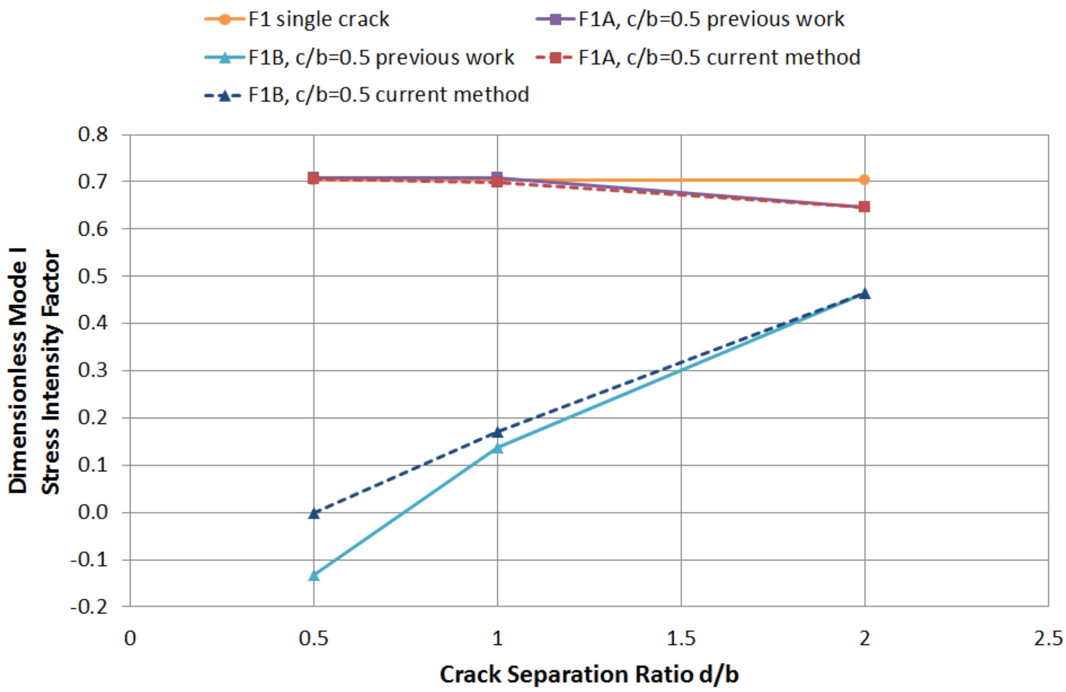

(a)

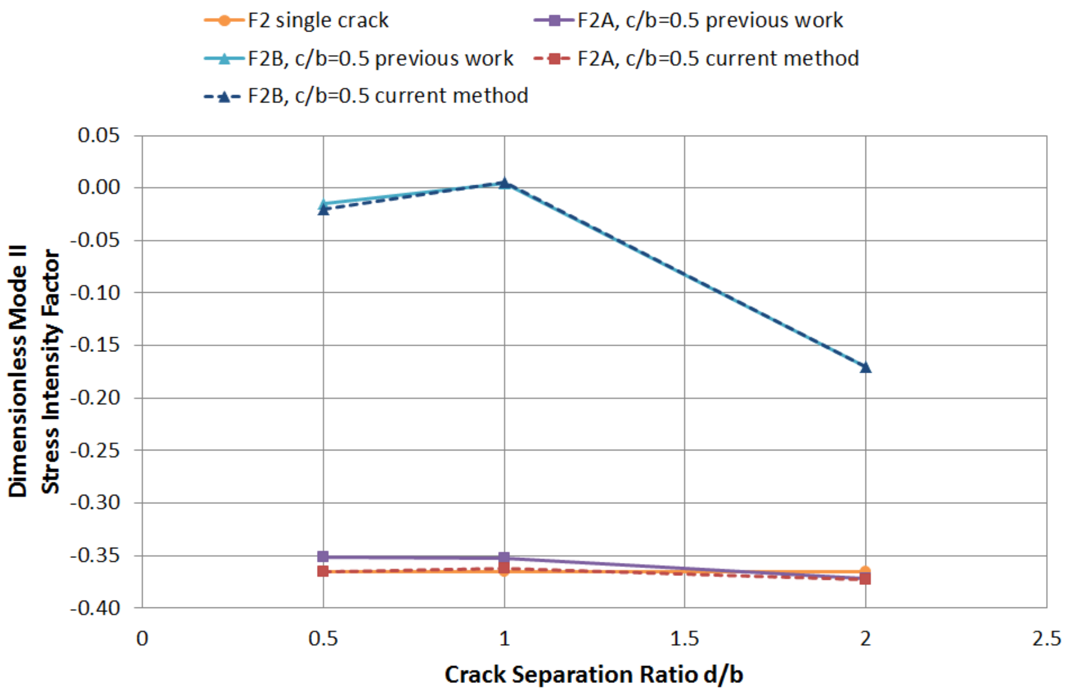

(b)

Figure 6.13: Comparison of, (a) mode I, and, (b) mode II, dimensionless stress intensity factors between Study Two and previous work by Jin et al. [140], two cracks of different sizes at 45° to the surface

6.4.2 Two Cracks at 30° to the Surface

This thesis increases our understanding of two crack interaction by investigating two different sized cracks at 30° to the surface, an angle more typical of RCF defects found within the railhead than those studied in the previous work [115, 140]. The crack size and separation ratios that have been considered at 30° to the surface are outlined in Table 6.3. Moreover, the results presented here increase understanding of how overlying and underlying cracks interact as their relative size and separation changes. The key findings are given in Table 6.4 and discussed in detail below.

Figure 6.14 shows the mode I dimensionless SIF for crack A (underlying crack) as the relative sizes between crack A and crack B change. For clarity Figure 6.14a shows the results when crack A is larger than crack B and Figure 6.14b shows the results when crack B is larger then crack A. The results for c/b=1 is shown in both graphs for ease of comparison.

When crack A is larger than crack B the mode I dimensionless SIF of crack A responds in a similar manner to that for cracks at 90° to the surface. That is, as crack B increases in size relative to crack A, the degree of shielding on crack A increases; the mode I dimensionless SIF of crack A reducing to approximately half that of the single crack case for crack separation ratio d=0.5b when c=b. As crack B decreases in size relative to crack A, the mode I dimensionless SIF of crack A tends towards the single crack case for small separation distances. This is because the act of crack A opening under the applied stress forces crack B towards closure (Figure 6.15). When crack B is closed it acts in an equivalent manner to solid material to the opening failure mode (mode I SIF). Therefore it no longer has any shielding effect on crack A, with the mode I dimensionless SIF of crack A equating to the single crack case.

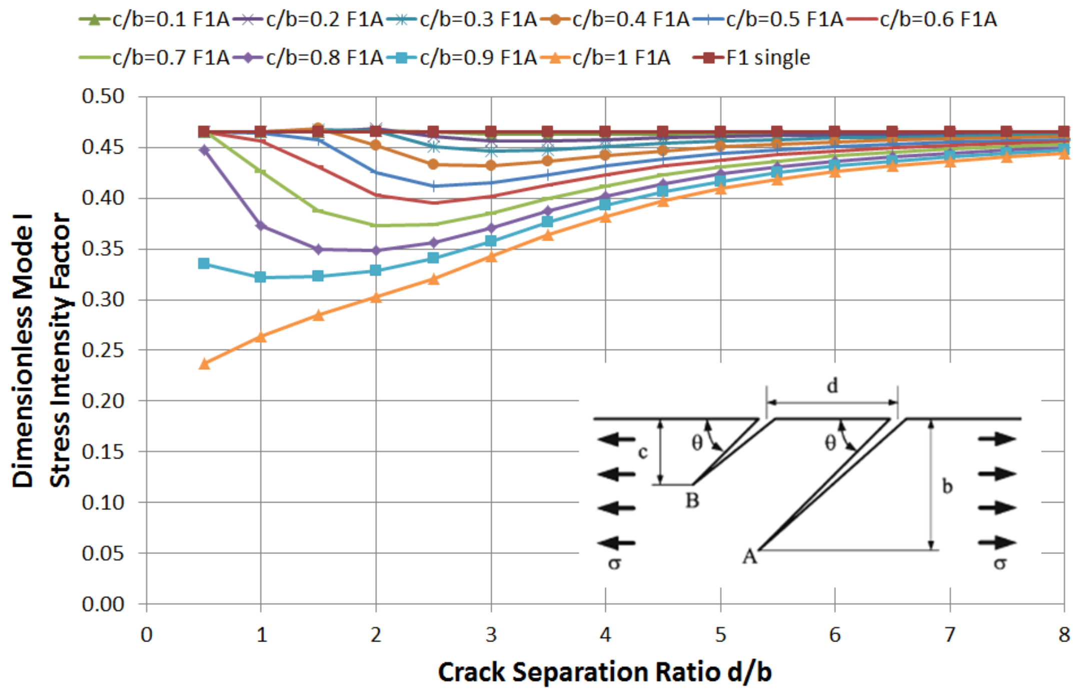

(a)

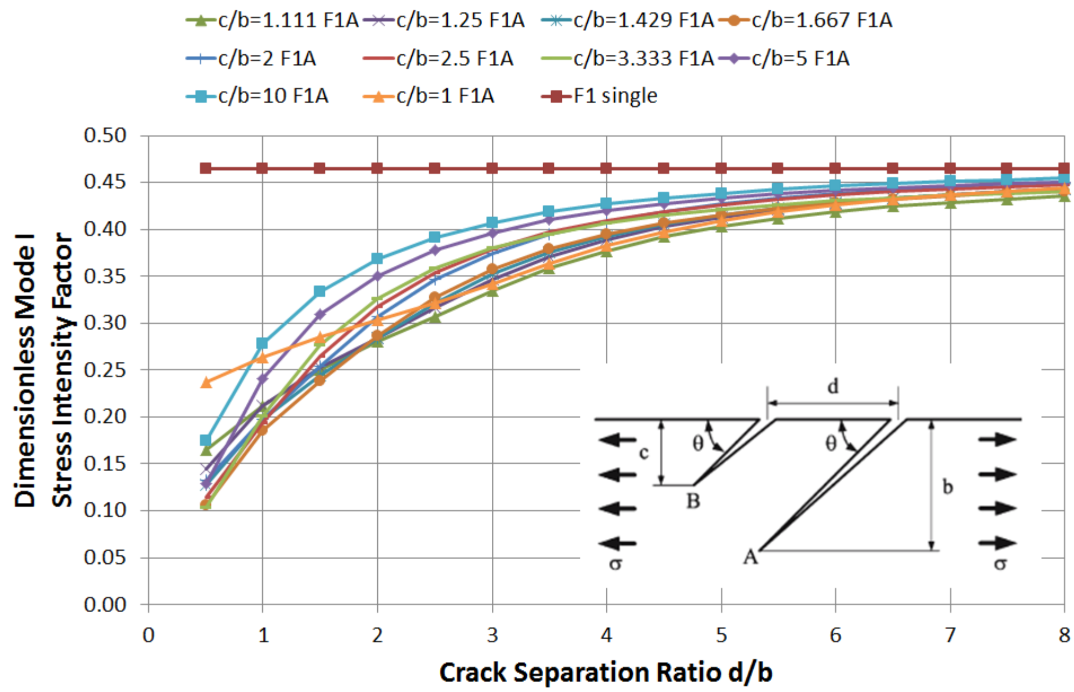

(b)

Figure 6.14: Mode I dimensionless stress intensity factor for crack A with neighbouring crack B of different relative sizes and separations. Both cracks at 30° to the surface. (a), crack A larger than crack B, (b), crack B larger than crack A

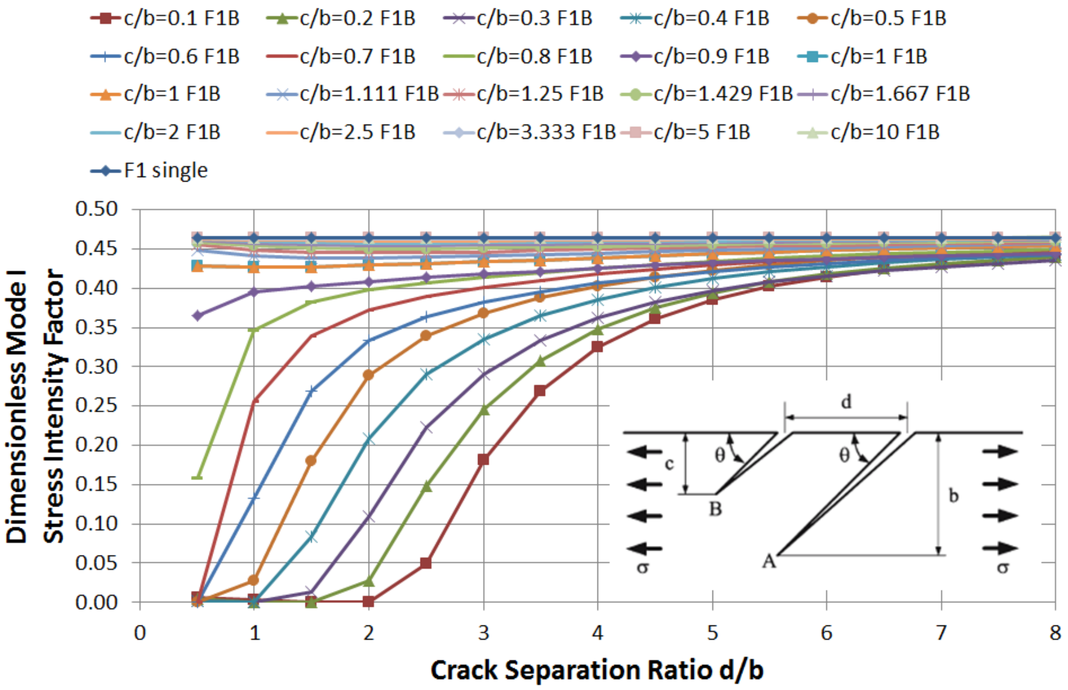

Figure 6.15: Mode I dimensionless stress intensity factor for crack B with neighbouring crack A of different relative sizes and separations. Both cracks at 30° to the surface

However, once the size of crack B is larger than crack A the trend of crack A is quite different. Crack B has an increased shielding effect on crack A up to the crack size ratio of c=3.33b. For this case, at a crack separation ratio of d=0.5b, the mode I dimensionless SIF of crack A is approximately half that of the case when c=b. However, above this crack size ratio, crack B has a decreased shielding effect on crack A. This is because, due to the orientation of the cracks, the crack tip of crack B becomes more remote from crack A as the size of crack B increases relative to crack A. The effect of crack separation also becomes more pronounced for the same reason, with the effect of a doubling of crack separation ratio from d=b to d=2b leading to a 33% increase in mode I dimensionless SIF of crack A for the case when c=10b. This is in comparison to the 15% increase in mode I dimensionless SIF of crack A for the same change in crack separation ratio for the case when c=b. Therefore the degree of shielding that is present at crack A increases to a limit, before reducing as the crack tip of crack B becomes more remote from the position of crack A.

Crack B (overlying crack) is shown in Figure 6.15 to behave quite differently to crack A. When crack B is larger than crack A, crack B behaves almost identically to a single crack, with minimal shielding effects from crack A. The relative size of crack A makes little difference to the dimensionless SIF of crack B when crack A is smaller than crack B. However once crack A is larger than crack B the degree of shielding experienced by crack B increases dramatically for crack separation ratios less than d=4b. Crack A becomes the dominant crack, forcing crack B to remain closed at significant separation ratios when crack B is less than half the size of crack A. In the case of c=0.1b crack B remains closed for separation ratios up to d=2b. The effect of increasing the crack separation ratio is also more pronounced, with the mode I dimensionless SIF of crack B tending rapidly towards a single crack case with increasing crack separation ratio once crack B opens.

Therefore, contrary to the findings for equally sized cracks, the effect of shielding on two unequally sized cracks is most pronounced for the overlying crack when it is smaller than the underlying crack. The shielding effect increases as the crack separation ratio decreases. For small crack separation ratios the underlying crack can force the overlying crack to remain closed at a considerable range of crack separation and size ratios. Only when the overlying crack is 80% of the size of the underlying crack will it remain open for crack separation ratios of d=0.5b. This closure of the overlying crack helps to explain why the underlying crack tends towards single crack behaviour as its size increases relative to the overlying crack for small crack separation ratios.

The mode II dimensionless SIF for crack A is shown in Figure 6.16a. In a similar manner to the crack opening failure mode, the results for the crack shear failure mode show increased crack shielding for crack A until crack B reaches crack size ratios of c=3.33b. However, unlike the crack opening failure mode, when crack B is larger than c=3.33b, crack A shows a consistent degree of shielding for mode II dimensionless SIF. This demonstrates that crack B continues to shield crack A from the shear failure mode, even though the crack tip of crack B becomes more remote from crack A. For these cases the effect of shielding is such that, at crack separation ratios of d=0.5b, the mode II dimensionless SIF of crack A is half the value that it would be if crack A was in isolation.

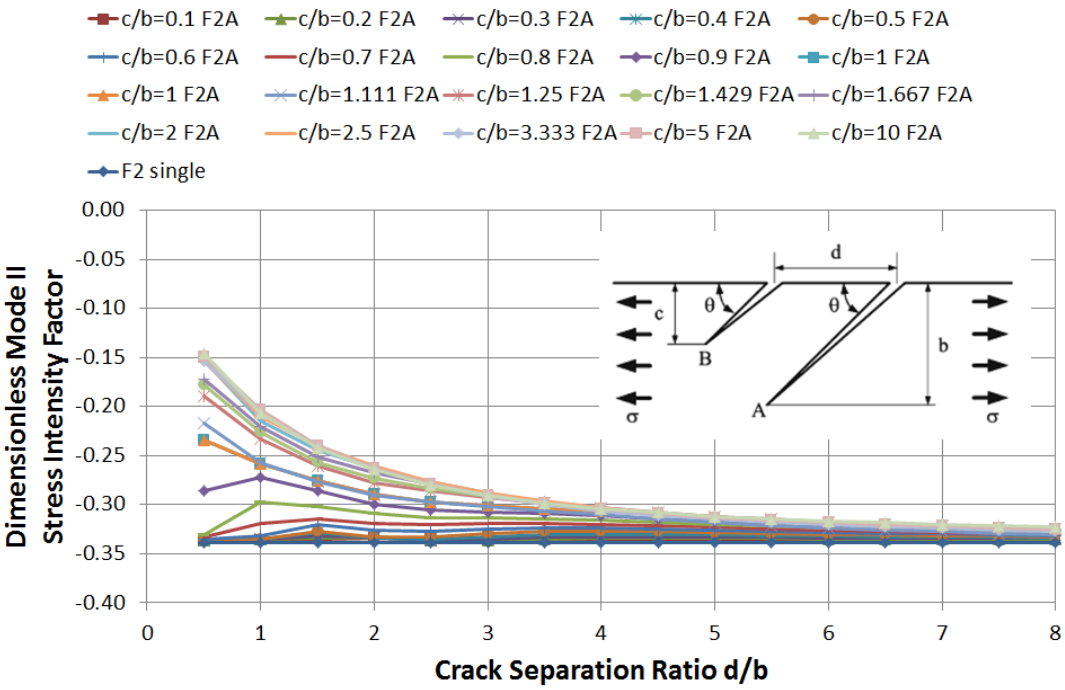

(a)

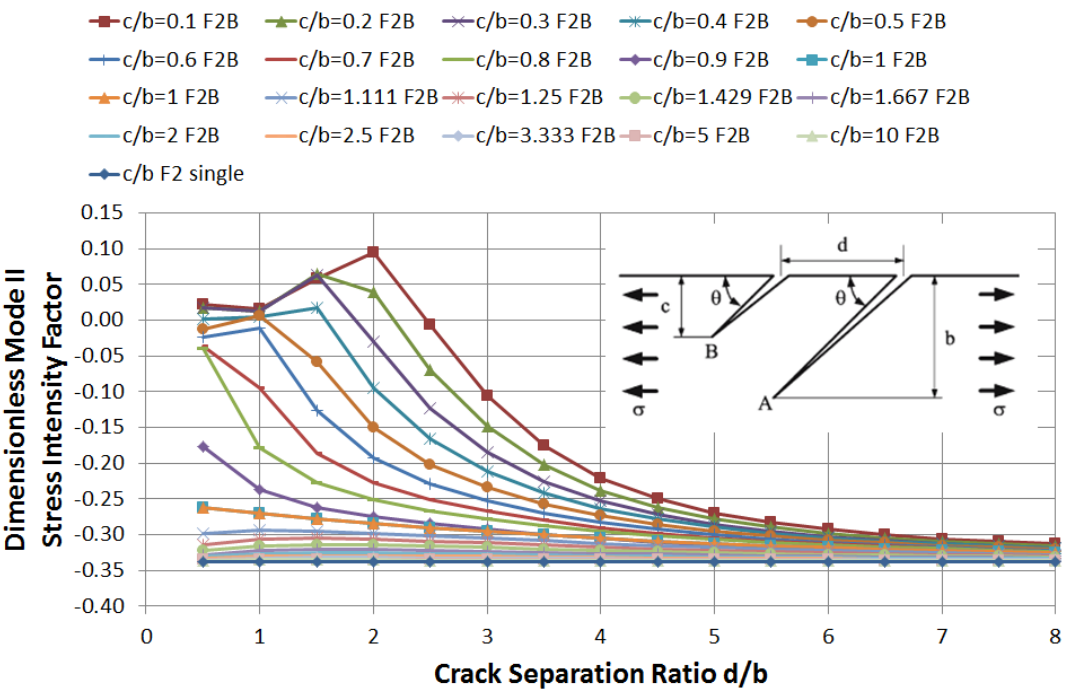

(b)

Figure 6.16: Mode II dimensionless stress intensity factor of two cracks at 30° to the surface with different relative sizes and separations. (a), crack A results, (b), crack B results

When crack A is larger than crack B the relative size of crack B has minimal effect on the mode II dimensionless SIF of crack A. The mode II dimensionless SIF of crack A remains almost identical to the single crack case for all separation ratios until crack B reaches 80% of the size of crack A. For all crack size ratios, once the crack separation ratio d=4b then the mode II dimensionless SIF of crack A differs by a maximum of 7%. Therefore the effect that the presence of crack B has on the mode II dimensionless SIF of crack A decreases rapidly with increasing crack separation ratio.

The mode II dimensionless SIF for crack B is shown in Figure 6.16b. It shows a similar trend to the mode I failure mode. When crack B is larger than crack A the effect of shielding on crack B is minimal, with the results almost identical to the single crack case. When the crack B is less than 80% of the size of crack A the presence of crack A greatly affects the mode II dimensionless SIF of crack B, especially at small crack separation ratios. For the cases where crack B is closed (Figure 6.15) the direction of the mode II dimensionless SIF of crack B (Figure 6.16b) reverses. This is because, as crack B is compressed shut by crack A, the faces of the crack are sliding relative to each other in the opposite manner to when crack B was open. Therefore, although cracks at this size ratio are closed and do not experience the mode I failure mode, the mode II failure mode is still present at the crack tip albeit significantly reduced in comparison to a single crack. The exact value for the mode II failure mode will be dependent on the friction coefficient between the crack faces when the crack is closed. As this is not the main focus here this has been kept constant at 0.3 throughout this work.

This Section has demonstrated the shielding effect that a crack has on its neighbour at an angle of 30° to the surface for a range of crack size and separation ratios. The key trends that have been found are given in Table 6.4. The range of dimensionless SIFs between the crack size and separation ratio intervals investigated are shown to be small. As a result the approximate, interpolated, results between these crack size and separation ratio intervals will retain good accuracy. To gain a clearer understanding of the shielding present between many similarly sized RCF defects in close proximity in the railhead Section 6.5 expands Study Two to investigate three different sized cracks. The additional shielding effect of a third crack has been demonstrated in Section 6.3.3.1 when considering three equally sized cracks.

Crack size ratio	Key trends
all c/b	Shielding effect is reduced with increasing crack separation ratio.
c/b≤0.7	Crack A (overlying crack) forces crack B (underlying crack) closed at crack separation ratios d/b=0.5. Crack A tends to single crack behaviour.
0.8≤c/b≤1	Shielding of crack A increases and shielding of crack B decreases as c/b increases. Effect of increasing crack separation ratio more pronounced for crack B.
c/b>1	Crack B behaves in similar manner to single crack. Effect of increasing crack separation ratio becomes more pronounced for crack A. Maximum shielding effect found for c/b=3.333.

Table 6.4: Key trends for two cracks at 30° to the surface with different size and separation ratios, c (crack depth of crack B), b (crack depth of crack A), d (crack separation ratio)

6.5 The Effect of Size and Separation Ratios for Three Cracks at 30° to the Surface

The detailed investigation of two cracks in Section 6.4.2 has demonstrated how the shielding effect on the cracks changes as the relative sizes of the cracks change. In order to better relate this to RCF defects the initial investigation into equally sized cracks showed a further shielding effect on the central crack of three (Section 6.3.3.1). This Section expands the two crack investigation to three cracks to further our understanding of similarly sized RCF type cracks in the railhead.

Equation 6.5 details the modelling requirements (N_{Models}) for the study. For the three crack investigation these requirements become significant, with the additional variants introduced by the third crack (Figure 6.17) increasing the modelling requirements for an exhaustive study to two hundred and forty times that of the two crack investigation.

$$N_{Models} = N_{Crack} \times (N_{CrackSizeRatio} \times N_{CrackSeparationRatio})^{(N_{Crack}-1)} \qquad (6.5)$$

Where N_{Crack} is the number of cracks considered, $N_{CrackSizeRatio}$ is the number of crack size ratios considered and $N_{CrackSeparationRatio}$ is the number of crack separation ratios considered.

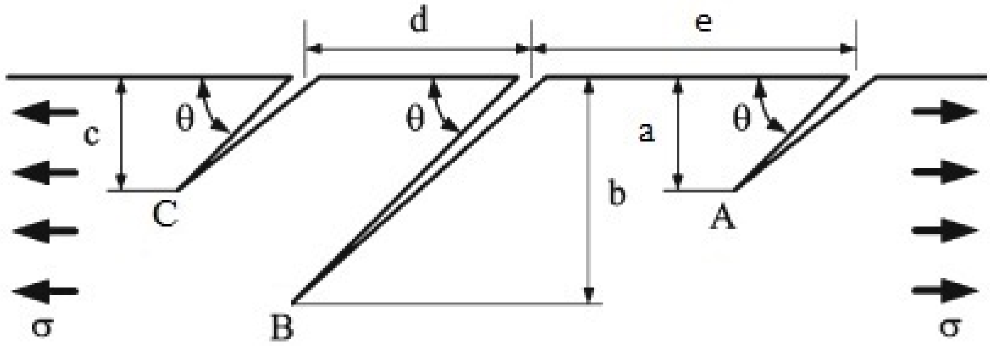

Figure 6.17: Diagram of crack configuration for three cracks in series under tensile stress σ, ϑ=30°. Figure adapted from Jin et al. [140]

To reduce the modelling requirements the three crack investigation only considers crack separation ratios of less than d=4b and e=4b, where the effect of crack separation was shown to be most significant for two cracks (Section 6.4). This reduced the modelling requirements for the three crack investigation by a factor of four to sixty times that of the two crack investigation.

The relative crack sizes and separations are shown in Figure 6.17. For each crack the relative size and separation of the other cracks are defined between size ratios of 0.1-1 and separation ratios of 0.5-4. From this a dimensionless SIF that is specific to the crack size and separation ratios, but is independent of the physical crack size, can be calculated. The results presented below are for the central crack B as this is most representative of a crack within a series of RCF defects. The results for crack A (overlying) and crack C (underlying) are shown in Appendix I.

6.5.1 Increasing Size of Crack A and Crack B Relative to Crack C

As in the previous Section key findings are presented in Table 6.5, with detailed description below. The mode I and mode II dimensionless SIF of the central crack B (F1B and F2B), as crack A and crack B increase in size relative to crack C until all cracks are of equal size, are shown in Figures 6.18-6.21, i.e. crack size ratios and crack separation ratios have been calculated using the fixed depth of crack C. Further results are given in Appendix I.2.

The results show that, as the crack separation ratio between crack C and crack B (d/c) increases, the degree of shielding experienced by crack B consistently decreases for all crack separation ratios between crack A and crack B (e/c). This is evident in Figure 6.18a where the dimensionless SIF of crack B when d=0.5c can be seen to be approximately half that when d=4c (effect is also seen in Figures I.7-6.21). Figure 6.18a also shows that when crack B is closed (mode I dimensionless SIF equal to zero) and that once crack B opens it rapidly tends towards a consistent degree of shielding (note the steep downward slope).

For all crack size ratios (b/c) where crack B is smaller than crack C and not forced closed by crack A the mode I and mode II dimensionless SIFs for d=0.5c are approximately 30% and 55% of the respective SIFs for the d=4c case. For the specific case when crack B is equal in size to crack C the respective mode I and mode II dimensionless SIFs for d=0.5c are approximately 60% and 75% of those for the d=4c case.

Increasing the size of crack A relative to crack B is shown to have an increased shielding effect on crack B as the separation ratio between crack A and crack B (e/c) decreases. This effect is seen regardless of the separation ratio between crack C and crack B (d/c). This increased shielding effect is shown to close crack B for cases when e<=2c (Figures 6.18 and 6.19, where the mode I dimensionless SIF of crack B is zero). However for all separation ratios the effect of crack A on crack B reduces significantly once crack B is 90% of the size of crack C.

When a=0.1c, the results are almost identical to the two crack case in Section 6.4.2. Therefore when crack A is 10% of the size of crack C, crack A has no effect on the behaviour of crack B for all crack separation ratios. The results showed that crack A has minimal shielding effect on the mode I and mode II dimensionless SIF of crack B whilst a<b, even when e=0.5c (Figure 6.18a). The shielding effect that crack A has on crack B reduces as the separation ratio (e/c) increases.

The results showed that when crack B (central crack) is smaller than crack C (overlying crack) but larger than crack A (underlying crack) the behaviour of the central crack is dominated by the overlying crack, with the crack separation ratio (d/c) dominating the degree of shielding of the central crack. However, when the underlying crack is greater than 90% of the size of the central crack, a further shielding effect on the central crack is present. For these cases the crack separation ratio between the underlying crack and the central crack (e/c) dominates whether or not crack closure of the central crack has occurred. As expected the shielding of the central crack reduces with increasing crack separation ratios for all cases. The findings when the overlying crack is the largest of the three are consistent with Section 6.4.2 when the central crack is more than 10% larger than the underlying crack. However, additional shielding is found when the underlying crack is greater than 90% of the size of the central crack. The main trends are summarised in Table 6.5.

Crack size or separation ratio	Key trends
d/c	Shielding effect is reduced with increasing crack separation ratios for all cases when crack B is open. Determines the extent to which crack B is shielded when crack B is open.
e/c	Shielding effect is reduced with increasing crack separation ratios when crack size ratio a/c>b/c. Determines the crack closure point of crack B.
a/c<b/c	Behaviour of crack B independent of crack size ratio a/c and separation ratio e/c. Degree of shielding of crack B is dictated by crack separation ratio d/c and is independent of crack size ratio b/c until b/c>0.9.
a/c>b/c	Crack B experiences increased shielding. Degree of shielding and closure of crack B is dominated by separation ratio e/c.

Table 6.5: Key trends for the central of three cracks at 30° to the surface with different size and separation ratios. Crack A (underlying) and crack B (central) increasing in size relative to crack C (overlying)

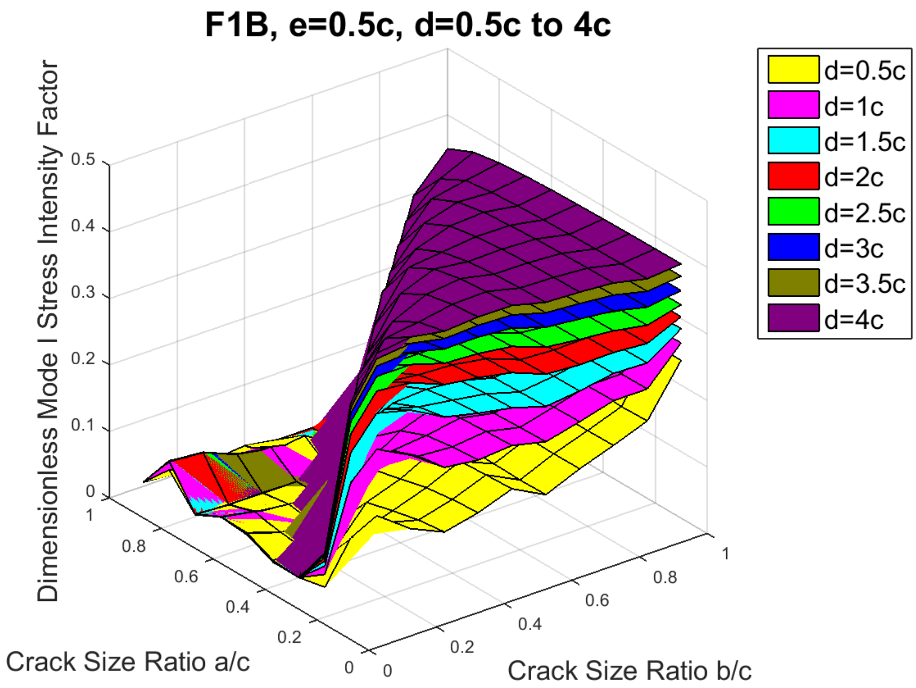

(a)

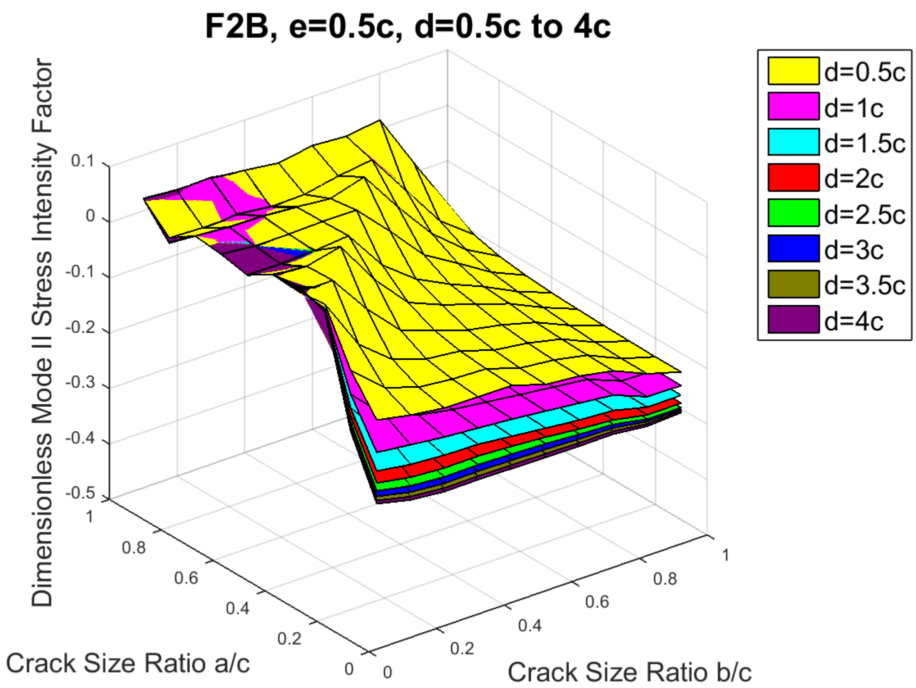

(b)

Figure 6.18: Mode I, (a), and mode II, (b), dimensionless stress intensity factor of Crack B as b=0.1c to 1c, a=0.1c to 1c and d=0.5c to 4c, e=0.5c

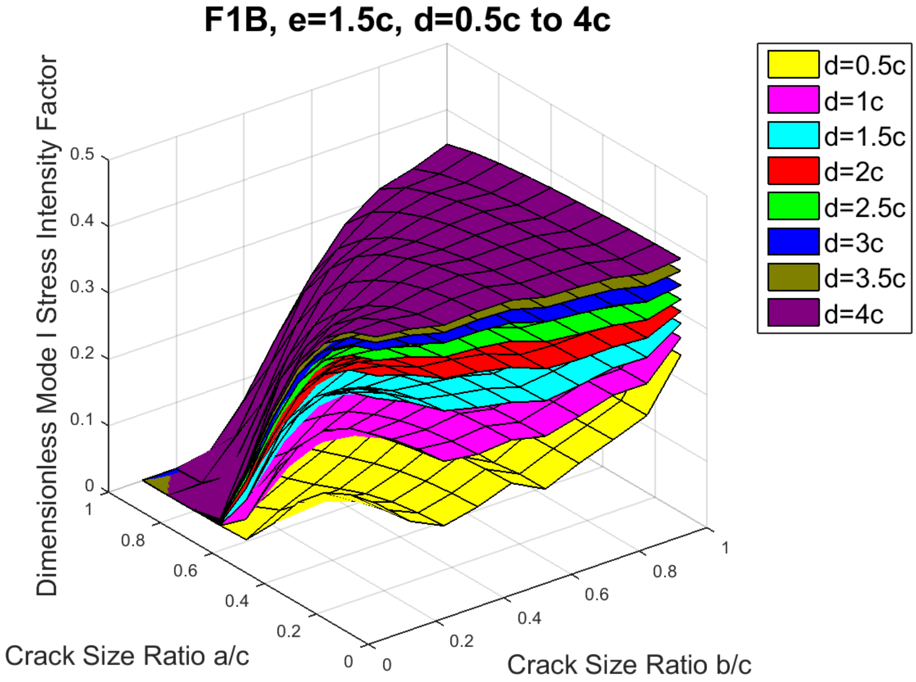

(a)

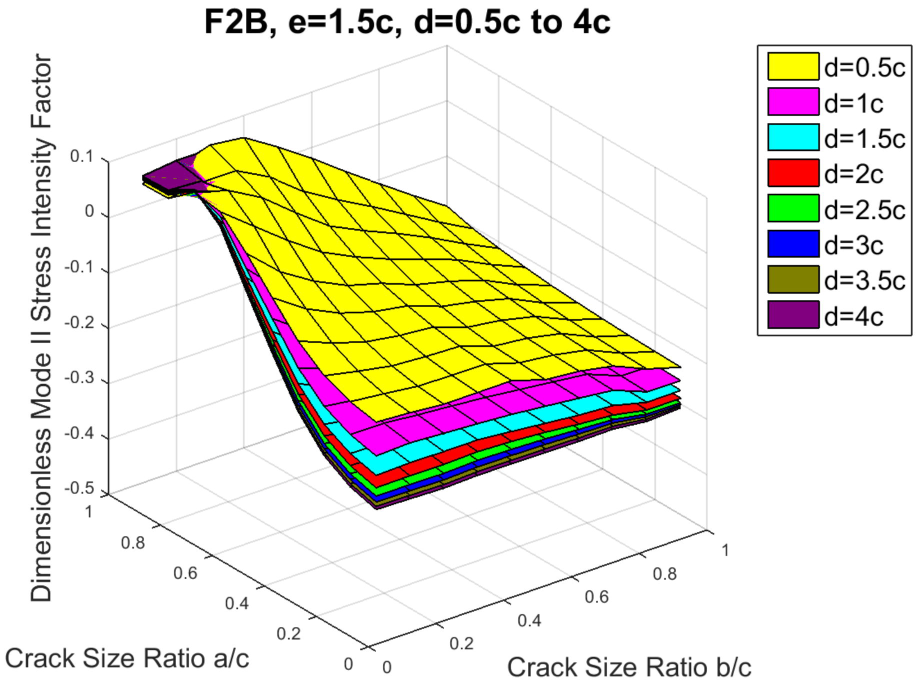

(b)

Figure 6.19: Mode I, (a), and mode II, (b), dimensionless stress intensity factor of Crack B as b=0.1c to 1c, a=0.1c to 1c and d=0.5c to 4c, e=1.5c

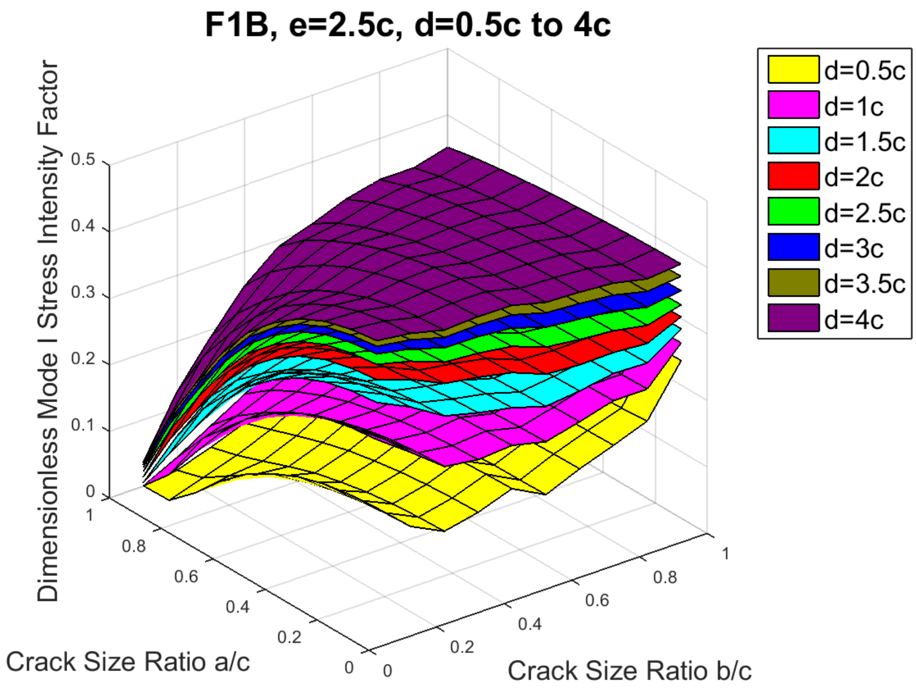

(a)

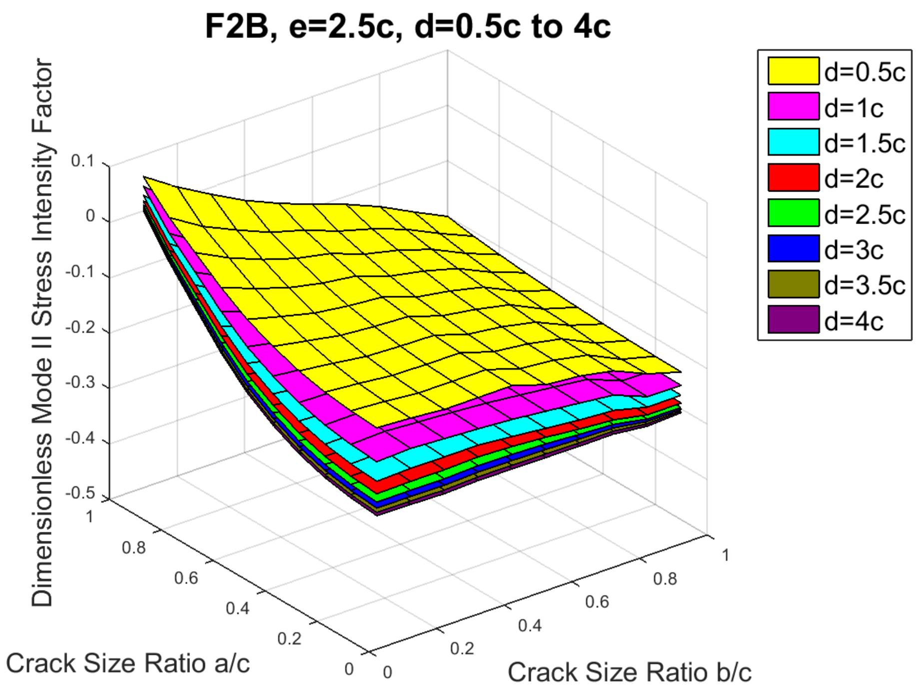

(b)

Figure 6.20: Mode I, (a), and mode II, (b), dimensionless stress intensity factor of Crack B as b=0.1c to 1c, a=0.1c to 1c and d=0.5c to 4c, e=2.5c

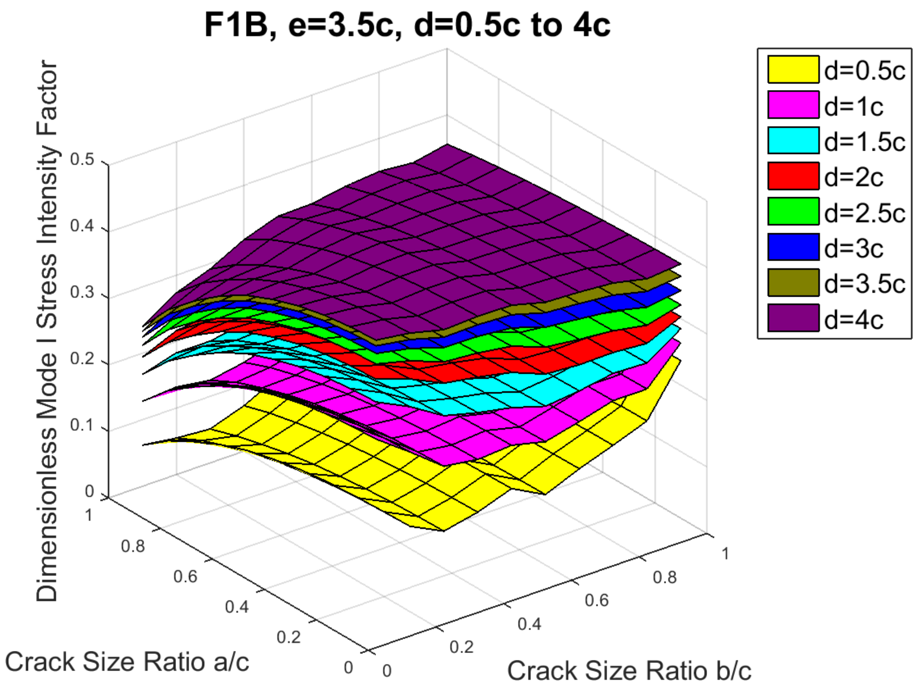

(a)

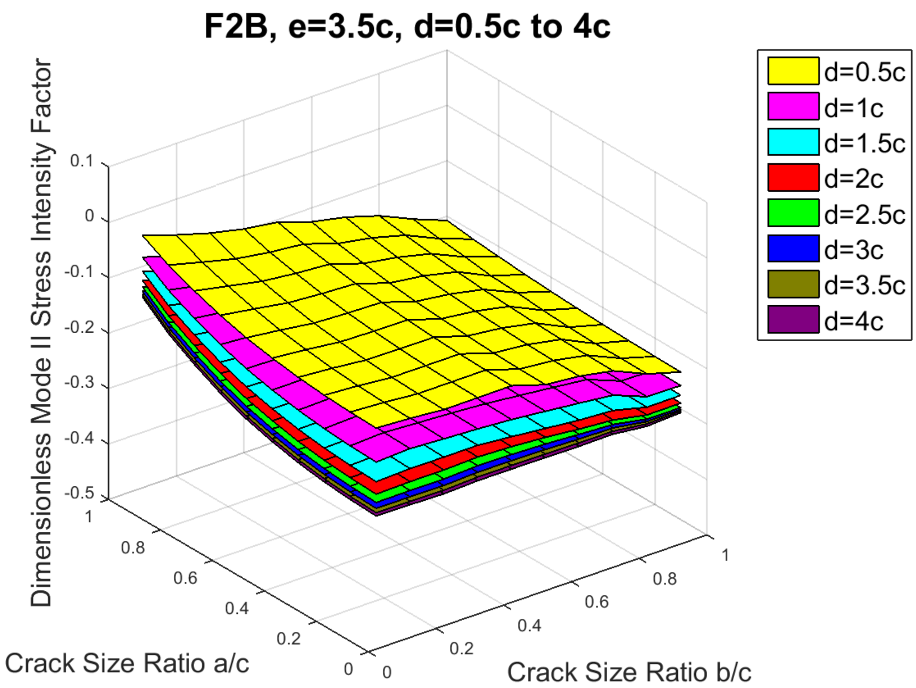

(b)

Figure 6.21: Mode I, (a), and mode II, (b), dimensionless stress intensity factor of Crack B as b=0.1c to 1c, a=0.1c to 1c and d=0.5c to 4c, e=3.5c

6.5.2 Increasing Size of Crack A and Crack C Relative to Crack B

The mode I and mode II dimensionless SIFs of crack B as crack A and crack C increase in size relative to crack B until all cracks are of equal size are shown in Figures 6.22-6.25, i.e. crack size ratios and crack separation ratios have been calculated using the fixed depth of crack B. Further results are given in Appendix I.2. The key findings are presented in Table 6.6, with detailed description below. For all separation ratios (both e/b and d/b) and size ratios (c/b) the mode I and mode II dimensionless SIF of crack B only reduce by 5% as the size ratio (a/b) of crack A increases from a=0.1b to a=0.8b (evident in the flat shape of the curve in Figure 6.22a as a/b increases). This increases to 20% reduction in mode I and mode II dimensionless SIFs of crack B when a=1b.

As the separation ratio (d/b) increased Crack C had an increased shielding effect on crack B as the crack size ratio (c/b) decreased. This is because Crack C became closed for smaller separation ratios and therefore no longer shielded crack B. Once crack C becomes large enough to open (crack size ratios c>=0.8b) then this trend is reversed, with decreasing separation ratio (d/b) increasing the shielding effect on crack B. This can be seen in Figure 6.22a where, for d=0.5b, the degree of shielding is unaffected by increasing crack size ratio c/b until c/b=0.8. At which point the degree of shielding on crack B increases significantly. This trend is consistent throughout Figures 6.22-6.25.

The results show that when the overlying crack (crack C) and the underlying crack (crack A) are smaller than the central crack (crack B) the behaviour of the central crack is dominated by the size and separation of the central crack relative to the overlying crack. The underlying crack did not add any further significant shielding effect onto the central crack until it was at least 90% of the size of the central crack, with the central crack's behaviour being independent of the crack separation ratio between the underlying and central cracks. It was also shown that, when the crack size ratio between the overlying and central cracks was reduced, the central crack tended towards single crack behaviour for any crack separation ratio between the overlying and central cracks. The findings when the central crack is the largest of the three are consistent with Section 6.4.2 where the behaviour of the underlying crack tended towards single crack behaviour when the overlying crack's relative sized decreased; the trend only varying from the two crack findings when the underlying crack was at least 90% of the size of the central crack. The main trends are summarised in Table 6.6.

Crack size or separation ratio	Key trends
d/b	As d/b increases, increased shielding of crack B for crack size ratios c/b<0.8, decreased shielding of crack B for c/b>=0.8. Dictates the point at which crack B enforces crack closure of crack C.
e/b	Behaviour of crack B independent of crack separation ratio e/b.
a/b	Behaviour of crack B independent of crack size ratio a/b for crack size ratios a<0.9b.
c/b	As crack size ratio c/b increases, increased shielding on crack B, especially as crack separation ratios d/b decreases. Behaviour of crack B independent of crack size ratio c/b when crack C is closed.

Table 6.6: Key trends for the central of three cracks at 30° to the surface with different size and separation ratios. Crack A (underlying) and crack C (overlying) increasing in size relative to crack B (central)

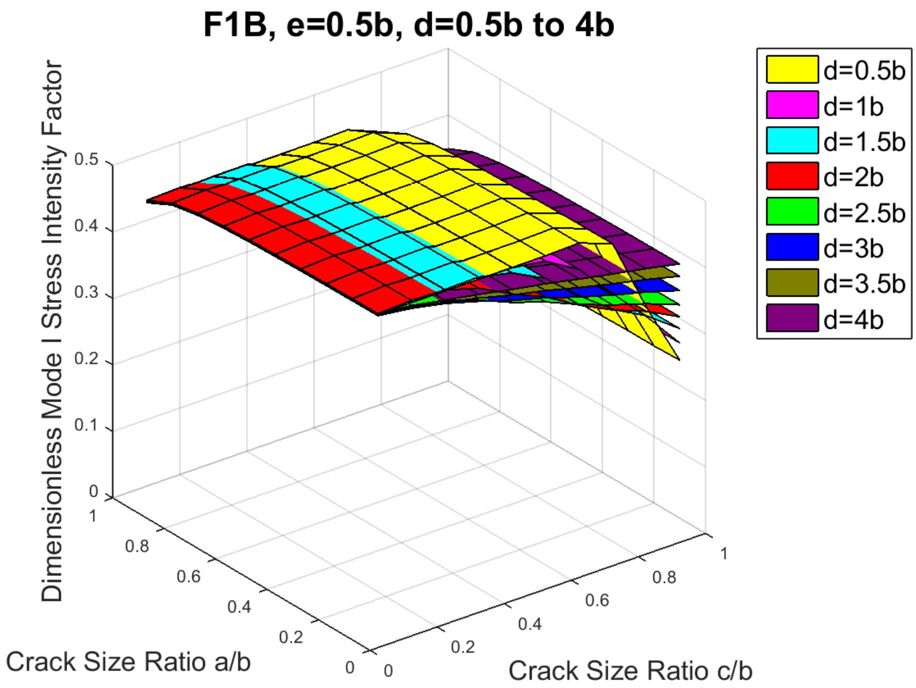

(a)

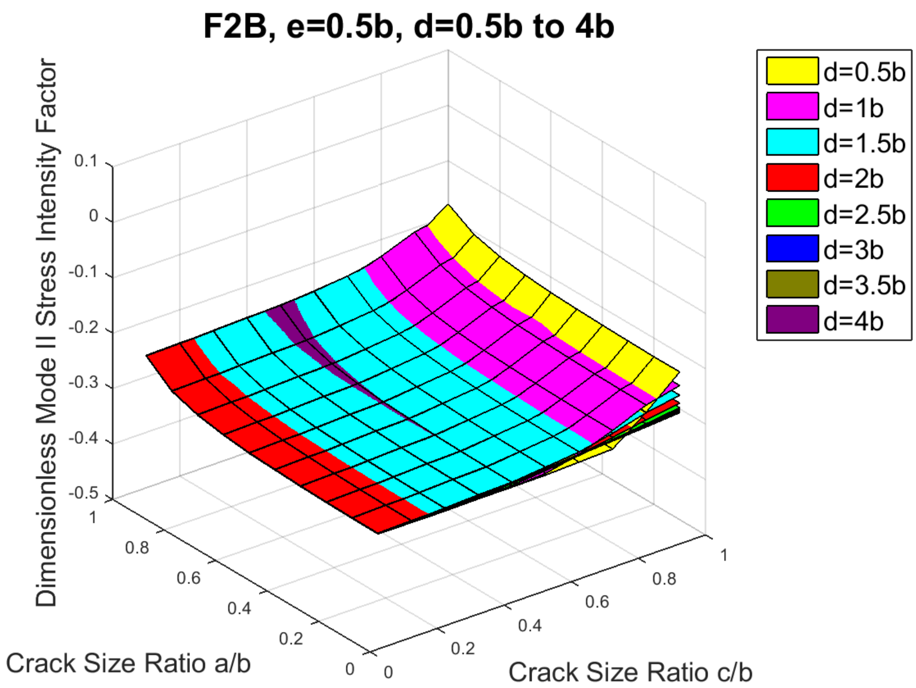

(b)

Figure 6.22: Mode I, (a), and mode II, (b), dimensionless stress intensity factor of Crack B as a=0.1b to 1b, c=0.1b to 1b and d=0.5b to 4b, e=0.5b

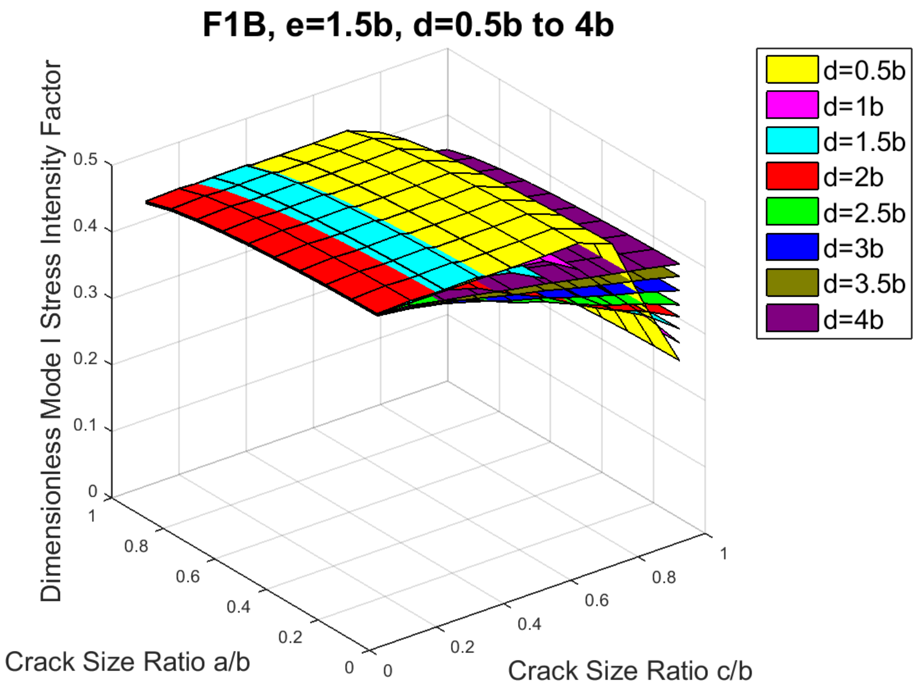

(a)

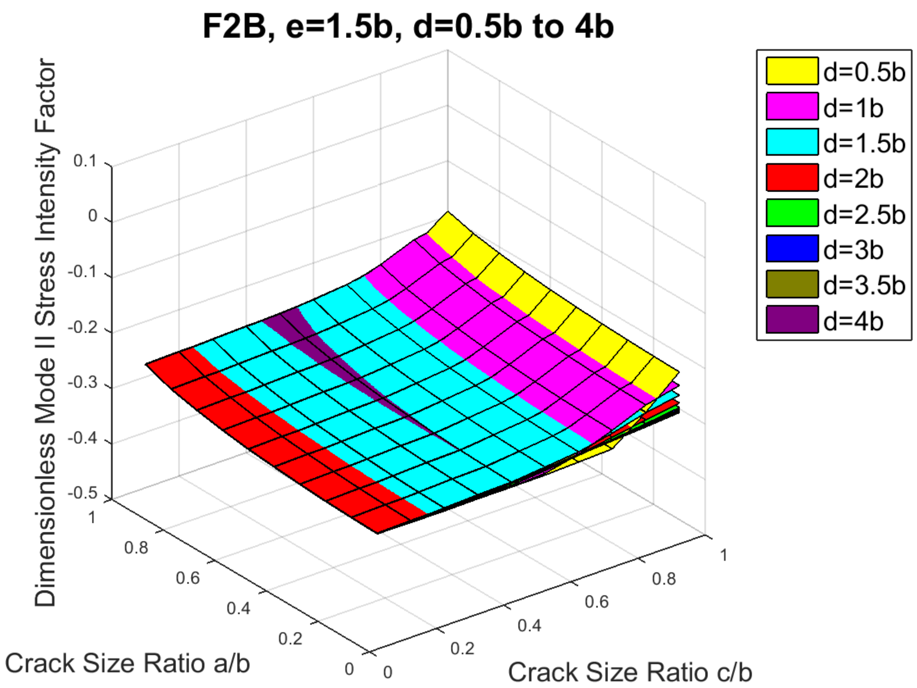

(b)

Figure 6.23: Mode I, (a), and mode II, (b), dimensionless stress intensity factor of Crack B as a=0.1b to 1b, c=0.1b to 1b and d=0.5b to 4b, e=1.5b

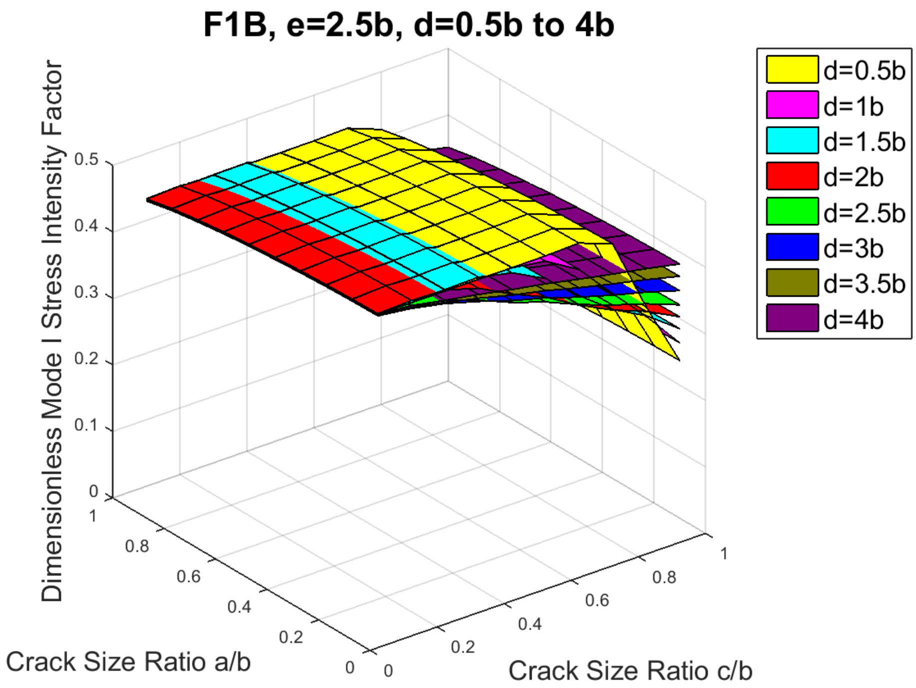

(a)

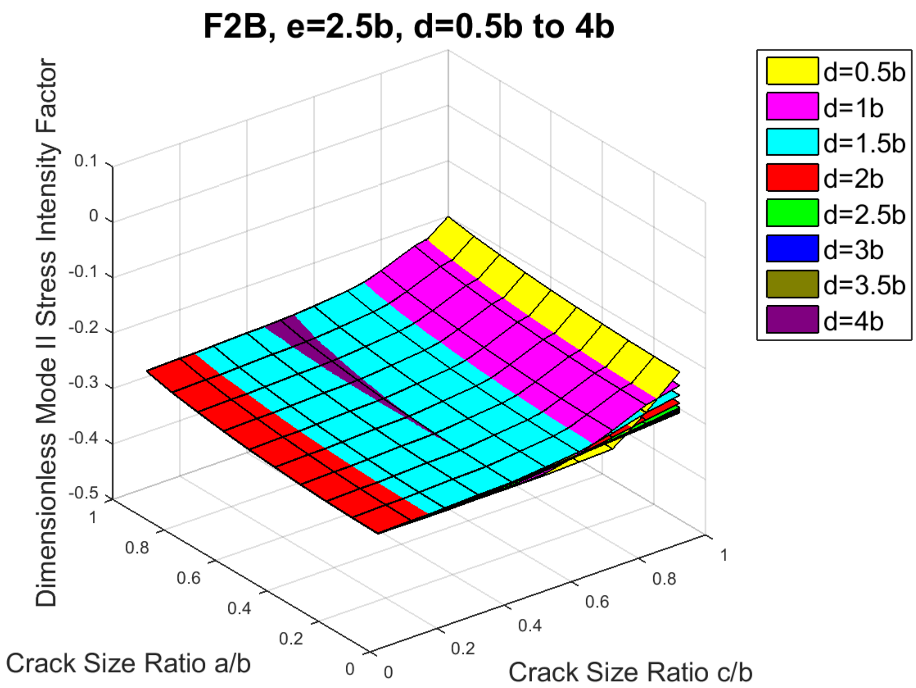

(b)

Figure 6.24: Mode I, (a), and mode II, (b), dimensionless stress intensity factor of Crack B as a=0.1b to 1b, c=0.1b to 1b and d=0.5b to 4b, e=2.5b

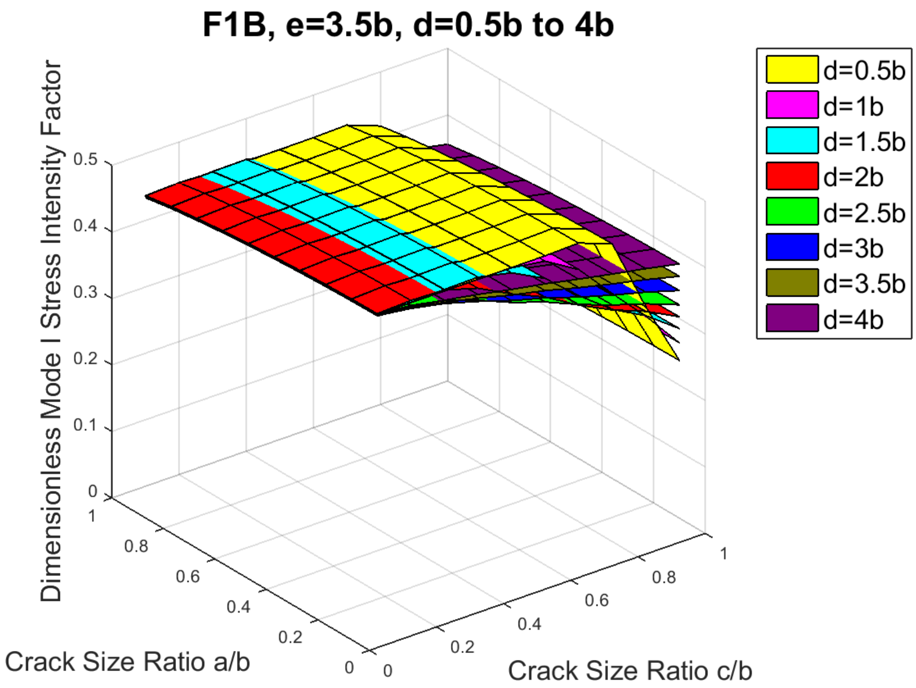

(a)

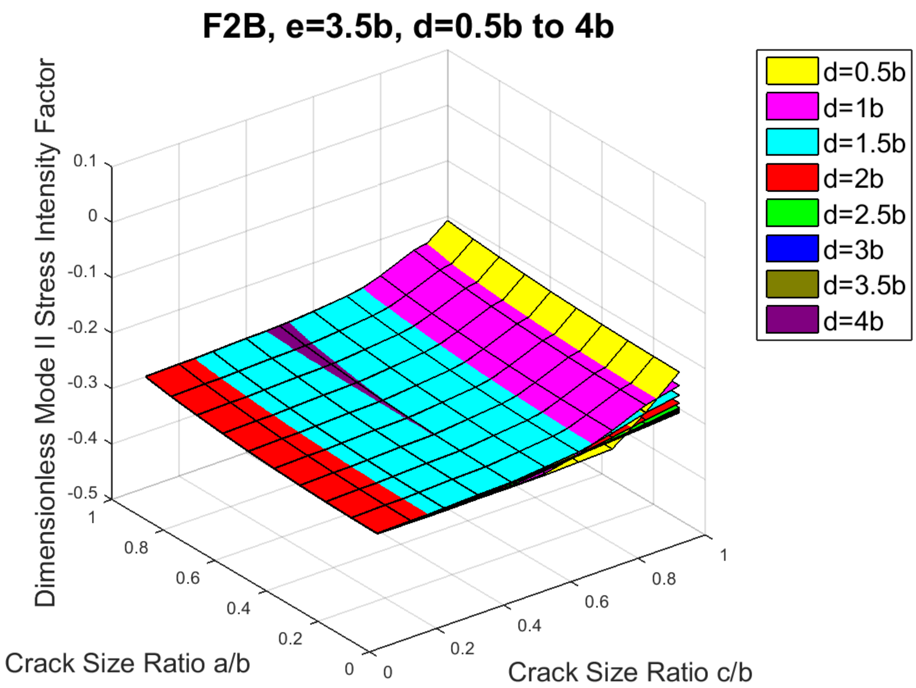

(b)

Figure 6.25: Mode I, (a), and mode II, (b), dimensionless stress intensity factor of Crack B as a=0.1b to 1b, c=0.1b to 1b and d=0.5b to 4b, e=3.5b

6.5.3 Increasing Size of Crack B and Crack C Relative to Crack A

The mode I and mode II dimensionless SIFs of crack B as crack B and crack C increase in size relative to crack A until all cracks are of equal size are shown in Figures 6.26-6.29, i.e. crack size ratios and crack separation ratios have been calculated using the fixed depth of crack A. Further results are given in Appendix I.2. The key findings are presented in Table 6.7, with detailed description below. For these results significant errors were found in the results for crack size ratio b=0.7a and b=0.9a so no data are available for these crack separation ratios. This was thought to be due to an error in model generation using the automatic script.

As can be seen when crack A is larger than crack B the crack size ratio (b/a) between crack B and crack A dictates the point of crack closure for crack B for all crack separation ratios (e/a and d/a). The crack size ratio (c/a) of crack C has negligible effect on mode I and mode II dimensionless SIFs of crack B when crack B is closed. However once crack B opens crack C has a further shielding effect on crack B over that of crack A in isolation. This occurs at all separation ratios (d/a and e/a), with the degree of shielding of crack B increasing as the crack separation ratio (d/a) between crack C and crack B decreases. The point at which the size ratio (c/a) of crack C is sufficient to impact the dimensionless SIF of crack B also varies depending on the crack separation ratio (d/a). For d=0.5a (Figure 6.26a) crack C significantly increases the shielding of crack B, but only for crack size ratios c>0.5b. This can be seen by the steep drop in the curves in Figure 6.26a. However, for d=3.5a (Figure 6.29) crack C increases the shielding of crack B at all size ratios (b/a and c/a), although to a lesser degree overall (these curves can be seen to be less steep than those in Figure 6.26a).

For example, when d=0.5a, e=4a, b=0.5a and c=1a (Figure 6.26a), the mode I dimensionless SIF of crack B decreases to 25% of that found when c=0.1a. When c=0.5a this increases to 54% of that found when c=0.1a. When c=0.2a this increases to approximately equal to that found when c=0.1a. However, when d=3.5a, e=4a, b=0.5a and c=1a (Figure 6.29), the mode I dimensionless SIF of crack B decreases to 87% of that found when c=0.1a. When c=0.5a this increases to 95% of that found when c=0.1a. When c=0.2a this increases to 99% of that found when c=0.1a.

The results show that when the central crack is smaller than the underlying crack the crack separation ratio between the central crack and the underlying crack determines the relative size at which the central crack will open. When the central crack is open the degree of shielding on the central crack decreases as the size ratio between the central crack and the underlying crack increases. In addition, the overlying crack further shields the central crack when the overlying crack is greater than 50% of the size of the central crack (i.e. when the overlying crack is open it additionally shields the central crack). This means that the central crack is forced closed by the shielding effect of nearby cracks for larger crack size ratios than those that occurred in the two crack investigation. The largest shielding effects from the overlying crack onto the central crack are found at the smallest crack separation ratios. The shielding effects decreases with increasing crack separation ratios.

The findings when the underlying crack is the largest of the three are consistent with Section 6.4.2 when the central crack is twice as large as the overlying crack. At this point the overlying crack is closed from the shielding from the central crack. However, additional shielding is found when the overlying crack is greater than half the size of the central crack. This additional shielding enforces crack closure of the central crack at larger size ratios than predicted by the two crack analysis. The main trends are summarised in Table 6.7.

Crack size or separation ratio	Key trends
d/a	Reduced additional shielding effect on crack B from crack C (for the cases when crack C is open) with increasing crack separation ratio.
e/a	Determines the point of crack opening for crack B. Shielding effect is reduced with increasing crack separation ratio.
b/a	Shielding effect on crack B is reduced with increasing crack size ratio. Especially for the cases when b<c as well
c/a	Shielding effect on crack B is increased with increasing crack size ratio. Enforces crack closure of crack B for larger sizes of crack B than predicted by the two crack analysis.

Table 6.7: Key trends for the central of three cracks at 30° to the surface with different size and separation ratios. Crack B (central) and crack C (overlying) increasing in size relative to crack A (underlying)

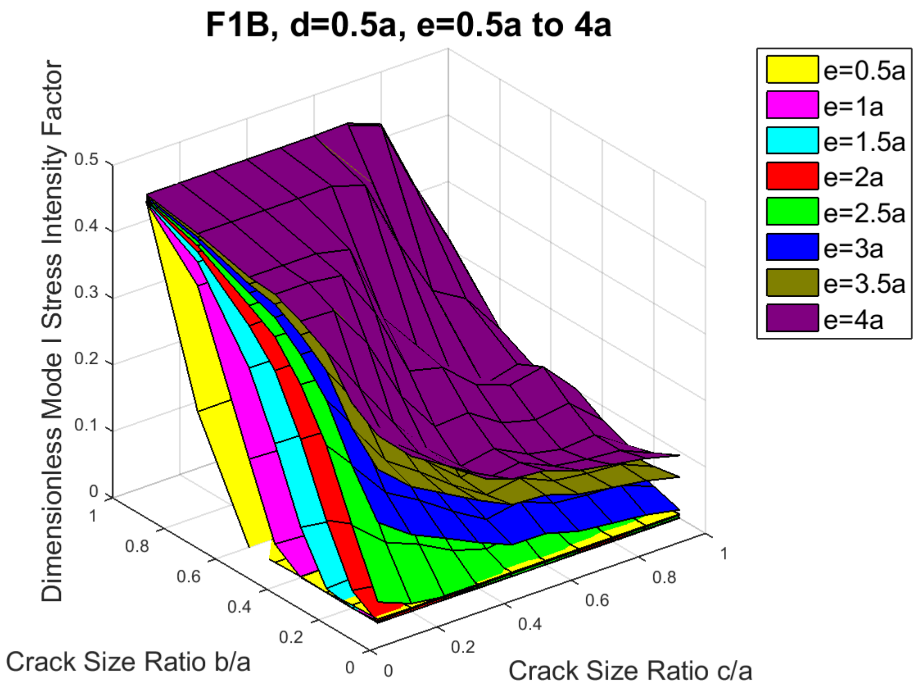

(a)

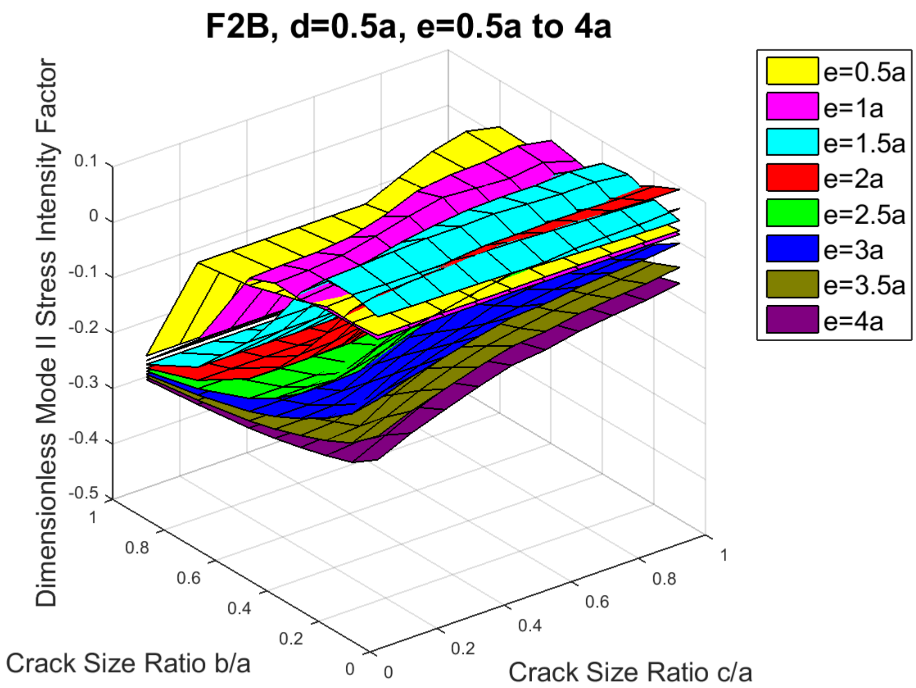

(b)

Figure 6.26: Mode I, (a), and mode II, (b), dimensionless stress intensity factor of Crack B as b=0.1a to 1a, c=0.1a to 1a and e=0.5a to 4a, d=0.5a

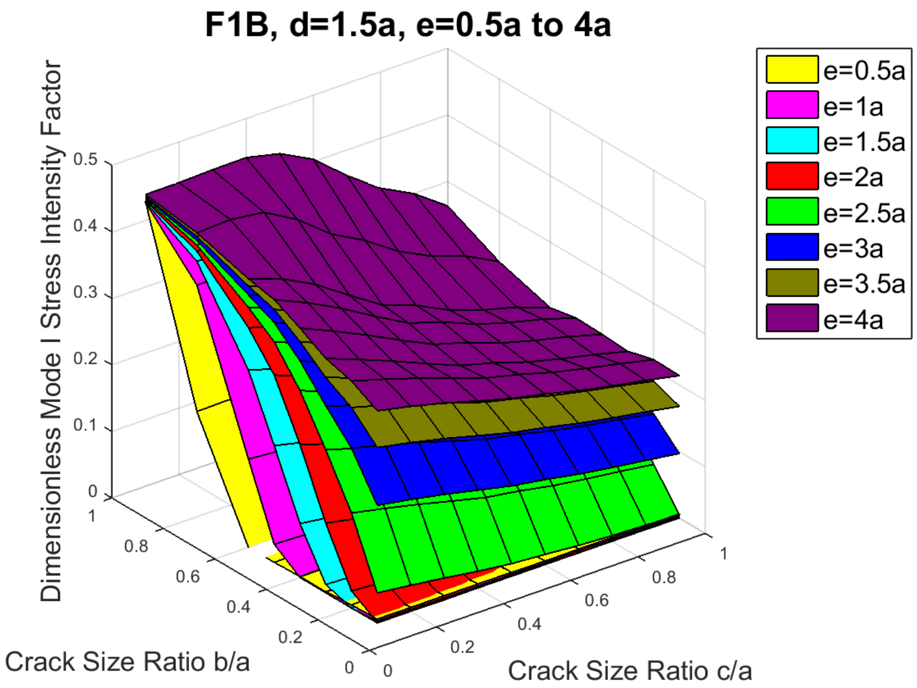

(a)

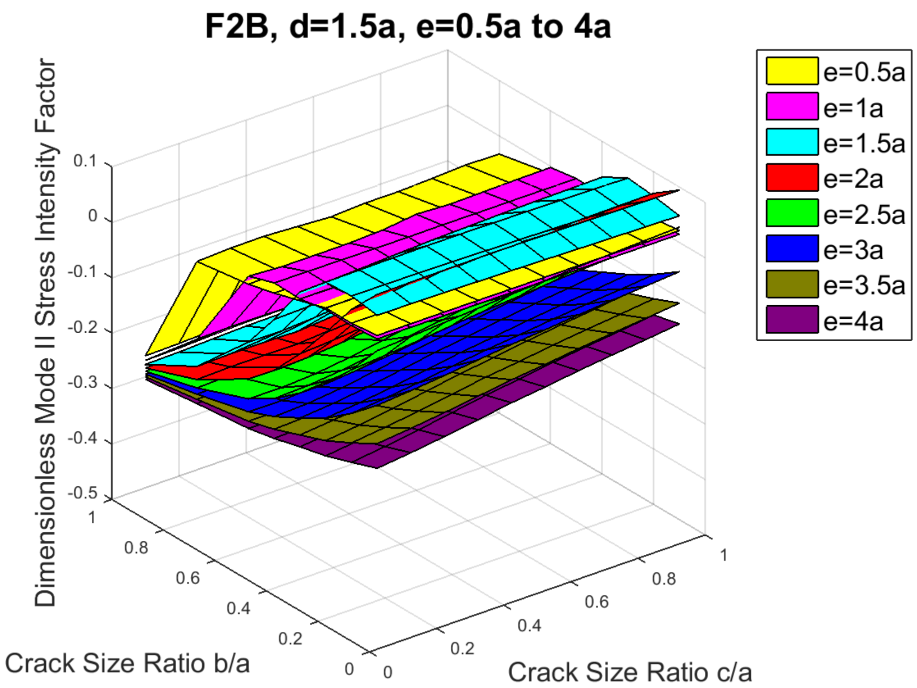

(b)

Figure 6.27: Mode I, (a), and mode II, (b), dimensionless stress intensity factor of Crack B as b=0.1a to 1a, c=0.1a to 1a and e=0.5a to 4a, d=1.5a

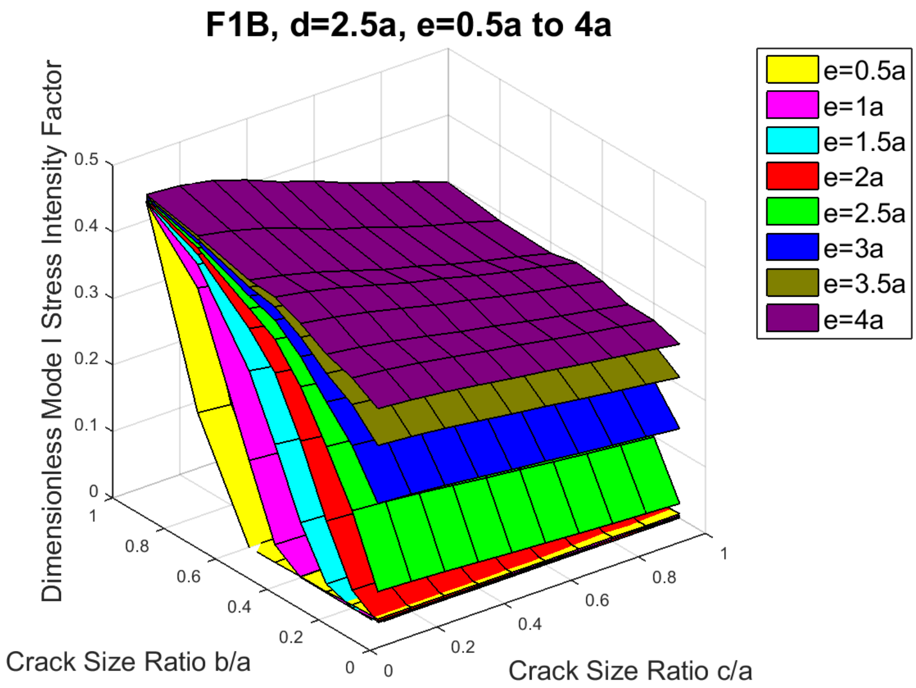

(a)

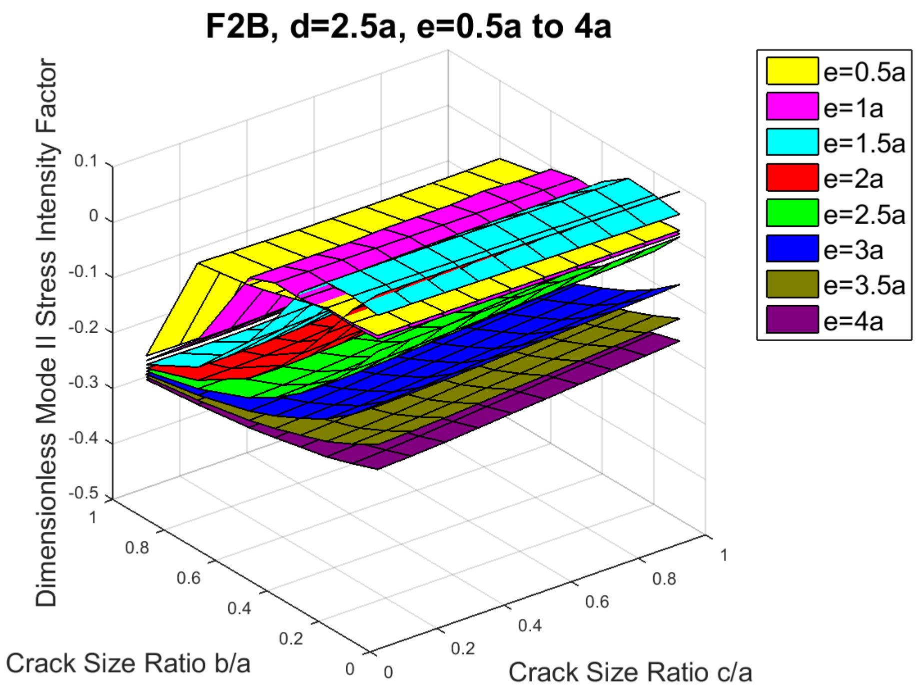

(b)

Figure 6.28: Mode I, (a), and mode II, (b), dimensionless stress intensity factor of Crack B as b=0.1a to 1a, c=0.1a to 1a and e=0.5a to 4a, d=2.5a

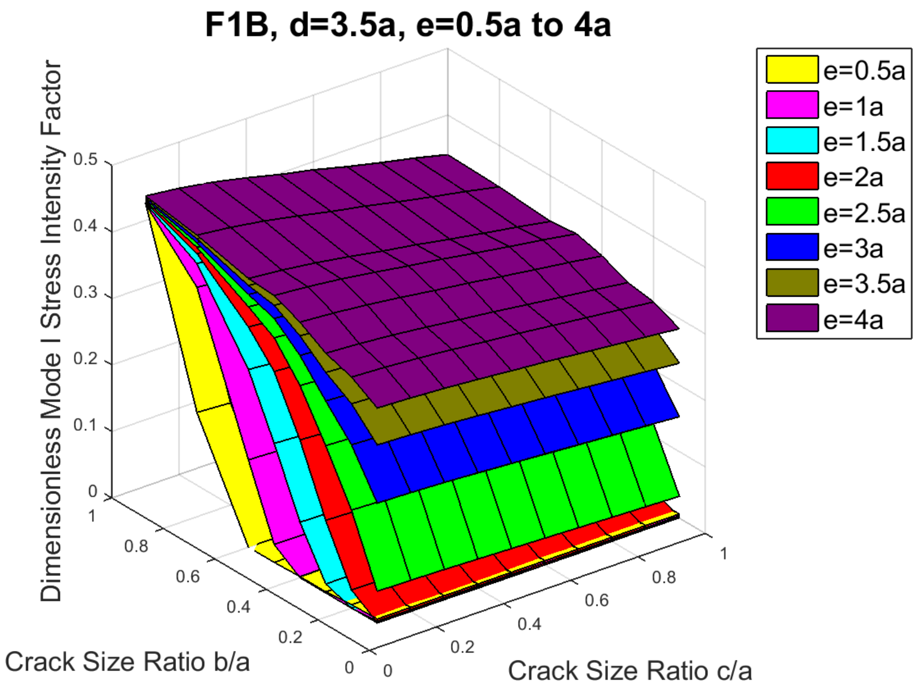

(a)

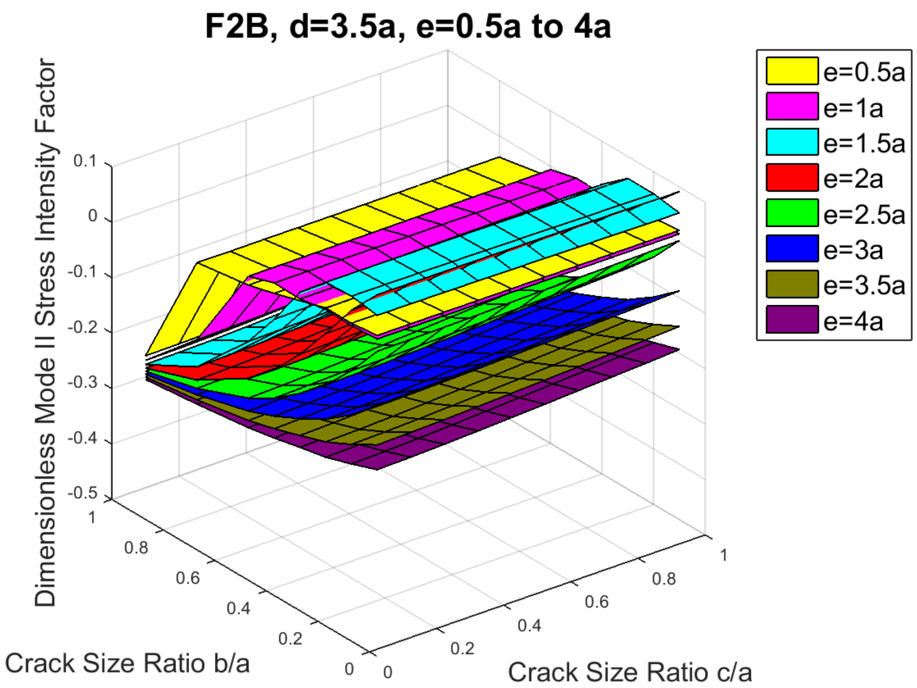

(b)

Figure 6.29: Mode I, (a), and mode II, (b), dimensionless stress intensity factor of Crack B as b=0.1a to 1a, c=0.1a to 1a and e=0.5a to 4a, d=3.5a

6.5.4 Point of Crack Closure: Multiple Cracks of Different Sizes

For the two dimensional study in the previous Sections an example where the central crack is at the point of closure is when the central crack is 8mm with overlying and underlying cracks of 10mm. In this Section the SIF for the semi-elliptical case of an 8mm central crack with overlying and underlying cracks of 10mm is investigated. As discussed in Chapter 5 the extensive run times of the three dimensional approach limited the number of crack configurations that it was practical to investigate and here only one case is presented.

In Figure 6.30 the case of three 10mm cracks with 5mm spacing is compared to three cracks with an 8mm central crack and overlying and underlying cracks of 10mm. The two dimensional SIF results for three cracks with an 8mm central crack and overlying and underlying cracks of 10mm is shown with the dashed horizontal lines in Figure 6.30.

The presence of a smaller central crack is shown to have an effect on the mode I and mode II SIF of all three cracks. The mode I and mode II SIF of both the overlying and underlying cracks has increased slightly and the SIF of the central crack has decreased. This is because the degree of shielding on the central crack has increased.

However, the SIF for the three dimensional case reduces by a factor of two in comparison to the factor of ten for the two dimensional case. This means that, unlike the two dimensional case, the 8mm central crack of three semi-elliptical cracks is not closed. Although the degree of shielding of the 8mm central crack has still increased significantly relative to the case of equally sized cracks, it is less significant than the reduction found with the two dimensional planar crack approximation. This demonstrates that the two dimensional planar crack approximation overestimates the degree of shielding between cracks in close proximity.

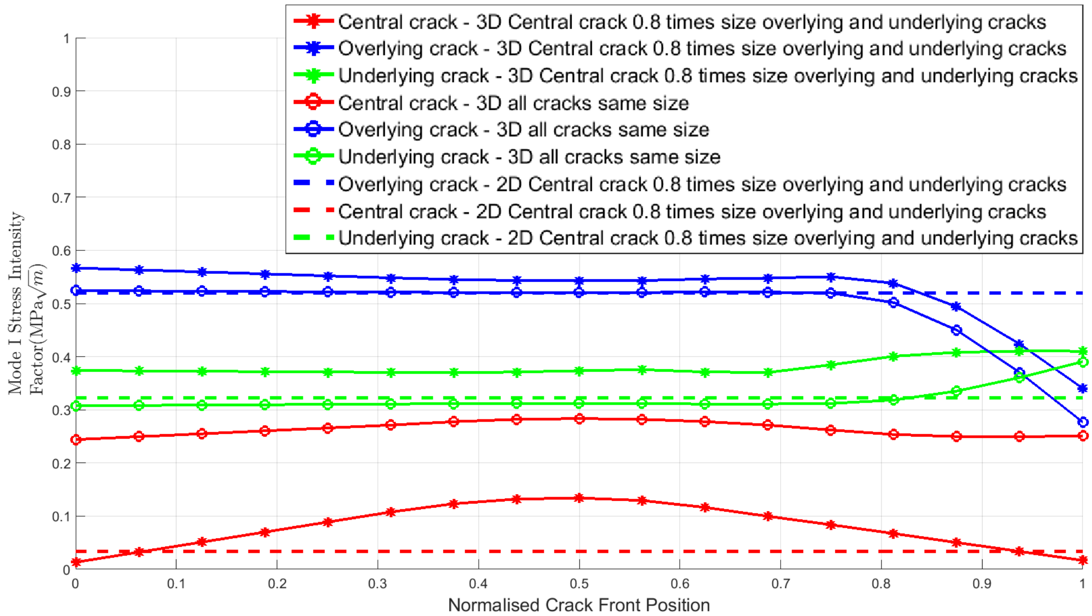

(a)

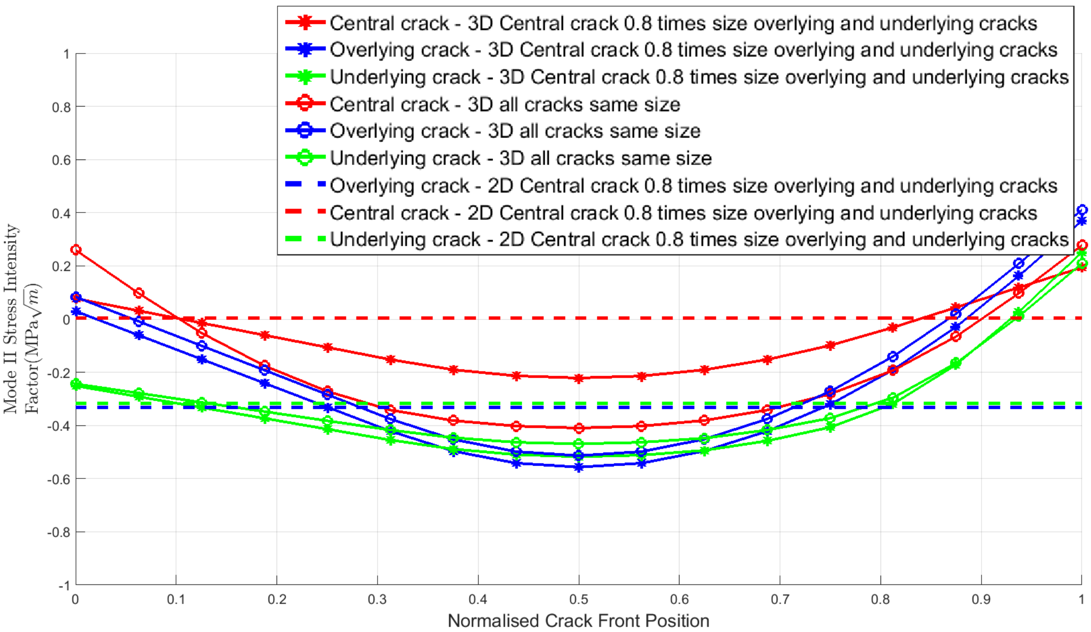

(b)

Figure 6.30: Comparison between stress intensity factor results from three 10mm cracks with 5mm spacing and three cracks with an 8mm central crack and overlying and underlying cracks of 10mm (both two dimensional and three dimensional), (a), mode I, (b), mode II

6.6 Conclusions

In this Chapter the shielding effects present when multiple cracks are in close proximity was investigated. Study One demonstrated that the BE approach is a suitable technique for this type of investigation. It was found that eleven equally sized cracks gave equivalent results to a hundred equally sized cracks in close proximity, but that the results for three cracks only overestimated the SIF by 10%. Therefore for studies designed to approximate hundreds of equally sized cracks in close proximity, the findings demonstrate that a minimum of three equally sized cracks are required in the model.

The comparison between the three dimensional and two dimensional approaches suggested that the thin planar geometry used in the two dimensional approach removed the need to apply the conversion factor to the mode II SIF. The relationship between the two dimensional approach and three dimensional approach was shown to hold true for multiple equally sized cracks in close proximity.

Study Two developed the method from Study One and was successfully validated against previous studies reported in the literature over a range of crack angles, sizes and separation ratios. For two cracks with varying size and separation ratios the interpolated results calculated from the method developed here showed good correlation with previous work. This means, providing that the solution intervals are small, a good approximation to the dimensionless SIF for any crack size and separation ratio, even in the transition between open and closed cracks, can be found. It is therefore possible to conclude that it is not necessary to give an explicit solution for each crack separation and sizing ratio.

In contrast to the findings for equally sized cracks, once the cracks are of unequal size, the effect of shielding is most pronounced on the overlying crack for cases when it is smaller than the underlying crack, especially at smaller separation ratios. For these cases the underlying crack can force the overlying crack to remain closed at a considerable range of crack separation and size ratios. Only when the overlying crack was 80% of the size of the underlying crack will it remain open for small crack separation ratios. The underlying crack was found to trend towards single crack behaviour when the overlying crack was closed.

New research into two equally sized cracks at 30° to the surface using Study Two demonstrated that the overlying crack experienced more shielding then the underlying crack. However, this was still to a lesser extent than for the central crack of three. Study Two was expanded to include three cracks of different size and separation ratios at 30° to the surface. This new research found that, when the central crack is smaller than the overlying crack but larger than the underlying crack, the behaviour of the central crack is dominated by the overlying crack. In these cases the crack separation ratio between the overlying crack and the central crack dominated the shielding of the central crack. However, when the underlying crack was also larger than the central crack a further shielding effect on the central crack was found to occur. With the crack separation ratio between the underlying crack and the central crack dominating whether the central crack was closed or open. As expected the central crack experienced reduced shielding as the crack separation ratios increased.

When the overlying crack and the underlying crack are smaller than the central crack the behaviour of the central crack is dominated by its relationship to the overlying crack. The underlying crack did not affect the amount of shielding of the central crack until it was 90% of the size of the central crack, with the central crack tending towards single crack behaviour as the crack separation ratio between the overlying crack and the central crack (c/b) decreased.

When the central crack was smaller than the underlying crack the behaviour of the central crack was determined by the separation ratio between the underlying crack and the central crack until the central crack was large enough to open. When the central crack was open the overlying crack additionally shielded the central crack when it was over 50% of the size of the central crack.

A greater level of crack stress shielding is experienced in two dimensional in comparison to three dimensional modelling of RCF cracks, although the SIF of the central semi-elliptical crack has still reduced significantly. However, this requires further investigation to corroborate and understand the significance to the results.

The new method developed here has furthered understanding of how multiple RCF cracks within the rail "communicate", i.e. influence one another's growth. It has demonstrated that, when cracks are of a similar size, they experience significant shielding effects from their overlying and underlying neighbours. When cracks are large compared with their neighbours they tend towards single crack behaviour. The next stage of development of this work is to investigate whether cracks continue to communicate under wheel loads, or if they act independently. It is expected that this may provide an explanation for the uniform crack separations frequently observed in rail RCF. However, while the work here informs and sets an agenda for this further investigation, developing and undertaking such a study is beyond the scope of this thesis.

Chapter 7

Concluding Remarks and Further Work

7.1 Introduction

This thesis builds upon the existing body of published work on the interaction of multiple cracks. It has shown how multiple cracks interact when they are of non-uniform size and occur at non-uniform separations. Both two dimensional and three dimensional boundary element approaches were developed and validated for the investigation. This has increased the understanding of rolling contact fatigue cracks within the rail, which tend to occur as a series of similarly sized, closely spaced cracks.

In addition, a new, geospatial, method sought locational correlation between rolling contact fatigue sites that were not generated by cornering forces or other known mechanisms and low adhesion events or underbridges. This analysis employed an investigatory method from the field of Geography and applied it to the rail scenario, providing a visual method for the display of locational correlations. Finally, a quasi-static approach was developed and used to find how the bending moment within the rail is affected by different types of support stiffness transitions, abrupt and gradual.

Each of the Chapters within this thesis draws its own conclusions. Here the main conclusions from each Chapter have been brought together. Avenues of further work that are possible using the approaches developed within this thesis are then discussed.

7.2 Summary of Conclusions

In Chapter 3 moving window filtering and geospatial techniques were used to investigate locational correlations between wheel slide protection events, rolling contact fatigue sites, underbridge and geographical data. It showed that there was a statistically significant increase in rolling contact fatigue adjacent to an underbridge and strong correlation between momentary slides and underbridge locations. However, no correlation between the likelihood of long slides and underbridge locations was found.

The increase in both the likelihood and the average number of momentary slide events per analysis window (i.e. per 80m examination length along the rail) in the same analysis window as a rolling contact fatigue site supports the hypothesis that locational correlation exists between momentary slides and rolling contact fatigue sites (but is not a causal link). This was corroborated by the geospatial distribution findings which demonstrated locational correlation at 40% of the rolling contact fatigue sites.

The geospatial analysis highlighted that braking on a descending track was the most likely track gradient to experience severe wheel slides. Nearby woodland, cuttings and nearby roads were highlighted as factors that correlated with low adhesion. The temporal analysis showed that low adhesion occurred outside the autumn period and therefore cannot be solely attributed to leaf fall. It was found that 55-60% of the annual total of wheel slide protection events occurred outside of the autumn period. It also showed that the time period where low adhesion is most prevalent falls within the busy morning period, but that the highest risk period for an individual train is the very early morning.

In Chapter 4 the effect of the proximity of wheel loads to each other (such as is the case with the bogie configuration) on the bending moment generated within the rail was investigated. The Winkler foundation approach found that the bending moment within the rail doubled in comparison to a single wheel load when a secondary nearby wheel load was considered. Improvements to the discrete support approach developed by Beagles [2] led to a removal of the need to consider the relative distance between the support and wheel positions.

Abrupt stiffness changes within the track were found to increase the peak positive bending moments within the rail in comparison to uniform stiffness ballasted track. The location of this peak positive bending moment was found to be dictated by the location of the stiffness change. The inclusion of a transition zone over a distance as short as ten sleepers (6m) led to a significant reduction of the whole rail bending in comparison to an abrupt stiffness change. It was found that the location of the peak positive rail bending moment was independent of the stiffness change with a gradual transition. Therefore the discrete support method successfully demonstrated the variation between different types of transitions using a simple quasi-static approach.

The inclusion of multiple wheel loads in close proximity to each other was found to be a critical factor that must be considered when investigating crack growth. The peak positive bending moment generated by multiple wheel loads in close proximity was found to increase the stress intensity factor of cracks within the rail by a factor of two. For multiple cracks within the rail (of 10mm radius and at 30° to the rail surface) this increased the equivalent stress intensity factor (ΔK_{eq}) generated by whole rail bending to above fatigue crack growth threshold levels (ΔK_{th}), leading to crack growth.

The peak negative rail bending moment was used within the three dimensional boundary element approach to investigate the mode II stress intensity factor of a single crack near to (but not directly underneath) the contact. The results suggested that use of this simple rail bending approach is sufficient to find an approximation to the peak negative mode II stress intensity factor used to calculate ΔK_{II} in the crack growth equations. Therefore, when calculating the crack growth rate, the amount of computing time required for a complex contact model can be approximately halved.

In Chapter 5 the considerations that need to be taken into account when developing a boundary element method were discussed. At the end of the Chapter the validity of the approach was demonstrated against published literature for the three dimensional method. Several scripts were developed to automate the load application, enabling many more runs to be undertaken than if this had been done manually. These scripts are given in Appendix D. The three dimensional approach also showed that the application of the bending moment could be approximated as a tensile stress for semi-elliptical defects with lengths as large as 10mm and inclined at 30° to the rail surface.

The effect of the presence of the crack on the wheel-rail contact pressure distribution was then investigated. Modelling of the wheel-rail contact was found to be extremely computationally expensive and other options were explored to reduce this burden. The

Herztian pressure profile was found to be a suitable approximation of the wheel-rail contact when over an RCF crack. Although preliminary results were found using this approach, it was still computationally expensive and it was therefore decided to pursue the two dimensional approach for the detailed multiple crack investigation.

In Chapter 6 the shielding effects present when multiple cracks are in close proximity were investigated. The approach was successfully validated against previous work over a range of crack angles, size ratios and separation ratios. Comparisons were drawn between the two dimensional and three dimensional boundary element approaches. The two dimensional approach was shown to give a good approximation of both the mode I (with conversion factor applied) and mode II (without conversion factor applied) SIF. The thin planar geometry used in the two dimensional representation of the rail meant that the 0.59 conversion factor did not need to be applied to the mode II SIF. The conversion factor was shown to hold true for multiple cracks in close proximity.

Comparisons between different numbers of cracks in series demonstrated that, in order to simulate rolling contact fatigue defects that occur as hundreds of closely spaced cracks in the rail, a minimum of three cracks was required to be incorporated within the model. The inclusion of a higher number of cracks does give an improved result, although eleven cracks were shown to give the same result as one hundred closely spaced cracks. However, the use of three cracks was shown to give a good enough approximation whilst minimising computational resources required for an exhaustive study on cracks of differing sizes. A greater level of crack stress shielding was found to be experienced in the two dimensional modelling in comparison to three dimensional modelling of RCF cracks. However the stress intensity factor of the central crack was still significantly reduced in the three dimensional case.

When two cracks, inclined at 30° to the rail surface, were of equal size the greatest level of shielding was experienced by the underlying crack. However, for the cases where the underlying crack was larger than the overlying crack the effect was reversed, with the overlying crack experiencing the greatest level of shielding.

The relationship between three cracks inclined at 30° to the rail surface was found to be complex once different size and separation ratios were included in the analysis. The main trends that were found for the different size and separation ratios (Tables 6.5-6.7) were that:

- When the central crack was smaller than the overlying crack but larger than the underlying crack, the behaviour of the central crack was found to be dominated by the overlying crack. However when the underlying crack was also larger than the central crack a further shielding effect on the central crack was found to occur.
- When the overlying crack and the underlying crack were smaller than the central crack the behaviour of the central crack was dominated by its relationship to the overlying crack. The underlying crack did not affect the amount of shielding of the central crack until it was 90% of the size of the central crack.
- When the central crack was smaller than the underlying crack the behaviour of the central crack was determined by the separation ratio between the underlying crack and the central crack until the central crack was large enough to open. When the central crack was open the overlying crack additionally shielded the central crack when it was over 50% of the size of the central crack.

7.3 Further Work

Within the rail defect management system data, in addition to rolling contact fatigue data there was also data on squat defects. Squats [110, 121] and studs [26] are thought to be thermally initiated. Geospatial correlation of the squat data to the wheel slide protection data used in Chapter 3 could highlight if these defect predominantly occur at areas of the line where heavy traction or braking is applied. Although further investigations on the link between weather conditions and wheel slides have been published in a recent paper by White et al. [63], the mechanistic link (humidity, leaf-fall, shade, bacteria or differences in vegetation) still requires further study. As well as highlighting areas where rolling contact fatigue cracks are present when they have not been predicted Figure 3.6 also demonstrates where rolling contact fatigue cracks are not present when they have been predicted. Investigations as to why this occurs could be undertaken to improve the prediction of rolling contact fatigue cracks within the rail.

The flexibility of the position and stiffness of the supports means that the discrete support approach for modelling rail bending can be adapted in several ways in future work. This could include the effect of a single unsupported sleeper, for example a decayed or broken sleeper in standard track or hanging sleepers that commonly develop near transition zones. The effect of changing the sleeper spacing within a transition zone could also be investigated. Changing the stiffness of the support structure at the point of the sleeper may prove to be a more maintainable solution then the sub-ballast concrete ramps currently used in transition zones. Investigations into adapting the discrete support approach to include dynamic effects such as train speed could be investigated. If proven to give good results this would be a much simpler method of investigating the dynamic effects of transition zones than finite element analysis techniques.

Now that the interactions between cracks of different sizes are better quantified, this could be used in the development of an approach to model the growth of multiple, similarly sized cracks. Further work is required to determine the extent to which the level of shielding affects the stress intensity factor when the cracks are underneath the wheel load. The growth analysis would add to understanding of why cracks appear as a row of similarly sized and spaced cracks within the rail.

The work in Chapter 5 identified that the next step is to ascertain if the cracks shield each other as the wheel passes over the cracks or if they act independently under compression. Preliminary investigations into this were undertaken but require further work. The boundary element approach is very flexible. During the design of the three dimensional method used in this thesis considerations were given to how the different aspects that affect crack growth, such as residual stress and the contact loading, could be combined into one model. This could be the focus of further work, which would investigate how these factors interact to generate cracks within the rail. The results within this thesis suggest that use of this simple rail bending approach is sufficient to find an approximation to the peak negative mode II stress intensity factor. However further work has been identified that would provide additional insight to this conclusion for different crack sizes. This is especially for the case of smaller cracks which are primarily driven by the contact stresses.

Rolling contact fatigue cracks in rails are common but the manner by which they interact as they propagate is complex. Preventative action to minimise the risk of accidents results in a large cost to maintain rail integrity as well as the potential to induce delays to the operational network. Increased knowledge and modelling of factors affecting rail rolling contact fatigue can lead to refinements of approaches to rail safety and reliability. Whilst this thesis had added to the body of knowledge, there remains much to be studied.

References

[1] A. D. Arnall, D. I. Fletcher, and R. Lewis, "Geospatial and temporal data mining to combine railway low adhesion and rail defect data," *Proceedings of the Institution of Civil Engineers - Transport*, vol. 0, no. 0, pp. 1–14, 0.

[2] A. E. Beagles, A. D. Arnall, and D. I. Fletcher, "Interaction of Multiple Cracks in Railheads," in *Proceedings of the 10th International Conference Contact Mechanics and Wear of Rail Wheel Systems*, (Colorado), p. 7, 2015.

[3] "Passenger rail usage 2018-19 q2 statistical release," tech. rep., Office of Rail and Road, 2018.

[4] "Network Rail Overview, https://www.networkrail.co.uk."

[5] S. Iwnicki, S. Bjorklund, and R. Enblom, "Wheel-rail contact mechanics," in *Wheel-Rail Interface Handbook* (R. Lewis and U. Olofsson, eds.), ch. 3, pp. 58–92, Woodhead Publishing Limited, 2009.

[6] H. Hertz, "Ueber die Beruehrung fester elastische Koerper (On the contact of elastic solids)," *Journal für die reine und angewandte Mathematik*, vol. 92, pp. 156–171, 1881.

[7] A. Love, *A Treatise on the Mathematical Theory of Elasticity*. Cambridge: Cambridge University Press, 1926.

[8] K. L. Johnson, "A review of the theory of rolling contact stresses," *Wear*, vol. 9, no. 1, pp. 4–19, 1966.

[9] D. H. Cooper, "Hertzian Contact-Stress Deformation Coefficients," *Journal of Applied Mechanics*, vol. 36, no. 2, p. 296, 1969.

[10] K. Johnson, *Contact Mechanics.* Cambridge: Cambridge University Press, 1985.

[11] J. Kalker, “Wheel-rail rolling contact theory,” *Wear*, vol. 144, no. 1-2, pp. 243–261, 1991.

[12] W. Yan and F. Fischer, “Applicability of the Hertz contact theory to rail-wheel contact problems,” *Applied Mechanics*, vol. 70, no. 4, pp. 255–268, 2000.

[13] J. Srivastava, P. Sarkar, and V. Ranjan, “Contact Stress Analysis in Wheel-Rail by Hertzian Method and Finite Element Method,” *Journal of The Institution of Engineers (India): Series C*, vol. 95, no. 4, pp. 319–325, 2014.

[14] K. L. Johnson, *A shakedown limit in rolling contact.* Division of Engineering, Brown University, 1962.

[15] K. Johnson and J. Jefferis, “Plastic flow and residual stresses in rolling and sliding contact,” in *Proc. Inst. Mech. Eng. symp. on rolling contact fatigue*, pp. 50–61, 1963.

[16] J. Kalker, *on the rolling contact of two elastic bodies in the presence of dry friction.* PhD thesis, Delft University of Technology, 1967.

[17] J. Ayasse and H. Chollet, “Determination of the wheel rail contact patch in semi-Hertzian conditions,” *Vehicle System Dynamics*, vol. 43, no. 3, pp. 161–172, 2005.

[18] T. Telliskivi and U. Olofsson, “Contact mechanics analysis of measured wheel-rail profiles using the finite element method,” *Proceedings of the Institution of Mechanical Engineers, Part F: Journal of Rail and Rapid Transit*, vol. 215, no. 2, pp. 65–72, 2001.

[19] M. Marshall, R. Lewis, R. Dwyer-Joyce, U. Olofsson, and S. Bjorklund, “Experimental Characterization of Wheel-Rail Contact Patch Evolution,” *Journal of Tribology*, vol. 128, no. 3, p. 493, 2006.

[20] F. Franklin, G. Weeda, A. Kapoor, and E. Hiensch, “Rolling contact fatigue and wear behaviour of the infrastar two-material rail,” *Wear*, vol. 258, no. 7-8, pp. 1048–1054, 2005.

[21] J. W. Ringsberg, F. J. Franklin, B. L. Josefson, A. Kapoor, and J. C. Nielsen, "Fatigue evaluation of surface coated railway rails using shakedown theory, finite element calculations, and lab and field trials," *International Journal of Fatigue*, vol. 27, no. 6, pp. 680–694, 2005.

[22] S. Lewis, R. Lewis, and D. Fletcher, "Assessment of laser cladding as an option for repairing/enhancing rails," *Wear*, vol. 330-331, pp. 581–591, 2015.

[23] S. Lewis, S. Fretwell-Smith, P. Goodwin, L. Smith, R. Lewis, M. Aslam, D. Fletcher, K. Murray, and R. Lambert, "Improving rail wear and RCF performance using laser cladding," *Wear*, vol. 366-367, pp. 268–278, 2016.

[24] "Rolling contact fatigue in rails: A guide to current understanding and practice," Tech. Rep. Issue 1, 2001.

[25] S. Andersson, "Friction and wear simulation of the whee-rail interface," in *Wheel-Rail Interface Handbook* (R. Lewis and U. Olofsson, eds.), ch. 4, pp. 93–124, Woodhead Publishing Limited, 2009.

[26] S. L. Grassie, D. I. Fletcher, E. A. Gallardo Hernandez, and P. Summers, "Studs: a squat-type defect in rails," *Proceedings of the Institution of Mechanical Engineers, Part F: Journal of Rail and Rapid Transit*, vol. 226, no. 3, pp. 243–256, 2012.

[27] "Bogie Catalogue, http://www.alstom.com," tech. rep., Alstom.

[28] "FLEXX Eco Bogies Technical Data, http://www.bombardier.com," tech. rep., Bombardier.

[29] "First Class Bogies, https://www.mobility.siemens.com," tech. rep., Siemens.

[30] J. Elkins and B. Eickhoff, "Advances in Nonlinear Wheel/Rail Force Prediction Methods and Their Validation," *Journal of Dynamic Systems, Measurement, and Control*, vol. 104, no. 2, p. 133, 1982.

[31] H. Tournay, "Supporting technologies vehicle track interaction," *Guidelines to Best Practice for Heavy Haul Operations: Wheel and Rail Interface Issues, International Heavy Haul Association. USA (Virginia)*, 2001.

[32] L. Smith, *Rolling Contact Fatigue in Wheel-Rail Contact.* PhD thesis, University of Newcastle upon Tyne, 2007.

[33] F. W. Carter, "On the action of a locomotive driving wheel," *Proc. R. Soc. London A*, vol. 112, no. 760, pp. 151–157, 1926.

[34] J. Kalker, "On the contact problem in elastostatics," in *Unilateral problems in structural analysis*, pp. 81–118, Springer, 1985.

[35] J. J. Kalker, *Wheel-rail wear calculations with the program CONTACT.* Faculty of Mathematics and Informatics, 1987.

[36] U. Olofsson, "Adhesion and friction modification," in *Wheel-Rail Interface Handbook* (R. Lewis and U. Olofsson, eds.), ch. 17, pp. 510–527, Woodhead Publishing Limited, 2009.

[37] S. Grassie, "Maintenance of the wheel-rail interface," in *Wheel-Rail Interface Handbook* (R. Lewis and U. Olofsson, eds.), ch. 20, pp. 576–607, Woodhead Publishing Limited, 2009.

[38] E. Gallardo-Hernandez and R. Lewis, "Twin disc assessment of wheel/rail adhesion," *Wear*, vol. 265, no. 9-10, pp. 1309–1316, 2008.

[39] D. Fletcher and S. Lewis, "Creep curve measurement to support wear and adhesion modelling, using a continuously variable creep twin disc machine," *Wear*, vol. 298-299, no. 1, pp. 57–65, 2013.

[40] D. F. Moore, "Principles and applications of tribology," 1975.

[41] U. Olofsson and K. Sundvall, "Influence of Leaves, Humidity and Applied Lubrication on Friction in the Wheel-Rail Contact: pin-on-disc experiments," 2006.

[42] W. Poole, "Characteristics of Railhead Leaf Contamination," tech. rep., RSSB, 2007.

[43] Y. Zhu, U. Olofsson, and R. Nilsson, "A field test study of leaf contamination on railhead surfaces," *Proceedings of the Institution of Mechanical Engineers, Part F: Journal of Rail and Rapid Transit*, vol. 228, no. 1, pp. 71–84, 2014.

[44] "ERTMS adhesion management: An Assessment of the Available Adhesion and Slip Risk for ERTMS," tech. rep., RSSB, 2003.

[45] D. Fletcher, F. Franklin, P. Hyde, and A. Kapoor, "Track Tests on Rail-Wheel Adhesion - RSSB 1121 (WP3) Characteristics of Railhead Leaf Contamination," tech. rep., AEA Technology Rail, 2006.

[46] T. Pearce and D. Watkins, "Adhesion and Leaves - A Review of the Problem and Potential Solutions," tech. rep., BRB Research Division, 1987.

[47] W. Wang, P. Shen, J. Song, J. Guo, Q. Liu, and X. Jin, "Experimental Study on Adhesion Behavior of Wheel/Rail under Dry and Water Conditions," *Wear*, vol. 271, no. 9-10, pp. 2699–2705, 2011.

[48] "Investigation into the Effect of Moisture on Rail Adhesion T1042," tech. rep., RSSB, 2014.

[49] T. Beagley, I. McEwen, and C. Pritchard, "Wheel/rail adhesion - Boundary lubrication by oily fluids," *Wear*, vol. 31, no. 1, pp. 77–88, 1975.

[50] C. Hardwick, R. Lewis, and U. Olofsson, "Low adhesion due to oxide formation in the presence of salt," *Proceedings of the Institution of Mechanical Engineers, Part F: Journal of Rail and Rapid Transit*, vol. 228, no. 8, pp. 887–897, 2014.

[51] T. Beagley, I. Mcewen, and C. Pritchard, "Wheel/rail adhesion - the influence of railhead debris," *Wear*, vol. 33, no. 1, pp. 141–152, 1975.

[52] T. Beagley and C. Pritchard, "A Basic Study of Wheel/Rail Adhesion 7 - Laboratory Studies on the Effects of Water," tech. rep., BRB Research and Development Division, 1973.

[53] S. Kumar, M. F. Alzoubi, and N. A. Allsayyed, "Wheel/Rail Adhesion Wear Investigation using a Quarter Scale Laboratory Testing Facility," in *Proceedings of the IEEE/ASME Joint Railroad Conference*, pp. 247–254, 1996.

[54] E. Niccolini and Y. Berthier, "Wheel/Rail Adhesion: laboratory study of "natural" third body role on locomotives wheels and rails," *Wear*, vol. 258, no. 7-8, pp. 1172–1178, 2005.

[55] P. Cann, “The "leaves on the line" problem: A study of leaf residue film formation and lubricity under laboratory test conditions,” *Tribology Letters*, vol. 24, no. 2, pp. 151–158, 2006.

[56] Z. Li, O. Arias-Cuevas, R. Lewis, and E. Gallardo-Hernandez, “Rolling-Sliding Laboratory Tests of Friction Modifiers in Leaf Contaminated Wheel-Rail Contacts,” *Tribology Letters*, vol. 33, no. 2, pp. 97–109, 2009.

[57] O. Arias-Cuevas, Z. Li, and R. Lewis, “A laboratory investigation on the influence of the particle size and slip during sanding on the adhesion and wear in the wheel-rail contact,” *Wear*, vol. 271, no. 1-2, pp. 14–24, 2011.

[58] T. Beagley and C. Pritchard, “Wheel/rail adhesion - the overriding influence of water,” *Wear*, vol. 35, no. 2, pp. 299–313, 1975.

[59] S. Watkins, “A Twelve Month Adhesion Survey on a 280km Route,” tech. rep., BRB Research and Development Division, 1976.

[60] L. Chapman, J. Thornes, Y. Huang, X. Cai, V. Sanderson, and S. White, “Modelling of rail surface temperatures: a preliminary study,” *Theoretical and Applied Climatology*, vol. 92, no. 1-2, pp. 121–131, 2007.

[61] “Dealing with the weather - autumn.”

[62] D. Fletcher, P. Hyde, and A. Kapoor, “Modelling and full-scale trials to investigate fluid pressurisation of rolling contact fatigue cracks,” *Wear*, vol. 265, no. 9-10, pp. 1317–1324, 2008.

[63] B. White, R. Nilsson, U. Olofsson, A. Arnall, M. Evans, T. Armitage, J. Fisk, D. Fletcher, and R. Lewis, “Effect of the presence of moisture at the wheel-rail interface during dew and damp conditions,” *Proceedings of the Institution of Mechanical Engineers, Part F: Journal of Rail and Rapid Transit*, vol. 232, no. Issue 4, 2018.

[64] F. Fischer and M. Wiest, “Approximate Analytical Model for Hertzian Elliptical Wheel-Rail or Wheel-Crossing Contact Problems,” *Journal of Tribology*, vol. 130, no. 4, 2008.

[65] N. Tanaka, "A new calculation method of hertz elliptical contact pressure," *Journal of tribology*, vol. 123, no. 4, pp. 887–889, 2001.

[66] G. Liu, Q. J. Wang, and C. Lin, "A Survey of Current Models for Simulating the Contact between Rough Surfaces," *Tribology Transactions*, vol. 42, no. 3, pp. 581–591, 1999.

[67] J. Kalker, "A Fast Algorithm for the Simplified Theory of Rolling Contact," *Vehicle System Dynamics*, vol. 11, no. 1, pp. 1–13, 1982.

[68] J. Kalker and J. Piotrowski, "Some New Results in Rolling Contact," *Vehicle System Dynamics*, vol. 18, no. 4, pp. 223–242, 1989.

[69] J. Kalker, *Three-Dimensional Elastic Bodies in Rolling Contact*, vol. 2 of *Solid Mechanics and Its Applications*. Springer Netherlands, 1990.

[70] W. Daves and F. Fischer, "Modelling of the plastification near the rough surface of a rail by the wheel-rail contact," *Wear*, vol. 253, no. 1-2, pp. 241–246, 2002.

[71] J. Blanco-Lorenzo, J. Santamaria, E. G. Vadillo, and N. Correa, "On the influence of conformity on wheel-rail rolling contact mechanics," *Tribology International*, vol. 103, pp. 647–667, 2016.

[72] P. Shackleton and S. Iwnicki, "Comparison of wheel-rail contact codes for railway vehicle simulation: an introduction to the Manchester Contact Benchmark and initial results," *Vehicle System Dynamics*, vol. 46, no. 1-2, pp. 129–149, 2008.

[73] F. Fischer, W. Daves, R. Pippan, and P. Pointer, "Some comments on surface cracks in rails," *Fatigue & Fracture of Engineering Materials and Structures*, vol. 29, no. 11, pp. 938–948, 2006.

[74] Y. Jiang, B. Xu, and H. Sehitoglu, "Three-Dimensional Elastic-Plastic Stress Analysis of Rolling Contact," *Journal of Tribology*, vol. 124, no. 4, p. 699, 2002.

[75] K. Van and M. Maitournam, "On some recent trends in modelling of contact fatigue and wear in rail," *Wear*, vol. 253, no. 1-2, pp. 219–227, 2002.

[76] J. W. Ringsberg and T. Lindback, "Rolling contact fatigue analysis of rails inculding numerical simulations of the rail manufacturing process and repeated wheel-

rail contact loads," *International Journal of Fatigue*, vol. 25, no. 6, pp. 547–558, 2003.

[77] K. D. Van and M. Maitournam, "Rolling contact in railways: modelling, simulation and damage prediction," *Fatigue & Fracture of Engineering Materials and Structures*, vol. 26, no. 10, pp. 939–948, 2003.

[78] J. Merwin and K. Johnson, "An Analysis of Plastic Deformation in Rolling Contact," *Proceedings of the Institution of Mechanical Engineers*, vol. 177, no. 1, pp. 676–690, 1963.

[79] G. Hamilton, "Plastic Flow in Rollers Loaded above the Yield Point," *Proceedings of the Institution of Mechanical Engineers*, vol. 177, no. 1, pp. 667–675, 1963.

[80] A. Ponter, A. Hearle, and K. Johnson, "Application of the kinematical shakedown theorem to rolling and sliding point contacts," *Journal of the Mechanics and Physics of Solids*, vol. 33, no. 4, pp. 339–362, 1985.

[81] G. Ham, C. Rubin, G. Hahn, and V. Bhargava, "Elasto-Plastic Finite Element Analysis of Repeated, Two-Dimensional Rolling-Sliding Contacts," *Journal of Tribology*, vol. 110, no. 1, p. 44, 1988.

[82] A. Bower and K. Johnson, "The influence of strain hardening on cumulative plastic deformation in rolling and sliding line contact," *Journal of the Mechanics and Physics of Solids*, vol. 37, no. 4, pp. 471–493, 1989.

[83] J. Evans and M. Burstow, "Vehicle/track interaction and rolling contact fatigue in rails in the UK," *Vehicle System Dynamics*, vol. 44, no. sup1, pp. 708–717, 2006.

[84] S. Way, "Pitting due to rolling contact," *ASME J. Applied Mechanics*, vol. 2, p. A49, 1935.

[85] M. Allery and P. Clayton, "A Review of Recent Work on Rolling Contact Fatigue (Squats) in Rails and Crossings," tech. rep., British Rail Research, 1979.

[86] P. Clayton and M. Allery, "Metallurgical Aspects of Surface Damage Problems in Rails," tech. rep., British Rail Research, 1981.

[87] P. Clayton, M. Allery, and P. Bold, "Surface Damage Phenomena in Rails," tech. rep., British Rail Research, 1982.

[88] A. Kapoor, F. Schmid, and D. Fletcher, "Managing the critical wheel/rail interface," *Railway Gazette International*, pp. 25–28, 2002.

[89] J. Ringsberg, "Life prediction of rolling contact fatigue crack initiation," *International Journal of Fatigue*, vol. 23, no. 7, pp. 575–586, 2001.

[90] A. Kapoor, "A Re-Evaluation of the Life to Rupture of Ductile Metals by Cyclic Plastic Strain," *Fatigue & Fracture of Engineering Materials and Structures*, vol. 17, no. 2, pp. 201–219, 1994.

[91] W. Tyfour, J. Beynon, and A. Kapoor, "Deterioration of rolling contact fatigue life of pearlitic rail steel due to dry-wet rolling-sliding line contact," *Wear*, vol. 197, no. 1-2, pp. 255–265, 1996.

[92] M. Busquet, L. Baillet, C. Bordreuil, and Y. Berthier, "3D finite element investigation on the plastic flows of rolling contacts - correlation with railhead microstructural observations," *Wear*, vol. 258, no. 7-8, pp. 1071–1080, 2005.

[93] Y. Jiraskova, J. Svoboda, O. Schneeweiss, W. Daves, and F. Fischer, "Microscopic investigation of surface layers on rails," *Applied Surface Science*, vol. 239, no. 2, pp. 132–141, 2005.

[94] A. Bower, "The Influence of Crack Face Friction and Trapped Fluid on Surface Initiated Rolling Contact Fatigue Cracks," *Journal of Tribology*, vol. 110, no. 4, p. 704, 1988.

[95] P. Bold, M. Brown, and R. Allen, "Shear mode crack growth and rolling contact fatigue," *Wear*, vol. 144, no. 1-2, pp. 307–317, 1991.

[96] J. Beynon, J. Garnham, and K. Sawley, "Rolling contact fatigue of three pearlitic rail steels," *Wear*, vol. 192, no. 1-2, pp. 94–111, 1996.

[97] K. Miller, "The Short Crack Problem," *Fatigue & Fracture of Engineering Materials and Structures*, vol. 5, no. 3, pp. 223–232, 1982.

[98] J. W. Ringsberg, “Shear mode growth of short surface-breaking RCF cracks,” *Wear*, vol. 258, no. 7-8, pp. 955–963, 2005.

[99] Y. Huang and E. Stein, “Prediction of the Fatigue Threshold for a Cracked Body Using Shakedown Theory,” *Fatigue & Fracture of Engineering Materials and Structures*, vol. 18, no. 3, pp. 363–370, 1995.

[100] D. Cannon, K.-O. Edel, S. Grassie, and K. Sawley, “Rail defects: an overview,” *Fatigue & Fracture of Engineering Materials & Structures*, vol. 26, no. 10, pp. 865–886, 2003.

[101] M. Kaneta, M. Suetsugu, and Y. Murakami, “Mechanism of Surface Crack Growth in Lubricated Rolling/Sliding Spherical Contact,” *Journal of Applied Mechanics*, vol. 53, no. 2, p. 354, 1986.

[102] D. Fletcher, L. Smith, and A. Kapoor, “Rail rolling contact fatigue dependence on friction, predicted using fracture mechanics with a three-dimensional boundary element model,” *Engineering Fracture Mechanics*, vol. 76, no. 17, pp. 2612–2625, 2009.

[103] C. Morbarigazzi and J. Stupnicki, “Measurement of microslips of subsurface fatigue crack faces due to rolling loads,” *The Journal of Strain Analysis for Engineering Design*, vol. 39, no. 2, pp. 161–171, 2004.

[104] S. Suresh, *Fatigue of materials.* Cambridge university press, 1998.

[105] T. L. Anderson, *Fracture mechanics: fundamentals and applications.* CRC press, 2017.

[106] G. R. Irwin, “Analysis of stresses and strains near the end of a crack traversing a plate,” *J. appl. Mech.*, 1957.

[107] D. Dowson, G. Higginson, and A. Whitaker, “Stress distribution in lubricated rolling contacts,” in *Symposium on Fatigue in Rolling Contact, Inst. Mech. Engrs*, 1963.

[108] E. Ollerton and J. Morey, “Fatigue strength of rail steel in rolling contact,” in *Proc. Symposium on Fatigue in Rolling Contact*, 1963.

[109] P. Walker, D. Dowson, M. Longfield, and V. Wright, "Rheological behaviour of human joints," *Rheologica Acta*, vol. 8, no. 2, pp. 234–239, 1969.

[110] S. Bogdanski and M. W. Brown, "Modelling the three-dimensional behaviour of shallow rolling contact fatigue cracks in rails," *Wear*, vol. 253, no. 1-2, pp. 17–25, 2002.

[111] I. I. Kudish and K. W. Burris, "Modeling of surface and subsurface crack behavior under contact load in the presence of lubricant," *International Journal of Fracture*, vol. 125, no. 1, pp. 125–147, 2004.

[112] M. Akama and T. MORI, "Boundary Element Analysis of Effects of Crack Face Friction and Trapped Fluid on Rolling Contact Fatigue Cracks," *Quarterly Report of RTRI*, vol. 46, no. 4, pp. 231–237, 2005.

[113] M. Kaneta and Y. Murakami, "Propagation of Semi-Elliptical Surface Cracks in Lubricated Rolling/Sliding Elliptical Contacts," *Journal of Tribology*, vol. 113, no. 2, p. 270, 1991.

[114] T. Goshima, S. Ishihara, and M. Shimizu, "The Influence of Crack-Face Fluid Pressure on the Fatigue Crack Propagation Due To Rolling Contact with Frictional Heat," *Journal of Thermal Stresses*, vol. 25, no. 4, pp. 373–388, 2002.

[115] Y. Murakami, *Stress intensity factors Handbook.* 1986.

[116] D. Fletcher and J. Beynon, "A simple method of stress intensity factor calculation for inclined surface-breaking cracks with crack face friction under contact loading," *Proceedings of the Institution of Mechanical Engineers, Part J: Journal of Engineering Tribology*, vol. 213, no. 6, pp. 481–486, 1999.

[117] J. Beynon and D. Fletcher, "A simple method of stress intensity factor calculation for inclined fluid-filled surface-breaking cracks under contact loading," *Proceedings of the Institution of Mechanical Engineers, Part J: Journal of Engineering Tribology*, vol. 213, no. 4, pp. 299–304, 1999.

[118] J. Rice, "A Path Independent Integral and the Approximate Analysis of Strain Concentration by Notches and Cracks," *Journal of Applied Mechanics*, vol. 35, no. 2, p. 379, 1968.

[119] A. Kapoor and F. Franklin, "Tribological layers and the wear of ductile materials," *Wear*, vol. 245, no. 1-2, pp. 204–215, 2000.

[120] F. Franklin, T. Chung, and A. Kapoor, "Ratcheting and fatigue-led wear in rail-wheel contact," *Fatigue & Fracture of Engineering Materials & Structures*, vol. 26, no. 10, pp. 949–955, 2003.

[121] S. Bogdanski and M. Brown, "Modelling of surface fatigue crack growth in ehd contact," in *Proceedings of the International Conference "Engineering Against Fatigue" Sheffield*, 1997.

[122] J. Ringsberg and A. Bergkvist, "On propagation of short rolling contact fatigue cracks," *Fatigue & Fracture of Engineering Materials and Structures*, vol. 26, no. 10, pp. 969–983, 2003.

[123] M. A. Golberg, *Boundary integral methods: numerical and mathematical aspects*, vol. 1. Computational Mechanics, 1999.

[124] M. Akama and T. Mori, "Boundary element analysis of surface initiated rolling contact fatigue cracks in wheel/rail contact systems," *Wear*, vol. 253, no. 1-2, pp. 35–41, 2002.

[125] D. Fletcher, P. Hyde, and A. Kapoor, "Growth of multiple rolling contact fatigue cracks driven by rail bending modelled using a boundary element technique," *Proceedings of the Institution of Mechanical Engineers, Part F: Journal of Rail and Rapid Transit*, vol. 218, no. 3, pp. 243–253, 2004.

[126] S. Mellings, J. Baynham, and R. A. Adey, "Automatic crack growth prediction in rails with BEM," *Engineering Fracture Mechanics*, vol. 72, no. 2, pp. 309–318, 2005.

[127] A. Kapoor and D. Fletcher, "The effect of residual stress on contact stress driven crack growth in rail Part 1: The model," tech. rep., NewRail, 2006.

[128] J. E. Garnham, D. I. Fletcher, C. L. Davis, and F. J. Franklin, "Visualization and modelling to understand rail rolling contact fatigue cracks in three dimensions," *Proceedings of the Institution of Mechanical Engineers, Part F: Journal of Rail and Rapid Transit*, vol. 225, no. 2, pp. 165–178, 2011.

[129] F. Franklin, A. Gahlot, D. Fletcher, J. Garnham, and C. Davis, "Three-dimensional modelling of rail steel microstructure and crack growth," *Wear*, vol. 271, no. 1-2, pp. 357–363, 2011.

[130] M. Burstow, "Experience of premium grade rail steels to resist rolling contact fatigue (RCF) on GB network," *Ironmaking & Steelmaking*, vol. 40, no. 2, pp. 103–107, 2013.

[131] D. Armstrong and M. Allery, "Rail Damage due to Wheelspin," tech. rep., BRB Research Division, 1987.

[132] A. Kapoor, K. Johnson, and J. Williams, "A model for the mild ratchetting wear of metals," *Wear*, vol. 200, no. 1-2, pp. 38–44, 1996.

[133] F. Franklin, I. Widiyarta, and A. Kapoor, "Computer simulation of wear and rolling contact fatigue," *Wear*, vol. 251, no. 1-12, pp. 949–955, 2001.

[134] M. Yu and T. Topper, "The Effects of Material Strength, Stress Ratio, and Compressive Overload on the Threshold Behavior of a SAE1045 Steel," *Journal of Engineering Materials and Technology*, vol. 107, no. 1, p. 19, 1985.

[135] R. Pippan, "The Growth of Short Cracks under Cyclic Compression," *Fatigue & Fracture of Engineering Materials and Structures*, vol. 9, no. 5, pp. 319–328, 1987.

[136] G. Girsch and R. Heyder, "Hsh rails for high-speed railway operations," *Eisenbahningenieur*, vol. 54, no. 10, pp. 6–15, 2003.

[137] R. Heyder and G. Girsch, "Testing of HSH rails in high-speed tracks to minimise rail damage," *Wear*, vol. 258, no. 7-8, pp. 1014–1021, 2005.

[138] J. Tillberg, F. Larsson, and K. Runesson, "A study of multiple crack interaction at rolling contact fatigue loading of rails," *Proceedings of the Institution of Mechanical Engineers, Part F: Journal of Rail and Rapid Transit*, vol. 223, no. 4, pp. 319–330, 2009.

[139] A. Martin-Meizoso, J. Martinez-Esnaola, and M. Fuentes-Perez, "Interactive effect of multiple crack growth on fatigue," *Theoretical and Applied Fracture Mechanics*, vol. 23, no. 3, pp. 219–233, 1995.

[140] X. Jin and L. M. Keer, "Solution of Multiple Edge Cracks in an Elastic Half Plane," *International Journal of Fracture*, vol. 137, no. 1-4, pp. 121–137, 2006.

[141] N.-a. Noda, M. Tsuru, and K. Oda, "Stress Intensity Factors of Double and Multiple Edge Cracks," *Japan Society of Mechanical Engineers International Journal*, vol. 40, no. 1, pp. 1–7, 1997.

[142] M. Wilks, D. Nowell, and D. Hills, "The evaluation of stress intensity factors for plane cracks in residual stress fields," *The Journal of Strain Analysis for Engineering Design*, vol. 28, no. 3, pp. 145–152, 1993.

[143] J. Williams, I. Dyson, and A. Kapoor, "Repeated Loading, Residual Stresses, Shakedown, and Tribology," *Journal of Materials Research*, vol. 14, no. 04, pp. 1548–1559, 1999.

[144] G. Schleinzer and F. Fischer, "Residual stress formation during the roller straightening of railway rails," *International Journal of Mechanical Sciences*, vol. 43, no. 10, pp. 2281–2295, 2001.

[145] "Train derailment at hatfield: A final report by the independent investigation board," tech. rep., Office of Rail Regulation, 2006.

[146] D. Fletcher and A. Kapoor, "Combination of bending and contact stresses," tech. rep., NewRail, 2006.

[147] D. Fletcher, A. Kapoor, F. Franklin, L. Smith, and P. Hyde, "Comparison of the Hatfield and alternative UK rails using models to assess the effect of residual stress on crack growth from rolling contact fatigue," tech. rep., NewRail, 2006.

[148] A. Kapoor and D. Fletcher, "The effect of residual stress on contact stress driven crack growth in rail Literature review," tech. rep., NewRail, 2006.

[149] A. Kapoor and D. Fletcher, "The effect of residual stress on contact stress driven crack growth in rail Part 2: Data," tech. rep., NewRail, 2006.

[150] A. Kapoor and D. Fletcher, "The effect of residual stress on contact stress driven crack growth in rail Part 3: Further Data," Tech. Rep. November, NewRail, 2006.

[151] J. Williams, *Engineering tribology.* Cambridge University Press, 2005.

[152] D. Fletcher, F. Franklin, and A. Kapoor, "Image analysis to reveal crack development using a computer simulation of wear and rolling contact fatigue," *Fatigue & Fracture of Engineering Materials and Structures*, vol. 26, no. 10, pp. 957–967, 2003.

[153] F. Hourlier and A. Pineau, "Fatigue Crack Propagation Behavior Under Complex Mode Loading," 1981.

[154] M. Dembosky and M. Burstow, "Track-Ex: A Comprehensive Track-Damage Management Tool," tech. rep., Network Rail, 2010.

[155] S. L. Grassie, "Rolling contact fatigue on the British railway system: treatment," *Wear*, vol. 258, no. 7-8, pp. 1310–1318, 2005.

[156] "The Treatment of Rolling Contact Fatigue by Hand Grinding: Good Practice Guide," Tech. Rep. Issue 1, 2001.

[157] S. Grassie, P. Nilsson, K. Bjurstrom, A. Frick, and L. G. Hansson, "Alleviation of rolling contact fatigue on Sweden's heavy haul railway," *Wear*, vol. 253, no. 1-2, pp. 42–53, 2002.

[158] S. Grassie and S. Cox, "The dynamic response of railway track with unsupported sleepers," *Proceedings of the Institution of Mechanical Engineers, Part D: Transport Engineering*, vol. 199, no. 24, pp. 123–136, 1985.

[159] A. Lundqvist and T. Dahlberg, "Load impact on railway track due to unsupported sleepers," *Proceedings of the Institution of Mechanical Engineers, Part F: Journal of Rail and Rapid Transit*, vol. 219, no. 2, pp. 67–77, 2005.

[160] M. Hendry, D. Hughes, L. Barbour, and M. Atkinson, "Train Induced Dynamic Response of Railway Track and Embankments Constructed Over Soft Peat Foundations," in *59th Canadian Geotechnical Conference*, pp. 947–954, 2006.

[161] W. Powrie and L. Le Pen, *A Guide to Track Stiffness.* Cross Industry Track Stiffness Working Group, 2016.

[162] B. Coelho, P. Holscher, and F. Barends, "Dynamic behaviour of transition zones in railways," in *Geotechnical Engineering: New Horizons: Proceedings of the 21st European Young Geotechnical Engineers' Conference*, (Rotterdam), 2011.

[163] B. Coelho, P. Holscher, J. Priest, W. Powrie, and F. Barends, "An assessment of transition zone performance," *Proceedings of the Institution of Mechanical Engineers, Part F: Journal of Rail and Rapid Transit*, vol. 225, no. 2, pp. 129–139, 2011.

[164] M. Banimahd, P. K. Woodward, J. Kennedy, and G. M. Medero, "Behaviour of train-track interaction in stiffness transitions," *Proceedings of the Institution of Civil Engineers - Transport*, vol. 165, no. 3, pp. 205–214, 2012.

[165] E. T. Selig and J. M. Waters, *Track geotechnology and substructure management*. Thomas Telford, 1994.

[166] M. El-Sibaie, W. GeMeiner, D. Clark, L. Al-Nazer, R. Arnold, S. Farritor, M. Fateh, S. Lu, and G. Carr, "Measurement of Vertical Track Modulus: Field Testing, Repeatability, and Effects of Track Geometry," in *IEEE/ASME/ASCE 2008 Joint Rail Conference*, pp. 151–158, ASME, 2008.

[167] E. G. Berggren, A. Nissen, and B. S. Paulsson, "Track deflection and stiffness measurements from a track recording car," *Proceedings of the Institution of Mechanical Engineers, Part F: Journal of Rail and Rapid Transit*, vol. 228, no. 6, pp. 570–580, 2014.

[168] L. Hall, "Simulations and analyses of train-induced ground vibrations in finite element models," *Soil Dynamics and Earthquake Engineering*, vol. 23, no. 5, pp. 403–413, 2003.

[169] J. Priest and W. Powrie, "Determination of Dynamic Track Modulus from Measurement of Track Velocity during Train Passage," *Journal of Geotechnical and Geoenvironmental Engineering*, vol. 135, no. 11, pp. 1732–1740, 2009.

[170] A. Paixao, E. Fortunato, and R. Calcada, "Transition zones to railway bridges: Track measurements and numerical modelling," *Engineering Structures*, vol. 80, pp. 435–443, 2014.

[171] "Cemex rail solutions, available from: http://www.cemex.co.uk," tech. rep., Cemex.

[172] R. Dukkipati and R. Dong, "Idealized steady state interaction between railway vehicle and track," *Proceedings of the Institution of Mechanical Engineers, Part F: Journal of Rail and Rapid Transit*, vol. 213, no. 1, pp. 15–29, 1999.

[173] S. Grassie, R. Gregory, D. Harrison, and K. Johnson, "The dynamic response of railway track to high frequency vertical excitation," *Journal of Mechanical Engineering Science*, vol. 24, no. 2, pp. 77–90, 1982.

[174] S. Grassie and S. Cox, "The dynamic response of railway track with flexible sleepers to high frequency vertical excitation," *Proceedings of the Institution of Mechanical Engineers*, vol. 198, no. 7, pp. 117–124, 1984.

[175] "Comparison of North American Rail Asset Life," tech. rep., Office of Rail Regulation, 2008.

[176] "BS EN 13674-1:2011 Railway applications - Track - Rail," 2011.

[177] J. J. Kalker, "Considerations on rail corrugation," *Vehicle System Dynamics*, vol. 23, no. 1, pp. 3–28, 1994.

[178] A. Igeland, "Railhead corrugation growth explained by dynamic interaction between track and bogie wheelsets," *Proceedings of the Institution of Mechanical Engineers, Part F: Journal of Rail and Rapid Transit*, vol. 210, no. 16, pp. 11–20, 1996.

[179] J. Hobbs, "Modelling of Bending Stresses in Rails," tech. rep., Office of Rail Regulation, 2004.

[180] E. Winkler, "Die lehre von der elastizitat und festigkeit (the theory of elasticity and stiffness)," *Dominicus, Prague*, 1867.

[181] K. Ishihara, *Soil behaviour in earthquake geotechnics*. Clarendon Press, 1996.

[182] M. Eisenberger and D. Z. Yankelevsky, "Exact stiffness matrix for beams on elastic foundation," *Computers & Structures*, vol. 21, no. 6, pp. 1355–1359, 1985.

[183] J. Clastornik, M. Eisenberger, D. Yankelevsky, and M. Adin, "Beams on Variable Winkler Elastic Foundation," *Journal of Applied Mechanics*, vol. 53, no. 4, p. 925, 1986.

[184] M. Eisenberger and J. Clastornik, “Beams on Variable Two-Parameter Elastic Foundation,” *Journal of Engineering Mechanics*, vol. 113, no. 10, pp. 1454–1466, 1987.

[185] N. Doyle, “Railway Track Design: A Review of Current Practice,” tech. rep., Bureau of Transport Economics, 1980.

[186] B. Van Dyk, J. Edwards, M. S. Dersch, C. J. Ruppert, and C. P. Barkan, “Evaluation of dynamic and impact wheel load factors and their application in design processes,” *Proceedings of the Institution of Mechanical Engineers, Part F: Journal of Rail and Rapid Transit*, vol. 231, no. 1, pp. 33–43, 2017.

[187] F. Birmann, “Track parameters, static and dynamic,” in *Proceedings of the Institution of Mechanical Engineers, Conference Proceedings*, vol. 180, pp. 73–85, 1965.

[188] G. Kouroussis, G. Gazetas, I. Anastasopoulos, C. Conti, and O. Verlinden, “Discrete modelling of vertical track-soil coupling for vehicle-track dynamics,” *Soil Dynamics and Earthquake Engineering*, vol. 31, no. 12, pp. 1711–1723, 2011.

[189] R. Dong, S. Sankar, and R. Dukkipati, “A finite element model of railway track and its application to the wheel flat problem,” *Proceedings of the Institution of Mechanical Engineers, Part F: Journal of Rail and Rapid Transit*, vol. 208, no. 16, pp. 61–72, 1994.

[190] L. Yang, W. Powrie, and J. Priest, “Dynamic Stress Analysis of a Ballasted Railway Track Bed during Train Passage,” *Journal of Geotechnical and Geoenvironmental Engineering*, vol. 135, no. 5, pp. 680–689, 2009.

[191] P. Grabe and C. Clayton, “Effects of principal stress rotation on permanent deformation in rail track foundations,” *Journal of Geotechnical and Geoenvironmental Engineering*, vol. 135, no. 4, pp. 555–565, 2009.

[192] J. N. Varandas, *Long-Term Behaviour of Railway Transitions Under Dynamic Loading.* PhD thesis, Universidade Nova de Lisboa, 2013.

[193] D. Li and D. Davis, "Transition of Railroad Bridge Approaches," *Journal of Geotechnical and Geoenvironmental Engineering*, vol. 131, no. 11, pp. 1392–1398, 2005.

[194] A. Arnall, D. Fletcher, and R. Lewis, "Geospatial and Temporal Analysis of Wheel Slide Events," in *Proceedings of the 10th International Conference Contact Mechanics and Wear of Rail Wheel Systems*, (Colorado), p. 7, 2015.

[195] S. Cohen, *Practical Statistics*. London: Edward Arnold, 1988.

[196] W. Poole, "ERTMS adhesion management: An overview of low adhesion factors for ERTMS," tech. rep., RSSB, 2003.

[197] D. I. Fletcher, "Numerical simulation of near surface rail cracks subject to thermal contact stress," *Wear*, vol. 314, no. 1-2, pp. 96–103, 2014.

[198] D. Scott, D. Fletcher, and B. Cardwell, "Simulation study of thermally initiated rail defects," *Proceedings of the Institution of Mechanical Engineers, Part F: Journal of Rail and Rapid Transit*, vol. 228, no. 2, pp. 113–127, 2014.

[199] "ArcGIS, http://www.esriuk.com/software/arcgis."

[200] C.-H. Lee, C.-R. Lin, and M.-S. Chen, "Sliding-Window Filtering: An Efficient Algorithm for Incremental Mining," in *International Conference on Information and Knowledge Management*, pp. 263–270, 2001.

[201] X. Wang, U. Kruger, and G. W. Irwin, "Process Monitoring Approach Using Fast Moving Window PCA," *Industrial & Engineering Chemistry Research*, vol. 44, no. 15, pp. 5691–5702, 2005.

[202] "West Coast Main Line, https://en.wikipedia.org/wiki/West_Coast_Main_Line."

[203] "Rail-View, http://www.rail-view.co.uk/RailView/Default.aspx."

[204] "West Coast Main Line Route Utilisation Strategy," Tech. Rep. July, Network Rail, 2011.

[205] "Garmin GPS, http://www8.garmin.com/aboutGPS/."

[206] "Compatibility Requirements for Braking Systems of Rail Vehicles - Railway Group Standard GMRT2045," tech. rep., RSSB, 2016.

[207] D. Li, D. Otter, and G. Carr, "Railway bridge approaches under heavy axle load traffic: problems, causes, and remedies," *Proceedings of the Institution of Mechanical Engineers, Part F: Journal of Rail and Rapid Transit*, vol. 224, no. 5, pp. 383–390, 2010.

[208] K. Hou, J. Kalousek, and R. Dong, "A dynamic model for an asymmetrical vehicle/track system," *Journal of Sound and Vibration*, vol. 267, no. 3, pp. 591–604, 2003.

[209] "The sustainable freight railway: Designing the freight vehicle - track system for higher delivered tonnage with improved availability at reduced cost," tech. rep., Sustrail, 2014.

[210] "Class 390, https://en.wikipedia.org/wiki/british_rail_class_390."

[211] "Intercity 125, https://en.wikipedia.org/wiki/intercity_125."

[212] "Intercity 225, https://en.wikipedia.org/wiki/intercity_225."

[213] "Class 390 - Virgin Trains West Coast, https://www.angeltrains.co.uk."

[214] F. Meissonnier, "European research for an optimised ballasted track: Final report," *Synthesis Part. Technical report, European Union, Contract number: BRPRCT97-0455. Project number: BE96-3263*, 2000.

[215] G. Hunt, "Eurobalt optimises ballasted track," *Railway Gazette International*, vol. 156, no. 12, pp. 813–816, 2000.

[216] T. Sussman, W. Ebersohn, and E. Selig, "Fundamental Nonlinear Track Load-Deflection Behavior for Condition Evaluation," *Transportation Research Record: Journal of the Transportation Research Board*, vol. 1742, no. June, pp. 61–67, 2001.

[217] W. Macaulay, "Note on the deflection of beams," *The Messenger of Mathematics*, vol. 48, pp. 129–130, 1919.

[218] "BM central load, https://en.wikipedia.org/wiki/Bending_moment."

[219] "Beasy software and services, https://www.beasy.com."

[220] D. I. Fletcher and S. H. Sanusi, "The potential for suppressing rail defect growth through tailoring rail thermo-mechanical properties," *Wear*, vol. 366-367, pp. 401–406, 2016.

[221] "P8 Wheel Profile Drawing," tech. rep., British Rail.

Appendices

Appendix A

Literature Review Additional Information

A.1 Rail and Wheel Profiles

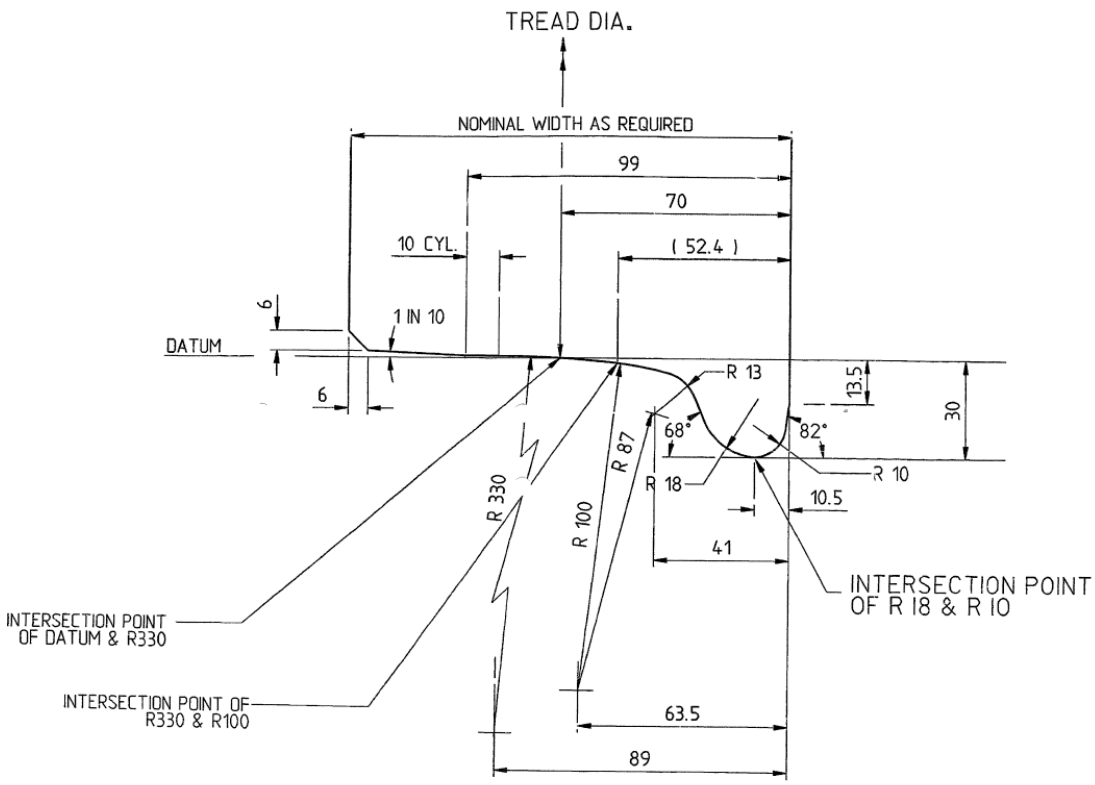

Figure A.1: P8 wheel profile [221]

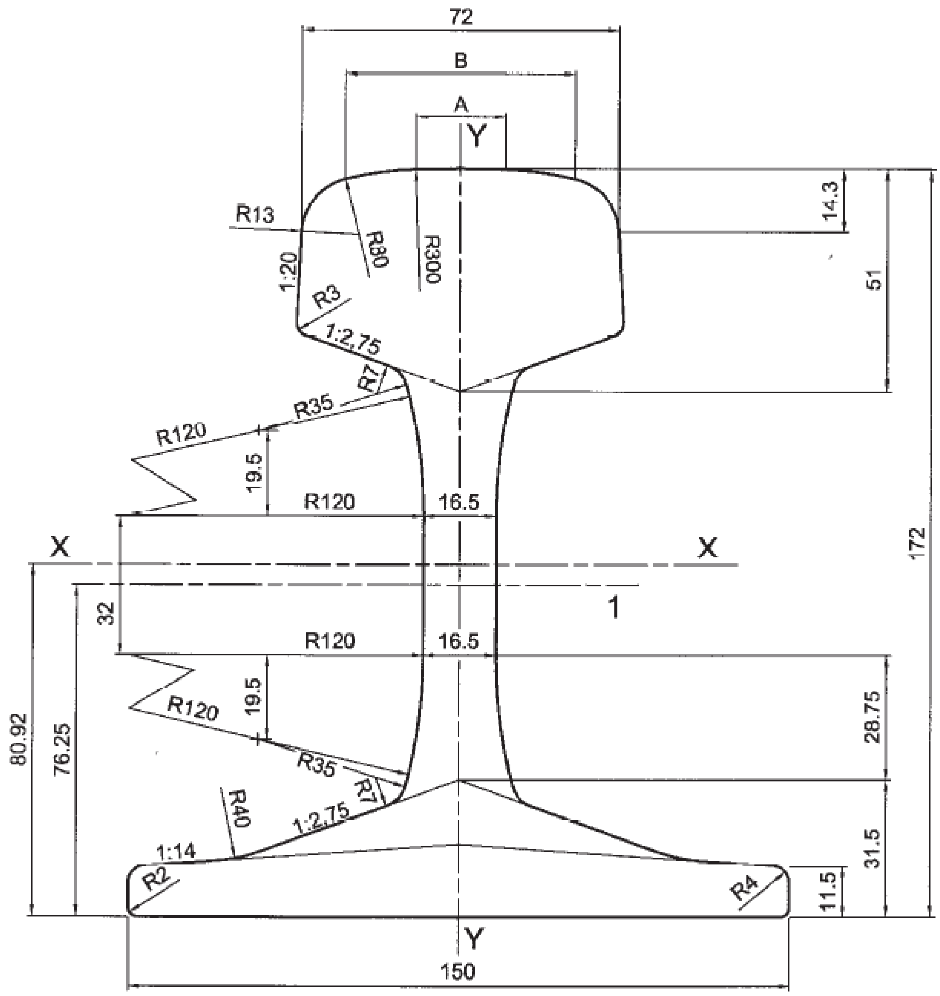

Key

1 centre line of branding

cross-sectional area	:	76,70	cm^2
mass per metre	:	60,21	kg/m
moment of inertia x-x axis	:	3 038,3	cm^4
section modulus - Head	:	333,6	cm^3
section modulus - Base	:	375,5	cm^3
moment of inertia y-y axis	:	512,3	cm^4
section modulus y-y axis	:	68,3	cm^3

indicative dimensions: A = 20,456 mm
B = 52,053 mm

Figure A.2: 60E1 rail profile [176]

A.2 Hertzian Contact Correction Factors for Elliptical Contacts

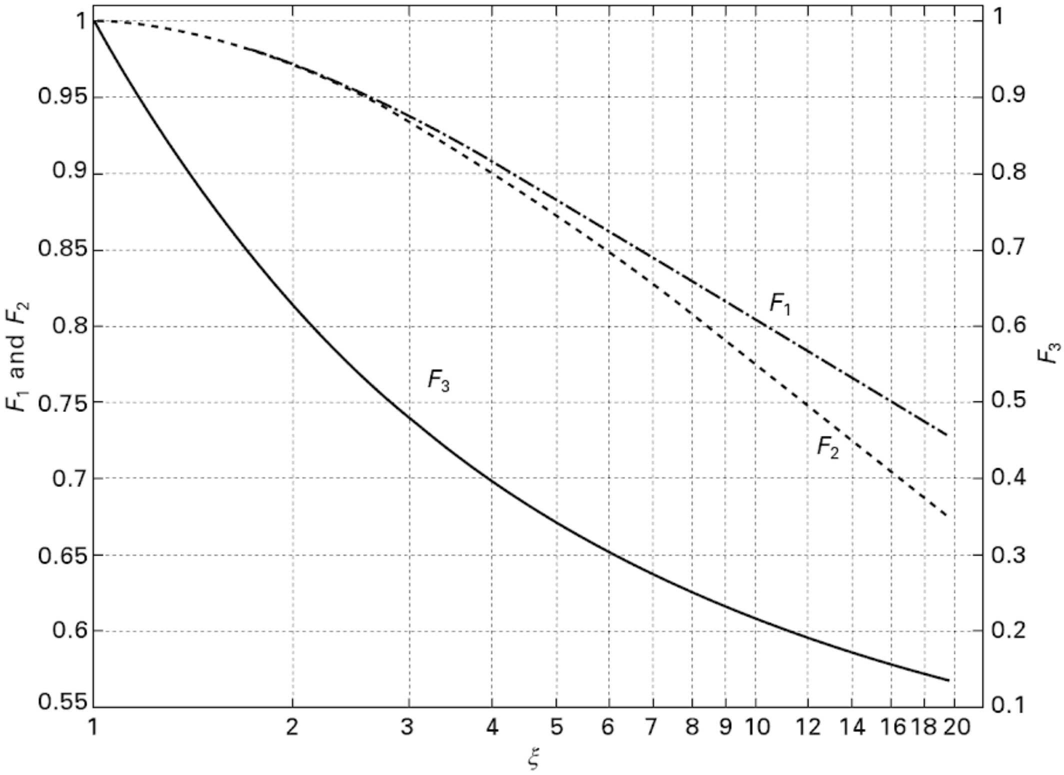

Figure A.3: Correction factors for elliptical contacts [5]

Appendix B

Geospatial and Temporal Data Mining to Combine Railway Low Adhesion and Rail Defect Data

In this Appendix the journal paper entitled Geospatial and Temporal Data Mining to Combine Railway Low Adhesion and Rail Defect Data is presented. This was published in the ICE Transport journal in June 2018 [1].

Cite this article
Arnall AD, Fletcher DI and Lewis R
Geospatial and temporal data mining to combine railway low adhesion and rail defect data.
Proceedings of the Institution of Civil Engineers – Transport,
https://doi.org/10.1680/jtran.17.00120

Research Article
Paper 1700120
Received 21/09/2017;
Accepted 08/06/2018

Keywords: environment/railway systems/railway tracks

Transport

ice publishing

Geospatial and temporal data mining to combine railway low adhesion and rail defect data

Andrew D. Arnall MEng
PhD student, Department of Mechanical Engineering, University of Sheffield, Sheffield, UK

David I. Fletcher BEng, PhD
Reader in Mechanical Engineering, Department of Mechanical Engineering, University of Sheffield, Sheffield, UK (corresponding author: d.i.fletcher@sheffield.ac.uk) (Orcid:0000-0002-1562-4655)

Roger Lewis MEng, PhD, CEng
Professor of Mechanical Engineering, Department of Mechanical Engineering, University of Sheffield, Sheffield, UK

Rolling contact fatigue (RCF) damage to rails and low adhesion at the rail–wheel interface remain significant problems in maintaining railway performance, fully utilising network capacity and reducing running costs. A novel approach has been developed to understand these problems through analysis of data on RCF and low-adhesion incidents from the UK rail network. This augments understanding of specific mechanisms such as the roles of rail plasticity in crack initiation and environmental moisture levels in low adhesion, which have not given sufficient information to prevent these problems to date. A moving-window filtering technique and temporal and geospatial approaches were used to identify correlations between sites of low rail–wheel adhesion subject to transient sliding contact, crack initiation and underbridge locations where vertical and lateral track stiffness typically change rapidly. The analysis showed that a high density of otherwise unexpected RCF defects occurred close to underbridges and that there was a strong correlation between momentary slides during braking and RCF sites. The temporal analysis indicated that, although concentrated in the autumn period, 55–60% of transient low-adhesion incidents occur outside that period, with the highest risk in the very early morning.

1. Introduction

Numerous investigations into rail rolling contact fatigue (RCF) have been conducted to understand how stresses at the contact patch contribute to the initiation and propagation of cracks, relevant examples being the studies by Fletcher and Beynon (2000), Kapoor *et al*. (2002), Grassie and Elkins (2005), Fischer *et al*. (2006) and Grassie (2015). With the development of harder rail steels, the forces present at the rail–wheel interface during normal operation generate much less extensive plastic flow than in conventional steel grades, thus restricting crack initiation or delaying the development of RCF unless some other factor is present to increase rail–wheel forces. It is known that residual stresses (Fletcher *et al*., 2006) or the lateral forces generated during cornering (Burstow, 2013) help drive RCF, yet a definitive picture of the factors influencing crack initiation and growth has not yet been established. Armstrong and Allery (1987) suggested that the location of RCF cracks is, in part, influenced by the occurrence of low adhesion, and this paper presents data analysis to establish if there is any correlation between low adhesion and RCF sites. It is hoped that better establishment of the factors that may contribute to crack formation and growth will focus future modelling of RCF damage.

Since the primary interest of this work was the factors that are not already well known to drive RCF damage, the Track-Ex package (Dembosky *et al*., 2011), which is based on the contact patch energy ($T\gamma$) approach, was used to remove from the analysis locations of RCF that are predicted, for example, at curves. Comparison of the Track-Ex prediction with data from Network Rail's rail defect management system (RDMS) highlighted RCF sites that were not predicted, supporting the existence of an alternative initiation process. Track-Ex makes several assumptions with regard to dynamics at the rail–wheel interface, focusing on lateral forces as a driver of damage. A key area in which vertical rather than lateral forces are increased is around underbridges (Evans and Burstow, 2006), where there are often rapid changes of track support stiffness and a high potential for vertical and lateral track misalignment. These can lead to wheel unloading and therefore an increased risk of a wheel reaching the adhesion limit. The influences of very localised stiffness change and misalignment on RCF cannot be predicted within Track-Ex, but removal of RCF sites that it does predict allowed this study to focus on these less-well-explored areas.

1.1 Geospatial approach

A moving-window filtering technique and a geospatial approach were used on data from a section of the UK rail network. These techniques were used to correlate locations where RCF occurs with the locations of factors that are known to increase rail–wheel forces or damage. These include

(*a*) wheel slides, during which there can be a high level of heat generated at the contact patch and material damage such as transformation of pearlite to brittle martensite;

this may subsequently lead to rail defects as described by Armstrong and Allery (1987), RSSB (2003), Fletcher (2014), and Scott *et al*. (2014)

(*b*) underbridges, where the higher support stiffness over the underbridge relative to the surrounding embankments means that the rail deforms less under lateral and vertical loads, leading to track misalignment, as described by Evans and Burstow (2006).

1.2 Temporal approach

In addition to geospatial correlation of RCF, the temporal distribution of wheel slide events was investigated using a methodology building on previous studies by the Rail Safety and Standards Board (RSSB, 2014), Arnall *et al*. (2015) and White *et al*. (2017). Although usually associated with autumn problems such as rail head leaf film described by Zhu *et al*. (2014), Poole (2007), Pearce and Watkins (1987) and Ishizaka *et al*. (2017), low adhesion also occurs outside the autumn period and therefore cannot be solely attributed to leaf fall. On an hourly timescale, reports of low adhesion are non-uniform throughout the day, but understanding of this is complicated since traffic density also varies throughout the day. The aim of the temporal analysis undertaken in this study was therefore to gain better understanding of low adhesion on two timescales (over a year and over a day), taking account of traffic levels.

2. Methodology

Within the analysis, two scenarios were considered in which the factors outlined in Section 1.1 are present (Figure 1). Correlation between RCF and wheel slide locations would be a result of either scenario 1a or scenario 1b. The data are unable to reveal directly whether wheel slides precede the later formation of RCF-type defects or whether wheelset dynamics when crossing the RCF site triggers a slide. The correlation between RCF and underbridge locations would demonstrate that alignment issues inherent in track where the support stiffness changes abruptly influence the formation of RCF (scenario 2).

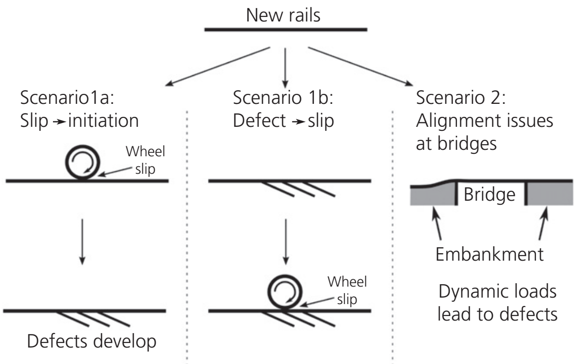

Figure 1. Relative slip at the rail–wheel interface and crack initiation scenarios for a newly installed rail initially free of damage. The stiffness and alignment fault at the bridge is exaggerated for clarity

Two types of wheel slides were considered as they were thought to have different causes and a different effect on the rail: (*a*) momentary sliding associated with traction peaks during low adhesion and its recovery and (*b*) longer periods of sliding associated with low adhesion over a large section of track. A location-based analysis was undertaken to identify whether these factors correlated with recorded RCF. It should be noted that these slides, identified by wheel slide protection (WSP) activations, are not caused by train faults but are a consequence of variations in rail–wheel adhesion and the reaction of train systems to this factor.

2.1 Data

Data collection focused on the UK West Coast Main Line (WCML), an overview of which is presented by Spoors (2012). The WCML is a busy mixed-traffic line connecting London with Birmingham, the north of England and Scotland. It carries a mix of high-speed intercity trains, regional passenger services and freight traffic, totalling some 2500 train movements each day. It has a mix of double and quadruple track layouts, is electrified at 25 kV AC, but also carries diesel-powered services. Due to hilly terrain and the history of construction by a series of different railway companies in the 1800s, 70% of the line is curved. In the early 2000s, the WCML was significantly upgraded to allow 200 km/h running over much of the line (Network Rail, 2011).

Rail surface damage data for RCF, together with locations, were collected over a 2-year period (2013–2015) through Network Rail's RDMS for the WCML 'down fast' line (i.e. the line travelling away from London, dominated by high-speed passenger traffic). Locations within this data set were specified using engineers' line references and track mileage, which were converted into global positioning system references using Omnicom Rail View (Omnicom Engineering, 2017).

Data on bridge locations focused on underbridges (i.e. where the railway goes over another feature). At these locations, the support structure of the track changes over a short distance, often leading to an abrupt change in track support stiffness and a high likelihood of dynamically generated forces as a train (and its suspension) crosses and reacts to the stiffness change. Minor alignment problems are also common near underbridges since both lateral and vertical stiffness change with the transition onto and off the structure. The combination of these factors is thought to increase rail damage in these areas. The underbridges considered within the analysis ranged from small culverts to large underbridges such as viaducts and bridges crossing motorways.

In addition to infrastructure data, WSP data were collected over a 5-year period (2009–2013) from class 390 passenger rolling stock that operates along the WCML. Only wheel slide events that occurred on the down fast line (the same track as the RCF) were considered. The WSP system on this rolling stock records a wheel slide event when the wheel speed on a free-rolling leading axle present on each train differs from that of one of the three remaining braked axles on the leading car. The majority of the data used within this study therefore represent an individual axle undergoing sliding and not the whole train experiencing a slide. The number of wheel slides found within the data was representative of any high-speed rolling stock operating within the UK (i.e. part of normal operation and not caused by a rolling stock fault).

During the period of data collection there were no major upgrades to the WCML and only routine maintenance was undertaken. The mix of rolling stock, their proportion in total traffic and the line speeds did not change significantly during the study period, meaning that locations with a high density of RCF-type defects would not be expected to change.

2.1.1 Filtering wheel slide data

Wheel slide is, by its nature, transient, but long slides potentially resulting in signals passed at danger and long sections of rail damage are of greatest concern from a safety perspective. Conversely, much shorter slide events have the potential to correlate with regions of RCF crack initiation, which range from a size comparable to the rail–wheel contact patch (~15–20 mm) to a few metres in cases where multiple RCF defects develop together. Long slides and momentary slides, both during braking, were therefore considered separately, with the aim that any correlation with underlying causes would be clearer than when also considering slides of intermediate length/duration. Two categories of long slides were defined as

- category LD: slide distance greater than 800 m (0·5 miles)
- category LT: slide time greater than 15 s.

The time criterion is based on the 800 m slide distance for a train travelling at a speed of 200 km/h (125 mph), the maximum line speed on the WCML. These severity criteria highlight events where the adhesion level available is insufficient over a prolonged distance or time.

Two categories of momentary slide were defined as

- category MD: slide distance less than 4·8 m (0·003 miles)
- category MT: slide time less than 0·1 s.

The momentary slide time criterion was based on the shortest time that it would be reasonable for the WSP system to detect and record 'an event' (i.e. a wheelset slide). The distance criterion is based on the 0·1 s slide time for a train speed of 200 km/h.

2.1.2 Filtering RCF data

A Track-Ex route fleet analysis was carried out for the down fast line at engineers' line references LEC1–LEC2 (London Euston to Stafford South), LEC4 (Stafford North to Crewe) and CGJ1–CGJ7 (Crewe to Carlisle). LEC3 (Stafford station area) and LEC5 (Crewe station area) are within-station areas only and were therefore not considered. RCF and adhesion data were removed from further analysis for sections of line where analysis of measured track geometry using Track-Ex predicted any RCF development. This is demonstrated in Figure 2: the example section of line shows how the RCF site at 0·7–0·9 km is predicted by the Track-Ex analysis and would therefore be removed from further consideration. This filtering process removed from the analysis RCF linked to macro-scale track geometry (i.e. curving). The remaining sites of observed RCF (grey bands in Figure 2) are not explained by Track-Ex and it is therefore of far greater interest to investigate potential causes further.

2.2 Geospatial distribution and visualisation

To gain an overview of the data and any locational correlations between low adhesion and RCF, the geospatial distribution of RCF sites that occurred within ±40 m of underbridges or wheel slides was examined using a geospatial visualisation. The choice of proximity distance was guided by research looking at track damage associated with the approaches to underbridges (Li *et al.*, 2010). Other track misalignments, for example at welds or rail joints, are known to excite the suspension of passing trains, with the potential for wheel unloading and peaks in rail–wheel load some distance further along the line from the cause of excitation (Hou *et al.*, 2003). The exact distances to the point of peak force or maximum damage will vary, for example depending on speed and

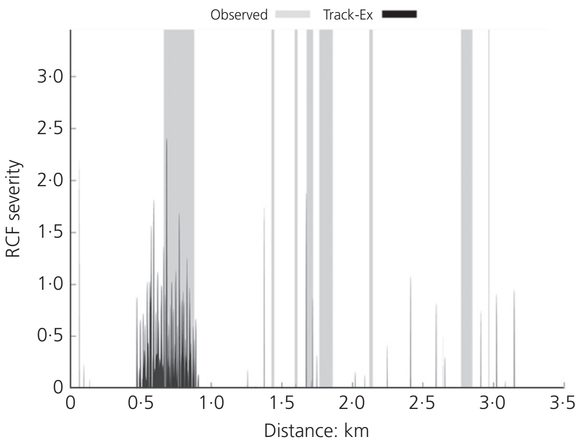

Figure 2. Predicted RCF from Track-Ex output against actual RCF sites from RDMS data, demonstrating which sites will be removed from the analysis

whether damage generated by surface contact pressure is of interest, or rail interior or foot damage. In mapping the location of low-adhesion incidents, the severity criteria outlined in Section 2.1.1 were used to define an 'event', which then becomes a single data point. Although this inherently means a loss of data in terms of the duration or severity of low-adhesion events, the data reduction is necessary to reveal the bigger picture and sufficient data remain to do this.

2.3 Moving-window correlation quantification

To quantify correlations revealed in the geospatial visualisations, a moving-window filtering technique (Figure 3) was used to ascertain if a correlation existed between the occurrence of underbridges, low-adhesion and RCF sites not already explained by the Track-Ex analysis. With track data segmented at 8 m intervals, the analysis window considered data from ten of these segments at any one time (80 m of track, for which chord and arc lengths are almost equal for any curve radius found on mainline track). As the analysis window 'slides along' the data, the model adapts as it iterates to include data from the newest point and discard data from the oldest point (Lee *et al.*, 2001; Wang *et al.*, 2005). Through this method of gradual introduction of new points and removal of old points, the distribution of quantities over distance is smoothed, permitting an improved analysis in determining proximity relationships.

The numbers of underbridges, RCF sites and low-adhesion events within each analysis window were counted. A baseline value of the likelihood that a factor would occur in any given analysis window and the average number that occurred per analysis window was obtained by consideration of the whole line. A comparison was then drawn between the baseline value and the value when both factors were present. For example, when considering the likelihood of locational correlation between RCF sites and underbridges, the proportion of analysis windows that contained both RCF sites and underbridges was compared with the baseline proportion of analysis windows that contained only RCF sites. From this, a relative likelihood ratio of the occurrence of RCF sites near underbridges was obtained and the degree of locational correlation was quantified.

2.4 Adhesion temporal analysis

In line with a methodology used in research on rail–wheel adhesion (RSSB, 2014), an analysis was undertaken on how the frequency of wheel slides varied over a year and over a day.

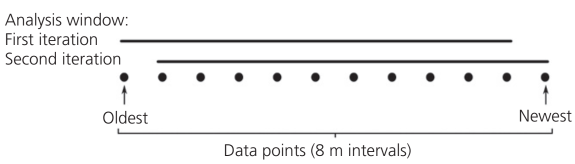

Figure 3. Schematic representation of the moving-window filtering technique

This highlighted the time periods for which wheel slide events are more prevalent and whether the trends observed remained consistent throughout the 5-year period studied. This allowed identification of whether there is a significant rise in wheel slide events during the autumn period when there are leaf layers present (Zhu *et al.*, 2014) or whether they are distributed more evenly throughout the year, indicating that other factors such as moisture on the rail head (RSSB, 2014) are a significant cause of wheel slides. A similar analysis was undertaken on hourly data for wheel slide events to determine if there are periods during the day when wheel slide events are more likely to occur. A comparison was drawn between the years to ascertain whether the pattern of wheel slide events remained consistent over the 5-year period studied.

3. Results and discussion

3.1 Geospatial distribution visualisation

Figures 4–6 show geospatial visualisations of RCF site locations on the WCML, filtered to remove RCF sites already predicted from track geometry using the method described in Section 2.1.2. For the London to Carlisle WCML, 67% of the RCF sites occurred within the area highlighted by a 10× zoom along the section of line between Crewe and Runcorn. This suggests that the characteristics of this section of line have led to an increased number of RCF sites occurring that have not been predicted by conventional consideration of track geometry. This section is just over 8% of the overall London to Carlisle distance and averages one underbridge every 1·6 km, compared with approximately one every 0·5 km for the line overall.

3.1.1 Underbridges and RCF

RCF sites where an underbridge was present within ±40 m are indicated by the larger shaded circles in Figure 4. It was found that 23% of the RCF sites had an underbridge within ±40 m, although quantified analysis (see Section 3.2.1) showed that only 10% of the 8 m line segments considered included an underbridge. This supports a strong correlation between bridges and RCF sites, although it does not pinpoint the physical cause. For example, if the railway crosses a busy road there may be contamination from traffic or the rail temperature may be lower on the bridge relative to the surrounding ground, leading to earlier dew formation that will reduce rail–wheel adhesion levels. Adhesion can vary with only minor changes in rail head condition and the change at a bridge is likely to be too rapid for train systems to respond, as described by Scott *et al.* (2014) for more general adhesion variations. The sites of RCF–underbridge coincidence were distributed throughout the study area, therefore the geospatial distribution did not highlight any other features as being influential (such as proximity to cities or the coast).

3.1.2 Long slides and RCF

In Figure 5, sites at which a long slide occurred within ±40 m of RCF damage are indicated by shaded circles. Over the

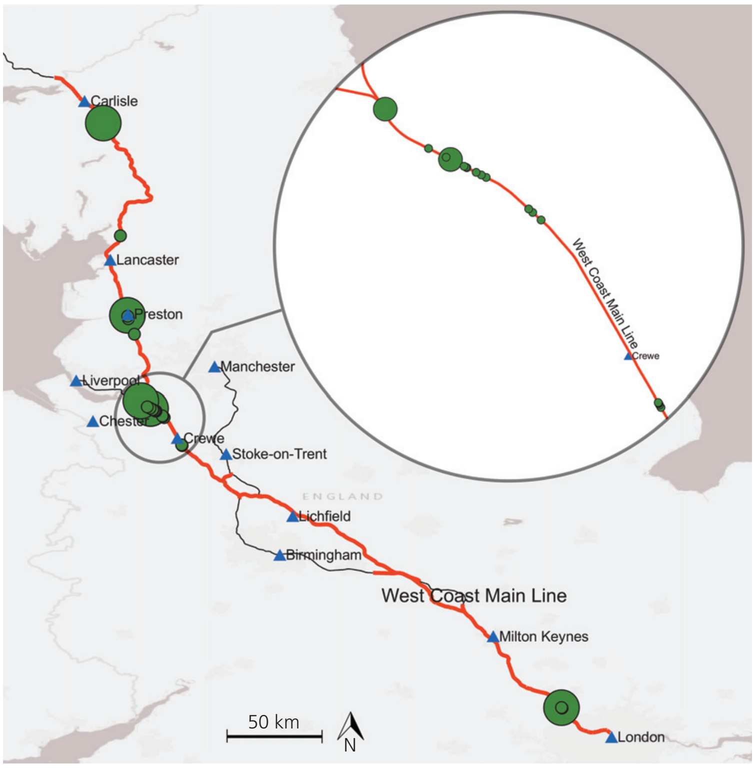

Figure 4. Distribution of RCF sites and underbridge locations. The size of the shaded circles indicates an underbridge within ±40 m of the RCF site (small, 0; large 1). The enlarged area (10× zoom) highlights the section of line with 67% of RCF sites

whole data set, it was found that 47% of the RCF sites had long slides within ±40 m. Of these, 78% occurred within the highlighted area, in which long slides occurred within ±40 m at 55% of the RCF sites. This supports a locational correlation between these two factors, which is further explored in Section 3.2.2.

3.1.3 Momentary slides and RCF

RCF sites at which momentary slides occurred within ±40 m are indicated with a filled circle in Figure 6. It was found that 37% of the RCF sites had momentary slides within ±40 m. Of these, 55% occurred within the highlighted area, for which momentary slides occurred within ±40 m at 30% of the RCF sites. This suggests locational correlation between these two factors and this is explored further in Section 3.2.2.

3.2 Moving-window correlation quantification

3.2.1 Underbridges and RCF

Figure 7 shows the proportion of 80 m analysis windows that contained RCF sites and each of the four categories of low-adhesion events discussed in Section 2.1.1. In the figure, quantification is on a positive/negative basis for the existence of RCF or low adhesion at a location and does not distinguish the number of occurrences within an analysis window. The presence of underbridges is indicated, with data plotted relative to the respective baseline values for each RCF or adhesion category for the whole line. The baseline case is included in the plot as a visual reminder, with unity representing the proportion of analysis windows that contained each type of event when considering the whole line, whether or not the analysis window included an underbridge. Analysis windows with underbridges present were just under 10% of the total line length considered.

As shown in Figure 7, when there were no underbridges in the analysis window, the occurrence of RCF and momentary slides was just slightly below the baseline. When the analysis window contained a single underbridge, the occurrence likelihood of RCF and momentary slide events increased to 1·3 times the baseline. When there were multiple underbridges within the analysis window, the percentage of cases that also contained a momentary slide event increased to 1·9 times the baseline. For both categories of long slides, the likelihood of their occurrence in the same analysis window as an underbridge was close to the baseline. When the severity criteria were not applied to

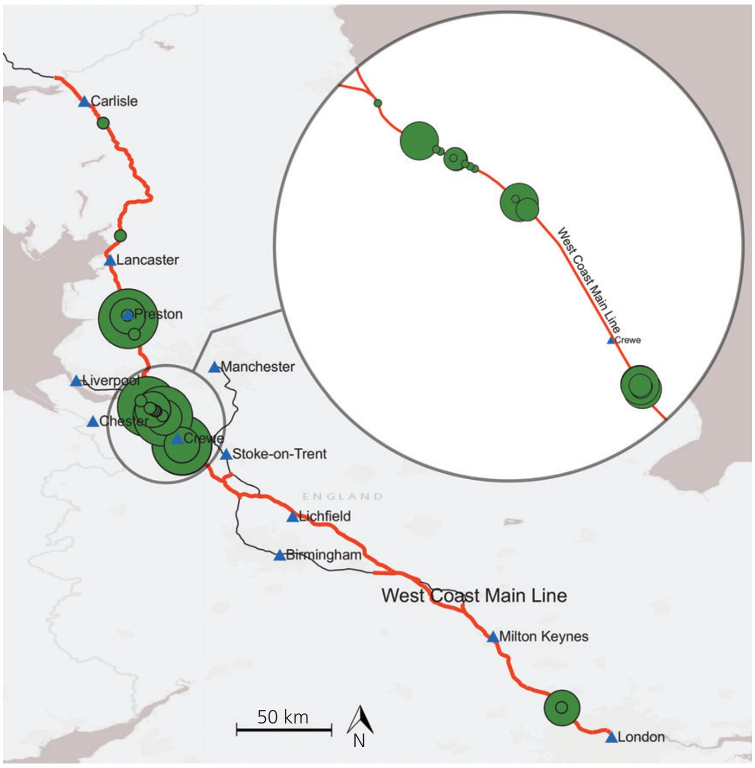

Figure 5. Distribution of RCF sites and long slides. The size of the shaded circles indicates the number of long slides within ±40 m of the RCF site (small, 0; medium, 1 or 2; large, 3+). The enlarged area (10× zoom) highlights the section of line with 67% of RCF sites

the low-adhesion events, the likelihood of their occurrence in the same analysis window as an underbridge was almost identical to the baseline.

Figure 8 shows the average number of RCF or low-adhesion events that occurred per analysis window, which gives a slightly different picture than the positive/negative approach used in Figure 7. All the results are relative to the baseline, the average number of events per analysis window that occurred when considering the whole line. The average number of RCF sites that occurred increased to 1·2 times the baseline when an underbridge was present. Taking the mean of the two categories of momentary slide, the number of events that occurred increased to 1·3 times the baseline in the same analysis window as a single underbridge. This further increased to 1·4 times the baseline when there was more than one underbridge. The average number of long slides increased to 1·1 times the baseline in the same analysis window as a single underbridge, but then decreased to 0·7 times the baseline when there was more than one underbridge. Without the severity criteria applied to the low-adhesion events, the average number that occurred in the same analysis window as a single underbridge increased to 1·2 times the baseline, further increasing to 1·6 times the baseline when there was more than one underbridge.

Of all the analysis windows that contained underbridges, 8% had multiple underbridges. Given that bridge sites made up just under 10% of the total line length, multiple bridge sites therefore make up only 0·8% of the line length. The limited number of analysis windows that matched this condition meant that no RCF sites met this criterion. However, the increase in both RCF site likelihood (on a positive/negative basis as in Figure 7) and the average number of sites per analysis window with a single underbridge (Figure 8) demonstrates the influence that an underbridge has on increasing RCF-type defects.

Without application of the severity criteria, the number of analysis windows that contained any type of slide event was 85% of the total number. This meant that when considering the likelihood of occurrence on a positive/negative categorical basis (Figure 7), the baseline analysis window was already likely to show positive, this measure being insensitive to the number of events. The increase in the average number of slide events indicated in Figure 8 (i.e. quantified on a continuous rather than categorical basis) better demonstrates the correlation of these events with underbridge locations.

When considering the categories of momentary slides and long slides, the numbers of analysis windows that contained

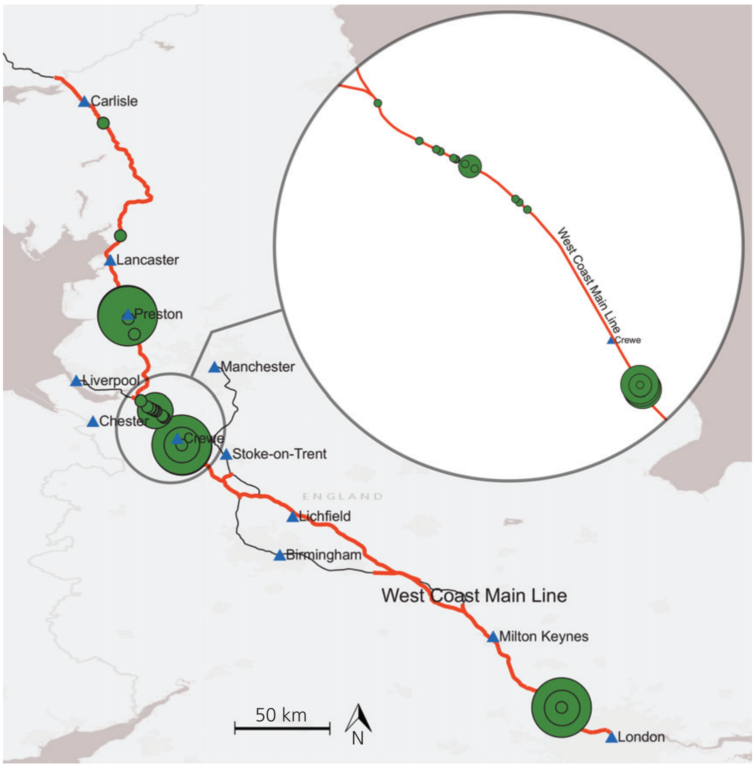

Figure 6. Distribution of RCF sites and momentary slides. The size of the shaded circles indicates the number of momentary slides within ±40 m of the RCF site (small, 0; medium, 1 or 2; large 3+). The enlarged area (10× zoom) highlights the section of line with 67% of RCF sites

these types of events were, respectively, 12% and 29% of the total number. These lower proportions permitted the likelihood (positive/negative) analysis in Figure 7 to demonstrate correlation of these events with bridge location.

The large increase in momentary wheel slide likelihood (Figure 7) and the average number of events per analysis window (Figure 8) when multiple underbridges were in the same analysis window supports a process where numerous stiffness changes and increased instances of track misalignment within a short section of line lead to momentary slide events, with the wheelset not able to accommodate the sudden changes in track alignment.

No correlation was found between the likelihood of long slides and underbridge locations. This was expected as the stiffness changes associated with underbridges are local and would not affect the adhesion level over 800 m of track, the criterion for a 'long' slide. The underlying cause of the negative correlation in the number of long slides that occurred in the same analysis window as multiple underbridges (Figure 8) cannot be confirmed with the available data. However, one observation is that a key influence behind this correlation would be the proportion of underbridges within heavy braking areas such as on the approach to stations or signals since a long slide would only be likely during braking. The different responses to the presence of an underbridge for the momentary and long categories of events support the hypothesis that they have different causes. In future work it may be useful to include locations dominated by braking as a factor in the analysis.

3.2.2 Low adhesion and RCF

The locational correlation between RCF sites and low-adhesion events is shown in Figure 9. For sites without RCF, the data were almost identical to the baseline values for the whole line. Without the severity criteria applied to the low-adhesion events, the likelihood of their occurrence (positive/negative basis) in the same analysis window as a site of RCF increased to 1·1 times the baseline. Filtering the adhesion data, the likelihood of a momentary slide occurring within the same analysis window as RCF was 2·4 times the baseline considering an average of the MD and MT categories. The likelihood of long slides occurring within the same analysis window as a site of RCF was 1·5 times the baseline when taking the LD and LT categories together.

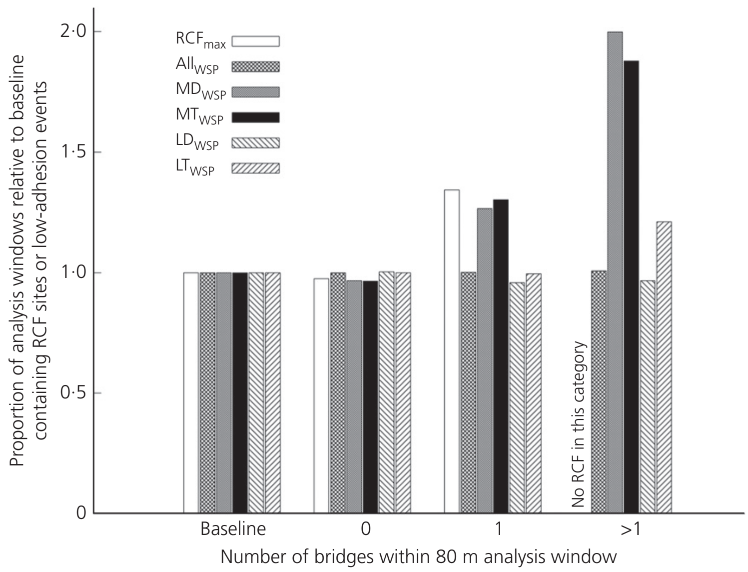

Figure 7. Comparison of the proportion of analysis windows that contain RCF sites or low-adhesion events that occurred in the same analysis window as an underbridge with the baseline. All_{WSP} represents adhesion event data without filtering by severity criteria

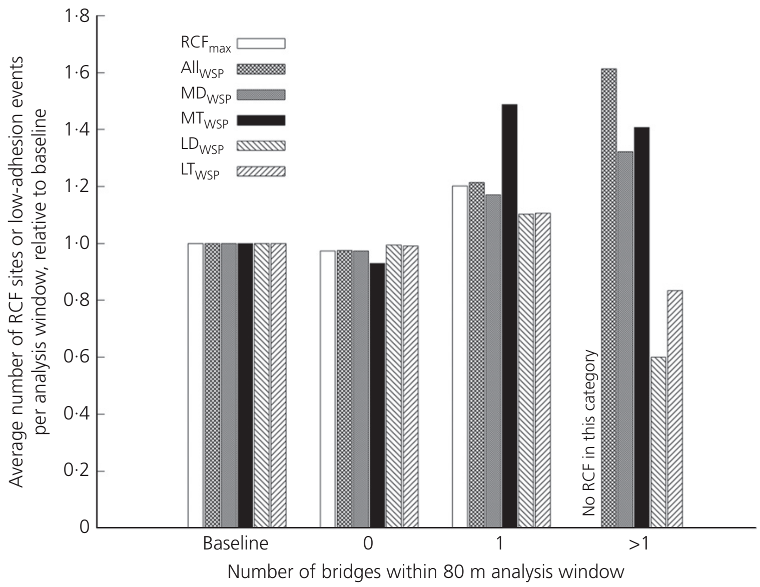

Figure 8. Comparison of the average number of RCF sites or low-adhesion events that occurred in the same analysis window as an underbridge with the baseline. All_{WSP} represents adhesion event data without filtering by severity criteria

Figure 10 shows how the average number of low-adhesion events is correlated with the presence of RCF. Without the severity criteria applied to the adhesion events (ALL_{WSP} in the figure), the average number of events that occurred in the same analysis window as a site of RCF increased to 2·3 times the baseline. The average number of momentary slide events that occurred within the same analysis window as RCF was 1·3 times the baseline, taking the average of the MD and MT categories. The average number of long slides that occurred within the same analysis window as RCF was 0·7 times the baseline

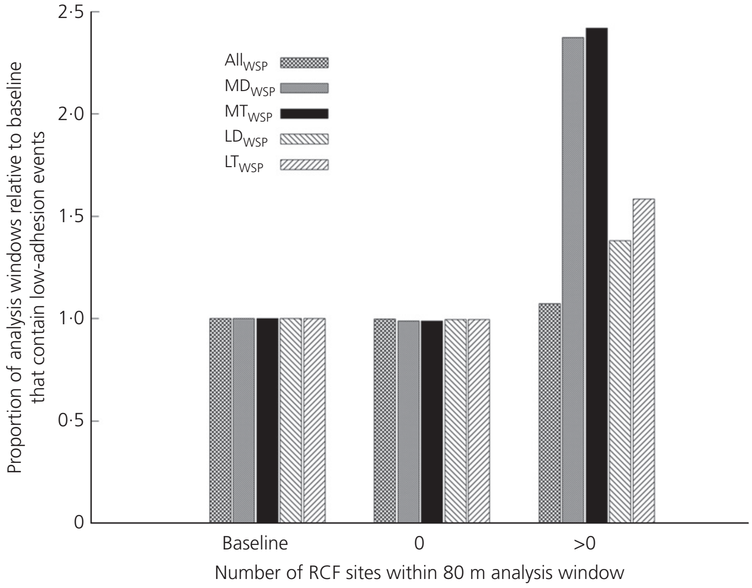

Figure 9. Comparison of the proportion of analysis windows that contain low-adhesion events in the same analysis window as a RCF site with the baseline

when taking the average for the LD and LT categories. As indicated by the subscript WSP in the figures, these slides all occurred under braking and were detected by WSP activation on the train.

Without application of the severity criteria, the number of analysis windows that contained low-adhesion events was 85% of the total number, making the binary method of quantification insensitive and leading to only small changes in the

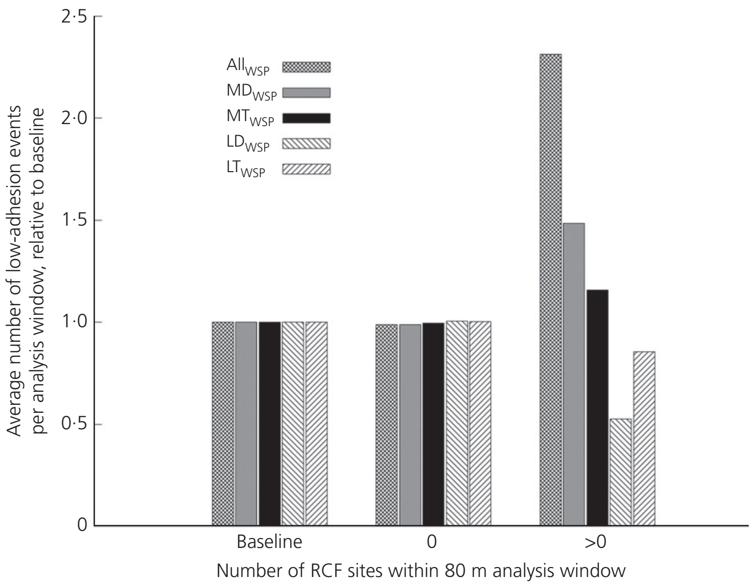

Figure 10. Comparison of the average number of low-adhesion events in the same analysis window as a RCF site with the baseline

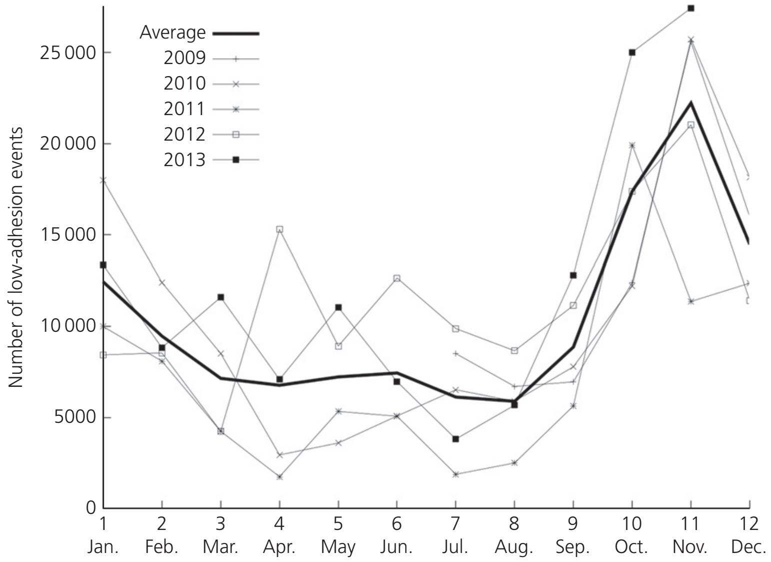

Figure 11. Number of wheel slide events occurring per month; these refer predominantly to momentary WSP events, not to safety-critical events such as signals passed at danger

likelihood results for RCF correlation in Figure 9. The change in the average number of low-adhesion events that occurred per analysis window shows much greater sensitivity. For momentary slides, the increase in both the likelihood (Figure 9) and the average number of events per analysis window (Figure 10) when coincident with RCF supports the hypothesis that a locational correlation exists between momentary slides and RCF sites, although this is not a causal link.

For longer slides, Figure 10 shows a reduction in the number of events when coincident with RCF, even though Figure 9 showed an increase in likelihood of occurrence on a positive/negative basis. The reason for the reduction in the number of long low-adhesion events when coincident with RCF could not be established from the data, but it is notable that the trend to increased likelihood (Figure 9) is much weaker for long slides than for momentary slides. It is possible that, although the data filtering applied helped to reveal the strong correlation between momentary slides and RCF locations, it also removed some potentially useful data on longer slides. The data visualisation for long slides in Figure 5 reveals that over three-quarters of the long slide events occurred in one geographical area. The binary analysis showing a positive correlation between long slides and RCF locations is most representative of this highly concentrated area, whereas the quantified analysis (showing a negative correlation) would better represent the rest of the area in which there was limited coincidence of long slides and RCF sites.

It is important to consider that although a single RCF crack would be classed as 'heavy' if having a visible surface crack length over 20 mm and 'severe' if over 30 mm (Railtrack, 2001), these cracks rarely occur in isolation but more often in significant quantity, giving them more potential to influence adhesion over a prolonged section of track. Together with the geospatial differences, this indicates that additional factors not captured in the quantified analysis need to be considered in order to obtain a deeper understanding of the links between long slides and RCF.

3.3 Temporal analysis

Building on the geospatial analysis, temporal analysis was conducted to assess both yearly and daily patterns in low-adhesion events. The monthly temporal analysis (Figure 11) highlighted periods during the year when wheel slide events occurred. It should be noted that these events refer predominantly to momentary WSP events, not to safety-critical events such as signals passed at danger. There was some variation between years, as would be expected since weather conditions are a key determinant of adhesion conditions, however, the behaviour for each year was similar and was represented well by the monthly average of the data (the dark line in Figure 11). Taking the mean of the data for each month took account of the fact that the data sets for 2009 and 2013 did not cover every month in those years. It was found that the 3-month autumn period (October to December) contained the greatest proportion of the yearly total of low-adhesion events (40–45%), with occurrence peaking in November. This is in line with the general understanding for the UK that low adhesion is a problem in the autumn. However, Figure 11 also shows that 55–60% of wheel slide events were distributed throughout the remaining 9 months of the year. Therefore, although fewer events occur per month, a greater number of events in total occur outside the autumn period.

In addition to the through-year analysis, an hourly temporal analysis was undertaken using two approaches.

In the first approach (Figure 12), the data are presented as the total number of wheel slide events in each hour summed across each year, expressed as the percentage of the total number of wheel slide events during each year. The data used to generate Figure 12 were analysed in conjunction with weather data presented by White *et al*. (2017). This approach indicates that the highest number of wheel slide events occurred between 06:00 and 10:00 – the morning ‘rush hour’ period when the consequences of delay can be severe due to the high traffic density and the potential for extensive knock-ons of delays to later in the day. A small evening peak in adhesion events was also noted, although this was much smaller than the morning peak. Traffic density data (presented later in this section) show similar amounts of traffic in the morning and evening peaks, so the distribution of adhesion events cannot be explained as simply a consequence of high traffic density in the morning peak. Other factors, such as rail surface oxide formation overnight when traffic is lighter, its subsequent removal by traffic during the day or differing rates of dew formation and evaporation, are also important. Rail temperature would be expected to vary throughout the day, potentially leading to dew to form railhead ice in colder periods. However, the running temperature of wheels is raised by frictional energy dissipation at the rail–wheel contact (Ertz and Knothe, 2002; Scott *et al*., 2014). Combined with pressure melting (Bottomley, 1872; Sanz *et al*., 2004), this makes it unlikely that ice would survive to influence adhesion events.

In the second approach (Figure 13) the low-adhesion event data summed across the years 2009–2013 are presented alongside hourly data on station stops attempted each day. The station stop data are mean values from timetable information for the whole UK network on Monday 28 October 2013 and Friday 3 January 2014. The intention here was not to match station stop data to exactly the trains on which low-adhesion incidents occurred, but rather to use it as an indication of traffic density throughout the day. Using this data, a value was generated (right-hand scale of Figure 13) by dividing national station stops each hour by the number of low-adhesion WSP activations observed per hour. It should be noted that this must be interpreted carefully since the differing data sources make strict interpretation as station stops per low-adhesion incident incorrect. It is also important to reiterate that the low-adhesion events refer predominantly to momentary low-adhesion wheel slide events, not to safety-critical events such as signals passed at danger.

The normalisation in the second approach (Figure 13) shows that the time period in which an individual train had the highest chance of experiencing a wheel slide low-adhesion problem was between 03:00 and 03:59, during which the lowest number of station stops take place (nationally) per low-adhesion incident observed. The number of low-adhesion events observed was low

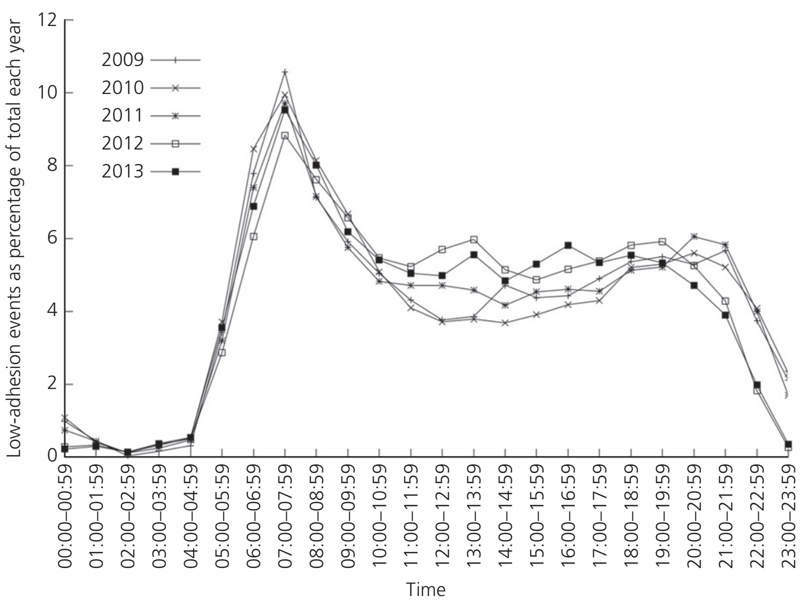

Figure 12. Number of wheel slide events that occurred per hour according to the first method (no normalisation)

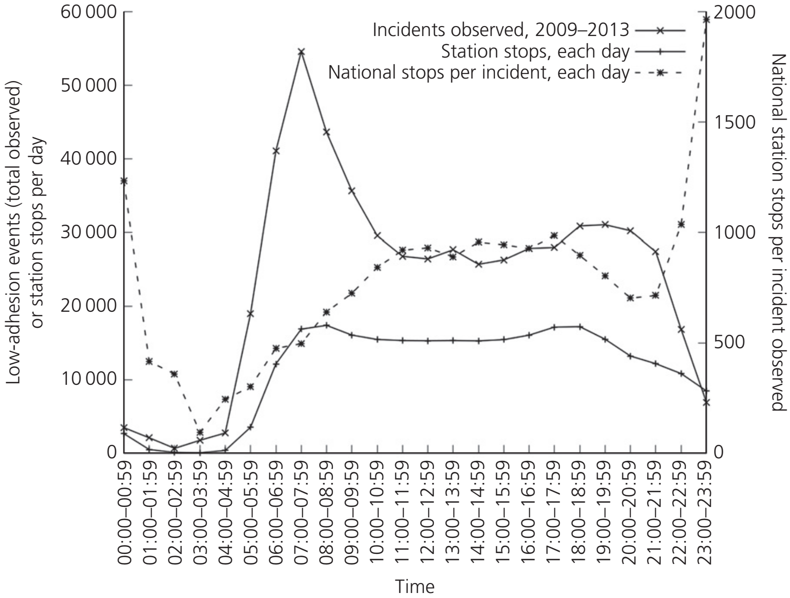

Figure 13. Number of wheel slide events occurring per hour for observed services in 2009–2013, normalised by the national number of station stops per hour

during this time (~1800) but, since traffic density is also low (indicated by ~110 station stops in that hour), each train has a higher chance of experiencing a problem than at other times of day. The figure for national station stops per observed incident rises gradually through the morning to reach a daytime plateaux by around 11:00. There was a small dip in the early evening, but the risk diminished greatly (i.e. more stops per incident) in the late evening. Normalisation of the low-adhesion data by traffic density supports the supposition from Figure 12 that traffic density is not the controlling factor since low-adhesion risk persisted through the morning peak in traffic but only marginally affected the evening peak.

4. Conclusions

Application of a moving-window filtering technique showed that there is a significant increase in RCF in the vicinity of an underbridge. Underbridge sites were characterised by an increase in RCF likelihood (i.e. the presence of any RCF) to 1·3 times the baseline, while there was an increase in the average number of RCF sites (a quantitative rather than a binary measure) to 1·2 times the baseline in the same 80 m analysis window as an underbridge. There was a strong correlation between momentary slides and underbridge locations, with an increase in the likelihood (presence/absence) of momentary slides to 1·9 times the baseline and an increase in the average number of events that occurred per analysis window (quantified basis) to 1·4 times the baseline in the same analysis window as multiple underbridges. The data showed no clear correlation between the likelihood of long slides and underbridge locations, with the likelihood of long slides remaining approximately equal to the baseline and the average number of events occurring per analysis window decreasing to 0·7 times the baseline in the same analysis window as multiple underbridges. The reasons for this decrease could not be established from the data available.

The increase in both the likelihood (2·4 times the baseline) and the average number (1·3 times the baseline) of momentary slide events per analysis window in the same analysis window as a RCF site supports the hypothesis that a locational correlation exists between momentary slides and RCF sites, although this is not necessarily a causal link. This was corroborated by geospatial distribution visualisations that presented data graphically on maps of the UK's WCML. The negative correlation between the average number (0·7 times the baseline) of long slides and RCF sites and the positive correlation between the likelihood (1·5 times the baseline) of long slides occurring and RCF sites did not support a direct locational correlation hypothesis. Geospatial visualisation in this case showed distinct differences in the level of correlation between different regions, suggesting additional factors need to be introduced into the analysis for better understanding of any correlation between long slides and RCF sites.

Temporal analysis indicated that low adhesion occurs both during and outside the autumn period and therefore cannot be solely attributed to leaf fall. With 40–45% of the yearly total of wheel slide low-adhesion events occurring during autumn, the analysis highlights that low adhesion is a problem that can affect train performance throughout the rest of the year, although at a lower rate of events per month.

When analysed in terms of the total number of incidents, it was found that the time period where low-adhesion events are most prevalent falls within the busy morning period, when the consequences of delays on passengers are the most severe. As the morning peak period may be influenced by both high traffic density and a high risk of low adhesion, a normalisation procedure based on national numbers of station stops was developed as a simple way of normalising the data for traffic density. This analysis showed that the highest risk of low adhesion for an individual train is in the very early morning (03:00–03.59). This risk was found to diminish by 11:00 (i.e. a rise in the number of station stops taking place on the network per incident observed) and the risk was found to rise only marginally in the evening peak traffic period.

Acknowledgements
The authors are grateful to Omnicom Engineering Ltd for the provision of access to Rail View software, to Michael Jacks at Virgin Trains for the provision of train-based data and to Mark Burstow, Brain Whitney and Andrew Cornish at Network Rail for helpful suggestions, the provision of track-based data and assistance with Track-Ex. Funding for this research was provided by Network Rail and an Engineering and Physical Sciences Research Council (EPSRC) doctoral training scholarship.

REFERENCES
Armstrong DS and Allery M (1987) *Rail Damage due to Wheelspin*. British Rail Research, Derby, UK, Report TM-TBC-009. See http://www.sparkrail.org (accessed 27/06/2018).

Arnall AD, Fletcher DI and Lewis R (2015) Geospatial and temporal analysis of wheel slide events. In *Proceedings of the 10th International Conference on Contact Mechanics and Wear of Rail Wheel Systems, Colorado Springs, CO, USA* (Tournay H (ed.)). Transportation Technology Center, Inc., Pueblo, CO, USA (CD-ROM).

Bottomley J (1872) Melting and regelation of ice. *Nature* **5(114)**: 185, https://doi.org/10.1038/005185a0.

Burstow M (2013) Experience of premium grade rail steels to resist rolling contact fatigue (RCF) on GB network. *Ironmaking & Steelmaking* **40(2)**: 103–107, https://doi.org/10.1179/1743281212Y.0000000042.

Dembosky MA, Greenwood SP and Doherty A (2011) Minimising rail lifecycle costs using Track-Ex damage and cost estimates. In *Proceedings of the World Congress Railway Research (WCRR), Lille, France*. SNCF, Saint-Denis, France. See https://www.sparkrail.org/Lists/Records/DispForm.aspx?ID=3432 (accessed 05/07/2018).

Ertz M and Knothe K (2002) A comparison of analytical and numerical methods for the calculation of temperatures in wheel–rail contact. *Wear* **253(3)**: 498–508, https://doi.org/10.1016/S0043-1648(02)00120-5.

Evans JR and Burstow MC (2006) Vehicle/track interaction and rolling contact fatigue in rails in the UK. *Vehicle System Dynamics* **44(sup1)**: 708–717, https://doi.org/10.1080/00423110600883652.

Fischer FD, Daves W, Pippan WR and Pointer P (2006) Some comments on surface cracks in rails. *Fatigue & Fracture of Engineering Materials & Structures.* **29(11)**: 938–948, https://doi.org/10.1111/j.1460-2695.2006.01051.x.

Fletcher DI (2014) Numerical simulation of near surface rail cracks subject to thermal contact stress. *Wear* **314(1–2)**: 96–103, https://doi.org/10.1016/j.wear.2013.11.021.

Fletcher DI and Beynon JH (2000) Equilibrium of crack growth and wear rates during unlubricated rolling-sliding contact of pearlitic rail steel. *Proceedings of the Institution of Mechanical Engineers, Part F: Journal of Rail and Rapid Transit* **214(2)**: 93–105, https://doi.org/10.1243/0954409001531360.

Fletcher DI, Kapoor A, Franklin FJ, Smith L and Hyde P (2006) *Comparison of the Hatfield and Alternative UK Rails Using Models to Assess the Effect of Residual Stress on Crack Growth from Rolling Contact Fatigue*. Her Majesty's Stationery Office, Norwich, UK, Research Report 461. See http://www.hse.gov.uk/research/rrpdf/rr461.pdf (accessed 27/06/2018).

Grassie SL (2015) Traction, curving and surface damage of rails, Part 2: Rail damage. *Proceedings of the Institution of Mechanical Engineers, Part F: Journal of Rail and Rapid Transit* **229(3)**: 330–339, https://doi.org/10.1177/0954409714541648.

Grassie SL and Elkins JA (2005) Tractive effort, curving and surface damage of rails. *Wear* **258(7–8)**: 1235–1244, https://doi.org/10.1016/j.wear.2004.03.064.

Hou K, Kalousek J and Dong R (2003) A dynamic model for an asymmetrical vehicle/track system. *Journal of Sound and Vibration* **267(3)**: 591–604, https://doi.org/10.1016/S0022-460X(03)00726-0.

Ishizaka K, Lewis SR and Lewis R (2017) The low adhesion problem due to leaf contamination in the wheel/rail contact: bonding and low adhesion mechanisms. *Wear* **378–379**: 183–197, https://doi.org/10.1016/j.wear.2017.02.044.

Kapoor A, Schmid F and Fletcher D (2002) Managing the critical wheel/rail interface. *Railway Gazette International* **158(1)**: 25–28.

Lee C, Lin C and Chen M (2001) Sliding-window filtering: an efficient algorithm for incremental mining. In *Proceedings of ACM Conference on Information and Knowledge Management* (Paques H and Liu L (eds)). ACM, New York, NY, USA, pp. 263–270.

Li D, Otter D and Carr G (2010) Railway bridge approaches under heavy axle load traffic: problems, causes, and remedies. *Proceedings of the Institution of Mechanical Engineers, Part F: Journal of Rail and Rapid Transit* **224(5)**: 383–390, https://doi.org/10.1243/09544097JRRT345.

Network Rail (2011) *West Coast Main Line Route Utilisation Strategy*. Network Rail, London, UK, RUS146/July 2011.

Omnicom Engineering (2017) *Omnicom Rail View*. See http://www.rail-view.co.uk/RailView/Default.aspx (accessed 20/09/2017).

Pearce TG and Watkins DJ (1987) *Adhesion and Leaves – A Review of the Problem and Potential Solutions*. British Rail Research, Derby, UK, Report TM-VTI-017, See http://www.sparkrail.org (accessed 27/06/2018).

Poole W (2007) *Characteristics of Railhead Leaf Contamination*. Rail Safety and Standards Board, London, UK, Summary report T354. See http://www.sparkrail.org (accessed 27/06/2018).

Railtrack (2001) *Rolling Contact Fatigue in Rails: A Guide to Current Understanding and Practice*. Railtrack Plc, London, UK, Report RT/PWG/001.

RSSB (Rail Safety and Standards Board) (2003) *ERTMS Adhesion Management: An Assessment of the Available Adhesion and Slip Risk for ERTMS*. RSSB, London, UK, Report T080. See http://www.sparkrail.org (accessed 27/06/2018).

RSSB (2014) *Investigation into the Effect of Moisture on Rail Adhesion*. RSSB, London, UK, Report T1042. See http://www.rssb.co.uk (accessed 27/06/2018).

Sanz E, Vega C, Abascal JL and MacDowell LG (2004) Phase diagram of water from computer simulation. *Physics Review Letters* **92(25)**: 255701-1–255701-4.

Scott D, Fletcher DI and Cardwell BJ (2014) Simulation study of thermally initiated rail defects. *Proceedings of the Institution of Mechanical Engineers, Part F: Journal of Rail and Rapid Transit* **228(2)**: 113–127, https://doi.org/10.1177/0954409712465697.

Spoors R (2012) Modern track renewal on the West Coast Main Line. *Rail Technology Review* **4**: 8–12.

Wang X, Kruger U and Irwin GW (2005) Process monitoring approach using fast moving window PCA. *Industrial & Engineering Chemistry Research* **44(15)**: 5691–5702, https://doi.org/10.1021/ie048873f.

White BT, Nilsson R, Olofsson U *et al.* (2017) A study into the effect of the presence of moisture at the wheel/rail interface during dew and damp conditions. *Proceedings of the Institution of Mechanical Engineers, Part F: Journal of Rail and Rapid Transit* **232(4)**: 979–989. doi.org/10.1177/0954409717706251.

Zhu Y, Olofsson U and Nilsson R (2014) A field test study of leaf contamination on railhead surfaces. *Proceedings of the Institution of Mechanical Engineers, Part F: Journal of Rail and Rapid Transit* **228(1)**: 71–84, https://doi.org/10.1177/0954409712464860.

Appendix C

Wheel Slide Protection Data Extraction Methodology

The wheel slide protection (WSP) data used in Chapter 3 was stored in an structured query language (SQL) database. To extract the required data from the initial tables into a format which could be interpreted by the mapping software the data-sets were linked through matching common values within the columns.

For the class 390 trains combining the tables assigned each wheel slide event with a global positioning system (GPS) location from the train management system (TMS) data-set and a line direction from the balise data-set. The balise data was linked with the balise ID present in both data-sets. To ascertain a location for the class 390 trains at the time of the WSP event the TMS data was linked using the vehicle number and date/time of event to identify the exact vehicle at the exact time of incident. The date/time columns were converted to a timestamp to allow for a numeric comparison instead of a date/time comparison to provide an easier approach when considering time intervals. A visual representation of the links between the tables is shown in Figure C.1. The results were returned only if the row fulfilled all of the criteria.

The initial application of time intervals to increase the amount of the WSP events which had been assigned a GPS location produced duplicate results where a WSP event had two or more TMS locations falling within this timestamp range, therefore listing the same event multiple times, one for each corresponding location. The duplicate WSP events were eliminated from the result-set using a group clause stating that only the maximum TMS location which fell within the time interval was returned in the results. It would have been more ideal to return the mode or smallest time interval but SQL does not have a function to ascertain the mode of a selection and returning the TMS location with the smallest time interval would have required a large amount of extra coding.

The data was split into five one yearly data-sets which covered the 2009-2013 period considered so the queries extracting the data into new tables could be run in parallel. To run this type of analysis in series on such a large data-set of one and a half million recorded WSP events to compare with seventy million recorded train locations in the TMS data would have taken excessive time even if it had not exceeded the database size limits within SQL.

To calculate a total of the WSP events at each balise the query counted the number of WSP events that occurred near each balise and returned the sum for every balise, even if it was zero, in the results. This was done for the class 221 and class 390 separately, as well as a combined total.

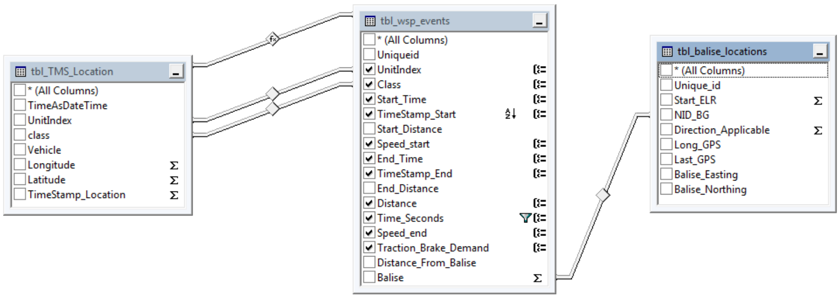

Figure C.1: Visual representation showing how the tables were linked within Structured Query Language to generate the results

Appendix D

Scripts for Automatic Application of Loads into BEASY

D.1 Application of Load Directly onto Patches Code

In this Appendix four sections of code are given. The first locates the mesh points associated with the element with the applied load, the second locates the coordinates of these mesh points and the third and fourth apply either the bending moment or the contact force. When the three for the desired patch loading (bending moment or contact force) are used in order on the dat file, these will generate the desired loading onto the rail model. The dat file must have a patch load already defined on the elements upon which the load will be applied, but this can be a constant (e.g. zero) value which is simple to apply in the main interface. The code given here was used to apply both the bending moment and the contact force within this thesis.

To find the mesh points associated with the element with the applied load:

```
'before starting: ensure .dat file is imported with:
'delimited columns,
'delimiter character - space,
'treat consectutive delimiters as one option deselected
Sub GetMeshPoints()
Application.ScreenUpdating = False

'Define variables
```

```
Dim ElArray As Variant
Dim ForceEl As Variant
Dim ElMP(5999, 5) As Variant
Dim MatchCol As Variant
Dim ActiveRow As Integer
Dim a As Integer
Dim b As Integer
Dim c As Integer
Dim d As Integer
Dim rows As Integer

'ensure correct workbook active
Workbooks("apply contact.xlsm").Activate
'ensure correct sheet active
Worksheets("Model_v6").Activate

'create array of rows/columns difining elements and mesh points within them,
'include all "Master" elements in zone 11,
'start from row after "Master" in zone 11,
'end on row before "Slave" in zone 11
ElArray = Range("A30160:BA37395")

Worksheets("get_load").Activate
rows = 6000
'create array of elements where load applied
ForceEl = Range("A3:A" & rows + 2)

'loop through each row to find mesh points within each element that has a load applied
For a = 1 To rows Step 1
    If Not ForceEl(a, 1) = "" Then 'if there is an element in row
'ensure looking in correct column of ElArray (dependant on number of digits)
        If ForceEl(a, 1) < 10 Then
            MatchCol = Application.index(ElArray, , 9)
        ElseIf ForceEl(a, 1) < 100 Then
            MatchCol = Application.index(ElArray, , 8)
        ElseIf ForceEl(a, 1) < 1000 Then
            MatchCol = Application.index(ElArray, , 7)
        ElseIf ForceEl(a, 1) < 10000 Then
            MatchCol = Application.index(ElArray, , 6)
        Else: MatchCol = Application.index(ElArray, , 5)
        End If

'find row in ElArray that contains element that force is applied to
        ActiveRow = Application.Match(ForceEl(a, 1), MatchCol, 0)

```

```
'reset counters
        c = 0
        d = 0

'loop through each column of ElArray to find mesh points within defined element
        For b = 9 To 53 Step 1
'find first 6 mesh points
            If c < 6 Then 'if not found first 6 mesh points
                If Not ElArray(ActiveRow, b) = "" Then 'if there is a mesh point in column
                    ElMP(a - 1, c) = Application.index(ElArray, ActiveRow, b) 'input this into output array
                    c = c + 1 'increase count so next mesh point is input into next column
                End If
            End If
'for reduced quadratic elements, 9 mesh points with 3 being on next line, find remaining 3
            If ElArray(ActiveRow, 1) = "Q3_8" Then 'if element type reduced quadratic
                If d < 3 Then 'if not found remaining 3 mesh points
                    If Not ElArray(ActiveRow + 1, b) = "" Then 'if there is a mesh point in column
                        ElMP(a, d) = Application.index(ElArray, ActiveRow + 1, b) 'input this into output array
                        d = d + 1 'increase count so next mesh point is input into next column
                    End If
                End If
            End If
        Next
    End If
Next

'paste output array into sheet
Range("C3:H" & rows + 2) = ElMP

Application.ScreenUpdating = True
End Sub
```

To find the coordinates of the mesh points associated with the element with the applied load:

```
'before starting: ensure run Sub GetMeshPoints()
Sub Getxy() 'or Getyz() for bending moment application
Application.ScreenUpdating = False

'define variables
Dim ElMP As Variant
Dim MPnum As Variant
'for contact load finding xy, for bending moment yz use appropiate Dim below
Dim MPxy As Variant
Dim MPyz As Variant
Dim MatchCol As Variant
Dim xy(5999, 12) As Variant
Dim yz(1263, 12) As Variant
Dim ActiveRow As Integer
Dim e As Integer
Dim f As Integer
Dim g As Integer
Dim h As Integer
Dim rows As Integer

'ensure correct workbook active
Workbooks("apply contact.xlsm").Activate
'ensure correct sheet active
Worksheets("Model_v6").Activate

'create array of rows/columns difining mesh points
MPnum = Range("E40:I26384")
'create array of rows/columns difining mesh point xy coordinates
MPxy = Range("G40:N26384")

Worksheets("get_load").Activate

rows = 6000
'create array of mesh points where load applied
ElMP = Range("C3:H" & rows + 2)

'loop through each row to find xy coordinates for mesh points that have a load applied
For e = 1 To rows Step 1 'loop through rows
    For f = 1 To 6 Step 1 'loop through columns
        If Not ElMP(e, f) = "" Then 'if there is a mesh point in cell
'ensure looking in correct column of ElMP (dependant on number of digits)
```

```
            If ElMP(e, f) < 10 Then
                MatchCol = Application.index(MPnum, , 5)
            ElseIf ElMP(e, f) < 100 Then
                MatchCol = Application.index(MPnum, , 4)
            ElseIf ElMP(e, f) < 1000 Then
                MatchCol = Application.index(MPnum, , 3)
            ElseIf ElMP(e, f) < 10000 Then
                MatchCol = Application.index(MPnum, , 2)
            Else: MatchCol = Application.index(MPnum, , 1)
            End If

'find row in ElMP that contains mesh point that force is applied to
            ActiveRow = Application.Match(ElMP(e, f), MatchCol, 0)

'loop through each column of MPxy to find xy coordinates (for contact load application)
            For g = 1 To 5 Step 1
                If Not MPxy(ActiveRow, g) = "" Then 'if there is a x coordinate in cell
                    xy(e - 1, f - 1) = MPxy(ActiveRow, g) 'x coordinate
                    xy(e - 1, f + 6) = MPxy(ActiveRow, g + 3) 'y coordinate (offset is constant as y always positive)
                    GoTo NextRow 'exit loop once found xy coordinates
                End If
            Next

'loop through each column of MPyz to find yz coordinates (for bending moment application)
                        For g = 8 To 4 Step -1
                                If Not MPyz(ActiveRow, g) = "" Then
                                        yz(e - 1, f + 6) = MPyz(ActiveRow, g)
                    yz(e - 1, f - 1) = MPyz(ActiveRow, g - 3)
                    GoTo NextRow
                End If
            Next
NextRow:
        End If
    Next
Next

'paste output array into sheet
Range("J3:V" & rows + 2) = xy 'or = yz for bending moment application

Application.ScreenUpdating = True
End Sub
```

For the application of the contact load the final script is:

```
'before starting: ensure run Sub GetMeshPoints() and Getxy()
Sub GetHertzian()
Application.ScreenUpdating = False

'define variables
Dim x As Variant
Dim y As Variant
Dim Direction As Variant
Dim u As Variant
Dim Hertz(5999, 2) As Variant
Dim a As Double
Dim b As Double
Dim p0 As Double
Dim xConCentre As Integer
Dim yConCentre As Integer
Dim ActiveRow As Integer
Dim i As Integer
Dim j As Integer
Dim k As Integer
Dim l As Integer
Dim LS As Integer
Dim rows As Integer
Dim ResultsSheet As String
Dim flg As Boolean
Dim sh As Worksheet

'ensure correct workbook active
Workbooks("apply contact.xlsm").Activate
'ensure correct sheet active
Worksheets("get_load").Activate

rows = 6000 'number of rows required to find all elements where load applied
a = 5.92 'major semi-axis
b = 3.94 'minor semi-axis
p0 = -1750 'max pressure
x = Range("J3:O" & rows + 2) 'mesh point x coordinate
y = Range("Q3:V" & rows + 2) 'mesh point y coordinate
Direction = Range("B3:B" & rows + 2) 'direction load applied in
u = 0.3 'friction coefficient

xConCentre = 0.000001599162 'centre of contact x direction
yConCentre = 86 'centre of contact y direction

```

```
For LS = 1 To 16 Step 1 'loop through load sets
        Worksheets("get_load").Activate
'loop through each row to calculate load applied at each mesh point
    For i = 1 To rows Step 3 'loop through rows
        For j = 1 To 6 Step 1 'loop through columns
            If Direction(i, 1) = 2 Then 'if direction y direction then calculate longitudinal traction
                If j <= 3 Then 'for first 3 columns
                    Hertz(i - 1, j - 1) = u * (p0 * (1 - ((x(i, j) - xConCentre) ^ 2 / b ^ 2) - ((y(i, j) - yConCentre) ^ 2 / a ^ 2) ^ 0.5)) 'first row
                    Hertz(i + 1, j - 1) = u * (p0 * (1 - ((x(i + 1, j) - xConCentre) ^ 2 / b ^ 2) - ((y(i + 1, j) - yConCentre) ^ 2 / a ^ 2) ^ 0.5)) 'second row
                Else: Hertz(i, j - 4) = u * (p0 * (1 - ((x(i, j) - xConCentre) ^ 2 / b ^ 2) - ((y(i, j) - yConCentre) ^ 2 / a ^ 2) ^ 0.5)) 'for columns 4-6
                End If
            ElseIf Direction(i, 1) = 3 Then 'if direction z direction then calculate vertical traction
                If j <= 3 Then 'for first 3 columns
                    Hertz(i - 1, j - 1) = p0 * (1 - ((x(i, j) - xConCentre) ^ 2 / b ^ 2) - ((y(i, j) - yConCentre) ^ 2 / a ^ 2) ^ 0.5) 'first row
                    Hertz(i + 1, j - 1) = p0 * (1 - ((x(i + 1, j) - xConCentre) ^ 2 / b ^ 2) - ((y(i + 1, j) - yConCentre) ^ 2 / a ^ 2) ^ 0.5) 'second row
                Else: Hertz(i, j - 4) = p0 * (1 - ((x(i, j) - xConCentre) ^ 2 / b ^ 2) - ((y(i, j) - yConCentre) ^ 2 / a ^ 2) ^ 0.5) 'for columns 4-6
                End If
            End If
        Next
    Next
'remove all postive values (ie those outside contact patch)
    For k = 1 To rows Step 1
        For l = 1 To 3 Step 1
            If Hertz(k - 1, l - 1) > 0 Then
                Hertz(k - 1, l - 1) = 0
            End If
        Next
    Next
'paste Hertz pressure profile into worksheet
    Range("X3:Z" & rows + 2) = Hertz

    Worksheets("Load set extra").Activate
```

```
'set correct spacing so dat file recognises load set ID
    If LS < 10 Then
        Range("A1") = "LOAD_SET     " & LS
    Else
        Range("A1") = "LOAD_SET    " & LS
    End If

    Range("A1:A44").Copy 'copy load set data defined before traction in dat file
        : e.g. load set ID and displacement BC's
'open/create sheet for load set contact
    ResultsSheet = "LoadSet" & LS
    flg = False
'check if worksheet defined already exists
    For Each sh In Worksheets
        If sh.Name = ResultsSheet Then
            flg = True: Exit For
        End If
    Next
'if sheet exists activate sheet else create sheet
    If flg = True Then
        Worksheets(ResultsSheet).Activate
    Else 'if sheet doesn't exist create before activating
        Worksheets.Add(After:=Sheets(Sheets.Count)).Name = ResultsSheet
        Worksheets(ResultsSheet).Activate
    End If

'paste load set data defined before traction in dat file: e.g. load set ID and
    displacement BC's
    Range("A1:A44").PasteSpecial

'copy loading into load set sheet ready for dat file
    Worksheets("get_load").Activate
    Range("AB3:AB" & rows + 2).Copy
    Worksheets(ResultsSheet).Activate
    Range("A45:A" & rows + 45).PasteSpecial xlPasteValues

'complete the load set sheet ready for dat file with load set data defined after
    traction in dat file: e.g. zone properties
    Worksheets("Load_set_extra").Activate
    Range("L1:L671").Copy
    Worksheets(ResultsSheet).Activate
    Range("A" & 45 + rows & ":A" & 45 + rows + 671).PasteSpecial xlPasteValues
    yConCentre = yConCentre + 2 'move centre of contact to next step
Next
Application.ScreenUpdating = True
End Sub
```

For the application of the bending moment the final script is:

```
'before starting: ensure run Sub GetMeshPoints() and Getyz()

Sub GetTract()
Application.ScreenUpdating = False

'define variables
Dim y As Variant
Dim z As Variant
Dim Tract(1263, 2) As Variant
Dim Mom As Variant
Dim NeutA As Double
Dim MomI As Double
Dim CrossA As Double
Dim ActiveRow As Integer
Dim i As Integer
Dim j As Integer
Dim k As Integer

'ensure correct workbook active
Workbooks("mesh_points_for_PL.xlsm").Activate
'ensure correct sheet active
Worksheets("get_load").Activate
Mom = 13000000
y = Range("J3:O1266")
z = Range("Q3:V1266")
NeutA = 80.92
MomI = 30383000
CrossA = 7590.09

'loop through each row to calculate load applied at each mesh point
For i = 1 To 1264 Step 1 'loop through rows
    For j = 1 To 6 Step 1 'loop through columns
        If Not z(i, j) = "" Then
            If y(i, j) = 0 Then 'for one end of model
                If i = 1 Then 'first row only
                    If j <= 3 Then 'for first 3 columns
                        Tract(i - 1, j - 1) = -(Mom * (z(i, j) - NeutA)) / MomI
                    Else: Tract(i, j - 4) = -(Mom * (z(i, j) - NeutA)) / MomI 'columns 4-6
                    End If
                ElseIf z(i - 1, j) = "" Then 'if i>1 then defines start of next element
                    If j <= 3 Then 'for first 3 columns
```

```
                    Tract(i - 1, j - 1) = -(Mom * (z(i, j) - NeutA)) / MomI
                Else: Tract(i, j - 4) = -(Mom * (z(i, j) - NeutA)) / MomI 'columns 4-6
                End If
            Else: Tract(i, j - 1) = -(Mom * (z(i, j) - NeutA)) / MomI 'defines load applied to mesh points 7-9
            End If
        ElseIf y(i, j) = 200 Then 'same process for the other end of model (loading reversed)
            If i = 1 Then
                If j <= 3 Then 'for first 3 columns
                    Tract(i - 1, j - 1) = (Mom * (z(i, j) - NeutA)) / MomI
                Else: Tract(i, j - 4) = (Mom * (z(i, j) - NeutA)) / MomI
                End If
            ElseIf z(i - 1, j) = "" Then
                If j <= 3 Then
                    Tract(i - 1, j - 1) = (Mom * (z(i, j) - NeutA)) / MomI
                Else: Tract(i, j - 4) = (Mom * (z(i, j) - NeutA)) / MomI
                End If
            Else: Tract(i, j - 1) = (Mom * (z(i, j) - NeutA)) / MomI
            End If
        End If
    End If
Next
Next
'paste loads into sheet
Range("X3:Z1266") = Tract

Application.ScreenUpdating = True
End Sub
```

D.2 Application of Load via Load Points Code

In this Appendix the method for automatically defining load points and the associated applied force is shown. Figure D.1 shows the base data required for this approach. On the left is the unique model extremities as calculated from the out file. From this the model extremities are calculated at 0.5mm intervals with curved geometry approximated to a triangular shape. This underestimated the boundary at the convex curvature and overestimated the geometry at the concave curvature. A manual check ensured all points remained in the geometry. The points that are required at each height are then defined on the right. The below code automatically increases z from the base of the rail to the top and returns the position and applied load of the load points which can then be copied directly into the dat file.

remove duplicates tool. Sort descending			model extremities at 0.5mm intervals			for z:	2
unique z	max x	min x	z	max x	min x		available x
172.00000	7.817056E-06	-7.817056E-06	0.00	0.000000E+00	0.000000E+00		-7.475000E+01
171.82570	1.022800E+01	-1.022800E+01	0.25	7.325000E+01	-7.325000E+01		-7.425000E+01
169.69780	2.602650E+01	-2.602650E+01	0.50	7.350000E+01	-7.350000E+01		-7.375000E+01
157.70000	3.600000E+01	-3.600000E+01	0.75	7.375000E+01	-7.375000E+01		-7.325000E+01
136.72470	3.704877E+01	-3.704877E+01	1.00	7.400000E+01	-7.400000E+01		-7.275000E+01
133.75550	3.507774E+01	-3.507774E+01	1.25	7.425000E+01	-7.425000E+01		-7.225000E+01
133.7555	3.507774E+01	-3.507774E+01	1.50	7.450000E+01	-7.450000E+01		-7.175000E+01
127.00060	1.650157E+01	-1.650157E+01	1.75	7.475000E+01	-7.475000E+01		-7.125000E+01
127.0006	1.650157E+01	-1.650157E+01	2.00	7.500000E+01	-7.500000E+01		-7.075000E+01
122.59000	1.223796E+01	-1.223796E+01	2.25	7.500000E+01	-7.500000E+01		-7.025000E+01
122.59	1.223796E+01	-1.223796E+01	2.50	7.500000E+01	-7.500000E+01		-6.975000E+01
119.77940	1.145046E+01	-1.145046E+01	2.75	7.500000E+01	-7.500000E+01		-6.925000E+01
119.7794	1.145046E+01	-1.145046E+01	3.00	7.500000E+01	-7.500000E+01		-6.875000E+01
92.25	8.250000E+00	-8.250000E+00	3.25	7.500000E+01	-7.500000E+01		-6.825000E+01
92.24999	8.250000E+00	-8.250000E+00	3.50	7.500000E+01	-7.500000E+01		-6.775000E+01
60.25	8.250000E+00	-8.250000E+00	3.75	7.500000E+01	-7.500000E+01		-6.725000E+01
32.72059	1.145046E+01	-1.145046E+01	4.00	7.500000E+01	-7.500000E+01		-6.675000E+01
29.90998	1.223796E+01	-1.223796E+01	4.25	7.500000E+01	-7.500000E+01		-6.625000E+01
25.49943	1.650157E+01	-1.650157E+01	4.50	7.500000E+01	-7.500000E+01		-6.575000E+01
14.85625	4.577031E+01	-4.577031E+01	4.75	7.500000E+01	-7.500000E+01		-6.525000E+01
14.85624	4.577033E+01	-4.577033E+01	5.00	7.500000E+01	-7.500000E+01		-6.475000E+01
12.54963	5.659015E+01	-5.659015E+01	5.25	7.500000E+01	-7.500000E+01		-6.425000E+01
11.5	7.128499E+01	-7.128499E+01	5.50	7.500000E+01	-7.500000E+01		-6.375000E+01
7.510165	7.500000E+01	-7.500000E+01	5.75	7.500000E+01	-7.500000E+01		-6.325000E+01
2	7.500000E+01	-7.500000E+01	6.00	7.500000E+01	-7.500000E+01		-6.275000E+01
1.70974E-14	7.300000E+01	-7.300000E+01	6.25	7.500000E+01	-7.500000E+01		-6.225000E+01
0	7.300000E+01	-7.300000E+01	6.50	7.500000E+01	-7.500000E+01		-6.175000E+01

Figure D.1: Model extremities for determining load point location

The below code defines the position of the load points:

```
Sub copy_x() 'copying points at increasing heights for both ends of model
Application.Calculation = xlCalculationAutomatic 'allow excel to calculate all
    formulas

Dim findrow0 As Range
Dim findrow1 As Range
Dim findrow2 As Range
Dim FindRowNumber0 As Long
Dim FindRowNumber1 As Long
Dim FindRowNumber2 As Long
Dim rowPC As Long
Dim PC() As Variant
Dim PointSep As Single

Workbooks("load distribution for bending.xlsm").Activate
Worksheets("applying body loads").Activate
```

```

'define point separation PointSep = 0.5
Range("AO1") = PointSep

Range("AB1").FormulaR1C1 = PointSep / 2 'define start height
Range("AF4").FormulaR1C1 = "endx" 'set top row for pasted values to ensure starts from top/has a start point if sheet blank

Application.Calculation = xlCalculationManual 'prevent excel to calculate formulas

While Range("AB1") < 172 'while height below model height copy values (endx used as row count)
    Range("AB3:AB500").Select 'select points at the height interval
    Selection.Copy 'copy points at the height interval
    Set findrow0 = Range("AF:AF").Find(What:="endx", LookIn:=xlValues) 'find end row of points at previous height interval
        FindRowNumber0 = findrow0.Row
    Range("AF" & FindRowNumber0).Select 'select row with "endx" in ie: next row for data
    Selection.PasteSpecial Paste:=xlPasteValues, Operation:=xlNone, SkipBlanks:=False, Transpose:=False 'paste points as values
    Range("AB1").Select 'select height interval
    Selection.Copy 'copy height interval
'find "endx" in cells just pasted for row of points at height interval
    Set findrow1 = Range("AF:AF").Find(What:="endx", LookIn:=xlValues)
    FindRowNumber1 = findrow1.Row - 1 'remove row with "endx" in
    Range("AH" & FindRowNumber0 & ":AH" & FindRowNumber1).Select 'select relavent rows for current height interval
'paste height interval value
    Selection.PasteSpecial Paste:=xlPasteValues, Operation:=xlNone, SkipBlanks:=False, Transpose:=False
    Range("AB1") = Range("AB1") + PointSep 'next point height interval
    Range("AB3:AB500").Calculate 'allow formula caluclation for points accross cross section
Wend

Range("AG4:AG" & FindRowNumber1) = 1 'include y value (distance into model)

Range("AF4:AH" & FindRowNumber1 + 1).Select 'select all data for first end of model (include "endx" row for later calcs)
Selection.Copy
Range("AF" & FindRowNumber1 + 1).Select 'paste in "endx" row (repeats point load locations at other end of model)
Selection.PasteSpecial Paste:=xlPasteValues, Operation:=xlNone, SkipBlanks:=False, Transpose:=False
```

```
Set findrow2 = Range("AF:AF").Find(What:="endx", LookIn:=xlValues) 'find end row of all points
FindRowNumber2 = findrow2.Row - 1 'remove "endx" row

Range("AG" & FindRowNumber1 + 1 & ":AG" & FindRowNumber2) = 199 'include y value for 2nd face (distance into model)

PC = Range("AE4:AE" & FindRowNumber2) 'create array of size of all rows populated
PC(1, 1) = 1 'set initial point count value

For rowPC = 2 To FindRowNumber2 - 3 'for loop to count number of load points and input into array
    PC(rowPC, 1) = PC(rowPC - 1, 1) + 1
Next rowPC

Range("AE4:AE" & FindRowNumber2) = PC 'paste array into excel to give load point id's

Application.Calculation = xlCalculationAutomatic 'allow excel to calculate all formulas
End Sub
```

The below code correctly formats the force applied to each load point, allowing it to be directly copied into the dat file. The force applied to each load point can then be calculated from the shear force generated by the bending moment:

```
Sub loads() 'separating LP's into the zones so loads applied to correct zone
 Application.Calculation = xlCalculationManual 'allow excel to calculate all formulas

Dim ARNLP As Long
Dim ARNZ1 As Long
Dim ARNZ2 As Long
Dim ARNZ3 As Long
Dim ARNZ4 As Long
Dim ARNZ12 As Long
Dim ARNZ13 As Long
Dim ARNZ14 As Long
Dim ARNZ15 As Long
Dim LP() As Variant
Dim ZONE1(12100, 1) As Variant '2 columns (count starts at zero) rows should be enough to contain all data
Dim ZONE2(12100, 1) As Variant
Dim ZONE3(12100, 1) As Variant
Dim ZONE4(12100, 1) As Variant
Dim ZONE12(12100, 1) As Variant
Dim ZONE13(12100, 1) As Variant
Dim ZONE14(12100, 1) As Variant
Dim ZONE15(12100, 1) As Variant

 Workbooks("load distribution for bending.xlsm").Activate
 Worksheets("applying body loads").Activate

 'define intial array row numbers for zone allocation
ARNZ1 = 0
ARNZ2 = 0
ARNZ3 = 0
ARNZ4 = 0
ARNZ12 = 0
ARNZ13 = 0
ARNZ14 = 0
ARNZ15 = 0

LP = Range("AE4", Range("AH4").End(xlDown)) 'define load point array

For ARNLP = 1 To UBound(LP) 'increase row count on search column
```

```
    If LP(ARNLP, 3) = 1 Then 'if in zone 1-4
        If LP(ARNLP, 4) < 29.9 Then 'if in zone 1 or 2
            If LP(ARNLP, 2) < 0 Then 'if in zone 1
                ZONE1(ARNZ1, 1) = LP(ARNLP, 1) 'insert point number into zone 1 array
                ZONE1(ARNZ1, 0) = "POINT FORCE"
                ARNZ1 = ARNZ1 + 1 'increase row count on zone 1 column
            Else: ZONE2(ARNZ2, 1) = LP(ARNLP, 1) 'else insert point number into zone 2 array
                ZONE2(ARNZ2, 0) = "POINT FORCE"
                ARNZ2 = ARNZ2 + 1 'increase row count on zone 2 column
            End If
        ElseIf LP(ARNLP, 4) < 122.6 Then 'else if in zone 3
            ZONE3(ARNZ3, 1) = LP(ARNLP, 1)
            ZONE3(ARNZ3, 0) = "POINT FORCE"
            ARNZ3 = ARNZ3 + 1 'increase row count on zone 3 column
        Else: ZONE4(ARNZ4, 1) = LP(ARNLP, 1)
            ZONE4(ARNZ4, 0) = "POINT FORCE"
            ARNZ4 = ARNZ4 + 1 'increase row count on zone 4 column
        End If
    ElseIf LP(ARNLP, 4) < 29.9 Then 'if in zone 12 or 13
        If LP(ARNLP, 2) < 0 Then 'if in zone 12
            ZONE12(ARNZ12, 1) = LP(ARNLP, 1) 'insert point number into zone 12 array
            ZONE12(ARNZ12, 0) = "POINT FORCE"
            ARNZ12 = ARNZ12 + 1 'increase row count on zone 12 column
        Else: ZONE13(ARNZ13, 1) = LP(ARNLP, 1) 'insert point number into zone 13 array
            ZONE13(ARNZ13, 0) = "POINT FORCE"
            ARNZ13 = ARNZ13 + 1 'increase row count on zone 13 column
        End If
    ElseIf LP(ARNLP, 4) < 122.6 Then 'if in zone 14
        ZONE14(ARNZ14, 1) = LP(ARNLP, 1) 'insert point number into zone 14 array
        ZONE14(ARNZ14, 0) = "POINT FORCE"
        ARNZ14 = ARNZ14 + 1 'increase row count on zone 14 column
    Else: ZONE15(ARNZ15, 1) = LP(ARNLP, 1) 'insert point number into zone 15 array
        ZONE15(ARNZ15, 0) = "POINT FORCE"
        ARNZ15 = ARNZ15 + 1 'increase row count on zone 15 column
    End If
Next ARNLP

'paste into correct columns
Range("AY4:AZ" & ARNZ1 + 4) = ZONE1
Range("BA4:BB" & ARNZ2 + 4) = ZONE2
Range("BC4:BD" & ARNZ3 + 4) = ZONE3
```

```
Range("BE4:BF" & ARNZ4 + 4) = ZONE4
Range("BG4:BH" & ARNZ12 + 4) = ZONE12
Range("BI4:BJ" & ARNZ13 + 4) = ZONE13
Range("BK4:BL" & ARNZ14 + 4) = ZONE14
Range("BM4:BN" & ARNZ15 + 4) = ZONE15

'recombine into 1 column including zone_ID row
Range("AY3:AZ" & ARNZ1 + 4).Select
Selection.Copy
Range("BP3").Select
ActiveSheet.Paste

Range("BA3:BB" & ARNZ2 + 4).Select
Selection.Copy
Range("BP4").End(xlDown).Offset(1, 0).Select 'find end row and paste in next row
ActiveSheet.Paste

Range("BC3:BD" & ARNZ3 + 4).Select
Selection.Copy
Range("BP4").End(xlDown).Offset(1, 0).Select
ActiveSheet.Paste

Range("BE3:BF" & ARNZ4 + 4).Select
Selection.Copy
Range("BP4").End(xlDown).Offset(1, 0).Select
ActiveSheet.Paste

Range("BG3:BH" & ARNZ12 + 4).Select
Selection.Copy
Range("BP4").End(xlDown).Offset(1, 0).Select
ActiveSheet.Paste

Range("BI3:BJ" & ARNZ13 + 4).Select
Selection.Copy
Range("BP4").End(xlDown).Offset(1, 0).Select
ActiveSheet.Paste

Range("BK3:BL" & ARNZ14 + 4).Select
Selection.Copy
Range("BP4").End(xlDown).Offset(1, 0).Select
ActiveSheet.Paste

Range("BM3:BN" & ARNZ15 + 4).Select
Selection.Copy
Range("BP4").End(xlDown).Offset(1, 0).Select
ActiveSheet.Paste
```

```

'zero force in x-direction - offset 1 column from range used to find end row
Range("BQ4", Range("BQ4").End(xlDown)).Offset(0, 1) = 0
'zero force in z-direction - offset 3 column from range used to find end row
Range("BQ4", Range("BQ4").End(xlDown)).Offset(0, 3) = 0
Range("BS1").Select
Selection.Copy
Range("BQ4", Range("BQ4").End(xlDown)).Offset(0, 2).Select 'offset 2 columns from range used to find end row
ActiveSheet.Paste 'paste formula in cell BS1 into all relavent cells

Application.Calculation = xlCalculationAutomatic 'allow excel to calculate all formulas
End Sub
```

Appendix E

Manually Adding Crack into a 3D Boundary Element Model

This can be done either directly within the base model or in a separate model which is then imported into the base model using the out file function within BEASY.

A crack can be manually added in BEASY as shown in Figure E.1. The crack surface patches need to be defined as outward pointing within the zone that they are in. There are several conditions that need to be met when meshing the crack that require consideration:

- All patches must face the same direction.
- All elements on the crack surface need to be quadrilateral.
- Elements in the crack and along crack front need to be continuous.
- Elements that will intersect the model edge need to be continuous with the elements on the model edge.

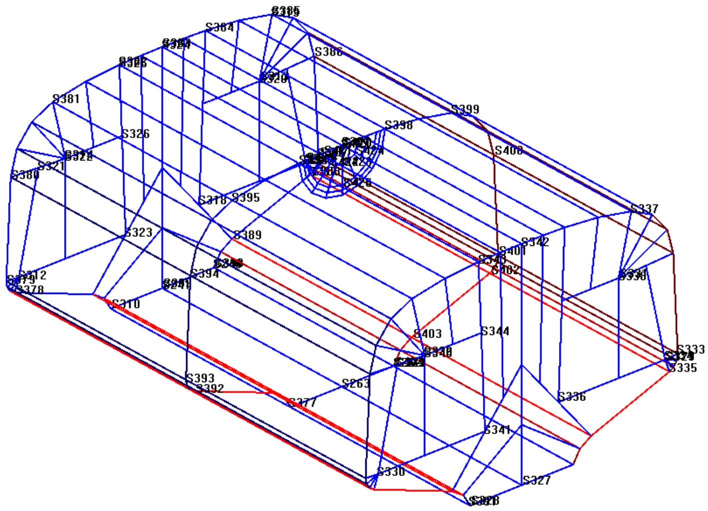

Figure E.1: Defining a crack within the base model

The crack can then be defined using the *preprocess* -> *fracture_data* menu within BEASY.

The contact between the crack faces and the crack face friction must be defined within the dat file. To include this, after the line:

ZONE INITIAL CRACK ELEMENTS GROUP

add in either:

USE NODE TO SURFACE CONTACT for non-conforming contact or USE NODE TO NODE CONTACT for conforming contact between the crack faces.

Then define the friction coefficient (which must be in scientific numeric form):

STATIC FRICTION COEFFICIENT 0.30000000E+00

DYNAMIC FRICTION COEFFICIENT 0.30000000E+00

The crack elements must also be defined as "dual" elements. This is done by adding a "1" to the end of the element definition line in the dat file, see Figure E.2.

```
Q3_8 4722 20150 20025 20027 20164 20151 20026 20165 20157 20158 4722 0
Q3_8 4723 20050 20160 20174 20052 20159 20167 20173 20051 20166 4723 0
Q3_8 4724 20160 20162 20176 20174 20161 20169 20175 20167 20168 4724 0
Q3_8 4725 20162 20164 20178 20176 20163 20171 20177 20169 20170 4725 0
Q3_8 4726 20164 20027 20029 20178 20165 20028 20179 20171 20172 4726 0
Q3_8 4727 20052 20174 20033 20034 20173 20181 19030 20053 20180 4727 0
Q3_8 4728 20174 20176 12245 20033 20175 20183 20032 20181 20182 4728 0
Q3_8 4729 20176 20178 15073 12245 20177 20185 20031 20183 20184 4729 0
Q3_8 4730 20178 20029 17579 15073 20179 20030 19029 20185 20186 4730 0
Q3_8 4731 21362 15508 20196 20190 21361 20193 20195 20201 20192 4731 1
Q3_8 4732 15508 21360 20215 20196 15507 20187 20197 20193 20194 4732 1
Q3_8 4733 20190 20196 20188 20189 20195 20199 20233 20191 20198 4733 1
Q3_8 4734 20196 20215 20227 20188 20197 20216 20232 20199 20200 4734 1
Q3_8 4735 21362 20190 20208 21864 20201 20205 20207 20863 20204 4735 1
Q3_8 4736 20190 20189 20250 20208 20191 20249 20209 20205 20206 4736 1
Q3_8 4737 21864 20208 20267 21865 20207 20211 20203 15493 20210 4737 1
Q3_8 4738 20208 20250 20262 20267 20209 20202 20266 20211 20212 4738 1
Q3_8 4739 21360 21358 20221 20215 21359 20218 20220 20187 20217 4739 1
Q3_8 4740 21358 21357 20285 20221 20366 20284 20222 20218 20219 4740 1
Q3_8 4741 20215 20221 20226 20227 20220 20224 20214 20216 20223 4741 1
Q3_8 4742 20221 20285 20287 20226 20222 20286 20213 20224 20225 4742 1
Q3_8 4743 20227 20226 20238 20188 20214 20235 20237 20232 20234 4743 1
Q3_8 4744 20226 20287 20229 20238 20213 20228 20239 20235 20236 4744 1
Q3_8 4745 20188 20238 20243 20189 20237 20241 20231 20233 20240 4745 1
Q3_8 4746 20238 20229 20295 20243 20239 20230 20244 20241 20242 4746 1
Q3_8 4747 20189 20243 20255 20250 20231 20252 20254 20249 20251 4747 1
Q3_8 4748 20243 20295 20245 20255 20244 20305 20256 20252 20253 4748 1
Q3_8 4749 20250 20255 20260 20262 20254 20258 20261 20202 20257 4749 1
Q3_8 4750 20255 20245 20247 20260 20256 20246 20248 20258 20259 4750 1
Q3_8 4751 20262 20260 20272 20267 20261 20269 20271 20266 20268 4751 1
Q3_8 4752 20260 20247 20264 20272 20248 20263 20273 20269 20270 4752 1
Q3_8 4753 20267 20272 15527 21865 20271 20275 20864 20203 20274 4753 1
Q3_8 4754 20272 20264 21866 15527 20273 20265 20865 20275 20276 4754 1
Q3_8 4755 21357 21356 20278 20285 15506 20277 20289 20284 20288 4755 1
Q3_8 4756 20285 20278 20280 20287 20289 20279 20291 20286 20290 4756 1
Q3_8 4757 20287 20280 20282 20229 20291 20281 20293 20228 20292 4757 1
Q3_8 4758 20229 20282 20297 20295 20293 20283 20296 20230 20294 4758 1
Q3_8 4759 20295 20297 20299 20245 20296 20298 20307 20305 20306 4759 1
Q3_8 4760 20245 20299 20301 20247 20307 20300 20309 20246 20308 4760 1
Q3_8 4761 20247 20301 20303 20264 20309 20302 20311 20263 20310 4761 1
Q3_8 4762 20264 20303 21867 21866 20311 20304 15494 20265 20312 4762 1
Q3_8 4763 20316 15449 20413 20368 15450 20404 20412 20367 20403 4763 0
Q3_8 4764 15449 15447 20415 20413 15448 20406 20414 20404 20405 4764 0
Q3_8 4765 15447 15446 20417 20415 20315 20408 20416 20406 20407 4765 0
Q3_8 4766 15446 15445 20419 20417 20314 20410 20418 20408 20409 4766 0
Q3_8 4767 15445 20313 20318 20419 15444 20317 20420 20410 20411 4767 0
Q3_8 4768 20368 20413 20431 20370 20412 20422 20430 20369 20421 4768 0
Q3_8 4769 20413 20415 20433 20431 20414 20424 20432 20422 20423 4769 0
Q3_8 4770 20415 20417 20435 20433 20416 20426 20434 20424 20425 4770 0
Q3_8 4771 20417 20419 20437 20435 20418 20428 20436 20426 20427 4771 0
```

Figure E.2: dat file extract showing "dual" elements defined on elements that make up the crack surface

Appendix F

Winkler Foundation Equations

The governing equation for an semi-infinite beam on an uniform Winkler foundation is given by:

$$0 = kw + EI\frac{d^4w}{dx^4} \tag{F.1}$$

Upon integration the deflection of the beam (w) is given by:

$$w = e^{\beta x}(C_1\sin(\beta x) + C_2\cos(\beta x)) + e^{-\beta x}(C_3\sin(\beta x) + C_4\cos(\beta x)) \tag{F.2}$$

where:

$$\beta = \sqrt[4]{\frac{k}{4EI}} \tag{F.3}$$

for ease of notation the following relationships are commonly used:

$$A_{\beta x} = e^{-\beta x}(\cos(\beta x) + \sin(\beta x)) \tag{F.4}$$

$$B_{\beta x} = e^{-\beta x}\sin(\beta x) \tag{F.5}$$

$$C_{\beta x} = e^{-\beta x}(\cos(\beta x) - \sin(\beta x)) \tag{F.6}$$

$$D_{\beta x} = e^{-\beta x}\cos(\beta x) \tag{F.7}$$

C_1 to C_4 are the constants of integration that are determined from the boundary conditions. At $x = \infty$ the deflection of the beam, w, equals zero. Therefore C_1 and $C_2 = 0$. C_3 and C_4 are solved by evaluating the bending moment and shear loading at $x = 0$ giving:

$$C_3 = \frac{2\beta^2 M_0}{k} \tag{F.8}$$

$$C_4 = \frac{2\beta P_0}{k} - \frac{2\beta^2 M_0}{k} \tag{F.9}$$

By inserting Equations F.8 and F.9 into F.2 using relationships F.4-F.7. The deflection (w) in the semi-infinite beam is therefore:

$$w = \frac{2\beta P_0}{k} D_{\beta x} - \frac{2\beta^2 M_0}{k} C_{\beta x} \tag{F.10}$$

Therefore the slope (θ), bending moment (M) and shear (V) is given by:

$$\theta = \frac{dw}{dx} = -\frac{2\beta^2 P_0}{k} A_{\beta x} + \frac{4\beta^3 M_0}{k} D_{\beta x} \tag{F.11}$$

$$M = -EI\frac{d^2 w}{dx^2} = -\frac{P_0}{\beta} B_{\beta x} + M_0 A_{\beta x} \tag{F.12}$$

$$V = -EI\frac{d^3 w}{dx^3} = -P_0 C_{\beta x} - \beta M_0 B_{\beta x} \tag{F.13}$$

For the infinite Winkler foundation the opposing sides of the infinite beam are assumed to act as symmetrical semi-infinite beams under a load $P_{0infinite} = P_{0semiinfinte}/2$. The slope of the beam, θ, is zero at $x = 0$ to ensure continuity of the beam. Therefore Equation F.11 becomes:

$$0 = -\frac{2\beta^2 (P_{0semi-infinite}/2)}{k} + \frac{4\beta^3 M_0}{k} \tag{F.14}$$

therefore:

$$M_0 = \frac{P_{0semi-infinite}}{4\beta} \tag{F.15}$$

substituting $P_{0infinite} = P_{0semiinfinte}/2$ and M_0 into Equation F.15 gives:

$$w = \frac{\beta P_{0semi-infinite}}{2k} A_{\beta x} \tag{F.16}$$

$$\theta = \frac{dw}{dx} = -\frac{\beta^2 P_{0semi-infinite}}{k} B_{\beta x} \tag{F.17}$$

$$M = -EI\frac{d^2w}{dx^2} = -\frac{P_{0semi-infinite}}{4\beta} C_{\beta x} \tag{F.18}$$

$$V = -EI\frac{d^3w}{dx^3} = -\frac{P_{0semi-infinite}}{2} D_{\beta x} \tag{F.19}$$

which describes the reaction of the infinite beam supported by a Winkler foundation under the point load P_0.

Appendix G

Euler-Bernoulli Beam on Discrete Support Equations

This method was developed by Adam Beagles. It was used in the co-authored paper between myself, Beagles and Fletcher [2] and a report on the sustainable freight railway [209]. Adam has kindly given his permission for me to use his method within this thesis. The theory behind it is explained here. These formulas allow the displacements and stresses in any point-loaded beam to be calculated.

A solution of the Euler-Bernoulli beam equation $EI\left(\frac{d^4y(x)}{dx^4}\right) = q(x)$ where $y(x)$ is the 'vertical' displacement, x is 'horizontal' distance along beam, the young's modulus (E) and second moment of area (I) are assumed to be constant along the beam, and the function $q(x)$ is the shear force produced by the loading.

The coordinate systems are defined in Figure G.1.

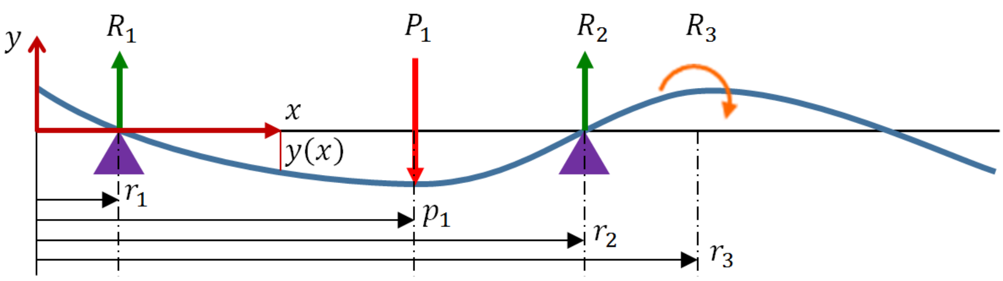

Figure G.1: Beam coordinates

Apart from at the points where point loads or restraints are applied the displacement of the beam is given by:

$$y(x) = \frac{1}{EI}\left(\sum_{k=1}^{N_R} R_k \cdot f(x, r_k, t_k + 2) - \sum_{k=1}^{N_P} P_k \cdot f(x, p_k, 3) + y_0 + y_0' \cdot x\right) \tag{G.1}$$

Where there are N_R reactions, R_k, resulting from constraints applied to the beam at distances r_k from the beginning ($x = 0$) of the beam. Each reaction has a type t_k, which is zero for a moment constraint or unity for a displacement constraint. The beam is loaded by N_P point loads, P_k, at positions p_k along the beam. At the beginning of the beam it has a displacement of y_0/EI and a slope y_0'/EI.

The 'Macaulay function' is:

$$f(x, y, m) = \begin{cases} \frac{(x-y)^m}{m!} & m \geq 0 \, and \, x > y \\ 0 & m < 0 \\ 0 & m > 0 \, and \, x \leq y \\ 1 & m = 0 \, and \, x = y \end{cases} \tag{G.2}$$

The derivatives of the displacement, Equation G.1, are as follows:

The first derivative is the slope of the beam and is given by:

$$y'(x) \equiv \frac{dy(x)}{dx} = \frac{1}{EI}\left(\sum_{k=1}^{N_R} R_k \cdot f(x, r_k, t_k + 1) - \sum_{k=1}^{N_P} P_k \cdot f(x, p_k, 2) + y_0'\right) \tag{G.3}$$

The second derivative multiplied by EI is the bending moment and is given by:

$$BM(x) \equiv EI\frac{d^2y(x)}{dx^2} = \sum_{k=1}^{N_R} R_k \cdot f(x, r_k, t_k) - \sum_{k=1}^{N_P} P_k \cdot f(x, p_k, 1) \tag{G.4}$$

The third derivative multiplied by EI is the shear force and is given by:

$$V(x) \equiv EI\frac{d^3y(x)}{dx^3} = \sum_{k=1}^{N_R} R_k \cdot f(x, r_k, t_k - 1) - \sum_{k=1}^{N_P} P_k \cdot f(x, p_k, 0) \tag{G.5}$$

In Equation G.1 there are $N_R + 2$ unknowns which can be written as a vector:

$$\underline{u} = \begin{pmatrix} R_1 \ldots & R_{N_R} & y_0 & y_0' \end{pmatrix}^T \tag{G.6}$$

The solution of a system of linear equations is therefore:

$$[A] \cdot \underline{u} = \underline{b} \tag{G.7}$$

The terms of matrix $[A]$ and vector $\underline{b}$ are derived from the equations for the N_R constraints, and the equilibrium of vertical forces and bending moment. Cases in which the constraints are rigid are considered first. If $y(r_i) = 0$ (type 1) then, multiplying Equation G.1 by EI the ith row of Equation G.7 is given by:

$$\begin{bmatrix} f(r_i, r_1, t_1 + 2) \ldots & f(r_i, r_{N_R}, t_{N_R} + 2) & 1 & r_i \end{bmatrix} \cdot \underline{u} = \sum_{k=1}^{N_P} P_k \cdot f(r_i, p_k, 3) \tag{G.8}$$

Similarly, if $y'(r_i) = 0$ (type 0) then the corresponding row of Equation G.7 is given by:

$$\begin{bmatrix} f(r_i, r_1, t_1 + 1) \ldots & f(r_i, r_{N_R}, t_{N_R} + 1) & 0 & 1 \end{bmatrix} \cdot \underline{u} = \sum_{k=1}^{N_P} P_k \cdot f(r_i, p_k, 2) \tag{G.9}$$

Equations G.8 and G.9 can be combined by incorporating the type of the constraint and noting that the last two terms in the row can be expressed using the Macaulay function:

$$\begin{bmatrix} f(r_i, r_1, t_i + t_1 + 1) \ldots & f(r_i, r_{N_R}, t_i + t_{N_R} + 1) & f(r_i, 0, t_i - 1) & f(r_i, 0, t_i) \end{bmatrix} \cdot \underline{u} = \sum_{k=1}^{N_P} P_k \cdot f(r_i, p_k, t_i + 2) \tag{G.10}$$

Note that, because $f(x, y, m) = 0$ if $x \geq y$ and $m > 0$, if the r_k are sorted so that $r_k \geq r_{(k-1)} \forall k$ the only non-zero terms in row i of matrix $[A]$ are in columns 1 to $i - 1$ (ignoring the last two columns).

If now we consider constraint i to have stiffness K_i (a displacement stiffness with dimension [Force]/[Distance] for type 1, or a moment stiffness with dimension [Force]*[Distance]/[angle] for type 0), then since a negative movement is associated with a larger reaction (see Figure G.1):

$$\begin{aligned} K_i \cdot y\left(r_i\right) &= -R_i \quad for\, type\, 1 \\ K_i \cdot y'\left(r_i\right) &= R_i \quad for\, type\, 0 \end{aligned} \tag{G.11}$$

Using Equation G.1 it is found that these equations are equivalent to the ith element on the diagonal of matrix $[A]$ (the coefficient of unknown R_i in the ith constraint equation, which was zero for rigid boundary conditions) being EI/K_i. If the stiffness of a support changes only one diagonal element of matrix $[A]$ needs to be changed.

The final two equations are moment and vertical equilibrium. These are achieved if the bending moment and shear force at the end of the beam ($x = end$) are both zero. Using EquationG.4 gives the moment equilibrium equation:

$$\left[\begin{array}{cccc} f\left(end, r_1, t_1\right)\ldots & f\left(end, r_{N_R}, t_{N_R}\right) & 0 & 0 \end{array}\right] \cdot \underline{u} = \sum_{k=1}^{N_P} P_k \cdot f\left(end, p_k, 1\right) \tag{G.12}$$

And, using Equation G.5, the vertical equilibrium equation:

$$\left[\begin{array}{cccc} f\left(end, r_1, t_1 - 1\right)\ldots & f\left(end, r_{N_R}, t_{N_R} - 1\right) & 0 & 0 \end{array}\right] \cdot \underline{u} = \sum_{k=1}^{N_P} P_k \cdot f\left(end, p_k, 0\right) \tag{G.13}$$

Appendix H

Script for Adding Cracks to the Base Model

The script within this Appendix generated the run files for the multiple crack analysis in Chapter 6. An extract of the base dat file is shown in Figure H.1. The script changes the dummy crack attachment mesh point for each crack (highlighted with the red box) with the correct mesh point for the desired spacing. The crack angle is also corrected. Along with the generated crack and joblist files, the corrected dat file is placed in the folder detailing the sizing and spacing combination for that run.

```
  ATTACH CRACK1
    ATTACHMENT MP C
    CRACK ELEVATION(Deg) 0
    CRACK SIZE FACTOR 1.0
    ZONE 1
USE GEOMETRY BASED SIF CALCULATION POSITIONS
LOADING DATA FOR CRACK GROUP
**Note: This model will use contact on the crack faces
**      Other keywords may be included for use in the wizard ONLY
**      Please do not edit this section manually
CRACK LOADING: USE CONTACT
CONTACT: NODE TO NODE:
DYNAMIC FRICTION: 0.3
STATIC FRICTION: 0.3
CRACK LOAD: START LOAD SET 1
**Note: This load set will not apply any traction to this crack face
**      Other keywords may be included for use in the wizard ONLY
**      Please do not edit this section manually
CRACK LOAD: NONE
CRACK LOAD: END LOAD SET 1
    CRACK FILENAME Model_v6.5_C1.crack
  END ATTACH CRACK
  ATTACH CRACK2
    ATTACHMENT MP B
    CRACK ELEVATION(Deg) 0
    CRACK SIZE FACTOR 1.0
    ZONE 1
USE GEOMETRY BASED SIF CALCULATION POSITIONS
LOADING DATA FOR CRACK GROUP
**Note: This model will not use loading on the crack faces
**      Other keywords may be included for use in the wizard ONLY
**      Please do not edit this section manually
CRACK LOADING: USE CONTACT
CONTACT: NODE TO NODE:
DYNAMIC FRICTION: 0.3
STATIC FRICTION: 0.3
CRACK LOAD: START LOAD SET 1
**Note: This load set will not apply any traction to this crack face
**      Other keywords may be included for use in the wizard ONLY
**      Please do not edit this section manually
CRACK LOAD: NONE
CRACK LOAD: END LOAD SET 1
    CRACK FILENAME Model_v6.5_C2.crack
  END ATTACH CRACK
  ATTACH CRACK3
    ATTACHMENT MP A
    CRACK ELEVATION(Deg) 0
    CRACK SIZE FACTOR 1.0
```

Figure H.1: Extract from base dat file with the dummy crack attachment mesh point highlighted. This is changed to the correct mesh point depending on crack separation desired

```
Sub fileamend()
 Application.ScreenUpdating = False
 Application.Calculation = xlCalculationAutomatic

Dim BaseFilePath As String
Dim FilePath0 As String
Dim FilePath1 As String
Dim FilePath2 As String
Dim FilePath3 As String
Dim FilePath4 As String
Dim FilePath5 As String
Dim FilePath6 As String
Dim FilePath7 As String
Dim FileContent As String
Dim TextFile As Integer
Dim a As Double
Dim b As Integer
Dim c As Double
Dim d As Double
Dim e As Double
Dim el As Integer
Dim bLoc As Integer
Dim FSO
Dim MpCrackA() As Variant
Dim MpCrackB() As Variant
Dim MpCrackC() As Variant
Dim LastRow As Long
Dim RN As Long
Dim CraData As String
Dim CraLenCount As Integer
Dim CraLen As Double
Dim CraLenC As Double
Dim CraLenB As Double
Dim CraLenA As Double
Dim Angle As Double

 Set FSO = CreateObject("Scripting.FileSystemObject") 'define FSO to find if folder exists and if not create new

 'filepaths
 Angle = Round(30, 0)
 BaseFilePath = "C:\this is your base file path"
 If Not FSO.FolderExists(BaseFilePath & "\" & Angle & "deg") Then
     FilePath0 = FSO.createfolder(BaseFilePath & "\" & Angle & "deg")
 Else: FilePath0 = BaseFilePath & "\" & Angle & "deg"
```

```
End If
FilePath1 = BaseFilePath & "\basefile"

CraData = ""
Workbooks("data for dat files.xlsm").Activate 'activate correct workbook

For bLoc = 1 To 3 Step 1 'define where crack b is in the set of cracks and set filepaths accordingly
    If bLoc = 1 Then
        If Not FSO.FolderExists(FilePath0 & "\bLHS") Then
            FilePath2 = FSO.createfolder(FilePath0 & "\bLHS")
        Else: FilePath2 = FilePath0 & "\bLHS"
        End If
    ElseIf bLoc = 2 Then
        If Not FSO.FolderExists(FilePath0 & "\bMID") Then
            FilePath2 = FSO.createfolder(FilePath0 & "\bMID")
        Else: FilePath2 = FilePath0 & "\bMID"
        End If
    ElseIf bLoc = 3 Then
        If Not FSO.FolderExists(FilePath0 & "\bRHS") Then
            FilePath2 = FSO.createfolder(FilePath0 & "\bRHS")
        Else: FilePath2 = FilePath0 & "\bRHS"
        End If
    End If
    For a = 0.1 To 1.01 Step 0.1
        a = Round(a, 1) 'was sometimes getting step sizes to many sf. this is to eliminate that
        Sheets("cralen_for_depth_at_angle").Activate 'activate correct sheet in workbook
        Range("G14") = a 'define a/b ratio in spreadsheet
        If Not FSO.FolderExists(FilePath2 & "\a=" & a & "b") Then
            FilePath3 = FSO.createfolder(FilePath2 & "\a=" & a & "b")
        Else: FilePath3 = FilePath2 & "\a=" & a & "b"
        End If
        For c = 0.1 To 1.01 Step 0.1 'size ratios considered
            c = Round(c, 1)
            Sheets("cralen_for_depth_at_angle").Activate 'activate correct sheet in workbook
            Range("G15") = c 'define c/b ratio in spreadsheet
            If Not FSO.FolderExists(FilePath3 & "\c=" & c & "b") Then
                FilePath4 = FSO.createfolder(FilePath3 & "\c=" & c & "b")
            Else: FilePath4 = FilePath3 & "\c=" & c & "b"
            End If
            For d = 0.5 To 4 Step 0.5 'spacing ratios considered between LHS and MID cracks
                d = Round(d, 1)
```

```
                Sheets("cralen_for_depth_at_angle").Activate 'activate correct sheet in workbook
                Range("G16") = d 'define d/b ratio in spreadsheet
                If Not FSO.FolderExists(FilePath4 & "\d=" & d & "b") Then
                    FilePath5 = FSO.createfolder(FilePath4 & "\d=" & d & "b")
                Else: FilePath5 = FilePath4 & "\d=" & d & "b"
                End If
                For e = 0.5 To 4 Step 0.5 'spacing ratios considered between MID and RHS cracks
                    e = Round(e, 1)
                 Sheets("cralen_for_depth_at_angle").Activate 'activate correct sheet in workbook
                    Range("G17") = e 'define e/b ratio in spreadsheet
'get mesh points for each crack depending on their position at spacings e,d for cracks A,B,C
                    MpCrackC = Range("N19:N23")
                    MpCrackB = Range("H19:H23")
                    MpCrackA = Range("T19:T23")
                    If Not FSO.FolderExists(FilePath5 & "\e=" & e & "b") Then
                        FilePath6 = FSO.createfolder(FilePath5 & "\e=" & e & "b")
                    Else: FilePath6 = FilePath5 & "\e=" & e & "b"
                    End If
                    For b = 1 To 5 Step 1
                        TextFile = FreeFile
                        If bLoc = 1 Then 'if largest crack LHS
'set crack length for crack C based on depth b
                            CraLenC = Round(b / Sin(WorksheetFunction.Radians(Angle)), 6)
'set crack length for crack B based on depth c
                            CraLenB = Round((b * c) / Sin(WorksheetFunction.Radians(Angle)), 6)
'set crack length for crack A based on depth a
                            CraLenA = Round((b * a) / Sin(WorksheetFunction.Radians(Angle)), 6)
                        ElseIf bLoc = 2 Then 'if largest crack MID
'set crack length for crack C based on depth c
                            CraLenC = Round((b * c) / Sin(WorksheetFunction.Radians(Angle)), 6)
'set crack length for crack B based on depth b
                            CraLenB = Round(b / Sin(WorksheetFunction.Radians(Angle)), 6)
'set crack length for crack A based on depth a
                            CraLenA = Round((b * a) / Sin(WorksheetFunction.Radians(Angle)), 6)
```

```
                        ElseIf bLoc = 3 Then 'if largest crack RHS
'set crack length for crack C based on depth c
                            CraLenC = Round((b * c) / Sin(WorksheetFunction.Radians(Angle)), 6)
'set crack length for crack B based on depth a
                            CraLenB = Round((b * a) / Sin(WorksheetFunction.Radians(Angle)), 6)
'set crack length for crack A based on depth b
                            CraLenA = Round(b / Sin(WorksheetFunction.Radians(Angle)), 6)
                        End If
                        If Not FSO.FolderExists(FilePath6 & "\b=" & b) Then
                            FilePath7 = FSO.createfolder(FilePath6 & "\b=" & b)
                        Else: FilePath7 = FilePath6 & "\b=" & b
                        End If
                        If Not FSO.FileExists(FilePath7 & "\Model_v6.5.dat") Then 'if .dat file not found create job files
'create .dat file by find and replace required mesh points from template file
                            Open FilePath1 & "\Model_v6.5.dat" For Input As TextFile
                                FileContent = Input(LOF(TextFile), TextFile) 'copy file into a text string
                            Close TextFile
'find/replace command replace mesh points to correct spacing
                            FileContent = Replace(FileContent, "    ATTACHMENT MP C", "    ATTACHMENT MP " & MpCrackC(b, 1))
                            FileContent = Replace(FileContent, "    ATTACHMENT MP B", "    ATTACHMENT MP " & MpCrackB(b, 1))
                            FileContent = Replace(FileContent, "    ATTACHMENT MP A", "    ATTACHMENT MP " & MpCrackA(b, 1))
                            FileContent = Replace(FileContent, "    CRACK ELEVATION(Deg) 0", "    CRACK ELEVATION(Deg) " & (90 - Angle))
                            TextFile = FreeFile
'create new .dat file
                            Open FilePath7 & "\Model_v6.5.dat" For Output As TextFile
                                Print #TextFile, FileContent
                            Close TextFile
                            TextFile = FreeFile
'count through each crack to set up .crack file per crack
                            For CraLenCount = 1 To 3 Step 1
                                If CraLenCount = 1 Then
                                    CraLen = Round(CraLenC, 6)
                                ElseIf CraLenCount = 2 Then
                                    CraLen = Round(CraLenB, 6)
```

```
                ElseIf CraLenCount = 3 Then
                    CraLen = Round(CraLenA, 6)
                End If
'activate correct sheet and filepath for crack size required
'define number of elements on cracks
                If CraLen <= 5 Then
                    Sheets("cra_el_20").Activate
                    el = 20
                Else: Sheets("cra_el_40").Activate
                    el = 40
                End If
                Range("B1") = Round(CraLen, 6)
                LastRow = Range("F1").End(xlDown).Row
'create new .crack file
                If CraLenCount = 1 Then
                    Open FilePath7 & "\Model_v6.5_C1.crack" For Output As TextFile
                ElseIf CraLenCount = 2 Then
                    Open FilePath7 & "\Model_v6.5_C2.crack" For Output As TextFile
                ElseIf CraLenCount = 3 Then
                    Open FilePath7 & "\Model_v6.5_C3.crack" For Output As TextFile
                End If
'copy required mesh points for crack into a string and paste into .crack file
'loop permits by row addition of data
                    For RN = 1 To LastRow
                        CraData = Range("F" & RN)
                        Print #TextFile, CraData
                        CraData = ""
                    Next RN
'add in the remainder of the .crack file from correct template file
                    Open FilePath1 & "\" & el & "el\Model_v6.5_C1.crack" For Input As TextFile + 1
                        FileContent = Input(LOF(TextFile + 1), TextFile + 1)
                    Close TextFile + 1
                    Print #TextFile, FileContent
                Close TextFile
                TextFile = FreeFile
            Next CraLenCount
'create joblist file by find and replace filepath from template file
            Open FilePath1 & "\Model_v6.5_joblist.txt" For Input As TextFile
                FileContent = Input(LOF(TextFile), TextFile)
            Close TextFile
```

```
                            FileContent = Replace(FileContent, "C:\dummy_file_path", FilePath7)
                            TextFile = FreeFile
'create new joblist file
                            Open FilePath7 & "\Model_v6.5_joblist.txt" For Output As TextFile
                                Print #TextFile, FileContent
                            Close TextFile
                            TextFile = FreeFile
'add filepath for joblist file to base of .bat file for multjob running
                            Open BaseFilePath & "\multjobs.txt" For Append As TextFile
                                Print #TextFile, "beasyq.exe -stopcode -joblistfile " & """" & FilePath7 & "\Model_v6.5_joblist.txt" & """"
                            Close TextFile
                        End If
                    Next b
                Next e
            Next d
        Next c
    Next a
Next bLoc

TextFile = FreeFile
'finish .bat file
Open BaseFilePath & "\multjobs.txt" For Append As TextFile
    Print #TextFile, "exit"
Close TextFile

Application.ScreenUpdating = True
End Sub
```

Appendix I

Full Results from the Effect of Crack Shielding on Cracks of Different Sizes and Spacings

I.1 Mode I and Mode II Stress Intensity Factor of Crack A

For completeness the mode I and mode II dimensionless SIF results for crack A in Chapter 6 are given here. These results are as crack A increases in size relative to crack C (Figures I.1 and I.2) and crack B (Figures I.3 and I.4) and when crack A is larger than both crack C and B (Figures I.5 and I.6). The full tabulated results are also given in the electronic version of this thesis.

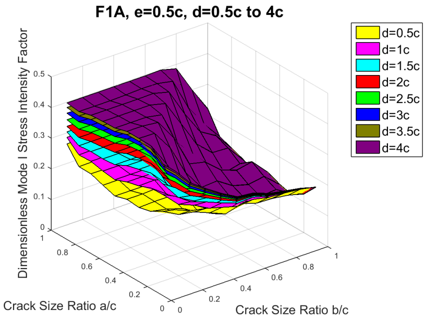

(a)

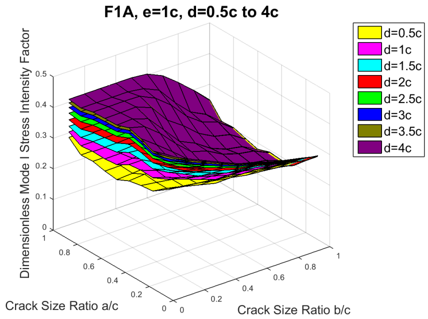

(b)

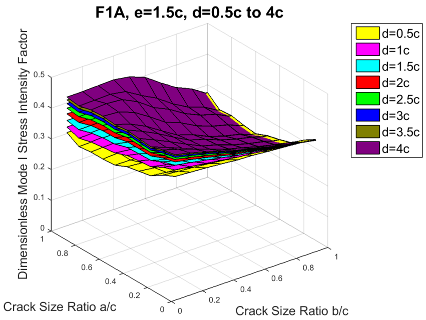

(c)

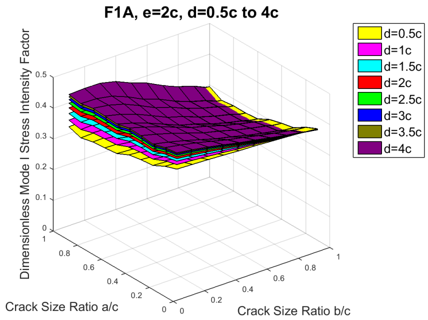

(d)

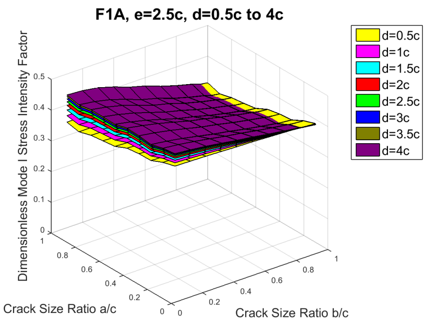

(e)

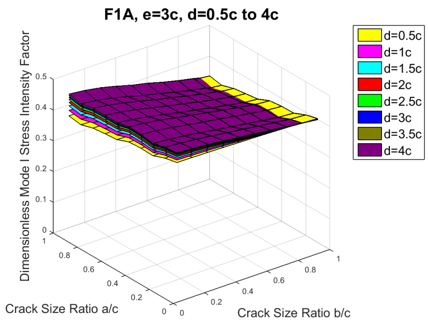

(f)

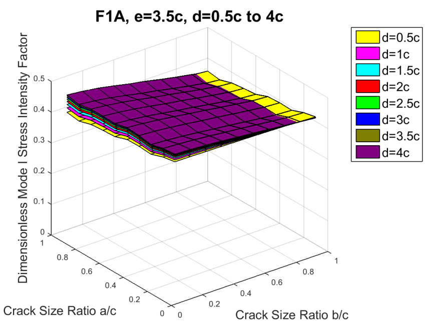

(g)

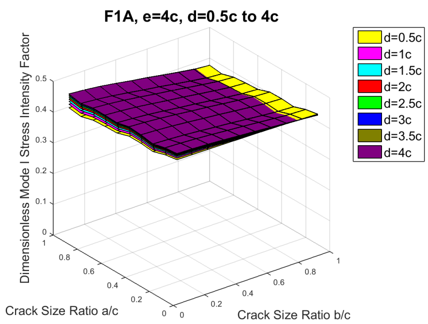

(h)

Figure I.1

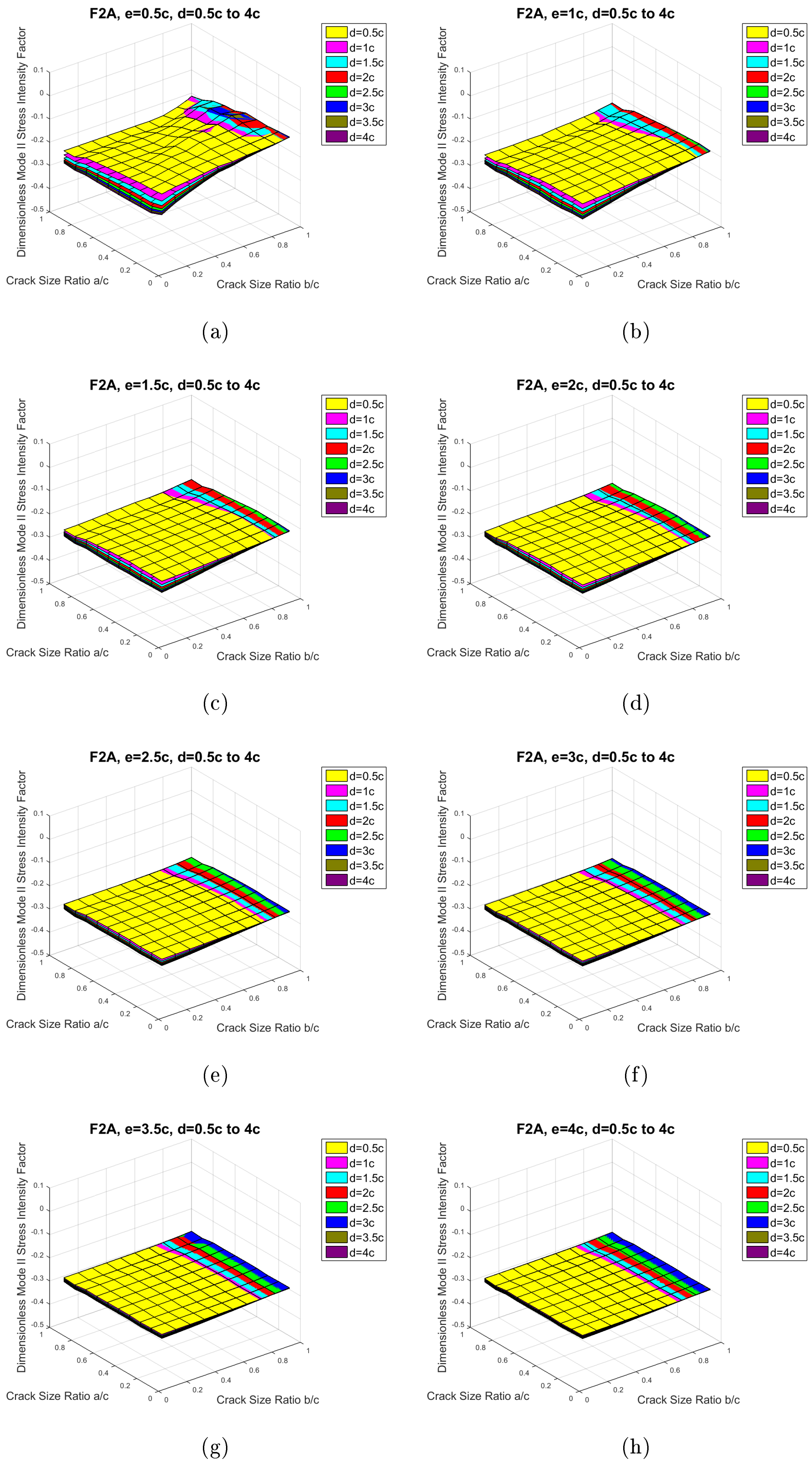
F2A, e=0.5c, d=0.5c to 4c
F2A, e=1c, d=0.5c to 4c
F2A, e=1.5c, d=0.5c to 4c
F2A, e=2c, d=0.5c to 4c
F2A, e=2.5c, d=0.5c to 4c
F2A, e=3c, d=0.5c to 4c
F2A, e=3.5c, d=0.5c to 4c
F2A, e=4c, d=0.5c to 4c
d=0.5c
d=1c
d=1.5c
d=2c
d=2.5c
d=3c
d=3.5c
d=4c
Dimensionless Mode II Stress Intensity Factor
Crack Size Ratio a/c
Crack Size Ratio b/c
(a)
(b)
(c)
(d)
(e)
(f)
(g)
(h)

Figure I.2

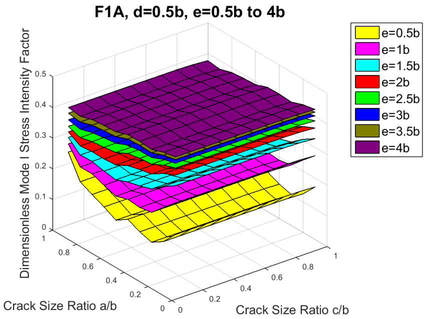

(a)

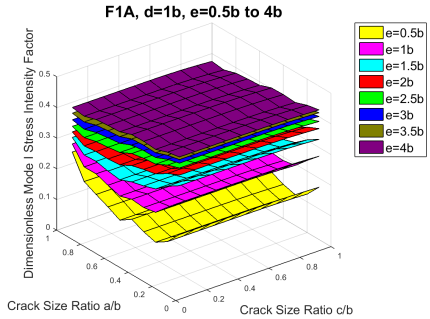

(b)

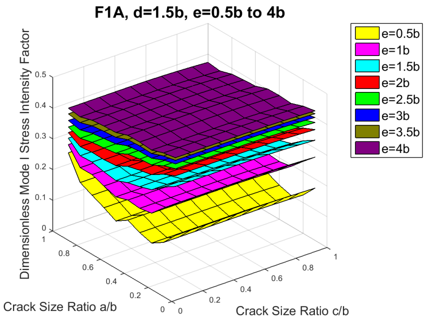

(c)

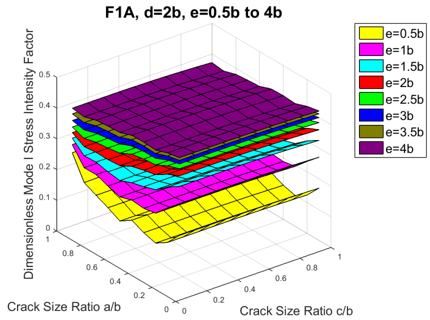

(d)

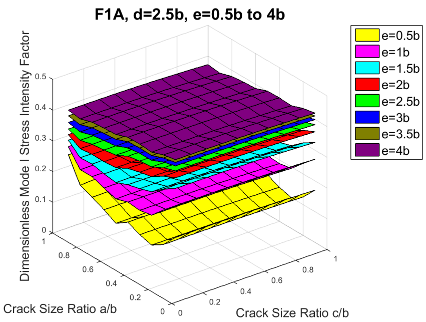

(e)

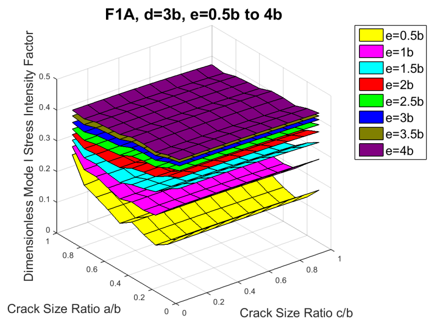

(f)

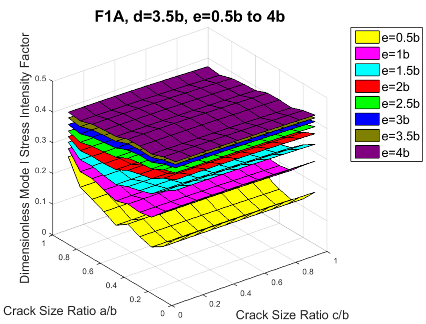

(g)

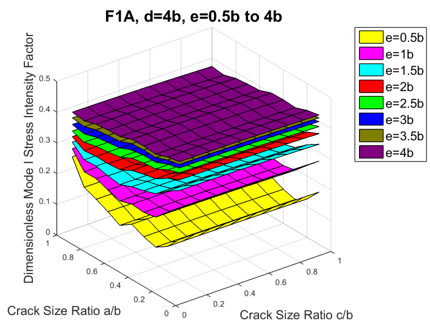

(h)

Figure I.3

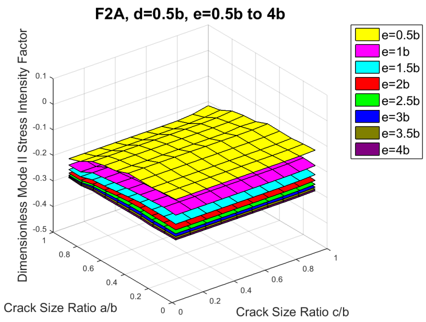

(a)

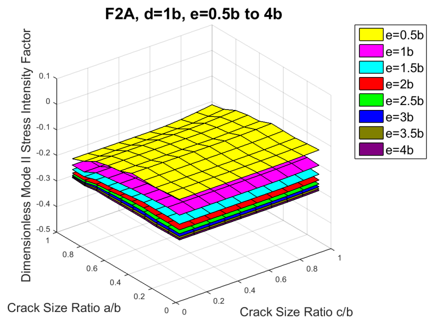

(b)

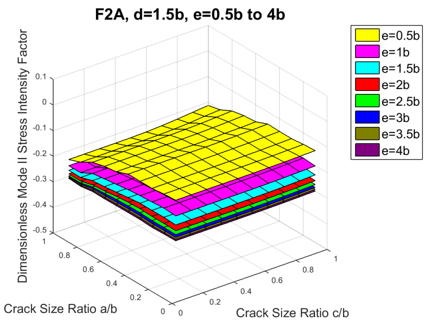

(c)

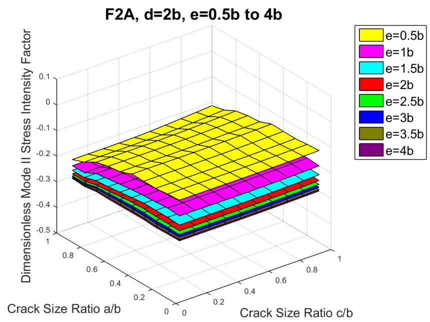

(d)

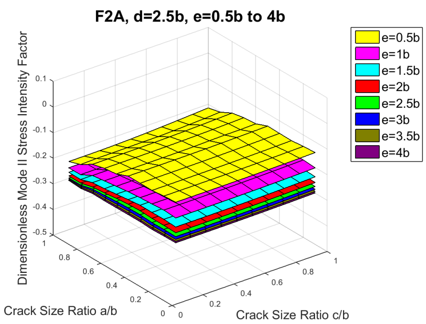

(e)

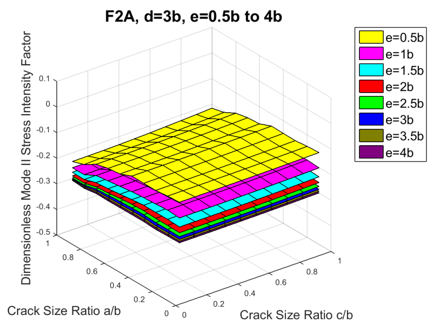

(f)

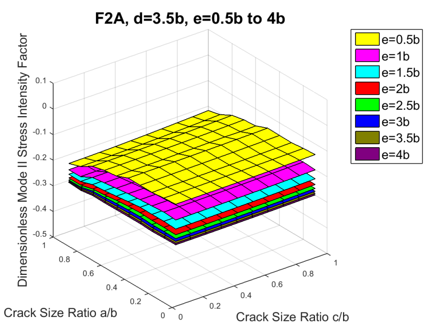

(g)

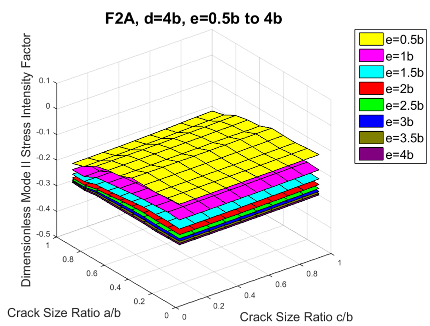

(h)

Figure I.4

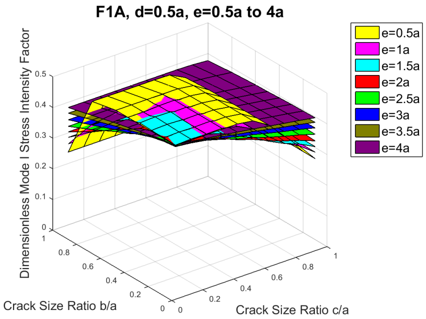

(a)

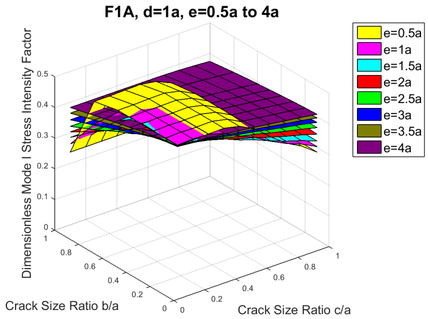

(b)

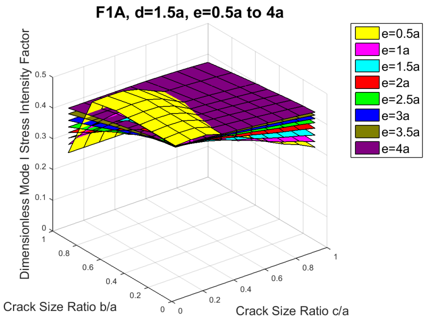

(c)

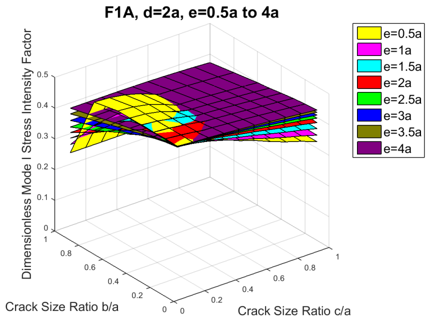

(d)

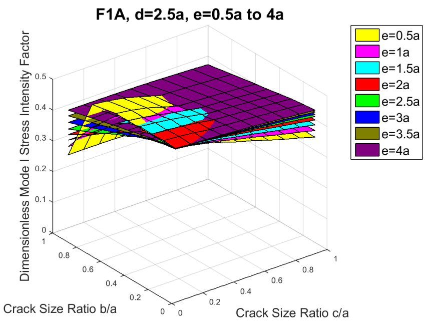

(e)

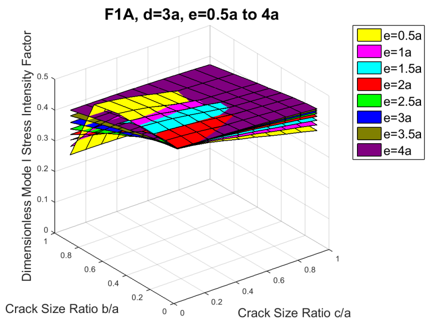

(f)

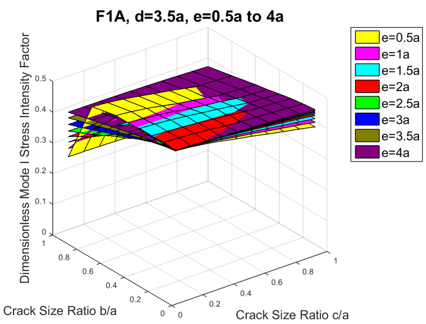

(g)

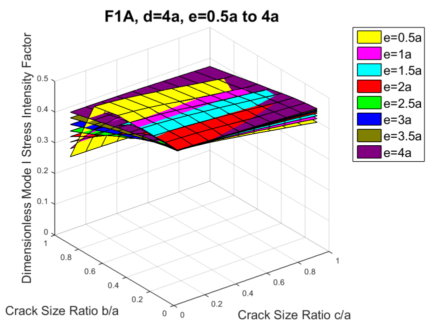

(h)

Figure I.5

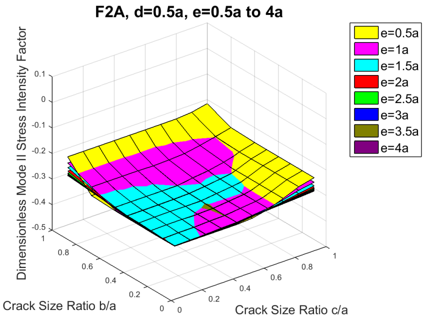

(a)

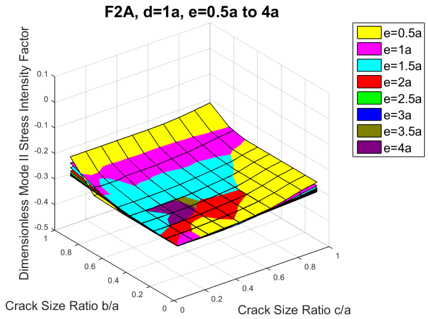

(b)

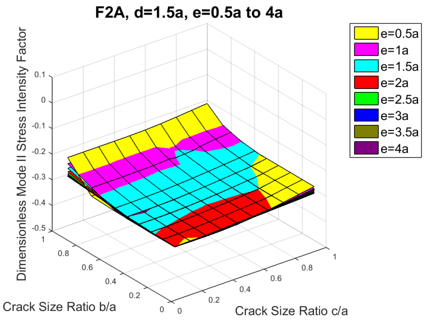

(c)

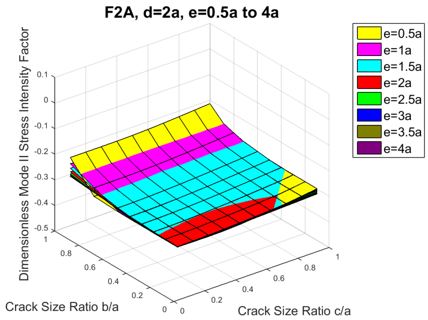

(d)

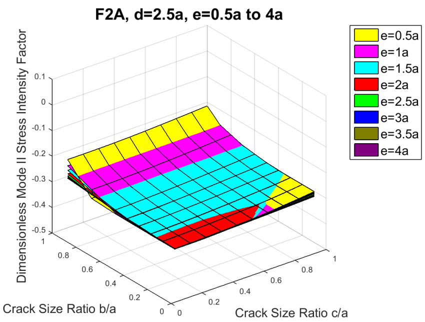

(e)

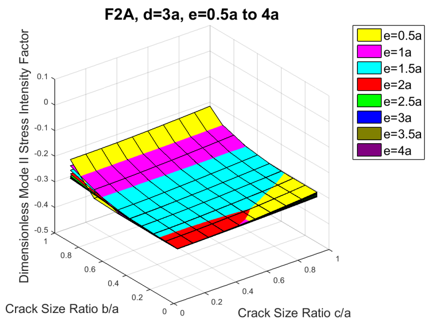

(f)

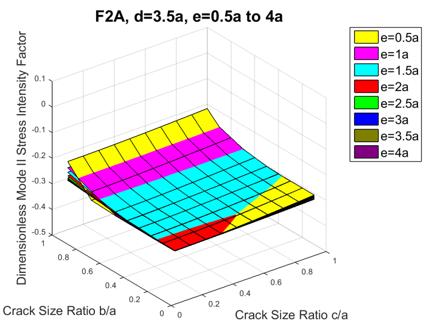

(g)

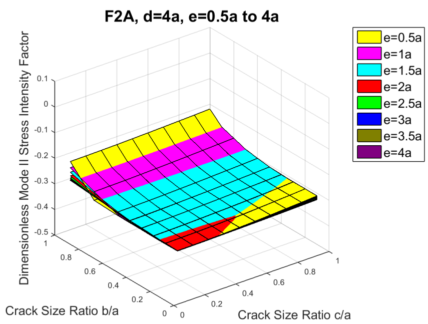

(h)

Figure I.6

The tabulated results show the dimensionless SIF to 4 significant figures. To calculate the SIF use Equations 2.12 and 2.13.

Figure I.1: F1A: e=0.5c & d=0.5c

	b/c									
	0.2553	0.2344	0.2248	0.2104	0.1961	0.2011	0.1905	0.187	0.1814	0.1715
	0.2271	0.1993	0.1904	0.1698	0.1485	0.1641	0.1487	0.1462	0.1392	0.1262
	0.2041	0.1941	0.1783	0.1521	0.1264	0.1447	0.1276	0.1234	0.1151	0.1011
	0.1939	0.1961	0.1959	0.177	0.1457	0.1606	0.1405	0.1369	0.1305	0.1118
a/c	0.1978	0.1977	0.2005	0.1977	0.1773	0.1787	0.1605	0.1565	0.1487	0.1293
	0.1855	0.1856	0.1855	0.1855	0.1647	0.1612	0.1373	0.1251	0.1119	0.09911
	0.1979	0.1979	0.1979	0.1981	0.1985	0.1896	0.1663	0.1548	0.1351	0.1224
	0.212	0.212	0.2121	0.212	0.2124	0.2129	0.1984	0.1813	0.1585	0.1382
	0.2124	0.2134	0.2129	0.2157	0.2227	0.2165	0.2176	0.2045	0.1778	0.1521
	0.2638	0.2638	0.2639	0.2638	0.2637	0.2641	0.264	0.2656	0.2516	0.2166

Figure I.1: F1A: e=0.5c & d=1c

	b/c									
	0.2994	0.2642	0.2457	0.2251	0.2065	0.2083	0.1947	0.189	0.1831	0.1706
	0.2819	0.2323	0.2121	0.184	0.1582	0.1719	0.1531	0.1484	0.146	0.1254
	0.2802	0.2434	0.2071	0.1688	0.1372	0.1546	0.134	0.1263	0.1309	0.1004
	0.2645	0.2659	0.2486	0.2035	0.1602	0.176	0.1505	0.1411	0.1477	0.1111
a/c	0.2542	0.2541	0.2541	0.2362	0.1988	0.1992	0.1793	0.1634	0.1662	0.1286
	0.2386	0.2386	0.2386	0.2367	0.2017	0.1899	0.1581	0.1304	0.1364	0.09833
	0.244	0.244	0.244	0.2442	0.2406	0.2189	0.1926	0.165	0.1645	0.1214
	0.2528	0.2528	0.2528	0.2528	0.2534	0.2503	0.2232	0.1986	0.1771	0.1368
	0.2507	0.2523	0.2528	0.255	0.2597	0.2555	0.2549	0.2285	0.1929	0.1523
	0.2849	0.2849	0.285	0.285	0.2849	0.2851	0.2852	0.2818	0.2522	0.2134

Figure I.1: F1A: e=0.5c & d=1.5c

	b/c									
	0.3275	0.2839	0.2591	0.2342	0.2127	0.2125	0.1972	0.1902	0.1837	0.1703
	0.3165	0.2543	0.226	0.1928	0.1641	0.1755	0.1553	0.1495	0.1476	0.1251
	0.3291	0.2766	0.2264	0.1792	0.1437	0.1586	0.1363	0.1274	0.1349	0.1002
	0.3182	0.3187	0.2857	0.2189	0.1689	0.1811	0.1533	0.1425	0.1526	0.1109
a/c	0.3074	0.3073	0.3056	0.272	0.212	0.2116	0.1798	0.1651	0.1719	0.1283
	0.2872	0.2873	0.2873	0.2836	0.2276	0.2056	0.1603	0.1326	0.1428	0.09806
	0.2837	0.2837	0.2837	0.2839	0.2804	0.2431	0.206	0.1682	0.1677	0.1212
	0.2846	0.2846	0.2846	0.2846	0.2856	0.2807	0.2421	0.2066	0.1833	0.1365
	0.2805	0.281	0.2816	0.2834	0.2866	0.2845	0.2828	0.2393	0.1994	0.1521
	0.3031	0.3031	0.3032	0.3032	0.3031	0.3032	0.304	0.2989	0.2584	0.2131

Figure I.1: F1A: e=0.5c & d=2c

	b/c									
	0.3464	0.2977	0.2688	0.2408	0.217	0.2152	0.1989	0.1912	0.1839	0.1702
	0.3393	0.2694	0.2357	0.199	0.168	0.1779	0.1567	0.1503	0.1477	0.1251
	0.3611	0.2993	0.2402	0.1867	0.1481	0.1613	0.1378	0.1283	0.1349	0.1001
	0.3544	0.3544	0.3096	0.2302	0.1749	0.1844	0.1552	0.1436	0.1547	0.1109
a/c	0.3468	0.3467	0.3433	0.2976	0.2212	0.2195	0.1823	0.1664	0.1739	0.1284
	0.3278	0.3279	0.3278	0.3222	0.2465	0.2142	0.1649	0.1343	0.1448	0.09808
	0.3217	0.3217	0.3218	0.322	0.3157	0.2639	0.2113	0.1715	0.1703	0.1212
	0.3171	0.3171	0.3171	0.3171	0.3182	0.3114	0.259	0.2138	0.1858	0.1367
	0.3076	0.3076	0.3082	0.3098	0.3128	0.3102	0.3086	0.2502	0.1989	0.1504
	0.321	0.321	0.321	0.321	0.3209	0.3211	0.3225	0.3164	0.2664	0.2147

Figure I.1: F1A: e=0.5c & d=2.5c

	b/c									
	0.3596	0.3076	0.2759	0.2458	0.2204	0.2173	0.2001	0.1919	0.1841	0.1703
	0.3552	0.2802	0.243	0.2038	0.1711	0.1798	0.1577	0.1509	0.1478	0.1251
	0.3829	0.3151	0.2499	0.1926	0.1516	0.1633	0.1388	0.1289	0.135	0.1001
	0.3793	0.3788	0.326	0.2388	0.1797	0.1871	0.1565	0.1443	0.1548	0.1109
a/c	0.3745	0.3744	0.37	0.3156	0.2286	0.2234	0.184	0.1673	0.1756	0.1284
	0.3578	0.3578	0.3578	0.3507	0.2612	0.2202	0.1681	0.1355	0.1465	0.09814
	0.3526	0.3526	0.3526	0.3529	0.3442	0.2804	0.2159	0.1747	0.1732	0.1214
	0.3469	0.3469	0.3469	0.3469	0.348	0.339	0.2734	0.2174	0.1832	0.137
	0.3349	0.3349	0.3352	0.3368	0.3395	0.3382	0.3345	0.2599	0.202	0.1516
	0.3424	0.3424	0.3424	0.3424	0.3424	0.3425	0.344	0.3363	0.2759	0.2166

Figure I.1: F1A: e=0.5c & d=3c

	b/c									
	0.3692	0.3149	0.2814	0.2498	0.2232	0.2191	0.2012	0.1924	0.1843	0.1703
	0.3665	0.2881	0.2484	0.2076	0.1737	0.1814	0.1587	0.1514	0.1479	0.1251
	0.3984	0.3266	0.2571	0.1973	0.1545	0.1651	0.1397	0.1294	0.1349	0.1001
	0.3969	0.3961	0.3379	0.2454	0.1836	0.1893	0.1577	0.1449	0.1547	0.1108
a/c	0.3941	0.394	0.389	0.329	0.2345	0.2265	0.1856	0.1681	0.1773	0.1284
	0.3794	0.3795	0.3795	0.3712	0.2726	0.2253	0.1697	0.1365	0.1481	0.09813
	0.3757	0.3757	0.3757	0.3761	0.3656	0.293	0.22	0.1767	0.1759	0.1214
	0.3707	0.3707	0.3707	0.3707	0.3718	0.361	0.2852	0.2205	0.186	0.1372
	0.3586	0.3586	0.3587	0.3603	0.3631	0.3618	0.3601	0.2684	0.2045	0.1516
	0.3639	0.3639	0.3639	0.3639	0.3638	0.364	0.3654	0.3557	0.2848	0.2183

Figure I.1: F1A: e=0.5c & d=3.5c

	b/c									
	0.3764	0.3204	0.2856	0.253	0.2255	0.2207	0.2022	0.193	0.1844	0.1703
	0.375	0.294	0.2526	0.2106	0.1758	0.1828	0.1595	0.1519	0.148	0.1251
	0.4096	0.3351	0.2626	0.2009	0.1568	0.1666	0.1406	0.1299	0.135	0.1001
	0.4096	0.4086	0.3466	0.2505	0.1867	0.1913	0.1588	0.1456	0.1548	0.1108
a/c	0.4084	0.4083	0.4028	0.3383	0.2392	0.2292	0.187	0.169	0.1787	0.1284
	0.3953	0.3953	0.3953	0.3863	0.2812	0.2296	0.1717	0.1376	0.1494	0.09818
	0.3929	0.3929	0.3929	0.3932	0.3816	0.3028	0.2235	0.179	0.1776	0.1215
	0.3889	0.3889	0.3889	0.3889	0.39	0.3778	0.2943	0.2235	0.1951	0.1374
	0.3775	0.3774	0.3775	0.3791	0.3828	0.3806	0.3699	0.2756	0.2067	0.1522
	0.3824	0.3824	0.3824	0.3824	0.3824	0.3825	0.384	0.3724	0.2927	0.2196

Figure I.1: F1A: e=0.5c & d=4c

	b/c									
	0.382	0.3247	0.289	0.2555	0.2275	0.2221	0.2032	0.1936	0.1847	0.1704
	0.3814	0.2986	0.2558	0.213	0.1775	0.184	0.1603	0.1524	0.1481	0.1252
	0.4181	0.3415	0.2668	0.2038	0.1588	0.1679	0.1415	0.1305	0.1352	0.1002
	0.4191	0.418	0.3533	0.2545	0.1893	0.193	0.1598	0.1462	0.155	0.1109
a/c	0.419	0.419	0.4131	0.3455	0.2429	0.2315	0.1884	0.1698	0.18	0.1285
	0.407	0.4071	0.407	0.3975	0.2881	0.233	0.1735	0.1386	0.1507	0.09832
	0.4057	0.4058	0.4058	0.406	0.3937	0.3101	0.2266	0.1811	0.1788	0.1218
	0.4027	0.4027	0.4028	0.4027	0.4039	0.3906	0.3017	0.2262	0.1961	0.1378
	0.3921	0.3921	0.3921	0.3936	0.3962	0.3952	0.3854	0.2818	0.2106	0.1529
	0.3973	0.3973	0.3974	0.3974	0.3973	0.3975	0.3989	0.3858	0.2991	0.2211

Figure I.1: F1A: e=1c & d=0.5c

	b/c									
a/c	0.3283	0.3206	0.3145	0.3068	0.2989	0.2969	0.2902	0.2857	0.2806	0.2732
	0.3013	0.2907	0.2832	0.2733	0.2634	0.2626	0.2546	0.25	0.2443	0.2363
	0.2703	0.2585	0.2502	0.2379	0.2254	0.2265	0.2167	0.2123	0.2065	0.1971
	0.2656	0.2583	0.2505	0.2361	0.2207	0.2234	0.2119	0.2069	0.2004	0.1898
	0.2577	0.2619	0.2587	0.2467	0.2295	0.2315	0.2182	0.2127	0.2054	0.1933
	0.2389	0.2422	0.246	0.2402	0.2247	0.2225	0.2086	0.2019	0.193	0.1801
	0.2439	0.2444	0.2482	0.2514	0.2441	0.2393	0.2245	0.2163	0.2056	0.1916
	0.2528	0.2527	0.2532	0.2569	0.2587	0.2564	0.2424	0.2326	0.2207	0.2043
	0.2507	0.2507	0.2507	0.2512	0.2541	0.2543	0.2443	0.2333	0.2196	0.2018
	0.2849	0.2849	0.2849	0.2879	0.2855	0.2904	0.2924	0.2853	0.2686	0.2498

Figure I.1: F1A: e=1c & d=1c

	b/c									
a/c	0.3597	0.3457	0.3341	0.3216	0.3098	0.3045	0.2948	0.2877	0.2811	0.2717
	0.3384	0.3194	0.3049	0.2893	0.2749	0.2705	0.2593	0.2521	0.2455	0.2349
	0.3138	0.2911	0.2741	0.2551	0.2375	0.235	0.2219	0.2146	0.2083	0.1959
	0.3156	0.2968	0.2785	0.2556	0.2342	0.2332	0.2177	0.2097	0.2041	0.1885
	0.3109	0.3108	0.2968	0.2715	0.2458	0.2441	0.2258	0.216	0.2109	0.1919
	0.2876	0.2912	0.2905	0.2747	0.2455	0.2398	0.2186	0.2062	0.2005	0.1786
	0.2835	0.2842	0.2875	0.2859	0.2708	0.2614	0.2382	0.2222	0.2139	0.1898
	0.2845	0.2845	0.2849	0.2866	0.2834	0.2775	0.259	0.2411	0.2258	0.2022
	0.2804	0.2804	0.2804	0.2804	0.2802	0.2774	0.2633	0.244	0.2272	0.1991
	0.303	0.303	0.3029	0.3029	0.3031	0.3042	0.3007	0.2906	0.2735	0.2462

Figure I.1: F1A: e=1c & d=1.5c

	b/c									
a/c	0.3808	0.3632	0.3475	0.3314	0.3168	0.3093	0.2977	0.2891	0.2814	0.271
	0.3632	0.3391	0.3195	0.2997	0.2822	0.2755	0.2623	0.2536	0.246	0.2343
	0.3427	0.3136	0.2903	0.2662	0.2452	0.2401	0.2249	0.216	0.209	0.1954
	0.3498	0.3239	0.2978	0.2683	0.2427	0.2388	0.2209	0.2112	0.2054	0.188
	0.3503	0.3454	0.3216	0.2875	0.2562	0.2507	0.2296	0.2178	0.2127	0.1913
	0.3283	0.3316	0.3257	0.2962	0.259	0.2485	0.2233	0.2084	0.2027	0.178
	0.3217	0.3224	0.3253	0.319	0.2909	0.274	0.2445	0.2251	0.2169	0.1892
	0.3171	0.3171	0.3176	0.3186	0.3108	0.297	0.2688	0.2451	0.2321	0.2015
	0.3077	0.3077	0.3077	0.3077	0.3057	0.2992	0.2765	0.2497	0.2313	0.1984
	0.321	0.321	0.321	0.321	0.3211	0.3198	0.3116	0.2971	0.2779	0.2453

Figure I.1: F1A: e=1c & d=2c

	b/c									
a/c	0.3956	0.3757	0.3574	0.3388	0.3219	0.3128	0.2999	0.2903	0.2818	0.2708
	0.3803	0.3532	0.3302	0.3074	0.2875	0.2789	0.2645	0.2547	0.2463	0.2342
	0.3626	0.3295	0.3022	0.2744	0.2507	0.2436	0.2271	0.2172	0.2093	0.1952
	0.3734	0.3431	0.3119	0.2778	0.2489	0.2426	0.2232	0.2125	0.2057	0.1879
	0.3779	0.3697	0.3398	0.2995	0.2638	0.2553	0.2323	0.2193	0.2135	0.1912
	0.3583	0.3613	0.3518	0.3125	0.269	0.2544	0.2267	0.2102	0.2041	0.1779
	0.3525	0.3532	0.3557	0.345	0.3055	0.2824	0.249	0.2274	0.2186	0.1891
	0.3468	0.3468	0.3474	0.3476	0.3353	0.3141	0.276	0.2483	0.2341	0.2015
	0.3349	0.335	0.3349	0.335	0.3314	0.321	0.2882	0.2542	0.2342	0.1985
	0.3424	0.3423	0.3423	0.3423	0.3424	0.34	0.3279	0.3071	0.282	0.2457

Figure I.1: F1A: e=1c & d=2.5c

	b/c									
a/c	0.4063	0.3851	0.365	0.3446	0.3261	0.3156	0.3016	0.2913	0.2821	0.2708
	0.3926	0.3635	0.3384	0.3135	0.2917	0.2817	0.2661	0.2557	0.2466	0.2342
	0.3768	0.3411	0.311	0.2809	0.2551	0.2464	0.2287	0.2181	0.2096	0.1952
	0.3901	0.3569	0.3224	0.2853	0.2538	0.2457	0.225	0.2135	0.206	0.1879
	0.3976	0.3872	0.3534	0.3089	0.2699	0.259	0.2344	0.2204	0.2139	0.1913
	0.38	0.3828	0.3705	0.3252	0.2771	0.2593	0.2294	0.2116	0.2047	0.1779
	0.3757	0.3764	0.3784	0.3642	0.3168	0.2897	0.2526	0.2293	0.22	0.1892
	0.3707	0.3706	0.3712	0.3708	0.3542	0.3267	0.2817	0.2508	0.2359	0.2017
	0.3586	0.3587	0.3586	0.3586	0.3537	0.3393	0.2971	0.258	0.2365	0.1989
	0.3638	0.3638	0.3638	0.3638	0.3638	0.3604	0.3448	0.3184	0.2863	0.2464

Figure I.1: F1A: e=1c & d=3c

	b/c									
a/c	0.4144	0.3921	0.3709	0.3493	0.3297	0.3181	0.3032	0.2922	0.2825	0.2708
	0.4017	0.3712	0.3447	0.3184	0.2953	0.2842	0.2677	0.2565	0.2469	0.2342
	0.3872	0.3498	0.3178	0.286	0.2588	0.2489	0.2302	0.2189	0.2098	0.1952
	0.4023	0.3672	0.3303	0.2911	0.2579	0.2484	0.2267	0.2143	0.2062	0.1879
	0.4119	0.4001	0.3636	0.3163	0.2749	0.2623	0.2363	0.2215	0.2142	0.1913
	0.3958	0.3986	0.3841	0.335	0.2837	0.2635	0.2318	0.2129	0.2052	0.178
	0.3928	0.3936	0.3955	0.3785	0.326	0.2957	0.2559	0.2309	0.2212	0.1893
	0.3889	0.3888	0.3894	0.3885	0.3687	0.3343	0.2867	0.2532	0.2376	0.2019
	0.3775	0.3775	0.3775	0.3775	0.3716	0.3675	0.3045	0.2614	0.2388	0.1993
	0.3824	0.3823	0.3823	0.3823	0.3823	0.378	0.3593	0.3273	0.2905	0.2471

Figure I.1: F1A: e=1c & d=3.5c

	b/c									
a/c	0.4206	0.3976	0.3756	0.3531	0.3326	0.3203	0.3047	0.2931	0.2829	0.2709
	0.4087	0.3772	0.3496	0.3223	0.2983	0.2864	0.2691	0.2574	0.2473	0.2343
	0.395	0.3563	0.3231	0.2901	0.2618	0.2511	0.2317	0.2198	0.2102	0.1953
	0.4115	0.3749	0.3364	0.2957	0.2613	0.2508	0.2282	0.2152	0.2066	0.188
	0.4226	0.4098	0.3714	0.322	0.279	0.2651	0.2381	0.2225	0.2146	0.1914
	0.4076	0.4103	0.3944	0.3426	0.2891	0.267	0.234	0.2142	0.2057	0.1781
	0.4057	0.4065	0.408	0.3893	0.3333	0.3005	0.2588	0.2326	0.2219	0.1896
	0.4027	0.4027	0.4032	0.4019	0.3798	0.3424	0.2908	0.2555	0.2393	0.2023
	0.3921	0.3922	0.3921	0.3921	0.3856	0.365	0.311	0.2647	0.2409	0.1998
	0.3973	0.3973	0.3972	0.3972	0.3972	0.3922	0.3709	0.3347	0.2947	0.2481

Figure I.1: F1A: e=1c & d=4c

	b/c									
a/c	0.4254	0.4019	0.3793	0.3562	0.3351	0.3222	0.3061	0.294	0.2834	0.2711
	0.414	0.3818	0.3534	0.3254	0.3008	0.2882	0.2705	0.2583	0.2478	0.2345
	0.401	0.3614	0.3272	0.2934	0.2644	0.2529	0.233	0.2206	0.2106	0.1955
	0.4184	0.3809	0.3412	0.2994	0.2641	0.2528	0.2296	0.2162	0.2071	0.1882
	0.4307	0.4172	0.3774	0.3266	0.2824	0.2675	0.2397	0.2236	0.2152	0.1917
	0.4166	0.4192	0.4023	0.3486	0.2934	0.27	0.236	0.2154	0.2063	0.1784
	0.4155	0.4163	0.4177	0.3976	0.3392	0.3045	0.2614	0.2342	0.2227	0.1899
	0.4133	0.4132	0.4138	0.4122	0.3883	0.3482	0.2944	0.2577	0.2409	0.2028
	0.4034	0.4035	0.4034	0.4034	0.3964	0.374	0.3164	0.2678	0.2426	0.2005
	0.4091	0.4091	0.4091	0.4091	0.4089	0.4034	0.3804	0.3408	0.2976	0.2492

Figure I.1: F1A: e=1.5c & d=0.5c

	b/c									
a/c	0.3661	0.3625	0.3591	0.3546	0.3497	0.3475	0.3428	0.339	0.3348	0.3288
	0.3476	0.3429	0.3386	0.333	0.3269	0.3248	0.3192	0.3151	0.3104	0.3038
	0.3225	0.3166	0.3116	0.3047	0.2974	0.2957	0.289	0.2845	0.2794	0.2721
	0.3146	0.3084	0.303	0.2951	0.2865	0.285	0.2777	0.2728	0.2674	0.2593
	0.3062	0.3017	0.297	0.2883	0.2784	0.2775	0.269	0.2639	0.2576	0.249
	0.2885	0.2878	0.2846	0.2763	0.2653	0.2645	0.2548	0.2494	0.2423	0.2328
	0.2855	0.2885	0.2893	0.2842	0.2742	0.2727	0.2622	0.2561	0.2482	0.2376
	0.2853	0.2883	0.2923	0.2921	0.2859	0.2831	0.2727	0.266	0.2572	0.2454
	0.2803	0.2811	0.2839	0.2865	0.2843	0.2817	0.2722	0.2649	0.2551	0.2417
	0.3029	0.3031	0.3043	0.308	0.3111	0.3123	0.3049	0.2983	0.2884	0.2741

Figure I.1: F1A: e=1.5c & d=1c

	b/c									
a/c	0.3875	0.3807	0.374	0.3663	0.3585	0.3537	0.3465	0.3405	0.3347	0.3269
	0.373	0.364	0.3556	0.3462	0.3367	0.3316	0.3233	0.3168	0.3106	0.3019
	0.352	0.3408	0.3308	0.3194	0.3082	0.303	0.2935	0.2864	0.2799	0.2703
	0.348	0.3356	0.3244	0.3112	0.2982	0.2932	0.2825	0.275	0.2682	0.2576
	0.3431	0.3322	0.3209	0.3062	0.2913	0.2867	0.2745	0.2663	0.2594	0.2473
	0.3281	0.322	0.3123	0.2968	0.28	0.2753	0.2613	0.2522	0.245	0.2309
	0.3236	0.3256	0.3217	0.309	0.2913	0.2857	0.2702	0.2595	0.2517	0.2355
	0.318	0.3215	0.3244	0.3199	0.3063	0.2989	0.2827	0.2702	0.2609	0.243
	0.3076	0.3088	0.3117	0.3126	0.3061	0.3007	0.2835	0.2702	0.2588	0.2388
	0.3209	0.3212	0.3229	0.3261	0.3272	0.3264	0.3163	0.3058	0.2912	0.2707

Figure I.1: F1A: e=1.5c & d=1.5c

	b/c									
a/c	0.4026	0.3938	0.3846	0.3744	0.3644	0.3579	0.349	0.3416	0.3348	0.326
	0.3907	0.3791	0.3676	0.3552	0.3433	0.3362	0.3261	0.318	0.3107	0.3011
	0.3725	0.3581	0.3442	0.3293	0.3154	0.3079	0.2965	0.2878	0.2802	0.2696
	0.3713	0.3551	0.3394	0.3221	0.306	0.2985	0.2857	0.2764	0.2687	0.2569
	0.3693	0.3543	0.338	0.3184	0.2999	0.2924	0.2779	0.2679	0.2601	0.2466
	0.3572	0.3473	0.3321	0.311	0.2899	0.2818	0.2652	0.254	0.2459	0.2301
	0.3544	0.3546	0.3453	0.3259	0.3031	0.2937	0.2747	0.2616	0.2528	0.2346
	0.3479	0.3512	0.3522	0.3423	0.3205	0.3093	0.2883	0.2729	0.2626	0.2421
	0.335	0.3362	0.339	0.3377	0.325	0.3143	0.2915	0.2735	0.2611	0.2377
	0.3424	0.3427	0.3445	0.3474	0.3464	0.3415	0.3273	0.3103	0.2936	0.2695

Figure I.1: F1A: e=1.5c & d=2c

	b/c									
a/c	0.4136	0.4036	0.3927	0.3807	0.369	0.361	0.351	0.3427	0.335	0.3257
	0.4033	0.3902	0.3767	0.3621	0.3483	0.3396	0.3282	0.3192	0.311	0.3008
	0.387	0.3707	0.3543	0.3369	0.3207	0.3115	0.2987	0.289	0.2805	0.2693
	0.3878	0.3693	0.3507	0.3304	0.3117	0.3023	0.288	0.2777	0.269	0.2566
	0.388	0.3704	0.3508	0.3277	0.3063	0.2966	0.2805	0.2693	0.2605	0.2463
	0.3782	0.3659	0.3471	0.3219	0.2973	0.2866	0.2681	0.2556	0.2465	0.2299
	0.3775	0.3761	0.3635	0.3391	0.312	0.2994	0.2782	0.2635	0.2538	0.2344
	0.3717	0.3748	0.374	0.3585	0.3316	0.3168	0.2926	0.2751	0.2638	0.2419
	0.3586	0.3598	0.3623	0.3588	0.34	0.3237	0.2973	0.2764	0.2626	0.2376
	0.3638	0.3642	0.3659	0.3685	0.3655	0.3567	0.3361	0.3141	0.2958	0.2693

Figure I.1: F1A: e=1.5c & d=2.5c

	b/c									
a/c	0.4218	0.411	0.3991	0.3858	0.3729	0.3637	0.3527	0.3436	0.3353	0.3256
	0.4127	0.3986	0.3838	0.3677	0.3524	0.3424	0.33	0.3201	0.3113	0.3008
	0.3977	0.3801	0.3622	0.343	0.3251	0.3145	0.3006	0.29	0.2808	0.2692
	0.3999	0.3798	0.3593	0.337	0.3165	0.3055	0.29	0.2788	0.2694	0.2566
	0.4017	0.3824	0.3605	0.3352	0.3116	0.3001	0.2826	0.2705	0.2609	0.2464
	0.3936	0.3798	0.3586	0.3306	0.3034	0.2906	0.2705	0.2569	0.2469	0.2299
	0.3946	0.3922	0.3772	0.3496	0.3195	0.3043	0.2811	0.2651	0.2545	0.2345
	0.3899	0.3929	0.3907	0.3715	0.3409	0.3229	0.2962	0.2771	0.265	0.242
	0.3775	0.3787	0.3809	0.3754	0.352	0.3318	0.302	0.2789	0.2641	0.2378
	0.3823	0.3827	0.3845	0.3867	0.3818	0.3696	0.3431	0.3174	0.2981	0.2697

Figure I.1: F1A: e=1.5c & d=3c

	b/c									
a/c	0.4281	0.4168	0.4041	0.39	0.3761	0.3661	0.3543	0.3445	0.3357	0.3257
	0.4199	0.4051	0.3894	0.3723	0.3559	0.345	0.3317	0.3211	0.3117	0.3008
	0.4058	0.3873	0.3683	0.3479	0.3289	0.3172	0.3023	0.291	0.2812	0.2693
	0.409	0.3878	0.366	0.3424	0.3205	0.3083	0.2918	0.2798	0.2698	0.2567
	0.4119	0.3914	0.3681	0.3411	0.316	0.3032	0.2845	0.2716	0.2613	0.2464
	0.4051	0.3902	0.3675	0.3375	0.3085	0.2942	0.2727	0.2581	0.2474	0.23
	0.4075	0.4044	0.3877	0.358	0.3256	0.3086	0.2837	0.2665	0.2551	0.2346
	0.4037	0.4067	0.4035	0.3817	0.3486	0.3282	0.2995	0.2789	0.266	0.2422
	0.3921	0.3934	0.3954	0.3884	0.3618	0.3388	0.3063	0.2813	0.2656	0.238
	0.3973	0.3976	0.3994	0.4013	0.3951	0.3797	0.3491	0.3206	0.3001	0.2701

Figure I.1: F1A: e=1.5c & d=3.5c

	b/c									
a/c	0.433	0.4213	0.4082	0.3935	0.3789	0.3683	0.3558	0.3455	0.3362	0.3258
	0.4254	0.4102	0.3938	0.376	0.3589	0.3472	0.3333	0.3221	0.3122	0.3009
	0.412	0.3929	0.3731	0.3519	0.332	0.3195	0.3039	0.292	0.2817	0.2694
	0.4159	0.394	0.3713	0.3467	0.3239	0.3108	0.2935	0.2809	0.2703	0.2568
	0.4197	0.3984	0.374	0.3459	0.3197	0.3059	0.2864	0.2727	0.2619	0.2466
	0.4139	0.3982	0.3743	0.343	0.3128	0.2973	0.2748	0.2594	0.248	0.2302
	0.4172	0.4136	0.3959	0.3646	0.3307	0.3123	0.2862	0.2681	0.2558	0.2348
	0.4143	0.4172	0.4133	0.3898	0.3549	0.3327	0.3026	0.2808	0.2669	0.2426
	0.4035	0.4047	0.4066	0.3986	0.3697	0.3449	0.3102	0.2837	0.2669	0.2385
	0.4091	0.4094	0.4112	0.4129	0.4056	0.3884	0.3544	0.3238	0.3021	0.2708

Figure I.1: F1A: e=1.5c & d=4c

	b/c									
a/c	0.437	0.425	0.4115	0.3963	0.3813	0.3702	0.3573	0.3465	0.3368	0.3261
	0.4298	0.4142	0.3974	0.379	0.3614	0.3492	0.3347	0.3231	0.3129	0.3012
	0.4169	0.3973	0.3769	0.3552	0.3347	0.3216	0.3055	0.293	0.2823	0.2697
	0.4213	0.3989	0.3755	0.3502	0.3267	0.313	0.2951	0.2819	0.2709	0.2571
	0.4257	0.4038	0.3786	0.3497	0.3227	0.3082	0.2881	0.2738	0.2625	0.2468
	0.4207	0.4045	0.3797	0.3474	0.3163	0.2999	0.2767	0.2606	0.2487	0.2305
	0.4248	0.4209	0.4023	0.3699	0.3349	0.3154	0.2885	0.2696	0.2566	0.2352
	0.4225	0.4254	0.421	0.3962	0.36	0.3366	0.3053	0.2826	0.2679	0.2431
	0.4123	0.4136	0.4153	0.4066	0.3761	0.3497	0.3137	0.286	0.2683	0.2392
	0.4184	0.4187	0.4206	0.4221	0.414	0.3949	0.3589	0.3267	0.3041	0.2717

Figure I.1: F1A: e=2c & d=0.5c

	b/c									
	0.39	0.388	0.386	0.3831	0.3799	0.3781	0.3747	0.3717	0.3683	0.3635
	0.3764	0.3739	0.3714	0.3679	0.364	0.3621	0.3581	0.3548	0.3509	0.3456
	0.3563	0.3531	0.3501	0.3459	0.3413	0.3392	0.3347	0.331	0.3267	0.3209
	0.3522	0.3486	0.3452	0.3403	0.3349	0.3329	0.3276	0.3237	0.3189	0.3126
a/c	0.3448	0.3411	0.3376	0.3322	0.326	0.324	0.3181	0.3139	0.3089	0.3019
	0.3262	0.3231	0.3198	0.314	0.3071	0.3054	0.2987	0.2943	0.2887	0.2812
	0.3217	0.3203	0.3179	0.3124	0.3051	0.3036	0.2964	0.2917	0.2854	0.2773
	0.3182	0.3192	0.3185	0.3146	0.3076	0.3061	0.2984	0.2933	0.2865	0.2777
	0.3086	0.3106	0.3119	0.31	0.3046	0.303	0.295	0.2895	0.2822	0.2724
	0.3218	0.3241	0.3272	0.3284	0.326	0.3247	0.3178	0.3123	0.3046	0.2941

Figure I.1: F1A: e=2c & d=1c

	b/c									
	0.4051	0.4012	0.397	0.392	0.3866	0.3829	0.3775	0.3726	0.3679	0.3615
	0.3941	0.3892	0.384	0.378	0.3716	0.3674	0.3612	0.3559	0.3507	0.3436
	0.3768	0.3707	0.3645	0.3573	0.3498	0.3452	0.3382	0.3323	0.3266	0.3188
	0.3756	0.3684	0.3613	0.3529	0.3443	0.3395	0.3316	0.3252	0.3192	0.3106
a/c	0.3709	0.3632	0.3555	0.3461	0.3363	0.3314	0.3226	0.3156	0.3093	0.2999
	0.3546	0.3473	0.3395	0.3293	0.3185	0.3135	0.3037	0.2962	0.2895	0.2791
	0.3513	0.3462	0.3395	0.3292	0.3176	0.3127	0.3018	0.2937	0.2866	0.275
	0.3478	0.3466	0.3425	0.3332	0.3213	0.3165	0.3047	0.2958	0.2881	0.2753
	0.3359	0.3377	0.3371	0.3311	0.3198	0.3148	0.3024	0.2925	0.284	0.2697
	0.3433	0.3461	0.3491	0.3484	0.3425	0.3381	0.3264	0.3158	0.3062	0.2909

Figure I.1: F1A: e=2c & d=1.5c

	b/c									
	0.4161	0.411	0.4051	0.3983	0.3913	0.3862	0.3795	0.3734	0.3677	0.3605
	0.4069	0.4004	0.3933	0.3851	0.3769	0.3711	0.3635	0.3568	0.3506	0.3426
	0.3915	0.3836	0.375	0.3653	0.3557	0.3494	0.3407	0.3333	0.3266	0.3179
	0.3923	0.3829	0.373	0.3618	0.3508	0.344	0.3343	0.3264	0.3193	0.3097
a/c	0.3896	0.3794	0.3685	0.3559	0.3434	0.3363	0.3255	0.317	0.3095	0.299
	0.3753	0.3653	0.354	0.3401	0.3263	0.3188	0.3069	0.2977	0.2898	0.2781
	0.3736	0.3659	0.3556	0.3412	0.3262	0.3186	0.3054	0.2953	0.2871	0.2741
	0.3712	0.3678	0.3602	0.3467	0.3311	0.3231	0.3087	0.2976	0.2887	0.2742
	0.3596	0.3605	0.3571	0.3463	0.331	0.3227	0.307	0.2946	0.2848	0.2685
	0.3649	0.3675	0.3698	0.3665	0.3554	0.3476	0.3318	0.3183	0.3074	0.2896

Figure I.1: F1A: e=2c & d=2c

	b/c									
	0.4244	0.4185	0.4115	0.4034	0.3951	0.3888	0.3811	0.3743	0.3678	0.3601
	0.4164	0.409	0.4005	0.3908	0.3811	0.374	0.3653	0.3577	0.3507	0.3422
	0.4023	0.3932	0.3831	0.3716	0.3603	0.3525	0.3427	0.3344	0.3268	0.3175
	0.4044	0.3937	0.382	0.3688	0.3558	0.3474	0.3365	0.3275	0.3195	0.3094
a/c	0.4032	0.3915	0.3785	0.3635	0.3489	0.34	0.3278	0.3182	0.3098	0.2986
	0.3904	0.3787	0.3651	0.3486	0.3323	0.3229	0.3094	0.299	0.2901	0.2778
	0.3902	0.3808	0.368	0.3507	0.333	0.3231	0.3082	0.2968	0.2875	0.2737
	0.3891	0.3842	0.3742	0.3574	0.3387	0.3283	0.3119	0.2993	0.2895	0.2739
	0.3784	0.3785	0.3728	0.3587	0.3399	0.3288	0.3107	0.2966	0.2857	0.2682
	0.3833	0.3859	0.3872	0.3813	0.3658	0.3549	0.3363	0.3207	0.3084	0.2893

Figure I.1: F1A: e=2c & d=2.5c

	b/c									
	0.4307	0.4243	0.4167	0.4076	0.3983	0.3911	0.3826	0.3751	0.3681	0.36
	0.4236	0.4156	0.4063	0.3955	0.3846	0.3766	0.3669	0.3586	0.351	0.3421
	0.4105	0.4007	0.3895	0.3768	0.3642	0.3552	0.3444	0.3353	0.3271	0.3174
	0.4136	0.402	0.3891	0.3744	0.3601	0.3504	0.3383	0.3285	0.3199	0.3093
a/c	0.4135	0.4007	0.3863	0.3697	0.3535	0.3432	0.3298	0.3193	0.3101	0.2986
	0.4018	0.389	0.3738	0.3555	0.3374	0.3264	0.3116	0.3002	0.2906	0.2778
	0.4027	0.3922	0.3778	0.3585	0.3387	0.327	0.3106	0.2982	0.288	0.2737
	0.4027	0.3969	0.3852	0.3663	0.3453	0.3328	0.3146	0.3008	0.2901	0.2739
	0.393	0.3925	0.3855	0.3689	0.3476	0.3341	0.314	0.2984	0.2867	0.2682
	0.3983	0.4007	0.4013	0.3931	0.3747	0.3614	0.3402	0.3229	0.3096	0.2894

Figure I.1: F1A: e=2c & d=3c

	b/c									
	0.4357	0.429	0.4208	0.4112	0.4012	0.3933	0.384	0.3759	0.3685	0.36
	0.4292	0.4208	0.4109	0.3994	0.3877	0.3789	0.3684	0.3595	0.3514	0.3421
	0.4168	0.4065	0.3946	0.3811	0.3676	0.3577	0.346	0.3363	0.3275	0.3174
	0.4206	0.4084	0.3947	0.3791	0.3637	0.353	0.3401	0.3295	0.3203	0.3093
a/c	0.4213	0.4078	0.3925	0.3748	0.3574	0.346	0.3317	0.3204	0.3106	0.2986
	0.4104	0.3968	0.3806	0.361	0.3417	0.3295	0.3136	0.3013	0.291	0.2778
	0.4123	0.401	0.3854	0.3647	0.3435	0.3305	0.3129	0.2995	0.2886	0.2738
	0.4131	0.4067	0.3938	0.3734	0.3508	0.3368	0.3172	0.3023	0.2907	0.274
	0.4043	0.4034	0.3953	0.3772	0.3541	0.3388	0.3171	0.3002	0.2875	0.2684
	0.4101	0.4125	0.4125	0.4025	0.3823	0.3671	0.344	0.3251	0.3109	0.2896

Figure I.1: F1A: e=2c & d=3.5c

	b/c									
	0.4396	0.4327	0.4242	0.4141	0.4036	0.3952	0.3854	0.3768	0.3689	0.3601
	0.4336	0.4249	0.4146	0.4026	0.3904	0.3809	0.3699	0.3605	0.3519	0.3423
	0.4218	0.4111	0.3987	0.3846	0.3704	0.36	0.3476	0.3373	0.328	0.3175
	0.4261	0.4135	0.3992	0.3829	0.3668	0.3554	0.3418	0.3306	0.3208	0.3095
a/c	0.4273	0.4134	0.3974	0.3789	0.3608	0.3486	0.3335	0.3215	0.3112	0.2988
	0.4171	0.403	0.386	0.3656	0.3453	0.3322	0.3155	0.3026	0.2917	0.278
	0.4197	0.4079	0.3915	0.3698	0.3476	0.3336	0.315	0.3008	0.2893	0.274
	0.4212	0.4143	0.4007	0.3792	0.3554	0.3403	0.3197	0.3039	0.2915	0.2743
	0.4131	0.4119	0.4031	0.3839	0.3595	0.3429	0.32	0.3021	0.2885	0.2687
	0.4194	0.4217	0.4213	0.4102	0.3887	0.372	0.3475	0.3274	0.3123	0.2901

Figure I.1: F1A: e=2c & d=4c

	b/c									
	0.4429	0.4357	0.427	0.4166	0.4058	0.397	0.3868	0.3778	0.3695	0.3604
	0.4372	0.4283	0.4177	0.4053	0.3927	0.3828	0.3714	0.3615	0.3525	0.3425
	0.4257	0.4147	0.402	0.3875	0.3729	0.3619	0.3491	0.3383	0.3287	0.3178
	0.4305	0.4175	0.4028	0.386	0.3694	0.3575	0.3433	0.3317	0.3215	0.3098
a/c	0.4321	0.4178	0.4013	0.3823	0.3636	0.3508	0.3352	0.3227	0.3119	0.2991
	0.4224	0.4079	0.3904	0.3693	0.3484	0.3347	0.3173	0.3038	0.2924	0.2784
	0.4255	0.4133	0.3963	0.3739	0.3509	0.3362	0.317	0.3022	0.2901	0.2744
	0.4275	0.4203	0.4061	0.3839	0.3593	0.3433	0.322	0.3055	0.2925	0.2748
	0.42	0.4186	0.4093	0.3893	0.364	0.3465	0.3227	0.3039	0.2896	0.2693
	0.4268	0.4291	0.4284	0.4164	0.394	0.3761	0.3506	0.3296	0.3137	0.2908

Figure I.1: F1A: e=2.5c & d=0.5c

	b/c									
	0.4064	0.4052	0.4038	0.4019	0.3997	0.3983	0.3958	0.3934	0.3907	0.3867
	0.3958	0.3943	0.3926	0.3903	0.3877	0.3861	0.3832	0.3806	0.3775	0.3732
	0.3788	0.3769	0.375	0.3723	0.3691	0.3675	0.3641	0.3612	0.3578	0.353
	0.378	0.3758	0.3736	0.3704	0.3668	0.365	0.3613	0.3581	0.3541	0.3491
a/c	0.3732	0.3708	0.3684	0.3648	0.3607	0.3589	0.3546	0.3512	0.347	0.3415
	0.3562	0.3537	0.3512	0.3473	0.3427	0.3409	0.3361	0.3324	0.3279	0.3219
	0.3514	0.3492	0.3469	0.3428	0.3378	0.3361	0.331	0.327	0.3222	0.3156
	0.3464	0.345	0.3433	0.3394	0.3342	0.3326	0.3271	0.3229	0.3177	0.3107
	0.335	0.3347	0.3337	0.3304	0.3253	0.3238	0.318	0.3136	0.308	0.3004
	0.3432	0.3444	0.3447	0.3429	0.3388	0.3376	0.3317	0.3274	0.3214	0.3134

Figure I.1: F1A: e=2.5c & d=1c

	b/c									
	0.4174	0.4149	0.4121	0.4086	0.4047	0.4018	0.3977	0.3939	0.39	0.3848
	0.4085	0.4054	0.4021	0.3979	0.3934	0.3902	0.3855	0.3812	0.377	0.3712
	0.3935	0.3897	0.3858	0.3809	0.3757	0.3721	0.3668	0.362	0.3573	0.3509
	0.3946	0.3902	0.3856	0.3801	0.3741	0.3702	0.3642	0.359	0.354	0.347
a/c	0.3919	0.387	0.3818	0.3755	0.3687	0.3646	0.358	0.3523	0.3469	0.3393
	0.3768	0.3715	0.366	0.359	0.3515	0.3471	0.3398	0.3337	0.3279	0.3197
	0.3734	0.3684	0.3629	0.3555	0.3474	0.3429	0.335	0.3284	0.3223	0.3133
	0.3693	0.3653	0.3604	0.353	0.3444	0.34	0.3315	0.3245	0.318	0.3082
	0.3581	0.3557	0.3519	0.345	0.3363	0.3321	0.3229	0.3154	0.3085	0.2978
	0.3646	0.3651	0.3636	0.3585	0.3505	0.3466	0.3372	0.3293	0.322	0.3104

Figure I.1: F1A: e=2.5c & d=1.5c

	b/c									
	0.4256	0.4223	0.4183	0.4135	0.4084	0.4044	0.3992	0.3944	0.3897	0.3838
	0.418	0.4139	0.4092	0.4035	0.3976	0.3931	0.3872	0.3819	0.3767	0.3701
	0.4043	0.3994	0.3938	0.3872	0.3804	0.3753	0.3687	0.3627	0.3571	0.3499
	0.4069	0.4011	0.3946	0.387	0.3793	0.3738	0.3664	0.3599	0.3538	0.346
a/c	0.4056	0.3991	0.3918	0.3832	0.3745	0.3685	0.3603	0.3533	0.3468	0.3383
	0.3919	0.3849	0.377	0.3674	0.3577	0.3514	0.3424	0.3348	0.3279	0.3186
	0.3899	0.383	0.3749	0.3647	0.3542	0.3476	0.3378	0.3296	0.3224	0.3122
	0.3869	0.381	0.3734	0.363	0.3518	0.3452	0.3346	0.3258	0.3182	0.3071
	0.3765	0.3724	0.366	0.356	0.3444	0.3377	0.3263	0.3169	0.3087	0.2965
	0.383	0.3822	0.3786	0.3702	0.3593	0.3528	0.3409	0.331	0.3223	0.3091

Figure I.1: F1A: e=2.5c & d=2c

	b/c									
	0.432	0.4281	0.4234	0.4176	0.4115	0.4066	0.4006	0.395	0.3897	0.3833
	0.4252	0.4205	0.4149	0.4081	0.401	0.3955	0.3887	0.3826	0.3767	0.3697
	0.4125	0.4069	0.4002	0.3922	0.3841	0.3779	0.3703	0.3635	0.3572	0.3494
	0.416	0.4094	0.4017	0.3926	0.3834	0.3766	0.3682	0.3608	0.354	0.3456
a/c	0.4158	0.4083	0.3996	0.3894	0.379	0.3717	0.3623	0.3543	0.347	0.3378
	0.4033	0.3951	0.3856	0.3742	0.3626	0.3548	0.3445	0.3359	0.3281	0.3182
	0.4023	0.3942	0.3844	0.3721	0.3595	0.3513	0.3401	0.3308	0.3226	0.3118
	0.4003	0.3932	0.3838	0.3711	0.3577	0.3492	0.3371	0.3272	0.3185	0.3067
	0.3907	0.3855	0.3774	0.3649	0.351	0.3422	0.3291	0.3184	0.3092	0.2961
	0.3978	0.396	0.3907	0.38	0.3665	0.3579	0.3441	0.3326	0.3229	0.3086

Figure I.1: F1A: e=2.5c & d=2.5c

	b/c									
	0.4369	0.4328	0.4275	0.421	0.4142	0.4085	0.4018	0.3957	0.3899	0.3831
	0.4308	0.4258	0.4195	0.4119	0.404	0.3976	0.3901	0.3833	0.3769	0.3695
	0.4188	0.4127	0.4053	0.3965	0.3874	0.3803	0.3718	0.3643	0.3574	0.3493
	0.4231	0.4159	0.4074	0.3973	0.387	0.3792	0.3698	0.3616	0.3542	0.3454
a/c	0.4237	0.4155	0.4059	0.3945	0.3829	0.3744	0.364	0.3552	0.3473	0.3377
	0.4119	0.403	0.3925	0.3798	0.3669	0.3578	0.3464	0.3369	0.3285	0.3181
	0.4118	0.4029	0.3919	0.3782	0.3642	0.3546	0.3421	0.3319	0.323	0.3117
	0.4106	0.4027	0.3921	0.3779	0.3629	0.3528	0.3394	0.3284	0.319	0.3066
	0.4018	0.3959	0.3865	0.3724	0.3567	0.3462	0.3316	0.3197	0.3098	0.296
	0.4094	0.407	0.4006	0.3883	0.3729	0.3624	0.3469	0.3342	0.3237	0.3086

Figure I.1: F1A: e=2.5c & d=3c

	b/c									
	0.4409	0.4365	0.4309	0.424	0.4165	0.4103	0.403	0.3964	0.3902	0.3831
	0.4353	0.4299	0.4232	0.4152	0.4066	0.3996	0.3914	0.3841	0.3773	0.3695
	0.4238	0.4174	0.4095	0.4	0.3902	0.3824	0.3733	0.3652	0.3578	0.3493
	0.4286	0.4211	0.412	0.4012	0.3901	0.3815	0.3714	0.3626	0.3546	0.3454
a/c	0.4298	0.4212	0.4109	0.3987	0.3862	0.3769	0.3657	0.3562	0.3477	0.3377
	0.4186	0.4093	0.398	0.3844	0.3706	0.3605	0.3482	0.338	0.3289	0.3181
	0.4192	0.4097	0.398	0.3833	0.3682	0.3575	0.3441	0.3331	0.3235	0.3117
	0.4186	0.4101	0.3987	0.3834	0.3672	0.3561	0.3415	0.3297	0.3196	0.3067
	0.4105	0.404	0.3938	0.3786	0.3616	0.3499	0.3341	0.3212	0.3104	0.2961
	0.4187	0.4158	0.4086	0.3951	0.3783	0.3665	0.3497	0.3359	0.3245	0.3088

Figure I.1: F1A: e=2.5c & d=3.5c

	b/c									
	0.4441	0.4396	0.4337	0.4264	0.4186	0.412	0.4043	0.3972	0.3906	0.3832
	0.4389	0.4333	0.4263	0.4179	0.4089	0.4014	0.3928	0.385	0.3777	0.3696
	0.4278	0.4211	0.4129	0.403	0.3927	0.3844	0.3747	0.3661	0.3583	0.3494
	0.433	0.4252	0.4157	0.4044	0.3928	0.3836	0.3729	0.3636	0.3552	0.3456
a/c	0.4346	0.4257	0.415	0.4022	0.3891	0.3792	0.3674	0.3573	0.3483	0.3379
	0.4239	0.4142	0.4024	0.3882	0.3737	0.363	0.35	0.3391	0.3295	0.3183
	0.425	0.4151	0.4028	0.3875	0.3716	0.3602	0.346	0.3344	0.3242	0.3119
	0.4249	0.416	0.404	0.388	0.371	0.359	0.3436	0.3311	0.3203	0.3069
	0.4173	0.4105	0.3997	0.3836	0.3657	0.3531	0.3364	0.3227	0.3112	0.2964
	0.426	0.4228	0.4151	0.4007	0.383	0.3702	0.3524	0.3376	0.3254	0.3091

Figure I.1: F1A: e=2.5c & d=4c

	b/c									
	0.4468	0.4421	0.436	0.4285	0.4205	0.4135	0.4055	0.3981	0.3912	0.3835
	0.4418	0.4361	0.4289	0.4202	0.4109	0.4031	0.394	0.3859	0.3783	0.3699
	0.431	0.4242	0.4157	0.4055	0.3949	0.3862	0.3761	0.3671	0.3589	0.3497
	0.4365	0.4285	0.4188	0.4071	0.3951	0.3855	0.3744	0.3646	0.3558	0.3459
a/c	0.4385	0.4294	0.4183	0.4052	0.3916	0.3812	0.3689	0.3584	0.349	0.3382
	0.4282	0.4182	0.406	0.3914	0.3764	0.3652	0.3517	0.3403	0.3303	0.3186
	0.4296	0.4195	0.4067	0.3909	0.3745	0.3625	0.3478	0.3356	0.325	0.3123
	0.4299	0.4208	0.4083	0.3918	0.3742	0.3616	0.3456	0.3324	0.3212	0.3073
	0.4228	0.4157	0.4044	0.3878	0.3692	0.3559	0.3386	0.3243	0.3122	0.2969
	0.4318	0.4285	0.4203	0.4054	0.3869	0.3733	0.3548	0.3394	0.3265	0.3097

Figure I.1: F1A: e=3c & d=0.5c

	b/c									
	0.4182	0.4174	0.4164	0.4151	0.4134	0.4124	0.4104	0.4085	0.4063	0.4031
	0.4095	0.4085	0.4074	0.4058	0.4038	0.4027	0.4005	0.3984	0.3959	0.3923
	0.3945	0.3933	0.392	0.3902	0.3879	0.3866	0.3841	0.3818	0.379	0.3751
	0.396	0.3946	0.3931	0.391	0.3767	0.387	0.3842	0.3816	0.3786	0.3744
a/c	0.3934	0.3918	0.3902	0.3878	0.3849	0.3833	0.3802	0.3774	0.3741	0.3695
	0.3782	0.3765	0.3747	0.372	0.3688	0.3672	0.3637	0.3607	0.3571	0.3522
	0.3746	0.3728	0.371	0.3681	0.3646	0.3629	0.3591	0.356	0.3521	0.3468
	0.3699	0.3683	0.3666	0.3636	0.3598	0.3583	0.3542	0.3508	0.3465	0.3409
	0.3578	0.3565	0.3551	0.3522	0.3482	0.3468	0.3424	0.3389	0.3344	0.3283
	0.3638	0.3633	0.3624	0.3599	0.3562	0.3549	0.3504	0.3468	0.3421	0.3357

Figure I.1: F1A: e=3c & d=1c

	b/c									
	0.4264	0.4247	0.4227	0.4201	0.4173	0.415	0.4118	0.4087	0.4056	0.4012
	0.4189	0.4168	0.4145	0.4115	0.4082	0.4057	0.4021	0.3986	0.3952	0.3904
	0.4053	0.4028	0.4001	0.3967	0.3929	0.3901	0.386	0.3822	0.3784	0.3731
	0.4082	0.4053	0.4022	0.3983	0.394	0.3909	0.3863	0.3822	0.378	0.3723
a/c	0.4071	0.4038	0.4003	0.3959	0.391	0.3877	0.3826	0.3781	0.3736	0.3674
	0.3933	0.3897	0.3858	0.3809	0.3755	0.3719	0.3664	0.3615	0.3567	0.3499
	0.391	0.3872	0.3831	0.3778	0.3719	0.3682	0.3622	0.3569	0.3517	0.3445
	0.3873	0.3836	0.3795	0.374	0.3677	0.3639	0.3574	0.3518	0.3464	0.3385
	0.3759	0.3727	0.3688	0.3632	0.3567	0.3529	0.3459	0.34	0.3342	0.3257
	0.3818	0.3796	0.3767	0.3715	0.365	0.3614	0.3542	0.3479	0.3419	0.3335

Figure I.1: F1A: e=3c & d=1.5c

	b/c									
	0.4327	0.4304	0.4275	0.424	0.4202	0.417	0.413	0.409	0.4052	0.4002
	0.4261	0.4233	0.42	0.4159	0.4115	0.408	0.4034	0.399	0.3948	0.3894
	0.4135	0.4102	0.4063	0.4016	0.3966	0.3926	0.3875	0.3827	0.378	0.372
	0.4173	0.4136	0.4091	0.4037	0.398	0.3937	0.388	0.3827	0.3777	0.3712
a/c	0.4173	0.413	0.4079	0.4019	0.3955	0.3908	0.3845	0.3788	0.3733	0.3663
	0.4047	0.3999	0.3943	0.3875	0.3805	0.3754	0.3684	0.3623	0.3565	0.3488
	0.4034	0.3983	0.3924	0.385	0.3773	0.3719	0.3644	0.3577	0.3516	0.3433
	0.4006	0.3956	0.3895	0.3818	0.3735	0.3679	0.3598	0.3527	0.3462	0.3373
	0.3901	0.3854	0.3796	0.3716	0.3629	0.3572	0.3485	0.341	0.3341	0.3245
	0.3963	0.3929	0.3879	0.3804	0.3716	0.3661	0.3569	0.349	0.3419	0.3316

Figure I.1: F1A: e=3c & d=2c

	b/c									
	0.4377	0.435	0.4315	0.4273	0.4226	0.4188	0.414	0.4095	0.4051	0.3998
	0.4317	0.4285	0.4245	0.4195	0.4142	0.4099	0.4046	0.3996	0.3947	0.3889
	0.4198	0.416	0.4113	0.4056	0.3996	0.3947	0.3888	0.3833	0.378	0.3715
	0.4244	0.42	0.4147	0.4082	0.4014	0.396	0.3894	0.3834	0.3777	0.3707
a/c	0.4251	0.4202	0.4141	0.4068	0.3992	0.3934	0.3861	0.3795	0.3734	0.3658
	0.4133	0.4078	0.4011	0.3929	0.3844	0.3782	0.3702	0.3631	0.3565	0.3483
	0.4128	0.4069	0.3997	0.3909	0.3816	0.3749	0.3663	0.3587	0.3517	0.3428
	0.4109	0.4049	0.3976	0.3881	0.3782	0.3712	0.3619	0.3538	0.3464	0.3368
	0.4011	0.3955	0.3883	0.3785	0.368	0.3608	0.3507	0.3421	0.3343	0.324
	0.4078	0.4035	0.3972	0.3878	0.3771	0.3699	0.3593	0.3503	0.3422	0.331

Figure I.1: F1A: e=3c & d=2.5c

	b/c									
	0.4416	0.4387	0.4349	0.4301	0.4248	0.4204	0.415	0.41	0.4052	0.3995
	0.4361	0.4327	0.4282	0.4227	0.4167	0.4117	0.4057	0.4001	0.3949	0.3887
	0.4248	0.4207	0.4155	0.4091	0.4023	0.3967	0.39	0.3839	0.3781	0.3713
	0.4299	0.4252	0.4192	0.412	0.4043	0.3982	0.3908	0.3841	0.3779	0.3705
a/c	0.4312	0.4258	0.4191	0.411	0.4024	0.3957	0.3875	0.3803	0.3736	0.3656
	0.42	0.414	0.4065	0.3975	0.388	0.3807	0.3718	0.3639	0.3568	0.3481
	0.4202	0.4137	0.4057	0.3958	0.3854	0.3777	0.368	0.3596	0.352	0.3427
	0.4188	0.4123	0.4041	0.3935	0.3823	0.3742	0.3637	0.3548	0.3467	0.3367
	0.4097	0.4035	0.3954	0.3844	0.3725	0.364	0.3528	0.3432	0.3347	0.3238
	0.417	0.412	0.4048	0.3941	0.382	0.3734	0.3616	0.3515	0.3426	0.3309

Figure I.1: F1A: e=3c & d=3c

	b/c									
	0.4448	0.4417	0.4377	0.4325	0.4268	0.4219	0.4161	0.4106	0.4054	0.3995
	0.4397	0.4361	0.4313	0.4253	0.4189	0.4133	0.4068	0.4008	0.3951	0.3886
	0.4287	0.4244	0.4189	0.412	0.4047	0.3985	0.3912	0.3846	0.3784	0.3713
	0.4343	0.4293	0.423	0.4152	0.4069	0.4001	0.3921	0.3849	0.3782	0.3705
a/c	0.4361	0.4304	0.4232	0.4145	0.4052	0.3978	0.389	0.3812	0.374	0.3656
	0.4253	0.419	0.411	0.4013	0.391	0.383	0.3733	0.3649	0.3572	0.3481
	0.426	0.4192	0.4106	0.4	0.3888	0.3802	0.3697	0.3606	0.3524	0.3427
	0.4251	0.4182	0.4093	0.398	0.386	0.3769	0.3656	0.3559	0.3472	0.3367
	0.4165	0.4099	0.4011	0.3893	0.3765	0.367	0.3548	0.3444	0.3352	0.3239
	0.4242	0.4189	0.411	0.3994	0.3863	0.3767	0.3638	0.3528	0.3432	0.331

Figure I.1: F1A: e=3c & d=3.5c

	b/c									
	0.4475	0.4443	0.44	0.4346	0.4286	0.4233	0.4171	0.4113	0.4058	0.3996
	0.4426	0.4388	0.4339	0.4276	0.4208	0.4149	0.408	0.4016	0.3955	0.3887
	0.432	0.4275	0.4217	0.4145	0.4068	0.4002	0.3925	0.3855	0.3788	0.3714
	0.4378	0.4327	0.426	0.4179	0.4092	0.402	0.3935	0.3858	0.3787	0.3706
a/c	0.44	0.4341	0.4266	0.4174	0.4077	0.3998	0.3905	0.3821	0.3745	0.3658
	0.4296	0.423	0.4147	0.4045	0.3937	0.3851	0.3749	0.3659	0.3577	0.3483
	0.4306	0.4235	0.4146	0.4035	0.3917	0.3825	0.3714	0.3617	0.353	0.3428
	0.4302	0.4229	0.4136	0.4018	0.3891	0.3794	0.3674	0.3571	0.3479	0.3369
	0.4219	0.415	0.4058	0.3934	0.3799	0.3697	0.3568	0.3457	0.3359	0.3241
	0.43	0.4244	0.416	0.4039	0.39	0.3796	0.366	0.3543	0.344	0.3313

Figure I.1: F1A: e=3c & d=4c

	b/c									
	0.4497	0.4464	0.442	0.4364	0.4302	0.4247	0.4182	0.4121	0.4063	0.3998
	0.4451	0.4412	0.436	0.4296	0.4225	0.4163	0.4091	0.4024	0.3961	0.389
	0.4346	0.43	0.4241	0.4167	0.4086	0.4018	0.3937	0.3863	0.3794	0.3716
	0.4407	0.4354	0.4286	0.4202	0.4112	0.4036	0.3948	0.3868	0.3793	0.3709
a/c	0.4432	0.4371	0.4294	0.4199	0.4099	0.4016	0.3918	0.3831	0.3751	0.3661
	0.4331	0.4263	0.4177	0.4072	0.396	0.387	0.3764	0.367	0.3584	0.3486
	0.4344	0.4271	0.4178	0.4064	0.3942	0.3845	0.373	0.3628	0.3537	0.3432
	0.4342	0.4268	0.4172	0.4049	0.3918	0.3816	0.3691	0.3583	0.3486	0.3373
	0.4263	0.4192	0.4096	0.3968	0.3828	0.3721	0.3586	0.3471	0.3368	0.3245
	0.4347	0.4289	0.4202	0.4075	0.3932	0.3822	0.368	0.3557	0.3449	0.3317

Figure I.1: F1A: e=3.5c & d=0.5c

	b/c									
a/c	0.427	0.4264	0.4257	0.4247	0.4234	0.4226	0.4211	0.4196	0.4177	0.4151
	0.4195	0.4188	0.418	0.4169	0.4154	0.4145	0.4128	0.4111	0.4091	0.4062
	0.4059	0.4051	0.4042	0.4028	0.4012	0.4002	0.3982	0.3964	0.3941	0.3909
	0.409	0.4081	0.407	0.4055	0.4036	0.4025	0.4003	0.3983	0.3958	0.3924
	0.408	0.4069	0.4058	0.404	0.402	0.4007	0.3984	0.3961	0.3934	0.3897
	0.3943	0.3931	0.3918	0.3899	0.3876	0.3863	0.3836	0.3812	0.3783	0.3742
	0.392	0.3907	0.3893	0.3872	0.3847	0.3833	0.3805	0.3779	0.3747	0.3704
	0.3882	0.3869	0.3855	0.3833	0.3805	0.3792	0.3761	0.3733	0.3699	0.3653
	0.3765	0.3753	0.3739	0.3716	0.3687	0.3673	0.364	0.3611	0.3575	0.3525
	0.3819	0.3809	0.3798	0.3776	0.3746	0.3733	0.3698	0.3669	0.3631	0.3578

Figure I.1: F1A: e=3.5c & d=1c

	b/c									
a/c	0.4332	0.432	0.4305	0.4286	0.4264	0.4246	0.4221	0.4195	0.4169	0.4133
	0.4267	0.4252	0.4235	0.4213	0.4188	0.4168	0.4139	0.4112	0.4083	0.4043
	0.414	0.4123	0.4103	0.4078	0.405	0.4028	0.3996	0.3965	0.3933	0.389
	0.4181	0.4161	0.4139	0.4111	0.4079	0.4054	0.4019	0.3985	0.3951	0.3904
	0.4182	0.416	0.4134	0.4102	0.4067	0.404	0.4001	0.3964	0.3927	0.3876
	0.4056	0.4031	0.4003	0.3967	0.3927	0.3899	0.3856	0.3816	0.3776	0.3721
	0.4043	0.4016	0.3986	0.3947	0.3903	0.3873	0.3826	0.3783	0.3741	0.3681
	0.4014	0.3986	0.3955	0.3913	0.3866	0.3835	0.3784	0.3739	0.3693	0.363
	0.3905	0.3877	0.3845	0.3802	0.3752	0.3719	0.3666	0.3617	0.3569	0.3501
	0.3963	0.3938	0.3909	0.3866	0.3814	0.3782	0.3726	0.3675	0.3625	0.3552

Figure I.1: F1A: e=3.5c & d=1.5c

	b/c									
a/c	0.4382	0.4365	0.4343	0.4316	0.4287	0.4262	0.4229	0.4197	0.4165	0.4124
	0.4323	0.4303	0.4278	0.4247	0.4214	0.4186	0.4149	0.4114	0.4078	0.4033
	0.4203	0.418	0.4152	0.4117	0.4079	0.4048	0.4007	0.3968	0.3929	0.388
	0.4251	0.4225	0.4193	0.4153	0.4111	0.4076	0.4031	0.3989	0.3947	0.3893
	0.426	0.423	0.4194	0.415	0.4102	0.4065	0.4015	0.3969	0.3924	0.3865
	0.4142	0.4109	0.4068	0.4019	0.3966	0.3926	0.3871	0.3821	0.3773	0.371
	0.4138	0.4101	0.4057	0.4003	0.3946	0.3902	0.3843	0.3789	0.3738	0.367
	0.4117	0.4078	0.4032	0.3974	0.3912	0.3866	0.3803	0.3745	0.3691	0.3618
	0.4015	0.3976	0.3929	0.3868	0.3801	0.3754	0.3686	0.3624	0.3566	0.3488
	0.4078	0.4042	0.3997	0.3935	0.3866	0.3819	0.3747	0.3683	0.3622	0.3539

Figure I.1: F1A: e=3.5c & d=2c

	b/c									
a/c	0.4421	0.4401	0.4376	0.4343	0.4307	0.4276	0.4237	0.42	0.4164	0.4119
	0.4367	0.4344	0.4314	0.4277	0.4236	0.4201	0.4158	0.4117	0.4077	0.4028
	0.4253	0.4226	0.4192	0.4149	0.4103	0.4065	0.4017	0.3972	0.3928	0.3874
	0.4306	0.4276	0.4237	0.4189	0.4137	0.4095	0.4043	0.3994	0.3946	0.3888
	0.4321	0.4286	0.4243	0.4189	0.4131	0.4085	0.4028	0.3974	0.3923	0.386
	0.4209	0.417	0.4122	0.4062	0.3998	0.3948	0.3885	0.3827	0.3772	0.3704
	0.4211	0.4168	0.4116	0.405	0.398	0.3927	0.3858	0.3796	0.3737	0.3664
	0.4196	0.4151	0.4095	0.4025	0.395	0.3893	0.3819	0.3753	0.3691	0.3612
	0.4101	0.4055	0.3997	0.3922	0.3842	0.3782	0.3703	0.3633	0.3567	0.3483
	0.4168	0.4125	0.407	0.3994	0.391	0.3849	0.3766	0.3692	0.3623	0.3533

Figure I.1: F1A: e=3.5c & d=2.5c

	b/c									
a/c	0.4453	0.4432	0.4403	0.4366	0.4325	0.4289	0.4246	0.4204	0.4164	0.4116
	0.4403	0.4377	0.4344	0.4302	0.4256	0.4216	0.4167	0.4122	0.4078	0.4026
	0.4293	0.4263	0.4225	0.4178	0.4125	0.4081	0.4027	0.3977	0.3929	0.3872
	0.435	0.4317	0.4274	0.422	0.4162	0.4113	0.4054	0.3999	0.3947	0.3886
	0.437	0.4332	0.4283	0.4223	0.4158	0.4104	0.404	0.398	0.3924	0.3858
	0.4262	0.422	0.4166	0.4099	0.4027	0.3969	0.3898	0.3834	0.3774	0.3702
	0.4269	0.4223	0.4164	0.409	0.4012	0.3949	0.3872	0.3804	0.3739	0.3662
	0.4259	0.421	0.4147	0.4068	0.3983	0.3917	0.3834	0.3761	0.3693	0.361
	0.4168	0.4118	0.4053	0.3969	0.3878	0.3808	0.372	0.3641	0.3569	0.3487
	0.424	0.4193	0.413	0.4044	0.3949	0.3878	0.3784	0.3702	0.3626	0.3531

Figure I.1: F1A: e=3.5c & d=3c

	b/c									
a/c	0.448	0.4457	0.4426	0.4386	0.4341	0.4302	0.4254	0.4209	0.4166	0.4116
	0.4432	0.4405	0.437	0.4324	0.4274	0.423	0.4177	0.4128	0.408	0.4025
	0.4325	0.4294	0.4253	0.4202	0.4145	0.4096	0.4038	0.3983	0.3931	0.3871
	0.4386	0.4351	0.4305	0.4247	0.4183	0.4129	0.4065	0.4006	0.395	0.3885
	0.4409	0.4369	0.4317	0.4252	0.4182	0.4123	0.4052	0.3988	0.3927	0.3857
	0.4305	0.426	0.4203	0.413	0.4053	0.3989	0.3912	0.3842	0.3777	0.3701
	0.4315	0.4266	0.4203	0.4125	0.404	0.397	0.3887	0.3812	0.3743	0.3662
	0.4309	0.4257	0.419	0.4105	0.4013	0.394	0.385	0.377	0.3697	0.361
	0.4223	0.4169	0.41	0.4009	0.3911	0.3833	0.3737	0.3651	0.3574	0.348
	0.4298	0.4248	0.4179	0.4087	0.3984	0.3904	0.3802	0.3713	0.3631	0.3531

Figure I.1: F1A: e=3.5c & d=3.5c

	b/c									
a/c	0.4501	0.4478	0.4445	0.4404	0.4357	0.4314	0.4264	0.4215	0.4169	0.4116
	0.4456	0.4428	0.4391	0.4344	0.429	0.4243	0.4187	0.4134	0.4083	0.4026
	0.4351	0.432	0.4277	0.4223	0.4163	0.411	0.4048	0.399	0.3935	0.3872
	0.4415	0.4378	0.433	0.4269	0.4203	0.4145	0.4077	0.4014	0.3954	0.3886
	0.444	0.4399	0.4345	0.4277	0.4203	0.4139	0.4065	0.3996	0.3932	0.3858
	0.434	0.4293	0.4233	0.4157	0.4076	0.4007	0.3925	0.3851	0.3782	0.3703
	0.4353	0.4302	0.4236	0.4154	0.4064	0.399	0.3902	0.3822	0.3748	0.3663
	0.435	0.4296	0.4226	0.4136	0.404	0.3961	0.3866	0.3781	0.3702	0.3611
	0.4266	0.4211	0.4138	0.4043	0.3939	0.3856	0.3754	0.3663	0.358	0.3482
	0.4345	0.4292	0.422	0.4123	0.4015	0.3929	0.3821	0.3725	0.3638	0.3534

Figure I.1: F1A: e=3.5c & d=4c

	b/c									
a/c	0.452	0.4495	0.4462	0.4419	0.437	0.4325	0.4273	0.4222	0.4173	0.4118
	0.4476	0.4448	0.4409	0.436	0.4305	0.4255	0.4197	0.4141	0.4088	0.4028
	0.4374	0.4341	0.4297	0.4241	0.4179	0.4124	0.4059	0.3998	0.394	0.3874
	0.4439	0.4401	0.4352	0.4289	0.422	0.4159	0.4088	0.4022	0.3959	0.3889
	0.4467	0.4424	0.4368	0.4298	0.4221	0.4155	0.4077	0.4005	0.3938	0.3861
	0.4368	0.432	0.4258	0.418	0.4095	0.4023	0.3938	0.386	0.3788	0.3706
	0.4384	0.4332	0.4264	0.4178	0.4085	0.4008	0.3916	0.3832	0.3755	0.3666
	0.4383	0.4328	0.4255	0.4163	0.4063	0.398	0.3881	0.3791	0.3709	0.3615
	0.4302	0.4245	0.4169	0.4071	0.3964	0.3876	0.377	0.3674	0.3587	0.3486
	0.4383	0.4329	0.4254	0.4153	0.4041	0.3951	0.3838	0.3737	0.3646	0.3538

Figure I.1: F1A: e=4c & d=0.5c

	b/c									
	0.4337	0.4332	0.4327	0.4319	0.431	0.4303	0.4291	0.4278	0.4263	0.4241
	0.4271	0.4266	0.426	0.4251	0.424	0.4233	0.4219	0.4205	0.4189	0.4164
	0.4144	0.4138	0.4132	0.4122	0.4109	0.4101	0.4086	0.407	0.4052	0.4025
	0.4187	0.418	0.4172	0.4161	0.4147	0.4138	0.4121	0.4105	0.4085	0.4056
a/c	0.4189	0.4181	0.4172	0.416	0.4144	0.4134	0.4116	0.4098	0.4076	0.4045
	0.4062	0.4054	0.4044	0.403	0.4013	0.4002	0.3982	0.3962	0.3939	0.3905
	0.405	0.4041	0.4031	0.4015	0.3996	0.3985	0.3962	0.3942	0.3916	0.388
	0.4022	0.4012	0.4001	0.3985	0.3964	0.3952	0.3929	0.3906	0.3879	0.384
	0.3912	0.3902	0.3891	0.3873	0.3851	0.3839	0.3813	0.379	0.3758	0.3719
	0.3969	0.3959	0.3949	0.3931	0.3908	0.3896	0.3869	0.3844	0.3813	0.377

Figure I.1: F1A: e=4c & d=1c

	b/c									
	0.4386	0.4376	0.4365	0.435	0.4333	0.4318	0.4298	0.4277	0.4255	0.4225
	0.4326	0.4316	0.4303	0.4286	0.4266	0.425	0.4227	0.4205	0.4181	0.4148
	0.4207	0.4194	0.4179	0.416	0.4138	0.4121	0.4095	0.407	0.4044	0.4008
	0.4256	0.4242	0.4226	0.4204	0.418	0.416	0.4132	0.4105	0.4076	0.4037
a/c	0.4266	0.425	0.4232	0.4208	0.418	0.4159	0.4128	0.4098	0.4068	0.4025
	0.4148	0.413	0.4109	0.4083	0.4053	0.403	0.3996	0.3964	0.393	0.3885
	0.4144	0.4124	0.4102	0.4073	0.404	0.4015	0.3978	0.3944	0.3908	0.3859
	0.4123	0.4102	0.4078	0.4047	0.4011	0.3985	0.3946	0.3909	0.3871	0.3818
	0.402	0.3998	0.3973	0.394	0.3902	0.3874	0.3832	0.3792	0.3752	0.3696
	0.4082	0.406	0.4035	0.4001	0.3961	0.3934	0.3889	0.3847	0.3805	0.3746

Figure I.1: F1A: e=4c & d=1.5c

	b/c									
	0.4425	0.4412	0.4395	0.4374	0.4351	0.4331	0.4304	0.4277	0.4251	0.4216
	0.4371	0.4356	0.4337	0.4313	0.4287	0.4264	0.4235	0.4205	0.4176	0.4138
	0.4256	0.4239	0.4218	0.4191	0.4161	0.4136	0.4103	0.4071	0.4039	0.3998
	0.4311	0.4292	0.4268	0.4238	0.4205	0.4178	0.4142	0.4107	0.4072	0.4027
a/c	0.4327	0.4305	0.4278	0.4245	0.4208	0.4178	0.4139	0.4101	0.4063	0.4015
	0.4215	0.4191	0.4161	0.4124	0.4083	0.4051	0.4008	0.3966	0.3926	0.3874
	0.4217	0.4191	0.4158	0.4117	0.4073	0.4038	0.3991	0.3947	0.3904	0.3847
	0.4203	0.4174	0.4139	0.4095	0.4047	0.401	0.396	0.3912	0.3867	0.3806
	0.4106	0.4076	0.4039	0.3992	0.394	0.3901	0.3847	0.3797	0.3748	0.3683
	0.4172	0.4142	0.4105	0.4056	0.4002	0.3962	0.3905	0.3852	0.3801	0.3733

Figure I.1: F1A: e=4c & d=2c

	b/c									
	0.4457	0.4442	0.4422	0.4396	0.4367	0.4342	0.431	0.428	0.4249	0.4211
	0.4406	0.4389	0.4366	0.4337	0.4305	0.4277	0.4242	0.4208	0.4174	0.4133
	0.4296	0.4276	0.425	0.4217	0.4181	0.415	0.4111	0.4074	0.4037	0.3992
	0.4355	0.4333	0.4304	0.4267	0.4227	0.4193	0.415	0.411	0.407	0.4022
a/c	0.4375	0.435	0.4317	0.4277	0.4232	0.4195	0.4149	0.4105	0.4062	0.4009
	0.4268	0.424	0.4204	0.4158	0.4109	0.4069	0.4018	0.3971	0.3925	0.3868
	0.4275	0.4244	0.4205	0.4155	0.4101	0.4058	0.4003	0.3952	0.3903	0.3842
	0.4265	0.4232	0.4189	0.4136	0.4078	0.4031	0.3973	0.3918	0.3866	0.3801
	0.4173	0.4138	0.4093	0.4036	0.3973	0.3924	0.3861	0.3803	0.3748	0.3677
	0.4244	0.4209	0.4163	0.4103	0.4037	0.3987	0.392	0.3859	0.3801	0.3726

Figure I.1: F1A: e=4c & d=2.5c

	b/c									
	0.4483	0.4466	0.4444	0.4415	0.4382	0.4353	0.4317	0.4283	0.4249	0.4208
	0.4435	0.4416	0.4391	0.4358	0.4321	0.4289	0.4249	0.4211	0.4174	0.413
	0.4328	0.4306	0.4277	0.424	0.4199	0.4163	0.4119	0.4078	0.4038	0.399
	0.439	0.4366	0.4334	0.4292	0.4247	0.4207	0.4159	0.4114	0.4071	0.4019
a/c	0.4414	0.4387	0.435	0.4304	0.4254	0.4211	0.4159	0.411	0.4063	0.4007
	0.431	0.428	0.4239	0.4188	0.4133	0.4086	0.4029	0.3976	0.3926	0.3865
	0.4321	0.4287	0.4243	0.4188	0.4127	0.4076	0.4015	0.3958	0.3904	0.3839
	0.4315	0.4279	0.4231	0.4171	0.4105	0.4052	0.3985	0.3925	0.3867	0.3798
	0.4228	0.4189	0.4139	0.4074	0.4003	0.3946	0.3875	0.381	0.3749	0.3675
	0.4302	0.4263	0.4211	0.4144	0.4069	0.401	0.3935	0.3867	0.3803	0.3724

Figure I.1: F1A: e=4c & d=3c

	b/c									
	0.4505	0.4487	0.4463	0.4432	0.4396	0.4363	0.4325	0.4287	0.425	0.4207
	0.4459	0.4439	0.4412	0.4376	0.4336	0.43	0.4257	0.4216	0.4176	0.4129
	0.4354	0.4332	0.43	0.4261	0.4216	0.4176	0.4128	0.4083	0.4039	0.3988
	0.442	0.4394	0.4359	0.4314	0.4265	0.4221	0.4169	0.412	0.4073	0.4018
a/c	0.4446	0.4417	0.4378	0.4328	0.4274	0.4226	0.4169	0.4116	0.4065	0.4006
	0.4345	0.4312	0.4269	0.4215	0.4154	0.4102	0.404	0.3983	0.3928	0.3865
	0.4359	0.4323	0.4276	0.4216	0.415	0.4094	0.4027	0.3965	0.3907	0.3839
	0.4356	0.4317	0.4267	0.4202	0.413	0.4071	0.3999	0.3932	0.387	0.3798
	0.4271	0.423	0.4176	0.4107	0.403	0.3967	0.3889	0.3818	0.3753	0.3674
	0.4349	0.4307	0.4252	0.4179	0.4098	0.4032	0.395	0.3876	0.3807	0.3724

Figure I.1: F1A: e=4c & d=3.5c

	b/c									
	0.4523	0.4505	0.448	0.4447	0.4409	0.4374	0.4332	0.4292	0.4253	0.4208
	0.4479	0.4459	0.443	0.4393	0.435	0.4312	0.4266	0.4222	0.4179	0.413
	0.4376	0.4353	0.432	0.4278	0.4231	0.4188	0.4138	0.4089	0.4042	0.3989
	0.4444	0.4417	0.438	0.4334	0.4281	0.4235	0.4179	0.4127	0.4076	0.4019
a/c	0.4472	0.4442	0.4401	0.4349	0.4291	0.424	0.418	0.4123	0.4069	0.4007
	0.4373	0.434	0.4295	0.4237	0.4173	0.4118	0.4052	0.3991	0.3932	0.3866
	0.439	0.4353	0.4303	0.424	0.4171	0.4111	0.404	0.3973	0.3911	0.384
	0.4389	0.4349	0.4296	0.4228	0.4153	0.4089	0.4012	0.3941	0.3875	0.3799
	0.4307	0.4265	0.4208	0.4135	0.4054	0.3986	0.3903	0.3828	0.3758	0.3676
	0.4387	0.4344	0.4285	0.4209	0.4123	0.4053	0.3965	0.3886	0.3812	0.3725

Figure I.1: F1A: e=4c & d=4c

	b/c									
	0.4539	0.452	0.4494	0.446	0.442	0.4384	0.434	0.4298	0.4257	0.4209
	0.4496	0.4475	0.4445	0.4407	0.4363	0.4322	0.4274	0.4228	0.4183	0.4132
	0.4395	0.4371	0.4337	0.4294	0.4245	0.42	0.4147	0.4096	0.4047	0.3991
	0.4464	0.4436	0.4398	0.435	0.4296	0.4247	0.4189	0.4134	0.4081	0.4021
a/c	0.4494	0.4463	0.4421	0.4367	0.4307	0.4254	0.419	0.4131	0.4074	0.4009
	0.4397	0.4362	0.4316	0.4256	0.419	0.4132	0.4063	0.3999	0.3938	0.3868
	0.4415	0.4377	0.4326	0.4261	0.4189	0.4126	0.4052	0.3982	0.3917	0.3842
	0.4417	0.4375	0.432	0.425	0.4172	0.4105	0.4025	0.3951	0.3881	0.3802
	0.4337	0.4293	0.4234	0.4159	0.4075	0.4003	0.3917	0.3838	0.3764	0.3679
	0.4418	0.4374	0.4314	0.4234	0.4146	0.4071	0.398	0.3897	0.3819	0.3729

Figure I.2: F2A: e=0.5c & d=0.5c

	b/c									
a/c	−0.197	−0.1859	−0.1792	−0.1705	−0.162	−0.1626	−0.1562	−0.153	−0.149	−0.1426
	−0.2019	−0.1923	−0.1825	−0.1743	−0.1673	−0.1637	−0.1586	−0.1547	−0.151	−0.1459
	−0.204	−0.2	−0.187	−0.1802	−0.1759	−0.1636	−0.1609	−0.1568	−0.1538	−0.1511
	−0.2098	−0.2067	−0.1946	−0.1831	−0.179	−0.1625	−0.1607	−0.1548	−0.1506	−0.1504
	−0.2143	−0.214	−0.2093	−0.1973	−0.1847	−0.1674	−0.1628	−0.1547	−0.1495	−0.1494
	−0.2204	−0.2205	−0.2206	−0.2201	−0.2186	−0.1955	−0.1882	−0.1815	−0.176	−0.1684
	−0.2268	−0.2268	−0.2269	−0.2274	−0.2273	−0.2155	−0.2019	−0.187	−0.18	−0.1722
	−0.2335	−0.2335	−0.2334	−0.2335	−0.2342	−0.2314	−0.2237	−0.2038	−0.1923	−0.1818
	−0.2571	−0.2564	−0.2567	−0.255	−0.2507	−0.2548	−0.2551	−0.2424	−0.2232	−0.2059
	−0.2582	−0.2582	−0.2581	−0.2581	−0.2582	−0.258	−0.2587	−0.2545	−0.239	−0.2158

Figure I.2: F2A: e=0.5c & d=1c

	b/c									
a/c	−0.2273	−0.2078	−0.1952	−0.182	−0.1702	−0.1683	−0.1595	−0.1545	−0.1502	−0.1417
	−0.2369	−0.2183	−0.2009	−0.1872	−0.1763	−0.1698	−0.1623	−0.1564	−0.1525	−0.145
	−0.2364	−0.2315	−0.2094	−0.1958	−0.1864	−0.1698	−0.1642	−0.1584	−0.1501	−0.1501
	−0.2391	−0.2355	−0.2184	−0.2015	−0.1916	−0.1673	−0.1627	−0.1559	−0.1433	−0.1493
	−0.2451	−0.2449	−0.2414	−0.2229	−0.2012	−0.1726	−0.1624	−0.1548	−0.1405	−0.1482
	−0.2514	−0.2515	−0.2514	−0.251	−0.2417	−0.2031	−0.1884	−0.182	−0.162	−0.1669
	−0.2574	−0.2576	−0.2576	−0.2577	−0.2591	−0.2367	−0.2052	−0.1882	−0.1649	−0.1704
	−0.2612	−0.2612	−0.2612	−0.2612	−0.2612	−0.2602	−0.2404	−0.2053	−0.1819	−0.1796
	−0.2764	−0.2755	−0.2752	−0.2742	−0.2725	−0.2735	−0.2729	−0.2514	−0.219	−0.2028
	−0.2759	−0.2758	−0.2758	−0.2758	−0.2759	−0.2758	−0.2758	−0.2744	−0.2484	−0.2123

Figure I.2: F2A: e=0.5c & d=1.5c

	b/c									
a/c	−0.247	−0.2227	−0.2058	−0.1893	−0.1753	−0.1717	−0.1616	−0.1555	−0.1506	−0.1414
	−0.2599	−0.2362	−0.2133	−0.1955	−0.1819	−0.1735	−0.1645	−0.1575	−0.1531	−0.1447
	−0.2594	−0.2536	−0.2246	−0.2059	−0.193	−0.174	−0.1668	−0.1595	−0.1494	−0.1497
	−0.2603	−0.2562	−0.235	−0.2143	−0.1997	−0.1723	−0.1657	−0.1573	−0.1415	−0.1489
	−0.2632	−0.2629	−0.259	−0.2352	−0.212	−0.1766	−0.1667	−0.1564	−0.138	−0.1477
	−0.2674	−0.2675	−0.2675	−0.2667	−0.2548	−0.2095	−0.1946	−0.1843	−0.1591	−0.1664
	−0.2736	−0.2737	−0.2737	−0.2737	−0.2741	−0.2479	−0.2096	−0.1915	−0.1635	−0.1698
	−0.2783	−0.2783	−0.2783	−0.2782	−0.2775	−0.2767	−0.2503	−0.2089	−0.1804	−0.179
	−0.2902	−0.2899	−0.2896	−0.289	−0.2878	−0.2872	−0.2853	−0.2606	−0.2192	−0.2022
	−0.2898	−0.2898	−0.2898	−0.2898	−0.2898	−0.2896	−0.2882	−0.2868	−0.2546	−0.2124

Figure I.2: F2A: e=0.5c & d=2c

	b/c									
a/c	−0.2604	−0.2332	−0.2135	−0.1947	−0.1789	−0.1741	−0.163	−0.1563	−0.1508	−0.1413
	−0.2756	−0.2488	−0.2223	−0.2016	−0.1859	−0.1761	−0.1661	−0.1583	−0.1533	−0.1446
	−0.2754	−0.2691	−0.2357	−0.2134	−0.1977	−0.177	−0.1686	−0.1605	−0.1497	−0.1496
	−0.276	−0.2716	−0.2487	−0.224	−0.2056	−0.1759	−0.1678	−0.1583	−0.1411	−0.1488
	−0.2773	−0.2771	−0.2732	−0.2454	−0.2201	−0.1796	−0.1693	−0.1577	−0.1376	−0.1476
	−0.2795	−0.2795	−0.2795	−0.2784	−0.2655	−0.2156	−0.1977	−0.1861	−0.1588	−0.1663
	−0.2832	−0.2832	−0.2832	−0.2832	−0.2837	−0.2539	−0.2152	−0.1936	−0.1634	−0.1698
	−0.2864	−0.2864	−0.2863	−0.2863	−0.2855	−0.2844	−0.2555	−0.2113	−0.1811	−0.1791
	−0.2977	−0.2976	−0.2973	−0.2966	−0.2954	−0.2951	−0.2922	−0.2664	−0.2238	−0.2029
	−0.2981	−0.2981	−0.298	−0.2981	−0.2981	−0.2977	−0.2957	−0.2938	−0.2586	−0.2133

Figure I.2: F2A: e=0.5c & d=2.5c

	b/c									
a/c	−0.2699	−0.2408	−0.2193	−0.1989	−0.1818	−0.1759	−0.1641	−0.1569	−0.151	−0.1413
	−0.2867	−0.2578	−0.2291	−0.2065	−0.1892	−0.1782	−0.1673	−0.1589	−0.1535	−0.1446
	−0.2869	−0.2802	−0.2441	−0.2192	−0.2016	−0.1794	−0.17	−0.1612	−0.15	−0.1496
	−0.2876	−0.283	−0.2591	−0.2315	−0.2103	−0.1787	−0.1694	−0.1591	−0.1415	−0.1488
	−0.2884	−0.2882	−0.2841	−0.2539	−0.2266	−0.1833	−0.1714	−0.1588	−0.1373	−0.1477
	−0.2895	−0.2895	−0.2895	−0.2882	−0.2744	−0.221	−0.2003	−0.1875	−0.1587	−0.1665
	−0.2914	−0.2914	−0.2915	−0.2914	−0.2919	−0.2592	−0.2195	−0.1949	−0.1628	−0.17
	−0.2926	−0.2926	−0.2926	−0.2925	−0.2917	−0.2903	−0.2594	−0.2145	−0.1839	−0.1795
	−0.3021	−0.3021	−0.3019	−0.3012	−0.3001	−0.2992	−0.2965	−0.2706	−0.2257	−0.2033
	−0.3014	−0.3014	−0.3014	−0.3014	−0.3014	−0.301	−0.2989	−0.2968	−0.2601	−0.2142

Figure I.2: F2A: e=0.5c & d=3c

	b/c									
a/c	−0.2768	−0.2465	−0.2237	−0.2023	−0.1842	−0.1775	−0.1651	−0.1574	−0.1512	−0.1412
	−0.2948	−0.2645	−0.2342	−0.2102	−0.1919	−0.18	−0.1684	−0.1595	−0.1537	−0.1446
	−0.2953	−0.2883	−0.2504	−0.2237	−0.2048	−0.1815	−0.1713	−0.1619	−0.1503	−0.1496
	−0.2963	−0.2916	−0.267	−0.2373	−0.2142	−0.1812	−0.1709	−0.1599	−0.1419	−0.1488
	−0.297	−0.2967	−0.2925	−0.2606	−0.2318	−0.1865	−0.1733	−0.1597	−0.1369	−0.1478
	−0.2975	−0.2976	−0.2976	−0.2961	−0.2815	−0.2256	−0.2032	−0.1888	−0.1585	−0.1666
	−0.2986	−0.2986	−0.2986	−0.2984	−0.299	−0.2642	−0.2234	−0.1965	−0.1623	−0.1702
	−0.2984	−0.2985	−0.2984	−0.2984	−0.2975	−0.296	−0.2632	−0.2174	−0.1838	−0.1799
	−0.3064	−0.3064	−0.3063	−0.3056	−0.3042	−0.3035	−0.2981	−0.2746	−0.2276	−0.2043
	−0.3041	−0.304	−0.304	−0.304	−0.304	−0.3036	−0.3015	−0.2992	−0.2614	−0.2153

Figure I.2: F2A: e=0.5c & d=3.5c

	b/c									
a/c	−0.2821	−0.2508	−0.2271	−0.2049	−0.1862	−0.179	−0.166	−0.158	−0.1514	−0.1413
	−0.3008	−0.2696	−0.2382	−0.2133	−0.1941	−0.1815	−0.1694	−0.1601	−0.154	−0.1446
	−0.3017	−0.2944	−0.2552	−0.2272	−0.2074	−0.1833	−0.1725	−0.1625	−0.1507	−0.1497
	−0.3029	−0.2981	−0.273	−0.2418	−0.2173	−0.1833	−0.1723	−0.1607	−0.1423	−0.1489
	−0.3036	−0.3033	−0.299	−0.2662	−0.236	−0.1893	−0.1751	−0.1607	−0.1368	−0.1479
	−0.304	−0.304	−0.304	−0.3025	−0.2872	−0.2294	−0.2056	−0.1901	−0.1586	−0.1668
	−0.3045	−0.3046	−0.3046	−0.3044	−0.3049	−0.2686	−0.2267	−0.1979	−0.1626	−0.1705
	−0.3037	−0.3037	−0.3037	−0.3036	−0.3027	−0.3011	−0.2671	−0.2201	−0.1809	−0.1803
	−0.3107	−0.3107	−0.3107	−0.31	−0.3085	−0.3078	−0.3069	−0.2785	−0.2298	−0.205
	−0.3071	−0.3071	−0.3071	−0.3071	−0.3071	−0.3067	−0.3045	−0.3021	−0.2628	−0.2168

Figure I.2: F2A: e=0.5c & d=4c

	b/c									
a/c	−0.2862	−0.2542	−0.2298	−0.2071	−0.1878	−0.1802	−0.1669	−0.1585	−0.1517	−0.1414
	−0.3055	−0.2735	−0.2413	−0.2157	−0.1959	−0.1829	−0.1704	−0.1607	−0.1543	−0.1447
	−0.3065	−0.2991	−0.2589	−0.2301	−0.2095	−0.1848	−0.1735	−0.1632	−0.1511	−0.1498
	−0.308	−0.3031	−0.2777	−0.2454	−0.2199	−0.1852	−0.1736	−0.1615	−0.1428	−0.1491
	−0.3087	−0.3085	−0.3041	−0.2705	−0.2394	−0.1916	−0.1766	−0.1616	−0.1369	−0.1481
	−0.3091	−0.3091	−0.3092	−0.3076	−0.2916	−0.2326	−0.2077	−0.1913	−0.1589	−0.1671
	−0.3095	−0.3095	−0.3095	−0.3094	−0.3097	−0.2725	−0.2296	−0.1992	−0.1632	−0.1709
	−0.3083	−0.3083	−0.3083	−0.3082	−0.3072	−0.3056	−0.2704	−0.2226	−0.1824	−0.1809
	−0.3146	−0.3147	−0.3147	−0.314	−0.3127	−0.3118	−0.3101	−0.282	−0.2309	−0.206
	−0.3103	−0.3103	−0.3103	−0.3103	−0.3103	−0.3098	−0.3077	−0.3053	−0.2651	−0.2184

Figure I.2: F2A: e=1c & d=0.5c

	b/c									
	−0.2392	−0.2347	−0.2309	−0.2261	−0.221	−0.2194	−0.215	−0.2118	−0.2082	−0.2031
	−0.2367	−0.2323	−0.2285	−0.2234	−0.2181	−0.2166	−0.212	−0.2087	−0.205	−0.1998
	−0.2392	−0.2362	−0.2327	−0.2278	−0.2225	−0.2204	−0.2157	−0.2121	−0.2084	−0.203
	−0.2389	−0.2384	−0.2354	−0.2317	−0.2273	−0.223	−0.2188	−0.2146	−0.2108	−0.2058
a/c	−0.2422	−0.24	−0.238	−0.2358	−0.233	−0.2261	−0.2228	−0.218	−0.214	−0.2095
	−0.2503	−0.2471	−0.2437	−0.2421	−0.2404	−0.2325	−0.2294	−0.2239	−0.2196	−0.2151
	−0.2573	−0.256	−0.2517	−0.2484	−0.2469	−0.2397	−0.2363	−0.2303	−0.2253	−0.2207
	−0.2612	−0.261	−0.2594	−0.2555	−0.253	−0.2469	−0.2438	−0.2371	−0.2313	−0.2261
	−0.2764	−0.2766	−0.2765	−0.276	−0.274	−0.2704	−0.2685	−0.262	−0.2551	−0.2483
	−0.2758	−0.2758	−0.2758	−0.2738	−0.2741	−0.268	−0.2649	−0.26	−0.2547	−0.2468

Figure I.2: F2A: e=1c & d=1c

	b/c									
	−0.2599	−0.2516	−0.2443	−0.2363	−0.2286	−0.2247	−0.2182	−0.2131	−0.2085	−0.2018
	−0.2585	−0.2501	−0.2425	−0.2341	−0.2259	−0.2221	−0.2152	−0.2101	−0.2055	−0.1985
	−0.2616	−0.2554	−0.2479	−0.2393	−0.2309	−0.2262	−0.2192	−0.2136	−0.2089	−0.2016
	−0.2607	−0.2589	−0.2524	−0.2447	−0.2367	−0.2295	−0.2227	−0.2163	−0.2111	−0.2043
a/c	−0.2602	−0.2586	−0.2551	−0.2502	−0.2437	−0.2332	−0.2268	−0.2197	−0.2132	−0.2079
	−0.2662	−0.2628	−0.2599	−0.2564	−0.2525	−0.2399	−0.2335	−0.2256	−0.2173	−0.2133
	−0.2734	−0.2719	−0.2681	−0.2647	−0.2599	−0.2472	−0.2404	−0.232	−0.2222	−0.2186
	−0.2782	−0.278	−0.2766	−0.2742	−0.27	−0.2578	−0.2485	−0.2386	−0.2285	−0.2236
	−0.2903	−0.2905	−0.2904	−0.2906	−0.2904	−0.2829	−0.2748	−0.2639	−0.2517	−0.2453
	−0.2899	−0.2898	−0.2898	−0.2897	−0.2895	−0.2858	−0.2789	−0.2659	−0.2522	−0.2432

Figure I.2: F2A: e=1c & d=1.5c

	b/c									
	−0.2741	−0.2635	−0.2536	−0.2432	−0.2336	−0.2282	−0.2202	−0.2141	−0.2087	−0.2012
	−0.2735	−0.2628	−0.2524	−0.2413	−0.2311	−0.2256	−0.2173	−0.211	−0.2057	−0.1979
	−0.2775	−0.2692	−0.2588	−0.2473	−0.2366	−0.2301	−0.2215	−0.2147	−0.2092	−0.201
	−0.2768	−0.2742	−0.2648	−0.2538	−0.2432	−0.2339	−0.2253	−0.2175	−0.2114	−0.2036
a/c	−0.2744	−0.2735	−0.2687	−0.2607	−0.2512	−0.2383	−0.2298	−0.2211	−0.2132	−0.2072
	−0.2782	−0.2748	−0.2719	−0.2681	−0.2611	−0.2457	−0.237	−0.2273	−0.217	−0.2125
	−0.2829	−0.2813	−0.2774	−0.2735	−0.2687	−0.2535	−0.2445	−0.2339	−0.2215	−0.2177
	−0.2863	−0.286	−0.2846	−0.2822	−0.2775	−0.2636	−0.2529	−0.2409	−0.2269	−0.2227
	−0.2977	−0.2979	−0.2978	−0.298	−0.2988	−0.2899	−0.2801	−0.2668	−0.251	−0.2443
	−0.2981	−0.2981	−0.298	−0.298	−0.298	−0.2956	−0.2874	−0.2703	−0.2519	−0.242

Figure I.2: F2A: e=1c & d=2c

	b/c									
	−0.2841	−0.2722	−0.2606	−0.2485	−0.2373	−0.2307	−0.2218	−0.215	−0.2089	−0.201
	−0.2842	−0.272	−0.2598	−0.2469	−0.235	−0.2282	−0.219	−0.2119	−0.2059	−0.1977
	−0.2889	−0.2794	−0.267	−0.2535	−0.2409	−0.233	−0.2233	−0.2156	−0.2094	−0.2008
	−0.2887	−0.2854	−0.2743	−0.261	−0.2482	−0.2372	−0.2273	−0.2186	−0.2117	−0.2034
a/c	−0.2854	−0.2851	−0.2793	−0.269	−0.257	−0.2421	−0.2322	−0.2223	−0.2136	−0.207
	−0.2881	−0.2847	−0.2816	−0.2775	−0.268	−0.2502	−0.2398	−0.2287	−0.2173	−0.2123
	−0.2911	−0.2894	−0.2855	−0.2811	−0.2764	−0.2588	−0.2479	−0.2357	−0.2218	−0.2175
	−0.2925	−0.2922	−0.2907	−0.2881	−0.2827	−0.2673	−0.2566	−0.2432	−0.2273	−0.2225
	−0.3021	−0.3023	−0.3022	−0.3023	−0.3033	−0.2934	−0.2837	−0.2697	−0.2516	−0.2441
	−0.3014	−0.3014	−0.3013	−0.3013	−0.3012	−0.2988	−0.29	−0.2719	−0.2526	−0.2419

Figure I.2: F2A: e=1c & d=2.5c

	b/c									
	−0.2915	−0.2787	−0.266	−0.2527	−0.2404	−0.2328	−0.2231	−0.2157	−0.2091	−0.201
	−0.292	−0.279	−0.2655	−0.2513	−0.2382	−0.2304	−0.2203	−0.2126	−0.2061	−0.1977
	−0.2973	−0.287	−0.2734	−0.2584	−0.2445	−0.2354	−0.2248	−0.2164	−0.2097	−0.2008
	−0.2975	−0.2939	−0.2816	−0.2667	−0.2524	−0.24	−0.229	−0.2195	−0.212	−0.2034
a/c	−0.2939	−0.2939	−0.2875	−0.2756	−0.2618	−0.2454	−0.2342	−0.2234	−0.214	−0.207
	−0.2961	−0.2927	−0.2898	−0.2851	−0.2737	−0.2542	−0.2422	−0.23	−0.2178	−0.2123
	−0.2983	−0.2965	−0.2925	−0.2881	−0.2831	−0.2634	−0.2508	−0.2373	−0.2222	−0.2176
	−0.2984	−0.2981	−0.2966	−0.2938	−0.2881	−0.2715	−0.26	−0.2452	−0.2279	−0.2227
	−0.3064	−0.3066	−0.3065	−0.3066	−0.3077	−0.297	−0.2876	−0.2724	−0.2524	−0.2444
	−0.304	−0.304	−0.3039	−0.3039	−0.3039	−0.3012	−0.2913	−0.2721	−0.2532	−0.2424

Figure I.2: F2A: e=1c & d=3c

	b/c									
	−0.2971	−0.2837	−0.2702	−0.2561	−0.243	−0.2346	−0.2243	−0.2163	−0.2094	−0.201
	−0.2979	−0.2842	−0.27	−0.2549	−0.241	−0.2324	−0.2216	−0.2133	−0.2064	−0.1977
	−0.3036	−0.2927	−0.2783	−0.2624	−0.2476	−0.2376	−0.2262	−0.2172	−0.2101	−0.2008
	−0.3042	−0.3004	−0.2873	−0.2713	−0.2559	−0.2425	−0.2306	−0.2204	−0.2124	−0.2034
a/c	−0.3005	−0.3007	−0.2938	−0.2809	−0.2659	−0.2483	−0.2361	−0.2245	−0.2145	−0.207
	−0.3025	−0.2991	−0.2963	−0.2912	−0.2785	−0.2576	−0.2444	−0.2313	−0.2184	−0.2125
	−0.3042	−0.3024	−0.2982	−0.2939	−0.2886	−0.2674	−0.2536	−0.2388	−0.2228	−0.2178
	−0.3037	−0.3033	−0.3018	−0.2989	−0.2931	−0.2767	−0.2633	−0.2472	−0.2285	−0.223
	−0.3107	−0.3109	−0.3107	−0.3108	−0.3119	−0.2892	−0.2915	−0.275	−0.2534	−0.2449
	−0.3071	−0.3071	−0.307	−0.307	−0.3069	−0.304	−0.2932	−0.2734	−0.2541	−0.243

Figure I.2: F2A: e=1c & d=3.5c

	b/c									
	−0.3014	−0.2876	−0.2736	−0.2589	−0.2452	−0.2363	−0.2255	−0.217	−0.2097	−0.2011
	−0.3025	−0.2883	−0.2735	−0.2578	−0.2433	−0.2341	−0.2228	−0.2141	−0.2068	−0.1978
	−0.3085	−0.2972	−0.2822	−0.2656	−0.2501	−0.2395	−0.2275	−0.218	−0.2105	−0.2009
	−0.3093	−0.3054	−0.2917	−0.275	−0.2588	−0.2447	−0.2322	−0.2214	−0.2129	−0.2036
a/c	−0.3056	−0.306	−0.2988	−0.2852	−0.2693	−0.2508	−0.2378	−0.2256	−0.2151	−0.2072
	−0.3076	−0.3042	−0.3015	−0.296	−0.2825	−0.2606	−0.2465	−0.2326	−0.2192	−0.2127
	−0.3091	−0.3072	−0.3031	−0.2988	−0.2932	−0.271	−0.2561	−0.2404	−0.2237	−0.2182
	−0.3082	−0.3079	−0.3063	−0.3033	−0.2975	−0.2804	−0.2664	−0.2492	−0.2294	−0.2234
	−0.3147	−0.3148	−0.3147	−0.3147	−0.3159	−0.3046	−0.2951	−0.2776	−0.2546	−0.2455
	−0.3103	−0.3103	−0.3102	−0.3102	−0.3101	−0.307	−0.2957	−0.2752	−0.255	−0.2439

Figure I.2: F2A: e=1c & d=4c

	b/c									
	−0.3048	−0.2906	−0.2762	−0.2611	−0.247	−0.2377	−0.2265	−0.2178	−0.2101	−0.2013
	−0.3061	−0.2915	−0.2763	−0.2602	−0.2452	−0.2356	−0.2239	−0.2149	−0.2072	−0.198
	−0.3123	−0.3008	−0.2853	−0.2682	−0.2522	−0.2411	−0.2287	−0.2189	−0.211	−0.2011
	−0.3134	−0.3093	−0.2953	−0.278	−0.2612	−0.2466	−0.2335	−0.2223	−0.2135	−0.2038
a/c	−0.3097	−0.3101	−0.3027	−0.2886	−0.2721	−0.253	−0.2394	−0.2267	−0.2158	−0.2076
	−0.3117	−0.3082	−0.3056	−0.2999	−0.2857	−0.2631	−0.2484	−0.2338	−0.22	−0.2131
	−0.3132	−0.3112	−0.3071	−0.3028	−0.297	−0.274	−0.2583	−0.2419	−0.2247	−0.2186
	−0.312	−0.3117	−0.3101	−0.3071	−0.3013	−0.2838	−0.2691	−0.251	−0.2304	−0.224
	−0.3182	−0.3183	−0.3182	−0.3182	−0.3194	−0.3079	−0.2983	−0.28	−0.2561	−0.2463
	−0.3133	−0.3133	−0.3132	−0.3132	−0.3131	−0.31	−0.2982	−0.2773	−0.2568	−0.245

Figure I.2: F2A: e=1.5c & d=0.5c

	b/c									
	−0.2633	−0.261	−0.2589	−0.256	−0.2527	−0.2513	−0.2481	−0.2455	−0.2425	−0.2383
	−0.2617	−0.2593	−0.2571	−0.254	−0.2506	−0.2491	−0.2458	−0.2431	−0.24	−0.2357
	−0.2621	−0.26	−0.2578	−0.2547	−0.2512	−0.2498	−0.2463	−0.2436	−0.2404	−0.236
	−0.2603	−0.2589	−0.2571	−0.2543	−0.251	−0.2493	−0.2459	−0.243	−0.2398	−0.2353
a/c	−0.2632	−0.2629	−0.2617	−0.2597	−0.2569	−0.2547	−0.2515	−0.2484	−0.245	−0.2406
	−0.2668	−0.2668	−0.2662	−0.2653	−0.2634	−0.2603	−0.2575	−0.2542	−0.2507	−0.2463
	−0.2721	−0.2705	−0.2697	−0.2696	−0.269	−0.2652	−0.2631	−0.2596	−0.256	−0.2518
	−0.2769	−0.2742	−0.2716	−0.2712	−0.2713	−0.2678	−0.2662	−0.2626	−0.259	−0.2549
	−0.29	−0.2886	−0.2857	−0.284	−0.2843	−0.2814	−0.2803	−0.2769	−0.2733	−0.2693
	−0.2897	−0.2889	−0.2865	−0.2829	−0.2811	−0.2783	−0.2783	−0.2751	−0.2716	−0.2676

Figure I.2: F2A: e=1.5c & d=1c

	b/c									
	−0.2776	−0.2732	−0.2689	−0.2639	−0.2587	−0.2555	−0.2506	−0.2464	−0.2424	−0.2369
	−0.2768	−0.2722	−0.2676	−0.2623	−0.2568	−0.2534	−0.2483	−0.244	−0.24	−0.2343
	−0.2776	−0.2732	−0.2687	−0.2633	−0.2576	−0.2542	−0.2489	−0.2445	−0.2404	−0.2345
	−0.2755	−0.2724	−0.2684	−0.2633	−0.2577	−0.2541	−0.2487	−0.244	−0.2398	−0.2337
a/c	−0.2775	−0.2763	−0.2734	−0.2691	−0.264	−0.2598	−0.2544	−0.2494	−0.245	−0.2388
	−0.2792	−0.2795	−0.278	−0.2751	−0.271	−0.2658	−0.2607	−0.2553	−0.2504	−0.2443
	−0.2817	−0.2806	−0.28	−0.2792	−0.2769	−0.2709	−0.2664	−0.2607	−0.2552	−0.2496
	−0.2849	−0.2821	−0.28	−0.2795	−0.2789	−0.273	−0.2693	−0.2636	−0.2575	−0.2524
	−0.2973	−0.2956	−0.2929	−0.2916	−0.2913	−0.2859	−0.2833	−0.2776	−0.2712	−0.2665
	−0.2978	−0.2968	−0.2942	−0.2913	−0.2893	−0.2843	−0.2811	−0.2749	−0.2691	−0.2644

Figure I.2: F2A: e=1.5c & d=1.5c

	b/c									
	−0.2877	−0.2822	−0.2762	−0.2695	−0.2629	−0.2583	−0.2523	−0.2471	−0.2424	−0.2362
	−0.2876	−0.2816	−0.2752	−0.2681	−0.2611	−0.2564	−0.2501	−0.2448	−0.24	−0.2336
	−0.2888	−0.2831	−0.2767	−0.2694	−0.2621	−0.2574	−0.2508	−0.2453	−0.2404	−0.2338
	−0.2869	−0.2826	−0.2769	−0.2698	−0.2625	−0.2574	−0.2506	−0.2449	−0.2398	−0.2329
a/c	−0.2886	−0.2868	−0.2824	−0.2761	−0.2692	−0.2634	−0.2566	−0.2504	−0.245	−0.2379
	−0.2895	−0.2899	−0.2874	−0.2828	−0.2767	−0.2698	−0.2631	−0.2563	−0.2504	−0.2434
	−0.29	−0.2894	−0.2889	−0.2871	−0.283	−0.2752	−0.269	−0.2618	−0.2551	−0.2486
	−0.2911	−0.2884	−0.2867	−0.2862	−0.2852	−0.2776	−0.2722	−0.2649	−0.2572	−0.2513
	−0.3017	−0.2999	−0.2973	−0.2963	−0.2964	−0.2899	−0.286	−0.279	−0.2706	−0.2653
	−0.3012	−0.3001	−0.2974	−0.2946	−0.293	−0.2878	−0.283	−0.2761	−0.2684	−0.263

Figure I.2: F2A: e=1.5c & d=2c

	b/c									
	−0.2952	−0.2889	−0.2818	−0.2739	−0.2661	−0.2606	−0.2537	−0.2478	−0.2425	−0.2359
	−0.2955	−0.2887	−0.2811	−0.2727	−0.2644	−0.2587	−0.2515	−0.2455	−0.2401	−0.2333
	−0.297	−0.2905	−0.283	−0.2742	−0.2656	−0.2598	−0.2523	−0.2461	−0.2406	−0.2335
	−0.2954	−0.2904	−0.2835	−0.275	−0.2663	−0.26	−0.2523	−0.2457	−0.24	−0.2326
a/c	−0.2971	−0.2949	−0.2895	−0.2818	−0.2734	−0.2663	−0.2584	−0.2513	−0.2452	−0.2376
	−0.2977	−0.2981	−0.295	−0.2891	−0.2814	−0.2731	−0.2651	−0.2574	−0.2507	−0.2431
	−0.2972	−0.2969	−0.2964	−0.2938	−0.2882	−0.2789	−0.2713	−0.263	−0.2554	−0.2483
	−0.2969	−0.2943	−0.2929	−0.2927	−0.2906	−0.2815	−0.2747	−0.2662	−0.2575	−0.251
	−0.3059	−0.3042	−0.3017	−0.3008	−0.3012	−0.2941	−0.2888	−0.2806	−0.2709	−0.2649
	−0.3038	−0.3027	−0.3	−0.2972	−0.2956	−0.29	−0.2852	−0.2779	−0.2686	−0.2626

Figure I.2: F2A: e=1.5c & d=2.5c

	b/c									
	−0.3009	−0.294	−0.2863	−0.2775	−0.2688	−0.2625	−0.2549	−0.2485	−0.2427	−0.2358
	−0.3014	−0.2941	−0.2858	−0.2765	−0.2672	−0.2607	−0.2528	−0.2462	−0.2403	−0.2332
	−0.3033	−0.2962	−0.2879	−0.2782	−0.2686	−0.2619	−0.2536	−0.2468	−0.2408	−0.2334
	−0.3019	−0.2965	−0.2888	−0.2793	−0.2695	−0.2623	−0.2537	−0.2465	−0.2403	−0.2325
a/c	−0.3037	−0.3013	−0.2952	−0.2865	−0.277	−0.2688	−0.26	−0.2522	−0.2456	−0.2376
	−0.3042	−0.3047	−0.3011	−0.2943	−0.2855	−0.276	−0.267	−0.2584	−0.2511	−0.243
	−0.3032	−0.3032	−0.3026	−0.2994	−0.2927	−0.2822	−0.2734	−0.2642	−0.2559	−0.2483
	−0.3022	−0.2996	−0.2984	−0.2984	−0.2955	−0.2852	−0.2772	−0.2676	−0.258	−0.251
	−0.3102	−0.3084	−0.306	−0.3054	−0.306	−0.298	−0.2915	−0.2822	−0.2715	−0.265
	−0.3068	−0.3057	−0.303	−0.3002	−0.2986	−0.2926	−0.2878	−0.2797	−0.2692	−0.2627

Figure I.2: F2A: e=1.5c & d=3c

	b/c									
	−0.3052	−0.2981	−0.2898	−0.2805	−0.2711	−0.2642	−0.256	−0.2492	−0.243	−0.2358
	−0.306	−0.2983	−0.2895	−0.2796	−0.2697	−0.2625	−0.254	−0.2469	−0.2406	−0.2332
	−0.3081	−0.3007	−0.2918	−0.2815	−0.2712	−0.2638	−0.2549	−0.2476	−0.2411	−0.2335
	−0.3069	−0.3012	−0.293	−0.2828	−0.2723	−0.2643	−0.2551	−0.2473	−0.2406	−0.2326
a/c	−0.3089	−0.3063	−0.2998	−0.2904	−0.2801	−0.2711	−0.2616	−0.2531	−0.246	−0.2376
	−0.3094	−0.3099	−0.3061	−0.2986	−0.289	−0.2786	−0.2688	−0.2595	−0.2516	−0.2431
	−0.3081	−0.3083	−0.3077	−0.3041	−0.2966	−0.2852	−0.2755	−0.2655	−0.2565	−0.2484
	−0.3067	−0.3042	−0.3031	−0.3032	−0.2998	−0.2886	−0.2795	−0.2691	−0.2587	−0.2511
	−0.3142	−0.3123	−0.3099	−0.3096	−0.3103	−0.3016	−0.2942	−0.2839	−0.2723	−0.2652
	−0.31	−0.3088	−0.3061	−0.3034	−0.3017	−0.2956	−0.2907	−0.2817	−0.2701	−0.263

Figure I.2: F2A: e=1.5c & d=3.5c

	b/c									
	−0.3087	−0.3012	−0.2927	−0.2829	−0.2731	−0.2658	−0.2572	−0.2499	−0.2433	−0.2359
	−0.3096	−0.3017	−0.2925	−0.2821	−0.2718	−0.2641	−0.2552	−0.2476	−0.241	−0.2333
	−0.3119	−0.3042	−0.2949	−0.2842	−0.2734	−0.2655	−0.2562	−0.2484	−0.2415	−0.2336
	−0.3109	−0.3049	−0.2964	−0.2857	−0.2747	−0.2662	−0.2564	−0.2482	−0.2411	−0.2327
a/c	−0.313	−0.3102	−0.3034	−0.2936	−0.2827	−0.2732	−0.2631	−0.2541	−0.2465	−0.2378
	−0.3136	−0.3141	−0.31	−0.3022	−0.292	−0.281	−0.2705	−0.2606	−0.2522	−0.2433
	−0.3121	−0.3124	−0.3118	−0.3079	−0.2999	−0.2878	−0.2774	−0.2668	−0.2572	−0.2487
	−0.3105	−0.308	−0.3071	−0.3072	−0.3034	−0.2916	−0.2818	−0.2706	−0.2596	−0.2515
	−0.3176	−0.3158	−0.3134	−0.3132	−0.314	−0.3048	−0.2968	−0.2856	−0.2733	−0.2657
	−0.313	−0.3118	−0.3091	−0.3064	−0.3047	−0.2984	−0.2934	−0.2837	−0.2712	−0.2636

Figure I.2: F2A: e=1.5c & d=4c

	b/c									
	−0.3114	−0.3038	−0.295	−0.2849	−0.2748	−0.2671	−0.2582	−0.2506	−0.2438	−0.2361
	−0.3125	−0.3044	−0.2949	−0.2842	−0.2735	−0.2656	−0.2562	−0.2484	−0.2415	−0.2335
	−0.3149	−0.307	−0.2975	−0.2864	−0.2753	−0.267	−0.2573	−0.2492	−0.2421	−0.2338
	−0.314	−0.3079	−0.2991	−0.2881	−0.2768	−0.2678	−0.2577	−0.2491	−0.2416	−0.233
a/c	−0.3163	−0.3134	−0.3064	−0.2963	−0.285	−0.275	−0.2645	−0.2551	−0.2471	−0.2381
	−0.3169	−0.3174	−0.3133	−0.3051	−0.2945	−0.283	−0.2721	−0.2617	−0.2529	−0.2437
	−0.3154	−0.3158	−0.3152	−0.3111	−0.3027	−0.2901	−0.2792	−0.268	−0.2581	−0.2491
	−0.3137	−0.3112	−0.3103	−0.3105	−0.3064	−0.2941	−0.2838	−0.272	−0.2606	−0.252
	−0.3207	−0.3188	−0.3164	−0.3163	−0.3172	−0.3076	−0.299	−0.2873	−0.2745	−0.2663
	−0.3158	−0.3146	−0.3118	−0.3091	−0.3074	−0.3011	−0.2959	−0.2857	−0.2725	−0.2644

Figure I.2: F2A: e=2c & d=0.5c

	b/c									
a/c	−0.279	−0.2777	−0.2763	−0.2744	−0.2723	−0.2711	−0.2688	−0.2667	−0.2643	−0.2609
	−0.2783	−0.2769	−0.2755	−0.2735	−0.2712	−0.2699	−0.2675	−0.2654	−0.2629	−0.2594
	−0.2788	−0.2774	−0.276	−0.274	−0.2716	−0.2703	−0.2678	−0.2656	−0.2631	−0.2595
	−0.2759	−0.2747	−0.2734	−0.2714	−0.269	−0.2678	−0.2653	−0.2631	−0.2604	−0.2568
	−0.2771	−0.2762	−0.2752	−0.2735	−0.2713	−0.2701	−0.2676	−0.2653	−0.2627	−0.259
	−0.2794	−0.2792	−0.2785	−0.2772	−0.2754	−0.274	−0.2716	−0.2694	−0.2667	−0.263
	−0.2832	−0.2832	−0.2829	−0.2823	−0.2811	−0.2795	−0.2775	−0.2752	−0.2724	−0.2688
	−0.2858	−0.2855	−0.2853	−0.2853	−0.2849	−0.283	−0.2814	−0.2791	−0.2764	−0.2729
	−0.2968	−0.2957	−0.2951	−0.2953	−0.2956	−0.2936	−0.2926	−0.2904	−0.2879	−0.2845
	−0.297	−0.295	−0.293	−0.2925	−0.2929	−0.2912	−0.2908	−0.2888	−0.2865	−0.2834

Figure I.2: F2A: e=2c & d=1c

	b/c									
a/c	−0.2891	−0.2865	−0.2838	−0.2804	−0.2768	−0.2743	−0.2706	−0.2672	−0.2639	−0.2595
	−0.289	−0.2863	−0.2833	−0.2797	−0.2759	−0.2733	−0.2694	−0.2659	−0.2626	−0.2579
	−0.29	−0.2871	−0.2841	−0.2804	−0.2765	−0.2738	−0.2698	−0.2662	−0.2628	−0.258
	−0.2871	−0.2845	−0.2816	−0.278	−0.274	−0.2713	−0.2673	−0.2636	−0.2601	−0.2552
	−0.2878	−0.2859	−0.2835	−0.2802	−0.2764	−0.2737	−0.2696	−0.2659	−0.2623	−0.2573
	−0.2894	−0.2884	−0.2867	−0.2839	−0.2805	−0.2777	−0.2737	−0.2699	−0.2662	−0.2611
	−0.2916	−0.2916	−0.2907	−0.2889	−0.2863	−0.2833	−0.2796	−0.2757	−0.2719	−0.2667
	−0.2921	−0.2922	−0.292	−0.2915	−0.2899	−0.2867	−0.2835	−0.2795	−0.2756	−0.2706
	−0.3013	−0.3004	−0.3001	−0.3003	−0.3001	−0.297	−0.2945	−0.2907	−0.2866	−0.282
	−0.3002	−0.2981	−0.2963	−0.2961	−0.2963	−0.2936	−0.2921	−0.2888	−0.2847	−0.2806

Figure I.2: F2A: e=2c & d=1.5c

	b/c									
a/c	−0.2966	−0.2932	−0.2894	−0.2848	−0.2801	−0.2766	−0.2719	−0.2677	−0.2638	−0.2587
	−0.297	−0.2933	−0.2892	−0.2843	−0.2793	−0.2756	−0.2708	−0.2665	−0.2624	−0.2571
	−0.2982	−0.2945	−0.2902	−0.2852	−0.28	−0.2762	−0.2712	−0.2668	−0.2626	−0.2572
	−0.2955	−0.2921	−0.288	−0.2829	−0.2777	−0.2739	−0.2688	−0.2642	−0.26	−0.2544
	−0.2961	−0.2935	−0.2899	−0.2852	−0.2802	−0.2763	−0.2712	−0.2665	−0.2622	−0.2564
	−0.2974	−0.296	−0.2932	−0.2892	−0.2845	−0.2805	−0.2754	−0.2705	−0.2661	−0.2602
	−0.2988	−0.2987	−0.2972	−0.2943	−0.2904	−0.2862	−0.2813	−0.2763	−0.2717	−0.2657
	−0.2982	−0.2986	−0.2982	−0.2968	−0.2941	−0.2898	−0.2853	−0.2802	−0.2753	−0.2695
	−0.3057	−0.3051	−0.3051	−0.3053	−0.3043	−0.3001	−0.2964	−0.2914	−0.2862	−0.2808
	−0.3029	−0.3009	−0.2994	−0.2994	−0.2998	−0.2964	−0.2939	−0.2894	−0.2841	−0.2792

Figure I.2: F2A: e=2c & d=2c

	b/c									
a/c	−0.3023	−0.2984	−0.2938	−0.2883	−0.2827	−0.2784	−0.2731	−0.2683	−0.2638	−0.2584
	−0.3029	−0.2988	−0.2938	−0.288	−0.282	−0.2775	−0.272	−0.2671	−0.2624	−0.2568
	−0.3045	−0.3002	−0.2951	−0.289	−0.2828	−0.2782	−0.2725	−0.2674	−0.2627	−0.2569
	−0.3019	−0.298	−0.293	−0.287	−0.2807	−0.276	−0.2701	−0.2648	−0.26	−0.254
	−0.3026	−0.2995	−0.2951	−0.2895	−0.2833	−0.2785	−0.2725	−0.2671	−0.2622	−0.256
	−0.3038	−0.3021	−0.2987	−0.2936	−0.2878	−0.2828	−0.2768	−0.2712	−0.2662	−0.2597
	−0.3048	−0.3047	−0.3027	−0.299	−0.294	−0.2887	−0.2829	−0.2771	−0.2718	−0.2653
	−0.3035	−0.3041	−0.3036	−0.3016	−0.2979	−0.2925	−0.287	−0.2811	−0.2754	−0.269
	−0.31	−0.3097	−0.31	−0.3099	−0.3081	−0.3029	−0.2982	−0.2923	−0.2863	−0.2803
	−0.3059	−0.304	−0.3028	−0.303	−0.3034	−0.2992	−0.2958	−0.2904	−0.2842	−0.2787

Figure I.2: F2A: e=2c & d=2.5c

	b/c									
a/c	−0.3067	−0.3025	−0.2974	−0.2913	−0.285	−0.28	−0.2741	−0.2688	−0.264	−0.2582
	−0.3076	−0.303	−0.2976	−0.2911	−0.2844	−0.2792	−0.2731	−0.2676	−0.2626	−0.2567
	−0.3093	−0.3046	−0.299	−0.2923	−0.2853	−0.28	−0.2736	−0.268	−0.2629	−0.2568
	−0.3069	−0.3026	−0.2971	−0.2904	−0.2833	−0.2778	−0.2712	−0.2655	−0.2602	−0.2539
	−0.3077	−0.3043	−0.2994	−0.293	−0.2861	−0.2805	−0.2738	−0.2678	−0.2625	−0.2559
	−0.3089	−0.3069	−0.3031	−0.2974	−0.2908	−0.285	−0.2782	−0.272	−0.2664	−0.2596
	−0.3098	−0.3096	−0.3073	−0.303	−0.2972	−0.2911	−0.2844	−0.2779	−0.2721	−0.2652
	−0.3081	−0.3088	−0.3082	−0.3058	−0.3013	−0.2951	−0.2887	−0.282	−0.2758	−0.2689
	−0.314	−0.3139	−0.3142	−0.3141	−0.3117	−0.3057	−0.3001	−0.2934	−0.2867	−0.2802
	−0.3091	−0.3073	−0.3063	−0.3068	−0.3069	−0.302	−0.2978	−0.2915	−0.2847	−0.2786

Figure I.2: F2A: e=2c & d=3c

	b/c									
a/c	−0.3101	−0.3057	−0.3003	−0.2938	−0.287	−0.2815	−0.2751	−0.2694	−0.2642	−0.2582
	−0.3112	−0.3064	−0.3006	−0.2937	−0.2865	−0.2808	−0.2741	−0.2682	−0.2629	−0.2567
	−0.3131	−0.3082	−0.3022	−0.295	−0.2875	−0.2816	−0.2747	−0.2687	−0.2632	−0.2568
	−0.3108	−0.3063	−0.3004	−0.2932	−0.2856	−0.2796	−0.2724	−0.2662	−0.2605	−0.2539
	−0.3117	−0.3081	−0.3029	−0.296	−0.2885	−0.2823	−0.2751	−0.2686	−0.2628	−0.2559
	−0.3129	−0.3109	−0.3068	−0.3006	−0.2935	−0.287	−0.2796	−0.2728	−0.2668	−0.2597
	−0.3138	−0.3136	−0.3111	−0.3064	−0.3	−0.2933	−0.286	−0.2789	−0.2725	−0.2652
	−0.312	−0.3128	−0.3121	−0.3093	−0.3044	−0.2975	−0.2905	−0.2831	−0.2763	−0.269
	−0.3175	−0.3175	−0.318	−0.3177	−0.3149	−0.3083	−0.302	−0.2946	−0.2873	−0.2803
	−0.3121	−0.3103	−0.3095	−0.3102	−0.3102	−0.3048	−0.2999	−0.2929	−0.2853	−0.2788

Figure I.2: F2A: e=2c & d=3.5c

	b/c									
a/c	−0.3129	−0.3083	−0.3026	−0.2958	−0.2887	−0.2829	−0.2761	−0.2701	−0.2646	−0.2583
	−0.3141	−0.3092	−0.3031	−0.2958	−0.2883	−0.2822	−0.2752	−0.2689	−0.2632	−0.2568
	−0.3161	−0.311	−0.3048	−0.2972	−0.2894	−0.2831	−0.2758	−0.2694	−0.2635	−0.2569
	−0.314	−0.3093	−0.3031	−0.2956	−0.2876	−0.2811	−0.2736	−0.2669	−0.2609	−0.254
	−0.3149	−0.3112	−0.3057	−0.2985	−0.2906	−0.284	−0.2763	−0.2694	−0.2633	−0.2561
	−0.3162	−0.3141	−0.3098	−0.3033	−0.2957	−0.2888	−0.281	−0.2737	−0.2673	−0.2598
	−0.3171	−0.3169	−0.3143	−0.3092	−0.3025	−0.2953	−0.2875	−0.2799	−0.2731	−0.2654
	−0.3152	−0.316	−0.3153	−0.3124	−0.3071	−0.2997	−0.2921	−0.2842	−0.277	−0.2692
	−0.3205	−0.3206	−0.3212	−0.3208	−0.3177	−0.3107	−0.3039	−0.2959	−0.2881	−0.2806
	−0.3149	−0.3131	−0.3123	−0.3132	−0.313	−0.3073	−0.3019	−0.2943	−0.2862	−0.2792

Figure I.2: F2A: e=2c & d=4c

	b/c									
a/c	−0.3151	−0.3104	−0.3046	−0.2976	−0.2902	−0.2841	−0.2771	−0.2708	−0.265	−0.2585
	−0.3164	−0.3114	−0.3051	−0.2977	−0.2899	−0.2835	−0.2762	−0.2696	−0.2637	−0.257
	−0.3185	−0.3134	−0.3069	−0.2991	−0.291	−0.2845	−0.2768	−0.2701	−0.264	−0.2571
	−0.3165	−0.3117	−0.3054	−0.2976	−0.2893	−0.2826	−0.2747	−0.2677	−0.2614	−0.2543
	−0.3175	−0.3137	−0.3081	−0.3006	−0.2924	−0.2855	−0.2775	−0.2703	−0.2638	−0.2564
	−0.3189	−0.3167	−0.3122	−0.3056	−0.2977	−0.2905	−0.2823	−0.2747	−0.2679	−0.2602
	−0.3198	−0.3196	−0.3169	−0.3116	−0.3046	−0.2971	−0.2889	−0.2809	−0.2738	−0.2658
	−0.3179	−0.3188	−0.318	−0.3149	−0.3093	−0.3017	−0.2937	−0.2854	−0.2778	−0.2697
	−0.3231	−0.3233	−0.3239	−0.3234	−0.3202	−0.3128	−0.3056	−0.2972	−0.289	−0.2811
	−0.3173	−0.3155	−0.3148	−0.3158	−0.3155	−0.3095	−0.3038	−0.2958	−0.2872	−0.2797

Figure I.2: F2A: e=2.5c & d=0.5c

	b/c									
a/c	−0.2898	−0.289	−0.2881	−0.2868	−0.2853	−0.2844	−0.2826	−0.281	−0.2791	−0.2763
	−0.2899	−0.289	−0.288	−0.2866	−0.285	−0.284	−0.2822	−0.2805	−0.2785	−0.2757
	−0.2908	−0.2899	−0.2889	−0.2875	−0.2858	−0.2848	−0.2829	−0.2812	−0.2791	−0.2762
	−0.2877	−0.2868	−0.2859	−0.2844	−0.2827	−0.2817	−0.2798	−0.278	−0.2758	−0.273
	−0.2881	−0.2873	−0.2865	−0.2851	−0.2835	−0.2825	−0.2806	−0.2788	−0.2766	−0.2737
	−0.2892	−0.2887	−0.288	−0.2868	−0.2853	−0.2844	−0.2825	−0.2808	−0.2786	−0.2756
	−0.2914	−0.2912	−0.2907	−0.2899	−0.2886	−0.2877	−0.286	−0.2842	−0.2821	−0.2791
	−0.2925	−0.2926	−0.2924	−0.2919	−0.291	−0.2901	−0.2886	−0.2869	−0.2848	−0.2819
	−0.3021	−0.3021	−0.3021	−0.302	−0.3016	−0.3006	−0.2995	−0.2979	−0.2958	−0.293
	−0.3009	−0.3005	−0.3003	−0.3005	−0.3006	−0.2996	−0.2988	−0.2974	−0.2955	−0.2929

Figure I.2: F2A: e=2.5c & d=1c

	b/c									
a/c	−0.2973	−0.2956	−0.2937	−0.2914	−0.2887	−0.2868	−0.2839	−0.2812	−0.2786	−0.2749
	−0.2977	−0.2959	−0.2939	−0.2914	−0.2886	−0.2865	−0.2836	−0.2808	−0.278	−0.2742
	−0.299	−0.2971	−0.295	−0.2924	−0.2895	−0.2874	−0.2843	−0.2815	−0.2786	−0.2747
	−0.2961	−0.2942	−0.2921	−0.2895	−0.2865	−0.2844	−0.2813	−0.2783	−0.2754	−0.2714
	−0.2963	−0.2946	−0.2927	−0.2902	−0.2873	−0.2852	−0.282	−0.2791	−0.2762	−0.272
	−0.2971	−0.2958	−0.2941	−0.2918	−0.2891	−0.2871	−0.2839	−0.281	−0.278	−0.2738
	−0.2984	−0.2977	−0.2965	−0.2947	−0.2923	−0.2903	−0.2873	−0.2844	−0.2814	−0.2772
	−0.2984	−0.2983	−0.2977	−0.2964	−0.2946	−0.2926	−0.2899	−0.287	−0.284	−0.2798
	−0.3065	−0.3067	−0.3066	−0.306	−0.3049	−0.303	−0.3006	−0.2978	−0.2949	−0.2908
	−0.3037	−0.3035	−0.3035	−0.3036	−0.3033	−0.3015	−0.2998	−0.2971	−0.2942	−0.2905

Figure I.2: F2A: e=2.5c & d=1.5c

	b/c									
a/c	−0.3029	−0.3007	−0.298	−0.2948	−0.2913	−0.2885	−0.2849	−0.2816	−0.2783	−0.2741
	−0.3037	−0.3013	−0.2984	−0.2949	−0.2913	−0.2884	−0.2846	−0.2811	−0.2778	−0.2734
	−0.3052	−0.3027	−0.2997	−0.2961	−0.2923	−0.2893	−0.2854	−0.2818	−0.2784	−0.2739
	−0.3025	−0.3	−0.297	−0.2933	−0.2894	−0.2864	−0.2824	−0.2787	−0.2752	−0.2706
	−0.3027	−0.3004	−0.2976	−0.294	−0.2902	−0.2872	−0.2832	−0.2794	−0.2759	−0.2712
	−0.3034	−0.3016	−0.2991	−0.2958	−0.2921	−0.2891	−0.2851	−0.2813	−0.2777	−0.2729
	−0.3043	−0.3033	−0.3014	−0.2986	−0.2953	−0.2924	−0.2885	−0.2847	−0.2811	−0.2762
	−0.3037	−0.3034	−0.3023	−0.3003	−0.2975	−0.2947	−0.2911	−0.2873	−0.2836	−0.2788
	−0.3109	−0.3112	−0.3108	−0.3097	−0.3078	−0.3051	−0.3018	−0.2981	−0.2944	−0.2897
	−0.3068	−0.3069	−0.307	−0.3069	−0.306	−0.3035	−0.3009	−0.2974	−0.2937	−0.2892

Figure I.2: F2A: e=2.5c & d=2c

	b/c									
a/c	−0.3073	−0.3047	−0.3015	−0.2976	−0.2934	−0.29	−0.2858	−0.282	−0.2783	−0.2737
	−0.3083	−0.3055	−0.3021	−0.2979	−0.2935	−0.2899	−0.2856	−0.2816	−0.2777	−0.2731
	−0.31	−0.3071	−0.3035	−0.2992	−0.2946	−0.2909	−0.2864	−0.2823	−0.2784	−0.2735
	−0.3074	−0.3045	−0.3009	−0.2965	−0.2918	−0.288	−0.2834	−0.2792	−0.2751	−0.2702
	−0.3077	−0.3051	−0.3017	−0.2973	−0.2926	−0.2889	−0.2842	−0.2799	−0.2759	−0.2708
	−0.3084	−0.3063	−0.3032	−0.2992	−0.2946	−0.2909	−0.2862	−0.2818	−0.2777	−0.2725
	−0.3092	−0.3079	−0.3055	−0.302	−0.2979	−0.2942	−0.2897	−0.2852	−0.2811	−0.2758
	−0.3083	−0.3079	−0.3064	−0.3038	−0.3002	−0.2966	−0.2923	−0.2878	−0.2836	−0.2783
	−0.3149	−0.3152	−0.3147	−0.3132	−0.3105	−0.3071	−0.3031	−0.2987	−0.2944	−0.2891
	−0.31	−0.3103	−0.3104	−0.3101	−0.3087	−0.3055	−0.3022	−0.298	−0.2936	−0.2886

Figure I.2: F2A: e=2.5c & d=2.5c

	b/c									
a/c	−0.3108	−0.308	−0.3044	−0.3	−0.2953	−0.2914	−0.2867	−0.2824	−0.2784	−0.2736
	−0.3119	−0.3089	−0.3051	−0.3004	−0.2954	−0.2914	−0.2865	−0.282	−0.2779	−0.2729
	−0.3138	−0.3107	−0.3067	−0.3018	−0.2966	−0.2924	−0.2873	−0.2828	−0.2785	−0.2734
	−0.3113	−0.3082	−0.3042	−0.2992	−0.2939	−0.2896	−0.2844	−0.2797	−0.2753	−0.27
	−0.3117	−0.3088	−0.305	−0.3001	−0.2948	−0.2905	−0.2852	−0.2804	−0.276	−0.2706
	−0.3124	−0.3101	−0.3067	−0.3021	−0.2969	−0.2926	−0.2873	−0.2824	−0.2779	−0.2723
	−0.3132	−0.3117	−0.309	−0.3051	−0.3003	−0.296	−0.2908	−0.2858	−0.2812	−0.2756
	−0.3121	−0.3116	−0.3099	−0.3069	−0.3027	−0.2985	−0.2935	−0.2885	−0.2838	−0.2781
	−0.3185	−0.3188	−0.3182	−0.3163	−0.3131	−0.309	−0.3044	−0.2994	−0.2946	−0.2889
	−0.3131	−0.3135	−0.3136	−0.3132	−0.3113	−0.3076	−0.3035	−0.2987	−0.2939	−0.2884

Figure I.2: F2A: e=2.5c & d=3c

	b/c									
a/c	−0.3135	−0.3106	−0.3067	−0.302	−0.2969	−0.2926	−0.2876	−0.2829	−0.2786	−0.2735
	−0.3148	−0.3117	−0.3076	−0.3026	−0.2972	−0.2927	−0.2874	−0.2826	−0.2781	−0.2729
	−0.3169	−0.3135	−0.3093	−0.304	−0.2984	−0.2938	−0.2883	−0.2833	−0.2787	−0.2733
	−0.3145	−0.3112	−0.3069	−0.3015	−0.2958	−0.291	−0.2854	−0.2802	−0.2755	−0.27
	−0.3149	−0.3119	−0.3078	−0.3026	−0.2968	−0.292	−0.2863	−0.2811	−0.2762	−0.2706
	−0.3157	−0.3132	−0.3095	−0.3046	−0.299	−0.2942	−0.2884	−0.2831	−0.2781	−0.2723
	−0.3164	−0.3148	−0.312	−0.3077	−0.3025	−0.2977	−0.292	−0.2866	−0.2816	−0.2756
	−0.3153	−0.3148	−0.3129	−0.3096	−0.305	−0.3003	−0.2948	−0.2893	−0.2841	−0.2781
	−0.3215	−0.3219	−0.3212	−0.3191	−0.3155	−0.311	−0.3058	−0.3002	−0.295	−0.289
	−0.3159	−0.3164	−0.3165	−0.3159	−0.3137	−0.3096	−0.305	−0.2997	−0.2944	−0.2885

Figure I.2: F2A: e=2.5c & d=3.5c

	b/c									
a/c	−0.3158	−0.3127	−0.3087	−0.3038	−0.2984	−0.2938	−0.2885	−0.2835	−0.2789	−0.2736
	−0.3172	−0.3139	−0.3096	−0.3044	−0.2987	−0.2939	−0.2883	−0.2832	−0.2784	−0.2729
	−0.3193	−0.3159	−0.3114	−0.3059	−0.3	−0.2951	−0.2892	−0.284	−0.279	−0.2734
	−0.317	−0.3136	−0.3091	−0.3035	−0.2974	−0.2924	−0.2864	−0.2809	−0.2759	−0.2701
	−0.3175	−0.3144	−0.3101	−0.3046	−0.2986	−0.2934	−0.2873	−0.2818	−0.2766	−0.2707
	−0.3184	−0.3158	−0.3119	−0.3067	−0.3008	−0.2957	−0.2895	−0.2838	−0.2786	−0.2724
	−0.3191	−0.3175	−0.3144	−0.3099	−0.3044	−0.2993	−0.2932	−0.2874	−0.282	−0.2758
	−0.318	−0.3174	−0.3154	−0.3119	−0.3071	−0.302	−0.296	−0.2901	−0.2847	−0.2783
	−0.3241	−0.3245	−0.3237	−0.3215	−0.3176	−0.3127	−0.3071	−0.3012	−0.2956	−0.2892
	−0.3183	−0.3188	−0.319	−0.3183	−0.3159	−0.3115	−0.3065	−0.3007	−0.295	−0.2887

Figure I.2: F2A: e=2.5c & d=4c

	b/c									
a/c	−0.3176	−0.3145	−0.3104	−0.3053	−0.2997	−0.2949	−0.2893	−0.2841	−0.2793	−0.2738
	−0.3191	−0.3157	−0.3114	−0.3059	−0.3001	−0.295	−0.2892	−0.2838	−0.2788	−0.2731
	−0.3213	−0.3178	−0.3132	−0.3075	−0.3014	−0.2962	−0.2902	−0.2846	−0.2795	−0.2736
	−0.3191	−0.3156	−0.311	−0.3052	−0.2989	−0.2936	−0.2873	−0.2816	−0.2763	−0.2703
	−0.3197	−0.3164	−0.312	−0.3063	−0.3001	−0.2947	−0.2883	−0.2825	−0.2771	−0.2709
	−0.3206	−0.3179	−0.3139	−0.3086	−0.3024	−0.297	−0.2906	−0.2846	−0.2791	−0.2727
	−0.3213	−0.3196	−0.3165	−0.3118	−0.3061	−0.3007	−0.2943	−0.2882	−0.2826	−0.2761
	−0.3202	−0.3196	−0.3176	−0.3139	−0.3088	−0.3035	−0.2973	−0.2911	−0.2853	−0.2786
	−0.3263	−0.3267	−0.3259	−0.3235	−0.3195	−0.3144	−0.3085	−0.3022	−0.2963	−0.2896
	−0.3204	−0.321	−0.3212	−0.3204	−0.3179	−0.3132	−0.308	−0.3018	−0.2958	−0.2891

Figure I.2: F2A: e=3c & d=0.5c

	b/c									
a/c	-0.2977	-0.2971	-0.2965	-0.2956	-0.2944	-0.2937	-0.2924	-0.2911	-0.2895	-0.2872
	-0.2982	-0.2976	-0.2969	-0.2959	-0.2947	-0.294	-0.2926	-0.2912	-0.2896	-0.2873
	-0.2996	-0.2989	-0.2982	-0.2972	-0.2959	-0.2952	-0.2937	-0.2923	-0.2906	-0.2882
	-0.2965	-0.2959	-0.2952	-0.2941	-0.2871	-0.2921	-0.2906	-0.2891	-0.2874	-0.285
	-0.2967	-0.2961	-0.2954	-0.2944	-0.2931	-0.2923	-0.2908	-0.2894	-0.2876	-0.2852
	-0.2973	-0.2968	-0.2962	-0.2952	-0.294	-0.2932	-0.2918	-0.2903	-0.2885	-0.2861
	-0.2985	-0.2981	-0.2976	-0.2968	-0.2957	-0.2949	-0.2935	-0.2921	-0.2904	-0.2879
	-0.2983	-0.2981	-0.2978	-0.2972	-0.2962	-0.2955	-0.2943	-0.2929	-0.2912	-0.2888
	-0.3065	-0.3065	-0.3063	-0.306	-0.3053	-0.3047	-0.3036	-0.3023	-0.3006	-0.2983
	-0.304	-0.304	-0.304	-0.3039	-0.3036	-0.303	-0.3021	-0.301	-0.2994	-0.2972

Figure I.2: F2A: e=3c & d=1c

	b/c									
a/c	-0.3033	-0.3021	-0.3008	-0.299	-0.2971	-0.2955	-0.2933	-0.2911	-0.2889	-0.2859
	-0.3041	-0.3029	-0.3014	-0.2996	-0.2975	-0.2959	-0.2936	-0.2913	-0.289	-0.2859
	-0.3057	-0.3044	-0.3029	-0.301	-0.2988	-0.2971	-0.2947	-0.2924	-0.2901	-0.2868
	-0.3029	-0.3015	-0.3	-0.298	-0.2958	-0.2941	-0.2916	-0.2892	-0.2868	-0.2835
	-0.303	-0.3017	-0.3002	-0.2983	-0.296	-0.2944	-0.2919	-0.2895	-0.287	-0.2836
	-0.3035	-0.3023	-0.301	-0.2991	-0.2969	-0.2953	-0.2928	-0.2904	-0.2879	-0.2845
	-0.3042	-0.3033	-0.3022	-0.3005	-0.2985	-0.2969	-0.2945	-0.2921	-0.2897	-0.2862
	-0.3035	-0.3029	-0.302	-0.3007	-0.2989	-0.2974	-0.2951	-0.2928	-0.2904	-0.287
	-0.3108	-0.3106	-0.3101	-0.3091	-0.3078	-0.3064	-0.3043	-0.3021	-0.2997	-0.2963
	-0.3071	-0.3072	-0.307	-0.3066	-0.3057	-0.3044	-0.3027	-0.3006	-0.2983	-0.2952

Figure I.2: F2A: e=3c & d=1.5c

	b/c									
a/c	-0.3077	-0.3061	-0.3041	-0.3017	-0.2991	-0.2969	-0.2941	-0.2913	-0.2886	-0.2851
	-0.3087	-0.307	-0.305	-0.3024	-0.2996	-0.2973	-0.2944	-0.2915	-0.2887	-0.2851
	-0.3105	-0.3088	-0.3066	-0.3039	-0.301	-0.2986	-0.2956	-0.2926	-0.2897	-0.286
	-0.3078	-0.306	-0.3038	-0.301	-0.298	-0.2956	-0.2925	-0.2894	-0.2865	-0.2827
	-0.308	-0.3063	-0.3041	-0.3013	-0.2983	-0.2959	-0.2927	-0.2897	-0.2867	-0.2828
	-0.3085	-0.3069	-0.3048	-0.3022	-0.2992	-0.2969	-0.2936	-0.2906	-0.2876	-0.2836
	-0.309	-0.3078	-0.306	-0.3036	-0.3008	-0.2985	-0.2954	-0.2923	-0.2893	-0.2853
	-0.3079	-0.3071	-0.3057	-0.3037	-0.3012	-0.299	-0.296	-0.2929	-0.29	-0.286
	-0.3148	-0.3144	-0.3135	-0.312	-0.3099	-0.3079	-0.3051	-0.3022	-0.2992	-0.2953
	-0.3103	-0.3104	-0.31	-0.3092	-0.3077	-0.3058	-0.3034	-0.3006	-0.2978	-0.2939

Figure I.2: F2A: e=3c & d=2c

	b/c									
a/c	-0.3111	-0.3093	-0.3069	-0.304	-0.3008	-0.2981	-0.2948	-0.2916	-0.2885	-0.2847
	-0.3124	-0.3104	-0.3079	-0.3048	-0.3014	-0.2986	-0.2951	-0.2918	-0.2886	-0.2847
	-0.3143	-0.3123	-0.3096	-0.3064	-0.3028	-0.2999	-0.2963	-0.2929	-0.2897	-0.2856
	-0.3117	-0.3096	-0.3069	-0.3036	-0.2999	-0.297	-0.2933	-0.2898	-0.2864	-0.2823
	-0.312	-0.31	-0.3073	-0.3039	-0.3003	-0.2973	-0.2935	-0.29	-0.2866	-0.2824
	-0.3125	-0.3106	-0.3081	-0.3049	-0.3012	-0.2982	-0.2945	-0.2909	-0.2875	-0.2831
	-0.313	-0.3114	-0.3092	-0.3062	-0.3028	-0.2999	-0.2962	-0.2926	-0.2892	-0.2848
	-0.3117	-0.3107	-0.3089	-0.3063	-0.3032	-0.3004	-0.2968	-0.2933	-0.2899	-0.2855
	-0.3182	-0.3178	-0.3166	-0.3146	-0.312	-0.3093	-0.306	-0.3025	-0.2991	-0.2948
	-0.3134	-0.3134	-0.3129	-0.3117	-0.3097	-0.3073	-0.3043	-0.301	-0.2976	-0.2934

Figure I.2: F2A: e=3c & d=2.5c

	b/c									
a/c	-0.3139	-0.3119	-0.3092	-0.3059	-0.3023	-0.2992	-0.2955	-0.2919	-0.2886	-0.2845
	-0.3153	-0.3131	-0.3103	-0.3068	-0.303	-0.2997	-0.2958	-0.2922	-0.2887	-0.2845
	-0.3173	-0.3151	-0.3122	-0.3085	-0.3045	-0.3011	-0.2971	-0.2933	-0.2897	-0.2855
	-0.3149	-0.3126	-0.3096	-0.3058	-0.3017	-0.2982	-0.2941	-0.2902	-0.2865	-0.2821
	-0.3152	-0.313	-0.31	-0.3062	-0.3021	-0.2986	-0.2944	-0.2904	-0.2867	-0.2822
	-0.3158	-0.3137	-0.3109	-0.3072	-0.3031	-0.2996	-0.2953	-0.2913	-0.2876	-0.283
	-0.3162	-0.3145	-0.312	-0.3086	-0.3047	-0.3013	-0.2971	-0.2931	-0.2893	-0.2846
	-0.3149	-0.3137	-0.3117	-0.3088	-0.3052	-0.3018	-0.2977	-0.2938	-0.29	-0.2853
	-0.3213	-0.3207	-0.3194	-0.317	-0.314	-0.3108	-0.3069	-0.303	-0.2992	-0.2945
	-0.3161	-0.3162	-0.3156	-0.3141	-0.3117	-0.3088	-0.3053	-0.3015	-0.2977	-0.2931

Figure I.2: F2A: e=3c & d=3c

	b/c									
a/c	-0.3161	-0.314	-0.3112	-0.3076	-0.3037	-0.3003	-0.2962	-0.2924	-0.2887	-0.2845
	-0.3176	-0.3153	-0.3124	-0.3086	-0.3044	-0.3009	-0.2966	-0.2926	-0.2888	-0.2845
	-0.3198	-0.3174	-0.3143	-0.3103	-0.306	-0.3023	-0.2979	-0.2938	-0.2899	-0.2854
	-0.3174	-0.315	-0.3118	-0.3077	-0.3033	-0.2994	-0.2949	-0.2907	-0.2867	-0.282
	-0.3178	-0.3154	-0.3123	-0.3082	-0.3037	-0.2998	-0.2952	-0.2909	-0.2869	-0.2821
	-0.3184	-0.3162	-0.3132	-0.3092	-0.3048	-0.3009	-0.2962	-0.2919	-0.2878	-0.2829
	-0.3189	-0.3171	-0.3144	-0.3107	-0.3065	-0.3027	-0.298	-0.2936	-0.2895	-0.2846
	-0.3175	-0.3163	-0.3141	-0.3109	-0.307	-0.3033	-0.2987	-0.2944	-0.2902	-0.2852
	-0.3238	-0.3232	-0.3218	-0.3192	-0.3158	-0.3123	-0.308	-0.3036	-0.2995	-0.2945
	-0.3185	-0.3186	-0.3179	-0.3162	-0.3136	-0.3103	-0.3064	-0.3021	-0.298	-0.2931

Figure I.2: F2A: e=3c & d=3.5c

	b/c									
a/c	-0.318	-0.3158	-0.3128	-0.3091	-0.305	-0.3013	-0.297	-0.2929	-0.289	-0.2845
	-0.3195	-0.3172	-0.3141	-0.3101	-0.3058	-0.3019	-0.2974	-0.2931	-0.2891	-0.2845
	-0.3218	-0.3193	-0.3161	-0.3119	-0.3074	-0.3034	-0.2987	-0.2943	-0.2902	-0.2855
	-0.3195	-0.317	-0.3136	-0.3094	-0.3047	-0.3006	-0.2957	-0.2912	-0.287	-0.2821
	-0.32	-0.3175	-0.3142	-0.3099	-0.3052	-0.301	-0.2961	-0.2915	-0.2872	-0.2822
	-0.3206	-0.3183	-0.3152	-0.311	-0.3063	-0.3021	-0.2972	-0.2925	-0.2881	-0.283
	-0.3211	-0.3192	-0.3164	-0.3125	-0.308	-0.3039	-0.299	-0.2943	-0.2899	-0.2847
	-0.3197	-0.3184	-0.3161	-0.3127	-0.3086	-0.3046	-0.2998	-0.295	-0.2906	-0.2853
	-0.326	-0.3254	-0.3238	-0.3211	-0.3175	-0.3137	-0.3091	-0.3044	-0.2999	-0.2946
	-0.3206	-0.3207	-0.3199	-0.3181	-0.3153	-0.3118	-0.3075	-0.3029	-0.2985	-0.2932

Figure I.2: F2A: e=3c & d=4c

	b/c									
a/c	-0.3195	-0.3173	-0.3142	-0.3104	-0.3061	-0.3022	-0.2977	-0.2934	-0.2893	-0.2847
	-0.3212	-0.3187	-0.3155	-0.3114	-0.3069	-0.3029	-0.2982	-0.2937	-0.2895	-0.2847
	-0.3235	-0.3209	-0.3176	-0.3133	-0.3086	-0.3044	-0.2995	-0.2949	-0.2906	-0.2857
	-0.3212	-0.3187	-0.3152	-0.3108	-0.3059	-0.3016	-0.2966	-0.2918	-0.2874	-0.2823
	-0.3217	-0.3192	-0.3158	-0.3114	-0.3064	-0.3021	-0.297	-0.2921	-0.2876	-0.2824
	-0.3225	-0.3201	-0.3168	-0.3125	-0.3076	-0.3033	-0.2981	-0.2932	-0.2885	-0.2832
	-0.323	-0.321	-0.3181	-0.3141	-0.3094	-0.3051	-0.2999	-0.295	-0.2903	-0.2849
	-0.3216	-0.3202	-0.3179	-0.3144	-0.31	-0.3058	-0.3008	-0.2958	-0.2911	-0.2856
	-0.3279	-0.3272	-0.3256	-0.3227	-0.3189	-0.315	-0.3101	-0.3052	-0.3005	-0.2949
	-0.3225	-0.3225	-0.3217	-0.3198	-0.3168	-0.3131	-0.3086	-0.3038	-0.2991	-0.2936

Figure I.2: F2A: e=3.5c & d=0.5c

	b/c									
	−0.3036	−0.3032	−0.3027	−0.302	−0.3011	−0.3005	−0.2995	−0.2984	−0.2971	−0.2953
	−0.3045	−0.304	−0.3035	−0.3028	−0.3019	−0.3013	−0.3002	−0.2991	−0.2977	−0.2958
	−0.3061	−0.3057	−0.3051	−0.3044	−0.3034	−0.3028	−0.3016	−0.3005	−0.2991	−0.2971
	−0.3032	−0.3028	−0.3022	−0.3014	−0.3004	−0.2998	−0.2986	−0.2975	−0.296	−0.294
a/c	−0.3034	−0.3029	−0.3024	−0.3016	−0.3006	−0.3	−0.2988	−0.2976	−0.2961	−0.2941
	−0.3038	−0.3034	−0.3029	−0.3021	−0.3011	−0.3005	−0.2993	−0.2981	−0.2966	−0.2945
	−0.3044	−0.3041	−0.3036	−0.3029	−0.302	−0.3014	−0.3002	−0.2991	−0.2976	−0.2955
	−0.3035	−0.3032	−0.3029	−0.3023	−0.3014	−0.3009	−0.2998	−0.2986	−0.2972	−0.2951
	−0.3108	−0.3106	−0.3104	−0.3099	−0.3092	−0.3087	−0.3077	−0.3066	−0.3052	−0.3032
	−0.3071	−0.307	−0.3069	−0.3066	−0.3061	−0.3056	−0.3047	−0.3038	−0.3024	−0.3005

Figure I.2: F2A: e=3.5c & d=1c

	b/c									
	−0.3079	−0.307	−0.306	−0.3047	−0.3032	−0.3019	−0.3001	−0.2984	−0.2965	−0.294
	−0.309	−0.3081	−0.307	−0.3056	−0.304	−0.3027	−0.3009	−0.299	−0.2971	−0.2945
	−0.3109	−0.3099	−0.3088	−0.3073	−0.3056	−0.3043	−0.3024	−0.3005	−0.2985	−0.2958
	−0.3081	−0.3071	−0.306	−0.3045	−0.3027	−0.3014	−0.2994	−0.2974	−0.2954	−0.2926
a/c	−0.3083	−0.3073	−0.3062	−0.3046	−0.3029	−0.3015	−0.2995	−0.2975	−0.2955	−0.2926
	−0.3087	−0.3078	−0.3066	−0.3051	−0.3034	−0.302	−0.3	−0.298	−0.296	−0.2931
	−0.3092	−0.3083	−0.3073	−0.3059	−0.3042	−0.3029	−0.3009	−0.2989	−0.2969	−0.294
	−0.3079	−0.3072	−0.3063	−0.3051	−0.3035	−0.3023	−0.3004	−0.2984	−0.2964	−0.2935
	−0.3147	−0.3142	−0.3135	−0.3125	−0.3112	−0.31	−0.3082	−0.3063	−0.3044	−0.3015
	−0.3102	−0.31	−0.3096	−0.3088	−0.3078	−0.3067	−0.3051	−0.3034	−0.3015	−0.2987

Figure I.2: F2A: e=3.5c & d=1.5c

	b/c									
	−0.3113	−0.3101	−0.3087	−0.3068	−0.3047	−0.303	−0.3007	−0.2984	−0.2962	−0.2933
	−0.3126	−0.3114	−0.3098	−0.3078	−0.3057	−0.3038	−0.3014	−0.2991	−0.2968	−0.2937
	−0.3146	−0.3133	−0.3117	−0.3096	−0.3074	−0.3055	−0.303	−0.3006	−0.2982	−0.2951
	−0.312	−0.3107	−0.309	−0.3068	−0.3045	−0.3026	−0.3	−0.2975	−0.2951	−0.2918
a/c	−0.3123	−0.3109	−0.3092	−0.3071	−0.3047	−0.3028	−0.3001	−0.2976	−0.2951	−0.2918
	−0.3127	−0.3114	−0.3097	−0.3076	−0.3052	−0.3033	−0.3007	−0.2981	−0.2956	−0.2923
	−0.3131	−0.3119	−0.3104	−0.3083	−0.306	−0.3041	−0.3015	−0.299	−0.2965	−0.2931
	−0.3116	−0.3107	−0.3093	−0.3075	−0.3053	−0.3035	−0.301	−0.2985	−0.296	−0.2926
	−0.3181	−0.3174	−0.3164	−0.3148	−0.3129	−0.3112	−0.3088	−0.3063	−0.3039	−0.3006
	−0.3132	−0.3129	−0.3121	−0.3109	−0.3094	−0.3078	−0.3056	−0.3033	−0.3009	−0.2977

Figure I.2: F2A: e=3.5c & d=2c

	b/c									
	−0.3141	−0.3127	−0.3109	−0.3086	−0.3061	−0.3039	−0.3013	−0.2986	−0.2961	−0.2929
	−0.3155	−0.3141	−0.3121	−0.3097	−0.3071	−0.3048	−0.302	−0.2993	−0.2966	−0.2934
	−0.3177	−0.3161	−0.3141	−0.3116	−0.3089	−0.3065	−0.3036	−0.3008	−0.2981	−0.2947
	−0.3151	−0.3136	−0.3115	−0.3089	−0.306	−0.3036	−0.3006	−0.2978	−0.2949	−0.2914
a/c	−0.3155	−0.3139	−0.3118	−0.3092	−0.3063	−0.3038	−0.3008	−0.2979	−0.295	−0.2914
	−0.316	−0.3144	−0.3124	−0.3098	−0.3069	−0.3044	−0.3013	−0.2984	−0.2955	−0.2918
	−0.3163	−0.3149	−0.313	−0.3105	−0.3077	−0.3053	−0.3022	−0.2992	−0.2963	−0.2927
	−0.3148	−0.3136	−0.3119	−0.3096	−0.307	−0.3046	−0.3016	−0.2987	−0.2958	−0.2921
	−0.3211	−0.3202	−0.3189	−0.3169	−0.3145	−0.3123	−0.3094	−0.3065	−0.3037	−0.3001
	−0.3159	−0.3155	−0.3145	−0.313	−0.3109	−0.3089	−0.3063	−0.3035	−0.3007	−0.2971

Figure I.2: F2A: e=3.5c & d=2.5c

	b/c									
	−0.3163	−0.3148	−0.3128	−0.3102	−0.3074	−0.3049	−0.3018	−0.2989	−0.2961	−0.2927
	−0.3178	−0.3163	−0.3141	−0.3114	−0.3084	−0.3058	−0.3026	−0.2996	−0.2967	−0.2932
	−0.3201	−0.3184	−0.3162	−0.3134	−0.3102	−0.3075	−0.3042	−0.3011	−0.2981	−0.2945
	−0.3177	−0.316	−0.3137	−0.3107	−0.3075	−0.3047	−0.3013	−0.2981	−0.295	−0.2912
a/c	−0.3181	−0.3163	−0.314	−0.3111	−0.3078	−0.3049	−0.3014	−0.2982	−0.295	−0.2912
	−0.3186	−0.3169	−0.3146	−0.3117	−0.3084	−0.3055	−0.302	−0.2987	−0.2955	−0.2916
	−0.3189	−0.3174	−0.3153	−0.3124	−0.3092	−0.3064	−0.3029	−0.2996	−0.2964	−0.2925
	−0.3174	−0.3161	−0.3142	−0.3116	−0.3085	−0.3058	−0.3023	−0.299	−0.2958	−0.2919
	−0.3236	−0.3227	−0.3211	−0.3188	−0.316	−0.3134	−0.3101	−0.3069	−0.3037	−0.3005
	−0.3183	−0.3178	−0.3167	−0.3149	−0.3125	−0.3101	−0.307	−0.3039	−0.3008	−0.2969

Figure I.2: F2A: e=3.5c & d=3c

	b/c									
	−0.3181	−0.3166	−0.3144	−0.3117	−0.3086	−0.3058	−0.3024	−0.2993	−0.2962	−0.2926
	−0.3198	−0.3181	−0.3158	−0.3129	−0.3096	−0.3067	−0.3033	−0.3	−0.2968	−0.2931
	−0.3221	−0.3203	−0.318	−0.3149	−0.3115	−0.3085	−0.3049	−0.3015	−0.2982	−0.2944
	−0.3198	−0.3179	−0.3155	−0.3123	−0.3088	−0.3057	−0.302	−0.2985	−0.2951	−0.2912
a/c	−0.3202	−0.3184	−0.3159	−0.3127	−0.3091	−0.306	−0.3022	−0.2986	−0.2952	−0.2912
	−0.3208	−0.319	−0.3166	−0.3135	−0.3098	−0.3066	−0.3028	−0.2991	−0.2956	−0.2915
	−0.3212	−0.3195	−0.3172	−0.3142	−0.3106	−0.3075	−0.3037	−0.3	−0.2965	−0.2924
	−0.3196	−0.3182	−0.3162	−0.3133	−0.31	−0.3069	−0.3031	−0.2995	−0.296	−0.2918
	−0.3258	−0.3248	−0.3231	−0.3206	−0.3175	−0.3146	−0.311	−0.3074	−0.3039	−0.2997
	−0.3204	−0.3198	−0.3186	−0.3166	−0.314	−0.3113	−0.3078	−0.3044	−0.301	−0.2968

Figure I.2: F2A: e=3.5c & d=3.5c

	b/c									
	−0.3197	−0.318	−0.3158	−0.3129	−0.3096	−0.3066	−0.3031	−0.2997	−0.2964	−0.2926
	−0.3214	−0.3196	−0.3173	−0.3142	−0.3108	−0.3076	−0.3039	−0.3004	−0.297	−0.2931
	−0.3238	−0.322	−0.3195	−0.3163	−0.3127	−0.3094	−0.3056	−0.302	−0.2985	−0.2945
	−0.3215	−0.3196	−0.317	−0.3137	−0.31	−0.3067	−0.3027	−0.2989	−0.2954	−0.2912
a/c	−0.322	−0.3201	−0.3175	−0.3141	−0.3103	−0.307	−0.3029	−0.2991	−0.2954	−0.2912
	−0.3226	−0.3208	−0.3182	−0.3148	−0.311	−0.3076	−0.3035	−0.2996	−0.2959	−0.2916
	−0.323	−0.3213	−0.3189	−0.3157	−0.3119	−0.3086	−0.3045	−0.3006	−0.2968	−0.2925
	−0.3215	−0.32	−0.3179	−0.3149	−0.3113	−0.308	−0.304	−0.3001	−0.2963	−0.2919
	−0.3276	−0.3266	−0.3248	−0.3222	−0.3189	−0.3157	−0.3118	−0.308	−0.3043	−0.2998
	−0.3222	−0.3216	−0.3203	−0.3182	−0.3154	−0.3124	−0.3087	−0.305	−0.3013	−0.2969

Figure I.2: F2A: e=3.5c & d=4c

	b/c									
	−0.321	−0.3193	−0.317	−0.314	−0.3106	−0.3074	−0.3037	−0.3002	−0.2967	−0.2928
	−0.3227	−0.3209	−0.3185	−0.3153	−0.3117	−0.3085	−0.3046	−0.3009	−0.2973	−0.2933
	−0.3252	−0.3233	−0.3207	−0.3174	−0.3137	−0.3103	−0.3063	−0.3025	−0.2988	−0.2946
	−0.323	−0.321	−0.3183	−0.3149	−0.311	−0.3076	−0.3034	−0.2995	−0.2957	−0.2914
a/c	−0.3235	−0.3215	−0.3188	−0.3154	−0.3114	−0.3079	−0.3037	−0.2996	−0.2958	−0.2914
	−0.3242	−0.3223	−0.3196	−0.3161	−0.3122	−0.3086	−0.3043	−0.3002	−0.2963	−0.2918
	−0.3246	−0.3228	−0.3203	−0.317	−0.3131	−0.3096	−0.3053	−0.3012	−0.2972	−0.2927
	−0.323	−0.3216	−0.3193	−0.3162	−0.3125	−0.309	−0.3048	−0.3007	−0.2967	−0.2921
	−0.3292	−0.3281	−0.3263	−0.3235	−0.3201	−0.3168	−0.3127	−0.3086	−0.3047	−0.3
	−0.3237	−0.3231	−0.3218	−0.3196	−0.3166	−0.3135	−0.3096	−0.3057	−0.3018	−0.2971

Figure I.2: F2A: e=4c & d=0.5c

	b/c									
	−0.308	−0.3077	−0.3074	−0.3068	−0.3062	−0.3057	−0.3048	−0.304	−0.3029	−0.3013
	−0.3092	−0.3089	−0.3085	−0.3079	−0.3072	−0.3067	−0.3059	−0.305	−0.3039	−0.3022
	−0.3112	−0.3108	−0.3104	−0.3098	−0.3091	−0.3086	−0.3077	−0.3067	−0.3056	−0.3038
	−0.3084	−0.308	−0.3076	−0.307	−0.3062	−0.3057	−0.3048	−0.3038	−0.3026	−0.3009
a/c	−0.3086	−0.3082	−0.3078	−0.3072	−0.3064	−0.3059	−0.3049	−0.3039	−0.3027	−0.301
	−0.309	−0.3086	−0.3082	−0.3076	−0.3068	−0.3063	−0.3053	−0.3043	−0.3031	−0.3013
	−0.3094	−0.3091	−0.3087	−0.3081	−0.3073	−0.3068	−0.3058	−0.3049	−0.3036	−0.3019
	−0.308	−0.3078	−0.3074	−0.3069	−0.3061	−0.3057	−0.3047	−0.3038	−0.3026	−0.3008
	−0.3148	−0.3146	−0.3143	−0.3138	−0.3132	−0.3127	−0.3118	−0.3109	−0.3097	−0.308
	−0.3102	−0.3101	−0.3099	−0.3095	−0.3089	−0.3085	−0.3077	−0.3069	−0.3057	−0.3041

Figure I.2: F2A: e=4c & d=1c

	b/c									
	−0.3114	−0.3108	−0.31	−0.309	−0.3078	−0.3067	−0.3053	−0.3038	−0.3023	−0.3002
	−0.3128	−0.3121	−0.3113	−0.3102	−0.3089	−0.3079	−0.3063	−0.3048	−0.3032	−0.301
	−0.3149	−0.3142	−0.3133	−0.3121	−0.3108	−0.3097	−0.3082	−0.3066	−0.305	−0.3027
	−0.3122	−0.3115	−0.3106	−0.3094	−0.308	−0.3069	−0.3053	−0.3037	−0.302	−0.2996
a/c	−0.3125	−0.3117	−0.3108	−0.3096	−0.3082	−0.3071	−0.3054	−0.3038	−0.3021	−0.2997
	−0.3129	−0.3122	−0.3113	−0.31	−0.3086	−0.3075	−0.3058	−0.3042	−0.3024	−0.3
	−0.3133	−0.3125	−0.3117	−0.3105	−0.3091	−0.308	−0.3064	−0.3047	−0.303	−0.3005
	−0.3117	−0.3111	−0.3103	−0.3092	−0.3079	−0.3068	−0.3052	−0.3035	−0.3018	−0.2993
	−0.3182	−0.3176	−0.3169	−0.316	−0.3148	−0.3138	−0.3122	−0.3106	−0.3089	−0.3065
	−0.3131	−0.3128	−0.3122	−0.3114	−0.3104	−0.3095	−0.308	−0.3065	−0.3049	−0.3025

Figure I.2: F2A: e=4c & d=1.5c

	b/c									
	−0.3142	−0.3133	−0.3121	−0.3107	−0.309	−0.3076	−0.3057	−0.3038	−0.3019	−0.2995
	−0.3157	−0.3147	−0.3135	−0.312	−0.3102	−0.3087	−0.3068	−0.3048	−0.3029	−0.3003
	−0.3179	−0.3169	−0.3156	−0.314	−0.3122	−0.3107	−0.3086	−0.3066	−0.3046	−0.302
	−0.3154	−0.3143	−0.313	−0.3113	−0.3094	−0.3079	−0.3058	−0.3037	−0.3016	−0.2989
a/c	−0.3157	−0.3146	−0.3133	−0.3116	−0.3097	−0.3081	−0.3059	−0.3038	−0.3017	−0.2989
	−0.3161	−0.3151	−0.3138	−0.312	−0.3101	−0.3085	−0.3063	−0.3042	−0.3021	−0.2992
	−0.3164	−0.3154	−0.3142	−0.3125	−0.3106	−0.309	−0.3068	−0.3047	−0.3026	−0.2997
	−0.3148	−0.3139	−0.3127	−0.3111	−0.3093	−0.3078	−0.3056	−0.3035	−0.3014	−0.2985
	−0.3211	−0.3204	−0.3193	−0.3179	−0.3162	−0.3147	−0.3126	−0.3106	−0.3085	−0.3056
	−0.3158	−0.3153	−0.3144	−0.3132	−0.3117	−0.3103	−0.3084	−0.3064	−0.3044	−0.3016

Figure I.2: F2A: e=4c & d=2c

	b/c									
	−0.3164	−0.3154	−0.314	−0.3122	−0.3101	−0.3084	−0.3061	−0.304	−0.3018	−0.2991
	−0.318	−0.3169	−0.3154	−0.3135	−0.3114	−0.3095	−0.3072	−0.305	−0.3027	−0.2999
	−0.3203	−0.3192	−0.3176	−0.3156	−0.3134	−0.3115	−0.3091	−0.3068	−0.3045	−0.3016
	−0.3179	−0.3167	−0.3151	−0.313	−0.3107	−0.3087	−0.3063	−0.3039	−0.3015	−0.2985
a/c	−0.3183	−0.317	−0.3154	−0.3133	−0.3109	−0.3089	−0.3064	−0.304	−0.3015	−0.2985
	−0.3188	−0.3176	−0.3159	−0.3138	−0.3114	−0.3094	−0.3068	−0.3044	−0.3019	−0.2988
	−0.3191	−0.3179	−0.3163	−0.3143	−0.3119	−0.3099	−0.3073	−0.3048	−0.3024	−0.2993
	−0.3174	−0.3164	−0.3149	−0.3129	−0.3106	−0.3087	−0.3061	−0.3036	−0.3012	−0.298
	−0.3236	−0.3227	−0.3214	−0.3196	−0.3175	−0.3156	−0.3131	−0.3107	−0.3083	−0.3051
	−0.3182	−0.3175	−0.3164	−0.3149	−0.3129	−0.3112	−0.3089	−0.3065	−0.3041	−0.301

Figure I.2: F2A: e=4c & d=2.5c

	b/c									
	−0.3182	−0.3171	−0.3155	−0.3135	−0.3112	−0.3091	−0.3066	−0.3042	−0.3018	−0.2989
	−0.3199	−0.3187	−0.3171	−0.3149	−0.3125	−0.3103	−0.3077	−0.3052	−0.3027	−0.2997
	−0.3223	−0.321	−0.3193	−0.3171	−0.3146	−0.3123	−0.3096	−0.307	−0.3045	−0.3014
	−0.32	−0.3186	−0.3168	−0.3145	−0.3119	−0.3096	−0.3068	−0.3041	−0.3015	−0.2983
a/c	−0.3204	−0.319	−0.3172	−0.3148	−0.3122	−0.3098	−0.307	−0.3042	−0.3015	−0.2983
	−0.321	−0.3196	−0.3179	−0.3154	−0.3127	−0.3103	−0.3074	−0.3046	−0.3019	−0.2986
	−0.3213	−0.32	−0.3182	−0.3159	−0.3132	−0.3108	−0.3079	−0.3051	−0.3024	−0.299
	−0.3196	−0.3185	−0.3168	−0.3145	−0.3119	−0.3096	−0.3067	−0.3039	−0.3012	−0.2978
	−0.3258	−0.3248	−0.3233	−0.3212	−0.3187	−0.3165	−0.3137	−0.3109	−0.3082	−0.3049
	−0.3203	−0.3195	−0.3183	−0.3164	−0.3142	−0.3121	−0.3094	−0.3068	−0.3041	−0.3008

Figure I.2: F2A: e=4c & d=3c

	b/c									
	−0.3198	−0.3186	−0.3169	−0.3147	−0.3122	−0.3099	−0.3071	−0.3045	−0.3018	−0.2988
	−0.3215	−0.3202	−0.3185	−0.3162	−0.3135	−0.3111	−0.3083	−0.3055	−0.3028	−0.2996
	−0.324	−0.3226	−0.3208	−0.3184	−0.3156	−0.3131	−0.3102	−0.3073	−0.3045	−0.3013
	−0.3217	−0.3203	−0.3183	−0.3158	−0.313	−0.3104	−0.3074	−0.3044	−0.3016	−0.2982
a/c	−0.3222	−0.3207	−0.3188	−0.3162	−0.3133	−0.3107	−0.3076	−0.3045	−0.3016	−0.2982
	−0.3228	−0.3214	−0.3194	−0.3168	−0.3139	−0.3112	−0.308	−0.305	−0.302	−0.2985
	−0.3231	−0.3218	−0.3198	−0.3173	−0.3144	−0.3117	−0.3085	−0.3055	−0.3025	−0.2989
	−0.3215	−0.3202	−0.3184	−0.316	−0.3131	−0.3105	−0.3074	−0.3043	−0.3013	−0.2977
	−0.3276	−0.3265	−0.3249	−0.3227	−0.32	−0.3175	−0.3144	−0.3113	−0.3084	−0.3048
	−0.322	−0.3212	−0.3199	−0.3179	−0.3154	−0.3131	−0.3101	−0.3071	−0.3042	−0.3007

Figure I.2: F2A: e=4c & d=3.5c

	b/c									
	−0.3211	−0.3198	−0.318	−0.3157	−0.3131	−0.3106	−0.3077	−0.3048	−0.302	−0.2988
	−0.3229	−0.3215	−0.3197	−0.3172	−0.3145	−0.3119	−0.3088	−0.3059	−0.303	−0.2997
	−0.3254	−0.324	−0.322	−0.3195	−0.3166	−0.3139	−0.3108	−0.3077	−0.3048	−0.3013
	−0.3231	−0.3217	−0.3196	−0.317	−0.314	−0.3113	−0.308	−0.3048	−0.3018	−0.2982
a/c	−0.3237	−0.3222	−0.3201	−0.3174	−0.3143	−0.3115	−0.3082	−0.305	−0.3019	−0.2982
	−0.3243	−0.3228	−0.3208	−0.318	−0.3149	−0.3121	−0.3087	−0.3054	−0.3022	−0.2985
	−0.3247	−0.3233	−0.3212	−0.3186	−0.3155	−0.3126	−0.3092	−0.3059	−0.3027	−0.299
	−0.3231	−0.3217	−0.3199	−0.3173	−0.3143	−0.3115	−0.3081	−0.3047	−0.3015	−0.2978
	−0.3292	−0.3281	−0.3264	−0.324	−0.3211	−0.3184	−0.3151	−0.3118	−0.3086	−0.3048
	−0.3236	−0.3227	−0.3213	−0.3192	−0.3166	−0.314	−0.3108	−0.3076	−0.3045	−0.3007

Figure I.2: F2A: e=4c & d=4c

	b/c									
	−0.3222	−0.3209	−0.319	−0.3166	−0.3139	−0.3113	−0.3082	−0.3052	−0.3023	−0.2989
	−0.324	−0.3226	−0.3207	−0.3182	−0.3153	−0.3126	−0.3094	−0.3063	−0.3033	−0.2998
	−0.3266	−0.3251	−0.3231	−0.3205	−0.3175	−0.3147	−0.3114	−0.3082	−0.305	−0.3015
	−0.3244	−0.3229	−0.3208	−0.318	−0.3149	−0.312	−0.3086	−0.3053	−0.3021	−0.2984
a/c	−0.3249	−0.3234	−0.3213	−0.3185	−0.3153	−0.3123	−0.3088	−0.3054	−0.3022	−0.2984
	−0.3256	−0.3241	−0.322	−0.3191	−0.3159	−0.3129	−0.3093	−0.3059	−0.3025	−0.2987
	−0.326	−0.3245	−0.3225	−0.3197	−0.3165	−0.3135	−0.3099	−0.3064	−0.3031	−0.2991
	−0.3244	−0.3231	−0.3211	−0.3184	−0.3153	−0.3123	−0.3088	−0.3053	−0.3019	−0.2979
	−0.3305	−0.3294	−0.3276	−0.3251	−0.3221	−0.3193	−0.3158	−0.3123	−0.309	−0.305
	−0.3249	−0.324	−0.3226	−0.3204	−0.3176	−0.3149	−0.3116	−0.3082	−0.3049	−0.3009

Figure I.3: F1A: e=0.5b & d=0.5b

	c/b									
a/b	0.1746	0.1746	0.1746	0.1746	0.1746	0.1746	0.1745	0.1745	0.1739	0.1715
	0.1288	0.1288	0.1288	0.1288	0.1288	0.1288	0.1288	0.1288	0.1283	0.1262
	0.1037	0.1037	0.1037	0.1037	0.1038	0.1037	0.1037	0.1037	0.1031	0.1011
	0.1147	0.1147	0.1146	0.1147	0.1147	0.1146	0.1146	0.1146	0.1140	0.1118
	0.1326	0.1326	0.1325	0.1325	0.1326	0.1325	0.1325	0.1325	0.1317	0.1293
	0.1067	0.1067	0.1057	0.1067	0.1068	0.1067	0.1067	0.1066	0.1135	0.0991
	0.1271	0.1271	0.1271	0.1271	0.1272	0.1271	0.1271	0.1270	0.1250	0.1224
	0.1449	0.1449	0.1448	0.1448	0.1449	0.1448	0.1447	0.1447	0.1431	0.1382
	0.1633	0.1633	0.1648	0.1641	0.1633	0.1644	0.1645	0.1644	0.1615	0.1521
	0.2372	0.2372	0.2370	0.2371	0.2373	0.2369	0.2369	0.2366	0.2307	0.2166

Figure I.3: F1A: e=0.5b & d=1b

	c/b									
a/b	0.1746	0.1746	0.1746	0.1746	0.1746	0.1746	0.1745	0.1740	0.1726	0.1706
	0.1288	0.1288	0.1288	0.1288	0.1288	0.1288	0.1287	0.1283	0.1271	0.1254
	0.1037	0.1037	0.1037	0.1037	0.1037	0.1037	0.1036	0.1031	0.1019	0.1004
	0.1147	0.1147	0.1147	0.1147	0.1147	0.1146	0.1145	0.1140	0.1127	0.1111
	0.1326	0.1326	0.1325	0.1325	0.1326	0.1325	0.1323	0.1317	0.1302	0.1286
	0.1067	0.1067	0.1067	0.1067	0.1067	0.1066	0.1055	0.1057	0.1042	0.0983
	0.1271	0.1271	0.1271	0.1271	0.1271	0.1270	0.1268	0.1258	0.1238	0.1214
	0.1449	0.1449	0.1448	0.1448	0.1449	0.1447	0.1444	0.1430	0.1401	0.1368
	0.1640	0.1633	0.1639	0.1633	0.1633	0.1644	0.1632	0.1582	0.1572	0.1523
	0.2372	0.2372	0.2371	0.2371	0.2372	0.2367	0.2351	0.2305	0.2221	0.2134

Figure I.3: F1A: e=0.5b & d=1.5b

	c/b									
a/b	0.1746	0.1745	0.1745	0.1745	0.1745	0.1744	0.1742	0.1733	0.1719	0.1703
	0.1288	0.1288	0.1287	0.1287	0.1287	0.1287	0.1284	0.1277	0.1265	0.1251
	0.1037	0.1037	0.1036	0.1036	0.1036	0.1036	0.1034	0.1027	0.1015	0.1002
	0.1147	0.1146	0.1146	0.1145	0.1146	0.1145	0.1143	0.1136	0.1123	0.1109
	0.1326	0.1325	0.1324	0.1323	0.1324	0.1323	0.1321	0.1313	0.1298	0.1283
	0.1067	0.1067	0.1066	0.1065	0.1066	0.1055	0.1052	0.1052	0.0997	0.0981
	0.1271	0.1271	0.1269	0.1269	0.1269	0.1268	0.1264	0.1251	0.1232	0.1212
	0.1449	0.1448	0.1446	0.1445	0.1446	0.1443	0.1437	0.1419	0.1393	0.1365
	0.1633	0.1632	0.1646	0.1636	0.1607	0.1601	0.1589	0.1563	0.1553	0.1521
	0.2371	0.2370	0.2366	0.2363	0.2363	0.2349	0.2321	0.2271	0.2205	0.2131

Figure I.3: F1A: e=0.5b & d=2b

	c/b									
a/b	0.1745	0.1745	0.1745	0.1746	0.1747	0.1744	0.1738	0.1729	0.1717	0.1702
	0.1288	0.1287	0.1287	0.1288	0.1289	0.1286	0.1281	0.1274	0.1263	0.1251
	0.1037	0.1036	0.1037	0.1038	0.1038	0.1036	0.1031	0.1023	0.1013	0.1001
	0.1147	0.1146	0.1146	0.1147	0.1148	0.1146	0.1141	0.1132	0.1121	0.1109
	0.1325	0.1325	0.1325	0.1326	0.1327	0.1324	0.1319	0.1310	0.1297	0.1284
	0.1067	0.1066	0.1057	0.1058	0.1059	0.1055	0.1058	0.1048	0.0995	0.0981
	0.1271	0.1270	0.1270	0.1272	0.1272	0.1267	0.1259	0.1246	0.1230	0.1212
	0.1448	0.1447	0.1447	0.1449	0.1449	0.1442	0.1430	0.1413	0.1391	0.1367
	0.1632	0.1639	0.1638	0.1639	0.1636	0.1595	0.1578	0.1553	0.1525	0.1504
	0.2370	0.2368	0.2368	0.2369	0.2361	0.2337	0.2303	0.2258	0.2206	0.2147

Figure I.3: F1A: e=0.5b & d=2.5b

	c/b									
a/b	0.1746	0.1746	0.1747	0.1747	0.1745	0.1741	0.1735	0.1726	0.1715	0.1703
	0.1288	0.1288	0.1289	0.1289	0.1288	0.1284	0.1278	0.1271	0.1262	0.1251
	0.1037	0.1038	0.1038	0.1039	0.1037	0.1034	0.1028	0.1021	0.1012	0.1001
	0.1147	0.1148	0.1148	0.1149	0.1147	0.1143	0.1138	0.1130	0.1120	0.1109
	0.1326	0.1326	0.1327	0.1328	0.1326	0.1322	0.1315	0.1307	0.1296	0.1284
	0.1058	0.1058	0.1059	0.1059	0.1057	0.1052	0.1054	0.1045	0.0994	0.0981
	0.1271	0.1272	0.1273	0.1273	0.1270	0.1264	0.1255	0.1243	0.1229	0.1214
	0.1449	0.1450	0.1450	0.1450	0.1445	0.1436	0.1424	0.1408	0.1390	0.1370
	0.1611	0.1640	0.1640	0.1637	0.1629	0.1588	0.1570	0.1549	0.1527	0.1516
	0.2372	0.2373	0.2372	0.2365	0.2349	0.2324	0.2292	0.2255	0.2214	0.2166

Figure I.3: F1A: e=0.5b & d=3b

	c/b									
a/b	0.1746	0.1746	0.1746	0.1745	0.1742	0.1738	0.1731	0.1723	0.1714	0.1703
	0.1288	0.1288	0.1288	0.1287	0.1285	0.1281	0.1275	0.1269	0.1261	0.1251
	0.1037	0.1038	0.1038	0.1037	0.1034	0.1030	0.1025	0.1018	0.1010	0.1001
	0.1147	0.1148	0.1148	0.1147	0.1144	0.1140	0.1134	0.1127	0.1118	0.1108
	0.1326	0.1327	0.1327	0.1325	0.1323	0.1318	0.1311	0.1303	0.1294	0.1284
	0.1058	0.1058	0.1058	0.1056	0.1053	0.1058	0.1050	0.1042	0.0992	0.0981
	0.1272	0.1272	0.1272	0.1269	0.1265	0.1259	0.1250	0.1239	0.1228	0.1214
	0.1449	0.1449	0.1448	0.1445	0.1439	0.1430	0.1418	0.1404	0.1389	0.1372
	0.1611	0.1639	0.1637	0.1631	0.1593	0.1580	0.1565	0.1547	0.1528	0.1516
	0.2372	0.2371	0.2365	0.2353	0.2335	0.2312	0.2284	0.2253	0.2220	0.2183

Figure I.3: F1A: e=0.5b & d=3.5b

	c/b									
a/b	0.1746	0.1746	0.1745	0.1743	0.1739	0.1735	0.1729	0.1721	0.1713	0.1703
	0.1288	0.1288	0.1287	0.1285	0.1282	0.1278	0.1273	0.1267	0.1260	0.1251
	0.1037	0.1037	0.1036	0.1035	0.1032	0.1028	0.1023	0.1016	0.1009	0.1001
	0.1147	0.1147	0.1146	0.1144	0.1141	0.1137	0.1131	0.1125	0.1117	0.1108
	0.1326	0.1326	0.1325	0.1323	0.1319	0.1315	0.1308	0.1301	0.1293	0.1284
	0.1058	0.1057	0.1056	0.1054	0.1060	0.1054	0.1048	0.1040	0.0991	0.0982
	0.1271	0.1271	0.1269	0.1266	0.1261	0.1255	0.1247	0.1237	0.1227	0.1215
	0.1449	0.1448	0.1445	0.1441	0.1434	0.1426	0.1415	0.1403	0.1390	0.1374
	0.1610	0.1608	0.1604	0.1598	0.1588	0.1577	0.1562	0.1547	0.1541	0.1522
	0.2371	0.2367	0.2359	0.2346	0.2327	0.2307	0.2282	0.2256	0.2228	0.2196

Figure I.3: F1A: e=0.5b & d=4b

	c/b									
a/b	0.1745	0.1745	0.1744	0.1741	0.1737	0.1733	0.1727	0.1720	0.1713	0.1704
	0.1288	0.1287	0.1286	0.1284	0.1281	0.1277	0.1272	0.1266	0.1260	0.1252
	0.1037	0.1037	0.1035	0.1033	0.1030	0.1026	0.1021	0.1015	0.1009	0.1002
	0.1147	0.1146	0.1145	0.1143	0.1139	0.1135	0.1130	0.1124	0.1117	0.1109
	0.1326	0.1325	0.1324	0.1321	0.1317	0.1313	0.1307	0.1300	0.1293	0.1285
	0.1057	0.1057	0.1055	0.1062	0.1057	0.1053	0.1046	0.1039	0.0992	0.0983
	0.1271	0.1270	0.1268	0.1264	0.1259	0.1253	0.1246	0.1237	0.1228	0.1218
	0.1448	0.1447	0.1444	0.1439	0.1432	0.1424	0.1414	0.1403	0.1392	0.1378
	0.1610	0.1607	0.1603	0.1595	0.1586	0.1576	0.1563	0.1550	0.1545	0.1529
	0.2370	0.2365	0.2356	0.2343	0.2326	0.2308	0.2286	0.2263	0.2239	0.2211

Figure I.3: F1A: e=1b & d=0.5b

	c/b									
a/b	0.2778	0.2778	0.2778	0.2778	0.2778	0.2778	0.2778	0.2777	0.2767	0.2732
	0.2406	0.2406	0.2406	0.2406	0.2406	0.2406	0.2406	0.2405	0.2396	0.2363
	0.2012	0.2012	0.2012	0.2012	0.2012	0.2012	0.2011	0.2011	0.2002	0.1971
	0.1939	0.1939	0.1939	0.1939	0.1939	0.1939	0.1939	0.1939	0.193	0.1898
	0.1978	0.1978	0.1978	0.1978	0.1978	0.1978	0.1977	0.1977	0.1967	0.1933
	0.1854	0.1854	0.1853	0.1854	0.1854	0.1853	0.1853	0.1852	0.1841	0.1801
	0.1978	0.1978	0.1978	0.1978	0.1979	0.1978	0.1977	0.1977	0.1963	0.1916
	0.212	0.212	0.212	0.212	0.212	0.2119	0.2119	0.2118	0.21	0.2043
	0.2116	0.2116	0.2116	0.2116	0.2117	0.2116	0.2115	0.2114	0.209	0.2018
	0.2638	0.2638	0.2637	0.2638	0.2638	0.2637	0.2636	0.2635	0.2597	0.2498

Figure I.3: F1A: e=1b & d=1b

	c/b									
a/b	0.2778	0.2778	0.2778	0.2778	0.2778	0.2778	0.2776	0.2766	0.2746	0.2717
	0.2406	0.2406	0.2406	0.2406	0.2406	0.2406	0.2404	0.2396	0.2376	0.2349
	0.2012	0.2012	0.2012	0.2012	0.2012	0.2012	0.201	0.2002	0.1984	0.1959
	0.1939	0.1939	0.1939	0.1939	0.1939	0.1939	0.1937	0.1929	0.191	0.1885
	0.1978	0.1978	0.1978	0.1978	0.1978	0.1978	0.1976	0.1967	0.1946	0.1919
	0.1854	0.1853	0.1853	0.1853	0.1854	0.1853	0.1851	0.184	0.1816	0.1786
	0.1978	0.1978	0.1978	0.1978	0.1978	0.1978	0.1975	0.1962	0.1934	0.1898
	0.212	0.212	0.212	0.212	0.212	0.2119	0.2115	0.2098	0.2064	0.2022
	0.2116	0.2116	0.2116	0.2116	0.2116	0.2115	0.2109	0.2088	0.2044	0.1991
	0.2638	0.2638	0.2637	0.2638	0.2638	0.2636	0.2626	0.2595	0.2533	0.2462

Figure I.3: F1A: e=1b & d=1.5b

	c/b									
a/b	0.2778	0.2778	0.2777	0.2777	0.2777	0.2775	0.2769	0.2756	0.2735	0.271
	0.2406	0.2406	0.2405	0.2405	0.2405	0.2404	0.2398	0.2386	0.2366	0.2343
	0.2012	0.2012	0.2011	0.2011	0.2011	0.201	0.2005	0.1993	0.1975	0.1954
	0.1939	0.1939	0.1938	0.1938	0.1938	0.1937	0.1932	0.192	0.1901	0.188
	0.1978	0.1977	0.1977	0.1976	0.1976	0.1975	0.1969	0.1957	0.1936	0.1913
	0.1853	0.1853	0.1852	0.1852	0.1852	0.185	0.1843	0.1828	0.1806	0.178
	0.1978	0.1978	0.1977	0.1976	0.1976	0.1973	0.1966	0.1948	0.1921	0.1892
	0.212	0.2119	0.2118	0.2117	0.2117	0.2113	0.2103	0.2082	0.205	0.2015
	0.2116	0.2116	0.2114	0.2113	0.2113	0.2107	0.2093	0.2065	0.2027	0.1984
	0.2638	0.2637	0.2635	0.2633	0.2633	0.2624	0.2602	0.2563	0.251	0.2453

Figure I.3: F1A: e=1b & d=2b

	c/b									
a/b	0.2778	0.2777	0.2777	0.2778	0.2778	0.2772	0.2763	0.2748	0.273	0.2708
	0.2406	0.2405	0.2405	0.2406	0.2406	0.2401	0.2393	0.2379	0.2362	0.2342
	0.2012	0.2011	0.2011	0.2012	0.2012	0.2007	0.1999	0.1987	0.1971	0.1952
	0.1939	0.1938	0.1938	0.194	0.1939	0.1935	0.1926	0.1914	0.1897	0.1879
	0.1977	0.1977	0.1977	0.1978	0.1978	0.1972	0.1964	0.195	0.1932	0.1912
	0.1853	0.1852	0.1852	0.1854	0.1853	0.1847	0.1837	0.1821	0.1801	0.1779
	0.1978	0.1977	0.1977	0.1978	0.1977	0.197	0.1958	0.1939	0.1917	0.1891
	0.2119	0.2118	0.2118	0.212	0.2118	0.2108	0.2093	0.2071	0.2045	0.2015
	0.2116	0.2115	0.2115	0.2116	0.2112	0.21	0.208	0.2053	0.2021	0.1985
	0.2637	0.2636	0.2636	0.2636	0.263	0.2611	0.2584	0.2547	0.2504	0.2457

Figure I.3: F1A: e=1b & d=2.5b

	c/b									
a/b	0.2778	0.2779	0.2779	0.2778	0.2775	0.2768	0.2757	0.2744	0.2727	0.2708
	0.2406	0.2407	0.2407	0.2407	0.2404	0.2397	0.2388	0.2375	0.236	0.2342
	0.2012	0.2013	0.2013	0.2013	0.201	0.2003	0.1994	0.1983	0.1969	0.1952
	0.1939	0.194	0.194	0.194	0.1937	0.1931	0.1922	0.191	0.1895	0.1879
	0.1978	0.1978	0.1979	0.1978	0.1975	0.1968	0.1958	0.1946	0.193	0.1913
	0.1854	0.1854	0.1855	0.1854	0.185	0.1842	0.1831	0.1816	0.1799	0.1779
	0.1978	0.1979	0.1979	0.1978	0.1973	0.1964	0.1951	0.1934	0.1915	0.1892
	0.212	0.2121	0.2121	0.2119	0.2113	0.2101	0.2085	0.2065	0.2043	0.2017
	0.2116	0.2117	0.2117	0.2114	0.2105	0.209	0.2071	0.2047	0.202	0.1989
	0.2638	0.2639	0.2637	0.2632	0.2619	0.2599	0.2572	0.2539	0.2504	0.2464

Figure I.3: F1A: e=1b & d=3b

	c/b									
a/b	0.2778	0.2779	0.2778	0.2775	0.277	0.2763	0.2752	0.274	0.2725	0.2708
	0.2406	0.2407	0.2406	0.2404	0.2399	0.2392	0.2383	0.2371	0.2358	0.2342
	0.2012	0.2013	0.2012	0.201	0.2005	0.1999	0.199	0.1979	0.1967	0.1952
	0.194	0.194	0.1939	0.1937	0.1933	0.1926	0.1917	0.1906	0.1894	0.1879
	0.1978	0.1978	0.1978	0.1975	0.197	0.1963	0.1954	0.1942	0.1929	0.1913
	0.1854	0.1854	0.1853	0.185	0.1844	0.1836	0.1825	0.1812	0.1797	0.178
	0.1979	0.1979	0.1977	0.1974	0.1967	0.1958	0.1945	0.193	0.1913	0.1893
	0.212	0.212	0.2118	0.2114	0.2105	0.2094	0.2079	0.2061	0.2042	0.2019
	0.2117	0.2116	0.2113	0.2107	0.2096	0.2082	0.2063	0.2042	0.2019	0.1993
	0.2638	0.2637	0.2632	0.2623	0.2607	0.2588	0.2563	0.2535	0.2506	0.2471

Figure I.3: F1A: e=1b & d=3.5b

	c/b									
a/b	0.2778	0.2778	0.2776	0.2772	0.2766	0.2759	0.2749	0.2737	0.2725	0.2709
	0.2406	0.2406	0.2404	0.2401	0.2395	0.2389	0.238	0.2369	0.2357	0.2343
	0.2012	0.2012	0.201	0.2007	0.2002	0.1995	0.1987	0.1977	0.1966	0.1953
	0.1939	0.1939	0.1937	0.1934	0.1929	0.1923	0.1914	0.1904	0.1893	0.188
	0.1978	0.1977	0.1976	0.1972	0.1967	0.196	0.195	0.194	0.1928	0.1914
	0.1853	0.1853	0.1851	0.1846	0.184	0.1832	0.1822	0.181	0.1797	0.1781
	0.1978	0.1977	0.1975	0.197	0.1962	0.1953	0.1941	0.1928	0.1913	0.1896
	0.212	0.2118	0.2115	0.2109	0.21	0.2089	0.2075	0.2059	0.2042	0.2023
	0.2116	0.2114	0.2109	0.2102	0.209	0.2077	0.206	0.2041	0.2021	0.1998
	0.2637	0.2634	0.2627	0.2616	0.2601	0.2583	0.256	0.2536	0.251	0.2481

Figure I.3: F1A: e=1b & d=4b

	c/b									
a/b	0.2778	0.2777	0.2774	0.2770	0.2764	0.2757	0.2747	0.2737	0.2725	0.2711
	0.2406	0.2405	0.2403	0.2399	0.2393	0.2387	0.2378	0.2368	0.2357	0.2345
	0.2012	0.2011	0.2009	0.2005	0.2000	0.1993	0.1985	0.1976	0.1967	0.1955
	0.1939	0.1938	0.1936	0.1932	0.1927	0.1921	0.1913	0.1904	0.1894	0.1882
	0.1978	0.1976	0.1974	0.1970	0.1964	0.1958	0.1949	0.1939	0.1929	0.1917
	0.1853	0.1852	0.1849	0.1844	0.1838	0.1830	0.1821	0.1810	0.1798	0.1784
	0.1978	0.1976	0.1973	0.1967	0.1960	0.1951	0.1940	0.1928	0.1915	0.1899
	0.2119	0.2117	0.2113	0.2106	0.2097	0.2087	0.2074	0.2060	0.2045	0.2028
	0.2116	0.2113	0.2107	0.2099	0.2088	0.2076	0.2060	0.2044	0.2026	0.2005
	0.2636	0.2632	0.2625	0.2613	0.2598	0.2582	0.2562	0.2541	0.2518	0.2492

Figure I.3: F1A: e=1.5b & d=0.5b

	c/b									
a/b	0.3338	0.3338	0.3338	0.3338	0.3338	0.3338	0.3337	0.3337	0.3325	0.3288
	0.3088	0.3088	0.3088	0.3088	0.3088	0.3088	0.3088	0.3087	0.3075	0.3038
	0.2772	0.2772	0.2772	0.2772	0.2772	0.2772	0.2771	0.2771	0.2759	0.2721
	0.2644	0.2644	0.2644	0.2644	0.2644	0.2644	0.2643	0.2643	0.2631	0.2593
	0.2542	0.2542	0.2542	0.2542	0.2542	0.2542	0.2542	0.2541	0.2529	0.249
	0.2384	0.2384	0.2384	0.2384	0.2384	0.2384	0.2383	0.2383	0.237	0.2328
	0.2439	0.2439	0.2439	0.2439	0.2439	0.2439	0.2438	0.2438	0.2423	0.2376
	0.2528	0.2527	0.2527	0.2527	0.2528	0.2527	0.2527	0.2526	0.2508	0.2454
	0.2505	0.2505	0.2505	0.2505	0.2505	0.2505	0.2504	0.2503	0.2481	0.2417
	0.2849	0.2849	0.2849	0.2849	0.2849	0.2849	0.2848	0.2847	0.282	0.2741

Figure I.3: F1A: e=1.5b & d=1b

	c/b									
a/b	0.3338	0.3338	0.3338	0.3338	0.3338	0.3338	0.3335	0.3324	0.3301	0.3269
	0.3088	0.3088	0.3088	0.3088	0.3088	0.3088	0.3085	0.3074	0.3051	0.3019
	0.2772	0.2772	0.2772	0.2772	0.2772	0.2772	0.2769	0.2758	0.2735	0.2703
	0.2644	0.2644	0.2644	0.2644	0.2644	0.2644	0.2641	0.263	0.2607	0.2576
	0.2542	0.2542	0.2542	0.2542	0.2542	0.2542	0.2539	0.2528	0.2505	0.2473
	0.2384	0.2384	0.2384	0.2384	0.2384	0.2384	0.2381	0.2369	0.2343	0.2309
	0.2439	0.2439	0.2439	0.2439	0.2439	0.2439	0.2435	0.2421	0.2393	0.2355
	0.2527	0.2527	0.2527	0.2527	0.2527	0.2527	0.2523	0.2506	0.2473	0.243
	0.2505	0.2505	0.2505	0.2505	0.2505	0.2504	0.2498	0.2479	0.2439	0.2388
	0.2849	0.2849	0.2849	0.2849	0.2849	0.2848	0.2841	0.2816	0.2767	0.2707

Figure I.3: F1A: e=1.5b & d=1.5b

	c/b									
a/b	0.3338	0.3338	0.3337	0.3337	0.3336	0.3334	0.3326	0.3311	0.3288	0.326
	0.3088	0.3088	0.3087	0.3087	0.3087	0.3084	0.3077	0.3061	0.3039	0.3011
	0.2772	0.2772	0.2771	0.277	0.277	0.2768	0.2761	0.2746	0.2723	0.2696
	0.2644	0.2643	0.2643	0.2642	0.2642	0.264	0.2633	0.2618	0.2595	0.2569
	0.2542	0.2542	0.2541	0.2541	0.2541	0.2538	0.2531	0.2516	0.2493	0.2466
	0.2384	0.2384	0.2383	0.2382	0.2382	0.2379	0.2372	0.2355	0.233	0.2301
	0.2439	0.2439	0.2438	0.2437	0.2437	0.2434	0.2425	0.2406	0.2378	0.2346
	0.2527	0.2527	0.2526	0.2525	0.2525	0.2521	0.251	0.2488	0.2457	0.2421
	0.2505	0.2504	0.2503	0.2502	0.2502	0.2496	0.2483	0.2457	0.242	0.2377
	0.2849	0.2849	0.2847	0.2846	0.2846	0.2838	0.2821	0.2789	0.2745	0.2695

Figure I.3: F1A: e=1.5b & d=2b

	c/b									
a/b	0.3338	0.3337	0.3337	0.3338	0.3336	0.3329	0.3318	0.3302	0.3281	0.3257
	0.3088	0.3087	0.3087	0.3088	0.3086	0.308	0.3069	0.3053	0.3033	0.3008
	0.2772	0.2771	0.2771	0.2772	0.277	0.2764	0.2753	0.2737	0.2717	0.2693
	0.2643	0.2643	0.2643	0.2644	0.2642	0.2636	0.2625	0.261	0.259	0.2566
	0.2542	0.2541	0.2541	0.2542	0.2541	0.2534	0.2524	0.2507	0.2487	0.2463
	0.2383	0.2383	0.2383	0.2384	0.2382	0.2375	0.2363	0.2346	0.2324	0.2299
	0.2439	0.2438	0.2438	0.2439	0.2437	0.2429	0.2415	0.2396	0.2372	0.2344
	0.2527	0.2526	0.2526	0.2527	0.2524	0.2515	0.2499	0.2477	0.245	0.2419
	0.2504	0.2503	0.2503	0.2504	0.25	0.2488	0.247	0.2443	0.2412	0.2376
	0.2849	0.2848	0.2848	0.2848	0.2843	0.2828	0.2804	0.2773	0.2736	0.2693

Figure I.3: F1A: e=1.5b & d=2.5b

	c/b									
a/b	0.3338	0.3338	0.3338	0.3337	0.3332	0.3324	0.3312	0.3296	0.3278	0.3256
	0.3088	0.3089	0.3089	0.3087	0.3083	0.3075	0.3063	0.3047	0.3029	0.3008
	0.2772	0.2772	0.2773	0.2771	0.2767	0.2759	0.2747	0.2732	0.2714	0.2692
	0.2644	0.2644	0.2644	0.2643	0.2639	0.2631	0.2619	0.2604	0.2587	0.2566
	0.2542	0.2543	0.2543	0.2542	0.2537	0.2529	0.2517	0.2502	0.2484	0.2464
	0.2384	0.2384	0.2385	0.2383	0.2378	0.2369	0.2357	0.234	0.2321	0.2299
	0.2439	0.244	0.244	0.2438	0.2432	0.2422	0.2408	0.239	0.2369	0.2345
	0.2527	0.2528	0.2528	0.2525	0.2519	0.2507	0.2491	0.2471	0.2447	0.242
	0.2505	0.2505	0.2505	0.2502	0.2493	0.2479	0.246	0.2436	0.2409	0.2378
	0.2849	0.285	0.2849	0.2844	0.2833	0.2816	0.2793	0.2765	0.2733	0.2697

Figure I.3: F1A: e=1.5b & d=3b

	c/b									
a/b	0.3338	0.3338	0.3337	0.3333	0.3327	0.3318	0.3306	0.3292	0.3276	0.3257
	0.3088	0.3088	0.3087	0.3084	0.3078	0.3069	0.3057	0.3043	0.3027	0.3008
	0.2772	0.2772	0.2771	0.2768	0.2762	0.2753	0.2742	0.2727	0.2712	0.2693
	0.2644	0.2644	0.2643	0.264	0.2634	0.2625	0.2614	0.26	0.2585	0.2567
	0.2542	0.2543	0.2541	0.2538	0.2532	0.2524	0.2512	0.2498	0.2483	0.2464
	0.2384	0.2384	0.2383	0.2379	0.2372	0.2363	0.2351	0.2336	0.232	0.23
	0.2439	0.2439	0.2437	0.2433	0.2426	0.2415	0.2402	0.2385	0.2367	0.2346
	0.2528	0.2527	0.2525	0.252	0.2512	0.25	0.2484	0.2466	0.2446	0.2422
	0.2505	0.2504	0.2502	0.2495	0.2485	0.2471	0.2452	0.2431	0.2408	0.238
	0.2849	0.2848	0.2845	0.2837	0.2823	0.2807	0.2785	0.276	0.2733	0.2701

Figure I.3: F1A: e=1.5b & d=3.5b

	c/b									
a/b	0.3338	0.3337	0.3334	0.333	0.3323	0.3314	0.3303	0.329	0.3275	0.3258
	0.3088	0.3087	0.3085	0.308	0.3074	0.3065	0.3054	0.3041	0.3027	0.3009
	0.2772	0.2771	0.2769	0.2764	0.2758	0.2749	0.2738	0.2725	0.2711	0.2694
	0.2644	0.2643	0.2641	0.2636	0.263	0.2621	0.2611	0.2598	0.2584	0.2568
	0.2542	0.2541	0.2539	0.2535	0.2528	0.252	0.2509	0.2496	0.2482	0.2466
	0.2384	0.2383	0.238	0.2375	0.2368	0.2359	0.2347	0.2334	0.2319	0.2302
	0.2439	0.2438	0.2435	0.2429	0.2421	0.2411	0.2398	0.2383	0.2367	0.2348
	0.2527	0.2526	0.2522	0.2516	0.2506	0.2495	0.2481	0.2464	0.2446	0.2426
	0.2504	0.2502	0.2498	0.249	0.2479	0.2466	0.2449	0.243	0.2409	0.2385
	0.2849	0.2846	0.2841	0.2831	0.2817	0.2802	0.2781	0.2759	0.2736	0.2708

Figure I.3: F1A: e=1.5b & d=4b

	c/b									
a/b	0.3338	0.3336	0.3333	0.3328	0.3321	0.3312	0.3302	0.329	0.3276	0.3261
	0.3088	0.3086	0.3083	0.3078	0.3071	0.3063	0.3053	0.3041	0.3028	0.3012
	0.2772	0.277	0.2767	0.2762	0.2755	0.2747	0.2737	0.2725	0.2712	0.2697
	0.2643	0.2642	0.2639	0.2634	0.2627	0.2619	0.2609	0.2598	0.2585	0.2571
	0.2542	0.254	0.2537	0.2533	0.2526	0.2518	0.2507	0.2496	0.2483	0.2468
	0.2383	0.2382	0.2379	0.2373	0.2366	0.2357	0.2346	0.2334	0.2321	0.2305
	0.2438	0.2436	0.2433	0.2427	0.2419	0.2409	0.2397	0.2384	0.2369	0.2352
	0.2527	0.2524	0.252	0.2513	0.2504	0.2493	0.248	0.2465	0.2449	0.2431
	0.2504	0.2501	0.2496	0.2488	0.2476	0.2464	0.2448	0.2431	0.2413	0.2392
	0.2848	0.2845	0.2838	0.2828	0.2815	0.28	0.2782	0.2762	0.2741	0.2717

Figure I.3: F1A: e=2b & d=0.5b

	c/b									
a/b	0.3683	0.3684	0.3684	0.3684	0.3684	0.3683	0.3683	0.3682	0.367	0.3635
	0.3506	0.3506	0.3506	0.3507	0.3506	0.3506	0.3506	0.3505	0.3493	0.3456
	0.3261	0.3261	0.3261	0.3261	0.3261	0.3261	0.326	0.326	0.3247	0.3209
	0.318	0.318	0.318	0.318	0.318	0.318	0.3179	0.3179	0.3166	0.3126
	0.3074	0.3074	0.3074	0.3074	0.3074	0.3074	0.3074	0.3073	0.306	0.3019
	0.287	0.287	0.287	0.287	0.287	0.2869	0.2869	0.2868	0.2855	0.2812
	0.2834	0.2834	0.2834	0.2834	0.2834	0.2834	0.2834	0.2833	0.2818	0.2773
	0.2845	0.2845	0.2845	0.2845	0.2845	0.2844	0.2844	0.2843	0.2827	0.2777
	0.2801	0.2801	0.2801	0.2801	0.2801	0.2801	0.28	0.28	0.2781	0.2724
	0.303	0.303	0.303	0.303	0.303	0.3029	0.3029	0.3028	0.3005	0.2941

Figure I.3: F1A: e=2b & d=1b

	c/b									
a/b	0.3683	0.3683	0.3683	0.3683	0.3683	0.3683	0.368	0.3669	0.3646	0.3615
	0.3506	0.3506	0.3506	0.3506	0.3506	0.3506	0.3503	0.3491	0.3468	0.3436
	0.3261	0.3261	0.3261	0.3261	0.3261	0.3261	0.3257	0.3246	0.3221	0.3188
	0.318	0.318	0.318	0.318	0.318	0.318	0.3176	0.3165	0.314	0.3106
	0.3074	0.3074	0.3074	0.3074	0.3074	0.3074	0.3071	0.3058	0.3033	0.2999
	0.287	0.287	0.287	0.287	0.287	0.2869	0.2866	0.2853	0.2827	0.2791
	0.2834	0.2834	0.2834	0.2834	0.2834	0.2834	0.283	0.2817	0.2788	0.275
	0.2845	0.2845	0.2844	0.2844	0.2845	0.2844	0.284	0.2825	0.2794	0.2753
	0.2801	0.2801	0.2801	0.2801	0.2801	0.2801	0.2796	0.2778	0.2743	0.2697
	0.303	0.303	0.3029	0.303	0.303	0.3029	0.3023	0.3002	0.2962	0.2909

Figure I.3: F1A: e=2b & d=1.5b

	c/b									
a/b	0.3683	0.3683	0.3683	0.3682	0.3682	0.3679	0.3671	0.3655	0.3633	0.3605
	0.3506	0.3506	0.3506	0.3505	0.3505	0.3502	0.3494	0.3477	0.3454	0.3426
	0.3261	0.3261	0.326	0.326	0.3259	0.3256	0.3248	0.3231	0.3208	0.3179
	0.318	0.318	0.3179	0.3179	0.3178	0.3175	0.3167	0.315	0.3126	0.3097
	0.3074	0.3074	0.3073	0.3073	0.3073	0.3069	0.3061	0.3044	0.3019	0.299
	0.2869	0.2869	0.2868	0.2868	0.2868	0.2864	0.2856	0.2838	0.2812	0.2781
	0.2834	0.2834	0.2833	0.2833	0.2832	0.2829	0.2819	0.28	0.2773	0.2741
	0.2844	0.2844	0.2843	0.2843	0.2842	0.2838	0.2828	0.2807	0.2777	0.2742
	0.2801	0.2801	0.28	0.2799	0.2799	0.2794	0.2781	0.2758	0.2724	0.2685
	0.3029	0.3029	0.3028	0.3027	0.3027	0.3021	0.3006	0.2978	0.294	0.2896

Figure I.3: F1A: e=2b & d=2b

	c/b									
a/b	0.3683	0.3683	0.3683	0.3683	0.3681	0.3674	0.3662	0.3646	0.3626	0.3601
	0.3506	0.3506	0.3506	0.3506	0.3504	0.3497	0.3485	0.3468	0.3447	0.3422
	0.3261	0.326	0.326	0.326	0.3258	0.3251	0.3239	0.3222	0.3201	0.3175
	0.318	0.3179	0.3179	0.3179	0.3178	0.317	0.3158	0.3141	0.3119	0.3094
	0.3074	0.3073	0.3073	0.3074	0.3072	0.3064	0.3052	0.3034	0.3012	0.2986
	0.2869	0.2869	0.2869	0.2869	0.2867	0.2859	0.2846	0.2828	0.2805	0.2778
	0.2834	0.2833	0.2833	0.2834	0.2831	0.2823	0.2809	0.279	0.2766	0.2737
	0.2844	0.2843	0.2843	0.2844	0.2841	0.2832	0.2817	0.2795	0.2769	0.2739
	0.2801	0.28	0.28	0.28	0.2797	0.2786	0.2769	0.2745	0.2716	0.2682
	0.3029	0.3028	0.3028	0.3028	0.3024	0.3011	0.2991	0.2963	0.2931	0.2893

Figure I.3: F1A: e=2b & d=2.5b

	c/b									
a/b	0.3683	0.3684	0.3683	0.3681	0.3676	0.3668	0.3655	0.364	0.3622	0.36
	0.3506	0.3507	0.3507	0.3505	0.3499	0.3491	0.3478	0.3462	0.3443	0.3421
	0.3261	0.3261	0.3261	0.3259	0.3254	0.3245	0.3232	0.3216	0.3197	0.3174
	0.318	0.318	0.318	0.3178	0.3173	0.3164	0.3151	0.3135	0.3116	0.3093
	0.3074	0.3075	0.3075	0.3073	0.3067	0.3058	0.3045	0.3028	0.3009	0.2986
	0.287	0.287	0.287	0.2868	0.2862	0.2853	0.2839	0.2822	0.2802	0.2778
	0.2834	0.2835	0.2835	0.2832	0.2826	0.2816	0.2802	0.2783	0.2762	0.2737
	0.2845	0.2845	0.2845	0.2842	0.2835	0.2824	0.2808	0.2788	0.2766	0.2739
	0.2801	0.2802	0.2801	0.2798	0.279	0.2777	0.2759	0.2737	0.2712	0.2682
	0.303	0.303	0.3029	0.3025	0.3016	0.3001	0.298	0.2955	0.2927	0.2894

Figure I.3: F1A: e=2b & d=3b

	c/b									
a/b	0.3684	0.3683	0.3682	0.3678	0.3671	0.3662	0.365	0.3636	0.3619	0.36
	0.3507	0.3506	0.3505	0.3501	0.3494	0.3485	0.3473	0.3458	0.3441	0.3421
	0.3261	0.3261	0.3259	0.3255	0.3249	0.3239	0.3227	0.3211	0.3194	0.3174
	0.318	0.318	0.3178	0.3175	0.3168	0.3158	0.3146	0.3131	0.3114	0.3093
	0.3074	0.3074	0.3073	0.3069	0.3062	0.3052	0.3039	0.3024	0.3007	0.2986
	0.287	0.2869	0.2868	0.2864	0.2856	0.2847	0.2833	0.2817	0.2799	0.2778
	0.2834	0.2834	0.2832	0.2828	0.282	0.281	0.2795	0.2779	0.276	0.2738
	0.2845	0.2844	0.2842	0.2837	0.2828	0.2817	0.2802	0.2784	0.2764	0.274
	0.2801	0.2801	0.2798	0.2792	0.2782	0.2769	0.2752	0.2732	0.271	0.2684
	0.303	0.3029	0.3026	0.3019	0.3007	0.2992	0.2973	0.295	0.2925	0.2896

Figure I.3: F1A: e=2b & d=3.5b

	c/b									
a/b	0.3683	0.3682	0.368	0.3675	0.3667	0.3659	0.3647	0.3634	0.3619	0.3601
	0.3506	0.3505	0.3502	0.3498	0.349	0.3481	0.3469	0.3456	0.3441	0.3423
	0.3261	0.326	0.3257	0.3252	0.3245	0.3235	0.3223	0.3209	0.3194	0.3175
	0.318	0.3179	0.3176	0.3171	0.3164	0.3154	0.3142	0.3128	0.3113	0.3095
	0.3074	0.3073	0.307	0.3065	0.3058	0.3048	0.3036	0.3022	0.3006	0.2988
	0.2869	0.2868	0.2865	0.286	0.2852	0.2842	0.283	0.2815	0.2799	0.278
	0.2834	0.2833	0.283	0.2824	0.2815	0.2805	0.2792	0.2777	0.276	0.274
	0.2844	0.2843	0.2839	0.2833	0.2824	0.2813	0.2798	0.2782	0.2764	0.2743
	0.2801	0.2799	0.2795	0.2788	0.2777	0.2765	0.2748	0.273	0.2711	0.2687
	0.3029	0.3027	0.3022	0.3013	0.3001	0.2987	0.2969	0.2949	0.2927	0.2901

Figure I.3: F1A: e=2b & d=4b

	c/b									
a/b	0.3683	0.3681	0.3678	0.3673	0.3665	0.3657	0.3646	0.3633	0.362	0.3604
	0.3506	0.3504	0.3501	0.3496	0.3488	0.3479	0.3468	0.3456	0.3442	0.3425
	0.3261	0.3259	0.3255	0.325	0.3242	0.3233	0.3222	0.3209	0.3195	0.3178
	0.318	0.3178	0.3174	0.3169	0.3161	0.3152	0.3141	0.3128	0.3114	0.3098
	0.3074	0.3072	0.3069	0.3063	0.3055	0.3046	0.3035	0.3022	0.3008	0.2991
	0.2869	0.2867	0.2864	0.2858	0.285	0.284	0.2828	0.2815	0.2801	0.2784
	0.2834	0.2832	0.2828	0.2822	0.2813	0.2803	0.2791	0.2777	0.2762	0.2744
	0.2844	0.2842	0.2837	0.2831	0.2821	0.2811	0.2797	0.2782	0.2766	0.2748
	0.28	0.2798	0.2793	0.2785	0.2775	0.2763	0.2748	0.2731	0.2714	0.2693
	0.3029	0.3025	0.302	0.3011	0.2999	0.2986	0.2969	0.295	0.2931	0.2908

Figure I.3: F1A: e=2.5b & d=0.5b

	c/b									
a/b	0.3912	0.3912	0.3912	0.3912	0.3913	0.3912	0.3913	0.3911	0.39	0.3867
	0.378	0.378	0.378	0.378	0.378	0.3779	0.378	0.3778	0.3766	0.3732
	0.358	0.358	0.358	0.358	0.358	0.358	0.358	0.3579	0.3567	0.353
	0.3543	0.3543	0.3543	0.3543	0.3543	0.3543	0.3543	0.3542	0.3529	0.3491
	0.3469	0.3469	0.3469	0.3469	0.3469	0.3469	0.3468	0.3468	0.3454	0.3415
	0.3276	0.3276	0.3276	0.3276	0.3276	0.3275	0.3275	0.3274	0.326	0.3219
	0.3216	0.3216	0.3216	0.3216	0.3216	0.3216	0.3215	0.3214	0.32	0.3156
	0.317	0.317	0.317	0.317	0.317	0.317	0.317	0.3169	0.3153	0.3107
	0.3073	0.3073	0.3073	0.3073	0.3073	0.3073	0.3072	0.3072	0.3055	0.3004
	0.3209	0.3209	0.3209	0.3209	0.3209	0.3209	0.3209	0.3208	0.3189	0.3134

Figure I.3: F1A: e=2.5b & d=1b

	c/b									
a/b	0.3912	0.3912	0.3912	0.3912	0.3912	0.3912	0.3909	0.3898	0.3877	0.3848
	0.378	0.378	0.3779	0.3779	0.378	0.3779	0.3776	0.3765	0.3742	0.3712
	0.358	0.358	0.358	0.358	0.358	0.358	0.3577	0.3565	0.3542	0.3509
	0.3543	0.3543	0.3543	0.3543	0.3543	0.3543	0.3539	0.3527	0.3503	0.347
	0.3469	0.3469	0.3469	0.3469	0.3469	0.3468	0.3465	0.3452	0.3427	0.3393
	0.3276	0.3276	0.3276	0.3276	0.3276	0.3275	0.3271	0.3258	0.3232	0.3197
	0.3216	0.3216	0.3216	0.3216	0.3216	0.3215	0.3211	0.3198	0.317	0.3133
	0.317	0.317	0.317	0.317	0.317	0.317	0.3166	0.3151	0.3122	0.3082
	0.3073	0.3073	0.3073	0.3073	0.3073	0.3073	0.3068	0.3052	0.302	0.2978
	0.3209	0.3209	0.3209	0.3209	0.3209	0.3209	0.3204	0.3186	0.3151	0.3104

Figure I.3: F1A: e=2.5b & d=1.5b

	c/b									
a/b	0.3912	0.3912	0.3912	0.3911	0.3911	0.3908	0.39	0.3885	0.3864	0.3838
	0.3779	0.3779	0.3779	0.3778	0.3778	0.3775	0.3766	0.3751	0.3729	0.3701
	0.358	0.358	0.358	0.3579	0.3579	0.3575	0.3567	0.355	0.3527	0.3499
	0.3543	0.3543	0.3542	0.3542	0.3542	0.3538	0.3529	0.3513	0.3489	0.346
	0.3469	0.3469	0.3468	0.3467	0.3467	0.3464	0.3455	0.3437	0.3413	0.3383
	0.3275	0.3275	0.3275	0.3274	0.3274	0.327	0.3261	0.3243	0.3217	0.3186
	0.3216	0.3215	0.3215	0.3214	0.3214	0.321	0.32	0.3181	0.3154	0.3122
	0.317	0.317	0.3169	0.3169	0.3168	0.3164	0.3153	0.3133	0.3105	0.3071
	0.3073	0.3073	0.3072	0.3071	0.3071	0.3066	0.3055	0.3033	0.3002	0.2965
	0.3209	0.3209	0.3208	0.3208	0.3207	0.3202	0.3189	0.3164	0.3131	0.3091

Figure I.3: F1A: e=2.5b & d=2b

	c/b									
a/b	0.3912	0.3912	0.3912	0.3912	0.3909	0.3902	0.3891	0.3876	0.3856	0.3833
	0.3779	0.3779	0.3779	0.3779	0.3776	0.3769	0.3758	0.3741	0.3721	0.3697
	0.358	0.358	0.358	0.358	0.3577	0.357	0.3558	0.3541	0.352	0.3494
	0.3543	0.3543	0.3543	0.3543	0.354	0.3533	0.352	0.3503	0.3481	0.3456
	0.3469	0.3468	0.3468	0.3468	0.3466	0.3458	0.3445	0.3427	0.3405	0.3378
	0.3275	0.3275	0.3275	0.3275	0.3272	0.3264	0.3251	0.3232	0.3209	0.3182
	0.3215	0.3215	0.3215	0.3215	0.3212	0.3204	0.319	0.317	0.3146	0.3118
	0.317	0.3169	0.3169	0.3169	0.3166	0.3157	0.3143	0.3122	0.3097	0.3067
	0.3073	0.3072	0.3072	0.3072	0.3069	0.3059	0.3043	0.302	0.2993	0.2961
	0.3209	0.3208	0.3208	0.3208	0.3204	0.3193	0.3175	0.3151	0.3121	0.3086

Figure I.3: F1A: e=2.5b & d=2.5b

	c/b									
a/b	0.3912	0.3913	0.3912	0.391	0.3905	0.3897	0.3885	0.387	0.3852	0.3831
	0.3779	0.378	0.3779	0.3777	0.3772	0.3763	0.3751	0.3735	0.3717	0.3695
	0.358	0.3581	0.358	0.3578	0.3572	0.3564	0.3551	0.3534	0.3515	0.3493
	0.3543	0.3544	0.3543	0.3541	0.3535	0.3526	0.3513	0.3497	0.3477	0.3454
	0.3469	0.3469	0.3469	0.3466	0.3461	0.3451	0.3438	0.3421	0.3401	0.3377
	0.3276	0.3276	0.3275	0.3273	0.3267	0.3257	0.3243	0.3226	0.3205	0.3181
	0.3216	0.3216	0.3216	0.3213	0.3207	0.3197	0.3182	0.3163	0.3142	0.3117
	0.317	0.317	0.317	0.3167	0.3161	0.315	0.3134	0.3115	0.3093	0.3066
	0.3073	0.3074	0.3073	0.307	0.3062	0.305	0.3034	0.3013	0.2989	0.296
	0.3209	0.321	0.3209	0.3205	0.3197	0.3184	0.3165	0.3142	0.3117	0.3086

Figure I.3: F1A: e=2.5b & d=3b

	c/b									
a/b	0.3912	0.3912	0.391	0.3907	0.39	0.3891	0.388	0.3866	0.385	0.3831
	0.378	0.3779	0.3777	0.3773	0.3767	0.3758	0.3746	0.3731	0.3715	0.3695
	0.358	0.358	0.3578	0.3574	0.3567	0.3558	0.3545	0.353	0.3513	0.3493
	0.3543	0.3543	0.3541	0.3537	0.353	0.352	0.3507	0.3492	0.3475	0.3454
	0.3469	0.3469	0.3467	0.3462	0.3455	0.3445	0.3432	0.3416	0.3399	0.3377
	0.3276	0.3275	0.3273	0.3269	0.3261	0.3251	0.3237	0.3221	0.3203	0.3181
	0.3216	0.3215	0.3213	0.3209	0.3201	0.319	0.3176	0.3159	0.314	0.3117
	0.317	0.3169	0.3168	0.3163	0.3154	0.3143	0.3128	0.311	0.309	0.3067
	0.3073	0.3073	0.307	0.3065	0.3055	0.3043	0.3027	0.3008	0.2987	0.2961
	0.3209	0.3209	0.3206	0.32	0.3189	0.3176	0.3158	0.3137	0.3115	0.3088

Figure I.3: F1A: e=2.5b & d=3.5b

	c/b									
a/b	0.3912	0.3911	0.3908	0.3904	0.3896	0.3888	0.3877	0.3864	0.3849	0.3832
	0.3779	0.3778	0.3775	0.377	0.3763	0.3754	0.3742	0.3729	0.3714	0.3696
	0.358	0.3579	0.3576	0.3571	0.3563	0.3554	0.3542	0.3528	0.3512	0.3494
	0.3543	0.3542	0.3539	0.3534	0.3526	0.3517	0.3504	0.349	0.3474	0.3456
	0.3469	0.3467	0.3464	0.3459	0.3451	0.3441	0.3429	0.3414	0.3398	0.3379
	0.3275	0.3274	0.3271	0.3265	0.3257	0.3247	0.3234	0.3219	0.3202	0.3183
	0.3215	0.3214	0.3211	0.3205	0.3196	0.3186	0.3172	0.3157	0.314	0.3119
	0.317	0.3167	0.3165	0.3159	0.3149	0.3138	0.3124	0.3108	0.309	0.3069
	0.3073	0.3071	0.3067	0.306	0.305	0.3039	0.3023	0.3006	0.2987	0.2964
	0.3209	0.3207	0.3203	0.3195	0.3184	0.3171	0.3154	0.3136	0.3115	0.3091

Figure I.3: F1A: e=2.5b & d=4b

	c/b									
a/b	0.3912	0.391	0.3907	0.3902	0.3895	0.3886	0.3876	0.3863	0.385	0.3835
	0.3779	0.3777	0.3774	0.3768	0.3761	0.3752	0.3741	0.3729	0.3715	0.3699
	0.358	0.3578	0.3575	0.3569	0.3561	0.3552	0.3541	0.3528	0.3514	0.3497
	0.3543	0.3541	0.3537	0.3532	0.3524	0.3515	0.3503	0.349	0.3476	0.3459
	0.3468	0.3466	0.3463	0.3457	0.3449	0.3439	0.3427	0.3414	0.34	0.3382
	0.3275	0.3273	0.3269	0.3263	0.3255	0.3245	0.3233	0.3219	0.3204	0.3186
	0.3215	0.3213	0.3209	0.3203	0.3194	0.3184	0.3171	0.3157	0.3141	0.3123
	0.317	0.3167	0.3163	0.3156	0.3147	0.3137	0.3123	0.3108	0.3093	0.3073
	0.3072	0.307	0.3065	0.3058	0.3048	0.3037	0.3022	0.3006	0.2989	0.2969
	0.3209	0.3206	0.3201	0.3193	0.3182	0.3169	0.3154	0.3137	0.3118	0.3097

Figure I.3: F1A: e=3b & d=0.5b

	c/b									
	0.4072	0.4072	0.4072	0.4072	0.4072	0.4072	0.4079	0.4071	0.4061	0.4031
	0.3967	0.3967	0.3967	0.3967	0.3967	0.3967	0.3966	0.3966	0.3955	0.3923
	0.3798	0.3798	0.3798	0.3798	0.3798	0.3798	0.3797	0.3797	0.3785	0.3751
	0.3792	0.3792	0.3792	0.3792	0.3792	0.3792	0.3792	0.3791	0.3779	0.3744
a/b	0.3746	0.3746	0.3746	0.3746	0.3746	0.3747	0.3746	0.3745	0.3732	0.3695
	0.3575	0.3575	0.3575	0.3575	0.3575	0.3575	0.3575	0.3574	0.356	0.3522
	0.3524	0.3524	0.3524	0.3524	0.3524	0.3524	0.3523	0.3523	0.3509	0.3468
	0.3468	0.3468	0.3468	0.3468	0.3468	0.3468	0.3468	0.3467	0.3452	0.3409
	0.3346	0.3346	0.3346	0.3346	0.3346	0.3346	0.3345	0.3345	0.3329	0.3283
	0.3424	0.3424	0.3424	0.3424	0.3424	0.3424	0.3423	0.3422	0.3405	0.3357

Figure I.3: F1A: e=3b & d=1b

	c/b									
	0.4072	0.4072	0.4072	0.4072	0.4072	0.4072	0.4069	0.4059	0.4039	0.4012
	0.3967	0.3967	0.3967	0.3967	0.3967	0.3967	0.3963	0.3953	0.3932	0.3904
	0.3798	0.3798	0.3798	0.3798	0.3798	0.3797	0.3794	0.3783	0.3761	0.3731
	0.3792	0.3792	0.3792	0.3792	0.3792	0.3792	0.3788	0.3777	0.3754	0.3723
a/b	0.3746	0.3746	0.3746	0.3746	0.3746	0.3746	0.3742	0.373	0.3707	0.3674
	0.3575	0.3575	0.3575	0.3575	0.3575	0.3575	0.3571	0.3558	0.3533	0.3499
	0.3524	0.3524	0.3524	0.3524	0.3524	0.3523	0.352	0.3506	0.348	0.3445
	0.3468	0.3468	0.3468	0.3468	0.3468	0.3468	0.3464	0.345	0.3423	0.3385
	0.3346	0.3346	0.3346	0.3346	0.3346	0.3346	0.3341	0.3326	0.3297	0.3257
	0.3424	0.3424	0.3424	0.3424	0.3424	0.3423	0.3418	0.3402	0.3371	0.3335

Figure I.3: F1A: e=3b & d=1.5b

	c/b									
	0.4072	0.4072	0.4071	0.4071	0.407	0.4067	0.406	0.4046	0.4027	0.4002
	0.3967	0.3967	0.3966	0.3966	0.3965	0.3962	0.3954	0.394	0.3919	0.3894
	0.3798	0.3797	0.3797	0.3797	0.3796	0.3793	0.3784	0.3769	0.3747	0.372
	0.3792	0.3792	0.3791	0.3791	0.379	0.3787	0.3778	0.3762	0.374	0.3712
a/b	0.3746	0.3746	0.3745	0.3745	0.3744	0.3741	0.3732	0.3715	0.3692	0.3663
	0.3575	0.3575	0.3574	0.3574	0.3573	0.357	0.356	0.3543	0.3518	0.3488
	0.3524	0.3524	0.3523	0.3523	0.3522	0.3518	0.3508	0.349	0.3464	0.3433
	0.3468	0.3468	0.3467	0.3467	0.3466	0.3462	0.3452	0.3433	0.3406	0.3373
	0.3346	0.3346	0.3345	0.3344	0.3344	0.3339	0.3328	0.3308	0.3279	0.3245
	0.3424	0.3423	0.3423	0.3422	0.3421	0.3417	0.3405	0.3383	0.3352	0.3316

Figure I.3: F1A: e=3b & d=2b

	c/b									
	0.4072	0.4071	0.4071	0.4071	0.4069	0.4062	0.4052	0.4037	0.4019	0.3998
	0.3967	0.3966	0.3966	0.3966	0.3963	0.3957	0.3946	0.393	0.3912	0.3889
	0.3797	0.3797	0.3797	0.3797	0.3794	0.3787	0.3775	0.3759	0.3739	0.3715
	0.3792	0.3792	0.3791	0.3791	0.3788	0.3781	0.3769	0.3753	0.3732	0.3707
a/b	0.3746	0.3746	0.3745	0.3745	0.3743	0.3735	0.3723	0.3705	0.3684	0.3658
	0.3575	0.3574	0.3574	0.3574	0.3571	0.3563	0.355	0.3532	0.351	0.3483
	0.3524	0.3523	0.3523	0.3523	0.352	0.3512	0.3498	0.3479	0.3456	0.3428
	0.3468	0.3468	0.3468	0.3467	0.3464	0.3455	0.3441	0.3422	0.3397	0.3368
	0.3346	0.3345	0.3345	0.3345	0.3341	0.3332	0.3317	0.3296	0.327	0.324
	0.3423	0.3423	0.3423	0.3422	0.3419	0.3408	0.3392	0.337	0.3343	0.331

Figure I.3: F1A: e=3b & d=2.5b

	c/b									
	0.4072	0.4072	0.4072	0.4069	0.4064	0.4057	0.4045	0.4031	0.4015	0.3995
	0.3967	0.3967	0.3966	0.3964	0.3959	0.3951	0.3939	0.3924	0.3907	0.3887
	0.3798	0.3798	0.3797	0.3795	0.3789	0.3781	0.3769	0.3753	0.3735	0.3713
	0.3792	0.3792	0.3792	0.3789	0.3784	0.3775	0.3762	0.3746	0.3728	0.3705
a/b	0.3746	0.3746	0.3746	0.3743	0.3738	0.3728	0.3715	0.3699	0.3679	0.3656
	0.3575	0.3575	0.3575	0.3572	0.3566	0.3557	0.3543	0.3525	0.3505	0.3481
	0.3524	0.3524	0.3524	0.3521	0.3515	0.3505	0.349	0.3472	0.3451	0.3427
	0.3468	0.3469	0.3468	0.3465	0.3459	0.3448	0.3433	0.3414	0.3393	0.3367
	0.3346	0.3346	0.3346	0.3342	0.3335	0.3324	0.3308	0.3288	0.3265	0.3238
	0.3424	0.3424	0.3423	0.342	0.3412	0.34	0.3383	0.3362	0.3338	0.3309

Figure I.3: F1A: e=3b & d=3b

	c/b									
	0.4072	0.4071	0.407	0.4066	0.406	0.4052	0.4041	0.4027	0.4013	0.3995
	0.3967	0.3966	0.3965	0.3961	0.3954	0.3946	0.3934	0.392	0.3905	0.3886
	0.3798	0.3797	0.3795	0.3791	0.3784	0.3776	0.3763	0.3749	0.3732	0.3713
	0.3792	0.3792	0.379	0.3786	0.3779	0.3769	0.3757	0.3742	0.3725	0.3705
a/b	0.3746	0.3746	0.3744	0.374	0.3732	0.3723	0.371	0.3694	0.3677	0.3656
	0.3575	0.3575	0.3573	0.3568	0.3561	0.3551	0.3537	0.3521	0.3503	0.3481
	0.3524	0.3523	0.3521	0.3517	0.3509	0.3498	0.3484	0.3467	0.3449	0.3427
	0.3468	0.3468	0.3466	0.3461	0.3452	0.3442	0.3427	0.3409	0.339	0.3367
	0.3346	0.3345	0.3343	0.3338	0.3329	0.3317	0.3302	0.3283	0.3263	0.3239
	0.3424	0.3423	0.342	0.3414	0.3405	0.3393	0.3376	0.3357	0.3335	0.331

Figure I.3: F1A: e=3b & d=3.5b

	c/b									
	0.4072	0.4071	0.4068	0.4063	0.4057	0.4049	0.4038	0.4026	0.4012	0.3996
	0.3967	0.3965	0.3963	0.3958	0.3951	0.3942	0.3931	0.3918	0.3904	0.3887
	0.3797	0.3796	0.3793	0.3788	0.3781	0.3772	0.376	0.3747	0.3732	0.3714
	0.3792	0.3791	0.3788	0.3782	0.3775	0.3766	0.3754	0.374	0.3725	0.3706
a/b	0.3746	0.3745	0.3742	0.3736	0.3728	0.3719	0.3706	0.3692	0.3676	0.3658
	0.3575	0.3573	0.357	0.3565	0.3556	0.3547	0.3533	0.3519	0.3502	0.3483
	0.3524	0.3522	0.3519	0.3513	0.3504	0.3494	0.3481	0.3465	0.3448	0.3428
	0.3468	0.3467	0.3463	0.3457	0.3448	0.3437	0.3423	0.3407	0.339	0.3369
	0.3346	0.3344	0.334	0.3334	0.3324	0.3313	0.3298	0.3281	0.3263	0.3241
	0.3423	0.3421	0.3417	0.341	0.34	0.3388	0.3372	0.3355	0.3335	0.3313

Figure I.3: F1A: e=3b & d=4b

	c/b									
	0.4071	0.407	0.4067	0.4062	0.4055	0.4047	0.4037	0.4025	0.4013	0.3998
	0.3966	0.3965	0.3961	0.3956	0.3949	0.3941	0.393	0.3918	0.3905	0.389
	0.3797	0.3795	0.3792	0.3786	0.3779	0.377	0.3759	0.3746	0.3733	0.3716
	0.3792	0.379	0.3786	0.3781	0.3773	0.3764	0.3753	0.374	0.3726	0.3709
a/b	0.3746	0.3744	0.374	0.3734	0.3726	0.3717	0.3705	0.3692	0.3678	0.3661
	0.3574	0.3572	0.3569	0.3563	0.3554	0.3545	0.3532	0.3519	0.3504	0.3486
	0.3523	0.3521	0.3517	0.3511	0.3502	0.3492	0.348	0.3465	0.345	0.3432
	0.3468	0.3466	0.3461	0.3455	0.3446	0.3436	0.3422	0.3408	0.3392	0.3373
	0.3345	0.3343	0.3338	0.3331	0.3322	0.3311	0.3297	0.3282	0.3265	0.3245
	0.3423	0.342	0.3415	0.3408	0.3398	0.3386	0.3372	0.3355	0.3338	0.3317

Figure I.3: F1A: e=3.5b & d=0.5b

	c/b									
	0.4187	0.4187	0.4187	0.4187	0.4187	0.4187	0.4188	0.4187	0.4177	0.4151
	0.4101	0.4101	0.4101	0.4101	0.4101	0.4101	0.41	0.41	0.409	0.4062
	0.3951	0.3951	0.3951	0.3951	0.3951	0.3951	0.3951	0.395	0.3939	0.3909
	0.3968	0.3968	0.3968	0.3968	0.3968	0.3968	0.3967	0.3967	0.3955	0.3924
a/b	0.3943	0.3943	0.3943	0.3943	0.3943	0.3943	0.3943	0.3942	0.393	0.3897
	0.3791	0.3791	0.3791	0.3791	0.3791	0.3791	0.3791	0.379	0.3778	0.3742
	0.3755	0.3755	0.3755	0.3755	0.3755	0.3755	0.3755	0.3754	0.3741	0.3704
	0.3707	0.3707	0.3707	0.3707	0.3707	0.3707	0.3706	0.3706	0.3692	0.3653
	0.3582	0.3582	0.3582	0.3582	0.3582	0.3582	0.3582	0.3581	0.3567	0.3525
	0.3639	0.3639	0.3639	0.3639	0.3639	0.3639	0.3638	0.3637	0.3622	0.3578

Figure I.3: F1A: e=3.5b & d=1b

	c/b									
	0.4187	0.4187	0.4187	0.4187	0.4187	0.4187	0.4184	0.4175	0.4158	0.4133
	0.4101	0.4101	0.4101	0.4101	0.4101	0.41	0.4097	0.4088	0.4069	0.4043
	0.3951	0.3951	0.3951	0.3951	0.3951	0.3951	0.3948	0.3937	0.3918	0.389
	0.3968	0.3968	0.3968	0.3968	0.3968	0.3967	0.3964	0.3953	0.3933	0.3904
a/b	0.3943	0.3943	0.3943	0.3943	0.3943	0.3943	0.3939	0.3928	0.3906	0.3876
	0.3791	0.3791	0.3791	0.3791	0.3791	0.3791	0.3787	0.3775	0.3753	0.3721
	0.3755	0.3755	0.3755	0.3755	0.3755	0.3755	0.3751	0.3739	0.3714	0.3681
	0.3707	0.3707	0.3707	0.3707	0.3707	0.3706	0.3703	0.369	0.3664	0.363
	0.3582	0.3582	0.3582	0.3582	0.3582	0.3582	0.3578	0.3564	0.3537	0.3501
	0.3639	0.3639	0.3639	0.3639	0.3639	0.3638	0.3634	0.3619	0.3591	0.3552

Figure I.3: F1A: e=3.5b & d=1.5b

	c/b									
	0.4187	0.4187	0.4187	0.4187	0.4186	0.4183	0.4176	0.4163	0.4146	0.4124
	0.4101	0.4101	0.41	0.41	0.4099	0.4096	0.4089	0.4075	0.4057	0.4033
	0.3951	0.3951	0.395	0.395	0.395	0.3946	0.3938	0.3924	0.3904	0.388
	0.3968	0.3967	0.3967	0.3967	0.3966	0.3963	0.3955	0.394	0.3919	0.3893
a/b	0.3943	0.3943	0.3943	0.3942	0.3942	0.3938	0.393	0.3914	0.3892	0.3865
	0.3791	0.3791	0.3791	0.379	0.379	0.3786	0.3777	0.3761	0.3738	0.371
	0.3755	0.3755	0.3754	0.3754	0.3753	0.375	0.374	0.3723	0.3699	0.367
	0.3707	0.3707	0.3706	0.3706	0.3705	0.3701	0.3691	0.3673	0.3648	0.3618
	0.3582	0.3582	0.3582	0.3581	0.358	0.3576	0.3566	0.3547	0.352	0.3488
	0.3639	0.3638	0.3638	0.3637	0.3637	0.3632	0.3621	0.3601	0.3573	0.3539

Figure I.3: F1A: e=3.5b & d=2b

	c/b									
	0.4187	0.4187	0.4187	0.4187	0.4184	0.4178	0.4169	0.4155	0.4139	0.4119
	0.4101	0.41	0.41	0.41	0.4097	0.4091	0.4081	0.4067	0.4049	0.4028
	0.3951	0.3951	0.395	0.395	0.3947	0.3941	0.393	0.3915	0.3897	0.3874
	0.3967	0.3967	0.3967	0.3967	0.3964	0.3957	0.3946	0.393	0.3911	0.3888
a/b	0.3943	0.3943	0.3943	0.3942	0.3939	0.3932	0.3921	0.3904	0.3884	0.386
	0.3791	0.3791	0.3791	0.379	0.3787	0.378	0.3767	0.375	0.3729	0.3704
	0.3755	0.3754	0.3754	0.3754	0.3751	0.3743	0.373	0.3712	0.3691	0.3664
	0.3707	0.3706	0.3706	0.3706	0.3703	0.3694	0.3681	0.3662	0.3639	0.3612
	0.3582	0.3582	0.3582	0.3581	0.3578	0.3569	0.3555	0.3535	0.3511	0.3483
	0.3638	0.3638	0.3638	0.3637	0.3634	0.3624	0.3609	0.3589	0.3564	0.3533

Figure I.3: F1A: e=3.5b & d=2.5b

	c/b									
	0.4187	0.4188	0.4187	0.4185	0.418	0.4173	0.4163	0.415	0.4135	0.4116
	0.4101	0.4101	0.41	0.4098	0.4093	0.4086	0.4075	0.4061	0.4045	0.4026
	0.3951	0.3951	0.3951	0.3948	0.3943	0.3935	0.3923	0.3909	0.3892	0.3872
	0.3968	0.3968	0.3967	0.3965	0.3959	0.3951	0.3939	0.3924	0.3907	0.3886
a/b	0.3943	0.3943	0.3943	0.394	0.3935	0.3926	0.3913	0.3898	0.388	0.3858
	0.3791	0.3791	0.3791	0.3788	0.3782	0.3773	0.376	0.3744	0.3725	0.3702
	0.3755	0.3755	0.3755	0.3752	0.3746	0.3736	0.3723	0.3705	0.3686	0.3662
	0.3707	0.3707	0.3706	0.3704	0.3697	0.3687	0.3673	0.3655	0.3635	0.361
	0.3582	0.3583	0.3582	0.3579	0.3572	0.3561	0.3546	0.3528	0.3506	0.3487
	0.3639	0.3639	0.3638	0.3635	0.3628	0.3616	0.36	0.3581	0.3558	0.3531

Figure I.3: F1A: e=3.5b & d=3b

	c/b									
	0.4187	0.4187	0.4185	0.4182	0.4176	0.4169	0.4158	0.4146	0.4132	0.4116
	0.4101	0.41	0.4099	0.4095	0.4089	0.4081	0.407	0.4057	0.4043	0.4025
	0.3951	0.3951	0.3949	0.3945	0.3938	0.393	0.3918	0.3905	0.389	0.3871
	0.3968	0.3967	0.3965	0.3961	0.3955	0.3946	0.3934	0.392	0.3904	0.3885
a/b	0.3943	0.3943	0.3941	0.3937	0.393	0.3921	0.3908	0.3893	0.3877	0.3857
	0.3791	0.3791	0.3789	0.3784	0.3777	0.3768	0.3755	0.3739	0.3722	0.3701
	0.3755	0.3755	0.3752	0.3748	0.374	0.373	0.3717	0.3701	0.3683	0.3662
	0.3707	0.3706	0.3704	0.3699	0.3691	0.3681	0.3667	0.365	0.3632	0.361
	0.3582	0.3582	0.3579	0.3574	0.3566	0.3555	0.354	0.3523	0.3504	0.348
	0.3639	0.3638	0.3635	0.363	0.3621	0.361	0.3594	0.3576	0.3556	0.3531

Figure I.3: F1A: e=3.5b & d=3.5b

	c/b									
	0.4187	0.4186	0.4184	0.4179	0.4173	0.4166	0.4155	0.4144	0.4131	0.4116
	0.41	0.4099	0.4097	0.4092	0.4086	0.4078	0.4067	0.4055	0.4042	0.4026
	0.3951	0.395	0.3947	0.3942	0.3935	0.3927	0.3915	0.3903	0.3889	0.3872
	0.3967	0.3966	0.3963	0.3958	0.3951	0.3942	0.3931	0.3918	0.3903	0.3886
a/b	0.3943	0.3942	0.3939	0.3934	0.3926	0.3917	0.3905	0.3891	0.3876	0.3858
	0.3791	0.379	0.3787	0.3781	0.3773	0.3764	0.3751	0.3737	0.3721	0.3703
	0.3755	0.3753	0.375	0.3744	0.3736	0.3726	0.3713	0.3699	0.3682	0.3663
	0.3707	0.3705	0.3702	0.3696	0.3687	0.3677	0.3663	0.3648	0.3631	0.3611
	0.3582	0.358	0.3577	0.3571	0.3561	0.3551	0.3536	0.3521	0.3503	0.3482
	0.3638	0.3636	0.3633	0.3626	0.3617	0.3605	0.359	0.3574	0.3555	0.3534

Figure I.3: F1A: e=3.5b & d=4b

	c/b									
	0.4187	0.4185	0.4183	0.4178	0.4171	0.4164	0.4155	0.4144	0.4132	0.4118
	0.41	0.4099	0.4096	0.4091	0.4084	0.4076	0.4066	0.4055	0.4043	0.4028
	0.3951	0.3949	0.3946	0.394	0.3933	0.3925	0.3914	0.3903	0.389	0.3874
	0.3967	0.3965	0.3962	0.3957	0.3949	0.3941	0.393	0.3918	0.3905	0.3889
a/b	0.3943	0.3941	0.3937	0.3932	0.3924	0.3915	0.3904	0.3891	0.3878	0.3861
	0.3791	0.3789	0.3785	0.3779	0.3771	0.3762	0.375	0.3737	0.3723	0.3706
	0.3755	0.3752	0.3749	0.3743	0.3734	0.3725	0.3712	0.3699	0.3684	0.3666
	0.3706	0.3704	0.37	0.3694	0.3685	0.3675	0.3662	0.3648	0.3633	0.3615
	0.3582	0.3579	0.3575	0.3568	0.3559	0.3549	0.3536	0.3521	0.3505	0.3486
	0.3638	0.3635	0.3631	0.3624	0.3614	0.3603	0.359	0.3574	0.3558	0.3538

Figure I.3: F1A: e=4b & d=0.5b

	c/b									
	0.4274	0.4274	0.4274	0.4274	0.4274	0.4274	0.4274	0.4273	0.4264	0.4241
	0.4199	0.4199	0.4199	0.4199	0.4199	0.4199	0.4199	0.4199	0.419	0.4164
	0.4063	0.4063	0.4063	0.4063	0.4063	0.4063	0.4063	0.4062	0.4052	0.4025
	0.4095	0.4095	0.4095	0.4095	0.4095	0.4095	0.4095	0.4094	0.4084	0.4056
a/b	0.4086	0.4086	0.4086	0.4086	0.4086	0.4086	0.4086	0.4085	0.4075	0.4045
	0.3949	0.3949	0.3949	0.3949	0.3949	0.3949	0.3949	0.3948	0.3937	0.3905
	0.3927	0.3927	0.3927	0.3927	0.3927	0.3927	0.3926	0.3926	0.3914	0.388
	0.3889	0.3889	0.3889	0.3889	0.3889	0.3889	0.3889	0.3888	0.3875	0.384
	0.3771	0.3771	0.3771	0.3771	0.3771	0.3771	0.377	0.3769	0.3756	0.3719
	0.3824	0.3824	0.3824	0.3824	0.3824	0.3824	0.3824	0.3823	0.3809	0.377

Figure I.3: F1A: e=4b & d=1b

	c/b									
	0.4274	0.4274	0.4274	0.4274	0.4274	0.4273	0.4271	0.4263	0.4247	0.4225
	0.4199	0.4199	0.4199	0.4199	0.4199	0.4199	0.4196	0.4188	0.4171	0.4148
	0.4063	0.4063	0.4063	0.4063	0.4063	0.4063	0.406	0.405	0.4033	0.4008
	0.4095	0.4095	0.4095	0.4095	0.4095	0.4095	0.4092	0.4082	0.4063	0.4037
a/b	0.4086	0.4086	0.4086	0.4086	0.4086	0.4086	0.4083	0.4073	0.4053	0.4025
	0.3949	0.3949	0.3949	0.3949	0.3949	0.3949	0.3945	0.3934	0.3914	0.3885
	0.3927	0.3927	0.3927	0.3927	0.3927	0.3926	0.3923	0.3911	0.3889	0.3859
	0.3889	0.3889	0.3889	0.3889	0.3889	0.3889	0.3885	0.3873	0.385	0.3818
	0.3771	0.3771	0.3771	0.3771	0.3771	0.377	0.3766	0.3754	0.3729	0.3696
	0.3824	0.3824	0.3824	0.3824	0.3824	0.3824	0.3819	0.3806	0.3781	0.3746

Figure I.3: F1A: e=4b & d=1.5b

	c/b									
	0.4274	0.4274	0.4273	0.4273	0.4273	0.427	0.4263	0.4252	0.4236	0.4216
	0.4199	0.4199	0.4199	0.4199	0.4198	0.4195	0.4188	0.4176	0.4159	0.4138
	0.4063	0.4063	0.4062	0.4062	0.4062	0.4059	0.4051	0.4038	0.402	0.3998
	0.4095	0.4095	0.4095	0.4094	0.4094	0.4091	0.4083	0.407	0.4051	0.4027
a/b	0.4086	0.4086	0.4086	0.4086	0.4085	0.4082	0.4074	0.4059	0.404	0.4015
	0.3949	0.3949	0.3949	0.3948	0.3948	0.3944	0.3936	0.3921	0.39	0.3874
	0.3927	0.3926	0.3926	0.3926	0.3925	0.3921	0.3913	0.3897	0.3875	0.3847
	0.3889	0.3889	0.3888	0.3888	0.3887	0.3884	0.3874	0.3858	0.3835	0.3806
	0.3771	0.377	0.377	0.377	0.3769	0.3765	0.3755	0.3738	0.3713	0.3683
	0.3824	0.3824	0.3823	0.3823	0.3822	0.3818	0.3808	0.3789	0.3764	0.3733

Figure I.3: F1A: e=4b & d=2b

	c/b									
	0.4274	0.4273	0.4273	0.4273	0.4271	0.4265	0.4256	0.4244	0.4229	0.4211
	0.4199	0.4199	0.4199	0.4199	0.4196	0.419	0.4181	0.4168	0.4152	0.4133
	0.4063	0.4063	0.4062	0.4062	0.4059	0.4053	0.4043	0.403	0.4013	0.3992
	0.4095	0.4095	0.4095	0.4094	0.4092	0.4085	0.4075	0.4061	0.4043	0.4022
a/b	0.4086	0.4086	0.4086	0.4085	0.4083	0.4076	0.4065	0.405	0.4032	0.4009
	0.3949	0.3949	0.3948	0.3948	0.3945	0.3938	0.3927	0.3911	0.3892	0.3868
	0.3926	0.3926	0.3926	0.3926	0.3923	0.3915	0.3903	0.3887	0.3866	0.3842
	0.3889	0.3888	0.3888	0.3888	0.3885	0.3877	0.3865	0.3847	0.3826	0.3801
	0.377	0.377	0.377	0.377	0.3766	0.3758	0.3745	0.3727	0.3704	0.3677
	0.3824	0.3823	0.3823	0.3823	0.3819	0.3811	0.3797	0.3778	0.3755	0.3726

Figure I.3: F1A: e=4b & d=2.5b

	c/b									
	0.4274	0.4274	0.4273	0.4271	0.4267	0.426	0.4251	0.4239	0.4225	0.4208
	0.4199	0.42	0.4199	0.4197	0.4192	0.4185	0.4175	0.4163	0.4148	0.413
	0.4063	0.4063	0.4062	0.406	0.4055	0.4048	0.4037	0.4024	0.4008	0.399
	0.4095	0.4095	0.4095	0.4092	0.4087	0.408	0.4069	0.4055	0.4039	0.4019
a/b	0.4086	0.4087	0.4086	0.4083	0.4078	0.407	0.4059	0.4044	0.4027	0.4007
	0.3949	0.3949	0.3949	0.3946	0.394	0.3932	0.392	0.3904	0.3887	0.3865
	0.3927	0.3927	0.3926	0.3923	0.3918	0.3909	0.3896	0.388	0.3862	0.3839
	0.3889	0.3889	0.3888	0.3886	0.388	0.387	0.3857	0.384	0.3821	0.3798
	0.3771	0.3771	0.377	0.3767	0.3761	0.3751	0.3737	0.3719	0.3699	0.3675
	0.3824	0.3824	0.3823	0.382	0.3813	0.3803	0.3788	0.377	0.3749	0.3724

Figure I.3: F1A: e=4b & d=3b

	c/b									
	0.4274	0.4273	0.4272	0.4268	0.4263	0.4256	0.4247	0.4235	0.4223	0.4207
	0.4199	0.4199	0.4197	0.4194	0.4188	0.4181	0.4171	0.4159	0.4146	0.4129
	0.4063	0.4062	0.4061	0.4057	0.4051	0.4043	0.4033	0.402	0.4006	0.3988
	0.4095	0.4095	0.4093	0.4089	0.4083	0.4075	0.4064	0.4051	0.4036	0.4018
a/b	0.4086	0.4086	0.4084	0.408	0.4074	0.4065	0.4054	0.404	0.4025	0.4006
	0.3949	0.3949	0.3947	0.3942	0.3936	0.3927	0.3914	0.39	0.3884	0.3865
	0.3927	0.3926	0.3924	0.392	0.3912	0.3903	0.389	0.3875	0.3859	0.3839
	0.3889	0.3888	0.3886	0.3882	0.3874	0.3865	0.3851	0.3836	0.3818	0.3798
	0.3771	0.377	0.3768	0.3763	0.3755	0.3745	0.3731	0.3715	0.3696	0.3674
	0.3824	0.3823	0.3821	0.3816	0.3807	0.3797	0.3782	0.3765	0.3746	0.3724

Figure I.3: F1A: e=4b & d=3.5b

	c/b									
	0.4274	0.4272	0.427	0.4266	0.426	0.4253	0.4244	0.4234	0.4222	0.4208
	0.4199	0.4198	0.4196	0.4191	0.4185	0.4178	0.4168	0.4157	0.4145	0.413
	0.4063	0.4061	0.4059	0.4054	0.4048	0.404	0.403	0.4018	0.4005	0.3989
	0.4095	0.4094	0.4091	0.4087	0.408	0.4072	0.4061	0.4049	0.4035	0.4019
a/b	0.4086	0.4085	0.4082	0.4077	0.407	0.4062	0.4051	0.4038	0.4024	0.4007
	0.3949	0.3947	0.3945	0.3939	0.3932	0.3923	0.3911	0.3898	0.3883	0.3866
	0.3926	0.3925	0.3922	0.3917	0.3909	0.39	0.3887	0.3873	0.3858	0.384
	0.3889	0.3887	0.3884	0.3878	0.387	0.3861	0.3848	0.3834	0.3818	0.3799
	0.377	0.3769	0.3765	0.376	0.3751	0.3741	0.3728	0.3712	0.3696	0.3676
	0.3824	0.3822	0.3818	0.3812	0.3803	0.3793	0.3779	0.3763	0.3746	0.3725

Figure I.3: F1A: e=4b & d=4b

	c/b									
	0.4273	0.4272	0.4269	0.4265	0.4259	0.4252	0.4243	0.4233	0.4222	0.4209
	0.4199	0.4197	0.4195	0.419	0.4184	0.4177	0.4167	0.4157	0.4145	0.4132
	0.4062	0.4061	0.4058	0.4053	0.4046	0.4039	0.4029	0.4018	0.4005	0.3991
	0.4095	0.4093	0.409	0.4085	0.4078	0.407	0.406	0.4048	0.4036	0.4021
a/b	0.4086	0.4084	0.4081	0.4076	0.4068	0.406	0.405	0.4038	0.4025	0.4009
	0.3949	0.3947	0.3943	0.3938	0.393	0.3922	0.391	0.3898	0.3884	0.3868
	0.3926	0.3924	0.3921	0.3915	0.3907	0.3898	0.3886	0.3873	0.3859	0.3842
	0.3888	0.3886	0.3883	0.3877	0.3868	0.3859	0.3847	0.3834	0.3819	0.3802
	0.377	0.3768	0.3764	0.3758	0.3749	0.3739	0.3726	0.3712	0.3697	0.3679
	0.3823	0.3821	0.3817	0.381	0.3801	0.3791	0.3778	0.3763	0.3748	0.3729

Figure I.4: F2A: e=0.5b & d=0.5b

	c/b									
a/b	−0.1454	−0.1454	−0.1454	−0.1454	−0.1454	−0.1454	−0.1453	−0.1453	−0.1447	−0.1426
	−0.1489	−0.1489	−0.1489	−0.1489	−0.1489	−0.1488	−0.1488	−0.1488	−0.1482	−0.1459
	−0.1541	−0.1541	−0.1542	−0.1541	−0.1541	−0.1541	−0.1541	−0.1541	−0.1534	−0.1511
	−0.1537	−0.1537	−0.1538	−0.1538	−0.1537	−0.1538	−0.1537	−0.1537	−0.153	−0.1504
	−0.1533	−0.1533	−0.1533	−0.1533	−0.1532	−0.1533	−0.1532	−0.1532	−0.1524	−0.1494
	−0.1717	−0.1717	−0.1725	−0.1717	−0.1717	−0.1717	−0.1716	−0.1716	−0.1662	−0.1684
	−0.1781	−0.1781	−0.1782	−0.1781	−0.1781	−0.1782	−0.178	−0.178	−0.1772	−0.1722
	−0.1897	−0.1897	−0.1897	−0.1897	−0.1896	−0.1897	−0.1896	−0.1895	−0.1878	−0.1818
	−0.2169	−0.2169	−0.2166	−0.2164	−0.2169	−0.2161	−0.2158	−0.2157	−0.2128	−0.2059
	−0.2338	−0.2339	−0.234	−0.2339	−0.2338	−0.234	−0.2337	−0.2334	−0.2284	−0.2158

Figure I.4: F2A: e=0.5b & d=1b

	c/b									
a/b	−0.1454	−0.1454	−0.1454	−0.1454	−0.1454	−0.1454	−0.1453	−0.1447	−0.1435	−0.1417
	−0.1489	−0.1489	−0.1489	−0.1489	−0.1489	−0.1489	−0.1487	−0.1481	−0.1468	−0.145
	−0.1542	−0.1542	−0.1542	−0.1542	−0.1541	−0.1542	−0.154	−0.1534	−0.152	−0.1501
	−0.1537	−0.1538	−0.1538	−0.1538	−0.1537	−0.1538	−0.1536	−0.153	−0.1515	−0.1493
	−0.1533	−0.1533	−0.1533	−0.1533	−0.1533	−0.1533	−0.1532	−0.1524	−0.1507	−0.1482
	−0.1717	−0.1717	−0.1717	−0.1717	−0.1717	−0.1717	−0.1723	−0.1705	−0.1684	−0.1669
	−0.1781	−0.1781	−0.1781	−0.1781	−0.1781	−0.1782	−0.1779	−0.1766	−0.174	−0.1704
	−0.1897	−0.1897	−0.1897	−0.1897	−0.1897	−0.1897	−0.1892	−0.1875	−0.1841	−0.1796
	−0.2161	−0.2169	−0.2161	−0.2169	−0.2169	−0.216	−0.2152	−0.2144	−0.2088	−0.2028
	−0.2339	−0.2339	−0.2339	−0.2339	−0.2338	−0.2338	−0.2323	−0.228	−0.2209	−0.2123

Figure I.4: F2A: e=0.5b & d=1.5b

	c/b									
a/b	−0.1454	−0.1454	−0.1453	−0.1453	−0.1453	−0.1452	−0.1449	−0.1441	−0.1429	−0.1414
	−0.1489	−0.1488	−0.1488	−0.1488	−0.1488	−0.1487	−0.1484	−0.1475	−0.1462	−0.1447
	−0.1541	−0.1541	−0.1541	−0.154	−0.1541	−0.154	−0.1536	−0.1527	−0.1513	−0.1497
	−0.1537	−0.1537	−0.1537	−0.1537	−0.1537	−0.1535	−0.1531	−0.1521	−0.1506	−0.1489
	−0.1533	−0.1533	−0.1532	−0.1532	−0.1532	−0.153	−0.1525	−0.1514	−0.1497	−0.1477
	−0.1717	−0.1717	−0.1716	−0.1716	−0.1716	−0.1722	−0.1715	−0.1693	−0.1688	−0.1664
	−0.1781	−0.1781	−0.178	−0.178	−0.178	−0.1777	−0.1768	−0.1751	−0.1726	−0.1698
	−0.1897	−0.1896	−0.1896	−0.1895	−0.1894	−0.189	−0.1877	−0.1855	−0.1825	−0.179
	−0.2169	−0.2168	−0.2164	−0.2158	−0.2176	−0.2168	−0.215	−0.2118	−0.206	−0.2022
	−0.2338	−0.2338	−0.2337	−0.2336	−0.2332	−0.2318	−0.2285	−0.2238	−0.2182	−0.2124

Figure I.4: F2A: e=0.5b & d=2b

	c/b									
a/b	−0.1454	−0.1453	−0.1453	−0.1454	−0.1454	−0.1451	−0.1446	−0.1437	−0.1426	−0.1413
	−0.1488	−0.1488	−0.1488	−0.1489	−0.1489	−0.1486	−0.148	−0.1471	−0.1459	−0.1446
	−0.1541	−0.1541	−0.1541	−0.1542	−0.1542	−0.1538	−0.1532	−0.1522	−0.151	−0.1496
	−0.1537	−0.1537	−0.1537	−0.1538	−0.1537	−0.1533	−0.1526	−0.1516	−0.1503	−0.1488
	−0.1533	−0.1532	−0.1532	−0.1533	−0.1532	−0.1527	−0.1519	−0.1507	−0.1493	−0.1476
	−0.1717	−0.1716	−0.1724	−0.1725	−0.1724	−0.1718	−0.17	−0.1686	−0.1684	−0.1663
	−0.1781	−0.178	−0.178	−0.1781	−0.1779	−0.1771	−0.1759	−0.1742	−0.1722	−0.1698
	−0.1896	−0.1895	−0.1895	−0.1896	−0.1892	−0.1882	−0.1866	−0.1845	−0.182	−0.1791
	−0.2168	−0.2159	−0.2159	−0.2159	−0.2154	−0.2158	−0.2135	−0.2105	−0.2071	−0.2029
	−0.2338	−0.2337	−0.2337	−0.2333	−0.232	−0.2297	−0.2262	−0.2221	−0.2179	−0.2133

Figure I.4: F2A: e=0.5b & d=2.5b

	c/b									
a/b	−0.1454	−0.1454	−0.1455	−0.1454	−0.1453	−0.1449	−0.1442	−0.1434	−0.1424	−0.1413
	−0.1489	−0.1489	−0.1489	−0.1489	−0.1487	−0.1483	−0.1476	−0.1468	−0.1458	−0.1446
	−0.1542	−0.1542	−0.1542	−0.1542	−0.154	−0.1535	−0.1528	−0.1519	−0.1509	−0.1496
	−0.1537	−0.1538	−0.1538	−0.1537	−0.1535	−0.153	−0.1522	−0.1513	−0.1501	−0.1488
	−0.1533	−0.1533	−0.1533	−0.1532	−0.1529	−0.1523	−0.1515	−0.1504	−0.1491	−0.1477
	−0.1725	−0.1725	−0.1725	−0.1724	−0.172	−0.1713	−0.1695	−0.1682	−0.1682	−0.1665
	−0.1781	−0.1782	−0.1781	−0.178	−0.1774	−0.1766	−0.1753	−0.1738	−0.172	−0.17
	−0.1897	−0.1897	−0.1896	−0.1893	−0.1886	−0.1875	−0.1859	−0.184	−0.1819	−0.1795
	−0.2181	−0.2162	−0.216	−0.2156	−0.2145	−0.2148	−0.2126	−0.21	−0.2072	−0.2033
	−0.2339	−0.2338	−0.2334	−0.2324	−0.2306	−0.2283	−0.2251	−0.2217	−0.2181	−0.2142

Figure I.4: F2A: e=0.5b & d=3b

	c/b									
a/b	−0.1454	−0.1454	−0.1454	−0.1453	−0.145	−0.1445	−0.1439	−0.1432	−0.1423	−0.1412
	−0.1489	−0.1489	−0.1489	−0.1487	−0.1484	−0.1479	−0.1473	−0.1465	−0.1456	−0.1446
	−0.1542	−0.1542	−0.1541	−0.154	−0.1536	−0.1532	−0.1525	−0.1517	−0.1507	−0.1496
	−0.1538	−0.1538	−0.1537	−0.1535	−0.1531	−0.1526	−0.1519	−0.151	−0.15	−0.1488
	−0.1533	−0.1533	−0.1532	−0.153	−0.1525	−0.1519	−0.1511	−0.1501	−0.149	−0.1478
	−0.1725	−0.1725	−0.1724	−0.1721	−0.1716	−0.17	−0.1691	−0.1679	−0.1681	−0.1666
	−0.1781	−0.1781	−0.1779	−0.1776	−0.1769	−0.176	−0.1748	−0.1735	−0.172	−0.1702
	−0.1897	−0.1896	−0.1894	−0.1888	−0.188	−0.1869	−0.1854	−0.1837	−0.182	−0.1799
	−0.2181	−0.216	−0.2156	−0.2149	−0.2155	−0.214	−0.212	−0.2097	−0.2074	−0.2043
	−0.2338	−0.2335	−0.2328	−0.2315	−0.2296	−0.2275	−0.2247	−0.2218	−0.2188	−0.2153

Figure I.4: F2A: e=0.5b & d=3.5b

	c/b									
a/b	−0.1454	−0.1454	−0.1453	−0.1451	−0.1447	−0.1443	−0.1437	−0.143	−0.1422	−0.1413
	−0.1489	−0.1488	−0.1487	−0.1485	−0.1481	−0.1477	−0.1471	−0.1464	−0.1456	−0.1446
	−0.1542	−0.1541	−0.154	−0.1538	−0.1534	−0.1529	−0.1522	−0.1515	−0.1507	−0.1497
	−0.1537	−0.1537	−0.1536	−0.1533	−0.1529	−0.1523	−0.1516	−0.1509	−0.15	−0.1489
	−0.1533	−0.1532	−0.153	−0.1527	−0.1522	−0.1517	−0.1509	−0.15	−0.149	−0.1479
	−0.1725	−0.1724	−0.1722	−0.1718	−0.1704	−0.1697	−0.1688	−0.1678	−0.1681	−0.1668
	−0.1781	−0.178	−0.1777	−0.1772	−0.1765	−0.1757	−0.1746	−0.1734	−0.1721	−0.1705
	−0.1896	−0.1895	−0.1891	−0.1885	−0.1876	−0.1865	−0.1852	−0.1837	−0.1822	−0.1803
	−0.218	−0.2177	−0.2172	−0.2163	−0.215	−0.2136	−0.2118	−0.2098	−0.2074	−0.205
	−0.2337	−0.2332	−0.2324	−0.231	−0.2292	−0.2273	−0.2249	−0.2224	−0.2198	−0.2168

Figure I.4: F2A: e=0.5b & d=4b

	c/b									
a/b	−0.1454	−0.1453	−0.1452	−0.1449	−0.1446	−0.1441	−0.1436	−0.1429	−0.1422	−0.1414
	−0.1488	−0.1488	−0.1486	−0.1484	−0.148	−0.1475	−0.147	−0.1463	−0.1456	−0.1447
	−0.1541	−0.1541	−0.1539	−0.1536	−0.1532	−0.1528	−0.1521	−0.1515	−0.1507	−0.1498
	−0.1537	−0.1536	−0.1534	−0.1531	−0.1527	−0.1522	−0.1516	−0.1508	−0.1501	−0.1491
	−0.1533	−0.1531	−0.1529	−0.1526	−0.1521	−0.1515	−0.1508	−0.15	−0.1492	−0.1481
	−0.1725	−0.1723	−0.1721	−0.1708	−0.1703	−0.1696	−0.1687	−0.1678	−0.1683	−0.1671
	−0.1781	−0.1779	−0.1776	−0.177	−0.1763	−0.1756	−0.1746	−0.1735	−0.1723	−0.1709
	−0.1896	−0.1894	−0.1889	−0.1883	−0.1874	−0.1864	−0.1852	−0.1839	−0.1826	−0.1809
	−0.218	−0.2176	−0.217	−0.2161	−0.2149	−0.2136	−0.2119	−0.2102	−0.2081	−0.206
	−0.2337	−0.2331	−0.2322	−0.2309	−0.2293	−0.2276	−0.2255	−0.2232	−0.221	−0.2184

Figure I.4: F2A: e=1b & d=0.5b

	c/b									
a/b	−0.2067	−0.2067	−0.2067	−0.2067	−0.2067	−0.2067	−0.2066	−0.2066	−0.2058	−0.2031
	−0.2035	−0.2035	−0.2035	−0.2035	−0.2035	−0.2035	−0.2034	−0.2034	−0.2025	−0.1998
	−0.207	−0.207	−0.207	−0.207	−0.207	−0.207	−0.2069	−0.2069	−0.206	−0.203
	−0.2101	−0.2101	−0.2101	−0.2101	−0.2101	−0.2101	−0.21	−0.21	−0.209	−0.2058
	−0.2143	−0.2143	−0.2143	−0.2143	−0.2143	−0.2143	−0.2142	−0.2142	−0.213	−0.2095
	−0.2205	−0.2205	−0.2205	−0.2205	−0.2205	−0.2205	−0.2204	−0.2203	−0.219	−0.2151
	−0.2268	−0.2268	−0.2268	−0.2268	−0.2268	−0.2268	−0.2268	−0.2267	−0.2252	−0.2207
	−0.2335	−0.2335	−0.2335	−0.2335	−0.2335	−0.2335	−0.2334	−0.2333	−0.2314	−0.2261
	−0.2575	−0.2575	−0.2575	−0.2575	−0.2575	−0.2575	−0.2574	−0.2573	−0.2549	−0.2483
	−0.2582	−0.2582	−0.2582	−0.2582	−0.2582	−0.2582	−0.2581	−0.2579	−0.2548	−0.2468

Figure I.4: F2A: e=1b & d=1b

	c/b									
a/b	−0.2067	−0.2067	−0.2067	−0.2067	−0.2067	−0.2067	−0.2065	−0.2057	−0.2041	−0.2018
	−0.2035	−0.2035	−0.2035	−0.2035	−0.2035	−0.2034	−0.2032	−0.2024	−0.2008	−0.1985
	−0.207	−0.207	−0.207	−0.207	−0.207	−0.207	−0.2067	−0.2059	−0.2041	−0.2016
	−0.2101	−0.2101	−0.2101	−0.2101	−0.2101	−0.2101	−0.2098	−0.2088	−0.2069	−0.2043
	−0.2143	−0.2143	−0.2143	−0.2143	−0.2143	−0.2143	−0.214	−0.2129	−0.2108	−0.2079
	−0.2205	−0.2205	−0.2205	−0.2205	−0.2205	−0.2204	−0.2201	−0.2189	−0.2165	−0.2133
	−0.2268	−0.2268	−0.2268	−0.2268	−0.2268	−0.2268	−0.2264	−0.2249	−0.2222	−0.2186
	−0.2335	−0.2335	−0.2335	−0.2335	−0.2335	−0.2334	−0.2329	−0.2312	−0.2279	−0.2236
	−0.2575	−0.2575	−0.2575	−0.2575	−0.2575	−0.2575	−0.2567	−0.2545	−0.2505	−0.2453
	−0.2582	−0.2582	−0.2582	−0.2582	−0.2582	−0.2581	−0.2571	−0.2543	−0.2494	−0.2432

Figure I.4: F2A: e=1b & d=1.5b

	c/b									
a/b	−0.2067	−0.2067	−0.2066	−0.2066	−0.2066	−0.2064	−0.2059	−0.2048	−0.2032	−0.2012
	−0.2034	−0.2034	−0.2034	−0.2033	−0.2033	−0.2032	−0.2026	−0.2015	−0.1999	−0.1979
	−0.207	−0.207	−0.2069	−0.2069	−0.2068	−0.2066	−0.2061	−0.2049	−0.2031	−0.201
	−0.2101	−0.2101	−0.21	−0.21	−0.21	−0.2097	−0.2091	−0.2078	−0.2059	−0.2036
	−0.2143	−0.2143	−0.2142	−0.2142	−0.2141	−0.2138	−0.2131	−0.2117	−0.2096	−0.2072
	−0.2205	−0.2204	−0.2204	−0.2203	−0.2203	−0.2199	−0.2191	−0.2175	−0.2152	−0.2125
	−0.2268	−0.2268	−0.2267	−0.2267	−0.2266	−0.2262	−0.2252	−0.2233	−0.2207	−0.2177
	−0.2335	−0.2334	−0.2334	−0.2333	−0.2332	−0.2327	−0.2314	−0.2292	−0.2262	−0.2227
	−0.2575	−0.2575	−0.2574	−0.2573	−0.2572	−0.2565	−0.2548	−0.2521	−0.2485	−0.2443
	−0.2582	−0.2581	−0.2581	−0.258	−0.2578	−0.2568	−0.2546	−0.2512	−0.247	−0.242

Figure I.4: F2A: e=1b & d=2b

	c/b									
a/b	−0.2067	−0.2066	−0.2066	−0.2067	−0.2066	−0.2061	−0.2054	−0.2042	−0.2028	−0.201
	−0.2034	−0.2034	−0.2034	−0.2034	−0.2033	−0.2029	−0.2021	−0.2009	−0.1994	−0.1977
	−0.207	−0.2069	−0.2069	−0.2069	−0.2068	−0.2063	−0.2055	−0.2042	−0.2026	−0.2008
	−0.2101	−0.21	−0.21	−0.2101	−0.2099	−0.2093	−0.2084	−0.207	−0.2054	−0.2034
	−0.2143	−0.2142	−0.2142	−0.2142	−0.2141	−0.2134	−0.2124	−0.2109	−0.2091	−0.207
	−0.2204	−0.2204	−0.2204	−0.2204	−0.2202	−0.2194	−0.2182	−0.2166	−0.2146	−0.2123
	−0.2268	−0.2267	−0.2267	−0.2267	−0.2264	−0.2255	−0.2242	−0.2223	−0.2201	−0.2175
	−0.2334	−0.2334	−0.2334	−0.2333	−0.2329	−0.2318	−0.2302	−0.228	−0.2255	−0.2225
	−0.2575	−0.2574	−0.2574	−0.2573	−0.2567	−0.2554	−0.2534	−0.2507	−0.2477	−0.2441
	−0.2581	−0.2581	−0.2581	−0.2578	−0.257	−0.2553	−0.2528	−0.2496	−0.2461	−0.2419

Figure I.4: F2A: e=1b & d=2.5b

	c/b									
a/b	−0.2067	−0.2067	−0.2067	−0.2067	−0.2063	−0.2058	−0.2049	−0.2038	−0.2026	−0.201
	−0.2035	−0.2035	−0.2035	−0.2034	−0.2031	−0.2025	−0.2016	−0.2005	−0.1992	−0.1977
	−0.207	−0.207	−0.207	−0.2069	−0.2065	−0.2059	−0.205	−0.2038	−0.2024	−0.2008
	−0.2101	−0.2101	−0.2101	−0.21	−0.2096	−0.2089	−0.2079	−0.2066	−0.2051	−0.2034
	−0.2143	−0.2143	−0.2143	−0.2141	−0.2137	−0.2129	−0.2118	−0.2104	−0.2088	−0.207
	−0.2205	−0.2205	−0.2205	−0.2202	−0.2197	−0.2188	−0.2176	−0.2161	−0.2144	−0.2123
	−0.2268	−0.2269	−0.2268	−0.2265	−0.2259	−0.2249	−0.2235	−0.2218	−0.2199	−0.2176
	−0.2335	−0.2335	−0.2334	−0.233	−0.2322	−0.231	−0.2294	−0.2274	−0.2252	−0.2227
	−0.2575	−0.2575	−0.2574	−0.2569	−0.2559	−0.2544	−0.2524	−0.25	−0.2475	−0.2444
	−0.2582	−0.2582	−0.2579	−0.2572	−0.2559	−0.2541	−0.2517	−0.2489	−0.2459	−0.2424

Figure I.4: F2A: e=1b & d=3b

	c/b									
a/b	−0.2067	−0.2067	−0.2066	−0.2064	−0.206	−0.2054	−0.2045	−0.2035	−0.2024	−0.201
	−0.2035	−0.2035	−0.2034	−0.2031	−0.2027	−0.2021	−0.2012	−0.2002	−0.1991	−0.1977
	−0.207	−0.207	−0.2069	−0.2066	−0.2061	−0.2055	−0.2046	−0.2035	−0.2023	−0.2008
	−0.2101	−0.2101	−0.21	−0.2097	−0.2091	−0.2084	−0.2074	−0.2063	−0.205	−0.2034
	−0.2143	−0.2143	−0.2141	−0.2138	−0.2132	−0.2124	−0.2113	−0.2101	−0.2087	−0.207
	−0.2205	−0.2204	−0.2203	−0.2199	−0.2192	−0.2183	−0.2171	−0.2158	−0.2143	−0.2125
	−0.2268	−0.2268	−0.2266	−0.2261	−0.2253	−0.2243	−0.223	−0.2215	−0.2198	−0.2178
	−0.2335	−0.2334	−0.2331	−0.2325	−0.2316	−0.2304	−0.2289	−0.2271	−0.2252	−0.223
	−0.2575	−0.2574	−0.257	−0.2563	−0.2551	−0.2537	−0.2518	−0.2497	−0.2475	−0.2449
	−0.2582	−0.258	−0.2574	−0.2565	−0.255	−0.2533	−0.2511	−0.2487	−0.2461	−0.243

Figure I.4: F2A: e=1b & d=3.5b

	c/b									
a/b	−0.2067	−0.2066	−0.2065	−0.2062	−0.2057	−0.2051	−0.2043	−0.2034	−0.2023	−0.2011
	−0.2034	−0.2034	−0.2032	−0.2029	−0.2024	−0.2018	−0.201	−0.2	−0.199	−0.1978
	−0.207	−0.2069	−0.2067	−0.2064	−0.2058	−0.2052	−0.2043	−0.2033	−0.2022	−0.2009
	−0.2101	−0.21	−0.2098	−0.2094	−0.2088	−0.2081	−0.2072	−0.2061	−0.205	−0.2036
	−0.2143	−0.2142	−0.2139	−0.2135	−0.2129	−0.2121	−0.2111	−0.2099	−0.2087	−0.2072
	−0.2204	−0.2203	−0.22	−0.2195	−0.2188	−0.218	−0.2169	−0.2156	−0.2143	−0.2127
	−0.2268	−0.2266	−0.2263	−0.2257	−0.2249	−0.224	−0.2227	−0.2214	−0.2199	−0.2182
	−0.2334	−0.2332	−0.2328	−0.2321	−0.2312	−0.2301	−0.2286	−0.2271	−0.2254	−0.2234
	−0.2575	−0.2572	−0.2567	−0.2558	−0.2547	−0.2533	−0.2516	−0.2498	−0.2478	−0.2455
	−0.2581	−0.2577	−0.2571	−0.256	−0.2546	−0.253	−0.251	−0.2489	−0.2466	−0.2439

Figure I.4: F2A: e=1b & d=4b

	c/b									
a/b	−0.2067	−0.2066	−0.2064	−0.206	−0.2055	−0.2049	−0.2042	−0.2033	−0.2024	−0.2013
	−0.2034	−0.2033	−0.2031	−0.2027	−0.2022	−0.2016	−0.2009	−0.2	−0.1991	−0.198
	−0.2069	−0.2068	−0.2066	−0.2062	−0.2057	−0.205	−0.2042	−0.2033	−0.2023	−0.2011
	−0.2101	−0.2099	−0.2097	−0.2092	−0.2086	−0.208	−0.2071	−0.2061	−0.2051	−0.2038
	−0.2143	−0.2141	−0.2138	−0.2133	−0.2127	−0.212	−0.211	−0.21	−0.2089	−0.2076
	−0.2204	−0.2202	−0.2199	−0.2194	−0.2187	−0.2179	−0.2168	−0.2157	−0.2145	−0.2131
	−0.2268	−0.2266	−0.2262	−0.2256	−0.2248	−0.2239	−0.2227	−0.2215	−0.2202	−0.2186
	−0.2334	−0.2331	−0.2327	−0.232	−0.231	−0.23	−0.2287	−0.2273	−0.2258	−0.224
	−0.2574	−0.2571	−0.2565	−0.2557	−0.2545	−0.2533	−0.2518	−0.2501	−0.2484	−0.2463
	−0.2581	−0.2576	−0.2569	−0.2559	−0.2545	−0.2531	−0.2513	−0.2494	−0.2474	−0.245

Figure I.4: F2A: e=1.5b & d=0.5b

	c/b									
	−0.2421	−0.2421	−0.2421	−0.2421	−0.242	−0.2421	−0.242	−0.242	−0.2411	−0.2383
	−0.2396	−0.2396	−0.2396	−0.2396	−0.2396	−0.2396	−0.2395	−0.2395	−0.2385	−0.2357
	−0.24	−0.24	−0.24	−0.24	−0.24	−0.24	−0.2399	−0.2399	−0.2389	−0.236
	−0.2395	−0.2395	−0.2395	−0.2395	−0.2395	−0.2395	−0.2395	−0.2394	−0.2384	−0.2353
a/b	−0.2452	−0.2452	−0.2452	−0.2452	−0.2452	−0.2452	−0.2451	−0.2451	−0.2439	−0.2406
	−0.2514	−0.2514	−0.2514	−0.2514	−0.2514	−0.2514	−0.2513	−0.2513	−0.25	−0.2463
	−0.2575	−0.2575	−0.2575	−0.2575	−0.2575	−0.2574	−0.2574	−0.2573	−0.2559	−0.2518
	−0.2612	−0.2612	−0.2612	−0.2612	−0.2612	−0.2612	−0.2612	−0.2611	−0.2594	−0.2549
	−0.2765	−0.2765	−0.2765	−0.2765	−0.2765	−0.2765	−0.2764	−0.2763	−0.2744	−0.2693
	−0.2758	−0.2758	−0.2758	−0.2758	−0.2758	−0.2758	−0.2758	−0.2756	−0.2734	−0.2676

Figure I.4: F2A: e=1.5b & d=1b

	c/b									
	−0.2421	−0.2421	−0.2421	−0.2421	−0.2421	−0.2421	−0.2418	−0.241	−0.2393	−0.2369
	−0.2396	−0.2396	−0.2396	−0.2396	−0.2396	−0.2395	−0.2393	−0.2384	−0.2367	−0.2343
	−0.24	−0.24	−0.24	−0.24	−0.24	−0.24	−0.2397	−0.2388	−0.237	−0.2345
	−0.2395	−0.2395	−0.2395	−0.2395	−0.2395	−0.2395	−0.2392	−0.2382	−0.2363	−0.2337
a/b	−0.2452	−0.2452	−0.2452	−0.2452	−0.2452	−0.2451	−0.2448	−0.2437	−0.2416	−0.2388
	−0.2514	−0.2514	−0.2514	−0.2514	−0.2514	−0.2513	−0.251	−0.2498	−0.2474	−0.2443
	−0.2575	−0.2575	−0.2575	−0.2575	−0.2575	−0.2574	−0.257	−0.2556	−0.253	−0.2496
	−0.2612	−0.2612	−0.2612	−0.2612	−0.2612	−0.2612	−0.2607	−0.2591	−0.2562	−0.2524
	−0.2765	−0.2765	−0.2765	−0.2765	−0.2765	−0.2764	−0.2758	−0.2741	−0.2708	−0.2665
	−0.2758	−0.2758	−0.2758	−0.2758	−0.2758	−0.2757	−0.2751	−0.2729	−0.2692	−0.2644

Figure I.4: F2A: e=1.5b & d=1.5b

	c/b									
	−0.2421	−0.2421	−0.242	−0.242	−0.242	−0.2418	−0.2412	−0.24	−0.2383	−0.2362
	−0.2396	−0.2395	−0.2395	−0.2395	−0.2394	−0.2392	−0.2386	−0.2374	−0.2357	−0.2336
	−0.24	−0.24	−0.2399	−0.2399	−0.2399	−0.2396	−0.239	−0.2377	−0.2359	−0.2338
	−0.2395	−0.2395	−0.2395	−0.2394	−0.2394	−0.2391	−0.2384	−0.2371	−0.2352	−0.2329
a/b	−0.2452	−0.2452	−0.2451	−0.2451	−0.245	−0.2447	−0.2439	−0.2424	−0.2404	−0.2379
	−0.2514	−0.2514	−0.2513	−0.2513	−0.2512	−0.2508	−0.2499	−0.2483	−0.2461	−0.2434
	−0.2575	−0.2574	−0.2574	−0.2573	−0.2573	−0.2568	−0.2558	−0.254	−0.2516	−0.2486
	−0.2612	−0.2612	−0.2611	−0.2611	−0.261	−0.2605	−0.2593	−0.2573	−0.2546	−0.2513
	−0.2765	−0.2765	−0.2764	−0.2764	−0.2762	−0.2756	−0.2743	−0.2719	−0.2689	−0.2653
	−0.2758	−0.2758	−0.2758	−0.2757	−0.2755	−0.2748	−0.2731	−0.2705	−0.2671	−0.263

Figure I.4: F2A: e=1.5b & d=2b

	c/b									
	−0.2421	−0.242	−0.242	−0.2421	−0.2419	−0.2414	−0.2405	−0.2393	−0.2378	−0.2359
	−0.2395	−0.2395	−0.2395	−0.2395	−0.2394	−0.2388	−0.238	−0.2367	−0.2352	−0.2333
	−0.24	−0.2399	−0.2399	−0.2399	−0.2398	−0.2392	−0.2383	−0.237	−0.2354	−0.2335
	−0.2395	−0.2395	−0.2395	−0.2395	−0.2393	−0.2387	−0.2377	−0.2363	−0.2346	−0.2326
a/b	−0.2452	−0.2451	−0.2451	−0.2451	−0.2449	−0.2442	−0.2431	−0.2416	−0.2398	−0.2376
	−0.2514	−0.2513	−0.2513	−0.2513	−0.251	−0.2502	−0.249	−0.2474	−0.2454	−0.2431
	−0.2574	−0.2574	−0.2574	−0.2573	−0.257	−0.2561	−0.2548	−0.253	−0.2508	−0.2483
	−0.2612	−0.2612	−0.2611	−0.2611	−0.2606	−0.2597	−0.2582	−0.2561	−0.2538	−0.251
	−0.2765	−0.2764	−0.2764	−0.2763	−0.2758	−0.2747	−0.2729	−0.2707	−0.2681	−0.2649
	−0.2758	−0.2758	−0.2757	−0.2756	−0.2749	−0.2736	−0.2716	−0.269	−0.2661	−0.2626

Figure I.4: F2A: e=1.5b & d=2.5b

	c/b									
	−0.2421	−0.2421	−0.2421	−0.242	−0.2416	−0.241	−0.24	−0.2389	−0.2375	−0.2358
	−0.2396	−0.2396	−0.2396	−0.2394	−0.239	−0.2384	−0.2375	−0.2363	−0.2349	−0.2332
	−0.24	−0.24	−0.24	−0.2398	−0.2394	−0.2387	−0.2378	−0.2366	−0.2351	−0.2334
	−0.2395	−0.2396	−0.2395	−0.2393	−0.2389	−0.2382	−0.2371	−0.2358	−0.2343	−0.2325
a/b	−0.2452	−0.2452	−0.2451	−0.2449	−0.2444	−0.2436	−0.2425	−0.2411	−0.2395	−0.2376
	−0.2514	−0.2514	−0.2513	−0.2511	−0.2505	−0.2496	−0.2484	−0.2468	−0.2451	−0.243
	−0.2575	−0.2575	−0.2574	−0.2571	−0.2564	−0.2555	−0.2541	−0.2524	−0.2505	−0.2483
	−0.2612	−0.2612	−0.2611	−0.2608	−0.26	−0.2589	−0.2574	−0.2555	−0.2534	−0.251
	−0.2765	−0.2765	−0.2764	−0.2759	−0.275	−0.2738	−0.272	−0.27	−0.2677	−0.265
	−0.2758	−0.2758	−0.2756	−0.2751	−0.274	−0.2726	−0.2706	−0.2683	−0.2657	−0.2627

Figure I.4: F2A: e=1.5b & d=3b

	c/b									
	−0.2421	−0.2421	−0.242	−0.2417	−0.2412	−0.2406	−0.2396	−0.2385	−0.2373	−0.2358
	−0.2396	−0.2395	−0.2394	−0.2391	−0.2386	−0.238	−0.237	−0.2359	−0.2347	−0.2332
	−0.24	−0.24	−0.2398	−0.2395	−0.239	−0.2383	−0.2374	−0.2362	−0.235	−0.2335
	−0.2395	−0.2395	−0.2394	−0.239	−0.2385	−0.2377	−0.2367	−0.2355	−0.2342	−0.2326
a/b	−0.2452	−0.2451	−0.245	−0.2446	−0.244	−0.2432	−0.242	−0.2408	−0.2393	−0.2376
	−0.2514	−0.2513	−0.2511	−0.2507	−0.25	−0.2491	−0.2479	−0.2465	−0.245	−0.2431
	−0.2575	−0.2574	−0.2572	−0.2567	−0.2559	−0.2549	−0.2536	−0.252	−0.2504	−0.2484
	−0.2612	−0.2611	−0.2609	−0.2603	−0.2594	−0.2583	−0.2568	−0.2551	−0.2533	−0.2511
	−0.2765	−0.2764	−0.276	−0.2754	−0.2744	−0.2731	−0.2715	−0.2696	−0.2676	−0.2652
	−0.2758	−0.2757	−0.2753	−0.2745	−0.2733	−0.2719	−0.27	−0.2679	−0.2657	−0.263

Figure I.4: F2A: e=1.5b & d=3.5b

	c/b									
	−0.2421	−0.242	−0.2418	−0.2415	−0.2409	−0.2403	−0.2394	−0.2384	−0.2373	−0.2359
	−0.2395	−0.2395	−0.2393	−0.2389	−0.2384	−0.2377	−0.2368	−0.2358	−0.2347	−0.2333
	−0.24	−0.2399	−0.2397	−0.2393	−0.2387	−0.238	−0.2371	−0.2361	−0.2349	−0.2336
	−0.2395	−0.2394	−0.2392	−0.2388	−0.2382	−0.2374	−0.2364	−0.2353	−0.2341	−0.2327
a/b	−0.2452	−0.245	−0.2448	−0.2443	−0.2436	−0.2428	−0.2418	−0.2406	−0.2393	−0.2378
	−0.2514	−0.2512	−0.2509	−0.2504	−0.2497	−0.2488	−0.2477	−0.2464	−0.245	−0.2433
	−0.2574	−0.2573	−0.2569	−0.2563	−0.2555	−0.2546	−0.2533	−0.2519	−0.2504	−0.2487
	−0.2612	−0.261	−0.2606	−0.2599	−0.259	−0.258	−0.2566	−0.2551	−0.2534	−0.2515
	−0.2764	−0.2762	−0.2758	−0.275	−0.274	−0.2728	−0.2713	−0.2696	−0.2678	−0.2657
	−0.2758	−0.2755	−0.275	−0.2741	−0.2729	−0.2715	−0.2698	−0.2679	−0.266	−0.2636

Figure I.4: F2A: e=1.5b & d=4b

	c/b									
	−0.2421	−0.2419	−0.2417	−0.2413	−0.2408	−0.2401	−0.2393	−0.2384	−0.2373	−0.2361
	−0.2395	−0.2394	−0.2392	−0.2387	−0.2382	−0.2375	−0.2367	−0.2358	−0.2348	−0.2335
	−0.2399	−0.2398	−0.2396	−0.2391	−0.2386	−0.2379	−0.237	−0.2361	−0.2351	−0.2338
	−0.2395	−0.2393	−0.2391	−0.2386	−0.238	−0.2373	−0.2364	−0.2354	−0.2343	−0.233
a/b	−0.2451	−0.245	−0.2447	−0.2442	−0.2435	−0.2427	−0.2417	−0.2407	−0.2395	−0.2381
	−0.2513	−0.2511	−0.2508	−0.2502	−0.2495	−0.2487	−0.2476	−0.2464	−0.2452	−0.2437
	−0.2574	−0.2572	−0.2568	−0.2562	−0.2554	−0.2545	−0.2533	−0.252	−0.2507	−0.2491
	−0.2612	−0.2609	−0.2605	−0.2598	−0.2589	−0.2579	−0.2566	−0.2552	−0.2537	−0.252
	−0.2764	−0.2761	−0.2756	−0.2749	−0.2738	−0.2727	−0.2713	−0.2698	−0.2682	−0.2663
	−0.2757	−0.2754	−0.2748	−0.2739	−0.2728	−0.2715	−0.2699	−0.2683	−0.2665	−0.2644

Figure I.4: F2A: e=2b & d=0.5b

	c/b									
a/b	−0.2645	−0.2645	−0.2645	−0.2645	−0.2644	−0.2645	−0.2645	−0.2644	−0.2635	−0.2609
	−0.2631	−0.2631	−0.2631	−0.2631	−0.2631	−0.2631	−0.263	−0.263	−0.2621	−0.2594
	−0.2633	−0.2633	−0.2633	−0.2633	−0.2633	−0.2633	−0.2633	−0.2632	−0.2623	−0.2595
	−0.2607	−0.2607	−0.2607	−0.2607	−0.2607	−0.2607	−0.2607	−0.2607	−0.2597	−0.2568
	−0.2632	−0.2632	−0.2632	−0.2632	−0.2632	−0.2632	−0.2631	−0.2631	−0.262	−0.259
	−0.2674	−0.2674	−0.2674	−0.2674	−0.2674	−0.2674	−0.2674	−0.2673	−0.2662	−0.263
	−0.2737	−0.2737	−0.2737	−0.2737	−0.2737	−0.2737	−0.2736	−0.2735	−0.2723	−0.2688
	−0.2782	−0.2782	−0.2782	−0.2782	−0.2782	−0.2782	−0.2782	−0.2781	−0.2767	−0.2729
	−0.2904	−0.2904	−0.2904	−0.2904	−0.2904	−0.2903	−0.2903	−0.2902	−0.2886	−0.2845
	−0.2899	−0.2899	−0.2899	−0.2898	−0.2898	−0.2898	−0.2898	−0.2897	−0.2879	−0.2834

Figure I.4: F2A: e=2b & d=1b

	c/b									
a/b	−0.2645	−0.2645	−0.2645	−0.2645	−0.2645	−0.2645	−0.2642	−0.2634	−0.2618	−0.2595
	−0.2631	−0.2631	−0.2631	−0.2631	−0.2631	−0.263	−0.2628	−0.2619	−0.2602	−0.2579
	−0.2633	−0.2633	−0.2633	−0.2633	−0.2633	−0.2633	−0.263	−0.2621	−0.2604	−0.258
	−0.2607	−0.2607	−0.2607	−0.2607	−0.2607	−0.2607	−0.2604	−0.2595	−0.2577	−0.2552
	−0.2632	−0.2632	−0.2632	−0.2632	−0.2632	−0.2631	−0.2628	−0.2618	−0.2599	−0.2573
	−0.2674	−0.2674	−0.2674	−0.2674	−0.2674	−0.2674	−0.2671	−0.266	−0.2639	−0.2611
	−0.2737	−0.2737	−0.2737	−0.2737	−0.2737	−0.2736	−0.2732	−0.272	−0.2698	−0.2667
	−0.2782	−0.2782	−0.2782	−0.2782	−0.2782	−0.2782	−0.2777	−0.2764	−0.2739	−0.2706
	−0.2904	−0.2904	−0.2904	−0.2904	−0.2904	−0.2903	−0.2898	−0.2883	−0.2856	−0.282
	−0.2899	−0.2899	−0.2899	−0.2898	−0.2898	−0.2898	−0.2892	−0.2876	−0.2846	−0.2806

Figure I.4: F2A: e=2b & d=1.5b

	c/b									
a/b	−0.2645	−0.2645	−0.2645	−0.2644	−0.2644	−0.2642	−0.2636	−0.2624	−0.2607	−0.2587
	−0.2631	−0.2631	−0.263	−0.263	−0.2629	−0.2627	−0.2621	−0.2609	−0.2592	−0.2571
	−0.2633	−0.2633	−0.2632	−0.2632	−0.2632	−0.2629	−0.2623	−0.261	−0.2593	−0.2572
	−0.2607	−0.2607	−0.2607	−0.2607	−0.2606	−0.2603	−0.2596	−0.2584	−0.2566	−0.2544
	−0.2632	−0.2631	−0.2631	−0.2631	−0.263	−0.2627	−0.262	−0.2606	−0.2587	−0.2564
	−0.2674	−0.2674	−0.2674	−0.2673	−0.2673	−0.2669	−0.2661	−0.2646	−0.2626	−0.2602
	−0.2737	−0.2736	−0.2736	−0.2736	−0.2735	−0.2731	−0.2722	−0.2706	−0.2684	−0.2657
	−0.2782	−0.2782	−0.2782	−0.2781	−0.278	−0.2776	−0.2765	−0.2748	−0.2724	−0.2695
	−0.2904	−0.2903	−0.2903	−0.2902	−0.2901	−0.2896	−0.2885	−0.2865	−0.2839	−0.2808
	−0.2898	−0.2898	−0.2898	−0.2897	−0.2896	−0.289	−0.2877	−0.2855	−0.2827	−0.2792

Figure I.4: F2A: e=2b & d=2b

	c/b									
a/b	−0.2645	−0.2645	−0.2645	−0.2645	−0.2643	−0.2638	−0.2629	−0.2617	−0.2602	−0.2584
	−0.2631	−0.263	−0.263	−0.263	−0.2628	−0.2623	−0.2614	−0.2602	−0.2587	−0.2568
	−0.2633	−0.2632	−0.2632	−0.2632	−0.263	−0.2625	−0.2616	−0.2603	−0.2588	−0.2569
	−0.2607	−0.2607	−0.2607	−0.2607	−0.2605	−0.2599	−0.2589	−0.2576	−0.256	−0.254
	−0.2632	−0.2631	−0.2631	−0.2631	−0.2628	−0.2622	−0.2612	−0.2598	−0.2581	−0.256
	−0.2674	−0.2674	−0.2674	−0.2673	−0.2671	−0.2664	−0.2653	−0.2637	−0.2619	−0.2597
	−0.2736	−0.2736	−0.2736	−0.2735	−0.2732	−0.2724	−0.2712	−0.2696	−0.2676	−0.2653
	−0.2782	−0.2782	−0.2782	−0.2781	−0.2777	−0.2768	−0.2755	−0.2737	−0.2716	−0.269
	−0.2903	−0.2903	−0.2903	−0.2902	−0.2897	−0.2888	−0.2873	−0.2853	−0.283	−0.2803
	−0.2898	−0.2898	−0.2898	−0.2896	−0.2891	−0.288	−0.2864	−0.2842	−0.2817	−0.2787

Figure I.4: F2A: e=2b & d=2.5b

	c/b									
a/b	−0.2645	−0.2645	−0.2645	−0.2643	−0.264	−0.2633	−0.2624	−0.2612	−0.2599	−0.2582
	−0.2631	−0.2631	−0.2631	−0.2629	−0.2625	−0.2618	−0.2609	−0.2597	−0.2583	−0.2567
	−0.2633	−0.2633	−0.2633	−0.2631	−0.2627	−0.262	−0.261	−0.2598	−0.2584	−0.2568
	−0.2607	−0.2608	−0.2607	−0.2605	−0.2601	−0.2594	−0.2584	−0.2571	−0.2556	−0.2539
	−0.2632	−0.2632	−0.2631	−0.2629	−0.2624	−0.2617	−0.2606	−0.2593	−0.2578	−0.2559
	−0.2674	−0.2674	−0.2674	−0.2671	−0.2666	−0.2658	−0.2646	−0.2632	−0.2616	−0.2596
	−0.2737	−0.2737	−0.2736	−0.2733	−0.2727	−0.2718	−0.2705	−0.269	−0.2673	−0.2652
	−0.2782	−0.2782	−0.2781	−0.2778	−0.2771	−0.2761	−0.2747	−0.2731	−0.2712	−0.2689
	−0.2904	−0.2903	−0.2902	−0.2898	−0.2891	−0.288	−0.2865	−0.2846	−0.2826	−0.2802
	−0.2899	−0.2898	−0.2897	−0.2892	−0.2884	−0.2872	−0.2855	−0.2835	−0.2813	−0.2786

Figure I.4: F2A: e=2b & d=3b

	c/b									
a/b	−0.2645	−0.2645	−0.2644	−0.2641	−0.2636	−0.2629	−0.262	−0.2609	−0.2597	−0.2582
	−0.2631	−0.263	−0.2629	−0.2626	−0.2621	−0.2614	−0.2605	−0.2594	−0.2582	−0.2567
	−0.2633	−0.2633	−0.2631	−0.2628	−0.2623	−0.2616	−0.2606	−0.2595	−0.2583	−0.2568
	−0.2607	−0.2607	−0.2606	−0.2602	−0.2597	−0.2589	−0.2579	−0.2568	−0.2555	−0.2539
	−0.2632	−0.2631	−0.263	−0.2626	−0.262	−0.2612	−0.2602	−0.2589	−0.2576	−0.2559
	−0.2674	−0.2674	−0.2672	−0.2668	−0.2661	−0.2653	−0.2642	−0.2629	−0.2614	−0.2597
	−0.2737	−0.2736	−0.2734	−0.2729	−0.2722	−0.2713	−0.2701	−0.2686	−0.2671	−0.2652
	−0.2782	−0.2781	−0.2779	−0.2774	−0.2766	−0.2756	−0.2742	−0.2727	−0.271	−0.269
	−0.2903	−0.2902	−0.29	−0.2894	−0.2885	−0.2874	−0.2859	−0.2843	−0.2825	−0.2803
	−0.2898	−0.2897	−0.2894	−0.2887	−0.2877	−0.2865	−0.2849	−0.2831	−0.2811	−0.2788

Figure I.4: F2A: e=2b & d=3.5b

	c/b									
a/b	−0.2645	−0.2644	−0.2642	−0.2638	−0.2633	−0.2626	−0.2618	−0.2607	−0.2596	−0.2583
	−0.2631	−0.263	−0.2628	−0.2624	−0.2618	−0.2611	−0.2603	−0.2592	−0.2581	−0.2568
	−0.2633	−0.2632	−0.263	−0.2626	−0.262	−0.2613	−0.2604	−0.2594	−0.2582	−0.2569
	−0.2607	−0.2606	−0.2604	−0.26	−0.2594	−0.2586	−0.2577	−0.2566	−0.2554	−0.254
	−0.2631	−0.263	−0.2628	−0.2623	−0.2617	−0.2609	−0.2599	−0.2588	−0.2576	−0.2561
	−0.2674	−0.2673	−0.267	−0.2665	−0.2658	−0.265	−0.2639	−0.2627	−0.2614	−0.2598
	−0.2736	−0.2735	−0.2732	−0.2726	−0.2719	−0.271	−0.2698	−0.2685	−0.2671	−0.2654
	−0.2782	−0.278	−0.2777	−0.2771	−0.2762	−0.2753	−0.274	−0.2726	−0.2711	−0.2692
	−0.2903	−0.2901	−0.2897	−0.2891	−0.2881	−0.2871	−0.2857	−0.2842	−0.2825	−0.2806
	−0.2898	−0.2896	−0.2891	−0.2884	−0.2873	−0.2862	−0.2847	−0.283	−0.2813	−0.2792

Figure I.4: F2A: e=2b & d=4b

	c/b									
a/b	−0.2645	−0.2644	−0.2641	−0.2637	−0.2631	−0.2625	−0.2617	−0.2607	−0.2597	−0.2585
	−0.263	−0.2629	−0.2626	−0.2622	−0.2617	−0.261	−0.2602	−0.2592	−0.2582	−0.257
	−0.2633	−0.2631	−0.2629	−0.2624	−0.2618	−0.2612	−0.2603	−0.2594	−0.2583	−0.2571
	−0.2607	−0.2606	−0.2603	−0.2598	−0.2592	−0.2585	−0.2576	−0.2566	−0.2555	−0.2543
	−0.2631	−0.263	−0.2627	−0.2622	−0.2615	−0.2608	−0.2599	−0.2588	−0.2577	−0.2564
	−0.2674	−0.2672	−0.2669	−0.2664	−0.2657	−0.2649	−0.2639	−0.2628	−0.2616	−0.2602
	−0.2736	−0.2734	−0.273	−0.2725	−0.2717	−0.2709	−0.2698	−0.2686	−0.2673	−0.2658
	−0.2782	−0.2779	−0.2775	−0.2769	−0.2761	−0.2752	−0.274	−0.2727	−0.2713	−0.2697
	−0.2903	−0.29	−0.2896	−0.2889	−0.288	−0.287	−0.2857	−0.2843	−0.2828	−0.2811
	−0.2898	−0.2895	−0.289	−0.2882	−0.2872	−0.2861	−0.2847	−0.2832	−0.2816	−0.2797

Figure I.4: F2A: e=2.5b & d=0.5b

	c/b									
	−0.2796	−0.2796	−0.2796	−0.2796	−0.2796	−0.2796	−0.2795	−0.2795	−0.2787	−0.2763
	−0.279	−0.279	−0.279	−0.279	−0.279	−0.279	−0.2789	−0.279	−0.2781	−0.2757
	−0.2796	−0.2796	−0.2796	−0.2796	−0.2796	−0.2796	−0.2796	−0.2796	−0.2787	−0.2762
	−0.2765	−0.2765	−0.2765	−0.2765	−0.2765	−0.2765	−0.2765	−0.2764	−0.2755	−0.273
a/b	−0.2774	−0.2774	−0.2774	−0.2774	−0.2774	−0.2774	−0.2774	−0.2773	−0.2763	−0.2737
	−0.2795	−0.2795	−0.2795	−0.2795	−0.2795	−0.2795	−0.2794	−0.2794	−0.2784	−0.2756
	−0.2832	−0.2832	−0.2832	−0.2832	−0.2832	−0.2832	−0.2832	−0.2831	−0.282	−0.2791
	−0.2863	−0.2863	−0.2863	−0.2862	−0.2863	−0.2863	−0.2863	−0.2862	−0.285	−0.2819
	−0.2978	−0.2978	−0.2978	−0.2978	−0.2978	−0.2978	−0.2978	−0.2977	−0.2964	−0.293
	−0.2981	−0.2981	−0.2981	−0.2981	−0.2981	−0.298	−0.298	−0.2979	−0.2965	−0.2929

Figure I.4: F2A: e=2.5b & d=1b

	c/b									
	−0.2796	−0.2796	−0.2796	−0.2796	−0.2796	−0.2796	−0.2793	−0.2785	−0.277	−0.2749
	−0.279	−0.279	−0.279	−0.279	−0.279	−0.279	−0.2788	−0.278	−0.2764	−0.2742
	−0.2796	−0.2796	−0.2796	−0.2796	−0.2796	−0.2796	−0.2794	−0.2785	−0.2769	−0.2747
	−0.2765	−0.2765	−0.2765	−0.2765	−0.2765	−0.2765	−0.2762	−0.2754	−0.2737	−0.2714
a/b	−0.2774	−0.2774	−0.2774	−0.2774	−0.2774	−0.2774	−0.2771	−0.2762	−0.2744	−0.272
	−0.2795	−0.2795	−0.2795	−0.2795	−0.2795	−0.2794	−0.2791	−0.2782	−0.2763	−0.2738
	−0.2832	−0.2832	−0.2832	−0.2832	−0.2832	−0.2832	−0.2829	−0.2818	−0.2799	−0.2772
	−0.2863	−0.2863	−0.2862	−0.2863	−0.2862	−0.2862	−0.2859	−0.2848	−0.2827	−0.2798
	−0.2978	−0.2978	−0.2978	−0.2978	−0.2978	−0.2977	−0.2973	−0.2961	−0.2939	−0.2908
	−0.2981	−0.2981	−0.2981	−0.2981	−0.2981	−0.298	−0.2975	−0.2962	−0.2938	−0.2905

Figure I.4: F2A: e=2.5b & d=1.5b

	c/b									
	−0.2796	−0.2796	−0.2796	−0.2795	−0.2795	−0.2792	−0.2787	−0.2776	−0.276	−0.2741
	−0.279	−0.279	−0.279	−0.279	−0.2789	−0.2787	−0.2781	−0.2769	−0.2754	−0.2734
	−0.2796	−0.2796	−0.2796	−0.2796	−0.2795	−0.2793	−0.2786	−0.2775	−0.2759	−0.2739
	−0.2765	−0.2765	−0.2765	−0.2764	−0.2764	−0.2761	−0.2755	−0.2743	−0.2726	−0.2706
a/b	−0.2774	−0.2774	−0.2773	−0.2773	−0.2773	−0.277	−0.2763	−0.275	−0.2733	−0.2712
	−0.2795	−0.2795	−0.2794	−0.2794	−0.2793	−0.279	−0.2783	−0.277	−0.2752	−0.2729
	−0.2832	−0.2832	−0.2832	−0.2831	−0.2831	−0.2827	−0.2819	−0.2805	−0.2786	−0.2762
	−0.2862	−0.2863	−0.2862	−0.2858	−0.2861	−0.2857	−0.2848	−0.2833	−0.2813	−0.2788
	−0.2978	−0.2978	−0.2977	−0.2977	−0.2976	−0.2972	−0.2962	−0.2945	−0.2924	−0.2897
	−0.298	−0.298	−0.298	−0.298	−0.2979	−0.2974	−0.2963	−0.2945	−0.2921	−0.2892

Figure I.4: F2A: e=2.5b & d=2b

	c/b									
	−0.2796	−0.2796	−0.2796	−0.2795	−0.2793	−0.2788	−0.278	−0.2769	−0.2755	−0.2737
	−0.279	−0.279	−0.279	−0.279	−0.2788	−0.2783	−0.2774	−0.2762	−0.2748	−0.2731
	−0.2796	−0.2796	−0.2796	−0.2796	−0.2794	−0.2788	−0.278	−0.2768	−0.2753	−0.2735
	−0.2765	−0.2765	−0.2765	−0.2764	−0.2762	−0.2757	−0.2748	−0.2735	−0.272	−0.2702
a/b	−0.2774	−0.2773	−0.2773	−0.2773	−0.2771	−0.2765	−0.2755	−0.2742	−0.2727	−0.2708
	−0.2795	−0.2794	−0.2794	−0.2794	−0.2791	−0.2785	−0.2775	−0.2761	−0.2745	−0.2725
	−0.2832	−0.2832	−0.2832	−0.2831	−0.2828	−0.2821	−0.2811	−0.2796	−0.2779	−0.2758
	−0.2863	−0.2863	−0.2864	−0.2861	−0.2858	−0.2851	−0.2839	−0.2824	−0.2805	−0.2783
	−0.2978	−0.2978	−0.2977	−0.2976	−0.2973	−0.2965	−0.2952	−0.2935	−0.2915	−0.2891
	−0.298	−0.298	−0.298	−0.2979	−0.2974	−0.2965	−0.2952	−0.2933	−0.2912	−0.2886

Figure I.4: F2A: e=2.5b & d=2.5b

	c/b									
	−0.2796	−0.2796	−0.2796	−0.2794	−0.279	−0.2784	−0.2775	−0.2764	−0.2751	−0.2736
	−0.279	−0.279	−0.279	−0.2788	−0.2784	−0.2778	−0.2769	−0.2758	−0.2745	−0.2729
	−0.2796	−0.2796	−0.2796	−0.2794	−0.279	−0.2784	−0.2775	−0.2763	−0.275	−0.2734
	−0.2765	−0.2765	−0.2765	−0.2763	−0.2759	−0.2752	−0.2742	−0.273	−0.2717	−0.27
a/b	−0.2774	−0.2774	−0.2773	−0.2771	−0.2767	−0.276	−0.275	−0.2737	−0.2723	−0.2706
	−0.2795	−0.2795	−0.2794	−0.2792	−0.2787	−0.278	−0.2769	−0.2756	−0.2741	−0.2723
	−0.2832	−0.2832	−0.2832	−0.2829	−0.2824	−0.2816	−0.2804	−0.2791	−0.2775	−0.2756
	−0.2863	−0.2864	−0.2863	−0.2859	−0.2853	−0.2845	−0.2832	−0.2818	−0.2801	−0.2781
	−0.2978	−0.2978	−0.2977	−0.2973	−0.2967	−0.2958	−0.2945	−0.2929	−0.2911	−0.2889
	−0.2981	−0.298	−0.2979	−0.2975	−0.2968	−0.2958	−0.2944	−0.2926	−0.2907	−0.2884

Figure I.4: F2A: e=2.5b & d=3b

	c/b									
	−0.2796	−0.2796	−0.2794	−0.2792	−0.2787	−0.278	−0.2771	−0.2761	−0.2749	−0.2735
	−0.279	−0.279	−0.2789	−0.2786	−0.2781	−0.2774	−0.2765	−0.2755	−0.2743	−0.2729
	−0.2796	−0.2796	−0.2795	−0.2792	−0.2786	−0.278	−0.2771	−0.276	−0.2748	−0.2733
	−0.2765	−0.2765	−0.2763	−0.276	−0.2755	−0.2748	−0.2738	−0.2727	−0.2715	−0.27
a/b	−0.2774	−0.2773	−0.2772	−0.2768	−0.2763	−0.2755	−0.2746	−0.2734	−0.2721	−0.2706
	−0.2795	−0.2794	−0.2792	−0.2789	−0.2783	−0.2775	−0.2765	−0.2753	−0.2739	−0.2723
	−0.2832	−0.2832	−0.283	−0.2826	−0.2819	−0.2811	−0.28	−0.2787	−0.2773	−0.2756
	−0.2863	−0.2814	−0.2859	−0.2856	−0.2848	−0.284	−0.2828	−0.2814	−0.2799	−0.2781
	−0.2978	−0.2977	−0.2974	−0.297	−0.2962	−0.2952	−0.294	−0.2925	−0.2909	−0.289
	−0.298	−0.2979	−0.2977	−0.2971	−0.2963	−0.2952	−0.2938	−0.2923	−0.2905	−0.2885

Figure I.4: F2A: e=2.5b & d=3.5b

	c/b									
	−0.2796	−0.2795	−0.2793	−0.2789	−0.2784	−0.2778	−0.2769	−0.276	−0.2749	−0.2736
	−0.279	−0.2789	−0.2787	−0.2784	−0.2778	−0.2772	−0.2763	−0.2753	−0.2742	−0.2729
	−0.2796	−0.2795	−0.2793	−0.2789	−0.2784	−0.2777	−0.2768	−0.2758	−0.2748	−0.2734
	−0.2765	−0.2764	−0.2762	−0.2758	−0.2752	−0.2745	−0.2736	−0.2726	−0.2714	−0.2701
a/b	−0.2774	−0.2772	−0.277	−0.2766	−0.276	−0.2753	−0.2743	−0.2733	−0.2721	−0.2707
	−0.2795	−0.2793	−0.2791	−0.2786	−0.278	−0.2772	−0.2762	−0.2751	−0.2739	−0.2724
	−0.2832	−0.2831	−0.2828	−0.2823	−0.2816	−0.2808	−0.2798	−0.2786	−0.2773	−0.2758
	−0.2862	−0.2882	−0.2858	−0.2853	−0.2845	−0.2837	−0.2825	−0.2813	−0.2799	−0.2783
	−0.2978	−0.2976	−0.2972	−0.2967	−0.2959	−0.2949	−0.2937	−0.2924	−0.2909	−0.2892
	−0.298	−0.2978	−0.2974	−0.2968	−0.2959	−0.2949	−0.2936	−0.2921	−0.2906	−0.2887

Figure I.4: F2A: e=2.5b & d=4b

	c/b									
	−0.2796	−0.2794	−0.2792	−0.2788	−0.2783	−0.2776	−0.2768	−0.2759	−0.275	−0.2738
	−0.279	−0.2789	−0.2786	−0.2782	−0.2777	−0.277	−0.2762	−0.2753	−0.2743	−0.2731
	−0.2796	−0.2795	−0.2792	−0.2788	−0.2782	−0.2776	−0.2768	−0.2758	−0.2748	−0.2736
	−0.2765	−0.2763	−0.2761	−0.2756	−0.2751	−0.2744	−0.2735	−0.2726	−0.2715	−0.2703
a/b	−0.2773	−0.2772	−0.2769	−0.2765	−0.2758	−0.2752	−0.2743	−0.2733	−0.2722	−0.2709
	−0.2794	−0.2793	−0.279	−0.2785	−0.2778	−0.2771	−0.2762	−0.2751	−0.274	−0.2727
	−0.2832	−0.283	−0.2827	−0.2822	−0.2815	−0.2807	−0.2797	−0.2786	−0.2775	−0.2761
	−0.2862	−0.2859	−0.2854	−0.2851	−0.2844	−0.2836	−0.2825	−0.2813	−0.2805	−0.2786
	−0.2977	−0.2975	−0.2971	−0.2965	−0.2957	−0.2948	−0.2937	−0.2925	−0.2911	−0.2896
	−0.298	−0.2977	−0.2973	−0.2967	−0.2958	−0.2948	−0.2936	−0.2923	−0.2908	−0.2891

Figure I.4: F2A: e=3b & d=0.5b

	c/b									
	−0.2902	−0.2902	−0.2902	−0.2902	−0.2902	−0.2902	−0.2889	−0.2901	−0.2894	−0.2872
	−0.2903	−0.2903	−0.2903	−0.2903	−0.2903	−0.2903	−0.2903	−0.2902	−0.2895	−0.2873
	−0.2913	−0.2913	−0.2913	−0.2913	−0.2913	−0.2913	−0.2913	−0.2913	−0.2905	−0.2882
	−0.2882	−0.2882	−0.2882	−0.2882	−0.2882	−0.2882	−0.2882	−0.2881	−0.2873	−0.285
a/b	−0.2885	−0.2885	−0.2885	−0.2885	−0.2885	−0.2884	−0.2884	−0.2884	−0.2875	−0.2852
	−0.2895	−0.2895	−0.2895	−0.2895	−0.2895	−0.2895	−0.2895	−0.2894	−0.2885	−0.2861
	−0.2915	−0.2915	−0.2915	−0.2915	−0.2915	−0.2915	−0.2914	−0.2914	−0.2905	−0.2879
	−0.2925	−0.2925	−0.2925	−0.2925	−0.2925	−0.2925	−0.2925	−0.2924	−0.2914	−0.2888
	−0.3022	−0.3022	−0.3022	−0.3022	−0.3022	−0.3022	−0.3022	−0.3021	−0.3011	−0.2983
	−0.3014	−0.3014	−0.3014	−0.3014	−0.3014	−0.3013	−0.3013	−0.3013	−0.3001	−0.2972

Figure I.4: F2A: e=3b & d=1b

	c/b									
	−0.2902	−0.2902	−0.2902	−0.2902	−0.2902	−0.2902	−0.29	−0.2892	−0.2878	−0.2859
	−0.2903	−0.2903	−0.2903	−0.2903	−0.2903	−0.2903	−0.29	−0.2893	−0.2879	−0.2859
	−0.2913	−0.2913	−0.2913	−0.2913	−0.2913	−0.2913	−0.2911	−0.2903	−0.2888	−0.2868
	−0.2882	−0.2882	−0.2882	−0.2882	−0.2882	−0.2881	−0.2879	−0.2871	−0.2856	−0.2835
a/b	−0.2885	−0.2885	−0.2885	−0.2885	−0.2885	−0.2884	−0.2882	−0.2874	−0.2858	−0.2836
	−0.2895	−0.2895	−0.2895	−0.2895	−0.2895	−0.2895	−0.2892	−0.2883	−0.2867	−0.2845
	−0.2915	−0.2915	−0.2915	−0.2915	−0.2915	−0.2914	−0.2912	−0.2903	−0.2886	−0.2862
	−0.2925	−0.2925	−0.2925	−0.2925	−0.2925	−0.2925	−0.2922	−0.2912	−0.2894	−0.287
	−0.3022	−0.3022	−0.3022	−0.3022	−0.3022	−0.3022	−0.3018	−0.3008	−0.2989	−0.2963
	−0.3014	−0.3014	−0.3014	−0.3014	−0.3014	−0.3013	−0.3009	−0.2998	−0.2978	−0.2952

Figure I.4: F2A: e=3b & d=1.5b

	c/b									
	−0.2902	−0.2902	−0.2902	−0.2901	−0.2901	−0.2899	−0.2893	−0.2883	−0.2869	−0.2851
	−0.2903	−0.2903	−0.2903	−0.2902	−0.2902	−0.29	−0.2894	−0.2883	−0.2869	−0.2851
	−0.2913	−0.2913	−0.2913	−0.2913	−0.2912	−0.291	−0.2904	−0.2893	−0.2879	−0.286
	−0.2882	−0.2882	−0.2881	−0.2881	−0.2881	−0.2878	−0.2872	−0.2861	−0.2846	−0.2827
a/b	−0.2885	−0.2884	−0.2884	−0.2884	−0.2883	−0.2881	−0.2874	−0.2863	−0.2847	−0.2828
	−0.2895	−0.2895	−0.2894	−0.2894	−0.2894	−0.2891	−0.2884	−0.2872	−0.2856	−0.2836
	−0.2915	−0.2915	−0.2914	−0.2914	−0.2913	−0.291	−0.2903	−0.2891	−0.2874	−0.2853
	−0.2925	−0.2925	−0.2925	−0.2924	−0.2924	−0.292	−0.2913	−0.29	−0.2882	−0.286
	−0.3022	−0.3022	−0.3022	−0.3021	−0.3021	−0.3017	−0.3009	−0.2995	−0.2976	−0.2953
	−0.3013	−0.3013	−0.3013	−0.3013	−0.3012	−0.3008	−0.2999	−0.2983	−0.2964	−0.2939

Figure I.4: F2A: e=3b & d=2b

	c/b									
	−0.2902	−0.2902	−0.2902	−0.2901	−0.29	−0.2895	−0.2887	−0.2876	−0.2863	−0.2847
	−0.2903	−0.2903	−0.2903	−0.2902	−0.29	−0.2896	−0.2888	−0.2877	−0.2863	−0.2847
	−0.2913	−0.2913	−0.2913	−0.2913	−0.2911	−0.2906	−0.2898	−0.2887	−0.2873	−0.2856
	−0.2882	−0.2881	−0.2881	−0.2881	−0.2879	−0.2874	−0.2865	−0.2854	−0.284	−0.2823
a/b	−0.2885	−0.2884	−0.2884	−0.2884	−0.2882	−0.2876	−0.2868	−0.2856	−0.2841	−0.2824
	−0.2895	−0.2895	−0.2894	−0.2894	−0.2892	−0.2886	−0.2877	−0.2865	−0.285	−0.2831
	−0.2915	−0.2914	−0.2914	−0.2914	−0.2911	−0.2905	−0.2896	−0.2883	−0.2867	−0.2848
	−0.2925	−0.2925	−0.2925	−0.2924	−0.2921	−0.2915	−0.2905	−0.2891	−0.2875	−0.2855
	−0.3022	−0.3022	−0.3022	−0.3021	−0.3018	−0.3011	−0.3	−0.2986	−0.2969	−0.2948
	−0.3013	−0.3013	−0.3013	−0.3012	−0.3008	−0.3001	−0.2989	−0.2974	−0.2956	−0.2934

Figure I.4: F2A: e=3b & d=2.5b

	c/b									
	−0.2902	−0.2902	−0.2902	−0.29	−0.2896	−0.2891	−0.2882	−0.2872	−0.286	−0.2845
	−0.2903	−0.2903	−0.2903	−0.2901	−0.2897	−0.2891	−0.2883	−0.2872	−0.286	−0.2845
	−0.2913	−0.2913	−0.2913	−0.2911	−0.2907	−0.2901	−0.2893	−0.2882	−0.287	−0.2855
	−0.2882	−0.2882	−0.2881	−0.2879	−0.2875	−0.2869	−0.286	−0.2849	−0.2836	−0.2821
a/b	−0.2885	−0.2885	−0.2884	−0.2882	−0.2878	−0.2872	−0.2862	−0.2851	−0.2838	−0.2822
	−0.2895	−0.2895	−0.2894	−0.2892	−0.2888	−0.2881	−0.2871	−0.286	−0.2846	−0.283
	−0.2915	−0.2915	−0.2914	−0.2912	−0.2907	−0.29	−0.289	−0.2878	−0.2863	−0.2846
	−0.2925	−0.2925	−0.2924	−0.2922	−0.2917	−0.2909	−0.2898	−0.2885	−0.2871	−0.2853
	−0.3022	−0.3022	−0.3021	−0.3018	−0.3013	−0.3005	−0.2994	−0.298	−0.2964	−0.2945
	−0.3014	−0.3013	−0.3012	−0.3009	−0.3003	−0.2995	−0.2982	−0.2968	−0.2951	−0.2931

Figure I.4: F2A: e=3b & d=3b

	c/b									
	−0.2902	−0.2902	−0.29	−0.2898	−0.2893	−0.2887	−0.2879	−0.2869	−0.2858	−0.2845
	−0.2903	−0.2903	−0.2901	−0.2898	−0.2894	−0.2888	−0.2879	−0.2869	−0.2858	−0.2845
	−0.2913	−0.2913	−0.2912	−0.2909	−0.2904	−0.2898	−0.2889	−0.2879	−0.2868	−0.2854
	−0.2882	−0.2881	−0.288	−0.2877	−0.2872	−0.2865	−0.2857	−0.2846	−0.2834	−0.282
a/b	−0.2885	−0.2884	−0.2883	−0.2879	−0.2874	−0.2868	−0.2858	−0.2848	−0.2836	−0.2821
	−0.2895	−0.2894	−0.2893	−0.2889	−0.2884	−0.2877	−0.2867	−0.2856	−0.2844	−0.2829
	−0.2915	−0.2914	−0.2912	−0.2909	−0.2903	−0.2896	−0.2886	−0.2874	−0.2861	−0.2846
	−0.2925	−0.2924	−0.2922	−0.2919	−0.2912	−0.2905	−0.2894	−0.2882	−0.2868	−0.2852
	−0.3022	−0.3021	−0.3019	−0.3015	−0.3008	−0.3	−0.2989	−0.2976	−0.2962	−0.2945
	−0.3013	−0.3013	−0.301	−0.3006	−0.2998	−0.299	−0.2978	−0.2964	−0.2949	−0.2931

Figure I.4: F2A: e=3b & d=3.5b

	c/b									
	−0.2902	−0.2901	−0.2899	−0.2896	−0.2891	−0.2885	−0.2877	−0.2868	−0.2857	−0.2845
	−0.2903	−0.2902	−0.29	−0.2896	−0.2891	−0.2885	−0.2877	−0.2868	−0.2858	−0.2845
	−0.2913	−0.2912	−0.291	−0.2907	−0.2901	−0.2895	−0.2887	−0.2878	−0.2867	−0.2855
	−0.2882	−0.2881	−0.2878	−0.2875	−0.2869	−0.2863	−0.2854	−0.2845	−0.2834	−0.2821
a/b	−0.2884	−0.2883	−0.2881	−0.2877	−0.2872	−0.2865	−0.2856	−0.2846	−0.2835	−0.2822
	−0.2895	−0.2894	−0.2891	−0.2887	−0.2881	−0.2874	−0.2865	−0.2855	−0.2844	−0.283
	−0.2914	−0.2913	−0.2911	−0.2906	−0.29	−0.2893	−0.2884	−0.2873	−0.2861	−0.2847
	−0.2925	−0.2923	−0.2921	−0.2916	−0.291	−0.2902	−0.2892	−0.288	−0.2868	−0.2853
	−0.3022	−0.302	−0.3017	−0.3012	−0.3005	−0.2997	−0.2987	−0.2975	−0.2962	−0.2946
	−0.3013	−0.3011	−0.3008	−0.3003	−0.2995	−0.2987	−0.2975	−0.2963	−0.2949	−0.2932

Figure I.4: F2A: e=3b & d=4b

	c/b									
	−0.2902	−0.29	−0.2898	−0.2894	−0.2889	−0.2883	−0.2876	−0.2867	−0.2858	−0.2847
	−0.2903	−0.2901	−0.2899	−0.2895	−0.289	−0.2884	−0.2876	−0.2868	−0.2858	−0.2847
	−0.2913	−0.2912	−0.2909	−0.2905	−0.29	−0.2894	−0.2886	−0.2877	−0.2868	−0.2857
	−0.2881	−0.288	−0.2877	−0.2873	−0.2868	−0.2862	−0.2854	−0.2845	−0.2835	−0.2823
a/b	−0.2884	−0.2883	−0.288	−0.2876	−0.287	−0.2864	−0.2855	−0.2846	−0.2836	−0.2824
	−0.2894	−0.2893	−0.289	−0.2886	−0.288	−0.2873	−0.2865	−0.2855	−0.2845	−0.2832
	−0.2914	−0.2913	−0.291	−0.2905	−0.2899	−0.2892	−0.2883	−0.2873	−0.2862	−0.2849
	−0.2925	−0.2923	−0.292	−0.2915	−0.2908	−0.2901	−0.2891	−0.2881	−0.2869	−0.2856
	−0.3022	−0.302	−0.3016	−0.3011	−0.3004	−0.2996	−0.2986	−0.2975	−0.2963	−0.2949
	−0.3013	−0.3011	−0.3007	−0.3002	−0.2994	−0.2986	−0.2975	−0.2963	−0.2951	−0.2936

Figure I.4: F2A: e=3.5b & d=0.5b

	c/b									
	−0.2979	−0.2979	−0.2979	−0.2979	−0.2979	−0.2979	−0.2977	−0.2979	−0.2972	−0.2953
	−0.2985	−0.2985	−0.2985	−0.2985	−0.2985	−0.2985	−0.2985	−0.2984	−0.2977	−0.2958
	−0.2999	−0.2999	−0.2999	−0.2999	−0.2999	−0.2999	−0.2999	−0.2999	−0.2991	−0.2971
	−0.2969	−0.2969	−0.2969	−0.2969	−0.2969	−0.2969	−0.2968	−0.2968	−0.2961	−0.294
a/b	−0.297	−0.297	−0.297	−0.297	−0.297	−0.297	−0.297	−0.2969	−0.2962	−0.2941
	−0.2976	−0.2976	−0.2976	−0.2976	−0.2976	−0.2976	−0.2976	−0.2975	−0.2967	−0.2945
	−0.2986	−0.2986	−0.2986	−0.2986	−0.2986	−0.2986	−0.2986	−0.2986	−0.2977	−0.2955
	−0.2984	−0.2984	−0.2984	−0.2984	−0.2984	−0.2984	−0.2983	−0.2983	−0.2974	−0.2951
	−0.3066	−0.3066	−0.3066	−0.3066	−0.3066	−0.3066	−0.3065	−0.3065	−0.3056	−0.3032
	−0.304	−0.304	−0.304	−0.304	−0.304	−0.304	−0.304	−0.3039	−0.303	−0.3005

Figure I.4: F2A: e=3.5b & d=1b

	c/b									
	−0.2979	−0.2979	−0.2979	−0.2979	−0.2979	−0.2979	−0.2977	−0.297	−0.2958	−0.294
	−0.2985	−0.2985	−0.2985	−0.2985	−0.2985	−0.2985	−0.2983	−0.2976	−0.2963	−0.2945
	−0.2999	−0.2999	−0.2999	−0.2999	−0.2999	−0.2999	−0.2997	−0.299	−0.2977	−0.2958
	−0.2969	−0.2969	−0.2969	−0.2969	−0.2969	−0.2968	−0.2966	−0.2959	−0.2945	−0.2926
a/b	−0.297	−0.297	−0.297	−0.297	−0.297	−0.297	−0.2967	−0.296	−0.2946	−0.2926
	−0.2976	−0.2976	−0.2976	−0.2976	−0.2976	−0.2976	−0.2973	−0.2965	−0.2951	−0.2931
	−0.2986	−0.2986	−0.2986	−0.2986	−0.2986	−0.2986	−0.2984	−0.2976	−0.2961	−0.294
	−0.2984	−0.2984	−0.2984	−0.2984	−0.2984	−0.2983	−0.2981	−0.2972	−0.2957	−0.2935
	−0.3066	−0.3066	−0.3066	−0.3066	−0.3066	−0.3065	−0.3062	−0.3054	−0.3038	−0.3015
	−0.304	−0.304	−0.304	−0.304	−0.304	−0.304	−0.3037	−0.3027	−0.3011	−0.2987

Figure I.4: F2A: e=3.5b & d=1.5b

	c/b									
	−0.2979	−0.2979	−0.2979	−0.2979	−0.2978	−0.2976	−0.2971	−0.2962	−0.2949	−0.2933
	−0.2985	−0.2985	−0.2985	−0.2985	−0.2984	−0.2982	−0.2977	−0.2967	−0.2954	−0.2937
	−0.2999	−0.2999	−0.2999	−0.2999	−0.2998	−0.2996	−0.2991	−0.2981	−0.2967	−0.2951
	−0.2969	−0.2969	−0.2968	−0.2968	−0.2968	−0.2965	−0.296	−0.295	−0.2936	−0.2918
a/b	−0.297	−0.297	−0.297	−0.2969	−0.2969	−0.2967	−0.2961	−0.295	−0.2936	−0.2918
	−0.2976	−0.2976	−0.2976	−0.2975	−0.2975	−0.2972	−0.2966	−0.2955	−0.2941	−0.2923
	−0.2986	−0.2986	−0.2986	−0.2986	−0.2985	−0.2983	−0.2976	−0.2965	−0.295	−0.2931
	−0.2984	−0.2984	−0.2983	−0.2983	−0.2982	−0.298	−0.2973	−0.2961	−0.2946	−0.2926
	−0.3066	−0.3066	−0.3065	−0.3065	−0.3064	−0.3061	−0.3054	−0.3042	−0.3026	−0.3006
	−0.304	−0.304	−0.304	−0.304	−0.3039	−0.3035	−0.3028	−0.3015	−0.2998	−0.2977

Figure I.4: F2A: e=3.5b & d=2b

	c/b									
	−0.2979	−0.2979	−0.2979	−0.2979	−0.2977	−0.2972	−0.2965	−0.2956	−0.2944	−0.2929
	−0.2985	−0.2985	−0.2985	−0.2984	−0.2983	−0.2978	−0.2971	−0.2961	−0.2949	−0.2934
	−0.2999	−0.2999	−0.2999	−0.2999	−0.2997	−0.2992	−0.2985	−0.2974	−0.2962	−0.2947
	−0.2969	−0.2968	−0.2968	−0.2968	−0.2966	−0.2961	−0.2954	−0.2943	−0.293	−0.2914
a/b	−0.297	−0.297	−0.297	−0.2969	−0.2969	−0.2962	−0.2954	−0.2944	−0.293	−0.2914
	−0.2976	−0.2976	−0.2975	−0.2975	−0.2973	−0.2968	−0.296	−0.2948	−0.2935	−0.2918
	−0.2986	−0.2986	−0.2986	−0.2986	−0.2983	−0.2978	−0.2969	−0.2958	−0.2944	−0.2927
	−0.2984	−0.2983	−0.2983	−0.2983	−0.298	−0.2975	−0.2966	−0.2954	−0.2939	−0.2921
	−0.3066	−0.3065	−0.3065	−0.3065	−0.3062	−0.3056	−0.3047	−0.3034	−0.3019	−0.3001
	−0.304	−0.304	−0.304	−0.3039	−0.3036	−0.303	−0.302	−0.3006	−0.2991	−0.2971

Figure I.4: F2A: e=3.5b & d=2.5b

	c/b									
	−0.2979	−0.2979	−0.2979	−0.2977	−0.2974	−0.2969	−0.2961	−0.2951	−0.294	−0.2927
	−0.2985	−0.2985	−0.2985	−0.2983	−0.298	−0.2974	−0.2966	−0.2957	−0.2945	−0.2932
	−0.2999	−0.2999	−0.2999	−0.2997	−0.2994	−0.2988	−0.298	−0.297	−0.2959	−0.2945
	−0.2969	−0.2969	−0.2968	−0.2966	−0.2963	−0.2957	−0.2949	−0.2939	−0.2927	−0.2912
a/b	−0.297	−0.297	−0.297	−0.2968	−0.2964	−0.2958	−0.295	−0.2939	−0.2927	−0.2912
	−0.2976	−0.2976	−0.2975	−0.2973	−0.2969	−0.2963	−0.2954	−0.2944	−0.2931	−0.2916
	−0.2986	−0.2986	−0.2986	−0.2984	−0.2979	−0.2973	−0.2964	−0.2953	−0.294	−0.2925
	−0.2984	−0.2984	−0.2983	−0.2981	−0.2976	−0.297	−0.296	−0.2948	−0.2935	−0.2919
	−0.3066	−0.3066	−0.3065	−0.3062	−0.3058	−0.3051	−0.3041	−0.3029	−0.3015	−0.3005
	−0.304	−0.304	−0.3039	−0.3037	−0.3031	−0.3024	−0.3014	−0.3001	−0.2986	−0.2969

Figure I.4: F2A: e=3.5b & d=3b

	c/b									
	−0.2979	−0.2979	−0.2978	−0.2975	−0.2971	−0.2965	−0.2958	−0.2949	−0.2938	−0.2926
	−0.2985	−0.2985	−0.2983	−0.2981	−0.2976	−0.2971	−0.2963	−0.2954	−0.2943	−0.2931
	−0.2999	−0.2999	−0.2998	−0.2995	−0.299	−0.2985	−0.2977	−0.2967	−0.2957	−0.2944
	−0.2969	−0.2968	−0.2967	−0.2964	−0.2959	−0.2953	−0.2945	−0.2936	−0.2925	−0.2912
a/b	−0.297	−0.297	−0.2968	−0.2965	−0.296	−0.2954	−0.2946	−0.2936	−0.2925	−0.2912
	−0.2976	−0.2975	−0.2974	−0.2971	−0.2966	−0.2959	−0.2951	−0.2941	−0.2929	−0.2915
	−0.2986	−0.2986	−0.2984	−0.2981	−0.2976	−0.2969	−0.296	−0.295	−0.2938	−0.2924
	−0.2984	−0.2983	−0.2981	−0.2978	−0.2972	−0.2965	−0.2956	−0.2945	−0.2933	−0.2918
	−0.3066	−0.3065	−0.3063	−0.3059	−0.3054	−0.3046	−0.3037	−0.3025	−0.3013	−0.2997
	−0.304	−0.3039	−0.3037	−0.3033	−0.3027	−0.302	−0.3009	−0.2997	−0.2984	−0.2968

Figure I.4: F2A: e=3.5b & d=3.5b

	c/b									
	−0.2979	−0.2978	−0.2976	−0.2973	−0.2969	−0.2963	−0.2956	−0.2947	−0.2938	−0.2926
	−0.2985	−0.2984	−0.2982	−0.2979	−0.2974	−0.2968	−0.2961	−0.2952	−0.2943	−0.2931
	−0.2999	−0.2998	−0.2996	−0.2993	−0.2988	−0.2982	−0.2975	−0.2966	−0.2956	−0.2945
	−0.2969	−0.2968	−0.2966	−0.2962	−0.2957	−0.2951	−0.2943	−0.2934	−0.2924	−0.2912
a/b	−0.297	−0.2969	−0.2967	−0.2963	−0.2958	−0.2952	−0.2944	−0.2934	−0.2924	−0.2912
	−0.2976	−0.2975	−0.2972	−0.2969	−0.2963	−0.2957	−0.2949	−0.2939	−0.2929	−0.2916
	−0.2986	−0.2985	−0.2983	−0.2979	−0.2973	−0.2967	−0.2958	−0.2948	−0.2938	−0.2925
	−0.2983	−0.2982	−0.298	−0.2976	−0.297	−0.2963	−0.2954	−0.2944	−0.2932	−0.2919
	−0.3065	−0.3064	−0.3062	−0.3057	−0.3051	−0.3044	−0.3034	−0.3024	−0.3012	−0.2998
	−0.304	−0.3038	−0.3036	−0.3031	−0.3025	−0.3017	−0.3007	−0.2996	−0.2984	−0.2969

Figure I.4: F2A: e=3.5b & d=4b

	c/b									
	−0.2979	−0.2978	−0.2976	−0.2972	−0.2967	−0.2962	−0.2955	−0.2947	−0.2938	−0.2928
	−0.2985	−0.2984	−0.2981	−0.2978	−0.2973	−0.2967	−0.296	−0.2952	−0.2943	−0.2933
	−0.2999	−0.2998	−0.2995	−0.2992	−0.2987	−0.2981	−0.2974	−0.2966	−0.2957	−0.2946
	−0.2968	−0.2967	−0.2965	−0.2961	−0.2956	−0.295	−0.2942	−0.2934	−0.2925	−0.2914
a/b	−0.297	−0.2968	−0.2966	−0.2962	−0.2957	−0.2951	−0.2943	−0.2934	−0.2925	−0.2914
	−0.2975	−0.2974	−0.2972	−0.2968	−0.2962	−0.2956	−0.2948	−0.2939	−0.2929	−0.2918
	−0.2986	−0.2985	−0.2982	−0.2978	−0.2972	−0.2966	−0.2957	−0.2948	−0.2938	−0.2927
	−0.2983	−0.2982	−0.2979	−0.2974	−0.2969	−0.2962	−0.2953	−0.2944	−0.2933	−0.2921
	−0.3065	−0.3064	−0.3061	−0.3056	−0.305	−0.3043	−0.3034	−0.3024	−0.3013	−0.3
	−0.304	−0.3038	−0.3035	−0.303	−0.3023	−0.3016	−0.3006	−0.2996	−0.2985	−0.2971

Figure I.4: F2A: e=4b & d=0.5b

	c/b									
a/b	−0.3037	−0.3037	−0.3037	−0.3037	−0.3037	−0.3037	−0.3037	−0.3037	−0.303	−0.3013
	−0.3047	−0.3047	−0.3047	−0.3047	−0.3047	−0.3047	−0.3046	−0.3046	−0.304	−0.3022
	−0.3064	−0.3064	−0.3064	−0.3064	−0.3064	−0.3064	−0.3064	−0.3063	−0.3057	−0.3038
	−0.3035	−0.3035	−0.3035	−0.3035	−0.3035	−0.3035	−0.3034	−0.3034	−0.3027	−0.3009
	−0.3036	−0.3036	−0.3036	−0.3036	−0.3036	−0.3036	−0.3036	−0.3035	−0.3029	−0.301
	−0.304	−0.304	−0.304	−0.304	−0.304	−0.304	−0.304	−0.304	−0.3033	−0.3013
	−0.3047	−0.3047	−0.3047	−0.3047	−0.3046	−0.3046	−0.3046	−0.3046	−0.3039	−0.3019
	−0.3036	−0.3036	−0.3036	−0.3036	−0.3036	−0.3036	−0.3036	−0.3036	−0.3028	−0.3008
	−0.3109	−0.3109	−0.3109	−0.3109	−0.3109	−0.3109	−0.3109	−0.3108	−0.3101	−0.308
	−0.3071	−0.3071	−0.3071	−0.3071	−0.3071	−0.3071	−0.3071	−0.307	−0.3062	−0.3041

Figure I.4: F2A: e=4b & d=1b

	c/b									
a/b	−0.3037	−0.3037	−0.3037	−0.3037	−0.3037	−0.3037	−0.3035	−0.3029	−0.3018	−0.3002
	−0.3047	−0.3047	−0.3047	−0.3047	−0.3047	−0.3046	−0.3044	−0.3038	−0.3027	−0.301
	−0.3064	−0.3064	−0.3064	−0.3064	−0.3064	−0.3064	−0.3062	−0.3055	−0.3043	−0.3027
	−0.3035	−0.3035	−0.3035	−0.3035	−0.3035	−0.3034	−0.3032	−0.3026	−0.3014	−0.2996
	−0.3036	−0.3036	−0.3036	−0.3036	−0.3036	−0.3036	−0.3034	−0.3027	−0.3014	−0.2997
	−0.304	−0.304	−0.304	−0.304	−0.304	−0.304	−0.3038	−0.3031	−0.3018	−0.3
	−0.3047	−0.3046	−0.3046	−0.3046	−0.3046	−0.3046	−0.3044	−0.3037	−0.3024	−0.3005
	−0.3036	−0.3036	−0.3036	−0.3036	−0.3036	−0.3036	−0.3034	−0.3026	−0.3013	−0.2993
	−0.3109	−0.3109	−0.3109	−0.3109	−0.3109	−0.3109	−0.3106	−0.3099	−0.3085	−0.3065
	−0.3071	−0.3071	−0.3071	−0.3071	−0.3071	−0.307	−0.3068	−0.306	−0.3045	−0.3025

Figure I.4: F2A: e=4b & d=1.5b

	c/b									
a/b	−0.3037	−0.3037	−0.3037	−0.3037	−0.3036	−0.3034	−0.3029	−0.3021	−0.3009	−0.2995
	−0.3047	−0.3046	−0.3046	−0.3046	−0.3046	−0.3044	−0.3039	−0.303	−0.3018	−0.3003
	−0.3064	−0.3064	−0.3064	−0.3063	−0.3063	−0.3061	−0.3056	−0.3047	−0.3035	−0.302
	−0.3035	−0.3035	−0.3034	−0.3034	−0.3034	−0.3032	−0.3026	−0.3017	−0.3005	−0.2989
	−0.3036	−0.3036	−0.3036	−0.3035	−0.3035	−0.3033	−0.3027	−0.3018	−0.3005	−0.2989
	−0.304	−0.304	−0.304	−0.304	−0.3039	−0.3037	−0.3032	−0.3022	−0.3009	−0.2992
	−0.3046	−0.3046	−0.3046	−0.3046	−0.3045	−0.3043	−0.3037	−0.3027	−0.3014	−0.2997
	−0.3036	−0.3036	−0.3036	−0.3036	−0.3035	−0.3033	−0.3027	−0.3017	−0.3003	−0.2985
	−0.3109	−0.3109	−0.3109	−0.3109	−0.3108	−0.3105	−0.3099	−0.3088	−0.3074	−0.3056
	−0.3071	−0.3071	−0.307	−0.307	−0.307	−0.3067	−0.306	−0.3049	−0.3034	−0.3016

Figure I.4: F2A: e=4b & d=2b

	c/b									
a/b	−0.3037	−0.3037	−0.3037	−0.3036	−0.3035	−0.3031	−0.3024	−0.3015	−0.3004	−0.2991
	−0.3046	−0.3046	−0.3046	−0.3046	−0.3044	−0.304	−0.3033	−0.3024	−0.3013	−0.2999
	−0.3064	−0.3064	−0.3064	−0.3063	−0.3061	−0.3057	−0.305	−0.3041	−0.303	−0.3016
	−0.3035	−0.3034	−0.3034	−0.3034	−0.3032	−0.3028	−0.3021	−0.3011	−0.2999	−0.2985
	−0.3036	−0.3036	−0.3036	−0.3035	−0.3033	−0.3029	−0.3022	−0.3012	−0.3	−0.2985
	−0.304	−0.304	−0.304	−0.304	−0.3038	−0.3033	−0.3026	−0.3015	−0.3003	−0.2988
	−0.3046	−0.3046	−0.3046	−0.3046	−0.3044	−0.3039	−0.3031	−0.3021	−0.3008	−0.2993
	−0.3036	−0.3036	−0.3036	−0.3036	−0.3033	−0.3028	−0.302	−0.3009	−0.2996	−0.298
	−0.3109	−0.3109	−0.3109	−0.3108	−0.3106	−0.3101	−0.3092	−0.3081	−0.3068	−0.3051
	−0.3071	−0.307	−0.307	−0.307	−0.3067	−0.3062	−0.3053	−0.3041	−0.3028	−0.301

Figure I.4: F2A: e=4b & d=2.5b

	c/b									
a/b	−0.3037	−0.3037	−0.3037	−0.3035	−0.3032	−0.3027	−0.302	−0.3011	−0.3001	−0.2989
	−0.3047	−0.3047	−0.3046	−0.3045	−0.3041	−0.3036	−0.3029	−0.302	−0.301	−0.2997
	−0.3064	−0.3064	−0.3063	−0.3062	−0.3059	−0.3053	−0.3046	−0.3037	−0.3027	−0.3014
	−0.3035	−0.3035	−0.3034	−0.3033	−0.3029	−0.3024	−0.3016	−0.3007	−0.2996	−0.2983
	−0.3036	−0.3036	−0.3036	−0.3034	−0.303	−0.3025	−0.3017	−0.3008	−0.2997	−0.2983
	−0.304	−0.304	−0.304	−0.3038	−0.3034	−0.3029	−0.3021	−0.3011	−0.3	−0.2986
	−0.3046	−0.3046	−0.3046	−0.3044	−0.304	−0.3034	−0.3026	−0.3016	−0.3005	−0.299
	−0.3036	−0.3036	−0.3036	−0.3034	−0.303	−0.3024	−0.3015	−0.3005	−0.2993	−0.2978
	−0.3109	−0.3109	−0.3108	−0.3106	−0.3102	−0.3096	−0.3087	−0.3076	−0.3064	−0.3049
	−0.3071	−0.3071	−0.307	−0.3068	−0.3063	−0.3057	−0.3047	−0.3036	−0.3024	−0.3008

Figure I.4: F2A: e=4b & d=3b

	c/b									
a/b	−0.3037	−0.3037	−0.3036	−0.3033	−0.3029	−0.3024	−0.3017	−0.3009	−0.2999	−0.2988
	−0.3047	−0.3046	−0.3045	−0.3042	−0.3038	−0.3033	−0.3026	−0.3018	−0.3008	−0.2996
	−0.3064	−0.3063	−0.3062	−0.306	−0.3056	−0.305	−0.3043	−0.3034	−0.3025	−0.3013
	−0.3035	−0.3034	−0.3033	−0.303	−0.3026	−0.3021	−0.3013	−0.3004	−0.2994	−0.2982
	−0.3036	−0.3036	−0.3034	−0.3032	−0.3027	−0.3021	−0.3014	−0.3005	−0.2995	−0.2982
	−0.304	−0.304	−0.3039	−0.3036	−0.3031	−0.3025	−0.3017	−0.3008	−0.2998	−0.2985
	−0.3046	−0.3046	−0.3045	−0.3042	−0.3037	−0.3031	−0.3023	−0.3013	−0.3002	−0.2989
	−0.3036	−0.3036	−0.3034	−0.3031	−0.3026	−0.302	−0.3012	−0.3002	−0.2991	−0.2977
	−0.3109	−0.3108	−0.3107	−0.3104	−0.3098	−0.3092	−0.3083	−0.3073	−0.3062	−0.3048
	−0.3071	−0.307	−0.3068	−0.3065	−0.3059	−0.3053	−0.3044	−0.3033	−0.3021	−0.3007

Figure I.4: F2A: e=4b & d=3.5b

	c/b									
a/b	−0.3037	−0.3036	−0.3034	−0.3031	−0.3027	−0.3022	−0.3015	−0.3007	−0.2999	−0.2988
	−0.3046	−0.3046	−0.3044	−0.3041	−0.3036	−0.3031	−0.3024	−0.3016	−0.3007	−0.2997
	−0.3064	−0.3063	−0.3061	−0.3058	−0.3054	−0.3048	−0.3041	−0.3033	−0.3024	−0.3013
	−0.3034	−0.3034	−0.3032	−0.3029	−0.3024	−0.3018	−0.3011	−0.3003	−0.2994	−0.2982
	−0.3036	−0.3035	−0.3033	−0.303	−0.3025	−0.3019	−0.3012	−0.3003	−0.2994	−0.2982
	−0.304	−0.3039	−0.3037	−0.3034	−0.3029	−0.3023	−0.3015	−0.3007	−0.2997	−0.2985
	−0.3046	−0.3045	−0.3043	−0.304	−0.3035	−0.3029	−0.3021	−0.3012	−0.3002	−0.299
	−0.3036	−0.3035	−0.3033	−0.3029	−0.3024	−0.3018	−0.3009	−0.3	−0.299	−0.2978
	−0.3109	−0.3108	−0.3105	−0.3102	−0.3096	−0.309	−0.3081	−0.3072	−0.3061	−0.3048
	−0.307	−0.3069	−0.3067	−0.3063	−0.3057	−0.305	−0.3041	−0.3031	−0.3021	−0.3007

Figure I.4: F2A: e=4b & d=4b

	c/b									
a/b	−0.3037	−0.3036	−0.3034	−0.303	−0.3026	−0.3021	−0.3014	−0.3007	−0.2999	−0.2989
	−0.3046	−0.3045	−0.3043	−0.304	−0.3035	−0.303	−0.3023	−0.3016	−0.3008	−0.2998
	−0.3064	−0.3062	−0.306	−0.3057	−0.3052	−0.3047	−0.304	−0.3033	−0.3025	−0.3015
	−0.3034	−0.3033	−0.3031	−0.3028	−0.3023	−0.3017	−0.301	−0.3003	−0.2994	−0.2984
	−0.3036	−0.3034	−0.3032	−0.3029	−0.3024	−0.3018	−0.3011	−0.3003	−0.2994	−0.2984
	−0.304	−0.3039	−0.3036	−0.3033	−0.3028	−0.3022	−0.3015	−0.3006	−0.2998	−0.2987
	−0.3046	−0.3045	−0.3042	−0.3039	−0.3033	−0.3028	−0.302	−0.3012	−0.3002	−0.2991
	−0.3036	−0.3035	−0.3032	−0.3028	−0.3023	−0.3017	−0.3009	−0.3	−0.2991	−0.2979
	−0.3109	−0.3107	−0.3105	−0.31	−0.3095	−0.3089	−0.308	−0.3072	−0.3062	−0.305
	−0.307	−0.3069	−0.3066	−0.3062	−0.3056	−0.3049	−0.3041	−0.3031	−0.3021	−0.3009

Figure I.5: F1A: e=0.5a & d=0.5a

	c/a									
b/a	0.4648	0.4647	0.4647	0.4647	0.4644	0.4569	0.4264	0.3731	0.3213	0.2638
	0.4648	0.4647	0.4647	0.4647	0.4644	0.4569	0.4264	0.3731	0.3213	0.2638
	0.4648	0.4648	0.4647	0.4647	0.4645	0.4569	0.4264	0.373	0.3212	0.2639
	0.4648	0.4648	0.4648	0.4647	0.4645	0.4569	0.4265	0.3733	0.3209	0.2638
	0.4647	0.4647	0.4647	0.4647	0.4644	0.457	0.4267	0.3731	0.3192	0.2637
	0.4649	0.4649	0.4649	0.4649	0.4646	0.4577	0.4258	0.3711	0.3186	0.2641
	0.4478	0.4476	0.4473	0.4473	0.4474	0.4461	0.4206	0.3688	0.3185	0.2656
	0.2372	0.2372	0.237	0.2371	0.2373	0.2369	0.2369	0.2366	0.2307	0.2166

Figure I.5: F1A: e=0.5a & d=1a

	c/a									
b/a	0.4647	0.4651	0.467	0.468	0.4569	0.4309	0.3875	0.3493	0.3223	0.2849
	0.4647	0.4651	0.467	0.468	0.4569	0.4309	0.3875	0.3493	0.3223	0.2849
	0.4648	0.4652	0.4671	0.4681	0.4569	0.4309	0.3875	0.3493	0.3223	0.285
	0.4648	0.4652	0.4671	0.4681	0.4569	0.431	0.3875	0.3493	0.3223	0.285
	0.4647	0.4651	0.467	0.468	0.4569	0.4309	0.3875	0.3493	0.3223	0.2849
	0.4649	0.4653	0.4672	0.4682	0.457	0.431	0.3876	0.3494	0.3224	0.2851
	0.4477	0.4481	0.4497	0.4507	0.4428	0.4204	0.3804	0.3441	0.3179	0.2818
	0.2372	0.2372	0.2371	0.2371	0.2372	0.2367	0.2351	0.2305	0.2221	0.2134

Figure I.5: F1A: e=0.5a & d=1.5a

	c/a									
b/a	0.4658	0.4681	0.4663	0.4514	0.4253	0.4029	0.3732	0.3483	0.3287	0.3031
	0.4658	0.4681	0.4663	0.4514	0.4253	0.4029	0.3732	0.3483	0.3287	0.3031
	0.4659	0.4682	0.4664	0.4514	0.4253	0.403	0.3733	0.3484	0.3288	0.3032
	0.4659	0.4682	0.4664	0.4514	0.4253	0.403	0.3733	0.3484	0.3288	0.3032
	0.4658	0.4681	0.4663	0.4513	0.4252	0.4029	0.3732	0.3483	0.3287	0.3031
	0.466	0.4682	0.4664	0.4515	0.4254	0.4031	0.3733	0.3485	0.3288	0.3032
	0.4485	0.4501	0.4488	0.4366	0.4139	0.3934	0.3658	0.3421	0.3232	0.2989
	0.2371	0.237	0.2366	0.2363	0.2363	0.2349	0.2321	0.2271	0.2205	0.2131

Figure I.5: F1A: e=0.5a & d=2a

	c/a									
b/a	0.4648	0.4606	0.4507	0.4335	0.4123	0.3956	0.3741	0.3558	0.3401	0.321
	0.4648	0.4606	0.4507	0.4335	0.4123	0.3956	0.3741	0.3558	0.3401	0.321
	0.4648	0.4606	0.4508	0.4335	0.4124	0.3956	0.3742	0.3559	0.3401	0.321
	0.4648	0.4606	0.4508	0.4335	0.4124	0.3956	0.3742	0.3559	0.3401	0.321
	0.4647	0.4605	0.4507	0.4334	0.4123	0.3956	0.3741	0.3558	0.3401	0.3209
	0.4649	0.4607	0.4509	0.4336	0.4125	0.3957	0.3743	0.356	0.3403	0.3211
	0.4478	0.4446	0.4364	0.4228	0.4025	0.3869	0.367	0.3496	0.3345	0.3164
	0.237	0.2368	0.2368	0.2369	0.2361	0.2337	0.2303	0.2258	0.2206	0.2147

Figure I.5: F1A: e=0.5a & d=2.5a

	c/a									
b/a	0.4628	0.4561	0.4459	0.4315	0.4151	0.4017	0.3852	0.3707	0.3576	0.3424
	0.4628	0.4561	0.4459	0.4315	0.4151	0.4017	0.3852	0.3707	0.3576	0.3424
	0.4628	0.4561	0.4459	0.4315	0.4151	0.4017	0.3853	0.3707	0.3576	0.3424
	0.4628	0.4561	0.4459	0.4315	0.4151	0.4018	0.3853	0.3707	0.3576	0.3424
	0.4627	0.456	0.4459	0.4315	0.4151	0.4017	0.3852	0.3707	0.3575	0.3424
	0.4629	0.4562	0.4461	0.4316	0.4152	0.4019	0.3854	0.3708	0.3577	0.3425
	0.4463	0.4407	0.4319	0.4192	0.4043	0.392	0.3767	0.3631	0.3507	0.3363
	0.2372	0.2373	0.2372	0.2365	0.2349	0.2324	0.2292	0.2255	0.2214	0.2166

Figure I.5: F1A: e=0.5a & d=3a

	c/a									
b/a	0.4625	0.4563	0.4477	0.4363	0.4235	0.4125	0.3994	0.3875	0.3764	0.3639
	0.4625	0.4563	0.4477	0.4363	0.4235	0.4126	0.3994	0.3875	0.3764	0.3639
	0.4626	0.4564	0.4478	0.4363	0.4235	0.4126	0.3995	0.3875	0.3765	0.3639
	0.4626	0.4564	0.4478	0.4363	0.4235	0.4126	0.3995	0.3876	0.3765	0.3639
	0.4625	0.4563	0.4477	0.4363	0.4234	0.4125	0.3994	0.3875	0.3764	0.3638
	0.4627	0.4565	0.4479	0.4364	0.4236	0.4127	0.3996	0.3877	0.3766	0.364
	0.4459	0.4406	0.433	0.4228	0.4112	0.4012	0.3891	0.3779	0.3675	0.3557
	0.2372	0.2371	0.2365	0.2353	0.2335	0.2312	0.2284	0.2253	0.222	0.2183

Figure I.5: F1A: e=0.5a & d=3.5a

	c/a									
b/a	0.4629	0.4579	0.4509	0.442	0.4318	0.4229	0.4123	0.4023	0.3929	0.3824
	0.4629	0.4579	0.451	0.442	0.4318	0.4229	0.4123	0.4023	0.3929	0.3824
	0.4629	0.4579	0.451	0.442	0.4319	0.4229	0.4123	0.4024	0.393	0.3824
	0.4629	0.4579	0.451	0.442	0.4319	0.4229	0.4123	0.4024	0.393	0.3824
	0.4628	0.4578	0.4509	0.4419	0.4318	0.4229	0.4122	0.4023	0.3929	0.3824
	0.463	0.458	0.4511	0.4421	0.432	0.423	0.4124	0.4025	0.3931	0.3825
	0.4461	0.4418	0.4356	0.4275	0.4183	0.41	0.4003	0.3911	0.3822	0.3724
	0.2371	0.2367	0.2359	0.2346	0.2327	0.2307	0.2282	0.2256	0.2228	0.2196

Figure I.5: F1A: e=0.5a & d=4a

	c/a									
b/a	0.4633	0.4593	0.4539	0.4467	0.4387	0.4313	0.4226	0.4143	0.4063	0.3973
	0.4633	0.4593	0.4539	0.4468	0.4387	0.4313	0.4226	0.4143	0.4063	0.3973
	0.4633	0.4594	0.4539	0.4468	0.4387	0.4313	0.4226	0.4143	0.4063	0.3974
	0.4633	0.4594	0.4539	0.4468	0.4387	0.4314	0.4226	0.4143	0.4063	0.3974
	0.4632	0.4593	0.4538	0.4467	0.4387	0.4313	0.4226	0.4143	0.4063	0.3973
	0.4634	0.4595	0.454	0.4469	0.4388	0.4315	0.4228	0.4145	0.4064	0.3975
	0.4465	0.443	0.438	0.4316	0.4242	0.4174	0.4094	0.4017	0.3942	0.3858
	0.237	0.2365	0.2356	0.2343	0.2326	0.2308	0.2286	0.2263	0.2239	0.2211

Figure I.5: F1A: e=1a & d=0.5a

	c/a									
b/a	0.4647	0.4651	0.467	0.468	0.4569	0.4309	0.3875	0.3493	0.3224	0.2849
	0.4647	0.4651	0.467	0.468	0.4569	0.4309	0.3875	0.3493	0.3224	0.2849
	0.4647	0.465	0.4669	0.468	0.4568	0.4309	0.3875	0.3493	0.3223	0.2849
	0.4647	0.465	0.4669	0.4679	0.4567	0.4307	0.3874	0.3492	0.3222	0.2879
	0.4644	0.4649	0.4671	0.4681	0.4568	0.4309	0.3883	0.3501	0.322	0.2855
	0.4569	0.4583	0.4612	0.4641	0.4571	0.4351	0.3936	0.3554	0.3286	0.2904
	0.3732	0.3732	0.3732	0.3732	0.3702	0.3727	0.3623	0.3408	0.3167	0.2853
	0.2638	0.2638	0.2637	0.2638	0.2638	0.2637	0.2636	0.2635	0.2597	0.2498

Figure I.5: F1A: e=1a & d=1a

	c/a									
b/a	0.4658	0.4681	0.4663	0.4514	0.4252	0.403	0.3733	0.3483	0.3288	0.303
	0.4658	0.4681	0.4663	0.4514	0.4251	0.403	0.3732	0.3483	0.3288	0.303
	0.4658	0.468	0.4663	0.4513	0.4251	0.4029	0.3732	0.3483	0.3287	0.3029
	0.4658	0.4681	0.4663	0.4513	0.4251	0.4029	0.3732	0.3483	0.3287	0.3029
	0.4656	0.4679	0.4662	0.4514	0.4252	0.4032	0.3734	0.3485	0.329	0.3031
	0.4584	0.4611	0.4609	0.4484	0.4237	0.4028	0.3737	0.3493	0.3299	0.3042
	0.3732	0.3567	0.3731	0.3728	0.3695	0.3634	0.3452	0.3282	0.3131	0.2906
	0.2638	0.2638	0.2637	0.2638	0.2638	0.2636	0.2626	0.2595	0.2533	0.2462

Figure I.5: F1A: e=1a & d=1.5a

	c/a									
b/a	0.4648	0.4606	0.4508	0.4335	0.4124	0.3956	0.3741	0.3558	0.3401	0.321
	0.4648	0.4606	0.4507	0.4335	0.4124	0.3956	0.3741	0.3558	0.3401	0.321
	0.4647	0.4605	0.4507	0.4334	0.4123	0.3956	0.3741	0.3558	0.3401	0.321
	0.4647	0.4605	0.4507	0.4334	0.4123	0.3956	0.3741	0.3558	0.3401	0.321
	0.4645	0.4603	0.4506	0.4334	0.4123	0.3956	0.3741	0.3558	0.3401	0.3211
	0.4571	0.4537	0.445	0.4289	0.409	0.3929	0.3718	0.3539	0.3385	0.3198
	0.3731	0.373	0.3726	0.3697	0.3607	0.352	0.324	0.3178	0.3125	0.2971
	0.2638	0.2637	0.2635	0.2633	0.2633	0.2624	0.2602	0.2563	0.251	0.2453

Figure I.5: F1A: e=1a & d=2a

	c/a									
b/a	0.4628	0.4561	0.4459	0.4315	0.4151	0.4017	0.3852	0.3707	0.3576	0.3424
	0.4628	0.4561	0.4459	0.4315	0.4151	0.4017	0.3852	0.3707	0.3576	0.3423
	0.4627	0.456	0.4458	0.4314	0.415	0.4017	0.3852	0.3706	0.3575	0.3423
	0.4627	0.456	0.4459	0.4314	0.415	0.4017	0.3852	0.3706	0.3575	0.3423
	0.4625	0.4558	0.4457	0.4313	0.415	0.4017	0.3852	0.3707	0.3576	0.3424
	0.4552	0.4492	0.4398	0.4262	0.4106	0.3977	0.3818	0.3677	0.3549	0.34
	0.3731	0.3725	0.3704	0.365	0.3567	0.349	0.3386	0.328	0.3183	0.3071
	0.2637	0.2636	0.2636	0.2636	0.263	0.2611	0.2584	0.2547	0.2504	0.2457

Figure I.5: F1A: e=1a & d=2.5a

	c/a									
b/a	0.4625	0.4563	0.4477	0.4363	0.4235	0.4126	0.3994	0.3875	0.3764	0.3638
	0.4625	0.4563	0.4477	0.4363	0.4234	0.4125	0.3994	0.3875	0.3764	0.3638
	0.4625	0.4563	0.4477	0.4362	0.4234	0.4125	0.3994	0.3874	0.3764	0.3638
	0.4625	0.4563	0.4477	0.4362	0.4234	0.4125	0.3994	0.3874	0.3764	0.3638
	0.4622	0.4561	0.4475	0.4361	0.4233	0.4124	0.3993	0.3874	0.3764	0.3638
	0.4549	0.4492	0.4411	0.4303	0.4181	0.4076	0.395	0.3836	0.3726	0.3604
	0.3728	0.3714	0.3687	0.3638	0.357	0.3509	0.3427	0.335	0.3272	0.3184
	0.2638	0.2639	0.2637	0.2632	0.2619	0.2599	0.2572	0.2539	0.2504	0.2464

Figure I.5: F1A: e=1a & d=3a

	c/a									
b/a	0.4629	0.4579	0.451	0.442	0.4318	0.4229	0.4123	0.4023	0.3929	0.3824
	0.4629	0.4578	0.4509	0.4419	0.4318	0.4229	0.4122	0.4023	0.3929	0.3823
	0.4628	0.4578	0.4509	0.4419	0.4318	0.4228	0.4122	0.4023	0.3929	0.3823
	0.4628	0.4578	0.4509	0.4419	0.4318	0.4228	0.4122	0.4023	0.3929	0.3823
	0.4626	0.4576	0.4507	0.4417	0.4316	0.4227	0.4121	0.4022	0.3928	0.3823
	0.4551	0.4504	0.4439	0.4354	0.4257	0.4171	0.4069	0.3973	0.3882	0.378
	0.3726	0.371	0.3682	0.3641	0.359	0.3536	0.3472	0.3409	0.3346	0.3273
	0.2638	0.2637	0.2632	0.2623	0.2607	0.2588	0.2563	0.2535	0.2506	0.2471

Figure I.5: F1A: e=1a & d=3.5a

	c/a									
b/a	0.4633	0.4593	0.4539	0.4468	0.4387	0.4313	0.4226	0.4143	0.4063	0.3973
	0.4633	0.4593	0.4538	0.4467	0.4387	0.4313	0.4226	0.4143	0.4063	0.3973
	0.4632	0.4593	0.4538	0.4467	0.4386	0.4312	0.4225	0.4142	0.4062	0.3972
	0.4632	0.4593	0.4538	0.4467	0.4386	0.4313	0.4225	0.4142	0.4062	0.3972
	0.463	0.459	0.4536	0.4465	0.4384	0.4311	0.4224	0.4141	0.4061	0.3972
	0.4555	0.4518	0.4466	0.4398	0.4321	0.425	0.4166	0.4086	0.4008	0.3922
	0.3726	0.371	0.3685	0.365	0.3607	0.3566	0.3515	0.346	0.3407	0.3347
	0.2637	0.2634	0.2627	0.2616	0.2601	0.2583	0.256	0.2536	0.251	0.2481

Figure I.5: F1A: e=1a & d=4a

	c/a									
b/a	0.4636	0.4605	0.4562	0.4505	0.4439	0.4378	0.4306	0.4236	0.4168	0.4091
	0.4636	0.4605	0.4561	0.4504	0.4439	0.4378	0.4306	0.4236	0.4168	0.4091
	0.4635	0.4604	0.4561	0.4504	0.4439	0.4378	0.4306	0.4235	0.4167	0.4091
	0.4635	0.4604	0.4561	0.4504	0.4439	0.4378	0.4306	0.4236	0.4167	0.4091
	0.4633	0.4602	0.4559	0.4502	0.4437	0.4376	0.4304	0.4234	0.4166	0.4089
	0.4558	0.4528	0.4487	0.4433	0.437	0.4311	0.4242	0.4174	0.4108	0.4034
	0.3726	0.3714	0.369	0.366	0.3624	0.3589	0.3546	0.3505	0.346	0.3408
	0.2636	0.2632	0.2625	0.2613	0.2598	0.2582	0.2562	0.2541	0.2518	0.2492

Figure I.5: F1A: e=1.5a & d=0.5a

	c/a									
b/a	0.4658	0.4681	0.4663	0.4513	0.4251	0.403	0.3733	0.3483	0.3288	0.3029
	0.4661	0.4683	0.4664	0.4515	0.4252	0.4031	0.3734	0.3485	0.3289	0.3031
	0.4683	0.4703	0.468	0.453	0.4267	0.4046	0.3748	0.3499	0.3303	0.3043
	0.4696	0.4718	0.4705	0.4564	0.4304	0.4086	0.3788	0.3538	0.3343	0.308
	0.4574	0.4579	0.458	0.4516	0.4302	0.4086	0.3807	0.3562	0.3355	0.3111
	0.4304	0.4311	0.4311	0.43	0.4197	0.4049	0.379	0.356	0.3375	0.3123
	0.3493	0.3493	0.3493	0.3493	0.3492	0.3491	0.3444	0.3324	0.3166	0.2983
	0.2849	0.2849	0.2849	0.2849	0.2849	0.2849	0.2848	0.2847	0.282	0.2741

Figure I.5: F1A: e=1.5a & d=1a

	c/a									
b/a	0.4648	0.4606	0.4508	0.4335	0.4123	0.3956	0.3741	0.3558	0.3401	0.3209
	0.4651	0.4609	0.4511	0.4338	0.4126	0.396	0.3745	0.3562	0.3405	0.3212
	0.467	0.4627	0.4529	0.4356	0.4144	0.3978	0.3762	0.3579	0.3421	0.3229
	0.4681	0.4643	0.455	0.4382	0.4173	0.4008	0.3794	0.361	0.3453	0.3261
	0.4572	0.4557	0.449	0.4346	0.4155	0.3998	0.3793	0.3615	0.346	0.3272
	0.431	0.431	0.4298	0.4218	0.4071	0.3938	0.3753	0.3589	0.3444	0.3264
	0.3493	0.3493	0.3492	0.3491	0.3483	0.3443	0.3371	0.3275	0.317	0.3058
	0.2849	0.2849	0.2849	0.2849	0.2849	0.2848	0.2841	0.2816	0.2767	0.2707

Figure I.5: F1A: e=1.5a & d=1.5a

	c/a									
b/a	0.4628	0.4561	0.4459	0.4315	0.4151	0.4017	0.3852	0.3707	0.3576	0.3424
	0.4631	0.4564	0.4463	0.4319	0.4155	0.4021	0.3856	0.371	0.3579	0.3427
	0.4651	0.4584	0.4482	0.4338	0.4174	0.404	0.3874	0.3728	0.3597	0.3445
	0.4662	0.4599	0.4501	0.436	0.4199	0.4066	0.3902	0.3757	0.3626	0.3474
	0.4559	0.4512	0.443	0.4305	0.4158	0.4032	0.3877	0.3738	0.3611	0.3464
	0.4309	0.4295	0.4246	0.4158	0.404	0.3932	0.3794	0.3668	0.3551	0.3415
	0.3492	0.3491	0.349	0.3488	0.3453	0.3404	0.3339	0.3265	0.3187	0.3103
	0.2849	0.2849	0.2847	0.2846	0.2846	0.2838	0.2821	0.2789	0.2745	0.2695

Figure I.5: F1A: e=1.5a & d=2a

	c/a									
b/a	0.4625	0.4563	0.4477	0.4363	0.4234	0.4126	0.3994	0.3875	0.3764	0.3638
	0.4629	0.4567	0.4481	0.4367	0.4238	0.4129	0.3998	0.3878	0.3768	0.3642
	0.4648	0.4586	0.45	0.4386	0.4257	0.4148	0.4016	0.3897	0.3786	0.3659
	0.4659	0.46	0.4516	0.4404	0.4278	0.417	0.404	0.3921	0.3811	0.3685
	0.4553	0.4504	0.4432	0.4332	0.4216	0.4116	0.3993	0.3881	0.3775	0.3655
	0.4303	0.4273	0.423	0.4154	0.4061	0.3976	0.3871	0.377	0.3676	0.3567
	0.3493	0.3492	0.3484	0.3464	0.3429	0.3385	0.333	0.327	0.321	0.3141
	0.2849	0.2848	0.2848	0.2848	0.2843	0.2828	0.2804	0.2773	0.2736	0.2693

Figure I.5: F1A: e=1.5a & d=2.5a

	c/a									
b/a	0.4629	0.4578	0.4509	0.4419	0.4318	0.4229	0.4122	0.4023	0.3929	0.3823
	0.4632	0.4582	0.4513	0.4423	0.4322	0.4233	0.4126	0.4027	0.3933	0.3827
	0.4652	0.4601	0.4532	0.4442	0.4341	0.4251	0.4145	0.4045	0.3951	0.3845
	0.4662	0.4613	0.4546	0.4458	0.4358	0.427	0.4164	0.4066	0.3972	0.3867
	0.4554	0.4512	0.4453	0.4373	0.4281	0.4199	0.4101	0.4007	0.3918	0.3818
	0.4301	0.4268	0.4232	0.4171	0.4095	0.4027	0.3943	0.3862	0.3784	0.3696
	0.3492	0.3486	0.3473	0.3448	0.3415	0.3377	0.333	0.3281	0.3231	0.3174
	0.2849	0.285	0.2849	0.2844	0.2833	0.2816	0.2793	0.2765	0.2733	0.2697

Figure I.5: F1A: e=1.5a & d=3a

	c/a									
b/a	0.4633	0.4593	0.4539	0.4467	0.4387	0.4313	0.4226	0.4143	0.4063	0.3973
	0.4636	0.4597	0.4542	0.4471	0.439	0.4317	0.4229	0.4146	0.4066	0.3976
	0.4656	0.4616	0.4561	0.449	0.4409	0.4335	0.4248	0.4165	0.4084	0.3994
	0.4666	0.4627	0.4574	0.4504	0.4424	0.4351	0.4265	0.4182	0.4103	0.4013
	0.4556	0.4522	0.4474	0.4411	0.4337	0.4269	0.4188	0.4111	0.4035	0.3951
	0.4301	0.4276	0.4235	0.4192	0.4133	0.4075	0.4004	0.3938	0.3877	0.3797
	0.3491	0.3482	0.3466	0.3442	0.3411	0.3379	0.3339	0.3297	0.3255	0.3206
	0.2849	0.2848	0.2845	0.2837	0.2823	0.2807	0.2785	0.276	0.2733	0.2701

Figure I.5: F1A: e=1.5a & d=3.5a

	c/a									
b/a	0.4636	0.4605	0.4561	0.4504	0.4439	0.4378	0.4306	0.4236	0.4167	0.4091
	0.464	0.4609	0.4565	0.4508	0.4443	0.4382	0.431	0.4239	0.4171	0.4094
	0.4659	0.4628	0.4584	0.4527	0.4462	0.4401	0.4328	0.4258	0.4189	0.4112
	0.4669	0.4639	0.4596	0.454	0.4475	0.4415	0.4343	0.4274	0.4206	0.4129
	0.4559	0.4531	0.4493	0.4441	0.4382	0.4325	0.4258	0.4193	0.4128	0.4056
	0.4302	0.428	0.4245	0.4204	0.4156	0.4116	0.4058	0.4001	0.3946	0.3884
	0.349	0.3481	0.3465	0.3443	0.3415	0.3387	0.3352	0.3316	0.328	0.3238
	0.2849	0.2846	0.2841	0.2831	0.2817	0.2802	0.2781	0.2759	0.2736	0.2708

Figure I.5: F1A: e=1.5a & d=4a

	c/a									
b/a	0.4638	0.4614	0.4579	0.4533	0.4479	0.4428	0.4368	0.4308	0.425	0.4184
	0.4642	0.4618	0.4583	0.4536	0.4483	0.4432	0.4372	0.4312	0.4253	0.4187
	0.4661	0.4637	0.4602	0.4555	0.4502	0.4451	0.439	0.4331	0.4272	0.4206
	0.4671	0.4647	0.4613	0.4567	0.4514	0.4464	0.4404	0.4345	0.4286	0.4221
	0.4561	0.4539	0.4507	0.4465	0.4416	0.4369	0.4313	0.4257	0.4202	0.414
	0.4303	0.4285	0.426	0.4221	0.418	0.4141	0.4099	0.4052	0.4003	0.3949
	0.349	0.3481	0.3467	0.3447	0.3422	0.3397	0.3367	0.3336	0.3304	0.3267
	0.2848	0.2845	0.2838	0.2828	0.2815	0.28	0.2782	0.2762	0.2741	0.2717

Figure I.5: F1A: e=2a & d=0.5a

	c/a									
b/a	0.4658	0.4615	0.4517	0.4344	0.4132	0.3966	0.3751	0.3567	0.341	0.3218
	0.4679	0.4637	0.454	0.4368	0.4157	0.3989	0.3775	0.3591	0.3433	0.3241
	0.4664	0.4639	0.4553	0.439	0.4184	0.4018	0.3805	0.3622	0.3464	0.3272
	0.4514	0.4513	0.4481	0.4362	0.4173	0.4012	0.3808	0.3629	0.3473	0.3284
	0.4252	0.4251	0.425	0.4211	0.409	0.3933	0.3754	0.3582	0.3424	0.326
	0.4031	0.4031	0.4031	0.4029	0.3983	0.3872	0.372	0.3564	0.3418	0.3247
	0.3484	0.3484	0.3484	0.3484	0.3483	0.3482	0.3452	0.3366	0.325	0.3123
	0.303	0.303	0.303	0.303	0.303	0.3029	0.3029	0.3028	0.3005	0.2941

Figure I.5: F1A: e=2a & d=1a

	c/a									
b/a	0.4638	0.4572	0.447	0.4326	0.4161	0.4028	0.3863	0.3717	0.3586	0.3433
	0.4662	0.4596	0.4496	0.4353	0.4189	0.4056	0.3891	0.3745	0.3614	0.3461
	0.465	0.4595	0.4503	0.4368	0.421	0.4079	0.3917	0.3773	0.3643	0.3491
	0.4512	0.4487	0.4422	0.4313	0.4172	0.4047	0.3895	0.3756	0.363	0.3484
	0.4251	0.4247	0.4217	0.4146	0.4041	0.393	0.38	0.3673	0.3555	0.3425
	0.403	0.4029	0.4024	0.3993	0.3923	0.3832	0.3719	0.3608	0.3503	0.3381
	0.3484	0.3484	0.3483	0.3482	0.3477	0.345	0.3398	0.3326	0.3245	0.3158
	0.303	0.303	0.3029	0.303	0.303	0.3029	0.3023	0.3002	0.2962	0.2909

Figure I.5: F1A: e=2a & d=1.5a

	c/a									
b/a	0.4636	0.4574	0.4488	0.4374	0.4246	0.4136	0.4005	0.3885	0.3774	0.3649
	0.4659	0.4599	0.4513	0.44	0.4272	0.4163	0.4032	0.3912	0.3801	0.3675
	0.4645	0.459	0.4511	0.4404	0.4281	0.4176	0.4048	0.3931	0.3822	0.3698
	0.4503	0.4466	0.4404	0.4316	0.421	0.4113	0.3996	0.3886	0.3783	0.3665
	0.4248	0.4228	0.4187	0.412	0.4034	0.395	0.385	0.3752	0.3659	0.3554
	0.4031	0.4025	0.4003	0.3959	0.3896	0.3825	0.3739	0.3653	0.3569	0.3476
	0.3483	0.3482	0.3482	0.3476	0.3456	0.3421	0.3372	0.3314	0.3252	0.3183
	0.3029	0.3029	0.3028	0.3027	0.3027	0.3021	0.3006	0.2978	0.294	0.2896

Figure I.5: F1A: e=2a & d=2a

	c/a									
b/a	0.464	0.4589	0.452	0.443	0.4329	0.424	0.4133	0.4034	0.3939	0.3833
	0.4663	0.4613	0.4545	0.4455	0.4354	0.4265	0.4159	0.4059	0.3965	0.3859
	0.4647	0.4601	0.4536	0.4451	0.4354	0.4268	0.4165	0.4068	0.3976	0.3872
	0.4501	0.4465	0.4412	0.4339	0.4255	0.4177	0.4084	0.3995	0.391	0.3813
	0.4244	0.4219	0.4178	0.412	0.4049	0.3982	0.3901	0.3822	0.3745	0.3658
	0.4028	0.4014	0.3987	0.3944	0.3889	0.3833	0.3765	0.3695	0.3626	0.3549
	0.3484	0.3483	0.3478	0.3463	0.3438	0.3404	0.3362	0.3314	0.3264	0.3207
	0.3029	0.3028	0.3028	0.3028	0.3024	0.3011	0.2991	0.2963	0.2931	0.2893

Figure I.5: F1A: e=2a & d=2.5a

	c/a									
b/a	0.4644	0.4604	0.4549	0.4478	0.4397	0.4324	0.4236	0.4153	0.4073	0.3983
	0.4667	0.4627	0.4573	0.4502	0.4421	0.4348	0.4261	0.4178	0.4097	0.4007
	0.465	0.4613	0.4561	0.4493	0.4416	0.4345	0.426	0.4179	0.4101	0.4013
	0.4503	0.4472	0.4427	0.4368	0.4299	0.4235	0.4158	0.4084	0.4012	0.3931
	0.4243	0.4219	0.4183	0.4134	0.4075	0.4019	0.3952	0.3886	0.3821	0.3747
	0.4026	0.4009	0.3983	0.3944	0.3897	0.385	0.3793	0.3736	0.3679	0.3614
	0.3483	0.3479	0.3469	0.3451	0.3426	0.3396	0.3359	0.3319	0.3277	0.3229
	0.303	0.303	0.3029	0.3025	0.3016	0.3001	0.298	0.2955	0.2927	0.2894

Figure I.5: F1A: e=2a & d=3a

	c/a									
b/a	0.4647	0.4616	0.4572	0.4515	0.445	0.4389	0.4316	0.4246	0.4178	0.4101
	0.467	0.4639	0.4596	0.4539	0.4474	0.4413	0.434	0.427	0.4202	0.4125
	0.4653	0.4623	0.4582	0.4527	0.4464	0.4405	0.4335	0.4267	0.42	0.4125
	0.4505	0.4479	0.4442	0.4394	0.4337	0.4283	0.4219	0.4157	0.4095	0.4025
	0.4244	0.4223	0.4192	0.4151	0.4102	0.4055	0.3998	0.3942	0.3886	0.3823
	0.4025	0.4009	0.3985	0.3952	0.3911	0.3871	0.3823	0.3774	0.3726	0.3671
	0.3482	0.3476	0.3464	0.3446	0.3421	0.3395	0.3362	0.3328	0.3292	0.3251
	0.303	0.3029	0.3026	0.3019	0.3007	0.2992	0.2973	0.295	0.2925	0.2896

Figure I.5: F1A: e=2a & d=3.5a

	c/a									
b/a	0.4649	0.4625	0.459	0.4543	0.449	0.4439	0.4378	0.4319	0.426	0.4194
	0.4672	0.4648	0.4613	0.4567	0.4513	0.4462	0.4402	0.4342	0.4284	0.4217
	0.4655	0.4631	0.4598	0.4553	0.4501	0.4452	0.4393	0.4335	0.4278	0.4213
	0.4506	0.4485	0.4455	0.4415	0.4368	0.4323	0.4269	0.4215	0.4162	0.4102
	0.4245	0.4227	0.4201	0.4166	0.4125	0.4085	0.4037	0.3989	0.3941	0.3887
	0.4026	0.4012	0.399	0.3962	0.3927	0.3893	0.3851	0.3809	0.3767	0.372
	0.3482	0.3474	0.3462	0.3445	0.3423	0.3399	0.3371	0.334	0.3309	0.3274
	0.3029	0.3027	0.3022	0.3013	0.3001	0.2987	0.2969	0.2949	0.2927	0.2901

Figure I.5: F1A: e=2a & d=4a

	c/a									
b/a	0.4651	0.4631	0.4603	0.4565	0.452	0.4478	0.4426	0.4376	0.4325	0.4268
	0.4674	0.4654	0.4626	0.4588	0.4544	0.4501	0.445	0.4399	0.4348	0.4291
	0.4657	0.4637	0.461	0.4573	0.453	0.4489	0.4439	0.4389	0.434	0.4284
	0.4508	0.449	0.4465	0.4432	0.4393	0.4354	0.4308	0.4262	0.4216	0.4164
	0.4246	0.4231	0.4209	0.418	0.4145	0.4111	0.407	0.4028	0.3987	0.394
	0.4026	0.4014	0.3996	0.3971	0.3941	0.3912	0.3876	0.384	0.3803	0.3761
	0.3481	0.3474	0.3463	0.3447	0.3427	0.3406	0.3381	0.3354	0.3327	0.3296
	0.3029	0.3025	0.302	0.3011	0.2999	0.2986	0.2969	0.295	0.2931	0.2908

Figure I.5: F1A: e=2.5a & d=0.5a

	c/a									
b/a	0.463	0.4566	0.4466	0.4322	0.4159	0.4026	0.3861	0.3716	0.3585	0.3432
	0.46	0.455	0.4458	0.4323	0.4164	0.4032	0.3869	0.3725	0.3595	0.3444
	0.4508	0.4491	0.4421	0.4303	0.4154	0.4023	0.3866	0.3726	0.3596	0.3447
	0.4335	0.4334	0.4312	0.4231	0.4106	0.3978	0.3833	0.3697	0.3569	0.3429
	0.4123	0.4123	0.4122	0.4097	0.4013	0.39	0.3769	0.3639	0.3515	0.3388
	0.3957	0.3957	0.3957	0.3956	0.393	0.3851	0.3737	0.362	0.3501	0.3376
	0.3559	0.3559	0.3559	0.3559	0.3558	0.3558	0.3535	0.3467	0.3375	0.3274
	0.3209	0.3209	0.3209	0.3209	0.3209	0.3209	0.3209	0.3208	0.3189	0.3134

Figure I.5: F1A: e=2.5a & d=1a

	c/a									
b/a	0.4627	0.4566	0.4482	0.4368	0.4241	0.4133	0.4002	0.3883	0.3772	0.3646
	0.4589	0.4536	0.4459	0.4353	0.4232	0.4126	0.3999	0.3883	0.3774	0.3651
	0.4499	0.4462	0.4397	0.4304	0.4193	0.4092	0.3973	0.3861	0.3756	0.3636
	0.4334	0.4318	0.4273	0.4199	0.4104	0.4011	0.3901	0.3796	0.3696	0.3585
	0.4123	0.4121	0.4101	0.4052	0.3978	0.3895	0.3798	0.3701	0.3607	0.3505
	0.3957	0.3956	0.3953	0.3932	0.3883	0.3816	0.3734	0.3647	0.3559	0.3466
	0.3559	0.3559	0.3558	0.3558	0.3554	0.3533	0.3491	0.3434	0.3366	0.3293
	0.3209	0.3209	0.3209	0.3209	0.3209	0.3209	0.3204	0.3186	0.3151	0.3104

Figure I.5: F1A: e=2.5a & d=1.5a

	c/a									
b/a	0.463	0.458	0.4512	0.4423	0.4323	0.4234	0.4128	0.4029	0.3935	0.383
	0.4589	0.4544	0.4481	0.4396	0.43	0.4215	0.4112	0.4016	0.3925	0.3822
	0.4495	0.4458	0.4403	0.4327	0.4239	0.4159	0.4063	0.3971	0.3884	0.3786
	0.4328	0.4303	0.4259	0.4196	0.412	0.4048	0.396	0.3876	0.3794	0.3702
	0.4121	0.4108	0.408	0.4032	0.397	0.3906	0.3829	0.3752	0.3677	0.3593
	0.3957	0.3954	0.3939	0.3907	0.386	0.3807	0.3741	0.3673	0.3605	0.3528
	0.3558	0.3558	0.3557	0.3553	0.3537	0.3509	0.3469	0.3421	0.3368	0.331
	0.3209	0.3209	0.3208	0.3208	0.3207	0.3202	0.3189	0.3164	0.3131	0.3091

Figure I.5: F1A: e=2.5a & d=2a

	c/a									
b/a	0.4633	0.4594	0.454	0.447	0.439	0.4317	0.423	0.4147	0.4067	0.3978
	0.4592	0.4556	0.4504	0.4437	0.436	0.4289	0.4205	0.4125	0.4047	0.396
	0.4496	0.4464	0.4418	0.4357	0.4285	0.4219	0.414	0.4064	0.3991	0.3907
	0.4327	0.4301	0.4263	0.421	0.4147	0.4088	0.4016	0.3946	0.3878	0.38
	0.4118	0.4101	0.4072	0.4029	0.3977	0.3925	0.3861	0.3798	0.3736	0.3665
	0.3955	0.3945	0.3926	0.3894	0.3852	0.3808	0.3754	0.3698	0.3642	0.3579
	0.3559	0.3559	0.3554	0.3543	0.3522	0.3495	0.3459	0.3419	0.3376	0.3326
	0.3209	0.3208	0.3208	0.3208	0.3204	0.3193	0.3175	0.3151	0.3121	0.3086

Figure I.5: F1A: e=2.5a & d=2.5a

	c/a									
b/a	0.4637	0.4606	0.4563	0.4506	0.4441	0.4381	0.4309	0.4239	0.4171	0.4094
	0.4595	0.4566	0.4525	0.447	0.4408	0.4349	0.4279	0.4211	0.4145	0.407
	0.4498	0.4472	0.4434	0.4384	0.4326	0.427	0.4205	0.414	0.4077	0.4006
	0.4327	0.4305	0.4272	0.4228	0.4176	0.4126	0.4066	0.4007	0.3949	0.3883
	0.4117	0.41	0.4074	0.4037	0.3992	0.3948	0.3895	0.3842	0.3789	0.3729
	0.3954	0.3942	0.3922	0.3892	0.3856	0.3818	0.3772	0.3725	0.3678	0.3624
	0.3558	0.3555	0.3547	0.3533	0.3511	0.3487	0.3455	0.342	0.3384	0.3342
	0.3209	0.321	0.3209	0.3205	0.3197	0.3184	0.3165	0.3142	0.3117	0.3086

Figure I.5: F1A: e=2.5a & d=3a

	c/a									
b/a	0.4639	0.4615	0.458	0.4534	0.4481	0.443	0.437	0.4311	0.4252	0.4187
	0.4597	0.4574	0.4541	0.4496	0.4445	0.4396	0.4337	0.4279	0.4222	0.4158
	0.45	0.4479	0.4448	0.4406	0.4358	0.4312	0.4256	0.4202	0.4147	0.4086
	0.4328	0.4309	0.4282	0.4245	0.4201	0.4159	0.4109	0.4058	0.4008	0.3951
	0.4118	0.4102	0.4079	0.4047	0.4009	0.3972	0.3927	0.3881	0.3835	0.3783
	0.3953	0.3941	0.3923	0.3897	0.3864	0.3832	0.3793	0.3752	0.3712	0.3665
	0.3557	0.3552	0.3543	0.3527	0.3507	0.3485	0.3457	0.3427	0.3395	0.3359
	0.3209	0.3209	0.3206	0.32	0.3189	0.3176	0.3158	0.3137	0.3115	0.3088

Figure I.5: F1A: e=2.5a & d=3.5a

	c/a									
b/a	0.4641	0.4621	0.4593	0.4555	0.4511	0.4468	0.4418	0.4367	0.4317	0.426
	0.4599	0.458	0.4553	0.4516	0.4473	0.4432	0.4382	0.4333	0.4284	0.4228
	0.4502	0.4484	0.4458	0.4424	0.4384	0.4344	0.4298	0.4251	0.4204	0.4151
	0.4329	0.4314	0.4291	0.426	0.4223	0.4187	0.4144	0.41	0.4057	0.4007
	0.4118	0.4105	0.4085	0.4058	0.4025	0.3993	0.3954	0.3915	0.3875	0.383
	0.3953	0.3942	0.3926	0.3903	0.3875	0.3847	0.3813	0.3778	0.3742	0.3702
	0.3557	0.3551	0.3541	0.3526	0.3507	0.3487	0.3462	0.3436	0.3408	0.3376
	0.3209	0.3207	0.3203	0.3195	0.3184	0.3171	0.3154	0.3136	0.3115	0.3091

Figure I.5: F1A: e=2.5a & d=4a

	c/a									
b/a	0.4642	0.4626	0.4603	0.4571	0.4534	0.4498	0.4455	0.4411	0.4368	0.4318
	0.46	0.4585	0.4562	0.4532	0.4496	0.446	0.4418	0.4376	0.4333	0.4285
	0.4503	0.4488	0.4467	0.4438	0.4404	0.4371	0.433	0.429	0.4249	0.4203
	0.433	0.4317	0.4298	0.4271	0.424	0.4209	0.4172	0.4135	0.4097	0.4054
	0.4119	0.4107	0.409	0.4067	0.4039	0.4011	0.3978	0.3944	0.3909	0.3869
	0.3954	0.3944	0.3929	0.3909	0.3885	0.3861	0.3831	0.38	0.3769	0.3733
	0.3557	0.3551	0.3541	0.3527	0.351	0.3492	0.347	0.3446	0.3422	0.3394
	0.3209	0.3206	0.3201	0.3193	0.3182	0.3169	0.3154	0.3137	0.3118	0.3097

Figure I.5: F1A: e=3a & d=0.5a

	c/a									
b/a	0.461	0.4552	0.4469	0.4357	0.4231	0.4123	0.3993	0.3874	0.3764	0.3638
	0.4556	0.4515	0.4441	0.4336	0.4216	0.4109	0.3982	0.3865	0.3756	0.3633
	0.446	0.4448	0.4394	0.4304	0.4193	0.4087	0.3966	0.3851	0.3743	0.3624
	0.4315	0.4315	0.4299	0.4237	0.4143	0.4043	0.3929	0.3818	0.3712	0.3599
	0.4151	0.4151	0.415	0.4131	0.4068	0.398	0.3876	0.3771	0.3668	0.3562
	0.4018	0.4018	0.4018	0.4018	0.3999	0.3936	0.3846	0.3751	0.3652	0.3549
	0.3707	0.3707	0.3707	0.3707	0.3707	0.3706	0.3687	0.3631	0.3553	0.3468
	0.3424	0.3424	0.3424	0.3424	0.3424	0.3424	0.3423	0.3422	0.3405	0.3357

Figure I.5: F1A: e=3a & d=1a

	c/a									
b/a	0.461	0.4562	0.4496	0.4408	0.4308	0.422	0.4115	0.4016	0.3923	0.3818
	0.4548	0.4507	0.4447	0.4365	0.4271	0.4187	0.4085	0.399	0.3899	0.3796
	0.4454	0.4426	0.4377	0.4306	0.422	0.414	0.4044	0.3953	0.3865	0.3767
	0.4315	0.4303	0.427	0.4213	0.414	0.4066	0.3978	0.3891	0.3808	0.3715
	0.4151	0.4149	0.4135	0.4097	0.404	0.3974	0.3896	0.3816	0.3736	0.365
	0.4018	0.4017	0.4015	0.3999	0.396	0.3907	0.384	0.3768	0.3694	0.3614
	0.3707	0.3707	0.3707	0.3707	0.3703	0.3686	0.3651	0.3602	0.3543	0.3479
	0.3424	0.3424	0.3424	0.3424	0.3424	0.3423	0.3418	0.3402	0.3371	0.3335

Figure I.5: F1A: e=3a & d=1.5a

	c/a									
b/a	0.4614	0.4576	0.4522	0.4452	0.4373	0.43	0.4214	0.4132	0.4052	0.3963
	0.4549	0.4514	0.4465	0.4399	0.4324	0.4255	0.4172	0.4092	0.4015	0.3929
	0.4451	0.4423	0.438	0.4322	0.4253	0.4188	0.4111	0.4035	0.3962	0.3879
	0.431	0.4291	0.4259	0.421	0.415	0.4091	0.402	0.395	0.3881	0.3804
	0.415	0.414	0.4118	0.4081	0.4032	0.398	0.3917	0.3852	0.3788	0.3716
	0.4018	0.4016	0.4004	0.3979	0.3941	0.3897	0.3843	0.3785	0.3726	0.3661
	0.3707	0.3706	0.3706	0.3703	0.3689	0.3665	0.3631	0.3589	0.3543	0.349
	0.3424	0.3423	0.3423	0.3422	0.3421	0.3417	0.3405	0.3383	0.3352	0.3316

Figure I.5: F1A: e=3a & d=2a

	c/a									
b/a	0.4617	0.4587	0.4544	0.4488	0.4423	0.4363	0.4292	0.4222	0.4155	0.4078
	0.4551	0.4523	0.4483	0.443	0.4368	0.431	0.4242	0.4175	0.4109	0.4035
	0.4451	0.4427	0.4391	0.4343	0.4286	0.4233	0.4168	0.4105	0.4042	0.3972
	0.4309	0.429	0.426	0.4218	0.4168	0.412	0.4061	0.4002	0.3944	0.3878
	0.4147	0.4134	0.4111	0.4077	0.4035	0.3992	0.3939	0.3886	0.3832	0.3771
	0.4017	0.4009	0.3994	0.3968	0.3934	0.3897	0.3851	0.3803	0.3755	0.3699
	0.3707	0.3707	0.3704	0.3694	0.3676	0.3653	0.3621	0.3585	0.3547	0.3503
	0.3423	0.3423	0.3423	0.3422	0.3419	0.3408	0.3392	0.337	0.3343	0.331

Figure I.5: F1A: e=3a & d=2.5a

	c/a									
b/a	0.4619	0.4595	0.4561	0.4515	0.4462	0.4412	0.4352	0.4293	0.4235	0.417
	0.4553	0.453	0.4497	0.4454	0.4403	0.4355	0.4297	0.424	0.4184	0.412
	0.4453	0.4432	0.4402	0.4362	0.4315	0.427	0.4216	0.4162	0.4109	0.4048
	0.4309	0.4292	0.4266	0.4231	0.4189	0.4147	0.4098	0.4048	0.3998	0.3941
	0.4146	0.4133	0.4112	0.4082	0.4045	0.4009	0.3964	0.3918	0.3873	0.382
	0.4015	0.4006	0.399	0.3966	0.3935	0.3903	0.3864	0.3823	0.3782	0.3734
	0.3707	0.3704	0.3698	0.3685	0.3667	0.3645	0.3617	0.3586	0.3553	0.3515
	0.3424	0.3424	0.3423	0.342	0.3412	0.34	0.3383	0.3362	0.3338	0.3309

Figure I.5: F1A: e=3a & d=3a

	c/a									
b/a	0.4621	0.4602	0.4573	0.4536	0.4492	0.445	0.4399	0.4349	0.4299	0.4242
	0.4555	0.4536	0.4509	0.4473	0.4431	0.439	0.4341	0.4293	0.4244	0.4189
	0.4454	0.4437	0.4412	0.4379	0.4339	0.4301	0.4255	0.4209	0.4162	0.411
	0.431	0.4295	0.4273	0.4243	0.4207	0.4172	0.4129	0.4086	0.4043	0.3994
	0.4147	0.4134	0.4115	0.4089	0.4058	0.4026	0.3987	0.3948	0.3909	0.3863
	0.4015	0.4005	0.399	0.3968	0.3941	0.3913	0.3879	0.3844	0.3808	0.3767
	0.3706	0.3702	0.3694	0.368	0.3662	0.3643	0.3617	0.359	0.3562	0.3528
	0.3424	0.3423	0.342	0.3414	0.3405	0.3393	0.3376	0.3357	0.3335	0.331

Figure I.5: F1A: e=3a & d=3.5a

	c/a									
b/a	0.4622	0.4606	0.4583	0.4552	0.4515	0.4479	0.4436	0.4393	0.4349	0.43
	0.4556	0.454	0.4518	0.4488	0.4453	0.4418	0.4376	0.4334	0.4292	0.4244
	0.4455	0.4441	0.442	0.4392	0.4358	0.4326	0.4286	0.4246	0.4206	0.416
	0.4311	0.4298	0.4279	0.4254	0.4223	0.4193	0.4156	0.4119	0.4081	0.4039
	0.4147	0.4136	0.412	0.4097	0.407	0.4042	0.4009	0.3975	0.394	0.39
	0.4015	0.4006	0.3992	0.3973	0.3949	0.3924	0.3895	0.3864	0.3832	0.3796
	0.3706	0.3701	0.3692	0.3679	0.3662	0.3644	0.3621	0.3597	0.3572	0.3543
	0.3423	0.3421	0.3417	0.341	0.34	0.3388	0.3372	0.3355	0.3335	0.3313

Figure I.5: F1A: e=3a & d=4a

	c/a									
b/a	0.4624	0.461	0.4591	0.4565	0.4533	0.4503	0.4466	0.4428	0.439	0.4347
	0.4557	0.4544	0.4525	0.45	0.447	0.444	0.4404	0.4368	0.4331	0.4289
	0.4456	0.4444	0.4426	0.4402	0.4374	0.4346	0.4312	0.4277	0.4242	0.4202
	0.4312	0.4301	0.4285	0.4263	0.4236	0.421	0.4178	0.4146	0.4113	0.4075
	0.4148	0.4138	0.4124	0.4104	0.408	0.4056	0.4027	0.3997	0.3967	0.3932
	0.4015	0.4007	0.3995	0.3978	0.3956	0.3935	0.3909	0.3882	0.3854	0.3822
	0.3706	0.37	0.3692	0.368	0.3664	0.3648	0.3627	0.3606	0.3583	0.3557
	0.3423	0.342	0.3415	0.3408	0.3398	0.3386	0.3372	0.3355	0.3338	0.3317

Figure I.5: F1A: e=3.5a & d=0.5a

	c/a									
b/a	0.4611	0.4565	0.4499	0.4411	0.4311	0.4223	0.4117	0.4018	0.3925	0.3819
	0.456	0.4528	0.4469	0.4388	0.4293	0.4205	0.4102	0.4005	0.3913	0.3809
	0.4478	0.4469	0.4427	0.4357	0.4269	0.4183	0.4085	0.399	0.3898	0.3798
	0.4364	0.4363	0.4351	0.4303	0.4228	0.4147	0.4054	0.3962	0.3872	0.3776
	0.4235	0.4235	0.4235	0.422	0.4169	0.4098	0.4013	0.3925	0.3838	0.3746
	0.4127	0.4127	0.4127	0.4126	0.4111	0.406	0.3985	0.3906	0.3822	0.3733
	0.3876	0.3876	0.3876	0.3876	0.3875	0.3875	0.3859	0.381	0.3743	0.3669
	0.3639	0.3639	0.3639	0.3639	0.3639	0.3639	0.3638	0.3637	0.3622	0.3578

Figure I.5: F1A: e=3.5a & d=1a

	c/a									
b/a	0.4612	0.4575	0.4522	0.4452	0.4373	0.43	0.4214	0.4132	0.4053	0.3963
	0.4554	0.4522	0.4475	0.4411	0.4336	0.4266	0.4183	0.4103	0.4025	0.3938
	0.4474	0.4452	0.4414	0.4358	0.4289	0.4223	0.4144	0.4067	0.3993	0.3909
	0.4363	0.4354	0.4328	0.4283	0.4224	0.4163	0.409	0.4017	0.3946	0.3866
	0.4235	0.4234	0.4222	0.4192	0.4145	0.4091	0.4026	0.3958	0.389	0.3814
	0.4127	0.4126	0.4124	0.4111	0.4079	0.4034	0.3978	0.3916	0.3852	0.3782
	0.3876	0.3876	0.3875	0.3875	0.3872	0.3857	0.3827	0.3784	0.3732	0.3675
	0.3639	0.3639	0.3639	0.3639	0.3639	0.3638	0.3634	0.3619	0.3591	0.3552

Figure I.5: F1A: e=3.5a & d=1.5a

	c/a									
b/a	0.4615	0.4585	0.4543	0.4487	0.4422	0.4362	0.4291	0.4222	0.4154	0.4078
	0.4555	0.4528	0.4488	0.4436	0.4375	0.4318	0.4249	0.4182	0.4116	0.4042
	0.4471	0.4449	0.4416	0.4369	0.4313	0.4259	0.4195	0.4131	0.4068	0.3997
	0.436	0.4345	0.4319	0.4279	0.423	0.4181	0.4122	0.4062	0.4002	0.3935
	0.4234	0.4227	0.4209	0.4178	0.4138	0.4094	0.404	0.3985	0.3929	0.3866
	0.4127	0.4125	0.4115	0.4095	0.4063	0.4025	0.3979	0.3929	0.3877	0.3819
	0.3875	0.3875	0.3875	0.3871	0.386	0.3839	0.3809	0.3771	0.373	0.3683
	0.3639	0.3638	0.3638	0.3637	0.3637	0.3632	0.3621	0.3601	0.3573	0.3539

Figure I.5: F1A: e=3.5a & d=2a

	c/a									
b/a	0.4617	0.4593	0.4559	0.4513	0.4461	0.4411	0.4351	0.4292	0.4234	0.4168
	0.4556	0.4534	0.4502	0.4459	0.4408	0.436	0.4302	0.4246	0.4189	0.4125
	0.4472	0.4452	0.4423	0.4384	0.4338	0.4292	0.4238	0.4184	0.413	0.407
	0.4359	0.4343	0.4319	0.4285	0.4243	0.4202	0.4152	0.4102	0.4051	0.3994
	0.4232	0.4221	0.4203	0.4175	0.4139	0.4102	0.4057	0.4011	0.3964	0.391
	0.4126	0.4119	0.4107	0.4085	0.4056	0.4024	0.3984	0.3942	0.3899	0.3849
	0.3876	0.3876	0.3872	0.3864	0.3848	0.3827	0.3799	0.3767	0.3732	0.3692
	0.3638	0.3638	0.3638	0.3637	0.3634	0.3624	0.3609	0.3589	0.3564	0.3533

Figure I.5: F1A: e=3.5a & d=2.5a

	c/a									
b/a	0.4619	0.4599	0.4571	0.4534	0.449	0.4448	0.4397	0.4347	0.4297	0.424
	0.4558	0.4539	0.4513	0.4477	0.4435	0.4394	0.4345	0.4297	0.4248	0.4193
	0.4472	0.4456	0.4432	0.4399	0.4359	0.4321	0.4275	0.4229	0.4182	0.413
	0.4359	0.4345	0.4323	0.4294	0.4258	0.4223	0.4181	0.4137	0.4094	0.4044
	0.4232	0.422	0.4203	0.4178	0.4146	0.4115	0.4076	0.4036	0.3996	0.3949
	0.4124	0.4116	0.4103	0.4082	0.4056	0.4028	0.3993	0.3957	0.392	0.3878
	0.3875	0.3873	0.3867	0.3856	0.384	0.382	0.3795	0.3767	0.3737	0.3702
	0.3639	0.3639	0.3638	0.3635	0.3628	0.3616	0.36	0.3581	0.3558	0.3531

Figure I.5: F1A: e=3.5a & d=3a

	c/a									
b/a	0.462	0.4604	0.4581	0.455	0.4513	0.4477	0.4434	0.4391	0.4347	0.4298
	0.4559	0.4544	0.4521	0.4492	0.4456	0.4421	0.438	0.4338	0.4296	0.4248
	0.4473	0.4459	0.4439	0.4411	0.4378	0.4345	0.4305	0.4265	0.4225	0.4179
	0.4359	0.4347	0.4329	0.4303	0.4273	0.4242	0.4205	0.4168	0.413	0.4087
	0.4232	0.4221	0.4205	0.4183	0.4156	0.4128	0.4095	0.406	0.4025	0.3984
	0.4124	0.4116	0.4103	0.4084	0.406	0.4036	0.4005	0.3974	0.3942	0.3904
	0.3875	0.3871	0.3864	0.3852	0.3835	0.3817	0.3795	0.377	0.3743	0.3713
	0.3639	0.3638	0.3635	0.363	0.3621	0.361	0.3594	0.3576	0.3556	0.3531

Figure I.5: F1A: e=3.5a & d=3.5a

	c/a									
b/a	0.4621	0.4608	0.4589	0.4563	0.4531	0.4501	0.4464	0.4426	0.4388	0.4345
	0.456	0.4547	0.4528	0.4503	0.4473	0.4443	0.4407	0.4371	0.4334	0.4292
	0.4474	0.4462	0.4445	0.4421	0.4393	0.4364	0.433	0.4295	0.426	0.422
	0.436	0.4349	0.4333	0.4311	0.4285	0.4259	0.4227	0.4194	0.4161	0.4123
	0.4232	0.4223	0.4208	0.4189	0.4165	0.4141	0.4112	0.4081	0.405	0.4015
	0.4124	0.4116	0.4104	0.4087	0.4066	0.4044	0.4018	0.399	0.3962	0.3929
	0.3874	0.387	0.3862	0.385	0.3835	0.3818	0.3798	0.3775	0.3752	0.3725
	0.3638	0.3636	0.3633	0.3626	0.3617	0.3605	0.359	0.3574	0.3555	0.3534

Figure I.5: F1A: e=3.5a & d=4a

	c/a									
b/a	0.4622	0.4611	0.4595	0.4572	0.4546	0.4519	0.4487	0.4454	0.4421	0.4383
	0.4561	0.455	0.4534	0.4512	0.4487	0.4461	0.443	0.4398	0.4366	0.4329
	0.4475	0.4465	0.445	0.443	0.4405	0.438	0.4351	0.432	0.4289	0.4254
	0.436	0.4351	0.4337	0.4319	0.4296	0.4273	0.4245	0.4216	0.4187	0.4153
	0.4232	0.4224	0.4212	0.4195	0.4174	0.4152	0.4127	0.41	0.4073	0.4041
	0.4124	0.4117	0.4106	0.4091	0.4072	0.4053	0.403	0.4005	0.398	0.3951
	0.3874	0.3869	0.3862	0.3851	0.3836	0.3821	0.3803	0.3783	0.3762	0.3737
	0.3638	0.3635	0.3631	0.3624	0.3614	0.3603	0.359	0.3574	0.3558	0.3538

Figure I.5: F1A: e=4a & d=0.5a

	c/a									
b/a	0.4618	0.4582	0.4529	0.446	0.438	0.4307	0.4221	0.4138	0.4058	0.3969
	0.4577	0.4551	0.4505	0.444	0.4364	0.4292	0.4208	0.4126	0.4047	0.3959
	0.4511	0.4504	0.4471	0.4415	0.4344	0.4274	0.4192	0.4112	0.4034	0.3949
	0.4421	0.442	0.4411	0.4372	0.4312	0.4245	0.4168	0.409	0.4014	0.3931
	0.4319	0.4319	0.4319	0.4307	0.4265	0.4207	0.4136	0.4062	0.3987	0.3908
	0.423	0.423	0.423	0.423	0.4217	0.4175	0.4112	0.4046	0.3973	0.3896
	0.4024	0.4024	0.4024	0.4024	0.4024	0.4024	0.4009	0.3968	0.391	0.3844
	0.3824	0.3824	0.3824	0.3824	0.3824	0.3824	0.3824	0.3823	0.3809	0.377

Figure I.5: F1A: e=4a & d=1a

	c/a									
b/a	0.4619	0.459	0.4548	0.4492	0.4427	0.4367	0.4296	0.4226	0.4159	0.4082
	0.4572	0.4547	0.4509	0.4457	0.4396	0.4339	0.4269	0.4202	0.4135	0.406
	0.4507	0.4491	0.446	0.4414	0.4359	0.4303	0.4238	0.4172	0.4108	0.4035
	0.442	0.4413	0.4392	0.4356	0.4307	0.4256	0.4195	0.4132	0.4071	0.4001
	0.4319	0.4318	0.4309	0.4284	0.4245	0.42	0.4144	0.4086	0.4027	0.3961
	0.423	0.423	0.4228	0.4217	0.419	0.4152	0.4104	0.4051	0.3995	0.3934
	0.4024	0.4024	0.4024	0.4024	0.4021	0.4008	0.3981	0.3943	0.3898	0.3847
	0.3824	0.3824	0.3824	0.3824	0.3824	0.3824	0.3819	0.3806	0.3781	0.3746

Figure I.5: F1A: e=4a & d=1.5a

	c/a									
b/a	0.4621	0.4597	0.4563	0.4518	0.4465	0.4415	0.4355	0.4296	0.4238	0.4172
	0.4572	0.4551	0.4519	0.4476	0.4426	0.4378	0.432	0.4263	0.4206	0.4142
	0.4505	0.4488	0.446	0.4422	0.4376	0.4331	0.4276	0.4221	0.4167	0.4105
	0.4418	0.4406	0.4384	0.4352	0.4311	0.4269	0.4218	0.4167	0.4115	0.4056
	0.4318	0.4312	0.4298	0.4272	0.4238	0.42	0.4154	0.4107	0.4058	0.4002
	0.423	0.4229	0.4221	0.4203	0.4176	0.4144	0.4103	0.4059	0.4014	0.3962
	0.4024	0.4024	0.4023	0.402	0.401	0.3992	0.3965	0.3932	0.3895	0.3852
	0.3824	0.3824	0.3823	0.3823	0.3822	0.3818	0.3808	0.3789	0.3764	0.3733

Figure I.5: F1A: e=4a & d=2a

	c/a									
b/a	0.4623	0.4603	0.4575	0.4538	0.4494	0.4452	0.4401	0.4351	0.4301	0.4244
	0.4573	0.4555	0.4529	0.4493	0.4451	0.4411	0.4362	0.4313	0.4264	0.4209
	0.4506	0.4490	0.4466	0.4433	0.4394	0.4356	0.4310	0.4263	0.4216	0.4163
	0.4417	0.4404	0.4384	0.4355	0.4320	0.4285	0.4242	0.4198	0.4154	0.4103
	0.4317	0.4308	0.4292	0.4268	0.4238	0.4206	0.4167	0.4126	0.4085	0.4037
	0.4229	0.4224	0.4213	0.4195	0.4169	0.4141	0.4107	0.4070	0.4031	0.3987
	0.4024	0.4024	0.4021	0.4014	0.4000	0.3981	0.3956	0.3927	0.3896	0.3859
	0.3824	0.3823	0.3823	0.3823	0.3819	0.3811	0.3797	0.3778	0.3755	0.3726

Figure I.5: F1A: e=4a & d=2.5a

	c/a									
b/a	0.4624	0.4608	0.4585	0.4554	0.4517	0.4481	0.4438	0.4395	0.4351	0.4302
	0.4574	0.4559	0.4537	0.4507	0.4472	0.4437	0.4396	0.4353	0.4311	0.4263
	0.4506	0.4492	0.4472	0.4444	0.4411	0.4378	0.4339	0.4298	0.4258	0.4211
	0.4417	0.4405	0.4387	0.4362	0.4332	0.4301	0.4264	0.4226	0.4188	0.4144
	0.4316	0.4307	0.4292	0.427	0.4243	0.4216	0.4182	0.4147	0.4111	0.4069
	0.4228	0.4222	0.421	0.4192	0.4169	0.4144	0.4114	0.4082	0.4048	0.401
	0.4024	0.4022	0.4017	0.4007	0.3992	0.3974	0.3952	0.3926	0.3899	0.3867
	0.3824	0.3824	0.3823	0.382	0.3813	0.3803	0.3788	0.377	0.3749	0.3724

Figure I.5: F1A: e=4a & d=3a

	c/a									
b/a	0.4625	0.4612	0.4593	0.4566	0.4535	0.4504	0.4467	0.443	0.4392	0.4349
	0.4575	0.4563	0.4544	0.4519	0.4489	0.4459	0.4423	0.4386	0.4349	0.4307
	0.4507	0.4495	0.4478	0.4454	0.4426	0.4397	0.4363	0.4328	0.4292	0.4252
	0.4417	0.4407	0.4391	0.4369	0.4343	0.4316	0.4284	0.4251	0.4218	0.4179
	0.4316	0.4307	0.4294	0.4274	0.4251	0.4226	0.4197	0.4166	0.4134	0.4098
	0.4228	0.4221	0.421	0.4193	0.4172	0.415	0.4123	0.4095	0.4066	0.4032
	0.4023	0.402	0.4013	0.4003	0.3988	0.3972	0.3951	0.3928	0.3904	0.3876
	0.3824	0.3823	0.3821	0.3816	0.3807	0.3797	0.3782	0.3765	0.3746	0.3724

Figure I.5: F1A: e=4a & d=3.5a

	c/a									
b/a	0.4626	0.4615	0.4599	0.4576	0.455	0.4523	0.4491	0.4458	0.4425	0.4387
	0.4576	0.4565	0.455	0.4528	0.4502	0.4476	0.4445	0.4413	0.4381	0.4344
	0.4507	0.4497	0.4483	0.4462	0.4438	0.4413	0.4383	0.4352	0.4321	0.4285
	0.4418	0.4408	0.4395	0.4376	0.4353	0.433	0.4302	0.4273	0.4243	0.4209
	0.4317	0.4308	0.4296	0.4279	0.4258	0.4237	0.4211	0.4184	0.4156	0.4123
	0.4228	0.4221	0.4211	0.4196	0.4177	0.4157	0.4134	0.4109	0.4083	0.4053
	0.4023	0.4019	0.4012	0.4001	0.3987	0.3972	0.3953	0.3933	0.3911	0.3886
	0.3824	0.3822	0.3818	0.3812	0.3803	0.3793	0.3779	0.3763	0.3746	0.3725

Figure I.5: F1A: e=4a & d=4a

	c/a									
b/a	0.4627	0.4617	0.4603	0.4584	0.4561	0.4538	0.451	0.4481	0.4452	0.4418
	0.4577	0.4568	0.4554	0.4535	0.4513	0.4491	0.4463	0.4435	0.4407	0.4374
	0.4508	0.4499	0.4487	0.4469	0.4448	0.4426	0.44	0.4373	0.4345	0.4314
	0.4418	0.441	0.4398	0.4382	0.4362	0.4341	0.4316	0.4291	0.4265	0.4234
	0.4317	0.431	0.4299	0.4284	0.4265	0.4246	0.4223	0.4199	0.4174	0.4146
	0.4228	0.4222	0.4212	0.4199	0.4182	0.4165	0.4143	0.4121	0.4098	0.4071
	0.4023	0.4019	0.4012	0.4002	0.3989	0.3975	0.3957	0.3939	0.392	0.3897
	0.3823	0.3821	0.3817	0.381	0.3801	0.3791	0.3778	0.3763	0.3748	0.3729

Figure I.6: F2A: e=0.5a & d=0.5a

	c/a									
b/a	−0.336	−0.336	−0.3359	−0.3359	−0.3359	−0.3324	−0.3192	−0.297	−0.2723	−0.2582
	−0.336	−0.336	−0.3359	−0.3359	−0.3359	−0.3324	−0.3192	−0.297	−0.2723	−0.2582
	−0.336	−0.336	−0.3359	−0.3359	−0.3358	−0.3324	−0.3191	−0.297	−0.2723	−0.2581
	−0.336	−0.336	−0.3359	−0.3359	−0.3358	−0.3324	−0.319	−0.2969	−0.2725	−0.2581
	−0.336	−0.336	−0.3359	−0.3359	−0.3358	−0.3323	−0.319	−0.2971	−0.2735	−0.2582
	−0.3354	−0.3355	−0.3354	−0.3354	−0.3353	−0.3314	−0.3195	−0.2981	−0.2736	−0.258
	−0.3306	−0.3307	−0.3308	−0.3307	−0.3308	−0.3286	−0.3172	−0.2943	−0.2685	−0.2545
	−0.2338	−0.2339	−0.234	−0.2339	−0.2338	−0.234	−0.2337	−0.2334	−0.2284	−0.2158

Figure I.6: F2A: e=0.5a & d=1a

	c/a									
b/a	−0.3358	−0.3345	−0.3315	−0.3288	−0.3272	−0.321	−0.3147	−0.3022	−0.2862	−0.2759
	−0.3358	−0.3345	−0.3315	−0.3288	−0.3272	−0.321	−0.3147	−0.3022	−0.2862	−0.2758
	−0.3357	−0.3344	−0.3315	−0.3287	−0.3272	−0.321	−0.3146	−0.3021	−0.2862	−0.2758
	−0.3357	−0.3344	−0.3315	−0.3287	−0.3272	−0.321	−0.3146	−0.3021	−0.2862	−0.2758
	−0.3357	−0.3345	−0.3315	−0.3288	−0.3272	−0.3211	−0.3147	−0.3022	−0.2863	−0.2759
	−0.3353	−0.3342	−0.3313	−0.3286	−0.3271	−0.3211	−0.3147	−0.3021	−0.2863	−0.2758
	−0.3306	−0.3299	−0.3279	−0.3258	−0.3242	−0.3184	−0.3123	−0.3001	−0.2843	−0.2744
	−0.2339	−0.2339	−0.2339	−0.2339	−0.2338	−0.2338	−0.2323	−0.228	−0.2209	−0.2123

Figure I.6: F2A: e=0.5a & d=1.5a

	c/a									
b/a	−0.3348	−0.333	−0.3326	−0.3339	−0.3333	−0.3265	−0.3193	−0.3096	−0.2993	−0.2898
	−0.3348	−0.333	−0.3326	−0.3339	−0.3333	−0.3265	−0.3193	−0.3096	−0.2993	−0.2898
	−0.3348	−0.333	−0.3326	−0.3339	−0.3332	−0.3264	−0.3192	−0.3095	−0.2992	−0.2898
	−0.3348	−0.333	−0.3326	−0.3339	−0.3332	−0.3265	−0.3193	−0.3096	−0.2993	−0.2898
	−0.3348	−0.333	−0.3326	−0.3339	−0.3332	−0.3265	−0.3193	−0.3096	−0.2993	−0.2898
	−0.3343	−0.3326	−0.3322	−0.3335	−0.3329	−0.3261	−0.319	−0.3093	−0.299	−0.2896
	−0.3298	−0.3285	−0.328	−0.3292	−0.3286	−0.3222	−0.3153	−0.306	−0.2959	−0.2868
	−0.2338	−0.2338	−0.2337	−0.2336	−0.2332	−0.2318	−0.2285	−0.2238	−0.2182	−0.2124

Figure I.6: F2A: e=0.5a & d=2a

	c/a									
b/a	−0.336	−0.3367	−0.337	−0.336	−0.3329	−0.3274	−0.321	−0.3136	−0.3061	−0.2981
	−0.336	−0.3367	−0.337	−0.336	−0.3329	−0.3274	−0.321	−0.3136	−0.3061	−0.2981
	−0.336	−0.3367	−0.3369	−0.336	−0.3329	−0.3273	−0.321	−0.3135	−0.3061	−0.298
	−0.336	−0.3367	−0.337	−0.336	−0.3329	−0.3274	−0.321	−0.3136	−0.3061	−0.2981
	−0.3359	−0.3367	−0.3369	−0.336	−0.3329	−0.3273	−0.321	−0.3136	−0.3061	−0.2981
	−0.3354	−0.3362	−0.3364	−0.3355	−0.3324	−0.3269	−0.3206	−0.3131	−0.3057	−0.2977
	−0.3306	−0.3312	−0.3313	−0.3289	−0.3274	−0.3221	−0.3159	−0.3088	−0.3016	−0.2938
	−0.2338	−0.2337	−0.2337	−0.2333	−0.232	−0.2297	−0.2262	−0.2221	−0.2179	−0.2133

Figure I.6: F2A: e=0.5a & d=2.5a

	c/a									
b/a	−0.3362	−0.3362	−0.3353	−0.3331	−0.3295	−0.3251	−0.3197	−0.3139	−0.308	−0.3014
	−0.3362	−0.3362	−0.3353	−0.3331	−0.3295	−0.3251	−0.3197	−0.3139	−0.308	−0.3014
	−0.3362	−0.3362	−0.3353	−0.333	−0.3295	−0.3251	−0.3197	−0.3138	−0.308	−0.3014
	−0.3362	−0.3362	−0.3353	−0.3331	−0.3295	−0.3251	−0.3197	−0.3138	−0.308	−0.3014
	−0.3362	−0.3362	−0.3353	−0.333	−0.3295	−0.3251	−0.3197	−0.3138	−0.308	−0.3014
	−0.3357	−0.3357	−0.3348	−0.3326	−0.329	−0.3246	−0.3192	−0.3134	−0.3076	−0.301
	−0.3307	−0.3307	−0.3297	−0.3275	−0.3241	−0.3197	−0.3145	−0.3088	−0.3032	−0.2968
	−0.2339	−0.2338	−0.2334	−0.2324	−0.2306	−0.2283	−0.2251	−0.2217	−0.2181	−0.2142

Figure I.6: F2A: e=0.5a & d=3a

	c/a									
b/a	−0.3359	−0.3352	−0.3336	−0.3311	−0.3276	−0.3238	−0.3192	−0.3144	−0.3096	−0.3041
	−0.3359	−0.3352	−0.3336	−0.331	−0.3276	−0.3238	−0.3192	−0.3144	−0.3096	−0.304
	−0.3359	−0.3351	−0.3336	−0.331	−0.3276	−0.3238	−0.3192	−0.3144	−0.3096	−0.304
	−0.3359	−0.3351	−0.3336	−0.331	−0.3276	−0.3238	−0.3192	−0.3144	−0.3096	−0.304
	−0.3358	−0.3351	−0.3336	−0.331	−0.3276	−0.3238	−0.3192	−0.3144	−0.3096	−0.304
	−0.3353	−0.3346	−0.3331	−0.3305	−0.3271	−0.3234	−0.3188	−0.314	−0.3092	−0.3036
	−0.3305	−0.3297	−0.3281	−0.3257	−0.3222	−0.3186	−0.3141	−0.3093	−0.3046	−0.2992
	−0.2338	−0.2335	−0.2328	−0.2315	−0.2296	−0.2275	−0.2247	−0.2218	−0.2188	−0.2153

Figure I.6: F2A: e=0.5a & d=3.5a

	c/a									
b/a	−0.3357	−0.3347	−0.333	−0.3305	−0.3273	−0.324	−0.3201	−0.316	−0.3119	−0.3071
	−0.3357	−0.3347	−0.333	−0.3305	−0.3273	−0.324	−0.32	−0.3159	−0.3118	−0.3071
	−0.3357	−0.3347	−0.333	−0.3304	−0.3273	−0.324	−0.32	−0.3159	−0.3118	−0.3071
	−0.3357	−0.3347	−0.333	−0.3305	−0.3273	−0.324	−0.32	−0.3159	−0.3118	−0.3071
	−0.3357	−0.3346	−0.3329	−0.3304	−0.3273	−0.324	−0.32	−0.3159	−0.3118	−0.3071
	−0.3352	−0.3341	−0.3324	−0.3299	−0.3268	−0.3236	−0.3195	−0.3155	−0.3114	−0.3067
	−0.3304	−0.3292	−0.3276	−0.3251	−0.322	−0.3188	−0.3149	−0.3109	−0.3069	−0.3021
	−0.2337	−0.2332	−0.2324	−0.231	−0.2292	−0.2273	−0.2249	−0.2224	−0.2198	−0.2168

Figure I.6: F2A: e=0.5a & d=4a

	c/a									
b/a	−0.3357	−0.3346	−0.333	−0.3307	−0.3278	−0.325	−0.3215	−0.318	−0.3144	−0.3103
	−0.3357	−0.3346	−0.333	−0.3307	−0.3278	−0.325	−0.3215	−0.318	−0.3144	−0.3103
	−0.3356	−0.3346	−0.3329	−0.3306	−0.3278	−0.3249	−0.3215	−0.3179	−0.3144	−0.3103
	−0.3357	−0.3346	−0.333	−0.3306	−0.3278	−0.325	−0.3215	−0.318	−0.3144	−0.3103
	−0.3356	−0.3346	−0.3329	−0.3306	−0.3278	−0.3249	−0.3215	−0.3179	−0.3144	−0.3103
	−0.3351	−0.3341	−0.3324	−0.3301	−0.3273	−0.3245	−0.321	−0.3175	−0.3139	−0.3098
	−0.3303	−0.3292	−0.3276	−0.3253	−0.3225	−0.3197	−0.3163	−0.3128	−0.3093	−0.3053
	−0.2337	−0.2331	−0.2322	−0.2309	−0.2293	−0.2276	−0.2255	−0.2232	−0.221	−0.2184

Figure I.6: F2A: e=1a & d=0.5a

	c/a									
b/a	−0.3358	−0.3344	−0.3315	−0.3288	−0.3272	−0.321	−0.3146	−0.3021	−0.2862	−0.2758
	−0.3357	−0.3344	−0.3315	−0.3288	−0.3272	−0.321	−0.3146	−0.3021	−0.2862	−0.2758
	−0.3357	−0.3343	−0.3314	−0.3287	−0.3271	−0.3209	−0.3146	−0.3021	−0.2861	−0.2758
	−0.3356	−0.3342	−0.3312	−0.3284	−0.3269	−0.3205	−0.3142	−0.3017	−0.2857	−0.2738
	−0.3356	−0.334	−0.3307	−0.3275	−0.3253	−0.3187	−0.3121	−0.2998	−0.2848	−0.2741
	−0.3321	−0.3304	−0.3275	−0.3244	−0.3207	−0.3116	−0.3047	−0.2927	−0.2762	−0.268
	−0.297	−0.2969	−0.297	−0.2969	−0.2986	−0.2966	−0.293	−0.282	−0.2688	−0.26
	−0.2582	−0.2582	−0.2582	−0.2582	−0.2582	−0.2582	−0.2581	−0.2579	−0.2548	−0.2468

Figure I.6: F2A: e=1a & d=1a

	c/a									
b/a	−0.3348	−0.333	−0.3326	−0.3339	−0.3333	−0.3264	−0.3193	−0.3096	−0.2993	−0.2899
	−0.3348	−0.333	−0.3326	−0.3339	−0.3333	−0.3264	−0.3193	−0.3095	−0.2992	−0.2898
	−0.3347	−0.3329	−0.3325	−0.3338	−0.3332	−0.3264	−0.3192	−0.3095	−0.2992	−0.2898
	−0.3347	−0.3329	−0.3324	−0.3337	−0.3331	−0.3263	−0.3191	−0.3094	−0.2991	−0.2897
	−0.3345	−0.3325	−0.332	−0.3333	−0.3328	−0.3258	−0.3187	−0.309	−0.2987	−0.2895
	−0.3309	−0.3286	−0.3273	−0.3285	−0.3284	−0.3211	−0.3144	−0.3048	−0.2944	−0.2858
	−0.297	−0.3085	−0.2969	−0.2967	−0.2963	−0.2915	−0.288	−0.2807	−0.2717	−0.2659
	−0.2582	−0.2582	−0.2582	−0.2582	−0.2582	−0.2581	−0.2571	−0.2543	−0.2494	−0.2432

Figure I.6: F2A: e=1a & d=1.5a

	c/a									
b/a	−0.336	−0.3367	−0.337	−0.336	−0.3329	−0.3274	−0.321	−0.3136	−0.3061	−0.2981
	−0.336	−0.3367	−0.337	−0.336	−0.3329	−0.3273	−0.321	−0.3136	−0.3061	−0.2981
	−0.3359	−0.3366	−0.3369	−0.3359	−0.3328	−0.3273	−0.3209	−0.3135	−0.306	−0.298
	−0.3359	−0.3366	−0.3369	−0.3359	−0.3328	−0.3273	−0.3209	−0.3135	−0.306	−0.298
	−0.3358	−0.3366	−0.3368	−0.3358	−0.3328	−0.3272	−0.3209	−0.3134	−0.306	−0.298
	−0.3322	−0.333	−0.3333	−0.3326	−0.3296	−0.3238	−0.3181	−0.3108	−0.3035	−0.2956
	−0.2969	−0.2969	−0.2966	−0.2958	−0.2948	−0.2907	−0.2978	−0.2835	−0.2757	−0.2703
	−0.2582	−0.2581	−0.2581	−0.258	−0.2578	−0.2568	−0.2546	−0.2512	−0.247	−0.242

Figure I.6: F2A: e=1a & d=2a

	c/a									
b/a	−0.3362	−0.3362	−0.3353	−0.3331	−0.3295	−0.3251	−0.3197	−0.3138	−0.308	−0.3014
	−0.3362	−0.3362	−0.3353	−0.3331	−0.3295	−0.3251	−0.3197	−0.3138	−0.308	−0.3014
	−0.3361	−0.3361	−0.3352	−0.333	−0.3294	−0.325	−0.3196	−0.3138	−0.3079	−0.3013
	−0.3361	−0.3361	−0.3352	−0.333	−0.3294	−0.325	−0.3196	−0.3137	−0.3079	−0.3013
	−0.336	−0.3361	−0.3351	−0.3329	−0.3294	−0.3249	−0.3196	−0.3137	−0.3079	−0.3012
	−0.3326	−0.3327	−0.3319	−0.3298	−0.3264	−0.3221	−0.3168	−0.3111	−0.3054	−0.2988
	−0.297	−0.2968	−0.296	−0.2947	−0.2927	−0.2893	−0.2855	−0.2814	−0.277	−0.2719
	−0.2581	−0.2581	−0.2581	−0.2578	−0.257	−0.2553	−0.2528	−0.2496	−0.2461	−0.2419

Figure I.6: F2A: e=1a & d=2.5a

	c/a									
b/a	−0.3359	−0.3352	−0.3336	−0.331	−0.3276	−0.3238	−0.3192	−0.3144	−0.3096	−0.304
	−0.3359	−0.3351	−0.3336	−0.331	−0.3276	−0.3238	−0.3192	−0.3144	−0.3096	−0.304
	−0.3358	−0.3351	−0.3335	−0.3309	−0.3275	−0.3237	−0.3191	−0.3143	−0.3095	−0.3039
	−0.3358	−0.335	−0.3335	−0.3309	−0.3275	−0.3237	−0.3191	−0.3143	−0.3095	−0.3039
	−0.3357	−0.335	−0.3335	−0.3309	−0.3274	−0.3237	−0.3191	−0.3143	−0.3095	−0.3039
	−0.3323	−0.3316	−0.3301	−0.3277	−0.3243	−0.3207	−0.3161	−0.311	−0.3067	−0.3012
	−0.2969	−0.2962	−0.2949	−0.293	−0.2906	−0.2876	−0.2841	−0.2803	−0.2765	−0.2721
	−0.2582	−0.2582	−0.2579	−0.2572	−0.2559	−0.2541	−0.2517	−0.2489	−0.2459	−0.2424

Figure I.6: F2A: e=1a & d=3a

	c/a									
b/a	−0.3357	−0.3347	−0.333	−0.3305	−0.3273	−0.324	−0.32	−0.3159	−0.3118	−0.3071
	−0.3357	−0.3347	−0.333	−0.3304	−0.3273	−0.324	−0.32	−0.3159	−0.3118	−0.3071
	−0.3356	−0.3346	−0.3329	−0.3304	−0.3272	−0.3239	−0.3199	−0.3158	−0.3118	−0.307
	−0.3356	−0.3346	−0.3329	−0.3303	−0.3272	−0.3239	−0.3199	−0.3158	−0.3117	−0.307
	−0.3355	−0.3345	−0.3328	−0.3303	−0.3271	−0.3239	−0.3199	−0.3158	−0.3117	−0.3069
	−0.3321	−0.3311	−0.3294	−0.327	−0.3239	−0.3207	−0.3168	−0.3127	−0.3087	−0.304
	−0.2967	−0.2959	−0.2944	−0.2923	−0.2896	−0.2871	−0.2839	−0.2806	−0.2772	−0.2734
	−0.2582	−0.258	−0.2574	−0.2565	−0.255	−0.2533	−0.2511	−0.2487	−0.2461	−0.243

Figure I.6: F2A: e=1a & d=3.5a

	c/a									
b/a	−0.3357	−0.3346	−0.333	−0.3306	−0.3278	−0.325	−0.3215	−0.3179	−0.3144	−0.3103
	−0.3356	−0.3346	−0.3329	−0.3306	−0.3278	−0.325	−0.3215	−0.3179	−0.3144	−0.3103
	−0.3356	−0.3345	−0.3329	−0.3306	−0.3277	−0.3249	−0.3214	−0.3179	−0.3143	−0.3102
	−0.3355	−0.3345	−0.3328	−0.3305	−0.3277	−0.3249	−0.3214	−0.3178	−0.3143	−0.3102
	−0.3355	−0.3344	−0.3328	−0.3305	−0.3277	−0.3248	−0.3213	−0.3178	−0.3142	−0.3101
	−0.332	−0.331	−0.3294	−0.3271	−0.3244	−0.3215	−0.3181	−0.3146	−0.3111	−0.307
	−0.2967	−0.2958	−0.2944	−0.2924	−0.2899	−0.2875	−0.2845	−0.2816	−0.2787	−0.2752
	−0.2581	−0.2577	−0.2571	−0.256	−0.2546	−0.253	−0.251	−0.2489	−0.2466	−0.2439

Figure I.6: F2A: e=1a & d=4a

	c/a									
b/a	−0.3357	−0.3347	−0.3332	−0.3311	−0.3286	−0.3261	−0.3231	−0.32	−0.3169	−0.3133
	−0.3357	−0.3347	−0.3332	−0.3311	−0.3286	−0.3261	−0.3231	−0.32	−0.3169	−0.3133
	−0.3356	−0.3346	−0.3331	−0.331	−0.3286	−0.3261	−0.323	−0.3199	−0.3168	−0.3132
	−0.3356	−0.3346	−0.3331	−0.331	−0.3285	−0.326	−0.323	−0.3199	−0.3168	−0.3132
	−0.3355	−0.3345	−0.333	−0.331	−0.3285	−0.326	−0.323	−0.3199	−0.3167	−0.3131
	−0.332	−0.3311	−0.3296	−0.3276	−0.3251	−0.3227	−0.3197	−0.3166	−0.3135	−0.31
	−0.2967	−0.2957	−0.2945	−0.2927	−0.2906	−0.2884	−0.2857	−0.2829	−0.2803	−0.2773
	−0.2581	−0.2576	−0.2569	−0.2559	−0.2545	−0.2531	−0.2513	−0.2494	−0.2474	−0.245

Figure I.6: F2A: e=1.5a & d=0.5a

	c/a									
b/a	−0.3346	−0.3328	−0.3324	−0.3337	−0.3331	−0.3263	−0.3191	−0.3094	−0.2991	−0.2897
	−0.3333	−0.3317	−0.3313	−0.3327	−0.3321	−0.3253	−0.3182	−0.3085	−0.2983	−0.2889
	−0.3301	−0.3285	−0.3283	−0.3296	−0.3291	−0.3223	−0.3154	−0.3058	−0.2956	−0.2865
	−0.3275	−0.3258	−0.3251	−0.3259	−0.3252	−0.3182	−0.3114	−0.302	−0.2916	−0.2829
	−0.3269	−0.3266	−0.3263	−0.3256	−0.3239	−0.3175	−0.3098	−0.3003	−0.2908	−0.2811
	−0.3213	−0.321	−0.321	−0.3211	−0.3206	−0.3136	−0.3067	−0.2973	−0.2867	−0.2783
	−0.3021	−0.3021	−0.3021	−0.3021	−0.3021	−0.3019	−0.2993	−0.2922	−0.2835	−0.2751
	−0.2758	−0.2758	−0.2758	−0.2758	−0.2758	−0.2758	−0.2758	−0.2756	−0.2734	−0.2676

Figure I.6: F2A: e=1.5a & d=1a

	c/a									
b/a	−0.3357	−0.3365	−0.3367	−0.3357	−0.3326	−0.3271	−0.3208	−0.3133	−0.3059	−0.2978
	−0.3344	−0.3352	−0.3354	−0.3345	−0.3314	−0.3259	−0.3196	−0.3122	−0.3048	−0.2968
	−0.3315	−0.3322	−0.3324	−0.3315	−0.3285	−0.323	−0.3168	−0.3095	−0.3021	−0.2942
	−0.3287	−0.3293	−0.3295	−0.3284	−0.3254	−0.3199	−0.3137	−0.3064	−0.2991	−0.2913
	−0.327	−0.3272	−0.3272	−0.3261	−0.3232	−0.3176	−0.3114	−0.3042	−0.2969	−0.2893
	−0.3209	−0.3209	−0.3204	−0.3194	−0.3169	−0.3115	−0.3057	−0.2987	−0.2915	−0.2843
	−0.3021	−0.3021	−0.3021	−0.302	−0.3013	−0.2988	−0.2942	−0.2884	−0.282	−0.2749
	−0.2758	−0.2758	−0.2758	−0.2758	−0.2758	−0.2757	−0.2751	−0.2729	−0.2692	−0.2644

Figure I.6: F2A: e=1.5a & d=1.5a

	c/a									
b/a	−0.3359	−0.336	−0.335	−0.3328	−0.3293	−0.3248	−0.3194	−0.3136	−0.3078	−0.3012
	−0.3346	−0.3347	−0.3337	−0.3315	−0.328	−0.3236	−0.3183	−0.3125	−0.3067	−0.3001
	−0.3317	−0.3317	−0.3308	−0.3286	−0.3251	−0.3208	−0.3154	−0.3097	−0.304	−0.2974
	−0.3289	−0.3289	−0.3279	−0.3257	−0.3222	−0.3178	−0.3125	−0.3068	−0.3011	−0.2946
	−0.3272	−0.3271	−0.3261	−0.3239	−0.3204	−0.316	−0.3108	−0.3051	−0.2994	−0.293
	−0.321	−0.3205	−0.3195	−0.3174	−0.3142	−0.3099	−0.305	−0.2995	−0.294	−0.2878
	−0.3021	−0.3021	−0.3019	−0.301	−0.2991	−0.296	−0.2918	−0.287	−0.2819	−0.2761
	−0.2758	−0.2758	−0.2758	−0.2757	−0.2755	−0.2748	−0.2731	−0.2705	−0.2671	−0.263

Figure I.6: F2A: e=1.5a & d=2a

	c/a									
b/a	−0.3356	−0.3349	−0.3333	−0.3308	−0.3273	−0.3236	−0.319	−0.3142	−0.3094	−0.3038
	−0.3343	−0.3336	−0.3321	−0.3295	−0.3261	−0.3224	−0.3178	−0.313	−0.3082	−0.3027
	−0.3313	−0.3306	−0.3291	−0.3266	−0.3232	−0.3195	−0.315	−0.3102	−0.3055	−0.3
	−0.3286	−0.3279	−0.3263	−0.3238	−0.3203	−0.3167	−0.3121	−0.3074	−0.3027	−0.2972
	−0.327	−0.3261	−0.3246	−0.322	−0.3186	−0.3149	−0.3104	−0.3057	−0.301	−0.2956
	−0.3208	−0.32	−0.3181	−0.3157	−0.3123	−0.3087	−0.3044	−0.2998	−0.2952	−0.29
	−0.3021	−0.302	−0.3013	−0.2998	−0.2974	−0.2945	−0.2908	−0.2868	−0.2827	−0.2779
	−0.2758	−0.2758	−0.2757	−0.2756	−0.2749	−0.2736	−0.2716	−0.269	−0.2661	−0.2626

Figure I.6: F2A: e=1.5a & d=2.5a

	c/a									
b/a	−0.3354	−0.3344	−0.3327	−0.3302	−0.327	−0.3238	−0.3198	−0.3157	−0.3116	−0.3068
	−0.3341	−0.3331	−0.3314	−0.3289	−0.3258	−0.3225	−0.3186	−0.3145	−0.3104	−0.3057
	−0.3312	−0.3302	−0.3285	−0.326	−0.3229	−0.3197	−0.3158	−0.3117	−0.3077	−0.303
	−0.3284	−0.3274	−0.3257	−0.3232	−0.3201	−0.3169	−0.313	−0.3089	−0.3049	−0.3002
	−0.3268	−0.3257	−0.324	−0.3215	−0.3183	−0.3152	−0.3112	−0.3072	−0.3032	−0.2986
	−0.3206	−0.3197	−0.3176	−0.3151	−0.3121	−0.3089	−0.305	−0.3011	−0.2971	−0.2926
	−0.302	−0.3015	−0.3006	−0.2988	−0.2965	−0.294	−0.2907	−0.2873	−0.2838	−0.2797
	−0.2758	−0.2758	−0.2756	−0.2751	−0.274	−0.2726	−0.2706	−0.2683	−0.2657	−0.2627

Figure I.6: F2A: e=1.5a & d=3a

	c/a									
b/a	−0.3354	−0.3343	−0.3327	−0.3304	−0.3276	−0.3247	−0.3212	−0.3177	−0.3141	−0.31
	−0.3341	−0.333	−0.3314	−0.3291	−0.3263	−0.3235	−0.32	−0.3165	−0.3129	−0.3088
	−0.3311	−0.3301	−0.3285	−0.3262	−0.3234	−0.3206	−0.3172	−0.3137	−0.3102	−0.3061
	−0.3284	−0.3273	−0.3257	−0.3234	−0.3207	−0.3178	−0.3144	−0.3109	−0.3074	−0.3034
	−0.3268	−0.3257	−0.324	−0.3217	−0.3189	−0.3161	−0.3127	−0.3092	−0.3057	−0.3017
	−0.3206	−0.3195	−0.318	−0.3154	−0.3125	−0.3097	−0.3065	−0.303	−0.2993	−0.2956
	−0.3019	−0.3013	−0.3002	−0.2985	−0.2963	−0.2941	−0.2912	−0.2883	−0.2852	−0.2817
	−0.2758	−0.2757	−0.2753	−0.2745	−0.2733	−0.2719	−0.27	−0.2679	−0.2657	−0.263

Figure I.6: F2A: e=1.5a & d=3.5a

	c/a									
b/a	−0.3354	−0.3344	−0.3329	−0.3309	−0.3284	−0.3259	−0.3229	−0.3198	−0.3166	−0.313
	−0.3341	−0.3331	−0.3316	−0.3296	−0.3271	−0.3246	−0.3216	−0.3185	−0.3154	−0.3118
	−0.3311	−0.3302	−0.3287	−0.3267	−0.3242	−0.3218	−0.3188	−0.3157	−0.3126	−0.3091
	−0.3284	−0.3274	−0.326	−0.3239	−0.3215	−0.319	−0.316	−0.313	−0.3099	−0.3064
	−0.3268	−0.3258	−0.3243	−0.3223	−0.3198	−0.3173	−0.3143	−0.3113	−0.3082	−0.3047
	−0.3206	−0.3196	−0.3183	−0.3162	−0.3137	−0.3109	−0.308	−0.305	−0.3019	−0.2984
	−0.3019	−0.3012	−0.3001	−0.2986	−0.2966	−0.2946	−0.2921	−0.2895	−0.2868	−0.2837
	−0.2758	−0.2755	−0.275	−0.2741	−0.2729	−0.2715	−0.2698	−0.2679	−0.266	−0.2636

Figure I.6: F2A: e=1.5a & d=4a

	c/a									
b/a	−0.3354	−0.3346	−0.3332	−0.3314	−0.3292	−0.3271	−0.3244	−0.3217	−0.3189	−0.3158
	−0.3341	−0.3333	−0.3319	−0.3301	−0.328	−0.3258	−0.3232	−0.3205	−0.3177	−0.3146
	−0.3312	−0.3303	−0.329	−0.3272	−0.3251	−0.3229	−0.3203	−0.3176	−0.3149	−0.3118
	−0.3284	−0.3276	−0.3263	−0.3245	−0.3223	−0.3202	−0.3176	−0.3149	−0.3122	−0.3091
	−0.3269	−0.326	−0.3247	−0.3228	−0.3207	−0.3185	−0.3159	−0.3132	−0.3105	−0.3074
	−0.3207	−0.3198	−0.3184	−0.3168	−0.3146	−0.3124	−0.3096	−0.3069	−0.3042	−0.3011
	−0.3019	−0.3012	−0.3002	−0.2988	−0.297	−0.2952	−0.293	−0.2907	−0.2884	−0.2857
	−0.2757	−0.2754	−0.2748	−0.2739	−0.2728	−0.2715	−0.2699	−0.2683	−0.2665	−0.2644

Figure I.6: F2A: e=2a & d=0.5a

	c/a									
b/a	−0.3348	−0.3355	−0.3358	−0.3348	−0.3317	−0.3262	−0.3198	−0.3124	−0.305	−0.297
	−0.3331	−0.3337	−0.3338	−0.3327	−0.3295	−0.3241	−0.3177	−0.3104	−0.303	−0.295
	−0.3326	−0.3328	−0.3325	−0.3311	−0.3277	−0.3222	−0.3158	−0.3084	−0.301	−0.293
	−0.3339	−0.3339	−0.3333	−0.3312	−0.3276	−0.3219	−0.3153	−0.3079	−0.3004	−0.2925
	−0.3333	−0.3333	−0.3332	−0.332	−0.3281	−0.323	−0.3161	−0.3087	−0.3014	−0.2929
	−0.3264	−0.3264	−0.3264	−0.3263	−0.3247	−0.3202	−0.3137	−0.3065	−0.299	−0.2912
	−0.3095	−0.3095	−0.3095	−0.3095	−0.3095	−0.3094	−0.3075	−0.3025	−0.296	−0.2888
	−0.2899	−0.2899	−0.2899	−0.2898	−0.2898	−0.2898	−0.2898	−0.2897	−0.2879	−0.2834

Figure I.6: F2A: e=2a & d=1a

	c/a									
b/a	−0.335	−0.335	−0.334	−0.3318	−0.3282	−0.3238	−0.3185	−0.3126	−0.3068	−0.3002
	−0.3332	−0.3331	−0.332	−0.3297	−0.3261	−0.3217	−0.3163	−0.3105	−0.3047	−0.2981
	−0.3326	−0.3323	−0.331	−0.3284	−0.3246	−0.3202	−0.3147	−0.3088	−0.303	−0.2963
	−0.3338	−0.3332	−0.3316	−0.3287	−0.3247	−0.3202	−0.3146	−0.3087	−0.3028	−0.2961
	−0.3333	−0.3331	−0.3319	−0.3293	−0.3252	−0.3207	−0.315	−0.309	−0.3032	−0.2963
	−0.3264	−0.3264	−0.326	−0.3244	−0.3211	−0.317	−0.3117	−0.306	−0.3001	−0.2936
	−0.3095	−0.3095	−0.3095	−0.3095	−0.309	−0.3072	−0.3038	−0.2994	−0.2945	−0.2888
	−0.2899	−0.2899	−0.2899	−0.2898	−0.2898	−0.2898	−0.2892	−0.2876	−0.2846	−0.2806

Figure I.6: F2A: e=2a & d=1.5a

	c/a									
b/a	−0.3347	−0.3339	−0.3324	−0.3298	−0.3264	−0.3226	−0.318	−0.3132	−0.3084	−0.3029
	−0.3329	−0.3321	−0.3305	−0.3279	−0.3244	−0.3206	−0.316	−0.3112	−0.3064	−0.3009
	−0.3324	−0.3314	−0.3297	−0.3269	−0.3232	−0.3194	−0.3147	−0.3098	−0.305	−0.2994
	−0.3336	−0.3325	−0.3306	−0.3275	−0.3236	−0.3197	−0.3149	−0.3099	−0.3051	−0.2994
	−0.3331	−0.3323	−0.3306	−0.3278	−0.3241	−0.3202	−0.3154	−0.3104	−0.3055	−0.2998
	−0.3264	−0.326	−0.3249	−0.3226	−0.3194	−0.3158	−0.3113	−0.3066	−0.3019	−0.2964
	−0.3095	−0.3095	−0.3094	−0.3089	−0.3074	−0.3051	−0.3019	−0.2981	−0.2941	−0.2894
	−0.2898	−0.2898	−0.2898	−0.2897	−0.2896	−0.289	−0.2877	−0.2855	−0.2827	−0.2792

Figure I.6: F2A: e=2a & d=2a

	c/a									
b/a	−0.3345	−0.3335	−0.3318	−0.3293	−0.3261	−0.3228	−0.3189	−0.3148	−0.3107	−0.3059
	−0.3327	−0.3317	−0.3299	−0.3274	−0.3242	−0.3209	−0.3169	−0.3128	−0.3088	−0.304
	−0.3322	−0.3311	−0.3293	−0.3266	−0.3233	−0.32	−0.3159	−0.3118	−0.3076	−0.3028
	−0.3335	−0.3323	−0.3303	−0.3275	−0.324	−0.3206	−0.3164	−0.3121	−0.3079	−0.303
	−0.333	−0.3319	−0.3301	−0.3275	−0.3241	−0.3208	−0.3167	−0.3125	−0.3083	−0.3034
	−0.3262	−0.3255	−0.324	−0.3218	−0.3188	−0.3157	−0.3118	−0.3079	−0.3039	−0.2992
	−0.3095	−0.3094	−0.309	−0.3079	−0.3061	−0.3039	−0.301	−0.2977	−0.2943	−0.2904
	−0.2898	−0.2898	−0.2898	−0.2896	−0.2891	−0.288	−0.2864	−0.2842	−0.2817	−0.2787

Figure I.6: F2A: e=2a & d=2.5a

	c/a									
b/a	−0.3344	−0.3334	−0.3318	−0.3294	−0.3266	−0.3238	−0.3203	−0.3168	−0.3132	−0.3091
	−0.3327	−0.3316	−0.3299	−0.3276	−0.3248	−0.3219	−0.3185	−0.3149	−0.3114	−0.3073
	−0.3322	−0.3311	−0.3294	−0.327	−0.324	−0.3211	−0.3176	−0.314	−0.3104	−0.3063
	−0.3335	−0.3323	−0.3305	−0.328	−0.325	−0.322	−0.3184	−0.3147	−0.311	−0.3068
	−0.3329	−0.3318	−0.3301	−0.3277	−0.3248	−0.3219	−0.3184	−0.3147	−0.3111	−0.3069
	−0.3261	−0.3252	−0.3238	−0.3217	−0.319	−0.3163	−0.3129	−0.3095	−0.306	−0.302
	−0.3095	−0.3091	−0.3084	−0.3071	−0.3053	−0.3033	−0.3007	−0.2979	−0.295	−0.2915
	−0.2899	−0.2898	−0.2897	−0.2892	−0.2884	−0.2872	−0.2855	−0.2835	−0.2813	−0.2786

Figure I.6: F2A: e=2a & d=3a

	c/a									
b/a	−0.3345	−0.3335	−0.332	−0.3299	−0.3274	−0.325	−0.3219	−0.3188	−0.3157	−0.3121
	−0.3327	−0.3317	−0.3302	−0.3281	−0.3256	−0.3231	−0.3201	−0.317	−0.3139	−0.3103
	−0.3322	−0.3312	−0.3297	−0.3275	−0.325	−0.3225	−0.3194	−0.3162	−0.3131	−0.3095
	−0.3335	−0.3325	−0.3309	−0.3287	−0.3261	−0.3235	−0.3203	−0.3171	−0.3139	−0.3102
	−0.3329	−0.3319	−0.3304	−0.3283	−0.3257	−0.3232	−0.3201	−0.317	−0.3138	−0.3102
	−0.3261	−0.3252	−0.3239	−0.3219	−0.3196	−0.3172	−0.3143	−0.3113	−0.3083	−0.3048
	−0.3094	−0.3089	−0.3081	−0.3068	−0.305	−0.3032	−0.3009	−0.2984	−0.2959	−0.2929
	−0.2898	−0.2897	−0.2894	−0.2887	−0.2877	−0.2865	−0.2849	−0.2831	−0.2811	−0.2788

Figure I.6: F2A: e=2a & d=3.5a

	c/a									
b/a	−0.3345	−0.3336	−0.3323	−0.3305	−0.3283	−0.3261	−0.3235	−0.3208	−0.318	−0.3149
	−0.3327	−0.3318	−0.3305	−0.3287	−0.3265	−0.3243	−0.3217	−0.319	−0.3162	−0.3131
	−0.3323	−0.3314	−0.33	−0.3282	−0.3259	−0.3237	−0.321	−0.3183	−0.3155	−0.3123
	−0.3336	−0.3326	−0.3312	−0.3293	−0.3271	−0.3248	−0.3221	−0.3193	−0.3164	−0.3132
	−0.333	−0.3321	−0.3307	−0.3289	−0.3267	−0.3244	−0.3218	−0.319	−0.3162	−0.313
	−0.3261	−0.3253	−0.3241	−0.3224	−0.3203	−0.3182	−0.3157	−0.313	−0.3104	−0.3073
	−0.3094	−0.3088	−0.308	−0.3067	−0.3051	−0.3035	−0.3014	−0.2992	−0.297	−0.2943
	−0.2898	−0.2896	−0.2891	−0.2884	−0.2873	−0.2862	−0.2847	−0.283	−0.2813	−0.2792

Figure I.6: F2A: e=2a & d=4a

	c/a									
b/a	−0.3345	−0.3338	−0.3326	−0.331	−0.3291	−0.3272	−0.3249	−0.3225	−0.3201	−0.3173
	−0.3328	−0.332	−0.3308	−0.3292	−0.3273	−0.3254	−0.3231	−0.3207	−0.3183	−0.3155
	−0.3323	−0.3315	−0.3303	−0.3287	−0.3268	−0.3249	−0.3225	−0.3201	−0.3176	−0.3148
	−0.3336	−0.3328	−0.3316	−0.3299	−0.328	−0.326	−0.3236	−0.3211	−0.3186	−0.3158
	−0.333	−0.3322	−0.3311	−0.3294	−0.3275	−0.3256	−0.3232	−0.3208	−0.3183	−0.3155
	−0.3262	−0.3254	−0.3243	−0.3228	−0.321	−0.3192	−0.3169	−0.3146	−0.3123	−0.3095
	−0.3094	−0.3088	−0.308	−0.3069	−0.3054	−0.3039	−0.3021	−0.3001	−0.2981	−0.2958
	−0.2898	−0.2895	−0.289	−0.2882	−0.2872	−0.2861	−0.2847	−0.2832	−0.2816	−0.2797

Figure I.6: F2A: e=2.5a & d=0.5a

	c/a									
	−0.3361	−0.336	−0.335	−0.3327	−0.3291	−0.3247	−0.3193	−0.3134	−0.3076	−0.3009
	−0.3367	−0.3363	−0.3352	−0.3326	−0.3289	−0.3245	−0.319	−0.3131	−0.3073	−0.3005
	−0.337	−0.3366	−0.3354	−0.3327	−0.3289	−0.3244	−0.3189	−0.3129	−0.3071	−0.3003
b/a	−0.336	−0.336	−0.3353	−0.333	−0.3291	−0.3247	−0.3191	−0.3131	−0.3073	−0.3005
	−0.3329	−0.3329	−0.3329	−0.3319	−0.3287	−0.3245	−0.3191	−0.3132	−0.3074	−0.3006
	−0.3274	−0.3274	−0.3274	−0.3273	−0.326	−0.3225	−0.3175	−0.3119	−0.3061	−0.2996
	−0.3136	−0.3136	−0.3136	−0.3136	−0.3135	−0.3135	−0.312	−0.3082	−0.3032	−0.2974
	−0.2981	−0.2981	−0.2981	−0.2981	−0.2981	−0.298	−0.298	−0.2979	−0.2965	−0.2929

Figure I.6: F2A: e=2.5a & d=1a

	c/a									
	−0.3358	−0.335	−0.3334	−0.3308	−0.3273	−0.3235	−0.3189	−0.3141	−0.3093	−0.3037
	−0.3365	−0.3356	−0.3339	−0.3311	−0.3274	−0.3236	−0.3189	−0.314	−0.3091	−0.3035
	−0.3368	−0.3359	−0.3341	−0.3313	−0.3276	−0.3238	−0.319	−0.314	−0.3091	−0.3035
b/a	−0.3359	−0.3353	−0.3339	−0.3312	−0.3276	−0.3238	−0.3191	−0.3142	−0.3093	−0.3036
	−0.3329	−0.3328	−0.3319	−0.3298	−0.3266	−0.323	−0.3185	−0.3137	−0.3089	−0.3033
	−0.3273	−0.3273	−0.3271	−0.3259	−0.3235	−0.3202	−0.3161	−0.3115	−0.3069	−0.3015
	−0.3136	−0.3136	−0.3135	−0.3135	−0.3131	−0.3118	−0.3092	−0.3057	−0.3018	−0.2971
	−0.2981	−0.2981	−0.2981	−0.2981	−0.2981	−0.298	−0.2975	−0.2962	−0.2938	−0.2905

Figure I.6: F2A: e=2.5a & d=1.5a

	c/a									
	−0.3357	−0.3346	−0.3329	−0.3303	−0.3271	−0.3238	−0.3198	−0.3157	−0.3116	−0.3068
	−0.3364	−0.3352	−0.3334	−0.3308	−0.3275	−0.3242	−0.3201	−0.3159	−0.3117	−0.3069
	−0.3366	−0.3355	−0.3337	−0.331	−0.3277	−0.3243	−0.3202	−0.316	−0.3118	−0.307
b/a	−0.3357	−0.3348	−0.3331	−0.3306	−0.3274	−0.3241	−0.32	−0.3159	−0.3117	−0.3069
	−0.3328	−0.3322	−0.3309	−0.3287	−0.3257	−0.3226	−0.3188	−0.3148	−0.3107	−0.306
	−0.3273	−0.3271	−0.3262	−0.3246	−0.3221	−0.3193	−0.3157	−0.3119	−0.308	−0.3035
	−0.3135	−0.3135	−0.3135	−0.313	−0.3119	−0.3101	−0.3076	−0.3045	−0.3012	−0.2974
	−0.298	−0.298	−0.298	−0.298	−0.2979	−0.2974	−0.2963	−0.2945	−0.2921	−0.2892

Figure I.6: F2A: e=2.5a & d=2a

	c/a									
	−0.3356	−0.3345	−0.3329	−0.3305	−0.3277	−0.3248	−0.3213	−0.3177	−0.3142	−0.31
	−0.3363	−0.3352	−0.3335	−0.3311	−0.3282	−0.3253	−0.3217	−0.3181	−0.3145	−0.3103
	−0.3366	−0.3355	−0.3338	−0.3313	−0.3284	−0.3255	−0.3219	−0.3183	−0.3146	−0.3104
b/a	−0.3356	−0.3346	−0.333	−0.3307	−0.3278	−0.325	−0.3215	−0.3179	−0.3143	−0.3101
	−0.3327	−0.3318	−0.3304	−0.3283	−0.3257	−0.323	−0.3197	−0.3162	−0.3127	−0.3087
	−0.3272	−0.3267	−0.3256	−0.3238	−0.3215	−0.319	−0.3159	−0.3127	−0.3094	−0.3055
	−0.3136	−0.3135	−0.3131	−0.3123	−0.3109	−0.3091	−0.3067	−0.3041	−0.3013	−0.298
	−0.298	−0.298	−0.298	−0.2979	−0.2974	−0.2965	−0.2952	−0.2933	−0.2912	−0.2886

Figure I.6: F2A: e=2.5a & d=2.5a

	c/a									
	−0.3356	−0.3346	−0.3331	−0.3311	−0.3285	−0.326	−0.323	−0.3199	−0.3167	−0.3131
	−0.3364	−0.3353	−0.3338	−0.3317	−0.3291	−0.3266	−0.3235	−0.3203	−0.3172	−0.3135
	−0.3366	−0.3356	−0.334	−0.3319	−0.3293	−0.3268	−0.3237	−0.3205	−0.3173	−0.3136
b/a	−0.3356	−0.3347	−0.3332	−0.3311	−0.3286	−0.3261	−0.3231	−0.3199	−0.3168	−0.3132
	−0.3326	−0.3318	−0.3304	−0.3285	−0.3262	−0.3238	−0.3209	−0.3179	−0.3148	−0.3113
	−0.3271	−0.3265	−0.3253	−0.3237	−0.3216	−0.3194	−0.3166	−0.3138	−0.3109	−0.3076
	−0.3135	−0.3132	−0.3127	−0.3116	−0.3102	−0.3085	−0.3064	−0.3041	−0.3016	−0.2987
	−0.2981	−0.298	−0.2979	−0.2975	−0.2968	−0.2958	−0.2944	−0.2926	−0.2907	−0.2884

Figure I.6: F2A: e=2.5a & d=3a

	c/a									
	−0.3357	−0.3348	−0.3334	−0.3316	−0.3294	−0.3272	−0.3245	−0.3218	−0.3191	−0.3159
	−0.3364	−0.3355	−0.3341	−0.3323	−0.3301	−0.3278	−0.3251	−0.3224	−0.3196	−0.3164
	−0.3366	−0.3357	−0.3344	−0.3325	−0.3303	−0.328	−0.3253	−0.3226	−0.3197	−0.3165
b/a	−0.3357	−0.3348	−0.3335	−0.3317	−0.3295	−0.3273	−0.3246	−0.3219	−0.3191	−0.3159
	−0.3326	−0.3318	−0.3306	−0.3289	−0.3268	−0.3247	−0.3222	−0.3195	−0.3168	−0.3137
	−0.3271	−0.3264	−0.3254	−0.3238	−0.3219	−0.32	−0.3176	−0.3151	−0.3125	−0.3096
	−0.3134	−0.3131	−0.3124	−0.3113	−0.3099	−0.3084	−0.3065	−0.3044	−0.3022	−0.2997
	−0.298	−0.2979	−0.2977	−0.2971	−0.2963	−0.2952	−0.2938	−0.2923	−0.2905	−0.2885

Figure I.6: F2A: e=2.5a & d=3.5a

	c/a									
	−0.3357	−0.3349	−0.3338	−0.3322	−0.3302	−0.3283	−0.326	−0.3236	−0.3211	−0.3183
	−0.3364	−0.3356	−0.3345	−0.3329	−0.3309	−0.3289	−0.3266	−0.3242	−0.3217	−0.3188
	−0.3367	−0.3359	−0.3347	−0.3331	−0.3311	−0.3292	−0.3268	−0.3243	−0.3219	−0.319
b/a	−0.3357	−0.3349	−0.3338	−0.3322	−0.3303	−0.3283	−0.326	−0.3236	−0.3211	−0.3183
	−0.3326	−0.3319	−0.3308	−0.3293	−0.3275	−0.3256	−0.3234	−0.3211	−0.3187	−0.3159
	−0.3271	−0.3265	−0.3255	−0.3241	−0.3224	−0.3207	−0.3186	−0.3164	−0.3141	−0.3115
	−0.3134	−0.313	−0.3123	−0.3113	−0.3099	−0.3085	−0.3068	−0.3049	−0.303	−0.3007
	−0.298	−0.2978	−0.2974	−0.2968	−0.2959	−0.2949	−0.2936	−0.2921	−0.2906	−0.2887

Figure I.6: F2A: e=2.5a & d=4a

	c/a									
	−0.3357	−0.3351	−0.334	−0.3327	−0.331	−0.3293	−0.3272	−0.3251	−0.3229	−0.3204
	−0.3365	−0.3358	−0.3348	−0.3333	−0.3316	−0.3299	−0.3278	−0.3257	−0.3235	−0.321
	−0.3367	−0.336	−0.335	−0.3336	−0.3319	−0.3301	−0.3281	−0.3259	−0.3237	−0.3212
b/a	−0.3357	−0.3351	−0.3341	−0.3327	−0.331	−0.3293	−0.3272	−0.3251	−0.3229	−0.3204
	−0.3327	−0.332	−0.3311	−0.3297	−0.3281	−0.3265	−0.3245	−0.3224	−0.3203	−0.3179
	−0.3271	−0.3266	−0.3257	−0.3244	−0.3229	−0.3213	−0.3195	−0.3175	−0.3155	−0.3132
	−0.3134	−0.313	−0.3123	−0.3113	−0.3101	−0.3089	−0.3073	−0.3056	−0.3039	−0.3018
	−0.298	−0.2977	−0.2973	−0.2967	−0.2958	−0.2948	−0.2936	−0.2923	−0.2908	−0.2891

Figure I.6: F2A: e=3a & d=0.5a

	c/a									
b/a	−0.3361	−0.3353	−0.3337	−0.3311	−0.3276	−0.3239	−0.3193	−0.3144	−0.3096	−0.304
	−0.3361	−0.3354	−0.3339	−0.3313	−0.3277	−0.324	−0.3193	−0.3145	−0.3097	−0.304
	−0.3353	−0.335	−0.3336	−0.3311	−0.3277	−0.3239	−0.3193	−0.3144	−0.3096	−0.304
	−0.3331	−0.3331	−0.3325	−0.3305	−0.3273	−0.3236	−0.3191	−0.3143	−0.3095	−0.3039
	−0.3295	−0.3295	−0.3295	−0.3287	−0.3262	−0.3228	−0.3185	−0.3138	−0.309	−0.3036
	−0.3251	−0.3251	−0.3251	−0.325	−0.3241	−0.3214	−0.3174	−0.313	−0.3083	−0.303
	−0.3138	−0.3138	−0.3138	−0.3138	−0.3138	−0.3138	−0.3127	−0.3097	−0.3056	−0.301
	−0.3014	−0.3014	−0.3014	−0.3014	−0.3014	−0.3013	−0.3013	−0.3013	−0.3001	−0.2972

Figure I.6: F2A: e=3a & d=1a

	c/a									
b/a	−0.3359	−0.3349	−0.3331	−0.3306	−0.3274	−0.3241	−0.3201	−0.316	−0.3119	−0.3071
	−0.3359	−0.3349	−0.3332	−0.3307	−0.3275	−0.3242	−0.3202	−0.3161	−0.312	−0.3072
	−0.3351	−0.3343	−0.3327	−0.3303	−0.3272	−0.324	−0.32	−0.3159	−0.3118	−0.307
	−0.333	−0.3326	−0.3314	−0.3292	−0.3263	−0.3232	−0.3193	−0.3153	−0.3113	−0.3066
	−0.3295	−0.3294	−0.3287	−0.3271	−0.3246	−0.3217	−0.3181	−0.3142	−0.3102	−0.3057
	−0.3251	−0.3251	−0.3249	−0.324	−0.3221	−0.3196	−0.3163	−0.3126	−0.3088	−0.3044
	−0.3138	−0.3138	−0.3138	−0.3138	−0.3135	−0.3125	−0.3104	−0.3076	−0.3044	−0.3006
	−0.3014	−0.3014	−0.3014	−0.3014	−0.3014	−0.3013	−0.3009	−0.2998	−0.2978	−0.2952

Figure I.6: F2A: e=3a & d=1.5a

	c/a									
b/a	−0.3359	−0.3348	−0.3331	−0.3308	−0.328	−0.3251	−0.3216	−0.318	−0.3145	−0.3103
	−0.3359	−0.3348	−0.3332	−0.3309	−0.328	−0.3252	−0.3217	−0.3181	−0.3145	−0.3104
	−0.335	−0.334	−0.3325	−0.3303	−0.3275	−0.3247	−0.3212	−0.3177	−0.3142	−0.31
	−0.3329	−0.3321	−0.3308	−0.3287	−0.3261	−0.3234	−0.3201	−0.3167	−0.3132	−0.3092
	−0.3294	−0.329	−0.3279	−0.3262	−0.3239	−0.3214	−0.3183	−0.315	−0.3116	−0.3077
	−0.3251	−0.3249	−0.3243	−0.323	−0.321	−0.3188	−0.3159	−0.3128	−0.3096	−0.3058
	−0.3138	−0.3138	−0.3138	−0.3134	−0.3126	−0.3111	−0.3091	−0.3066	−0.3039	−0.3006
	−0.3013	−0.3013	−0.3013	−0.3013	−0.3012	−0.3008	−0.2999	−0.2983	−0.2964	−0.2939

Figure I.6: F2A: e=3a & d=2a

	c/a									
b/a	−0.3359	−0.3349	−0.3334	−0.3313	−0.3288	−0.3263	−0.3232	−0.3201	−0.317	−0.3134
	−0.3359	−0.3349	−0.3334	−0.3314	−0.3288	−0.3263	−0.3233	−0.3202	−0.3171	−0.3134
	−0.335	−0.334	−0.3326	−0.3306	−0.3282	−0.3257	−0.3227	−0.3196	−0.3165	−0.3129
	−0.3328	−0.332	−0.3307	−0.3288	−0.3265	−0.3241	−0.3212	−0.3182	−0.3152	−0.3117
	−0.3293	−0.3287	−0.3276	−0.3259	−0.3238	−0.3216	−0.3189	−0.316	−0.3131	−0.3097
	−0.325	−0.3246	−0.3237	−0.3224	−0.3205	−0.3185	−0.316	−0.3133	−0.3105	−0.3073
	−0.3138	−0.3138	−0.3135	−0.3128	−0.3117	−0.3103	−0.3083	−0.3061	−0.3038	−0.301
	−0.3013	−0.3013	−0.3013	−0.3012	−0.3008	−0.3001	−0.2989	−0.2974	−0.2956	−0.2934

Figure I.6: F2A: e=3a & d=2.5a

	c/a									
b/a	−0.3359	−0.335	−0.3337	−0.3319	−0.3297	−0.3275	−0.3248	−0.3221	−0.3193	−0.3161
	−0.3359	−0.335	−0.3337	−0.3319	−0.3297	−0.3275	−0.3249	−0.3221	−0.3194	−0.3162
	−0.335	−0.3341	−0.3329	−0.3311	−0.3289	−0.3268	−0.3241	−0.3214	−0.3187	−0.3156
	−0.3328	−0.332	−0.3308	−0.3291	−0.3271	−0.325	−0.3224	−0.3198	−0.3172	−0.3141
	−0.3293	−0.3286	−0.3275	−0.326	−0.3241	−0.3222	−0.3197	−0.3172	−0.3147	−0.3117
	−0.3249	−0.3244	−0.3235	−0.3222	−0.3205	−0.3187	−0.3164	−0.3141	−0.3116	−0.3088
	−0.3138	−0.3136	−0.3131	−0.3123	−0.3111	−0.3098	−0.308	−0.306	−0.3039	−0.3015
	−0.3014	−0.3013	−0.3012	−0.3009	−0.3003	−0.2995	−0.2982	−0.2968	−0.2951	−0.2931

Figure I.6: F2A: e=3a & d=3a

	c/a									
b/a	−0.3359	−0.3352	−0.334	−0.3324	−0.3305	−0.3286	−0.3262	−0.3238	−0.3214	−0.3185
	−0.336	−0.3352	−0.334	−0.3324	−0.3305	−0.3286	−0.3262	−0.3238	−0.3214	−0.3186
	−0.335	−0.3343	−0.3331	−0.3316	−0.3297	−0.3278	−0.3255	−0.3231	−0.3207	−0.3179
	−0.3328	−0.3321	−0.331	−0.3295	−0.3277	−0.3259	−0.3236	−0.3213	−0.319	−0.3162
	−0.3293	−0.3286	−0.3277	−0.3263	−0.3246	−0.3228	−0.3207	−0.3185	−0.3162	−0.3136
	−0.3249	−0.3244	−0.3235	−0.3223	−0.3207	−0.3191	−0.3171	−0.315	−0.3128	−0.3103
	−0.3138	−0.3135	−0.3129	−0.312	−0.3109	−0.3096	−0.308	−0.3062	−0.3043	−0.3021
	−0.3013	−0.3013	−0.301	−0.3006	−0.2998	−0.299	−0.2978	−0.2964	−0.2949	−0.2931

Figure I.6: F2A: e=3a & d=3.5a

	c/a									
b/a	−0.336	−0.3353	−0.3343	−0.3329	−0.3312	−0.3295	−0.3274	−0.3253	−0.3232	−0.3206
	−0.336	−0.3353	−0.3343	−0.3329	−0.3312	−0.3295	−0.3275	−0.3253	−0.3232	−0.3207
	−0.3351	−0.3344	−0.3334	−0.332	−0.3304	−0.3287	−0.3267	−0.3246	−0.3224	−0.3199
	−0.3328	−0.3322	−0.3313	−0.3299	−0.3283	−0.3267	−0.3247	−0.3227	−0.3206	−0.3181
	−0.3293	−0.3287	−0.3278	−0.3266	−0.3251	−0.3235	−0.3216	−0.3196	−0.3176	−0.3153
	−0.3249	−0.3244	−0.3236	−0.3224	−0.321	−0.3196	−0.3178	−0.3159	−0.314	−0.3118
	−0.3137	−0.3134	−0.3128	−0.312	−0.3108	−0.3097	−0.3082	−0.3066	−0.3049	−0.3029
	−0.3013	−0.3011	−0.3008	−0.3003	−0.2995	−0.2987	−0.2975	−0.2963	−0.2949	−0.2932

Figure I.6: F2A: e=3a & d=4a

	c/a									
b/a	−0.336	−0.3354	−0.3345	−0.3333	−0.3318	−0.3303	−0.3285	−0.3266	−0.3247	−0.3225
	−0.336	−0.3354	−0.3345	−0.3333	−0.3318	−0.3304	−0.3285	−0.3266	−0.3247	−0.3225
	−0.3351	−0.3345	−0.3336	−0.3324	−0.331	−0.3295	−0.3277	−0.3258	−0.3239	−0.3217
	−0.3329	−0.3323	−0.3315	−0.3303	−0.3289	−0.3274	−0.3257	−0.3239	−0.322	−0.3198
	−0.3293	−0.3288	−0.328	−0.3269	−0.3255	−0.3242	−0.3225	−0.3207	−0.3189	−0.3168
	−0.3249	−0.3244	−0.3237	−0.3227	−0.3214	−0.3201	−0.3185	−0.3168	−0.3151	−0.3131
	−0.3137	−0.3134	−0.3128	−0.312	−0.311	−0.3099	−0.3085	−0.3071	−0.3056	−0.3038
	−0.3013	−0.3011	−0.3007	−0.3002	−0.2994	−0.2986	−0.2975	−0.2963	−0.2951	−0.2936

Figure I.6: F2A: e=3.5a & d=0.5a

	c/a									
b/a	−0.3356	−0.3346	−0.333	−0.3305	−0.3273	−0.324	−0.32	−0.3159	−0.3118	−0.3071
	−0.3351	−0.3343	−0.3327	−0.3303	−0.3272	−0.3239	−0.32	−0.3159	−0.3118	−0.307
	−0.3336	−0.3333	−0.3321	−0.3299	−0.3269	−0.3237	−0.3197	−0.3157	−0.3116	−0.3069
	−0.3311	−0.331	−0.3306	−0.3289	−0.3262	−0.3231	−0.3193	−0.3153	−0.3112	−0.3066
	−0.3276	−0.3276	−0.3276	−0.3269	−0.3249	−0.3221	−0.3185	−0.3146	−0.3106	−0.3061
	−0.3239	−0.3239	−0.3239	−0.3238	−0.3231	−0.3209	−0.3176	−0.3139	−0.31	−0.3056
	−0.3144	−0.3144	−0.3144	−0.3144	−0.3144	−0.3144	−0.3135	−0.311	−0.3077	−0.3038
	−0.304	−0.304	−0.304	−0.304	−0.304	−0.304	−0.304	−0.3039	−0.303	−0.3005

Figure I.6: F2A: e=3.5a & d=1a

	c/a									
b/a	−0.3356	−0.3345	−0.3329	−0.3306	−0.3278	−0.3249	−0.3215	−0.3179	−0.3143	−0.3102
	−0.3349	−0.3339	−0.3324	−0.3302	−0.3274	−0.3246	−0.3212	−0.3176	−0.3141	−0.31
	−0.3335	−0.3328	−0.3314	−0.3293	−0.3267	−0.324	−0.3206	−0.3171	−0.3136	−0.3096
	−0.331	−0.3307	−0.3297	−0.3279	−0.3255	−0.3229	−0.3196	−0.3162	−0.3128	−0.3088
	−0.3276	−0.3275	−0.327	−0.3257	−0.3236	−0.3212	−0.3182	−0.315	−0.3116	−0.3078
	−0.3239	−0.3238	−0.3237	−0.323	−0.3215	−0.3194	−0.3167	−0.3136	−0.3104	−0.3067
	−0.3144	−0.3144	−0.3144	−0.3144	−0.3142	−0.3133	−0.3116	−0.3093	−0.3066	−0.3034
	−0.304	−0.304	−0.304	−0.304	−0.304	−0.304	−0.3037	−0.3027	−0.3011	−0.2987

Figure I.6: F2A: e=3.5a & d=1.5a

	c/a									
b/a	−0.3356	−0.3346	−0.3331	−0.3311	−0.3286	−0.3261	−0.323	−0.3199	−0.3168	−0.3132
	−0.3349	−0.3339	−0.3325	−0.3305	−0.3281	−0.3256	−0.3226	−0.3195	−0.3164	−0.3129
	−0.3334	−0.3326	−0.3313	−0.3294	−0.327	−0.3246	−0.3217	−0.3187	−0.3157	−0.3121
	−0.3309	−0.3303	−0.3292	−0.3275	−0.3253	−0.3231	−0.3203	−0.3174	−0.3144	−0.3109
	−0.3275	−0.3272	−0.3263	−0.3249	−0.323	−0.3209	−0.3183	−0.3155	−0.3127	−0.3094
	−0.3239	−0.3237	−0.3232	−0.3222	−0.3206	−0.3187	−0.3163	−0.3137	−0.311	−0.3078
	−0.3144	−0.3144	−0.3143	−0.3141	−0.3134	−0.3122	−0.3105	−0.3084	−0.3061	−0.3033
	−0.304	−0.304	−0.304	−0.304	−0.3039	−0.3035	−0.3028	−0.3015	−0.2998	−0.2977

Figure I.6: F2A: e=3.5a & d=2a

	c/a									
b/a	−0.3356	−0.3347	−0.3334	−0.3316	−0.3294	−0.3272	−0.3246	−0.3219	−0.3191	−0.3159
	−0.3349	−0.334	−0.3327	−0.331	−0.3288	−0.3267	−0.324	−0.3213	−0.3186	−0.3155
	−0.3334	−0.3326	−0.3314	−0.3297	−0.3276	−0.3255	−0.323	−0.3203	−0.3176	−0.3145
	−0.3308	−0.3302	−0.3291	−0.3275	−0.3256	−0.3236	−0.3211	−0.3186	−0.316	−0.313
	−0.3274	−0.3269	−0.326	−0.3247	−0.3229	−0.3211	−0.3188	−0.3163	−0.3138	−0.3109
	−0.3238	−0.3234	−0.3228	−0.3216	−0.3201	−0.3184	−0.3163	−0.314	−0.3117	−0.3089
	−0.3144	−0.3144	−0.3142	−0.3136	−0.3127	−0.3115	−0.3098	−0.308	−0.3059	−0.3035
	−0.304	−0.304	−0.304	−0.3039	−0.3036	−0.303	−0.302	−0.3006	−0.2991	−0.2971

Figure I.6: F2A: e=3.5a & d=2.5a

	c/a									
b/a	−0.3356	−0.3349	−0.3337	−0.3321	−0.3302	−0.3283	−0.326	−0.3236	−0.3211	−0.3183
	−0.3349	−0.3342	−0.333	−0.3315	−0.3296	−0.3277	−0.3254	−0.323	−0.3206	−0.3178
	−0.3334	−0.3327	−0.3316	−0.3301	−0.3283	−0.3264	−0.3241	−0.3218	−0.3194	−0.3167
	−0.3308	−0.3302	−0.3292	−0.3278	−0.3261	−0.3243	−0.3221	−0.3199	−0.3176	−0.3149
	−0.3274	−0.3269	−0.326	−0.3247	−0.3231	−0.3215	−0.3194	−0.3173	−0.3151	−0.3125
	−0.3237	−0.3233	−0.3226	−0.3215	−0.32	−0.3185	−0.3166	−0.3146	−0.3125	−0.3101
	−0.3144	−0.3142	−0.3138	−0.3132	−0.3122	−0.311	−0.3095	−0.3078	−0.306	−0.3039
	−0.304	−0.304	−0.3039	−0.3037	−0.3031	−0.3024	−0.3014	−0.3001	−0.2986	−0.2969

Figure I.6: F2A: e=3.5a & d=3a

	c/a									
b/a	−0.3357	−0.335	−0.334	−0.3326	−0.3309	−0.3292	−0.3272	−0.3251	−0.3229	−0.3204
	−0.3349	−0.3343	−0.3333	−0.3319	−0.3303	−0.3286	−0.3265	−0.3244	−0.3223	−0.3198
	−0.3334	−0.3328	−0.3318	−0.3305	−0.3289	−0.3272	−0.3252	−0.3232	−0.3211	−0.3186
	−0.3309	−0.3303	−0.3294	−0.3281	−0.3266	−0.325	−0.3231	−0.3211	−0.319	−0.3166
	−0.3274	−0.3269	−0.3261	−0.3249	−0.3235	−0.322	−0.3202	−0.3182	−0.3163	−0.314
	−0.3237	−0.3233	−0.3225	−0.3215	−0.3202	−0.3188	−0.3171	−0.3153	−0.3134	−0.3113
	−0.3143	−0.3141	−0.3136	−0.3129	−0.3119	−0.3108	−0.3094	−0.3079	−0.3063	−0.3044
	−0.304	−0.3039	−0.3037	−0.3033	−0.3027	−0.302	−0.3009	−0.2997	−0.2984	−0.2968

Figure I.6: F2A: e=3.5a & d=3.5a

	c/a									
b/a	−0.3357	−0.3351	−0.3342	−0.333	−0.3315	−0.33	−0.3282	−0.3263	−0.3244	−0.3222
	−0.335	−0.3344	−0.3335	−0.3323	−0.3309	−0.3294	−0.3276	−0.3257	−0.3238	−0.3216
	−0.3334	−0.3329	−0.332	−0.3309	−0.3294	−0.328	−0.3262	−0.3244	−0.3225	−0.3203
	−0.3309	−0.3303	−0.3295	−0.3284	−0.327	−0.3256	−0.3239	−0.3221	−0.3203	−0.3182
	−0.3274	−0.3269	−0.3262	−0.3251	−0.3238	−0.3225	−0.3209	−0.3192	−0.3174	−0.3154
	−0.3237	−0.3233	−0.3226	−0.3216	−0.3205	−0.3192	−0.3177	−0.3161	−0.3144	−0.3124
	−0.3143	−0.314	−0.3136	−0.3128	−0.3119	−0.3109	−0.3096	−0.3082	−0.3067	−0.305
	−0.304	−0.3038	−0.3036	−0.3031	−0.3025	−0.3017	−0.3007	−0.2996	−0.2984	−0.2969

Figure I.6: F2A: e=3.5a & d=4a

	c/a									
b/a	−0.3357	−0.3352	−0.3344	−0.3334	−0.3321	−0.3307	−0.3291	−0.3275	−0.3257	−0.3237
	−0.335	−0.3345	−0.3337	−0.3327	−0.3314	−0.3301	−0.3285	−0.3268	−0.3251	−0.3231
	−0.3335	−0.333	−0.3322	−0.3312	−0.3299	−0.3286	−0.3271	−0.3254	−0.3237	−0.3218
	−0.3309	−0.3304	−0.3297	−0.3287	−0.3275	−0.3262	−0.3247	−0.3231	−0.3215	−0.3196
	−0.3274	−0.327	−0.3263	−0.3254	−0.3242	−0.323	−0.3216	−0.32	−0.3184	−0.3166
	−0.3237	−0.3233	−0.3227	−0.3218	−0.3207	−0.3196	−0.3182	−0.3168	−0.3153	−0.3135
	−0.3143	−0.314	−0.3135	−0.3128	−0.312	−0.311	−0.3098	−0.3086	−0.3072	−0.3057
	−0.304	−0.3038	−0.3035	−0.303	−0.3023	−0.3016	−0.3006	−0.2996	−0.2985	−0.2971

Figure I.6: F2A: e=4a & d=0.5a

	c/a									
b/a	−0.3354	−0.3344	−0.3328	−0.3306	−0.3277	−0.3249	−0.3214	−0.3179	−0.3143	−0.3102
	−0.3346	−0.3339	−0.3324	−0.3302	−0.3275	−0.3247	−0.3212	−0.3177	−0.3142	−0.3101
	−0.333	−0.3328	−0.3317	−0.3297	−0.3271	−0.3243	−0.3209	−0.3174	−0.3139	−0.3099
	−0.3305	−0.3305	−0.3301	−0.3286	−0.3263	−0.3236	−0.3204	−0.317	−0.3135	−0.3095
	−0.3273	−0.3273	−0.3273	−0.3268	−0.3251	−0.3226	−0.3196	−0.3163	−0.3128	−0.3089
	−0.3241	−0.3241	−0.3241	−0.324	−0.3234	−0.3216	−0.3188	−0.3157	−0.3123	−0.3085
	−0.316	−0.316	−0.316	−0.316	−0.3159	−0.3159	−0.3152	−0.3131	−0.3102	−0.3069
	−0.3071	−0.3071	−0.3071	−0.3071	−0.3071	−0.3071	−0.3071	−0.307	−0.3062	−0.3041

Figure I.6: F2A: e=4a & d=1a

	c/a									
b/a	−0.3354	−0.3345	−0.333	−0.331	−0.3285	−0.326	−0.323	−0.3199	−0.3168	−0.3131
	−0.3345	−0.3336	−0.3323	−0.3303	−0.3279	−0.3255	−0.3225	−0.3194	−0.3163	−0.3128
	−0.3329	−0.3323	−0.3311	−0.3293	−0.327	−0.3247	−0.3218	−0.3188	−0.3158	−0.3122
	−0.3305	−0.3302	−0.3293	−0.3278	−0.3258	−0.3235	−0.3208	−0.3178	−0.3149	−0.3114
	−0.3273	−0.3272	−0.3268	−0.3257	−0.324	−0.3219	−0.3194	−0.3166	−0.3137	−0.3104
	−0.3241	−0.324	−0.3239	−0.3234	−0.3221	−0.3203	−0.318	−0.3154	−0.3126	−0.3095
	−0.316	−0.316	−0.3159	−0.3159	−0.3157	−0.315	−0.3136	−0.3116	−0.3093	−0.3065
	−0.3071	−0.3071	−0.3071	−0.3071	−0.3071	−0.307	−0.3068	−0.306	−0.3045	−0.3025

Figure I.6: F2A: e=4a & d=1.5a

	c/a									
b/a	−0.3354	−0.3346	−0.3333	−0.3315	−0.3293	−0.3271	−0.3245	−0.3218	−0.319	−0.3158
	−0.3344	−0.3336	−0.3324	−0.3307	−0.3285	−0.3264	−0.3238	−0.3211	−0.3184	−0.3153
	−0.3328	−0.3321	−0.331	−0.3294	−0.3274	−0.3253	−0.3228	−0.3202	−0.3175	−0.3144
	−0.3304	−0.3298	−0.3289	−0.3275	−0.3256	−0.3237	−0.3213	−0.3188	−0.3162	−0.3132
	−0.3273	−0.327	−0.3263	−0.3251	−0.3235	−0.3217	−0.3194	−0.3171	−0.3146	−0.3117
	−0.3241	−0.324	−0.3235	−0.3227	−0.3213	−0.3197	−0.3177	−0.3154	−0.3131	−0.3103
	−0.3159	−0.3159	−0.3159	−0.3157	−0.3151	−0.3141	−0.3126	−0.3108	−0.3088	−0.3064
	−0.3071	−0.3071	−0.307	−0.307	−0.307	−0.3067	−0.306	−0.3049	−0.3034	−0.3016

Figure I.6: F2A: e=4a & d=2a

	c/a									
b/a	−0.3355	−0.3347	−0.3336	−0.332	−0.3301	−0.3282	−0.3258	−0.3234	−0.321	−0.3182
	−0.3345	−0.3337	−0.3326	−0.3311	−0.3292	−0.3273	−0.3251	−0.3227	−0.3203	−0.3175
	−0.3328	−0.3321	−0.3311	−0.3296	−0.3279	−0.326	−0.3238	−0.3215	−0.3192	−0.3164
	−0.3303	−0.3297	−0.3288	−0.3275	−0.3258	−0.3241	−0.322	−0.3198	−0.3175	−0.3149
	−0.3272	−0.3268	−0.326	−0.3249	−0.3234	−0.3218	−0.3198	−0.3177	−0.3155	−0.3129
	−0.324	−0.3237	−0.3232	−0.3222	−0.3209	−0.3195	−0.3176	−0.3157	−0.3136	−0.3112
	−0.316	−0.3159	−0.3157	−0.3153	−0.3145	−0.3134	−0.312	−0.3104	−0.3086	−0.3065
	−0.3071	−0.307	−0.307	−0.307	−0.3067	−0.3062	−0.3053	−0.3041	−0.3028	−0.301

Figure I.6: F2A: e=4a & d=2.5a

	c/a									
b/a	−0.3355	−0.3348	−0.3338	−0.3324	−0.3308	−0.3291	−0.327	−0.3249	−0.3228	−0.3203
	−0.3345	−0.3338	−0.3329	−0.3315	−0.3299	−0.3282	−0.3262	−0.3241	−0.322	−0.3195
	−0.3328	−0.3322	−0.3313	−0.33	−0.3284	−0.3268	−0.3248	−0.3228	−0.3207	−0.3183
	−0.3303	−0.3298	−0.3289	−0.3277	−0.3262	−0.3247	−0.3228	−0.3208	−0.3188	−0.3164
	−0.3272	−0.3267	−0.326	−0.3249	−0.3235	−0.3221	−0.3203	−0.3184	−0.3165	−0.3142
	−0.324	−0.3236	−0.323	−0.322	−0.3208	−0.3195	−0.3179	−0.3161	−0.3143	−0.3121
	−0.3159	−0.3158	−0.3155	−0.3149	−0.314	−0.313	−0.3117	−0.3102	−0.3086	−0.3068
	−0.3071	−0.3071	−0.307	−0.3068	−0.3063	−0.3057	−0.3047	−0.3036	−0.3024	−0.3008

Figure I.6: F2A: e=4a & d=3a

	c/a									
b/a	−0.3355	−0.3349	−0.3341	−0.3329	−0.3314	−0.3299	−0.3281	−0.3262	−0.3243	−0.322
	−0.3345	−0.3339	−0.3331	−0.3319	−0.3304	−0.329	−0.3272	−0.3253	−0.3234	−0.3212
	−0.3328	−0.3323	−0.3315	−0.3303	−0.3289	−0.3275	−0.3257	−0.3239	−0.322	−0.3199
	−0.3303	−0.3298	−0.329	−0.328	−0.3266	−0.3252	−0.3236	−0.3218	−0.32	−0.3179
	−0.3272	−0.3267	−0.326	−0.325	−0.3238	−0.3225	−0.3209	−0.3192	−0.3175	−0.3154
	−0.3239	−0.3236	−0.323	−0.3221	−0.3209	−0.3197	−0.3182	−0.3167	−0.315	−0.3131
	−0.3159	−0.3157	−0.3153	−0.3147	−0.3138	−0.3129	−0.3116	−0.3103	−0.3088	−0.3071
	−0.3071	−0.307	−0.3068	−0.3065	−0.3059	−0.3053	−0.3044	−0.3033	−0.3021	−0.3007

Figure I.6: F2A: e=4a & d=3.5a

	c/a									
b/a	−0.3356	−0.335	−0.3343	−0.3332	−0.3319	−0.3306	−0.329	−0.3273	−0.3256	−0.3236
	−0.3345	−0.334	−0.3333	−0.3322	−0.3309	−0.3296	−0.3281	−0.3264	−0.3247	−0.3227
	−0.3329	−0.3324	−0.3316	−0.3306	−0.3294	−0.3281	−0.3265	−0.3249	−0.3232	−0.3213
	−0.3303	−0.3299	−0.3292	−0.3282	−0.327	−0.3258	−0.3243	−0.3227	−0.3211	−0.3192
	−0.3272	−0.3267	−0.3261	−0.3252	−0.3241	−0.3229	−0.3215	−0.32	−0.3184	−0.3166
	−0.3239	−0.3236	−0.323	−0.3222	−0.3211	−0.32	−0.3187	−0.3173	−0.3158	−0.314
	−0.3159	−0.3156	−0.3152	−0.3146	−0.3138	−0.3129	−0.3117	−0.3105	−0.3092	−0.3076
	−0.307	−0.3069	−0.3067	−0.3063	−0.3057	−0.305	−0.3041	−0.3031	−0.3021	−0.3007

Figure I.6: F2A: e=4a & d=4a

	c/a									
b/a	−0.3356	−0.3351	−0.3344	−0.3335	−0.3324	−0.3312	−0.3297	−0.3283	−0.3267	−0.3249
	−0.3346	−0.3341	−0.3334	−0.3325	−0.3314	−0.3302	−0.3288	−0.3273	−0.3258	−0.324
	−0.3329	−0.3324	−0.3318	−0.3309	−0.3298	−0.3286	−0.3272	−0.3258	−0.3243	−0.3226
	−0.3303	−0.3299	−0.3293	−0.3284	−0.3274	−0.3263	−0.3249	−0.3235	−0.3221	−0.3204
	−0.3272	−0.3268	−0.3262	−0.3254	−0.3244	−0.3233	−0.322	−0.3207	−0.3193	−0.3176
	−0.3239	−0.3236	−0.3231	−0.3223	−0.3214	−0.3204	−0.3191	−0.3179	−0.3165	−0.3149
	−0.3159	−0.3156	−0.3152	−0.3146	−0.3138	−0.313	−0.3119	−0.3108	−0.3096	−0.3082
	−0.307	−0.3069	−0.3066	−0.3062	−0.3056	−0.3049	−0.3041	−0.3031	−0.3021	−0.3009

I.2 Mode I and Mode II Stress Intensity Factor of Crack B

The remaining results for the mode I and mode II dimensionless SIF results for crack B in Chapter 6 are given here.

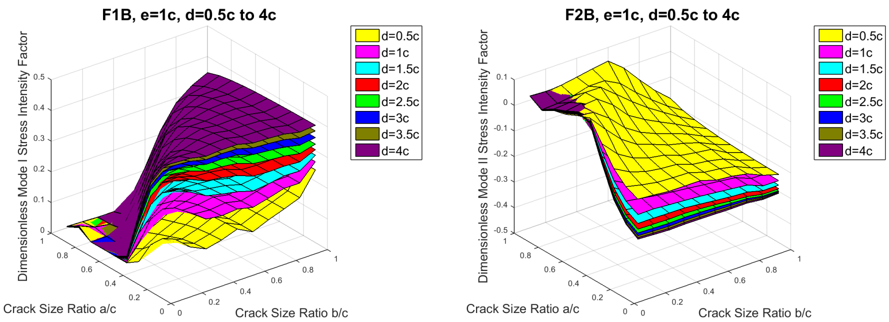

(a) (b)

Figure I.7: Mode I, (a), and mode II, (b), dimensionless stress intensity factor of Crack B as b=0.1c to 1c, a=0.1c to 1c and d=0.5c to 4c, e=1c

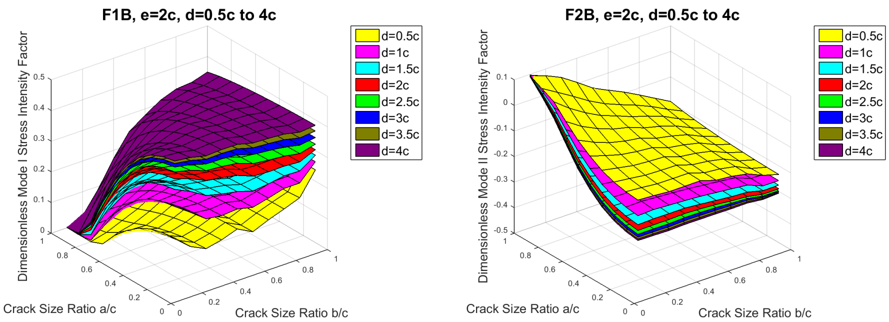

(a) (b)

Figure I.8: Mode I, (a), and mode II, (b), dimensionless stress intensity factor of Crack B as b=0.1c to 1c, a=0.1c to 1c and d=0.5c to 4c, e=2c

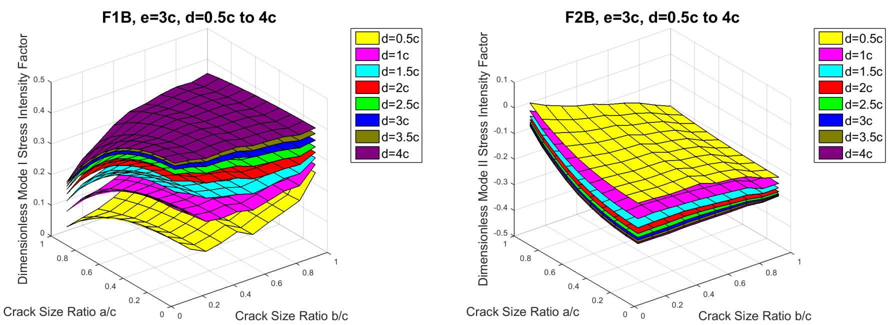

(a) (b)

Figure I.9: Mode I, (a), and mode II, (b), dimensionless stress intensity factor of Crack B as b=0.1c to 1c, a=0.1c to 1c and d=0.5c to 4c, e=3c

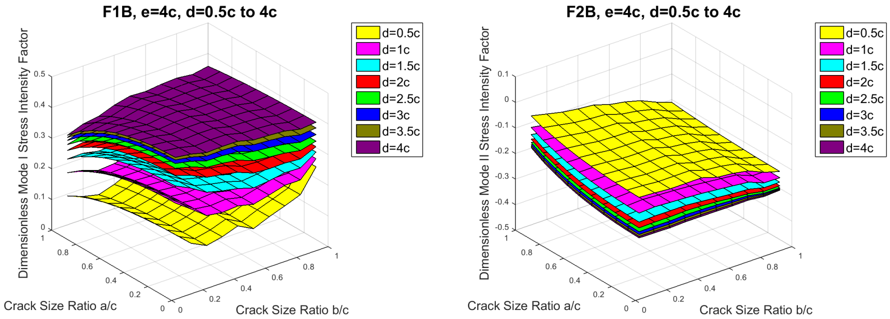

(a) (b)

Figure I.10: Mode I, (a), and mode II, (b), dimensionless stress intensity factor of Crack B as b=0.1c to 1c, a=0.1c to 1c and d=0.5c to 4c, e=4c

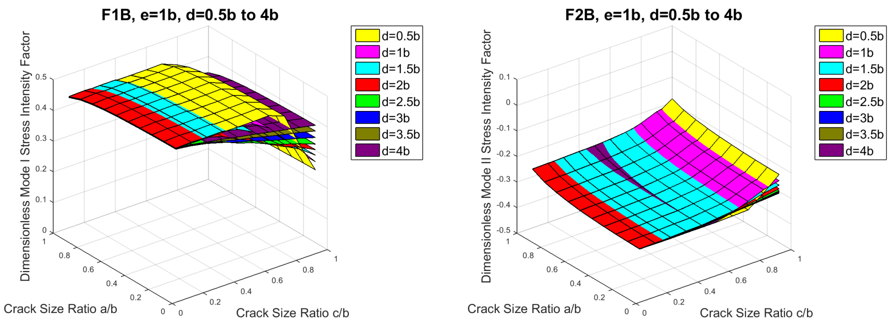

(a) (b)

Figure I.11: Mode I, (a), and mode II, (b), dimensionless stress intensity factor of Crack B as a=0.1b to 1b, c=0.1b to 1b and d=0.5b to 4b, e=1b

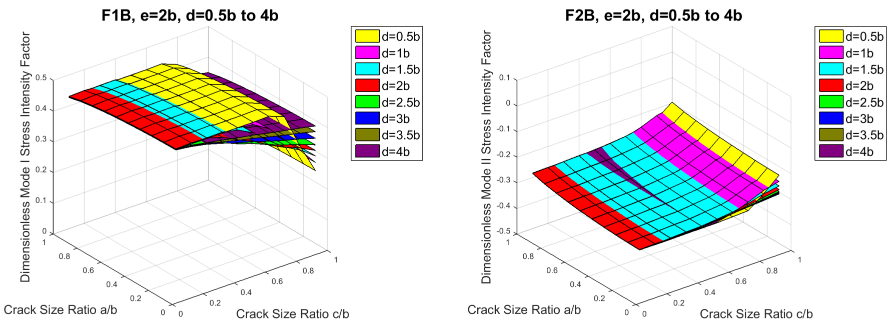

(a) (b)

Figure I.12: Mode I, (a), and mode II, (b), dimensionless stress intensity factor of Crack B as a=0.1b to 1b, c=0.1b to 1b and d=0.5b to 4b, e=2b

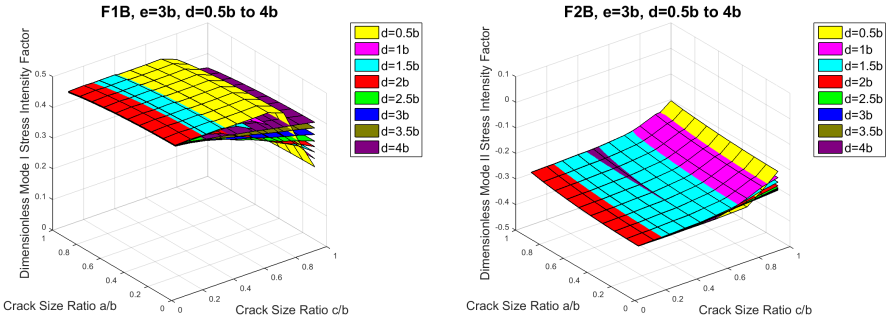

(a) (b)

Figure I.13: Mode I, (a), and mode II, (b), dimensionless stress intensity factor of Crack B as a=0.1b to 1b, c=0.1b to 1b and d=0.5b to 4b, e=3b

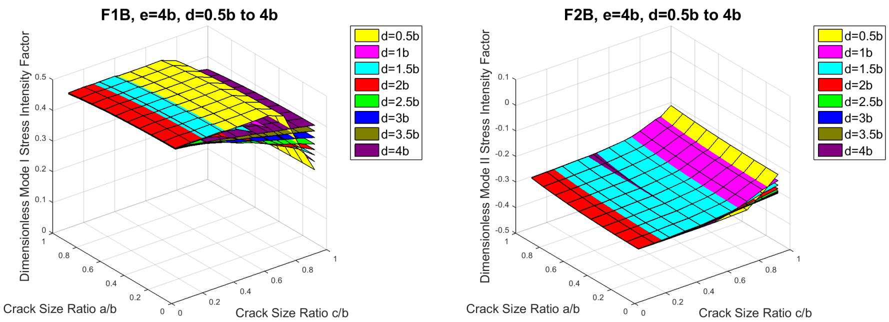

(a) (b)

Figure I.14: Mode I, (a), and mode II, (b), dimensionless stress intensity factor of Crack B as a=0.1b to 1b, c=0.1b to 1b and d=0.5b to 4b, e=4b

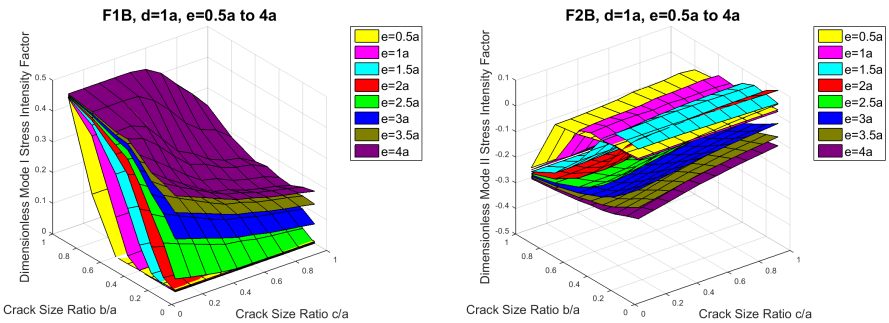

(a) (b)

Figure I.15: Mode I, (a), and mode II, (b), dimensionless stress intensity factor of Crack B as b=0.1a to 1a, c=0.1a to 1a and e=0.5a to 4a, d=1a

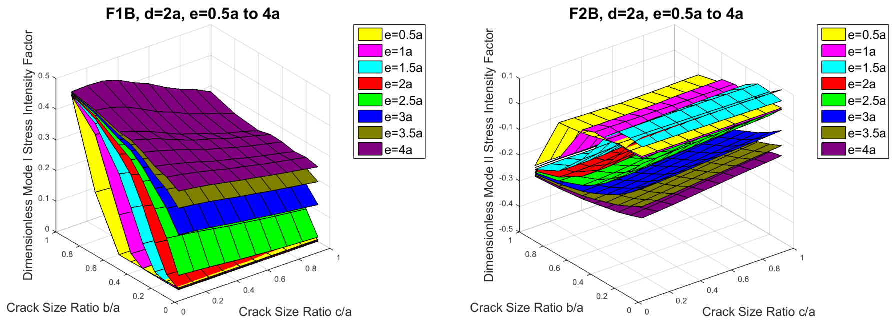

(a) (b)

Figure I.16: Mode I, (a), and mode II, (b), dimensionless stress intensity factor of Crack B as b=0.1a to 1a, c=0.1a to 1a and e=0.5a to 4a, d=2a

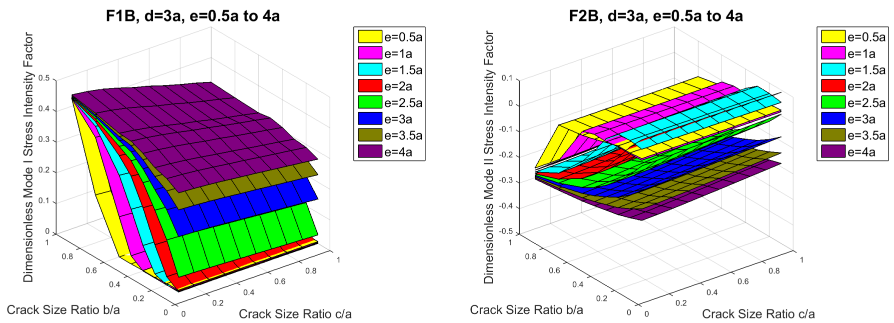

(a) (b)

Figure I.17: Mode I, (a), and mode II, (b), dimensionless stress intensity factor of Crack B as b=0.1a to 1a, c=0.1a to 1a and e=0.5a to 4a, d=3a

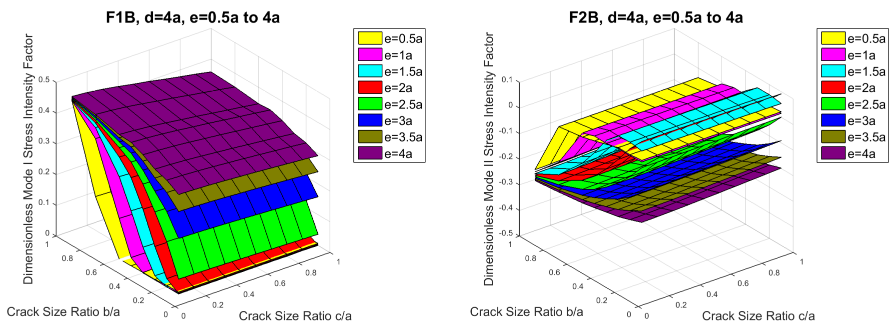

(a) (b)

Figure I.18: Mode I, (a), and mode II, (b), dimensionless stress intensity factor of Crack B as b=0.1a to 1a, c=0.1a to 1a and e=0.5a to 4a, d=4a

The tabulated results show the dimensionless SIF to 4 significant figures. To calculate the SIF use Equations 2.12 and 2.13.

Figure 6.18a: F1B: e=0.5c & d=0.5c

	b/c									
	0.162	0.1249	0.1022	0.1137	0.1319	0.1056	0.1269	0.1446	0.1638	0.2375
	0.1058	0.1107	0.09738	0.1107	0.1301	0.1049	0.1267	0.144	0.1624	0.2361
	0.00859	0.07174	0.0884	0.1055	0.1276	0.1063	0.1275	0.1439	0.1651	0.236
	0.00025	0.02108	0.0781	0.09585	0.1216	0.1069	0.1283	0.1432	0.1651	0.2351
a/c	0.00342	0.00033	0.02951	0.08617	0.1074	0.1122	0.1294	0.1438	0.1665	0.2336
	0.02182	0.00471	0.00021	0.02178	0.08108	0.09822	0.1243	0.1385	0.1622	0.2325
	0.02273	0.01241	0.00661	0.00200	0.02157	0.08443	0.1149	0.1362	0.1597	0.2296
	0.00287	0.00120	0.00104	6.7e−05	0.00050	0.02636	0.09612	0.126	0.1553	0.2252
	0.04758	0.03311	0.01155	0.02127	0.02873	−0.0004	0.02638	0.09454	0.1419	0.2179
	0.00623	0.00229	0.00365	0.00826	8.3e−05	0.00027	0.00115	0.03472	0.1231	0.1982

Figure 6.18a: F1B: e=0.5c & d=1c

	b/c									
	0.2617	0.2355	0.1993	0.1929	0.1971	0.1852	0.1977	0.2118	0.2118	0.2636
	0.1889	0.2169	0.1933	0.1898	0.1954	0.1839	0.1969	0.2111	0.2116	0.2631
	0.02785	0.1618	0.1788	0.184	0.1926	0.1822	0.1959	0.2105	0.2117	0.2628
	0.00021	0.04235	0.1364	0.1682	0.1861	0.1786	0.1937	0.209	0.2118	0.262
a/c	0.00183	0.00010	0.04757	0.1365	0.1703	0.1768	0.1879	0.2066	0.2146	0.2608
	0.02128	0.00138	0.00012	0.0432	0.1337	0.1609	0.1857	0.2036	0.2116	0.2597
	0.02305	0.01373	0.00152	0.00046	0.04318	0.1368	0.1702	0.1985	0.2094	0.2571
	0.00373	0.00022	6.2e−05	6.1e−05	0.00046	0.05009	0.1436	0.1829	0.2087	0.2532
	0.06154	0.05046	0.03135	0.02965	0.01809	0.00011	0.04389	0.1387	0.1831	0.2459
	0.00650	0.00505	0.00270	0.00439	5.0e−05	−3e−05	−0.0003	0.05791	0.1664	0.2281

Figure 6.18a: F1B: e=0.5c & d=1.5c

	b/c									
	0.3159	0.303	0.2751	0.2633	0.2536	0.2383	0.244	0.2528	0.2509	0.285
	0.2343	0.282	0.2674	0.2599	0.2519	0.2371	0.2432	0.2522	0.2505	0.2846
	0.04029	0.2185	0.25	0.2534	0.249	0.2355	0.2422	0.2515	0.25	0.2843
	0.00029	0.06251	0.1929	0.2356	0.2422	0.2319	0.2401	0.2501	0.2502	0.2836
a/c	0.00145	0.00044	0.07022	0.1872	0.2252	0.2259	0.2363	0.2478	0.2515	0.2825
	0.02055	0.00032	0.00036	0.06286	0.1807	0.2101	0.2311	0.2449	0.249	0.2814
	0.02321	0.01285	0.00047	0.00044	0.05928	0.1752	0.2139	0.2392	0.2479	0.279
	0.00386	0.00022	−5e−05	−7e−05	−0.0001	0.06498	0.1778	0.2226	0.2441	0.2754
	0.06113	0.05395	0.03282	0.02782	0.01096	−0.0003	0.05867	0.1775	0.2217	0.2684
	0.00651	0.00517	0.00235	0.00297	2.6e−05	−4e−05	0.00051	0.0715	0.1951	0.2514

Figure 6.18a: F1B: e=0.5c & d=2c

	b/c									
	0.3493	0.3444	0.3238	0.3167	0.3066	0.2868	0.2833	0.2843	0.2804	0.3028
	0.262	0.3219	0.3156	0.3131	0.3048	0.2855	0.2826	0.2838	0.28	0.3025
	0.04798	0.2533	0.2961	0.306	0.3017	0.2838	0.2816	0.2831	0.2795	0.3022
	0.0001	0.0757	0.2323	0.2867	0.2944	0.2801	0.2795	0.2818	0.2785	0.3016
a/c	0.0009	0.00042	0.08736	0.2293	0.276	0.2724	0.2757	0.2796	0.2794	0.3005
	0.01983	−0.0003	0.00035	0.08202	0.226	0.2566	0.2699	0.2767	0.2772	0.2995
	0.02289	0.01199	0.00042	0.00069	0.07903	0.2128	0.2529	0.2704	0.2755	0.2973
	0.00384	0.00011	0.00012	8e−05	0.00032	0.08035	0.2092	0.2534	0.2714	0.2938
	0.06079	0.05666	0.03407	0.02765	0.00993	−0.0009	0.07075	0.2058	0.2504	0.2873
	0.00641	0.00513	0.00232	0.00269	3.6e−05	0.00031	0.00015	0.08161	0.216	0.2703

Figure 6.18a: F1B: e=0.5c & d=2.5c

	b/c									
	0.3714	0.3714	0.3557	0.3529	0.346	0.3274	0.3215	0.3169	0.3076	0.3209
	0.2803	0.3479	0.3471	0.3491	0.3441	0.3261	0.3207	0.3163	0.3072	0.3206
	0.05293	0.2758	0.3266	0.3417	0.3408	0.3243	0.3197	0.3157	0.3067	0.3203
	−7e−05	0.08437	0.2587	0.3215	0.3331	0.3204	0.3175	0.3143	0.3058	0.3196
a/c	0.00060	0.00030	0.09915	0.2586	0.3138	0.3123	0.3136	0.3121	0.3058	0.3187
	0.0193	−0.0003	0.00047	0.09614	0.2601	0.2957	0.3074	0.3092	0.3038	0.3177
	0.02265	0.01128	0.00028	7.2e−05	0.09552	0.246	0.2899	0.3024	0.3017	0.3156
	0.00382	1.9e−05	0.00010	0.00025	0.00066	0.09612	0.2409	0.2854	0.2978	0.3122
	0.06047	0.0566	0.03515	0.02772	0.0114	−0.0008	0.08246	0.2346	0.2768	0.3056
	0.00660	0.00517	0.00220	0.00263	0.00012	4.2e−05	−0.0002	0.09324	0.2372	0.2889

Figure 6.18a: F1B: e=0.5c & d=3c

	b/c									
	0.3867	0.3899	0.3775	0.3778	0.3737	0.3573	0.3523	0.3467	0.3349	0.3423
	0.2928	0.3658	0.3686	0.3738	0.3717	0.356	0.3515	0.3461	0.3345	0.342
	0.05629	0.2912	0.3474	0.3662	0.3683	0.3541	0.3504	0.3455	0.334	0.3417
	0.00011	0.09025	0.2767	0.3453	0.3603	0.3501	0.3482	0.3441	0.3331	0.3411
a/c	0.00045	0.00049	0.1072	0.2787	0.3404	0.3418	0.3442	0.3418	0.3326	0.3401
	0.01893	−0.0004	0.00037	0.1061	0.2841	0.3246	0.3377	0.3388	0.3307	0.3391
	0.02247	0.01097	0.00013	0.00058	0.1076	0.2708	0.3197	0.3318	0.3282	0.337
	0.00379	4.2e−05	0.00015	0.00028	0.00026	0.1089	0.2671	0.3143	0.324	0.3337
	0.06017	0.05624	0.036	0.02772	0.0107	−0.0008	0.09268	0.261	0.3031	0.3272
	0.00666	0.00513	0.00216	0.00249	−3e−05	−0.0001	0.00061	0.1056	0.2601	0.3101

Figure 6.18a: F1B: e=0.5c & d=3.5c

	b/c									
	0.3978	0.4032	0.3928	0.3953	0.3934	0.379	0.3754	0.3705	0.3586	0.3638
	0.3019	0.3785	0.3838	0.3913	0.3913	0.3777	0.3747	0.37	0.3582	0.3635
	0.05865	0.3021	0.3621	0.3834	0.3878	0.3757	0.3735	0.3693	0.3577	0.3632
	0.00038	0.09439	0.2895	0.362	0.3797	0.3716	0.3713	0.3679	0.3568	0.3626
a/c	0.00047	0.00032	0.1128	0.2932	0.3593	0.3631	0.3672	0.3656	0.3559	0.3616
	0.01867	−6e−06	0.00024	0.1131	0.3012	0.3454	0.3605	0.3625	0.354	0.3606
	0.02234	0.01062	−0.0005	0.00076	0.1161	0.2892	0.342	0.3551	0.3515	0.3585
	0.00379	5.3e−05	0.00018	0.00046	0.00026	0.1183	0.2871	0.3374	0.3463	0.3551
	0.05996	0.05595	0.0364	0.0277	0.00761	−0.0008	0.109	0.2823	0.3261	0.3485
	0.00627	0.00507	0.00209	0.00241	0.00013	−0.0003	0.00019	0.1163	0.2799	0.3312

Figure 6.18a: F1B: e=0.5c & d=4c

	b/c									
	0.4060	0.4129	0.4041	0.4080	0.4076	0.3948	0.3926	0.3887	0.3775	0.3823
	0.3086	0.3879	0.3949	0.4039	0.4055	0.3935	0.3918	0.3882	0.3771	0.3820
	0.0604	0.3101	0.3729	0.3960	0.4020	0.3915	0.3907	0.3875	0.3766	0.3817
	0.0004	0.0974	0.2988	0.3742	0.3937	0.3873	0.3884	0.3860	0.3756	0.3811
a/c	0.0004	0.0005	0.1169	0.3037	0.3730	0.3786	0.3842	0.3837	0.3744	0.3801
	0.0185	−0.0003	0.0004	0.1181	0.3134	0.3606	0.3774	0.3805	0.3726	0.3791
	0.0223	0.0102	0.0003	0.0003	0.1223	0.3029	0.3586	0.3729	0.3700	0.3769
	0.0038	0.0000	0.0002	0.0003	0.0003	0.1253	0.3019	0.3550	0.3650	0.3735
	0.0598	0.0558	0.0359	0.0275	0.0117	0.0002	0.1147	0.2985	0.3443	0.3668
	0.0067	0.0053	0.0020	0.0023	0.0001	−0.0002	0.0006	0.1248	0.2964	0.3492

Figure I.7a: F1B: e=1c & d=0.5c

	b/c									
a/c	0.1693	0.1263	0.1024	0.1137	0.1318	0.1055	0.1269	0.1446	0.1637	0.2369
	0.1488	0.1171	0.0976	0.1105	0.1296	0.1053	0.1260	0.1437	0.1634	0.2361
	0.1056	0.0993	0.0889	0.1048	0.1259	0.1022	0.1239	0.1423	0.1628	0.2348
	0.0273	0.0645	0.0741	0.0947	0.1197	0.0997	0.1232	0.1503	0.1623	0.2332
	0.0004	0.0284	0.0588	0.0812	0.1098	0.0995	0.1222	0.1384	0.1613	0.2314
	0.0000	0.0080	0.0422	0.0676	0.0953	0.0977	0.1196	0.1358	0.1603	0.2293
	0.0002	0.0001	0.0172	0.0481	0.0745	0.0906	0.1154	0.1312	0.1588	0.2254
	−0.0001	0.0002	−0.0001	0.0174	0.0500	0.0770	0.1078	0.1262	0.1541	0.2201
	0.0300	0.0075	−0.0001	0.0001	0.0149	0.0487	0.0880	0.1128	0.1450	0.2129
	0.0047	0.0026	0.0001	−0.0010	−0.0004	0.0180	0.0574	0.0965	0.1369	0.1991

Figure I.7a: F1B: e=1c & d=1c

	b/c									
a/c	0.2711	0.2372	0.1995	0.1928	0.1970	0.1851	0.1976	0.2117	0.2117	0.2635
	0.2450	0.2248	0.1933	0.1891	0.1945	0.1833	0.1963	0.2107	0.2111	0.2629
	0.1894	0.2005	0.1821	0.1826	0.1905	0.1805	0.1943	0.2092	0.2102	0.2618
	0.0858	0.1525	0.1608	0.1710	0.1836	0.1759	0.1912	0.2068	0.2090	0.2604
	0.0032	0.0705	0.1207	0.1503	0.1722	0.1687	0.1865	0.2036	0.2076	0.2586
	0.0003	0.0165	0.0731	0.1165	0.1547	0.1593	0.1803	0.1995	0.2054	0.2564
	0.0003	0.0003	0.0262	0.0814	0.1235	0.1437	0.1692	0.1922	0.2030	0.2528
	0.0000	0.0003	−0.0001	0.0371	0.0918	0.1277	0.1550	0.1809	0.2016	0.2478
	0.0284	0.0084	−0.0001	0.0008	0.0383	0.0915	0.1291	0.1632	0.1871	0.2407
	0.0041	−0.0001	0.0001	−0.0003	0.0043	0.0492	0.1053	0.1478	0.1814	0.2275

Figure I.7a: F1B: e=1c & d=1.5c

	b/c									
a/c	0.3264	0.3049	0.2753	0.2631	0.2534	0.2382	0.2438	0.2527	0.2509	0.2849
	0.2977	0.2910	0.2679	0.2589	0.2508	0.2364	0.2425	0.2517	0.2501	0.2843
	0.2360	0.2634	0.2543	0.2516	0.2466	0.2336	0.2406	0.2502	0.2489	0.2834
	0.1200	0.2088	0.2289	0.2384	0.2392	0.2289	0.2374	0.2479	0.2472	0.2821
	0.0090	0.1104	0.1817	0.2146	0.2268	0.2214	0.2327	0.2446	0.2456	0.2803
	0.0006	0.0300	0.1108	0.1746	0.2073	0.2106	0.2262	0.2405	0.2434	0.2782
	0.0003	0.0002	0.0406	0.1118	0.1680	0.1907	0.2144	0.2331	0.2397	0.2748
	0.0001	0.0001	0.0006	0.0483	0.1154	0.1618	0.1960	0.2215	0.2342	0.2699
	0.0274	0.0078	−0.0001	0.0012	0.0487	0.1150	0.1648	0.2026	0.2223	0.2630
	0.0039	0.0001	0.0002	0.0001	0.0051	0.0611	0.1300	0.1789	0.2119	0.2501

Figure I.7a: F1B: e=1c & d=2c

	b/c									
a/c	0.3605	0.3464	0.3241	0.3165	0.3064	0.2866	0.2832	0.2842	0.2803	0.3028
	0.3302	0.3316	0.3161	0.3119	0.3036	0.2847	0.2819	0.2832	0.2795	0.3022
	0.2647	0.3021	0.3014	0.3040	0.2990	0.2817	0.2799	0.2818	0.2785	0.3013
	0.1410	0.2438	0.2733	0.2896	0.2910	0.2768	0.2767	0.2796	0.2768	0.3001
	0.0136	0.1375	0.2222	0.2638	0.2775	0.2689	0.2719	0.2763	0.2744	0.2984
	0.0003	0.0401	0.1391	0.2198	0.2562	0.2573	0.2652	0.2721	0.2717	0.2964
	0.0003	0.0003	0.0537	0.1409	0.2122	0.2355	0.2529	0.2648	0.2679	0.2930
	0.0001	0.0003	0.0021	0.0626	0.1429	0.1969	0.2324	0.2529	0.2619	0.2883
	0.0263	0.0069	−0.0002	0.0042	0.0639	0.1383	0.1969	0.2334	0.2499	0.2816
	0.0040	0.0002	0.0001	0.0002	0.0079	0.0709	0.1475	0.2017	0.2360	0.2688

Figure I.7a: F1B: e=1c & d=2.5c

	b/c									
a/c	0.3830	0.3735	0.3560	0.3528	0.3458	0.3272	0.3213	0.3167	0.3075	0.3208
	0.3517	0.3582	0.3477	0.3480	0.3428	0.3252	0.3200	0.3158	0.3068	0.3202
	0.2836	0.3275	0.3323	0.3396	0.3379	0.3221	0.3179	0.3143	0.3057	0.3194
	0.1545	0.2666	0.3029	0.3245	0.3295	0.3169	0.3146	0.3121	0.3041	0.3182
	0.0168	0.1553	0.2490	0.2974	0.3153	0.3085	0.3095	0.3087	0.3017	0.3165
	0.0004	0.0471	0.1590	0.2509	0.2927	0.2963	0.3026	0.3045	0.2989	0.3146
	0.0001	0.0003	0.0632	0.1632	0.2461	0.2725	0.2897	0.2969	0.2944	0.3113
	0.0001	0.0003	0.0045	0.0741	0.1670	0.2289	0.2676	0.2847	0.2882	0.3067
	0.0253	0.0066	−0.0002	0.0074	0.0779	0.1621	0.2292	0.2644	0.2762	0.3000
	0.0036	0.0002	0.0000	0.0000	0.0118	0.0831	0.1677	0.2260	0.2598	0.2874

Figure I.7a: F1B: e=1c & d=3c

	b/c									
a/c	0.3987	0.3921	0.3777	0.3776	0.3734	0.3571	0.3521	0.3465	0.3348	0.3422
	0.3667	0.3764	0.3692	0.3726	0.3704	0.3551	0.3507	0.3456	0.3341	0.3416
	0.2967	0.3448	0.3533	0.3640	0.3653	0.3518	0.3486	0.3441	0.3330	0.3408
	0.1638	0.2822	0.3231	0.3485	0.3567	0.3465	0.3452	0.3417	0.3313	0.3396
	0.0189	0.1672	0.2672	0.3204	0.3420	0.3378	0.3399	0.3383	0.3289	0.3380
	0.0008	0.0518	0.1728	0.2723	0.3185	0.3251	0.3327	0.3339	0.3260	0.3360
	0.0001	0.0003	0.0697	0.1791	0.2701	0.3001	0.3194	0.3261	0.3210	0.3328
	0.0001	0.0005	0.0062	0.0826	0.1848	0.2554	0.2960	0.3135	0.3145	0.3281
	0.0245	0.0061	−0.0001	0.0101	0.0885	0.1819	0.2558	0.2924	0.3022	0.3214
	0.0037	0.0002	0.0001	0.0000	0.0154	0.0937	0.1861	0.2498	0.2842	0.3086

Figure I.7a: F1B: e=1c & d=3.5c

	b/c									
a/c	0.4100	0.4054	0.3931	0.3951	0.3931	0.3788	0.3753	0.3704	0.3585	0.3637
	0.3774	0.3894	0.3844	0.3900	0.3900	0.3767	0.3738	0.3694	0.3577	0.3631
	0.3060	0.3572	0.3682	0.3812	0.3848	0.3734	0.3716	0.3678	0.3566	0.3623
	0.1703	0.2933	0.3374	0.3654	0.3760	0.3678	0.3681	0.3654	0.3549	0.3611
	0.0205	0.1756	0.2800	0.3367	0.3609	0.3590	0.3628	0.3619	0.3525	0.3594
	0.0004	0.0552	0.1827	0.2873	0.3368	0.3459	0.3554	0.3574	0.3495	0.3574
	0.0003	0.0003	0.0746	0.1905	0.2872	0.3204	0.3416	0.3494	0.3444	0.3541
	0.0000	−0.0001	0.0075	0.0886	0.1979	0.2733	0.3177	0.3365	0.3373	0.3494
	0.0239	0.0057	0.0002	0.0121	0.0962	0.1957	0.2760	0.3148	0.3248	0.3425
	0.0037	0.0002	0.0001	−0.0001	0.0181	0.1019	0.2007	0.2694	0.3054	0.3295

Figure I.7a: F1B: e=1c & d=4c

	b/c									
a/c	0.4185	0.4152	0.4043	0.4078	0.4074	0.3946	0.3924	0.3886	0.3773	0.3822
	0.3854	0.3989	0.3955	0.4027	0.4042	0.3924	0.3910	0.3875	0.3766	0.3816
	0.3130	0.3662	0.3791	0.3938	0.3989	0.3891	0.3887	0.3860	0.3755	0.3808
	0.1751	0.3014	0.3478	0.3776	0.3899	0.3835	0.3852	0.3836	0.3737	0.3796
	0.0216	0.1817	0.2893	0.3485	0.3746	0.3745	0.3797	0.3800	0.3713	0.3779
	0.0000	0.0576	0.1898	0.2982	0.3501	0.3612	0.3722	0.3754	0.3682	0.3759
	0.0003	0.0005	0.0780	0.1989	0.2996	0.3351	0.3582	0.3672	0.3630	0.3725
	0.0001	0.0001	0.0084	0.0931	0.2076	0.2869	0.3338	0.3540	0.3555	0.3677
	0.0235	0.0054	−0.0001	0.0135	0.1018	0.2064	0.2910	0.3319	0.3430	0.3607
	0.0035	0.0001	0.0002	0.0000	0.0201	0.1081	0.2118	0.2846	0.3230	0.3474

Figure 6.19a: F1B: e=1.5c & d=0.5c

	b/c									
	0.1719	0.1273	0.1029	0.1140	0.1320	0.1055	0.1269	0.1446	0.1637	0.2369
	0.1621	0.1219	0.0995	0.1114	0.1301	0.1053	0.1259	0.1437	0.1631	0.2362
	0.1420	0.1114	0.0933	0.1069	0.1268	0.0996	0.1244	0.1423	0.1621	0.2349
	0.1049	0.0925	0.0824	0.0990	0.1212	0.0995	0.1217	0.1400	0.1610	0.2327
a/c	0.0488	0.0635	0.0670	0.0876	0.1133	0.0965	0.1188	0.1370	0.1577	0.2301
	0.0027	0.0297	0.0507	0.0744	0.1035	0.0930	0.1169	0.1338	0.1561	0.2274
	0.0010	0.0121	0.0370	0.0599	0.0880	0.0883	0.1121	0.1297	0.1560	0.2235
	0.0009	0.0033	0.0246	0.0458	0.0683	0.0804	0.1072	0.1240	0.1523	0.2186
	−0.0002	0.0000	0.0101	0.0286	0.0516	0.0699	0.0983	0.1155	0.1459	0.2123
	0.0003	0.0004	0.0002	0.0103	0.0306	0.0538	0.0863	0.1068	0.1377	0.2018

Figure 6.19a: F1B: e=1.5c & d=1c

	b/c									
	0.2743	0.2385	0.2001	0.1930	0.1971	0.1851	0.1976	0.2117	0.2117	0.2635
	0.2617	0.2310	0.1955	0.1899	0.1948	0.1834	0.1963	0.2107	0.2109	0.2628
	0.2360	0.2165	0.1873	0.1845	0.1910	0.1806	0.1942	0.2090	0.2097	0.2616
	0.1885	0.1904	0.1729	0.1752	0.1847	0.1760	0.1907	0.2062	0.2079	0.2597
a/c	0.1160	0.1499	0.1510	0.1614	0.1756	0.1695	0.1859	0.2026	0.2056	0.2573
	0.0336	0.0971	0.1213	0.1432	0.1639	0.1614	0.1803	0.1984	0.2029	0.2547
	0.0009	0.0332	0.0769	0.1132	0.1449	0.1494	0.1714	0.1919	0.1987	0.2509
	0.0009	0.0046	0.0400	0.0792	0.1169	0.1341	0.1594	0.1831	0.1951	0.2459
	0.0003	0.0004	0.0138	0.0515	0.0903	0.1130	0.1454	0.1713	0.1884	0.2396
	0.0006	0.0004	−0.0002	0.0266	0.0667	0.0989	0.1282	0.1523	0.1800	0.2293

Figure 6.19a: F1B: e=1.5c & d=1.5c

	b/c									
	0.3299	0.3064	0.2759	0.2634	0.2535	0.2382	0.2438	0.2527	0.2508	0.2849
	0.3161	0.2979	0.2705	0.2598	0.2511	0.2364	0.2425	0.2516	0.2500	0.2842
	0.2879	0.2814	0.2606	0.2535	0.2469	0.2335	0.2403	0.2499	0.2486	0.2831
	0.2358	0.2520	0.2432	0.2429	0.2401	0.2287	0.2367	0.2471	0.2464	0.2813
a/c	0.1557	0.2060	0.2170	0.2270	0.2301	0.2218	0.2318	0.2434	0.2436	0.2790
	0.0622	0.1452	0.1819	0.2057	0.2171	0.2133	0.2259	0.2392	0.2409	0.2765
	0.0019	0.0610	0.1260	0.1704	0.1958	0.1995	0.2166	0.2325	0.2369	0.2727
	0.0009	0.0127	0.0652	0.1188	0.1638	0.1800	0.2034	0.2234	0.2314	0.2679
	0.0000	0.0001	0.0233	0.0721	0.1228	0.1522	0.1857	0.2110	0.2233	0.2616
	0.0003	0.0000	0.0004	0.0323	0.0808	0.1233	0.1593	0.1897	0.2132	0.2514

Figure 6.19a: F1B: e=1.5c & d=2c

	b/c									
	0.3641	0.3480	0.3247	0.3168	0.3065	0.2866	0.2832	0.2842	0.2803	0.3028
	0.3497	0.3389	0.3189	0.3129	0.3038	0.2847	0.2818	0.2831	0.2794	0.3020
	0.3201	0.3215	0.3081	0.3061	0.2993	0.2815	0.2795	0.2814	0.2780	0.3009
	0.2651	0.2901	0.2894	0.2945	0.2918	0.2764	0.2759	0.2786	0.2759	0.2992
a/c	0.1804	0.2411	0.2606	0.2771	0.2809	0.2691	0.2709	0.2750	0.2731	0.2970
	0.0802	0.1758	0.2222	0.2537	0.2667	0.2599	0.2647	0.2706	0.2699	0.2946
	0.0043	0.0826	0.1610	0.2150	0.2433	0.2451	0.2550	0.2639	0.2651	0.2909
	0.0003	0.0202	0.0869	0.1573	0.2080	0.2231	0.2411	0.2546	0.2594	0.2861
	−0.0002	0.0004	0.0338	0.0948	0.1587	0.1925	0.2215	0.2418	0.2510	0.2800
	0.0006	0.0004	0.0024	0.0429	0.1000	0.1490	0.1890	0.2197	0.2392	0.2699

Figure 6.19a: F1B: e=1.5c & d=2.5c

	b/c									
	0.3868	0.3751	0.3567	0.3530	0.3459	0.3272	0.3213	0.3167	0.3075	0.3207
	0.3719	0.3658	0.3506	0.3490	0.3430	0.3252	0.3198	0.3156	0.3066	0.3200
	0.3413	0.3476	0.3393	0.3417	0.3382	0.3218	0.3174	0.3138	0.3052	0.3190
	0.2845	0.3151	0.3198	0.3296	0.3303	0.3164	0.3136	0.3111	0.3031	0.3173
a/c	0.1967	0.2642	0.2897	0.3113	0.3188	0.3087	0.3084	0.3073	0.3003	0.3152
	0.0919	0.1958	0.2490	0.2866	0.3037	0.2990	0.3019	0.3028	0.2971	0.3128
	0.0066	0.0976	0.1846	0.2459	0.2790	0.2832	0.2917	0.2959	0.2921	0.3092
	0.0009	0.0258	0.1027	0.1849	0.2415	0.2598	0.2771	0.2863	0.2857	0.3044
	0.0002	0.0004	0.0420	0.1133	0.1881	0.2265	0.2560	0.2729	0.2771	0.2983
	0.0006	0.0003	0.0049	0.0523	0.1178	0.1742	0.2203	0.2499	0.2640	0.2882

Figure 6.19a: F1B: e=1.5c & d=3c

	b/c									
	0.4026	0.3938	0.3784	0.3779	0.3735	0.3571	0.3521	0.3465	0.3348	0.3421
	0.3874	0.3842	0.3722	0.3737	0.3706	0.3550	0.3506	0.3454	0.3339	0.3415
	0.3561	0.3656	0.3606	0.3662	0.3656	0.3516	0.3481	0.3435	0.3325	0.3404
	0.2980	0.3323	0.3406	0.3537	0.3575	0.3460	0.3442	0.3407	0.3303	0.3387
a/c	0.2079	0.2800	0.3096	0.3349	0.3455	0.3380	0.3387	0.3368	0.3275	0.3366
	0.0997	0.2095	0.2673	0.3093	0.3299	0.3278	0.3320	0.3322	0.3242	0.3342
	0.0083	0.1078	0.2008	0.2672	0.3042	0.3114	0.3214	0.3250	0.3191	0.3305
	0.0009	0.0297	0.1139	0.2039	0.2653	0.2871	0.3061	0.3150	0.3122	0.3258
	−0.0002	0.0008	0.0479	0.1268	0.2094	0.2519	0.2842	0.3011	0.3031	0.3195
	0.0006	0.0005	0.0069	0.0595	0.1315	0.1949	0.2463	0.2771	0.2894	0.3093

Figure 6.19a: F1B: e=1.5c & d=3.5c

	b/c									
	0.4140	0.4071	0.3938	0.3954	0.3932	0.3788	0.3752	0.3703	0.3584	0.3636
	0.3986	0.3973	0.3874	0.3911	0.3902	0.3766	0.3737	0.3692	0.3575	0.3629
	0.3667	0.3784	0.3757	0.3835	0.3851	0.3731	0.3711	0.3673	0.3561	0.3618
	0.3076	0.3445	0.3552	0.3707	0.3767	0.3673	0.3671	0.3643	0.3539	0.3602
a/c	0.2159	0.2912	0.3237	0.3515	0.3645	0.3591	0.3615	0.3603	0.3510	0.3580
	0.1052	0.2192	0.2802	0.3253	0.3485	0.3487	0.3546	0.3556	0.3476	0.3555
	0.0095	0.1149	0.2122	0.2822	0.3222	0.3319	0.3437	0.3482	0.3424	0.3518
	0.0009	0.0325	0.1218	0.2174	0.2823	0.3069	0.3280	0.3380	0.3353	0.3469
	0.0004	0.0015	0.0522	0.1365	0.2247	0.2703	0.3054	0.3236	0.3258	0.3406
	0.0006	0.0002	0.0084	0.0649	0.1418	0.2100	0.2662	0.2990	0.3114	0.3301

Figure 6.19a: F1B: e=1.5c & d=4c

	b/c									
	0.4225	0.4169	0.4050	0.4081	0.4075	0.3946	0.3924	0.3885	0.3773	0.3822
	0.4069	0.4070	0.3986	0.4037	0.4044	0.3924	0.3908	0.3873	0.3764	0.3814
	0.3747	0.3879	0.3867	0.3960	0.3993	0.3888	0.3882	0.3854	0.3749	0.3803
	0.3148	0.3535	0.3659	0.3830	0.3908	0.3829	0.3841	0.3824	0.3727	0.3786
a/c	0.2217	0.2995	0.3340	0.3635	0.3784	0.3746	0.3784	0.3783	0.3697	0.3764
	0.1092	0.2262	0.2896	0.3370	0.3621	0.3640	0.3714	0.3735	0.3662	0.3739
	0.0104	0.1200	0.2204	0.2931	0.3353	0.3469	0.3602	0.3660	0.3609	0.3701
	0.0009	0.0346	0.1277	0.2271	0.2946	0.3214	0.3442	0.3555	0.3537	0.3652
	0.0004	0.0019	0.0553	0.1436	0.2359	0.2841	0.3212	0.3408	0.3440	0.3587
	0.0003	0.0003	0.0096	0.0688	0.1494	0.2219	0.2810	0.3158	0.3290	0.3480

Figure I.8a: F1B: e=2c & d=0.5c

	b/c									
a/c	0.1730	0.1278	0.1032	0.1142	0.1321	0.1056	0.1269	0.1447	0.1637	0.2370
	0.1674	0.1244	0.1008	0.1123	0.1306	0.1046	0.1261	0.1438	0.1602	0.2362
	0.1565	0.1180	0.0966	0.1089	0.1280	0.1039	0.1246	0.1425	0.1600	0.2350
	0.1367	0.1065	0.0891	0.1031	0.1235	0.1002	0.1223	0.1404	0.1614	0.2335
	0.1060	0.0892	0.0782	0.0948	0.1173	0.0966	0.1187	0.1374	0.1596	0.2303
	0.0675	0.0674	0.0648	0.0845	0.1097	0.0935	0.1163	0.1341	0.1570	0.2273
	0.0166	0.0362	0.0484	0.0706	0.0987	0.0882	0.1123	0.1288	0.1544	0.2232
	0.0005	0.0132	0.0344	0.0552	0.0847	0.0815	0.1069	0.1247	0.1501	0.2184
	0.0008	0.0054	0.0240	0.0433	0.0678	0.0742	0.1010	0.1184	0.1463	0.2129
	0.0013	0.0020	0.0151	0.0308	0.0502	0.0649	0.0926	0.1100	0.1401	0.2046

Figure I.8a: F1B: e=2c & d=1c

	b/c									
a/c	0.2757	0.2392	0.2005	0.1933	0.1972	0.1852	0.1977	0.2118	0.2117	0.2635
	0.2684	0.2344	0.1972	0.1909	0.1954	0.1837	0.1965	0.2108	0.2109	0.2628
	0.2543	0.2252	0.1913	0.1867	0.1922	0.1813	0.1945	0.2091	0.2097	0.2616
	0.2287	0.2092	0.1814	0.1796	0.1870	0.1772	0.1913	0.2065	0.2077	0.2597
	0.1892	0.1849	0.1666	0.1694	0.1795	0.1716	0.1869	0.2029	0.2052	0.2571
	0.1389	0.1537	0.1478	0.1566	0.1705	0.1648	0.1817	0.1989	0.2023	0.2543
	0.0703	0.1089	0.1203	0.1378	0.1573	0.1551	0.1744	0.1931	0.1984	0.2504
	0.0055	0.0536	0.0842	0.1129	0.1399	0.1424	0.1649	0.1859	0.1935	0.2457
	0.0007	0.0158	0.0491	0.0824	0.1180	0.1281	0.1532	0.1769	0.1882	0.2401
	0.0013	0.0013	0.0223	0.0545	0.0870	0.1074	0.1358	0.1633	0.1812	0.2317

Figure I.8a: F1B: e=2c & d=1.5c

	b/c									
a/c	0.3314	0.3072	0.2764	0.2636	0.2537	0.2383	0.2439	0.2527	0.2509	0.2849
	0.3234	0.3017	0.2725	0.2609	0.2516	0.2367	0.2426	0.2517	0.2500	0.2842
	0.3079	0.2913	0.2654	0.2560	0.2481	0.2341	0.2405	0.2500	0.2486	0.2830
	0.2800	0.2731	0.2533	0.2478	0.2423	0.2298	0.2372	0.2473	0.2463	0.2811
	0.2367	0.2454	0.2354	0.2358	0.2341	0.2237	0.2326	0.2436	0.2434	0.2787
	0.1812	0.2098	0.2128	0.2209	0.2240	0.2165	0.2272	0.2394	0.2401	0.2759
	0.1052	0.1586	0.1802	0.1988	0.2092	0.2060	0.2194	0.2335	0.2360	0.2721
	0.0230	0.0947	0.1370	0.1693	0.1895	0.1921	0.2094	0.2259	0.2309	0.2674
	0.0001	0.0355	0.0865	0.1322	0.1642	0.1744	0.1967	0.2165	0.2244	0.2619
	0.0019	0.0042	0.0389	0.0824	0.1252	0.1483	0.1772	0.2020	0.2152	0.2535

Figure I.8a: F1B: e=2c & d=2c

	b/c									
a/c	0.3657	0.3488	0.3252	0.3171	0.3067	0.2867	0.2832	0.2842	0.2803	0.3027
	0.3574	0.3430	0.3210	0.3140	0.3044	0.2850	0.2819	0.2831	0.2794	0.3020
	0.3411	0.3319	0.3134	0.3086	0.3005	0.2821	0.2797	0.2814	0.2780	0.3009
	0.3118	0.3125	0.3003	0.2996	0.2942	0.2775	0.2762	0.2787	0.2758	0.2990
	0.2664	0.2832	0.2809	0.2865	0.2851	0.2710	0.2715	0.2750	0.2728	0.2966
	0.2078	0.2452	0.2560	0.2701	0.2740	0.2632	0.2658	0.2708	0.2695	0.2940
	0.1273	0.1904	0.2203	0.2459	0.2577	0.2518	0.2577	0.2647	0.2648	0.2902
	0.0383	0.1219	0.1733	0.2134	0.2360	0.2368	0.2472	0.2569	0.2589	0.2856
	0.0010	0.0524	0.1177	0.1722	0.2078	0.2174	0.2337	0.2472	0.2522	0.2801
	0.0012	0.0093	0.0555	0.1114	0.1642	0.1877	0.2127	0.2323	0.2425	0.2717

Figure I.8a: F1B: e=2c & d=2.5c

	b/c									
a/c	0.3884	0.3760	0.3572	0.3533	0.3460	0.3273	0.3213	0.3167	0.3075	0.3207
	0.3799	0.3700	0.3528	0.3501	0.3437	0.3255	0.3199	0.3156	0.3066	0.3200
	0.3631	0.3585	0.3448	0.3444	0.3395	0.3224	0.3176	0.3139	0.3052	0.3189
	0.3329	0.3384	0.3311	0.3350	0.3328	0.3175	0.3140	0.3110	0.3030	0.3171
	0.2861	0.3080	0.3109	0.3212	0.3232	0.3106	0.3089	0.3072	0.3000	0.3147
	0.2254	0.2685	0.2849	0.3039	0.3114	0.3023	0.3030	0.3028	0.2966	0.3121
	0.1420	0.2115	0.2470	0.2783	0.2941	0.2902	0.2944	0.2966	0.2918	0.3084
	0.0489	0.1399	0.1978	0.2441	0.2710	0.2742	0.2833	0.2885	0.2859	0.3038
	0.0026	0.0655	0.1386	0.2004	0.2410	0.2534	0.2689	0.2784	0.2784	0.2982
	0.0012	0.0135	0.0684	0.1352	0.1946	0.2211	0.2467	0.2628	0.2681	0.2899

Figure I.8a: F1B: e=2c & d=3c

	b/c									
a/c	0.4042	0.3947	0.3789	0.3782	0.3737	0.3572	0.3521	0.3465	0.3348	0.3421
	0.3955	0.3885	0.3744	0.3749	0.3712	0.3554	0.3507	0.3454	0.3339	0.3414
	0.3784	0.3767	0.3662	0.3690	0.3670	0.3522	0.3483	0.3435	0.3324	0.3402
	0.3476	0.3562	0.3522	0.3592	0.3600	0.3470	0.3445	0.3406	0.3301	0.3384
	0.2998	0.3250	0.3314	0.3450	0.3500	0.3399	0.3392	0.3367	0.3271	0.3361
	0.2375	0.2845	0.3046	0.3271	0.3378	0.3312	0.3330	0.3321	0.3236	0.3334
	0.1520	0.2260	0.2653	0.3007	0.3199	0.3187	0.3241	0.3256	0.3187	0.3297
	0.0560	0.1523	0.2145	0.2653	0.2959	0.3020	0.3125	0.3172	0.3126	0.3250
	0.0038	0.0746	0.1533	0.2201	0.2647	0.2803	0.2975	0.3066	0.3049	0.3194
	0.0012	0.0168	0.0779	0.1525	0.2165	0.2466	0.2742	0.2904	0.2936	0.3109

Figure I.8a: F1B: e=2c & d=3.5c

	b/c									
a/c	0.4157	0.4080	0.3943	0.3957	0.3934	0.3789	0.3753	0.3704	0.3584	0.3636
	0.4068	0.4017	0.3897	0.3923	0.3908	0.3769	0.3738	0.3692	0.3575	0.3629
	0.3895	0.3898	0.3814	0.3863	0.3865	0.3737	0.3713	0.3673	0.3560	0.3617
	0.3582	0.3689	0.3671	0.3763	0.3793	0.3684	0.3674	0.3643	0.3537	0.3599
	0.3096	0.3372	0.3459	0.3618	0.3691	0.3611	0.3620	0.3602	0.3506	0.3574
	0.2463	0.2959	0.3186	0.3436	0.3566	0.3522	0.3556	0.3555	0.3470	0.3547
	0.1591	0.2362	0.2785	0.3166	0.3382	0.3393	0.3464	0.3488	0.3420	0.3509
	0.0611	0.1610	0.2264	0.2804	0.3136	0.3222	0.3344	0.3402	0.3356	0.3462
	0.0048	0.0811	0.1636	0.2340	0.2816	0.2999	0.3190	0.3293	0.3277	0.3404
	0.0012	0.0192	0.0848	0.1648	0.2322	0.2652	0.2951	0.3125	0.3157	0.3317

Figure I.8a: F1B: e=2c & d=4c

	b/c									
a/c	0.4242	0.4178	0.4056	0.4084	0.4076	0.3947	0.3924	0.3886	0.3773	0.3822
	0.4153	0.4114	0.4009	0.4050	0.4051	0.3927	0.3909	0.3874	0.3764	0.3814
	0.3977	0.3994	0.3924	0.3989	0.4006	0.3894	0.3884	0.3854	0.3748	0.3802
	0.3661	0.3783	0.3780	0.3888	0.3934	0.3840	0.3844	0.3824	0.3724	0.3783
	0.3169	0.3462	0.3565	0.3741	0.3830	0.3766	0.3789	0.3782	0.3693	0.3758
	0.2527	0.3043	0.3288	0.3555	0.3703	0.3675	0.3724	0.3734	0.3656	0.3731
	0.1643	0.2438	0.2881	0.3281	0.3516	0.3544	0.3630	0.3665	0.3605	0.3692
	0.0647	0.1674	0.2351	0.2913	0.3266	0.3369	0.3508	0.3578	0.3540	0.3644
	0.0055	0.0859	0.1712	0.2441	0.2940	0.3142	0.3350	0.3466	0.3459	0.3584
	0.0012	0.0209	0.0898	0.1737	0.2436	0.2789	0.3106	0.3295	0.3336	0.3496

Figure 6.20a: F1B: e=2.5c & d=0.5c

	b/c									
	0.1735	0.1281	0.1034	0.1143	0.1322	0.1057	0.1270	0.1447	0.1637	0.2370
	0.1700	0.1259	0.1017	0.1129	0.1310	0.1048	0.1262	0.1440	0.1603	0.2363
	0.1633	0.1216	0.0987	0.1104	0.1290	0.1044	0.1250	0.1428	0.1594	0.2351
	0.1515	0.1142	0.0935	0.1062	0.1256	0.1021	0.1230	0.1409	0.1626	0.2333
a/c	0.1333	0.1032	0.0859	0.1000	0.1207	0.0990	0.1201	0.1384	0.1570	0.2308
	0.1100	0.0891	0.0765	0.0925	0.1148	0.0944	0.1169	0.1353	0.1552	0.2281
	0.0766	0.0689	0.0632	0.0818	0.1065	0.0906	0.1132	0.1312	0.1540	0.2242
	0.0359	0.0438	0.0486	0.0691	0.0962	0.0849	0.1091	0.1257	0.1502	0.2197
	0.0018	0.0181	0.0344	0.0554	0.0842	0.0787	0.1035	0.1206	0.1477	0.2146
	0.0009	0.0066	0.0237	0.0425	0.0670	0.0708	0.0968	0.1141	0.1422	0.2069

Figure 6.20a: F1B: e=2.5c & d=1c

	b/c									
	0.2763	0.2396	0.2007	0.1934	0.1973	0.1853	0.1978	0.2118	0.2118	0.2636
	0.2717	0.2363	0.1984	0.1916	0.1959	0.1841	0.1967	0.2109	0.2110	0.2629
	0.2629	0.2302	0.1941	0.1884	0.1933	0.1820	0.1950	0.2095	0.2099	0.2617
	0.2474	0.2196	0.1870	0.1831	0.1892	0.1786	0.1922	0.2071	0.2080	0.2599
a/c	0.2238	0.2038	0.1766	0.1754	0.1832	0.1739	0.1884	0.2039	0.2056	0.2574
	0.1933	0.1837	0.1636	0.1659	0.1761	0.1683	0.1839	0.2002	0.2027	0.2547
	0.1498	0.1547	0.1449	0.1524	0.1659	0.1604	0.1776	0.1950	0.1989	0.2510
	0.0962	0.1183	0.1212	0.1353	0.1532	0.1506	0.1699	0.1888	0.1943	0.2465
	0.0405	0.0775	0.0936	0.1150	0.1381	0.1390	0.1608	0.1815	0.1890	0.2414
	0.0005	0.0259	0.0561	0.0858	0.1163	0.1234	0.1477	0.1710	0.1826	0.2345

Figure 6.20a: F1B: e=2.5c & d=1.5c

	b/c									
	0.3321	0.3077	0.2767	0.2638	0.2538	0.2384	0.2439	0.2527	0.2509	0.2849
	0.3270	0.3039	0.2739	0.2617	0.2522	0.2371	0.2428	0.2518	0.2501	0.2842
	0.3173	0.2969	0.2687	0.2579	0.2493	0.2348	0.2410	0.2503	0.2488	0.2831
	0.3004	0.2848	0.2601	0.2516	0.2446	0.2312	0.2380	0.2478	0.2467	0.2813
a/c	0.2745	0.2667	0.2474	0.2426	0.2380	0.2261	0.2340	0.2444	0.2438	0.2789
	0.2410	0.2437	0.2314	0.2314	0.2299	0.2200	0.2292	0.2406	0.2406	0.2762
	0.1931	0.2106	0.2089	0.2155	0.2185	0.2114	0.2225	0.2352	0.2364	0.2725
	0.1341	0.1689	0.1806	0.1952	0.2041	0.2007	0.2143	0.2287	0.2316	0.2681
	0.0718	0.1217	0.1473	0.1710	0.1868	0.1879	0.2045	0.2209	0.2260	0.2630
	0.0052	0.0580	0.1001	0.1360	0.1617	0.1692	0.1903	0.2099	0.2183	0.2558

Figure 6.20a: F1B: e=2.5c & d=2c

	b/c									
	0.3665	0.3493	0.3255	0.3173	0.3068	0.2868	0.2833	0.2842	0.2803	0.3028
	0.3611	0.3453	0.3225	0.3149	0.305	0.2853	0.2821	0.2833	0.2795	0.3021
	0.351	0.3378	0.3169	0.3108	0.3018	0.2829	0.2802	0.2817	0.2782	0.3009
	0.3332	0.325	0.3075	0.3038	0.2966	0.2789	0.2771	0.2792	0.2761	0.2992
a/c	0.3061	0.3058	0.2938	0.2939	0.2893	0.2734	0.2728	0.2757	0.2732	0.2968
	0.2709	0.2812	0.2764	0.2815	0.2804	0.2668	0.2678	0.2718	0.27	0.2941
	0.2206	0.246	0.2517	0.264	0.2677	0.2575	0.2607	0.2663	0.2656	0.2904
	0.1583	0.2015	0.2205	0.2417	0.2518	0.2458	0.252	0.2595	0.2602	0.2861
	0.09212	0.1507	0.1842	0.2148	0.2326	0.2318	0.2416	0.2516	0.2539	0.281
	0.01387	0.08251	0.1328	0.1761	0.2046	0.2114	0.2266	0.2402	0.2457	0.2738

Figure 6.20a: F1B: e=2.5c & d=2.5c

	b/c									
	0.3892	0.3765	0.3575	0.3535	0.3462	0.3274	0.3214	0.3168	0.3075	0.3208
	0.3837	0.3724	0.3543	0.3511	0.3442	0.3258	0.3202	0.3158	0.3067	0.3201
	0.3733	0.3646	0.3485	0.3466	0.3409	0.3232	0.3181	0.3141	0.3053	0.3189
	0.355	0.3513	0.3387	0.3393	0.3353	0.319	0.3148	0.3113	0.3032	0.3172
a/c	0.3271	0.3314	0.3243	0.3288	0.3275	0.3131	0.3103	0.3079	0.3003	0.3148
	0.2908	0.3059	0.3062	0.3158	0.318	0.306	0.3049	0.3038	0.297	0.3121
	0.2389	0.2694	0.2803	0.2973	0.3046	0.2961	0.2975	0.2981	0.2925	0.3085
	0.1745	0.2232	0.2473	0.2737	0.2877	0.2837	0.2883	0.2911	0.2871	0.3041
	0.1057	0.1702	0.209	0.2453	0.2671	0.2686	0.2772	0.2828	0.2806	0.2991
	0.02196	0.09913	0.1553	0.2045	0.2374	0.2468	0.2612	0.2708	0.2715	0.2919

Figure 6.20a: F1B: e=2.5c & d=3c

	b/c									
	0.4051	0.3952	0.3793	0.3784	0.3738	0.3573	0.3522	0.3466	0.3348	0.3422
	0.3995	0.3909	0.376	0.3758	0.3718	0.3557	0.3509	0.3455	0.3339	0.3415
	0.3888	0.383	0.37	0.3713	0.3683	0.353	0.3488	0.3438	0.3325	0.3403
	0.3702	0.3694	0.3599	0.3637	0.3626	0.3486	0.3453	0.3411	0.3303	0.3385
a/c	0.3417	0.349	0.3451	0.3528	0.3545	0.3424	0.3406	0.3374	0.3274	0.3361
	0.3046	0.3229	0.3265	0.3394	0.3446	0.335	0.335	0.3331	0.324	0.3334
	0.2516	0.2855	0.2999	0.3203	0.3307	0.3247	0.3272	0.3271	0.3194	0.3297
	0.1857	0.2381	0.2659	0.296	0.3131	0.3117	0.3176	0.3198	0.3137	0.3253
	0.115	0.1836	0.2262	0.2665	0.2918	0.296	0.306	0.3111	0.3071	0.3202
	0.02825	0.1106	0.1708	0.2243	0.2609	0.2733	0.2893	0.2987	0.2976	0.3129

Figure 6.20a: F1B: e=2.5c & d=3.5c

	b/c									
	0.4165	0.4085	0.3947	0.3959	0.3935	0.3790	0.3753	0.3704	0.3585	0.3636
	0.4108	0.4042	0.3913	0.3933	0.3914	0.3773	0.3740	0.3693	0.3576	0.3629
	0.4000	0.3961	0.3852	0.3886	0.3878	0.3745	0.3718	0.3675	0.3561	0.3617
	0.3811	0.3823	0.3750	0.3809	0.3820	0.3700	0.3682	0.3647	0.3539	0.3599
a/c	0.3523	0.3616	0.3599	0.3698	0.3737	0.3636	0.3634	0.3609	0.3508	0.3575
	0.3146	0.3351	0.3410	0.3561	0.3636	0.3561	0.3576	0.3565	0.3474	0.3547
	0.2607	0.2970	0.3138	0.3366	0.3493	0.3454	0.3496	0.3503	0.3426	0.3509
	0.1938	0.2488	0.2792	0.3117	0.3313	0.3321	0.3397	0.3428	0.3368	0.3464
	0.1216	0.1931	0.2384	0.2816	0.3094	0.3160	0.3278	0.3339	0.3299	0.3411
	0.0329	0.1187	0.1818	0.2384	0.2777	0.2926	0.3105	0.3210	0.3201	0.3336

Figure 6.20a: F1B: e=2.5c & d=4c

	b/c									
	0.425	0.4184	0.4059	0.4086	0.4078	0.3948	0.3925	0.3886	0.3773	0.3822
	0.4193	0.414	0.4025	0.406	0.4057	0.3931	0.3912	0.3875	0.3764	0.3814
	0.4084	0.4058	0.3963	0.4012	0.402	0.3902	0.3889	0.3857	0.375	0.3802
	0.3893	0.3918	0.386	0.3934	0.3961	0.3856	0.3853	0.3828	0.3727	0.3783
a/c	0.3602	0.3709	0.3707	0.3822	0.3876	0.3792	0.3803	0.3789	0.3695	0.3758
	0.322	0.344	0.3515	0.3682	0.3773	0.3714	0.3744	0.3744	0.366	0.373
	0.2675	0.3055	0.324	0.3484	0.3629	0.3606	0.3662	0.3681	0.3611	0.3692
	0.1997	0.2566	0.2889	0.3232	0.3445	0.3471	0.3561	0.3604	0.3552	0.3646
	0.1264	0.2001	0.2473	0.2926	0.3222	0.3306	0.3439	0.3512	0.3481	0.3592
	0.0363	0.1246	0.1899	0.2487	0.2901	0.3068	0.3264	0.3381	0.3381	0.3515

Figure I.9a: F1B: e=3c & d=0.5c

	b/c									
a/c	0.1738	0.1283	0.1035	0.1144	0.1323	0.1057	0.127	0.1447	0.1637	0.237
	0.1714	0.1267	0.1023	0.1134	0.1314	0.105	0.1264	0.1441	0.1604	0.2364
	0.167	0.1238	0.1001	0.1115	0.1298	0.1049	0.1254	0.1431	0.1596	0.2354
	0.1593	0.1187	0.0964	0.1083	0.1295	0.103	0.1237	0.1415	0.1589	0.2337
	0.1477	0.1112	0.09099	0.1038	0.1233	0.09951	0.1211	0.1393	0.1602	0.2315
	0.1328	0.1018	0.08425	0.09814	0.1188	0.09643	0.1174	0.1367	0.1555	0.229
	0.1112	0.08818	0.07472	0.09022	0.1124	0.09279	0.1149	0.1331	0.153	0.2255
	0.08406	0.07107	0.06271	0.08037	0.1045	0.08846	0.1113	0.1288	0.1522	0.2214
	0.05345	0.0515	0.0504	0.06905	0.09535	0.08303	0.1065	0.1227	0.1489	0.2168
	0.01264	0.02468	0.03575	0.05564	0.0827	0.07607	0.1005	0.118	0.1442	0.2105

Figure I.9a: F1B: e=3c & d=1c

	b/c									
a/c	0.2767	0.2399	0.2009	0.1935	0.1974	0.1853	0.1978	0.2118	0.2118	0.2636
	0.2736	0.2375	0.1992	0.1922	0.1963	0.1844	0.197	0.2111	0.2112	0.263
	0.2676	0.2332	0.196	0.1897	0.1942	0.1827	0.1955	0.2098	0.2101	0.2619
	0.2574	0.2259	0.1908	0.1857	0.1909	0.1799	0.1931	0.2078	0.2084	0.2602
	0.2421	0.215	0.1832	0.1798	0.1862	0.176	0.1899	0.205	0.2062	0.258
	0.2224	0.2012	0.1738	0.1726	0.1806	0.1714	0.186	0.2017	0.2036	0.2555
	0.1941	0.1815	0.1605	0.1625	0.1726	0.165	0.1807	0.1972	0.2	0.252
	0.1584	0.1567	0.1437	0.1499	0.1628	0.1571	0.1743	0.1918	0.1959	0.2479
	0.1177	0.1279	0.1241	0.1351	0.1513	0.148	0.1668	0.1856	0.1911	0.2432
	0.06307	0.08836	0.09677	0.1145	0.1354	0.1353	0.1565	0.177	0.1847	0.2273

Figure I.9a: F1B: e=3c & d=1.5c

	b/c									
a/c	0.3325	0.308	0.2769	0.2639	0.2539	0.2384	0.244	0.2528	0.2509	0.285
	0.329	0.3052	0.2748	0.2623	0.2526	0.2374	0.2431	0.252	0.2502	0.2843
	0.3225	0.3002	0.271	0.2594	0.2503	0.2355	0.2415	0.2506	0.249	0.2833
	0.3112	0.2918	0.2646	0.2545	0.2465	0.2325	0.239	0.2484	0.2471	0.2816
	0.2944	0.2793	0.2553	0.2476	0.2412	0.2282	0.2354	0.2455	0.2446	0.2794
	0.2727	0.2635	0.2438	0.2391	0.2347	0.2231	0.2313	0.242	0.2416	0.2768
	0.2417	0.2409	0.2274	0.2271	0.2257	0.2161	0.2256	0.2373	0.2376	0.2733
	0.2024	0.2124	0.207	0.212	0.2146	0.2075	0.2187	0.2316	0.2331	0.2692
	0.1573	0.1792	0.1834	0.1944	0.2015	0.1973	0.2106	0.225	0.228	0.2646
	0.09715	0.1338	0.1506	0.1698	0.1832	0.1833	0.1995	0.2159	0.2213	0.2583

Figure I.9a: F1B: e=3c & d=2c

	b/c									
a/c	0.3669	0.3496	0.3257	0.3174	0.3069	0.2868	0.2833	0.2843	0.2803	0.3028
	0.3632	0.3467	0.3234	0.3156	0.3054	0.2857	0.2823	0.2834	0.2796	0.3022
	0.3564	0.3414	0.3193	0.3123	0.3029	0.2836	0.2807	0.282	0.2784	0.3011
	0.3446	0.3324	0.3123	0.307	0.2987	0.2803	0.278	0.2798	0.2765	0.2994
	0.3269	0.319	0.3023	0.2993	0.2927	0.2756	0.2743	0.2767	0.2739	0.2972
	0.3042	0.3022	0.2897	0.2898	0.2856	0.2701	0.2699	0.2732	0.2709	0.2947
	0.2716	0.2782	0.2719	0.2765	0.2756	0.2624	0.2638	0.2683	0.2668	0.2912
	0.2303	0.2478	0.2494	0.2599	0.2631	0.253	0.2565	0.2624	0.262	0.2871
	0.1828	0.2123	0.2232	0.2404	0.2485	0.2419	0.2479	0.2555	0.2564	0.2825
	0.1195	0.1638	0.1876	0.2131	0.2282	0.2265	0.2361	0.2462	0.2488	0.2762

Figure I.9a: F1B: e=3c & d=2.5c

	b/c									
a/c	0.3897	0.3769	0.3577	0.3537	0.3463	0.3274	0.3214	0.3168	0.3075	0.3208
	0.3859	0.3738	0.3553	0.3517	0.3447	0.3262	0.3204	0.3159	0.3068	0.3201
	0.3788	0.3683	0.3509	0.3483	0.342	0.324	0.3186	0.3145	0.3055	0.3191
	0.3667	0.3589	0.3437	0.3426	0.3375	0.3204	0.3157	0.3121	0.3036	0.3174
	0.3485	0.3452	0.3331	0.3345	0.3312	0.3154	0.3118	0.3089	0.3009	0.3151
	0.3251	0.3277	0.32	0.3245	0.3235	0.3095	0.3071	0.3052	0.2979	0.3126
	0.2916	0.3027	0.3013	0.3105	0.3128	0.3013	0.3007	0.3001	0.2937	0.3092
	0.249	0.2712	0.2779	0.2929	0.2996	0.2911	0.2929	0.2939	0.2888	0.3051
	0.1999	0.2343	0.2502	0.2722	0.284	0.2793	0.2838	0.2868	0.283	0.3005
	0.1346	0.184	0.2126	0.2434	0.2623	0.2628	0.2711	0.2769	0.2752	0.2941

Figure I.9a: F1B: e=3c & d=3c

	b/c									
a/c	0.4055	0.3955	0.3795	0.3785	0.374	0.3574	0.3523	0.3466	0.3348	0.3422
	0.4017	0.3924	0.377	0.3765	0.3723	0.3561	0.3512	0.3457	0.334	0.3415
	0.3944	0.3868	0.3725	0.373	0.3695	0.3538	0.3493	0.3442	0.3328	0.3405
	0.3821	0.3772	0.3651	0.3671	0.3648	0.35	0.3463	0.3417	0.3307	0.3388
	0.3636	0.3631	0.3542	0.3587	0.3582	0.3448	0.3421	0.3384	0.328	0.3365
	0.3397	0.3452	0.3407	0.3484	0.3503	0.3386	0.3373	0.3345	0.3249	0.3339
	0.3055	0.3197	0.3215	0.3339	0.3392	0.33	0.3305	0.3291	0.3205	0.3304
	0.262	0.2874	0.2974	0.3157	0.3254	0.3195	0.3223	0.3227	0.3154	0.3262
	0.2118	0.2496	0.2689	0.2943	0.3092	0.3071	0.3128	0.3152	0.3095	0.3215
	0.1451	0.198	0.2299	0.2645	0.2867	0.2899	0.2996	0.305	0.3014	0.315

Figure I.9a: F1B: e=3c & d=3.5c

	b/c									
a/c	0.4170	0.4089	0.3949	0.3961	0.3936	0.3790	0.3754	0.3704	0.3585	0.3637
	0.4130	0.4057	0.3924	0.3940	0.3919	0.3777	0.3743	0.3695	0.3577	0.3630
	0.4057	0.4000	0.3878	0.3904	0.3890	0.3753	0.3723	0.3679	0.3564	0.3619
	0.3932	0.3903	0.3802	0.3844	0.3842	0.3715	0.3692	0.3654	0.3543	0.3602
	0.3745	0.3759	0.3692	0.3758	0.3775	0.3661	0.3649	0.3619	0.3515	0.3578
	0.3503	0.3577	0.3554	0.3652	0.3693	0.3597	0.3599	0.3579	0.3482	0.3552
	0.3156	0.3318	0.3359	0.3504	0.3580	0.3509	0.3530	0.3524	0.3438	0.3516
	0.2715	0.2990	0.3113	0.3319	0.3439	0.3400	0.3445	0.3457	0.3385	0.3473
	0.2204	0.2605	0.2822	0.3100	0.3272	0.3273	0.3347	0.3380	0.3324	0.3424
	0.1526	0.2080	0.2423	0.2796	0.3042	0.3096	0.3210	0.3274	0.3240	0.3358

Figure I.9a: F1B: e=3c & d=4c

	b/c									
a/c	0.4255	0.4187	0.4062	0.4088	0.4079	0.3949	0.3926	0.3886	0.3774	0.3822
	0.4215	0.4155	0.4036	0.4067	0.4062	0.3935	0.3914	0.3877	0.3765	0.3815
	0.4142	0.4097	0.399	0.403	0.4032	0.391	0.3894	0.386	0.3752	0.3804
	0.4015	0.3999	0.3913	0.3969	0.3984	0.3871	0.3863	0.3835	0.3731	0.3786
	0.3826	0.3854	0.3801	0.3882	0.3915	0.3817	0.3819	0.3799	0.3702	0.3762
	0.3581	0.367	0.3661	0.3775	0.3832	0.3752	0.3767	0.3758	0.3668	0.3735
	0.323	0.3408	0.3463	0.3625	0.3716	0.3662	0.3696	0.3702	0.3623	0.3698
	0.2785	0.3076	0.3214	0.3437	0.3573	0.3551	0.361	0.3634	0.3569	0.3654
	0.2268	0.2685	0.2919	0.3214	0.3404	0.3421	0.351	0.3555	0.3506	0.3605
	0.1581	0.2154	0.2513	0.2906	0.3169	0.324	0.337	0.3446	0.342	0.3537

Figure 6.21a: F1B: e=3.5c & d=0.5c

	b/c									
a/c	0.1740	0.1284	0.1036	0.1145	0.1324	0.1057	0.1270	0.1448	0.1638	0.2370
	0.1723	0.1273	0.1027	0.1137	0.1316	0.1052	0.1265	0.1443	0.1633	0.2365
	0.1692	0.1251	0.1010	0.1122	0.1304	0.1043	0.1257	0.1434	0.1597	0.2356
	0.1639	0.1215	0.0983	0.1098	0.1283	0.1037	0.1243	0.1420	0.1586	0.2342
	0.1559	0.1162	0.0943	0.1064	0.1253	0.1016	0.1223	0.1402	0.1581	0.2322
	0.1458	0.1096	0.0894	0.1021	0.1217	0.0982	0.1194	0.1379	0.1589	0.2299
	0.1313	0.1000	0.0824	0.0961	0.1167	0.0948	0.1167	0.1349	0.1538	0.2268
	0.1129	0.0881	0.0737	0.0887	0.1106	0.0914	0.1132	0.1312	0.1539	0.2232
	0.0914	0.0740	0.0636	0.0801	0.1035	0.0871	0.1097	0.1270	0.1506	0.2191
	0.0618	0.0548	0.0510	0.0684	0.0938	0.0812	0.1044	0.1206	0.1463	0.2135

Figure 6.21a: F1B: e=3.5c & d=1c

	b/c									
a/c	0.277	0.2401	0.201	0.1936	0.1975	0.1854	0.1979	0.2119	0.2118	0.2636
	0.2747	0.2383	0.1997	0.1926	0.1966	0.1846	0.1971	0.2112	0.2113	0.263
	0.2705	0.2351	0.1973	0.1906	0.1949	0.1832	0.1959	0.2101	0.2103	0.2621
	0.2633	0.2298	0.1933	0.1875	0.1923	0.181	0.1939	0.2084	0.2089	0.2606
	0.2527	0.2219	0.1877	0.183	0.1886	0.1778	0.1912	0.206	0.2069	0.2586
	0.2392	0.2121	0.1807	0.1774	0.184	0.174	0.1879	0.2031	0.2045	0.2563
	0.22	0.1982	0.1709	0.1697	0.1777	0.1688	0.1835	0.1993	0.2014	0.2532
	0.1955	0.1806	0.1585	0.1601	0.17	0.1624	0.1781	0.1946	0.1976	0.2495
	0.1668	0.1599	0.1441	0.1489	0.161	0.155	0.1719	0.1893	0.1934	0.2453
	0.1276	0.1316	0.1242	0.1335	0.1487	0.1449	0.1635	0.1821	0.1878	0.2397

Figure 6.21a: F1B: e=3.5c & d=1.5c

	b/c									
a/c	0.3328	0.3082	0.277	0.264	0.254	0.2385	0.244	0.2528	0.2509	0.285
	0.3302	0.3061	0.2754	0.2627	0.2529	0.2376	0.2433	0.2521	0.2503	0.2844
	0.3256	0.3024	0.2725	0.2604	0.251	0.2361	0.2419	0.2509	0.2493	0.2835
	0.3176	0.2962	0.2676	0.2566	0.248	0.2336	0.2398	0.2491	0.2476	0.282
	0.3059	0.2872	0.2607	0.2512	0.2437	0.23	0.2368	0.2465	0.2453	0.2799
	0.2911	0.2758	0.252	0.2446	0.2385	0.2258	0.2333	0.2435	0.2427	0.2776
	0.2699	0.2597	0.2399	0.2354	0.2313	0.22	0.2284	0.2393	0.2391	0.2745
	0.2429	0.2395	0.2246	0.2239	0.2225	0.213	0.2226	0.2344	0.2348	0.2707
	0.2113	0.2156	0.207	0.2104	0.2122	0.2047	0.2158	0.2287	0.2303	0.2665
	0.1681	0.183	0.183	0.192	0.1981	0.1936	0.2067	0.221	0.2244	0.2609

Figure 6.21a: F1B: e=3.5c & d=2c

	b/c									
a/c	0.3672	0.3498	0.3259	0.3175	0.307	0.2869	0.2834	0.2843	0.2804	0.3028
	0.3645	0.3476	0.3241	0.3161	0.3058	0.2859	0.2825	0.2836	0.2797	0.3022
	0.3596	0.3437	0.3209	0.3135	0.3037	0.2842	0.2811	0.2824	0.2786	0.3013
	0.3512	0.337	0.3156	0.3093	0.3003	0.2814	0.2788	0.2804	0.2769	0.2998
	0.339	0.3274	0.308	0.3033	0.2955	0.2776	0.2756	0.2777	0.2746	0.2977
	0.3234	0.3153	0.2986	0.2959	0.2897	0.273	0.2719	0.2746	0.2719	0.2954
	0.3011	0.2981	0.2853	0.2856	0.2817	0.2666	0.2667	0.2703	0.2683	0.2922
	0.2728	0.2765	0.2688	0.2729	0.2718	0.2588	0.2605	0.2651	0.2639	0.2885
	0.2395	0.251	0.2492	0.2579	0.2602	0.2498	0.2533	0.2592	0.259	0.2843
	0.1942	0.2162	0.2226	0.2374	0.2445	0.2375	0.2435	0.2513	0.2523	0.2786

Figure 6.21a: F1B: e=3.5c & d=2.5c

	b/c									
a/c	0.39	0.3771	0.3579	0.3538	0.3464	0.3275	0.3215	0.3168	0.3075	0.3208
	0.3872	0.3748	0.356	0.3523	0.3451	0.3264	0.3206	0.3161	0.3069	0.3202
	0.3821	0.3707	0.3526	0.3495	0.3428	0.3246	0.3191	0.3148	0.3058	0.3193
	0.3736	0.3638	0.3471	0.345	0.3392	0.3216	0.3166	0.3127	0.304	0.3178
	0.3609	0.3538	0.3391	0.3387	0.3341	0.3175	0.3132	0.3099	0.3017	0.3157
	0.3448	0.3412	0.3292	0.3309	0.3279	0.3125	0.3092	0.3066	0.2989	0.3134
	0.3219	0.3234	0.3154	0.32	0.3193	0.3057	0.3037	0.3021	0.2952	0.3102
	0.2928	0.301	0.298	0.3065	0.3087	0.2973	0.297	0.2967	0.2907	0.3064
	0.2585	0.2745	0.2775	0.2906	0.2964	0.2876	0.2893	0.2905	0.2856	0.3022
	0.2118	0.2384	0.2496	0.269	0.2795	0.2744	0.2789	0.2822	0.2788	0.2964

Figure 6.21a: F1B: e=3.5c & d=3c

	b/c									
a/c	0.4058	0.3958	0.3797	0.3787	0.3741	0.3575	0.3523	0.3466	0.3348	0.3422
	0.403	0.3934	0.3777	0.377	0.3727	0.3563	0.3514	0.3458	0.3342	0.3416
	0.3978	0.3892	0.3743	0.3742	0.3704	0.3544	0.3498	0.3445	0.333	0.3406
	0.3891	0.3822	0.3686	0.3696	0.3666	0.3513	0.3472	0.3423	0.3312	0.3391
	0.3762	0.3719	0.3604	0.363	0.3612	0.347	0.3436	0.3394	0.3287	0.337
	0.3598	0.359	0.3502	0.3549	0.3548	0.3418	0.3394	0.3359	0.3259	0.3346
	0.3365	0.3408	0.3359	0.3436	0.3458	0.3346	0.3336	0.3312	0.322	0.3313
	0.3068	0.3179	0.3181	0.3297	0.3348	0.3259	0.3266	0.3256	0.3173	0.3275
	0.2717	0.2907	0.297	0.3133	0.322	0.3157	0.3186	0.3191	0.3121	0.3231
	0.2242	0.2538	0.2683	0.2909	0.3045	0.3019	0.3076	0.3103	0.305	0.3172

Figure 6.21a: F1B: e=3.5c & d=3.5c

	b/c									
a/c	0.4173	0.4091	0.3951	0.3962	0.3937	0.3791	0.3754	0.3705	0.3585	0.3637
	0.4144	0.4067	0.3931	0.3945	0.3923	0.378	0.3745	0.3696	0.3578	0.3631
	0.4092	0.4024	0.3896	0.3916	0.3899	0.376	0.3728	0.3682	0.3566	0.3621
	0.4003	0.3953	0.3838	0.3869	0.386	0.3728	0.3701	0.366	0.3548	0.3605
	0.3873	0.3849	0.3754	0.3802	0.3806	0.3683	0.3665	0.363	0.3522	0.3583
	0.3707	0.3718	0.3651	0.3719	0.3739	0.3629	0.3621	0.3594	0.3492	0.3559
	0.347	0.3533	0.3505	0.3604	0.3648	0.3556	0.3561	0.3545	0.3452	0.3525
	0.3169	0.33	0.3323	0.3461	0.3535	0.3466	0.3489	0.3487	0.3404	0.3486
	0.2813	0.3024	0.3109	0.3294	0.3403	0.3361	0.3406	0.342	0.335	0.3441
	0.2331	0.2648	0.2816	0.3065	0.3224	0.3219	0.3293	0.3329	0.3276	0.3381

Figure 6.21a: F1B: e=3.5c & d=4c

	b/c									
a/c	0.4258	0.4189	0.4063	0.4089	0.408	0.3949	0.3926	0.3887	0.3774	0.3822
	0.4229	0.4165	0.4043	0.4072	0.4066	0.3937	0.3916	0.3878	0.3767	0.3816
	0.4176	0.4122	0.4008	0.4043	0.4041	0.3917	0.3899	0.3864	0.3754	0.3805
	0.4087	0.405	0.3949	0.3995	0.4002	0.3884	0.3872	0.3841	0.3735	0.3789
	0.3955	0.3944	0.3864	0.3927	0.3946	0.3839	0.3834	0.381	0.3709	0.3767
	0.3788	0.3812	0.3759	0.3843	0.3879	0.3784	0.379	0.3773	0.3679	0.3742
	0.3548	0.3625	0.3612	0.3726	0.3785	0.3709	0.3729	0.3723	0.3638	0.3708
	0.3245	0.3389	0.3428	0.3581	0.3671	0.3617	0.3655	0.3663	0.3589	0.3667
	0.2885	0.311	0.321	0.3411	0.3537	0.3511	0.357	0.3595	0.3533	0.3621
	0.2397	0.273	0.2914	0.3179	0.3354	0.3366	0.3454	0.3502	0.3457	0.356

Figure I.10a: F1B: e=4c & d=0.5c

	b/c									
	0.1741	0.1285	0.1037	0.1146	0.1324	0.1058	0.1271	0.1448	0.1638	0.2371
	0.1729	0.1276	0.1029	0.1139	0.1318	0.1053	0.1266	0.1444	0.1634	0.2366
	0.1706	0.1260	0.1017	0.1128	0.1308	0.1046	0.1259	0.1436	0.1599	0.2358
	0.1667	0.1233	0.0996	0.1109	0.1292	0.1043	0.1248	0.1425	0.1590	0.2345
a/c	0.1610	0.1194	0.0966	0.1082	0.1268	0.1026	0.1231	0.1409	0.1583	0.2328
	0.1538	0.1146	0.0929	0.1049	0.1240	0.0996	0.1212	0.1390	0.1565	0.2308
	0.1436	0.1077	0.0877	0.1004	0.1200	0.0977	0.1185	0.1364	0.1575	0.2281
	0.1307	0.0990	0.0811	0.0947	0.1152	0.0934	0.1141	0.1333	0.1551	0.2249
	0.1154	0.0888	0.0735	0.0881	0.1096	0.0894	0.1115	0.1297	0.1528	0.2212
	0.0943	0.0747	0.0631	0.0791	0.1020	0.0856	0.1081	0.1251	0.1485	0.2164

Figure I.10a: F1B: e=4c & d=1c

	b/c									
	0.2771	0.2402	0.2011	0.1937	0.1975	0.1854	0.1979	0.2119	0.2118	0.2636
	0.2754	0.2388	0.2001	0.1928	0.1968	0.1848	0.1973	0.2114	0.2114	0.2631
	0.2723	0.2364	0.1982	0.1913	0.1955	0.1836	0.1963	0.2104	0.2105	0.2623
	0.267	0.2324	0.1951	0.1888	0.1933	0.1818	0.1946	0.2089	0.2093	0.261
a/c	0.2593	0.2265	0.1908	0.1853	0.1903	0.1792	0.1923	0.2069	0.2075	0.2592
	0.2496	0.2193	0.1854	0.1809	0.1867	0.1761	0.1896	0.2044	0.2055	0.2572
	0.2359	0.209	0.178	0.1749	0.1817	0.1718	0.1858	0.2011	0.2027	0.2544
	0.2185	0.1961	0.1687	0.1675	0.1755	0.1665	0.1813	0.1971	0.1994	0.2511
	0.198	0.1809	0.1577	0.1587	0.1683	0.1605	0.1761	0.1926	0.1956	0.2473
	0.1698	0.1602	0.1428	0.1469	0.1586	0.1524	0.1691	0.1865	0.1907	0.2424

Figure I.10a: F1B: e=4c & d=1.5c

	b/c									
	0.333	0.3083	0.2771	0.2641	0.254	0.2386	0.2441	0.2528	0.251	0.285
	0.331	0.3067	0.2758	0.2631	0.2531	0.2378	0.2434	0.2522	0.2504	0.2845
	0.3275	0.3039	0.2735	0.2612	0.2516	0.2365	0.2423	0.2512	0.2495	0.2837
	0.3217	0.2992	0.2698	0.2582	0.2492	0.2344	0.2405	0.2496	0.2481	0.2823
a/c	0.3132	0.2924	0.2644	0.2539	0.2457	0.2315	0.2379	0.2474	0.2461	0.2805
	0.3025	0.2839	0.2578	0.2487	0.2415	0.228	0.2349	0.2448	0.2437	0.2784
	0.2873	0.272	0.2485	0.2414	0.2357	0.2232	0.2308	0.2412	0.2406	0.2756
	0.2681	0.2571	0.237	0.2325	0.2285	0.2174	0.2259	0.2369	0.2368	0.2722
	0.2454	0.2395	0.2234	0.222	0.2203	0.2107	0.2202	0.232	0.2326	0.2685
	0.2143	0.2155	0.2051	0.2077	0.2091	0.2016	0.2126	0.2255	0.2273	0.2634

Figure I.10a: F1B: e=4c & d=2c

	b/c									
	0.3674	0.35	0.326	0.3176	0.307	0.2869	0.2834	0.2843	0.2804	0.3028
	0.3653	0.3483	0.3246	0.3164	0.306	0.2861	0.2827	0.2837	0.2798	0.3023
	0.3616	0.3452	0.3221	0.3144	0.3043	0.2847	0.2815	0.2826	0.2789	0.3015
	0.3555	0.3402	0.318	0.311	0.3016	0.2824	0.2795	0.281	0.2774	0.3001
a/c	0.3465	0.3329	0.3121	0.3062	0.2976	0.2792	0.2768	0.2786	0.2753	0.2983
	0.3352	0.3239	0.3048	0.3004	0.2929	0.2753	0.2736	0.2759	0.273	0.2962
	0.3193	0.3111	0.2947	0.2922	0.2864	0.27	0.2692	0.2722	0.2697	0.2933
	0.2991	0.2952	0.282	0.2822	0.2784	0.2636	0.2639	0.2677	0.2659	0.29
	0.2752	0.2764	0.2672	0.2705	0.2691	0.2561	0.2578	0.2626	0.2615	0.2861
	0.2426	0.2507	0.247	0.2547	0.2566	0.2461	0.2497	0.2558	0.2556	0.2811

Figure I.10a: F1B: e=4c & d=2.5c

	b/c									
	0.3902	0.3772	0.358	0.3539	0.3464	0.3276	0.3215	0.3169	0.3076	0.3208
	0.3881	0.3754	0.3565	0.3526	0.3454	0.3267	0.3208	0.3162	0.307	0.3203
	0.3842	0.3723	0.3538	0.3504	0.3435	0.3251	0.3194	0.3151	0.306	0.3194
	0.3779	0.367	0.3495	0.3468	0.3405	0.3226	0.3174	0.3133	0.3045	0.3181
a/c	0.3687	0.3595	0.3433	0.3417	0.3363	0.3191	0.3144	0.3108	0.3024	0.3162
	0.3571	0.3501	0.3357	0.3356	0.3313	0.315	0.311	0.308	0.2999	0.3141
	0.3406	0.3369	0.3251	0.3269	0.3243	0.3093	0.3063	0.304	0.2966	0.3112
	0.3199	0.3203	0.3118	0.3163	0.3157	0.3024	0.3006	0.2993	0.2926	0.3078
	0.2953	0.3008	0.2963	0.3039	0.3058	0.2943	0.2941	0.294	0.2881	0.304
	0.2617	0.2742	0.2751	0.2871	0.2923	0.2835	0.2854	0.2868	0.2821	0.2988

Figure I.10a: F1B: e=4c & d=3c

	b/c									
	0.4060	0.3959	0.3798	0.3787	0.3741	0.3575	0.3524	0.3467	0.3349	0.3422
	0.4039	0.3941	0.3782	0.3774	0.3730	0.3566	0.3515	0.3460	0.3343	0.3417
	0.4000	0.3908	0.3755	0.3751	0.3711	0.3549	0.3502	0.3448	0.3332	0.3408
	0.3935	0.3855	0.3710	0.3714	0.3680	0.3523	0.3480	0.3429	0.3316	0.3394
a/c	0.3841	0.3777	0.3647	0.3661	0.3636	0.3487	0.3449	0.3403	0.3294	0.3375
	0.3723	0.3681	0.3568	0.3597	0.3583	0.3443	0.3413	0.3373	0.3269	0.3353
	0.3555	0.3546	0.3459	0.3508	0.3510	0.3384	0.3363	0.3332	0.3234	0.3324
	0.3344	0.3377	0.3323	0.3398	0.3421	0.3311	0.3304	0.3283	0.3193	0.3289
	0.3093	0.3176	0.3162	0.3270	0.3317	0.3227	0.3235	0.3226	0.3146	0.3249
	0.2751	0.2904	0.2945	0.3096	0.3177	0.3114	0.3143	0.3151	0.3083	0.3197

Figure I.10a: F1B: e=4c & d=3.5c

	b/c									
	0.4175	0.4092	0.3952	0.3963	0.3938	0.3792	0.3755	0.3705	0.3585	0.3637
	0.4153	0.4074	0.3936	0.3949	0.3926	0.3782	0.3747	0.3698	0.3579	0.3632
	0.4113	0.4041	0.3908	0.3926	0.3907	0.3765	0.3732	0.3686	0.3569	0.3623
	0.4048	0.3986	0.3863	0.3888	0.3875	0.3738	0.3709	0.3666	0.3552	0.3608
a/c	0.3953	0.3908	0.3798	0.3834	0.383	0.3701	0.3678	0.3639	0.3529	0.3589
	0.3833	0.381	0.3718	0.3768	0.3775	0.3656	0.364	0.3608	0.3503	0.3566
	0.3663	0.3673	0.3606	0.3677	0.3701	0.3594	0.3589	0.3565	0.3467	0.3536
	0.3449	0.3501	0.3468	0.3565	0.3609	0.3519	0.3527	0.3514	0.3424	0.35
	0.3194	0.3297	0.3304	0.3433	0.3503	0.3432	0.3456	0.3456	0.3376	0.3459
	0.2848	0.3021	0.3083	0.3256	0.3359	0.3316	0.3362	0.3378	0.3311	0.3405

Figure I.10a: F1B: e=4c & d=4c

	b/c									
	0.426	0.4191	0.4064	0.409	0.4081	0.395	0.3927	0.3887	0.3774	0.3822
	0.4238	0.4172	0.4048	0.4077	0.4069	0.394	0.3918	0.388	0.3768	0.3817
	0.4198	0.4139	0.402	0.4053	0.4049	0.3923	0.3903	0.3867	0.3757	0.3807
	0.4132	0.4083	0.3974	0.4014	0.4016	0.3895	0.388	0.3847	0.374	0.3793
a/c	0.4036	0.4004	0.3908	0.3959	0.397	0.3857	0.3848	0.382	0.3716	0.3773
	0.3915	0.3905	0.3827	0.3893	0.3915	0.3811	0.3809	0.3788	0.3689	0.375
	0.3744	0.3766	0.3714	0.38	0.3839	0.3748	0.3757	0.3744	0.3652	0.3718
	0.3527	0.3592	0.3574	0.3686	0.3746	0.3672	0.3694	0.3691	0.3609	0.3681
	0.327	0.3386	0.3408	0.3553	0.3638	0.3583	0.3621	0.3632	0.3559	0.364
	0.292	0.3107	0.3184	0.3372	0.3492	0.3465	0.3524	0.3552	0.3492	0.3584

Figure 6.18b: F2B: e=0.5c & d=0.5c

	b/c									
a/c	−0.1306	−0.1426	−0.1510	−0.1521	−0.1523	−0.1717	−0.1776	−0.1894	−0.2159	−0.2334
	−0.0687	−0.1205	−0.1408	−0.1474	−0.1499	−0.1696	−0.1762	−0.1886	−0.2158	−0.2337
	0.0237	−0.0701	−0.1183	−0.1384	−0.1453	−0.1646	−0.1731	−0.1869	−0.2139	−0.2327
	0.0183	0.0179	−0.0544	−0.1138	−0.1353	−0.1559	−0.1678	−0.1842	−0.2109	−0.2317
	0.0214	0.0162	0.0302	−0.0501	−0.1128	−0.1378	−0.1581	−0.1781	−0.2061	−0.2300
	−0.0062	−0.0102	−0.0045	0.0013	−0.0727	−0.1190	−0.1492	−0.1747	−0.2049	−0.2280
	0.0037	−0.0026	−0.0022	−0.0005	−0.0008	−0.0604	−0.1240	−0.1599	−0.1974	−0.2238
	0.0094	0.0027	0.0032	−0.0017	−0.0076	0.0102	−0.0654	−0.1341	−0.1837	−0.2173
	−0.0219	−0.0244	−0.0237	−0.0290	−0.0277	−0.0156	−0.0074	−0.0834	−0.1595	−0.2051
	0.0217	0.0153	0.0162	0.0094	0.0015	0.0118	0.0075	0.0161	−0.0824	−0.1775

Figure 6.18b: F2B: e=0.5c & d=1c

	b/c									
a/c	−0.1888	−0.1961	−0.2032	−0.2081	−0.2131	−0.2196	−0.2262	−0.2331	−0.2570	−0.2580
	−0.1118	−0.1697	−0.1911	−0.2023	−0.2099	−0.2175	−0.2249	−0.2322	−0.2562	−0.2576
	0.0164	−0.1062	−0.1650	−0.1911	−0.2043	−0.2139	−0.2227	−0.2307	−0.2548	−0.2568
	0.0214	0.0124	−0.0929	−0.1636	−0.1920	−0.2068	−0.2186	−0.2280	−0.2521	−0.2556
	0.0216	0.0119	0.0123	−0.0938	−0.1643	−0.1902	−0.2111	−0.2234	−0.2464	−0.2536
	−0.0064	−0.0090	−0.0052	−0.0152	−0.1127	−0.1672	−0.1989	−0.2178	−0.2435	−0.2514
	0.0037	−0.0022	−0.0075	−0.0102	−0.0261	−0.1005	−0.1718	−0.2028	−0.2341	−0.2468
	0.0092	0.0047	0.0035	−0.0045	−0.0185	−0.0119	−0.1058	−0.1756	−0.2175	−0.2397
	−0.0314	−0.0280	−0.0209	−0.0283	−0.0376	−0.0208	−0.0300	−0.1189	−0.1971	−0.2264
	0.0215	0.0164	0.0176	0.0069	−0.0013	−0.0027	−0.0061	−0.0141	−0.1163	−0.1962

Figure 6.18b: F2B: e=0.5c & d=1.5c

	b/c									
a/c	−0.2226	−0.2316	−0.2360	−0.2374	−0.2439	−0.2505	−0.2568	−0.2608	−0.2760	−0.2756
	−0.1366	−0.2025	−0.2234	−0.2312	−0.2405	−0.2482	−0.2554	−0.2598	−0.2752	−0.2751
	0.0128	−0.1307	−0.1951	−0.2192	−0.2344	−0.2443	−0.2530	−0.2582	−0.2741	−0.2743
	0.0237	0.0087	−0.1160	−0.1894	−0.2211	−0.2365	−0.2485	−0.2553	−0.2714	−0.2729
	0.0219	0.0127	0.0098	−0.1130	−0.1909	−0.2205	−0.2402	−0.2503	−0.2664	−0.2708
	−0.0064	−0.0085	−0.0050	−0.0198	−0.1335	−0.1947	−0.2281	−0.2442	−0.2630	−0.2685
	0.0038	−0.0022	−0.0098	−0.0125	−0.0344	−0.1222	−0.1983	−0.2288	−0.2532	−0.2637
	0.0091	0.0046	0.0020	−0.0081	−0.0269	−0.0279	−0.1300	−0.1997	−0.2373	−0.2562
	−0.0311	−0.0305	−0.0230	−0.0313	−0.0467	−0.0333	−0.0449	−0.1379	−0.2128	−0.2424
	0.0215	0.0164	0.0174	0.0045	−0.0060	−0.0131	−0.0252	−0.0328	−0.1326	−0.2107

Figure 6.18b: F2B: e=0.5c & d=2c

	b/c									
a/c	−0.2439	−0.2547	−0.2591	−0.2586	−0.2619	−0.2665	−0.2730	−0.2779	−0.2899	−0.2896
	−0.1522	−0.2239	−0.2459	−0.2521	−0.2583	−0.2642	−0.2715	−0.2768	−0.2891	−0.2891
	0.0112	−0.1465	−0.2163	−0.2395	−0.2520	−0.2602	−0.2690	−0.2751	−0.2879	−0.2883
	0.0253	0.0065	−0.1321	−0.2082	−0.2382	−0.2521	−0.2644	−0.2721	−0.2858	−0.2869
	0.0221	0.0128	0.0053	−0.1267	−0.2067	−0.2360	−0.2559	−0.2669	−0.2810	−0.2847
	−0.0064	−0.0080	−0.0035	−0.0218	−0.1453	−0.2088	−0.2434	−0.2606	−0.2773	−0.2823
	0.0039	−0.0021	−0.0092	−0.0125	−0.0354	−0.1334	−0.2123	−0.2449	−0.2675	−0.2773
	0.0091	0.0044	0.0008	−0.0090	−0.0279	−0.0296	−0.1410	−0.2145	−0.2513	−0.2695
	−0.0308	−0.0323	−0.0244	−0.0326	−0.0486	−0.0418	−0.0496	−0.1497	−0.2256	−0.2554
	0.0215	0.0164	0.0174	0.0039	−0.0076	−0.0182	−0.0325	−0.0416	−0.1450	−0.2226

Figure 6.18b: F2B: e=0.5c & d=2.5c

	b/c									
a/c	−0.2583	−0.2704	−0.2753	−0.2743	−0.2760	−0.2785	−0.2826	−0.2859	−0.2973	−0.2979
	−0.1625	−0.2384	−0.2616	−0.2676	−0.2724	−0.2762	−0.2810	−0.2849	−0.2965	−0.2973
	0.0105	−0.1572	−0.2309	−0.2546	−0.2660	−0.2721	−0.2785	−0.2832	−0.2953	−0.2965
	0.0265	0.0052	−0.1431	−0.2221	−0.2517	−0.2639	−0.2738	−0.2801	−0.2931	−0.2950
	0.0223	0.0138	0.0041	−0.1373	−0.2193	−0.2475	−0.2652	−0.2749	−0.2887	−0.2928
	−0.0064	−0.0075	−0.0030	−0.0234	−0.1546	−0.2194	−0.2526	−0.2684	−0.2848	−0.2904
	0.0040	−0.0021	−0.0102	−0.0128	−0.0363	−0.1419	−0.2207	−0.2526	−0.2750	−0.2852
	0.0090	0.0043	0.0001	−0.0097	−0.0281	−0.0291	−0.1468	−0.2215	−0.2596	−0.2773
	−0.0306	−0.0323	−0.0258	−0.0338	−0.0505	−0.0382	−0.0498	−0.1548	−0.2322	−0.2630
	0.0217	0.0165	0.0174	0.0036	−0.0080	−0.0203	−0.0330	−0.0409	−0.1500	−0.2295

Figure 6.18b: F2B: e=0.5c & d=3c

	b/c									
a/c	−0.2684	−0.2815	−0.2869	−0.2859	−0.2871	−0.2885	−0.2908	−0.2922	−0.3017	−0.3012
	−0.1698	−0.2486	−0.2729	−0.2791	−0.2834	−0.2861	−0.2892	−0.2911	−0.3009	−0.3006
	0.0101	−0.1647	−0.2413	−0.2658	−0.2769	−0.2820	−0.2867	−0.2894	−0.2997	−0.2998
	0.0273	0.0044	−0.1509	−0.2325	−0.2623	−0.2737	−0.2820	−0.2863	−0.2975	−0.2983
	0.0224	0.0134	0.0033	−0.1449	−0.2290	−0.2570	−0.2732	−0.2810	−0.2933	−0.2960
	−0.0064	−0.0072	−0.0031	−0.0246	−0.1619	−0.2282	−0.2604	−0.2745	−0.2893	−0.2936
	0.0041	−0.0021	−0.0107	−0.0168	−0.0370	−0.1496	−0.2279	−0.2585	−0.2795	−0.2885
	0.0090	0.0041	−0.0004	−0.0102	−0.0283	−0.0291	−0.1518	−0.2269	−0.2642	−0.2805
	−0.0303	−0.0322	−0.0269	−0.0348	−0.0509	−0.0386	−0.0441	−0.1585	−0.2363	−0.2660
	0.0218	0.0166	0.0173	0.0034	−0.0083	−0.0198	−0.0326	−0.0396	−0.1522	−0.2323

Figure 6.18b: F2B: e=0.5c & d=3.5c

	b/c									
a/c	−0.2757	−0.2896	−0.2954	−0.2946	−0.2956	−0.2966	−0.2979	−0.2980	−0.3060	−0.3038
	−0.1750	−0.2560	−0.2811	−0.2877	−0.2919	−0.2942	−0.2964	−0.2969	−0.3052	−0.3033
	0.0099	−0.1700	−0.2489	−0.2741	−0.2852	−0.2900	−0.2938	−0.2952	−0.3040	−0.3024
	0.0279	0.0040	−0.1565	−0.2401	−0.2704	−0.2816	−0.2890	−0.2921	−0.3018	−0.3010
	0.0225	0.0139	0.0028	−0.1506	−0.2365	−0.2647	−0.2802	−0.2868	−0.2978	−0.2987
	−0.0061	−0.0070	−0.0033	−0.0255	−0.1675	−0.2353	−0.2672	−0.2802	−0.2937	−0.2963
	0.0041	−0.0021	−0.0113	−0.0149	−0.0378	−0.1544	−0.2342	−0.2642	−0.2839	−0.2911
	0.0090	0.0040	−0.0009	−0.0107	−0.0287	−0.0293	−0.1562	−0.2321	−0.2674	−0.2831
	−0.0302	−0.0320	−0.0276	−0.0355	−0.0480	−0.0390	−0.0520	−0.1622	−0.2402	−0.2685
	0.0219	0.0166	0.0172	0.0032	−0.0086	−0.0200	−0.0326	−0.0383	−0.1568	−0.2347

Figure 6.18b: F2B: e=0.5c & d=4c

	b/c									
a/c	−0.2813	−0.2957	−0.3018	−0.3012	−0.3022	−0.3030	−0.3039	−0.3033	−0.3103	−0.3069
	−0.1789	−0.2616	−0.2873	−0.2942	−0.2984	−0.3006	−0.3023	−0.3022	−0.3095	−0.3063
	0.0098	−0.1740	−0.2546	−0.2804	−0.2917	−0.2964	−0.2998	−0.3005	−0.3083	−0.3055
	0.0283	0.0037	−0.1607	−0.2460	−0.2767	−0.2879	−0.2949	−0.2974	−0.3061	−0.3040
	0.0226	0.0139	0.0024	−0.1549	−0.2423	−0.2708	−0.2860	−0.2920	−0.3022	−0.3017
	−0.0062	−0.0069	−0.0033	−0.0261	−0.1719	−0.2410	−0.2729	−0.2854	−0.2981	−0.2993
	0.0042	−0.0021	−0.0091	−0.0132	−0.0382	−0.1583	−0.2395	−0.2692	−0.2882	−0.2941
	0.0090	0.0040	−0.0012	−0.0110	−0.0290	−0.0296	−0.1599	−0.2367	−0.2713	−0.2861
	−0.0300	−0.0319	−0.0275	−0.0361	−0.0531	−0.0395	−0.0493	−0.1656	−0.2438	−0.2715
	0.0220	0.0167	0.0171	0.0025	−0.0090	−0.0217	−0.0329	−0.0372	−0.1591	−0.2374

Figure I.7b: F2B: e=1c & d=0.5c

	b/c									
	−0.1402	−0.1455	−0.1519	−0.1523	−0.1522	−0.1716	−0.1775	−0.1892	−0.2158	−0.2336
	−0.1192	−0.1331	−0.1441	−0.1474	−0.1490	−0.1682	−0.1756	−0.1878	−0.2147	−0.2328
	−0.0765	−0.1094	−0.1300	−0.1392	−0.1438	−0.1649	−0.1731	−0.1859	−0.2126	−0.2319
	−0.0063	−0.0672	−0.1038	−0.1248	−0.1349	−0.1576	−0.1674	−0.1756	−0.2096	−0.2301
a/c	0.0668	0.0014	−0.0585	−0.0991	−0.1204	−0.1438	−0.1587	−0.1771	−0.2050	−0.2274
	0.0486	0.0402	−0.0032	−0.0616	−0.1008	−0.1271	−0.1483	−0.1705	−0.2001	−0.2241
	0.0261	0.0387	0.0438	0.0002	−0.0623	−0.0987	−0.1299	−0.1591	−0.1912	−0.2191
	0.0138	0.0183	0.0422	0.0411	−0.0073	−0.0569	−0.1017	−0.1409	−0.1790	−0.2120
	−0.0133	−0.0119	0.0016	0.0182	0.0186	−0.0132	−0.0689	−0.1188	−0.1644	−0.2024
	0.0149	0.0105	0.0155	0.0260	0.0373	0.0466	−0.0013	−0.0690	−0.1314	−0.1845

Figure I.7b: F2B: e=1c & d=1c

	b/c									
	−0.2007	−0.1996	−0.2043	−0.2083	−0.2130	−0.2194	−0.2260	−0.2329	−0.2569	−0.2579
	−0.1755	−0.1850	−0.1951	−0.2024	−0.2090	−0.2166	−0.2240	−0.2314	−0.2556	−0.2570
	−0.1234	−0.1567	−0.1781	−0.1921	−0.2025	−0.2121	−0.2208	−0.2291	−0.2537	−0.2557
	−0.0364	−0.1055	−0.1474	−0.1742	−0.1914	−0.2046	−0.2157	−0.2254	−0.2506	−0.2536
a/c	0.0590	−0.0294	−0.0971	−0.1447	−0.1735	−0.1927	−0.2078	−0.2198	−0.2458	−0.2506
	0.0528	0.0332	−0.0332	−0.1039	−0.1490	−0.1765	−0.1978	−0.2131	−0.2405	−0.2472
	0.0302	0.0401	0.0294	−0.0350	−0.1042	−0.1463	−0.1799	−0.2014	−0.2308	−0.2415
	0.0158	0.0190	0.0321	0.0168	−0.0411	−0.0974	−0.1501	−0.1840	−0.2165	−0.2337
	−0.0127	−0.0098	0.0006	0.0072	−0.0038	−0.0426	−0.1105	−0.1595	−0.2020	−0.2232
	0.0149	0.0116	0.0124	0.0083	0.0150	0.0181	−0.0364	−0.1030	−0.1620	−0.2033

Figure I.7b: F2B: e=1c & d=1.5c

	b/c									
	−0.2356	−0.2354	−0.2371	−0.2377	−0.2438	−0.2504	−0.2566	−0.2606	−0.2758	−0.2754
	−0.2084	−0.2196	−0.2273	−0.2313	−0.2395	−0.2472	−0.2544	−0.2589	−0.2745	−0.2744
	−0.1510	−0.1885	−0.2094	−0.2204	−0.2324	−0.2423	−0.2509	−0.2564	−0.2726	−0.2730
	−0.0542	−0.1321	−0.1764	−0.2011	−0.2204	−0.2341	−0.2453	−0.2524	−0.2696	−0.2708
a/c	0.0529	−0.0483	−0.1212	−0.1693	−0.2011	−0.2211	−0.2367	−0.2464	−0.2647	−0.2676
	0.0554	0.0261	−0.0515	−0.1246	−0.1743	−0.2039	−0.2258	−0.2391	−0.2592	−0.2640
	0.0326	0.0423	0.0241	−0.0504	−0.1262	−0.1724	−0.2065	−0.2265	−0.2498	−0.2580
	0.0167	0.0203	0.0332	0.0110	−0.0578	−0.1220	−0.1759	−0.2077	−0.2363	−0.2498
	−0.0122	−0.0091	0.0004	0.0040	−0.0168	−0.0621	−0.1344	−0.1813	−0.2196	−0.2387
	0.0149	0.0116	0.0114	0.0041	0.0054	−0.0022	−0.0596	−0.1260	−0.1808	−0.2178

Figure I.7b: F2B: e=1c & d=2c

	b/c									
	−0.2578	−0.2587	−0.2603	−0.2588	−0.2618	−0.2664	−0.2728	−0.2777	−0.2897	−0.2895
	−0.2292	−0.2421	−0.2500	−0.2522	−0.2573	−0.2632	−0.2705	−0.2759	−0.2884	−0.2885
	−0.1684	−0.2093	−0.2311	−0.2408	−0.2500	−0.2580	−0.2669	−0.2733	−0.2864	−0.2870
	−0.0652	−0.1495	−0.1969	−0.2207	−0.2376	−0.2496	−0.2611	−0.2691	−0.2833	−0.2847
a/c	0.0495	−0.0598	−0.1384	−0.1872	−0.2175	−0.2362	−0.2522	−0.2628	−0.2787	−0.2813
	0.0578	0.0216	−0.0631	−0.1397	−0.1894	−0.2183	−0.2408	−0.2552	−0.2732	−0.2776
	0.0347	0.0442	0.0201	−0.0617	−0.1391	−0.1856	−0.2208	−0.2421	−0.2635	−0.2714
	0.0176	0.0216	0.0347	0.0082	−0.0670	−0.1341	−0.1894	−0.2225	−0.2498	−0.2628
	−0.0117	−0.0084	0.0010	0.0043	−0.0186	−0.0716	−0.1454	−0.1949	−0.2324	−0.2513
	0.0150	0.0117	0.0114	0.0043	0.0050	−0.0047	−0.0689	−0.1391	−0.1940	−0.2297

Figure I.7b: F2B: e=1c & d=2.5c

	b/c									
	−0.2727	−0.2746	−0.2765	−0.2746	−0.2760	−0.2784	−0.2824	−0.2858	−0.2972	−0.2977
	−0.2431	−0.2574	−0.2660	−0.2678	−0.2714	−0.2751	−0.2800	−0.2840	−0.2958	−0.2966
	−0.1800	−0.2234	−0.2464	−0.2560	−0.2639	−0.2699	−0.2764	−0.2813	−0.2937	−0.2951
	−0.0725	−0.1612	−0.2110	−0.2353	−0.2511	−0.2613	−0.2704	−0.2770	−0.2905	−0.2927
a/c	0.0477	−0.0674	−0.1505	−0.2007	−0.2305	−0.2477	−0.2614	−0.2707	−0.2859	−0.2893
	0.0599	0.0189	−0.0717	−0.1511	−0.2014	−0.2293	−0.2499	−0.2629	−0.2804	−0.2855
	0.0364	0.0458	0.0174	−0.0699	−0.1492	−0.1960	−0.2295	−0.2496	−0.2709	−0.2792
	0.0184	0.0227	0.0345	0.0060	−0.0739	−0.1436	−0.1976	−0.2297	−0.2569	−0.2704
	−0.0113	−0.0078	0.0023	0.0048	−0.0198	−0.0774	−0.1524	−0.2015	−0.2391	−0.2587
	0.0152	0.0119	0.0116	0.0047	0.0055	−0.0052	−0.0723	−0.1443	−0.2006	−0.2366

Figure I.7b: F2B: e=1c & d=3c

	b/c									
	−0.2832	−0.2858	−0.2881	−0.2862	−0.2870	−0.2884	−0.2906	−0.2920	−0.3015	−0.3010
	−0.2530	−0.2682	−0.2773	−0.2793	−0.2824	−0.2851	−0.2882	−0.2902	−0.3002	−0.2999
	−0.1881	−0.2333	−0.2573	−0.2672	−0.2747	−0.2798	−0.2845	−0.2875	−0.2981	−0.2984
	−0.0774	−0.1694	−0.2210	−0.2461	−0.2617	−0.2710	−0.2785	−0.2832	−0.2949	−0.2960
a/c	0.0466	−0.0727	−0.1590	−0.2106	−0.2407	−0.2572	−0.2694	−0.2768	−0.2902	−0.2926
	0.0615	0.0173	−0.0776	−0.1594	−0.2108	−0.2384	−0.2577	−0.2690	−0.2847	−0.2887
	0.0377	0.0471	0.0164	−0.0757	−0.1571	−0.2046	−0.2370	−0.2555	−0.2753	−0.2824
	0.0190	0.0235	0.0352	0.0046	−0.0793	−0.1507	−0.2046	−0.2353	−0.2613	−0.2735
	−0.0109	−0.0073	0.0019	0.0055	−0.0205	−0.0386	−0.1583	−0.2068	−0.2433	−0.2617
	0.0154	0.0120	0.0116	0.0050	0.0058	−0.0056	−0.0753	−0.1487	−0.2046	−0.2395

Figure I.7b: F2B: e=1c & d=3.5c

	b/c									
	−0.2909	−0.2940	−0.2967	−0.2949	−0.2956	−0.2965	−0.2977	−0.2978	−0.3059	−0.3037
	−0.2601	−0.2761	−0.2857	−0.2879	−0.2908	−0.2931	−0.2953	−0.2960	−0.3045	−0.3026
	−0.1940	−0.2405	−0.2653	−0.2756	−0.2831	−0.2877	−0.2916	−0.2933	−0.3024	−0.3011
	−0.0809	−0.1754	−0.2284	−0.2541	−0.2699	−0.2789	−0.2856	−0.2890	−0.2992	−0.2987
a/c	0.0460	−0.0764	−0.1652	−0.2180	−0.2485	−0.2649	−0.2763	−0.2825	−0.2945	−0.2952
	0.0628	0.0162	−0.0817	−0.1656	−0.2180	−0.2458	−0.2645	−0.2746	−0.2889	−0.2914
	0.0386	0.0481	0.0152	−0.0799	−0.1631	−0.2114	−0.2435	−0.2611	−0.2795	−0.2850
	0.0194	0.0242	0.0358	0.0036	−0.0833	−0.1564	−0.2106	−0.2406	−0.2656	−0.2761
	−0.0106	−0.0069	0.0020	0.0059	−0.0237	−0.0862	−0.1634	−0.2117	−0.2474	−0.2643
	0.0155	0.0121	0.0117	0.0051	0.0062	−0.0061	−0.0786	−0.1530	−0.2086	−0.2419

Figure I.7b: F2B: e=1c & d=4c

	b/c									
	−0.2967	−0.3001	−0.3031	−0.3015	−0.3021	−0.3029	−0.3037	−0.3031	−0.3101	−0.3067
	−0.2655	−0.2820	−0.2920	−0.2944	−0.2974	−0.2995	−0.3013	−0.3013	−0.3087	−0.3057
	−0.1984	−0.2459	−0.2714	−0.2820	−0.2895	−0.2941	−0.2975	−0.2986	−0.3067	−0.3041
	−0.0835	−0.1798	−0.2339	−0.2602	−0.2762	−0.2851	−0.2914	−0.2942	−0.3034	−0.3017
a/c	0.0456	−0.0791	−0.1698	−0.2236	−0.2545	−0.2710	−0.2821	−0.2877	−0.2987	−0.2983
	0.0638	0.0156	−0.0847	−0.1702	−0.2236	−0.2517	−0.2701	−0.2797	−0.2931	−0.2944
	0.0394	0.0489	0.0146	−0.0830	−0.1678	−0.2169	−0.2489	−0.2661	−0.2836	−0.2880
	0.0198	0.0247	0.0362	0.0031	−0.0864	−0.1610	−0.2157	−0.2454	−0.2698	−0.2791
	−0.0104	−0.0066	0.0021	0.0062	−0.0248	−0.0890	−0.1676	−0.2161	−0.2513	−0.2672
	0.0156	0.0122	0.0117	0.0053	0.0064	−0.0066	−0.0809	−0.1568	−0.2121	−0.2447

Figure 6.19b: F2B: e=1.5c & d=0.5c

	b/c									
a/c	−0.1430	−0.1470	−0.1527	−0.1527	−0.1525	−0.1717	−0.1776	−0.1892	−0.2158	−0.2335
	−0.1335	−0.1402	−0.1478	−0.1492	−0.1498	−0.1687	−0.1758	−0.1878	−0.2145	−0.2326
	−0.1141	−0.1270	−0.1385	−0.1428	−0.1452	−0.1663	−0.1728	−0.1856	−0.2125	−0.2312
	−0.0790	−0.1037	−0.1225	−0.1323	−0.1378	−0.1593	−0.1681	−0.1822	−0.2092	−0.2292
	−0.0283	−0.0694	−0.0983	−0.1168	−0.1271	−0.1495	−0.1616	−0.1774	−0.2062	−0.2264
	0.0246	−0.0300	−0.0680	−0.0970	−0.1140	−0.1377	−0.1526	−0.1717	−0.2010	−0.2231
	0.0718	0.0247	−0.0222	−0.0643	−0.0939	−0.1190	−0.1398	−0.1624	−0.1921	−0.2180
	0.0797	0.0619	0.0278	−0.0208	−0.0658	−0.0951	−0.1214	−0.1501	−0.1820	−0.2114
	0.0411	0.0494	0.0489	0.0166	−0.0306	−0.0669	−0.1000	−0.1351	−0.1705	−0.2034
	0.0397	0.0498	0.0679	0.0602	0.0221	−0.0192	−0.0644	−0.1074	−0.1500	−0.1904

Figure 6.19b: F2B: e=1.5c & d=1c

	b/c									
a/c	−0.2039	−0.2013	−0.2053	−0.2088	−0.2133	−0.2196	−0.2261	−0.2330	−0.2569	−0.2579
	−0.1926	−0.1933	−0.1994	−0.2045	−0.2100	−0.2171	−0.2241	−0.2314	−0.2556	−0.2568
	−0.1695	−0.1777	−0.1882	−0.1966	−0.2043	−0.2128	−0.2209	−0.2288	−0.2534	−0.2551
	−0.1274	−0.1501	−0.1690	−0.1834	−0.1950	−0.2059	−0.2158	−0.2249	−0.2501	−0.2527
	−0.0658	−0.1090	−0.1405	−0.1642	−0.1816	−0.1962	−0.2086	−0.2195	−0.2455	−0.2494
	−0.0032	−0.0615	−0.1057	−0.1404	−0.1653	−0.1844	−0.2002	−0.2132	−0.2403	−0.2457
	0.0631	0.0014	−0.0564	−0.1048	−0.1401	−0.1658	−0.1872	−0.2036	−0.2327	−0.2401
	0.0822	0.0560	0.0049	−0.0564	−0.1065	−0.1399	−0.1693	−0.1907	−0.2211	−0.2329
	0.0472	0.0514	0.0375	−0.0077	−0.0651	−0.1075	−0.1462	−0.1746	−0.2081	−0.2241
	0.0464	0.0549	0.0619	0.0424	0.0020	−0.0509	−0.1045	−0.1470	−0.1850	−0.2096

Figure 6.19b: F2B: e=1.5c & d=1.5c

	b/c									
a/c	−0.2391	−0.2373	−0.2382	−0.2383	−0.2442	−0.2505	−0.2567	−0.2607	−0.2758	−0.2754
	−0.2270	−0.2286	−0.2319	−0.2336	−0.2406	−0.2477	−0.2545	−0.2589	−0.2744	−0.2743
	−0.2019	−0.2116	−0.2200	−0.2251	−0.2344	−0.2430	−0.2510	−0.2561	−0.2722	−0.2725
	−0.1563	−0.1816	−0.1998	−0.2111	−0.2243	−0.2355	−0.2453	−0.2519	−0.2688	−0.2699
	−0.0889	−0.1367	−0.1691	−0.1904	−0.2099	−0.2249	−0.2375	−0.2460	−0.2643	−0.2664
	−0.0189	−0.0837	−0.1308	−0.1647	−0.1921	−0.2120	−0.2283	−0.2391	−0.2587	−0.2624
	0.0558	−0.0171	−0.0772	−0.1260	−0.1647	−0.1921	−0.2141	−0.2287	−0.2503	−0.2565
	0.0816	0.0476	−0.0118	−0.0765	−0.1280	−0.1646	−0.1948	−0.2148	−0.2394	−0.2489
	0.0489	0.0509	0.0305	−0.0236	−0.0847	−0.1305	−0.1702	−0.1973	−0.2262	−0.2395
	0.0482	0.0563	0.0614	0.0355	−0.0196	−0.0734	−0.1277	−0.1682	−0.2027	−0.2242

Figure 6.19b: F2B: e=1.5c & d=2c

	b/c									
a/c	−0.2615	−0.2607	−0.2614	−0.2594	−0.2621	−0.2665	−0.2729	−0.2777	−0.2897	−0.2895
	−0.2488	−0.2516	−0.2548	−0.2545	−0.2584	−0.2637	−0.2707	−0.2759	−0.2883	−0.2883
	−0.2225	−0.2338	−0.2424	−0.2457	−0.2520	−0.2588	−0.2669	−0.2730	−0.2860	−0.2865
	−0.1747	−0.2023	−0.2211	−0.2311	−0.2416	−0.2511	−0.2611	−0.2685	−0.2824	−0.2837
	−0.1036	−0.1550	−0.1894	−0.2095	−0.2266	−0.2401	−0.2530	−0.2623	−0.2777	−0.2800
	−0.0286	−0.0985	−0.1489	−0.1825	−0.2081	−0.2267	−0.2434	−0.2552	−0.2722	−0.2759
	0.0510	−0.0280	−0.0910	−0.1417	−0.1796	−0.2061	−0.2286	−0.2443	−0.2639	−0.2697
	0.0818	0.0416	−0.0241	−0.0894	−0.1411	−0.1780	−0.2086	−0.2298	−0.2526	−0.2618
	0.0506	0.0508	0.0246	−0.0345	−0.0962	−0.1423	−0.1833	−0.2116	−0.2390	−0.2521
	0.0497	0.0573	0.0610	0.0308	−0.0282	−0.0846	−0.1409	−0.1812	−0.2154	−0.2362

Figure 6.19b: F2B: e=1.5c & d=2.5c

	b/c									
a/c	−0.2765	−0.2767	−0.2776	−0.2752	−0.2763	−0.2786	−0.2825	−0.2858	−0.2972	−0.2977
	−0.2635	−0.2673	−0.2708	−0.2701	−0.2725	−0.2756	−0.2802	−0.2840	−0.2957	−0.2965
	−0.2364	−0.2489	−0.2581	−0.2611	−0.2660	−0.2707	−0.2764	−0.2810	−0.2933	−0.2946
	−0.1870	−0.2164	−0.2362	−0.2460	−0.2553	−0.2628	−0.2705	−0.2764	−0.2897	−0.2918
	−0.1134	−0.1674	−0.2034	−0.2238	−0.2399	−0.2516	−0.2622	−0.2702	−0.2849	−0.2880
	−0.0349	−0.1084	−0.1616	−0.1959	−0.2209	−0.2379	−0.2524	−0.2629	−0.2793	−0.2838
	0.0480	−0.0349	−0.1012	−0.1536	−0.1915	−0.2168	−0.2374	−0.2519	−0.2709	−0.2775
	0.0825	0.0377	−0.0322	−0.0990	−0.1517	−0.1879	−0.2171	−0.2371	−0.2598	−0.2694
	0.0523	0.0511	0.0204	−0.0422	−0.1050	−0.1514	−0.1912	−0.2185	−0.2459	−0.2595
	0.0510	0.0584	0.0606	0.0271	−0.0351	−0.0930	−0.1481	−0.1876	−0.2223	−0.2432

Figure 6.19b: F2B: e=1.5c & d=3c

	b/c									
a/c	−0.2871	−0.2879	−0.2893	−0.2868	−0.2874	−0.2886	−0.2907	−0.2920	−0.3015	−0.3010
	−0.2738	−0.2784	−0.2823	−0.2817	−0.2835	−0.2856	−0.2884	−0.2902	−0.3001	−0.2998
	−0.2462	−0.2596	−0.2693	−0.2725	−0.2768	−0.2806	−0.2845	−0.2872	−0.2977	−0.2979
	−0.1956	−0.2264	−0.2469	−0.2571	−0.2660	−0.2725	−0.2786	−0.2826	−0.2941	−0.2950
	−0.1202	−0.1761	−0.2134	−0.2344	−0.2503	−0.2611	−0.2702	−0.2763	−0.2892	−0.2912
	−0.0391	−0.1154	−0.1706	−0.2057	−0.2308	−0.2472	−0.2603	−0.2689	−0.2836	−0.2870
	0.0463	−0.0396	−0.1085	−0.1623	−0.2008	−0.2258	−0.2451	−0.2578	−0.2752	−0.2806
	0.0833	0.0352	−0.0377	−0.1061	−0.1599	−0.1963	−0.2244	−0.2429	−0.2641	−0.2725
	0.0537	0.0515	0.0177	−0.0477	−0.1117	−0.1590	−0.1980	−0.2240	−0.2502	−0.2625
	0.0523	0.0594	0.0605	0.0244	−0.0404	−0.0997	−0.1544	−0.1927	−0.2263	−0.2461

Figure 6.19b: F2B: e=1.5c & d=3.5c

	b/c									
a/c	−0.2949	−0.2961	−0.2978	−0.2955	−0.2959	−0.2966	−0.2978	−0.2979	−0.3059	−0.3037
	−0.2814	−0.2864	−0.2908	−0.2903	−0.2920	−0.2936	−0.2955	−0.2960	−0.3044	−0.3025
	−0.2533	−0.2674	−0.2776	−0.2810	−0.2852	−0.2885	−0.2916	−0.2930	−0.3020	−0.3005
	−0.2019	−0.2336	−0.2548	−0.2653	−0.2742	−0.2804	−0.2856	−0.2884	−0.2983	−0.2977
	−0.1250	−0.1825	−0.2207	−0.2423	−0.2583	−0.2689	−0.2772	−0.2820	−0.2934	−0.2939
	−0.0421	−0.1204	−0.1772	−0.2131	−0.2385	−0.2548	−0.2671	−0.2746	−0.2878	−0.2896
	0.0452	−0.0429	−0.1138	−0.1688	−0.2079	−0.2330	−0.2517	−0.2633	−0.2793	−0.2832
	0.0841	0.0336	−0.0416	−0.1113	−0.1663	−0.2030	−0.2307	−0.2483	−0.2681	−0.2750
	0.0550	0.0519	0.0159	−0.0516	−0.1168	−0.1652	−0.2040	−0.2292	−0.2542	−0.2650
	0.0533	0.0603	0.0605	0.0226	−0.0443	−0.1047	−0.1598	−0.1976	−0.2304	−0.2486

Figure 6.19b: F2B: e=1.5c & d=4c

	b/c									
a/c	−0.3007	−0.3023	−0.3042	−0.3021	−0.3025	−0.3031	−0.3038	−0.3031	−0.3102	−0.3067
	−0.2870	−0.2925	−0.2971	−0.2969	−0.2986	−0.3000	−0.3015	−0.3013	−0.3086	−0.3055
	−0.2586	−0.2732	−0.2837	−0.2874	−0.2917	−0.2949	−0.2976	−0.2982	−0.3062	−0.3036
	−0.2066	−0.2390	−0.2608	−0.2716	−0.2806	−0.2867	−0.2915	−0.2936	−0.3026	−0.3007
	−0.1286	−0.1872	−0.2262	−0.2483	−0.2645	−0.2750	−0.2830	−0.2872	−0.2976	−0.2969
	−0.0442	−0.1241	−0.1821	−0.2186	−0.2444	−0.2608	−0.2728	−0.2797	−0.2920	−0.2926
	0.0445	−0.0452	−0.1177	−0.1737	−0.2135	−0.2387	−0.2573	−0.2684	−0.2834	−0.2862
	0.0848	0.0326	−0.0444	−0.1152	−0.1711	−0.2084	−0.2361	−0.2532	−0.2722	−0.2780
	0.0560	0.0524	0.0147	−0.0544	−0.1207	−0.1699	−0.2089	−0.2339	−0.2582	−0.2679
	0.0541	0.0611	0.0606	0.0213	−0.0473	−0.1085	−0.1643	−0.2019	−0.2343	−0.2514

Figure I.8b: F2B: e=2c & d=0.5c

	b/c									
a/c	−0.1440	−0.1477	−0.1532	−0.1530	−0.1527	−0.1719	−0.1777	−0.1893	−0.2158	−0.2336
	−0.1388	−0.1437	−0.1500	−0.1505	−0.1507	−0.1701	−0.1762	−0.1881	−0.2166	−0.2327
	−0.1286	−0.1358	−0.1439	−0.1460	−0.1472	−0.1662	−0.1737	−0.1861	−0.2144	−0.2312
	−0.1100	−0.1221	−0.1335	−0.1384	−0.1414	−0.1619	−0.1700	−0.1829	−0.2099	−0.2288
	−0.0817	−0.1014	−0.1182	−0.1274	−0.1331	−0.1546	−0.1645	−0.1785	−0.2054	−0.2261
	−0.0471	−0.0761	−0.0992	−0.1141	−0.1232	−0.1451	−0.1573	−0.1735	−0.2011	−0.2229
	−0.0018	−0.0418	−0.0713	−0.0945	−0.1091	−0.1322	−0.1470	−0.1665	−0.1948	−0.2184
	0.0477	0.0013	−0.0369	−0.0691	−0.0914	−0.1159	−0.1344	−0.1567	−0.1871	−0.2127
	0.0725	0.0362	−0.0004	−0.0392	−0.0713	−0.0963	−0.1192	−0.1456	−0.1772	−0.2058
	0.0957	0.0738	0.0461	0.0057	−0.0371	−0.0668	−0.0956	−0.1280	−0.1622	−0.1956

Figure I.8b: F2B: e=2c & d=1c

	b/c									
a/c	−0.2051	−0.2022	−0.2058	−0.2092	−0.2136	−0.2198	−0.2262	−0.2330	−0.2570	−0.2579
	−0.1989	−0.1973	−0.2020	−0.2061	−0.2111	−0.2177	−0.2246	−0.2316	−0.2557	−0.2569
	−0.1866	−0.1880	−0.1947	−0.2004	−0.2066	−0.2142	−0.2217	−0.2293	−0.2537	−0.2552
	−0.1645	−0.1717	−0.1821	−0.1910	−0.1994	−0.2085	−0.2172	−0.2256	−0.2505	−0.2527
	−0.1306	−0.1472	−0.1636	−0.1772	−0.1890	−0.2004	−0.2109	−0.2206	−0.2462	−0.2494
	−0.0885	−0.1168	−0.1407	−0.1606	−0.1766	−0.1910	−0.2036	−0.2149	−0.2413	−0.2457
	−0.0336	−0.0753	−0.1087	−0.1369	−0.1589	−0.1775	−0.1933	−0.2068	−0.2344	−0.2405
	0.0249	−0.0287	−0.0703	−0.1076	−0.1367	−0.1604	−0.1803	−0.1966	−0.2257	−0.2341
	0.0636	0.0172	−0.0302	−0.0754	−0.1112	−0.1394	−0.1648	−0.1846	−0.2152	−0.2265
	0.0976	0.0694	0.0277	−0.0245	−0.0728	−0.1074	−0.1409	−0.1663	−0.1986	−0.2152

Figure I.8b: F2B: e=2c & d=1.5c

	b/c									
a/c	−0.2405	−0.2382	−0.2388	−0.2387	−0.2444	−0.2507	−0.2568	−0.2607	−0.2758	−0.2754
	−0.2338	−0.2329	−0.2346	−0.2353	−0.2417	−0.2485	−0.2550	−0.2592	−0.2746	−0.2744
	−0.2205	−0.2228	−0.2268	−0.2293	−0.2369	−0.2446	−0.2519	−0.2567	−0.2725	−0.2726
	−0.1967	−0.2052	−0.2135	−0.2191	−0.2290	−0.2383	−0.2469	−0.2527	−0.2692	−0.2699
	−0.1600	−0.1785	−0.1939	−0.2044	−0.2178	−0.2295	−0.2400	−0.2472	−0.2648	−0.2663
	−0.1141	−0.1453	−0.1693	−0.1864	−0.2043	−0.2191	−0.2320	−0.2409	−0.2598	−0.2624
	−0.0540	−0.0997	−0.1344	−0.1610	−0.1851	−0.2043	−0.2206	−0.2321	−0.2524	−0.2568
	0.0081	−0.0480	−0.0923	−0.1292	−0.1610	−0.1856	−0.2064	−0.2211	−0.2433	−0.2500
	0.0550	−0.0003	−0.0503	−0.0941	−0.1331	−0.1635	−0.1894	−0.2080	−0.2326	−0.2420
	0.0945	0.0613	0.0131	−0.0430	−0.0922	−0.1296	−0.1636	−0.1881	−0.2162	−0.2300

Figure I.8b: F2B: e=2c & d=2c

	b/c									
a/c	−0.2629	−0.2617	−0.2620	−0.2598	−0.2624	−0.2667	−0.2730	−0.2778	−0.2898	−0.2895
	−0.2559	−0.2562	−0.2576	−0.2563	−0.2596	−0.2644	−0.2711	−0.2762	−0.2885	−0.2884
	−0.2421	−0.2456	−0.2495	−0.2500	−0.2546	−0.2604	−0.2679	−0.2735	−0.2862	−0.2866
	−0.2172	−0.2271	−0.2356	−0.2395	−0.2464	−0.2539	−0.2627	−0.2693	−0.2828	−0.2838
	−0.1789	−0.1992	−0.2150	−0.2241	−0.2348	−0.2448	−0.2555	−0.2636	−0.2782	−0.2800
	−0.1306	−0.1642	−0.1894	−0.2053	−0.2208	−0.2341	−0.2472	−0.2571	−0.2729	−0.2759
	−0.0672	−0.1161	−0.1529	−0.1787	−0.2009	−0.2187	−0.2354	−0.2478	−0.2656	−0.2700
	−0.0016	−0.0612	−0.1083	−0.1453	−0.1758	−0.1994	−0.2206	−0.2363	−0.2565	−0.2629
	0.0495	−0.0108	−0.0632	−0.1081	−0.1466	−0.1764	−0.2030	−0.2226	−0.2455	−0.2546
	0.0927	0.0545	0.0012	−0.0562	−0.1039	−0.1416	−0.1763	−0.2019	−0.2286	−0.2421

Figure I.8b: F2B: e=2c & d=2.5c

	b/c									
a/c	−0.2780	−0.2776	−0.2783	−0.2756	−0.2766	−0.2788	−0.2826	−0.2859	−0.2972	−0.2977
	−0.2708	−0.2720	−0.2738	−0.2720	−0.2737	−0.2764	−0.2806	−0.2843	−0.2959	−0.2966
	−0.2566	−0.2611	−0.2654	−0.2655	−0.2686	−0.2723	−0.2773	−0.2815	−0.2936	−0.2947
	−0.2310	−0.2421	−0.2511	−0.2547	−0.2602	−0.2657	−0.2721	−0.2773	−0.2901	−0.2918
	−0.1916	−0.2133	−0.2299	−0.2389	−0.2483	−0.2564	−0.2648	−0.2714	−0.2854	−0.2880
	−0.1417	−0.1771	−0.2035	−0.2195	−0.2339	−0.2454	−0.2563	−0.2648	−0.2800	−0.2837
	−0.0759	−0.1273	−0.1660	−0.1920	−0.2135	−0.2297	−0.2443	−0.2554	−0.2726	−0.2778
	−0.0072	−0.0701	−0.1197	−0.1575	−0.1876	−0.2099	−0.2293	−0.2437	−0.2633	−0.2705
	0.0457	−0.0188	−0.0717	−0.1187	−0.1574	−0.1863	−0.2113	−0.2298	−0.2524	−0.2620
	0.0919	0.0499	−0.0064	−0.0651	−0.1133	−0.1511	−0.1841	−0.2087	−0.2353	−0.2492

Figure I.8b: F2B: e=2c & d=3c

	b/c									
a/c	−0.2886	−0.2889	−0.2899	−0.2872	−0.2876	−0.2887	−0.2908	−0.2921	−0.3016	−0.3010
	−0.2813	−0.2831	−0.2854	−0.2836	−0.2847	−0.2864	−0.2889	−0.2905	−0.3002	−0.2999
	−0.2668	−0.2720	−0.2768	−0.2770	−0.2795	−0.2822	−0.2855	−0.2877	−0.2980	−0.2980
	−0.2408	−0.2526	−0.2622	−0.2659	−0.2710	−0.2755	−0.2802	−0.2834	−0.2944	−0.2951
	−0.2005	−0.2233	−0.2406	−0.2498	−0.2589	−0.2660	−0.2728	−0.2775	−0.2897	−0.2912
	−0.1494	−0.1862	−0.2135	−0.2300	−0.2442	−0.2549	−0.2642	−0.2708	−0.2843	−0.2869
	−0.0820	−0.1351	−0.1754	−0.2019	−0.2233	−0.2389	−0.2521	−0.2613	−0.2768	−0.2809
	−0.0122	−0.0764	−0.1279	−0.1665	−0.1969	−0.2187	−0.2368	−0.2495	−0.2675	−0.2736
	0.0435	−0.0234	−0.0782	−0.1265	−0.1658	−0.1946	−0.2185	−0.2354	−0.2564	−0.2651
	0.0917	0.0468	−0.0130	−0.0715	−0.1206	−0.1586	−0.1908	−0.2141	−0.2395	−0.2522

Figure I.8b: F2B: e=2c & d=3.5c

	b/c									
a/c	−0.2964	−0.2971	−0.2985	−0.2959	−0.2962	−0.2968	−0.2980	−0.2980	−0.3059	−0.3037
	−0.2890	−0.2913	−0.2939	−0.2922	−0.2932	−0.2944	−0.2960	−0.2963	−0.3045	−0.3025
	−0.2743	−0.2800	−0.2852	−0.2855	−0.2879	−0.2902	−0.2926	−0.2936	−0.3023	−0.3007
	−0.2479	−0.2603	−0.2704	−0.2743	−0.2793	−0.2834	−0.2872	−0.2892	−0.2987	−0.2977
	−0.2070	−0.2305	−0.2484	−0.2580	−0.2670	−0.2738	−0.2798	−0.2833	−0.2939	−0.2938
	−0.1550	−0.1928	−0.2209	−0.2378	−0.2521	−0.2625	−0.2711	−0.2765	−0.2885	−0.2895
	−0.0863	−0.1408	−0.1821	−0.2092	−0.2309	−0.2464	−0.2588	−0.2669	−0.2809	−0.2835
	−0.0150	−0.0808	−0.1338	−0.1732	−0.2040	−0.2259	−0.2433	−0.2550	−0.2716	−0.2762
	0.0419	−0.0265	−0.0830	−0.1324	−0.1724	−0.2014	−0.2248	−0.2408	−0.2604	−0.2676
	0.0918	0.0448	−0.0164	−0.0762	−0.1263	−0.1648	−0.1967	−0.2193	−0.2437	−0.2546

Figure I.8b: F2B: e=2c & d=4c

	b/c									
a/c	−0.3022	−0.3033	−0.3049	−0.3025	−0.3028	−0.3033	−0.3039	−0.3032	−0.3102	−0.3068
	−0.2947	−0.2974	−0.3002	−0.2988	−0.2998	−0.3008	−0.3019	−0.3016	−0.3088	−0.3056
	−0.2799	−0.2860	−0.2915	−0.2920	−0.2945	−0.2966	−0.2985	−0.2988	−0.3065	−0.3037
	−0.2532	−0.2661	−0.2765	−0.2807	−0.2857	−0.2897	−0.2931	−0.2944	−0.3030	−0.3008
	−0.2118	−0.2360	−0.2543	−0.2642	−0.2733	−0.2801	−0.2856	−0.2885	−0.2981	−0.2969
	−0.1591	−0.1977	−0.2264	−0.2438	−0.2582	−0.2686	−0.2768	−0.2816	−0.2927	−0.2925
	−0.0895	−0.1450	−0.1871	−0.2148	−0.2368	−0.2523	−0.2644	−0.2720	−0.2851	−0.2865
	−0.0170	−0.0841	−0.1382	−0.1783	−0.2095	−0.2316	−0.2488	−0.2600	−0.2756	−0.2791
	0.0409	−0.0288	−0.0865	−0.1368	−0.1774	−0.2067	−0.2300	−0.2456	−0.2645	−0.2705
	0.0920	0.0434	−0.0182	−0.0797	−0.1307	−0.1697	−0.2017	−0.2239	−0.2476	−0.2575

Figure 6.24b: F2B: e=2.5c & d=0.5c

	b/c									
	−0.1446	−0.1481	−0.1535	−0.1532	−0.1528	−0.1720	−0.1777	−0.1893	−0.2159	−0.2336
	−0.1413	−0.1455	−0.1513	−0.1514	−0.1513	−0.1706	−0.1766	−0.1883	−0.2169	−0.2328
	−0.1352	−0.1404	−0.1472	−0.1482	−0.1487	−0.1674	−0.1745	−0.1866	−0.2152	−0.2315
	−0.1243	−0.1317	−0.1402	−0.1427	−0.1443	−0.1634	−0.1712	−0.1839	−0.2108	−0.2294
a/c	−0.1076	−0.1187	−0.1299	−0.1348	−0.1380	−0.1578	−0.1672	−0.1801	−0.2087	−0.2267
	−0.0863	−0.1023	−0.1170	−0.1252	−0.1304	−0.1517	−0.1616	−0.1757	−0.2044	−0.2236
	−0.0564	−0.0792	−0.0988	−0.1116	−0.1198	−0.1411	−0.1531	−0.1696	−0.1974	−0.2193
	−0.0209	−0.0513	−0.0755	−0.0945	−0.1067	−0.1290	−0.1430	−0.1625	−0.1908	−0.2142
	0.0150	−0.0222	−0.0498	−0.0750	−0.0921	−0.1150	−0.1320	−0.1538	−0.1825	−0.2084
	0.0615	0.0216	−0.0127	−0.0449	−0.0712	−0.0943	−0.1153	−0.1405	−0.1712	−0.2004

Figure 6.24b: F2B: e=2.5c & d=1c

	b/c									
	−0.2057	−0.2026	−0.2062	−0.2095	−0.2137	−0.2199	−0.2263	−0.2331	−0.2570	−0.2579
	−0.2019	−0.1994	−0.2035	−0.2072	−0.2118	−0.2183	−0.2250	−0.2319	−0.2560	−0.2570
	−0.1944	−0.1934	−0.1985	−0.2031	−0.2085	−0.2155	−0.2226	−0.2299	−0.2542	−0.2555
	−0.1813	−0.1830	−0.1900	−0.1963	−0.2029	−0.2110	−0.2188	−0.2268	−0.2514	−0.2532
a/c	−0.1613	−0.1675	−0.1775	−0.1864	−0.1950	−0.2045	−0.2136	−0.2224	−0.2475	−0.2501
	−0.1356	−0.1479	−0.1619	−0.1742	−0.1855	−0.1968	−0.2074	−0.2173	−0.2430	−0.2465
	−0.0995	−0.1202	−0.1399	−0.1572	−0.1721	−0.1862	−0.1988	−0.2103	−0.2369	−0.2417
	−0.0562	−0.0866	−0.1129	−0.1363	−0.1557	−0.1731	−0.1884	−0.2019	−0.2295	−0.2359
	−0.0137	−0.0516	−0.0835	−0.1129	−0.1371	−0.1582	−0.1765	−0.1922	−0.2212	−0.2294
	0.0438	−0.0047	−0.0441	−0.0804	−0.1109	−0.1364	−0.1595	−0.1784	−0.2085	−0.2200

Figure 6.24b: F2B: e=2.5c & d=1.5c

	b/c									
	−0.2411	−0.2387	−0.2391	−0.2389	−0.2446	−0.2508	−0.2569	−0.2608	−0.2759	−0.2755
	−0.2369	−0.2352	−0.2362	−0.2365	−0.2426	−0.2491	−0.2554	−0.2595	−0.2748	−0.2745
	−0.2289	−0.2287	−0.2309	−0.2321	−0.2389	−0.2460	−0.2528	−0.2574	−0.2729	−0.2729
	−0.2148	−0.2174	−0.2219	−0.2248	−0.2329	−0.2410	−0.2487	−0.2539	−0.2700	−0.2705
a/c	−0.1932	−0.2006	−0.2086	−0.2141	−0.2243	−0.2339	−0.2429	−0.2491	−0.2660	−0.2671
	−0.1655	−0.1792	−0.1919	−0.2011	−0.2139	−0.2255	−0.2361	−0.2436	−0.2614	−0.2633
	−0.1263	−0.1491	−0.1683	−0.1828	−0.1994	−0.2138	−0.2267	−0.2359	−0.2550	−0.2581
	−0.0792	−0.1123	−0.1390	−0.1602	−0.1815	−0.1994	−0.2153	−0.2267	−0.2472	−0.2520
	−0.0321	−0.0734	−0.1067	−0.1349	−0.1613	−0.1830	−0.2022	−0.2162	−0.2383	−0.2450
	0.0279	−0.0234	−0.0634	−0.0998	−0.1327	−0.1597	−0.1835	−0.2011	−0.2255	−0.2351

Figure 6.24b: F2B: e=2.5c & d=2c

	b/c									
	−0.2636	−0.2622	−0.2624	−0.2601	−0.2626	−0.2669	−0.2731	−0.2779	−0.2898	−0.2896
	−0.2592	−0.2585	−0.2593	−0.2576	−0.2604	−0.2651	−0.2716	−0.2765	−0.2887	−0.2886
	−0.2508	−0.2517	−0.2537	−0.2530	−0.2566	−0.2619	−0.2689	−0.2742	−0.2867	−0.2869
	−0.2361	−0.2399	−0.2443	−0.2453	−0.2504	−0.2567	−0.2646	−0.2706	−0.2837	−0.2843
a/c	−0.2136	−0.2223	−0.2304	−0.2342	−0.2415	−0.2494	−0.2585	−0.2656	−0.2795	−0.2808
	−0.1846	−0.1999	−0.2129	−0.2206	−0.2307	−0.2406	−0.2515	−0.2598	−0.2747	−0.2768
	−0.1436	−0.1683	−0.1884	−0.2015	−0.2157	−0.2285	−0.2417	−0.2518	−0.2681	−0.2714
	−0.0942	−0.1296	−0.1578	−0.1779	−0.1972	−0.2137	−0.2298	−0.2422	−0.2602	−0.2650
	−0.0443	−0.0883	−0.1236	−0.1512	−0.1760	−0.1967	−0.2162	−0.2311	−0.2512	−0.2577
	0.0172	−0.0354	−0.0778	−0.1143	−0.1463	−0.1725	−0.1967	−0.2154	−0.2380	−0.2474

Figure 6.24b: F2B: e=2.5c & d=2.5c

	b/c									
	−0.2787	−0.2781	−0.2787	−0.2759	−0.2768	−0.2789	−0.2827	−0.2859	−0.2973	−0.2978
	−0.2742	−0.2744	−0.2755	−0.2733	−0.2746	−0.2770	−0.2811	−0.2846	−0.2961	−0.2968
	−0.2656	−0.2674	−0.2698	−0.2685	−0.2707	−0.2738	−0.2784	−0.2823	−0.2941	−0.2951
	−0.2505	−0.2553	−0.2601	−0.2607	−0.2643	−0.2685	−0.2740	−0.2787	−0.2910	−0.2924
a/c	−0.2274	−0.2372	−0.2457	−0.2493	−0.2552	−0.2610	−0.2678	−0.2735	−0.2867	−0.2888
	−0.1975	−0.2141	−0.2278	−0.2353	−0.2441	−0.2521	−0.2606	−0.2676	−0.2818	−0.2847
	−0.1554	−0.1815	−0.2025	−0.2156	−0.2287	−0.2397	−0.2507	−0.2594	−0.2751	−0.2792
	−0.1043	−0.1415	−0.1712	−0.1912	−0.2096	−0.2246	−0.2386	−0.2496	−0.2670	−0.2726
	−0.0525	−0.0986	−0.1357	−0.1636	−0.1878	−0.2071	−0.2247	−0.2384	−0.2579	−0.2652
	0.0103	−0.0438	−0.0882	−0.1255	−0.1572	−0.1824	−0.2049	−0.2224	−0.2448	−0.2546

Figure 6.24b: F2B: e=2.5c & d=3c

	b/c									
	−0.2893	−0.2894	−0.2903	−0.2875	−0.2879	−0.2889	−0.2909	−0.2922	−0.3017	−0.3011
	−0.2848	−0.2856	−0.2871	−0.2849	−0.2856	−0.2870	−0.2893	−0.2908	−0.3005	−0.3001
	−0.2760	−0.2785	−0.2813	−0.2801	−0.2817	−0.2837	−0.2865	−0.2885	−0.2985	−0.2983
	−0.2606	−0.2661	−0.2714	−0.2721	−0.2751	−0.2783	−0.2821	−0.2847	−0.2953	−0.2957
a/c	−0.2372	−0.2477	−0.2568	−0.2604	−0.2658	−0.2707	−0.2759	−0.2796	−0.2910	−0.2920
	−0.2067	−0.2241	−0.2384	−0.2461	−0.2546	−0.2617	−0.2686	−0.2736	−0.2860	−0.2879
	−0.1636	−0.1908	−0.2126	−0.2260	−0.2388	−0.2491	−0.2585	−0.2654	−0.2793	−0.2823
	−0.1114	−0.1499	−0.1806	−0.2011	−0.2194	−0.2336	−0.2462	−0.2555	−0.2712	−0.2757
	−0.0582	−0.1058	−0.1444	−0.1728	−0.1971	−0.2159	−0.2321	−0.2442	−0.2619	−0.2682
	0.0059	−0.0496	−0.0957	−0.1338	−0.1658	−0.1907	−0.2120	−0.2280	−0.2488	−0.2576

Figure 6.24b: F2B: e=2.5c & d=3.5c

	b/c									
	−0.2971	−0.2977	−0.2989	−0.2962	−0.2964	−0.2970	−0.2981	−0.2980	−0.3060	−0.3037
	−0.2925	−0.2938	−0.2957	−0.2935	−0.2941	−0.2951	−0.2964	−0.2967	−0.3048	−0.3027
	−0.2836	−0.2865	−0.2897	−0.2886	−0.2901	−0.2917	−0.2936	−0.2943	−0.3028	−0.3010
	−0.2680	−0.2741	−0.2797	−0.2805	−0.2835	−0.2863	−0.2891	−0.2905	−0.2996	−0.2983
a/c	−0.2443	−0.2553	−0.2648	−0.2688	−0.2741	−0.2786	−0.2829	−0.2853	−0.2952	−0.2946
	−0.2133	−0.2314	−0.2462	−0.2542	−0.2626	−0.2694	−0.2755	−0.2793	−0.2903	−0.2905
	−0.1696	−0.1976	−0.2200	−0.2338	−0.2467	−0.2567	−0.2653	−0.2710	−0.2835	−0.2849
	−0.1165	−0.1560	−0.1875	−0.2085	−0.2270	−0.2410	−0.2529	−0.2610	−0.2753	−0.2783
	−0.0622	−0.1110	−0.1507	−0.1797	−0.2043	−0.2229	−0.2386	−0.2496	−0.2660	−0.2707
	0.0035	−0.0538	−0.1012	−0.1400	−0.1725	−0.1974	−0.2183	−0.2333	−0.2528	−0.2600

Figure 6.24b: F2B: e=2.5c & d=4c

	b/c									
	−0.3029	−0.3038	−0.3053	−0.3028	−0.3030	−0.3034	−0.3040	−0.3033	−0.3103	−0.3068
	−0.2983	−0.2999	−0.3021	−0.3001	−0.3007	−0.3015	−0.3024	−0.3019	−0.3091	−0.3058
	−0.2893	−0.2926	−0.2961	−0.2952	−0.2966	−0.2981	−0.2996	−0.2995	−0.3070	−0.3040
	−0.2736	−0.2800	−0.2859	−0.2870	−0.2900	−0.2926	−0.2950	−0.2958	−0.3038	−0.3013
a/c	−0.2496	−0.2611	−0.2709	−0.2751	−0.2805	−0.2849	−0.2887	−0.2905	−0.2995	−0.2977
	−0.2183	−0.2368	−0.2521	−0.2604	−0.2689	−0.2756	−0.2813	−0.2844	−0.2945	−0.2935
	−0.1740	−0.2026	−0.2256	−0.2397	−0.2527	−0.2627	−0.2710	−0.2761	−0.2876	−0.2879
	−0.1203	−0.1605	−0.1926	−0.2141	−0.2328	−0.2469	−0.2584	−0.2660	−0.2794	−0.2812
	−0.0652	−0.1149	−0.1555	−0.1849	−0.2098	−0.2286	−0.2440	−0.2545	−0.2700	−0.2736
	0.0009	−0.0569	−0.1053	−0.1447	−0.1776	−0.2027	−0.2235	−0.2380	−0.2567	−0.2629

Figure I.9b: F2B: e=3c & d=0.5c

	b/c									
a/c	−0.1448	−0.1484	−0.1537	−0.1533	−0.1529	−0.1721	−0.1778	−0.1894	−0.2159	−0.2336
	−0.1427	−0.1465	−0.1521	−0.1520	−0.1518	−0.1710	−0.1769	−0.1886	−0.2170	−0.2329
	−0.1386	−0.1431	−0.1492	−0.1496	−0.1498	−0.1683	−0.1752	−0.1871	−0.2157	−0.2318
	−0.1316	−0.1372	−0.1443	−0.1456	−0.1474	−0.1652	−0.1725	−0.1849	−0.2133	−0.2300
	−0.1210	−0.1285	−0.1371	−0.1399	−0.1416	−0.1615	−0.1690	−0.1817	−0.2085	−0.2275
	−0.1075	−0.1176	−0.1281	−0.1328	−0.1358	−0.1562	−0.1650	−0.1779	−0.2065	−0.2246
	−0.0881	−0.1019	−0.1154	−0.1228	−0.1277	−0.1487	−0.1585	−0.1728	−0.2014	−0.2208
	−0.0638	−0.0825	−0.0997	−0.1106	−0.1178	−0.1385	−0.1500	−0.1666	−0.1947	−0.2162
	−0.0371	−0.0609	−0.0811	−0.0966	−0.1065	−0.1278	−0.1411	−0.1600	−0.1874	−0.2110
	−0.0014	−0.0317	−0.0549	−0.0761	−0.0909	−0.1127	−0.1286	−0.1494	−0.1781	−0.2040

Figure I.9b: F2B: e=3c & d=1c

	b/c									
a/c	−0.2061	−0.2029	−0.2064	−0.2096	−0.2139	−0.2200	−0.2264	−0.2332	−0.2571	−0.2580
	−0.2034	−0.2006	−0.2044	−0.2079	−0.2124	−0.2187	−0.2253	−0.2322	−0.2562	−0.2572
	−0.1985	−0.1965	−0.2009	−0.2049	−0.2098	−0.2165	−0.2234	−0.2305	−0.2547	−0.2559
	−0.1900	−0.1895	−0.1949	−0.1999	−0.2056	−0.2129	−0.2203	−0.2279	−0.2522	−0.2538
	−0.1772	−0.1790	−0.1861	−0.1926	−0.1995	−0.2078	−0.2160	−0.2242	−0.2489	−0.2510
	−0.1608	−0.1659	−0.1751	−0.1836	−0.1922	−0.2017	−0.2109	−0.2198	−0.2450	−0.2478
	−0.1373	−0.1472	−0.1596	−0.1711	−0.1819	−0.1932	−0.2038	−0.2139	−0.2397	−0.2434
	−0.1079	−0.1238	−0.1404	−0.1556	−0.1694	−0.1829	−0.1953	−0.2067	−0.2333	−0.2382
	−0.0751	−0.0976	−0.1185	−0.1380	−0.1551	−0.1712	−0.1856	−0.1986	−0.2261	−0.2324
	−0.0318	−0.0623	−0.0889	−0.1139	−0.1354	−0.1550	−0.1723	−0.1875	−0.2162	−0.2307

Figure I.9b: F2B: e=3c & d=1.5c

	b/c									
a/c	−0.2415	−0.2390	−0.2394	−0.2391	−0.2448	−0.2510	−0.2570	−0.2609	−0.2760	−0.2755
	−0.2386	−0.2365	−0.2373	−0.2373	−0.2432	−0.2496	−0.2558	−0.2598	−0.2750	−0.2747
	−0.2333	−0.2320	−0.2334	−0.2340	−0.2403	−0.2471	−0.2537	−0.2580	−0.2734	−0.2733
	−0.2241	−0.2244	−0.2270	−0.2286	−0.2357	−0.2431	−0.2503	−0.2551	−0.2709	−0.2711
	−0.2103	−0.2130	−0.2176	−0.2207	−0.2291	−0.2375	−0.2455	−0.2510	−0.2674	−0.2681
	−0.1926	−0.1987	−0.2059	−0.2111	−0.2211	−0.2308	−0.2399	−0.2463	−0.2634	−0.2647
	−0.1672	−0.1783	−0.1894	−0.1976	−0.2100	−0.2214	−0.2321	−0.2398	−0.2579	−0.2600
	−0.1354	−0.1528	−0.1687	−0.1810	−0.1963	−0.2101	−0.2227	−0.2319	−0.2511	−0.2544
	−0.0997	−0.1240	−0.1449	−0.1620	−0.1807	−0.1971	−0.2121	−0.2231	−0.2435	−0.2483
	−0.0526	−0.0854	−0.1127	−0.1360	−0.1593	−0.1793	−0.1974	−0.2110	−0.2329	−0.2398

Figure I.9b: F2B: e=3c & d=2c

	b/c									
a/c	−0.2639	−0.2625	−0.2626	−0.2603	−0.2627	−0.2670	−0.2732	−0.2779	−0.2899	−0.2896
	−0.2610	−0.2599	−0.2604	−0.2584	−0.2611	−0.2655	−0.2720	−0.2768	−0.2889	−0.2887
	−0.2554	−0.2552	−0.2564	−0.2549	−0.2581	−0.2630	−0.2698	−0.2749	−0.2872	−0.2873
	−0.2458	−0.2472	−0.2496	−0.2493	−0.2533	−0.2589	−0.2662	−0.2718	−0.2846	−0.2850
	−0.2314	−0.2353	−0.2398	−0.2411	−0.2465	−0.2531	−0.2613	−0.2676	−0.2809	−0.2818
	−0.2129	−0.2203	−0.2275	−0.2311	−0.2382	−0.2461	−0.2554	−0.2626	−0.2767	−0.2782
	−0.1865	−0.1989	−0.2103	−0.2170	−0.2266	−0.2364	−0.2473	−0.2558	−0.2709	−0.2733
	−0.1532	−0.1722	−0.1887	−0.1996	−0.2124	−0.2247	−0.2375	−0.2476	−0.2640	−0.2676
	−0.1157	−0.1419	−0.1640	−0.1796	−0.1962	−0.2112	−0.2264	−0.2383	−0.2562	−0.2611
	−0.0665	−0.1013	−0.1301	−0.1524	−0.1740	−0.1928	−0.2112	−0.2256	−0.2456	−0.2522

Figure I.9b: F2B: e=3c & d=2.5c

	b/c									
a/c	−0.2791	−0.2785	−0.2789	−0.2761	−0.2769	−0.2790	−0.2828	−0.2860	−0.2973	−0.2978
	−0.2760	−0.2758	−0.2766	−0.2741	−0.2752	−0.2775	−0.2815	−0.2849	−0.2963	−0.2969
	−0.2703	−0.2710	−0.2725	−0.2706	−0.2722	−0.2749	−0.2792	−0.2829	−0.2946	−0.2954
	−0.2605	−0.2627	−0.2656	−0.2648	−0.2673	−0.2707	−0.2756	−0.2798	−0.2919	−0.2931
	−0.2457	−0.2505	−0.2555	−0.2563	−0.2603	−0.2648	−0.2706	−0.2755	−0.2882	−0.2899
	−0.2267	−0.2350	−0.2428	−0.2460	−0.2517	−0.2577	−0.2646	−0.2704	−0.2838	−0.2862
	−0.1995	−0.2131	−0.2250	−0.2315	−0.2399	−0.2478	−0.2564	−0.2635	−0.2779	−0.2811
	−0.1653	−0.1856	−0.2028	−0.2136	−0.2253	−0.2358	−0.2464	−0.2552	−0.2709	−0.2752
	−0.1267	−0.1542	−0.1774	−0.1930	−0.2086	−0.2220	−0.2351	−0.2457	−0.2630	−0.2686
	−0.0759	−0.1124	−0.1425	−0.1649	−0.1857	−0.2031	−0.2196	−0.2328	−0.2521	−0.2595

Figure I.9b: F2B: e=3c & d=3c

	b/c									
a/c	−0.2897	−0.2897	−0.2906	−0.2877	−0.2880	−0.2890	−0.2910	−0.2923	−0.3017	−0.3011
	−0.2866	−0.2871	−0.2882	−0.2857	−0.2863	−0.2875	−0.2897	−0.2911	−0.3007	−0.3002
	−0.2808	−0.2821	−0.2840	−0.2821	−0.2832	−0.2849	−0.2874	−0.2891	−0.2990	−0.2987
	−0.2708	−0.2737	−0.2770	−0.2762	−0.2782	−0.2806	−0.2838	−0.2860	−0.2962	−0.2963
	−0.2558	−0.2613	−0.2667	−0.2676	−0.2710	−0.2746	−0.2787	−0.2816	−0.2925	−0.2931
	−0.2364	−0.2455	−0.2538	−0.2571	−0.2623	−0.2673	−0.2726	−0.2765	−0.2881	−0.2894
	−0.2088	−0.2231	−0.2356	−0.2423	−0.2502	−0.2573	−0.2642	−0.2695	−0.2822	−0.2843
	−0.1739	−0.1951	−0.2129	−0.2240	−0.2354	−0.2450	−0.2542	−0.2611	−0.2751	−0.2783
	−0.1344	−0.1630	−0.1869	−0.2029	−0.2184	−0.2310	−0.2427	−0.2515	−0.2671	−0.2717
	−0.0826	−0.1202	−0.1515	−0.1743	−0.1950	−0.2118	−0.2269	−0.2385	−0.2562	−0.2625

Figure I.9b: F2B: e=3c & d=3.5c

	b/c									
a/c	−0.2975	−0.2980	−0.2991	−0.2964	−0.2965	−0.2971	−0.2982	−0.2981	−0.3060	−0.3038
	−0.2943	−0.2953	−0.2968	−0.2944	−0.2948	−0.2956	−0.2968	−0.2970	−0.3050	−0.3029
	−0.2885	−0.2902	−0.2925	−0.2907	−0.2917	−0.2929	−0.2945	−0.2950	−0.3033	−0.3014
	−0.2784	−0.2817	−0.2854	−0.2847	−0.2866	−0.2886	−0.2908	−0.2918	−0.3005	−0.2990
	−0.2632	−0.2692	−0.2749	−0.2760	−0.2793	−0.2825	−0.2857	−0.2874	−0.2967	−0.2957
	−0.2435	−0.2531	−0.2618	−0.2653	−0.2705	−0.2751	−0.2795	−0.2822	−0.2923	−0.2920
	−0.2155	−0.2304	−0.2434	−0.2503	−0.2583	−0.2649	−0.2711	−0.2751	−0.2863	−0.2869
	−0.1801	−0.2020	−0.2204	−0.2317	−0.2432	−0.2525	−0.2609	−0.2666	−0.2792	−0.2809
	−0.1400	−0.1694	−0.1940	−0.2104	−0.2259	−0.2383	−0.2493	−0.2570	−0.2712	−0.2742
	−0.0874	−0.1259	−0.1582	−0.1812	−0.2022	−0.2189	−0.2333	−0.2438	−0.2602	−0.2650

Figure I.9b: F2B: e=3c & d=4c

	b/c									
a/c	−0.3033	−0.3041	−0.3056	−0.3030	−0.3031	−0.3035	−0.3041	−0.3034	−0.3103	−0.3068
	−0.3002	−0.3014	−0.3032	−0.3010	−0.3014	−0.3020	−0.3028	−0.3022	−0.3093	−0.3059
	−0.2942	−0.2963	−0.2989	−0.2973	−0.2982	−0.2993	−0.3005	−0.3002	−0.3075	−0.3044
	−0.2840	−0.2878	−0.2917	−0.2912	−0.2931	−0.2949	−0.2968	−0.2970	−0.3048	−0.3020
	−0.2687	−0.2751	−0.2811	−0.2825	−0.2858	−0.2887	−0.2915	−0.2926	−0.3010	−0.2987
	−0.2489	−0.2589	−0.2679	−0.2716	−0.2769	−0.2813	−0.2853	−0.2874	−0.2965	−0.2950
	−0.2205	−0.2359	−0.2493	−0.2564	−0.2645	−0.2711	−0.2768	−0.2802	−0.2905	−0.2899
	−0.1848	−0.2071	−0.2260	−0.2377	−0.2492	−0.2585	−0.2665	−0.2717	−0.2833	−0.2839
	−0.1441	−0.1741	−0.1992	−0.2160	−0.2317	−0.2442	−0.2548	−0.2620	−0.2753	−0.2771
	−0.0909	−0.1302	−0.1631	−0.1866	−0.2078	−0.2245	−0.2387	−0.2487	−0.2642	−0.2679

Figure 6.21b: F2B: e=3.5c & d=0.5c

	b/c									
a/c	−0.1450	−0.1485	−0.1538	−0.1534	−0.1530	−0.1722	−0.1779	−0.1894	−0.2160	−0.2337
	−0.1435	−0.1471	−0.1526	−0.1524	−0.1521	−0.1713	−0.1771	−0.1888	−0.2153	−0.2331
	−0.1407	−0.1447	−0.1505	−0.1506	−0.1505	−0.1698	−0.1758	−0.1876	−0.2160	−0.2321
	−0.1358	−0.1405	−0.1469	−0.1476	−0.1480	−0.1666	−0.1736	−0.1857	−0.2142	−0.2305
	−0.1287	−0.1345	−0.1417	−0.1433	−0.1443	−0.1631	−0.1705	−0.1830	−0.2112	−0.2283
	−0.1195	−0.1268	−0.1352	−0.1380	−0.1398	−0.1596	−0.1673	−0.1799	−0.2067	−0.2258
	−0.1065	−0.1159	−0.1261	−0.1306	−0.1336	−0.1537	−0.1617	−0.1756	−0.2040	−0.2224
	−0.0900	−0.1023	−0.1147	−0.1214	−0.1259	−0.1458	−0.1558	−0.1704	−0.1974	−0.2183
	−0.0708	−0.0865	−0.1015	−0.1109	−0.1171	−0.1373	−0.1482	−0.1646	−0.1917	−0.2137
	−0.0448	−0.0650	−0.0828	−0.0964	−0.1051	−0.1256	−0.1384	−0.1569	−0.1841	−0.2076

Figure 6.21b: F2B: e=3.5c & d=1c

	b/c									
a/c	−0.2063	−0.2031	−0.2065	−0.2097	−0.214	−0.2201	−0.2265	−0.2332	−0.2571	−0.258
	−0.2044	−0.2014	−0.2051	−0.2084	−0.2128	−0.2191	−0.2256	−0.2324	−0.2564	−0.2573
	−0.2009	−0.1984	−0.2024	−0.2061	−0.2108	−0.2173	−0.224	−0.231	−0.2551	−0.2562
	−0.195	−0.1934	−0.1981	−0.2023	−0.2075	−0.2144	−0.2215	−0.2288	−0.253	−0.2544
	−0.1863	−0.186	−0.1916	−0.1968	−0.2028	−0.2104	−0.2179	−0.2257	−0.2501	−0.252
	−0.1752	−0.1768	−0.1837	−0.1901	−0.1971	−0.2055	−0.2138	−0.222	−0.2468	−0.2491
	−0.1593	−0.1637	−0.1724	−0.1807	−0.1891	−0.1987	−0.208	−0.217	−0.2422	−0.2452
	−0.1392	−0.1472	−0.1584	−0.1691	−0.1794	−0.1905	−0.201	−0.211	−0.2368	−0.2407
	−0.1158	−0.1281	−0.1422	−0.1557	−0.1682	−0.1811	−0.193	−0.2042	−0.2306	−0.2355
	−0.0841	−0.1022	−0.1202	−0.1374	−0.153	−0.1683	−0.1822	−0.195	−0.2222	−0.2286

Figure 6.21b: F2B: e=3.5c & d=1.5c

	b/c									
a/c	−0.2417	−0.2392	−0.2395	−0.2392	−0.2449	−0.251	−0.2571	−0.2609	−0.276	−0.2756
	−0.2397	−0.2374	−0.2379	−0.2378	−0.2436	−0.2499	−0.2561	−0.26	−0.2752	−0.2748
	−0.2359	−0.2341	−0.2351	−0.2353	−0.2414	−0.248	−0.2544	−0.2585	−0.2738	−0.2736
	−0.2295	−0.2286	−0.2303	−0.2312	−0.2378	−0.2448	−0.2516	−0.2561	−0.2717	−0.2717
	−0.22	−0.2206	−0.2235	−0.2253	−0.2326	−0.2403	−0.2477	−0.2527	−0.2687	−0.2691
	−0.208	−0.2105	−0.2149	−0.218	−0.2264	−0.2349	−0.243	−0.2487	−0.2652	−0.2661
	−0.1908	−0.1961	−0.2029	−0.2079	−0.2178	−0.2274	−0.2366	−0.2432	−0.2605	−0.2619
	−0.1691	−0.1782	−0.1881	−0.1953	−0.2071	−0.2184	−0.2289	−0.2366	−0.2548	−0.257
	−0.1437	−0.1573	−0.1706	−0.1809	−0.1949	−0.208	−0.2201	−0.2291	−0.2482	−0.2516
	−0.1094	−0.129	−0.1466	−0.1612	−0.1784	−0.1939	−0.2082	−0.219	−0.2393	−0.2442

Figure 6.21b: F2B: e=3.5c & d=2c

	b/c									
a/c	−0.2642	−0.2627	−0.2627	−0.2604	−0.2628	−0.2671	−0.2733	−0.278	−0.2899	−0.2896
	−0.262	−0.2608	−0.2611	−0.2589	−0.2615	−0.2659	−0.2723	−0.2771	−0.2891	−0.2889
	−0.2581	−0.2573	−0.2581	−0.2563	−0.2592	−0.2639	−0.2704	−0.2755	−0.2877	−0.2876
	−0.2514	−0.2516	−0.2531	−0.252	−0.2555	−0.2606	−0.2675	−0.2729	−0.2854	−0.2856
	−0.2415	−0.2432	−0.2459	−0.2458	−0.2501	−0.2559	−0.2635	−0.2693	−0.2823	−0.2829
	−0.229	−0.2326	−0.237	−0.2382	−0.2437	−0.2503	−0.2586	−0.2651	−0.2786	−0.2797
	−0.2111	−0.2176	−0.2244	−0.2276	−0.2347	−0.2426	−0.252	−0.2594	−0.2736	−0.2754
	−0.1884	−0.1988	−0.2087	−0.2145	−0.2236	−0.2332	−0.2439	−0.2525	−0.2677	−0.2703
	−0.1619	−0.1768	−0.1905	−0.1994	−0.211	−0.2224	−0.2348	−0.2446	−0.2609	−0.2645
	−0.126	−0.1471	−0.1658	−0.1788	−0.1938	−0.2078	−0.2224	−0.2341	−0.2519	−0.2568

Figure 6.21b: F2B: e=3.5c & d=2.5c

	b/c									
a/c	−0.2793	−0.2786	−0.2791	−0.2762	−0.277	−0.2791	−0.2829	−0.2861	−0.2974	−0.2979
	−0.2771	−0.2767	−0.2773	−0.2747	−0.2757	−0.2779	−0.2818	−0.2851	−0.2965	−0.2971
	−0.273	−0.2732	−0.2742	−0.272	−0.2733	−0.2758	−0.2799	−0.2835	−0.2951	−0.2958
	−0.2662	−0.2672	−0.2691	−0.2675	−0.2695	−0.2725	−0.277	−0.2809	−0.2927	−0.2937
	−0.2561	−0.2586	−0.2617	−0.2612	−0.264	−0.2677	−0.2728	−0.2772	−0.2895	−0.2909
	−0.2432	−0.2477	−0.2525	−0.2534	−0.2574	−0.262	−0.2679	−0.273	−0.2858	−0.2877
	−0.2248	−0.2323	−0.2395	−0.2424	−0.2481	−0.2541	−0.2611	−0.2671	−0.2807	−0.2832
	−0.2015	−0.2129	−0.2234	−0.2289	−0.2368	−0.2445	−0.253	−0.2601	−0.2746	−0.278
	−0.1743	−0.1903	−0.2046	−0.2133	−0.2238	−0.2334	−0.2436	−0.2521	−0.2678	−0.2722
	−0.1374	−0.1597	−0.1791	−0.1921	−0.2061	−0.2185	−0.231	−0.2414	−0.2585	−0.2642

Figure 6.21b: F2B: e=3.5c & d=3c

	b/c									
a/c	−0.29	−0.2899	−0.2907	−0.2878	−0.2881	−0.2891	−0.2911	−0.2923	−0.3018	−0.3012
	−0.2877	−0.288	−0.289	−0.2863	−0.2867	−0.2879	−0.29	−0.2913	−0.3009	−0.3004
	−0.2836	−0.2843	−0.2858	−0.2835	−0.2843	−0.2858	−0.2881	−0.2897	−0.2994	−0.2991
	−0.2766	−0.2783	−0.2806	−0.279	−0.2804	−0.2823	−0.2851	−0.287	−0.2971	−0.297
	−0.2663	−0.2695	−0.273	−0.2725	−0.2748	−0.2775	−0.2809	−0.2834	−0.2939	−0.2942
	−0.2532	−0.2584	−0.2636	−0.2645	−0.2681	−0.2717	−0.2759	−0.2791	−0.2901	−0.2909
	−0.2345	−0.2427	−0.2504	−0.2534	−0.2586	−0.2637	−0.2691	−0.2731	−0.2849	−0.2864
	−0.2108	−0.2229	−0.2339	−0.2397	−0.2471	−0.2539	−0.2608	−0.266	−0.2788	−0.2811
	−0.183	−0.1999	−0.2148	−0.2237	−0.2338	−0.2426	−0.2513	−0.258	−0.2719	−0.2752
	−0.1455	−0.1687	−0.1888	−0.2021	−0.2158	−0.2274	−0.2385	−0.2471	−0.2626	−0.2668

Figure 6.21b: F2B: e=3.5c & d=3.5c

	b/c									
a/c	−0.2977	−0.2982	−0.2993	−0.2966	−0.2966	−0.2972	−0.2982	−0.2982	−0.3061	−0.3038
	−0.2955	−0.2962	−0.2975	−0.295	−0.2953	−0.296	−0.2971	−0.2972	−0.3052	−0.3031
	−0.2913	−0.2925	−0.2943	−0.2922	−0.2928	−0.2938	−0.2952	−0.2955	−0.3037	−0.3017
	−0.2843	−0.2864	−0.289	−0.2876	−0.2888	−0.2903	−0.2922	−0.2929	−0.3014	−0.2997
	−0.2738	−0.2775	−0.2814	−0.281	−0.2832	−0.2854	−0.288	−0.2892	−0.2981	−0.2968
	−0.2605	−0.2662	−0.2718	−0.2729	−0.2763	−0.2795	−0.2829	−0.2848	−0.2943	−0.2935
	−0.2416	−0.2503	−0.2584	−0.2616	−0.2668	−0.2714	−0.276	−0.2788	−0.2891	−0.289
	−0.2176	−0.2303	−0.2417	−0.2477	−0.2551	−0.2615	−0.2676	−0.2716	−0.283	−0.2837
	−0.1894	−0.2069	−0.2222	−0.2315	−0.2416	−0.2501	−0.258	−0.2635	−0.276	−0.2777
	−0.1514	−0.1752	−0.1959	−0.2095	−0.2233	−0.2347	−0.245	−0.2525	−0.2666	−0.2697

Figure 6.21b: F2B: e=3.5c & d=4c

	b/c									
a/c	−0.3036	−0.3043	−0.3057	−0.3032	−0.3032	−0.3036	−0.3042	−0.3034	−0.3104	−0.3069
	−0.3013	−0.3023	−0.3039	−0.3016	−0.3018	−0.3024	−0.3031	−0.3025	−0.3095	−0.3061
	−0.2971	−0.2986	−0.3007	−0.2988	−0.2994	−0.3002	−0.3012	−0.3008	−0.308	−0.3048
	−0.29	−0.2925	−0.2954	−0.2941	−0.2954	−0.2967	−0.2981	−0.2981	−0.3056	−0.3027
	−0.2795	−0.2835	−0.2876	−0.2875	−0.2896	−0.2918	−0.2939	−0.2944	−0.3024	−0.2998
	−0.266	−0.2721	−0.278	−0.2793	−0.2827	−0.2858	−0.2888	−0.29	−0.2985	−0.2965
	−0.2469	−0.256	−0.2645	−0.2679	−0.2731	−0.2776	−0.2817	−0.2839	−0.2933	−0.292
	−0.2227	−0.2358	−0.2476	−0.2538	−0.2612	−0.2676	−0.2733	−0.2767	−0.2871	−0.2867
	−0.1942	−0.2121	−0.2279	−0.2374	−0.2476	−0.2561	−0.2636	−0.2685	−0.2801	−0.2807
	−0.1558	−0.1801	−0.2012	−0.2152	−0.2291	−0.2405	−0.2505	−0.2574	−0.2707	−0.2726

Figure I.10b: F2B: e=4c & d=0.5c

	b/c									
a/c	−0.1451	−0.1486	−0.1539	−0.1535	−0.1531	−0.1722	−0.1779	−0.1895	−0.2160	−0.2337
	−0.1440	−0.1476	−0.1530	−0.1527	−0.1524	−0.1715	−0.1773	−0.1889	−0.2154	−0.2332
	−0.1419	−0.1457	−0.1513	−0.1513	−0.1511	−0.1703	−0.1762	−0.1879	−0.2164	−0.2326
	−0.1384	−0.1427	−0.1486	−0.1490	−0.1491	−0.1676	−0.1744	−0.1863	−0.2148	−0.2308
	−0.1333	−0.1382	−0.1447	−0.1457	−0.1462	−0.1648	−0.1719	−0.1841	−0.2124	−0.2290
	−0.1269	−0.1327	−0.1399	−0.1417	−0.1427	−0.1622	−0.1690	−0.1815	−0.2090	−0.2268
	−0.1177	−0.1248	−0.1331	−0.1360	−0.1378	−0.1567	−0.1655	−0.1779	−0.2046	−0.2239
	−0.1061	−0.1150	−0.1247	−0.1290	−0.1318	−0.1517	−0.1604	−0.1736	−0.2000	−0.2203
	−0.0925	−0.1034	−0.1149	−0.1209	−0.1249	−0.1452	−0.1543	−0.1687	−0.1962	−0.2163
	−0.0737	−0.0877	−0.1015	−0.1099	−0.1156	−0.1352	−0.1458	−0.1621	−0.1889	−0.2110

Figure I.10b: F2B: e=4c & d=1c

	b/c									
a/c	−0.2064	−0.2032	−0.2066	−0.2098	−0.214	−0.2201	−0.2265	−0.2333	−0.2572	−0.258
	−0.205	−0.2019	−0.2055	−0.2088	−0.2131	−0.2193	−0.2258	−0.2326	−0.2565	−0.2574
	−0.2024	−0.1997	−0.2035	−0.207	−0.2115	−0.2179	−0.2245	−0.2314	−0.2554	−0.2565
	−0.1981	−0.1959	−0.2002	−0.204	−0.2089	−0.2156	−0.2224	−0.2295	−0.2537	−0.2549
	−0.1918	−0.1905	−0.1953	−0.1998	−0.2052	−0.2123	−0.2195	−0.227	−0.2512	−0.2528
	−0.1839	−0.1837	−0.1894	−0.1946	−0.2007	−0.2084	−0.2161	−0.2239	−0.2484	−0.2503
	−0.1727	−0.1742	−0.181	−0.1874	−0.1945	−0.2029	−0.2113	−0.2197	−0.2445	−0.247
	−0.1585	−0.1623	−0.1705	−0.1785	−0.1868	−0.1963	−0.2056	−0.2147	−0.2398	−0.243
	−0.1418	−0.1483	−0.1584	−0.1682	−0.178	−0.1887	−0.199	−0.2089	−0.2345	−0.2384
	−0.1189	−0.1292	−0.1419	−0.1542	−0.1661	−0.1785	−0.1902	−0.2012	−0.2274	−0.2324

Figure I.10b: F2B: e=4c & d=1.5c

	b/c									
a/c	−0.2419	−0.2393	−0.2396	−0.2393	−0.2449	−0.2511	−0.2571	−0.261	−0.276	−0.2756
	−0.2403	−0.2379	−0.2384	−0.2382	−0.2439	−0.2502	−0.2563	−0.2602	−0.2754	−0.275
	−0.2375	−0.2354	−0.2362	−0.2362	−0.2422	−0.2486	−0.2549	−0.2589	−0.2742	−0.2739
	−0.2328	−0.2313	−0.2326	−0.233	−0.2393	−0.246	−0.2526	−0.2569	−0.2724	−0.2723
	−0.226	−0.2254	−0.2274	−0.2285	−0.2352	−0.2424	−0.2494	−0.2541	−0.2698	−0.27
	−0.2174	−0.218	−0.221	−0.2229	−0.2303	−0.238	−0.2456	−0.2507	−0.2668	−0.2674
	−0.2052	−0.2076	−0.212	−0.2151	−0.2235	−0.232	−0.2403	−0.2461	−0.2628	−0.2638
	−0.1898	−0.1945	−0.2008	−0.2055	−0.2151	−0.2247	−0.2339	−0.2405	−0.2579	−0.2595
	−0.1717	−0.1792	−0.1878	−0.1943	−0.2055	−0.2163	−0.2267	−0.2342	−0.2524	−0.2547
	−0.1469	−0.1583	−0.17	−0.1792	−0.1925	−0.205	−0.2169	−0.2258	−0.2448	−0.2482

Figure I.10b: F2B: e=4c & d=2c

	b/c									
a/c	−0.2643	−0.2628	−0.2629	−0.2605	−0.2629	−0.2671	−0.2734	−0.278	−0.29	−0.2897
	−0.2627	−0.2613	−0.2616	−0.2593	−0.2618	−0.2662	−0.2725	−0.2773	−0.2893	−0.289
	−0.2598	−0.2587	−0.2592	−0.2573	−0.26	−0.2645	−0.271	−0.2759	−0.2881	−0.2879
	−0.2549	−0.2544	−0.2554	−0.2539	−0.257	−0.2619	−0.2686	−0.2738	−0.2861	−0.2862
	−0.2477	−0.2482	−0.25	−0.2491	−0.2528	−0.2581	−0.2652	−0.2708	−0.2834	−0.2838
	−0.2388	−0.2404	−0.2433	−0.2433	−0.2477	−0.2536	−0.2613	−0.2672	−0.2803	−0.281
	−0.226	−0.2295	−0.2338	−0.2351	−0.2406	−0.2474	−0.2558	−0.2624	−0.276	−0.2773
	−0.21	−0.2158	−0.2221	−0.2251	−0.2319	−0.2398	−0.2491	−0.2566	−0.2709	−0.2728
	−0.191	−0.1997	−0.2084	−0.2134	−0.2219	−0.2311	−0.2416	−0.25	−0.2651	−0.2678
	−0.1652	−0.1778	−0.1898	−0.1976	−0.2084	−0.2193	−0.2314	−0.2411	−0.2574	−0.261

Figure I.10b: F2B: e=4c & d=2.5c

	b/c									
a/c	−0.2795	−0.2788	−0.2792	−0.2763	−0.2771	−0.2792	−0.2829	−0.2861	−0.2974	−0.2979
	−0.2778	−0.2773	−0.2778	−0.2751	−0.276	−0.2782	−0.282	−0.2853	−0.2967	−0.2972
	−0.2748	−0.2746	−0.2754	−0.273	−0.2741	−0.2765	−0.2805	−0.2839	−0.2954	−0.2961
	−0.2698	−0.2702	−0.2715	−0.2695	−0.2711	−0.2738	−0.2781	−0.2818	−0.2935	−0.2943
	−0.2624	−0.2638	−0.2659	−0.2646	−0.2667	−0.2699	−0.2746	−0.2787	−0.2907	−0.2919
	−0.2532	−0.2558	−0.2589	−0.2585	−0.2615	−0.2653	−0.2706	−0.2751	−0.2875	−0.289
	−0.2402	−0.2445	−0.2492	−0.2501	−0.2542	−0.2589	−0.265	−0.2702	−0.2832	−0.2852
	−0.2237	−0.2304	−0.2372	−0.2398	−0.2453	−0.2512	−0.2582	−0.2643	−0.2779	−0.2806
	−0.2042	−0.2138	−0.223	−0.2277	−0.235	−0.2422	−0.2505	−0.2575	−0.272	−0.2754
	−0.1777	−0.1913	−0.2039	−0.2114	−0.221	−0.2303	−0.2402	−0.2485	−0.2641	−0.2685

Figure I.10b: F2B: e=4c & d=3c

	b/c									
a/c	−0.2901	−0.2901	−0.2908	−0.2879	−0.2882	−0.2892	−0.2911	−0.2924	−0.3018	−0.3012
	−0.2884	−0.2885	−0.2895	−0.2867	−0.2871	−0.2882	−0.2902	−0.2915	−0.3011	−0.3005
	−0.2854	−0.2858	−0.287	−0.2845	−0.2852	−0.2865	−0.2887	−0.2902	−0.2998	−0.2994
	−0.2803	−0.2813	−0.283	−0.281	−0.282	−0.2837	−0.2862	−0.2879	−0.2978	−0.2976
	−0.2728	−0.2748	−0.2773	−0.276	−0.2776	−0.2798	−0.2827	−0.2848	−0.2951	−0.2951
	−0.2634	−0.2666	−0.2702	−0.2698	−0.2722	−0.275	−0.2786	−0.2812	−0.2918	−0.2923
	−0.2502	−0.2552	−0.2603	−0.2613	−0.2648	−0.2686	−0.273	−0.2762	−0.2874	−0.2884
	−0.2334	−0.2408	−0.248	−0.2507	−0.2557	−0.2607	−0.2661	−0.2702	−0.2822	−0.2837
	−0.2135	−0.2239	−0.2336	−0.2384	−0.2452	−0.2516	−0.2583	−0.2634	−0.2762	−0.2785
	−0.1865	−0.2009	−0.2141	−0.2217	−0.231	−0.2394	−0.2478	−0.2543	−0.2682	−0.2716

Figure I.10b: F2B: e=4c & d=3.5c

	b/c									
a/c	−0.2979	−0.2983	−0.2994	−0.2966	−0.2967	−0.2973	−0.2983	−0.2982	−0.3061	−0.3039
	−0.2962	−0.2968	−0.298	−0.2954	−0.2956	−0.2963	−0.2974	−0.2974	−0.3054	−0.3032
	−0.2931	−0.294	−0.2956	−0.2932	−0.2936	−0.2945	−0.2958	−0.296	−0.3041	−0.302
	−0.2879	−0.2894	−0.2915	−0.2896	−0.2905	−0.2917	−0.2933	−0.2938	−0.3021	−0.3002
	−0.2804	−0.2828	−0.2857	−0.2845	−0.286	−0.2877	−0.2898	−0.2906	−0.2993	−0.2978
	−0.2709	−0.2746	−0.2785	−0.2783	−0.2806	−0.2829	−0.2856	−0.287	−0.2961	−0.2949
	−0.2575	−0.2629	−0.2685	−0.2696	−0.273	−0.2764	−0.2799	−0.2819	−0.2916	−0.291
	−0.2405	−0.2484	−0.256	−0.2588	−0.2638	−0.2684	−0.273	−0.2759	−0.2863	−0.2863
	−0.2204	−0.2312	−0.2413	−0.2464	−0.2531	−0.2592	−0.265	−0.269	−0.2803	−0.2811
	−0.193	−0.208	−0.2215	−0.2295	−0.2387	−0.2468	−0.2544	−0.2598	−0.2723	−0.2741

Figure I.10b: F2B: e=4c & d=4c

	b/c									
a/c	−0.3037	−0.3045	−0.3059	−0.3033	−0.3033	−0.3037	−0.3043	−0.3035	−0.3104	−0.3069
	−0.302	−0.3029	−0.3045	−0.302	−0.3022	−0.3027	−0.3034	−0.3027	−0.3097	−0.3062
	−0.2989	−0.3001	−0.302	−0.2998	−0.3002	−0.3009	−0.3018	−0.3013	−0.3084	−0.3051
	−0.2937	−0.2955	−0.2979	−0.2962	−0.297	−0.2981	−0.2992	−0.299	−0.3064	−0.3033
	−0.2861	−0.2888	−0.292	−0.291	−0.2925	−0.2941	−0.2957	−0.2959	−0.3036	−0.3008
	−0.2765	−0.2805	−0.2847	−0.2847	−0.287	−0.2892	−0.2915	−0.2921	−0.3003	−0.2979
	−0.2629	−0.2688	−0.2746	−0.2759	−0.2794	−0.2826	−0.2857	−0.2871	−0.2958	−0.294
	−0.2458	−0.2541	−0.262	−0.2651	−0.2701	−0.2745	−0.2787	−0.281	−0.2905	−0.2893
	−0.2255	−0.2368	−0.2472	−0.2524	−0.2593	−0.2652	−0.2707	−0.274	−0.2844	−0.284
	−0.1979	−0.2133	−0.2272	−0.2354	−0.2447	−0.2527	−0.26	−0.2648	−0.2764	−0.277

Figure 6.22a: F1B: e=0.5b & d=0.5b

	c/b									
a/b	0.4646	0.4646	0.4647	0.4647	0.4646	0.4648	0.4664	0.4477	0.3352	0.2375
	0.4643	0.4643	0.4644	0.4644	0.4643	0.4645	0.4661	0.4474	0.3348	0.2361
	0.464	0.464	0.464	0.4641	0.464	0.4642	0.4657	0.447	0.3344	0.236
	0.4633	0.4633	0.4634	0.4634	0.4633	0.4635	0.4651	0.4463	0.3336	0.2351
	0.4623	0.4623	0.4623	0.4624	0.4623	0.4625	0.464	0.4451	0.3323	0.2336
	0.4612	0.4612	0.4612	0.4612	0.4611	0.4613	0.4629	0.4439	0.3248	0.2325
	0.4589	0.4589	0.4589	0.4589	0.4589	0.459	0.4606	0.4414	0.3275	0.2296
	0.4552	0.4552	0.4552	0.4552	0.4552	0.4553	0.4569	0.4374	0.3235	0.2252
	0.4478	0.4479	0.4478	0.4479	0.4478	0.448	0.4494	0.4296	0.3146	0.2179
	0.4288	0.4288	0.4288	0.4288	0.4288	0.4289	0.4303	0.4097	0.2957	0.1982

Figure 6.22a: F1B: e=0.5b & d=1b

	c/b									
a/b	0.4646	0.4646	0.4646	0.4646	0.4643	0.4567	0.4266	0.3729	0.3211	0.2636
	0.4643	0.4643	0.4643	0.4643	0.464	0.4564	0.426	0.3724	0.3206	0.2631
	0.464	0.464	0.4639	0.4639	0.4637	0.4561	0.4256	0.3721	0.3203	0.2628
	0.4633	0.4633	0.4633	0.4633	0.463	0.4554	0.4248	0.3712	0.3195	0.262
	0.4623	0.4623	0.4622	0.4622	0.462	0.4543	0.4237	0.3698	0.3183	0.2608
	0.4612	0.4612	0.4611	0.4611	0.4608	0.4532	0.4223	0.3684	0.317	0.2597
	0.4589	0.4589	0.4588	0.4588	0.4585	0.4508	0.4197	0.3655	0.3144	0.2571
	0.4552	0.4552	0.4551	0.4551	0.4548	0.447	0.4157	0.361	0.3104	0.2532
	0.4479	0.4478	0.4478	0.4478	0.4475	0.4395	0.4078	0.3526	0.3028	0.2459
	0.4288	0.4288	0.4287	0.4287	0.4284	0.4202	0.3878	0.3318	0.284	0.2281

Figure 6.22a: F1B: e=0.5b & d=1.5b

	c/b									
a/b	0.4646	0.465	0.4669	0.4679	0.4567	0.4307	0.3873	0.3491	0.3221	0.285
	0.4643	0.4647	0.4666	0.4676	0.4564	0.4303	0.3869	0.3487	0.3217	0.2846
	0.464	0.4644	0.4663	0.4672	0.456	0.4299	0.3865	0.3484	0.3214	0.2843
	0.4633	0.4637	0.4656	0.4665	0.4553	0.4291	0.3857	0.3476	0.3206	0.2836
	0.4623	0.4627	0.4645	0.4654	0.4541	0.4279	0.3845	0.3464	0.3195	0.2825
	0.4611	0.4615	0.4634	0.4643	0.4528	0.4265	0.3832	0.3451	0.3183	0.2814
	0.4589	0.4592	0.4611	0.4619	0.4503	0.4238	0.3805	0.3426	0.3159	0.279
	0.4552	0.4555	0.4574	0.458	0.4462	0.4196	0.3764	0.3386	0.3121	0.2754
	0.4478	0.4482	0.4499	0.4505	0.4384	0.4116	0.3686	0.3312	0.3049	0.2684
	0.4288	0.4291	0.4308	0.431	0.4181	0.3912	0.3488	0.3122	0.2868	0.2514

Figure 6.22a: F1B: e=0.5b & d=2b

	c/b									
a/b	0.4657	0.468	0.4662	0.4512	0.425	0.4027	0.3731	0.3482	0.3285	0.3028
	0.4654	0.4677	0.4658	0.4509	0.4247	0.4024	0.3727	0.3478	0.3282	0.3025
	0.4651	0.4673	0.4655	0.4505	0.4243	0.402	0.3724	0.3475	0.3279	0.3022
	0.4644	0.4666	0.4648	0.4498	0.4236	0.4013	0.3717	0.3468	0.3272	0.3016
	0.4633	0.4656	0.4637	0.4486	0.4224	0.4002	0.3705	0.3457	0.3262	0.3005
	0.4622	0.4644	0.4625	0.4474	0.4212	0.399	0.3694	0.3446	0.3251	0.2995
	0.4599	0.4621	0.46	0.4449	0.4187	0.3965	0.367	0.3423	0.3228	0.2973
	0.4562	0.4583	0.4561	0.4409	0.4147	0.3926	0.3632	0.3386	0.3192	0.2938
	0.4488	0.4509	0.4485	0.4332	0.4071	0.3852	0.356	0.3316	0.3124	0.2873
	0.4297	0.4316	0.4289	0.4134	0.3875	0.366	0.3373	0.3135	0.2949	0.2703

Figure 6.22a: F1B: e=0.5b & d=2.5b

	c/b									
a/b	0.4646	0.4604	0.4506	0.4333	0.4122	0.3954	0.374	0.3557	0.3399	0.3209
	0.4643	0.4601	0.4503	0.433	0.4119	0.3951	0.3737	0.3554	0.3396	0.3206
	0.464	0.4598	0.4499	0.4327	0.4115	0.3948	0.3733	0.3551	0.3393	0.3203
	0.4633	0.4591	0.4492	0.432	0.4109	0.3941	0.3727	0.3544	0.3387	0.3196
	0.4623	0.458	0.4482	0.4309	0.4098	0.3931	0.3717	0.3534	0.3377	0.3187
	0.4611	0.4569	0.447	0.4297	0.4087	0.3919	0.3706	0.3523	0.3367	0.3177
	0.4588	0.4545	0.4446	0.4274	0.4063	0.3897	0.3683	0.3502	0.3345	0.3156
	0.4551	0.4508	0.4409	0.4236	0.4026	0.386	0.3648	0.3467	0.3311	0.3122
	0.4478	0.4434	0.4335	0.4163	0.3954	0.3789	0.3578	0.3399	0.3245	0.3056
	0.4286	0.4241	0.4142	0.3972	0.3766	0.3605	0.3397	0.3222	0.3072	0.2889

Figure 6.22a: F1B: e=0.5b & d=3b

	c/b									
a/b	0.4626	0.4559	0.4458	0.4313	0.4149	0.4016	0.3851	0.3706	0.3574	0.3423
	0.4623	0.4556	0.4454	0.431	0.4146	0.4013	0.3848	0.3703	0.3571	0.342
	0.462	0.4553	0.4451	0.4307	0.4143	0.4009	0.3845	0.37	0.3568	0.3417
	0.4613	0.4546	0.4444	0.43	0.4137	0.4003	0.3838	0.3693	0.3562	0.3411
	0.4603	0.4536	0.4434	0.429	0.4126	0.3993	0.3828	0.3684	0.3553	0.3401
	0.4592	0.4525	0.4423	0.4279	0.4115	0.3982	0.3818	0.3673	0.3543	0.3391
	0.4569	0.4502	0.44	0.4256	0.4093	0.396	0.3796	0.3652	0.3521	0.337
	0.4532	0.4464	0.4363	0.422	0.4057	0.3924	0.3761	0.3617	0.3487	0.3337
	0.4459	0.4391	0.429	0.4148	0.3986	0.3854	0.3692	0.3549	0.3421	0.3272
	0.4267	0.4201	0.4101	0.396	0.3801	0.3672	0.3512	0.3373	0.3248	0.3101

Figure 6.22a: F1B: e=0.5b & d=3.5b

	c/b									
a/b	0.4624	0.4562	0.4476	0.4362	0.4233	0.4124	0.3993	0.3874	0.3763	0.3638
	0.4621	0.4559	0.4473	0.4359	0.423	0.4121	0.399	0.3871	0.376	0.3635
	0.4618	0.4556	0.447	0.4355	0.4227	0.4118	0.3987	0.3868	0.3757	0.3632
	0.4611	0.4549	0.4463	0.4349	0.4221	0.4112	0.3981	0.3862	0.3751	0.3626
	0.4601	0.4539	0.4453	0.4339	0.4211	0.4102	0.3971	0.3852	0.3741	0.3616
	0.4589	0.4528	0.4441	0.4327	0.42	0.4091	0.396	0.3841	0.3731	0.3606
	0.4566	0.4505	0.4419	0.4305	0.4177	0.4069	0.3938	0.382	0.3709	0.3585
	0.4529	0.4468	0.4382	0.4269	0.4141	0.4033	0.3903	0.3785	0.3675	0.3551
	0.4457	0.4395	0.431	0.4197	0.4071	0.3963	0.3834	0.3717	0.3608	0.3485
	0.4266	0.4205	0.4121	0.401	0.3885	0.378	0.3653	0.3538	0.3432	0.3312

Figure 6.22a: F1B: e=0.5b & d=4b

	c/b									
a/b	0.4627	0.4577	0.4508	0.4418	0.4317	0.4228	0.4121	0.4022	0.3928	0.3823
	0.4624	0.4574	0.4505	0.4415	0.4314	0.4225	0.4119	0.4019	0.3925	0.3820
	0.4621	0.4571	0.4502	0.4412	0.4311	0.4221	0.4115	0.4016	0.3922	0.3817
	0.4614	0.4564	0.4495	0.4406	0.4305	0.4215	0.4109	0.4010	0.3916	0.3811
	0.4604	0.4554	0.4485	0.4395	0.4294	0.4205	0.4099	0.4000	0.3906	0.3801
	0.4593	0.4543	0.4474	0.4384	0.4283	0.4194	0.4088	0.3989	0.3896	0.3791
	0.4570	0.4520	0.4451	0.4362	0.4261	0.4172	0.4066	0.3968	0.3874	0.3769
	0.4533	0.4483	0.4414	0.4325	0.4225	0.4136	0.4031	0.3933	0.3840	0.3735
	0.4460	0.4411	0.4342	0.4254	0.4154	0.4066	0.3961	0.3864	0.3772	0.3668
	0.4269	0.4220	0.4153	0.4066	0.3968	0.3882	0.3779	0.3684	0.3593	0.3492

Figure I.11a: F1B: e=1b & d=0.5b

	c/b									
a/b	0.4645	0.4645	0.4646	0.4646	0.4645	0.4647	0.4663	0.4476	0.3351	0.2369
	0.4639	0.4639	0.464	0.464	0.4639	0.4641	0.4657	0.447	0.3344	0.2361
	0.463	0.463	0.4631	0.4631	0.463	0.4632	0.4648	0.446	0.3334	0.2348
	0.4617	0.4617	0.4618	0.4618	0.4617	0.4619	0.4635	0.4446	0.3319	0.2332
	0.4599	0.4599	0.4599	0.4599	0.4598	0.46	0.4616	0.4426	0.3298	0.2314
	0.4577	0.4577	0.4577	0.4578	0.4577	0.4579	0.4594	0.4403	0.3274	0.2293
	0.4541	0.4541	0.4541	0.4541	0.454	0.4542	0.4557	0.4364	0.3236	0.2254
	0.4489	0.4489	0.4489	0.4489	0.4489	0.449	0.4505	0.431	0.318	0.2201
	0.4412	0.4412	0.4413	0.4413	0.4412	0.4414	0.4428	0.423	0.3104	0.2129
	0.4268	0.4269	0.4269	0.4269	0.4268	0.427	0.4284	0.408	0.2987	0.1991

Figure I.11a: F1B: e=1b & d=1b

	c/b									
a/b	0.4645	0.4645	0.4645	0.4645	0.4642	0.4566	0.4265	0.3728	0.321	0.2635
	0.4639	0.4639	0.4639	0.4639	0.4636	0.456	0.4256	0.3721	0.3203	0.2629
	0.463	0.463	0.463	0.463	0.4627	0.4551	0.4246	0.3709	0.3193	0.2618
	0.4617	0.4617	0.4617	0.4617	0.4614	0.4538	0.4231	0.3693	0.3178	0.2604
	0.4599	0.4599	0.4598	0.4598	0.4595	0.4519	0.4211	0.3671	0.3159	0.2586
	0.4577	0.4577	0.4576	0.4576	0.4574	0.4497	0.4187	0.3646	0.3137	0.2564
	0.4541	0.454	0.454	0.454	0.4537	0.446	0.4148	0.3604	0.3099	0.2528
	0.4489	0.4489	0.4488	0.4488	0.4485	0.4407	0.4094	0.3545	0.3046	0.2478
	0.4412	0.4412	0.4412	0.4412	0.4409	0.4329	0.4013	0.3463	0.2972	0.2407
	0.4269	0.4268	0.4268	0.4268	0.4264	0.4184	0.3862	0.3308	0.2832	0.2275

Figure I.11a: F1B: e=1b & d=1.5b

	c/b									
a/b	0.4645	0.4649	0.4668	0.4678	0.4567	0.4306	0.3872	0.349	0.322	0.2849
	0.4639	0.4643	0.4662	0.4672	0.456	0.4299	0.3865	0.3483	0.3214	0.2843
	0.463	0.4634	0.4653	0.4662	0.455	0.4288	0.3854	0.3473	0.3204	0.2834
	0.4617	0.4621	0.4639	0.4648	0.4535	0.4273	0.3839	0.3459	0.319	0.2821
	0.4598	0.4602	0.4621	0.4629	0.4515	0.4252	0.3819	0.3439	0.3172	0.2803
	0.4577	0.4581	0.4599	0.4607	0.4491	0.4228	0.3795	0.3417	0.315	0.2782
	0.454	0.4544	0.4562	0.457	0.4452	0.4187	0.3756	0.3379	0.3114	0.2748
	0.4489	0.4492	0.451	0.4516	0.4396	0.413	0.37	0.3326	0.3064	0.2699
	0.4412	0.4416	0.4433	0.4438	0.4315	0.4048	0.3621	0.3251	0.2992	0.263
	0.4268	0.4272	0.4289	0.4291	0.4162	0.3894	0.3473	0.3109	0.2857	0.2501

Figure I.11a: F1B: e=1b & d=2b

	c/b									
a/b	0.4656	0.4679	0.4661	0.4511	0.4249	0.4027	0.373	0.3481	0.3285	0.3028
	0.465	0.4673	0.4654	0.4505	0.4243	0.402	0.3723	0.3475	0.3278	0.3022
	0.4641	0.4664	0.4645	0.4495	0.4233	0.401	0.3714	0.3466	0.327	0.3013
	0.4628	0.465	0.4631	0.448	0.4218	0.3996	0.37	0.3452	0.3257	0.3001
	0.4609	0.4631	0.4611	0.446	0.4199	0.3977	0.3682	0.3434	0.3239	0.2984
	0.4587	0.4609	0.4589	0.4437	0.4176	0.3955	0.366	0.3413	0.3219	0.2964
	0.4551	0.4572	0.4551	0.4398	0.4137	0.3917	0.3623	0.3378	0.3184	0.293
	0.4499	0.4519	0.4497	0.4344	0.4083	0.3864	0.3572	0.3328	0.3136	0.2883
	0.4422	0.4442	0.4418	0.4264	0.4004	0.3788	0.3498	0.3256	0.3067	0.2816
	0.4278	0.4296	0.4269	0.4114	0.3857	0.3644	0.3358	0.3121	0.2935	0.2688

Figure I.11a: F1B: e=1b & d=2.5b

	c/b									
a/b	0.4645	0.4603	0.4505	0.4332	0.4121	0.3953	0.3739	0.3556	0.3399	0.3208
	0.4639	0.4597	0.4499	0.4326	0.4115	0.3947	0.3733	0.355	0.3393	0.3202
	0.463	0.4588	0.449	0.4317	0.4106	0.3938	0.3724	0.3542	0.3385	0.3194
	0.4617	0.4574	0.4476	0.4303	0.4092	0.3925	0.3711	0.3529	0.3372	0.3182
	0.4598	0.4556	0.4457	0.4285	0.4074	0.3907	0.3694	0.3512	0.3355	0.3165
	0.4576	0.4534	0.4435	0.4263	0.4052	0.3886	0.3673	0.3491	0.3335	0.3146
	0.454	0.4497	0.4398	0.4226	0.4016	0.385	0.3638	0.3457	0.3302	0.3113
	0.4488	0.4444	0.4345	0.4174	0.3965	0.38	0.3589	0.3409	0.3255	0.3067
	0.4411	0.4367	0.4268	0.4098	0.389	0.3727	0.3517	0.3339	0.3186	0.3
	0.4266	0.4222	0.4124	0.3954	0.3749	0.3589	0.3382	0.3207	0.3057	0.2874

Figure I.11a: F1B: e=1b & d=3b

	c/b									
a/b	0.4625	0.4558	0.4457	0.4313	0.4149	0.4015	0.3850	0.3705	0.3574	0.3422
	0.4619	0.4552	0.4451	0.4306	0.4143	0.4009	0.3844	0.3699	0.3568	0.3416
	0.4610	0.4543	0.4442	0.4298	0.4134	0.4000	0.3836	0.3691	0.3560	0.3408
	0.4597	0.4530	0.4428	0.4284	0.4121	0.3987	0.3823	0.3678	0.3547	0.3396
	0.4579	0.4512	0.4410	0.4266	0.4103	0.3970	0.3806	0.3661	0.3531	0.3380
	0.4557	0.4490	0.4388	0.4245	0.4082	0.3949	0.3785	0.3641	0.3511	0.3360
	0.4520	0.4453	0.4352	0.4209	0.4046	0.3914	0.3751	0.3607	0.3478	0.3328
	0.4469	0.4402	0.4301	0.4158	0.3996	0.3865	0.3702	0.3559	0.3431	0.3281
	0.4392	0.4325	0.4225	0.4083	0.3922	0.3792	0.3631	0.3489	0.3362	0.3214
	0.4248	0.4182	0.4083	0.3942	0.3784	0.3655	0.3496	0.3357	0.3231	0.3086

Figure I.11a: F1B: e=1b & d=3.5b

	c/b									
a/b	0.4623	0.4561	0.4475	0.4361	0.4233	0.4123	0.3992	0.3873	0.3762	0.3637
	0.4617	0.4555	0.4469	0.4355	0.4227	0.4117	0.3986	0.3867	0.3756	0.3631
	0.4608	0.4546	0.446	0.4346	0.4218	0.4109	0.3978	0.3859	0.3748	0.3623
	0.4595	0.4533	0.4447	0.4333	0.4205	0.4096	0.3965	0.3846	0.3736	0.3611
	0.4576	0.4515	0.4429	0.4315	0.4187	0.4078	0.3948	0.3829	0.3719	0.3594
	0.4555	0.4493	0.4407	0.4293	0.4166	0.4058	0.3927	0.3809	0.3699	0.3574
	0.4518	0.4457	0.4371	0.4258	0.4131	0.4023	0.3893	0.3775	0.3665	0.3541
	0.4467	0.4405	0.432	0.4207	0.4081	0.3973	0.3844	0.3727	0.3618	0.3494
	0.439	0.4329	0.4244	0.4132	0.4007	0.39	0.3772	0.3655	0.3547	0.3425
	0.4246	0.4186	0.4102	0.3992	0.3868	0.3763	0.3636	0.3522	0.3415	0.3295

Figure I.11a: F1B: e=1b & d=4b

	c/b									
a/b	0.4626	0.4576	0.4507	0.4417	0.4316	0.4227	0.4121	0.4021	0.3927	0.3822
	0.462	0.457	0.4501	0.4411	0.431	0.4221	0.4115	0.4016	0.3922	0.3816
	0.4611	0.4561	0.4492	0.4403	0.4302	0.4212	0.4106	0.4007	0.3913	0.3808
	0.4598	0.4548	0.4479	0.439	0.4289	0.4199	0.4093	0.3995	0.3901	0.3796
	0.458	0.453	0.4461	0.4371	0.4271	0.4182	0.4076	0.3977	0.3883	0.3779
	0.4558	0.4508	0.444	0.435	0.425	0.4161	0.4055	0.3957	0.3863	0.3759
	0.4522	0.4472	0.4404	0.4314	0.4214	0.4126	0.402	0.3922	0.3829	0.3725
	0.447	0.4421	0.4352	0.4264	0.4164	0.4076	0.3971	0.3873	0.3781	0.3677
	0.4394	0.4344	0.4277	0.4189	0.4089	0.4002	0.3898	0.3801	0.371	0.3607
	0.425	0.4201	0.4134	0.4047	0.395	0.3863	0.3761	0.3666	0.3575	0.3474

Figure 6.23a: F1B: e=1.5b & d=0.5b

	c/b									
a/b	0.4645	0.4645	0.4645	0.4645	0.4645	0.4647	0.4662	0.4476	0.3351	0.2369
	0.4637	0.4637	0.4638	0.4638	0.4637	0.4639	0.4655	0.4468	0.3342	0.2362
	0.4625	0.4625	0.4626	0.4626	0.4625	0.4627	0.4643	0.4455	0.333	0.2349
	0.4607	0.4607	0.4607	0.4607	0.4607	0.4609	0.4624	0.4436	0.331	0.2327
	0.4583	0.4583	0.4583	0.4583	0.4583	0.4584	0.46	0.441	0.3285	0.2301
	0.4556	0.4556	0.4556	0.4556	0.4556	0.4557	0.4573	0.4382	0.3257	0.2274
	0.4515	0.4515	0.4515	0.4515	0.4515	0.4516	0.4531	0.4339	0.3216	0.2235
	0.4461	0.4461	0.4461	0.4461	0.4461	0.4463	0.4478	0.4283	0.3181	0.2186
	0.439	0.439	0.439	0.4391	0.439	0.4392	0.4406	0.421	0.3093	0.2123
	0.4275	0.4275	0.4275	0.4275	0.4275	0.4276	0.429	0.409	0.2978	0.2018

Figure 6.23a: F1B: e=1.5b & d=1b

	c/b									
a/b	0.4645	0.4645	0.4644	0.4644	0.4642	0.4566	0.4265	0.3728	0.321	0.2635
	0.4637	0.4637	0.4636	0.4637	0.4634	0.4558	0.4254	0.372	0.3202	0.2628
	0.4625	0.4625	0.4625	0.4625	0.4622	0.4546	0.4241	0.3706	0.319	0.2616
	0.4607	0.4607	0.4606	0.4606	0.4604	0.4527	0.4221	0.3684	0.317	0.2597
	0.4583	0.4583	0.4582	0.4582	0.4579	0.4503	0.4195	0.3656	0.3145	0.2573
	0.4556	0.4556	0.4555	0.4555	0.4552	0.4475	0.4166	0.3625	0.3118	0.2547
	0.4515	0.4515	0.4514	0.4514	0.4511	0.4434	0.4123	0.358	0.3078	0.2509
	0.4461	0.4461	0.446	0.446	0.4457	0.4379	0.4067	0.3522	0.3025	0.2459
	0.439	0.439	0.439	0.439	0.4386	0.4308	0.3994	0.3447	0.2958	0.2396
	0.4275	0.4275	0.4274	0.4274	0.4271	0.4192	0.3874	0.3324	0.2849	0.2293

Figure 6.23a: F1B: e=1.5b & d=1.5b

	c/b									
a/b	0.4645	0.4649	0.4668	0.4678	0.4566	0.4306	0.3872	0.349	0.322	0.2849
	0.4637	0.4641	0.466	0.4669	0.4558	0.4297	0.3863	0.3482	0.3212	0.2842
	0.4625	0.4629	0.4648	0.4657	0.4545	0.4284	0.385	0.3469	0.32	0.2831
	0.4607	0.4611	0.4629	0.4638	0.4525	0.4263	0.383	0.345	0.3182	0.2813
	0.4583	0.4586	0.4605	0.4613	0.4499	0.4236	0.3804	0.3425	0.3158	0.279
	0.4556	0.4559	0.4578	0.4585	0.4469	0.4206	0.3775	0.3397	0.3132	0.2765
	0.4515	0.4518	0.4536	0.4543	0.4425	0.4161	0.3732	0.3356	0.3093	0.2727
	0.4461	0.4464	0.4482	0.4488	0.4368	0.4103	0.3676	0.3303	0.3042	0.2679
	0.439	0.4393	0.4411	0.4415	0.4293	0.4028	0.3603	0.3234	0.2977	0.2616
	0.4275	0.4278	0.4295	0.4298	0.4171	0.3905	0.3486	0.3123	0.287	0.2514

Figure 6.23a: F1B: e=1.5b & d=2b

	c/b									
a/b	0.4656	0.4678	0.466	0.4511	0.4249	0.4026	0.3729	0.3481	0.3284	0.3028
	0.4648	0.467	0.4652	0.4502	0.4241	0.4018	0.3722	0.3473	0.3277	0.302
	0.4636	0.4658	0.464	0.449	0.4228	0.4006	0.371	0.3462	0.3266	0.3009
	0.4617	0.464	0.462	0.447	0.4209	0.3987	0.3691	0.3443	0.3248	0.2992
	0.4593	0.4615	0.4595	0.4444	0.4183	0.3962	0.3667	0.342	0.3225	0.297
	0.4566	0.4588	0.4567	0.4416	0.4155	0.3934	0.364	0.3394	0.32	0.2946
	0.4525	0.4546	0.4524	0.4372	0.4112	0.3893	0.36	0.3355	0.3163	0.2909
	0.4471	0.4491	0.4468	0.4316	0.4056	0.3839	0.3547	0.3304	0.3113	0.2861
	0.44	0.4419	0.4395	0.4242	0.3984	0.3768	0.3479	0.3239	0.305	0.28
	0.4284	0.4302	0.4276	0.4123	0.3867	0.3654	0.3369	0.3131	0.2946	0.2699

Figure 6.23a: F1B: e=1.5b & d=2.5b

	c/b									
a/b	0.4645	0.4603	0.4505	0.4332	0.4121	0.3953	0.3739	0.3556	0.3398	0.3207
	0.4637	0.4595	0.4497	0.4324	0.4113	0.3945	0.3731	0.3548	0.3391	0.32
	0.4625	0.4583	0.4485	0.4312	0.4101	0.3934	0.372	0.3537	0.338	0.319
	0.4607	0.4564	0.4466	0.4293	0.4083	0.3916	0.3702	0.352	0.3364	0.3173
	0.4582	0.454	0.4441	0.4269	0.4059	0.3892	0.3679	0.3498	0.3341	0.3152
	0.4555	0.4512	0.4414	0.4242	0.4032	0.3866	0.3654	0.3473	0.3317	0.3128
	0.4514	0.4471	0.4372	0.4201	0.3992	0.3827	0.3615	0.3435	0.328	0.3092
	0.446	0.4416	0.4318	0.4147	0.3939	0.3775	0.3564	0.3385	0.3232	0.3044
	0.4389	0.4345	0.4247	0.4077	0.387	0.3707	0.3498	0.3321	0.3169	0.2983
	0.4273	0.4228	0.4131	0.3962	0.3757	0.3597	0.3391	0.3216	0.3066	0.2882

Figure 6.23a: F1B: e=1.5b & d=3b

	c/b									
a/b	0.4625	0.4558	0.4456	0.4312	0.4148	0.4014	0.385	0.3704	0.3573	0.3421
	0.4617	0.455	0.4448	0.4304	0.4141	0.4007	0.3842	0.3697	0.3566	0.3415
	0.4605	0.4538	0.4437	0.4293	0.4129	0.3996	0.3831	0.3686	0.3555	0.3404
	0.4587	0.452	0.4418	0.4275	0.4111	0.3978	0.3814	0.3669	0.3539	0.3387
	0.4563	0.4496	0.4394	0.4251	0.4088	0.3955	0.3791	0.3647	0.3517	0.3366
	0.4536	0.4469	0.4367	0.4224	0.4062	0.3929	0.3766	0.3622	0.3492	0.3342
	0.4495	0.4428	0.4327	0.4184	0.4022	0.389	0.3727	0.3584	0.3455	0.3305
	0.4441	0.4374	0.4273	0.4131	0.397	0.3839	0.3677	0.3535	0.3406	0.3258
	0.437	0.4303	0.4203	0.4062	0.3902	0.3772	0.3611	0.347	0.3343	0.3195
	0.4255	0.4189	0.4089	0.395	0.3791	0.3663	0.3504	0.3364	0.3239	0.3093

Figure 6.23a: F1B: e=1.5b & d=3.5b

	c/b									
a/b	0.4623	0.4561	0.4474	0.436	0.4232	0.4123	0.3992	0.3873	0.3762	0.3636
	0.4615	0.4553	0.4467	0.4353	0.4225	0.4115	0.3984	0.3865	0.3754	0.3629
	0.4603	0.4541	0.4455	0.4341	0.4213	0.4104	0.3973	0.3854	0.3744	0.3618
	0.4585	0.4523	0.4437	0.4323	0.4195	0.4086	0.3956	0.3837	0.3727	0.3602
	0.456	0.4499	0.4413	0.4299	0.4172	0.4063	0.3933	0.3815	0.3704	0.358
	0.4533	0.4472	0.4386	0.4273	0.4146	0.4037	0.3907	0.3789	0.368	0.3555
	0.4493	0.4431	0.4346	0.4233	0.4106	0.3998	0.3869	0.3751	0.3642	0.3518
	0.4439	0.4378	0.4293	0.418	0.4054	0.3947	0.3818	0.3701	0.3593	0.3469
	0.4368	0.4307	0.4223	0.4111	0.3986	0.3879	0.3752	0.3636	0.3528	0.3406
	0.4253	0.4193	0.4109	0.3998	0.3874	0.377	0.3643	0.3528	0.3422	0.3301

Figure 6.23a: F1B: e=1.5b & d=4b

	c/b									
a/b	0.4626	0.4576	0.4507	0.4417	0.4316	0.4226	0.412	0.4021	0.3927	0.3822
	0.4618	0.4568	0.4499	0.4409	0.4308	0.4219	0.4113	0.4014	0.392	0.3814
	0.4606	0.4556	0.4487	0.4398	0.4297	0.4207	0.4101	0.4002	0.3909	0.3803
	0.4588	0.4538	0.4469	0.438	0.4279	0.419	0.4084	0.3985	0.3891	0.3786
	0.4564	0.4514	0.4445	0.4356	0.4255	0.4166	0.4061	0.3962	0.3869	0.3764
	0.4537	0.4487	0.4419	0.4329	0.4229	0.414	0.4035	0.3937	0.3844	0.3739
	0.4496	0.4446	0.4378	0.4289	0.4189	0.4101	0.3996	0.3898	0.3805	0.3701
	0.4442	0.4393	0.4325	0.4236	0.4137	0.4049	0.3945	0.3847	0.3755	0.3652
	0.4371	0.4322	0.4255	0.4167	0.4068	0.3981	0.3877	0.3781	0.3689	0.3587
	0.4256	0.4208	0.4141	0.4054	0.3956	0.387	0.3768	0.3672	0.3582	0.348

Figure I.12a: F1B: e=2b & d=0.5b

	c/b									
a/b	0.4645	0.4645	0.4645	0.4645	0.4644	0.4646	0.4662	0.4476	0.3351	0.237
	0.4637	0.4637	0.4637	0.4637	0.4636	0.4638	0.4654	0.4467	0.3342	0.2362
	0.4623	0.4624	0.4624	0.4624	0.4623	0.4625	0.4641	0.4453	0.3329	0.235
	0.4603	0.4603	0.4604	0.4604	0.4604	0.4605	0.4621	0.4432	0.3308	0.2335
	0.4576	0.4576	0.4577	0.4577	0.4576	0.4578	0.4594	0.4404	0.3281	0.2303
	0.4546	0.4546	0.4547	0.4547	0.4546	0.4548	0.4563	0.4373	0.3251	0.2273
	0.4504	0.4504	0.4505	0.4505	0.4504	0.4506	0.4521	0.4329	0.321	0.2232
	0.4452	0.4452	0.4452	0.4452	0.4452	0.4453	0.4468	0.4276	0.3158	0.2184
	0.4387	0.4387	0.4388	0.4388	0.4387	0.4389	0.4403	0.4209	0.3095	0.2129
	0.4291	0.4291	0.4292	0.4292	0.4291	0.4293	0.4307	0.411	0.3005	0.2046

Figure I.12a: F1B: e=2b & d=1b

	c/b									
a/b	0.4645	0.4645	0.4644	0.4644	0.4642	0.4566	0.4265	0.3728	0.321	0.2635
	0.4637	0.4636	0.4636	0.4636	0.4633	0.4558	0.4254	0.372	0.3202	0.2628
	0.4623	0.4623	0.4623	0.4623	0.462	0.4544	0.424	0.3705	0.3189	0.2616
	0.4603	0.4603	0.4603	0.4603	0.46	0.4524	0.4218	0.3683	0.3169	0.2597
	0.4576	0.4576	0.4576	0.4576	0.4573	0.4497	0.419	0.3653	0.3143	0.2571
	0.4546	0.4546	0.4546	0.4546	0.4543	0.4466	0.4158	0.362	0.3113	0.2543
	0.4504	0.4504	0.4504	0.4504	0.4501	0.4424	0.4114	0.3574	0.3072	0.2504
	0.4452	0.4452	0.4451	0.4451	0.4448	0.4371	0.4061	0.3518	0.3022	0.2457
	0.4387	0.4387	0.4387	0.4387	0.4384	0.4306	0.3994	0.3451	0.2962	0.2401
	0.4291	0.4291	0.4291	0.4291	0.4287	0.4209	0.3895	0.3351	0.2873	0.2317

Figure I.12a: F1B: e=2b & d=1.5b

	c/b									
a/b	0.4645	0.4649	0.4668	0.4677	0.4566	0.4306	0.3872	0.349	0.322	0.2849
	0.4636	0.464	0.4659	0.4669	0.4557	0.4297	0.3863	0.3482	0.3212	0.2842
	0.4623	0.4627	0.4646	0.4655	0.4543	0.4282	0.3849	0.3469	0.32	0.283
	0.4603	0.4607	0.4626	0.4635	0.4522	0.426	0.3828	0.3448	0.318	0.2811
	0.4576	0.458	0.4598	0.4607	0.4493	0.4231	0.3799	0.3421	0.3154	0.2787
	0.4546	0.455	0.4568	0.4576	0.4461	0.4198	0.3768	0.3391	0.3126	0.2759
	0.4504	0.4508	0.4526	0.4533	0.4415	0.4152	0.3724	0.3349	0.3086	0.2721
	0.4452	0.4455	0.4473	0.4479	0.436	0.4096	0.367	0.3298	0.3037	0.2674
	0.4387	0.4391	0.4408	0.4413	0.4292	0.4028	0.3605	0.3236	0.2979	0.2619
	0.4291	0.4295	0.4311	0.4315	0.4191	0.3927	0.3508	0.3144	0.2891	0.2535

Figure I.12a: F1B: e=2b & d=2b

	c/b									
a/b	0.4655	0.4678	0.466	0.4511	0.4249	0.4026	0.3729	0.3481	0.3284	0.3027
	0.4647	0.467	0.4652	0.4502	0.424	0.4018	0.3721	0.3473	0.3277	0.302
	0.4634	0.4657	0.4638	0.4488	0.4227	0.4005	0.3708	0.346	0.3265	0.3009
	0.4614	0.4636	0.4617	0.4467	0.4206	0.3984	0.3689	0.3441	0.3246	0.299
	0.4587	0.4609	0.4589	0.4438	0.4177	0.3957	0.3662	0.3416	0.3221	0.2966
	0.4557	0.4578	0.4558	0.4407	0.4146	0.3926	0.3633	0.3387	0.3194	0.294
	0.4514	0.4535	0.4514	0.4362	0.4103	0.3884	0.3592	0.3347	0.3155	0.2902
	0.4462	0.4482	0.446	0.4308	0.4049	0.3832	0.3541	0.3298	0.3108	0.2856
	0.4397	0.4417	0.4393	0.4241	0.3984	0.3768	0.348	0.3239	0.305	0.2801
	0.4301	0.4319	0.4294	0.4141	0.3886	0.3673	0.3388	0.315	0.2964	0.2717

Figure I.12a: F1B: e=2b & d=2.5b

	c/b									
a/b	0.4645	0.4603	0.4505	0.4332	0.4121	0.3953	0.3739	0.3556	0.3398	0.3207
	0.4637	0.4595	0.4496	0.4324	0.4112	0.3945	0.3731	0.3548	0.3391	0.32
	0.4623	0.4581	0.4483	0.431	0.41	0.3932	0.3718	0.3536	0.3379	0.3189
	0.4603	0.4561	0.4462	0.429	0.408	0.3913	0.3699	0.3517	0.3361	0.3171
	0.4576	0.4533	0.4435	0.4263	0.4053	0.3887	0.3674	0.3493	0.3337	0.3147
	0.4546	0.4503	0.4405	0.4233	0.4024	0.3858	0.3646	0.3465	0.331	0.3121
	0.4503	0.446	0.4362	0.4191	0.3982	0.3817	0.3606	0.3426	0.3272	0.3084
	0.4451	0.4407	0.4309	0.4139	0.3931	0.3767	0.3557	0.3379	0.3225	0.3038
	0.4386	0.4342	0.4245	0.4075	0.3868	0.3706	0.3498	0.332	0.3168	0.2982
	0.4289	0.4245	0.4148	0.398	0.3775	0.3615	0.3408	0.3233	0.3083	0.2899

Figure I.12a: F1B: e=2b & d=3b

	c/b									
a/b	0.4625	0.4558	0.4456	0.4312	0.4148	0.4014	0.385	0.3704	0.3573	0.3421
	0.4617	0.455	0.4448	0.4304	0.414	0.4006	0.3842	0.3697	0.3566	0.3414
	0.4603	0.4537	0.4435	0.4291	0.4128	0.3994	0.383	0.3685	0.3554	0.3402
	0.4583	0.4516	0.4415	0.4271	0.4108	0.3975	0.3811	0.3666	0.3535	0.3384
	0.4556	0.4489	0.4388	0.4245	0.4082	0.3949	0.3785	0.3641	0.3511	0.3361
	0.4526	0.446	0.4358	0.4215	0.4053	0.3921	0.3758	0.3614	0.3484	0.3334
	0.4484	0.4417	0.4317	0.4174	0.4012	0.3881	0.3718	0.3575	0.3446	0.3297
	0.4432	0.4365	0.4265	0.4123	0.3962	0.3831	0.367	0.3527	0.3399	0.325
	0.4367	0.4301	0.4201	0.406	0.39	0.377	0.361	0.3469	0.3342	0.3194
	0.4271	0.4205	0.4106	0.3967	0.3808	0.368	0.3521	0.3381	0.3255	0.3109

Figure I.12a: F1B: e=2b & d=3.5b

	c/b									
a/b	0.4622	0.4561	0.4474	0.436	0.4232	0.4123	0.3992	0.3873	0.3762	0.3636
	0.4614	0.4552	0.4466	0.4352	0.4224	0.4115	0.3984	0.3865	0.3754	0.3629
	0.4601	0.4539	0.4453	0.4339	0.4211	0.4102	0.3972	0.3853	0.3742	0.3617
	0.4581	0.4519	0.4434	0.4319	0.4192	0.4083	0.3952	0.3834	0.3723	0.3599
	0.4554	0.4492	0.4407	0.4293	0.4166	0.4057	0.3927	0.3809	0.3699	0.3574
	0.4524	0.4463	0.4377	0.4264	0.4137	0.4029	0.3899	0.3781	0.3671	0.3547
	0.4482	0.4421	0.4335	0.4223	0.4096	0.3989	0.3859	0.3742	0.3633	0.3509
	0.443	0.4369	0.4284	0.4172	0.4046	0.3939	0.381	0.3693	0.3585	0.3462
	0.4365	0.4305	0.422	0.4109	0.3984	0.3877	0.375	0.3634	0.3526	0.3404
	0.4269	0.4209	0.4126	0.4015	0.3891	0.3786	0.3659	0.3545	0.3438	0.3317

Figure I.12a: F1B: e=2b & d=4b

	c/b									
a/b	0.4626	0.4576	0.4507	0.4417	0.4316	0.4226	0.412	0.4021	0.3927	0.3822
	0.4618	0.4568	0.4499	0.4409	0.4308	0.4218	0.4112	0.4013	0.3919	0.3814
	0.4605	0.4554	0.4486	0.4396	0.4295	0.4206	0.41	0.4001	0.3907	0.3802
	0.4584	0.4534	0.4465	0.4376	0.4275	0.4186	0.408	0.3982	0.3888	0.3783
	0.4557	0.4508	0.4439	0.435	0.4249	0.416	0.4055	0.3956	0.3863	0.3758
	0.4528	0.4478	0.4409	0.432	0.422	0.4131	0.4026	0.3928	0.3835	0.3731
	0.4485	0.4436	0.4368	0.4279	0.4179	0.4091	0.3986	0.3888	0.3796	0.3692
	0.4433	0.4384	0.4316	0.4228	0.4128	0.4041	0.3936	0.3839	0.3747	0.3644
	0.4369	0.432	0.4252	0.4165	0.4066	0.3979	0.3875	0.3779	0.3687	0.3584
	0.4273	0.4224	0.4157	0.407	0.3973	0.3886	0.3784	0.3688	0.3598	0.3496

Figure 6.24a: F1B: e=2.5b & d=0.5b

	c/b									
a/b	0.4645	0.4645	0.4645	0.4646	0.4645	0.4647	0.4663	0.4476	0.3351	0.237
	0.4637	0.4637	0.4637	0.4638	0.4637	0.4639	0.4654	0.4468	0.3343	0.2363
	0.4624	0.4624	0.4624	0.4624	0.4624	0.4625	0.4641	0.4454	0.333	0.2351
	0.4604	0.4604	0.4604	0.4604	0.4603	0.4605	0.4621	0.4433	0.3311	0.2333
	0.4576	0.4576	0.4577	0.4577	0.4576	0.4578	0.4594	0.4405	0.3284	0.2308
	0.4546	0.4546	0.4546	0.4546	0.4546	0.4547	0.4563	0.4374	0.3254	0.2281
	0.4504	0.4504	0.4504	0.4504	0.4504	0.4505	0.4521	0.433	0.3216	0.2242
	0.4454	0.4454	0.4454	0.4456	0.4454	0.4455	0.4465	0.4279	0.3166	0.2197
	0.4395	0.4395	0.4395	0.4395	0.4395	0.4396	0.4411	0.4219	0.3109	0.2146
	0.4312	0.4312	0.4312	0.4312	0.4311	0.4313	0.4327	0.4133	0.3034	0.2069

Figure 6.24a: F1B: e=2.5b & d=1b

	c/b									
a/b	0.4645	0.4645	0.4644	0.4644	0.4642	0.4566	0.4265	0.3728	0.321	0.2636
	0.4637	0.4637	0.4636	0.4636	0.4634	0.4558	0.4254	0.372	0.3203	0.2629
	0.4624	0.4624	0.4623	0.4623	0.4621	0.4545	0.4241	0.3707	0.319	0.2617
	0.4604	0.4603	0.4603	0.4603	0.46	0.4524	0.422	0.3685	0.3171	0.2599
	0.4576	0.4576	0.4576	0.4576	0.4573	0.4497	0.4191	0.3656	0.3145	0.2574
	0.4546	0.4545	0.4545	0.4545	0.4542	0.4466	0.4159	0.3623	0.3116	0.2547
	0.4504	0.4504	0.4503	0.4503	0.45	0.4424	0.4115	0.3579	0.3076	0.251
	0.4454	0.4454	0.4453	0.4453	0.445	0.4373	0.4065	0.3526	0.3029	0.2465
	0.4395	0.4395	0.4394	0.4394	0.4391	0.4314	0.4005	0.3465	0.2975	0.2414
	0.4312	0.4311	0.4311	0.4311	0.4308	0.423	0.3919	0.3379	0.2898	0.2345

Figure 6.24a: F1B: e=2.5b & d=1.5b

	c/b									
a/b	0.4645	0.4649	0.4668	0.4678	0.4566	0.4306	0.3872	0.349	0.322	0.2849
	0.4637	0.4641	0.466	0.4669	0.4558	0.4297	0.3864	0.3482	0.3213	0.2842
	0.4624	0.4627	0.4646	0.4656	0.4544	0.4283	0.385	0.347	0.3201	0.2831
	0.4603	0.4607	0.4626	0.4635	0.4522	0.4262	0.3829	0.345	0.3182	0.2813
	0.4576	0.458	0.4599	0.4607	0.4494	0.4233	0.3801	0.3423	0.3157	0.2789
	0.4546	0.4549	0.4568	0.4576	0.4461	0.42	0.377	0.3393	0.3128	0.2762
	0.4504	0.4507	0.4526	0.4533	0.4417	0.4155	0.3727	0.3353	0.3089	0.2725
	0.4454	0.4457	0.4475	0.4481	0.4364	0.4101	0.3676	0.3304	0.3043	0.2681
	0.4395	0.4398	0.4416	0.4421	0.4302	0.4039	0.3616	0.3248	0.299	0.263
	0.4311	0.4315	0.4332	0.4336	0.4214	0.3952	0.3533	0.3169	0.2915	0.2558

Figure 6.24a: F1B: e=2.5b & d=2b

	c/b									
a/b	0.4656	0.4678	0.466	0.4511	0.4249	0.4026	0.373	0.3481	0.3284	0.3028
	0.4648	0.467	0.4652	0.4503	0.4241	0.4018	0.3722	0.3473	0.3277	0.3021
	0.4634	0.4657	0.4638	0.4489	0.4227	0.4005	0.3709	0.3461	0.3265	0.3009
	0.4614	0.4636	0.4617	0.4468	0.4206	0.3985	0.369	0.3442	0.3247	0.2992
	0.4587	0.4609	0.4589	0.4439	0.4179	0.3958	0.3663	0.3417	0.3223	0.2968
	0.4556	0.4578	0.4558	0.4407	0.4147	0.3927	0.3634	0.3388	0.3195	0.2941
	0.4514	0.4535	0.4514	0.4363	0.4104	0.3886	0.3594	0.3349	0.3157	0.2904
	0.4464	0.4484	0.4462	0.4311	0.4053	0.3836	0.3545	0.3303	0.3112	0.2861
	0.4404	0.4424	0.4402	0.425	0.3993	0.3778	0.3489	0.3249	0.306	0.281
	0.4321	0.434	0.4316	0.4164	0.3909	0.3696	0.3411	0.3173	0.2986	0.2738

Figure 6.24a: F1B: e=2.5b & d=2.5b

	c/b									
a/b	0.4645	0.4603	0.4505	0.4332	0.4121	0.3953	0.3739	0.3556	0.3398	0.3208
	0.4637	0.4595	0.4497	0.4324	0.4113	0.3946	0.3731	0.3549	0.3391	0.3201
	0.4624	0.4582	0.4483	0.4311	0.41	0.3933	0.3719	0.3537	0.338	0.3189
	0.4603	0.4561	0.4463	0.4291	0.408	0.3914	0.37	0.3518	0.3362	0.3172
	0.4576	0.4534	0.4435	0.4264	0.4054	0.3888	0.3675	0.3493	0.3337	0.3148
	0.4545	0.4503	0.4405	0.4233	0.4024	0.3858	0.3646	0.3466	0.331	0.3121
	0.4503	0.446	0.4362	0.4192	0.3983	0.3818	0.3607	0.3427	0.3273	0.3085
	0.4453	0.441	0.4312	0.4142	0.3934	0.3771	0.3561	0.3382	0.3229	0.3041
	0.4393	0.435	0.4253	0.4083	0.3877	0.3715	0.3506	0.3329	0.3177	0.2991
	0.431	0.4266	0.4169	0.4001	0.3796	0.3636	0.3429	0.3254	0.3103	0.2919

Figure 6.24a: F1B: e=2.5b & d=3b

	c/b									
a/b	0.4625	0.4558	0.4456	0.4312	0.4148	0.4014	0.385	0.3704	0.3573	0.3422
	0.4617	0.455	0.4448	0.4304	0.4141	0.4007	0.3842	0.3697	0.3566	0.3415
	0.4604	0.4537	0.4435	0.4292	0.4128	0.3995	0.383	0.3685	0.3554	0.3403
	0.4584	0.4517	0.4415	0.4272	0.4108	0.3975	0.3811	0.3667	0.3536	0.3385
	0.4556	0.449	0.4388	0.4245	0.4082	0.395	0.3786	0.3642	0.3512	0.3361
	0.4526	0.4459	0.4358	0.4215	0.4053	0.3921	0.3758	0.3614	0.3484	0.3334
	0.4484	0.4417	0.4317	0.4174	0.4013	0.3881	0.3719	0.3576	0.3447	0.3297
	0.4434	0.4367	0.4267	0.4125	0.3964	0.3834	0.3672	0.353	0.3402	0.3253
	0.4375	0.4309	0.4209	0.4068	0.3908	0.3778	0.3618	0.3477	0.3349	0.3202
	0.4292	0.4226	0.4127	0.3987	0.3828	0.37	0.3541	0.3401	0.3275	0.3129

Figure 6.24a: F1B: e=2.5b & d=3.5b

	c/b									
a/b	0.4623	0.4561	0.4475	0.436	0.4232	0.4123	0.3992	0.3873	0.3762	0.3636
	0.4615	0.4553	0.4467	0.4352	0.4225	0.4115	0.3984	0.3865	0.3754	0.3629
	0.4602	0.454	0.4454	0.434	0.4212	0.4103	0.3972	0.3853	0.3743	0.3617
	0.4581	0.452	0.4434	0.432	0.4192	0.4084	0.3953	0.3834	0.3724	0.3599
	0.4554	0.4493	0.4407	0.4293	0.4166	0.4058	0.3927	0.3809	0.3699	0.3575
	0.4523	0.4462	0.4377	0.4263	0.4137	0.4029	0.3899	0.3781	0.3671	0.3547
	0.4482	0.4421	0.4335	0.4223	0.4096	0.3989	0.3859	0.3742	0.3633	0.3509
	0.4432	0.4371	0.4286	0.4174	0.4048	0.3941	0.3812	0.3696	0.3587	0.3464
	0.4373	0.4312	0.4228	0.4116	0.3991	0.3885	0.3757	0.3641	0.3533	0.3411
	0.429	0.423	0.4146	0.4035	0.3911	0.3806	0.3679	0.3564	0.3458	0.3336

Figure 6.24a: F1B: e=2.5b & d=4b

	c/b									
a/b	0.4626	0.4576	0.4507	0.4417	0.4316	0.4226	0.412	0.4021	0.3927	0.3822
	0.4618	0.4568	0.4499	0.4409	0.4308	0.4219	0.4113	0.4014	0.392	0.3814
	0.4605	0.4555	0.4486	0.4396	0.4295	0.4206	0.41	0.4001	0.3907	0.3802
	0.4585	0.4535	0.4466	0.4376	0.4276	0.4187	0.4081	0.3982	0.3888	0.3783
	0.4557	0.4508	0.4439	0.435	0.4249	0.416	0.4055	0.3957	0.3863	0.3758
	0.4527	0.4477	0.4409	0.432	0.422	0.4131	0.4026	0.3928	0.3835	0.373
	0.4485	0.4436	0.4367	0.4279	0.4179	0.4091	0.3986	0.3888	0.3796	0.3692
	0.4435	0.4386	0.4318	0.423	0.413	0.4043	0.3938	0.3841	0.3749	0.3646
	0.4376	0.4327	0.426	0.4172	0.4073	0.3986	0.3882	0.3786	0.3694	0.3592
	0.4293	0.4245	0.4178	0.4091	0.3993	0.3906	0.3804	0.3708	0.3617	0.3515

Figure I.13a: F1B: e=3b & d=0.5b

	c/b									
	0.4645	0.4645	0.4646	0.4646	0.4645	0.4647	0.4663	0.4476	0.3351	0.237
	0.4638	0.4638	0.4638	0.4638	0.4638	0.4639	0.4655	0.4469	0.3344	0.2364
	0.4625	0.4625	0.4626	0.4626	0.4625	0.4627	0.4643	0.4456	0.3332	0.2354
	0.4606	0.4606	0.4607	0.4607	0.4606	0.4608	0.4624	0.4436	0.3314	0.2337
a/b	0.458	0.458	0.4581	0.4581	0.458	0.4591	0.4597	0.4409	0.329	0.2315
	0.4551	0.4551	0.4551	0.4551	0.455	0.4552	0.4567	0.4379	0.3262	0.229
	0.451	0.451	0.4511	0.4511	0.451	0.4512	0.4527	0.4338	0.3226	0.2255
	0.4463	0.4463	0.4463	0.4463	0.4463	0.4464	0.4479	0.429	0.318	0.2214
	0.4408	0.4409	0.4409	0.4409	0.4408	0.441	0.4424	0.4234	0.3129	0.2168
	0.4334	0.4334	0.4335	0.4335	0.4334	0.4336	0.435	0.4159	0.3059	0.2105

Figure I.13a: F1B: e=3b & d=1b

	c/b									
	0.4645	0.4645	0.4645	0.4645	0.4642	0.4566	0.4265	0.3729	0.3211	0.2636
	0.4638	0.4638	0.4637	0.4637	0.4635	0.4559	0.4255	0.3721	0.3203	0.263
	0.4625	0.4625	0.4625	0.4625	0.4622	0.4546	0.4243	0.3709	0.3192	0.2619
	0.4606	0.4606	0.4605	0.4606	0.4603	0.4527	0.4223	0.3689	0.3175	0.2602
a/b	0.458	0.458	0.4579	0.458	0.4577	0.4501	0.4196	0.3662	0.3151	0.258
	0.4551	0.455	0.455	0.455	0.4547	0.4471	0.4166	0.3631	0.3123	0.2555
	0.451	0.451	0.451	0.451	0.4507	0.4431	0.4124	0.359	0.3086	0.252
	0.4463	0.4463	0.4462	0.4462	0.4459	0.4383	0.4076	0.3541	0.3043	0.2479
	0.4408	0.4408	0.4408	0.4408	0.4405	0.4328	0.4021	0.3485	0.2993	0.2432
	0.4334	0.4334	0.4334	0.4334	0.4331	0.4254	0.3946	0.3409	0.2926	0.2273

Figure I.13a: F1B: e=3b & d=1.5b

	c/b									
	0.4645	0.4649	0.4668	0.4678	0.4567	0.4306	0.3872	0.349	0.322	0.285
	0.4638	0.4641	0.466	0.467	0.4559	0.4298	0.3865	0.3483	0.3213	0.2843
	0.4625	0.4629	0.4648	0.4658	0.4546	0.4285	0.3852	0.3472	0.3202	0.2833
	0.4606	0.461	0.4629	0.4638	0.4526	0.4265	0.3833	0.3453	0.3185	0.2816
a/b	0.458	0.4584	0.4602	0.4611	0.4498	0.4238	0.3807	0.3428	0.3161	0.2794
	0.455	0.4554	0.4573	0.4581	0.4467	0.4206	0.3777	0.34	0.3135	0.2768
	0.451	0.4514	0.4532	0.454	0.4425	0.4164	0.3736	0.3362	0.3098	0.2733
	0.4463	0.4466	0.4484	0.4491	0.4375	0.4114	0.3688	0.3317	0.3055	0.2692
	0.4408	0.4412	0.443	0.4436	0.4318	0.4057	0.3634	0.3265	0.3007	0.2646
	0.4334	0.4338	0.4355	0.436	0.424	0.3979	0.356	0.3204	0.294	0.2583

Figure I.13a: F1B: e=3b & d=2b

	c/b									
	0.4656	0.4679	0.4661	0.4511	0.4249	0.4027	0.373	0.3481	0.3285	0.3028
	0.4648	0.4671	0.4653	0.4503	0.4242	0.4019	0.3723	0.3474	0.3278	0.3022
	0.4636	0.4659	0.464	0.4491	0.4229	0.4007	0.3711	0.3463	0.3267	0.3011
	0.4617	0.4639	0.462	0.4471	0.421	0.3988	0.3693	0.3445	0.325	0.2994
a/b	0.459	0.4612	0.4593	0.4444	0.4183	0.3963	0.3668	0.3421	0.3227	0.2972
	0.4561	0.4583	0.4563	0.4413	0.4153	0.3933	0.364	0.3394	0.3201	0.2947
	0.4521	0.4542	0.4522	0.4371	0.4112	0.3894	0.3602	0.3357	0.3165	0.2912
	0.4473	0.4494	0.4473	0.4322	0.4064	0.3847	0.3557	0.3314	0.3123	0.2871
	0.4418	0.4439	0.4416	0.4266	0.4009	0.3794	0.3505	0.3264	0.3075	0.2825
	0.4344	0.4363	0.434	0.4189	0.3934	0.3721	0.3435	0.3197	0.301	0.2762

Figure I.13a: F1B: e=3b & d=2.5b

	c/b									
	0.4645	0.4603	0.4505	0.4332	0.4121	0.3953	0.3739	0.3556	0.3399	0.3208
	0.4638	0.4596	0.4497	0.4325	0.4114	0.3946	0.3732	0.3549	0.3392	0.3201
	0.4625	0.4583	0.4485	0.4313	0.4102	0.3935	0.3721	0.3538	0.3381	0.3191
	0.4606	0.4564	0.4466	0.4294	0.4083	0.3916	0.3703	0.3521	0.3364	0.3174
a/b	0.458	0.4538	0.4441	0.4269	0.4058	0.3892	0.3679	0.3497	0.3337	0.3151
	0.455	0.4508	0.441	0.4238	0.4029	0.3864	0.3652	0.3471	0.3315	0.3126
	0.451	0.4467	0.4369	0.4199	0.399	0.3826	0.3614	0.3435	0.328	0.3092
	0.4462	0.4419	0.4322	0.4152	0.3944	0.3781	0.3571	0.3392	0.3238	0.3051
	0.4407	0.4364	0.4267	0.4098	0.3892	0.3729	0.3521	0.3343	0.3191	0.3005
	0.4333	0.429	0.4193	0.4025	0.382	0.3659	0.3452	0.3277	0.3126	0.2941

Figure I.13a: F1B: e=3b & d=3b

	c/b									
	0.4625	0.4558	0.4457	0.4312	0.4149	0.4015	0.385	0.3705	0.3574	0.3422
	0.4618	0.4551	0.4449	0.4305	0.4141	0.4008	0.3843	0.3698	0.3567	0.3415
	0.4605	0.4539	0.4437	0.4293	0.413	0.3996	0.3832	0.3687	0.3556	0.3405
	0.4586	0.4519	0.4418	0.4274	0.4111	0.3978	0.3814	0.3669	0.3539	0.3388
a/b	0.456	0.4493	0.4392	0.4249	0.4086	0.3953	0.379	0.3646	0.3516	0.3365
	0.4531	0.4464	0.4363	0.422	0.4058	0.3926	0.3763	0.3619	0.3489	0.3339
	0.449	0.4424	0.4323	0.4181	0.4019	0.3888	0.3725	0.3582	0.3453	0.3304
	0.4443	0.4377	0.4277	0.4135	0.3974	0.3843	0.3682	0.3539	0.3411	0.3262
	0.4388	0.4322	0.4223	0.4082	0.3922	0.3792	0.3631	0.349	0.3363	0.3215
	0.4314	0.4249	0.415	0.401	0.3851	0.3723	0.3563	0.3423	0.3297	0.315

Figure I.13a: F1B: e=3b & d=3.5b

	c/b									
	0.4623	0.4561	0.4475	0.4361	0.4232	0.4123	0.3992	0.3873	0.3762	0.3637
	0.4615	0.4554	0.4467	0.4353	0.4225	0.4116	0.3985	0.3866	0.3755	0.363
	0.4603	0.4541	0.4455	0.4341	0.4213	0.4104	0.3974	0.3855	0.3744	0.3619
	0.4584	0.4522	0.4436	0.4322	0.4195	0.4086	0.3956	0.3837	0.3726	0.3602
a/b	0.4558	0.4496	0.4411	0.4297	0.417	0.4061	0.3931	0.3813	0.3703	0.3578
	0.4528	0.4467	0.4382	0.4268	0.4141	0.4033	0.3904	0.3786	0.3676	0.3552
	0.4488	0.4427	0.4342	0.4229	0.4103	0.3995	0.3866	0.3749	0.3639	0.3516
	0.4441	0.438	0.4295	0.4183	0.4057	0.395	0.3822	0.3705	0.3596	0.3473
	0.4386	0.4326	0.4242	0.413	0.4005	0.3899	0.3771	0.3655	0.3547	0.3424
	0.4312	0.4252	0.4169	0.4058	0.3934	0.3828	0.3701	0.3586	0.3479	0.3358

Figure I.13a: F1B: e=3b & d=4b

	c/b									
	0.4626	0.4576	0.4507	0.4417	0.4316	0.4227	0.4120	0.4021	0.3927	0.3822
	0.4619	0.4569	0.4500	0.4410	0.4309	0.4219	0.4113	0.4014	0.3920	0.3815
	0.4606	0.4556	0.4488	0.4398	0.4297	0.4208	0.4102	0.4003	0.3909	0.3804
	0.4587	0.4537	0.4469	0.4379	0.4278	0.4189	0.4083	0.3985	0.3891	0.3786
a/b	0.4561	0.4511	0.4443	0.4354	0.4253	0.4164	0.4059	0.3960	0.3867	0.3762
	0.4532	0.4482	0.4414	0.4325	0.4224	0.4136	0.4031	0.3932	0.3839	0.3735
	0.4492	0.4442	0.4374	0.4285	0.4186	0.4097	0.3993	0.3895	0.3802	0.3698
	0.4444	0.4395	0.4327	0.4239	0.4140	0.4052	0.3947	0.3850	0.3758	0.3654
	0.4390	0.4341	0.4273	0.4186	0.4087	0.4000	0.3896	0.3799	0.3708	0.3605
	0.4316	0.4267	0.4200	0.4113	0.4015	0.3929	0.3826	0.3730	0.3639	0.3537

Figure 6.25a: F1B: e=3.5b & d=0.5b

	c/b									
a/b	0.4645	0.4646	0.4646	0.4646	0.4645	0.4647	0.4663	0.4476	0.3351	0.237
	0.4639	0.4639	0.4639	0.4639	0.4638	0.464	0.4656	0.4469	0.3345	0.2365
	0.4627	0.4627	0.4628	0.4628	0.4627	0.4629	0.4645	0.4458	0.3335	0.2356
	0.461	0.461	0.461	0.461	0.4609	0.4611	0.4627	0.444	0.3318	0.2342
	0.4585	0.4586	0.4586	0.4586	0.4585	0.4587	0.4603	0.4415	0.3296	0.2322
	0.4558	0.4558	0.4558	0.4558	0.4558	0.4559	0.4575	0.4387	0.3271	0.2299
	0.4521	0.4521	0.4521	0.4521	0.452	0.4522	0.4537	0.4349	0.3238	0.2268
	0.4476	0.4477	0.4477	0.4477	0.4476	0.4478	0.4493	0.4304	0.3197	0.2232
	0.4426	0.4426	0.4427	0.4427	0.4426	0.4428	0.4442	0.4254	0.315	0.2191
	0.4359	0.436	0.436	0.436	0.4359	0.4361	0.4375	0.4186	0.3088	0.2135

Figure 6.25a: F1B: e=3.5b & d=1b

	c/b									
a/b	0.4645	0.4645	0.4645	0.4645	0.4642	0.4567	0.4266	0.3729	0.3211	0.2636
	0.4639	0.4638	0.4638	0.4638	0.4635	0.456	0.4259	0.3722	0.32	0.263
	0.4627	0.4627	0.4627	0.4627	0.4624	0.4548	0.4245	0.3711	0.3195	0.2621
	0.461	0.4609	0.4609	0.4609	0.4606	0.4531	0.4227	0.3693	0.3179	0.2606
	0.4586	0.4585	0.4585	0.4585	0.4582	0.4506	0.4202	0.3669	0.3157	0.2586
	0.4558	0.4558	0.4557	0.4557	0.4555	0.4479	0.4174	0.3641	0.3132	0.2563
	0.4521	0.452	0.452	0.452	0.4517	0.4441	0.4136	0.3603	0.3098	0.2532
	0.4476	0.4476	0.4476	0.4476	0.4473	0.4397	0.4091	0.3558	0.3059	0.2495
	0.4426	0.4426	0.4426	0.4426	0.4423	0.4347	0.4041	0.3508	0.3014	0.2453
	0.4359	0.4359	0.4359	0.4359	0.4356	0.428	0.3974	0.344	0.2983	0.2397

Figure 6.25a: F1B: e=3.5b & d=1.5b

	c/b									
a/b	0.4645	0.4649	0.4668	0.4678	0.4567	0.4306	0.3872	0.3491	0.322	0.285
	0.4638	0.4642	0.4661	0.4671	0.456	0.4299	0.3866	0.3484	0.3214	0.2844
	0.4627	0.4631	0.465	0.466	0.4548	0.4288	0.3854	0.3474	0.3205	0.2835
	0.4609	0.4613	0.4632	0.4641	0.4529	0.4269	0.3837	0.3457	0.3189	0.282
	0.4585	0.4589	0.4608	0.4617	0.4504	0.4244	0.3813	0.3435	0.3167	0.2799
	0.4558	0.4561	0.458	0.4589	0.4475	0.4215	0.3786	0.3409	0.3143	0.2776
	0.452	0.4524	0.4542	0.4551	0.4436	0.4176	0.3748	0.3374	0.3109	0.2745
	0.4476	0.448	0.4498	0.4505	0.439	0.413	0.3705	0.3332	0.307	0.2707
	0.4426	0.443	0.4448	0.4454	0.4338	0.4078	0.3655	0.3285	0.3026	0.2665
	0.4359	0.4363	0.438	0.4386	0.4268	0.4009	0.3589	0.3223	0.2967	0.2609

Figure 6.25a: F1B: e=3.5b & d=2b

	c/b									
a/b	0.4656	0.4679	0.4661	0.4511	0.425	0.4027	0.373	0.3481	0.3285	0.3028
	0.4649	0.4672	0.4654	0.4504	0.4243	0.402	0.3724	0.3475	0.3279	0.3022
	0.4638	0.4661	0.4642	0.4493	0.4231	0.4009	0.3713	0.3465	0.3269	0.3013
	0.462	0.4643	0.4624	0.4474	0.4213	0.3992	0.3696	0.3449	0.3254	0.2998
	0.4596	0.4618	0.4599	0.445	0.4189	0.3968	0.3674	0.3427	0.3233	0.2977
	0.4568	0.459	0.4571	0.4421	0.4161	0.3941	0.3648	0.3402	0.3208	0.2954
	0.4531	0.4552	0.4532	0.4383	0.4124	0.3905	0.3613	0.3368	0.3176	0.2922
	0.4486	0.4508	0.4487	0.4337	0.4079	0.3862	0.3571	0.3328	0.3137	0.2885
	0.4436	0.4457	0.4435	0.4285	0.4029	0.3813	0.3524	0.3283	0.3093	0.2843
	0.4369	0.4389	0.4367	0.4217	0.3961	0.3748	0.3462	0.3222	0.3035	0.2786

Figure 6.25a: F1B: e=3.5b & d=2.5b

	c/b									
a/b	0.4646	0.4604	0.4505	0.4333	0.4121	0.3954	0.3739	0.3556	0.3399	0.3208
	0.4639	0.4597	0.4498	0.4326	0.4115	0.3947	0.3733	0.355	0.3393	0.3202
	0.4627	0.4585	0.4487	0.4315	0.4104	0.3937	0.3723	0.354	0.3383	0.3193
	0.4609	0.4567	0.4469	0.4297	0.4087	0.392	0.3706	0.3524	0.3368	0.3178
	0.4585	0.4543	0.4445	0.4273	0.4063	0.3897	0.3684	0.3503	0.3347	0.3157
	0.4558	0.4515	0.4417	0.4246	0.4037	0.3871	0.3659	0.3478	0.3323	0.3134
	0.452	0.4478	0.438	0.4209	0.4001	0.3836	0.3625	0.3445	0.329	0.3102
	0.4476	0.4433	0.4336	0.4166	0.3958	0.3795	0.3584	0.3405	0.3252	0.3064
	0.4425	0.4383	0.4286	0.4116	0.391	0.3748	0.3538	0.3361	0.3208	0.3022
	0.4358	0.4315	0.4219	0.4051	0.3845	0.3685	0.3477	0.3301	0.315	0.2964

Figure 6.25a: F1B: e=3.5b & d=3b

	c/b									
a/b	0.4625	0.4559	0.4457	0.4313	0.4149	0.4015	0.385	0.3705	0.3574	0.3422
	0.4619	0.4552	0.445	0.4306	0.4142	0.4009	0.3844	0.3699	0.3568	0.3416
	0.4607	0.454	0.4439	0.4295	0.4132	0.3998	0.3834	0.3689	0.3558	0.3406
	0.459	0.4523	0.4421	0.4278	0.4115	0.3981	0.3817	0.3673	0.3542	0.3391
	0.4566	0.4499	0.4398	0.4254	0.4092	0.3959	0.3795	0.3651	0.3521	0.337
	0.4538	0.4471	0.437	0.4228	0.4065	0.3933	0.377	0.3626	0.3496	0.3346
	0.4501	0.4434	0.4334	0.4191	0.403	0.3898	0.3735	0.3592	0.3463	0.3313
	0.4457	0.439	0.429	0.4149	0.3988	0.3857	0.3695	0.3552	0.3424	0.3275
	0.4406	0.434	0.4241	0.41	0.394	0.381	0.3649	0.3507	0.338	0.3231
	0.434	0.4274	0.4175	0.4035	0.3876	0.3747	0.3587	0.3447	0.332	0.3172

Figure 6.25a: F1B: e=3.5b & d=3.5b

	c/b									
a/b	0.4623	0.4561	0.4475	0.4361	0.4233	0.4123	0.3992	0.3873	0.3762	0.3637
	0.4616	0.4555	0.4468	0.4354	0.4226	0.4117	0.3986	0.3867	0.3756	0.3631
	0.4605	0.4543	0.4457	0.4343	0.4215	0.4106	0.3975	0.3856	0.3746	0.3621
	0.4587	0.4526	0.444	0.4326	0.4198	0.409	0.3959	0.384	0.373	0.3605
	0.4563	0.4502	0.4416	0.4302	0.4175	0.4067	0.3936	0.3818	0.3708	0.3583
	0.4536	0.4474	0.4389	0.4276	0.4149	0.4041	0.3911	0.3793	0.3683	0.3559
	0.4498	0.4437	0.4352	0.4239	0.4113	0.4005	0.3876	0.3758	0.3649	0.3525
	0.4454	0.4394	0.4309	0.4196	0.4071	0.3964	0.3835	0.3718	0.3609	0.3486
	0.4404	0.4344	0.4259	0.4148	0.4022	0.3916	0.3788	0.3672	0.3564	0.3441
	0.4338	0.4277	0.4194	0.4083	0.3958	0.3853	0.3726	0.361	0.3503	0.3381

Figure 6.25a: F1B: e=3.5b & d=4b

	c/b									
a/b	0.4627	0.4576	0.4507	0.4417	0.4316	0.4227	0.4121	0.4022	0.3927	0.3822
	0.462	0.457	0.4501	0.4411	0.431	0.422	0.4114	0.4015	0.3921	0.3816
	0.4608	0.4558	0.4489	0.44	0.4299	0.4209	0.4104	0.4005	0.3911	0.3805
	0.4591	0.4541	0.4472	0.4382	0.4282	0.4192	0.4087	0.3988	0.3894	0.3789
	0.4567	0.4517	0.4448	0.4359	0.4258	0.4169	0.4064	0.3965	0.3872	0.3767
	0.4539	0.4489	0.4421	0.4332	0.4232	0.4143	0.4038	0.394	0.3846	0.3742
	0.4502	0.4452	0.4384	0.4295	0.4196	0.4107	0.4002	0.3905	0.3812	0.3708
	0.4458	0.4409	0.4341	0.4252	0.4153	0.4065	0.3961	0.3863	0.3771	0.3667
	0.4408	0.4359	0.4291	0.4203	0.4104	0.4017	0.3913	0.3816	0.3724	0.3621
	0.4341	0.4292	0.4225	0.4138	0.404	0.3953	0.385	0.3754	0.3662	0.356

Figure I.14a: F1B: e=4b & d=0.5b

	c/b									
	0.4646	0.4646	0.4646	0.4646	0.4646	0.4647	0.4663	0.4477	0.3352	0.2371
	0.464	0.464	0.464	0.464	0.4639	0.4641	0.4657	0.447	0.3346	0.2366
	0.4629	0.4629	0.463	0.463	0.4629	0.4631	0.4647	0.446	0.3337	0.2358
	0.4613	0.4613	0.4614	0.4614	0.4612	0.4615	0.4631	0.4443	0.3322	0.2345
a/b	0.4591	0.4591	0.4592	0.4592	0.4591	0.4593	0.4609	0.4421	0.3303	0.2328
	0.4566	0.4566	0.4567	0.4567	0.4566	0.4568	0.4583	0.4396	0.328	0.2308
	0.4532	0.4532	0.4532	0.4533	0.4532	0.4534	0.4549	0.4361	0.3251	0.2281
	0.4492	0.4492	0.4492	0.4492	0.4491	0.4493	0.4508	0.4321	0.3214	0.2249
	0.4446	0.4446	0.4446	0.4447	0.4446	0.4448	0.4462	0.4274	0.3172	0.2212
	0.4386	0.4386	0.4386	0.4386	0.4385	0.4387	0.4401	0.4213	0.3117	0.2164

Figure I.14a: F1B: e=4b & d=1b

	c/b									
	0.4646	0.4646	0.4645	0.4645	0.4642	0.4567	0.4266	0.3729	0.3211	0.2636
	0.464	0.4639	0.4639	0.4639	0.4636	0.4561	0.426	0.3723	0.3206	0.2631
	0.4629	0.4629	0.4629	0.4629	0.4626	0.455	0.4247	0.3714	0.3196	0.2623
	0.4613	0.4613	0.4613	0.4613	0.461	0.4534	0.4231	0.3698	0.3183	0.261
a/b	0.4591	0.4591	0.4591	0.4591	0.4588	0.4512	0.4209	0.3676	0.3163	0.2592
	0.4566	0.4566	0.4565	0.4566	0.4563	0.4487	0.4183	0.3651	0.3141	0.2572
	0.4532	0.4532	0.4531	0.4531	0.4529	0.4453	0.4149	0.3617	0.3111	0.2544
	0.4492	0.4492	0.4491	0.4491	0.4488	0.4413	0.4108	0.3577	0.3063	0.2511
	0.4446	0.4446	0.4445	0.4445	0.4443	0.4367	0.4063	0.3531	0.3035	0.2473
	0.4386	0.4385	0.4385	0.4385	0.4382	0.4306	0.4003	0.3471	0.2981	0.2424

Figure I.14a: F1B: e=4b & d=1.5b

	c/b									
	0.4646	0.4649	0.4668	0.4678	0.4567	0.4307	0.3873	0.3491	0.3221	0.285
	0.4639	0.4643	0.4662	0.4672	0.4561	0.43	0.3867	0.3485	0.3215	0.2845
	0.4629	0.4633	0.4652	0.4662	0.455	0.429	0.3857	0.3476	0.3206	0.2837
	0.4613	0.4617	0.4636	0.4645	0.4533	0.4273	0.3841	0.3461	0.3192	0.2823
a/b	0.4591	0.4595	0.4614	0.4623	0.4511	0.4251	0.3819	0.3441	0.3173	0.2805
	0.4566	0.457	0.4588	0.4597	0.4484	0.4225	0.3795	0.3418	0.3151	0.2784
	0.4532	0.4536	0.4554	0.4562	0.4449	0.4189	0.3761	0.3386	0.3121	0.2756
	0.4492	0.4495	0.4513	0.4521	0.4407	0.4148	0.3722	0.3349	0.3086	0.2722
	0.4446	0.4449	0.4467	0.4475	0.4359	0.4101	0.3677	0.3307	0.3046	0.2685
	0.4385	0.4389	0.4407	0.4413	0.4296	0.4038	0.3618	0.3251	0.2993	0.2634

Figure I.14a: F1B: e=4b & d=2b

	c/b									
	0.4656	0.4679	0.4661	0.4512	0.425	0.4027	0.373	0.3482	0.3285	0.3028
	0.465	0.4673	0.4655	0.4505	0.4244	0.4021	0.3725	0.3476	0.328	0.3023
	0.464	0.4663	0.4644	0.4495	0.4233	0.4011	0.3715	0.3467	0.3271	0.3015
	0.4624	0.4646	0.4628	0.4478	0.4217	0.3996	0.37	0.3453	0.3257	0.3001
a/b	0.4602	0.4624	0.4605	0.4456	0.4195	0.3975	0.368	0.3433	0.3238	0.2983
	0.4576	0.4599	0.4579	0.443	0.417	0.395	0.3656	0.341	0.3216	0.2962
	0.4542	0.4564	0.4544	0.4395	0.4136	0.3917	0.3625	0.338	0.3187	0.2933
	0.4502	0.4523	0.4503	0.4354	0.4096	0.3878	0.3587	0.3344	0.3152	0.29
	0.4456	0.4477	0.4456	0.4307	0.405	0.3834	0.3544	0.3303	0.3112	0.2861
	0.4395	0.4416	0.4394	0.4245	0.3989	0.3775	0.3488	0.3248	0.306	0.2811

Figure I.14a: F1B: e=4b & d=2.5b

	c/b									
	0.4646	0.4604	0.4505	0.4333	0.4121	0.3954	0.3739	0.3556	0.3399	0.3208
	0.464	0.4598	0.4499	0.4327	0.4116	0.3948	0.3734	0.3551	0.3394	0.3203
	0.4629	0.4587	0.4489	0.4317	0.4106	0.3939	0.3725	0.3542	0.3385	0.3194
	0.4613	0.4571	0.4473	0.4301	0.409	0.3924	0.371	0.3528	0.3371	0.3181
a/b	0.4591	0.4549	0.4451	0.4279	0.4069	0.3903	0.369	0.3508	0.3352	0.3162
	0.4566	0.4524	0.4426	0.4255	0.4045	0.3879	0.3667	0.3486	0.333	0.3141
	0.4532	0.4489	0.4392	0.4221	0.4012	0.3848	0.3636	0.3456	0.3301	0.3112
	0.4491	0.4449	0.4352	0.4181	0.3974	0.381	0.3599	0.342	0.3266	0.3078
	0.4445	0.4403	0.4306	0.4137	0.393	0.3767	0.3558	0.3379	0.3226	0.304
	0.4385	0.4342	0.4246	0.4077	0.3872	0.371	0.3503	0.3326	0.3174	0.2988

Figure I.14a: F1B: e=4b & d=3b

	c/b									
	0.4626	0.4559	0.4457	0.4313	0.4149	0.4015	0.3850	0.3705	0.3574	0.3422
	0.4620	0.4553	0.4451	0.4307	0.4143	0.4009	0.3845	0.3700	0.3569	0.3417
	0.4609	0.4542	0.4441	0.4297	0.4133	0.4000	0.3835	0.3690	0.3560	0.3408
	0.4593	0.4526	0.4425	0.4281	0.4118	0.3985	0.3821	0.3676	0.3545	0.3394
a/b	0.4571	0.4505	0.4404	0.4260	0.4097	0.3964	0.3801	0.3656	0.3526	0.3375
	0.4546	0.4480	0.4379	0.4236	0.4073	0.3941	0.3778	0.3634	0.3504	0.3353
	0.4512	0.4446	0.4345	0.4203	0.4041	0.3909	0.3746	0.3603	0.3474	0.3324
	0.4472	0.4406	0.4306	0.4164	0.4003	0.3871	0.3709	0.3567	0.3438	0.3289
	0.4426	0.4360	0.4261	0.4119	0.3959	0.3829	0.3668	0.3526	0.3398	0.3249
	0.4366	0.4300	0.4201	0.4061	0.3902	0.3772	0.3612	0.3472	0.3345	0.3197

Figure I.14a: F1B: e=4b & d=3.5b

	c/b									
	0.4623	0.4561	0.4475	0.4361	0.4233	0.4124	0.3993	0.3873	0.3762	0.3637
	0.4617	0.4555	0.4469	0.4355	0.4227	0.4118	0.3987	0.3868	0.3757	0.3632
	0.4607	0.4545	0.4459	0.4345	0.4217	0.4108	0.3977	0.3858	0.3748	0.3623
	0.4591	0.4529	0.4443	0.4329	0.4202	0.4093	0.3962	0.3844	0.3733	0.3608
a/b	0.4569	0.4508	0.4422	0.4308	0.4181	0.4072	0.3942	0.3824	0.3713	0.3589
	0.4544	0.4483	0.4397	0.4284	0.4157	0.4049	0.3919	0.38	0.3691	0.3566
	0.451	0.4449	0.4364	0.4251	0.4124	0.4016	0.3887	0.3769	0.366	0.3536
	0.447	0.4409	0.4324	0.4211	0.4085	0.3978	0.3849	0.3732	0.3623	0.35
	0.4424	0.4363	0.4279	0.4167	0.4042	0.3935	0.3807	0.369	0.3582	0.3459
	0.4364	0.4303	0.422	0.4108	0.3984	0.3878	0.3751	0.3635	0.3527	0.3405

Figure I.14a: F1B: e=4b & d=4b

	c/b									
	0.4627	0.4577	0.4508	0.4418	0.4317	0.4227	0.4121	0.4022	0.3928	0.3822
	0.4621	0.4571	0.4502	0.4412	0.4311	0.4221	0.4115	0.4016	0.3922	0.3817
	0.461	0.456	0.4491	0.4402	0.4301	0.4211	0.4105	0.4006	0.3913	0.3807
	0.4594	0.4544	0.4476	0.4386	0.4285	0.4196	0.409	0.3991	0.3898	0.3793
a/b	0.4572	0.4523	0.4454	0.4365	0.4264	0.4175	0.407	0.3971	0.3877	0.3773
	0.4547	0.4498	0.4429	0.434	0.424	0.4151	0.4046	0.3947	0.3854	0.375
	0.4513	0.4464	0.4396	0.4307	0.4207	0.4118	0.4013	0.3916	0.3823	0.3718
	0.4473	0.4424	0.4356	0.4267	0.4168	0.408	0.3975	0.3878	0.3785	0.3681
	0.4427	0.4378	0.4311	0.4223	0.4124	0.4036	0.3932	0.3835	0.3743	0.364
	0.4367	0.4318	0.4251	0.4164	0.4065	0.3978	0.3875	0.3779	0.3687	0.3584

Figure 6.22b: F2B: e=0.5b & d=0.5b

	c/b									
a/b	−0.3358	−0.3358	−0.3358	−0.3358	−0.3357	−0.3352	−0.3328	−0.3304	−0.2852	−0.2334
	−0.3352	−0.3352	−0.3352	−0.3352	−0.3352	−0.3346	−0.3323	−0.3298	−0.2847	−0.2337
	−0.3343	−0.3343	−0.3343	−0.3343	−0.3343	−0.3338	−0.3314	−0.3289	−0.2839	−0.2327
	−0.3328	−0.3328	−0.3328	−0.3328	−0.3328	−0.3323	−0.3299	−0.3275	−0.2826	−0.2317
	−0.3304	−0.3304	−0.3304	−0.3304	−0.3304	−0.3299	−0.3275	−0.3252	−0.2805	−0.23
	−0.3278	−0.3278	−0.3278	−0.3278	−0.3278	−0.3273	−0.3249	−0.3226	−0.2836	−0.228
	−0.3225	−0.3225	−0.3224	−0.3225	−0.3224	−0.3219	−0.3196	−0.3174	−0.2743	−0.2238
	−0.314	−0.314	−0.314	−0.314	−0.314	−0.3135	−0.3112	−0.3091	−0.2665	−0.2173
	−0.2986	−0.2986	−0.2984	−0.2986	−0.2986	−0.2981	−0.2959	−0.2939	−0.2533	−0.2051
	−0.2622	−0.2622	−0.2622	−0.2622	−0.2622	−0.2617	−0.2597	−0.2582	−0.2198	−0.1775

Figure 6.22b: F2B: e=0.5b & d=1b

	c/b									
a/b	−0.3358	−0.3358	−0.3357	−0.3357	−0.3356	−0.3322	−0.3187	−0.2968	−0.2721	−0.258
	−0.3352	−0.3352	−0.3351	−0.3351	−0.3351	−0.3316	−0.3184	−0.2964	−0.2717	−0.2576
	−0.3343	−0.3343	−0.3343	−0.3342	−0.3342	−0.3307	−0.3175	−0.2956	−0.2709	−0.2568
	−0.3328	−0.3328	−0.3327	−0.3327	−0.3327	−0.3292	−0.3161	−0.2942	−0.2696	−0.2556
	−0.3304	−0.3304	−0.3303	−0.3303	−0.3303	−0.3269	−0.3138	−0.2921	−0.2675	−0.2536
	−0.3278	−0.3278	−0.3278	−0.3277	−0.3277	−0.3243	−0.3113	−0.2898	−0.2652	−0.2514
	−0.3225	−0.3225	−0.3224	−0.3224	−0.3223	−0.3189	−0.3062	−0.285	−0.2604	−0.2468
	−0.314	−0.314	−0.3139	−0.3139	−0.3139	−0.3105	−0.2979	−0.2774	−0.253	−0.2397
	−0.2987	−0.2986	−0.2986	−0.2985	−0.2985	−0.2952	−0.2832	−0.2635	−0.2391	−0.2264
	−0.2622	−0.2622	−0.2622	−0.2621	−0.2621	−0.259	−0.2482	−0.2305	−0.2074	−0.1962

Figure 6.22b: F2B: e=0.5b & d=1.5b

	c/b									
a/b	−0.3355	−0.3342	−0.3313	−0.3286	−0.327	−0.3264	−0.3208	−0.3145	−0.302	−0.2861	−0.2756
	−0.3349	−0.3337	−0.3307	−0.328	−0.3264	−0.3203	−0.314	−0.3014	−0.2855	−0.2751
	−0.3341	−0.3328	−0.3298	−0.3271	−0.3256	−0.3195	−0.3131	−0.3006	−0.2847	−0.2743
	−0.3326	−0.3313	−0.3284	−0.3257	−0.3241	−0.3181	−0.3117	−0.2992	−0.2834	−0.2729
	−0.3302	−0.3289	−0.326	−0.3233	−0.3218	−0.3158	−0.3095	−0.297	−0.2812	−0.2708
	−0.3276	−0.3263	−0.3234	−0.3208	−0.3193	−0.3133	−0.307	−0.2946	−0.2789	−0.2685
	−0.3222	−0.321	−0.3181	−0.3155	−0.3141	−0.3082	−0.302	−0.2896	−0.2739	−0.2637
	−0.3137	−0.3125	−0.3097	−0.3072	−0.3059	−0.3001	−0.2939	−0.2817	−0.2662	−0.2562
	−0.2984	−0.2972	−0.2942	−0.292	−0.2911	−0.2855	−0.2795	−0.2675	−0.2523	−0.2424
	−0.262	−0.2608	−0.2583	−0.2562	−0.2556	−0.2505	−0.2449	−0.2337	−0.2194	−0.2107

Figure 6.22b: F2B: e=0.5b & d=2b

	c/b									
a/b	−0.3346	−0.3328	−0.3324	−0.3337	−0.3331	−0.3263	−0.3191	−0.3094	−0.2991	−0.2896
	−0.334	−0.3322	−0.3318	−0.3331	−0.3325	−0.3257	−0.3185	−0.3088	−0.2985	−0.2891
	−0.3331	−0.3314	−0.331	−0.3323	−0.3316	−0.3248	−0.3177	−0.308	−0.2977	−0.2883
	−0.3316	−0.3299	−0.3295	−0.3308	−0.3302	−0.3234	−0.3162	−0.3065	−0.2963	−0.2869
	−0.3293	−0.3275	−0.3271	−0.3285	−0.3278	−0.321	−0.3139	−0.3042	−0.294	−0.2847
	−0.3267	−0.3249	−0.3246	−0.3259	−0.3253	−0.3185	−0.3114	−0.3017	−0.2916	−0.2823
	−0.3213	−0.3196	−0.3193	−0.3206	−0.32	−0.3133	−0.3062	−0.2966	−0.2865	−0.2773
	−0.3129	−0.3112	−0.3109	−0.3123	−0.3117	−0.305	−0.298	−0.2885	−0.2786	−0.2695
	−0.2975	−0.296	−0.2958	−0.2972	−0.2966	−0.2901	−0.2832	−0.274	−0.2643	−0.2554
	−0.2612	−0.2598	−0.2597	−0.2612	−0.2607	−0.2545	−0.2481	−0.2396	−0.2306	−0.2226

Figure 6.22b: F2B: e=0.5b & d=2.5b

	c/b									
a/b	−0.3358	−0.3365	−0.3367	−0.3358	−0.3327	−0.3271	−0.3208	−0.3133	−0.3059	−0.2979
	−0.3352	−0.3359	−0.3362	−0.3352	−0.3321	−0.3266	−0.3202	−0.3128	−0.3054	−0.2973
	−0.3343	−0.3351	−0.3353	−0.3343	−0.3312	−0.3257	−0.3193	−0.3119	−0.3045	−0.2965
	−0.3328	−0.3336	−0.3338	−0.3328	−0.3297	−0.3242	−0.3179	−0.3105	−0.3031	−0.295
	−0.3304	−0.3312	−0.3314	−0.3304	−0.3274	−0.3218	−0.3155	−0.3081	−0.3008	−0.2928
	−0.3278	−0.3286	−0.3288	−0.3278	−0.3248	−0.3193	−0.313	−0.3056	−0.2983	−0.2904
	−0.3225	−0.3232	−0.3235	−0.3225	−0.3194	−0.314	−0.3077	−0.3004	−0.2931	−0.2852
	−0.314	−0.3148	−0.315	−0.314	−0.311	−0.3056	−0.2994	−0.2922	−0.2851	−0.2773
	−0.2987	−0.2994	−0.2997	−0.2988	−0.2958	−0.2906	−0.2846	−0.2776	−0.2706	−0.263
	−0.2623	−0.263	−0.2633	−0.2625	−0.2597	−0.2548	−0.2493	−0.2428	−0.2364	−0.2295

Figure 6.22b: F2B: e=0.5b & d=3b

	c/b									
a/b	−0.336	−0.336	−0.3351	−0.3328	−0.3293	−0.3249	−0.3195	−0.3136	−0.3078	−0.3012
	−0.3354	−0.3354	−0.3345	−0.3323	−0.3287	−0.3243	−0.3189	−0.3131	−0.3073	−0.3006
	−0.3345	−0.3345	−0.3336	−0.3314	−0.3278	−0.3234	−0.318	−0.3122	−0.3064	−0.2998
	−0.333	−0.333	−0.3321	−0.3299	−0.3263	−0.3219	−0.3166	−0.3107	−0.305	−0.2983
	−0.3306	−0.3306	−0.3297	−0.3275	−0.324	−0.3196	−0.3142	−0.3084	−0.3026	−0.296
	−0.328	−0.328	−0.3271	−0.3249	−0.3214	−0.317	−0.3117	−0.3059	−0.3002	−0.2936
	−0.3227	−0.3227	−0.3218	−0.3196	−0.3161	−0.3117	−0.3064	−0.3007	−0.295	−0.2885
	−0.3142	−0.3142	−0.3133	−0.3111	−0.3076	−0.3033	−0.2981	−0.2925	−0.2869	−0.2805
	−0.2989	−0.2989	−0.298	−0.2959	−0.2925	−0.2884	−0.2833	−0.2778	−0.2724	−0.266
	−0.2624	−0.2624	−0.2616	−0.2597	−0.2565	−0.2527	−0.248	−0.243	−0.2383	−0.2323

Figure 6.22b: F2B: e=0.5b & d=3.5b

	c/b									
a/b	−0.3357	−0.3349	−0.3334	−0.3308	−0.3274	−0.3236	−0.319	−0.3142	−0.3094	−0.3038
	−0.3351	−0.3344	−0.3328	−0.3302	−0.3268	−0.323	−0.3184	−0.3136	−0.3088	−0.3033
	−0.3342	−0.3335	−0.3319	−0.3294	−0.3259	−0.3222	−0.3176	−0.3128	−0.308	−0.3024
	−0.3327	−0.332	−0.3304	−0.3279	−0.3244	−0.3207	−0.3161	−0.3113	−0.3065	−0.301
	−0.3303	−0.3296	−0.328	−0.3255	−0.322	−0.3183	−0.3137	−0.309	−0.3042	−0.2987
	−0.3277	−0.327	−0.3254	−0.3229	−0.3195	−0.3158	−0.3112	−0.3064	−0.3018	−0.2963
	−0.3223	−0.3216	−0.3201	−0.3176	−0.3142	−0.3105	−0.306	−0.3012	−0.2965	−0.2911
	−0.3139	−0.3132	−0.3116	−0.3091	−0.3058	−0.3022	−0.2977	−0.293	−0.2884	−0.2831
	−0.2986	−0.2979	−0.2964	−0.294	−0.2907	−0.2872	−0.2829	−0.2784	−0.2737	−0.2685
	−0.2621	−0.2615	−0.2601	−0.2578	−0.2548	−0.2516	−0.2476	−0.2435	−0.2394	−0.2347

Figure 6.22b: F2B: e=0.5b & d=4b

	c/b									
a/b	−0.3355	−0.3345	−0.3328	−0.3302	−0.3271	−0.3238	−0.3198	−0.3157	−0.3116	−0.3069
	−0.3349	−0.3339	−0.3322	−0.3297	−0.3265	−0.3232	−0.3193	−0.3152	−0.3111	−0.3063
	−0.334	−0.333	−0.3313	−0.3288	−0.3256	−0.3224	−0.3184	−0.3143	−0.3102	−0.3055
	−0.3325	−0.3315	−0.3298	−0.3273	−0.3241	−0.3209	−0.3169	−0.3128	−0.3088	−0.304
	−0.3301	−0.3291	−0.3274	−0.3249	−0.3218	−0.3185	−0.3146	−0.3105	−0.3064	−0.3017
	−0.3275	−0.3265	−0.3248	−0.3223	−0.3192	−0.316	−0.312	−0.308	−0.304	−0.2993
	−0.3222	−0.3212	−0.3195	−0.317	−0.3139	−0.3107	−0.3068	−0.3028	−0.2988	−0.2941
	−0.3137	−0.3127	−0.311	−0.3086	−0.3055	−0.3024	−0.2985	−0.2946	−0.2906	−0.2861
	−0.2984	−0.2975	−0.2958	−0.2935	−0.2905	−0.2874	−0.2837	−0.2798	−0.2759	−0.2715
	−0.2619	−0.261	−0.2595	−0.2574	−0.2546	−0.2518	−0.2484	−0.2449	−0.2414	−0.2374

Figure I.11b: F2B: e=1b & d=0.5b

	c/b									
	−0.3356	−0.3356	−0.3356	−0.3356	−0.3356	−0.3351	−0.3327	−0.3302	−0.285	−0.2336
	−0.3345	−0.3345	−0.3345	−0.3345	−0.3345	−0.3339	−0.3316	−0.3291	−0.2841	−0.2328
	−0.3329	−0.3329	−0.3329	−0.3329	−0.3329	−0.3323	−0.33	−0.3276	−0.2827	−0.2319
	−0.3304	−0.3304	−0.3304	−0.3304	−0.3304	−0.3298	−0.3275	−0.3251	−0.2805	−0.2301
a/b	−0.3268	−0.3268	−0.3268	−0.3268	−0.3268	−0.3263	−0.3239	−0.3216	−0.2773	−0.2274
	−0.3228	−0.3228	−0.3227	−0.3228	−0.3227	−0.3222	−0.3199	−0.3177	−0.2738	−0.2241
	−0.3161	−0.3161	−0.316	−0.3161	−0.316	−0.3155	−0.3133	−0.3111	−0.2678	−0.2191
	−0.3067	−0.3067	−0.3067	−0.3067	−0.3067	−0.3062	−0.304	−0.302	−0.2596	−0.212
	−0.2941	−0.2941	−0.2941	−0.2941	−0.2941	−0.2936	−0.2915	−0.2896	−0.2484	−0.2024
	−0.2704	−0.2704	−0.2704	−0.2704	−0.2704	−0.27	−0.2679	−0.2664	−0.2254	−0.1845

Figure I.11b: F2B: e=1b & d=1b

	c/b									
	−0.3356	−0.3356	−0.3355	−0.3355	−0.3355	−0.332	−0.3185	−0.2967	−0.272	−0.2579
	−0.3345	−0.3345	−0.3344	−0.3344	−0.3344	−0.3309	−0.3177	−0.2957	−0.271	−0.257
	−0.3329	−0.3329	−0.3328	−0.3328	−0.3328	−0.3293	−0.3162	−0.2944	−0.2697	−0.2557
	−0.3304	−0.3304	−0.3303	−0.3303	−0.3303	−0.3268	−0.3138	−0.2922	−0.2675	−0.2536
a/b	−0.3268	−0.3268	−0.3267	−0.3267	−0.3267	−0.3233	−0.3103	−0.2889	−0.2643	−0.2506
	−0.3228	−0.3228	−0.3227	−0.3227	−0.3226	−0.3192	−0.3065	−0.2853	−0.2608	−0.2472
	−0.3161	−0.3161	−0.316	−0.316	−0.3159	−0.3126	−0.3	−0.2793	−0.2549	−0.2415
	−0.3067	−0.3067	−0.3067	−0.3066	−0.3066	−0.3033	−0.291	−0.271	−0.2467	−0.2337
	−0.2941	−0.2941	−0.2941	−0.294	−0.294	−0.2908	−0.279	−0.2596	−0.2357	−0.2232
	−0.2704	−0.2704	−0.2704	−0.2703	−0.2703	−0.2672	−0.2563	−0.2383	−0.2149	−0.2033

Figure I.11b: F2B: e=1b & d=1.5b

	c/b									
	−0.3354	−0.3341	−0.3311	−0.3284	−0.3268	−0.3207	−0.3143	−0.3018	−0.2859	−0.2754
	−0.3342	−0.3329	−0.33	−0.3273	−0.3257	−0.3196	−0.3133	−0.3008	−0.2849	−0.2744
	−0.3326	−0.3314	−0.3284	−0.3257	−0.3242	−0.3181	−0.3118	−0.2993	−0.2834	−0.273
	−0.3301	−0.3289	−0.326	−0.3233	−0.3218	−0.3158	−0.3095	−0.297	−0.2812	−0.2708
a/b	−0.3266	−0.3253	−0.3224	−0.3198	−0.3183	−0.3124	−0.3061	−0.2937	−0.2779	−0.2676
	−0.3225	−0.3213	−0.3184	−0.3158	−0.3144	−0.3085	−0.3023	−0.2899	−0.2742	−0.264
	−0.3158	−0.3146	−0.3117	−0.3092	−0.3079	−0.3022	−0.296	−0.2837	−0.2681	−0.258
	−0.3065	−0.3053	−0.3025	−0.3	−0.2989	−0.2933	−0.2872	−0.2751	−0.2597	−0.2498
	−0.2939	−0.2927	−0.29	−0.2876	−0.2867	−0.2813	−0.2753	−0.2634	−0.2483	−0.2387
	−0.2702	−0.269	−0.2665	−0.2643	−0.2638	−0.2586	−0.2529	−0.2414	−0.2269	−0.2178

Figure I.11b: F2B: e=1b & d=2b

	c/b									
	−0.3344	−0.3327	−0.3322	−0.3335	−0.3329	−0.3261	−0.3189	−0.3092	−0.2989	−0.2895
	−0.3333	−0.3315	−0.3311	−0.3324	−0.3318	−0.325	−0.3178	−0.3081	−0.2979	−0.2885
	−0.3317	−0.33	−0.3296	−0.3309	−0.3303	−0.3235	−0.3163	−0.3066	−0.2963	−0.287
	−0.3292	−0.3275	−0.3271	−0.3284	−0.3278	−0.321	−0.3139	−0.3042	−0.294	−0.2847
a/b	−0.3257	−0.3239	−0.3236	−0.3249	−0.3243	−0.3175	−0.3104	−0.3008	−0.2906	−0.2813
	−0.3216	−0.3199	−0.3196	−0.3209	−0.3203	−0.3136	−0.3065	−0.2969	−0.2868	−0.2776
	−0.3149	−0.3133	−0.313	−0.3144	−0.3138	−0.307	−0.3	−0.2905	−0.2805	−0.2714
	−0.3056	−0.304	−0.3038	−0.3052	−0.3046	−0.2979	−0.291	−0.2817	−0.2718	−0.2628
	−0.293	−0.2915	−0.2913	−0.2928	−0.2922	−0.2857	−0.2789	−0.2697	−0.26	−0.2513
	−0.2694	−0.268	−0.2679	−0.2694	−0.2689	−0.2625	−0.256	−0.2472	−0.238	−0.2297

Figure I.11b: F2B: e=1b & d=2.5b

	c/b									
	−0.3356	−0.3363	−0.3366	−0.3356	−0.3325	−0.327	−0.3206	−0.3132	−0.3058	−0.2977
	−0.3345	−0.3352	−0.3355	−0.3345	−0.3314	−0.3259	−0.3195	−0.3121	−0.3047	−0.2966
	−0.3329	−0.3336	−0.3339	−0.3329	−0.3298	−0.3243	−0.3179	−0.3105	−0.3031	−0.2951
	−0.3304	−0.3311	−0.3314	−0.3304	−0.3273	−0.3218	−0.3155	−0.3081	−0.3007	−0.2927
a/b	−0.3268	−0.3276	−0.3278	−0.3268	−0.3238	−0.3183	−0.312	−0.3046	−0.2973	−0.2893
	−0.3228	−0.3235	−0.3238	−0.3228	−0.3198	−0.3143	−0.308	−0.3007	−0.2934	−0.2855
	−0.3161	−0.3168	−0.3171	−0.3161	−0.3131	−0.3077	−0.3015	−0.2942	−0.287	−0.2792
	−0.3068	−0.3075	−0.3078	−0.3068	−0.3038	−0.2985	−0.2924	−0.2852	−0.2781	−0.2704
	−0.2942	−0.2949	−0.2952	−0.2943	−0.2913	−0.2861	−0.2801	−0.2731	−0.2662	−0.2587
	−0.2705	−0.2713	−0.2715	−0.2707	−0.2679	−0.2628	−0.2571	−0.2504	−0.2438	−0.2366

Figure I.11b: F2B: e=1b & d=3b

	c/b									
	−0.3358	−0.3358	−0.3349	−0.3327	−0.3291	−0.3247	−0.3193	−0.3135	−0.3077	−0.301
	−0.3347	−0.3347	−0.3338	−0.3316	−0.328	−0.3236	−0.3182	−0.3124	−0.3066	−0.2999
	−0.3331	−0.3331	−0.3322	−0.33	−0.3264	−0.322	−0.3166	−0.3108	−0.305	−0.2984
	−0.3306	−0.3306	−0.3297	−0.3275	−0.3239	−0.3195	−0.3142	−0.3084	−0.3026	−0.296
a/b	−0.327	−0.327	−0.3261	−0.3239	−0.3204	−0.316	−0.3107	−0.3049	−0.2992	−0.2926
	−0.323	−0.323	−0.3221	−0.3199	−0.3164	−0.312	−0.3067	−0.301	−0.2953	−0.2887
	−0.3163	−0.3163	−0.3154	−0.3132	−0.3097	−0.3054	−0.3001	−0.2945	−0.2888	−0.2824
	−0.3069	−0.307	−0.306	−0.3039	−0.3005	−0.2962	−0.291	−0.2854	−0.2799	−0.2735
	−0.2943	−0.2944	−0.2935	−0.2914	−0.288	−0.2838	−0.2788	−0.2733	−0.2679	−0.2617
	−0.2706	−0.2707	−0.2698	−0.2678	−0.2646	−0.2606	−0.2558	−0.2505	−0.2454	−0.2395

Figure I.11b: F2B: e=1b & d=3.5b

	c/b									
	−0.3355	−0.3348	−0.3332	−0.3307	−0.3272	−0.3235	−0.3189	−0.314	−0.3092	−0.3037
	−0.3344	−0.3336	−0.3321	−0.3295	−0.3261	−0.3224	−0.3177	−0.3129	−0.3081	−0.3026
	−0.3328	−0.332	−0.3305	−0.3279	−0.3245	−0.3208	−0.3162	−0.3114	−0.3066	−0.3011
	−0.3303	−0.3296	−0.328	−0.3255	−0.322	−0.3183	−0.3137	−0.3089	−0.3042	−0.2987
a/b	−0.3267	−0.326	−0.3244	−0.3219	−0.3185	−0.3148	−0.3102	−0.3055	−0.3007	−0.2952
	−0.3226	−0.3219	−0.3204	−0.3179	−0.3145	−0.3108	−0.3063	−0.3015	−0.2968	−0.2914
	−0.3159	−0.3152	−0.3137	−0.3112	−0.3078	−0.3042	−0.2997	−0.295	−0.2904	−0.285
	−0.3066	−0.3059	−0.3044	−0.3019	−0.2986	−0.295	−0.2906	−0.286	−0.2814	−0.2761
	−0.294	−0.2933	−0.2919	−0.2894	−0.2862	−0.2827	−0.2784	−0.2739	−0.2694	−0.2643
	−0.2703	−0.2697	−0.2682	−0.2659	−0.2628	−0.2595	−0.2553	−0.2511	−0.2468	−0.2419

Figure I.11b: F2B: e=1b & d=4b

	c/b									
	−0.3353	−0.3343	−0.3326	−0.3301	−0.3269	−0.3237	−0.3197	−0.3156	−0.3115	−0.3067
	−0.3342	−0.3332	−0.3315	−0.329	−0.3258	−0.3225	−0.3186	−0.3145	−0.3104	−0.3057
	−0.3326	−0.3316	−0.3299	−0.3274	−0.3242	−0.321	−0.317	−0.3129	−0.3088	−0.3041
	−0.3301	−0.3291	−0.3274	−0.3249	−0.3217	−0.3185	−0.3145	−0.3105	−0.3064	−0.3017
a/b	−0.3265	−0.3255	−0.3238	−0.3213	−0.3182	−0.315	−0.311	−0.307	−0.3029	−0.2983
	−0.3225	−0.3215	−0.3198	−0.3173	−0.3142	−0.311	−0.3071	−0.3031	−0.299	−0.2944
	−0.3158	−0.3148	−0.3131	−0.3106	−0.3075	−0.3044	−0.3005	−0.2965	−0.2926	−0.288
	−0.3064	−0.3055	−0.3038	−0.3014	−0.2983	−0.2952	−0.2914	−0.2875	−0.2836	−0.2791
	−0.2938	−0.2929	−0.2913	−0.2889	−0.2859	−0.2829	−0.2792	−0.2753	−0.2715	−0.2672
	−0.2702	−0.2692	−0.2677	−0.2654	−0.2626	−0.2597	−0.2561	−0.2525	−0.2489	−0.2447

Figure 6.23b: F2B: e=1.5b & d=0.5b

	c/b									
a/b	−0.3356	−0.3356	−0.3356	−0.3356	−0.3356	−0.3351	−0.3327	−0.3302	−0.285	−0.2335
	−0.3344	−0.3343	−0.3343	−0.3343	−0.3343	−0.3338	−0.3314	−0.329	−0.2839	−0.2326
	−0.3324	−0.3324	−0.3323	−0.3323	−0.3323	−0.3318	−0.3294	−0.3271	−0.2822	−0.2312
	−0.3294	−0.3294	−0.3294	−0.3294	−0.3293	−0.3288	−0.3265	−0.3241	−0.2796	−0.2292
	−0.3254	−0.3254	−0.3254	−0.3254	−0.3254	−0.3248	−0.3225	−0.3202	−0.2761	−0.2264
	−0.3209	−0.3209	−0.3209	−0.3209	−0.3209	−0.3204	−0.3181	−0.3159	−0.2722	−0.2231
	−0.3143	−0.3143	−0.3142	−0.3142	−0.3142	−0.3137	−0.3115	−0.3093	−0.2663	−0.218
	−0.3056	−0.3056	−0.3056	−0.3056	−0.3056	−0.3051	−0.3029	−0.3009	−0.2573	−0.2114
	−0.295	−0.295	−0.295	−0.295	−0.295	−0.2945	−0.2924	−0.2905	−0.2493	−0.2034
	−0.2777	−0.2777	−0.2777	−0.2777	−0.2777	−0.2772	−0.2752	−0.2735	−0.2341	−0.1904

Figure 6.23b: F2B: e=1.5b & d=1b

	c/b									
a/b	−0.3356	−0.3356	−0.3355	−0.3355	−0.3355	−0.332	−0.3185	−0.2967	−0.272	−0.2579
	−0.3344	−0.3343	−0.3343	−0.3342	−0.3342	−0.3307	−0.3175	−0.2955	−0.2709	−0.2568
	−0.3324	−0.3324	−0.3323	−0.3322	−0.3322	−0.3288	−0.3156	−0.2938	−0.2691	−0.2551
	−0.3294	−0.3294	−0.3293	−0.3293	−0.3292	−0.3258	−0.3128	−0.2912	−0.2666	−0.2527
	−0.3254	−0.3254	−0.3253	−0.3253	−0.3253	−0.3218	−0.309	−0.2877	−0.2631	−0.2494
	−0.3209	−0.3209	−0.3208	−0.3208	−0.3208	−0.3174	−0.3048	−0.2837	−0.2593	−0.2457
	−0.3143	−0.3142	−0.3142	−0.3141	−0.3141	−0.3108	−0.2983	−0.2778	−0.2534	−0.2401
	−0.3056	−0.3056	−0.3056	−0.3055	−0.3055	−0.3022	−0.29	−0.2701	−0.2459	−0.2329
	−0.295	−0.295	−0.295	−0.2949	−0.2949	−0.2917	−0.2799	−0.2605	−0.2366	−0.2241
	−0.2777	−0.2777	−0.2776	−0.2776	−0.2776	−0.2744	−0.2633	−0.2451	−0.2215	−0.2096

Figure 6.23b: F2B: e=1.5b & d=1.5b

	c/b									
a/b	−0.3354	−0.3341	−0.3311	−0.3284	−0.3268	−0.3207	−0.3143	−0.3018	−0.2859	−0.2754
	−0.3341	−0.3328	−0.3298	−0.3271	−0.3256	−0.3195	−0.3131	−0.3006	−0.2847	−0.2743
	−0.3321	−0.3308	−0.3279	−0.3252	−0.3236	−0.3176	−0.3113	−0.2988	−0.2829	−0.2725
	−0.3291	−0.3278	−0.3249	−0.3223	−0.3208	−0.3148	−0.3085	−0.2961	−0.2803	−0.2699
	−0.3251	−0.3239	−0.321	−0.3184	−0.317	−0.311	−0.3048	−0.2924	−0.2766	−0.2664
	−0.3207	−0.3194	−0.3166	−0.314	−0.3127	−0.3068	−0.3006	−0.2883	−0.2726	−0.2624
	−0.314	−0.3128	−0.3099	−0.3074	−0.3062	−0.3005	−0.2943	−0.2821	−0.2665	−0.2565
	−0.3054	−0.3042	−0.3014	−0.299	−0.2979	−0.2923	−0.2862	−0.2741	−0.2587	−0.2489
	−0.2948	−0.2936	−0.2909	−0.2885	−0.2876	−0.2822	−0.2762	−0.2643	−0.2492	−0.2395
	−0.2775	−0.2763	−0.2737	−0.2715	−0.2709	−0.2656	−0.2599	−0.2483	−0.2335	−0.2242

Figure 6.23b: F2B: e=1.5b & d=2b

	c/b									
a/b	−0.3344	−0.3326	−0.3322	−0.3335	−0.3329	−0.3261	−0.3189	−0.3092	−0.2989	−0.2895
	−0.3331	−0.3314	−0.331	−0.3323	−0.3317	−0.3248	−0.3177	−0.308	−0.2977	−0.2883
	−0.3312	−0.3294	−0.329	−0.3303	−0.3297	−0.3229	−0.3158	−0.3061	−0.2958	−0.2865
	−0.3282	−0.3265	−0.3261	−0.3274	−0.3268	−0.32	−0.3129	−0.3032	−0.293	−0.2837
	−0.3242	−0.3225	−0.3222	−0.3235	−0.3229	−0.3161	−0.309	−0.2994	−0.2893	−0.28
	−0.3198	−0.3181	−0.3178	−0.3191	−0.3185	−0.3118	−0.3047	−0.2952	−0.2851	−0.2759
	−0.3131	−0.3115	−0.3112	−0.3126	−0.312	−0.3053	−0.2983	−0.2888	−0.2788	−0.2697
	−0.3045	−0.3029	−0.3027	−0.3041	−0.3035	−0.2969	−0.29	−0.2806	−0.2708	−0.2618
	−0.2939	−0.2924	−0.2922	−0.2937	−0.2931	−0.2866	−0.2798	−0.2706	−0.2609	−0.2521
	−0.2767	−0.2752	−0.2752	−0.2766	−0.2761	−0.2697	−0.2631	−0.2541	−0.2447	−0.2362

Figure 6.23b: F2B: e=1.5b & d=2.5b

	c/b									
a/b	−0.3356	−0.3363	−0.3366	−0.3356	−0.3325	−0.327	−0.3206	−0.3132	−0.3058	−0.2977
	−0.3343	−0.3351	−0.3353	−0.3343	−0.3312	−0.3257	−0.3194	−0.312	−0.3045	−0.2965
	−0.3323	−0.3331	−0.3333	−0.3323	−0.3293	−0.3238	−0.3174	−0.31	−0.3026	−0.2946
	−0.3294	−0.3301	−0.3304	−0.3294	−0.3263	−0.3208	−0.3145	−0.3071	−0.2998	−0.2918
	−0.3254	−0.3261	−0.3264	−0.3254	−0.3224	−0.3169	−0.3106	−0.3033	−0.2959	−0.288
	−0.3209	−0.3217	−0.3219	−0.321	−0.3179	−0.3125	−0.3062	−0.2989	−0.2917	−0.2838
	−0.3143	−0.315	−0.3153	−0.3143	−0.3113	−0.3059	−0.2997	−0.2925	−0.2853	−0.2775
	−0.3057	−0.3064	−0.3067	−0.3057	−0.3028	−0.2974	−0.2913	−0.2842	−0.2771	−0.2694
	−0.2951	−0.2958	−0.2961	−0.2952	−0.2922	−0.287	−0.281	−0.274	−0.267	−0.2595
	−0.2778	−0.2785	−0.2788	−0.2779	−0.2751	−0.2699	−0.2641	−0.2573	−0.2505	−0.2432

Figure 6.23b: F2B: e=1.5b & d=3b

	c/b									
a/b	−0.3358	−0.3358	−0.3349	−0.3327	−0.3291	−0.3247	−0.3193	−0.3135	−0.3077	−0.301
	−0.3345	−0.3346	−0.3336	−0.3314	−0.3279	−0.3234	−0.3181	−0.3122	−0.3064	−0.2998
	−0.3326	−0.3326	−0.3316	−0.3294	−0.3259	−0.3215	−0.3161	−0.3103	−0.3045	−0.2979
	−0.3296	−0.3296	−0.3287	−0.3265	−0.3229	−0.3185	−0.3132	−0.3074	−0.3016	−0.295
	−0.3256	−0.3256	−0.3247	−0.3225	−0.319	−0.3146	−0.3093	−0.3035	−0.2978	−0.2912
	−0.3211	−0.3211	−0.3202	−0.318	−0.3145	−0.3102	−0.3049	−0.2992	−0.2935	−0.287
	−0.3144	−0.3145	−0.3136	−0.3114	−0.3079	−0.3036	−0.2984	−0.2927	−0.2871	−0.2806
	−0.3058	−0.3059	−0.305	−0.3028	−0.2994	−0.2951	−0.2899	−0.2844	−0.2788	−0.2725
	−0.2952	−0.2953	−0.2944	−0.2923	−0.2889	−0.2847	−0.2796	−0.2742	−0.2687	−0.2625
	−0.2779	−0.2779	−0.2771	−0.275	−0.2717	−0.2677	−0.2628	−0.2574	−0.2522	−0.2461

Figure 6.23b: F2B: e=1.5b & d=3.5b

	c/b									
a/b	−0.3355	−0.3348	−0.3332	−0.3306	−0.3272	−0.3234	−0.3188	−0.314	−0.3092	−0.3037
	−0.3342	−0.3335	−0.3319	−0.3294	−0.3259	−0.3222	−0.3176	−0.3128	−0.308	−0.3025
	−0.3322	−0.3315	−0.33	−0.3274	−0.324	−0.3202	−0.3156	−0.3109	−0.3061	−0.3005
	−0.3293	−0.3285	−0.327	−0.3244	−0.321	−0.3173	−0.3127	−0.308	−0.3032	−0.2977
	−0.3253	−0.3245	−0.323	−0.3205	−0.3171	−0.3134	−0.3088	−0.3041	−0.2993	−0.2939
	−0.3208	−0.3201	−0.3186	−0.316	−0.3126	−0.309	−0.3044	−0.2997	−0.295	−0.2896
	−0.3141	−0.3134	−0.3119	−0.3094	−0.306	−0.3024	−0.2979	−0.2933	−0.2886	−0.2832
	−0.3055	−0.3048	−0.3033	−0.3008	−0.2975	−0.2939	−0.2895	−0.2849	−0.2803	−0.275
	−0.2949	−0.2942	−0.2928	−0.2903	−0.287	−0.2835	−0.2792	−0.2747	−0.2702	−0.265
	−0.2776	−0.2769	−0.2755	−0.2731	−0.2699	−0.2665	−0.2623	−0.258	−0.2536	−0.2486

Figure 6.23b: F2B: e=1.5b & d=4b

	c/b									
a/b	−0.3353	−0.3343	−0.3326	−0.3301	−0.3269	−0.3236	−0.3197	−0.3156	−0.3115	−0.3067
	−0.334	−0.333	−0.3313	−0.3288	−0.3256	−0.3224	−0.3184	−0.3143	−0.3102	−0.3055
	−0.3321	−0.331	−0.3293	−0.3268	−0.3237	−0.3204	−0.3165	−0.3124	−0.3083	−0.3036
	−0.3291	−0.3281	−0.3264	−0.3239	−0.3207	−0.3175	−0.3135	−0.3095	−0.3054	−0.3007
	−0.3251	−0.3241	−0.3224	−0.3199	−0.3168	−0.3136	−0.3096	−0.3056	−0.3015	−0.2969
	−0.3206	−0.3196	−0.3179	−0.3155	−0.3124	−0.3092	−0.3053	−0.3013	−0.2972	−0.2926
	−0.314	−0.313	−0.3113	−0.3088	−0.3058	−0.3026	−0.2987	−0.2948	−0.2908	−0.2862
	−0.3053	−0.3044	−0.3027	−0.3003	−0.2972	−0.2941	−0.2903	−0.2864	−0.2825	−0.278
	−0.2947	−0.2938	−0.2922	−0.2898	−0.2868	−0.2837	−0.28	−0.2762	−0.2723	−0.2679
	−0.2774	−0.2765	−0.2749	−0.2726	−0.2697	−0.2667	−0.2631	−0.2594	−0.2557	−0.2514

Figure I.12b: F2B: e=2b & d=0.5b

	c/b									
a/b	−0.3357	−0.3356	−0.3356	−0.3356	−0.3356	−0.3351	−0.3327	−0.3302	−0.2851	−0.2336
	−0.3345	−0.3344	−0.3344	−0.3344	−0.3344	−0.3339	−0.3315	−0.3291	−0.284	−0.2327
	−0.3325	−0.3325	−0.3324	−0.3325	−0.3324	−0.3319	−0.3295	−0.3272	−0.2823	−0.2312
	−0.3294	−0.3294	−0.3294	−0.3294	−0.3293	−0.3289	−0.3265	−0.3242	−0.2797	−0.2288
	−0.3254	−0.3254	−0.3253	−0.3254	−0.3253	−0.3248	−0.3225	−0.3202	−0.2761	−0.2261
	−0.3209	−0.3209	−0.3208	−0.3209	−0.3208	−0.3203	−0.318	−0.3158	−0.2722	−0.2229
	−0.3146	−0.3146	−0.3145	−0.3146	−0.3145	−0.314	−0.3118	−0.3097	−0.2666	−0.2184
	−0.3069	−0.3069	−0.3068	−0.3069	−0.3068	−0.3063	−0.3041	−0.3021	−0.2599	−0.2127
	−0.2978	−0.2978	−0.2977	−0.2978	−0.2978	−0.2973	−0.2951	−0.2932	−0.252	−0.2058
	−0.2842	−0.2842	−0.2842	−0.2842	−0.2842	−0.2837	−0.2816	−0.2799	−0.2399	−0.1956

Figure I.12b: F2B: e=2b & d=1b

	c/b									
a/b	−0.3357	−0.3356	−0.3356	−0.3355	−0.3355	−0.332	−0.3185	−0.2967	−0.272	−0.2579
	−0.3344	−0.3344	−0.3344	−0.3343	−0.3343	−0.3308	−0.3176	−0.2956	−0.271	−0.2569
	−0.3325	−0.3325	−0.3324	−0.3324	−0.3323	−0.3289	−0.3157	−0.2939	−0.2692	−0.2552
	−0.3294	−0.3294	−0.3294	−0.3293	−0.3293	−0.3259	−0.3128	−0.2912	−0.2666	−0.2527
	−0.3254	−0.3254	−0.3253	−0.3253	−0.3252	−0.3218	−0.3089	−0.2876	−0.2631	−0.2494
	−0.3209	−0.3209	−0.3208	−0.3208	−0.3207	−0.3173	−0.3047	−0.2836	−0.2592	−0.2457
	−0.3146	−0.3146	−0.3145	−0.3145	−0.3144	−0.3111	−0.2987	−0.2781	−0.2537	−0.2405
	−0.3069	−0.3069	−0.3068	−0.3068	−0.3067	−0.3034	−0.2912	−0.2712	−0.247	−0.2341
	−0.2978	−0.2978	−0.2977	−0.2977	−0.2976	−0.2944	−0.2825	−0.2631	−0.2391	−0.2265
	−0.2842	−0.2842	−0.2841	−0.2841	−0.2841	−0.2809	−0.2695	−0.2509	−0.2273	−0.2152

Figure I.12b: F2B: e=2b & d=1.5b

	c/b									
a/b	−0.3354	−0.3341	−0.3311	−0.3284	−0.3268	−0.3207	−0.3143	−0.3018	−0.2859	−0.2754
	−0.3342	−0.3329	−0.3299	−0.3272	−0.3257	−0.3196	−0.3132	−0.3007	−0.2848	−0.2744
	−0.3322	−0.3309	−0.328	−0.3253	−0.3237	−0.3177	−0.3114	−0.2989	−0.283	−0.2726
	−0.3292	−0.3279	−0.325	−0.3223	−0.3208	−0.3148	−0.3085	−0.2961	−0.2803	−0.2699
	−0.3251	−0.3238	−0.321	−0.3183	−0.3169	−0.311	−0.3047	−0.2924	−0.2766	−0.2663
	−0.3206	−0.3194	−0.3165	−0.3139	−0.3126	−0.3067	−0.3005	−0.2882	−0.2726	−0.2624
	−0.3143	−0.3131	−0.3103	−0.3077	−0.3065	−0.3008	−0.2946	−0.2824	−0.2669	−0.2568
	−0.3066	−0.3054	−0.3026	−0.3002	−0.2991	−0.2935	−0.2874	−0.2753	−0.2599	−0.25
	−0.2975	−0.2963	−0.2936	−0.2913	−0.2903	−0.2848	−0.2788	−0.2669	−0.2517	−0.242
	−0.2839	−0.2828	−0.2801	−0.2779	−0.2772	−0.2719	−0.266	−0.2543	−0.2394	−0.23

Figure I.12b: F2B: e=2b & d=2b

	c/b									
a/b	−0.3344	−0.3327	−0.3323	−0.3335	−0.3329	−0.3261	−0.3189	−0.3092	−0.2989	−0.2895
	−0.3332	−0.3315	−0.3311	−0.3324	−0.3317	−0.3249	−0.3178	−0.3081	−0.2978	−0.2884
	−0.3313	−0.3295	−0.3291	−0.3304	−0.3298	−0.323	−0.3159	−0.3062	−0.2959	−0.2866
	−0.3283	−0.3265	−0.3262	−0.3275	−0.3268	−0.3201	−0.3129	−0.3033	−0.2931	−0.2838
	−0.3242	−0.3225	−0.3222	−0.3235	−0.3229	−0.3161	−0.309	−0.2994	−0.2893	−0.28
	−0.3197	−0.318	−0.3177	−0.3191	−0.3185	−0.3117	−0.3047	−0.2951	−0.2851	−0.2759
	−0.3134	−0.3118	−0.3115	−0.3129	−0.3123	−0.3056	−0.2986	−0.2892	−0.2791	−0.27
	−0.3057	−0.3042	−0.3039	−0.3053	−0.3047	−0.2981	−0.2912	−0.2818	−0.2719	−0.2629
	−0.2967	−0.2951	−0.295	−0.2964	−0.2958	−0.2892	−0.2824	−0.2732	−0.2635	−0.2546
	−0.2831	−0.2817	−0.2816	−0.283	−0.2825	−0.276	−0.2693	−0.2603	−0.2507	−0.2421

Figure I.12b: F2B: e=2b & d=2.5b

	c/b									
a/b	−0.3356	−0.3364	−0.3366	−0.3356	−0.3325	−0.327	−0.3206	−0.3132	−0.3058	−0.2977
	−0.3344	−0.3352	−0.3354	−0.3344	−0.3313	−0.3258	−0.3195	−0.3121	−0.3046	−0.2966
	−0.3324	−0.3332	−0.3334	−0.3325	−0.3294	−0.3239	−0.3175	−0.3101	−0.3027	−0.2947
	−0.3294	−0.3302	−0.3304	−0.3294	−0.3264	−0.3209	−0.3146	−0.3072	−0.2998	−0.2918
	−0.3254	−0.3261	−0.3264	−0.3254	−0.3223	−0.3169	−0.3106	−0.3033	−0.2959	−0.288
	−0.3209	−0.3216	−0.3219	−0.3209	−0.3179	−0.3124	−0.3062	−0.2989	−0.2916	−0.2837
	−0.3146	−0.3153	−0.3156	−0.3146	−0.3116	−0.3062	−0.3	−0.2928	−0.2856	−0.2778
	−0.3069	−0.3076	−0.3079	−0.307	−0.304	−0.2986	−0.2925	−0.2854	−0.2782	−0.2705
	−0.2978	−0.2986	−0.2988	−0.2979	−0.295	−0.2897	−0.2836	−0.2766	−0.2696	−0.262
	−0.2842	−0.285	−0.2853	−0.2844	−0.2815	−0.2763	−0.2704	−0.2635	−0.2567	−0.2492

Figure I.12b: F2B: e=2b & d=3b

	c/b									
a/b	−0.3358	−0.3359	−0.3349	−0.3327	−0.3291	−0.3247	−0.3193	−0.3135	−0.3077	−0.301
	−0.3346	−0.3347	−0.3337	−0.3315	−0.3279	−0.3235	−0.3181	−0.3123	−0.3065	−0.2999
	−0.3327	−0.3327	−0.3318	−0.3295	−0.326	−0.3216	−0.3162	−0.3104	−0.3046	−0.298
	−0.3296	−0.3297	−0.3287	−0.3265	−0.323	−0.3186	−0.3132	−0.3075	−0.3017	−0.2951
	−0.3256	−0.3256	−0.3247	−0.3225	−0.3189	−0.3146	−0.3093	−0.3035	−0.2978	−0.2912
	−0.3211	−0.3211	−0.3202	−0.318	−0.3145	−0.3101	−0.3048	−0.2991	−0.2934	−0.2869
	−0.3148	−0.3148	−0.3139	−0.3117	−0.3082	−0.3039	−0.2987	−0.293	−0.2874	−0.2809
	−0.3071	−0.3071	−0.3062	−0.304	−0.3006	−0.2963	−0.2911	−0.2855	−0.28	−0.2736
	−0.298	−0.298	−0.2971	−0.295	−0.2916	−0.2874	−0.2823	−0.2768	−0.2713	−0.2651
	−0.2844	−0.2844	−0.2835	−0.2815	−0.2781	−0.274	−0.269	−0.2636	−0.2583	−0.2522

Figure I.12b: F2B: e=2b & d=3.5b

	c/b									
a/b	−0.3355	−0.3348	−0.3332	−0.3307	−0.3272	−0.3235	−0.3189	−0.3141	−0.3093	−0.3037
	−0.3343	−0.3336	−0.332	−0.3295	−0.326	−0.3223	−0.3177	−0.3129	−0.3081	−0.3025
	−0.3323	−0.3316	−0.3301	−0.3275	−0.3241	−0.3203	−0.3158	−0.311	−0.3062	−0.3007
	−0.3293	−0.3286	−0.327	−0.3245	−0.3211	−0.3174	−0.3128	−0.308	−0.3032	−0.2977
	−0.3252	−0.3245	−0.323	−0.3205	−0.317	−0.3133	−0.3088	−0.3041	−0.2993	−0.2938
	−0.3207	−0.32	−0.3185	−0.316	−0.3126	−0.3089	−0.3044	−0.2997	−0.295	−0.2895
	−0.3144	−0.3137	−0.3122	−0.3097	−0.3063	−0.3027	−0.2982	−0.2936	−0.2889	−0.2835
	−0.3067	−0.306	−0.3045	−0.3021	−0.2987	−0.2951	−0.2907	−0.2861	−0.2815	−0.2762
	−0.2977	−0.297	−0.2955	−0.293	−0.2898	−0.2862	−0.2819	−0.2773	−0.2728	−0.2676
	−0.2841	−0.2834	−0.2819	−0.2795	−0.2763	−0.2729	−0.2686	−0.2642	−0.2597	−0.2546

Figure I.12b: F2B: e=2b & d=4b

	c/b									
a/b	−0.3353	−0.3343	−0.3326	−0.3301	−0.3269	−0.3237	−0.3197	−0.3156	−0.3115	−0.3068
	−0.3341	−0.3331	−0.3314	−0.3289	−0.3257	−0.3225	−0.3185	−0.3144	−0.3103	−0.3056
	−0.3322	−0.3311	−0.3294	−0.3269	−0.3238	−0.3205	−0.3166	−0.3125	−0.3084	−0.3037
	−0.3291	−0.3281	−0.3264	−0.3239	−0.3208	−0.3176	−0.3136	−0.3095	−0.3055	−0.3008
	−0.3251	−0.3241	−0.3224	−0.3199	−0.3168	−0.3135	−0.3096	−0.3056	−0.3015	−0.2969
	−0.3206	−0.3196	−0.3179	−0.3154	−0.3123	−0.3091	−0.3052	−0.3012	−0.2972	−0.2925
	−0.3143	−0.3133	−0.3116	−0.3092	−0.3061	−0.3029	−0.299	−0.2951	−0.2911	−0.2865
	−0.3066	−0.3056	−0.3039	−0.3015	−0.2985	−0.2953	−0.2915	−0.2876	−0.2837	−0.2791
	−0.2975	−0.2965	−0.2949	−0.2925	−0.2895	−0.2864	−0.2826	−0.2788	−0.2749	−0.2705
	−0.2839	−0.2829	−0.2814	−0.279	−0.2761	−0.2731	−0.2694	−0.2656	−0.2618	−0.2575

Figure 6.24b: F2B: e=2.5b & d=0.5b

	c/b									
a/b	−0.3357	−0.3357	−0.3357	−0.3357	−0.3357	−0.3351	−0.3327	−0.3303	−0.2851	−0.2336
	−0.3346	−0.3346	−0.3346	−0.3346	−0.3346	−0.3341	−0.3317	−0.3292	−0.2842	−0.2328
	−0.3328	−0.3328	−0.3328	−0.3328	−0.3328	−0.3323	−0.3299	−0.3275	−0.2826	−0.2315
	−0.33	−0.33	−0.33	−0.33	−0.33	−0.3295	−0.3271	−0.3248	−0.2802	−0.2294
	−0.3262	−0.3262	−0.3262	−0.3262	−0.3262	−0.3257	−0.3233	−0.321	−0.2769	−0.2267
	−0.3219	−0.3219	−0.3219	−0.3219	−0.3219	−0.3214	−0.3191	−0.3168	−0.2731	−0.2236
	−0.316	−0.316	−0.316	−0.316	−0.316	−0.3155	−0.3132	−0.3111	−0.2679	−0.2193
	−0.3091	−0.3091	−0.309	−0.3084	−0.309	−0.3085	−0.3075	−0.3042	−0.2618	−0.2142
	−0.3011	−0.3011	−0.3011	−0.3011	−0.3011	−0.3006	−0.2984	−0.2965	−0.255	−0.2084
	−0.2899	−0.2899	−0.2899	−0.2899	−0.2899	−0.2894	−0.2873	−0.2855	−0.245	−0.2004

Figure 6.24b: F2B: e=2.5b & d=1b

	c/b									
a/b	−0.3357	−0.3357	−0.3356	−0.3356	−0.3355	−0.3321	−0.3186	−0.2967	−0.272	−0.2579
	−0.3346	−0.3346	−0.3345	−0.3345	−0.3345	−0.331	−0.3178	−0.2958	−0.2711	−0.257
	−0.3328	−0.3328	−0.3327	−0.3327	−0.3327	−0.3292	−0.316	−0.2942	−0.2695	−0.2555
	−0.33	−0.33	−0.3299	−0.3299	−0.3299	−0.3264	−0.3134	−0.2917	−0.2671	−0.2532
	−0.3262	−0.3262	−0.3261	−0.3261	−0.3261	−0.3226	−0.3098	−0.2883	−0.2638	−0.2501
	−0.3219	−0.3219	−0.3218	−0.3218	−0.3218	−0.3184	−0.3057	−0.2845	−0.2601	−0.2465
	−0.316	−0.316	−0.316	−0.3159	−0.3159	−0.3125	−0.3001	−0.2793	−0.255	−0.2417
	−0.3091	−0.3091	−0.309	−0.309	−0.3089	−0.3056	−0.2933	−0.2731	−0.249	−0.2359
	−0.3011	−0.3011	−0.3011	−0.301	−0.301	−0.2977	−0.2857	−0.2661	−0.2421	−0.2294
	−0.2899	−0.2899	−0.2898	−0.2898	−0.2898	−0.2866	−0.2751	−0.2561	−0.2324	−0.22

Figure 6.24b: F2B: e=2.5b & d=1.5b

	c/b									
a/b	−0.3354	−0.3341	−0.3312	−0.3285	−0.3269	−0.3207	−0.3144	−0.3019	−0.286	−0.2755
	−0.3344	−0.3331	−0.3301	−0.3274	−0.3258	−0.3197	−0.3134	−0.3009	−0.285	−0.2745
	−0.3326	−0.3313	−0.3283	−0.3256	−0.3241	−0.318	−0.3117	−0.2992	−0.2834	−0.2729
	−0.3298	−0.3285	−0.3256	−0.3229	−0.3214	−0.3154	−0.3091	−0.2966	−0.2808	−0.2705
	−0.326	−0.3247	−0.3218	−0.3192	−0.3177	−0.3118	−0.3055	−0.2931	−0.2774	−0.2671
	−0.3217	−0.3204	−0.3175	−0.3149	−0.3136	−0.3077	−0.3015	−0.2892	−0.2735	−0.2633
	−0.3158	−0.3145	−0.3117	−0.3092	−0.3079	−0.3021	−0.296	−0.2838	−0.2682	−0.2581
	−0.3088	−0.3076	−0.3048	−0.3024	−0.3012	−0.2955	−0.2894	−0.2773	−0.2619	−0.252
	−0.3009	−0.2997	−0.2969	−0.2946	−0.2935	−0.288	−0.282	−0.27	−0.2548	−0.245
	−0.2897	−0.2885	−0.2858	−0.2836	−0.2827	−0.2773	−0.2714	−0.2597	−0.2446	−0.2351

Figure 6.24b: F2B: e=2.5b & d=2b

	c/b									
a/b	−0.3345	−0.3327	−0.3323	−0.3336	−0.333	−0.3262	−0.319	−0.3093	−0.299	−0.2896
	−0.3334	−0.3317	−0.3312	−0.3325	−0.3319	−0.3251	−0.3179	−0.3082	−0.298	−0.2886
	−0.3316	−0.3299	−0.3295	−0.3308	−0.3302	−0.3234	−0.3162	−0.3065	−0.2963	−0.2869
	−0.3288	−0.3271	−0.3267	−0.328	−0.3274	−0.3206	−0.3135	−0.3039	−0.2936	−0.2843
	−0.325	−0.3233	−0.323	−0.3243	−0.3237	−0.3169	−0.3098	−0.3002	−0.2901	−0.2808
	−0.3207	−0.3191	−0.3187	−0.3201	−0.3195	−0.3127	−0.3057	−0.2961	−0.286	−0.2768
	−0.3149	−0.3132	−0.313	−0.3143	−0.3137	−0.307	−0.3	−0.2906	−0.2805	−0.2714
	−0.3079	−0.3063	−0.3061	−0.3075	−0.3069	−0.3002	−0.2933	−0.2839	−0.274	−0.265
	−0.3	−0.2985	−0.2983	−0.2997	−0.2991	−0.2925	−0.2857	−0.2764	−0.2666	−0.2577
	−0.2889	−0.2874	−0.2872	−0.2886	−0.2881	−0.2816	−0.2749	−0.2657	−0.2561	−0.2474

Figure 6.24b: F2B: e=2.5b & d=2.5b

	c/b									
a/b	−0.3357	−0.3364	−0.3367	−0.3357	−0.3326	−0.327	−0.3207	−0.3133	−0.3058	−0.2978
	−0.3346	−0.3353	−0.3356	−0.3346	−0.3315	−0.326	−0.3196	−0.3122	−0.3048	−0.2968
	−0.3328	−0.3335	−0.3338	−0.3328	−0.3297	−0.3242	−0.3179	−0.3105	−0.3031	−0.2951
	−0.33	−0.3307	−0.331	−0.33	−0.3269	−0.3214	−0.3151	−0.3078	−0.3004	−0.2924
	−0.3262	−0.3269	−0.3272	−0.3262	−0.3232	−0.3177	−0.3114	−0.3041	−0.2967	−0.2888
	−0.3219	−0.3226	−0.3229	−0.3219	−0.3189	−0.3135	−0.3072	−0.2999	−0.2926	−0.2847
	−0.316	−0.3168	−0.3171	−0.3161	−0.3131	−0.3077	−0.3015	−0.2942	−0.287	−0.2792
	−0.3091	−0.3098	−0.3101	−0.3091	−0.3062	−0.3008	−0.2947	−0.2875	−0.2803	−0.2726
	−0.3012	−0.3019	−0.3022	−0.3012	−0.2983	−0.293	−0.2869	−0.2799	−0.2728	−0.2652
	−0.29	−0.2907	−0.291	−0.2901	−0.2872	−0.282	−0.276	−0.269	−0.2621	−0.2546

Figure 6.24b: F2B: e=2.5b & d=3b

	c/b									
a/b	−0.3359	−0.3359	−0.335	−0.3327	−0.3292	−0.3248	−0.3194	−0.3135	−0.3077	−0.3011
	−0.3348	−0.3348	−0.3339	−0.3317	−0.3281	−0.3237	−0.3183	−0.3125	−0.3067	−0.3001
	−0.333	−0.333	−0.3321	−0.3299	−0.3263	−0.3219	−0.3166	−0.3107	−0.305	−0.2983
	−0.3302	−0.3302	−0.3293	−0.3271	−0.3236	−0.3192	−0.3138	−0.308	−0.3023	−0.2957
	−0.3264	−0.3264	−0.3255	−0.3233	−0.3198	−0.3154	−0.3101	−0.3043	−0.2986	−0.292
	−0.3221	−0.3221	−0.3212	−0.319	−0.3155	−0.3112	−0.3059	−0.3001	−0.2944	−0.2879
	−0.3162	−0.3163	−0.3153	−0.3132	−0.3097	−0.3054	−0.3001	−0.2945	−0.2888	−0.2823
	−0.3093	−0.3099	−0.3084	−0.3062	−0.3028	−0.2985	−0.2933	−0.2877	−0.2821	−0.2757
	−0.3013	−0.3014	−0.3005	−0.2983	−0.2949	−0.2907	−0.2856	−0.28	−0.2745	−0.2682
	−0.2901	−0.2901	−0.2893	−0.2872	−0.2838	−0.2797	−0.2746	−0.2692	−0.2638	−0.2576

Figure 6.24b: F2B: e=2.5b & d=3.5b

	c/b									
a/b	−0.3356	−0.3348	−0.3333	−0.3307	−0.3273	−0.3235	−0.3189	−0.3141	−0.3093	−0.3037
	−0.3345	−0.3338	−0.3322	−0.3297	−0.3262	−0.3225	−0.3179	−0.3131	−0.3083	−0.3027
	−0.3327	−0.332	−0.3304	−0.3279	−0.3244	−0.3207	−0.3161	−0.3113	−0.3065	−0.301
	−0.3299	−0.3292	−0.3276	−0.3251	−0.3216	−0.3179	−0.3134	−0.3086	−0.3038	−0.2983
	−0.3261	−0.3254	−0.3238	−0.3213	−0.3179	−0.3142	−0.3096	−0.3049	−0.3001	−0.2946
	−0.3218	−0.3211	−0.3195	−0.317	−0.3136	−0.3099	−0.3054	−0.3007	−0.296	−0.2905
	−0.3159	−0.3152	−0.3137	−0.3112	−0.3078	−0.3042	−0.2997	−0.295	−0.2903	−0.2849
	−0.309	−0.308	−0.3067	−0.3042	−0.3009	−0.2973	−0.2929	−0.2882	−0.2836	−0.2783
	−0.301	−0.3003	−0.2988	−0.2964	−0.2931	−0.2895	−0.2851	−0.2806	−0.276	−0.2707
	−0.2898	−0.2891	−0.2877	−0.2852	−0.282	−0.2785	−0.2742	−0.2697	−0.2652	−0.26

Figure 6.24b: F2B: e=2.5b & d=4b

	c/b									
a/b	−0.3354	−0.3344	−0.3327	−0.3301	−0.327	−0.3237	−0.3197	−0.3156	−0.3115	−0.3068
	−0.3343	−0.3333	−0.3316	−0.3291	−0.3259	−0.3227	−0.3187	−0.3146	−0.3105	−0.3058
	−0.3325	−0.3315	−0.3298	−0.3273	−0.3241	−0.3209	−0.3169	−0.3128	−0.3088	−0.304
	−0.3297	−0.3287	−0.327	−0.3245	−0.3214	−0.3181	−0.3142	−0.3101	−0.306	−0.3013
	−0.3259	−0.3249	−0.3232	−0.3207	−0.3176	−0.3144	−0.3104	−0.3064	−0.3023	−0.2977
	−0.3216	−0.3206	−0.3189	−0.3164	−0.3133	−0.3101	−0.3062	−0.3022	−0.2982	−0.2935
	−0.3157	−0.3147	−0.3131	−0.3106	−0.3075	−0.3044	−0.3005	−0.2965	−0.2925	−0.2879
	−0.3088	−0.3078	−0.3062	−0.3037	−0.3006	−0.2975	−0.2937	−0.2897	−0.2857	−0.2812
	−0.3008	−0.2999	−0.2982	−0.2958	−0.2928	−0.2897	−0.2859	−0.282	−0.2781	−0.2736
	−0.2896	−0.2887	−0.2871	−0.2847	−0.2817	−0.2787	−0.2749	−0.2711	−0.2673	−0.2629

Figure I.13b: F2B: e=3b & d=0.5b

	c/b									
a/b	−0.3357	−0.3357	−0.3357	−0.3357	−0.3357	−0.3352	−0.3328	−0.3303	−0.2851	−0.2336
	−0.3348	−0.3348	−0.3348	−0.3348	−0.3348	−0.3342	−0.3319	−0.3294	−0.2843	−0.2329
	−0.3332	−0.3332	−0.3332	−0.3332	−0.3332	−0.3327	−0.3303	−0.3278	−0.283	−0.2318
	−0.3307	−0.3307	−0.3307	−0.3307	−0.3307	−0.3302	−0.3278	−0.3255	−0.2808	−0.23
	−0.3273	−0.3273	−0.3273	−0.3273	−0.3273	−0.3261	−0.3244	−0.3221	−0.2778	−0.2275
	−0.3234	−0.3234	−0.3234	−0.3234	−0.3234	−0.3229	−0.3206	−0.3183	−0.2744	−0.2246
	−0.3181	−0.3181	−0.3181	−0.3181	−0.3181	−0.3176	−0.3153	−0.3131	−0.2697	−0.2208
	−0.3118	−0.3118	−0.3118	−0.3118	−0.3118	−0.3113	−0.3091	−0.3069	−0.2643	−0.2162
	−0.3048	−0.3048	−0.3047	−0.3048	−0.3047	−0.3043	−0.3021	−0.3	−0.2581	−0.211
	−0.2952	−0.2952	−0.2951	−0.2951	−0.2951	−0.2946	−0.2925	−0.2906	−0.2498	−0.204

Figure I.13b: F2B: e=3b & d=1b

	c/b									
a/b	−0.3357	−0.3357	−0.3357	−0.3356	−0.3356	−0.3321	−0.3186	−0.2968	−0.2721	−0.258
	−0.3348	−0.3348	−0.3347	−0.3347	−0.3346	−0.3312	−0.3179	−0.296	−0.2713	−0.2572
	−0.3332	−0.3332	−0.3331	−0.3331	−0.3331	−0.3296	−0.3164	−0.2945	−0.2699	−0.2559
	−0.3307	−0.3307	−0.3306	−0.3306	−0.3306	−0.3271	−0.3141	−0.2923	−0.2678	−0.2538
	−0.3273	−0.3273	−0.3272	−0.3272	−0.3272	−0.3238	−0.3108	−0.2893	−0.2648	−0.251
	−0.3234	−0.3234	−0.3233	−0.3233	−0.3233	−0.3199	−0.3071	−0.2858	−0.2614	−0.2478
	−0.3181	−0.3181	−0.318	−0.318	−0.318	−0.3146	−0.3021	−0.2811	−0.2568	−0.2434
	−0.3118	−0.3118	−0.3117	−0.3117	−0.3117	−0.3084	−0.296	−0.2756	−0.2514	−0.2382
	−0.3048	−0.3048	−0.3047	−0.3047	−0.3046	−0.3014	−0.2892	−0.2693	−0.2453	−0.2324
	−0.2952	−0.2952	−0.2951	−0.295	−0.295	−0.2918	−0.28	−0.2608	−0.237	−0.2307

Figure I.13b: F2B: e=3b & d=1.5b

	c/b									
a/b	−0.3355	−0.3342	−0.3312	−0.3285	−0.3269	−0.3208	−0.3144	−0.3019	−0.286	−0.2755
	−0.3345	−0.3332	−0.3303	−0.3276	−0.326	−0.3199	−0.3135	−0.301	−0.2852	−0.2747
	−0.333	−0.3317	−0.3287	−0.326	−0.3245	−0.3184	−0.3121	−0.2996	−0.2837	−0.2733
	−0.3305	−0.3292	−0.3263	−0.3236	−0.3221	−0.316	−0.3097	−0.2973	−0.2815	−0.2711
	−0.3271	−0.3258	−0.3229	−0.3202	−0.3188	−0.3128	−0.3065	−0.2942	−0.2784	−0.2681
	−0.3232	−0.3219	−0.319	−0.3164	−0.315	−0.3091	−0.3029	−0.2906	−0.2749	−0.2647
	−0.3179	−0.3166	−0.3138	−0.3112	−0.3099	−0.3041	−0.2979	−0.2857	−0.2701	−0.26
	−0.3116	−0.3103	−0.3075	−0.3051	−0.3038	−0.2981	−0.292	−0.2799	−0.2644	−0.2544
	−0.3045	−0.3033	−0.3006	−0.2981	−0.297	−0.2914	−0.2854	−0.2734	−0.2581	−0.2483
	−0.2949	−0.2937	−0.291	−0.2887	−0.2878	−0.2823	−0.2764	−0.264	−0.2494	−0.2398

Figure I.13b: F2B: e=3b & d=2b

	c/b									
a/b	−0.3345	−0.3328	−0.3323	−0.3336	−0.333	−0.3262	−0.319	−0.3093	−0.299	−0.2896
	−0.3336	−0.3318	−0.3314	−0.3327	−0.3321	−0.3253	−0.3181	−0.3084	−0.2981	−0.2887
	−0.332	−0.3303	−0.3299	−0.3312	−0.3305	−0.3237	−0.3166	−0.3069	−0.2966	−0.2873
	−0.3295	−0.3278	−0.3274	−0.3287	−0.3281	−0.3213	−0.3142	−0.3045	−0.2943	−0.285
	−0.3261	−0.3244	−0.3241	−0.3254	−0.3248	−0.318	−0.3109	−0.3013	−0.2911	−0.2818
	−0.3222	−0.3206	−0.3202	−0.3215	−0.3209	−0.3142	−0.3071	−0.2976	−0.2875	−0.2782
	−0.317	−0.3153	−0.315	−0.3163	−0.3157	−0.309	−0.302	−0.2925	−0.2825	−0.2733
	−0.3107	−0.3091	−0.3088	−0.3102	−0.3096	−0.3029	−0.296	−0.2866	−0.2766	−0.2676
	−0.3037	−0.3021	−0.3018	−0.3032	−0.3027	−0.2961	−0.2892	−0.2799	−0.27	−0.2611
	−0.2941	−0.2925	−0.2924	−0.2938	−0.2932	−0.2867	−0.2799	−0.2707	−0.261	−0.2522

Figure I.13b: F2B: e=3b & d=2.5b

	c/b									
a/b	−0.3357	−0.3364	−0.3367	−0.3357	−0.3326	−0.3271	−0.3207	−0.3133	−0.3059	−0.2978
	−0.3348	−0.3355	−0.3358	−0.3348	−0.3317	−0.3262	−0.3198	−0.3124	−0.305	−0.2969
	−0.3332	−0.3339	−0.3342	−0.3332	−0.3301	−0.3246	−0.3183	−0.3109	−0.3035	−0.2954
	−0.3307	−0.3314	−0.3317	−0.3307	−0.3276	−0.3222	−0.3158	−0.3085	−0.3011	−0.2931
	−0.3273	−0.3281	−0.3282	−0.3273	−0.3243	−0.3188	−0.3125	−0.3052	−0.2981	−0.2899
	−0.3234	−0.3242	−0.3244	−0.3234	−0.3204	−0.3149	−0.3087	−0.3014	−0.2941	−0.2862
	−0.3181	−0.3189	−0.3191	−0.3182	−0.3151	−0.3097	−0.3035	−0.2963	−0.289	−0.2811
	−0.3118	−0.3126	−0.3128	−0.3119	−0.3089	−0.3035	−0.2974	−0.2902	−0.283	−0.2752
	−0.3048	−0.3056	−0.3058	−0.3049	−0.3019	−0.2966	−0.2905	−0.2834	−0.2763	−0.2686
	−0.2952	−0.296	−0.2962	−0.2953	−0.2924	−0.2871	−0.2811	−0.2741	−0.2671	−0.2595

Figure I.13b: F2B: e=3b & d=3b

	c/b									
a/b	−0.3359	−0.3359	−0.335	−0.3328	−0.3292	−0.3248	−0.3194	−0.3136	−0.3078	−0.3011
	−0.335	−0.335	−0.3341	−0.3319	−0.3283	−0.3239	−0.3185	−0.3127	−0.3069	−0.3002
	−0.3334	−0.3334	−0.3325	−0.3303	−0.3267	−0.3223	−0.3169	−0.3111	−0.3053	−0.2987
	−0.3309	−0.3309	−0.33	−0.3278	−0.3243	−0.3199	−0.3145	−0.3087	−0.3029	−0.2963
	−0.3275	−0.3275	−0.3266	−0.3244	−0.3209	−0.3165	−0.3112	−0.3054	−0.2997	−0.2931
	−0.3236	−0.3236	−0.3227	−0.3205	−0.317	−0.3127	−0.3074	−0.3016	−0.2959	−0.2894
	−0.3183	−0.3183	−0.3174	−0.3152	−0.3118	−0.3074	−0.3022	−0.2965	−0.2908	−0.2843
	−0.312	−0.312	−0.3111	−0.309	−0.3055	−0.3012	−0.296	−0.2904	−0.2848	−0.2783
	−0.305	−0.305	−0.3041	−0.302	−0.2985	−0.2943	−0.2891	−0.2836	−0.278	−0.2717
	−0.2954	−0.2954	−0.2945	−0.2924	−0.289	−0.2848	−0.2797	−0.2742	−0.2688	−0.2625

Figure I.13b: F2B: e=3b & d=3.5b

	c/b									
a/b	−0.3356	−0.3349	−0.3333	−0.3308	−0.3273	−0.3236	−0.319	−0.3142	−0.3093	−0.3038
	−0.3347	−0.3339	−0.3324	−0.3298	−0.3264	−0.3226	−0.318	−0.3132	−0.3084	−0.3029
	−0.3331	−0.3324	−0.3308	−0.3283	−0.3248	−0.3211	−0.3165	−0.3117	−0.3069	−0.3014
	−0.3306	−0.3299	−0.3283	−0.3258	−0.3223	−0.3186	−0.3141	−0.3093	−0.3045	−0.299
	−0.3272	−0.3265	−0.3249	−0.3224	−0.319	−0.3153	−0.3107	−0.306	−0.3012	−0.2957
	−0.3233	−0.3226	−0.321	−0.3185	−0.3151	−0.3114	−0.3069	−0.3022	−0.2974	−0.292
	−0.318	−0.3173	−0.3158	−0.3132	−0.3099	−0.3062	−0.3017	−0.297	−0.2923	−0.2869
	−0.3117	−0.311	−0.3095	−0.307	−0.3037	−0.3	−0.2956	−0.2909	−0.2863	−0.2809
	−0.3047	−0.304	−0.3025	−0.3	−0.2967	−0.2931	−0.2887	−0.2841	−0.2795	−0.2742
	−0.295	−0.2943	−0.2929	−0.2904	−0.2872	−0.2836	−0.2793	−0.2747	−0.2702	−0.265

Figure I.13b: F2B: e=3b & d=4b

	c/b									
a/b	−0.3354	−0.3344	−0.3327	−0.3302	−0.327	−0.3238	−0.3198	−0.3157	−0.3116	−0.3068
	−0.3345	−0.3335	−0.3318	−0.3293	−0.3261	−0.3228	−0.3189	−0.3148	−0.3107	−0.3059
	−0.3329	−0.3319	−0.3302	−0.3277	−0.3245	−0.3213	−0.3173	−0.3132	−0.3091	−0.3044
	−0.3304	−0.3294	−0.3277	−0.3252	−0.3221	−0.3188	−0.3149	−0.3108	−0.3067	−0.302
	−0.327	−0.326	−0.3243	−0.3218	−0.3187	−0.3155	−0.3115	−0.3075	−0.3034	−0.2987
	−0.3231	−0.3221	−0.3204	−0.3179	−0.3148	−0.3116	−0.3077	−0.3037	−0.2996	−0.295
	−0.3178	−0.3168	−0.3151	−0.3127	−0.3096	−0.3064	−0.3025	−0.2985	−0.2945	−0.2899
	−0.3115	−0.3105	−0.3089	−0.3064	−0.3034	−0.3002	−0.2964	−0.2924	−0.2884	−0.2839
	−0.3045	−0.3035	−0.3019	−0.2994	−0.2964	−0.2933	−0.2895	−0.2856	−0.2816	−0.2771
	−0.2949	−0.2939	−0.2923	−0.2899	−0.2869	−0.2838	−0.2801	−0.2762	−0.2723	−0.2679

Figure 6.25b: F2B: e=3.5b & d=0.5b

	c/b									
	−0.3358	−0.3358	−0.3357	−0.3358	−0.3357	−0.3352	−0.3328	−0.3304	−0.2852	−0.2337
	−0.335	−0.335	−0.3349	−0.335	−0.3349	−0.3344	−0.332	−0.3296	−0.2845	−0.2331
	−0.3336	−0.3336	−0.3336	−0.3336	−0.3336	−0.333	−0.3307	−0.3282	−0.2833	−0.2321
	−0.3314	−0.3314	−0.3314	−0.3314	−0.3314	−0.3309	−0.3285	−0.3262	−0.2814	−0.2305
a/b	−0.3284	−0.3284	−0.3284	−0.3284	−0.3284	−0.3279	−0.3255	−0.3232	−0.2788	−0.2283
	−0.325	−0.325	−0.325	−0.325	−0.3249	−0.3244	−0.3221	−0.3198	−0.2758	−0.2258
	−0.3203	−0.3203	−0.3203	−0.3203	−0.3203	−0.3198	−0.3175	−0.3152	−0.2716	−0.2224
	−0.3147	−0.3147	−0.3147	−0.3147	−0.3147	−0.3142	−0.312	−0.3098	−0.2668	−0.2183
	−0.3085	−0.3085	−0.3085	−0.3085	−0.3085	−0.308	−0.3058	−0.3037	−0.2614	−0.2137
	−0.3001	−0.3001	−0.3001	−0.3001	−0.3001	−0.2996	−0.2974	−0.2955	−0.2541	−0.2076

Figure 6.25b: F2B: e=3.5b & d=1b

	c/b									
	−0.3358	−0.3358	−0.3357	−0.3357	−0.3356	−0.3322	−0.3187	−0.2968	−0.2721	−0.258
	−0.335	−0.335	−0.3349	−0.3349	−0.3348	−0.3314	−0.3179	−0.2961	−0.2715	−0.2573
	−0.3336	−0.3336	−0.3335	−0.3335	−0.3334	−0.33	−0.3168	−0.2948	−0.2702	−0.2562
	−0.3314	−0.3314	−0.3313	−0.3313	−0.3313	−0.3278	−0.3147	−0.2929	−0.2684	−0.2544
a/b	−0.3284	−0.3284	−0.3284	−0.3283	−0.3283	−0.3249	−0.3119	−0.2903	−0.2658	−0.252
	−0.325	−0.325	−0.3249	−0.3249	−0.3248	−0.3214	−0.3086	−0.2872	−0.2628	−0.2491
	−0.3203	−0.3203	−0.3202	−0.3202	−0.3201	−0.3168	−0.3041	−0.2831	−0.2588	−0.2452
	−0.3147	−0.3147	−0.3147	−0.3146	−0.3146	−0.3112	−0.2989	−0.2781	−0.254	−0.2407
	−0.3085	−0.3085	−0.3084	−0.3084	−0.3083	−0.305	−0.2928	−0.2726	−0.2486	−0.2355
	−0.3001	−0.3001	−0.3	−0.3	−0.3	−0.2967	−0.2848	−0.2651	−0.24	−0.2286

Figure 6.25b: F2B: e=3.5b & d=1.5b

	c/b									
	−0.3355	−0.3342	−0.3313	−0.3285	−0.3269	−0.3208	−0.3145	−0.3019	−0.286	−0.2756
	−0.3347	−0.3334	−0.3305	−0.3277	−0.3262	−0.3201	−0.3137	−0.3012	−0.2853	−0.2748
	−0.3333	−0.332	−0.3291	−0.3264	−0.3248	−0.3187	−0.3124	−0.2999	−0.2841	−0.2736
	−0.3312	−0.3299	−0.3269	−0.3243	−0.3227	−0.3167	−0.3104	−0.2979	−0.2821	−0.2717
a/b	−0.3282	−0.3269	−0.324	−0.3213	−0.3199	−0.3139	−0.3076	−0.2952	−0.2794	−0.2691
	−0.3247	−0.3235	−0.3206	−0.318	−0.3165	−0.3106	−0.3043	−0.292	−0.2763	−0.2661
	−0.32	−0.3188	−0.3159	−0.3134	−0.312	−0.3061	−0.2999	−0.2877	−0.2721	−0.2619
	−0.3145	−0.3132	−0.3104	−0.3079	−0.3066	−0.3009	−0.2947	−0.2826	−0.2671	−0.257
	−0.3082	−0.307	−0.3042	−0.3018	−0.3006	−0.2949	−0.2889	−0.2768	−0.2615	−0.2516
	−0.2999	−0.2987	−0.2959	−0.2935	−0.2925	−0.287	−0.281	−0.2691	−0.2539	−0.2442

Figure 6.25b: F2B: e=3.5b & d=2b

	c/b									
	−0.3346	−0.3328	−0.3324	−0.3337	−0.3331	−0.3262	−0.3191	−0.3093	−0.2991	−0.2896
	−0.3338	−0.332	−0.3316	−0.3329	−0.3323	−0.3255	−0.3183	−0.3086	−0.2983	−0.2889
	−0.3324	−0.3306	−0.3302	−0.3315	−0.3309	−0.3241	−0.3169	−0.3073	−0.297	−0.2876
	−0.3302	−0.3285	−0.3281	−0.3294	−0.3288	−0.322	−0.3149	−0.3052	−0.295	−0.2856
a/b	−0.3273	−0.3255	−0.3252	−0.3265	−0.3259	−0.3191	−0.312	−0.3024	−0.2922	−0.2829
	−0.3238	−0.3221	−0.3218	−0.3231	−0.3225	−0.3157	−0.3087	−0.2991	−0.2889	−0.2797
	−0.3191	−0.3175	−0.3171	−0.3185	−0.3179	−0.3112	−0.3041	−0.2946	−0.2846	−0.2754
	−0.3136	−0.312	−0.3117	−0.313	−0.3124	−0.3058	−0.2988	−0.2894	−0.2794	−0.2703
	−0.3074	−0.3058	−0.3055	−0.3069	−0.3063	−0.2997	−0.2928	−0.2834	−0.2735	−0.2645
	−0.299	−0.2975	−0.2972	−0.2986	−0.2981	−0.2915	−0.2847	−0.2755	−0.2657	−0.2568

Figure 6.25b: F2B: e=3.5b & d=2.5b

	c/b									
	−0.3357	−0.3365	−0.3367	−0.3358	−0.3327	−0.3271	−0.3208	−0.3133	−0.3059	−0.2979
	−0.3349	−0.3357	−0.3359	−0.3349	−0.3319	−0.3263	−0.32	−0.3126	−0.3051	−0.2971
	−0.3336	−0.3343	−0.3346	−0.3336	−0.3305	−0.325	−0.3186	−0.3112	−0.3038	−0.2958
	−0.3314	−0.3321	−0.3324	−0.3314	−0.3283	−0.3228	−0.3165	−0.3091	−0.3017	−0.2937
a/b	−0.3284	−0.3292	−0.3294	−0.3284	−0.3254	−0.3199	−0.3136	−0.3062	−0.2989	−0.2909
	−0.325	−0.3257	−0.326	−0.325	−0.322	−0.3165	−0.3102	−0.3029	−0.2956	−0.2877
	−0.3203	−0.321	−0.3213	−0.3203	−0.3173	−0.3119	−0.3056	−0.2984	−0.2911	−0.2832
	−0.3147	−0.3155	−0.3157	−0.3148	−0.3118	−0.3064	−0.3002	−0.293	−0.2858	−0.278
	−0.3085	−0.3093	−0.3095	−0.3086	−0.3056	−0.3002	−0.2941	−0.287	−0.2798	−0.2722
	−0.3001	−0.3009	−0.3011	−0.3002	−0.2973	−0.292	−0.2859	−0.2789	−0.2718	−0.2642

Figure 6.25b: F2B: e=3.5b & d=3b

	c/b									
	−0.336	−0.336	−0.3351	−0.3328	−0.3293	−0.3249	−0.3195	−0.3136	−0.3078	−0.3012
	−0.3352	−0.3352	−0.3342	−0.332	−0.3285	−0.3241	−0.3187	−0.3128	−0.307	−0.3004
	−0.3338	−0.3338	−0.3329	−0.3307	−0.3271	−0.3227	−0.3173	−0.3115	−0.3057	−0.2991
	−0.3316	−0.3316	−0.3307	−0.3285	−0.325	−0.3206	−0.3152	−0.3094	−0.3036	−0.297
a/b	−0.3286	−0.3286	−0.3277	−0.3255	−0.322	−0.3176	−0.3123	−0.3065	−0.3007	−0.2942
	−0.3252	−0.3252	−0.3243	−0.3221	−0.3186	−0.3142	−0.3089	−0.3032	−0.2974	−0.2909
	−0.3205	−0.3205	−0.3196	−0.3174	−0.3139	−0.3096	−0.3043	−0.2986	−0.2929	−0.2864
	−0.3149	−0.315	−0.314	−0.3119	−0.3084	−0.3041	−0.2989	−0.2932	−0.2876	−0.2811
	−0.3087	−0.3087	−0.3078	−0.3057	−0.3022	−0.298	−0.2928	−0.2872	−0.2816	−0.2752
	−0.3003	−0.3003	−0.2994	−0.2973	−0.2939	−0.2897	−0.2846	−0.279	−0.2735	−0.2668

Figure 6.25b: F2B: e=3.5b & d=3.5b

	c/b									
	−0.3356	−0.3349	−0.3334	−0.3308	−0.3274	−0.3236	−0.319	−0.3142	−0.3094	−0.3038
	−0.3348	−0.3341	−0.3326	−0.33	−0.3265	−0.3228	−0.3182	−0.3134	−0.3086	−0.3031
	−0.3335	−0.3327	−0.3312	−0.3286	−0.3252	−0.3215	−0.3169	−0.3121	−0.3073	−0.3017
	−0.3313	−0.3306	−0.329	−0.3265	−0.323	−0.3193	−0.3147	−0.31	−0.3052	−0.2997
a/b	−0.3283	−0.3276	−0.3261	−0.3235	−0.3201	−0.3164	−0.3118	−0.3071	−0.3023	−0.2968
	−0.3249	−0.3241	−0.3226	−0.3201	−0.3167	−0.313	−0.3084	−0.3037	−0.299	−0.2935
	−0.3202	−0.3195	−0.3179	−0.3154	−0.312	−0.3084	−0.3039	−0.2991	−0.2944	−0.289
	−0.3146	−0.3139	−0.3124	−0.3099	−0.3065	−0.3029	−0.2984	−0.2937	−0.2891	−0.2837
	−0.3084	−0.3077	−0.3062	−0.3037	−0.3004	−0.2968	−0.2923	−0.2877	−0.2831	−0.2777
	−0.3	−0.2993	−0.2978	−0.2954	−0.2921	−0.2885	−0.2841	−0.2796	−0.275	−0.2697

Figure 6.25b: F2B: e=3.5b & d=4b

	c/b									
	−0.3355	−0.3345	−0.3327	−0.3302	−0.3271	−0.3238	−0.3198	−0.3157	−0.3116	−0.3069
	−0.3347	−0.3336	−0.3319	−0.3294	−0.3263	−0.323	−0.319	−0.3149	−0.3108	−0.3061
	−0.3333	−0.3323	−0.3306	−0.3281	−0.3249	−0.3216	−0.3177	−0.3136	−0.3095	−0.3048
	−0.3311	−0.3301	−0.3284	−0.3259	−0.3227	−0.3195	−0.3155	−0.3115	−0.3074	−0.3027
a/b	−0.3281	−0.3271	−0.3254	−0.3229	−0.3198	−0.3166	−0.3126	−0.3086	−0.3045	−0.2998
	−0.3247	−0.3237	−0.322	−0.3195	−0.3164	−0.3132	−0.3092	−0.3052	−0.3012	−0.2965
	−0.32	−0.319	−0.3173	−0.3149	−0.3117	−0.3086	−0.3047	−0.3006	−0.2966	−0.292
	−0.3144	−0.3134	−0.3118	−0.3093	−0.3062	−0.3031	−0.2992	−0.2952	−0.2913	−0.2867
	−0.3082	−0.3072	−0.3056	−0.3031	−0.3001	−0.2969	−0.2931	−0.2892	−0.2852	−0.2807
	−0.2998	−0.2988	−0.2972	−0.2948	−0.2918	−0.2887	−0.2849	−0.281	−0.2771	−0.2726

Figure I.14b: F2B: e=4b & d=0.5b

	c/b									
	−0.3358	−0.3358	−0.3358	−0.3358	−0.3358	−0.3353	−0.3329	−0.3304	−0.2852	−0.2337
	−0.3351	−0.3351	−0.3351	−0.3351	−0.3351	−0.3346	−0.3322	−0.3298	−0.2846	−0.2332
	−0.3339	−0.3339	−0.3339	−0.3339	−0.3339	−0.3334	−0.331	−0.3286	−0.2836	−0.2326
	−0.332	−0.332	−0.332	−0.332	−0.332	−0.3315	−0.3291	−0.3268	−0.2819	−0.2308
a/b	−0.3295	−0.3294	−0.3294	−0.3294	−0.3294	−0.3289	−0.3265	−0.3242	−0.2797	−0.229
	−0.3264	−0.3264	−0.3264	−0.3264	−0.3264	−0.3259	−0.3236	−0.3213	−0.2771	−0.2268
	−0.3223	−0.3223	−0.3223	−0.3223	−0.3223	−0.3218	−0.3195	−0.3172	−0.2734	−0.2239
	−0.3175	−0.3175	−0.3174	−0.3175	−0.3174	−0.3169	−0.3147	−0.3125	−0.2692	−0.2203
	−0.312	−0.312	−0.312	−0.312	−0.312	−0.3115	−0.3093	−0.3071	−0.2644	−0.2163
	−0.3047	−0.3047	−0.3047	−0.3047	−0.3047	−0.3042	−0.302	−0.2999	−0.2582	−0.211

Figure I.14b: F2B: e=4b & d=1b

	c/b									
	−0.3358	−0.3358	−0.3357	−0.3357	−0.3357	−0.3322	−0.3187	−0.2969	−0.2721	−0.258
	−0.3351	−0.3351	−0.335	−0.335	−0.335	−0.3315	−0.318	−0.2962	−0.2715	−0.2574
	−0.3339	−0.3339	−0.3338	−0.3338	−0.3338	−0.3303	−0.3171	−0.2951	−0.2706	−0.2565
	−0.332	−0.332	−0.332	−0.3319	−0.3319	−0.3284	−0.3153	−0.2935	−0.2689	−0.2549
a/b	−0.3295	−0.3294	−0.3294	−0.3293	−0.3293	−0.3259	−0.3128	−0.2912	−0.2667	−0.2528
	−0.3264	−0.3264	−0.3263	−0.3263	−0.3263	−0.3229	−0.31	−0.2885	−0.2641	−0.2503
	−0.3223	−0.3223	−0.3223	−0.3222	−0.3222	−0.3188	−0.3061	−0.2849	−0.2605	−0.247
	−0.3175	−0.3175	−0.3174	−0.3174	−0.3173	−0.314	−0.3015	−0.2805	−0.2567	−0.243
	−0.312	−0.312	−0.3119	−0.3119	−0.3118	−0.3085	−0.2961	−0.2757	−0.2516	−0.2384
	−0.3047	−0.3047	−0.3046	−0.3046	−0.3045	−0.3013	−0.2891	−0.2692	−0.2453	−0.2324

Figure I.14b: F2B: e=4b & d=1.5b

	c/b									
	−0.3356	−0.3343	−0.3313	−0.3286	−0.327	−0.3209	−0.3145	−0.302	−0.2861	−0.2756
	−0.3349	−0.3336	−0.3306	−0.3279	−0.3263	−0.3202	−0.3138	−0.3013	−0.2854	−0.275
	−0.3337	−0.3324	−0.3294	−0.3267	−0.3251	−0.3191	−0.3127	−0.3002	−0.2844	−0.2739
	−0.3318	−0.3305	−0.3276	−0.3249	−0.3233	−0.3173	−0.3109	−0.2985	−0.2827	−0.2723
a/b	−0.3292	−0.3279	−0.325	−0.3223	−0.3208	−0.3148	−0.3085	−0.2961	−0.2803	−0.27
	−0.3262	−0.3249	−0.322	−0.3194	−0.3179	−0.3119	−0.3057	−0.2933	−0.2776	−0.2674
	−0.3221	−0.3208	−0.318	−0.3154	−0.314	−0.3081	−0.3019	−0.2896	−0.274	−0.2638
	−0.3172	−0.316	−0.3131	−0.3106	−0.3093	−0.3034	−0.2973	−0.2851	−0.2696	−0.2595
	−0.3117	−0.3105	−0.3077	−0.3052	−0.304	−0.2982	−0.2921	−0.28	−0.2646	−0.2547
	−0.3044	−0.3032	−0.3005	−0.298	−0.2969	−0.2913	−0.2853	−0.2733	−0.2581	−0.2482

Figure I.14b: F2B: e=4b & d=2b

	c/b									
	−0.3346	−0.3328	−0.3324	−0.3337	−0.3331	−0.3263	−0.3191	−0.3094	−0.2991	−0.2897
	−0.3339	−0.3321	−0.3317	−0.333	−0.3324	−0.3256	−0.3184	−0.3087	−0.2984	−0.289
	−0.3327	−0.331	−0.3306	−0.3318	−0.3312	−0.3244	−0.3173	−0.3076	−0.2973	−0.2879
	−0.3308	−0.3291	−0.3287	−0.33	−0.3294	−0.3226	−0.3154	−0.3058	−0.2956	−0.2862
a/b	−0.3283	−0.3265	−0.3261	−0.3275	−0.3268	−0.3201	−0.313	−0.3033	−0.2931	−0.2838
	−0.3253	−0.3235	−0.3232	−0.3245	−0.3239	−0.3171	−0.3101	−0.3005	−0.2903	−0.281
	−0.3212	−0.3195	−0.3191	−0.3205	−0.3199	−0.3132	−0.3061	−0.2966	−0.2865	−0.2773
	−0.3163	−0.3147	−0.3143	−0.3157	−0.3151	−0.3084	−0.3014	−0.292	−0.2819	−0.2728
	−0.3109	−0.3092	−0.3089	−0.3103	−0.3097	−0.3031	−0.2961	−0.2868	−0.2768	−0.2678
	−0.3036	−0.302	−0.3017	−0.3031	−0.3026	−0.296	−0.2891	−0.2798	−0.27	−0.261

Figure I.14b: F2B: e=4b & d=2.5b

	c/b									
	−0.3358	−0.3365	−0.3368	−0.3358	−0.3327	−0.3272	−0.3208	−0.3134	−0.3059	−0.2979
	−0.3351	−0.3358	−0.3361	−0.3351	−0.332	−0.3265	−0.3201	−0.3127	−0.3053	−0.2972
	−0.3339	−0.3346	−0.3349	−0.3339	−0.3308	−0.3253	−0.3189	−0.3115	−0.3041	−0.2961
	−0.332	−0.3328	−0.333	−0.332	−0.329	−0.3234	−0.3171	−0.3097	−0.3023	−0.2943
a/b	−0.3294	−0.3302	−0.3304	−0.3294	−0.3264	−0.3209	−0.3146	−0.3072	−0.2999	−0.2919
	−0.3264	−0.3272	−0.3274	−0.3264	−0.3234	−0.3179	−0.3116	−0.3043	−0.297	−0.289
	−0.3223	−0.3231	−0.3233	−0.3224	−0.3193	−0.3139	−0.3076	−0.3004	−0.2931	−0.2852
	−0.3175	−0.3182	−0.3185	−0.3175	−0.3145	−0.3091	−0.3029	−0.2957	−0.2884	−0.2806
	−0.312	−0.3127	−0.313	−0.312	−0.3091	−0.3037	−0.2975	−0.2904	−0.2832	−0.2754
	−0.3047	−0.3055	−0.3057	−0.3048	−0.3018	−0.2965	−0.2904	−0.2833	−0.2762	−0.2685

Figure I.14b: F2B: e=4b & d=3b

	c/b									
	−0.336	−0.336	−0.3351	−0.3329	−0.3293	−0.3249	−0.3195	−0.3137	−0.3078	−0.3012
	−0.3353	−0.3353	−0.3344	−0.3322	−0.3286	−0.3242	−0.3188	−0.313	−0.3072	−0.3005
	−0.3341	−0.3341	−0.3332	−0.331	−0.3274	−0.323	−0.3176	−0.3118	−0.306	−0.2994
	−0.3322	−0.3322	−0.3313	−0.3291	−0.3256	−0.3212	−0.3158	−0.31	−0.3042	−0.2976
a/b	−0.3296	−0.3297	−0.3287	−0.3265	−0.323	−0.3186	−0.3133	−0.3075	−0.3017	−0.2951
	−0.3266	−0.3266	−0.3257	−0.3235	−0.32	−0.3156	−0.3103	−0.3046	−0.2988	−0.2923
	−0.3225	−0.3226	−0.3216	−0.3195	−0.316	−0.3116	−0.3063	−0.3006	−0.2949	−0.2884
	−0.3177	−0.3177	−0.3168	−0.3146	−0.3111	−0.3068	−0.3016	−0.2959	−0.2902	−0.2837
	−0.3122	−0.3122	−0.3113	−0.3091	−0.3057	−0.3014	−0.2962	−0.2906	−0.285	−0.2785
	−0.3049	−0.3049	−0.304	−0.3019	−0.2985	−0.2942	−0.2891	−0.2835	−0.2779	−0.2716

Figure I.14b: F2B: e=4b & d=3.5b

	c/b									
	−0.3357	−0.335	−0.3334	−0.3308	−0.3274	−0.3236	−0.319	−0.3142	−0.3094	−0.3039
	−0.335	−0.3343	−0.3327	−0.3301	−0.3267	−0.323	−0.3183	−0.3135	−0.3087	−0.3032
	−0.3338	−0.3331	−0.3315	−0.329	−0.3255	−0.3218	−0.3172	−0.3124	−0.3076	−0.302
	−0.3319	−0.3312	−0.3296	−0.3271	−0.3236	−0.3199	−0.3153	−0.3106	−0.3058	−0.3002
a/b	−0.3293	−0.3286	−0.3271	−0.3245	−0.3211	−0.3174	−0.3128	−0.308	−0.3033	−0.2978
	−0.3263	−0.3256	−0.3241	−0.3215	−0.3181	−0.3144	−0.3099	−0.3051	−0.3004	−0.2949
	−0.3222	−0.3215	−0.32	−0.3175	−0.3141	−0.3104	−0.3059	−0.3011	−0.2964	−0.291
	−0.3173	−0.3166	−0.3151	−0.3126	−0.3092	−0.3056	−0.3011	−0.2964	−0.2917	−0.2863
	−0.3119	−0.3112	−0.3097	−0.3072	−0.3038	−0.3002	−0.2957	−0.2911	−0.2864	−0.2811
	−0.3046	−0.3039	−0.3024	−0.2999	−0.2966	−0.293	−0.2886	−0.284	−0.2794	−0.2741

Figure I.14b: F2B: e=4b & d=4b

	c/b									
	−0.3355	−0.3345	−0.3328	−0.3303	−0.3271	−0.3238	−0.3199	−0.3158	−0.3117	−0.3069
	−0.3348	−0.3338	−0.3321	−0.3296	−0.3264	−0.3232	−0.3192	−0.3151	−0.311	−0.3062
	−0.3336	−0.3326	−0.3309	−0.3284	−0.3252	−0.322	−0.318	−0.3139	−0.3098	−0.3051
	−0.3317	−0.3307	−0.329	−0.3265	−0.3234	−0.3201	−0.3162	−0.3121	−0.308	−0.3033
a/b	−0.3291	−0.3281	−0.3264	−0.3239	−0.3208	−0.3176	−0.3136	−0.3096	−0.3055	−0.3008
	−0.3261	−0.3251	−0.3234	−0.321	−0.3178	−0.3146	−0.3107	−0.3066	−0.3026	−0.2979
	−0.322	−0.321	−0.3194	−0.3169	−0.3138	−0.3106	−0.3067	−0.3026	−0.2986	−0.294
	−0.3172	−0.3162	−0.3145	−0.3121	−0.309	−0.3058	−0.3019	−0.2979	−0.2939	−0.2893
	−0.3117	−0.3107	−0.309	−0.3066	−0.3035	−0.3004	−0.2965	−0.2926	−0.2886	−0.284
	−0.3044	−0.3034	−0.3018	−0.2994	−0.2963	−0.2932	−0.2894	−0.2855	−0.2815	−0.277

Figure 6.26a: F1B: e=0.5a & d=0.5a

	c/a									
	0.0065	0.0059	0.0066	0.0064	0.0066	0.0065	0.0065	0.0065	0.0064	0.0062
	0.0047	0.0049	0.0063	0.0050	0.0053	0.0062	0.0042	0.0049	0.0060	0.0023
	0.0007	0.0010	0.0017	0.0015	0.0026	0.0010	−0.0001	0.0039	0.0068	0.0036
b/a	0.0018	0.0019	0.0022	0.0019	0.0021	0.0013	0.0036	0.0068	0.0107	0.0083
	0.0001	0.0002	0.0003	0.0001	0.0002	0.0002	0.0000	0.0149	0.0202	0.0001
	−0.0004	0.0001	0.0001	−0.0002	−0.0001	−0.0001	0.0002	0.0002	0.0001	0.0003
	0.1579	0.1583	0.1590	0.1590	0.1587	0.1434	0.0941	0.0631	0.0478	0.0347
	0.4288	0.4288	0.4288	0.4288	0.4288	0.4289	0.4303	0.4097	0.2957	0.1982

Figure I.15a: F1B: e=0.5a & d=1a

	c/a									
	0.0066	0.0066	0.0066	0.0065	0.0066	0.0065	0.0065	0.0065	0.0064	0.0065
	0.0052	0.0052	0.0052	0.0051	0.0051	0.0052	0.0050	0.0051	0.0049	0.0050
	0.0019	0.0024	0.0029	0.0026	0.0022	0.0031	0.0028	0.0030	0.0030	0.0027
b/a	0.0021	0.0026	0.0035	0.0032	0.0034	0.0050	0.0047	0.0047	0.0055	0.0044
	0.0002	0.0001	0.0000	0.0001	0.0000	−0.0001	0.0000	0.0000	0.0002	0.0001
	−0.0001	−0.0004	0.0001	−0.0001	0.0003	0.0000	0.0000	−0.0001	−0.0003	0.0000
	0.1581	0.1577	0.1565	0.1544	0.1423	0.1218	0.0973	0.0806	0.0722	0.0579
	0.4288	0.4288	0.4287	0.4287	0.4284	0.4202	0.3878	0.3318	0.2840	0.2281

Figure 6.27a: F1B: e=0.5a & d=1.5a

	c/a									
	0.0066	0.0065	0.0066	0.0066	0.0065	0.0059	0.0063	0.0063	0.0063	0.0065
	0.0050	0.0051	0.0052	0.0051	0.0052	0.0051	0.0051	0.0051	0.0052	0.0052
	0.0017	0.0018	0.0018	0.0018	0.0019	0.0020	0.0021	0.0022	0.0023	0.0024
b/a	0.0018	0.0019	0.0020	0.0020	0.0022	0.0024	0.0025	0.0027	0.0029	0.0030
	0.0002	0.0002	0.0002	0.0002	0.0000	0.0000	−0.0001	0.0000	0.0000	0.0000
	−0.0005	−0.0004	−0.0004	−0.0002	0.0001	−0.0004	−0.0005	−0.0001	0.0001	0.0000
	0.1581	0.1592	0.1574	0.1456	0.1275	0.1152	0.1000	0.0893	0.0825	0.0715
	0.4288	0.4291	0.4308	0.4310	0.4181	0.3912	0.3488	0.3122	0.2868	0.2514

Figure I.16a: F1B: e=0.5a & d=2a

	c/a									
	0.0065	0.0066	0.0066	0.0065	0.0065	0.0061	0.0065	0.0064	0.0065	0.0064
	0.0051	0.0050	0.0052	0.0049	0.0052	0.0051	0.0050	0.0051	0.0052	0.0051
	0.0017	0.0017	0.0018	0.0019	0.0020	0.0020	0.0021	0.0022	0.0022	0.0023
b/a	0.0017	0.0018	0.0019	0.0020	0.0021	0.0022	0.0023	0.0024	0.0026	0.0027
	0.0001	0.0002	0.0002	0.0002	−0.0001	−0.0001	0.0000	0.0000	−0.0001	0.0000
	0.0001	−0.0001	−0.0001	−0.0002	−0.0001	−0.0001	−0.0001	−0.0004	0.0001	0.0003
	0.1580	0.1545	0.1472	0.1363	0.1227	0.1146	0.1039	0.0960	0.0899	0.0816
	0.4297	0.4316	0.4289	0.4134	0.3875	0.3660	0.3373	0.3135	0.2949	0.2703

Figure 6.28a: F1B: e=0.5a & d=2.5a

	c/a									
	0.0066	0.0066	0.0066	0.0064	0.0064	0.0061	0.0065	0.0065	0.0061	0.0066
	0.0050	0.0052	0.0052	0.0049	0.0051	0.0051	0.0052	0.0051	0.0052	0.0052
	0.0018	0.0018	0.0018	0.0018	0.0019	0.0020	0.0021	0.0021	0.0022	0.0022
b/a	0.0017	0.0018	0.0018	0.0020	0.0021	0.0022	0.0023	0.0024	0.0025	0.0026
	0.0002	0.0002	0.0002	0.0000	0.0002	0.0000	0.0001	0.0001	0.0001	0.0001
	−0.0001	0.0001	−0.0001	−0.0004	−0.0001	−0.0002	0.0001	−0.0004	−0.0001	0.0000
	0.1563	0.1514	0.1447	0.1357	0.1265	0.1198	0.1118	0.1053	0.0998	0.0932
	0.4286	0.4241	0.4142	0.3972	0.3766	0.3605	0.3397	0.3222	0.3072	0.2889

Figure I.17a: F1B: e=0.5a & d=3a

	c/a									
	0.0065	0.0065	0.0064	0.0066	0.0066	0.0066	0.0066	0.0066	0.0066	0.0067
	0.0050	0.0052	0.0050	0.0050	0.0052	0.0051	0.0051	0.0050	0.0053	0.0051
	0.0017	0.0017	0.0018	0.0019	0.0019	0.0019	0.0020	0.0021	0.0021	0.0022
b/a	0.0018	0.0018	0.0019	0.0020	0.0021	0.0021	0.0022	0.0023	0.0024	0.0025
	0.0002	0.0002	0.0003	0.0002	0.0001	0.0000	0.0000	0.0001	−0.0001	0.0000
	0.0001	−0.0004	−0.0004	−0.0007	−0.0001	0.0001	−0.0003	0.0004	−0.0001	−0.0001
	0.1564	0.1522	0.1470	0.1404	0.1334	0.1279	0.1215	0.1160	0.1111	0.1056
	0.4267	0.4201	0.4101	0.3960	0.3801	0.3672	0.3512	0.3373	0.3248	0.3101

Figure 6.29a: F1B: e=0.5a & d=3.5a

	c/a									
	0.0066	0.0066	0.0066	0.0065	0.0066	0.0065	0.0066	0.0066	0.0067	0.0063
	0.0052	0.0051	0.0050	0.0051	0.0051	0.0052	0.0052	0.0051	0.0053	0.0051
	0.0017	0.0018	0.0018	0.0018	0.0019	0.0019	0.0019	0.0020	0.0020	0.0021
b/a	0.0017	0.0018	0.0018	0.0019	0.0020	0.0020	0.0021	0.0022	0.0023	0.0024
	0.0002	0.0001	0.0002	0.0000	0.0003	0.0001	0.0001	0.0000	0.0001	0.0001
	−0.0001	0.0001	−0.0004	−0.0001	−0.0004	0.0001	−0.0001	−0.0001	0.0001	−0.0003
	0.1568	0.1537	0.1498	0.1448	0.1395	0.1350	0.1298	0.1252	0.1210	0.1163
	0.4266	0.4205	0.4121	0.4010	0.3885	0.3780	0.3653	0.3538	0.3432	0.3312

Figure I.18a: F1B: e=0.5a & d=4a

	c/a									
	0.0065	0.0066	0.0065	0.0066	0.0065	0.0066	0.0066	0.0067	0.0067	0.0067
	0.0051	0.0052	0.0051	0.0052	0.0051	0.0050	0.0053	0.0052	0.0052	0.0053
	0.0018	0.0018	0.0017	0.0018	0.0018	0.0019	0.0019	0.0020	0.0020	0.0020
b/a	0.0018	0.0018	0.0019	0.0019	0.0020	0.0020	0.0021	0.0022	0.0022	0.0023
	0.0002	0.0002	0.0001	0.0002	0.0002	0.0000	0.0001	0.0000	0.0001	0.0001
	−0.0001	−0.0001	−0.0004	−0.0001	−0.0001	0.0001	−0.0004	−0.0004	−0.0003	−0.0002
	0.1571	0.1548	0.1519	0.1482	0.1440	0.1404	0.1362	0.1323	0.1287	0.1248
	0.4269	0.4220	0.4153	0.4066	0.3968	0.3882	0.3779	0.3684	0.3593	0.3492

Figure 6.26a: F1B: e=1a & d=0.5a

	c/a									
b/a	0.0035	0.0041	0.0043	0.0042	0.0043	0.0042	0.0042	0.0042	0.0044	0.0047
	0.0001	0.0001	0.0003	0.0001	0.0004	0.0013	0.0026	0.0011	0.0025	0.0026
	0.0004	0.0000	0.0002	0.0001	0.0001	0.0002	0.0001	0.0002	−0.0001	0.0001
	0.0005	0.0000	−0.0001	−0.0003	−0.0003	0.0001	−0.0005	0.0003	−0.0003	−0.0010
	0.0277	0.0246	0.0152	0.0109	0.0058	0.0012	−0.0003	−0.0002	0.0056	−0.0004
	0.1325	0.1300	0.1233	0.1088	0.0738	0.0473	0.0336	0.0261	0.0215	0.0180
	0.3471	0.3471	0.3471	0.3471	0.3497	0.3298	0.2305	0.1523	0.1296	0.0965
	0.4268	0.4269	0.4269	0.4269	0.4268	0.4270	0.4284	0.4080	0.2987	0.1991

Figure I.15a: F1B: e=1a & d=1a

	c/a									
b/a	0.0034	0.0034	0.0033	0.0031	0.0035	0.0037	0.0038	0.0038	0.0039	0.0041
	0.0001	0.0001	0.0001	0.0000	0.0001	0.0000	0.0002	0.0001	0.0002	−0.0001
	0.0000	−0.0001	0.0000	−0.0001	−0.0002	−0.0001	−0.0001	0.0001	−0.0001	0.0001
	−0.0001	0.0001	0.0001	−0.0003	0.0001	0.0001	0.0002	0.0002	−0.0001	−0.0003
	0.0260	0.0271	0.0263	0.0211	0.0152	0.0127	0.0093	0.0073	0.0072	0.0043
	0.1296	0.1287	0.1256	0.1113	0.0931	0.0817	0.0699	0.0616	0.0582	0.0492
	0.3471	0.3495	0.3474	0.3437	0.3106	0.2655	0.2205	0.1886	0.1728	0.1478
	0.4269	0.4268	0.4268	0.4268	0.4264	0.4184	0.3862	0.3308	0.2832	0.2275

Figure 6.27a: F1B: e=1a & d=1.5a

	c/a									
b/a	0.0034	0.0034	0.0032	0.0033	0.0036	0.0034	0.0037	0.0038	0.0039	0.0039
	0.0001	0.0000	0.0000	0.0000	0.0002	0.0001	0.0002	0.0001	0.0002	0.0001
	0.0001	0.0000	0.0001	0.0000	0.0001	0.0000	0.0001	0.0000	0.0002	0.0002
	0.0003	0.0001	0.0000	0.0001	0.0000	−0.0001	0.0000	0.0000	0.0001	0.0001
	0.0274	0.0254	0.0222	0.0179	0.0138	0.0122	0.0095	0.0080	0.0070	0.0051
	0.1325	0.1283	0.1200	0.1076	0.0953	0.0889	0.0793	0.0728	0.0684	0.0611
	0.3479	0.3494	0.3415	0.3146	0.2816	0.2585	0.2317	0.2192	0.1986	0.1789
	0.4268	0.4272	0.4289	0.4291	0.4162	0.3894	0.3473	0.3109	0.2857	0.2501

Figure I.16a: F1B: e=1a & d=2a

	c/a									
b/a	0.0031	0.0034	0.0035	0.0035	0.0036	0.0036	0.0037	0.0038	0.0038	0.0040
	0.0001	0.0002	0.0001	0.0001	0.0001	0.0001	0.0001	−0.0001	0.0002	0.0002
	0.0000	0.0000	0.0002	0.0003	0.0002	0.0000	−0.0001	0.0000	0.0002	0.0001
	0.0001	0.0004	0.0000	0.0002	−0.0001	0.0001	0.0002	0.0001	0.0000	0.0002
	0.0265	0.0243	0.0217	0.0186	0.0157	0.0141	0.0119	0.0105	0.0093	0.0079
	0.1303	0.1246	0.1175	0.1086	0.0996	0.0940	0.0867	0.0812	0.0766	0.0709
	0.3461	0.3380	0.3232	0.3019	0.2791	0.2636	0.2442	0.2290	0.2170	0.2017
	0.4278	0.4296	0.4269	0.4114	0.3857	0.3644	0.3358	0.3121	0.2935	0.2688

Figure 6.28a: F1B: e=1a & d=2.5a

	c/a									
b/a	0.0033	0.0033	0.0034	0.0035	0.0036	0.0036	0.0034	0.0036	0.0038	0.0036
	0.0001	0.0002	0.0001	0.0002	0.0001	0.0002	0.0002	0.0002	0.0002	0.0002
	0.0001	0.0001	0.0000	0.0001	0.0001	0.0001	0.0001	0.0002	0.0002	0.0000
	0.0004	0.0000	0.0002	0.0003	0.0004	0.0003	0.0000	0.0003	0.0001	0.0000
	0.0267	0.0251	0.0232	0.0211	0.0189	0.0174	0.0157	0.0143	0.0131	0.0118
	0.1305	0.1261	0.1208	0.1143	0.1077	0.1028	0.0969	0.0923	0.0879	0.0831
	0.3439	0.3347	0.3221	0.3060	0.2895	0.2769	0.2620	0.2494	0.2386	0.2260
	0.4266	0.4222	0.4124	0.3954	0.3749	0.3589	0.3382	0.3207	0.3057	0.2874

Figure I.17a: F1B: e=1a & d=3a

	c/a									
b/a	0.0033	0.0031	0.0034	0.0035	0.0034	0.0036	0.0035	0.0037	0.0034	0.0037
	0.0001	0.0001	0.0001	0.0001	0.0002	0.0002	0.0001	0.0002	0.0001	0.0002
	0.0000	−0.0001	−0.0001	0.0000	0.0001	0.0002	0.0001	0.0000	0.0002	0.0001
	0.0000	−0.0001	0.0002	0.0000	−0.0003	−0.0003	0.0002	0.0002	0.0002	0.0000
	0.0269	0.0259	0.0246	0.0230	0.0214	0.0202	0.0188	0.0176	0.0165	0.0154
	0.1310	0.1279	0.1240	0.1193	0.1143	0.1103	0.1056	0.1015	0.0978	0.0937
	0.3442	0.3369	0.3273	0.3152	0.3024	0.2923	0.2803	0.2698	0.2604	0.2498
	0.4248	0.4182	0.4083	0.3942	0.3784	0.3655	0.3496	0.3357	0.3231	0.3086

Figure 6.29a: F1B: e=1a & d=3.5a

	c/a									
b/a	0.0034	0.0031	0.0033	0.0035	0.0035	0.0032	0.0032	0.0036	0.0034	0.0037
	0.0001	0.0000	0.0001	0.0001	0.0002	0.0002	0.0001	0.0001	0.0001	0.0002
	0.0000	0.0002	0.0001	0.0001	0.0000	0.0001	−0.0001	0.0003	0.0000	0.0001
	0.0001	0.0001	−0.0001	0.0004	0.0002	0.0002	−0.0002	−0.0003	0.0002	−0.0001
	0.0271	0.0264	0.0254	0.0243	0.0231	0.0221	0.0210	0.0200	0.0191	0.0181
	0.1314	0.1292	0.1264	0.1229	0.1191	0.1158	0.1121	0.1086	0.1055	0.1019
	0.3450	0.3395	0.3323	0.3232	0.3133	0.3049	0.2952	0.2865	0.2784	0.2694
	0.4246	0.4186	0.4102	0.3992	0.3868	0.3763	0.3636	0.3522	0.3415	0.3295

Figure I.18a: F1B: e=1a & d=4a

	c/a									
b/a	0.0034	0.0034	0.0033	0.0035	0.0034	0.0033	0.0035	0.0036	0.0037	0.0035
	0.0001	0.0001	0.0001	0.0001	0.0002	0.0002	0.0001	0.0001	0.0002	0.0001
	0.0002	0.0000	−0.0001	0.0001	0.0001	0.0001	0.0001	−0.0001	0.0001	0.0002
	0.0000	−0.0001	−0.0002	0.0000	0.0002	−0.0001	−0.0001	0.0003	0.0002	0.0000
	0.0272	0.0267	0.0260	0.0252	0.0243	0.0235	0.0225	0.0217	0.0209	0.0201
	0.1316	0.1300	0.1279	0.1253	0.1223	0.1197	0.1167	0.1138	0.1111	0.1081
	0.3455	0.3414	0.3360	0.3291	0.3215	0.3146	0.3067	0.2991	0.2922	0.2846
	0.4250	0.4201	0.4134	0.4047	0.3950	0.3863	0.3761	0.3666	0.3575	0.3474

Figure 6.26a: F1B: e=1.5a & d=0.5a

	c/a									
	0.0007	0.0007	0.0007	0.0002	0.0003	0.0006	0.0003	0.0003	0.0001	0.0003
	0.0005	0.0005	0.0005	0.0002	0.0008	0.0009	0.0001	0.0002	0.0005	0.0004
	0.0066	0.0092	0.0094	0.0064	0.0042	0.0023	0.0021	0.0009	0.0027	0.0002
b/a	0.0758	0.0682	0.0564	0.0393	0.0282	0.0206	0.0167	0.0132	0.0139	0.0103
	0.1787	0.1771	0.1715	0.1289	0.0822	0.0741	0.0531	0.0433	0.0566	0.0306
	0.2697	0.2685	0.2686	0.2588	0.1760	0.1209	0.0907	0.0729	0.0715	0.0538
	0.3829	0.3829	0.3830	0.3829	0.3840	0.3661	0.2618	0.1770	0.1532	0.1068
	0.4275	0.4275	0.4275	0.4275	0.4275	0.4276	0.4290	0.4090	0.2978	0.2018

Figure I.15a: F1B: e=1.5a & d=1a

	c/a									
	0.0007	0.0003	0.0007	0.0007	0.0007	0.0006	0.0006	0.0003	0.0006	0.0006
	0.0003	0.0003	0.0003	0.0002	0.0003	0.0003	0.0005	0.0005	0.0004	0.0004
	0.0136	0.0112	0.0086	0.0052	0.0025	0.0023	0.0009	0.0003	0.0001	−0.0002
b/a	0.0841	0.0775	0.0685	0.0569	0.0466	0.0443	0.0376	0.0340	0.0324	0.0266
	0.1810	0.1729	0.1540	0.1303	0.1099	0.1018	0.0890	0.0810	0.0776	0.0667
	0.2690	0.2691	0.2488	0.2084	0.1726	0.1545	0.1339	0.1203	0.1142	0.0989
	0.3829	0.3829	0.3833	0.3799	0.3455	0.2999	0.2438	0.2065	0.1892	0.1523
	0.4275	0.4275	0.4274	0.4274	0.4271	0.4192	0.3874	0.3324	0.2849	0.2293

Figure 6.27a: F1B: e=1.5a & d=1.5a

	c/a									
	0.0007	0.0007	0.0003	0.0007	0.0007	0.0006	0.0006	0.0006	0.0006	0.0003
	0.0003	0.0002	0.0003	0.0005	0.0000	0.0002	0.0003	0.0004	0.0002	0.0000
	0.0127	0.0105	0.0083	0.0059	0.0039	0.0030	0.0018	0.0011	0.0006	0.0004
b/a	0.0813	0.0747	0.0676	0.0594	0.0519	0.0482	0.0427	0.0391	0.0362	0.0323
	0.1757	0.1638	0.1504	0.1346	0.1200	0.1125	0.1018	0.0945	0.0888	0.0808
	0.2661	0.2514	0.2321	0.2070	0.1841	0.1718	0.1554	0.1440	0.1357	0.1233
	0.3838	0.3856	0.3777	0.3486	0.3115	0.2861	0.2538	0.2302	0.2144	0.1897
	0.4275	0.4278	0.4295	0.4298	0.4171	0.3905	0.3486	0.3123	0.2870	0.2514

Figure I.16a: F1B: e=1.5a & d=2a

	c/a									
	0.0007	0.0007	0.0002	0.0007	0.0007	0.0006	0.0006	0.0006	0.0006	0.0006
	0.0003	0.0005	0.0003	0.0003	0.0003	0.0003	0.0005	0.0000	0.0003	0.0004
	0.0130	0.0116	0.0100	0.0083	0.0067	0.0057	0.0046	0.0038	0.0031	0.0024
b/a	0.0820	0.0776	0.0726	0.0668	0.0611	0.0574	0.0529	0.0493	0.0463	0.0429
	0.1762	0.1676	0.1579	0.1467	0.1358	0.1286	0.1197	0.1128	0.1069	0.1000
	0.2639	0.2520	0.2365	0.2194	0.2027	0.1918	0.1783	0.1681	0.1593	0.1490
	0.3819	0.3735	0.3579	0.3345	0.3089	0.2915	0.2693	0.2519	0.2378	0.2197
	0.4284	0.4302	0.4276	0.4123	0.3867	0.3654	0.3369	0.3131	0.2946	0.2699

Figure 6.28a: F1B: e=1.5a & d=2.5a

	c/a									
	−0.0002	0.0007	0.0007	0.0003	0.0003	0.0007	0.0006	0.0006	0.0006	0.0006
	0.0005	0.0003	0.0003	0.0003	0.0002	0.0000	0.0003	0.0003	0.0003	0.0003
	0.0133	0.0124	0.0113	0.0101	0.0089	0.0081	0.0071	0.0063	0.0056	0.0049
b/a	0.0828	0.0799	0.0764	0.0723	0.0681	0.0650	0.0613	0.0581	0.0554	0.0523
	0.1775	0.1718	0.1649	0.1569	0.1488	0.1426	0.1353	0.1292	0.1238	0.1178
	0.2651	0.2572	0.2456	0.2334	0.2214	0.2116	0.2007	0.1916	0.1833	0.1742
	0.3796	0.3699	0.3566	0.3394	0.3210	0.3073	0.2904	0.2764	0.2642	0.2499
	0.4273	0.4228	0.4131	0.3962	0.3757	0.3597	0.3391	0.3216	0.3066	0.2882

Figure I.17a: F1B: e=1.5a & d=3a

	c/a									
	0.0002	0.0007	0.0007	0.0007	0.0007	0.0003	0.0007	0.0006	0.0003	0.0006
	0.0005	0.0005	0.0002	0.0003	0.0003	0.0003	0.0003	0.0003	0.0002	0.0005
	0.0134	0.0128	0.0121	0.0113	0.0104	0.0097	0.0089	0.0082	0.0076	0.0069
b/a	0.0832	0.0813	0.0789	0.0759	0.0728	0.0702	0.0672	0.0646	0.0622	0.0595
	0.1784	0.1745	0.1696	0.1638	0.1576	0.1526	0.1467	0.1415	0.1368	0.1315
	0.2664	0.2606	0.2537	0.2436	0.2341	0.2265	0.2181	0.2099	0.2022	0.1949
	0.3799	0.3722	0.3620	0.3493	0.3355	0.3244	0.3112	0.2996	0.2890	0.2771
	0.4255	0.4189	0.4089	0.3950	0.3791	0.3663	0.3504	0.3364	0.3239	0.3093

Figure 6.29a: F1B: e=1.5a & d=3.5a

	c/a									
	0.0007	0.0007	0.0007	0.0003	0.0002	0.0003	0.0002	0.0007	0.0009	0.0006
	0.0003	0.0003	0.0003	0.0000	0.0005	0.0005	0.0003	0.0005	0.0005	0.0002
	0.0135	0.0131	0.0126	0.0120	0.0113	0.0108	0.0101	0.0095	0.0090	0.0084
b/a	0.0834	0.0821	0.0804	0.0782	0.0758	0.0737	0.0714	0.0692	0.0671	0.0649
	0.1789	0.1762	0.1727	0.1683	0.1635	0.1594	0.1547	0.1504	0.1463	0.1418
	0.2671	0.2629	0.2583	0.2514	0.2441	0.2369	0.2298	0.2232	0.2171	0.2100
	0.3807	0.3749	0.3673	0.3577	0.3472	0.3382	0.3276	0.3180	0.3090	0.2990
	0.4253	0.4193	0.4109	0.3998	0.3874	0.3770	0.3643	0.3528	0.3422	0.3301

Figure I.18a: F1B: e=1.5a & d=4a

	c/a									
	0.0003	0.0007	0.0007	0.0007	0.0007	0.0007	0.0007	0.0002	0.0009	0.0003
	0.0003	0.0005	0.0004	0.0003	0.0003	0.0000	0.0005	0.0005	0.0001	0.0003
	0.0135	0.0133	0.0129	0.0124	0.0119	0.0115	0.0110	0.0105	0.0101	0.0096
b/a	0.0836	0.0826	0.0813	0.0797	0.0779	0.0762	0.0743	0.0724	0.0707	0.0688
	0.1793	0.1773	0.1747	0.1713	0.1676	0.1642	0.1604	0.1567	0.1532	0.1494
	0.2676	0.2644	0.2606	0.2562	0.2505	0.2452	0.2385	0.2328	0.2277	0.2219
	0.3813	0.3770	0.3712	0.3639	0.3557	0.3484	0.3399	0.3319	0.3242	0.3158
	0.4256	0.4208	0.4141	0.4054	0.3956	0.3870	0.3768	0.3672	0.3582	0.3480

Figure 6.26a: F1B: e=2a & d=0.5a

	c/a									
	0.0013	0.0005	0.0013	0.0014	0.0004	0.0004	0.0013	0.0013	0.0013	0.0013
	0.0266	0.0188	0.0153	0.0087	0.0045	0.0069	0.0039	0.0033	0.0043	0.0020
	0.1092	0.0845	0.0615	0.0424	0.0312	0.0302	0.0238	0.0204	0.0240	0.0151
b/a	0.2082	0.2059	0.1570	0.0943	0.0672	0.0623	0.0482	0.0410	0.0466	0.0308
	0.2886	0.2885	0.2821	0.2160	0.1299	0.1284	0.0931	0.0809	0.0942	0.0502
	0.3329	0.3329	0.3329	0.3217	0.2131	0.1624	0.1130	0.0875	0.0945	0.0649
	0.3979	0.3979	0.3980	0.3980	0.3990	0.3815	0.2758	0.1907	0.1648	0.1100
	0.4291	0.4291	0.4292	0.4292	0.4291	0.4293	0.4307	0.4110	0.3005	0.2046

Figure I.15a: F1B: e=2a & d=1a

	c/a									
	0.0013	0.0013	0.0013	0.0013	0.0014	0.0005	0.0013	0.0004	0.0013	0.0013
	0.0244	0.0184	0.0136	0.0088	0.0053	0.0044	0.0026	0.0019	0.0015	0.0013
	0.1014	0.0846	0.0707	0.0561	0.0442	0.0412	0.0338	0.0301	0.0274	0.0223
b/a	0.2014	0.1746	0.1473	0.1179	0.0959	0.0904	0.0766	0.0694	0.0652	0.0545
	0.2904	0.2753	0.2417	0.1982	0.1599	0.1489	0.1253	0.1125	0.1066	0.0870
	0.3334	0.3340	0.3121	0.2603	0.2091	0.1884	0.1589	0.1398	0.1300	0.1074
	0.3979	0.3979	0.3984	0.3951	0.3618	0.3154	0.2582	0.2200	0.2020	0.1633
	0.4291	0.4291	0.4291	0.4291	0.4287	0.4209	0.3895	0.3351	0.2873	0.2317

Figure 6.27a: F1B: e=2a & d=1.5a

	c/a									
	0.0013	0.0013	0.0013	0.0013	0.0013	0.0013	0.0005	0.0013	0.0013	0.0019
	0.0259	0.0224	0.0188	0.0151	0.0119	0.0101	0.0080	0.0066	0.0054	0.0042
	0.1049	0.0951	0.0850	0.0744	0.0648	0.0593	0.0524	0.0476	0.0435	0.0389
b/a	0.2004	0.1835	0.1658	0.1462	0.1282	0.1188	0.1063	0.0977	0.0909	0.0824
	0.2816	0.2625	0.2406	0.2151	0.1912	0.1786	0.1606	0.1483	0.1385	0.1252
	0.3299	0.3135	0.2896	0.2588	0.2290	0.2136	0.1917	0.1765	0.1652	0.1483
	0.3989	0.4008	0.3933	0.3649	0.3265	0.3005	0.2676	0.2435	0.2273	0.2020
	0.4291	0.4295	0.4311	0.4315	0.4191	0.3927	0.3508	0.3144	0.2891	0.2535

Figure I.16a: F1B: e=2a & d=2a

	c/a									
	0.0013	0.0013	0.0013	0.0013	0.0013	0.0013	0.0005	0.0004	0.0012	0.0012
	0.0267	0.0246	0.0223	0.0196	0.0171	0.0154	0.0134	0.0119	0.0106	0.0093
	0.1071	0.1013	0.0947	0.0872	0.0799	0.0748	0.0688	0.0641	0.0600	0.0555
b/a	0.2037	0.1936	0.1821	0.1689	0.1558	0.1467	0.1358	0.1271	0.1196	0.1114
	0.2831	0.2704	0.2558	0.2387	0.2219	0.2103	0.1962	0.1851	0.1754	0.1642
	0.3273	0.3133	0.2963	0.2760	0.2557	0.2421	0.2251	0.2122	0.2010	0.1877
	0.3970	0.3885	0.3729	0.3492	0.3232	0.3055	0.2828	0.2651	0.2507	0.2323
	0.4301	0.4319	0.4294	0.4141	0.3886	0.3673	0.3388	0.3150	0.2964	0.2717

Figure 6.28a: F1B: e=2a & d=2.5a

	c/a									
	0.0013	0.0013	0.0013	0.0013	0.0013	0.0013	0.0013	0.0004	0.0012	0.0012
	0.0271	0.0258	0.0242	0.0224	0.0205	0.0190	0.0174	0.0160	0.0148	0.0135
	0.1082	0.1046	0.1001	0.0948	0.0895	0.0852	0.0803	0.0762	0.0724	0.0684
b/a	0.2055	0.1992	0.1916	0.1824	0.1729	0.1655	0.1568	0.1494	0.1426	0.1352
	0.2851	0.2770	0.2670	0.2552	0.2430	0.2334	0.2223	0.2127	0.2041	0.1946
	0.3288	0.3192	0.3074	0.2931	0.2784	0.2671	0.2538	0.2425	0.2324	0.2211
	0.3946	0.3848	0.3714	0.3539	0.3353	0.3213	0.3042	0.2899	0.2774	0.2628
	0.4289	0.4245	0.4148	0.3980	0.3775	0.3615	0.3408	0.3233	0.3083	0.2899

Figure I.17a: F1B: e=2a & d=3a

	c/a									
	0.0013	−0.0004	0.0005	0.0013	0.0013	0.0004	0.0012	0.0012	0.0012	0.0012
	0.0273	0.0265	0.0254	0.0240	0.0226	0.0215	0.0201	0.0190	0.0179	0.0168
	0.1087	0.1063	0.1032	0.0994	0.0954	0.0920	0.0881	0.0846	0.0813	0.0779
b/a	0.2065	0.2023	0.1970	0.1905	0.1835	0.1775	0.1707	0.1645	0.1588	0.1525
	0.2864	0.2809	0.2740	0.2655	0.2564	0.2487	0.2399	0.2319	0.2246	0.2165
	0.3302	0.3236	0.3152	0.3050	0.2940	0.2849	0.2744	0.2649	0.2562	0.2466
	0.3949	0.3871	0.3768	0.3639	0.3499	0.3386	0.3251	0.3133	0.3025	0.2904
	0.4271	0.4205	0.4106	0.3967	0.3808	0.3680	0.3521	0.3381	0.3255	0.3109

Figure 6.29a: F1B: e=2a & d=3.5a

	c/a									
	0.0013	0.0005	0.0013	0.0013	0.0013	0.0004	0.0012	0.0012	0.0012	0.0012
	0.0274	0.0268	0.0260	0.0251	0.0240	0.0231	0.0220	0.0210	0.0201	0.0192
	0.1090	0.1074	0.1051	0.1023	0.0993	0.0965	0.0934	0.0905	0.0878	0.0848
b/a	0.2070	0.2041	0.2003	0.1955	0.1901	0.1854	0.1800	0.1749	0.1701	0.1648
	0.2871	0.2833	0.2782	0.2719	0.2650	0.2589	0.2518	0.2453	0.2390	0.2322
	0.3310	0.3264	0.3203	0.3127	0.3044	0.2971	0.2886	0.2808	0.2734	0.2652
	0.3957	0.3898	0.3821	0.3724	0.3617	0.3525	0.3418	0.3320	0.3228	0.3125
	0.4269	0.4209	0.4126	0.4015	0.3891	0.3786	0.3659	0.3545	0.3438	0.3317

Figure I.18a: F1B: e=2a & d=4a

	c/a									
	0.0013	0.0013	0.0013	0.0013	0.0013	0.0013	0.0012	0.0012	0.0012	0.0012
	0.0275	0.0271	0.0265	0.0257	0.0249	0.0242	0.0233	0.0225	0.0217	0.0209
	0.1092	0.1080	0.1063	0.1042	0.1018	0.0996	0.0971	0.0947	0.0923	0.0898
b/a	0.2073	0.2053	0.2024	0.1987	0.1946	0.1908	0.1864	0.1822	0.1782	0.1737
	0.2875	0.2847	0.2810	0.2762	0.2708	0.2659	0.2602	0.2547	0.2494	0.2436
	0.3315	0.3282	0.3236	0.3178	0.3114	0.3055	0.2986	0.2921	0.2858	0.2789
	0.3963	0.3919	0.3861	0.3786	0.3703	0.3629	0.3542	0.3460	0.3382	0.3295
	0.4273	0.4224	0.4157	0.4070	0.3973	0.3886	0.3784	0.3688	0.3598	0.3496

Figure 6.26a: F1B: e=2.5a & d=0.5a

	c/a									
b/a	0.0320	0.0122	0.0053	0.0012	0.0007	0.0002	0.0003	−0.0002	0.0008	0.0009
	0.1245	0.0812	0.0609	0.0341	0.0189	0.0252	0.0152	0.0132	0.0140	0.0066
	0.2220	0.1667	0.1216	0.0757	0.0511	0.0551	0.0396	0.0337	0.0384	0.0237
	0.2903	0.2880	0.2284	0.1481	0.0953	0.1011	0.0740	0.0616	0.0721	0.0425
	0.3393	0.3392	0.3325	0.2616	0.1674	0.1605	0.1210	0.1053	0.1171	0.0670
	0.3633	0.3633	0.3633	0.3521	0.2354	0.1802	0.1287	0.0981	0.1106	0.0708
	0.4073	0.4073	0.4073	0.4073	0.4084	0.3911	0.2856	0.1994	0.1724	0.1141
	0.4312	0.4312	0.4312	0.4312	0.4311	0.4313	0.4327	0.4133	0.3034	0.2069

Figure I.15a: F1B: e=2.5a & d=1a

	c/a									
b/a	0.0426	0.0311	0.0210	0.0120	0.0066	0.0044	0.0024	0.0011	0.0007	0.0005
	0.1367	0.1163	0.0981	0.0790	0.0621	0.0554	0.0441	0.0374	0.0324	0.0259
	0.2078	0.1791	0.1543	0.1281	0.1052	0.0978	0.0822	0.0732	0.0663	0.0561
	0.2824	0.2506	0.2176	0.1817	0.1507	0.1419	0.1213	0.1100	0.1024	0.0858
	0.3416	0.3257	0.2888	0.2417	0.2006	0.1871	0.1610	0.1461	0.1383	0.1163
	0.3638	0.3649	0.3431	0.2893	0.2352	0.2121	0.1787	0.1586	0.1499	0.1234
	0.4072	0.4072	0.4077	0.4046	0.3722	0.3252	0.2673	0.2286	0.2101	0.1710
	0.4312	0.4311	0.4311	0.4311	0.4308	0.4230	0.3919	0.3379	0.2898	0.2345

Figure 6.27a: F1B: e=2.5a & d=1.5a

	c/a									
b/a	0.0459	0.0398	0.0332	0.0257	0.0196	0.0159	0.0118	0.0091	0.0071	0.0052
	0.1430	0.1324	0.1210	0.1083	0.0963	0.0884	0.0787	0.0714	0.0650	0.0580
	0.2151	0.2001	0.1842	0.1669	0.1506	0.1404	0.1276	0.1180	0.1098	0.1001
	0.2812	0.2618	0.2414	0.2190	0.1980	0.1858	0.1697	0.1580	0.1481	0.1360
	0.3318	0.3112	0.2875	0.2602	0.2346	0.2205	0.2011	0.1875	0.1764	0.1617
	0.3604	0.3435	0.3186	0.2866	0.2558	0.2389	0.2156	0.1994	0.1871	0.1692
	0.4082	0.4103	0.4030	0.3746	0.3359	0.3095	0.2763	0.2519	0.2354	0.2099
	0.4311	0.4315	0.4332	0.4336	0.4214	0.3952	0.3533	0.3169	0.2915	0.2558

Figure I.16a: F1B: e=2.5a & d=2a

	c/a									
b/a	0.0472	0.0437	0.0394	0.0346	0.0296	0.0261	0.0222	0.0189	0.0164	0.0139
	0.1454	0.1393	0.1320	0.1235	0.1149	0.1083	0.1007	0.0944	0.0887	0.0825
	0.2186	0.2100	0.1998	0.1882	0.1764	0.1677	0.1574	0.1489	0.1412	0.1328
	0.2851	0.2737	0.2605	0.2454	0.2303	0.2194	0.2065	0.1960	0.1866	0.1761
	0.3334	0.3199	0.3041	0.2859	0.2678	0.2552	0.2399	0.2276	0.2169	0.2046
	0.3576	0.3431	0.3254	0.3044	0.2833	0.2690	0.2514	0.2375	0.2255	0.2114
	0.4064	0.3980	0.3822	0.3583	0.3321	0.3142	0.2913	0.2734	0.2588	0.2402
	0.4321	0.4340	0.4316	0.4164	0.3909	0.3696	0.3411	0.3173	0.2986	0.2738

Figure 6.28a: F1B: e=2.5a & d=2.5a

	c/a									
b/a	0.0478	0.0456	0.0428	0.0394	0.0359	0.0331	0.0298	0.0270	0.0246	0.0220
	0.1464	0.1426	0.1377	0.1318	0.1256	0.1204	0.1145	0.1092	0.1044	0.0991
	0.2202	0.2148	0.2080	0.1998	0.1913	0.1843	0.1762	0.1690	0.1624	0.1553
	0.2872	0.2800	0.2712	0.2607	0.2497	0.2408	0.2306	0.2217	0.2135	0.2045
	0.3356	0.3269	0.3162	0.3035	0.2903	0.2800	0.2678	0.2574	0.2479	0.2374
	0.3591	0.3492	0.3369	0.3221	0.3069	0.2951	0.2812	0.2694	0.2588	0.2468
	0.4039	0.3940	0.3805	0.3629	0.3441	0.3300	0.3127	0.2983	0.2856	0.2708
	0.4310	0.4266	0.4169	0.4001	0.3796	0.3636	0.3429	0.3254	0.3103	0.2919

Figure I.17a: F1B: e=2.5a & d=3a

	c/a									
b/a	0.0481	0.0467	0.0447	0.0423	0.0397	0.0375	0.0350	0.0327	0.0305	0.0283
	0.1470	0.1444	0.1410	0.1367	0.1321	0.1280	0.1233	0.1190	0.1150	0.1106
	0.2210	0.2174	0.2126	0.2067	0.2003	0.1947	0.1883	0.1824	0.1769	0.1708
	0.2883	0.2835	0.2773	0.2697	0.2615	0.2545	0.2463	0.2389	0.2319	0.2243
	0.3369	0.3311	0.3236	0.3144	0.3046	0.2963	0.2866	0.2779	0.2698	0.2609
	0.3605	0.3537	0.3450	0.3344	0.3230	0.3135	0.3025	0.2926	0.2834	0.2733
	0.4042	0.3963	0.3860	0.3729	0.3588	0.3474	0.3338	0.3219	0.3110	0.2987
	0.4292	0.4226	0.4127	0.3987	0.3828	0.3700	0.3541	0.3401	0.3275	0.3129

Figure 6.29a: F1B: e=2.5a & d=3.5a

	c/a									
b/a	0.0483	0.0473	0.0459	0.0441	0.0422	0.0405	0.0385	0.0366	0.0348	0.0329
	0.1473	0.1455	0.1430	0.1398	0.1362	0.1330	0.1293	0.1258	0.1224	0.1187
	0.2215	0.2189	0.2154	0.2110	0.2061	0.2016	0.1965	0.1916	0.1870	0.1818
	0.2889	0.2855	0.2810	0.2754	0.2691	0.2634	0.2569	0.2508	0.2449	0.2384
	0.3377	0.3336	0.3281	0.3213	0.3138	0.3071	0.2994	0.2922	0.2853	0.2777
	0.3613	0.3566	0.3502	0.3423	0.3337	0.3260	0.3172	0.3090	0.3012	0.2926
	0.4050	0.3991	0.3913	0.3815	0.3707	0.3614	0.3506	0.3406	0.3313	0.3210
	0.4290	0.4230	0.4146	0.4035	0.3911	0.3806	0.3679	0.3564	0.3458	0.3336

Figure I.18a: F1B: e=2.5a & d=4a

	c/a									
b/a	0.0484	0.0477	0.0466	0.0453	0.0438	0.0424	0.0409	0.0394	0.0379	0.0363
	0.1475	0.1462	0.1443	0.1418	0.1391	0.1365	0.1335	0.1306	0.1277	0.1246
	0.2217	0.2198	0.2172	0.2138	0.2100	0.2064	0.2022	0.1981	0.1942	0.1899
	0.2893	0.2868	0.2834	0.2790	0.2741	0.2696	0.2643	0.2592	0.2542	0.2487
	0.3381	0.3351	0.3310	0.3258	0.3200	0.3146	0.3083	0.3023	0.2965	0.2901
	0.3619	0.3584	0.3537	0.3476	0.3409	0.3375	0.3275	0.3207	0.3141	0.3068
	0.4056	0.4012	0.3953	0.3878	0.3794	0.3718	0.3630	0.3548	0.3469	0.3381
	0.4293	0.4245	0.4178	0.4091	0.3993	0.3906	0.3804	0.3708	0.3617	0.3515

Figure 6.26a: F1B: e=3a & d=0.5a

	c/a									
b/a	0.1519	0.1158	0.0930	0.0689	0.0480	0.0472	0.0333	0.0279	0.0226	0.0126
	0.2141	0.1563	0.1273	0.0930	0.0632	0.0725	0.0524	0.0471	0.0446	0.0247
	0.2903	0.2249	0.1694	0.1176	0.0793	0.0898	0.0659	0.0570	0.0624	0.0358
	0.3357	0.3335	0.2696	0.1821	0.1231	0.1289	0.0980	0.0862	0.0951	0.0556
	0.3684	0.3683	0.3615	0.2889	0.1902	0.1808	0.1396	0.1224	0.1336	0.0827
	0.3819	0.3820	0.3819	0.3707	0.2509	0.1948	0.1406	0.1099	0.1201	0.0761
	0.4143	0.4143	0.4143	0.4143	0.4154	0.3984	0.2932	0.2063	0.1782	0.1180
	0.4334	0.4334	0.4335	0.4335	0.4334	0.4336	0.4350	0.4159	0.3059	0.2105

Figure I.15a: F1B: e=3a & d=1a

	c/a									
b/a	0.1727	0.1561	0.1399	0.1229	0.1073	0.0985	0.0868	0.0786	0.0714	0.0631
	0.2324	0.2074	0.1850	0.1621	0.1416	0.1319	0.1171	0.1074	0.0990	0.0884
	0.2725	0.2395	0.2111	0.1819	0.1564	0.1471	0.1295	0.1188	0.1102	0.0968
	0.3274	0.2930	0.2571	0.2187	0.1857	0.1754	0.1534	0.1409	0.1322	0.1145
	0.3710	0.3551	0.3164	0.2673	0.2245	0.2098	0.1826	0.1668	0.1581	0.1354
	0.3825	0.3839	0.3625	0.3075	0.2521	0.2279	0.1936	0.1728	0.1629	0.1353
	0.4143	0.4143	0.4148	0.4119	0.3801	0.3328	0.2744	0.2352	0.2164	0.1770
	0.4334	0.4334	0.4334	0.4334	0.4331	0.4254	0.3946	0.3409	0.2926	0.2273

Figure 6.27a: F1B: e=3a & d=1.5a

	c/a									
b/a	0.1775	0.1687	0.1588	0.1476	0.1365	0.1284	0.119	0.1113	0.1045	0.09715
	0.2404	0.2277	0.2139	0.1986	0.1838	0.1736	0.1614	0.1518	0.1433	0.1338
	0.2814	0.2643	0.2463	0.227	0.2088	0.1971	0.1826	0.1714	0.1617	0.1506
	0.3259	0.3052	0.2833	0.2594	0.2371	0.2237	0.2064	0.1937	0.1829	0.1698
	0.3606	0.3392	0.3145	0.2862	0.2597	0.2448	0.2246	0.2103	0.1986	0.1832
	0.3791	0.362	0.3366	0.3039	0.2724	0.2549	0.2311	0.2144	0.2016	0.1833
	0.4153	0.4175	0.4105	0.382	0.3431	0.3165	0.283	0.2584	0.2416	0.2159
	0.4334	0.4338	0.4355	0.436	0.424	0.3979	0.356	0.3204	0.294	0.2583

Figure I.16a: F1B: e=3a & d=2a

	c/a									
b/a	0.1793	0.174	0.1676	0.1599	0.152	0.1455	0.1382	0.1317	0.1258	0.1195
	0.2433	0.2359	0.227	0.2166	0.206	0.1976	0.1879	0.1796	0.172	0.1638
	0.2854	0.2756	0.2641	0.2509	0.2377	0.2277	0.216	0.2062	0.1973	0.1876
	0.3301	0.3179	0.3039	0.2878	0.2718	0.26	0.2461	0.2347	0.2245	0.2131
	0.3623	0.3482	0.3319	0.313	0.2943	0.2811	0.2652	0.2523	0.2411	0.2282
	0.3761	0.3613	0.3433	0.3218	0.3003	0.2856	0.2676	0.2533	0.241	0.2265
	0.4135	0.4051	0.3893	0.3653	0.3389	0.3209	0.2978	0.2797	0.265	0.2462
	0.4344	0.4363	0.434	0.4189	0.3934	0.3721	0.3435	0.3197	0.301	0.2762

Figure 6.28a: F1B: e=3a & d=2.5a

	c/a									
b/a	0.1801	0.1767	0.1723	0.1668	0.161	0.1559	0.1501	0.1449	0.1399	0.1346
	0.2445	0.2398	0.2338	0.2264	0.2186	0.212	0.2043	0.1974	0.191	0.184
	0.2872	0.281	0.2733	0.264	0.2542	0.2461	0.2368	0.2286	0.2209	0.2126
	0.3323	0.3247	0.3153	0.3041	0.2923	0.2828	0.2718	0.2621	0.2532	0.2434
	0.3646	0.3556	0.3445	0.3313	0.3177	0.3068	0.2942	0.2833	0.2733	0.2623
	0.3777	0.3675	0.355	0.34	0.3244	0.3123	0.2981	0.286	0.275	0.2628
	0.4109	0.401	0.3875	0.3698	0.3509	0.3366	0.3192	0.3047	0.2919	0.2769
	0.4333	0.429	0.4193	0.4025	0.382	0.3659	0.3452	0.3277	0.3126	0.2941

Figure I.17a: F1B: e=3a & d=3a

	c/a									
b/a	0.1806	0.1782	0.175	0.171	0.1666	0.1626	0.158	0.1537	0.1496	0.1451
	0.2452	0.242	0.2377	0.2323	0.2264	0.2211	0.215	0.2093	0.2039	0.198
	0.2881	0.2839	0.2785	0.2717	0.2643	0.2578	0.2503	0.2435	0.237	0.2299
	0.3335	0.3284	0.3218	0.3136	0.3048	0.2972	0.2884	0.2804	0.2728	0.2645
	0.3659	0.3599	0.3521	0.3426	0.3324	0.3237	0.3137	0.3046	0.296	0.2867
	0.3791	0.3722	0.3633	0.3524	0.3408	0.3311	0.3198	0.3096	0.3002	0.2899
	0.4112	0.4033	0.3929	0.3798	0.3656	0.3541	0.3404	0.3284	0.3174	0.305
	0.4314	0.4249	0.415	0.401	0.3851	0.3723	0.3563	0.3423	0.3297	0.315

Figure 6.29a: F1B: e=3a & d=3.5a

	c/a									
b/a	0.1808	0.1791	0.1767	0.1737	0.1703	0.1671	0.1634	0.1598	0.1564	0.1526
	0.2456	0.2432	0.24	0.236	0.2314	0.2272	0.2223	0.2176	0.213	0.208
	0.2886	0.2856	0.2816	0.2765	0.2708	0.2656	0.2595	0.2538	0.2483	0.2423
	0.3341	0.3305	0.3257	0.3196	0.3128	0.3067	0.2997	0.293	0.2866	0.2796
	0.3667	0.3625	0.3568	0.3497	0.3419	0.3349	0.3269	0.3193	0.3121	0.3042
	0.38	0.3751	0.3686	0.3605	0.3517	0.3438	0.3348	0.3264	0.3184	0.3096
	0.412	0.4061	0.3983	0.3884	0.3775	0.3682	0.3572	0.3472	0.3379	0.3274
	0.4312	0.4252	0.4169	0.4058	0.3934	0.3828	0.3701	0.3586	0.3479	0.3358

Figure I.18a: F1B: e=3a & d=4a

	c/a									
b/a	0.181	0.1797	0.1779	0.1755	0.1728	0.1702	0.1672	0.1642	0.1613	0.1581
	0.2458	0.2441	0.2416	0.2384	0.2348	0.2314	0.2274	0.2235	0.2196	0.2154
	0.2889	0.2867	0.2836	0.2797	0.2752	0.2709	0.266	0.2612	0.2565	0.2513
	0.3345	0.3319	0.3282	0.3235	0.3182	0.3133	0.3075	0.3019	0.2965	0.2906
	0.3672	0.3641	0.3598	0.3544	0.3483	0.3426	0.3361	0.3298	0.3237	0.3169
	0.3805	0.377	0.3721	0.3659	0.359	0.3527	0.3453	0.3383	0.3315	0.324
	0.4126	0.4082	0.4023	0.3947	0.3862	0.3786	0.3698	0.3614	0.3535	0.3446
	0.4316	0.4267	0.42	0.4113	0.4015	0.3929	0.3826	0.373	0.3639	0.3537

Figure 6.26a: F1B: e=3.5a & d=0.5a

	c/a									
b/a	0.2317	0.1879	0.1601	0.1322	0.1081	0.1051	0.0887	0.0812	0.0739	0.0618
	0.2709	0.2041	0.1699	0.1323	0.1002	0.1079	0.0861	0.0796	0.0759	0.0548
	0.3341	0.2634	0.2000	0.1446	0.1034	0.1133	0.0882	0.0784	0.0829	0.0510
	0.3651	0.3631	0.2969	0.2046	0.1430	0.1473	0.1153	0.1026	0.1109	0.0684
	0.3883	0.3882	0.3815	0.3080	0.2061	0.1948	0.1525	0.1346	0.1452	0.0938
	0.3955	0.3955	0.3955	0.3843	0.2627	0.2061	0.1519	0.1181	0.1277	0.0812
	0.4203	0.4203	0.4204	0.4203	0.4214	0.4046	0.2994	0.2121	0.1831	0.1206
	0.4359	0.4360	0.4360	0.4360	0.4359	0.4361	0.4375	0.4186	0.3088	0.2135

Figure I.15a: F1B: e=3.5a & d=1a

	c/a									
b/a	0.2586	0.2393	0.2204	0.2007	0.1824	0.1714	0.1574	0.1471	0.138	0.1276
	0.2924	0.2647	0.2399	0.2147	0.1922	0.1809	0.1645	0.1533	0.1436	0.1316
	0.3142	0.2785	0.2473	0.2159	0.1889	0.1784	0.1596	0.1479	0.1385	0.1242
	0.3567	0.3207	0.2829	0.2429	0.2086	0.1973	0.1744	0.1611	0.1518	0.1335
	0.3911	0.3753	0.3354	0.2849	0.2409	0.2254	0.1975	0.1811	0.1719	0.1487
	0.3961	0.3977	0.3766	0.3208	0.2644	0.2394	0.2045	0.1832	0.1728	0.1449
	0.4203	0.4203	0.4208	0.418	0.3868	0.3393	0.2804	0.2409	0.2217	0.1821
	0.4359	0.4359	0.4359	0.4359	0.4356	0.428	0.3974	0.344	0.2983	0.2397

Figure 6.27a: F1B: e=3.5a & d=1.5a

	c/a									
b/a	0.2644	0.2542	0.2426	0.2295	0.2164	0.2066	0.1953	0.1858	0.1773	0.1681
	0.3016	0.2877	0.2725	0.2557	0.2394	0.2279	0.2144	0.2034	0.1937	0.183
	0.3238	0.3057	0.2865	0.2657	0.2461	0.2331	0.2175	0.2055	0.195	0.183
	0.3549	0.3333	0.3105	0.2857	0.2626	0.2485	0.2305	0.2171	0.2057	0.192
	0.3804	0.3585	0.3331	0.3041	0.2769	0.2614	0.2407	0.2259	0.2138	0.1981
	0.3928	0.3755	0.3496	0.3164	0.2844	0.2665	0.2423	0.2252	0.2121	0.1936
	0.4214	0.4236	0.4168	0.3884	0.3493	0.3224	0.2887	0.2639	0.2469	0.221
	0.4359	0.4363	0.438	0.4386	0.4268	0.4009	0.3589	0.3223	0.2967	0.2609

Figure I.16a: F1B: e=3.5a & d=2a

	c/a									
b/a	0.2664	0.2603	0.2527	0.2437	0.2342	0.2264	0.2174	0.2095	0.2022	0.1942
	0.3048	0.2967	0.2869	0.2755	0.2637	0.2543	0.2435	0.2341	0.2255	0.2162
	0.3281	0.3178	0.3056	0.2916	0.2773	0.2664	0.2537	0.243	0.2332	0.2226
	0.3593	0.3467	0.3321	0.3154	0.2988	0.2865	0.272	0.2601	0.2494	0.2374
	0.3821	0.3677	0.3509	0.3316	0.3124	0.2988	0.2825	0.2693	0.2577	0.2445
	0.3896	0.3746	0.3563	0.3345	0.3127	0.2977	0.2794	0.2648	0.2523	0.2375
	0.4196	0.4112	0.3953	0.3712	0.3447	0.3265	0.3033	0.2851	0.2702	0.2513
	0.4369	0.4389	0.4367	0.4217	0.3961	0.3748	0.3462	0.3222	0.3035	0.2786

Figure 6.28a: F1B: e=3.5a & d=2.5a

	c/a									
b/a	0.2674	0.2633	0.2581	0.2516	0.2445	0.2384	0.2313	0.2247	0.2186	0.2118
	0.3061	0.301	0.2943	0.2862	0.2775	0.27	0.2614	0.2536	0.2463	0.2384
	0.33	0.3235	0.3153	0.3054	0.295	0.2862	0.2762	0.2671	0.2587	0.2496
	0.3616	0.3537	0.3439	0.3323	0.3201	0.3101	0.2987	0.2885	0.2792	0.269
	0.3844	0.3752	0.3639	0.3504	0.3364	0.3253	0.3123	0.3011	0.2909	0.2795
	0.3912	0.3809	0.3681	0.3529	0.3371	0.3248	0.3104	0.298	0.2869	0.2744
	0.417	0.407	0.3934	0.3756	0.3566	0.3422	0.3248	0.3101	0.2972	0.2822
	0.4358	0.4315	0.4219	0.4051	0.3845	0.3685	0.3477	0.3301	0.315	0.2964

Figure I.17a: F1B: e=3.5a & d=3a

	c/a									
b/a	0.2679	0.2651	0.2612	0.2564	0.251	0.2461	0.2404	0.235	0.2298	0.2242
	0.3069	0.3033	0.2985	0.2925	0.2859	0.28	0.2731	0.2667	0.2605	0.2538
	0.331	0.3266	0.3207	0.3135	0.3056	0.2987	0.2906	0.2832	0.276	0.2683
	0.3628	0.3575	0.3506	0.3422	0.3331	0.3251	0.316	0.3075	0.2996	0.2909
	0.3858	0.3796	0.3717	0.3619	0.3515	0.3426	0.3322	0.3229	0.3141	0.3045
	0.3926	0.3856	0.3766	0.3655	0.3537	0.3439	0.3324	0.3221	0.3125	0.3019
	0.4172	0.4093	0.3988	0.3856	0.3714	0.3598	0.346	0.3339	0.3228	0.3103
	0.434	0.4274	0.4175	0.4035	0.3876	0.3747	0.3587	0.3447	0.332	0.3172

Figure 6.29a: F1B: e=3.5a & d=3.5a

	c/a									
b/a	0.2682	0.2661	0.2632	0.2595	0.2553	0.2513	0.2467	0.2423	0.2379	0.2331
	0.3073	0.3047	0.3011	0.2965	0.2914	0.2866	0.2811	0.2757	0.2705	0.2648
	0.3315	0.3283	0.324	0.3186	0.3125	0.3069	0.3004	0.2942	0.2882	0.2816
	0.3634	0.3597	0.3547	0.3484	0.3413	0.335	0.3276	0.3206	0.3139	0.3065
	0.3866	0.3823	0.3765	0.3692	0.3612	0.354	0.3457	0.338	0.3305	0.3224
	0.3935	0.3885	0.382	0.3738	0.3648	0.3568	0.3476	0.339	0.3309	0.3219
	0.418	0.4121	0.4042	0.3943	0.3834	0.374	0.363	0.3529	0.3434	0.3329
	0.4338	0.4277	0.4194	0.4083	0.3958	0.3853	0.3726	0.361	0.3503	0.3381

Figure I.18a: F1B: e=3.5a & d=4a

	c/a									
b/a	0.2684	0.2668	0.2646	0.2616	0.2582	0.255	0.2512	0.2475	0.2438	0.2397
	0.3075	0.3056	0.3028	0.2993	0.2952	0.2913	0.2867	0.2822	0.2779	0.273
	0.3318	0.3295	0.3262	0.3219	0.3171	0.3126	0.3072	0.3021	0.297	0.2914
	0.3639	0.3611	0.3573	0.3524	0.3469	0.3417	0.3357	0.3299	0.3242	0.3179
	0.3871	0.3839	0.3795	0.374	0.3677	0.3619	0.3551	0.3487	0.3424	0.3354
	0.394	0.3904	0.3855	0.3792	0.3722	0.3658	0.3583	0.3511	0.3442	0.3366
	0.4186	0.4142	0.4082	0.4006	0.3921	0.3845	0.3755	0.3671	0.3591	0.3502
	0.4341	0.4292	0.4225	0.4138	0.404	0.3953	0.385	0.3754	0.3662	0.356

Figure 6.26a: F1B: e=4a & d=0.5a

	c/a									
b/a	0.2823	0.2337	0.2027	0.1725	0.1466	0.1421	0.1244	0.1158	0.1075	0.09428
	0.3079	0.2352	0.1975	0.1579	0.1242	0.1309	0.1082	0.1009	0.09658	0.07474
	0.3635	0.2898	0.221	0.1629	0.1202	0.1292	0.1033	0.09286	0.09693	0.06309
	0.3857	0.3839	0.3161	0.2205	0.1569	0.1602	0.1274	0.1142	0.122	0.07906
	0.403	0.4029	0.3962	0.3221	0.2177	0.2051	0.162	0.1436	0.1537	0.102
	0.406	0.4061	0.406	0.3949	0.2739	0.2147	0.1591	0.1213	0.1345	0.08555
	0.4257	0.4257	0.4257	0.4257	0.4268	0.4101	0.3048	0.217	0.1873	0.1251
	0.4386	0.4386	0.4386	0.4386	0.4385	0.4387	0.4401	0.4213	0.3117	0.2164

Figure I.15a: F1B: e=4a & d=1a

	c/a									
b/a	0.3133	0.2923	0.2717	0.2503	0.2306	0.2183	0.203	0.1915	0.1814	0.1698
	0.3315	0.302	0.2755	0.2489	0.2252	0.2128	0.1955	0.1835	0.173	0.1602
	0.3422	0.3048	0.2721	0.2393	0.2108	0.1994	0.1799	0.1677	0.1576	0.1428
	0.3773	0.3402	0.301	0.2598	0.2246	0.2126	0.1892	0.1754	0.1657	0.1469
	0.406	0.3903	0.3495	0.2979	0.2531	0.2369	0.2084	0.1916	0.1821	0.1586
	0.4067	0.4085	0.3876	0.3311	0.2739	0.2483	0.2129	0.1912	0.1805	0.1524
	0.4256	0.4256	0.4261	0.4234	0.3927	0.3448	0.2856	0.2457	0.2263	0.1865
	0.4386	0.4385	0.4385	0.4385	0.4382	0.4306	0.4003	0.3471	0.2981	0.2424

Figure 6.27a: F1B: e=4a & d=1.5a

	c/a									
b/a	0.3196	0.3086	0.296	0.2818	0.2676	0.2568	0.2444	0.234	0.2245	0.2143
	0.3414	0.3267	0.3106	0.2929	0.2757	0.2634	0.2491	0.2374	0.227	0.2155
	0.3523	0.3334	0.3135	0.292	0.2716	0.2581	0.2417	0.2289	0.2177	0.2051
	0.3753	0.3531	0.3296	0.3042	0.2804	0.2658	0.2474	0.2336	0.2218	0.2077
	0.395	0.3727	0.3468	0.3173	0.2896	0.2737	0.2527	0.2375	0.2251	0.2091
	0.4034	0.386	0.3598	0.3261	0.2938	0.2755	0.251	0.2337	0.2204	0.2016
	0.4267	0.4291	0.4224	0.3939	0.3546	0.3276	0.2936	0.2686	0.2515	0.2255
	0.4385	0.4389	0.4407	0.4413	0.4296	0.4038	0.3618	0.3251	0.2993	0.2634

Figure I.16a: F1B: e=4a & d=2a

	c/a									
b/a	0.3218	0.3152	0.307	0.2971	0.2868	0.2782	0.2684	0.2596	0.2514	0.2426
	0.3447	0.3362	0.3259	0.3138	0.3014	0.2914	0.2799	0.2699	0.2607	0.2507
	0.3568	0.3461	0.3335	0.3189	0.3042	0.2928	0.2796	0.2684	0.2582	0.247
	0.3798	0.3669	0.3519	0.3348	0.3178	0.3051	0.2903	0.278	0.2669	0.2547
	0.3967	0.3821	0.365	0.3454	0.3259	0.312	0.2954	0.2819	0.2701	0.2566
	0.4001	0.3849	0.3664	0.3443	0.3223	0.3071	0.2886	0.2738	0.2611	0.2461
	0.4249	0.4166	0.4007	0.3764	0.3498	0.3315	0.3081	0.2898	0.2748	0.2558
	0.4395	0.4416	0.4394	0.4245	0.3989	0.3775	0.3488	0.3248	0.306	0.2811

Figure 6.28a: F1B: e=4a & d=2.5a

	c/a									
b/a	0.3228	0.3185	0.3127	0.3056	0.2979	0.2911	0.2833	0.2761	0.2692	0.2617
	0.3462	0.3407	0.3337	0.3251	0.3159	0.3079	0.2988	0.2905	0.2827	0.2742
	0.3588	0.3521	0.3436	0.3333	0.3225	0.3134	0.3029	0.2935	0.2847	0.2751
	0.3822	0.3741	0.3641	0.3522	0.3397	0.3294	0.3177	0.3072	0.2976	0.2871
	0.3991	0.3897	0.3782	0.3645	0.3503	0.3389	0.3258	0.3143	0.3039	0.2923
	0.4017	0.3913	0.3784	0.363	0.347	0.3345	0.32	0.3074	0.2962	0.2835
	0.4223	0.4123	0.3986	0.3808	0.3616	0.3472	0.3296	0.3149	0.3019	0.2868
	0.4385	0.4342	0.4246	0.4077	0.3872	0.371	0.3503	0.3326	0.3174	0.2988

Figure I.17a: F1B: e=4a & d=3a

	c/a									
b/a	0.3234	0.3203	0.3161	0.3108	0.3049	0.2994	0.2932	0.2872	0.2814	0.2751
	0.347	0.3432	0.3381	0.3318	0.3247	0.3184	0.3111	0.3042	0.2976	0.2904
	0.3598	0.3552	0.3492	0.3417	0.3335	0.3262	0.3179	0.3101	0.3026	0.2945
	0.3834	0.378	0.371	0.3623	0.3529	0.3448	0.3354	0.3267	0.3185	0.3096
	0.4005	0.3942	0.3861	0.3763	0.3656	0.3565	0.346	0.3365	0.3276	0.3177
	0.4031	0.396	0.3869	0.3758	0.3639	0.3538	0.3422	0.3318	0.3221	0.3114
	0.4226	0.4146	0.4041	0.3908	0.3765	0.3648	0.351	0.3388	0.3276	0.3151
	0.4366	0.43	0.4201	0.4061	0.3902	0.3772	0.3612	0.3472	0.3345	0.3197

Figure 6.29a: F1B: e=4a & d=3.5a

	c/a									
b/a	0.3237	0.3214	0.3183	0.3142	0.3095	0.3051	0.3000	0.2950	0.2901	0.2848
	0.3474	0.3446	0.3408	0.3360	0.3305	0.3254	0.3195	0.3138	0.3082	0.3021
	0.3603	0.3571	0.3526	0.3469	0.3406	0.3347	0.3280	0.3215	0.3152	0.3083
	0.3841	0.3803	0.3751	0.3686	0.3614	0.3548	0.3472	0.3401	0.3332	0.3256
	0.4013	0.3969	0.3910	0.3836	0.3755	0.3682	0.3597	0.3518	0.3442	0.3359
	0.4040	0.3990	0.3924	0.3841	0.3750	0.3669	0.3576	0.3489	0.3407	0.3316
	0.4233	0.4174	0.4095	0.3995	0.3885	0.3791	0.3680	0.3579	0.3483	0.3378
	0.4364	0.4303	0.4220	0.4108	0.3984	0.3878	0.3751	0.3635	0.3527	0.3405

Figure I.18a: F1B: e=4a & d=4a

	c/a									
b/a	0.3239	0.3222	0.3197	0.3165	0.3127	0.3091	0.3049	0.3007	0.2966	0.292
	0.3477	0.3456	0.3427	0.3388	0.3345	0.3303	0.3254	0.3206	0.3159	0.3107
	0.3607	0.3582	0.3548	0.3504	0.3454	0.3406	0.3351	0.3296	0.3243	0.3184
	0.3845	0.3817	0.3778	0.3727	0.3671	0.3617	0.3555	0.3495	0.3437	0.3372
	0.4018	0.3986	0.3941	0.3885	0.3821	0.3762	0.3693	0.3627	0.3563	0.3492
	0.4046	0.4009	0.396	0.3896	0.3825	0.376	0.3684	0.3612	0.3542	0.3465
	0.4239	0.4195	0.4135	0.4058	0.3973	0.3896	0.3806	0.3722	0.3641	0.3552
	0.4367	0.4318	0.4251	0.4164	0.4065	0.3978	0.3875	0.3779	0.3687	0.3584

Figure 6.26b: F2B: e=0.5a & d=0.5a

	c/a									
b/a	0.0221	0.0222	0.0223	0.0222	0.0220	0.0224	0.0224	0.0225	0.0223	0.0217
	0.0176	0.0179	0.0194	0.0180	0.0148	0.0194	0.0165	0.0181	0.0174	0.0153
	0.0190	0.0213	0.0247	0.0217	0.0154	0.0235	0.0163	0.0226	0.0245	0.0162
	0.0019	0.0052	0.0085	0.0071	0.0032	0.0067	0.0048	0.0188	0.0229	0.0094
	−0.0111	−0.0113	−0.0094	−0.0090	−0.0110	−0.0109	−0.0049	0.0122	0.0164	0.0015
	−0.0254	−0.0252	−0.0255	−0.0244	−0.0249	−0.0184	0.0015	0.0197	0.0286	0.0118
	−0.0388	−0.0388	−0.0389	−0.0389	−0.0386	−0.0388	−0.0118	0.0143	0.0290	0.0161
	−0.2622	−0.2622	−0.2622	−0.2622	−0.2622	−0.2617	−0.2597	−0.2582	−0.2198	−0.1775

Figure I.15b: F2B: e=0.5a & d=1a

	c/a									
b/a	0.0221	0.0222	0.0223	0.0223	0.0223	0.0223	0.0220	0.0218	0.0217	0.0215
	0.0168	0.0168	0.0169	0.0169	0.0168	0.0168	0.0167	0.0166	0.0164	0.0164
	0.0172	0.0175	0.0177	0.0175	0.0171	0.0177	0.0175	0.0177	0.0175	0.0176
	0.0035	0.0053	0.0068	0.0063	0.0052	0.0083	0.0074	0.0080	0.0080	0.0069
	−0.0088	−0.0051	−0.0036	−0.0029	−0.0034	0.0001	−0.0017	−0.0003	0.0008	−0.0013
	−0.0234	−0.0171	−0.0133	−0.0109	−0.0079	−0.0014	−0.0031	−0.0028	0.0011	−0.0027
	−0.0384	−0.0378	−0.0348	−0.0308	−0.0267	−0.0172	−0.0168	−0.0142	−0.0074	−0.0141
	−0.2622	−0.2622	−0.2622	−0.2621	−0.2621	−0.2590	−0.2482	−0.2305	−0.2074	−0.1962

Figure 6.27b: F2B: e=0.5a & d=1.5a

	c/a									
b/a	0.0221	0.0221	0.0221	0.0220	0.0219	0.0218	0.0217	0.0216	0.0215	0.0215
	0.0167	0.0167	0.0167	0.0167	0.0166	0.0166	0.0165	0.0164	0.0164	0.0164
	0.0168	0.0168	0.0168	0.0168	0.0170	0.0170	0.0171	0.0172	0.0173	0.0174
	0.0024	0.0025	0.0026	0.0022	0.0025	0.0034	0.0036	0.0040	0.0041	0.0045
	−0.0115	−0.0111	−0.0109	−0.0106	−0.0091	−0.0080	−0.0076	−0.0068	−0.0065	−0.0060
	−0.0229	−0.0219	−0.0210	−0.0216	−0.0200	−0.0199	−0.0172	−0.0148	−0.0139	−0.0131
	−0.0368	−0.0339	−0.0335	−0.0369	−0.0405	−0.0372	−0.0373	−0.0348	−0.0317	−0.0328
	−0.2620	−0.2608	−0.2583	−0.2562	−0.2556	−0.2505	−0.2449	−0.2337	−0.2194	−0.2107

Figure I.16b: F2B: e=0.5a & d=2a

	c/a									
b/a	0.0221	0.0220	0.0220	0.0219	0.0218	0.0217	0.0217	0.0216	0.0216	0.0215
	0.0167	0.0167	0.0167	0.0166	0.0166	0.0166	0.0165	0.0165	0.0164	0.0164
	0.0168	0.0168	0.0169	0.0170	0.0170	0.0171	0.0172	0.0173	0.0173	0.0174
	0.0023	0.0023	0.0024	0.0020	0.0023	0.0026	0.0033	0.0034	0.0036	0.0039
	−0.0121	−0.0120	−0.0118	−0.0104	−0.0098	−0.0092	−0.0086	−0.0083	−0.0080	−0.0076
	−0.0247	−0.0248	−0.0246	−0.0237	−0.0230	−0.0219	−0.0208	−0.0211	−0.0193	−0.0182
	−0.0385	−0.0406	−0.0427	−0.0441	−0.0466	−0.0452	−0.0451	−0.0437	−0.0419	−0.0416
	−0.2612	−0.2598	−0.2597	−0.2612	−0.2607	−0.2545	−0.2481	−0.2396	−0.2306	−0.2226

Figure 6.28b: F2B: e=0.5a & d=2.5a

	c/a									
b/a	0.0221	0.0220	0.0220	0.0219	0.0218	0.0218	0.0217	0.0217	0.0217	0.0217
	0.0167	0.0167	0.0167	0.0166	0.0166	0.0166	0.0166	0.0165	0.0165	0.0165
	0.0168	0.0168	0.0169	0.0170	0.0170	0.0171	0.0172	0.0172	0.0173	0.0174
	0.0023	0.0024	0.0025	0.0020	0.0023	0.0025	0.0032	0.0033	0.0034	0.0036
	−0.0120	−0.0119	−0.0116	−0.0103	−0.0098	−0.0095	−0.0090	−0.0085	−0.0084	−0.0080
	−0.0247	−0.0246	−0.0242	−0.0234	−0.0226	−0.0219	−0.0222	−0.0203	−0.0209	−0.0203
	−0.0396	−0.0410	−0.0422	−0.0434	−0.0436	−0.0437	−0.0435	−0.0429	−0.0421	−0.0409
	−0.2623	−0.2630	−0.2633	−0.2625	−0.2597	−0.2548	−0.2493	−0.2428	−0.2364	−0.2295

Figure I.17b: F2B: e=0.5a & d=3a

	c/a									
b/a	0.0221	0.0220	0.0220	0.0220	0.0219	0.0219	0.0218	0.0218	0.0218	0.0218
	0.0167	0.0167	0.0167	0.0167	0.0166	0.0166	0.0166	0.0166	0.0166	0.0166
	0.0168	0.0168	0.0169	0.0169	0.0170	0.0170	0.0171	0.0171	0.0172	0.0173
	0.0023	0.0024	0.0025	0.0020	0.0021	0.0023	0.0025	0.0032	0.0032	0.0034
	−0.0120	−0.0119	−0.0116	−0.0104	−0.0100	−0.0097	−0.0091	−0.0088	−0.0085	−0.0083
	−0.0246	−0.0244	−0.0240	−0.0232	−0.0226	−0.0220	−0.0219	−0.0207	−0.0201	−0.0198
	−0.0389	−0.0401	−0.0406	−0.0406	−0.0409	−0.0407	−0.0405	−0.0406	−0.0401	−0.0396
	−0.2624	−0.2624	−0.2616	−0.2597	−0.2565	−0.2527	−0.2480	−0.2430	−0.2383	−0.2323

Figure 6.29b: F2B: e=0.5a & d=3.5a

	c/a									
b/a	0.0221	0.0220	0.0220	0.0220	0.0220	0.0219	0.0219	0.0219	0.0219	0.0219
	0.0167	0.0167	0.0167	0.0167	0.0167	0.0167	0.0166	0.0166	0.0166	0.0166
	0.0168	0.0168	0.0169	0.0169	0.0169	0.0170	0.0170	0.0171	0.0171	0.0172
	0.0023	0.0024	0.0024	0.0025	0.0020	0.0021	0.0023	0.0024	0.0031	0.0032
	−0.0120	−0.0119	−0.0117	−0.0105	−0.0103	−0.0100	−0.0096	−0.0094	−0.0089	−0.0086
	−0.0246	−0.0244	−0.0241	−0.0236	−0.0228	−0.0223	−0.0226	−0.0218	−0.0217	−0.0200
	−0.0387	−0.0394	−0.0392	−0.0393	−0.0393	−0.0392	−0.0391	−0.0387	−0.0383	−0.0383
	−0.2621	−0.2615	−0.2601	−0.2578	−0.2548	−0.2516	−0.2476	−0.2435	−0.2394	−0.2347

Figure I.18b: F2B: e=0.5a & d=4a

	c/a									
b/a	0.0221	0.0221	0.0220	0.0220	0.0220	0.0220	0.0220	0.0220	0.0220	0.0220
	0.0167	0.0167	0.0167	0.0167	0.0167	0.0167	0.0167	0.0167	0.0167	0.0167
	0.0168	0.0168	0.0168	0.0169	0.0169	0.0169	0.0170	0.0170	0.0171	0.0171
	0.0023	0.0023	0.0024	0.0025	0.0019	0.0020	0.0021	0.0022	0.0023	0.0025
	−0.0120	−0.0119	−0.0118	−0.0116	−0.0104	−0.0102	−0.0100	−0.0097	−0.0096	−0.0090
	−0.0246	−0.0244	−0.0241	−0.0238	−0.0233	−0.0226	−0.0230	−0.0225	−0.0218	−0.0217
	−0.0386	−0.0392	−0.0387	−0.0387	−0.0386	−0.0384	−0.0382	−0.0379	−0.0376	−0.0372
	−0.2619	−0.2610	−0.2595	−0.2574	−0.2546	−0.2518	−0.2484	−0.2449	−0.2414	−0.2374

Figure 6.26b: F2B: e=1a & d=0.5a

	c/a									
	0.0152	0.0147	0.0145	0.0148	0.0153	0.0147	0.0148	0.0146	0.0147	0.0149
	0.0140	0.0143	0.0145	0.0137	0.0115	0.0143	0.0124	0.0125	0.0125	0.0105
	0.0130	0.0193	0.0194	0.0184	0.0167	0.0238	0.0232	0.0199	0.0238	0.0155
b/a	0.0043	0.0099	0.0160	0.0201	0.0276	0.0356	0.0319	0.0289	0.0341	0.0260
	0.0065	0.0087	0.0146	0.0279	0.0432	0.0557	0.0516	0.0478	0.0556	0.0373
	−0.0123	−0.0092	−0.0079	−0.0013	0.0155	0.0398	0.0478	0.0501	0.0575	0.0466
	−0.1783	−0.1782	−0.1782	−0.1782	−0.1772	−0.1772	−0.1503	−0.1137	−0.0770	−0.0690
	−0.2704	−0.2704	−0.2704	−0.2704	−0.2704	−0.2700	−0.2679	−0.2664	−0.2254	−0.1845

Figure I.15b: F2B: e=1a & d=1a

	c/a									
	0.0158	0.0159	0.0159	0.0157	0.0154	0.0153	0.0152	0.0150	0.0150	0.0149
	0.0124	0.0125	0.0125	0.0123	0.0121	0.0121	0.0119	0.0118	0.0117	0.0116
	0.0150	0.0154	0.0158	0.0154	0.0147	0.0154	0.0145	0.0128	0.0128	0.0124
b/a	0.0081	0.0107	0.0118	0.0111	0.0089	0.0116	0.0099	0.0102	0.0102	0.0083
	0.0111	0.0161	0.0189	0.0185	0.0161	0.0210	0.0185	0.0188	0.0195	0.0150
	−0.0068	−0.0006	0.0027	0.0036	0.0068	0.0147	0.0154	0.0179	0.0218	0.0181
	−0.1782	−0.1827	−0.1766	−0.1749	−0.1741	−0.1597	−0.1445	−0.1279	−0.1102	−0.1030
	−0.2704	−0.2704	−0.2704	−0.2703	−0.2703	−0.2672	−0.2563	−0.2383	−0.2149	−0.2033

Figure 6.27b: F2B: e=1a & d=1.5a

	c/a									
	0.0158	0.0157	0.0156	0.0154	0.0153	0.0152	0.0151	0.0150	0.0149	0.0149
	0.0123	0.0123	0.0122	0.0120	0.0119	0.0118	0.0117	0.0117	0.0116	0.0116
	0.0138	0.0137	0.0136	0.0134	0.0128	0.0128	0.0127	0.0127	0.0113	0.0114
b/a	0.0056	0.0053	0.0051	0.0046	0.0042	0.0045	0.0043	0.0043	0.0043	0.0041
	0.0071	0.0065	0.0062	0.0056	0.0053	0.0059	0.0057	0.0057	0.0057	0.0054
	−0.0083	−0.0122	−0.0123	−0.0121	−0.0094	−0.0021	−0.0051	−0.0039	−0.0027	−0.0022
	−0.1771	−0.1756	−0.1760	−0.1769	−0.1729	−0.1617	−0.1574	−0.1375	−0.1326	−0.1260
	−0.2702	−0.2690	−0.2665	−0.2643	−0.2638	−0.2586	−0.2529	−0.2414	−0.2269	−0.2178

Figure I.16b: F2B: e=1a & d=2a

	c/a									
	0.0158	0.0157	0.0156	0.0155	0.0153	0.0153	0.0152	0.0151	0.0151	0.0150
	0.0123	0.0122	0.0122	0.0121	0.0120	0.0119	0.0118	0.0118	0.0118	0.0117
	0.0138	0.0137	0.0136	0.0134	0.0129	0.0129	0.0128	0.0128	0.0114	0.0114
b/a	0.0054	0.0052	0.0050	0.0048	0.0045	0.0045	0.0044	0.0044	0.0043	0.0043
	0.0068	0.0064	0.0061	0.0057	0.0055	0.0054	0.0053	0.0052	0.0051	0.0050
	−0.0119	−0.0123	−0.0123	−0.0118	−0.0111	−0.0100	−0.0066	−0.0059	−0.0053	−0.0047
	−0.1786	−0.1795	−0.1791	−0.1765	−0.1717	−0.1650	−0.1582	−0.1520	−0.1460	−0.1391
	−0.2694	−0.2680	−0.2679	−0.2694	−0.2689	−0.2625	−0.2560	−0.2472	−0.2380	−0.2297

Figure 6.28b: F2B: e=1a & d=2.5a

	c/a									
	0.0158	0.0157	0.0156	0.0155	0.0155	0.0154	0.0154	0.0153	0.0153	0.0152
	0.0123	0.0123	0.0122	0.0121	0.0121	0.0120	0.0120	0.0119	0.0119	0.0119
	0.0138	0.0137	0.0137	0.0136	0.0135	0.0134	0.0134	0.0133	0.0115	0.0116
b/a	0.0054	0.0053	0.0052	0.0050	0.0049	0.0049	0.0048	0.0047	0.0047	0.0047
	0.0069	0.0067	0.0065	0.0063	0.0060	0.0059	0.0058	0.0057	0.0056	0.0055
	−0.0115	−0.0115	−0.0112	−0.0108	−0.0076	−0.0071	−0.0066	−0.0020	−0.0057	−0.0052
	−0.1784	−0.1780	−0.1764	−0.1734	−0.1691	−0.1647	−0.1593	−0.1544	−0.1496	−0.1443
	−0.2705	−0.2713	−0.2715	−0.2707	−0.2679	−0.2628	−0.2571	−0.2504	−0.2438	−0.2366

Figure I.17b: F2B: e=1a & d=3a

	c/a									
	0.0158	0.0157	0.0157	0.0156	0.0156	0.0155	0.0155	0.0154	0.0154	0.0154
	0.0123	0.0123	0.0122	0.0122	0.0122	0.0121	0.0121	0.0121	0.0120	0.0120
	0.0138	0.0138	0.0137	0.0137	0.0136	0.0136	0.0135	0.0135	0.0116	0.0116
b/a	0.0055	0.0054	0.0053	0.0052	0.0051	0.0051	0.0051	0.0050	0.0050	0.0050
	0.0069	0.0068	0.0067	0.0066	0.0065	0.0064	0.0062	0.0060	0.0059	0.0058
	−0.0085	−0.0084	−0.0082	−0.0079	−0.0076	−0.0072	−0.0068	−0.0064	−0.0060	−0.0056
	−0.1780	−0.1769	−0.1750	−0.1722	−0.1686	−0.1652	−0.1610	−0.1571	−0.1531	−0.1487
	−0.2706	−0.2707	−0.2698	−0.2678	−0.2646	−0.2606	−0.2558	−0.2505	−0.2454	−0.2395

Figure 6.29b: F2B: e=1a & d=3.5a

	c/a									
	0.0158	0.0157	0.0157	0.0157	0.0156	0.0156	0.0156	0.0155	0.0155	0.0155
	0.0123	0.0123	0.0123	0.0122	0.0122	0.0122	0.0122	0.0121	0.0121	0.0121
	0.0138	0.0138	0.0138	0.0137	0.0137	0.0137	0.0137	0.0136	0.0116	0.0117
b/a	0.0055	0.0054	0.0054	0.0053	0.0053	0.0052	0.0052	0.0052	0.0052	0.0051
	0.0070	0.0069	0.0068	0.0067	0.0067	0.0066	0.0065	0.0064	0.0063	0.0062
	−0.0085	−0.0084	−0.0082	−0.0080	−0.0077	−0.0074	−0.0071	−0.0068	−0.0064	−0.0061
	−0.1779	−0.1766	−0.1749	−0.1724	−0.1695	−0.1668	−0.1631	−0.1599	−0.1568	−0.1530
	−0.2703	−0.2697	−0.2682	−0.2659	−0.2628	−0.2595	−0.2553	−0.2511	−0.2468	−0.2419

Figure I.18b: F2B: e=1a & d=4a

	c/a									
	0.0158	0.0158	0.0157	0.0157	0.0157	0.0157	0.0156	0.0156	0.0156	0.0156
	0.0123	0.0123	0.0123	0.0123	0.0122	0.0122	0.0122	0.0122	0.0122	0.0122
	0.0138	0.0138	0.0138	0.0138	0.0137	0.0137	0.0137	0.0137	0.0116	0.0117
b/a	0.0055	0.0055	0.0054	0.0054	0.0054	0.0054	0.0053	0.0053	0.0053	0.0053
	0.0070	0.0069	0.0069	0.0068	0.0068	0.0067	0.0066	0.0065	0.0065	0.0064
	−0.0085	−0.0084	−0.0083	−0.0081	−0.0078	−0.0076	−0.0073	−0.0071	−0.0068	−0.0066
	−0.1779	−0.1768	−0.1752	−0.1731	−0.1707	−0.1683	−0.1655	−0.1627	−0.1599	−0.1568
	−0.2702	−0.2692	−0.2677	−0.2654	−0.2626	−0.2597	−0.2561	−0.2525	−0.2489	−0.2447

Figure 6.26b: F2B: e=1.5a & d=0.5a

	c/a									
b/a	0.0559	0.0539	0.0527	0.0518	0.0507	0.0466	0.0450	0.0425	0.0409	0.0397
	0.0679	0.0661	0.0657	0.0651	0.0627	0.0613	0.0580	0.0553	0.0528	0.0498
	0.0689	0.0721	0.0761	0.0794	0.0791	0.0812	0.0778	0.0749	0.0751	0.0679
	0.0173	0.0216	0.0311	0.0446	0.0541	0.0612	0.0630	0.0627	0.0659	0.0602
	−0.0591	−0.0591	−0.0565	−0.0405	−0.0196	0.0075	0.0124	0.0175	0.0323	0.0221
	−0.1266	−0.1269	−0.1267	−0.1263	−0.1115	−0.0756	−0.0512	−0.0367	−0.0196	−0.0192
	−0.2275	−0.2275	−0.2275	−0.2274	−0.2266	−0.2258	−0.1960	−0.1558	−0.1139	−0.1074
	−0.2777	−0.2777	−0.2777	−0.2777	−0.2777	−0.2772	−0.2752	−0.2735	−0.2341	−0.1904

Figure I.15b: F2B: e=1.5a & d=1a

	c/a									
b/a	0.0585	0.0585	0.0579	0.0566	0.0550	0.0532	0.0514	0.0496	0.0482	0.0464
	0.0656	0.0659	0.0657	0.0651	0.0638	0.0621	0.0603	0.0584	0.0567	0.0549
	0.0631	0.0642	0.0658	0.0671	0.0676	0.0670	0.0662	0.0649	0.0635	0.0619
	0.0179	0.0193	0.0240	0.0294	0.0340	0.0376	0.0398	0.0414	0.0418	0.0424
	−0.0575	−0.0579	−0.0525	−0.0434	−0.0336	−0.0233	−0.0166	−0.0109	−0.0066	0.0020
	−0.1257	−0.1244	−0.1247	−0.1193	−0.1060	−0.0888	−0.0766	−0.0658	−0.0563	−0.0509
	−0.2275	−0.2272	−0.2257	−0.2236	−0.2222	−0.2057	−0.1914	−0.1735	−0.1535	−0.1470
	−0.2777	−0.2777	−0.2776	−0.2776	−0.2776	−0.2744	−0.2633	−0.2451	−0.2215	−0.2096

Figure 6.27b: F2B: e=1.5a & d=1.5a

	c/a									
b/a	0.0585	0.0581	0.0573	0.0561	0.0548	0.0535	0.0520	0.0507	0.0496	0.0482
	0.0657	0.0655	0.0651	0.0642	0.0631	0.0619	0.0605	0.0591	0.0578	0.0563
	0.0634	0.0641	0.0648	0.0653	0.0654	0.0649	0.0643	0.0634	0.0625	0.0614
	0.0181	0.0201	0.0228	0.0260	0.0289	0.0306	0.0326	0.0338	0.0345	0.0355
	−0.0589	−0.0571	−0.0530	−0.0471	−0.0409	−0.0360	−0.0308	−0.0266	−0.0233	−0.0196
	−0.1272	−0.1280	−0.1244	−0.1184	−0.1101	−0.1015	−0.0933	−0.0858	−0.0798	−0.0734
	−0.2262	−0.2245	−0.2248	−0.2261	−0.2212	−0.2092	−0.1990	−0.1875	−0.1764	−0.1682
	−0.2775	−0.2763	−0.2737	−0.2715	−0.2709	−0.2656	−0.2599	−0.2483	−0.2335	−0.2242

Figure I.16b: F2B: e=1.5a & d=2a

	c/a									
b/a	0.0584	0.0579	0.0572	0.0562	0.0551	0.0541	0.0529	0.0518	0.0508	0.0497
	0.0656	0.0652	0.0647	0.0638	0.0628	0.0619	0.0607	0.0596	0.0585	0.0573
	0.0632	0.0635	0.0638	0.0639	0.0638	0.0635	0.0630	0.0624	0.0617	0.0610
	0.0182	0.0196	0.0214	0.0235	0.0254	0.0267	0.0282	0.0292	0.0300	0.0308
	−0.0582	−0.0560	−0.0529	−0.0488	−0.0445	−0.0412	−0.0373	−0.0341	−0.0313	−0.0282
	−0.1264	−0.1249	−0.1217	−0.1171	−0.1112	−0.1060	−0.1000	−0.0947	−0.0900	−0.0846
	−0.2278	−0.2288	−0.2281	−0.2251	−0.2197	−0.2122	−0.2044	−0.1963	−0.1889	−0.1812
	−0.2767	−0.2752	−0.2752	−0.2766	−0.2761	−0.2697	−0.2631	−0.2541	−0.2447	−0.2362

Figure 6.28b: F2B: e=1.5a & d=2.5a

	c/a									
b/a	0.0584	0.0580	0.0574	0.0566	0.0557	0.0548	0.0538	0.0529	0.0520	0.0510
	0.0655	0.0652	0.0646	0.0639	0.0631	0.0623	0.0613	0.0603	0.0594	0.0584
	0.0631	0.0632	0.0632	0.0631	0.0629	0.0626	0.0622	0.0617	0.0612	0.0606
	0.0180	0.0189	0.0201	0.0214	0.0228	0.0237	0.0248	0.0257	0.0264	0.0271
	−0.0582	−0.0565	−0.0542	−0.0512	−0.0481	−0.0455	−0.0426	−0.0400	−0.0377	−0.0351
	−0.1260	−0.1242	−0.1215	−0.1176	−0.1130	−0.1098	−0.1053	−0.1011	−0.0973	−0.0930
	−0.2276	−0.2271	−0.2251	−0.2216	−0.2168	−0.2116	−0.2056	−0.1996	−0.1940	−0.1876
	−0.2778	−0.2785	−0.2788	−0.2779	−0.2751	−0.2699	−0.2641	−0.2573	−0.2505	−0.2432

Figure I.17b: F2B: e=1.5a & d=3a

	c/a									
b/a	0.0585	0.0581	0.0576	0.0569	0.0562	0.0555	0.0547	0.0539	0.0531	0.0523
	0.0655	0.0652	0.0648	0.0641	0.0634	0.0627	0.0619	0.0611	0.0603	0.0594
	0.0630	0.0630	0.0629	0.0628	0.0625	0.0622	0.0618	0.0614	0.0610	0.0605
	0.0178	0.0184	0.0192	0.0201	0.0210	0.0218	0.0226	0.0232	0.0238	0.0244
	−0.0584	−0.0571	−0.0554	−0.0533	−0.0509	−0.0489	−0.0466	−0.0445	−0.0425	−0.0404
	−0.1260	−0.1243	−0.1221	−0.1193	−0.1159	−0.1128	−0.1091	−0.1064	−0.1028	−0.0997
	−0.2272	−0.2259	−0.2236	−0.2203	−0.2162	−0.2121	−0.2073	−0.2025	−0.1979	−0.1927
	−0.2779	−0.2779	−0.2771	−0.2750	−0.2717	−0.2677	−0.2628	−0.2574	−0.2522	−0.2461

Figure 6.29b: F2B: e=1.5a & d=3.5a

	c/a									
b/a	0.0585	0.0582	0.0578	0.0573	0.0566	0.0560	0.0553	0.0547	0.0540	0.0533
	0.0656	0.0653	0.0649	0.0644	0.0638	0.0632	0.0625	0.0618	0.0611	0.0603
	0.0630	0.0629	0.0628	0.0626	0.0624	0.0621	0.0617	0.0614	0.0610	0.0605
	0.0177	0.0181	0.0186	0.0193	0.0199	0.0205	0.0211	0.0216	0.0221	0.0226
	−0.0585	−0.0576	−0.0563	−0.0547	−0.0529	−0.0513	−0.0495	−0.0478	−0.0461	−0.0443
	−0.1261	−0.1249	−0.1231	−0.1208	−0.1181	−0.1157	−0.1128	−0.1101	−0.1074	−0.1047
	−0.2270	−0.2256	−0.2235	−0.2206	−0.2171	−0.2138	−0.2097	−0.2058	−0.2020	−0.1976
	−0.2776	−0.2769	−0.2755	−0.2731	−0.2699	−0.2665	−0.2623	−0.2580	−0.2536	−0.2486

Figure I.18b: F2B: e=1.5a & d=4a

	c/a									
b/a	0.0585	0.0583	0.0579	0.0575	0.0570	0.0564	0.0559	0.0553	0.0548	0.0541
	0.0656	0.0653	0.0650	0.0646	0.0641	0.0636	0.0630	0.0624	0.0618	0.0611
	0.0630	0.0629	0.0628	0.0626	0.0623	0.0621	0.0617	0.0614	0.0610	0.0606
	0.0177	0.0179	0.0183	0.0187	0.0192	0.0196	0.0201	0.0205	0.0209	0.0213
	−0.0586	−0.0579	−0.0569	−0.0557	−0.0543	−0.0531	−0.0516	−0.0502	−0.0488	−0.0473
	−0.1262	−0.1254	−0.1237	−0.1220	−0.1198	−0.1178	−0.1156	−0.1133	−0.1111	−0.1085
	−0.2270	−0.2258	−0.2239	−0.2214	−0.2185	−0.2157	−0.2123	−0.2090	−0.2057	−0.2019
	−0.2774	−0.2765	−0.2749	−0.2726	−0.2697	−0.2667	−0.2631	−0.2594	−0.2557	−0.2514

Figure 6.26b: F2B: e=2a & d=0.5a

	c/a									
b/a	0.0955	0.0991	0.1016	0.1048	0.1069	0.1024	0.1020	0.0991	0.0967	0.0957
	0.0412	0.0497	0.0589	0.0676	0.0733	0.0733	0.0752	0.0749	0.0732	0.0738
	−0.0289	−0.0228	−0.0007	0.0149	0.0270	0.0347	0.0400	0.0428	0.0460	0.0461
	−0.0941	−0.0920	−0.0800	−0.0603	−0.0375	−0.0205	−0.0108	−0.0030	0.0058	0.0057
	−0.1504	−0.1501	−0.1468	−0.1273	−0.1069	−0.0669	−0.0566	−0.0455	−0.0247	−0.0371
	−0.1932	−0.1932	−0.1932	−0.1925	−0.1820	−0.1328	−0.1088	−0.0926	−0.0667	−0.0668
	−0.2512	−0.2512	−0.2512	−0.2511	−0.2503	−0.2492	−0.2182	−0.1747	−0.1316	−0.1280
	−0.2842	−0.2842	−0.2842	−0.2842	−0.2842	−0.2837	−0.2816	−0.2799	−0.2399	−0.1956

Figure I.15b: F2B: e=2a & d=1a

	c/a									
b/a	0.0969	0.0993	0.1012	0.1027	0.1035	0.1025	0.1019	0.1005	0.0991	0.0976
	0.0428	0.0486	0.0542	0.0600	0.0647	0.0657	0.0680	0.0687	0.0689	0.0694
	−0.0279	−0.0211	−0.0122	−0.0007	0.0081	0.0119	0.0176	0.0213	0.0238	0.0277
	−0.0954	−0.0932	−0.0843	−0.0728	−0.0606	−0.0514	−0.0425	−0.0356	−0.0306	−0.0245
	−0.1487	−0.1503	−0.1444	−0.1338	−0.1214	−0.1062	−0.0962	−0.0865	−0.0784	−0.0728
	−0.1921	−0.1902	−0.1901	−0.1852	−0.1725	−0.1519	−0.1383	−0.1258	−0.1142	−0.1074
	−0.2512	−0.2508	−0.2494	−0.2470	−0.2447	−0.2278	−0.2127	−0.1939	−0.1730	−0.1663
	−0.2842	−0.2842	−0.2841	−0.2841	−0.2841	−0.2809	−0.2695	−0.2509	−0.2273	−0.2152

Figure 6.27b: F2B: e=2a & d=1.5a

	c/a									
b/a	0.0962	0.0971	0.0979	0.0985	0.0986	0.0981	0.0976	0.0967	0.0957	0.0945
	0.0417	0.0449	0.0484	0.0520	0.0552	0.0567	0.0587	0.0598	0.0605	0.0613
	−0.0279	−0.0233	−0.0168	−0.0116	−0.0052	−0.0006	0.0031	0.0071	0.0107	0.0131
	−0.0934	−0.0897	−0.0843	−0.0774	−0.0703	−0.0647	−0.0582	−0.0529	−0.0484	−0.0430
	−0.1507	−0.1486	−0.1433	−0.1355	−0.1270	−0.1194	−0.1115	−0.1045	−0.0988	−0.0922
	−0.1939	−0.1945	−0.1909	−0.1837	−0.1745	−0.1640	−0.1543	−0.1452	−0.1375	−0.1296
	−0.2499	−0.2480	−0.2482	−0.2487	−0.2442	−0.2317	−0.2210	−0.2088	−0.1971	−0.1881
	−0.2839	−0.2828	−0.2801	−0.2779	−0.2772	−0.2719	−0.2660	−0.2543	−0.2394	−0.2300

Figure I.16b: F2B: e=2a & d=2a

	c/a									
b/a	0.0959	0.0961	0.0963	0.0964	0.0962	0.0957	0.0952	0.0944	0.0936	0.0927
	0.0409	0.0427	0.0448	0.0470	0.0491	0.0504	0.0519	0.0530	0.0537	0.0545
	−0.0286	−0.0257	−0.0223	−0.0171	−0.0139	−0.0109	−0.0064	−0.0043	−0.0007	0.0012
	−0.0933	−0.0903	−0.0864	−0.0816	−0.0766	−0.0726	−0.0680	−0.0640	−0.0604	−0.0562
	−0.1495	−0.1467	−0.1424	−0.1367	−0.1306	−0.1253	−0.1193	−0.1140	−0.1093	−0.1039
	−0.1930	−0.1911	−0.1872	−0.1814	−0.1746	−0.1682	−0.1611	−0.1543	−0.1483	−0.1416
	−0.2514	−0.2525	−0.2517	−0.2485	−0.2428	−0.2349	−0.2267	−0.2181	−0.2102	−0.2019
	−0.2831	−0.2817	−0.2816	−0.2830	−0.2825	−0.2760	−0.2693	−0.2603	−0.2507	−0.2421

Figure 6.28b: F2B: e=2a & d=2.5a

	c/a									
b/a	0.0957	0.0957	0.0957	0.0955	0.0951	0.0947	0.0941	0.0934	0.0927	0.0919
	0.0406	0.0416	0.0429	0.0443	0.0456	0.0466	0.0477	0.0485	0.0492	0.0499
	−0.0290	−0.0272	−0.0249	−0.0222	−0.0179	−0.0162	−0.0140	−0.0118	−0.0097	−0.0064
	−0.0937	−0.0915	−0.0887	−0.0852	−0.0814	−0.0783	−0.0746	−0.0714	−0.0684	−0.0651
	−0.1495	−0.1471	−0.1437	−0.1395	−0.1348	−0.1307	−0.1260	−0.1217	−0.1177	−0.1133
	−0.1924	−0.1902	−0.1867	−0.1821	−0.1768	−0.1720	−0.1665	−0.1613	−0.1565	−0.1511
	−0.2513	−0.2507	−0.2487	−0.2449	−0.2398	−0.2343	−0.2279	−0.2215	−0.2155	−0.2087
	−0.2842	−0.2850	−0.2853	−0.2844	−0.2815	−0.2763	−0.2704	−0.2635	−0.2567	−0.2492

Figure I.17b: F2B: e=2a & d=3a

	c/a									
b/a	0.0957	0.0956	0.0954	0.0951	0.0947	0.0943	0.0937	0.0931	0.0924	0.0917
	0.0404	0.0410	0.0418	0.0427	0.0436	0.0443	0.0451	0.0457	0.0463	0.0468
	−0.0293	−0.0281	−0.0265	−0.0245	−0.0224	−0.0206	−0.0173	−0.0161	−0.0147	−0.0130
	−0.0939	−0.0923	−0.0903	−0.0877	−0.0848	−0.0823	−0.0794	−0.0767	−0.0742	−0.0715
	−0.1497	−0.1478	−0.1453	−0.1420	−0.1383	−0.1351	−0.1313	−0.1277	−0.1244	−0.1206
	−0.1925	−0.1905	−0.1876	−0.1839	−0.1797	−0.1759	−0.1714	−0.1672	−0.1632	−0.1586
	−0.2508	−0.2495	−0.2471	−0.2436	−0.2392	−0.2349	−0.2297	−0.2246	−0.2197	−0.2141
	−0.2844	−0.2844	−0.2835	−0.2815	−0.2781	−0.2740	−0.2690	−0.2636	−0.2583	−0.2522

Figure 6.29b: F2B: e=2a & d=3.5a

	c/a									
b/a	0.0956	0.0955	0.0953	0.0950	0.0946	0.0941	0.0936	0.0931	0.0925	0.0918
	0.0403	0.0407	0.0412	0.0418	0.0424	0.0429	0.0435	0.0439	0.0444	0.0448
	−0.0295	−0.0286	−0.0275	−0.0260	−0.0245	−0.0231	−0.0215	−0.0182	−0.0173	−0.0164
	−0.0941	−0.0929	−0.0914	−0.0894	−0.0872	−0.0852	−0.0828	−0.0806	−0.0785	−0.0762
	−0.1499	−0.1485	−0.1465	−0.1439	−0.1410	−0.1384	−0.1353	−0.1323	−0.1295	−0.1263
	−0.1926	−0.1910	−0.1887	−0.1857	−0.1824	−0.1792	−0.1756	−0.1720	−0.1686	−0.1648
	−0.2507	−0.2492	−0.2470	−0.2439	−0.2402	−0.2366	−0.2323	−0.2281	−0.2240	−0.2193
	−0.2841	−0.2834	−0.2819	−0.2795	−0.2763	−0.2729	−0.2686	−0.2642	−0.2597	−0.2546

Figure I.18b: F2B: e=2a & d=4a

	c/a									
b/a	0.0956	0.0955	0.0953	0.0950	0.0946	0.0942	0.0937	0.0932	0.0926	0.0920
	0.0402	0.0405	0.0408	0.0412	0.0417	0.0420	0.0424	0.0428	0.0431	0.0434
	−0.0296	−0.0289	−0.0281	−0.0270	−0.0258	−0.0247	−0.0234	−0.0222	−0.0211	−0.0182
	−0.0942	−0.0933	−0.0921	−0.0906	−0.0888	−0.0872	−0.0853	−0.0835	−0.0817	−0.0797
	−0.1500	−0.1489	−0.1473	−0.1453	−0.1430	−0.1408	−0.1383	−0.1358	−0.1334	−0.1307
	−0.1927	−0.1914	−0.1896	−0.1872	−0.1845	−0.1819	−0.1788	−0.1758	−0.1729	−0.1697
	−0.2507	−0.2494	−0.2474	−0.2448	−0.2416	−0.2386	−0.2350	−0.2314	−0.2279	−0.2239
	−0.2839	−0.2829	−0.2814	−0.2790	−0.2761	−0.2731	−0.2694	−0.2656	−0.2618	−0.2575

Figure 6.26b: F2B: e=2.5a & d=0.5a

	c/a									
b/a	0.0007	0.0150	0.0268	0.0396	0.0494	0.0496	0.0552	0.0568	0.0579	0.0615
	−0.0678	−0.0518	−0.0343	−0.0192	−0.0049	0.0004	0.0087	0.0129	0.0151	0.0216
	−0.1215	−0.1177	−0.0894	−0.0706	−0.0532	−0.0398	−0.0309	−0.0229	−0.0167	−0.0127
	−0.1651	−0.1621	−0.1460	−0.1223	−0.1026	−0.0746	−0.0660	−0.0578	−0.0420	−0.0449
	−0.2015	−0.2013	−0.1976	−0.1737	−0.1489	−0.1059	−0.0939	−0.0809	−0.0581	−0.0712
	−0.2290	−0.2290	−0.2290	−0.2280	−0.2181	−0.1647	−0.1387	−0.1229	−0.0913	−0.0943
	−0.2664	−0.2664	−0.2664	−0.2663	−0.2654	−0.2642	−0.2316	−0.1867	−0.1429	−0.1405
	−0.2899	−0.2899	−0.2899	−0.2899	−0.2899	−0.2894	−0.2873	−0.2855	−0.2450	−0.2004

Figure I.15b: F2B: e=2.5a & d=1a

	c/a									
b/a	−0.0035	0.0038	0.0107	0.0187	0.0262	0.0299	0.0354	0.0386	0.0411	0.0438
	−0.0655	−0.0572	−0.0485	−0.0390	−0.0302	−0.0253	−0.0186	−0.0140	−0.0100	−0.0047
	−0.1207	−0.1126	−0.1017	−0.0895	−0.0780	−0.0705	−0.0618	−0.0554	−0.0503	−0.0441
	−0.1666	−0.1635	−0.1523	−0.1386	−0.1253	−0.1135	−0.1032	−0.0944	−0.0877	−0.0804
	−0.1994	−0.2009	−0.1943	−0.1819	−0.1675	−0.1503	−0.1385	−0.1272	−0.1177	−0.1109
	−0.2278	−0.2255	−0.2249	−0.2195	−0.2060	−0.1844	−0.1703	−0.1565	−0.1429	−0.1364
	−0.2663	−0.2660	−0.2645	−0.2620	−0.2590	−0.2418	−0.2263	−0.2070	−0.1856	−0.1784
	−0.2899	−0.2899	−0.2898	−0.2898	−0.2898	−0.2866	−0.2751	−0.2561	−0.2324	−0.2200

Figure 6.27b: F2B: e=2.5a & d=1.5a

	c/a									
b/a	−0.0052	−0.0008	0.0033	0.0078	0.0122	0.0156	0.0195	0.0226	0.0253	0.0279
	−0.0672	−0.0623	−0.0568	−0.0505	−0.0443	−0.0400	−0.0349	−0.0308	−0.0273	−0.0234
	−0.1203	−0.1146	−0.1078	−0.0997	−0.0917	−0.0859	−0.0791	−0.0736	−0.0688	−0.0634
	−0.1642	−0.1593	−0.1523	−0.1435	−0.1344	−0.1272	−0.1191	−0.1123	−0.1064	−0.0998
	−0.2018	−0.1993	−0.1931	−0.1842	−0.1742	−0.1653	−0.1559	−0.1476	−0.1406	−0.1327
	−0.2297	−0.2303	−0.2263	−0.2185	−0.2084	−0.1974	−0.1869	−0.1769	−0.1684	−0.1597
	−0.2650	−0.2630	−0.2631	−0.2636	−0.2589	−0.2462	−0.2351	−0.2225	−0.2105	−0.2011
	−0.2897	−0.2885	−0.2858	−0.2836	−0.2827	−0.2773	−0.2714	−0.2597	−0.2446	−0.2351

Figure I.16b: F2B: e=2.5a & d=2a

	c/a									
b/a	−0.0059	−0.0038	−0.0007	0.0019	0.0051	0.0079	0.0103	0.0127	0.0149	0.0172
	−0.0681	−0.0651	−0.0615	−0.0572	−0.0527	−0.0493	−0.0453	−0.0418	−0.0388	−0.0354
	−0.1211	−0.1173	−0.1126	−0.1071	−0.1012	−0.0966	−0.0912	−0.0866	−0.0824	−0.0778
	−0.1641	−0.1602	−0.1551	−0.1489	−0.1422	−0.1368	−0.1305	−0.1249	−0.1199	−0.1143
	−0.2005	−0.1972	−0.1922	−0.1856	−0.1784	−0.1722	−0.1650	−0.1586	−0.1528	−0.1463
	−0.2287	−0.2267	−0.2224	−0.2161	−0.2086	−0.2016	−0.1938	−0.1865	−0.1799	−0.1725
	−0.2666	−0.2676	−0.2668	−0.2636	−0.2576	−0.2495	−0.2411	−0.2322	−0.2240	−0.2154
	−0.2889	−0.2874	−0.2872	−0.2886	−0.2881	−0.2816	−0.2749	−0.2657	−0.2561	−0.2474

Figure 6.28b: F2B: e=2.5a & d=2.5a

	c/a									
b/a	−0.0062	−0.0049	−0.0032	−0.0006	0.0011	0.0034	0.0050	0.0067	0.0087	0.0103
	−0.0685	−0.0666	−0.0641	−0.0611	−0.0578	−0.0551	−0.0520	−0.0492	−0.0466	−0.0438
	−0.1216	−0.1191	−0.1158	−0.1117	−0.1074	−0.1037	−0.0995	−0.0957	−0.0921	−0.0882
	−0.1645	−0.1617	−0.1579	−0.1533	−0.1483	−0.1440	−0.1390	−0.1344	−0.1302	−0.1255
	−0.2005	−0.1977	−0.1938	−0.1888	−0.1832	−0.1784	−0.1727	−0.1675	−0.1626	−0.1572
	−0.2282	−0.2257	−0.2219	−0.2168	−0.2110	−0.2058	−0.1996	−0.1938	−0.1884	−0.1824
	−0.2665	−0.2659	−0.2638	−0.2599	−0.2546	−0.2490	−0.2424	−0.2357	−0.2295	−0.2224
	−0.2900	−0.2907	−0.2910	−0.2901	−0.2872	−0.2820	−0.2760	−0.2690	−0.2621	−0.2546

Figure I.17b: F2B: e=2.5a & d=3a

	c/a									
b/a	−0.0064	−0.0055	−0.0044	−0.0022	−0.0007	0.0002	0.0017	0.0036	0.0045	0.0059
	−0.0688	−0.0675	−0.0657	−0.0635	−0.0610	−0.0589	−0.0564	−0.0541	−0.0520	−0.0496
	−0.1219	−0.1201	−0.1178	−0.1148	−0.1115	−0.1085	−0.1051	−0.1020	−0.0990	−0.0957
	−0.1648	−0.1627	−0.1600	−0.1565	−0.1526	−0.1491	−0.1451	−0.1413	−0.1377	−0.1338
	−0.2008	−0.1985	−0.1955	−0.1916	−0.1873	−0.1834	−0.1788	−0.1745	−0.1704	−0.1658
	−0.2282	−0.2260	−0.2229	−0.2188	−0.2142	−0.2100	−0.2050	−0.2002	−0.1957	−0.1907
	−0.2660	−0.2646	−0.2622	−0.2585	−0.2540	−0.2495	−0.2442	−0.2389	−0.2338	−0.2280
	−0.2901	−0.2901	−0.2893	−0.2872	−0.2838	−0.2797	−0.2746	−0.2692	−0.2638	−0.2576

Figure 6.29b: F2B: e=2.5a & d=3.5a

	c/a									
b/a	−0.0065	−0.0059	−0.0051	−0.0041	−0.0022	−0.0009	−0.0003	0.0007	0.0017	0.0035
	−0.0690	−0.0680	−0.0667	−0.0650	−0.0632	−0.0614	−0.0595	−0.0576	−0.0558	−0.0538
	−0.1221	−0.1208	−0.1190	−0.1167	−0.1142	−0.1118	−0.1091	−0.1065	−0.1040	−0.1012
	−0.1650	−0.1635	−0.1614	−0.1587	−0.1556	−0.1528	−0.1495	−0.1464	−0.1433	−0.1400
	−0.2010	−0.1993	−0.1969	−0.1938	−0.1904	−0.1872	−0.1834	−0.1799	−0.1764	−0.1725
	−0.2283	−0.2266	−0.2241	−0.2208	−0.2171	−0.2136	−0.2095	−0.2055	−0.2017	−0.1974
	−0.2659	−0.2644	−0.2620	−0.2588	−0.2550	−0.2513	−0.2468	−0.2424	−0.2382	−0.2333
	−0.2898	−0.2891	−0.2877	−0.2852	−0.2820	−0.2785	−0.2742	−0.2697	−0.2652	−0.2600

Figure I.18b: F2B: e=2.5a & d=4a

	c/a									
b/a	−0.0066	−0.0062	−0.0056	−0.0048	−0.0039	−0.0031	−0.0010	−0.0007	0.0000	0.0009
	−0.0691	−0.0683	−0.0673	−0.0661	−0.0646	−0.0632	−0.0616	−0.0601	−0.0585	−0.0569
	−0.1223	−0.1213	−0.1199	−0.1181	−0.1161	−0.1142	−0.1119	−0.1097	−0.1076	−0.1053
	−0.1652	−0.1640	−0.1623	−0.1602	−0.1578	−0.1554	−0.1527	−0.1501	−0.1475	−0.1447
	−0.2011	−0.1998	−0.1979	−0.1955	−0.1927	−0.1901	−0.1870	−0.1839	−0.1810	−0.1776
	−0.2285	−0.2271	−0.2250	−0.2224	−0.2193	−0.2080	−0.2130	−0.2097	−0.2064	−0.2027
	−0.2659	−0.2645	−0.2625	−0.2597	−0.2565	−0.2534	−0.2496	−0.2459	−0.2422	−0.2380
	−0.2896	−0.2887	−0.2871	−0.2847	−0.2817	−0.2787	−0.2749	−0.2711	−0.2673	−0.2629

Figure 6.26b: F2B: e=3a & d=0.5a

	c/a									
	−0.0936	−0.0739	−0.0586	−0.0430	−0.0295	−0.0259	−0.0169	−0.0121	−0.0082	−0.0014
	−0.1464	−0.1245	−0.1015	−0.0827	−0.0681	−0.0586	−0.0495	−0.0427	−0.0386	−0.0317
	−0.1825	−0.1780	−0.1446	−0.1216	−0.1049	−0.0842	−0.0756	−0.0674	−0.0573	−0.0549
b/a	−0.2103	−0.2067	−0.1878	−0.1606	−0.1392	−0.1076	−0.0980	−0.0873	−0.0704	−0.0761
	−0.2340	−0.2337	−0.2298	−0.2029	−0.1756	−0.1305	−0.1169	−0.1028	−0.0788	−0.0909
	−0.2523	−0.2524	−0.2524	−0.2512	−0.2408	−0.1841	−0.1573	−0.1396	−0.1083	−0.1127
	−0.2777	−0.2777	−0.2777	−0.2776	−0.2766	−0.2754	−0.2416	−0.1955	−0.1513	−0.1494
	−0.2952	−0.2952	−0.2951	−0.2951	−0.2951	−0.2946	−0.2925	−0.2906	−0.2498	−0.2040

Figure I.15b: F2B: e=3a & d=1a

	c/a									
	−0.1014	−0.0918	−0.0820	−0.0714	−0.0615	−0.0555	−0.0479	−0.0423	−0.0374	−0.0318
	−0.1437	−0.1330	−0.1216	−0.1091	−0.0975	−0.0904	−0.0814	−0.0747	−0.0691	−0.0623
	−0.1826	−0.1732	−0.1602	−0.1457	−0.1320	−0.1226	−0.1119	−0.1037	−0.0970	−0.0889
b/a	−0.2118	−0.2083	−0.1959	−0.1806	−0.1655	−0.1523	−0.1405	−0.1304	−0.1225	−0.1139
	−0.2316	−0.2329	−0.2259	−0.2126	−0.1970	−0.1787	−0.1658	−0.1535	−0.1431	−0.1354
	−0.2510	−0.2485	−0.2475	−0.2418	−0.2276	−0.2052	−0.1903	−0.1758	−0.1619	−0.1550
	−0.2777	−0.2773	−0.2758	−0.2731	−0.2696	−0.2522	−0.2364	−0.2168	−0.1950	−0.1875
	−0.2952	−0.2952	−0.2951	−0.2950	−0.2950	−0.2918	−0.2800	−0.2608	−0.2370	−0.2307

Figure 6.27b: F2B: e=3a & d=1.5a

	c/a									
	−0.1038	−0.0986	−0.0924	−0.0854	−0.0783	−0.0731	−0.0670	−0.0620	−0.0575	−0.0526
	−0.1461	−0.1398	−0.1326	−0.1242	−0.1159	−0.1097	−0.1025	−0.0966	−0.0913	−0.0854
	−0.1821	−0.1756	−0.1676	−0.1581	−0.1484	−0.1412	−0.1327	−0.1258	−0.1196	−0.1127
b/a	−0.2093	−0.2038	−0.1960	−0.1861	−0.1759	−0.1677	−0.1584	−0.1506	−0.1437	−0.1360
	−0.2342	−0.2316	−0.2249	−0.2153	−0.2046	−0.1949	−0.1847	−0.1757	−0.1679	−0.1593
	−0.2530	−0.2536	−0.2494	−0.2413	−0.2307	−0.2191	−0.2081	−0.1976	−0.1886	−0.1793
	−0.2763	−0.2742	−0.2741	−0.2746	−0.2698	−0.2569	−0.2456	−0.2329	−0.2205	−0.2110
	−0.2949	−0.2937	−0.2910	−0.2887	−0.2878	−0.2823	−0.2764	−0.2640	−0.2494	−0.2398

Figure I.16b: F2B: e=3a & d=2a

	c/a									
	−0.1048	−0.1016	−0.0975	−0.0927	−0.0876	−0.0835	−0.0787	−0.0745	−0.0707	−0.0665
	−0.1472	−0.1433	−0.1385	−0.1326	−0.1266	−0.1216	−0.1159	−0.1109	−0.1063	−0.1013
	−0.1830	−0.1786	−0.1732	−0.1666	−0.1596	−0.1538	−0.1472	−0.1413	−0.1360	−0.1301
b/a	−0.2092	−0.2049	−0.1992	−0.1921	−0.1846	−0.1784	−0.1712	−0.1648	−0.1589	−0.1524
	−0.2329	−0.2293	−0.2240	−0.2169	−0.2091	−0.2023	−0.1945	−0.1875	−0.1811	−0.1740
	−0.2521	−0.2499	−0.2455	−0.2388	−0.2310	−0.2236	−0.2153	−0.2076	−0.2006	−0.1928
	−0.2779	−0.2789	−0.2781	−0.2748	−0.2688	−0.2605	−0.2519	−0.2428	−0.2344	−0.2256
	−0.2941	−0.2925	−0.2924	−0.2938	−0.2932	−0.2867	−0.2799	−0.2707	−0.2610	−0.2522

Figure 6.28b: F2B: e=3a & d=2.5a

	c/a									
	−0.1053	−0.1032	−0.1004	−0.0969	−0.0931	−0.0899	−0.0861	−0.0827	−0.0795	−0.0759
	−0.1478	−0.1452	−0.1418	−0.1376	−0.1331	−0.1292	−0.1246	−0.1205	−0.1166	−0.1124
	−0.1836	−0.1806	−0.1767	−0.1719	−0.1667	−0.1622	−0.1569	−0.1521	−0.1475	−0.1425
b/a	−0.2096	−0.2064	−0.2023	−0.1970	−0.1913	−0.1864	−0.1806	−0.1753	−0.1704	−0.1649
	−0.2329	−0.2299	−0.2256	−0.2202	−0.2142	−0.2089	−0.2028	−0.1971	−0.1917	−0.1857
	−0.2515	−0.2489	−0.2449	−0.2396	−0.2335	−0.2279	−0.2214	−0.2153	−0.2096	−0.2031
	−0.2778	−0.2772	−0.2750	−0.2711	−0.2657	−0.2599	−0.2532	−0.2464	−0.2400	−0.2328
	−0.2952	−0.2960	−0.2962	−0.2953	−0.2924	−0.2871	−0.2811	−0.2741	−0.2671	−0.2595

Figure I.17b: F2B: e=3a & d=3a

	c/a									
	−0.1056	−0.1041	−0.1021	−0.0995	−0.0966	−0.0940	−0.0911	−0.0882	−0.0855	−0.0826
	−0.1481	−0.1463	−0.1438	−0.1407	−0.1372	−0.1341	−0.1305	−0.1271	−0.1238	−0.1202
	−0.1839	−0.1818	−0.1790	−0.1754	−0.1714	−0.1678	−0.1636	−0.1596	−0.1558	−0.1515
b/a	−0.2100	−0.2076	−0.2045	−0.2005	−0.1961	−0.1921	−0.1874	−0.1831	−0.1789	−0.1743
	−0.2331	−0.2308	−0.2275	−0.2233	−0.2186	−0.2143	−0.2093	−0.2046	−0.2001	−0.1950
	−0.2515	−0.2492	−0.2460	−0.2417	−0.2368	−0.2323	−0.2271	−0.2220	−0.2172	−0.2118
	−0.2773	−0.2759	−0.2734	−0.2697	−0.2651	−0.2605	−0.2551	−0.2496	−0.2444	−0.2385
	−0.2954	−0.2954	−0.2945	−0.2924	−0.2890	−0.2848	−0.2797	−0.2742	−0.2688	−0.2625

Figure 6.29b: F2B: e=3a & d=3.5a

	c/a									
	−0.1058	−0.1047	−0.1031	−0.1012	−0.0989	−0.0969	−0.0945	−0.0921	−0.0899	−0.0874
	−0.1483	−0.1470	−0.1451	−0.1427	−0.1400	−0.1375	−0.1345	−0.1317	−0.1290	−0.1259
	−0.1842	−0.1826	−0.1804	−0.1777	−0.1745	−0.1716	−0.1682	−0.1649	−0.1618	−0.1582
b/a	−0.2102	−0.2084	−0.2060	−0.2029	−0.1994	−0.1962	−0.1924	−0.1887	−0.1852	−0.1812
	−0.2334	−0.2315	−0.2290	−0.2256	−0.2219	−0.2184	−0.2143	−0.2103	−0.2065	−0.2022
	−0.2517	−0.2498	−0.2472	−0.2437	−0.2398	−0.2361	−0.2317	−0.2275	−0.2235	−0.2189
	−0.2772	−0.2756	−0.2733	−0.2700	−0.2661	−0.2623	−0.2577	−0.2532	−0.2488	−0.2438
	−0.2950	−0.2943	−0.2929	−0.2904	−0.2872	−0.2836	−0.2793	−0.2747	−0.2702	−0.2650

Figure I.18b: F2B: e=3a & d=4a

	c/a									
	−0.1059	−0.1050	−0.1039	−0.1023	−0.1005	−0.0989	−0.0969	−0.0949	−0.0930	−0.0909
	−0.1485	−0.1474	−0.1460	−0.1441	−0.1419	−0.1399	−0.1375	−0.1351	−0.1328	−0.1302
	−0.1843	−0.1831	−0.1814	−0.1792	−0.1767	−0.1743	−0.1715	−0.1688	−0.1661	−0.1631
b/a	−0.2104	−0.2090	−0.2071	−0.2047	−0.2018	−0.1992	−0.1960	−0.1930	−0.1899	−0.1866
	−0.2335	−0.2321	−0.2300	−0.2274	−0.2243	−0.2215	−0.2180	−0.2147	−0.2114	−0.2078
	−0.2518	−0.2503	−0.2482	−0.2454	−0.2422	−0.2391	−0.2355	−0.2319	−0.2284	−0.2245
	−0.2772	−0.2758	−0.2737	−0.2709	−0.2676	−0.2644	−0.2606	−0.2567	−0.2530	−0.2487
	−0.2949	−0.2939	−0.2923	−0.2899	−0.2869	−0.2838	−0.2801	−0.2762	−0.2723	−0.2679

Figure 6.26b: F2B: e=3.5a & d=0.5a

	c/a									
b/a	−0.1596	−0.1354	−0.1165	−0.0980	−0.0819	−0.0763	−0.0652	−0.0586	−0.0532	−0.0448
	−0.1994	−0.1738	−0.1473	−0.1257	−0.1088	−0.0976	−0.0868	−0.0786	−0.0733	−0.0650
	−0.2225	−0.2173	−0.1816	−0.1557	−0.1374	−0.1147	−0.1047	−0.0953	−0.0842	−0.0828
	−0.2409	−0.2369	−0.2160	−0.1866	−0.1632	−0.1302	−0.1194	−0.1078	−0.0900	−0.0964
	−0.2568	−0.2565	−0.2525	−0.2234	−0.1943	−0.1478	−0.1332	−0.1182	−0.0936	−0.1051
	−0.2694	−0.2694	−0.2694	−0.2681	−0.2571	−0.1978	−0.1697	−0.1522	−0.1204	−0.1256
	−0.2870	−0.2870	−0.2870	−0.2869	−0.2859	−0.2845	−0.2498	−0.2027	−0.1581	−0.1569
	−0.3001	−0.3001	−0.3001	−0.3001	−0.3001	−0.2996	−0.2974	−0.2955	−0.2541	−0.2076

Figure I.15b: F2B: e=3.5a & d=1a

	c/a									
b/a	−0.1700	−0.1586	−0.1468	−0.1342	−0.1222	−0.1145	−0.1050	−0.0977	−0.0914	−0.0841
	−0.1965	−0.1843	−0.1713	−0.1572	−0.1439	−0.1355	−0.1250	−0.1170	−0.1103	−0.1022
	−0.2232	−0.2130	−0.1991	−0.1836	−0.1685	−0.1580	−0.1462	−0.1369	−0.1293	−0.1202
	−0.2424	−0.2386	−0.2255	−0.2092	−0.1931	−0.1790	−0.1663	−0.1554	−0.1468	−0.1374
	−0.2542	−0.2554	−0.2481	−0.2342	−0.2178	−0.1988	−0.1852	−0.1723	−0.1614	−0.1530
	−0.2680	−0.2652	−0.2640	−0.2580	−0.2434	−0.2204	−0.2051	−0.1900	−0.1757	−0.1683
	−0.2869	−0.2866	−0.2850	−0.2823	−0.2782	−0.2607	−0.2447	−0.2248	−0.2027	−0.1950
	−0.3001	−0.3001	−0.3000	−0.3000	−0.3000	−0.2967	−0.2848	−0.2651	−0.2400	−0.2286

Figure 6.27b: F2B: e=3.5a & d=1.5a

	c/a									
b/a	−0.1729	−0.1666	−0.1592	−0.1508	−0.1422	−0.1356	−0.128	−0.1215	−0.1157	−0.1094
	−0.1993	−0.1922	−0.1839	−0.1745	−0.1649	−0.1577	−0.1493	−0.1423	−0.136	−0.129
	−0.2227	−0.2155	−0.2068	−0.1966	−0.1863	−0.1784	−0.1692	−0.1614	−0.1544	−0.1466
	−0.2398	−0.2341	−0.2257	−0.2152	−0.2043	−0.1955	−0.1856	−0.177	−0.1696	−0.1612
	−0.257	−0.2542	−0.2473	−0.2373	−0.2261	−0.2159	−0.2052	−0.1957	−0.1875	−0.1784
	−0.27	−0.2706	−0.2663	−0.258	−0.247	−0.2351	−0.2237	−0.2129	−0.2035	−0.1939
	−0.2855	−0.2834	−0.2832	−0.2836	−0.2788	−0.2658	−0.2543	−0.2413	−0.2288	−0.219
	−0.2999	−0.2987	−0.2959	−0.2935	−0.2925	−0.287	−0.281	−0.2691	−0.2539	−0.2442

Figure I.16b: F2B: e=3.5a & d=2a

	c/a									
b/a	−0.1741	−0.1702	−0.1653	−0.1594	−0.1531	−0.1479	−0.1418	−0.1365	−0.1315	−0.126
	−0.2006	−0.1961	−0.1906	−0.1839	−0.1769	−0.1712	−0.1645	−0.1586	−0.1531	−0.1471
	−0.2236	−0.2189	−0.2129	−0.2057	−0.1981	−0.1919	−0.1846	−0.1782	−0.1723	−0.1658
	−0.2397	−0.2351	−0.2291	−0.2216	−0.2136	−0.2069	−0.1991	−0.1922	−0.1859	−0.1788
	−0.2557	−0.2519	−0.2463	−0.2389	−0.2307	−0.2236	−0.2155	−0.2081	−0.2013	−0.1938
	−0.2691	−0.2669	−0.2623	−0.2555	−0.2474	−0.2398	−0.2312	−0.2232	−0.216	−0.2078
	−0.2872	−0.2882	−0.2873	−0.284	−0.2779	−0.2695	−0.2607	−0.2515	−0.243	−0.2341
	−0.299	−0.2975	−0.2972	−0.2986	−0.2981	−0.2915	−0.2847	−0.2755	−0.2657	−0.2568

Figure 6.28b: F2B: e=3.5a & d=2.5a

	c/a									
b/a	−0.1747	−0.1721	−0.1686	−0.1643	−0.1596	−0.1555	−0.1507	−0.1462	−0.142	−0.1374
	−0.2012	−0.1983	−0.1943	−0.1895	−0.1842	−0.1796	−0.1743	−0.1694	−0.1648	−0.1597
	−0.2243	−0.221	−0.2168	−0.2115	−0.2057	−0.2008	−0.195	−0.1897	−0.1847	−0.1791
	−0.2402	−0.2368	−0.2324	−0.2268	−0.2207	−0.2153	−0.2091	−0.2034	−0.1981	−0.1921
	−0.2556	−0.2525	−0.2481	−0.2424	−0.2361	−0.2306	−0.2241	−0.218	−0.2124	−0.2061
	−0.2685	−0.2658	−0.2618	−0.2563	−0.25	−0.2442	−0.2375	−0.2311	−0.2252	−0.2185
	−0.2871	−0.2865	−0.2843	−0.2803	−0.2748	−0.269	−0.2621	−0.2552	−0.2487	−0.2414
	−0.3001	−0.3009	−0.3011	−0.3002	−0.2973	−0.292	−0.2859	−0.2789	−0.2718	−0.2642

Figure I.17b: F2B: e=3.5a & d=3a

	c/a									
b/a	−0.175	−0.1731	−0.1706	−0.1674	−0.1637	−0.1604	−0.1566	−0.1529	−0.1494	−0.1455
	−0.2016	−0.1995	−0.1966	−0.193	−0.1889	−0.1852	−0.181	−0.1769	−0.173	−0.1687
	−0.2247	−0.2224	−0.2192	−0.2152	−0.2108	−0.2068	−0.2021	−0.1977	−0.1935	−0.1888
	−0.2406	−0.2381	−0.2347	−0.2305	−0.2257	−0.2214	−0.2164	−0.2117	−0.2071	−0.2021
	−0.2559	−0.2534	−0.25	−0.2456	−0.2406	−0.2361	−0.2309	−0.2259	−0.2211	−0.2158
	−0.2686	−0.2662	−0.2628	−0.2584	−0.2534	−0.2487	−0.2433	−0.2381	−0.2331	−0.2274
	−0.2866	−0.2851	−0.2826	−0.2789	−0.2742	−0.2695	−0.264	−0.2585	−0.2532	−0.2471
	−0.3003	−0.3003	−0.2994	−0.2973	−0.2939	−0.2897	−0.2846	−0.279	−0.2735	−0.2668

Figure 6.29b: F2B: e=3.5a & d=3.5a

	c/a									
b/a	−0.1752	−0.1738	−0.1719	−0.1694	−0.1665	−0.1638	−0.1607	−0.1577	−0.1547	−0.1514
	−0.2018	−0.2003	−0.1981	−0.1953	−0.1921	−0.1891	−0.1856	−0.1822	−0.1789	−0.1752
	−0.2249	−0.2232	−0.2208	−0.2177	−0.2142	−0.2109	−0.2071	−0.2034	−0.1999	−0.1959
	−0.2408	−0.2389	−0.2364	−0.233	−0.2293	−0.2258	−0.2216	−0.2177	−0.2138	−0.2095
	−0.2561	−0.2542	−0.2515	−0.248	−0.2441	−0.2404	−0.236	−0.2319	−0.2278	−0.2233
	−0.2687	−0.2668	−0.2641	−0.2605	−0.2564	−0.2526	−0.2481	−0.2437	−0.2395	−0.2347
	−0.2864	−0.2849	−0.2825	−0.2792	−0.2752	−0.2713	−0.2667	−0.2621	−0.2576	−0.2525
	−0.3	−0.2993	−0.2978	−0.2954	−0.2921	−0.2885	−0.2841	−0.2796	−0.275	−0.2697

Figure I.18b: F2B: e=3.5a & d=4a

	c/a									
b/a	−0.1753	−0.1743	−0.1728	−0.1708	−0.1685	−0.1663	−0.1637	−0.1611	−0.1586	−0.1558
	−0.202	−0.2008	−0.1991	−0.1968	−0.1943	−0.1918	−0.1889	−0.1861	−0.1833	−0.1801
	−0.2251	−0.2238	−0.2219	−0.2194	−0.2166	−0.2139	−0.2108	−0.2077	−0.2046	−0.2012
	−0.241	−0.2395	−0.2375	−0.2349	−0.2318	−0.2289	−0.2255	−0.2222	−0.2189	−0.2152
	−0.2563	−0.2548	−0.2526	−0.2498	−0.2466	−0.2436	−0.24	−0.2364	−0.233	−0.2291
	−0.2688	−0.2673	−0.2651	−0.2622	−0.2589	−0.2557	−0.2519	−0.2482	−0.2446	−0.2405
	−0.2865	−0.285	−0.2829	−0.2801	−0.2767	−0.2735	−0.2695	−0.2657	−0.2618	−0.2574
	−0.2998	−0.2988	−0.2972	−0.2948	−0.2918	−0.2887	−0.2849	−0.281	−0.2771	−0.2726

Figure 6.26b: F2B: e=4a & d=0.5a

	c/a									
b/a	−0.2021	−0.1750	−0.1540	−0.1336	−0.1160	−0.1093	−0.0970	−0.0894	−0.0831	−0.0737
	−0.2343	−0.2063	−0.1775	−0.1541	−0.1358	−0.1236	−0.1118	−0.1028	−0.0967	−0.0877
	−0.2495	−0.2437	−0.2064	−0.1788	−0.1592	−0.1354	−0.1246	−0.1144	−0.1027	−0.1015
	−0.2624	−0.2581	−0.2358	−0.2047	−0.1800	−0.1460	−0.1345	−0.1223	−0.1040	−0.1099
	−0.2734	−0.2731	−0.2690	−0.2382	−0.2079	−0.1604	−0.1451	−0.1296	−0.1044	−0.1156
	−0.2824	−0.2824	−0.2824	−0.2809	−0.2679	−0.2082	−0.1797	−0.1629	−0.1288	−0.1352
	−0.2947	−0.2947	−0.2947	−0.2946	−0.2936	−0.2922	−0.2566	−0.2087	−0.1637	−0.1621
	−0.3047	−0.3047	−0.3047	−0.3047	−0.3047	−0.3042	−0.3020	−0.2999	−0.2582	−0.2110

Figure I.15b: F2B: e=4a & d=1a

	c/a									
b/a	−0.2142	−0.2017	−0.1887	−0.1749	−0.1618	−0.1531	−0.1425	−0.1343	−0.1271	−0.1189
	−0.2313	−0.2181	−0.2041	−0.189	−0.1747	−0.1655	−0.1542	−0.1455	−0.138	−0.1292
	−0.2506	−0.2398	−0.2252	−0.2088	−0.1933	−0.1821	−0.1696	−0.1598	−0.1516	−0.1419
	−0.2639	−0.2599	−0.2462	−0.2292	−0.2125	−0.1978	−0.1846	−0.1731	−0.164	−0.1542
	−0.2707	−0.2717	−0.2643	−0.2499	−0.233	−0.2136	−0.1994	−0.1861	−0.1748	−0.1661
	−0.2809	−0.2779	−0.2764	−0.2703	−0.2553	−0.232	−0.2162	−0.2008	−0.1862	−0.1785
	−0.2946	−0.2943	−0.2927	−0.2899	−0.2855	−0.2678	−0.2515	−0.2314	−0.2091	−0.2012
	−0.3047	−0.3047	−0.3046	−0.3046	−0.3045	−0.3013	−0.2891	−0.2692	−0.2453	−0.2324

Figure 6.27b: F2B: e=4a & d=1.5a

	c/a									
b/a	−0.2175	−0.2106	−0.2025	−0.1931	−0.1837	−0.1764	−0.1679	−0.1606	−0.1541	−0.1469
	−0.2343	−0.2267	−0.2179	−0.2077	−0.1975	−0.1896	−0.1805	−0.1729	−0.1659	−0.1583
	−0.2501	−0.2426	−0.2334	−0.2227	−0.2118	−0.2034	−0.1938	−0.1856	−0.1783	−0.17
	−0.2612	−0.2552	−0.2465	−0.2357	−0.2243	−0.2151	−0.2047	−0.1958	−0.188	−0.1792
	−0.2736	−0.2708	−0.2636	−0.2533	−0.2418	−0.2313	−0.2203	−0.2104	−0.2019	−0.1925
	−0.2829	−0.2835	−0.2792	−0.2706	−0.2595	−0.2473	−0.2356	−0.2245	−0.2149	−0.205
	−0.2932	−0.291	−0.2908	−0.2911	−0.2862	−0.2731	−0.2615	−0.2484	−0.2357	−0.2258
	−0.3044	−0.3032	−0.3005	−0.298	−0.2969	−0.2913	−0.2853	−0.2733	−0.2581	−0.2482

Figure I.16b: F2B: e=4a & d=2a

	c/a									
b/a	−0.2187	−0.2145	−0.209	−0.2025	−0.1956	−0.1897	−0.183	−0.177	−0.1713	−0.1652
	−0.2357	−0.231	−0.225	−0.2179	−0.2103	−0.204	−0.1968	−0.1904	−0.1844	−0.1778
	−0.2512	−0.2462	−0.2399	−0.2323	−0.2243	−0.2176	−0.2099	−0.2031	−0.1968	−0.1898
	−0.2612	−0.2564	−0.2501	−0.2423	−0.2339	−0.2269	−0.2188	−0.2116	−0.205	−0.1976
	−0.2722	−0.2684	−0.2626	−0.255	−0.2466	−0.2393	−0.2308	−0.2232	−0.2162	−0.2084
	−0.2821	−0.2798	−0.2751	−0.2681	−0.2599	−0.2521	−0.2433	−0.2351	−0.2277	−0.2193
	−0.2949	−0.2959	−0.295	−0.2916	−0.2854	−0.277	−0.2681	−0.2588	−0.2502	−0.2411
	−0.3036	−0.302	−0.3017	−0.3031	−0.3026	−0.296	−0.2891	−0.2798	−0.27	−0.261

Figure 6.28b: F2B: e=4a & d=2.5a

	c/a									
b/a	−0.2194	−0.2165	−0.2127	−0.2079	−0.2027	−0.198	−0.1926	−0.1876	−0.1829	−0.1777
	−0.2364	−0.2332	−0.229	−0.2238	−0.2181	−0.2131	−0.2073	−0.202	−0.1969	−0.1913
	−0.2518	−0.2484	−0.2439	−0.2383	−0.2323	−0.227	−0.2208	−0.2152	−0.2098	−0.2039
	−0.2616	−0.2581	−0.2535	−0.2477	−0.2413	−0.2357	−0.2293	−0.2233	−0.2177	−0.2114
	−0.2722	−0.269	−0.2644	−0.2586	−0.2521	−0.2464	−0.2397	−0.2334	−0.2276	−0.221
	−0.2815	−0.2787	−0.2746	−0.269	−0.2625	−0.2566	−0.2497	−0.2432	−0.2371	−0.2303
	−0.2948	−0.2942	−0.292	−0.2879	−0.2824	−0.2765	−0.2695	−0.2626	−0.256	−0.2485
	−0.3047	−0.3055	−0.3057	−0.3048	−0.3018	−0.2965	−0.2904	−0.2833	−0.2762	−0.2685

Figure I.17b: F2B: e=4a & d=3a

	c/a									
b/a	−0.2197	−0.2177	−0.2148	−0.2112	−0.2072	−0.2034	−0.1991	−0.195	−0.191	−0.1865
	−0.2368	−0.2345	−0.2314	−0.2275	−0.2231	−0.2191	−0.2144	−0.21	−0.2057	−0.2009
	−0.2523	−0.2498	−0.2465	−0.2422	−0.2375	−0.2333	−0.2283	−0.2236	−0.2191	−0.2141
	−0.262	−0.2594	−0.2559	−0.2515	−0.2465	−0.242	−0.2368	−0.2318	−0.227	−0.2217
	−0.2725	−0.2699	−0.2664	−0.2619	−0.2568	−0.2521	−0.2467	−0.2415	−0.2365	−0.231
	−0.2815	−0.2791	−0.2756	−0.2711	−0.266	−0.2612	−0.2556	−0.2503	−0.2451	−0.2394
	−0.2943	−0.2928	−0.2903	−0.2865	−0.2818	−0.2771	−0.2714	−0.2659	−0.2605	−0.2543
	−0.3049	−0.3049	−0.304	−0.3019	−0.2985	−0.2942	−0.2891	−0.2835	−0.2779	−0.2716

Figure 6.29b: F2B: e=4a & d=3.5a

	c/a									
b/a	−0.2199	−0.2184	−0.2162	−0.2134	−0.2102	−0.2072	−0.2036	−0.2002	−0.1968	−0.193
	−0.2371	−0.2354	−0.233	−0.2299	−0.2264	−0.2232	−0.2194	−0.2156	−0.212	−0.208
	−0.2525	−0.2507	−0.2481	−0.2449	−0.2411	−0.2377	−0.2336	−0.2297	−0.2258	−0.2215
	−0.2623	−0.2603	−0.2576	−0.2542	−0.2502	−0.2465	−0.2422	−0.2381	−0.234	−0.2295
	−0.2727	−0.2707	−0.268	−0.2644	−0.2603	−0.2565	−0.252	−0.2477	−0.2434	−0.2387
	−0.2816	−0.2797	−0.2769	−0.2733	−0.2691	−0.2652	−0.2605	−0.2561	−0.2517	−0.2468
	−0.2942	−0.2926	−0.2902	−0.2868	−0.2828	−0.2789	−0.2742	−0.2695	−0.265	−0.2598
	−0.3046	−0.3039	−0.3024	−0.2999	−0.2966	−0.293	−0.2886	−0.284	−0.2794	−0.2741

Figure I.18b: F2B: e=4a & d=4a

	c/a									
b/a	−0.2201	−0.2189	−0.2172	−0.2149	−0.2124	−0.2099	−0.2069	−0.204	−0.2011	−0.1979
	−0.2372	−0.2359	−0.234	−0.2316	−0.2288	−0.2261	−0.2229	−0.2198	−0.2167	−0.2133
	−0.2527	−0.2513	−0.2493	−0.2467	−0.2437	−0.2408	−0.2374	−0.2341	−0.2309	−0.2272
	−0.2624	−0.2609	−0.2588	−0.256	−0.2529	−0.2498	−0.2462	−0.2427	−0.2393	−0.2354
	−0.2729	−0.2713	−0.2691	−0.2662	−0.2629	−0.2598	−0.256	−0.2524	−0.2488	−0.2447
	−0.2818	−0.2802	−0.278	−0.275	−0.2716	−0.2683	−0.2645	−0.2607	−0.2569	−0.2527
	−0.2942	−0.2927	−0.2906	−0.2877	−0.2843	−0.281	−0.277	−0.2731	−0.2692	−0.2648
	−0.3044	−0.3034	−0.3018	−0.2994	−0.2963	−0.2932	−0.2894	−0.2855	−0.2815	−0.277

I.3 Mode I and Mode II Stress Intensity Factor of Crack C

For completeness the mode I and mode II dimensionless SIF results for crack C in Chapter 6 are given here. These results are when crack C is larger than both crack B and A (Figures I.19 and I.20) and as crack C increases in size relative to crack B (Figures I.21 and I.22) and crack A (Figures I.23 and I.24).

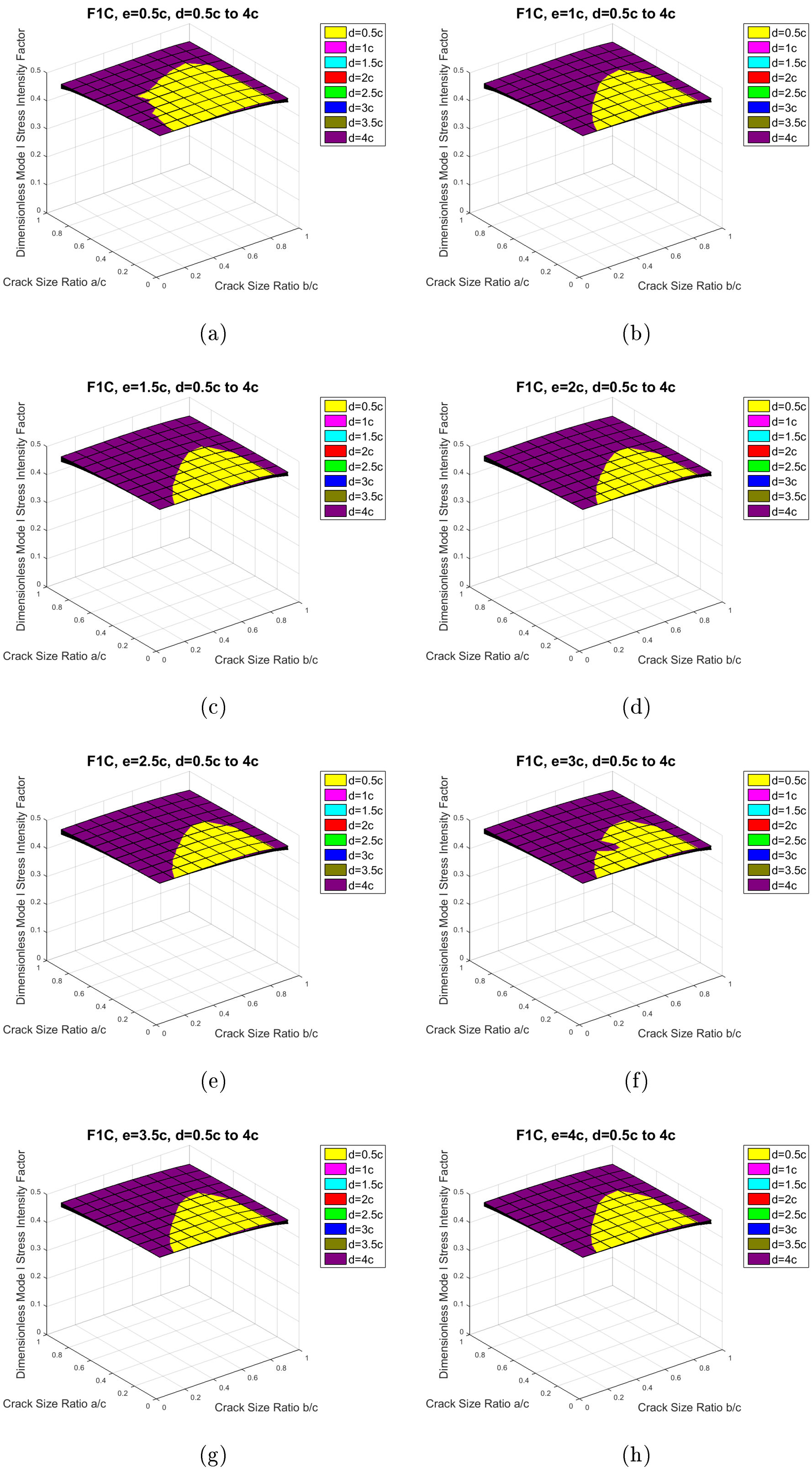
F1C, e=0.5c, d=0.5c to 4c
F1C, e=1c, d=0.5c to 4c
F1C, e=1.5c, d=0.5c to 4c
F1C, e=2c, d=0.5c to 4c
F1C, e=2.5c, d=0.5c to 4c
F1C, e=3c, d=0.5c to 4c
F1C, e=3.5c, d=0.5c to 4c
F1C, e=4c, d=0.5c to 4c
Dimensionless Mode I Stress Intensity Factor
Crack Size Ratio a/c
Crack Size Ratio b/c
d=0.5c
d=1c
d=1.5c
d=2c
d=2.5c
d=3c
d=3.5c
d=4c
(a)
(b)
(c)
(d)
(e)
(f)
(g)
(h)

Figure I.19

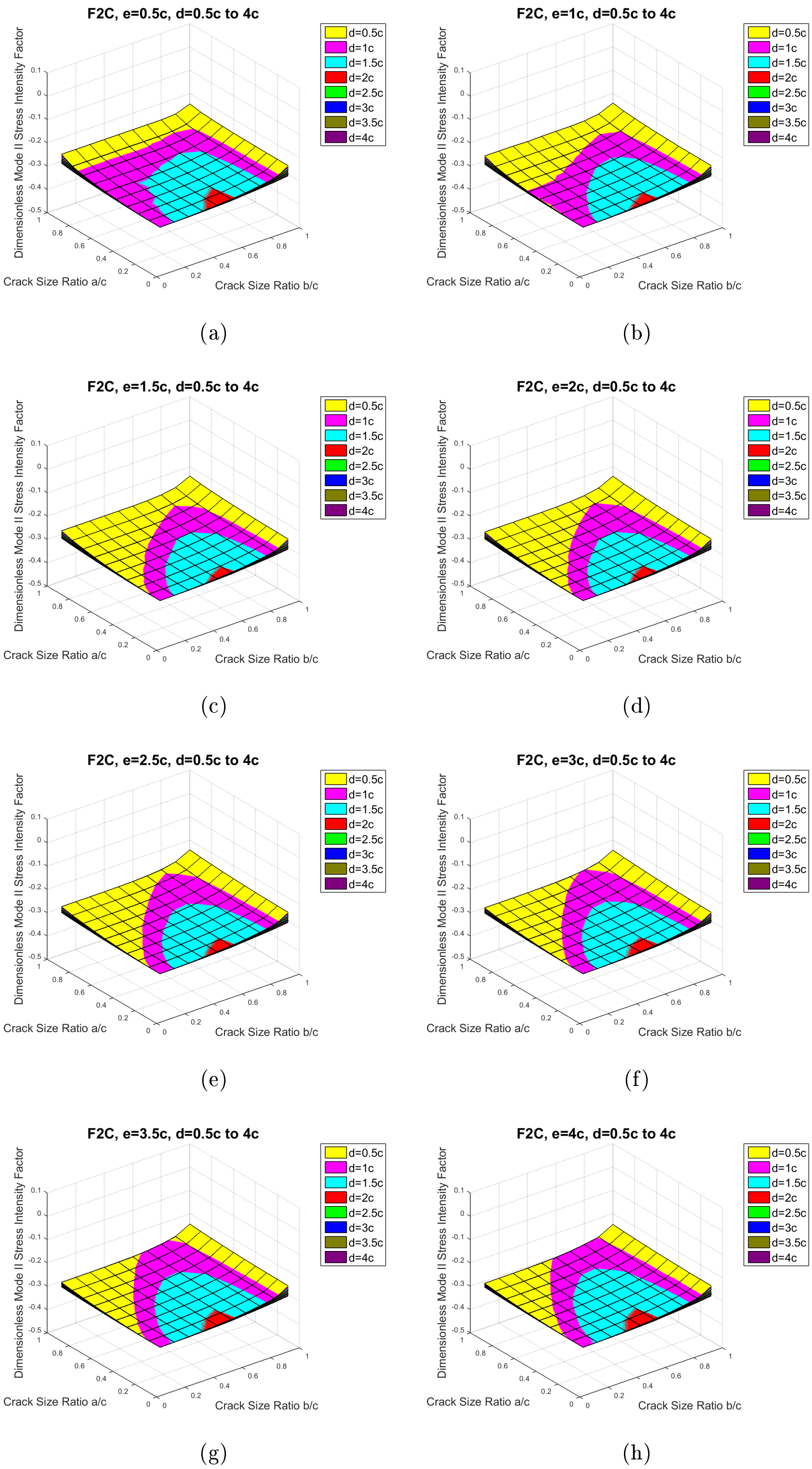
F2C, e=0.5c, d=0.5c to 4c
F2C, e=1c, d=0.5c to 4c
F2C, e=1.5c, d=0.5c to 4c
F2C, e=2c, d=0.5c to 4c
F2C, e=2.5c, d=0.5c to 4c
F2C, e=3c, d=0.5c to 4c
F2C, e=3.5c, d=0.5c to 4c
F2C, e=4c, d=0.5c to 4c
d=0.5c
d=1c
d=1.5c
d=2c
d=2.5c
d=3c
d=3.5c
d=4c
Dimensionless Mode II Stress Intensity Factor
Crack Size Ratio a/c
Crack Size Ratio b/c
(a)
(b)
(c)
(d)
(e)
(f)
(g)
(h)

Figure I.20

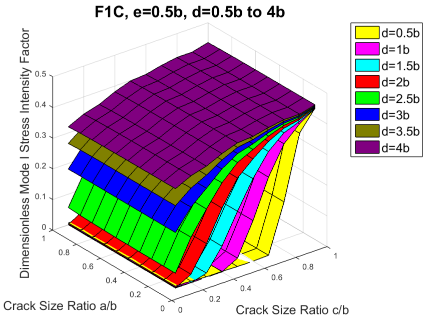

(a)

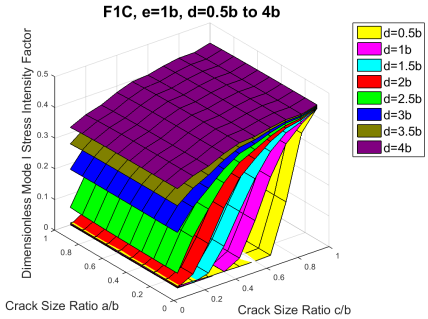

(b)

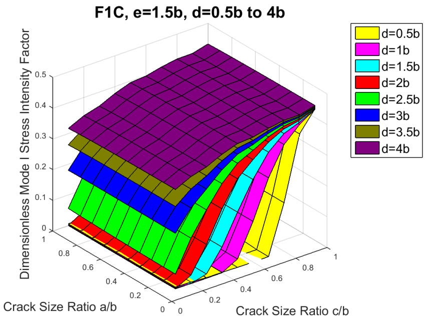

(c)

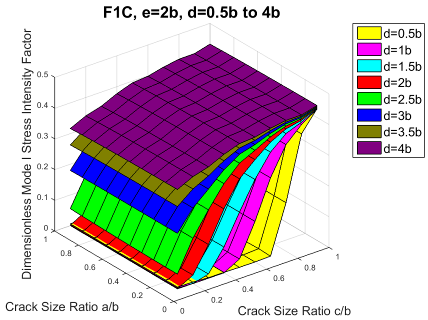

(d)

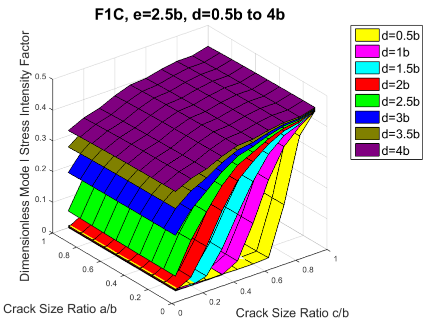

(e)

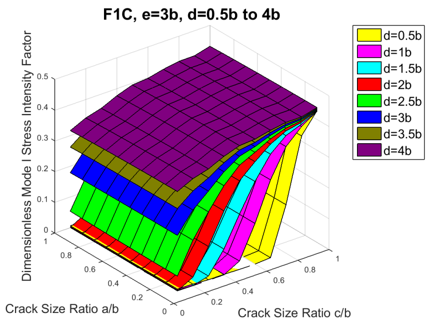

(f)

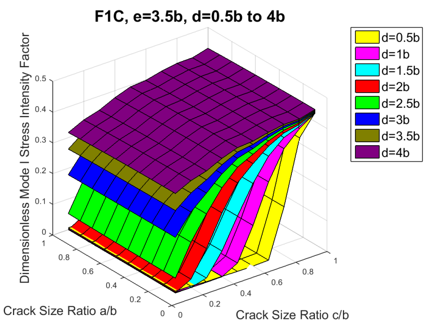

(g)

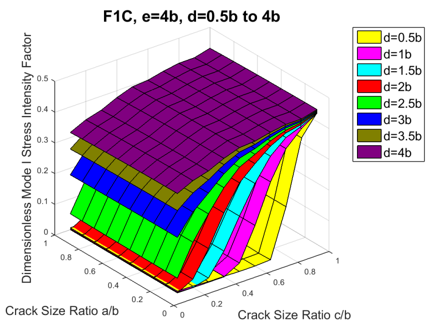

(h)

Figure I.21

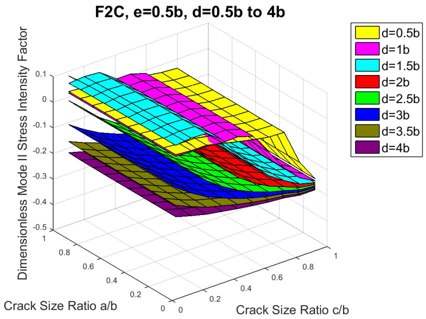

(a)

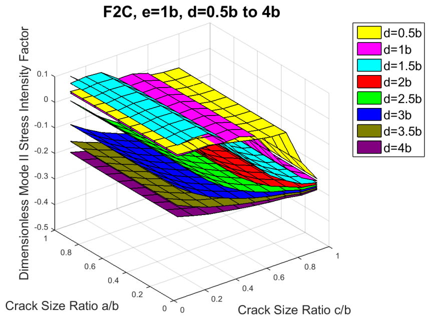

(b)

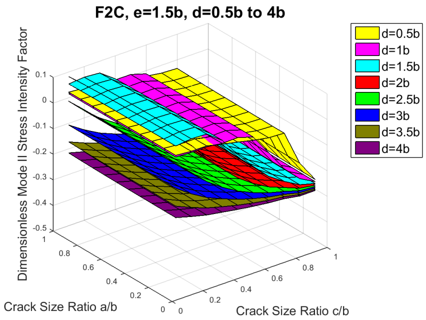

(c)

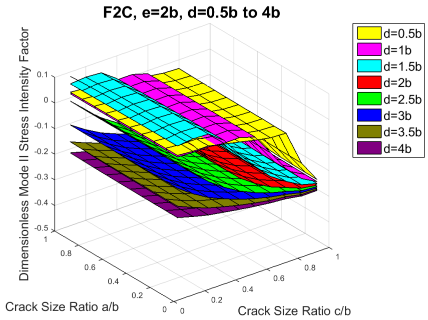

(d)

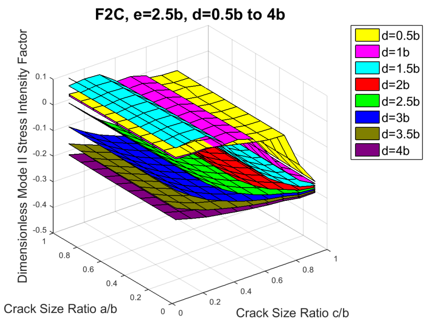

(e)

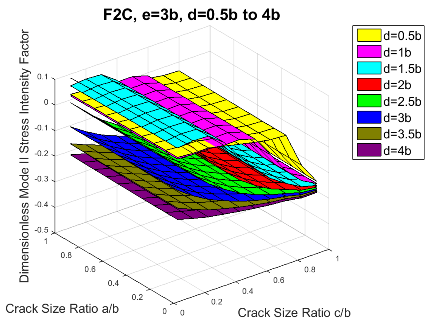

(f)

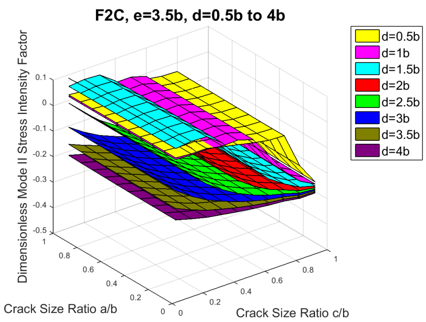

(g)

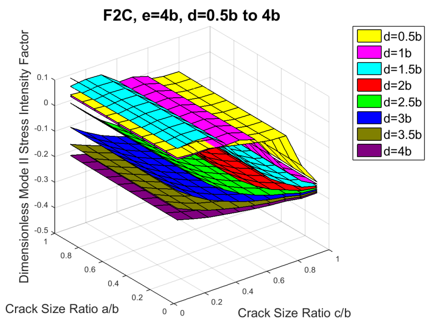

(h)

Figure I.22

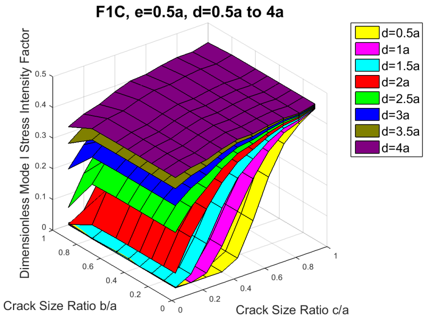

(a)

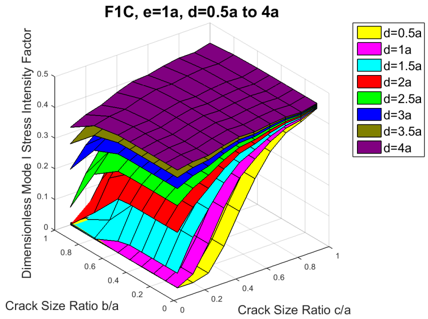

(b)

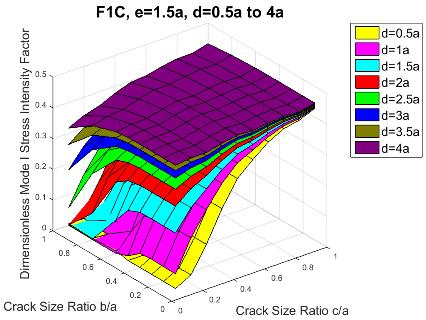

(c)

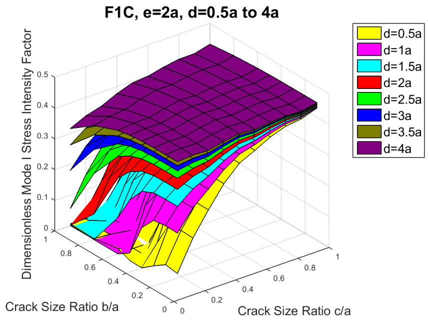

(d)

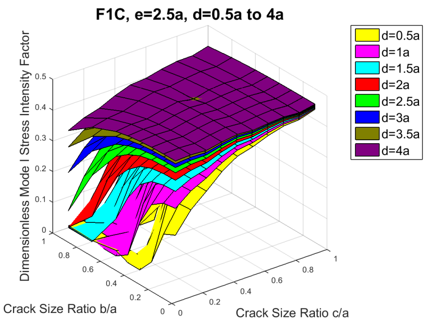

(e)

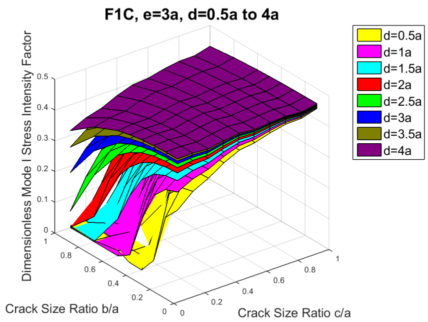

(f)

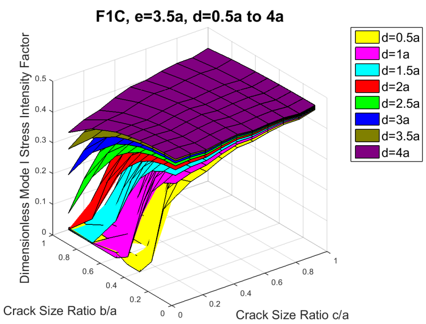

(g)

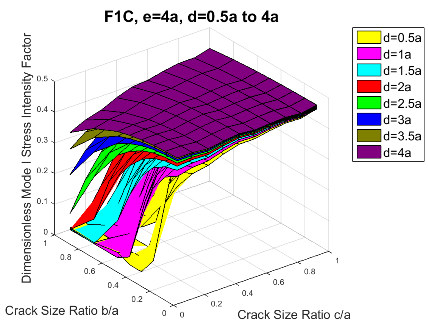

(h)

Figure I.23

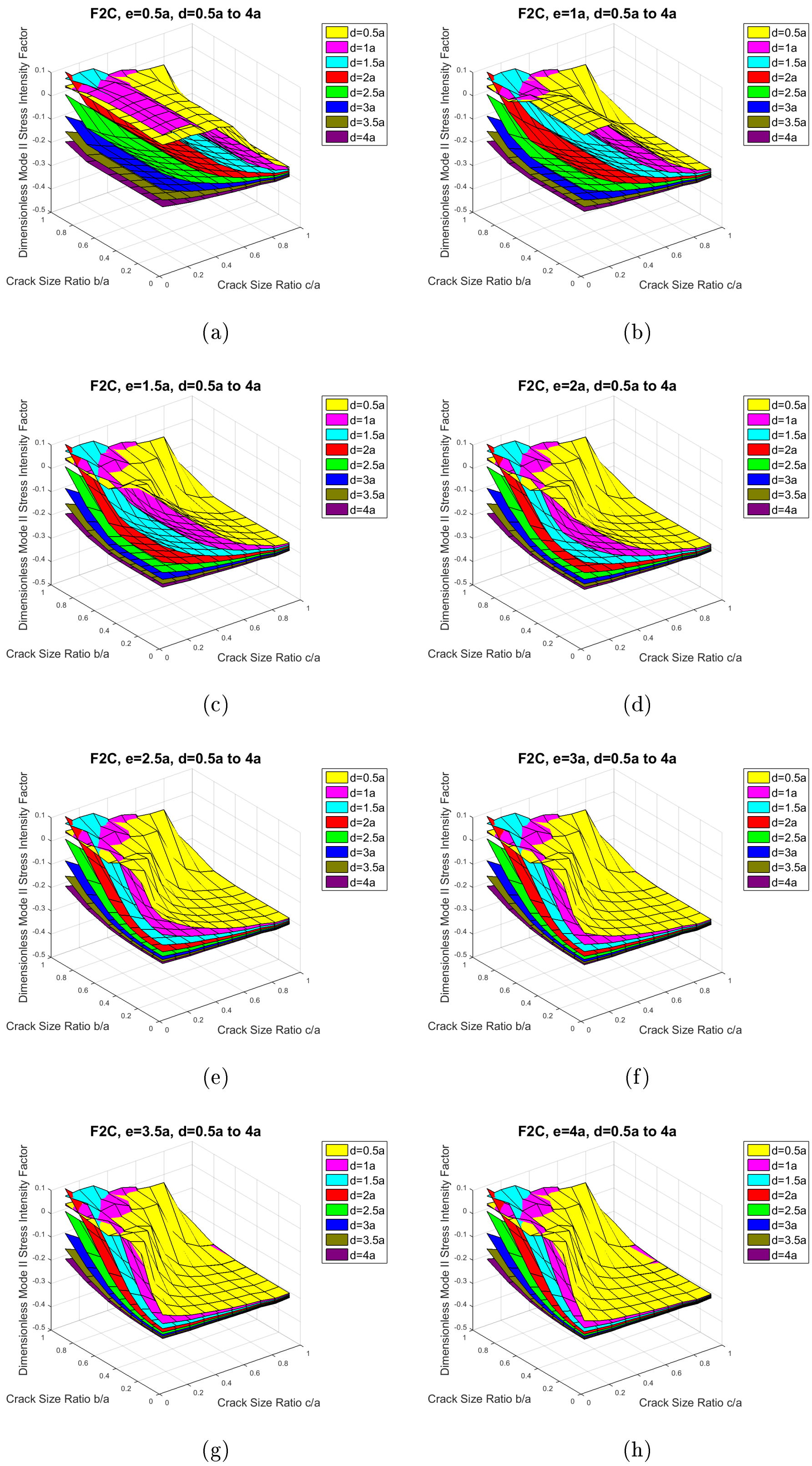

(a) (b) (c) (d) (e) (f) (g) (h)

Figure I.24

The tabulated results show the dimensionless SIF to 4 significant figures. To calculate the SIF use Equations 2.12 and 2.13.

Figure I.19: F1C: e=0.5c & d=0.5c

	b/c									
	0.4644	0.4642	0.4639	0.4632	0.4622	0.4611	0.4588	0.4551	0.4478	0.4285
	0.4639	0.4637	0.4635	0.4629	0.4619	0.4608	0.4585	0.4549	0.4476	0.4286
	0.4631	0.463	0.4629	0.4624	0.4615	0.4603	0.4581	0.4545	0.4472	0.4284
	0.4617	0.4617	0.4617	0.4614	0.4607	0.4596	0.4575	0.4539	0.4467	0.428
a/c	0.4599	0.4599	0.4599	0.4598	0.4593	0.4584	0.4564	0.453	0.4459	0.4274
	0.4577	0.4577	0.4577	0.4577	0.4576	0.4569	0.4553	0.452	0.4452	0.4268
	0.4541	0.4541	0.4541	0.4541	0.4541	0.4539	0.4528	0.4499	0.4435	0.4256
	0.4489	0.4489	0.4489	0.4489	0.4489	0.4489	0.4486	0.4466	0.4408	0.4237
	0.4412	0.4412	0.4412	0.4411	0.441	0.4411	0.4411	0.4404	0.4361	0.4205
	0.4269	0.4269	0.4269	0.4269	0.4269	0.4268	0.4269	0.4268	0.4253	0.4136

Figure I.19: F1C: e=0.5c & d=1c

	b/c									
	0.4643	0.4638	0.4629	0.4616	0.4598	0.4576	0.454	0.4488	0.4412	0.4268
	0.4637	0.4633	0.4625	0.4613	0.4595	0.4574	0.4538	0.4487	0.441	0.4267
	0.4625	0.4624	0.4619	0.4608	0.4591	0.457	0.4535	0.4484	0.4408	0.4266
	0.4607	0.4607	0.4606	0.4598	0.4584	0.4564	0.453	0.4479	0.4404	0.4263
a/c	0.4583	0.4583	0.4583	0.4581	0.4571	0.4553	0.4521	0.4472	0.4397	0.4258
	0.4556	0.4556	0.4556	0.4556	0.4553	0.4539	0.4511	0.4465	0.4391	0.4254
	0.4515	0.4515	0.4515	0.4515	0.4516	0.451	0.449	0.4448	0.4378	0.4245
	0.4461	0.4461	0.4461	0.4461	0.4461	0.4461	0.4453	0.4423	0.4358	0.4232
	0.439	0.439	0.439	0.4389	0.4388	0.4389	0.4388	0.4376	0.4328	0.421
	0.4275	0.4275	0.4275	0.4275	0.4275	0.4275	0.4275	0.4274	0.4254	0.4167

Figure I.19: F1C: e=0.5c & d=1.5c

	b/c									
	0.4642	0.4634	0.4623	0.4605	0.4581	0.4554	0.4513	0.4459	0.4388	0.4274
	0.4635	0.463	0.4619	0.4602	0.4579	0.4552	0.4511	0.4458	0.4387	0.4273
	0.4622	0.4621	0.4613	0.4597	0.4575	0.4549	0.4509	0.4456	0.4385	0.4271
	0.4602	0.4602	0.46	0.4588	0.4568	0.4543	0.4504	0.4452	0.4382	0.4269
a/c	0.4575	0.4575	0.4575	0.4571	0.4557	0.4534	0.4497	0.4446	0.4376	0.4265
	0.4545	0.4545	0.4545	0.4545	0.454	0.4522	0.4489	0.444	0.4372	0.4262
	0.4503	0.4503	0.4503	0.4503	0.4503	0.4496	0.4472	0.4427	0.4361	0.4255
	0.4451	0.4451	0.4451	0.4451	0.4451	0.445	0.4441	0.4407	0.4346	0.4245
	0.4386	0.4386	0.4386	0.4386	0.4384	0.4385	0.4384	0.437	0.4324	0.4228
	0.429	0.429	0.429	0.429	0.429	0.429	0.429	0.4289	0.4268	0.4198

Figure I.19: F1C: e=0.5c & d=2c

	b/c									
	0.4644	0.4636	0.4623	0.4603	0.4576	0.4546	0.4504	0.4452	0.4388	0.4292
	0.4637	0.4631	0.462	0.46	0.4574	0.4545	0.4503	0.4451	0.4387	0.4291
	0.4625	0.4623	0.4614	0.4596	0.4571	0.4542	0.4501	0.4449	0.4385	0.429
	0.4604	0.4604	0.4601	0.4588	0.4566	0.4537	0.4497	0.4446	0.4383	0.4288
a/c	0.4577	0.4577	0.4577	0.4572	0.4555	0.453	0.4491	0.4442	0.4378	0.4285
	0.4547	0.4547	0.4547	0.4546	0.454	0.4519	0.4484	0.4437	0.4374	0.4282
	0.4505	0.4505	0.4505	0.4505	0.4504	0.4496	0.447	0.4426	0.4366	0.4276
	0.4455	0.4455	0.4455	0.4455	0.4455	0.4454	0.4443	0.441	0.4353	0.4269
	0.4396	0.4396	0.4396	0.4395	0.4394	0.4396	0.4393	0.4379	0.4337	0.4256
	0.4313	0.4313	0.4313	0.4313	0.4313	0.4313	0.4312	0.4311	0.4292	0.4232

Figure I.19: F1C: e=0.5c & d=2.5c

	b/c									
	0.4644	0.4637	0.4624	0.4604	0.4577	0.4546	0.4505	0.4455	0.4396	0.4313
	0.4638	0.4633	0.4621	0.4602	0.4575	0.4545	0.4503	0.4454	0.4395	0.4312
	0.4626	0.4625	0.4615	0.4598	0.4572	0.4543	0.4502	0.4452	0.4394	0.4311
	0.4607	0.4607	0.4604	0.4591	0.4567	0.4538	0.4499	0.445	0.4391	0.431
a/c	0.4581	0.4581	0.4581	0.4576	0.4558	0.4532	0.4494	0.4446	0.4388	0.4307
	0.4552	0.4552	0.4552	0.4552	0.4544	0.4523	0.4488	0.4441	0.4384	0.4305
	0.4512	0.4512	0.4512	0.4512	0.4511	0.4502	0.4475	0.4433	0.4377	0.43
	0.4464	0.4464	0.4464	0.4464	0.4464	0.4464	0.4452	0.4419	0.4367	0.4293
	0.441	0.441	0.441	0.4409	0.4408	0.4409	0.4408	0.4393	0.4354	0.4283
	0.4336	0.4336	0.4336	0.4336	0.4336	0.4336	0.4336	0.4335	0.4316	0.4264

Figure I.19: F1C: e=0.5c & d=3c

	b/c									
	0.4645	0.4638	0.4626	0.4607	0.4581	0.4552	0.4512	0.4465	0.441	0.4337
	0.464	0.4634	0.4623	0.4605	0.458	0.455	0.4511	0.4464	0.4409	0.4336
	0.4629	0.4627	0.4618	0.4602	0.4577	0.4548	0.4509	0.4462	0.4408	0.4335
	0.4611	0.4611	0.4608	0.4595	0.4573	0.4545	0.4507	0.446	0.4406	0.4334
a/c	0.4587	0.4587	0.4587	0.4582	0.4565	0.4539	0.4502	0.4457	0.4403	0.4332
	0.456	0.456	0.456	0.4559	0.4552	0.4531	0.4497	0.4453	0.4401	0.433
	0.4522	0.4522	0.4522	0.4522	0.4522	0.4513	0.4486	0.4446	0.4395	0.4325
	0.4479	0.4479	0.4479	0.4479	0.4478	0.4478	0.4466	0.4434	0.4386	0.432
	0.4428	0.4428	0.4428	0.4428	0.4427	0.4428	0.4426	0.4412	0.4375	0.4311
	0.4362	0.4362	0.4362	0.4362	0.4362	0.4362	0.4362	0.436	0.4343	0.4295

Figure I.19: F1C: e=0.5c & d=3.5c

	b/c									
	0.4646	0.464	0.4629	0.4611	0.4587	0.456	0.4523	0.4479	0.4429	0.4362
	0.4641	0.4636	0.4626	0.4609	0.4586	0.4559	0.4522	0.4478	0.4428	0.4362
	0.4631	0.463	0.4622	0.4606	0.4584	0.4557	0.452	0.4477	0.4427	0.4361
	0.4615	0.4615	0.4612	0.4601	0.458	0.4554	0.4518	0.4475	0.4426	0.436
a/c	0.4594	0.4594	0.4594	0.4589	0.4573	0.4549	0.4514	0.4472	0.4423	0.4358
	0.4568	0.4569	0.4569	0.4568	0.4561	0.4542	0.451	0.4469	0.4421	0.4356
	0.4535	0.4535	0.4535	0.4535	0.4534	0.4525	0.45	0.4462	0.4415	0.4353
	0.4494	0.4494	0.4494	0.4494	0.4494	0.4494	0.4483	0.4452	0.4408	0.4348
	0.4449	0.4449	0.4449	0.4448	0.4447	0.4448	0.4448	0.4433	0.4398	0.4341
	0.4389	0.4389	0.4389	0.4389	0.4389	0.4389	0.4389	0.4387	0.4371	0.4327

Figure I.19: F1C: e=0.5c & d=4c

	b/c									
	0.4647	0.4641	0.4631	0.4616	0.4594	0.4569	0.4535	0.4495	0.4449	0.439
	0.4643	0.4638	0.4629	0.4614	0.4593	0.4568	0.4534	0.4494	0.4449	0.4389
	0.4634	0.4632	0.4625	0.4611	0.4591	0.4566	0.4533	0.4493	0.4448	0.4388
	0.462	0.462	0.4617	0.4606	0.4587	0.4563	0.4531	0.4492	0.4447	0.4387
a/c	0.46	0.46	0.46	0.4596	0.4581	0.4559	0.4527	0.4489	0.4444	0.4386
	0.4577	0.4577	0.4577	0.4577	0.4571	0.4553	0.4524	0.4486	0.4442	0.4384
	0.4547	0.4547	0.4547	0.4547	0.4546	0.4538	0.4515	0.4481	0.4438	0.4381
	0.451	0.451	0.451	0.451	0.451	0.451	0.4499	0.4472	0.4431	0.4377
	0.4469	0.4469	0.4469	0.4469	0.4468	0.4469	0.4468	0.4455	0.4423	0.4371
	0.4415	0.4415	0.4415	0.4415	0.4415	0.4415	0.4415	0.4414	0.4399	0.4359

Figure I.19: F1C: e=1c & d=0.5c

	b/c									
a/c	0.4644	0.4641	0.4638	0.4631	0.4621	0.461	0.4587	0.455	0.4477	0.4287
	0.4636	0.4634	0.4631	0.4625	0.4615	0.4604	0.4582	0.4545	0.4473	0.4283
	0.4625	0.4623	0.4621	0.4616	0.4607	0.4596	0.4574	0.4538	0.4466	0.4278
	0.4607	0.4607	0.4605	0.4601	0.4593	0.4583	0.4562	0.4541	0.4456	0.427
	0.4583	0.4583	0.4582	0.458	0.4574	0.4565	0.4545	0.4512	0.4443	0.4257
	0.4556	0.4555	0.4555	0.4555	0.4551	0.4543	0.4526	0.4494	0.4427	0.4247
	0.4515	0.4515	0.4514	0.4514	0.4513	0.4507	0.4493	0.4465	0.4401	0.4227
	0.4461	0.4461	0.4461	0.446	0.446	0.4457	0.4448	0.4424	0.4365	0.4199
	0.439	0.439	0.439	0.439	0.4389	0.4389	0.4384	0.4367	0.4316	0.4159
	0.4275	0.4275	0.4275	0.4257	0.4274	0.4273	0.4272	0.4263	0.4226	0.4091

Figure I.19: F1C: e=1c & d=1c

	b/c									
a/c	0.4643	0.4637	0.4628	0.4615	0.4597	0.4576	0.4539	0.4488	0.4411	0.4268
	0.4635	0.463	0.4622	0.461	0.4592	0.4571	0.4535	0.4484	0.4408	0.4265
	0.4623	0.4619	0.4612	0.4601	0.4584	0.4564	0.4529	0.4478	0.4403	0.4261
	0.4603	0.4602	0.4597	0.4588	0.4572	0.4553	0.4519	0.447	0.4396	0.4255
	0.4577	0.4576	0.4574	0.4568	0.4555	0.4537	0.4506	0.4458	0.4385	0.4247
	0.4547	0.4546	0.4546	0.4543	0.4534	0.4519	0.449	0.4444	0.4373	0.4237
	0.4504	0.4504	0.4504	0.4503	0.4499	0.4488	0.4464	0.4422	0.4353	0.4222
	0.4452	0.4452	0.4452	0.4452	0.4451	0.4444	0.4427	0.4391	0.4327	0.4202
	0.4388	0.4388	0.4388	0.4388	0.4388	0.4385	0.4375	0.4348	0.4292	0.4174
	0.4292	0.4292	0.4292	0.4292	0.4292	0.4291	0.4287	0.4271	0.4228	0.4127

Figure I.19: F1C: e=1c & d=1.5c

	b/c									
a/c	0.4641	0.4634	0.4622	0.4604	0.458	0.4553	0.4513	0.4459	0.4388	0.4273
	0.4634	0.4627	0.4616	0.4599	0.4576	0.4549	0.4509	0.4456	0.4385	0.4271
	0.4622	0.4617	0.4607	0.4591	0.4569	0.4543	0.4504	0.4451	0.4381	0.4268
	0.4602	0.46	0.4593	0.4579	0.4559	0.4534	0.4496	0.4444	0.4375	0.4263
	0.4575	0.4575	0.4571	0.4561	0.4544	0.4521	0.4485	0.4435	0.4367	0.4256
	0.4545	0.4545	0.4544	0.4538	0.4525	0.4505	0.4472	0.4424	0.4357	0.4248
	0.4503	0.4503	0.4503	0.4501	0.4494	0.4479	0.445	0.4406	0.4342	0.4236
	0.4453	0.4453	0.4453	0.4452	0.445	0.4441	0.442	0.4381	0.4321	0.4221
	0.4394	0.4394	0.4394	0.4394	0.4394	0.439	0.4378	0.4348	0.4294	0.42
	0.4311	0.4311	0.4311	0.4311	0.4311	0.431	0.4305	0.4287	0.4245	0.4164

Figure I.19: F1C: e=1c & d=2c

	b/c									
a/c	0.4643	0.4635	0.4622	0.4602	0.4576	0.4546	0.4504	0.4452	0.4387	0.4292
	0.4636	0.4629	0.4617	0.4598	0.4572	0.4543	0.4501	0.4449	0.4385	0.429
	0.4625	0.462	0.4609	0.4591	0.4566	0.4537	0.4497	0.4445	0.4382	0.4287
	0.4607	0.4604	0.4596	0.458	0.4557	0.453	0.449	0.444	0.4377	0.4283
	0.4581	0.458	0.4576	0.4564	0.4544	0.4518	0.4481	0.4432	0.437	0.4277
	0.4551	0.4551	0.455	0.4543	0.4528	0.4505	0.447	0.4423	0.4362	0.4271
	0.4511	0.4511	0.4511	0.4509	0.45	0.4482	0.4452	0.4408	0.435	0.4261
	0.4464	0.4464	0.4464	0.4464	0.4461	0.445	0.4426	0.4388	0.4333	0.4249
	0.4409	0.4409	0.4409	0.441	0.4409	0.4405	0.4391	0.436	0.4311	0.4232
	0.4336	0.4336	0.4336	0.4336	0.4336	0.4335	0.433	0.4311	0.4272	0.4203

Figure I.19: F1C: e=1c & d=2.5c

	b/c									
a/c	0.4644	0.4636	0.4623	0.4603	0.4576	0.4546	0.4504	0.4454	0.4395	0.4313
	0.4638	0.4631	0.4619	0.4599	0.4573	0.4543	0.4502	0.4452	0.4393	0.4311
	0.4627	0.4622	0.4611	0.4593	0.4568	0.4539	0.4498	0.4449	0.4391	0.4309
	0.4611	0.4608	0.46	0.4584	0.456	0.4532	0.4492	0.4444	0.4387	0.4305
	0.4587	0.4586	0.4582	0.4569	0.4549	0.4522	0.4484	0.4437	0.4381	0.4301
	0.4559	0.4559	0.4558	0.4551	0.4534	0.451	0.4475	0.4429	0.4374	0.4295
	0.4522	0.4522	0.4522	0.452	0.451	0.4491	0.446	0.4417	0.4364	0.4287
	0.4478	0.4478	0.4478	0.4478	0.4474	0.4463	0.4438	0.44	0.435	0.4276
	0.4428	0.4428	0.4428	0.4428	0.4428	0.4423	0.4408	0.4377	0.4332	0.4262
	0.4361	0.4361	0.4361	0.4361	0.4361	0.436	0.4355	0.4336	0.4299	0.4239

Figure I.19: F1C: e=1c & d=3c

	b/c									
a/c	0.4645	0.4638	0.4626	0.4607	0.4581	0.4551	0.4511	0.4464	0.441	0.4336
	0.4639	0.4633	0.4621	0.4603	0.4578	0.4549	0.4509	0.4462	0.4408	0.4335
	0.463	0.4625	0.4615	0.4598	0.4573	0.4545	0.4506	0.446	0.4406	0.4333
	0.4615	0.4612	0.4604	0.4589	0.4566	0.4539	0.4501	0.4455	0.4402	0.433
	0.4593	0.4592	0.4588	0.4576	0.4556	0.4531	0.4494	0.4449	0.4397	0.4326
	0.4568	0.4568	0.4566	0.4559	0.4543	0.452	0.4486	0.4443	0.4392	0.4321
	0.4534	0.4534	0.4534	0.4531	0.4522	0.4503	0.4473	0.4432	0.4383	0.4314
	0.4494	0.4494	0.4494	0.4493	0.449	0.4478	0.4454	0.4418	0.4371	0.4305
	0.4448	0.4448	0.4448	0.4448	0.4448	0.4443	0.4428	0.4398	0.4356	0.4293
	0.4388	0.4388	0.4388	0.4388	0.4388	0.4387	0.4381	0.4363	0.4328	0.4274

Figure I.19: F1C: e=1c & d=3.5c

	b/c									
a/c	0.4646	0.4639	0.4628	0.4611	0.4587	0.4559	0.4522	0.4479	0.4429	0.4362
	0.4641	0.4635	0.4624	0.4608	0.4584	0.4557	0.452	0.4477	0.4427	0.4361
	0.4632	0.4628	0.4619	0.4603	0.458	0.4554	0.4518	0.4474	0.4425	0.4359
	0.4619	0.4616	0.4609	0.4595	0.4574	0.4549	0.4513	0.4471	0.4422	0.4357
	0.4599	0.4599	0.4595	0.4584	0.4566	0.4541	0.4507	0.4466	0.4418	0.4353
	0.4577	0.4576	0.4575	0.4569	0.4554	0.4532	0.45	0.446	0.4413	0.4349
	0.4546	0.4546	0.4546	0.4544	0.4535	0.4517	0.4488	0.4451	0.4405	0.4343
	0.451	0.451	0.451	0.4509	0.4506	0.4495	0.4472	0.4438	0.4395	0.4335
	0.4468	0.4468	0.4468	0.4468	0.4468	0.4464	0.4449	0.4421	0.4382	0.4325
	0.4414	0.4414	0.4414	0.4414	0.4414	0.4414	0.4408	0.4391	0.4358	0.4308

Figure I.19: F1C: e=1c & d=4c

	b/c									
a/c	0.4647	0.4641	0.4631	0.4615	0.4594	0.4568	0.4535	0.4495	0.4449	0.4389
	0.4642	0.4637	0.4628	0.4612	0.4591	0.4566	0.4533	0.4493	0.4448	0.4388
	0.4635	0.4631	0.4622	0.4608	0.4588	0.4563	0.453	0.4491	0.4446	0.4387
	0.4623	0.462	0.4614	0.4601	0.4582	0.4559	0.4527	0.4488	0.4443	0.4384
	0.4605	0.4605	0.4601	0.4591	0.4574	0.4552	0.4521	0.4483	0.4439	0.4381
	0.4585	0.4585	0.4584	0.4578	0.4564	0.4544	0.4515	0.4478	0.4435	0.4378
	0.4557	0.4557	0.4557	0.4555	0.4547	0.4531	0.4504	0.447	0.4428	0.4372
	0.4525	0.4525	0.4525	0.4524	0.4522	0.4511	0.449	0.4459	0.442	0.4366
	0.4488	0.4488	0.4488	0.4488	0.4487	0.4483	0.447	0.4444	0.4408	0.4357
	0.4439	0.4439	0.4439	0.4439	0.4439	0.4439	0.4433	0.4417	0.4387	0.4342

Figure I.19: F1C: e=1.5c & d=0.5c

	b/c									
	0.4644	0.4641	0.4638	0.4631	0.4621	0.4609	0.4587	0.455	0.4477	0.4286
	0.4636	0.4633	0.463	0.4624	0.4614	0.4602	0.458	0.4544	0.4471	0.4281
	0.4623	0.462	0.4618	0.4612	0.4603	0.4592	0.457	0.4534	0.4462	0.4274
	0.4603	0.4601	0.4599	0.4594	0.4586	0.4576	0.4555	0.452	0.4449	0.4263
a/c	0.4576	0.4576	0.4574	0.4571	0.4563	0.4554	0.4534	0.4501	0.4432	0.4249
	0.4546	0.4546	0.4546	0.4543	0.4538	0.4529	0.4511	0.4479	0.4412	0.4233
	0.4504	0.4504	0.4504	0.4503	0.4499	0.4492	0.4476	0.4447	0.4383	0.4209
	0.4452	0.4451	0.4451	0.4451	0.4449	0.4444	0.4431	0.4405	0.4345	0.4177
	0.4387	0.4387	0.4387	0.4386	0.4386	0.4383	0.4373	0.4351	0.4296	0.4137
	0.4291	0.4291	0.429	0.429	0.4289	0.4288	0.4283	0.4266	0.422	0.4074

Figure I.19: F1C: e=1.5c & d=1c

	b/c									
	0.4643	0.4637	0.4628	0.4615	0.4597	0.4575	0.4539	0.4487	0.4411	0.4268
	0.4635	0.463	0.4621	0.4609	0.4591	0.4569	0.4534	0.4483	0.4407	0.4264
	0.4623	0.4618	0.461	0.4598	0.4581	0.456	0.4525	0.4475	0.44	0.4258
	0.4603	0.4599	0.4593	0.4582	0.4566	0.4547	0.4513	0.4464	0.439	0.425
a/c	0.4576	0.4574	0.457	0.4561	0.4547	0.4529	0.4496	0.4449	0.4376	0.4238
	0.4546	0.4545	0.4543	0.4536	0.4524	0.4508	0.4478	0.4432	0.4361	0.4226
	0.4504	0.4504	0.4503	0.45	0.4491	0.4477	0.445	0.4407	0.4337	0.4208
	0.4454	0.4454	0.4453	0.4452	0.4447	0.4437	0.4414	0.4375	0.431	0.4184
	0.4395	0.4395	0.4394	0.4394	0.4392	0.4385	0.4368	0.4334	0.4274	0.4155
	0.4312	0.4312	0.4311	0.4311	0.431	0.4307	0.4296	0.427	0.4218	0.4109

Figure I.19: F1C: e=1.5c & d=1.5c

	b/c									
	0.4642	0.4634	0.4622	0.4604	0.458	0.4553	0.4512	0.4459	0.4388	0.4273
	0.4634	0.4627	0.4616	0.4598	0.4575	0.4548	0.4508	0.4455	0.4384	0.427
	0.4622	0.4616	0.4606	0.4589	0.4566	0.454	0.4501	0.4448	0.4379	0.4265
	0.4604	0.4599	0.459	0.4575	0.4554	0.4529	0.4491	0.4439	0.437	0.4258
a/c	0.4579	0.4576	0.4569	0.4556	0.4537	0.4514	0.4477	0.4427	0.436	0.4249
	0.4549	0.4548	0.4544	0.4534	0.4517	0.4496	0.4462	0.4413	0.4348	0.4239
	0.4509	0.4509	0.4508	0.4501	0.4489	0.447	0.4439	0.4393	0.433	0.4224
	0.4462	0.4462	0.4461	0.4459	0.4451	0.4436	0.4409	0.4367	0.4307	0.4206
	0.4407	0.4407	0.4407	0.4406	0.4403	0.4393	0.4371	0.4335	0.4279	0.4183
	0.4334	0.4333	0.4333	0.4333	0.4332	0.4327	0.4313	0.4285	0.4235	0.4147

Figure I.19: F1C: e=1.5c & d=2c

	b/c									
	0.4644	0.4635	0.4622	0.4602	0.4576	0.4546	0.4504	0.4452	0.4387	0.4291
	0.4637	0.4629	0.4617	0.4597	0.4571	0.4542	0.45	0.4448	0.4384	0.4289
	0.4626	0.4619	0.4608	0.4589	0.4564	0.4535	0.4494	0.4443	0.438	0.4285
	0.4609	0.4604	0.4594	0.4577	0.4553	0.4525	0.4485	0.4435	0.4373	0.4279
a/c	0.4586	0.4582	0.4575	0.456	0.4538	0.4512	0.4474	0.4425	0.4364	0.4271
	0.4559	0.4557	0.4552	0.454	0.4521	0.4497	0.4461	0.4414	0.4354	0.4263
	0.4521	0.4521	0.4519	0.4511	0.4496	0.4475	0.4442	0.4397	0.4339	0.4251
	0.4477	0.4477	0.4477	0.4473	0.4463	0.4446	0.4417	0.4376	0.4321	0.4236
	0.4427	0.4427	0.4427	0.4426	0.4421	0.4409	0.4385	0.4349	0.4298	0.4217
	0.4361	0.436	0.436	0.436	0.4359	0.4352	0.4337	0.4308	0.4262	0.4188

Figure I.19: F1C: e=1.5c & d=2.5c

	b/c									
	0.4644	0.4636	0.4623	0.4603	0.4576	0.4546	0.4504	0.4454	0.4395	0.4313
	0.4638	0.4631	0.4618	0.4599	0.4572	0.4542	0.4501	0.4451	0.4393	0.431
	0.4629	0.4622	0.461	0.4592	0.4566	0.4536	0.4496	0.4447	0.4389	0.4307
	0.4613	0.4608	0.4598	0.4581	0.4556	0.4528	0.4488	0.444	0.4383	0.4302
a/c	0.4592	0.4589	0.4581	0.4566	0.4543	0.4517	0.4478	0.4431	0.4375	0.4295
	0.4567	0.4566	0.456	0.4548	0.4529	0.4504	0.4467	0.4422	0.4367	0.4288
	0.4533	0.4533	0.4531	0.4522	0.4506	0.4484	0.4451	0.4408	0.4355	0.4278
	0.4493	0.4493	0.4492	0.4488	0.4477	0.4459	0.443	0.439	0.4339	0.4265
	0.4447	0.4447	0.4447	0.4446	0.444	0.4427	0.4403	0.4367	0.432	0.4249
	0.4387	0.4387	0.4387	0.4387	0.4385	0.4378	0.4362	0.4333	0.429	0.4225

Figure I.19: F1C: e=1.5c & d=3c

	b/c									
	0.4645	0.4638	0.4626	0.4606	0.4581	0.4551	0.4511	0.4464	0.441	0.4336
	0.464	0.4633	0.4621	0.4602	0.4577	0.4548	0.4508	0.4462	0.4407	0.4334
	0.4631	0.4625	0.4614	0.4596	0.4572	0.4543	0.4504	0.4458	0.4404	0.4331
	0.4617	0.4612	0.4603	0.4586	0.4563	0.4536	0.4498	0.4452	0.4399	0.4327
a/c	0.4598	0.4595	0.4588	0.4573	0.4552	0.4526	0.4489	0.4444	0.4392	0.4321
	0.4576	0.4574	0.4569	0.4558	0.4539	0.4514	0.4479	0.4436	0.4385	0.4315
	0.4545	0.4545	0.4542	0.4535	0.4519	0.4497	0.4465	0.4424	0.4375	0.4306
	0.4509	0.4509	0.4508	0.4504	0.4493	0.4475	0.4447	0.4408	0.4361	0.4295
	0.4468	0.4468	0.4467	0.4466	0.446	0.4447	0.4423	0.4389	0.4345	0.4282
	0.4414	0.4413	0.4413	0.4413	0.4411	0.4404	0.4388	0.4359	0.432	0.4261

Figure I.19: F1C: e=1.5c & d=3.5c

	b/c									
	0.4646	0.4639	0.4628	0.4611	0.4587	0.4559	0.4522	0.4478	0.4428	0.4362
	0.4641	0.4635	0.4624	0.4607	0.4584	0.4556	0.452	0.4476	0.4426	0.436
	0.4633	0.4628	0.4618	0.4601	0.4579	0.4552	0.4516	0.4473	0.4423	0.4358
	0.4621	0.4617	0.4608	0.4593	0.4571	0.4545	0.451	0.4468	0.4419	0.4354
a/c	0.4604	0.4601	0.4594	0.4581	0.4561	0.4537	0.4502	0.4461	0.4413	0.4349
	0.4584	0.4583	0.4578	0.4567	0.4549	0.4527	0.4494	0.4454	0.4407	0.4344
	0.4557	0.4556	0.4554	0.4546	0.4532	0.4512	0.4481	0.4443	0.4398	0.4336
	0.4524	0.4524	0.4523	0.4519	0.4509	0.4492	0.4465	0.4429	0.4386	0.4326
	0.4487	0.4487	0.4487	0.4485	0.448	0.4467	0.4445	0.4413	0.4372	0.4315
	0.4439	0.4438	0.4438	0.4438	0.4436	0.443	0.4413	0.4387	0.435	0.4297

Figure I.19: F1C: e=1.5c & d=4c

	b/c									
	0.4647	0.4641	0.4631	0.4615	0.4593	0.4568	0.4535	0.4495	0.4449	0.4389
	0.4643	0.4637	0.4627	0.4612	0.4591	0.4566	0.4532	0.4493	0.4447	0.4388
	0.4636	0.4631	0.4622	0.4607	0.4586	0.4562	0.4529	0.449	0.4445	0.4385
	0.4625	0.4621	0.4613	0.4599	0.4579	0.4556	0.4524	0.4485	0.4441	0.4382
a/c	0.461	0.4607	0.4601	0.4589	0.457	0.4548	0.4517	0.4479	0.4436	0.4378
	0.4592	0.459	0.4586	0.4576	0.456	0.4539	0.4509	0.4473	0.443	0.4373
	0.4567	0.4567	0.4565	0.4558	0.4545	0.4526	0.4498	0.4463	0.4422	0.4366
	0.4538	0.4538	0.4537	0.4534	0.4524	0.4509	0.4484	0.4451	0.4412	0.4357
	0.4505	0.4504	0.4504	0.4503	0.4498	0.4487	0.4466	0.4436	0.4399	0.4347
	0.4461	0.4461	0.4461	0.4461	0.4459	0.4453	0.4438	0.4413	0.438	0.4332

Figure I.19: F1C: e=2c & d=0.5c

	b/c									
	0.4644	0.4641	0.4638	0.4631	0.4621	0.4609	0.4587	0.455	0.4477	0.4286
	0.4636	0.4633	0.463	0.4623	0.4613	0.4602	0.458	0.4543	0.4472	0.4281
	0.4623	0.462	0.4617	0.4611	0.4602	0.4591	0.4569	0.4533	0.4461	0.4272
	0.4603	0.4601	0.4598	0.4593	0.4584	0.4573	0.4552	0.4517	0.4446	0.4257
a/c	0.4576	0.4574	0.4572	0.4568	0.456	0.455	0.4529	0.4496	0.4427	0.4243
	0.4546	0.4545	0.4543	0.454	0.4533	0.4524	0.4504	0.4472	0.4405	0.4225
	0.4504	0.4504	0.4503	0.4501	0.4495	0.4487	0.447	0.4439	0.4374	0.4199
	0.4454	0.4454	0.4454	0.4452	0.4448	0.4442	0.4427	0.4398	0.4337	0.4167
	0.4395	0.4394	0.4394	0.4394	0.4392	0.4387	0.4374	0.4349	0.4291	0.4128
	0.4312	0.4311	0.4311	0.4311	0.431	0.4307	0.4297	0.4276	0.4224	0.4072

Figure I.19: F1C: e=2c & d=1c

	b/c									
	0.4643	0.4637	0.4628	0.4615	0.4597	0.4575	0.4539	0.4487	0.4411	0.4267
	0.4636	0.463	0.4622	0.4609	0.4591	0.4569	0.4533	0.4482	0.4406	0.4263
	0.4624	0.4618	0.461	0.4598	0.458	0.456	0.4524	0.4474	0.4398	0.4257
	0.4605	0.46	0.4593	0.4581	0.4565	0.4545	0.4511	0.4461	0.4387	0.4247
a/c	0.4579	0.4576	0.457	0.4559	0.4544	0.4525	0.4492	0.4444	0.4372	0.4233
	0.455	0.4548	0.4543	0.4535	0.4521	0.4503	0.4472	0.4426	0.4355	0.4219
	0.4511	0.4509	0.4507	0.45	0.4488	0.4473	0.4444	0.44	0.4331	0.4199
	0.4463	0.4463	0.4462	0.4457	0.4449	0.4435	0.4409	0.4368	0.4303	0.4175
	0.4409	0.4409	0.4408	0.4406	0.44	0.439	0.4367	0.433	0.4268	0.4145
	0.4335	0.4334	0.4334	0.4334	0.4331	0.4324	0.4306	0.4274	0.4217	0.4101

Figure I.19: F1C: e=2c & d=1.5c

	b/c									
	0.4642	0.4634	0.4622	0.4604	0.458	0.4553	0.4512	0.4459	0.4388	0.4273
	0.4635	0.4628	0.4616	0.4598	0.4575	0.4548	0.4507	0.4454	0.4384	0.4269
	0.4624	0.4617	0.4606	0.4589	0.4566	0.454	0.45	0.4447	0.4377	0.4264
	0.4607	0.4601	0.4591	0.4574	0.4552	0.4527	0.4488	0.4437	0.4368	0.4255
a/c	0.4583	0.4578	0.457	0.4555	0.4535	0.4511	0.4473	0.4423	0.4356	0.4245
	0.4556	0.4553	0.4546	0.4533	0.4515	0.4492	0.4457	0.4408	0.4342	0.4233
	0.4519	0.4518	0.4513	0.4503	0.4487	0.4466	0.4433	0.4387	0.4323	0.4217
	0.4476	0.4475	0.4473	0.4465	0.4453	0.4435	0.4405	0.4361	0.43	0.4197
	0.4425	0.4425	0.4424	0.442	0.4411	0.4397	0.437	0.433	0.4272	0.4173
	0.4359	0.4358	0.4358	0.4357	0.4352	0.4342	0.432	0.4285	0.4232	0.4139

Figure I.19: F1C: e=2c & d=2c

	b/c									
	0.4644	0.4636	0.4622	0.4602	0.4576	0.4546	0.4504	0.4452	0.4387	0.4292
	0.4638	0.463	0.4617	0.4597	0.4571	0.4541	0.45	0.4448	0.4384	0.4288
	0.4628	0.462	0.4608	0.4589	0.4563	0.4534	0.4493	0.4442	0.4378	0.4283
	0.4612	0.4605	0.4594	0.4576	0.4552	0.4524	0.4483	0.4433	0.437	0.4277
a/c	0.4591	0.4585	0.4576	0.4559	0.4536	0.4509	0.4471	0.4422	0.436	0.4268
	0.4566	0.4562	0.4554	0.454	0.4519	0.4494	0.4456	0.4409	0.4349	0.4258
	0.4533	0.453	0.4525	0.4513	0.4495	0.4472	0.4437	0.4391	0.4333	0.4244
	0.4493	0.4492	0.4489	0.448	0.4465	0.4445	0.4413	0.437	0.4314	0.4228
	0.4447	0.4447	0.4446	0.444	0.4429	0.4412	0.4384	0.4344	0.4291	0.4208
	0.4387	0.4387	0.4386	0.4384	0.4378	0.4365	0.4342	0.4307	0.4258	0.418

Figure I.19: F1C: e=2c & d=2.5c

	b/c									
	0.4644	0.4636	0.4623	0.4603	0.4576	0.4546	0.4504	0.4454	0.4395	0.4312
	0.4639	0.4631	0.4619	0.4599	0.4572	0.4542	0.4501	0.4451	0.4392	0.431
	0.463	0.4623	0.4611	0.4591	0.4565	0.4536	0.4495	0.4446	0.4388	0.4306
	0.4616	0.461	0.4598	0.458	0.4555	0.4526	0.4487	0.4438	0.4381	0.43
a/c	0.4597	0.4592	0.4582	0.4565	0.4542	0.4514	0.4475	0.4428	0.4372	0.4292
	0.4575	0.4571	0.4563	0.4548	0.4526	0.45	0.4463	0.4417	0.4362	0.4284
	0.4544	0.4542	0.4536	0.4524	0.4505	0.4481	0.4446	0.4402	0.4349	0.4272
	0.4508	0.4508	0.4504	0.4495	0.4479	0.4458	0.4426	0.4384	0.4333	0.4258
	0.4467	0.4467	0.4465	0.446	0.4448	0.443	0.4401	0.4362	0.4313	0.4241
	0.4413	0.4413	0.4413	0.441	0.4403	0.4389	0.4365	0.4331	0.4286	0.4218

Figure I.19: F1C: e=2c & d=3c

	b/c									
	0.4645	0.4638	0.4626	0.4607	0.4581	0.4551	0.4511	0.4464	0.441	0.4336
	0.464	0.4633	0.4621	0.4603	0.4577	0.4548	0.4508	0.4461	0.4407	0.4334
	0.4632	0.4626	0.4614	0.4596	0.4571	0.4542	0.4503	0.4457	0.4403	0.433
	0.462	0.4614	0.4603	0.4586	0.4562	0.4534	0.4496	0.445	0.4397	0.4325
a/c	0.4603	0.4598	0.4588	0.4573	0.455	0.4523	0.4486	0.4441	0.4389	0.4318
	0.4583	0.4579	0.4571	0.4557	0.4537	0.4511	0.4476	0.4432	0.4381	0.4311
	0.4556	0.4554	0.4548	0.4536	0.4518	0.4494	0.4461	0.4419	0.4369	0.4301
	0.4523	0.4522	0.4519	0.451	0.4495	0.4474	0.4443	0.4403	0.4356	0.4289
	0.4486	0.4486	0.4484	0.4479	0.4467	0.4449	0.4421	0.4384	0.4339	0.4273
	0.4438	0.4438	0.4437	0.4435	0.4427	0.4414	0.439	0.4357	0.4315	0.4254

Figure I.19: F1C: e=2c & d=3.5c

	b/c									
	0.4646	0.464	0.4628	0.4611	0.4587	0.4559	0.4522	0.4478	0.4428	0.4362
	0.4642	0.4635	0.4624	0.4607	0.4584	0.4556	0.4519	0.4476	0.4426	0.436
	0.4635	0.4629	0.4618	0.4601	0.4578	0.4551	0.4515	0.4472	0.4423	0.4357
	0.4623	0.4618	0.4608	0.4592	0.457	0.4544	0.4509	0.4466	0.4417	0.4352
a/c	0.4608	0.4604	0.4595	0.458	0.456	0.4535	0.45	0.4458	0.441	0.4346
	0.459	0.4587	0.458	0.4567	0.4548	0.4524	0.4491	0.445	0.4403	0.434
	0.4566	0.4564	0.4559	0.4548	0.4531	0.4509	0.4477	0.4439	0.4393	0.4331
	0.4537	0.4536	0.4533	0.4525	0.451	0.4491	0.4462	0.4425	0.4381	0.432
	0.4504	0.4504	0.4502	0.4497	0.4486	0.4469	0.4443	0.4408	0.4366	0.4308
	0.446	0.446	0.446	0.4458	0.4451	0.4438	0.4415	0.4384	0.4346	0.429

Figure I.19: F1C: e=2c & d=4c

	b/c									
	0.4647	0.4641	0.4631	0.4615	0.4593	0.4568	0.4534	0.4495	0.4449	0.4389
	0.4643	0.4637	0.4628	0.4612	0.4591	0.4566	0.4532	0.4492	0.4447	0.4387
	0.4637	0.4631	0.4622	0.4607	0.4586	0.4561	0.4528	0.4489	0.4444	0.4385
	0.4627	0.4622	0.4613	0.4599	0.4579	0.4555	0.4522	0.4484	0.4439	0.438
a/c	0.4613	0.4609	0.4601	0.4588	0.4569	0.4546	0.4515	0.4477	0.4433	0.4375
	0.4597	0.4594	0.4588	0.4576	0.4558	0.4537	0.4506	0.4469	0.4427	0.4369
	0.4575	0.4574	0.4569	0.4559	0.4543	0.4523	0.4495	0.4459	0.4417	0.4361
	0.4549	0.4549	0.4546	0.4538	0.4525	0.4507	0.4481	0.4447	0.4407	0.4352
	0.452	0.452	0.4518	0.4513	0.4503	0.4488	0.4464	0.4432	0.4394	0.4341
	0.4481	0.4481	0.4481	0.4479	0.4472	0.446	0.4439	0.4411	0.4376	0.4326

Figure I.19: F1C: e=2.5c & d=0.5c

	b/c									
	0.4644	0.4641	0.4638	0.4631	0.4621	0.461	0.4587	0.455	0.4477	0.4286
	0.4637	0.4634	0.463	0.4624	0.4614	0.4603	0.458	0.4543	0.4471	0.4281
	0.4624	0.4622	0.4619	0.4612	0.4602	0.4591	0.4569	0.4533	0.4461	0.4272
	0.4605	0.4603	0.46	0.4594	0.4585	0.4574	0.4552	0.4517	0.4446	0.4259
a/c	0.4579	0.4577	0.4575	0.457	0.4561	0.4551	0.453	0.4495	0.4426	0.4241
	0.455	0.4548	0.4547	0.4542	0.4534	0.4524	0.4504	0.4471	0.4404	0.4222
	0.451	0.4509	0.4508	0.4504	0.4497	0.4489	0.447	0.4438	0.4373	0.4196
	0.4463	0.4463	0.4462	0.4459	0.4453	0.4446	0.4429	0.4399	0.4336	0.4164
	0.4409	0.4409	0.4408	0.4407	0.4402	0.4396	0.4381	0.4353	0.4293	0.4127
	0.4335	0.4334	0.4334	0.4334	0.4331	0.4326	0.4314	0.4289	0.4234	0.4076

Figure I.19: F1C: e=2.5c & d=1c

	b/c									
	0.4643	0.4637	0.4629	0.4615	0.4597	0.4575	0.4539	0.4487	0.4411	0.4267
	0.4637	0.4631	0.4622	0.4609	0.4591	0.457	0.4534	0.4482	0.4406	0.4263
	0.4626	0.462	0.4612	0.4599	0.4581	0.456	0.4525	0.4474	0.4398	0.4256
	0.4608	0.4603	0.4595	0.4583	0.4566	0.4545	0.4511	0.4461	0.4386	0.4246
a/c	0.4584	0.458	0.4573	0.4562	0.4545	0.4526	0.4492	0.4444	0.437	0.4232
	0.4557	0.4553	0.4547	0.4537	0.4522	0.4504	0.4472	0.4424	0.4353	0.4216
	0.452	0.4518	0.4513	0.4504	0.4491	0.4474	0.4444	0.4398	0.4329	0.4195
	0.4476	0.4475	0.4472	0.4465	0.4453	0.4438	0.441	0.4367	0.43	0.4171
	0.4427	0.4426	0.4424	0.4419	0.441	0.4397	0.4371	0.4331	0.4267	0.4142
	0.436	0.436	0.4359	0.4357	0.435	0.4339	0.4318	0.4281	0.4221	0.4101

Figure I.19: F1C: e=2.5c & d=1.5c

	b/c									
	0.4642	0.4634	0.4622	0.4604	0.458	0.4553	0.4512	0.4459	0.4388	0.4273
	0.4636	0.4628	0.4617	0.4599	0.4575	0.4548	0.4508	0.4454	0.4384	0.4269
	0.4626	0.4619	0.4607	0.459	0.4566	0.454	0.45	0.4447	0.4377	0.4263
	0.461	0.4603	0.4593	0.4576	0.4553	0.4528	0.4488	0.4436	0.4367	0.4255
a/c	0.4588	0.4582	0.4573	0.4557	0.4536	0.4511	0.4473	0.4422	0.4354	0.4243
	0.4564	0.4559	0.455	0.4536	0.4516	0.4492	0.4456	0.4406	0.434	0.423
	0.453	0.4526	0.4519	0.4507	0.4489	0.4467	0.4432	0.4385	0.432	0.4213
	0.449	0.4488	0.4483	0.4473	0.4457	0.4437	0.4405	0.4359	0.4297	0.4193
	0.4445	0.4444	0.444	0.4433	0.4419	0.4402	0.4372	0.433	0.427	0.4169
	0.4385	0.4385	0.4383	0.4378	0.4368	0.4354	0.4328	0.4289	0.4233	0.4137

Figure I.19: F1C: e=2.5c & d=2c

	b/c									
	0.4644	0.4636	0.4623	0.4602	0.4576	0.4546	0.4504	0.4452	0.4387	0.4291
	0.4639	0.463	0.4618	0.4598	0.4571	0.4542	0.45	0.4448	0.4384	0.4288
	0.4629	0.4622	0.4609	0.459	0.4564	0.4535	0.4493	0.4442	0.4378	0.4283
	0.4615	0.4608	0.4596	0.4577	0.4552	0.4524	0.4483	0.4433	0.437	0.4276
a/c	0.4596	0.4589	0.4579	0.4561	0.4537	0.4509	0.447	0.4418	0.4359	0.4266
	0.4573	0.4568	0.4558	0.4542	0.452	0.4493	0.4455	0.4407	0.4347	0.4255
	0.4543	0.4539	0.4531	0.4517	0.4496	0.4472	0.4435	0.4389	0.433	0.4241
	0.4507	0.4505	0.4499	0.4487	0.4468	0.4446	0.4412	0.4368	0.4311	0.4224
	0.4466	0.4465	0.4461	0.4452	0.4436	0.4416	0.4385	0.4343	0.4289	0.4204
	0.4412	0.4412	0.441	0.4404	0.4392	0.4375	0.4347	0.4309	0.4258	0.4177

Figure I.19: F1C: e=2.5c & d=2.5c

	b/c									
	0.4645	0.4637	0.4624	0.4603	0.4576	0.4546	0.4504	0.4454	0.4395	0.4312
	0.464	0.4632	0.4619	0.4599	0.4572	0.4542	0.4501	0.4451	0.4392	0.431
	0.4632	0.4624	0.4612	0.4592	0.4566	0.4536	0.4495	0.4446	0.4387	0.4305
	0.4619	0.4612	0.46	0.4581	0.4556	0.4527	0.4486	0.4438	0.438	0.4299
a/c	0.4602	0.4595	0.4584	0.4567	0.4542	0.4514	0.4475	0.4427	0.4371	0.429
	0.4581	0.4576	0.4566	0.455	0.4527	0.45	0.4462	0.4416	0.436	0.4281
	0.4554	0.455	0.4542	0.4528	0.4506	0.4481	0.4445	0.44	0.4346	0.4269
	0.4522	0.4519	0.4513	0.4501	0.4482	0.4459	0.4425	0.4382	0.433	0.4254
	0.4485	0.4484	0.448	0.447	0.4454	0.4433	0.4401	0.4361	0.4311	0.4237
	0.4437	0.4437	0.4434	0.4428	0.4415	0.4397	0.4369	0.4332	0.4285	0.4214

Figure I.19: F1C: e=2.5c & d=3c

	b/c									
	0.4645	0.4638	0.4626	0.4607	0.4581	0.4551	0.4511	0.4464	0.441	0.4336
	0.4641	0.4634	0.4622	0.4603	0.4577	0.4548	0.4508	0.4461	0.4407	0.4334
	0.4634	0.4627	0.4615	0.4597	0.4571	0.4542	0.4503	0.4457	0.4403	0.433
	0.4622	0.4616	0.4605	0.4587	0.4562	0.4534	0.4496	0.445	0.4397	0.4324
a/c	0.4607	0.4601	0.4591	0.4574	0.455	0.4523	0.4486	0.444	0.4388	0.4317
	0.4589	0.4584	0.4575	0.4559	0.4537	0.4511	0.4474	0.443	0.4379	0.4309
	0.4565	0.4561	0.4553	0.4539	0.4519	0.4494	0.4459	0.4417	0.4367	0.4298
	0.4536	0.4533	0.4527	0.4515	0.4497	0.4474	0.4442	0.4401	0.4352	0.4285
	0.4503	0.4501	0.4497	0.4488	0.4472	0.4452	0.4421	0.4382	0.4336	0.427
	0.446	0.4459	0.4457	0.445	0.4438	0.442	0.4393	0.4357	0.4313	0.4251

Figure I.19: F1C: e=2.5c & d=3.5c

	b/c									
	0.4646	0.464	0.4628	0.4611	0.4587	0.4559	0.4522	0.4478	0.4428	0.4362
	0.4642	0.4636	0.4625	0.4607	0.4584	0.4556	0.4519	0.4476	0.4426	0.436
	0.4636	0.463	0.4619	0.4602	0.4578	0.4552	0.4515	0.4472	0.4422	0.4357
	0.4626	0.462	0.461	0.4593	0.4571	0.4544	0.4508	0.4466	0.4417	0.4351
a/c	0.4612	0.4606	0.4597	0.4582	0.456	0.4534	0.4499	0.4457	0.4409	0.4345
	0.4596	0.4591	0.4583	0.4568	0.4548	0.4523	0.4489	0.4449	0.4401	0.4338
	0.4574	0.457	0.4563	0.4551	0.4532	0.4509	0.4476	0.4436	0.439	0.4328
	0.4548	0.4546	0.454	0.4529	0.4512	0.4491	0.446	0.4422	0.4378	0.4317
	0.4519	0.4517	0.4513	0.4505	0.449	0.4471	0.4442	0.4406	0.4363	0.4304
	0.448	0.448	0.4478	0.4471	0.446	0.4443	0.4417	0.4384	0.4344	0.4287

Figure I.19: F1C: e=2.5c & d=4c

	b/c									
	0.4647	0.4641	0.4631	0.4615	0.4593	0.4568	0.4535	0.4495	0.4449	0.4389
	0.4644	0.4638	0.4628	0.4612	0.4591	0.4566	0.4532	0.4492	0.4447	0.4387
	0.4638	0.4632	0.4623	0.4607	0.4586	0.4561	0.4528	0.4489	0.4444	0.4384
	0.4629	0.4623	0.4614	0.4599	0.4579	0.4555	0.4522	0.4483	0.4439	0.438
a/c	0.4616	0.4612	0.4603	0.4589	0.4569	0.4546	0.4514	0.4476	0.4432	0.4374
	0.4602	0.4598	0.459	0.4577	0.4559	0.4536	0.4505	0.4468	0.4425	0.4367
	0.4582	0.4579	0.4573	0.4561	0.4544	0.4523	0.4493	0.4457	0.4415	0.4359
	0.4559	0.4557	0.4552	0.4542	0.4527	0.4507	0.4479	0.4445	0.4404	0.4349
	0.4533	0.4532	0.4528	0.452	0.4507	0.4489	0.4463	0.443	0.4391	0.4338
	0.4499	0.4498	0.4496	0.4491	0.448	0.4465	0.4441	0.441	0.4373	0.4322

Figure I.19: F1C: e=3c & d=0.5c

	b/c									
a/c	0.4644	0.4641	0.4638	0.4631	0.4621	0.461	0.4587	0.455	0.4477	0.4286
	0.4637	0.4635	0.4631	0.4625	0.4615	0.4603	0.4581	0.4544	0.4472	0.4281
	0.4626	0.4623	0.462	0.4614	0.4604	0.4593	0.457	0.4534	0.4462	0.4273
	0.4609	0.4606	0.4603	0.4597	0.4549	0.4576	0.4554	0.4519	0.4448	0.426
	0.4585	0.4582	0.458	0.4574	0.4564	0.4554	0.4533	0.4498	0.4428	0.4243
	0.4557	0.4555	0.4553	0.4547	0.4539	0.4529	0.4508	0.4474	0.4406	0.4223
	0.452	0.4518	0.4516	0.4512	0.4504	0.4495	0.4475	0.4443	0.4376	0.4197
	0.4476	0.4475	0.4474	0.447	0.4463	0.4455	0.4436	0.4405	0.434	0.4166
	0.4426	0.4426	0.4425	0.4422	0.4416	0.4408	0.4392	0.4363	0.43	0.4131
	0.436	0.4359	0.4359	0.4357	0.4352	0.4346	0.4331	0.4305	0.4246	0.4083

Figure I.19: F1C: e=3c & d=1c

	b/c									
a/c	0.4644	0.4638	0.4629	0.4616	0.4597	0.4576	0.4539	0.4488	0.4411	0.4268
	0.4638	0.4632	0.4623	0.461	0.4592	0.457	0.4534	0.4483	0.4406	0.4263
	0.4627	0.4622	0.4613	0.46	0.4582	0.4561	0.4526	0.4475	0.4399	0.4257
	0.4611	0.4606	0.4598	0.4585	0.4568	0.4547	0.4512	0.4462	0.4387	0.4246
	0.459	0.4585	0.4577	0.4565	0.4549	0.4529	0.4494	0.4445	0.4372	0.4232
	0.4565	0.456	0.4553	0.4542	0.4527	0.4507	0.4474	0.4426	0.4354	0.4217
	0.4531	0.4527	0.4521	0.4511	0.4497	0.4479	0.4447	0.4401	0.433	0.4196
	0.4491	0.4488	0.4483	0.4475	0.4462	0.4445	0.4415	0.4371	0.4303	0.4171
	0.4446	0.4444	0.444	0.4433	0.4422	0.4407	0.4379	0.4337	0.4271	0.4143
	0.4386	0.4385	0.4382	0.4377	0.4368	0.4355	0.433	0.4291	0.4229	0.4109

Figure I.19: F1C: e=3c & d=1.5c

	b/c									
a/c	0.4642	0.4634	0.4623	0.4604	0.458	0.4553	0.4512	0.4459	0.4388	0.4273
	0.4637	0.4629	0.4617	0.4599	0.4575	0.4549	0.4508	0.4454	0.4384	0.4269
	0.4628	0.462	0.4609	0.4591	0.4567	0.4541	0.4501	0.4448	0.4378	0.4264
	0.4613	0.4606	0.4595	0.4578	0.4555	0.4529	0.449	0.4437	0.4368	0.4255
	0.4594	0.4587	0.4577	0.456	0.4538	0.4513	0.4475	0.4423	0.4355	0.4243
	0.4571	0.4565	0.4556	0.454	0.4519	0.4495	0.4458	0.4407	0.434	0.423
	0.4541	0.4536	0.4527	0.4513	0.4494	0.4471	0.4435	0.4386	0.4321	0.4213
	0.4505	0.4501	0.4494	0.4481	0.4463	0.4442	0.4408	0.4361	0.4298	0.4192
	0.4464	0.4461	0.4456	0.4445	0.4429	0.441	0.4378	0.4333	0.4272	0.4169
	0.441	0.4409	0.4405	0.4396	0.4383	0.4366	0.4337	0.4295	0.4237	0.4138

Figure I.19: F1C: e=3c & d=2c

	b/c									
a/c	0.4644	0.4636	0.4623	0.4603	0.4576	0.4546	0.4504	0.4452	0.4387	0.4292
	0.4639	0.4631	0.4618	0.4598	0.4572	0.4542	0.45	0.4448	0.4384	0.4288
	0.4631	0.4623	0.461	0.4591	0.4565	0.4535	0.4494	0.4442	0.4378	0.4283
	0.4618	0.4611	0.4598	0.4579	0.4554	0.4525	0.4484	0.4433	0.437	0.4276
	0.4601	0.4594	0.4582	0.4564	0.4539	0.4511	0.4471	0.4421	0.4359	0.4266
	0.4581	0.4574	0.4563	0.4546	0.4523	0.4496	0.4457	0.4408	0.4347	0.4255
	0.4553	0.4548	0.4538	0.4522	0.45	0.4475	0.4437	0.439	0.433	0.424
	0.4521	0.4517	0.4509	0.4494	0.4474	0.445	0.4414	0.4369	0.4311	0.4223
	0.4484	0.4481	0.4475	0.4462	0.4444	0.4422	0.4388	0.4345	0.4289	0.4203
	0.4436	0.4434	0.443	0.442	0.4404	0.4385	0.4354	0.4313	0.426	0.4177

Figure I.19: F1C: e=3c & d=2.5c

	b/c									
a/c	0.4645	0.4637	0.4624	0.4603	0.4576	0.4546	0.4504	0.4454	0.4395	0.4313
	0.464	0.4633	0.462	0.46	0.4573	0.4542	0.4501	0.4451	0.4392	0.431
	0.4633	0.4625	0.4613	0.4593	0.4566	0.4536	0.4495	0.4446	0.4388	0.4306
	0.4622	0.4614	0.4602	0.4583	0.4557	0.4527	0.4487	0.4438	0.438	0.4299
	0.4606	0.4599	0.4588	0.4569	0.4544	0.4515	0.4476	0.4428	0.4371	0.429
	0.4588	0.4582	0.4571	0.4553	0.4529	0.4502	0.4463	0.4416	0.436	0.4281
	0.4563	0.4558	0.4548	0.4532	0.451	0.4483	0.4446	0.44	0.4346	0.4268
	0.4535	0.453	0.4522	0.4508	0.4487	0.4462	0.4426	0.4382	0.4329	0.4253
	0.4502	0.4498	0.4492	0.4479	0.446	0.4437	0.4404	0.4362	0.431	0.4236
	0.4459	0.4457	0.4452	0.4442	0.4425	0.4405	0.4374	0.4334	0.4285	0.4214

Figure I.19: F1C: e=3c & d=3c

	b/c									
a/c	0.4646	0.4638	0.4626	0.4607	0.4581	0.4551	0.4511	0.4464	0.441	0.4336
	0.4642	0.4634	0.4622	0.4603	0.4577	0.4548	0.4508	0.4461	0.4407	0.4334
	0.4635	0.4628	0.4616	0.4597	0.4572	0.4543	0.4504	0.4457	0.4403	0.433
	0.4625	0.4618	0.4606	0.4588	0.4563	0.4535	0.4496	0.445	0.4397	0.4324
	0.4611	0.4604	0.4594	0.4576	0.4552	0.4524	0.4486	0.4441	0.4388	0.4316
	0.4595	0.4589	0.4579	0.4562	0.4539	0.4512	0.4475	0.443	0.4379	0.4308
	0.4573	0.4568	0.4559	0.4543	0.4522	0.4496	0.446	0.4417	0.4366	0.4297
	0.4547	0.4543	0.4535	0.4521	0.4501	0.4477	0.4443	0.4401	0.4352	0.4284
	0.4518	0.4514	0.4508	0.4496	0.4478	0.4455	0.4423	0.4383	0.4335	0.4269
	0.4479	0.4477	0.4472	0.4463	0.4447	0.4427	0.4397	0.4359	0.4314	0.4249

Figure I.19: F1C: e=3c & d=3.5c

	b/c									
a/c	0.4646	0.464	0.4628	0.4611	0.4587	0.4559	0.4522	0.4478	0.4428	0.4362
	0.4643	0.4636	0.4625	0.4608	0.4584	0.4557	0.452	0.4476	0.4426	0.436
	0.4637	0.4631	0.462	0.4602	0.4579	0.4552	0.4515	0.4472	0.4422	0.4356
	0.4628	0.4622	0.4611	0.4594	0.4571	0.4545	0.4509	0.4466	0.4417	0.4351
	0.4615	0.4609	0.4599	0.4583	0.4561	0.4535	0.45	0.4458	0.4409	0.4344
	0.4601	0.4595	0.4586	0.4571	0.455	0.4524	0.449	0.4449	0.4401	0.4337
	0.4581	0.4577	0.4568	0.4554	0.4534	0.451	0.4477	0.4436	0.439	0.4327
	0.4558	0.4554	0.4547	0.4534	0.4516	0.4493	0.4461	0.4422	0.4377	0.4315
	0.4532	0.4529	0.4523	0.4512	0.4495	0.4474	0.4444	0.4406	0.4363	0.4302
	0.4497	0.4496	0.4491	0.4482	0.4467	0.4448	0.442	0.4385	0.4343	0.4285

Figure I.19: F1C: e=3c & d=4c

	b/c									
a/c	0.4647	0.4641	0.4631	0.4615	0.4594	0.4568	0.4535	0.4495	0.4449	0.4389
	0.4644	0.4638	0.4628	0.4612	0.4591	0.4566	0.4532	0.4492	0.4447	0.4387
	0.4639	0.4633	0.4623	0.4608	0.4586	0.4562	0.4528	0.4489	0.4444	0.4384
	0.4631	0.4625	0.4616	0.46	0.458	0.4555	0.4522	0.4483	0.4438	0.438
	0.4619	0.4614	0.4605	0.4591	0.457	0.4547	0.4514	0.4476	0.4432	0.4373
	0.4606	0.4602	0.4593	0.4579	0.456	0.4537	0.4505	0.4468	0.4424	0.4367
	0.4589	0.4585	0.4577	0.4564	0.4546	0.4524	0.4494	0.4457	0.4414	0.4358
	0.4568	0.4565	0.4558	0.4547	0.453	0.4509	0.448	0.4444	0.4403	0.4347
	0.4545	0.4542	0.4537	0.4526	0.4511	0.4492	0.4464	0.443	0.439	0.4336
	0.4514	0.4512	0.4508	0.45	0.4486	0.4469	0.4443	0.4411	0.4373	0.4321

Figure I.19: F1C: e=3.5c & d=0.5c

	b/c									
	0.4644	0.4641	0.4638	0.4632	0.4621	0.461	0.4587	0.455	0.4477	0.4286
	0.4638	0.4635	0.4632	0.4626	0.4615	0.4604	0.4581	0.4545	0.4472	0.4282
	0.4628	0.4625	0.4622	0.4616	0.4606	0.4594	0.4572	0.4535	0.4463	0.4274
	0.4612	0.4609	0.4606	0.46	0.459	0.4579	0.4557	0.4521	0.445	0.4262
a/c	0.459	0.4588	0.4585	0.4579	0.4569	0.4559	0.4537	0.4502	0.4432	0.4245
	0.4565	0.4563	0.456	0.4555	0.4545	0.4535	0.4514	0.448	0.441	0.4227
	0.4531	0.4529	0.4527	0.4522	0.4513	0.4504	0.4483	0.445	0.4382	0.4201
	0.4491	0.4489	0.4488	0.4483	0.4475	0.4466	0.4447	0.4415	0.4349	0.4172
	0.4446	0.4444	0.4443	0.4439	0.4432	0.4424	0.4405	0.4375	0.4311	0.4139
	0.4385	0.4385	0.4384	0.4381	0.4374	0.4367	0.4351	0.4322	0.4261	0.4094

Figure I.19: F1C: e=3.5c & d=1c

	b/c									
	0.4644	0.4638	0.4629	0.4616	0.4597	0.4576	0.4539	0.4488	0.4411	0.4268
	0.4638	0.4632	0.4624	0.4611	0.4592	0.4571	0.4535	0.4483	0.4407	0.4264
	0.4629	0.4623	0.4615	0.4602	0.4584	0.4562	0.4527	0.4476	0.44	0.4257
	0.4615	0.4609	0.4601	0.4588	0.4571	0.455	0.4514	0.4464	0.4389	0.4247
a/c	0.4595	0.459	0.4582	0.457	0.4553	0.4532	0.4498	0.4448	0.4374	0.4234
	0.4573	0.4568	0.456	0.4549	0.4532	0.4512	0.4479	0.443	0.4357	0.4219
	0.4542	0.4538	0.4531	0.452	0.4504	0.4486	0.4453	0.4406	0.4334	0.4198
	0.4506	0.4502	0.4496	0.4486	0.4472	0.4454	0.4423	0.4377	0.4308	0.4175
	0.4465	0.4462	0.4457	0.4448	0.4435	0.4419	0.4389	0.4345	0.4278	0.4148
	0.4411	0.4409	0.4405	0.4398	0.4386	0.4371	0.4344	0.4303	0.4238	0.4112

Figure I.19: F1C: e=3.5c & d=1.5c

	b/c									
	0.4642	0.4635	0.4623	0.4604	0.458	0.4553	0.4512	0.4459	0.4388	0.4273
	0.4637	0.463	0.4618	0.46	0.4576	0.4549	0.4508	0.4455	0.4384	0.4269
	0.4629	0.4622	0.461	0.4592	0.4569	0.4542	0.4502	0.4448	0.4378	0.4264
	0.4616	0.4609	0.4598	0.458	0.4557	0.4531	0.4491	0.4438	0.4369	0.4256
a/c	0.4599	0.4592	0.4581	0.4564	0.4542	0.4516	0.4477	0.4425	0.4356	0.4244
	0.4579	0.4572	0.4562	0.4546	0.4524	0.4499	0.4461	0.441	0.4342	0.4231
	0.4551	0.4545	0.4536	0.4521	0.45	0.4476	0.4439	0.439	0.4323	0.4214
	0.4519	0.4514	0.45	0.4491	0.4472	0.4449	0.4414	0.4366	0.4302	0.4194
	0.4482	0.4478	0.447	0.4458	0.444	0.4419	0.4385	0.4339	0.4277	0.4172
	0.4434	0.4431	0.4425	0.4414	0.4398	0.4379	0.4347	0.4304	0.4244	0.4143

Figure I.19: F1C: e=3.5c & d=2c

	b/c									
	0.4644	0.4636	0.4623	0.4603	0.4576	0.4546	0.4504	0.4452	0.4387	0.4292
	0.464	0.4632	0.4619	0.4599	0.4572	0.4542	0.45	0.4448	0.4384	0.4289
	0.4633	0.4625	0.4612	0.4592	0.4566	0.4536	0.4494	0.4443	0.4379	0.4284
	0.4621	0.4613	0.4601	0.4581	0.4555	0.4526	0.4485	0.4434	0.4371	0.4276
a/c	0.4605	0.4598	0.4586	0.4567	0.4542	0.4513	0.4473	0.4423	0.436	0.4267
	0.4587	0.458	0.4569	0.4551	0.4526	0.4499	0.4459	0.441	0.4348	0.4256
	0.4563	0.4556	0.4546	0.4529	0.4505	0.4479	0.4441	0.4392	0.4332	0.4241
	0.4534	0.4528	0.4519	0.4503	0.4481	0.4456	0.4419	0.4372	0.4313	0.4224
	0.4501	0.4496	0.4488	0.4473	0.4453	0.4429	0.4394	0.4349	0.4292	0.4205
	0.4458	0.4454	0.4447	0.4435	0.4417	0.4395	0.4362	0.4319	0.4264	0.418

Figure I.19: F1C: e=3.5c & d=2.5c

	b/c									
	0.4645	0.4637	0.4624	0.4604	0.4577	0.4546	0.4504	0.4454	0.4395	0.4313
	0.4641	0.4633	0.462	0.46	0.4573	0.4543	0.4501	0.4451	0.4392	0.431
	0.4634	0.4627	0.4614	0.4594	0.4567	0.4537	0.4496	0.4446	0.4388	0.4306
	0.4624	0.4617	0.4604	0.4585	0.4558	0.4529	0.4488	0.4439	0.4381	0.4299
a/c	0.461	0.4603	0.4591	0.4572	0.4546	0.4517	0.4477	0.4429	0.4372	0.4291
	0.4594	0.4587	0.4576	0.4557	0.4533	0.4504	0.4465	0.4417	0.4361	0.4281
	0.4572	0.4566	0.4555	0.4538	0.4514	0.4487	0.4449	0.4402	0.4347	0.4268
	0.4546	0.454	0.4531	0.4515	0.4492	0.4467	0.443	0.4385	0.4331	0.4254
	0.4516	0.4512	0.4503	0.4489	0.4468	0.4444	0.4408	0.4365	0.4313	0.4237
	0.4478	0.4474	0.4467	0.4455	0.4436	0.4413	0.438	0.4339	0.4289	0.4215

Figure I.19: F1C: e=3.5c & d=3c

	b/c									
	0.4646	0.4638	0.4626	0.4607	0.4581	0.4551	0.4511	0.4464	0.441	0.4336
	0.4642	0.4635	0.4623	0.4604	0.4578	0.4548	0.4509	0.4462	0.4407	0.4334
	0.4636	0.4629	0.4617	0.4598	0.4573	0.4544	0.4504	0.4457	0.4403	0.433
	0.4627	0.462	0.4608	0.459	0.4565	0.4536	0.4497	0.4451	0.4397	0.4324
a/c	0.4614	0.4608	0.4596	0.4578	0.4554	0.4526	0.4487	0.4442	0.4389	0.4317
	0.46	0.4593	0.4583	0.4565	0.4542	0.4514	0.4477	0.4432	0.438	0.4308
	0.458	0.4574	0.4564	0.4548	0.4525	0.4499	0.4462	0.4418	0.4367	0.4297
	0.4557	0.4552	0.4543	0.4528	0.4506	0.4481	0.4445	0.4403	0.4353	0.4284
	0.4531	0.4526	0.4518	0.4504	0.4484	0.446	0.4427	0.4385	0.4337	0.4269
	0.4496	0.4493	0.4486	0.4474	0.4456	0.4434	0.4402	0.4362	0.4316	0.4271

Figure I.19: F1C: e=3.5c & d=3.5c

	b/c									
	0.4647	0.464	0.4629	0.4611	0.4587	0.4559	0.4522	0.4478	0.4428	0.4362
	0.4643	0.4637	0.4626	0.4608	0.4584	0.4557	0.452	0.4476	0.4426	0.436
	0.4638	0.4631	0.462	0.4603	0.458	0.4552	0.4516	0.4472	0.4423	0.4357
	0.463	0.4623	0.4613	0.4596	0.4572	0.4546	0.4509	0.4466	0.4417	0.4352
a/c	0.4618	0.4612	0.4602	0.4585	0.4563	0.4537	0.4501	0.4458	0.441	0.4345
	0.4605	0.46	0.459	0.4574	0.4552	0.4526	0.4491	0.4449	0.4401	0.4337
	0.4588	0.4582	0.4573	0.4558	0.4537	0.4512	0.4478	0.4438	0.439	0.4327
	0.4567	0.4562	0.4554	0.454	0.452	0.4496	0.4463	0.4424	0.4378	0.4316
	0.4543	0.4539	0.4532	0.4519	0.4501	0.4478	0.4447	0.4408	0.4364	0.4303
	0.4512	0.4509	0.4503	0.4492	0.4475	0.4454	0.4425	0.4388	0.4345	0.4286

Figure I.19: F1C: e=3.5c & d=4c

	b/c									
	0.4648	0.4641	0.4631	0.4615	0.4594	0.4568	0.4535	0.4495	0.4449	0.4389
	0.4645	0.4639	0.4629	0.4613	0.4591	0.4566	0.4532	0.4492	0.4447	0.4387
	0.464	0.4634	0.4624	0.4608	0.4587	0.4562	0.4529	0.4489	0.4444	0.4384
	0.4632	0.4627	0.4617	0.4602	0.458	0.4556	0.4523	0.4484	0.4439	0.438
a/c	0.4622	0.4617	0.4607	0.4592	0.4572	0.4548	0.4515	0.4476	0.4432	0.4374
	0.461	0.4605	0.4596	0.4582	0.4562	0.4539	0.4507	0.4468	0.4425	0.4367
	0.4595	0.459	0.4581	0.4568	0.4549	0.4526	0.4495	0.4458	0.4415	0.4358
	0.4576	0.4572	0.4564	0.4551	0.4533	0.4512	0.4482	0.4445	0.4403	0.4347
	0.4555	0.4551	0.4544	0.4533	0.4516	0.4495	0.4467	0.4432	0.4391	0.4336
	0.4527	0.4524	0.4519	0.4508	0.4493	0.4474	0.4447	0.4413	0.4374	0.4321

Figure I.19: F1C: e=4c & d=0.5c

	b/c									
	0.4645	0.4642	0.4638	0.4632	0.4621	0.461	0.4587	0.455	0.4477	0.4286
	0.4639	0.4636	0.4633	0.4626	0.4616	0.4605	0.4582	0.4545	0.4472	0.4282
	0.463	0.4627	0.4624	0.4617	0.4607	0.4596	0.4573	0.4537	0.4465	0.4268
	0.4616	0.4613	0.461	0.4603	0.4593	0.4582	0.456	0.4524	0.4452	0.4267
a/c	0.4596	0.4593	0.459	0.4584	0.4574	0.4564	0.4542	0.4506	0.4436	0.4249
	0.4573	0.4571	0.4568	0.4562	0.4552	0.4542	0.4521	0.4486	0.4417	0.4231
	0.4542	0.454	0.4538	0.4532	0.4523	0.4513	0.4492	0.4458	0.4389	0.4207
	0.4506	0.4504	0.4502	0.4497	0.4488	0.4479	0.4459	0.4426	0.4359	0.418
	0.4465	0.4463	0.4461	0.4457	0.4449	0.444	0.4421	0.4389	0.4323	0.4149
	0.4411	0.441	0.4408	0.4404	0.4397	0.4389	0.4371	0.4341	0.4278	0.4108

Figure I.19: F1C: e=4c & d=1c

	b/c									
	0.4644	0.4638	0.4629	0.4616	0.4598	0.4576	0.454	0.4488	0.4411	0.4268
	0.4639	0.4633	0.4624	0.4611	0.4593	0.4571	0.4535	0.4484	0.4407	0.4264
	0.4631	0.4625	0.4616	0.4603	0.4585	0.4564	0.4528	0.4477	0.4401	0.4258
	0.4618	0.4612	0.4604	0.4591	0.4573	0.4552	0.4517	0.4466	0.439	0.4249
a/c	0.46	0.4595	0.4587	0.4574	0.4557	0.4536	0.4501	0.4451	0.4377	0.4236
	0.458	0.4575	0.4567	0.4555	0.4538	0.4518	0.4484	0.4434	0.4361	0.4222
	0.4553	0.4548	0.454	0.4529	0.4513	0.4493	0.446	0.4412	0.434	0.4202
	0.452	0.4516	0.4509	0.4498	0.4483	0.4464	0.4432	0.4385	0.4315	0.418
	0.4483	0.4479	0.4473	0.4463	0.4449	0.4431	0.4401	0.4355	0.4287	0.4155
	0.4435	0.4432	0.4426	0.4418	0.4404	0.4388	0.4359	0.4316	0.425	0.4121

Figure I.19: F1C: e=4c & d=1.5c

	b/c									
	0.4643	0.4635	0.4623	0.4605	0.4581	0.4553	0.4513	0.4459	0.4388	0.4273
	0.4638	0.463	0.4619	0.46	0.4576	0.4549	0.4509	0.4455	0.4384	0.427
	0.4631	0.4623	0.4611	0.4593	0.457	0.4543	0.4503	0.4449	0.4379	0.4265
	0.4619	0.4612	0.46	0.4583	0.4559	0.4533	0.4493	0.444	0.437	0.4257
a/c	0.4603	0.4596	0.4585	0.4568	0.4545	0.4519	0.448	0.4428	0.4358	0.4246
	0.4585	0.4578	0.4568	0.4551	0.4529	0.4503	0.4465	0.4413	0.4345	0.4234
	0.4561	0.4554	0.4544	0.4528	0.4507	0.4482	0.4444	0.4394	0.4327	0.4217
	0.4532	0.4526	0.4516	0.4501	0.4481	0.4457	0.4421	0.4372	0.4306	0.4198
	0.4499	0.4493	0.4485	0.4471	0.4452	0.4429	0.4394	0.4347	0.4283	0.4177
	0.4455	0.4451	0.4444	0.4431	0.4413	0.4392	0.4359	0.4314	0.4252	0.4149

Figure I.19: F1C: e=4c & d=2c

	b/c									
	0.4644	0.4636	0.4623	0.4603	0.4576	0.4546	0.4504	0.4452	0.4387	0.4292
	0.464	0.4632	0.4619	0.4599	0.4572	0.4543	0.4501	0.4449	0.4384	0.4289
	0.4634	0.4626	0.4613	0.4593	0.4567	0.4537	0.4495	0.4444	0.438	0.4284
	0.4624	0.4616	0.4603	0.4583	0.4557	0.4528	0.4487	0.4435	0.4372	0.4277
a/c	0.4609	0.4602	0.4589	0.457	0.4545	0.4516	0.4475	0.4425	0.4362	0.4268
	0.4593	0.4586	0.4574	0.4555	0.453	0.4502	0.4462	0.4412	0.435	0.4257
	0.4571	0.4564	0.4553	0.4535	0.4511	0.4484	0.4445	0.4396	0.4335	0.4243
	0.4545	0.4539	0.4528	0.4511	0.4488	0.4462	0.4424	0.4377	0.4317	0.4227
	0.4516	0.451	0.45	0.4485	0.4463	0.4438	0.4401	0.4355	0.4297	0.4208
	0.4477	0.4472	0.4464	0.4449	0.4429	0.4406	0.4371	0.4327	0.4271	0.4184

Figure I.19: F1C: e=4c & d=2.5c

	b/c									
	0.4645	0.4637	0.4624	0.4604	0.4577	0.4546	0.4504	0.4454	0.4395	0.4313
	0.4641	0.4634	0.4621	0.46	0.4573	0.4543	0.4501	0.4451	0.4393	0.431
	0.4636	0.4628	0.4615	0.4595	0.4568	0.4538	0.4497	0.4447	0.4388	0.4306
	0.4626	0.4619	0.4606	0.4586	0.456	0.453	0.4489	0.444	0.4382	0.43
a/c	0.4614	0.4606	0.4594	0.4575	0.4549	0.4519	0.4479	0.443	0.4373	0.4292
	0.4599	0.4592	0.458	0.4561	0.4536	0.4507	0.4468	0.442	0.4363	0.4283
	0.4579	0.4573	0.4561	0.4543	0.4519	0.4491	0.4452	0.4405	0.4349	0.427
	0.4556	0.455	0.4539	0.4522	0.4499	0.4472	0.4434	0.4388	0.4334	0.4256
	0.453	0.4524	0.4514	0.4498	0.4476	0.4451	0.4414	0.437	0.4316	0.424
	0.4495	0.449	0.4482	0.4467	0.4447	0.4422	0.4388	0.4345	0.4293	0.4219

Figure I.19: F1C: e=4c & d=3c

	b/c									
	0.4646	0.4638	0.4626	0.4607	0.4581	0.4551	0.4511	0.4464	0.441	0.4336
	0.4643	0.4635	0.4623	0.4604	0.4578	0.4549	0.4509	0.4462	0.4407	0.4334
	0.4637	0.463	0.4618	0.4599	0.4573	0.4544	0.4505	0.4458	0.4404	0.433
	0.4629	0.4622	0.461	0.4591	0.4566	0.4537	0.4498	0.4451	0.4398	0.4325
a/c	0.4618	0.4611	0.4599	0.4581	0.4556	0.4528	0.4489	0.4443	0.439	0.4318
	0.4604	0.4598	0.4587	0.4569	0.4545	0.4517	0.4479	0.4433	0.4381	0.4309
	0.4587	0.458	0.457	0.4553	0.4529	0.4502	0.4465	0.4421	0.4369	0.4298
	0.4566	0.456	0.455	0.4534	0.4512	0.4485	0.4449	0.4406	0.4355	0.4286
	0.4542	0.4537	0.4528	0.4513	0.4491	0.4466	0.4431	0.4389	0.434	0.4272
	0.4511	0.4507	0.4499	0.4485	0.4465	0.4441	0.4408	0.4367	0.432	0.4253

Figure I.19: F1C: e=4c & d=3.5c

	b/c									
	0.4647	0.464	0.4629	0.4611	0.4587	0.456	0.4522	0.4479	0.4428	0.4362
	0.4644	0.4637	0.4626	0.4608	0.4584	0.4557	0.452	0.4476	0.4426	0.436
	0.4639	0.4632	0.4621	0.4604	0.458	0.4553	0.4516	0.4473	0.4423	0.4357
	0.4631	0.4625	0.4614	0.4597	0.4574	0.4547	0.451	0.4467	0.4418	0.4352
a/c	0.4621	0.4615	0.4604	0.4588	0.4565	0.4538	0.4502	0.4459	0.4411	0.4345
	0.4609	0.4603	0.4593	0.4577	0.4554	0.4528	0.4493	0.4451	0.4403	0.4338
	0.4593	0.4588	0.4578	0.4562	0.4541	0.4515	0.4481	0.4439	0.4392	0.4328
	0.4575	0.4569	0.456	0.4546	0.4525	0.45	0.4467	0.4426	0.438	0.4317
	0.4553	0.4549	0.454	0.4526	0.4507	0.4483	0.4451	0.4411	0.4366	0.4304
	0.4526	0.4522	0.4514	0.4501	0.4483	0.4461	0.443	0.4392	0.4348	0.4288

Figure I.19: F1C: e=4c & d=4c

	b/c									
	0.4648	0.4642	0.4631	0.4615	0.4594	0.4569	0.4535	0.4495	0.4449	0.4389
	0.4645	0.4639	0.4629	0.4613	0.4591	0.4566	0.4533	0.4493	0.4447	0.4387
	0.4641	0.4635	0.4625	0.4609	0.4587	0.4563	0.4529	0.4489	0.4444	0.4385
	0.4634	0.4628	0.4618	0.4603	0.4581	0.4557	0.4524	0.4484	0.4439	0.4379
a/c	0.4625	0.4619	0.4609	0.4594	0.4573	0.4549	0.4516	0.4477	0.4433	0.4374
	0.4614	0.4609	0.4599	0.4585	0.4564	0.454	0.4508	0.447	0.4426	0.4367
	0.46	0.4595	0.4586	0.4572	0.4552	0.4529	0.4497	0.4459	0.4416	0.4359
	0.4583	0.4578	0.457	0.4556	0.4537	0.4515	0.4484	0.4447	0.4405	0.4348
	0.4564	0.4559	0.4552	0.4539	0.4521	0.45	0.447	0.4434	0.4393	0.4337
	0.4539	0.4535	0.4528	0.4517	0.45	0.448	0.4451	0.4417	0.4377	0.4322

Figure I.20: F2C: e=0.5c & d=0.5c

	b/c									
a/c	−0.3354	−0.3349	−0.3341	−0.3326	−0.3303	−0.3277	−0.3223	−0.3139	−0.2985	−0.2623
	−0.3345	−0.3341	−0.3334	−0.3321	−0.3298	−0.3272	−0.3219	−0.3135	−0.2983	−0.262
	−0.3329	−0.3328	−0.3323	−0.3312	−0.329	−0.3265	−0.3213	−0.313	−0.2976	−0.2617
	−0.3304	−0.3304	−0.3303	−0.3295	−0.3277	−0.3252	−0.3202	−0.3121	−0.2969	−0.2612
	−0.3269	−0.3269	−0.3268	−0.3266	−0.3255	−0.3232	−0.3186	−0.3107	−0.2956	−0.2604
	−0.3228	−0.3228	−0.3228	−0.3228	−0.3225	−0.3208	−0.3167	−0.3093	−0.2947	−0.2597
	−0.3161	−0.3161	−0.3161	−0.3161	−0.3161	−0.3156	−0.3128	−0.3061	−0.2923	−0.2581
	−0.3068	−0.3068	−0.3068	−0.3068	−0.3068	−0.3067	−0.3058	−0.3011	−0.2886	−0.2559
	−0.2941	−0.2941	−0.2941	−0.2939	−0.2935	−0.2938	−0.2937	−0.2919	−0.2824	−0.2521
	−0.2705	−0.2705	−0.2705	−0.2705	−0.2705	−0.2704	−0.2705	−0.2704	−0.2668	−0.2444

Figure I.20: F2C: e=0.5c & d=1c

	b/c									
a/c	−0.3353	−0.3343	−0.3327	−0.3303	−0.3267	−0.3227	−0.316	−0.3067	−0.2941	−0.2704
	−0.3343	−0.3335	−0.3321	−0.3298	−0.3263	−0.3223	−0.3157	−0.3065	−0.2939	−0.2703
	−0.3324	−0.3322	−0.3311	−0.3291	−0.3258	−0.3218	−0.3153	−0.3061	−0.2935	−0.2701
	−0.3294	−0.3294	−0.3291	−0.3276	−0.3247	−0.3209	−0.3146	−0.3055	−0.293	−0.2698
	−0.3254	−0.3254	−0.3254	−0.3249	−0.3229	−0.3194	−0.3136	−0.3047	−0.292	−0.2693
	−0.321	−0.321	−0.321	−0.321	−0.3202	−0.3175	−0.3121	−0.3037	−0.2913	−0.2688
	−0.3143	−0.3143	−0.3143	−0.3143	−0.3143	−0.3132	−0.3093	−0.3016	−0.2897	−0.2678
	−0.3057	−0.3057	−0.3057	−0.3057	−0.3057	−0.3056	−0.3041	−0.2984	−0.2871	−0.2664
	−0.2951	−0.2949	−0.2949	−0.2948	−0.2945	−0.2948	−0.2945	−0.2923	−0.2841	−0.264
	−0.2778	−0.2778	−0.2778	−0.2778	−0.2778	−0.2778	−0.2778	−0.2776	−0.2738	−0.2595

Figure I.20: F2C: e=0.5c & d=1.5c

	b/c									
a/c	−0.3354	−0.3343	−0.3323	−0.3294	−0.3254	−0.321	−0.3143	−0.3057	−0.2951	−0.2778
	−0.3345	−0.3336	−0.3318	−0.329	−0.3251	−0.3207	−0.3141	−0.3055	−0.2949	−0.2777
	−0.3326	−0.3323	−0.331	−0.3284	−0.3247	−0.3203	−0.3138	−0.3053	−0.2947	−0.2776
	−0.3296	−0.3296	−0.3291	−0.3272	−0.3238	−0.3196	−0.3133	−0.3049	−0.2943	−0.2773
	−0.3255	−0.3255	−0.3255	−0.3248	−0.3223	−0.3185	−0.3124	−0.3042	−0.2936	−0.2769
	−0.321	−0.321	−0.321	−0.321	−0.32	−0.317	−0.3114	−0.3035	−0.2931	−0.2766
	−0.3147	−0.3147	−0.3147	−0.3147	−0.3147	−0.3134	−0.3093	−0.302	−0.2919	−0.2758
	−0.307	−0.307	−0.307	−0.307	−0.307	−0.3069	−0.3052	−0.2996	−0.2901	−0.2748
	−0.2979	−0.2979	−0.2978	−0.2977	−0.2975	−0.2977	−0.2975	−0.2951	−0.2879	−0.2732
	−0.2843	−0.2843	−0.2843	−0.2843	−0.2843	−0.2843	−0.2843	−0.2841	−0.2807	−0.27

Figure I.20: F2C: e=0.5c & d=2c

	b/c									
a/c	−0.3355	−0.3343	−0.3324	−0.3294	−0.3254	−0.3209	−0.3146	−0.3069	−0.2978	−0.2843
	−0.3346	−0.3337	−0.332	−0.3291	−0.3251	−0.3207	−0.3144	−0.3068	−0.2977	−0.2842
	−0.3329	−0.3326	−0.3312	−0.3286	−0.3248	−0.3204	−0.3142	−0.3066	−0.2975	−0.2841
	−0.3301	−0.3301	−0.3296	−0.3276	−0.3241	−0.3198	−0.3138	−0.3063	−0.2973	−0.2839
	−0.3263	−0.3263	−0.3263	−0.3255	−0.3228	−0.3189	−0.3131	−0.3057	−0.2967	−0.2836
	−0.322	−0.322	−0.322	−0.322	−0.3208	−0.3177	−0.3123	−0.3052	−0.2963	−0.2833
	−0.3161	−0.3161	−0.3161	−0.3161	−0.3161	−0.3147	−0.3106	−0.304	−0.2954	−0.2827
	−0.3092	−0.3092	−0.3092	−0.3092	−0.3092	−0.3091	−0.3073	−0.3022	−0.294	−0.2819
	−0.3012	−0.3012	−0.3012	−0.3011	−0.3009	−0.3012	−0.3009	−0.2986	−0.2924	−0.2807
	−0.29	−0.29	−0.29	−0.29	−0.29	−0.29	−0.29	−0.2898	−0.2869	−0.2782

Figure I.20: F2C: e=0.5c & d=2.5c

	b/c									
a/c	−0.3356	−0.3346	−0.3328	−0.33	−0.3263	−0.322	−0.3161	−0.3092	−0.3012	−0.2901
	−0.3348	−0.3341	−0.3324	−0.3298	−0.3261	−0.3218	−0.316	−0.3091	−0.3011	−0.29
	−0.3333	−0.3331	−0.3318	−0.3293	−0.3257	−0.3215	−0.3158	−0.3089	−0.301	−0.2899
	−0.3309	−0.3308	−0.3304	−0.3285	−0.3252	−0.3211	−0.3154	−0.3086	−0.3008	−0.2897
	−0.3275	−0.3275	−0.3274	−0.3267	−0.3241	−0.3203	−0.3149	−0.3082	−0.3004	−0.2895
	−0.3235	−0.3235	−0.3235	−0.3235	−0.3224	−0.3193	−0.3142	−0.3078	−0.3	−0.2892
	−0.3182	−0.3182	−0.3182	−0.3182	−0.3182	−0.3168	−0.3129	−0.3068	−0.2993	−0.2888
	−0.312	−0.312	−0.312	−0.312	−0.312	−0.3119	−0.3101	−0.3053	−0.2981	−0.2881
	−0.3049	−0.3049	−0.3049	−0.3048	−0.3047	−0.3048	−0.3047	−0.3024	−0.2969	−0.2871
	−0.2953	−0.2953	−0.2953	−0.2953	−0.2953	−0.2953	−0.2953	−0.2951	−0.2925	−0.2852

Figure I.20: F2C: e=0.5c & d=3c

	b/c									
a/c	−0.3357	−0.3348	−0.3333	−0.3308	−0.3274	−0.3235	−0.3182	−0.312	−0.3049	−0.2953
	−0.335	−0.3344	−0.3329	−0.3306	−0.3273	−0.3234	−0.3181	−0.3119	−0.3048	−0.2953
	−0.3337	−0.3335	−0.3324	−0.3302	−0.327	−0.3232	−0.318	−0.3118	−0.3047	−0.2952
	−0.3316	−0.3316	−0.3311	−0.3294	−0.3265	−0.3228	−0.3177	−0.3115	−0.3045	−0.2951
	−0.3286	−0.3286	−0.3286	−0.3279	−0.3256	−0.3221	−0.3172	−0.3112	−0.3042	−0.2949
	−0.3251	−0.3251	−0.3251	−0.3251	−0.3241	−0.3213	−0.3167	−0.3108	−0.3039	−0.2947
	−0.3205	−0.3205	−0.3205	−0.3205	−0.3204	−0.3191	−0.3155	−0.31	−0.3033	−0.2943
	−0.3149	−0.3149	−0.3149	−0.3149	−0.3149	−0.3148	−0.3132	−0.3088	−0.3024	−0.2937
	−0.3087	−0.3087	−0.3087	−0.3086	−0.3085	−0.3086	−0.3083	−0.3063	−0.3013	−0.2929
	−0.3003	−0.3003	−0.3003	−0.3003	−0.3003	−0.3003	−0.3003	−0.3001	−0.2977	−0.2913

Figure I.20: F2C: e=0.5c & d=3.5c

	b/c									
a/c	−0.3358	−0.335	−0.3337	−0.3316	−0.3286	−0.3251	−0.3205	−0.3149	−0.3087	−0.3004
	−0.3352	−0.3347	−0.3334	−0.3314	−0.3285	−0.325	−0.3204	−0.3149	−0.3086	−0.3003
	−0.3341	−0.3339	−0.3329	−0.331	−0.3282	−0.3248	−0.3202	−0.3147	−0.3085	−0.3002
	−0.3322	−0.3322	−0.3319	−0.3304	−0.3278	−0.3245	−0.32	−0.3146	−0.3084	−0.3001
	−0.3297	−0.3297	−0.3296	−0.329	−0.327	−0.324	−0.3196	−0.3143	−0.3081	−0.2999
	−0.3266	−0.3266	−0.3266	−0.3266	−0.3257	−0.3232	−0.3191	−0.3139	−0.3079	−0.2998
	−0.3226	−0.3226	−0.3226	−0.3226	−0.3225	−0.3214	−0.3181	−0.3133	−0.3073	−0.2994
	−0.3177	−0.3177	−0.3177	−0.3177	−0.3177	−0.3176	−0.3161	−0.3122	−0.3066	−0.299
	−0.3122	−0.3122	−0.3122	−0.3122	−0.312	−0.3122	−0.3121	−0.3101	−0.3056	−0.2983
	−0.305	−0.305	−0.305	−0.305	−0.305	−0.3049	−0.3049	−0.3048	−0.3026	−0.2969

Figure I.20: F2C: e=0.5c & d=4c

	b/c									
a/c	−0.3359	−0.3353	−0.3341	−0.3322	−0.3297	−0.3267	−0.3226	−0.3177	−0.3122	−0.305
	−0.3354	−0.3349	−0.3338	−0.3321	−0.3295	−0.3265	−0.3225	−0.3177	−0.3122	−0.305
	−0.3345	−0.3343	−0.3334	−0.3318	−0.3293	−0.3264	−0.3224	−0.3176	−0.3121	−0.3049
	−0.3328	−0.3328	−0.3325	−0.3312	−0.329	−0.3261	−0.3222	−0.3174	−0.312	−0.3048
	−0.3306	−0.3306	−0.3306	−0.3301	−0.3283	−0.3256	−0.3218	−0.3171	−0.3118	−0.3046
	−0.328	−0.328	−0.328	−0.3279	−0.3272	−0.325	−0.3214	−0.3169	−0.3115	−0.3045
	−0.3244	−0.3244	−0.3244	−0.3244	−0.3244	−0.3234	−0.3205	−0.3163	−0.3111	−0.3042
	−0.3202	−0.3202	−0.3202	−0.3202	−0.3202	−0.3201	−0.3188	−0.3154	−0.3104	−0.3038
	−0.3154	−0.3154	−0.3154	−0.3154	−0.3153	−0.3154	−0.3152	−0.3135	−0.3096	−0.3032
	−0.3091	−0.3091	−0.3091	−0.3091	−0.3091	−0.3091	−0.3091	−0.3089	−0.307	−0.302

Figure I.20: F2C: e=1c & d=0.5c

	b/c									
a/c	−0.3354	−0.3348	−0.334	−0.3325	−0.3301	−0.3276	−0.3222	−0.3138	−0.2985	−0.2621
	−0.3342	−0.3337	−0.333	−0.3316	−0.3293	−0.3267	−0.3215	−0.3131	−0.2978	−0.2617
	−0.3323	−0.332	−0.3314	−0.3301	−0.328	−0.3255	−0.3204	−0.3121	−0.297	−0.2611
	−0.3294	−0.3293	−0.3289	−0.3279	−0.326	−0.3236	−0.3187	−0.3086	−0.2956	−0.2602
	−0.3254	−0.3254	−0.3252	−0.3246	−0.323	−0.3209	−0.3162	−0.3085	−0.2938	−0.2592
	−0.3209	−0.3209	−0.3209	−0.3206	−0.3195	−0.3176	−0.3134	−0.3061	−0.2917	−0.2574
	−0.3143	−0.3143	−0.3142	−0.3142	−0.3137	−0.3123	−0.3088	−0.3021	−0.2882	−0.2551
	−0.3057	−0.3057	−0.3056	−0.3056	−0.3055	−0.3048	−0.3023	−0.2965	−0.2838	−0.252
	−0.2951	−0.2951	−0.2951	−0.295	−0.295	−0.2949	−0.2935	−0.2891	−0.2779	−0.2479
	−0.2777	−0.2777	−0.2777	−0.2796	−0.2777	−0.2776	−0.2774	−0.2751	−0.2664	−0.2405

Figure I.20: F2C: e=1c & d=1c

	b/c									
a/c	−0.3353	−0.3342	−0.3326	−0.3302	−0.3266	−0.3226	−0.3159	−0.3066	−0.294	−0.2704
	−0.3342	−0.3332	−0.3318	−0.3294	−0.3259	−0.322	−0.3154	−0.3061	−0.2936	−0.2701
	−0.3324	−0.3316	−0.3304	−0.3282	−0.3249	−0.3211	−0.3146	−0.3055	−0.293	−0.2696
	−0.3295	−0.3291	−0.3282	−0.3264	−0.3234	−0.3197	−0.3134	−0.3045	−0.2922	−0.269
	−0.3254	−0.3254	−0.3249	−0.3236	−0.3211	−0.3177	−0.3117	−0.303	−0.2909	−0.2681
	−0.3209	−0.3209	−0.3208	−0.3202	−0.3182	−0.3152	−0.3097	−0.3014	−0.2895	−0.2671
	−0.3146	−0.3146	−0.3146	−0.3144	−0.3134	−0.3112	−0.3065	−0.2988	−0.2872	−0.2655
	−0.3069	−0.3069	−0.3069	−0.3069	−0.3065	−0.3052	−0.3017	−0.2951	−0.2839	−0.2634
	−0.2978	−0.2978	−0.2978	−0.2978	−0.2978	−0.2973	−0.2953	−0.2901	−0.2803	−0.2607
	−0.2842	−0.2842	−0.2842	−0.2842	−0.2842	−0.2841	−0.2834	−0.2803	−0.2725	−0.2559

Figure I.20: F2C: e=1c & d=1.5c

	b/c									
a/c	−0.3354	−0.3342	−0.3323	−0.3293	−0.3254	−0.3209	−0.3142	−0.3057	−0.295	−0.2778
	−0.3344	−0.3333	−0.3315	−0.3287	−0.3248	−0.3204	−0.3138	−0.3053	−0.2947	−0.2775
	−0.3328	−0.332	−0.3303	−0.3277	−0.324	−0.3197	−0.3132	−0.3048	−0.2943	−0.2772
	−0.3301	−0.3297	−0.3285	−0.3262	−0.3227	−0.3186	−0.3123	−0.304	−0.2937	−0.2767
	−0.3264	−0.3263	−0.3256	−0.3239	−0.3209	−0.3171	−0.311	−0.303	−0.2927	−0.276
	−0.322	−0.322	−0.3219	−0.3209	−0.3185	−0.3151	−0.3095	−0.3017	−0.2917	−0.2753
	−0.3162	−0.3162	−0.3161	−0.3159	−0.3146	−0.3119	−0.307	−0.2998	−0.29	−0.2741
	−0.3092	−0.3092	−0.3092	−0.3092	−0.3088	−0.3072	−0.3034	−0.297	−0.2878	−0.2725
	−0.3013	−0.3013	−0.3013	−0.3013	−0.3013	−0.3006	−0.2984	−0.2933	−0.285	−0.2704
	−0.2901	−0.2901	−0.2901	−0.2901	−0.2901	−0.29	−0.2891	−0.286	−0.2793	−0.2669

Figure I.20: F2C: e=1c & d=2c

	b/c									
a/c	−0.3355	−0.3343	−0.3323	−0.3293	−0.3253	−0.3208	−0.3145	−0.3069	−0.2978	−0.2842
	−0.3346	−0.3335	−0.3317	−0.3288	−0.3249	−0.3204	−0.3142	−0.3066	−0.2975	−0.284
	−0.3331	−0.3323	−0.3307	−0.328	−0.3242	−0.3199	−0.3137	−0.3062	−0.2972	−0.2838
	−0.3308	−0.3303	−0.3291	−0.3267	−0.3232	−0.319	−0.313	−0.3056	−0.2967	−0.2834
	−0.3274	−0.3273	−0.3266	−0.3248	−0.3216	−0.3177	−0.312	−0.3047	−0.296	−0.2828
	−0.3235	−0.3235	−0.3233	−0.3222	−0.3197	−0.3161	−0.3108	−0.3037	−0.2952	−0.2822
	−0.3182	−0.3182	−0.3182	−0.3178	−0.3164	−0.3135	−0.3088	−0.3022	−0.2939	−0.2813
	−0.3119	−0.3119	−0.3119	−0.3119	−0.3114	−0.3097	−0.3059	−0.3	−0.2921	−0.28
	−0.3049	−0.3049	−0.3049	−0.3049	−0.3048	−0.3042	−0.3018	−0.297	−0.2899	−0.2784
	−0.2953	−0.2953	−0.2953	−0.2953	−0.2953	−0.2952	−0.2943	−0.2914	−0.2855	−0.2756

Figure I.20: F2C: e=1c & d=2.5c

	b/c									
a/c	−0.3356	−0.3345	−0.3328	−0.33	−0.3262	−0.3219	−0.3161	−0.3091	−0.3012	−0.29
	−0.3348	−0.3339	−0.3322	−0.3295	−0.3258	−0.3216	−0.3158	−0.3089	−0.301	−0.2899
	−0.3336	−0.3328	−0.3314	−0.3288	−0.3253	−0.3211	−0.3154	−0.3086	−0.3007	−0.2896
	−0.3315	−0.3311	−0.33	−0.3277	−0.3244	−0.3204	−0.3148	−0.3081	−0.3003	−0.2893
	−0.3286	−0.3285	−0.3278	−0.3261	−0.3231	−0.3193	−0.3139	−0.3074	−0.2997	−0.2888
	−0.3251	−0.3251	−0.3249	−0.3238	−0.3214	−0.318	−0.3129	−0.3066	−0.2991	−0.2883
	−0.3204	−0.3204	−0.3204	−0.3201	−0.3186	−0.3158	−0.3113	−0.3053	−0.298	−0.2876
	−0.3149	−0.3149	−0.3149	−0.3148	−0.3143	−0.3126	−0.3089	−0.3035	−0.2966	−0.2865
	−0.3086	−0.3086	−0.3086	−0.3086	−0.3086	−0.3079	−0.3055	−0.3011	−0.2948	−0.2852
	−0.3003	−0.3003	−0.3003	−0.3003	−0.3003	−0.3001	−0.2992	−0.2965	−0.2913	−0.2829

Figure I.20: F2C: e=1c & d=3c

	b/c									
a/c	−0.3357	−0.3348	−0.3332	−0.3308	−0.3274	−0.3235	−0.3182	−0.3119	−0.3049	−0.2953
	−0.335	−0.3342	−0.3327	−0.3304	−0.3271	−0.3232	−0.318	−0.3117	−0.3047	−0.2952
	−0.3339	−0.3333	−0.332	−0.3298	−0.3266	−0.3228	−0.3176	−0.3115	−0.3045	−0.295
	−0.3322	−0.3318	−0.3308	−0.3288	−0.3258	−0.3222	−0.3171	−0.311	−0.3041	−0.2947
	−0.3296	−0.3295	−0.3289	−0.3274	−0.3247	−0.3213	−0.3164	−0.3105	−0.3036	−0.2943
	−0.3266	−0.3266	−0.3264	−0.3254	−0.3233	−0.3201	−0.3155	−0.3098	−0.3031	−0.2939
	−0.3225	−0.3225	−0.3225	−0.3222	−0.3208	−0.3183	−0.3141	−0.3087	−0.3022	−0.2932
	−0.3177	−0.3177	−0.3176	−0.3176	−0.3171	−0.3155	−0.3121	−0.3072	−0.301	−0.2924
	−0.3122	−0.3122	−0.3122	−0.3122	−0.3121	−0.3115	−0.3092	−0.3051	−0.2995	−0.2912
	−0.3049	−0.3049	−0.3049	−0.3049	−0.3049	−0.3048	−0.3039	−0.3014	−0.2966	−0.2893

Figure I.20: F2C: e=1c & d=3.5c

	b/c									
a/c	−0.3358	−0.335	−0.3337	−0.3315	−0.3286	−0.3251	−0.3204	−0.3149	−0.3087	−0.3003
	−0.3352	−0.3345	−0.3332	−0.3312	−0.3283	−0.3249	−0.3202	−0.3147	−0.3085	−0.3002
	−0.3343	−0.3337	−0.3326	−0.3307	−0.3279	−0.3245	−0.32	−0.3145	−0.3083	−0.3001
	−0.3328	−0.3325	−0.3316	−0.3298	−0.3272	−0.324	−0.3195	−0.3141	−0.308	−0.2998
	−0.3305	−0.3305	−0.33	−0.3286	−0.3262	−0.3232	−0.3189	−0.3136	−0.3076	−0.2995
	−0.3279	−0.3279	−0.3277	−0.3269	−0.325	−0.3222	−0.3181	−0.313	−0.3071	−0.2991
	−0.3244	−0.3244	−0.3243	−0.3241	−0.3229	−0.3206	−0.3169	−0.3121	−0.3064	−0.2985
	−0.3201	−0.3201	−0.3201	−0.3201	−0.3197	−0.3182	−0.3152	−0.3108	−0.3053	−0.2978
	−0.3153	−0.3153	−0.3153	−0.3153	−0.3153	−0.3147	−0.3127	−0.309	−0.3041	−0.2968
	−0.309	−0.309	−0.309	−0.309	−0.309	−0.3089	−0.3081	−0.3058	−0.3016	−0.2952

Figure I.20: F2C: e=1c & d=4c

	b/c									
a/c	−0.3359	−0.3352	−0.3341	−0.3322	−0.3296	−0.3266	−0.3226	−0.3177	−0.3122	−0.305
	−0.3354	−0.3348	−0.3337	−0.3319	−0.3294	−0.3264	−0.3224	−0.3176	−0.3121	−0.3049
	−0.3346	−0.3341	−0.3331	−0.3314	−0.329	−0.3261	−0.3221	−0.3174	−0.3119	−0.3047
	−0.3333	−0.333	−0.3322	−0.3307	−0.3285	−0.3256	−0.3217	−0.317	−0.3117	−0.3045
	−0.3313	−0.3313	−0.3308	−0.3296	−0.3276	−0.3249	−0.3212	−0.3166	−0.3113	−0.3042
	−0.3291	−0.329	−0.3289	−0.3282	−0.3265	−0.3241	−0.3205	−0.3161	−0.3109	−0.3039
	−0.326	−0.326	−0.3259	−0.3257	−0.3247	−0.3227	−0.3195	−0.3153	−0.3102	−0.3034
	−0.3223	−0.3223	−0.3223	−0.3223	−0.3219	−0.3206	−0.318	−0.3141	−0.3093	−0.3027
	−0.3181	−0.3181	−0.3181	−0.3181	−0.3181	−0.3176	−0.3158	−0.3126	−0.3082	−0.3019
	−0.3127	−0.3127	−0.3126	−0.3126	−0.3126	−0.3125	−0.3119	−0.3098	−0.3061	−0.3005

Figure I.20: F2C: e=1.5c & d=0.5c

	b/c									
	−0.3354	−0.3349	−0.334	−0.3325	−0.3301	−0.3275	−0.3222	−0.3138	−0.2984	−0.2621
	−0.3342	−0.3337	−0.3329	−0.3315	−0.3291	−0.3266	−0.3213	−0.313	−0.2977	−0.2615
	−0.3323	−0.3319	−0.3312	−0.3298	−0.3276	−0.3252	−0.32	−0.3117	−0.2967	−0.2607
	−0.3294	−0.3291	−0.3285	−0.3273	−0.3253	−0.3229	−0.318	−0.3099	−0.295	−0.2595
a/c	−0.3254	−0.3252	−0.3249	−0.3239	−0.3221	−0.3199	−0.3152	−0.3074	−0.2929	−0.258
	−0.3209	−0.3209	−0.3207	−0.32	−0.3185	−0.3165	−0.3121	−0.3047	−0.2905	−0.2562
	−0.3146	−0.3146	−0.3145	−0.3142	−0.3131	−0.3114	−0.3075	−0.3006	−0.2867	−0.2536
	−0.3069	−0.3068	−0.3068	−0.3067	−0.3062	−0.3049	−0.3016	−0.2953	−0.2822	−0.2503
	−0.2978	−0.2978	−0.2977	−0.2977	−0.2975	−0.2967	−0.2941	−0.2888	−0.2767	−0.2462
	−0.2842	−0.2842	−0.2841	−0.2841	−0.2841	−0.2838	−0.2823	−0.2782	−0.2678	−0.2398

Figure I.20: F2C: e=1.5c & d=1c

	b/c									
	−0.3353	−0.3342	−0.3326	−0.3302	−0.3266	−0.3226	−0.3159	−0.3066	−0.294	−0.2703
	−0.3343	−0.3332	−0.3317	−0.3293	−0.3258	−0.3219	−0.3152	−0.306	−0.2935	−0.27
	−0.3326	−0.3316	−0.3303	−0.328	−0.3246	−0.3208	−0.3143	−0.3052	−0.2927	−0.2694
	−0.3299	−0.3292	−0.328	−0.3259	−0.3228	−0.3191	−0.3128	−0.3039	−0.2916	−0.2685
a/c	−0.3262	−0.3258	−0.3249	−0.3232	−0.3203	−0.3169	−0.3108	−0.3022	−0.2901	−0.2673
	−0.3219	−0.3218	−0.3212	−0.3199	−0.3175	−0.3143	−0.3086	−0.3002	−0.2885	−0.2661
	−0.3161	−0.3161	−0.3159	−0.3151	−0.3132	−0.3105	−0.3053	−0.2974	−0.2863	−0.2642
	−0.3091	−0.3091	−0.3091	−0.3088	−0.3076	−0.3054	−0.301	−0.2938	−0.2828	−0.2619
	−0.3012	−0.3011	−0.3011	−0.3011	−0.3005	−0.2991	−0.2955	−0.2892	−0.279	−0.259
	−0.29	−0.2899	−0.2899	−0.2899	−0.2898	−0.289	−0.2868	−0.282	−0.2727	−0.2546

Figure I.20: F2C: e=1.5c & d=1.5c

	b/c									
	−0.3355	−0.3342	−0.3323	−0.3293	−0.3253	−0.3209	−0.3142	−0.3056	−0.295	−0.2777
	−0.3346	−0.3334	−0.3315	−0.3286	−0.3247	−0.3203	−0.3137	−0.3052	−0.2946	−0.2774
	−0.333	−0.332	−0.3302	−0.3275	−0.3237	−0.3194	−0.313	−0.3045	−0.2941	−0.277
	−0.3307	−0.3298	−0.3283	−0.3258	−0.3223	−0.3181	−0.3118	−0.3035	−0.2932	−0.2763
a/c	−0.3274	−0.3269	−0.3257	−0.3235	−0.3202	−0.3164	−0.3103	−0.3022	−0.2921	−0.2754
	−0.3236	−0.3233	−0.3225	−0.3208	−0.3179	−0.3143	−0.3086	−0.3008	−0.2908	−0.2744
	−0.3183	−0.3182	−0.3179	−0.3167	−0.3145	−0.3113	−0.306	−0.2986	−0.289	−0.273
	−0.312	−0.312	−0.3119	−0.3114	−0.3099	−0.3073	−0.3027	−0.2958	−0.2866	−0.2712
	−0.3049	−0.3049	−0.3049	−0.3048	−0.304	−0.3023	−0.2984	−0.2923	−0.2837	−0.2689
	−0.2953	−0.2953	−0.2953	−0.2952	−0.2951	−0.2942	−0.2917	−0.2869	−0.279	−0.2655

Figure I.20: F2C: e=1.5c & d=2c

	b/c									
	−0.3355	−0.3343	−0.3323	−0.3293	−0.3253	−0.3208	−0.3145	−0.3068	−0.2978	−0.2843
	−0.3347	−0.3336	−0.3317	−0.3288	−0.3248	−0.3203	−0.3141	−0.3065	−0.2974	−0.284
	−0.3334	−0.3324	−0.3306	−0.3278	−0.324	−0.3196	−0.3135	−0.3059	−0.297	−0.2836
	−0.3313	−0.3305	−0.329	−0.3264	−0.3227	−0.3185	−0.3126	−0.3051	−0.2963	−0.283
a/c	−0.3284	−0.3279	−0.3267	−0.3244	−0.3211	−0.3171	−0.3113	−0.3041	−0.2954	−0.2823
	−0.3251	−0.3248	−0.324	−0.3221	−0.3191	−0.3154	−0.3099	−0.3029	−0.2944	−0.2815
	−0.3204	−0.3204	−0.32	−0.3187	−0.3162	−0.3129	−0.3078	−0.3012	−0.2929	−0.2803
	−0.3148	−0.3148	−0.3147	−0.3141	−0.3124	−0.3097	−0.3052	−0.2989	−0.291	−0.2788
	−0.3086	−0.3086	−0.3085	−0.3084	−0.3075	−0.3055	−0.3017	−0.2962	−0.2887	−0.277
	−0.3002	−0.3002	−0.3002	−0.3002	−0.2999	−0.2989	−0.2964	−0.2918	−0.285	−0.2743

Figure I.20: F2C: e=1.5c & d=2.5c

	b/c									
	−0.3356	−0.3345	−0.3328	−0.33	−0.3262	−0.3219	−0.3161	−0.3091	−0.3012	−0.29
	−0.3349	−0.3339	−0.3322	−0.3295	−0.3258	−0.3215	−0.3157	−0.3088	−0.3009	−0.2898
	−0.3338	−0.3329	−0.3313	−0.3287	−0.3251	−0.3209	−0.3152	−0.3083	−0.3005	−0.2895
	−0.332	−0.3313	−0.3299	−0.3275	−0.324	−0.32	−0.3144	−0.3077	−0.2999	−0.289
a/c	−0.3295	−0.329	−0.3279	−0.3258	−0.3226	−0.3188	−0.3134	−0.3068	−0.2992	−0.2884
	−0.3265	−0.3263	−0.3255	−0.3238	−0.321	−0.3174	−0.3122	−0.3058	−0.2984	−0.2877
	−0.3225	−0.3224	−0.322	−0.3208	−0.3185	−0.3153	−0.3105	−0.3044	−0.2972	−0.2867
	−0.3176	−0.3176	−0.3175	−0.3169	−0.3152	−0.3125	−0.3082	−0.3025	−0.2956	−0.2855
	−0.3121	−0.3121	−0.3121	−0.3119	−0.311	−0.309	−0.3054	−0.3002	−0.2937	−0.284
	−0.3048	−0.3048	−0.3048	−0.3048	−0.3045	−0.3035	−0.3009	−0.2966	−0.2907	−0.2817

Figure I.20: F2C: e=1.5c & d=3c

	b/c									
	−0.3357	−0.3348	−0.3332	−0.3307	−0.3274	−0.3235	−0.3182	−0.3119	−0.3049	−0.2953
	−0.3351	−0.3342	−0.3327	−0.3303	−0.327	−0.3231	−0.3179	−0.3117	−0.3047	−0.2951
	−0.3341	−0.3333	−0.3319	−0.3296	−0.3264	−0.3226	−0.3174	−0.3113	−0.3043	−0.2948
	−0.3326	−0.332	−0.3307	−0.3286	−0.3255	−0.3218	−0.3168	−0.3107	−0.3038	−0.2944
a/c	−0.3304	−0.33	−0.329	−0.3271	−0.3243	−0.3208	−0.3159	−0.31	−0.3032	−0.2939
	−0.3279	−0.3277	−0.327	−0.3254	−0.3228	−0.3196	−0.3149	−0.3091	−0.3025	−0.2933
	−0.3243	−0.3243	−0.3239	−0.3228	−0.3207	−0.3178	−0.3134	−0.3079	−0.3015	−0.2925
	−0.3201	−0.3201	−0.32	−0.3194	−0.3179	−0.3154	−0.3115	−0.3063	−0.3002	−0.2914
	−0.3153	−0.3153	−0.3153	−0.3151	−0.3142	−0.3124	−0.3091	−0.3044	−0.2986	−0.2902
	−0.309	−0.309	−0.3089	−0.3089	−0.3086	−0.3076	−0.3053	−0.3013	−0.296	−0.2882

Figure I.20: F2C: e=1.5c & d=3.5c

	b/c									
	−0.3358	−0.335	−0.3337	−0.3315	−0.3285	−0.3251	−0.3204	−0.3149	−0.3086	−0.3003
	−0.3353	−0.3346	−0.3332	−0.3311	−0.3282	−0.3248	−0.3202	−0.3147	−0.3085	−0.3002
	−0.3344	−0.3338	−0.3325	−0.3305	−0.3277	−0.3243	−0.3198	−0.3143	−0.3082	−0.2999
	−0.3331	−0.3326	−0.3315	−0.3296	−0.3269	−0.3237	−0.3192	−0.3138	−0.3077	−0.2996
a/c	−0.3312	−0.3309	−0.33	−0.3284	−0.3259	−0.3228	−0.3184	−0.3132	−0.3072	−0.2991
	−0.329	−0.3288	−0.3282	−0.3269	−0.3246	−0.3217	−0.3176	−0.3125	−0.3066	−0.2986
	−0.3259	−0.3259	−0.3256	−0.3246	−0.3228	−0.3202	−0.3163	−0.3114	−0.3057	−0.2979
	−0.3222	−0.3222	−0.3222	−0.3217	−0.3203	−0.3181	−0.3146	−0.31	−0.3046	−0.297
	−0.3181	−0.3181	−0.318	−0.3179	−0.3171	−0.3155	−0.3125	−0.3083	−0.3032	−0.2959
	−0.3126	−0.3126	−0.3126	−0.3125	−0.3123	−0.3114	−0.3092	−0.3057	−0.301	−0.2942

Figure I.20: F2C: e=1.5c & d=4c

	b/c									
	−0.3359	−0.3352	−0.3341	−0.3322	−0.3296	−0.3266	−0.3225	−0.3177	−0.3122	−0.305
	−0.3355	−0.3348	−0.3337	−0.3319	−0.3293	−0.3264	−0.3223	−0.3175	−0.312	−0.3048
	−0.3347	−0.3341	−0.3331	−0.3313	−0.3289	−0.326	−0.322	−0.3172	−0.3118	−0.3046
	−0.3336	−0.3331	−0.3321	−0.3305	−0.3282	−0.3254	−0.3215	−0.3168	−0.3114	−0.3043
a/c	−0.3319	−0.3316	−0.3309	−0.3294	−0.3273	−0.3246	−0.3208	−0.3162	−0.3109	−0.3039
	−0.33	−0.3298	−0.3293	−0.3281	−0.3262	−0.3236	−0.32	−0.3156	−0.3104	−0.3034
	−0.3273	−0.3273	−0.327	−0.3262	−0.3246	−0.3223	−0.3189	−0.3146	−0.3096	−0.3028
	−0.3241	−0.3241	−0.324	−0.3236	−0.3224	−0.3205	−0.3175	−0.3134	−0.3086	−0.302
	−0.3205	−0.3204	−0.3204	−0.3203	−0.3196	−0.3182	−0.3156	−0.3119	−0.3074	−0.301
	−0.3157	−0.3157	−0.3157	−0.3156	−0.3154	−0.3146	−0.3127	−0.3096	−0.3055	−0.2996

Figure I.20: F2C: e=2c & d=0.5c

	b/c									
a/c	−0.3355	−0.3349	−0.334	−0.3325	−0.3302	−0.3276	−0.3222	−0.3138	−0.2985	−0.2621
	−0.3344	−0.3339	−0.333	−0.3316	−0.3292	−0.3267	−0.3214	−0.313	−0.2978	−0.2615
	−0.3326	−0.3321	−0.3313	−0.3299	−0.3277	−0.3252	−0.32	−0.3117	−0.2966	−0.2606
	−0.3299	−0.3294	−0.3288	−0.3275	−0.3253	−0.3229	−0.3178	−0.3098	−0.2947	−0.2595
	−0.3261	−0.3258	−0.3252	−0.3241	−0.3221	−0.3199	−0.315	−0.3072	−0.2925	−0.2576
	−0.3219	−0.3217	−0.3213	−0.3203	−0.3186	−0.3165	−0.3119	−0.3043	−0.29	−0.2557
	−0.3161	−0.316	−0.3158	−0.3151	−0.3136	−0.3118	−0.3075	−0.3004	−0.2864	−0.253
	−0.3091	−0.3091	−0.309	−0.3086	−0.3075	−0.3059	−0.3021	−0.2955	−0.2821	−0.2498
	−0.3011	−0.3012	−0.3012	−0.301	−0.3003	−0.299	−0.2957	−0.2897	−0.277	−0.246
	−0.2899	−0.2899	−0.2899	−0.2899	−0.2896	−0.2888	−0.2863	−0.2811	−0.2696	−0.2404

Figure I.20: F2C: e=2c & d=1c

	b/c									
a/c	−0.3354	−0.3343	−0.3327	−0.3302	−0.3266	−0.3226	−0.3159	−0.3066	−0.294	−0.2703
	−0.3345	−0.3334	−0.3318	−0.3294	−0.3259	−0.3219	−0.3153	−0.306	−0.2935	−0.2699
	−0.3329	−0.3319	−0.3304	−0.3281	−0.3247	−0.3208	−0.3142	−0.3051	−0.2927	−0.2693
	−0.3305	−0.3296	−0.3283	−0.3261	−0.3228	−0.319	−0.3127	−0.3037	−0.2914	−0.2683
	−0.3272	−0.3265	−0.3253	−0.3233	−0.3203	−0.3167	−0.3106	−0.3018	−0.2898	−0.267
	−0.3233	−0.3228	−0.3219	−0.3202	−0.3175	−0.3141	−0.3083	−0.2998	−0.288	−0.2656
	−0.3181	−0.3179	−0.3173	−0.3159	−0.3135	−0.3105	−0.305	−0.297	−0.2855	−0.2636
	−0.3119	−0.3118	−0.3115	−0.3106	−0.3087	−0.3061	−0.3011	−0.2935	−0.2825	−0.2612
	−0.3048	−0.3048	−0.3048	−0.3043	−0.3029	−0.3007	−0.2964	−0.2894	−0.2789	−0.2584
	−0.2952	−0.2952	−0.2952	−0.2951	−0.2944	−0.2929	−0.2894	−0.2833	−0.2735	−0.2545

Figure I.20: F2C: e=2c & d=1.5c

	b/c									
a/c	−0.3355	−0.3343	−0.3323	−0.3293	−0.3254	−0.3209	−0.3142	−0.3056	−0.295	−0.2777
	−0.3347	−0.3335	−0.3316	−0.3287	−0.3247	−0.3203	−0.3137	−0.3052	−0.2946	−0.2774
	−0.3334	−0.3322	−0.3304	−0.3276	−0.3237	−0.3194	−0.3129	−0.3044	−0.294	−0.2769
	−0.3313	−0.3302	−0.3286	−0.3259	−0.3222	−0.318	−0.3117	−0.3033	−0.293	−0.2761
	−0.3284	−0.3275	−0.3261	−0.3236	−0.3202	−0.3162	−0.31	−0.3019	−0.2918	−0.275
	−0.325	−0.3244	−0.3232	−0.321	−0.3179	−0.3141	−0.3082	−0.3003	−0.2904	−0.2739
	−0.3204	−0.3201	−0.3192	−0.3174	−0.3147	−0.3112	−0.3057	−0.2981	−0.2885	−0.2724
	−0.3149	−0.3148	−0.3143	−0.313	−0.3107	−0.3077	−0.3026	−0.2954	−0.2861	−0.2705
	−0.3086	−0.3086	−0.3084	−0.3077	−0.3059	−0.3034	−0.2988	−0.2922	−0.2833	−0.2683
	−0.3003	−0.3003	−0.3003	−0.3	−0.299	−0.2972	−0.2934	−0.2875	−0.2793	−0.2651

Figure I.20: F2C: e=2c & d=2c

	b/c									
a/c	−0.3355	−0.3343	−0.3324	−0.3293	−0.3253	−0.3208	−0.3145	−0.3068	−0.2977	−0.2842
	−0.3348	−0.3337	−0.3318	−0.3288	−0.3248	−0.3203	−0.3141	−0.3065	−0.2974	−0.2839
	−0.3337	−0.3326	−0.3307	−0.3279	−0.324	−0.3196	−0.3134	−0.3059	−0.2969	−0.2835
	−0.3318	−0.3309	−0.3292	−0.3264	−0.3227	−0.3184	−0.3124	−0.305	−0.2961	−0.2828
	−0.3293	−0.3285	−0.327	−0.3245	−0.321	−0.3169	−0.3111	−0.3038	−0.2951	−0.2819
	−0.3264	−0.3258	−0.3246	−0.3223	−0.319	−0.3152	−0.3096	−0.3025	−0.294	−0.281
	−0.3224	−0.322	−0.3211	−0.3193	−0.3164	−0.3128	−0.3075	−0.3007	−0.2924	−0.2797
	−0.3176	−0.3174	−0.3169	−0.3155	−0.313	−0.3099	−0.305	−0.2985	−0.2906	−0.2782
	−0.3121	−0.3121	−0.3118	−0.3109	−0.309	−0.3063	−0.3019	−0.2959	−0.2883	−0.2764
	−0.3048	−0.3048	−0.3048	−0.3044	−0.3032	−0.3012	−0.2975	−0.2921	−0.285	−0.2737

Figure I.20: F2C: e=2c & d=2.5c

	b/c									
a/c	−0.3356	−0.3346	−0.3328	−0.33	−0.3262	−0.3219	−0.3161	−0.3091	−0.3012	−0.29
	−0.335	−0.334	−0.3322	−0.3295	−0.3258	−0.3215	−0.3157	−0.3088	−0.3009	−0.2898
	−0.334	−0.333	−0.3314	−0.3287	−0.325	−0.3209	−0.3151	−0.3083	−0.3004	−0.2894
	−0.3324	−0.3316	−0.33	−0.3275	−0.324	−0.3199	−0.3143	−0.3075	−0.2998	−0.2888
	−0.3303	−0.3295	−0.3282	−0.3258	−0.3225	−0.3186	−0.3131	−0.3065	−0.2989	−0.2881
	−0.3277	−0.3272	−0.326	−0.324	−0.3209	−0.3171	−0.3119	−0.3054	−0.298	−0.2873
	−0.3242	−0.3239	−0.3231	−0.3213	−0.3186	−0.3151	−0.3101	−0.3039	−0.2967	−0.2862
	−0.32	−0.3199	−0.3194	−0.3181	−0.3157	−0.3126	−0.308	−0.3021	−0.2951	−0.2849
	−0.3152	−0.3152	−0.315	−0.3141	−0.3123	−0.3096	−0.3054	−0.2999	−0.2933	−0.2834
	−0.3089	−0.3089	−0.3089	−0.3085	−0.3073	−0.3053	−0.3017	−0.2967	−0.2905	−0.2811

Figure I.20: F2C: e=2c & d=3c

	b/c									
a/c	−0.3357	−0.3348	−0.3332	−0.3308	−0.3274	−0.3235	−0.3182	−0.3119	−0.3049	−0.2953
	−0.3352	−0.3343	−0.3328	−0.3303	−0.327	−0.3231	−0.3179	−0.3117	−0.3046	−0.2951
	−0.3343	−0.3335	−0.332	−0.3296	−0.3264	−0.3226	−0.3174	−0.3112	−0.3042	−0.2948
	−0.333	−0.3322	−0.3308	−0.3286	−0.3254	−0.3217	−0.3166	−0.3106	−0.3037	−0.2943
	−0.3311	−0.3304	−0.3292	−0.3272	−0.3242	−0.3206	−0.3157	−0.3097	−0.3029	−0.2936
	−0.3289	−0.3284	−0.3274	−0.3255	−0.3227	−0.3193	−0.3146	−0.3088	−0.3021	−0.2929
	−0.3258	−0.3255	−0.3248	−0.3232	−0.3207	−0.3176	−0.3131	−0.3075	−0.301	−0.292
	−0.3222	−0.3221	−0.3216	−0.3204	−0.3183	−0.3155	−0.3112	−0.3059	−0.2997	−0.2909
	−0.318	−0.318	−0.3178	−0.317	−0.3153	−0.3129	−0.309	−0.304	−0.2981	−0.2897
	−0.3125	−0.3125	−0.3125	−0.3121	−0.311	−0.3091	−0.3058	−0.3013	−0.2958	−0.2877

Figure I.20: F2C: e=2c & d=3.5c

	b/c									
a/c	−0.3358	−0.335	−0.3337	−0.3315	−0.3285	−0.3251	−0.3204	−0.3149	−0.3086	−0.3003
	−0.3354	−0.3346	−0.3333	−0.3311	−0.3282	−0.3248	−0.3202	−0.3147	−0.3084	−0.3001
	−0.3346	−0.3339	−0.3326	−0.3305	−0.3277	−0.3243	−0.3197	−0.3143	−0.3081	−0.2998
	−0.3334	−0.3328	−0.3316	−0.3296	−0.3268	−0.3236	−0.3191	−0.3137	−0.3076	−0.2994
	−0.3318	−0.3312	−0.3302	−0.3284	−0.3257	−0.3226	−0.3182	−0.313	−0.3069	−0.2988
	−0.3298	−0.3294	−0.3286	−0.3269	−0.3245	−0.3215	−0.3173	−0.3121	−0.3062	−0.2982
	−0.3272	−0.327	−0.3263	−0.3249	−0.3228	−0.32	−0.316	−0.311	−0.3053	−0.2974
	−0.324	−0.3239	−0.3235	−0.3225	−0.3206	−0.3181	−0.3144	−0.3096	−0.3041	−0.2964
	−0.3204	−0.3204	−0.3202	−0.3195	−0.318	−0.3158	−0.3124	−0.308	−0.3027	−0.2953
	−0.3156	−0.3156	−0.3156	−0.3153	−0.3143	−0.3126	−0.3097	−0.3057	−0.3007	−0.2936

Figure I.20: F2C: e=2c & d=4c

	b/c									
a/c	−0.3359	−0.3352	−0.3341	−0.3322	−0.3296	−0.3266	−0.3225	−0.3177	−0.3122	−0.305
	−0.3355	−0.3349	−0.3337	−0.3319	−0.3293	−0.3263	−0.3223	−0.3175	−0.312	−0.3048
	−0.3349	−0.3342	−0.3331	−0.3313	−0.3289	−0.3259	−0.3219	−0.3171	−0.3117	−0.3045
	−0.3338	−0.3333	−0.3322	−0.3305	−0.3281	−0.3253	−0.3213	−0.3166	−0.3113	−0.3042
	−0.3324	−0.3319	−0.331	−0.3294	−0.3272	−0.3244	−0.3206	−0.316	−0.3107	−0.3037
	−0.3307	−0.3303	−0.3296	−0.3282	−0.3261	−0.3234	−0.3198	−0.3153	−0.3101	−0.3031
	−0.3284	−0.3282	−0.3276	−0.3264	−0.3245	−0.3221	−0.3186	−0.3143	−0.3092	−0.3024
	−0.3256	−0.3255	−0.3252	−0.3243	−0.3227	−0.3205	−0.3172	−0.3131	−0.3082	−0.3015
	−0.3224	−0.3224	−0.3222	−0.3216	−0.3204	−0.3185	−0.3155	−0.3116	−0.307	−0.3005
	−0.3183	−0.3183	−0.3182	−0.318	−0.3171	−0.3156	−0.3131	−0.3096	−0.3052	−0.299

Figure I.20: F2C: e=2.5c & d=0.5c

	b/c									
	−0.3355	−0.3349	−0.3341	−0.3326	−0.3302	−0.3276	−0.3222	−0.3138	−0.2985	−0.2621
	−0.3346	−0.334	−0.3332	−0.3317	−0.3293	−0.3268	−0.3215	−0.3131	−0.2979	−0.2615
	−0.333	−0.3325	−0.3317	−0.3302	−0.3279	−0.3254	−0.3202	−0.3119	−0.2968	−0.2607
	−0.3305	−0.3301	−0.3293	−0.3279	−0.3257	−0.3233	−0.3182	−0.31	−0.2947	−0.2594
a/c	−0.3272	−0.3268	−0.3261	−0.3248	−0.3227	−0.3204	−0.3154	−0.3075	−0.2927	−0.2576
	−0.3233	−0.323	−0.3224	−0.3213	−0.3194	−0.3172	−0.3124	−0.3047	−0.2902	−0.2557
	−0.3181	−0.3178	−0.3174	−0.3165	−0.3147	−0.3127	−0.3083	−0.3009	−0.2868	−0.2531
	−0.3118	−0.3117	−0.3115	−0.3107	−0.3093	−0.3075	−0.3033	−0.2964	−0.2828	−0.25
	−0.3048	−0.3048	−0.3047	−0.3042	−0.303	−0.3014	−0.2977	−0.2912	−0.2781	−0.2464
	−0.2952	−0.2952	−0.2952	−0.295	−0.2942	−0.293	−0.2897	−0.2839	−0.2716	−0.2415

Figure I.20: F2C: e=2.5c & d=1c

	b/c									
	−0.3354	−0.3343	−0.3327	−0.3302	−0.3267	−0.3226	−0.3159	−0.3066	−0.294	−0.2703
	−0.3346	−0.3335	−0.332	−0.3295	−0.326	−0.322	−0.3153	−0.3061	−0.2935	−0.2699
	−0.3332	−0.3322	−0.3307	−0.3283	−0.3248	−0.3209	−0.3143	−0.3052	−0.2927	−0.2693
	−0.3311	−0.3301	−0.3287	−0.3264	−0.3231	−0.3192	−0.3128	−0.3038	−0.2915	−0.2683
a/c	−0.3282	−0.3273	−0.326	−0.3239	−0.3207	−0.317	−0.3108	−0.3019	−0.2898	−0.2669
	−0.3248	−0.3241	−0.3229	−0.321	−0.318	−0.3145	−0.3085	−0.2999	−0.288	−0.2654
	−0.3202	−0.3196	−0.3187	−0.317	−0.3143	−0.3111	−0.3054	−0.2971	−0.2856	−0.2634
	−0.3147	−0.3144	−0.3137	−0.3123	−0.3099	−0.307	−0.3017	−0.2938	−0.2826	−0.2611
	−0.3085	−0.3084	−0.3079	−0.3069	−0.3049	−0.3024	−0.2974	−0.29	−0.2793	−0.2584
	−0.3002	−0.3002	−0.3	−0.2994	−0.2979	−0.2958	−0.2915	−0.2847	−0.2746	−0.2548

Figure I.20: F2C: e=2.5c & d=1.5c

	b/c									
	−0.3355	−0.3343	−0.3323	−0.3293	−0.3254	−0.3209	−0.3142	−0.3056	−0.295	−0.2777
	−0.3349	−0.3336	−0.3317	−0.3287	−0.3248	−0.3204	−0.3138	−0.3052	−0.2946	−0.2774
	−0.3337	−0.3325	−0.3306	−0.3277	−0.3239	−0.3195	−0.313	−0.3045	−0.294	−0.2769
	−0.3318	−0.3307	−0.3289	−0.3262	−0.3224	−0.3182	−0.3117	−0.3034	−0.293	−0.276
a/c	−0.3293	−0.3283	−0.3266	−0.3241	−0.3205	−0.3164	−0.3101	−0.3019	−0.2917	−0.2749
	−0.3263	−0.3255	−0.324	−0.3216	−0.3182	−0.3143	−0.3083	−0.3003	−0.2903	−0.2737
	−0.3223	−0.3217	−0.3205	−0.3183	−0.3152	−0.3116	−0.3058	−0.2981	−0.2884	−0.2721
	−0.3175	−0.3171	−0.3162	−0.3144	−0.3116	−0.3083	−0.3029	−0.2955	−0.2861	−0.2702
	−0.3121	−0.3119	−0.3112	−0.3098	−0.3075	−0.3045	−0.2995	−0.2925	−0.2834	−0.2681
	−0.3049	−0.3048	−0.3045	−0.3036	−0.3017	−0.2992	−0.2948	−0.2884	−0.2798	−0.2651

Figure I.20: F2C: e=2.5c & d=2c

	b/c									
	−0.3355	−0.3344	−0.3324	−0.3294	−0.3253	−0.3208	−0.3145	−0.3068	−0.2978	−0.2842
	−0.3349	−0.3338	−0.3318	−0.3289	−0.3248	−0.3204	−0.3141	−0.3065	−0.2974	−0.2839
	−0.3339	−0.3328	−0.3309	−0.328	−0.3241	−0.3196	−0.3135	−0.3059	−0.2969	−0.2835
	−0.3323	−0.3313	−0.3295	−0.3267	−0.3228	−0.3185	−0.3124	−0.305	−0.2961	−0.2828
a/c	−0.3301	−0.3292	−0.3275	−0.3249	−0.3212	−0.317	−0.3111	−0.3039	−0.295	−0.2818
	−0.3276	−0.3267	−0.3253	−0.3228	−0.3193	−0.3153	−0.3096	−0.3024	−0.2938	−0.2808
	−0.3241	−0.3234	−0.3222	−0.32	−0.3168	−0.313	−0.3075	−0.3006	−0.2922	−0.2795
	−0.3199	−0.3195	−0.3185	−0.3166	−0.3137	−0.3103	−0.3051	−0.2985	−0.2904	−0.2779
	−0.3152	−0.3149	−0.3142	−0.3127	−0.3102	−0.3071	−0.3023	−0.296	−0.2882	−0.2761
	−0.3089	−0.3088	−0.3084	−0.3074	−0.3054	−0.3028	−0.2984	−0.2926	−0.2852	−0.2736

Figure I.20: F2C: e=2.5c & d=2.5c

	b/c									
	−0.3357	−0.3346	−0.3328	−0.33	−0.3262	−0.3219	−0.3161	−0.3091	−0.3012	−0.29
	−0.3351	−0.3341	−0.3323	−0.3296	−0.3258	−0.3215	−0.3157	−0.3088	−0.3009	−0.2898
	−0.3342	−0.3332	−0.3315	−0.3288	−0.3251	−0.3209	−0.3151	−0.3083	−0.3004	−0.2894
	−0.3329	−0.3319	−0.3303	−0.3277	−0.3241	−0.3199	−0.3143	−0.3075	−0.2997	−0.2888
a/c	−0.3309	−0.3301	−0.3286	−0.3261	−0.3226	−0.3187	−0.3131	−0.3065	−0.2988	−0.288
	−0.3287	−0.328	−0.3266	−0.3243	−0.321	−0.3172	−0.3118	−0.3053	−0.2978	−0.2871
	−0.3257	−0.3251	−0.324	−0.3219	−0.3189	−0.3152	−0.3101	−0.3038	−0.2965	−0.2859
	−0.3221	−0.3217	−0.3208	−0.319	−0.3163	−0.3129	−0.308	−0.302	−0.2949	−0.2846
	−0.3179	−0.3177	−0.3171	−0.3156	−0.3133	−0.3102	−0.3057	−0.2999	−0.2931	−0.2831
	−0.3125	−0.3124	−0.312	−0.311	−0.3091	−0.3065	−0.3024	−0.297	−0.2906	−0.2809

Figure I.20: F2C: e=2.5c & d=3c

	b/c									
	−0.3358	−0.3348	−0.3332	−0.3308	−0.3274	−0.3235	−0.3182	−0.3119	−0.3049	−0.2953
	−0.3353	−0.3344	−0.3328	−0.3304	−0.327	−0.3231	−0.3179	−0.3117	−0.3046	−0.2951
	−0.3345	−0.3336	−0.3321	−0.3297	−0.3264	−0.3226	−0.3174	−0.3112	−0.3042	−0.2947
	−0.3333	−0.3325	−0.331	−0.3287	−0.3255	−0.3218	−0.3166	−0.3105	−0.3036	−0.2942
a/c	−0.3316	−0.3309	−0.3296	−0.3274	−0.3243	−0.3206	−0.3156	−0.3096	−0.3028	−0.2935
	−0.3297	−0.3291	−0.3279	−0.3258	−0.3229	−0.3194	−0.3145	−0.3087	−0.302	−0.2928
	−0.3271	−0.3266	−0.3255	−0.3237	−0.321	−0.3177	−0.313	−0.3073	−0.3008	−0.2918
	−0.3239	−0.3236	−0.3228	−0.3212	−0.3187	−0.3157	−0.3112	−0.3058	−0.2994	−0.2906
	−0.3203	−0.3201	−0.3195	−0.3183	−0.3161	−0.3133	−0.3092	−0.304	−0.2979	−0.2893
	−0.3156	−0.3155	−0.3152	−0.3142	−0.3125	−0.3101	−0.3064	−0.3015	−0.2957	−0.2874

Figure I.20: F2C: e=2.5c & d=3.5c

	b/c									
	−0.3359	−0.3351	−0.3337	−0.3315	−0.3286	−0.3251	−0.3204	−0.3149	−0.3086	−0.3003
	−0.3355	−0.3347	−0.3333	−0.3312	−0.3282	−0.3248	−0.3202	−0.3147	−0.3084	−0.3001
	−0.3348	−0.334	−0.3327	−0.3306	−0.3277	−0.3243	−0.3197	−0.3143	−0.3081	−0.2998
	−0.3337	−0.333	−0.3317	−0.3297	−0.3269	−0.3236	−0.3191	−0.3137	−0.3075	−0.2993
a/c	−0.3323	−0.3316	−0.3304	−0.3285	−0.3258	−0.3226	−0.3182	−0.3129	−0.3068	−0.2987
	−0.3306	−0.33	−0.329	−0.3272	−0.3246	−0.3215	−0.3172	−0.312	−0.3061	−0.2981
	−0.3283	−0.3278	−0.3269	−0.3253	−0.3229	−0.32	−0.3159	−0.3109	−0.3051	−0.2972
	−0.3255	−0.3252	−0.3245	−0.3231	−0.321	−0.3183	−0.3143	−0.3095	−0.3039	−0.2962
	−0.3224	−0.3222	−0.3217	−0.3206	−0.3187	−0.3162	−0.3125	−0.3079	−0.3025	−0.295
	−0.3182	−0.3182	−0.3179	−0.3171	−0.3155	−0.3134	−0.3101	−0.3058	−0.3006	−0.2934

Figure I.20: F2C: e=2.5c & d=4c

	b/c									
	−0.336	−0.3353	−0.3341	−0.3322	−0.3296	−0.3266	−0.3225	−0.3177	−0.3122	−0.305
	−0.3356	−0.3349	−0.3337	−0.3319	−0.3293	−0.3264	−0.3223	−0.3175	−0.312	−0.3048
	−0.335	−0.3343	−0.3332	−0.3314	−0.3289	−0.3259	−0.3219	−0.3171	−0.3117	−0.3045
	−0.3341	−0.3335	−0.3324	−0.3306	−0.3282	−0.3253	−0.3213	−0.3166	−0.3112	−0.3041
a/c	−0.3328	−0.3322	−0.3312	−0.3296	−0.3272	−0.3244	−0.3206	−0.3159	−0.3106	−0.3035
	−0.3313	−0.3308	−0.3299	−0.3284	−0.3261	−0.3234	−0.3197	−0.3151	−0.3099	−0.303
	−0.3293	−0.3289	−0.3281	−0.3267	−0.3247	−0.3221	−0.3185	−0.3141	−0.309	−0.3022
	−0.3269	−0.3266	−0.326	−0.3248	−0.3229	−0.3206	−0.3171	−0.3129	−0.308	−0.3012
	−0.3241	−0.324	−0.3235	−0.3225	−0.3209	−0.3188	−0.3156	−0.3115	−0.3067	−0.3002
	−0.3205	−0.3204	−0.3202	−0.3195	−0.3181	−0.3163	−0.3134	−0.3096	−0.3051	−0.2988

Figure I.20: F2C: e=3c & d=0.5c

	b/c									
a/c	−0.3355	−0.335	−0.3341	−0.3326	−0.3302	−0.3276	−0.3223	−0.3138	−0.2985	−0.2621
	−0.3347	−0.3342	−0.3333	−0.3318	−0.3295	−0.3269	−0.3216	−0.3132	−0.298	−0.2616
	−0.3334	−0.3328	−0.332	−0.3305	−0.3282	−0.3257	−0.3204	−0.3121	−0.297	−0.2608
	−0.3312	−0.3307	−0.3299	−0.3285	−0.3255	−0.3238	−0.3186	−0.3104	−0.2953	−0.2596
	−0.3283	−0.3278	−0.3271	−0.3257	−0.3235	−0.3212	−0.3161	−0.3081	−0.2931	−0.2579
	−0.3248	−0.3244	−0.3238	−0.3225	−0.3205	−0.3182	−0.3133	−0.3054	−0.2908	−0.2561
	−0.3202	−0.3198	−0.3193	−0.3182	−0.3163	−0.3141	−0.3094	−0.3019	−0.2877	−0.2536
	−0.3147	−0.3144	−0.314	−0.313	−0.3113	−0.3094	−0.3049	−0.2977	−0.2837	−0.2506
	−0.3085	−0.3083	−0.308	−0.3072	−0.3057	−0.304	−0.2998	−0.2931	−0.2796	−0.2473
	−0.3001	−0.3001	−0.2999	−0.2994	−0.2981	−0.2966	−0.2929	−0.2866	−0.2738	−0.2428

Figure I.20: F2C: e=3c & d=1c

	b/c									
a/c	−0.3354	−0.3343	−0.3327	−0.3302	−0.3267	−0.3226	−0.3159	−0.3066	−0.294	−0.2704
	−0.3347	−0.3336	−0.3321	−0.3296	−0.3261	−0.322	−0.3154	−0.3061	−0.2936	−0.27
	−0.3336	−0.3325	−0.331	−0.3285	−0.325	−0.3211	−0.3145	−0.3053	−0.2928	−0.2693
	−0.3317	−0.3307	−0.3292	−0.3269	−0.3234	−0.3196	−0.3131	−0.304	−0.2916	−0.2684
	−0.3292	−0.3282	−0.3268	−0.3246	−0.3213	−0.3175	−0.3112	−0.3023	−0.2901	−0.2671
	−0.3262	−0.3253	−0.324	−0.3219	−0.3188	−0.3152	−0.309	−0.3003	−0.2883	−0.2656
	−0.3221	−0.3214	−0.3203	−0.3184	−0.3154	−0.312	−0.3061	−0.2976	−0.286	−0.2636
	−0.3173	−0.3168	−0.3158	−0.3141	−0.3114	−0.3083	−0.3026	−0.2945	−0.2832	−0.2614
	−0.3119	−0.3115	−0.3108	−0.3093	−0.3069	−0.3041	−0.2988	−0.291	−0.2801	−0.2588
	−0.3047	−0.3045	−0.304	−0.3029	−0.3008	−0.2984	−0.2935	−0.2863	−0.2758	−0.2564

Figure I.20: F2C: e=3c & d=1.5c

	b/c									
a/c	−0.3356	−0.3343	−0.3323	−0.3294	−0.3254	−0.3209	−0.3143	−0.3056	−0.295	−0.2777
	−0.335	−0.3337	−0.3318	−0.3288	−0.3249	−0.3204	−0.3138	−0.3052	−0.2947	−0.2774
	−0.3339	−0.3327	−0.3308	−0.3279	−0.324	−0.3196	−0.3131	−0.3046	−0.2941	−0.2769
	−0.3323	−0.3312	−0.3293	−0.3265	−0.3227	−0.3184	−0.3119	−0.3035	−0.2931	−0.2761
	−0.3301	−0.329	−0.3273	−0.3246	−0.3209	−0.3167	−0.3104	−0.3021	−0.2919	−0.275
	−0.3275	−0.3266	−0.3249	−0.3224	−0.3188	−0.3148	−0.3086	−0.3005	−0.2905	−0.2738
	−0.324	−0.3232	−0.3217	−0.3194	−0.316	−0.3122	−0.3063	−0.2984	−0.2886	−0.2722
	−0.3199	−0.3192	−0.3179	−0.3158	−0.3127	−0.3092	−0.3035	−0.2959	−0.2864	−0.2703
	−0.3151	−0.3146	−0.3136	−0.3118	−0.309	−0.3057	−0.3004	−0.2931	−0.2839	−0.2682
	−0.3089	−0.3086	−0.3078	−0.3064	−0.304	−0.3011	−0.2961	−0.2893	−0.2805	−0.2654

Figure I.20: F2C: e=3c & d=2c

	b/c									
a/c	−0.3356	−0.3344	−0.3324	−0.3294	−0.3253	−0.3208	−0.3145	−0.3069	−0.2978	−0.2842
	−0.335	−0.3339	−0.3319	−0.3289	−0.3249	−0.3204	−0.3142	−0.3065	−0.2974	−0.2839
	−0.3342	−0.333	−0.3311	−0.3281	−0.3242	−0.3197	−0.3135	−0.3059	−0.2969	−0.2835
	−0.3328	−0.3316	−0.3298	−0.3269	−0.323	−0.3187	−0.3126	−0.3051	−0.2961	−0.2828
	−0.3308	−0.3298	−0.328	−0.3253	−0.3215	−0.3173	−0.3113	−0.3039	−0.2951	−0.2819
	−0.3286	−0.3276	−0.326	−0.3234	−0.3198	−0.3157	−0.3098	−0.3026	−0.2939	−0.2809
	−0.3255	−0.3247	−0.3233	−0.3208	−0.3174	−0.3135	−0.3078	−0.3008	−0.2923	−0.2795
	−0.3219	−0.3213	−0.32	−0.3178	−0.3146	−0.3109	−0.3055	−0.2987	−0.2905	−0.2779
	−0.3178	−0.3173	−0.3163	−0.3143	−0.3114	−0.308	−0.3029	−0.2964	−0.2884	−0.2761
	−0.3124	−0.312	−0.3113	−0.3097	−0.3072	−0.3041	−0.2994	−0.2933	−0.2857	−0.2738

Figure I.20: F2C: e=3c & d=2.5c

	b/c									
a/c	−0.3357	−0.3346	−0.3328	−0.33	−0.3262	−0.3219	−0.3161	−0.3091	−0.3012	−0.29
	−0.3352	−0.3342	−0.3324	−0.3296	−0.3258	−0.3216	−0.3157	−0.3088	−0.3009	−0.2898
	−0.3344	−0.3334	−0.3317	−0.3289	−0.3252	−0.321	−0.3152	−0.3083	−0.3005	−0.2894
	−0.3332	−0.3322	−0.3305	−0.3279	−0.3242	−0.3201	−0.3144	−0.3076	−0.2998	−0.2888
	−0.3315	−0.3306	−0.329	−0.3264	−0.3229	−0.3188	−0.3133	−0.3066	−0.2989	−0.288
	−0.3296	−0.3287	−0.3272	−0.3248	−0.3214	−0.3175	−0.312	−0.3054	−0.2979	−0.2871
	−0.3269	−0.3262	−0.3248	−0.3226	−0.3194	−0.3156	−0.3103	−0.3039	−0.2965	−0.2859
	−0.3238	−0.3232	−0.322	−0.32	−0.317	−0.3134	−0.3083	−0.3021	−0.2949	−0.2845
	−0.3202	−0.3197	−0.3188	−0.317	−0.3142	−0.3109	−0.3061	−0.3002	−0.2932	−0.283
	−0.3155	−0.3152	−0.3144	−0.313	−0.3106	−0.3076	−0.3031	−0.2975	−0.2908	−0.281

Figure I.20: F2C: e=3c & d=3c

	b/c									
a/c	−0.3358	−0.3348	−0.3333	−0.3308	−0.3274	−0.3235	−0.3182	−0.3119	−0.3049	−0.2953
	−0.3354	−0.3344	−0.3329	−0.3304	−0.3271	−0.3232	−0.3179	−0.3117	−0.3046	−0.2951
	−0.3347	−0.3338	−0.3322	−0.3298	−0.3265	−0.3227	−0.3174	−0.3112	−0.3042	−0.2947
	−0.3336	−0.3328	−0.3313	−0.3289	−0.3256	−0.3219	−0.3167	−0.3106	−0.3036	−0.2942
	−0.3322	−0.3313	−0.3299	−0.3277	−0.3245	−0.3208	−0.3157	−0.3097	−0.3029	−0.2935
	−0.3304	−0.3297	−0.3284	−0.3262	−0.3232	−0.3196	−0.3146	−0.3087	−0.302	−0.2927
	−0.3281	−0.3275	−0.3263	−0.3243	−0.3214	−0.318	−0.3132	−0.3074	−0.3008	−0.2917
	−0.3254	−0.3248	−0.3238	−0.322	−0.3193	−0.316	−0.3115	−0.3059	−0.2994	−0.2905
	−0.3222	−0.3218	−0.321	−0.3194	−0.3169	−0.3139	−0.3095	−0.3041	−0.2979	−0.2892
	−0.3181	−0.3178	−0.3172	−0.3159	−0.3137	−0.311	−0.3069	−0.3018	−0.2959	−0.2874

Figure I.20: F2C: e=3c & d=3.5c

	b/c									
a/c	−0.3359	−0.3351	−0.3337	−0.3315	−0.3286	−0.3251	−0.3204	−0.3149	−0.3086	−0.3003
	−0.3355	−0.3347	−0.3334	−0.3312	−0.3283	−0.3248	−0.3202	−0.3147	−0.3084	−0.3001
	−0.3349	−0.3341	−0.3328	−0.3307	−0.3278	−0.3244	−0.3198	−0.3143	−0.3081	−0.2998
	−0.334	−0.3332	−0.3319	−0.3299	−0.327	−0.3237	−0.3191	−0.3137	−0.3076	−0.2993
	−0.3327	−0.332	−0.3308	−0.3288	−0.326	−0.3227	−0.3183	−0.3129	−0.3069	−0.2987
	−0.3312	−0.3305	−0.3294	−0.3275	−0.3248	−0.3217	−0.3173	−0.3121	−0.3061	−0.298
	−0.3291	−0.3286	−0.3276	−0.3258	−0.3233	−0.3202	−0.316	−0.3109	−0.305	−0.2971
	−0.3267	−0.3263	−0.3254	−0.3238	−0.3214	−0.3186	−0.3145	−0.3095	−0.3038	−0.2961
	−0.324	−0.3236	−0.3229	−0.3215	−0.3193	−0.3166	−0.3128	−0.308	−0.3025	−0.2949
	−0.3204	−0.3201	−0.3196	−0.3184	−0.3165	−0.3141	−0.3105	−0.306	−0.3007	−0.2933

Figure I.20: F2C: e=3c & d=4c

	b/c									
a/c	−0.336	−0.3353	−0.3341	−0.3322	−0.3296	−0.3266	−0.3225	−0.3177	−0.3122	−0.305
	−0.3357	−0.335	−0.3338	−0.3319	−0.3294	−0.3264	−0.3223	−0.3175	−0.312	−0.3048
	−0.3351	−0.3344	−0.3333	−0.3315	−0.3289	−0.326	−0.3219	−0.3172	−0.3117	−0.3045
	−0.3343	−0.3336	−0.3325	−0.3307	−0.3283	−0.3253	−0.3214	−0.3166	−0.3112	−0.3041
	−0.3332	−0.3325	−0.3315	−0.3298	−0.3274	−0.3245	−0.3206	−0.3159	−0.3106	−0.3035
	−0.3318	−0.3313	−0.3303	−0.3286	−0.3263	−0.3236	−0.3198	−0.3152	−0.3099	−0.3029
	−0.33	−0.3296	−0.3287	−0.3271	−0.3249	−0.3223	−0.3186	−0.3141	−0.309	−0.3021
	−0.3279	−0.3275	−0.3267	−0.3254	−0.3233	−0.3208	−0.3173	−0.3129	−0.3079	−0.3011
	−0.3255	−0.3252	−0.3245	−0.3233	−0.3215	−0.3191	−0.3157	−0.3116	−0.3067	−0.3001
	−0.3223	−0.3221	−0.3216	−0.3206	−0.319	−0.3169	−0.3137	−0.3098	−0.3051	−0.2987

Figure I.20: F2C: e=3.5c & d=0.5c

	b/c									
a/c	−0.3356	−0.335	−0.3341	−0.3326	−0.3302	−0.3276	−0.3223	−0.3138	−0.2985	−0.2621
	−0.3349	−0.3343	−0.3335	−0.332	−0.3296	−0.327	−0.3217	−0.3133	−0.298	−0.2617
	−0.3337	−0.3331	−0.3323	−0.3308	−0.3285	−0.3259	−0.3207	−0.3123	−0.2972	−0.2609
	−0.3318	−0.3313	−0.3305	−0.329	−0.3267	−0.3242	−0.319	−0.3108	−0.2958	−0.2598
	−0.3292	−0.3287	−0.328	−0.3266	−0.3244	−0.3219	−0.3168	−0.3087	−0.2937	−0.2583
	−0.3263	−0.3258	−0.3251	−0.3238	−0.3216	−0.3193	−0.3143	−0.3063	−0.2915	−0.2566
	−0.3222	−0.3218	−0.3211	−0.3199	−0.3179	−0.3156	−0.3109	−0.3031	−0.2887	−0.2542
	−0.3174	−0.317	−0.3165	−0.3154	−0.3134	−0.3114	−0.3068	−0.2993	−0.2851	−0.2515
	−0.3119	−0.3116	−0.3112	−0.3102	−0.3085	−0.3065	−0.3022	−0.295	−0.2813	−0.2485
	−0.3047	−0.3045	−0.3041	−0.3033	−0.3018	−0.3001	−0.296	−0.2894	−0.2761	−0.2444

Figure I.20: F2C: e=3.5c & d=1c

	b/c									
a/c	−0.3355	−0.3344	−0.3328	−0.3303	−0.3267	−0.3226	−0.3159	−0.3066	−0.294	−0.2704
	−0.3349	−0.3338	−0.3322	−0.3297	−0.3262	−0.3221	−0.3155	−0.3062	−0.2936	−0.27
	−0.3338	−0.3328	−0.3312	−0.3288	−0.3253	−0.3213	−0.3146	−0.3054	−0.2929	−0.2694
	−0.3322	−0.3312	−0.3297	−0.3273	−0.3238	−0.3199	−0.3134	−0.3042	−0.2919	−0.2685
	−0.33	−0.329	−0.3275	−0.3252	−0.3219	−0.3181	−0.3116	−0.3027	−0.2904	−0.2673
	−0.3274	−0.3265	−0.3251	−0.3229	−0.3196	−0.3159	−0.3096	−0.3008	−0.2888	−0.2659
	−0.3239	−0.323	−0.3218	−0.3197	−0.3166	−0.3131	−0.307	−0.2984	−0.2866	−0.2641
	−0.3197	−0.319	−0.3178	−0.3159	−0.313	−0.3097	−0.3038	−0.2955	−0.284	−0.2619
	−0.315	−0.3143	−0.3134	−0.3117	−0.309	−0.3058	−0.3003	−0.2923	−0.2811	−0.2595
	−0.3087	−0.3082	−0.3075	−0.306	−0.3036	−0.3008	−0.2956	−0.288	−0.2772	−0.2563

Figure I.20: F2C: e=3.5c & d=1.5c

	b/c									
a/c	−0.3356	−0.3343	−0.3324	−0.3294	−0.3254	−0.3209	−0.3143	−0.3057	−0.295	−0.2778
	−0.3351	−0.3338	−0.3319	−0.3289	−0.3249	−0.3205	−0.3139	−0.3053	−0.2947	−0.2775
	−0.3342	−0.333	−0.331	−0.3281	−0.3242	−0.3198	−0.3132	−0.3047	−0.2941	−0.277
	−0.3328	−0.3316	−0.3297	−0.3268	−0.323	−0.3186	−0.3121	−0.3037	−0.2933	−0.2762
	−0.3308	−0.3297	−0.3279	−0.3251	−0.3214	−0.3171	−0.3107	−0.3024	−0.2921	−0.2752
	−0.3286	−0.3275	−0.3258	−0.3231	−0.3195	−0.3154	−0.3091	−0.3009	−0.2908	−0.274
	−0.3255	−0.3246	−0.323	−0.3204	−0.3169	−0.313	−0.3069	−0.2989	−0.289	−0.2725
	−0.3219	−0.321	−0.3201	−0.3172	−0.314	−0.3102	−0.3043	−0.2966	−0.2869	−0.2707
	−0.3178	−0.317	−0.3158	−0.3136	−0.3106	−0.307	−0.3014	−0.2939	−0.2845	−0.2687
	−0.3123	−0.3118	−0.3107	−0.3089	−0.3061	−0.3029	−0.2976	−0.2905	−0.2814	−0.266

Figure I.20: F2C: e=3.5c & d=2c

	b/c									
a/c	−0.3356	−0.3344	−0.3324	−0.3294	−0.3254	−0.3208	−0.3146	−0.3069	−0.2978	−0.2842
	−0.3351	−0.3339	−0.332	−0.329	−0.325	−0.3205	−0.3142	−0.3065	−0.2975	−0.284
	−0.3343	−0.3332	−0.3313	−0.3283	−0.3243	−0.3198	−0.3136	−0.306	−0.297	−0.2835
	−0.3331	−0.332	−0.3301	−0.3272	−0.3233	−0.3189	−0.3127	−0.3052	−0.2962	−0.2829
	−0.3314	−0.3304	−0.3285	−0.3257	−0.3219	−0.3176	−0.3115	−0.3041	−0.2952	−0.282
	−0.3295	−0.3285	−0.3267	−0.324	−0.3203	−0.3161	−0.3102	−0.3028	−0.2941	−0.281
	−0.3268	−0.3259	−0.3243	−0.3217	−0.3181	−0.3141	−0.3083	−0.3011	−0.2926	−0.2797
	−0.3237	−0.3228	−0.3214	−0.319	−0.3156	−0.3117	−0.3061	−0.2992	−0.2908	−0.2781
	−0.3201	−0.3194	−0.3181	−0.3159	−0.3127	−0.3091	−0.3037	−0.297	−0.2889	−0.2764
	−0.3153	−0.3148	−0.3137	−0.3118	−0.3089	−0.3055	−0.3005	−0.2941	−0.2863	−0.2741

Figure I.20: F2C: e=3.5c & d=2.5c

	b/c									
a/c	−0.3357	−0.3346	−0.3328	−0.33	−0.3262	−0.3219	−0.3161	−0.3091	−0.3012	−0.29
	−0.3353	−0.3342	−0.3324	−0.3297	−0.3259	−0.3216	−0.3158	−0.3088	−0.3009	−0.2898
	−0.3346	−0.3336	−0.3318	−0.3291	−0.3253	−0.3211	−0.3153	−0.3084	−0.3005	−0.2894
	−0.3335	−0.3325	−0.3308	−0.3281	−0.3244	−0.3202	−0.3145	−0.3077	−0.2999	−0.2888
	−0.3321	−0.3311	−0.3294	−0.3268	−0.3232	−0.3191	−0.3135	−0.3067	−0.299	−0.288
	−0.3303	−0.3294	−0.3278	−0.3253	−0.3218	−0.3178	−0.3123	−0.3056	−0.298	−0.2872
	−0.328	−0.3272	−0.3257	−0.3233	−0.3199	−0.3161	−0.3107	−0.3042	−0.2967	−0.286
	−0.3253	−0.3245	−0.3232	−0.3209	−0.3177	−0.314	−0.3088	−0.3025	−0.2952	−0.2847
	−0.3221	−0.3215	−0.3203	−0.3182	−0.3152	−0.3117	−0.3067	−0.3006	−0.2935	−0.2832
	−0.318	−0.3175	−0.3165	−0.3147	−0.3119	−0.3087	−0.304	−0.2981	−0.2913	−0.2812

Figure I.20: F2C: e=3.5c & d=3c

	b/c									
a/c	−0.3358	−0.3349	−0.3333	−0.3308	−0.3274	−0.3235	−0.3182	−0.3119	−0.3049	−0.2953
	−0.3354	−0.3345	−0.3329	−0.3305	−0.3271	−0.3232	−0.3179	−0.3117	−0.3046	−0.2951
	−0.3348	−0.3339	−0.3324	−0.3299	−0.3266	−0.3227	−0.3175	−0.3113	−0.3043	−0.2948
	−0.3339	−0.333	−0.3315	−0.3291	−0.3258	−0.322	−0.3168	−0.3107	−0.3037	−0.2942
	−0.3326	−0.3317	−0.3303	−0.3279	−0.3247	−0.321	−0.3159	−0.3098	−0.3029	−0.2936
	−0.3311	−0.3303	−0.3289	−0.3267	−0.3235	−0.3199	−0.3148	−0.3089	−0.3021	−0.2928
	−0.329	−0.3283	−0.327	−0.3249	−0.3219	−0.3183	−0.3135	−0.3076	−0.3009	−0.2918
	−0.3266	−0.326	−0.3248	−0.3228	−0.3199	−0.3165	−0.3118	−0.3061	−0.2996	−0.2906
	−0.3239	−0.3233	−0.3222	−0.3204	−0.3177	−0.3145	−0.31	−0.3045	−0.2981	−0.2893
	−0.3203	−0.3198	−0.3189	−0.3173	−0.3149	−0.3119	−0.3076	−0.3023	−0.2962	−0.2857

Figure I.20: F2C: e=3.5c & d=3.5c

	b/c									
a/c	−0.3359	−0.3351	−0.3337	−0.3315	−0.3286	−0.3251	−0.3204	−0.3149	−0.3086	−0.3003
	−0.3356	−0.3348	−0.3334	−0.3313	−0.3283	−0.3249	−0.3202	−0.3147	−0.3084	−0.3001
	−0.335	−0.3342	−0.3329	−0.3308	−0.3278	−0.3244	−0.3198	−0.3143	−0.3081	−0.2998
	−0.3342	−0.3334	−0.3321	−0.33	−0.3271	−0.3238	−0.3192	−0.3138	−0.3076	−0.2994
	−0.3331	−0.3323	−0.331	−0.329	−0.3262	−0.3229	−0.3184	−0.313	−0.3069	−0.2988
	−0.3317	−0.331	−0.3298	−0.3279	−0.3251	−0.3219	−0.3175	−0.3122	−0.3062	−0.2981
	−0.3299	−0.3293	−0.3282	−0.3263	−0.3237	−0.3205	−0.3162	−0.311	−0.3051	−0.2972
	−0.3278	−0.3272	−0.3262	−0.3245	−0.322	−0.319	−0.3148	−0.3097	−0.304	−0.2961
	−0.3254	−0.3249	−0.324	−0.3224	−0.32	−0.3172	−0.3132	−0.3083	−0.3026	−0.295
	−0.3222	−0.3218	−0.321	−0.3196	−0.3175	−0.3148	−0.311	−0.3063	−0.3009	−0.2934

Figure I.20: F2C: e=3.5c & d=4c

	b/c									
a/c	−0.336	−0.3353	−0.3341	−0.3322	−0.3296	−0.3266	−0.3226	−0.3177	−0.3122	−0.305
	−0.3357	−0.335	−0.3338	−0.332	−0.3294	−0.3264	−0.3223	−0.3175	−0.312	−0.3048
	−0.3352	−0.3345	−0.3334	−0.3315	−0.329	−0.326	−0.322	−0.3172	−0.3117	−0.3045
	−0.3345	−0.3338	−0.3327	−0.3309	−0.3284	−0.3254	−0.3214	−0.3167	−0.3113	−0.3041
	−0.3335	−0.3328	−0.3317	−0.33	−0.3275	−0.3246	−0.3207	−0.316	−0.3107	−0.3036
	−0.3323	−0.3317	−0.3306	−0.3289	−0.3266	−0.3237	−0.3199	−0.3153	−0.31	−0.3029
	−0.3307	−0.3301	−0.3292	−0.3276	−0.3253	−0.3225	−0.3188	−0.3143	−0.3091	−0.3021
	−0.3288	−0.3283	−0.3274	−0.3259	−0.3238	−0.3211	−0.3175	−0.3131	−0.308	−0.3012
	−0.3267	−0.3262	−0.3255	−0.3241	−0.322	−0.3196	−0.3161	−0.3118	−0.3068	−0.3001
	−0.3239	−0.3235	−0.3229	−0.3216	−0.3198	−0.3175	−0.3142	−0.3101	−0.3053	−0.2988

Figure I.20: F2C: e=4c & d=0.5c

	b/c									
	−0.3356	−0.335	−0.3342	−0.3327	−0.3303	−0.3277	−0.3223	−0.3139	−0.2985	−0.2621
	−0.335	−0.3344	−0.3336	−0.3321	−0.3297	−0.3271	−0.3218	−0.3133	−0.2981	−0.2617
	−0.334	−0.3334	−0.3326	−0.3311	−0.3287	−0.3262	−0.3209	−0.3125	−0.2973	−0.2618
	−0.3323	−0.3318	−0.331	−0.3295	−0.3272	−0.3247	−0.3194	−0.3111	−0.2961	−0.2597
a/c	−0.3301	−0.3296	−0.3288	−0.3274	−0.3251	−0.3226	−0.3175	−0.3093	−0.2943	−0.2587
	−0.3275	−0.327	−0.3262	−0.3249	−0.3227	−0.3203	−0.3152	−0.3072	−0.2925	−0.2571
	−0.324	−0.3235	−0.3228	−0.3215	−0.3194	−0.3171	−0.3121	−0.3043	−0.2896	−0.255
	−0.3198	−0.3193	−0.3187	−0.3175	−0.3155	−0.3133	−0.3086	−0.3009	−0.2866	−0.2525
	−0.315	−0.3146	−0.3141	−0.313	−0.3111	−0.309	−0.3045	−0.2971	−0.2828	−0.2497
	−0.3087	−0.3084	−0.3079	−0.307	−0.3052	−0.3033	−0.299	−0.292	−0.2784	−0.246

Figure I.20: F2C: e=4c & d=1c

	b/c									
	−0.3355	−0.3344	−0.3328	−0.3303	−0.3267	−0.3227	−0.316	−0.3066	−0.294	−0.2704
	−0.335	−0.3339	−0.3323	−0.3298	−0.3262	−0.3222	−0.3155	−0.3062	−0.2937	−0.2701
	−0.3341	−0.333	−0.3314	−0.329	−0.3254	−0.3214	−0.3148	−0.3056	−0.293	−0.2695
	−0.3327	−0.3316	−0.3301	−0.3277	−0.3242	−0.3202	−0.3137	−0.3045	−0.2921	−0.2687
a/c	−0.3307	−0.3297	−0.3282	−0.3259	−0.3224	−0.3186	−0.3121	−0.3031	−0.2908	−0.2676
	−0.3285	−0.3275	−0.3261	−0.3238	−0.3204	−0.3167	−0.3103	−0.3014	−0.2893	−0.2663
	−0.3254	−0.3245	−0.3231	−0.321	−0.3177	−0.3141	−0.3079	−0.2992	−0.2872	−0.2646
	−0.3218	−0.3209	−0.3197	−0.3176	−0.3145	−0.311	−0.305	−0.2965	−0.2848	−0.2626
	−0.3176	−0.3169	−0.3157	−0.3138	−0.3109	−0.3076	−0.3018	−0.2936	−0.2822	−0.2603
	−0.3122	−0.3115	−0.3105	−0.3088	−0.3062	−0.3031	−0.2976	−0.2897	−0.2787	−0.2573

Figure I.20: F2C: e=4c & d=1.5c

	b/c									
	−0.3356	−0.3344	−0.3324	−0.3294	−0.3254	−0.321	−0.3143	−0.3057	−0.295	−0.2778
	−0.3352	−0.3339	−0.3319	−0.329	−0.325	−0.3206	−0.3139	−0.3053	−0.2947	−0.2775
	−0.3344	−0.3331	−0.3312	−0.3283	−0.3243	−0.3199	−0.3133	−0.3048	−0.2942	−0.277
	−0.3332	−0.3319	−0.33	−0.3271	−0.3233	−0.3189	−0.3123	−0.3039	−0.2934	−0.2763
a/c	−0.3315	−0.3303	−0.3284	−0.3256	−0.3218	−0.3175	−0.3111	−0.3027	−0.2923	−0.2754
	−0.3295	−0.3284	−0.3266	−0.3238	−0.3201	−0.3159	−0.3096	−0.3013	−0.2911	−0.2743
	−0.3268	−0.3258	−0.3241	−0.3214	−0.3178	−0.3138	−0.3076	−0.2995	−0.2894	−0.2728
	−0.3237	−0.3227	−0.3211	−0.3186	−0.3151	−0.3112	−0.3052	−0.2973	−0.2875	−0.2711
	−0.3201	−0.3192	−0.3177	−0.3154	−0.3121	−0.3084	−0.3026	−0.2949	−0.2853	−0.2692
	−0.3153	−0.3146	−0.3133	−0.3112	−0.3081	−0.3046	−0.2991	−0.2917	−0.2824	−0.2667

Figure I.20: F2C: e=4c & d=2c

	b/c									
	−0.3356	−0.3344	−0.3324	−0.3294	−0.3254	−0.3208	−0.3146	−0.3069	−0.2978	−0.2842
	−0.3352	−0.334	−0.3321	−0.329	−0.325	−0.3205	−0.3143	−0.3066	−0.2975	−0.284
	−0.3345	−0.3333	−0.3314	−0.3284	−0.3244	−0.32	−0.3137	−0.3061	−0.2971	−0.2836
	−0.3334	−0.3323	−0.3304	−0.3274	−0.3235	−0.3191	−0.3129	−0.3053	−0.2964	−0.283
a/c	−0.332	−0.3308	−0.329	−0.3261	−0.3222	−0.3179	−0.3118	−0.3043	−0.2954	−0.2821
	−0.3302	−0.3292	−0.3274	−0.3246	−0.3208	−0.3165	−0.3105	−0.3031	−0.2944	−0.2812
	−0.3279	−0.3269	−0.3252	−0.3225	−0.3188	−0.3147	−0.3088	−0.3016	−0.293	−0.2799
	−0.3251	−0.3242	−0.3226	−0.3201	−0.3165	−0.3125	−0.3068	−0.2997	−0.2913	−0.2785
	−0.322	−0.3211	−0.3197	−0.3173	−0.3139	−0.3101	−0.3046	−0.2977	−0.2894	−0.2768
	−0.3179	−0.3171	−0.3158	−0.3136	−0.3105	−0.3069	−0.3016	−0.295	−0.287	−0.2747

Figure I.20: F2C: e=4c & d=2.5c

	b/c									
	−0.3357	−0.3346	−0.3328	−0.33	−0.3262	−0.3219	−0.3161	−0.3091	−0.3012	−0.29
	−0.3353	−0.3343	−0.3325	−0.3297	−0.3259	−0.3216	−0.3158	−0.3089	−0.3009	−0.2898
	−0.3347	−0.3337	−0.3319	−0.3292	−0.3254	−0.3211	−0.3153	−0.3084	−0.3005	−0.2894
	−0.3338	−0.3328	−0.331	−0.3283	−0.3246	−0.3204	−0.3146	−0.3078	−0.2999	−0.2889
a/c	−0.3325	−0.3315	−0.3298	−0.3271	−0.3235	−0.3193	−0.3137	−0.3069	−0.2991	−0.2882
	−0.331	−0.33	−0.3284	−0.3258	−0.3222	−0.3182	−0.3126	−0.3059	−0.2982	−0.2873
	−0.3289	−0.328	−0.3265	−0.324	−0.3205	−0.3166	−0.3111	−0.3045	−0.297	−0.2862
	−0.3265	−0.3257	−0.3242	−0.3218	−0.3185	−0.3147	−0.3094	−0.3029	−0.2955	−0.2849
	−0.3238	−0.323	−0.3216	−0.3194	−0.3162	−0.3126	−0.3074	−0.3012	−0.2939	−0.2835
	−0.3201	−0.3195	−0.3183	−0.3162	−0.3133	−0.3098	−0.3049	−0.2988	−0.2918	−0.2816

Figure I.20: F2C: e=4c & d=3c

	b/c									
	−0.3358	−0.3349	−0.3333	−0.3308	−0.3274	−0.3235	−0.3182	−0.3119	−0.3049	−0.2953
	−0.3355	−0.3346	−0.333	−0.3305	−0.3271	−0.3232	−0.318	−0.3117	−0.3047	−0.2951
	−0.3349	−0.334	−0.3325	−0.33	−0.3267	−0.3228	−0.3176	−0.3113	−0.3043	−0.2948
	−0.3341	−0.3332	−0.3317	−0.3293	−0.326	−0.3221	−0.3169	−0.3108	−0.3038	−0.2943
a/c	−0.333	−0.3321	−0.3306	−0.3282	−0.325	−0.3212	−0.3161	−0.31	−0.3031	−0.2937
	−0.3316	−0.3308	−0.3293	−0.327	−0.3239	−0.3202	−0.3151	−0.3091	−0.3022	−0.2929
	−0.3298	−0.329	−0.3277	−0.3254	−0.3223	−0.3187	−0.3138	−0.3079	−0.3012	−0.2919
	−0.3277	−0.327	−0.3257	−0.3235	−0.3206	−0.3171	−0.3123	−0.3065	−0.2999	−0.2908
	−0.3253	−0.3246	−0.3234	−0.3214	−0.3186	−0.3152	−0.3106	−0.3049	−0.2985	−0.2895
	−0.3221	−0.3215	−0.3204	−0.3186	−0.316	−0.3128	−0.3083	−0.3029	−0.2966	−0.2879

Figure I.20: F2C: e=4c & d=3.5c

	b/c									
	−0.3359	−0.3351	−0.3337	−0.3315	−0.3286	−0.3251	−0.3204	−0.3149	−0.3087	−0.3003
	−0.3356	−0.3348	−0.3334	−0.3313	−0.3283	−0.3249	−0.3202	−0.3147	−0.3085	−0.3001
	−0.3351	−0.3343	−0.333	−0.3309	−0.3279	−0.3245	−0.3199	−0.3144	−0.3081	−0.2999
	−0.3344	−0.3336	−0.3323	−0.3302	−0.3273	−0.3239	−0.3193	−0.3138	−0.3077	−0.2994
a/c	−0.3334	−0.3326	−0.3313	−0.3293	−0.3264	−0.3231	−0.3185	−0.3131	−0.307	−0.2988
	−0.3322	−0.3315	−0.3302	−0.3282	−0.3254	−0.3221	−0.3177	−0.3123	−0.3063	−0.2982
	−0.3306	−0.3299	−0.3287	−0.3268	−0.3241	−0.3209	−0.3165	−0.3113	−0.3053	−0.2973
	−0.3287	−0.3281	−0.3269	−0.3251	−0.3225	−0.3194	−0.3152	−0.31	−0.3042	−0.2963
	−0.3266	−0.326	−0.3249	−0.3232	−0.3207	−0.3178	−0.3136	−0.3086	−0.3029	−0.2951
	−0.3238	−0.3233	−0.3223	−0.3207	−0.3184	−0.3156	−0.3116	−0.3068	−0.3013	−0.2937

Figure I.20: F2C: e=4c & d=4c

	b/c									
	−0.336	−0.3353	−0.3341	−0.3322	−0.3297	−0.3266	−0.3226	−0.3177	−0.3122	−0.305
	−0.3357	−0.335	−0.3339	−0.332	−0.3294	−0.3264	−0.3224	−0.3175	−0.312	−0.3048
	−0.3353	−0.3346	−0.3335	−0.3316	−0.3291	−0.3261	−0.322	−0.3172	−0.3118	−0.3046
	−0.3346	−0.334	−0.3328	−0.331	−0.3285	−0.3255	−0.3215	−0.3167	−0.3113	−0.3042
a/c	−0.3337	−0.3331	−0.332	−0.3302	−0.3277	−0.3248	−0.3208	−0.3161	−0.3107	−0.3036
	−0.3327	−0.3321	−0.331	−0.3292	−0.3268	−0.324	−0.3201	−0.3154	−0.3101	−0.303
	−0.3313	−0.3307	−0.3296	−0.328	−0.3256	−0.3228	−0.319	−0.3144	−0.3092	−0.3022
	−0.3296	−0.329	−0.3281	−0.3265	−0.3242	−0.3215	−0.3178	−0.3133	−0.3082	−0.3013
	−0.3277	−0.3272	−0.3263	−0.3248	−0.3226	−0.3201	−0.3164	−0.3121	−0.307	−0.3003
	−0.3252	−0.3248	−0.324	−0.3226	−0.3206	−0.3181	−0.3147	−0.3104	−0.3056	−0.2989

Figure I.21: F1C: e=0.5b & d=0.5b

	c/b									
	0.0064	0.0050	0.0017	0.0017	0.0002	−0.0001	0.0015	0.1580	0.3643	0.4285
	0.0061	0.0052	0.0018	0.0017	0.0001	−0.0002	0.0015	0.1579	0.3641	0.4286
	0.0061	0.0050	0.0017	0.0017	0.0001	−0.0001	0.0015	0.1579	0.3640	0.4284
	0.0065	0.0050	0.0017	0.0017	0.0002	−0.0004	0.0016	0.1580	0.3637	0.4280
a/b	0.0065	0.0050	0.0017	0.0017	0.0001	−0.0002	0.0015	0.1580	0.3632	0.4274
	0.0065	0.0051	0.0017	0.0017	0.0001	−0.0001	0.0016	0.1580	0.3628	0.4268
	0.0065	0.0050	0.0017	0.0017	0.0002	−0.0001	0.0035	0.1580	0.3625	0.4256
	0.0059	0.0051	0.0017	0.0017	0.0002	−0.0004	0.0038	0.1580	0.3607	0.4237
	0.0064	0.0051	0.0017	0.0018	0.0001	0.0001	0.0026	0.1575	0.3577	0.4205
	0.0064	0.0049	0.0017	0.0019	0.0002	0.0001	0.0033	0.1559	0.3492	0.4136

Figure I.21: F1C: e=0.5b & d=1b

	c/b									
	0.0029	0.0001	−0.0001	0.0003	0.0274	0.1322	0.2564	0.3471	0.3947	0.4268
	0.0030	0.0001	0.0002	0.0004	0.0274	0.1322	0.2563	0.3470	0.3946	0.4267
	0.0029	0.0002	0.0000	0.0000	0.0274	0.1322	0.2563	0.3469	0.3944	0.4266
	0.0029	0.0001	0.0001	0.0003	0.0275	0.1321	0.2561	0.3467	0.3941	0.4263
a/b	0.0032	0.0001	0.0000	−0.0002	0.0276	0.1321	0.2559	0.3464	0.3936	0.4258
	0.0029	0.0002	0.0001	−0.0001	0.0277	0.1321	0.2558	0.3460	0.3931	0.4254
	0.0029	0.0001	0.0001	0.0002	0.0279	0.1319	0.2553	0.3453	0.3921	0.4245
	0.0032	0.0000	0.0000	−0.0001	0.0282	0.1317	0.2545	0.3442	0.3907	0.4232
	0.0032	0.0002	0.0002	0.0001	0.0286	0.1310	0.2528	0.3420	0.3881	0.4210
	0.0029	0.0002	0.0001	0.0004	0.0292	0.1290	0.2483	0.3369	0.3828	0.4167

Figure I.21: F1C: e=0.5b & d=1.5b

	c/b									
	0.0003	0.0002	0.0137	0.0840	0.1800	0.2689	0.3400	0.3830	0.4023	0.4274
	0.0007	0.0004	0.0137	0.0840	0.1800	0.2689	0.3399	0.3829	0.4022	0.4273
	0.0007	0.0002	0.0137	0.0841	0.1800	0.2688	0.3398	0.3827	0.4021	0.4271
	0.0007	−0.0001	0.0138	0.0841	0.1800	0.2687	0.3396	0.3825	0.4018	0.4269
a/b	0.0007	−0.0001	0.0139	0.0842	0.1801	0.2686	0.3394	0.3822	0.4014	0.4265
	0.0007	0.0002	0.0140	0.0842	0.1800	0.2684	0.3390	0.3818	0.4010	0.4262
	0.0007	0.0004	0.0142	0.0842	0.1799	0.2681	0.3384	0.3810	0.4003	0.4255
	0.0007	0.0004	0.0145	0.0843	0.1797	0.2675	0.3374	0.3799	0.3992	0.4245
	0.0007	0.0002	0.0148	0.0842	0.1791	0.2663	0.3356	0.3780	0.3974	0.4228
	0.0006	0.0002	0.0154	0.0835	0.1774	0.2632	0.3316	0.3739	0.3937	0.4198

Figure I.21: F1C: e=0.5b & d=2b

	c/b									
	0.0004	0.0277	0.1099	0.2082	0.2885	0.3331	0.3725	0.3980	0.4087	0.4292
	0.0013	0.0278	0.1099	0.2083	0.2885	0.3331	0.3725	0.3979	0.4086	0.4291
	0.0013	0.0278	0.1100	0.2083	0.2884	0.3330	0.3723	0.3978	0.4085	0.4290
	0.0013	0.0280	0.1101	0.2083	0.2884	0.3328	0.3721	0.3976	0.4083	0.4288
a/b	0.0004	0.0281	0.1103	0.2084	0.2883	0.3326	0.3719	0.3973	0.4080	0.4285
	0.0012	0.0283	0.1104	0.2084	0.2881	0.3323	0.3715	0.3969	0.4077	0.4282
	0.0012	0.0286	0.1107	0.2085	0.2877	0.3318	0.3709	0.3963	0.4070	0.4276
	0.0004	0.0290	0.1110	0.2084	0.2872	0.3309	0.3699	0.3954	0.4062	0.4269
	0.0004	0.0295	0.1114	0.2080	0.2860	0.3294	0.3683	0.3938	0.4048	0.4256
	0.0011	0.0304	0.1115	0.2066	0.2831	0.3260	0.3649	0.3907	0.4020	0.4232

Figure I.21: F1C: e=0.5b & d=2.5b

	c/b									
	0.0485	0.1480	0.2227	0.2902	0.3392	0.3636	0.3897	0.4074	0.4137	0.4313
	0.0486	0.1481	0.2227	0.2902	0.3391	0.3635	0.3896	0.4073	0.4136	0.4312
	0.0488	0.1481	0.2227	0.2902	0.3391	0.3634	0.3895	0.4072	0.4135	0.4311
	0.0491	0.1483	0.2227	0.2901	0.3389	0.3632	0.3893	0.4070	0.4133	0.4310
a/b	0.0496	0.1485	0.2227	0.2900	0.3387	0.3630	0.3891	0.4067	0.4131	0.4307
	0.0500	0.1487	0.2227	0.2898	0.3385	0.3627	0.3888	0.4064	0.4128	0.4305
	0.0509	0.1491	0.2226	0.2895	0.3380	0.3621	0.3882	0.4059	0.4123	0.4300
	0.0520	0.1495	0.2224	0.2889	0.3373	0.3613	0.3874	0.4051	0.4116	0.4293
	0.0537	0.1498	0.2219	0.2879	0.3359	0.3599	0.3860	0.4039	0.4104	0.4283
	0.0565	0.1499	0.2202	0.2853	0.3330	0.3570	0.3833	0.4014	0.4082	0.4264

Figure I.21: F1C: e=0.5b & d=3b

	c/b									
	0.1811	0.2463	0.2903	0.3355	0.3683	0.3823	0.4013	0.4145	0.4180	0.4337
	0.1812	0.2464	0.2903	0.3355	0.3682	0.3822	0.4012	0.4144	0.4179	0.4336
	0.1812	0.2464	0.2902	0.3354	0.3681	0.3821	0.4011	0.4143	0.4178	0.4335
	0.1813	0.2464	0.2902	0.3353	0.3680	0.3820	0.4010	0.4141	0.4177	0.4334
a/b	0.1815	0.2464	0.2901	0.3351	0.3678	0.3817	0.4007	0.4139	0.4175	0.4332
	0.1816	0.2463	0.2899	0.3349	0.3675	0.3814	0.4005	0.4137	0.4172	0.4330
	0.1818	0.2462	0.2896	0.3345	0.3670	0.3810	0.4000	0.4132	0.4168	0.4325
	0.1821	0.2460	0.2891	0.3338	0.3663	0.3802	0.3993	0.4125	0.4162	0.4320
	0.1821	0.2454	0.2881	0.3326	0.3651	0.3790	0.3982	0.4115	0.4152	0.4311
	0.1816	0.2437	0.2858	0.3300	0.3625	0.3766	0.3959	0.4095	0.4132	0.4295

Figure I.21: F1C: e=0.5b & d=3.5b

	c/b									
	0.2685	0.3081	0.3334	0.3649	0.3882	0.3959	0.4104	0.4205	0.4221	0.4362
	0.2685	0.3081	0.3333	0.3649	0.3881	0.3958	0.4104	0.4205	0.422	0.4362
	0.2685	0.308	0.3332	0.3648	0.388	0.3957	0.4103	0.4204	0.422	0.4361
	0.2684	0.308	0.3331	0.3646	0.3879	0.3956	0.4101	0.4203	0.4218	0.436
a/b	0.2684	0.3078	0.333	0.3644	0.3877	0.3954	0.4099	0.4201	0.4216	0.4358
	0.2683	0.3077	0.3328	0.3642	0.3875	0.3951	0.4097	0.4198	0.4214	0.4356
	0.2682	0.3074	0.3324	0.3638	0.387	0.3947	0.4093	0.4194	0.4211	0.4353
	0.2679	0.3069	0.3318	0.3631	0.3864	0.3941	0.4087	0.4189	0.4205	0.4348
	0.2672	0.3059	0.3307	0.362	0.3853	0.393	0.4077	0.418	0.4197	0.4341
	0.2653	0.3037	0.3283	0.3597	0.383	0.391	0.4058	0.4163	0.4182	0.4327

Figure I.21: F1C: e=0.5b & d=4b

	c/b									
	0.324	0.3482	0.3623	0.3856	0.4029	0.4065	0.418	0.4259	0.426	0.439
	0.3239	0.3482	0.3623	0.3855	0.4029	0.4065	0.418	0.4259	0.426	0.4389
	0.3239	0.3481	0.3622	0.3854	0.4028	0.4064	0.4179	0.4258	0.4259	0.4388
	0.3238	0.348	0.3621	0.3853	0.4027	0.4063	0.4178	0.4257	0.4258	0.4387
a/b	0.3237	0.3478	0.3619	0.3851	0.4025	0.4061	0.4176	0.4255	0.4256	0.4386
	0.3235	0.3476	0.3617	0.3849	0.4022	0.4059	0.4174	0.4253	0.4254	0.4384
	0.3232	0.3473	0.3613	0.3845	0.4018	0.4055	0.417	0.425	0.4251	0.4381
	0.3227	0.3467	0.3607	0.3839	0.4012	0.4049	0.4165	0.4245	0.4247	0.4377
	0.3217	0.3456	0.3596	0.3828	0.4003	0.404	0.4156	0.4237	0.4239	0.4371
	0.3195	0.3434	0.3574	0.3808	0.3983	0.4022	0.414	0.4223	0.4226	0.4359

Figure I.21: F1C: e=1b & d=0.5b

	c/b									
a/b	0.0065	0.0051	0.0016	0.0017	0.0002	−0.0001	0.0015	0.1579	0.3643	0.4287
	0.0063	0.0049	0.0017	0.0016	0.0002	−0.0004	0.0017	0.1579	0.3640	0.4283
	0.0064	0.0051	0.0017	0.0017	0.0003	−0.0002	0.0015	0.1578	0.3635	0.4278
	0.0065	0.0051	0.0018	0.0017	0.0002	−0.0001	0.0032	0.1577	0.3629	0.4270
	0.0065	0.0050	0.0017	0.0017	0.0001	−0.0004	0.0016	0.1577	0.3620	0.4257
	0.0065	0.0050	0.0017	0.0017	0.0002	0.0001	0.0018	0.1576	0.3609	0.4247
	0.0063	0.0050	0.0017	0.0016	0.0002	−0.0001	0.0037	0.1573	0.3591	0.4227
	0.0060	0.0049	0.0017	0.0017	0.0002	−0.0004	0.0040	0.1569	0.3566	0.4199
	0.0063	0.0051	0.0017	0.0018	0.0002	−0.0001	0.0026	0.1561	0.3528	0.4159
	0.0064	0.0050	0.0017	0.0018	0.0002	−0.0006	0.0032	0.1545	0.3451	0.4091

Figure I.21: F1C: e=1b & d=1b

	c/b									
a/b	0.0029	0.0001	0.0000	−0.0003	0.0274	0.1322	0.2564	0.3471	0.3946	0.4268
	0.0029	0.0002	0.0001	0.0002	0.0274	0.1321	0.2562	0.3468	0.3943	0.4265
	0.0031	0.0001	0.0001	0.0001	0.0275	0.1321	0.2560	0.3466	0.3939	0.4261
	0.0032	0.0002	0.0000	0.0000	0.0276	0.1320	0.2557	0.3461	0.3933	0.4255
	0.0032	0.0001	0.0001	−0.0001	0.0277	0.1318	0.2552	0.3455	0.3924	0.4247
	0.0032	0.0000	0.0001	0.0003	0.0278	0.1316	0.2548	0.3447	0.3915	0.4237
	0.0031	0.0001	0.0001	0.0002	0.0280	0.1313	0.2539	0.3434	0.3898	0.4222
	0.0029	0.0001	0.0000	0.0002	0.0283	0.1308	0.2525	0.3415	0.3876	0.4202
	0.0032	−0.0001	0.0003	0.0001	0.0286	0.1299	0.2504	0.3388	0.3846	0.4174
	0.0031	0.0002	0.0001	0.0000	0.0290	0.1282	0.2465	0.3339	0.3791	0.4127

Figure I.21: F1C: e=1b & d=1.5b

	c/b									
a/b	0.0003	0.0002	0.0137	0.0840	0.1800	0.2688	0.3399	0.3829	0.4022	0.4273
	0.0007	0.0004	0.0137	0.0840	0.1800	0.2687	0.3397	0.3827	0.4020	0.4271
	0.0007	0.0003	0.0138	0.0840	0.1799	0.2686	0.3395	0.3824	0.4017	0.4268
	0.0007	0.0000	0.0139	0.0841	0.1799	0.2684	0.3391	0.3819	0.4012	0.4263
	0.0003	0.0002	0.0140	0.0841	0.1798	0.2681	0.3385	0.3812	0.4004	0.4256
	0.0007	0.0002	0.0141	0.0841	0.1796	0.2676	0.3378	0.3804	0.3996	0.4248
	0.0007	0.0002	0.0144	0.0841	0.1793	0.2670	0.3367	0.3791	0.3984	0.4236
	0.0007	−0.0001	0.0146	0.0840	0.1788	0.2659	0.3352	0.3774	0.3967	0.4221
	0.0007	−0.0001	0.0149	0.0837	0.1779	0.2642	0.3329	0.3749	0.3943	0.4200
	0.0006	0.0004	0.0154	0.0831	0.1764	0.2612	0.3288	0.3707	0.3903	0.4164

Figure I.21: F1C: e=1b & d=2b

	c/b									
a/b	0.0013	0.0277	0.1098	0.2082	0.2885	0.3331	0.3725	0.3980	0.4087	0.4292
	0.0013	0.0278	0.1099	0.2082	0.2884	0.3329	0.3723	0.3978	0.4085	0.4290
	0.0004	0.0279	0.1101	0.2082	0.2883	0.3327	0.3720	0.3975	0.4082	0.4287
	0.0004	0.0281	0.1102	0.2083	0.2881	0.3324	0.3716	0.3971	0.4078	0.4283
	0.0012	0.0283	0.1104	0.2082	0.2877	0.3318	0.3710	0.3964	0.4072	0.4277
	−0.0004	0.0285	0.1105	0.2081	0.2873	0.3312	0.3703	0.3957	0.4065	0.4271
	0.0012	0.0289	0.1107	0.2080	0.2866	0.3303	0.3693	0.3946	0.4054	0.4261
	0.0012	0.0293	0.1110	0.2076	0.2856	0.3289	0.3678	0.3932	0.4040	0.4249
	0.0012	0.0297	0.1110	0.2069	0.2841	0.3269	0.3657	0.3911	0.4021	0.4232
	0.0003	0.0305	0.1112	0.2054	0.2812	0.3234	0.3620	0.3877	0.3990	0.4203

Figure I.21: F1C: e=1b & d=2.5b

	c/b									
a/b	0.04845	0.148	0.2226	0.2902	0.3391	0.3635	0.3896	0.4073	0.4136	0.4313
	0.04869	0.1481	0.2226	0.2901	0.339	0.3633	0.3895	0.4072	0.4135	0.4311
	0.04906	0.1482	0.2226	0.29	0.3388	0.3631	0.3892	0.4069	0.4132	0.4309
	0.04957	0.1484	0.2226	0.2898	0.3385	0.3628	0.3888	0.4065	0.4129	0.4305
	0.05019	0.1487	0.2225	0.2895	0.3381	0.3622	0.3883	0.406	0.4123	0.4301
	0.05081	0.1489	0.2223	0.2891	0.3375	0.3617	0.3877	0.4054	0.4118	0.4295
	0.05185	0.1492	0.222	0.2884	0.3367	0.3607	0.3867	0.4044	0.4109	0.4287
	0.05317	0.1494	0.2216	0.2875	0.3355	0.3594	0.3854	0.4032	0.4097	0.4276
	0.05455	0.1495	0.2206	0.286	0.3337	0.3576	0.3836	0.4015	0.4082	0.4262
	0.05693	0.1494	0.2189	0.2834	0.3306	0.3544	0.3806	0.3987	0.4056	0.4239

Figure I.21: F1C: e=1b & d=3b

	c/b									
a/b	0.1811	0.2463	0.2903	0.3355	0.3682	0.3822	0.4013	0.4144	0.418	0.4336
	0.1811	0.2463	0.2902	0.3353	0.3681	0.3821	0.4011	0.4143	0.4178	0.4335
	0.1813	0.2463	0.2901	0.3352	0.3679	0.3819	0.4009	0.4141	0.4176	0.4333
	0.1814	0.2462	0.2899	0.3349	0.3676	0.3815	0.4005	0.4137	0.4173	0.433
	0.1815	0.2461	0.2896	0.3345	0.3671	0.381	0.4001	0.4133	0.4168	0.4326
	0.1816	0.2459	0.2892	0.334	0.3666	0.3805	0.3995	0.4127	0.4164	0.4321
	0.1818	0.2456	0.2886	0.3332	0.3657	0.3796	0.3987	0.4119	0.4156	0.4314
	0.1818	0.245	0.2877	0.3322	0.3646	0.3785	0.3975	0.4109	0.4146	0.4305
	0.1815	0.2441	0.2863	0.3306	0.3629	0.3768	0.396	0.4094	0.4133	0.4293
	0.181	0.2423	0.2839	0.3278	0.3601	0.3741	0.3934	0.4071	0.4112	0.4274

Figure I.21: F1C: e=1b & d=3.5b

	c/b									
a/b	0.2684	0.3081	0.3333	0.3649	0.3882	0.3959	0.4104	0.4205	0.4221	0.4362
	0.2684	0.308	0.3332	0.3647	0.388	0.3957	0.4103	0.4204	0.4219	0.4361
	0.2684	0.3079	0.3331	0.3645	0.3878	0.3955	0.4101	0.4202	0.4218	0.4359
	0.2683	0.3077	0.3328	0.3643	0.3875	0.3952	0.4098	0.4199	0.4215	0.4357
	0.2681	0.3074	0.3324	0.3638	0.3871	0.3948	0.4093	0.4195	0.4211	0.4353
	0.2679	0.307	0.332	0.3634	0.3866	0.3943	0.4089	0.419	0.4207	0.4349
	0.2675	0.3064	0.3313	0.3626	0.3858	0.3935	0.4081	0.4183	0.42	0.4343
	0.2669	0.3055	0.3303	0.3615	0.3847	0.3925	0.4071	0.4174	0.4192	0.4335
	0.2658	0.3042	0.3288	0.36	0.3832	0.3911	0.4058	0.4162	0.418	0.4325
	0.2639	0.3018	0.3262	0.3574	0.3807	0.3887	0.4036	0.4142	0.4162	0.4308

Figure I.21: F1C: e=1b & d=4b

	c/b									
a/b	0.3239	0.3482	0.3623	0.3855	0.4029	0.4065	0.4180	0.4259	0.4260	0.4389
	0.3238	0.3481	0.3622	0.3854	0.4028	0.4064	0.4179	0.4258	0.4259	0.4388
	0.3237	0.3479	0.3620	0.3852	0.4026	0.4062	0.4177	0.4256	0.4257	0.4387
	0.3235	0.3477	0.3617	0.3849	0.4023	0.4059	0.4174	0.4254	0.4255	0.4384
	0.3232	0.3473	0.3613	0.3845	0.4019	0.4055	0.4170	0.4250	0.4251	0.4381
	0.3228	0.3469	0.3609	0.3841	0.4014	0.4051	0.4166	0.4246	0.4248	0.4378
	0.3222	0.3462	0.3601	0.3833	0.4007	0.4044	0.4159	0.4240	0.4242	0.4372
	0.3213	0.3452	0.3591	0.3823	0.3997	0.4034	0.4151	0.4231	0.4234	0.4366
	0.3200	0.3438	0.3577	0.3809	0.3984	0.4022	0.4139	0.4221	0.4225	0.4357
	0.3176	0.3413	0.3553	0.3786	0.3962	0.4001	0.4120	0.4204	0.4209	0.4342

Figure I.21: F1C: e=1.5b & d=0.5b

	c/b									
	0.0065	0.0050	0.0017	0.0017	0.0003	−0.0002	0.0001	0.1578	0.3642	0.4286
	0.0065	0.0051	0.0017	0.0016	0.0002	−0.0001	0.0001	0.1578	0.3638	0.4281
	0.0060	0.0050	0.0017	0.0017	0.0002	−0.0004	0.0032	0.1577	0.3632	0.4274
	0.0059	0.0051	0.0017	0.0017	0.0002	−0.0001	0.0015	0.1575	0.3623	0.4263
a/b	0.0065	0.0050	0.0017	0.0018	0.0002	−0.0002	0.0001	0.1573	0.3610	0.4249
	0.0065	0.0049	0.0017	0.0017	−0.0001	0.0001	0.0019	0.1570	0.3596	0.4233
	0.0064	0.0051	0.0017	0.0017	0.0002	−0.0004	0.0020	0.1566	0.3574	0.4209
	0.0059	0.0050	0.0017	0.0018	0.0001	−0.0001	0.0038	0.1560	0.3541	0.4177
	0.0064	0.0050	0.0017	0.0018	0.0000	−0.0001	0.0026	0.1551	0.3509	0.4137
	0.0062	0.0049	0.0017	0.0018	0.0002	−0.0001	0.0030	0.1536	0.3451	0.4074

Figure I.21: F1C: e=1.5b & d=1b

	c/b									
	0.0032	0.0001	0.0000	0.0002	0.0274	0.1322	0.2563	0.3470	0.3946	0.4268
	0.0029	0.0001	−0.0001	0.0000	0.0274	0.1321	0.2561	0.3467	0.3942	0.4264
	0.0031	0.0002	0.0000	0.0002	0.0275	0.1320	0.2558	0.3463	0.3936	0.4258
	0.0029	0.0001	0.0001	0.0002	0.0275	0.1318	0.2553	0.3456	0.3927	0.4250
a/b	0.0029	0.0001	−0.0001	−0.0001	0.0277	0.1315	0.2547	0.3447	0.3916	0.4238
	0.0031	0.0001	0.0001	0.0004	0.0278	0.1312	0.2540	0.3436	0.3903	0.4226
	0.0029	0.0001	0.0002	−0.0001	0.0280	0.1308	0.2529	0.3421	0.3884	0.4208
	0.0032	0.0001	0.0000	0.0002	0.0282	0.1302	0.2513	0.3399	0.3859	0.4184
	0.0028	0.0001	0.0002	0.0002	0.0284	0.1292	0.2492	0.3371	0.3827	0.4155
	0.0032	0.0002	0.0001	0.0000	0.0287	0.1277	0.2457	0.3327	0.3777	0.4109

Figure I.21: F1C: e=1.5b & d=1.5b

	c/b									
	0.0007	0.0004	0.0137	0.0840	0.1800	0.2688	0.3399	0.3829	0.4022	0.4273
	0.0002	0.0002	0.0137	0.0840	0.1799	0.2686	0.3396	0.3826	0.4019	0.4270
	0.0003	0.0002	0.0138	0.0840	0.1798	0.2684	0.3392	0.3821	0.4014	0.4265
	0.0007	0.0002	0.0139	0.0840	0.1797	0.2680	0.3387	0.3814	0.4007	0.4258
a/b	0.0007	0.0000	0.0140	0.0840	0.1795	0.2676	0.3379	0.3805	0.3997	0.4249
	0.0007	0.0004	0.0142	0.0839	0.1792	0.2670	0.3370	0.3794	0.3987	0.4239
	0.0003	0.0002	0.0144	0.0838	0.1788	0.2660	0.3356	0.3779	0.3971	0.4224
	0.0007	0.0002	0.0146	0.0836	0.1781	0.2648	0.3338	0.3759	0.3951	0.4206
	0.0006	0.0003	0.0148	0.0833	0.1771	0.2630	0.3314	0.3733	0.3926	0.4183
	0.0006	0.0003	0.0152	0.0827	0.1757	0.2603	0.3276	0.3692	0.3887	0.4147

Figure I.21: F1C: e=1.5b & d=2b

	c/b									
	0.0013	0.0277	0.1098	0.2082	0.2885	0.3330	0.3725	0.3979	0.4087	0.4291
	0.0013	0.0278	0.1099	0.2081	0.2883	0.3328	0.3722	0.3977	0.4084	0.4289
	0.0013	0.0279	0.1100	0.2081	0.2881	0.3325	0.3718	0.3972	0.4080	0.4285
	0.0012	0.0281	0.1101	0.2080	0.2877	0.3319	0.3712	0.3966	0.4073	0.4279
a/b	0.0012	0.0283	0.1103	0.2079	0.2872	0.3313	0.3704	0.3958	0.4065	0.4271
	0.0004	0.0286	0.1104	0.2077	0.2867	0.3305	0.3695	0.3949	0.4057	0.4263
	0.0012	0.0289	0.1105	0.2074	0.2858	0.3292	0.3681	0.3935	0.4043	0.4251
	0.0012	0.0292	0.1106	0.2069	0.2845	0.3277	0.3664	0.3918	0.4027	0.4236
	0.0003	0.0296	0.1106	0.2060	0.2828	0.3255	0.3642	0.3896	0.4006	0.4217
	0.0011	0.0302	0.1105	0.2046	0.2802	0.3223	0.3607	0.3862	0.3975	0.4188

Figure I.21: F1C: e=1.5b & d=2.5b

	c/b									
	0.0484	0.1479	0.2226	0.2902	0.3391	0.3635	0.3896	0.4073	0.4136	0.4313
	0.0487	0.1480	0.2226	0.2900	0.3389	0.3633	0.3894	0.4071	0.4134	0.4310
	0.0490	0.1481	0.2225	0.2898	0.3386	0.3629	0.3890	0.4067	0.4130	0.4307
	0.0496	0.1483	0.2224	0.2895	0.3381	0.3624	0.3885	0.4061	0.4125	0.4302
a/b	0.0503	0.1485	0.2222	0.2890	0.3375	0.3617	0.3877	0.4054	0.4118	0.4295
	0.0510	0.1487	0.2219	0.2885	0.3368	0.3609	0.3869	0.4046	0.4110	0.4288
	0.0520	0.1489	0.2214	0.2876	0.3357	0.3597	0.3857	0.4034	0.4099	0.4278
	0.0532	0.1490	0.2208	0.2865	0.3343	0.3582	0.3842	0.4020	0.4085	0.4265
	0.0544	0.1489	0.2198	0.2849	0.3324	0.3562	0.3822	0.4001	0.4068	0.4249
	0.0563	0.1488	0.2181	0.2824	0.3295	0.3531	0.3792	0.3973	0.4042	0.4225

Figure I.21: F1C: e=1.5b & d=3b

	c/b									
	0.181	0.2463	0.2902	0.3354	0.3682	0.3822	0.4012	0.4144	0.4179	0.4336
	0.1811	0.2462	0.2901	0.3353	0.368	0.382	0.401	0.4142	0.4177	0.4334
	0.1811	0.2461	0.2899	0.335	0.3677	0.3816	0.4007	0.4139	0.4174	0.4331
	0.1813	0.246	0.2896	0.3346	0.3672	0.3812	0.4002	0.4134	0.417	0.4327
a/b	0.1814	0.2458	0.2892	0.334	0.3666	0.3805	0.3995	0.4127	0.4164	0.4321
	0.1814	0.2455	0.2886	0.3334	0.3659	0.3798	0.3988	0.4121	0.4157	0.4315
	0.1814	0.245	0.2878	0.3324	0.3648	0.3787	0.3977	0.411	0.4147	0.4306
	0.1813	0.2443	0.2867	0.3311	0.3634	0.3773	0.3964	0.4098	0.4136	0.4295
	0.1809	0.2432	0.2852	0.3294	0.3616	0.3755	0.3947	0.4082	0.4121	0.4282
	0.1803	0.2415	0.2829	0.3267	0.3589	0.3728	0.3921	0.4058	0.4099	0.4261

Figure I.21: F1C: e=1.5b & d=3.5b

	c/b									
	0.2684	0.308	0.3333	0.3648	0.3881	0.3958	0.4104	0.4205	0.4221	0.4362
	0.2683	0.3079	0.3331	0.3646	0.3879	0.3956	0.4102	0.4203	0.4219	0.436
	0.2682	0.3077	0.3329	0.3644	0.3876	0.3953	0.4099	0.42	0.4216	0.4358
	0.268	0.3074	0.3325	0.3639	0.3872	0.3949	0.4094	0.4196	0.4212	0.4354
a/b	0.2678	0.307	0.332	0.3633	0.3866	0.3943	0.4088	0.419	0.4207	0.4349
	0.2674	0.3064	0.3313	0.3627	0.3859	0.3936	0.4082	0.4184	0.4201	0.4344
	0.2669	0.3057	0.3304	0.3617	0.3849	0.3926	0.4073	0.4175	0.4192	0.4336
	0.2661	0.3046	0.3292	0.3604	0.3836	0.3914	0.4061	0.4164	0.4182	0.4326
	0.2649	0.3031	0.3276	0.3588	0.382	0.3898	0.4046	0.415	0.4169	0.4315
	0.263	0.3009	0.3251	0.3562	0.3795	0.3874	0.4024	0.413	0.415	0.4297

Figure I.21: F1C: e=1.5b & d=4b

	c/b									
	0.3239	0.3482	0.3623	0.3855	0.4029	0.4065	0.418	0.4259	0.426	0.4389
	0.3238	0.348	0.3621	0.3853	0.4027	0.4063	0.4178	0.4257	0.4258	0.4388
	0.3236	0.3477	0.3618	0.385	0.4024	0.406	0.4175	0.4255	0.4256	0.4385
	0.3232	0.3474	0.3614	0.3846	0.402	0.4056	0.4171	0.4251	0.4252	0.4382
a/b	0.3228	0.3469	0.3609	0.3841	0.4014	0.4051	0.4166	0.4246	0.4247	0.4378
	0.3223	0.3463	0.3603	0.3834	0.4008	0.4045	0.416	0.424	0.4242	0.4373
	0.3215	0.3454	0.3593	0.3825	0.3999	0.4036	0.4152	0.4233	0.4235	0.4366
	0.3204	0.3442	0.3581	0.3813	0.3987	0.4025	0.4141	0.4223	0.4226	0.4357
	0.3189	0.3426	0.3565	0.3798	0.3972	0.4011	0.4128	0.4211	0.4215	0.4347
	0.3166	0.3402	0.3542	0.3774	0.395	0.399	0.4109	0.4192	0.4198	0.4332

Figure I.21: F1C: e=2b & d=0.5b

	c/b									
a/b	0.0065	0.0051	0.0017	0.0017	0.0004	0.0001	0.0015	0.1578	0.3642	0.4286
	0.0065	0.0051	0.0017	0.0017	−0.0001	0.0001	0.0031	0.1578	0.3638	0.4281
	0.0065	0.0051	0.0017	0.0017	0.0002	0.0001	0.0017	0.1576	0.3631	0.4272
	0.0065	0.0050	0.0017	0.0017	0.0002	0.0001	0.0000	0.1574	0.3620	0.4257
	0.0063	0.0051	0.0017	0.0017	0.0001	−0.0001	0.0033	0.1570	0.3605	0.4243
	0.0059	0.0051	0.0017	0.0017	0.0002	0.0001	0.0035	0.1566	0.3589	0.4225
	0.0060	0.0050	0.0017	0.0017	0.0002	−0.0004	0.0036	0.1561	0.3566	0.4199
	0.0063	0.0049	0.0017	0.0018	0.0001	0.0001	0.0038	0.1554	0.3538	0.4167
	0.0064	0.0050	0.0017	0.0018	0.0001	−0.0001	0.0025	0.1544	0.3503	0.4128
	0.0062	0.0050	0.0017	0.0019	0.0001	−0.0004	0.0028	0.1530	0.3450	0.4072

Figure I.21: F1C: e=2b & d=1b

	c/b									
a/b	0.0032	0.0001	0.0000	0.0001	0.0274	0.1322	0.2563	0.3470	0.3946	0.4267
	0.0032	0.0001	0.0002	0.0001	0.0274	0.1321	0.2561	0.3467	0.3942	0.4263
	0.0032	0.0001	0.0001	0.0003	0.0274	0.1319	0.2557	0.3461	0.3935	0.4257
	0.0032	0.0002	0.0001	0.0001	0.0275	0.1317	0.2551	0.3453	0.3925	0.4247
	0.0032	0.0002	0.0002	0.0002	0.0276	0.1313	0.2543	0.3442	0.3911	0.4233
	0.0032	0.0001	−0.0001	−0.0001	0.0277	0.1310	0.2535	0.3430	0.3896	0.4219
	0.0032	0.0001	0.0001	−0.0002	0.0278	0.1304	0.2522	0.3413	0.3875	0.4199
	0.0032	0.0002	−0.0001	0.0002	0.0280	0.1297	0.2506	0.3391	0.3850	0.4175
	0.0029	0.0001	0.0003	0.0002	0.0281	0.1288	0.2486	0.3364	0.3819	0.4145
	0.0031	0.0002	0.0001	0.0001	0.0283	0.1275	0.2455	0.3324	0.3773	0.4101

Figure I.21: F1C: e=2b & d=1.5b

	c/b									
a/b	0.0007	0.0004	0.0137	0.0840	0.1800	0.2688	0.3399	0.3829	0.4022	0.4273
	0.0007	0.0004	0.0137	0.0840	0.1799	0.2686	0.3396	0.3825	0.4018	0.4269
	0.0007	0.0002	0.0138	0.0839	0.1797	0.2682	0.3391	0.3820	0.4013	0.4264
	0.0007	0.0002	0.0139	0.0839	0.1795	0.2678	0.3384	0.3811	0.4004	0.4255
	0.0007	0.0002	0.0140	0.0838	0.1792	0.2671	0.3374	0.3800	0.3993	0.4245
	0.0007	0.0002	0.0141	0.0837	0.1788	0.2664	0.3364	0.3788	0.3981	0.4233
	0.0007	0.0004	0.0143	0.0835	0.1783	0.2654	0.3349	0.3771	0.3963	0.4217
	0.0007	0.0002	0.0145	0.0833	0.1776	0.2641	0.3330	0.3750	0.3943	0.4197
	0.0003	0.0005	0.0147	0.0830	0.1766	0.2624	0.3307	0.3725	0.3917	0.4173
	0.0006	0.0002	0.0150	0.0825	0.1753	0.2599	0.3272	0.3687	0.3881	0.4139

Figure I.21: F1C: e=2b & d=2b

	c/b									
a/b	0.0013	0.0277	0.1098	0.2081	0.2884	0.3330	0.3724	0.3979	0.4086	0.4292
	0.0004	0.0278	0.1098	0.2081	0.2882	0.3328	0.3721	0.3976	0.4083	0.4288
	0.0004	0.0279	0.1099	0.2080	0.2879	0.3323	0.3717	0.3971	0.4078	0.4283
	0.0012	0.0280	0.1100	0.2078	0.2875	0.3317	0.3709	0.3964	0.4071	0.4277
	0.0012	0.0282	0.1100	0.2076	0.2869	0.3309	0.3700	0.3954	0.4061	0.4268
	0.0004	0.0285	0.1101	0.2073	0.2862	0.3299	0.3689	0.3943	0.4051	0.4258
	0.0012	0.0287	0.1102	0.2069	0.2852	0.3286	0.3675	0.3928	0.4036	0.4244
	0.0012	0.0291	0.1102	0.2063	0.2839	0.3269	0.3656	0.3910	0.4019	0.4228
	0.0012	0.0294	0.1101	0.2054	0.2822	0.3248	0.3634	0.3888	0.3998	0.4208
	0.0011	0.0298	0.1100	0.2041	0.2798	0.3218	0.3602	0.3856	0.3968	0.4180

Figure I.21: F1C: e=2b & d=2.5b

	c/b									
a/b	0.0484	0.1479	0.2226	0.2902	0.3391	0.3635	0.3896	0.4073	0.4136	0.4312
	0.0486	0.1480	0.2225	0.2900	0.3389	0.3632	0.3893	0.4070	0.4133	0.4310
	0.0489	0.1480	0.2224	0.2897	0.3385	0.3628	0.3889	0.4066	0.4129	0.4306
	0.0495	0.1481	0.2221	0.2892	0.3379	0.3621	0.3882	0.4059	0.4123	0.4300
	0.0501	0.1483	0.2218	0.2886	0.3371	0.3613	0.3873	0.4050	0.4114	0.4292
	0.0508	0.1484	0.2215	0.2880	0.3363	0.3604	0.3864	0.4041	0.4105	0.4284
	0.0518	0.1485	0.2210	0.2870	0.3351	0.3591	0.3851	0.4028	0.4093	0.4272
	0.0529	0.1486	0.2202	0.2858	0.3336	0.3574	0.3834	0.4012	0.4078	0.4258
	0.0539	0.1484	0.2192	0.2842	0.3317	0.3555	0.3814	0.3993	0.4060	0.4241
	0.0554	0.1482	0.2177	0.2819	0.3290	0.3526	0.3786	0.3966	0.4035	0.4218

Figure I.21: F1C: e=2b & d=3b

	c/b									
a/b	0.1810	0.2463	0.2902	0.3354	0.3682	0.3822	0.4012	0.4144	0.4179	0.4336
	0.1810	0.2462	0.2901	0.3352	0.3680	0.3819	0.4010	0.4142	0.4177	0.4334
	0.1810	0.2460	0.2898	0.3349	0.3676	0.3815	0.4006	0.4138	0.4173	0.4330
	0.1811	0.2458	0.2894	0.3343	0.3670	0.3809	0.4000	0.4132	0.4168	0.4325
	0.1811	0.2454	0.2888	0.3336	0.3662	0.3801	0.3992	0.4124	0.4160	0.4318
	0.1811	0.2450	0.2882	0.3329	0.3654	0.3793	0.3983	0.4116	0.4153	0.4311
	0.1810	0.2445	0.2873	0.3318	0.3642	0.3781	0.3972	0.4105	0.4142	0.4301
	0.1808	0.2437	0.2861	0.3304	0.3627	0.3766	0.3957	0.4091	0.4129	0.4289
	0.1804	0.2426	0.2846	0.3287	0.3609	0.3748	0.3940	0.4074	0.4114	0.4273
	0.1798	0.2410	0.2825	0.3262	0.3583	0.3722	0.3915	0.4051	0.4092	0.4254

Figure I.21: F1C: e=2b & d=3.5b

	c/b									
a/b	0.2684	0.308	0.3333	0.3648	0.3881	0.3958	0.4104	0.4205	0.422	0.4362
	0.2683	0.3079	0.3331	0.3646	0.3879	0.3956	0.4101	0.4203	0.4218	0.436
	0.2681	0.3076	0.3328	0.3642	0.3875	0.3952	0.4098	0.4199	0.4215	0.4357
	0.2678	0.3072	0.3322	0.3637	0.387	0.3947	0.4092	0.4194	0.421	0.4352
	0.2674	0.3066	0.3316	0.363	0.3862	0.3939	0.4085	0.4187	0.4204	0.4346
	0.267	0.306	0.3309	0.3622	0.3854	0.3932	0.4078	0.418	0.4197	0.434
	0.2664	0.3051	0.3299	0.3611	0.3843	0.3921	0.4067	0.417	0.4187	0.4331
	0.2655	0.304	0.3286	0.3598	0.383	0.3907	0.4054	0.4158	0.4176	0.432
	0.2643	0.3025	0.327	0.3581	0.3813	0.3891	0.4039	0.4143	0.4163	0.4308
	0.2626	0.3004	0.3246	0.3557	0.3789	0.3868	0.4017	0.4123	0.4144	0.429

Figure I.21: F1C: e=2b & d=4b

	c/b									
a/b	0.3239	0.3482	0.3623	0.3855	0.4029	0.4065	0.418	0.4259	0.426	0.4389
	0.3237	0.3479	0.3621	0.3853	0.4027	0.4063	0.4177	0.4257	0.4258	0.4387
	0.3234	0.3476	0.3617	0.3849	0.4023	0.4059	0.4174	0.4254	0.4255	0.4385
	0.323	0.3472	0.3612	0.3844	0.4018	0.4054	0.4169	0.4249	0.425	0.438
	0.3225	0.3465	0.3605	0.3837	0.4011	0.4048	0.4163	0.4243	0.4245	0.4375
	0.3218	0.3458	0.3598	0.383	0.4004	0.404	0.4156	0.4237	0.4239	0.4369
	0.3209	0.3448	0.3588	0.3819	0.3993	0.403	0.4147	0.4228	0.423	0.4361
	0.3198	0.3436	0.3575	0.3807	0.3981	0.4019	0.4135	0.4217	0.422	0.4352
	0.3183	0.342	0.3559	0.3791	0.3966	0.4004	0.4122	0.4204	0.4208	0.4341
	0.3161	0.3397	0.3536	0.3768	0.3944	0.3983	0.4102	0.4186	0.4191	0.4326

Figure I.21: F1C: e=2.5b & d=0.5b

	c/b									
	0.0065	0.0050	0.0017	0.0017	0.0002	0.0001	0.0030	0.1578	0.3642	0.4286
	0.0065	0.0051	0.0016	0.0017	0.0003	−0.0001	0.0015	0.1577	0.3638	0.4281
	0.0065	0.0051	0.0017	0.0017	0.0000	−0.0001	0.0015	0.1576	0.3630	0.4272
	0.0065	0.0049	0.0017	0.0017	0.0001	0.0001	0.0015	0.1573	0.3619	0.4259
a/b	0.0065	0.0049	0.0017	0.0017	0.0002	−0.0004	0.0016	0.1569	0.3604	0.4241
	0.0060	0.0050	0.0017	0.0018	0.0001	−0.0001	0.0034	0.1564	0.3587	0.4222
	0.0064	0.0048	0.0017	0.0017	0.0001	−0.0004	0.0019	0.1558	0.3562	0.4196
	0.0064	0.0048	0.0017	0.0010	0.0001	−0.0002	0.0024	0.1550	0.3535	0.4164
	0.0063	0.0051	0.0017	0.0018	0.0002	0.0001	0.0040	0.1540	0.3502	0.4127
	0.0064	0.0051	0.0018	0.0018	0.0002	0.0001	0.0026	0.1527	0.3455	0.4076

Figure I.21: F1C: e=2.5b & d=1b

	c/b									
	0.0032	0.0001	0.0001	0.0001	0.0274	0.1322	0.2563	0.3470	0.3946	0.4267
	0.0029	0.0001	−0.0001	−0.0001	0.0274	0.1320	0.2561	0.3466	0.3942	0.4263
	0.0032	0.0001	0.0002	0.0000	0.0274	0.1319	0.2556	0.3461	0.3935	0.4256
	0.0028	0.0001	0.0001	0.0002	0.0274	0.1316	0.2550	0.3452	0.3924	0.4246
a/b	0.0032	0.0001	0.0002	0.0003	0.0275	0.1312	0.2541	0.3440	0.3910	0.4232
	0.0032	0.0002	−0.0001	0.0003	0.0276	0.1308	0.2532	0.3427	0.3894	0.4216
	0.0029	0.0001	0.0000	0.0002	0.0277	0.1302	0.2519	0.3409	0.3872	0.4195
	0.0029	0.0001	0.0000	−0.0004	0.0278	0.1295	0.2503	0.3387	0.3847	0.4171
	0.0029	0.0001	0.0001	−0.0002	0.0279	0.1286	0.2484	0.3361	0.3817	0.4142
	0.0029	0.0001	0.0001	0.0002	0.0280	0.1274	0.2456	0.3325	0.3775	0.4101

Figure I.21: F1C: e=2.5b & d=1.5b

	c/b									
	0.0007	0.0002	0.0137	0.0840	0.1800	0.2688	0.3399	0.3829	0.4022	0.4273
	0.0007	0.0002	0.0137	0.0839	0.1798	0.2686	0.3396	0.3825	0.4018	0.4269
	0.0003	0.0002	0.0137	0.0839	0.1796	0.2682	0.3390	0.3819	0.4012	0.4263
	0.0007	0.0000	0.0138	0.0838	0.1793	0.2676	0.3383	0.3810	0.4003	0.4255
a/b	0.0003	0.0005	0.0139	0.0837	0.1790	0.2669	0.3372	0.3799	0.3991	0.4243
	0.0007	0.0003	0.0140	0.0835	0.1785	0.2661	0.3361	0.3786	0.3978	0.4230
	0.0003	0.0004	0.0142	0.0833	0.1780	0.2650	0.3345	0.3768	0.3960	0.4213
	0.0007	0.0005	0.0143	0.0834	0.1772	0.2637	0.3326	0.3747	0.3939	0.4193
	0.0006	0.0005	0.0145	0.0828	0.1763	0.2621	0.3304	0.3722	0.3914	0.4169
	0.0006	0.0004	0.0147	0.0823	0.1750	0.2597	0.3272	0.3687	0.3880	0.4137

Figure I.21: F1C: e=2.5b & d=2b

	c/b									
	0.0013	0.0277	0.1098	0.2081	0.2884	0.3330	0.3724	0.3979	0.4086	0.4291
	0.0013	0.0278	0.1098	0.2080	0.2882	0.3327	0.3721	0.3976	0.4083	0.4288
	0.0013	0.0278	0.1098	0.2079	0.2879	0.3323	0.3716	0.3971	0.4078	0.4283
	0.0012	0.0280	0.1098	0.2076	0.2873	0.3316	0.3708	0.3963	0.4070	0.4276
a/b	0.0012	0.0281	0.1098	0.2073	0.2866	0.3307	0.3698	0.3952	0.4060	0.4266
	0.0012	0.0283	0.1098	0.2070	0.2859	0.3296	0.3687	0.3941	0.4048	0.4255
	0.0012	0.0285	0.1098	0.2065	0.2848	0.3282	0.3671	0.3925	0.4033	0.4241
	0.0012	0.0288	0.1098	0.2058	0.2835	0.3266	0.3653	0.3906	0.4015	0.4224
	0.0012	0.0291	0.1097	0.2050	0.2819	0.3245	0.3631	0.3884	0.3994	0.4204
	0.0011	0.0294	0.1095	0.2038	0.2796	0.3217	0.3601	0.3854	0.3965	0.4177

Figure I.21: F1C: e=2.5b & d=2.5b

	c/b									
	0.04841	0.1479	0.2226	0.2902	0.3391	0.3635	0.3896	0.4073	0.4136	0.4312
	0.04857	0.1479	0.2225	0.2899	0.3388	0.3632	0.3893	0.407	0.4133	0.431
	0.04883	0.1479	0.2223	0.2896	0.3384	0.3627	0.3889	0.4065	0.4129	0.4305
	0.04926	0.148	0.222	0.2891	0.3378	0.362	0.3881	0.4058	0.4122	0.4299
a/b	0.04982	0.148	0.2216	0.2884	0.337	0.3611	0.3872	0.4049	0.4113	0.429
	0.05045	0.148	0.2212	0.2877	0.336	0.3601	0.3861	0.4039	0.4103	0.4281
	0.05127	0.1481	0.2206	0.2867	0.3348	0.3587	0.3847	0.4025	0.409	0.4269
	0.05224	0.148	0.2198	0.2854	0.3332	0.3571	0.3831	0.4008	0.4074	0.4254
	0.0532	0.1479	0.2188	0.2839	0.3314	0.3551	0.3811	0.3989	0.4056	0.4237
	0.05451	0.1476	0.2174	0.2818	0.3289	0.3524	0.3784	0.3963	0.4032	0.4214

Figure I.21: F1C: e=2.5b & d=3b

	c/b									
	0.181	0.2463	0.2902	0.3354	0.3682	0.3822	0.4012	0.4144	0.4179	0.4336
	0.181	0.2461	0.29	0.3352	0.3679	0.3819	0.401	0.4141	0.4177	0.4334
	0.181	0.2459	0.2897	0.3348	0.3675	0.3815	0.4005	0.4137	0.4173	0.433
	0.1809	0.2456	0.2892	0.3342	0.3669	0.3808	0.3999	0.4131	0.4167	0.4324
a/b	0.1808	0.2452	0.2886	0.3335	0.3661	0.38	0.399	0.4123	0.4159	0.4317
	0.1807	0.2447	0.2879	0.3326	0.3651	0.379	0.3981	0.4114	0.415	0.4309
	0.1806	0.2441	0.2869	0.3314	0.3639	0.3778	0.3968	0.4101	0.4139	0.4298
	0.1803	0.2432	0.2857	0.3301	0.3624	0.3762	0.3953	0.4087	0.4125	0.4285
	0.1799	0.2422	0.2843	0.3284	0.3606	0.3745	0.3936	0.407	0.411	0.427
	0.1793	0.2407	0.2823	0.326	0.3581	0.372	0.3912	0.4048	0.4088	0.4251

Figure I.21: F1C: e=2.5b & d=3.5b

	c/b									
	0.2684	0.308	0.3333	0.3648	0.3881	0.3958	0.4104	0.4205	0.422	0.4362
	0.2683	0.3078	0.3331	0.3646	0.3879	0.3956	0.4101	0.4203	0.4218	0.436
	0.268	0.3075	0.3327	0.3642	0.3875	0.3952	0.4097	0.4199	0.4215	0.4357
	0.2677	0.3071	0.3322	0.3636	0.3869	0.3946	0.4092	0.4193	0.4209	0.4351
a/b	0.2672	0.3064	0.3314	0.3628	0.3861	0.3938	0.4084	0.4186	0.4202	0.4345
	0.2667	0.3057	0.3306	0.362	0.3852	0.3929	0.4075	0.4178	0.4195	0.4338
	0.266	0.3048	0.3295	0.3608	0.384	0.3918	0.4064	0.4167	0.4184	0.4328
	0.2651	0.3036	0.3282	0.3594	0.3826	0.3904	0.4051	0.4154	0.4172	0.4317
	0.2639	0.3022	0.3266	0.3578	0.3809	0.3888	0.4035	0.414	0.4159	0.4304
	0.2623	0.3002	0.3244	0.3555	0.3787	0.3865	0.4014	0.412	0.414	0.4287

Figure I.21: F1C: e=2.5b & d=4b

	c/b									
	0.3239	0.3481	0.3623	0.3855	0.4029	0.4065	0.4180	0.4259	0.4260	0.4389
	0.3237	0.3479	0.3620	0.3853	0.4026	0.4062	0.4177	0.4257	0.4258	0.4387
	0.3234	0.3476	0.3617	0.3849	0.4023	0.4059	0.4174	0.4253	0.4254	0.4384
	0.3229	0.3471	0.3611	0.3843	0.4017	0.4053	0.4169	0.4248	0.4250	0.4380
a/b	0.3223	0.3463	0.3604	0.3836	0.4010	0.4046	0.4162	0.4242	0.4243	0.4374
	0.3216	0.3456	0.3596	0.3828	0.4001	0.4038	0.4154	0.4234	0.4237	0.4367
	0.3206	0.3445	0.3584	0.3816	0.3990	0.4027	0.4144	0.4225	0.4227	0.4359
	0.3194	0.3432	0.3571	0.3803	0.3977	0.4015	0.4132	0.4213	0.4217	0.4349
	0.3180	0.3417	0.3555	0.3787	0.3962	0.4000	0.4118	0.4200	0.4205	0.4338
	0.3159	0.3395	0.3534	0.3766	0.3941	0.3980	0.4099	0.4183	0.4188	0.4322

Figure I.21: F1C: e=3b & d=0.5b

	c/b									
	0.0065	0.0050	0.0016	0.0016	0.0001	−0.0001	0.0031	0.1578	0.3642	0.4286
	0.0065	0.0051	0.0017	0.0017	−0.0026	−0.0002	0.0030	0.1577	0.3638	0.4281
	0.0065	0.0051	0.0016	0.0017	0.0002	−0.0004	0.0031	0.1575	0.3631	0.4273
	0.0060	0.0051	0.0017	0.0017	0.0002	−0.0002	0.0031	0.1572	0.3620	0.4260
a/b	0.0058	0.0051	0.0017	0.0016	0.0001	−0.0004	0.0017	0.1568	0.3605	0.4243
	0.0063	0.0048	0.0017	0.0017	0.0003	−0.0002	0.0017	0.1563	0.3588	0.4223
	0.0064	0.0051	0.0017	0.0018	0.0001	0.0001	0.0019	0.1556	0.3564	0.4197
	0.0063	0.0051	0.0017	0.0018	0.0002	−0.0001	0.0036	0.1548	0.3537	0.4166
	0.0064	0.0049	0.0017	0.0018	0.0002	−0.0004	0.0038	0.1539	0.3506	0.4131
	0.0064	0.0050	0.0017	0.0019	0.0002	−0.0006	0.0040	0.1526	0.3464	0.4083

Figure I.21: F1C: e=3b & d=1b

	c/b									
	0.0031	0.0001	−0.0001	0.0002	0.0273	0.1322	0.2563	0.3470	0.3946	0.4268
	0.0031	0.0001	−0.0001	−0.0003	0.0274	0.1320	0.2561	0.3467	0.3942	0.4263
	0.0032	0.0001	0.0002	0.0001	0.0274	0.1319	0.2556	0.3461	0.3935	0.4257
	0.0032	0.0000	0.0001	0.0002	0.0274	0.1316	0.2550	0.3452	0.3924	0.4246
a/b	0.0031	0.0001	0.0001	−0.0003	0.0274	0.1312	0.2541	0.3440	0.3910	0.4232
	0.0032	0.0002	0.0001	0.0000	0.0275	0.1307	0.2531	0.3427	0.3894	0.4217
	0.0031	0.0002	0.0002	0.0003	0.0276	0.1301	0.2519	0.3408	0.3873	0.4196
	0.0028	0.0001	0.0000	0.0002	0.0276	0.1294	0.2503	0.3387	0.3848	0.4171
	0.0032	0.0001	0.0000	0.0002	0.0277	0.1286	0.2485	0.3362	0.3819	0.4143
	0.0032	0.0002	0.0003	0.0001	0.0278	0.1274	0.2459	0.3329	0.3780	0.4109

Figure I.21: F1C: e=3b & d=1.5b

	c/b									
	0.0007	0.0000	0.0137	0.0840	0.1800	0.2688	0.3399	0.3829	0.4022	0.4273
	0.0007	−0.0001	0.0137	0.0839	0.1798	0.2686	0.3396	0.3825	0.4019	0.4269
	0.0007	0.0005	0.0137	0.0839	0.1796	0.2682	0.3391	0.3820	0.4013	0.4264
	−0.0002	0.0002	0.0138	0.0838	0.1793	0.2676	0.3383	0.3811	0.4004	0.4255
a/b	0.0003	0.0005	0.0138	0.0836	0.1789	0.2669	0.3372	0.3799	0.3992	0.4243
	0.0007	0.0005	0.0139	0.0834	0.1784	0.2660	0.3360	0.3786	0.3978	0.4230
	0.0007	0.0005	0.0140	0.0832	0.1778	0.2649	0.3345	0.3768	0.3960	0.4213
	0.0007	0.0003	0.0142	0.0829	0.1770	0.2635	0.3326	0.3747	0.3939	0.4192
	0.0007	0.0003	0.0143	0.0826	0.1761	0.2619	0.3304	0.3723	0.3915	0.4169
	0.0006	0.0002	0.0145	0.0821	0.1749	0.2598	0.3275	0.3689	0.3882	0.4138

Figure I.21: F1C: e=3b & d=2b

	c/b									
	0.0004	0.0277	0.1098	0.2081	0.2884	0.3330	0.3724	0.3979	0.4086	0.4292
	0.0013	0.0277	0.1098	0.2080	0.2882	0.3327	0.3721	0.3976	0.4083	0.4288
	0.0013	0.0278	0.1098	0.2078	0.2879	0.3323	0.3716	0.3971	0.4078	0.4283
	0.0013	0.0279	0.1097	0.2076	0.2873	0.3316	0.3708	0.3963	0.4070	0.4276
a/b	0.0012	0.0280	0.1097	0.2072	0.2866	0.3306	0.3698	0.3952	0.4060	0.4266
	0.0012	0.0281	0.1096	0.2068	0.2858	0.3296	0.3686	0.3940	0.4048	0.4255
	0.0012	0.0283	0.1095	0.2062	0.2846	0.3282	0.3671	0.3924	0.4032	0.4240
	0.0004	0.0286	0.1094	0.2055	0.2833	0.3265	0.3652	0.3905	0.4014	0.4223
	0.0012	0.0288	0.1093	0.2047	0.2818	0.3245	0.3631	0.3884	0.3994	0.4203
	0.0011	0.0291	0.1091	0.2035	0.2796	0.3219	0.3602	0.3855	0.3966	0.4177

Figure I.21: F1C: e=3b & d=2.5b

	c/b									
	0.0484	0.1479	0.2226	0.2902	0.3391	0.3635	0.3896	0.4073	0.4136	0.4313
	0.0485	0.1479	0.2225	0.2899	0.3389	0.3632	0.3893	0.4070	0.4133	0.4310
	0.0487	0.1479	0.2223	0.2896	0.3384	0.3627	0.3889	0.4065	0.4129	0.4306
	0.0491	0.1478	0.2219	0.2891	0.3378	0.3620	0.3881	0.4058	0.4122	0.4299
a/b	0.0495	0.1478	0.2214	0.2884	0.3369	0.3611	0.3872	0.4049	0.4113	0.4290
	0.0501	0.1478	0.2210	0.2876	0.3360	0.3601	0.3861	0.4038	0.4103	0.4281
	0.0508	0.1477	0.2203	0.2865	0.3347	0.3586	0.3847	0.4024	0.4089	0.4268
	0.0516	0.1476	0.2195	0.2853	0.3331	0.3570	0.3830	0.4007	0.4073	0.4253
	0.0524	0.1474	0.2186	0.2838	0.3314	0.3551	0.3810	0.3989	0.4055	0.4236
	0.0535	0.1471	0.2172	0.2818	0.3290	0.3525	0.3785	0.3964	0.4031	0.4214

Figure I.21: F1C: e=3b & d=3b

	c/b									
	0.181	0.2463	0.2902	0.3354	0.3682	0.3822	0.4012	0.4144	0.4179	0.4336
	0.181	0.2461	0.29	0.3352	0.3679	0.3819	0.401	0.4141	0.4177	0.4334
	0.1809	0.2459	0.2897	0.3348	0.3675	0.3815	0.4005	0.4137	0.4173	0.433
	0.1808	0.2456	0.2892	0.3342	0.3669	0.3808	0.3999	0.4131	0.4167	0.4324
a/b	0.1806	0.2451	0.2885	0.3334	0.366	0.38	0.399	0.4122	0.4159	0.4316
	0.1805	0.2446	0.2878	0.3325	0.3651	0.379	0.398	0.4113	0.415	0.4308
	0.1802	0.2439	0.2868	0.3313	0.3638	0.3777	0.3967	0.41	0.4138	0.4297
	0.1799	0.243	0.2856	0.3299	0.3623	0.3761	0.3952	0.4086	0.4124	0.4284
	0.1795	0.242	0.2842	0.3283	0.3605	0.3744	0.3935	0.4069	0.4108	0.4269
	0.1789	0.2406	0.2822	0.3261	0.3582	0.372	0.3912	0.4047	0.4087	0.4249

Figure I.21: F1C: e=3b & d=3.5b

	c/b									
	0.2684	0.308	0.3333	0.3648	0.3881	0.3958	0.4104	0.4205	0.422	0.4362
	0.2682	0.3078	0.3331	0.3646	0.3879	0.3956	0.4101	0.4203	0.4218	0.436
	0.268	0.3075	0.3327	0.3642	0.3875	0.3952	0.4097	0.4199	0.4215	0.4356
	0.2676	0.307	0.3321	0.3636	0.3869	0.3946	0.4091	0.4193	0.4209	0.4351
a/b	0.2671	0.3064	0.3314	0.3628	0.386	0.3938	0.4084	0.4186	0.4202	0.4344
	0.2666	0.3056	0.3305	0.3619	0.3851	0.3929	0.4075	0.4177	0.4194	0.4337
	0.2658	0.3046	0.3294	0.3607	0.3839	0.3917	0.4063	0.4166	0.4183	0.4327
	0.2648	0.3034	0.3281	0.3593	0.3825	0.3903	0.405	0.4153	0.4171	0.4315
	0.2637	0.302	0.3265	0.3577	0.3808	0.3887	0.4034	0.4138	0.4157	0.4302
	0.2622	0.3001	0.3244	0.3555	0.3787	0.3865	0.4014	0.4119	0.4139	0.4285

Figure I.21: F1C: e=3b & d=4b

	c/b									
	0.3239	0.3481	0.3623	0.3855	0.4029	0.4065	0.418	0.4259	0.426	0.4389
	0.3237	0.3479	0.362	0.3853	0.4026	0.4062	0.4177	0.4257	0.4258	0.4387
	0.3234	0.3476	0.3617	0.3849	0.4023	0.4059	0.4174	0.4253	0.4254	0.4384
	0.3229	0.347	0.3611	0.3843	0.4017	0.4053	0.4168	0.4248	0.4249	0.438
a/b	0.3222	0.3463	0.3603	0.3835	0.4009	0.4046	0.4161	0.4241	0.4243	0.4373
	0.3215	0.3455	0.3595	0.3827	0.4001	0.4038	0.4153	0.4234	0.4236	0.4367
	0.3204	0.3444	0.3583	0.3815	0.3989	0.4026	0.4143	0.4224	0.4226	0.4358
	0.3192	0.3431	0.357	0.3802	0.3976	0.4014	0.4131	0.4212	0.4215	0.4347
	0.3178	0.3416	0.3554	0.3786	0.3961	0.3999	0.4117	0.4199	0.4203	0.4336
	0.3159	0.3395	0.3534	0.3766	0.3941	0.398	0.4098	0.4182	0.4187	0.4321

Figure I.21: F1C: e=3.5b & d=0.5b

	c/b									
a/b	0.0063	0.0051	0.0017	0.0017	0.0000	−0.0001	0.0015	0.1579	0.3642	0.4286
	0.0064	0.0050	0.0017	0.0016	0.0001	0.0001	0.0015	0.1577	0.3638	0.4282
	0.0065	0.0050	0.0016	0.0016	0.0002	0.0001	0.0015	0.1575	0.3632	0.4274
	0.0060	0.0051	0.0017	0.0016	0.0001	−0.0001	0.0016	0.1572	0.3621	0.4262
	0.0065	0.0051	0.0017	0.0017	0.0000	−0.0004	0.0015	0.1568	0.3607	0.4245
	0.0065	0.0049	0.0017	0.0017	0.0001	−0.0001	0.0016	0.1563	0.3591	0.4227
	0.0060	0.0049	0.0017	0.0017	0.0001	−0.0007	0.0017	0.1556	0.3568	0.4201
	0.0060	0.0051	0.0017	0.0017	0.0002	−0.0004	0.0035	0.1548	0.3542	0.4172
	0.0064	0.0051	0.0017	0.0018	0.0002	−0.0007	0.0038	0.1538	0.3513	0.4139
	0.0064	0.0050	0.0017	0.0018	0.0002	−0.0002	0.0039	0.1526	0.3474	0.4094

Figure I.21: F1C: e=3.5b & d=1b

	c/b									
a/b	0.0028	0.0001	0.0000	0.0003	0.0273	0.1322	0.2563	0.3470	0.3946	0.4268
	0.0029	0.0002	−0.0001	0.0001	0.0274	0.1321	0.2561	0.3467	0.3938	0.4264
	0.0031	0.0001	0.0001	0.0000	0.0274	0.1319	0.2557	0.3461	0.3935	0.4257
	0.0031	0.0001	0.0001	0.0000	0.0274	0.1316	0.2551	0.3453	0.3926	0.4247
	0.0031	0.0001	0.0001	0.0002	0.0274	0.1312	0.2542	0.3441	0.3912	0.4234
	0.0029	0.0001	0.0003	0.0001	0.0274	0.1307	0.2532	0.3428	0.3897	0.4219
	0.0028	0.0001	−0.0001	0.0001	0.0275	0.1302	0.2519	0.3411	0.3876	0.4198
	0.0031	−0.0002	0.0001	0.0002	0.0275	0.1295	0.2505	0.3390	0.3852	0.4175
	0.0029	0.0002	0.0002	0.0001	0.0275	0.1286	0.2488	0.3366	0.3825	0.4148
	0.0032	0.0002	0.0002	0.0000	0.0276	0.1276	0.2464	0.3335	0.3769	0.4112

Figure I.21: F1C: e=3.5b & d=1.5b

	c/b									
a/b	0.0003	0.0003	0.0137	0.0840	0.1800	0.2688	0.3399	0.3829	0.4022	0.4273
	0.0002	0.0002	0.0137	0.0839	0.1798	0.2686	0.3396	0.3826	0.4019	0.4269
	0.0007	0.0002	0.0137	0.0839	0.1796	0.2682	0.3391	0.3820	0.4013	0.4264
	0.0007	0.0002	0.0137	0.0837	0.1793	0.2676	0.3383	0.3812	0.4005	0.4256
	0.0007	0.0003	0.0138	0.0836	0.1789	0.2669	0.3373	0.3800	0.3993	0.4244
	0.0007	0.0003	0.0139	0.0834	0.1784	0.2660	0.3362	0.3787	0.3980	0.4231
	0.0003	0.0002	0.0139	0.0831	0.1777	0.2649	0.3346	0.3770	0.3963	0.4214
	0.0007	0.0002	0.0141	0.0828	0.1770	0.2636	0.3328	0.3749	0.3941	0.4194
	0.0007	0.0004	0.0142	0.0825	0.1761	0.2620	0.3307	0.3726	0.3918	0.4172
	0.0006	0.0004	0.0143	0.0820	0.1749	0.2600	0.3279	0.3696	0.3888	0.4143

Figure I.21: F1C: e=3.5b & d=2b

	c/b									
a/b	0.0013	0.0277	0.1098	0.2081	0.2884	0.3330	0.3725	0.3979	0.4087	0.4292
	0.0013	0.0277	0.1098	0.2080	0.2882	0.3328	0.3722	0.3976	0.4083	0.4289
	0.0013	0.0278	0.1097	0.2078	0.2879	0.3323	0.3717	0.3971	0.4079	0.4284
	0.0013	0.0278	0.1097	0.2075	0.2873	0.3316	0.3709	0.3964	0.4071	0.4276
	0.0012	0.0279	0.1096	0.2071	0.2866	0.3307	0.3699	0.3953	0.4061	0.4267
	0.0012	0.0280	0.1095	0.2067	0.2858	0.3297	0.3688	0.3942	0.4049	0.4256
	0.0012	0.0282	0.1093	0.2061	0.2847	0.3283	0.3672	0.3926	0.4034	0.4241
	−0.0004	0.0283	0.1091	0.2054	0.2834	0.3266	0.3654	0.3907	0.4016	0.4224
	0.0012	0.0285	0.1090	0.2045	0.2818	0.3248	0.3634	0.3887	0.3996	0.4205
	0.0003	0.0287	0.1087	0.2034	0.2798	0.3223	0.3607	0.3859	0.3969	0.4180

Figure I.21: F1C: e=3.5b & d=2.5b

	c/b									
a/b	0.0484	0.1479	0.2226	0.2902	0.3391	0.3635	0.3896	0.4073	0.4136	0.4313
	0.0485	0.1479	0.2225	0.2899	0.3389	0.3632	0.3893	0.4070	0.4133	0.4310
	0.0487	0.1478	0.2222	0.2896	0.3385	0.3628	0.3889	0.4066	0.4129	0.4306
	0.0489	0.1478	0.2219	0.2891	0.3378	0.3621	0.3882	0.4059	0.4122	0.4299
	0.0493	0.1477	0.2215	0.2884	0.3370	0.3612	0.3873	0.4050	0.4113	0.4291
	0.0497	0.1476	0.2210	0.2876	0.3360	0.3601	0.3862	0.4039	0.4103	0.4281
	0.0503	0.1474	0.2203	0.2866	0.3347	0.3588	0.3848	0.4025	0.4090	0.4268
	0.0509	0.1473	0.2194	0.2853	0.3332	0.3571	0.3831	0.4009	0.4074	0.4254
	0.0517	0.1470	0.2185	0.2839	0.3315	0.3553	0.3813	0.3991	0.4057	0.4237
	0.0526	0.1467	0.2172	0.2819	0.3292	0.3529	0.3788	0.3966	0.4034	0.4215

Figure I.21: F1C: e=3.5b & d=3b

	c/b									
a/b	0.181	0.2463	0.2902	0.3354	0.3682	0.3822	0.4012	0.4144	0.4179	0.4336
	0.181	0.2461	0.29	0.3352	0.368	0.3819	0.401	0.4142	0.4177	0.4334
	0.1809	0.2459	0.2897	0.3348	0.3676	0.3815	0.4006	0.4138	0.4173	0.433
	0.1807	0.2455	0.2892	0.3343	0.3669	0.3809	0.3999	0.4131	0.4167	0.4324
	0.1805	0.2451	0.2886	0.3335	0.3661	0.38	0.3991	0.4123	0.4159	0.4317
	0.1803	0.2445	0.2878	0.3326	0.3651	0.3791	0.3981	0.4114	0.415	0.4308
	0.18	0.2438	0.2868	0.3314	0.3639	0.3778	0.3968	0.4101	0.4138	0.4297
	0.1797	0.2429	0.2856	0.33	0.3624	0.3763	0.3953	0.4087	0.4125	0.4284
	0.1792	0.2419	0.2842	0.3284	0.3607	0.3745	0.3937	0.4071	0.4109	0.4269
	0.1786	0.2406	0.2824	0.3263	0.3584	0.3723	0.3914	0.4049	0.4089	0.4271

Figure I.21: F1C: e=3.5b & d=3.5b

	c/b									
a/b	0.2684	0.308	0.3333	0.3648	0.3881	0.3958	0.4104	0.4205	0.4221	0.4362
	0.2682	0.3078	0.3331	0.3646	0.3879	0.3956	0.4101	0.4203	0.4218	0.436
	0.268	0.3075	0.3327	0.3642	0.3875	0.3952	0.4098	0.4199	0.4215	0.4357
	0.2676	0.307	0.3322	0.3636	0.3869	0.3946	0.4092	0.4193	0.4209	0.4352
	0.2671	0.3064	0.3314	0.3628	0.3861	0.3938	0.4084	0.4186	0.4202	0.4345
	0.2665	0.3056	0.3306	0.362	0.3852	0.3929	0.4075	0.4178	0.4194	0.4337
	0.2657	0.3046	0.3295	0.3608	0.384	0.3917	0.4064	0.4166	0.4184	0.4327
	0.2648	0.3034	0.3281	0.3594	0.3826	0.3903	0.405	0.4153	0.4171	0.4316
	0.2637	0.3021	0.3266	0.3578	0.381	0.3888	0.4035	0.4139	0.4158	0.4303
	0.2622	0.3003	0.3246	0.3557	0.3789	0.3867	0.4015	0.412	0.414	0.4286

Figure I.21: F1C: e=3.5b & d=4b

	c/b									
a/b	0.3239	0.3482	0.3623	0.3855	0.4029	0.4065	0.4180	0.4259	0.4260	0.4389
	0.3237	0.3479	0.3621	0.3853	0.4027	0.4063	0.4177	0.4257	0.4258	0.4387
	0.3234	0.3476	0.3617	0.3849	0.4023	0.4059	0.4174	0.4254	0.4255	0.4384
	0.3229	0.3471	0.3611	0.3843	0.4017	0.4054	0.4169	0.4248	0.4250	0.4380
	0.3222	0.3463	0.3604	0.3836	0.4010	0.4046	0.4162	0.4242	0.4243	0.4374
	0.3215	0.3455	0.3595	0.3827	0.4001	0.4038	0.4154	0.4234	0.4236	0.4367
	0.3205	0.3444	0.3584	0.3816	0.3990	0.4027	0.4143	0.4224	0.4227	0.4358
	0.3193	0.3431	0.3571	0.3802	0.3977	0.4014	0.4131	0.4212	0.4216	0.4347
	0.3179	0.3416	0.3555	0.3787	0.3962	0.4000	0.4117	0.4199	0.4203	0.4336
	0.3161	0.3397	0.3535	0.3767	0.3942	0.3981	0.4099	0.4182	0.4187	0.4321

Figure I.21: F1C: e=4b & d=0.5b

	c/b									
a/b	0.0060	0.0051	0.0016	0.0017	0.0001	0.0001	0.0030	0.1578	0.3643	0.4286
	0.0065	0.0051	0.0017	0.0017	−0.0001	0.0001	0.0014	0.1578	0.3639	0.4282
	0.0063	0.0050	0.0017	0.0017	0.0001	−0.0005	0.0031	0.1576	0.3633	0.4268
	0.0065	0.0051	0.0017	0.0016	0.0003	−0.0001	0.0031	0.1573	0.3623	0.4267
	0.0065	0.0050	0.0017	0.0017	0.0001	−0.0001	0.0015	0.1568	0.3609	0.4249
	0.0063	0.0051	0.0017	0.0016	0.0002	−0.0001	0.0032	0.1563	0.3594	0.4231
	0.0064	0.0049	0.0017	0.0017	0.0002	−0.0004	0.0017	0.1556	0.3573	0.4207
	0.0064	0.0049	0.0017	0.0017	0.0003	−0.0001	0.0034	0.1549	0.3549	0.4180
	0.0063	0.0050	0.0017	0.0018	0.0001	−0.0004	0.0020	0.1540	0.3521	0.4149
	0.0064	0.0048	0.0017	0.0018	0.0001	−0.0001	0.0037	0.1528	0.3486	0.4108

Figure I.21: F1C: e=4b & d=1b

	c/b									
a/b	0.0028	0.0002	0.0001	0.0001	0.0273	0.1322	0.2564	0.3470	0.3946	0.4268
	0.0032	0.0002	0.0002	0.0001	0.0273	0.1321	0.2561	0.3467	0.3942	0.4264
	0.0032	0.0001	0.0000	0.0003	0.0273	0.1319	0.2557	0.3462	0.3938	0.4258
	0.0029	0.0001	−0.0001	0.0001	0.0274	0.1316	0.2551	0.3454	0.3927	0.4249
	0.0031	0.0000	0.0002	0.0002	0.0274	0.1312	0.2543	0.3443	0.3915	0.4236
	0.0030	0.0001	0.0001	0.0003	0.0274	0.1308	0.2534	0.3431	0.3900	0.4222
	0.0029	0.0001	0.0001	−0.0003	0.0274	0.1302	0.2522	0.3414	0.3881	0.4202
	0.0028	0.0001	0.0001	0.0003	0.0274	0.1296	0.2508	0.3394	0.3870	0.4180
	0.0032	0.0001	0.0003	0.0000	0.0274	0.1288	0.2492	0.3372	0.3832	0.4155
	0.0032	0.0001	0.0002	0.0001	0.0274	0.1278	0.2470	0.3343	0.3799	0.4121

Figure I.21: F1C: e=4b & d=1.5b

	c/b									
a/b	0.0007	0.0002	0.0137	0.0840	0.1800	0.2688	0.3399	0.3829	0.4022	0.4273
	0.0007	0.0002	0.0137	0.0839	0.1798	0.2686	0.3396	0.3826	0.4019	0.4270
	0.0007	0.0004	0.0137	0.0839	0.1796	0.2682	0.3391	0.3821	0.4014	0.4265
	0.0007	0.0002	0.0137	0.0837	0.1793	0.2677	0.3384	0.3813	0.4006	0.4257
	0.0003	0.0002	0.0138	0.0836	0.1789	0.2670	0.3375	0.3802	0.3995	0.4246
	0.0007	0.0003	0.0138	0.0834	0.1784	0.2661	0.3364	0.3790	0.3982	0.4234
	0.0002	0.0002	0.0139	0.0831	0.1777	0.2651	0.3349	0.3773	0.3965	0.4217
	0.0007	0.0004	0.0139	0.0828	0.1770	0.2638	0.3331	0.3754	0.3946	0.4198
	0.0003	0.0002	0.0140	0.0825	0.1761	0.2623	0.3312	0.3732	0.3924	0.4177
	0.0003	0.0002	0.0141	0.0820	0.1750	0.2604	0.3286	0.3703	0.3895	0.4149

Figure I.21: F1C: e=4b & d=2b

	c/b									
a/b	0.0004	0.0277	0.1098	0.2081	0.2884	0.3330	0.3725	0.3979	0.4087	0.4292
	0.0004	0.0277	0.1098	0.2080	0.2882	0.3328	0.3722	0.3977	0.4084	0.4289
	0.0013	0.0277	0.1097	0.2078	0.2879	0.3324	0.3717	0.3972	0.4079	0.4284
	0.0013	0.0278	0.1096	0.2075	0.2874	0.3317	0.3710	0.3965	0.4072	0.4277
	0.0012	0.0279	0.1095	0.2071	0.2867	0.3308	0.3700	0.3955	0.4062	0.4268
	0.0012	0.0279	0.1094	0.2067	0.2859	0.3299	0.3690	0.3944	0.4051	0.4257
	0.0012	0.0280	0.1092	0.2060	0.2848	0.3285	0.3675	0.3928	0.4036	0.4243
	0.0012	0.0282	0.1090	0.2053	0.2835	0.3269	0.3658	0.3911	0.4019	0.4227
	0.0012	0.0283	0.1087	0.2045	0.2821	0.3252	0.3638	0.3891	0.4000	0.4208
	0.0004	0.0285	0.1084	0.2034	0.2802	0.3228	0.3613	0.3865	0.3975	0.4184

Figure I.21: F1C: e=4b & d=2.5b

	c/b									
a/b	0.0484	0.1479	0.2226	0.2902	0.3391	0.3635	0.3896	0.4073	0.4136	0.4313
	0.0485	0.1479	0.2225	0.2900	0.3389	0.3632	0.3894	0.4071	0.4134	0.4310
	0.0486	0.1478	0.2223	0.2896	0.3385	0.3628	0.3889	0.4066	0.4130	0.4306
	0.0488	0.1477	0.2219	0.2891	0.3379	0.3622	0.3883	0.4060	0.4123	0.4300
	0.0491	0.1476	0.2215	0.2885	0.3371	0.3613	0.3874	0.4051	0.4115	0.4292
	0.0494	0.1474	0.2210	0.2877	0.3362	0.3603	0.3864	0.4041	0.4105	0.4283
	0.0499	0.1473	0.2203	0.2867	0.3349	0.3590	0.3850	0.4027	0.4092	0.4270
	0.0504	0.1470	0.2195	0.2855	0.3335	0.3574	0.3834	0.4012	0.4077	0.4256
	0.0510	0.1467	0.2185	0.2841	0.3319	0.3557	0.3816	0.3994	0.4060	0.4240
	0.0518	0.1464	0.2173	0.2823	0.3297	0.3534	0.3793	0.3971	0.4038	0.4219

Figure I.21: F1C: e=4b & d=3b

	c/b									
a/b	0.1810	0.2463	0.2902	0.3354	0.3682	0.3822	0.4012	0.4144	0.4180	0.4336
	0.1809	0.2461	0.2900	0.3352	0.3680	0.3820	0.4010	0.4142	0.4177	0.4334
	0.1808	0.2459	0.2897	0.3349	0.3676	0.3816	0.4006	0.4138	0.4174	0.4330
	0.1807	0.2456	0.2893	0.3343	0.3670	0.3810	0.4000	0.4132	0.4168	0.4325
	0.1805	0.2451	0.2886	0.3336	0.3662	0.3801	0.3992	0.4124	0.4160	0.4318
	0.1802	0.2445	0.2879	0.3327	0.3653	0.3792	0.3983	0.4115	0.4151	0.4309
	0.1799	0.2438	0.2869	0.3316	0.3640	0.3780	0.3970	0.4103	0.4140	0.4298
	0.1795	0.2430	0.2857	0.3302	0.3626	0.3765	0.3956	0.4089	0.4127	0.4286
	0.1790	0.2420	0.2844	0.3287	0.3610	0.3749	0.3940	0.4073	0.4112	0.4272
	0.1784	0.2407	0.2827	0.3267	0.3589	0.3727	0.3918	0.4053	0.4092	0.4253

Figure I.21: F1C: e=4b & d=3.5b

	c/b									
a/b	0.2684	0.308	0.3333	0.3648	0.3881	0.3958	0.4104	0.4205	0.4221	0.4362
	0.2682	0.3078	0.3331	0.3646	0.3879	0.3956	0.4102	0.4203	0.4218	0.436
	0.268	0.3075	0.3327	0.3643	0.3875	0.3952	0.4098	0.4199	0.4215	0.4357
	0.2676	0.3071	0.3322	0.3637	0.387	0.3947	0.4092	0.4194	0.421	0.4352
	0.2671	0.3064	0.3315	0.3629	0.3862	0.3939	0.4085	0.4187	0.4203	0.4345
	0.2665	0.3057	0.3307	0.3621	0.3853	0.393	0.4077	0.4179	0.4195	0.4338
	0.2658	0.3047	0.3296	0.3609	0.3841	0.3919	0.4065	0.4168	0.4185	0.4328
	0.2648	0.3036	0.3283	0.3596	0.3828	0.3905	0.4052	0.4155	0.4173	0.4317
	0.2638	0.3023	0.3269	0.3581	0.3812	0.389	0.4037	0.4141	0.416	0.4304
	0.2624	0.3005	0.325	0.3561	0.3792	0.387	0.4018	0.4123	0.4142	0.4288

Figure I.21: F1C: e=4b & d=4b

	c/b									
a/b	0.3239	0.3482	0.3623	0.3855	0.4029	0.4065	0.418	0.4259	0.426	0.4389
	0.3237	0.348	0.3621	0.3853	0.4027	0.4063	0.4178	0.4257	0.4258	0.4387
	0.3234	0.3476	0.3617	0.3849	0.4023	0.4059	0.4174	0.4254	0.4255	0.4385
	0.3229	0.3471	0.3612	0.3844	0.4018	0.4054	0.4169	0.4249	0.425	0.4379
	0.3223	0.3464	0.3605	0.3837	0.4011	0.4047	0.4162	0.4242	0.4244	0.4374
	0.3216	0.3456	0.3596	0.3828	0.4002	0.4039	0.4155	0.4235	0.4237	0.4367
	0.3206	0.3445	0.3585	0.3817	0.3991	0.4028	0.4144	0.4225	0.4228	0.4359
	0.3194	0.3433	0.3572	0.3804	0.3979	0.4016	0.4132	0.4214	0.4217	0.4348
	0.3181	0.3419	0.3558	0.379	0.3964	0.4002	0.4119	0.4201	0.4205	0.4337
	0.3163	0.34	0.3539	0.3771	0.3945	0.3984	0.4102	0.4184	0.4189	0.4322

Figure I.22: F2C: e=0.5b & d=0.5b

	c/b									
a/b	0.0218	0.0165	0.0166	0.0023	−0.0121	−0.0248	−0.0360	−0.0386	−0.1773	−0.2623
	0.0215	0.0163	0.0164	0.0045	−0.0112	−0.0248	−0.0360	−0.0386	−0.1772	−0.2620
	0.0218	0.0165	0.0166	0.0031	−0.0121	−0.0247	−0.0359	−0.0390	−0.1770	−0.2617
	0.0216	0.0164	0.0165	0.0022	−0.0120	−0.0246	−0.0357	−0.0384	−0.1766	−0.2612
	0.0215	0.0163	0.0164	0.0022	−0.0111	−0.0245	−0.0356	−0.0382	−0.1761	−0.2604
	0.0217	0.0164	0.0165	0.0023	−0.0111	−0.0241	−0.0353	−0.0380	−0.1762	−0.2597
	0.0216	0.0164	0.0165	0.0023	−0.0110	−0.0241	−0.0348	−0.0376	−0.1726	−0.2581
	0.0216	0.0164	0.0165	0.0023	−0.0117	−0.0234	−0.0341	−0.0370	−0.1710	−0.2559
	0.0214	0.0163	0.0165	0.0024	−0.0107	−0.0229	−0.0330	−0.0366	−0.1685	−0.2521
	0.0214	0.0162	0.0164	0.0025	−0.0100	−0.0218	−0.0306	−0.0351	−0.1644	−0.2444

Figure I.22: F2C: e=0.5b & d=1b

	c/b									
a/b	0.0155	0.0120	0.0132	0.0053	0.0069	−0.0117	−0.0942	−0.1783	−0.2376	−0.2704
	0.0153	0.0119	0.0131	0.0053	0.0069	−0.0118	−0.0950	−0.1783	−0.2375	−0.2703
	0.0155	0.0120	0.0132	0.0054	0.0069	−0.0117	−0.0949	−0.1781	−0.2373	−0.2701
	0.0154	0.0120	0.0132	0.0054	0.0068	−0.0118	−0.0950	−0.1779	−0.2370	−0.2698
	0.0153	0.0119	0.0131	0.0053	0.0068	−0.0119	−0.0949	−0.1777	−0.2366	−0.2693
	0.0154	0.0120	0.0132	0.0054	0.0067	−0.0119	−0.0948	−0.1774	−0.2361	−0.2688
	0.0153	0.0120	0.0132	0.0055	0.0066	−0.0121	−0.0947	−0.1768	−0.2353	−0.2678
	0.0153	0.0120	0.0136	0.0055	0.0065	−0.0123	−0.0940	−0.1759	−0.2340	−0.2664
	0.0153	0.0119	0.0113	0.0056	0.0062	−0.0128	−0.0936	−0.1743	−0.2318	−0.2640
	0.0152	0.0119	0.0115	0.0058	0.0054	−0.0137	−0.0927	−0.1709	−0.2273	−0.2595

Figure I.22: F2C: e=0.5b & d=1.5b

	c/b									
a/b	0.0583	0.0654	0.0627	0.0173	−0.0589	−0.1268	−0.1869	−0.2276	−0.2616	−0.2778
	0.0581	0.0652	0.0625	0.0172	−0.0590	−0.1268	−0.1869	−0.2275	−0.2615	−0.2777
	0.0582	0.0653	0.0625	0.0171	−0.0590	−0.1268	−0.1868	−0.2274	−0.2613	−0.2776
	0.0580	0.0650	0.0622	0.0169	−0.0592	−0.1268	−0.1867	−0.2272	−0.2611	−0.2773
	0.0578	0.0647	0.0618	0.0165	−0.0594	−0.1267	−0.1865	−0.2269	−0.2608	−0.2769
	0.0575	0.0645	0.0615	0.0161	−0.0595	−0.1267	−0.1862	−0.2265	−0.2604	−0.2766
	0.0571	0.0639	0.0607	0.0154	−0.0599	−0.1266	−0.1858	−0.2259	−0.2597	−0.2758
	0.0565	0.0631	0.0596	0.0144	−0.0604	−0.1264	−0.1852	−0.2250	−0.2587	−0.2748
	0.0555	0.0617	0.0577	0.0127	−0.0611	−0.1260	−0.1840	−0.2235	−0.2570	−0.2732
	0.0533	0.0586	0.0538	0.0097	−0.0623	−0.1249	−0.1814	−0.2202	−0.2536	−0.2700

Figure I.22: F2C: e=0.5b & d=2b

	c/b									
a/b	0.0954	0.0399	−0.0300	−0.0947	−0.1505	−0.1933	−0.2276	−0.2513	−0.2750	−0.2843
	0.0952	0.0397	−0.0302	−0.0948	−0.1505	−0.1932	−0.2276	−0.2512	−0.2750	−0.2842
	0.0950	0.0395	−0.0303	−0.0948	−0.1505	−0.1932	−0.2275	−0.2511	−0.2748	−0.2841
	0.0946	0.0392	−0.0305	−0.0948	−0.1505	−0.1931	−0.2274	−0.2509	−0.2746	−0.2839
	0.0940	0.0386	−0.0308	−0.0950	−0.1505	−0.1929	−0.2271	−0.2507	−0.2744	−0.2836
	0.0935	0.0381	−0.0311	−0.0950	−0.1504	−0.1927	−0.2269	−0.2504	−0.2741	−0.2833
	0.0923	0.0370	−0.0318	−0.0952	−0.1503	−0.1924	−0.2264	−0.2498	−0.2735	−0.2827
	0.0907	0.0355	−0.0326	−0.0954	−0.1501	−0.1919	−0.2257	−0.2491	−0.2727	−0.2819
	0.0879	0.0332	−0.0338	−0.0956	−0.1496	−0.1910	−0.2245	−0.2478	−0.2714	−0.2807
	0.0823	0.0286	−0.0360	−0.0956	−0.1482	−0.1888	−0.2219	−0.2451	−0.2688	−0.2782

Figure I.22: F2C: e=0.5b & d=2.5b

	c/b									
a/b	−0.0073	−0.0696	−0.1229	−0.1658	−0.2017	−0.2291	−0.2511	−0.2665	−0.2847	−0.2901
	−0.0074	−0.0697	−0.1229	−0.1658	−0.2017	−0.2290	−0.2511	−0.2664	−0.2847	−0.2900
	−0.0075	−0.0698	−0.1230	−0.1658	−0.2016	−0.2289	−0.2510	−0.2663	−0.2846	−0.2899
	−0.0078	−0.0699	−0.1230	−0.1657	−0.2015	−0.2288	−0.2508	−0.2662	−0.2844	−0.2897
	−0.0082	−0.0702	−0.1231	−0.1657	−0.2014	−0.2287	−0.2506	−0.2660	−0.2842	−0.2895
	−0.0086	−0.0703	−0.1231	−0.1656	−0.2013	−0.2285	−0.2504	−0.2657	−0.2839	−0.2892
	−0.0093	−0.0707	−0.1233	−0.1655	−0.2010	−0.2281	−0.2499	−0.2652	−0.2835	−0.2888
	−0.0102	−0.0712	−0.1233	−0.1653	−0.2006	−0.2275	−0.2493	−0.2646	−0.2828	−0.2881
	−0.0113	−0.0718	−0.1233	−0.1648	−0.1997	−0.2265	−0.2482	−0.2635	−0.2817	−0.2871
	−0.0143	−0.0727	−0.1229	−0.1635	−0.1979	−0.2244	−0.2460	−0.2613	−0.2796	−0.2852

Figure I.22: F2C: e=0.5b & d=3b

	c/b									
a/b	−0.1067	−0.1492	−0.1848	−0.2111	−0.2342	−0.2524	−0.2674	−0.2779	−0.2926	−0.2953
	−0.1068	−0.1492	−0.1848	−0.211	−0.2341	−0.2524	−0.2673	−0.2778	−0.2925	−0.2953
	−0.1068	−0.1492	−0.1847	−0.211	−0.2341	−0.2523	−0.2673	−0.2777	−0.2925	−0.2952
	−0.107	−0.1493	−0.1847	−0.2109	−0.234	−0.2522	−0.2671	−0.2776	−0.2923	−0.2951
	−0.1071	−0.1493	−0.1847	−0.2108	−0.2338	−0.252	−0.2669	−0.2774	−0.2921	−0.2949
	−0.1072	−0.1493	−0.1846	−0.2107	−0.2336	−0.2518	−0.2667	−0.2772	−0.2919	−0.2947
	−0.1075	−0.1493	−0.1845	−0.2104	−0.2333	−0.2514	−0.2663	−0.2768	−0.2915	−0.2943
	−0.1077	−0.1493	−0.1842	−0.21	−0.2328	−0.2509	−0.2658	−0.2762	−0.291	−0.2937
	−0.1079	−0.1491	−0.1837	−0.2093	−0.232	−0.25	−0.2648	−0.2753	−0.2901	−0.2929
	−0.108	−0.1483	−0.1823	−0.2076	−0.2301	−0.2481	−0.2629	−0.2735	−0.2885	−0.2913

Figure I.22: F2C: e=0.5b & d=3.5b

	c/b									
a/b	−0.1763	−0.2028	−0.2256	−0.2417	−0.257	−0.2695	−0.28	−0.2872	−0.2994	−0.3004
	−0.1763	−0.2028	−0.2256	−0.2417	−0.2569	−0.2694	−0.2799	−0.2871	−0.2994	−0.3003
	−0.1763	−0.2027	−0.2255	−0.2417	−0.2569	−0.2694	−0.2798	−0.2871	−0.2993	−0.3002
	−0.1763	−0.2027	−0.2255	−0.2416	−0.2568	−0.2693	−0.2797	−0.287	−0.2992	−0.3001
	−0.1763	−0.2027	−0.2253	−0.2414	−0.2566	−0.2691	−0.2796	−0.2868	−0.299	−0.2999
	−0.1763	−0.2026	−0.2252	−0.2413	−0.2564	−0.2689	−0.2794	−0.2866	−0.2989	−0.2998
	−0.1762	−0.2024	−0.225	−0.241	−0.2561	−0.2686	−0.279	−0.2862	−0.2985	−0.2994
	−0.1761	−0.2021	−0.2246	−0.2405	−0.2556	−0.2681	−0.2785	−0.2857	−0.298	−0.299
	−0.1756	−0.2015	−0.2238	−0.2397	−0.2548	−0.2672	−0.2777	−0.285	−0.2973	−0.2983
	−0.1744	−0.2	−0.2222	−0.238	−0.253	−0.2655	−0.2761	−0.2834	−0.2958	−0.2969

Figure I.22: F2C: e=0.5b & d=4b

	c/b									
a/b	−0.2212	−0.2381	−0.2532	−0.2633	−0.2736	−0.2824	−0.29	−0.295	−0.3054	−0.305
	−0.2212	−0.238	−0.2532	−0.2632	−0.2736	−0.2824	−0.2899	−0.2949	−0.3054	−0.305
	−0.2211	−0.238	−0.2531	−0.2632	−0.2735	−0.2823	−0.2899	−0.2949	−0.3053	−0.3049
	−0.2211	−0.2379	−0.253	−0.2631	−0.2734	−0.2822	−0.2898	−0.2947	−0.3052	−0.3048
	−0.221	−0.2378	−0.2529	−0.2629	−0.2732	−0.2821	−0.2896	−0.2946	−0.3051	−0.3046
	−0.2209	−0.2377	−0.2527	−0.2628	−0.2731	−0.2819	−0.2894	−0.2944	−0.3049	−0.3045
	−0.2207	−0.2374	−0.2524	−0.2624	−0.2728	−0.2816	−0.2891	−0.2941	−0.3046	−0.3042
	−0.2203	−0.237	−0.252	−0.262	−0.2723	−0.2811	−0.2887	−0.2937	−0.3042	−0.3038
	−0.2196	−0.2363	−0.2512	−0.2612	−0.2715	−0.2804	−0.2879	−0.293	−0.3035	−0.3032
	−0.218	−0.2346	−0.2496	−0.2596	−0.27	−0.2789	−0.2865	−0.2917	−0.3023	−0.302

Figure I.22: F2C: e=1b & d=0.5b

	c/b									
	0.0219	0.0166	0.0166	0.0023	−0.0112	−0.0248	−0.0360	−0.0390	−0.1772	−0.2621
	0.0218	0.0165	0.0166	0.0022	−0.0121	−0.0247	−0.0359	−0.0390	−0.1770	−0.2617
	0.0215	0.0163	0.0164	0.0022	−0.0111	−0.0247	−0.0358	−0.0384	−0.1766	−0.2611
	0.0214	0.0162	0.0163	0.0022	−0.0112	−0.0245	−0.0356	−0.0382	−0.1760	−0.2602
a/b	0.0215	0.0163	0.0164	0.0022	−0.0109	−0.0243	−0.0352	−0.0378	−0.1751	−0.2592
	0.0216	0.0164	0.0165	0.0023	−0.0119	−0.0240	−0.0347	−0.0374	−0.1740	−0.2574
	0.0216	0.0164	0.0165	0.0023	−0.0117	−0.0236	−0.0341	−0.0369	−0.1725	−0.2551
	0.0215	0.0163	0.0165	0.0024	−0.0106	−0.0231	−0.0333	−0.0361	−0.1703	−0.2520
	0.0216	0.0164	0.0165	0.0024	−0.0103	−0.0230	−0.0322	−0.0352	−0.1673	−0.2479
	0.0214	0.0162	0.0164	0.0025	−0.0099	−0.0216	−0.0303	−0.0337	−0.1615	−0.2405

Figure I.22: F2C: e=1b & d=1b

	c/b									
	0.0155	0.0121	0.0132	0.0054	0.0069	−0.0116	−0.0942	−0.1783	−0.2375	−0.2704
	0.0155	0.0120	0.0132	0.0054	0.0069	−0.0117	−0.0949	−0.1781	−0.2373	−0.2701
	0.0153	0.0119	0.0131	0.0053	0.0068	−0.0118	−0.0949	−0.1779	−0.2369	−0.2696
	0.0152	0.0119	0.0131	0.0053	0.0067	−0.0119	−0.0948	−0.1775	−0.2364	−0.2690
a/b	0.0153	0.0119	0.0131	0.0054	0.0067	−0.0119	−0.0946	−0.1769	−0.2356	−0.2681
	0.0154	0.0120	0.0135	0.0055	0.0067	−0.0120	−0.0944	−0.1763	−0.2347	−0.2671
	0.0153	0.0120	0.0136	0.0055	0.0066	−0.0121	−0.0939	−0.1753	−0.2333	−0.2655
	0.0153	0.0120	0.0136	0.0056	0.0064	−0.0123	−0.0931	−0.1739	−0.2314	−0.2634
	0.0153	0.0120	0.0114	0.0057	0.0062	−0.0125	−0.0924	−0.1720	−0.2288	−0.2607
	0.0152	0.0118	0.0115	0.0059	0.0057	−0.0130	−0.0913	−0.1686	−0.2242	−0.2559

Figure I.22: F2C: e=1b & d=1.5b

	c/b									
	0.0583	0.0654	0.0627	0.0174	−0.0589	−0.1267	−0.1869	−0.2275	−0.2615	−0.2778
	0.0582	0.0653	0.0625	0.0172	−0.0590	−0.1267	−0.1868	−0.2273	−0.2613	−0.2775
	0.0579	0.0650	0.0622	0.0169	−0.0591	−0.1267	−0.1866	−0.2271	−0.2610	−0.2772
	0.0577	0.0646	0.0617	0.0165	−0.0593	−0.1266	−0.1863	−0.2267	−0.2605	−0.2767
a/b	0.0574	0.0643	0.0612	0.0160	−0.0595	−0.1265	−0.1859	−0.2261	−0.2599	−0.2760
	0.0570	0.0639	0.0607	0.0155	−0.0597	−0.1263	−0.1854	−0.2254	−0.2591	−0.2753
	0.0565	0.0631	0.0597	0.0146	−0.0601	−0.1260	−0.1846	−0.2244	−0.2580	−0.2741
	0.0557	0.0621	0.0583	0.0135	−0.0605	−0.1255	−0.1836	−0.2230	−0.2564	−0.2725
	0.0548	0.0608	0.0567	0.0121	−0.0609	−0.1248	−0.1821	−0.2210	−0.2543	−0.2704
	0.0530	0.0583	0.0535	0.0097	−0.0616	−0.1235	−0.1794	−0.2177	−0.2507	−0.2669

Figure I.22: F2C: e=1b & d=2b

	c/b									
	0.0954	0.0399	−0.0300	−0.0947	−0.1505	−0.1932	−0.2276	−0.2513	−0.2750	−0.2842
	0.0951	0.0396	−0.0302	−0.0947	−0.1505	−0.1931	−0.2275	−0.2511	−0.2748	−0.2840
	0.0946	0.0392	−0.0305	−0.0948	−0.1504	−0.1930	−0.2273	−0.2509	−0.2746	−0.2838
	0.0939	0.0386	−0.0308	−0.0949	−0.1503	−0.1928	−0.2270	−0.2505	−0.2742	−0.2834
a/b	0.0931	0.0378	−0.0312	−0.0949	−0.1502	−0.1924	−0.2265	−0.2500	−0.2736	−0.2828
	0.0922	0.0370	−0.0316	−0.0950	−0.1500	−0.1920	−0.2260	−0.2494	−0.2730	−0.2822
	0.0907	0.0357	−0.0324	−0.0951	−0.1496	−0.1914	−0.2252	−0.2485	−0.2720	−0.2813
	0.0887	0.0340	−0.0333	−0.0951	−0.1492	−0.1905	−0.2240	−0.2472	−0.2708	−0.2800
	0.0861	0.0319	−0.0343	−0.0950	−0.1483	−0.1893	−0.2225	−0.2455	−0.2691	−0.2784
	0.0815	0.0281	−0.0359	−0.0949	−0.1470	−0.1870	−0.2198	−0.2426	−0.2662	−0.2756

Figure I.22: F2C: e=1b & d=2.5b

	c/b									
	−0.0073	−0.0696	−0.1229	−0.1658	−0.2017	−0.2290	−0.2511	−0.2665	−0.2847	−0.2900
	−0.0075	−0.0697	−0.1229	−0.1657	−0.2016	−0.2289	−0.2509	−0.2663	−0.2845	−0.2899
	−0.0078	−0.0699	−0.1230	−0.1657	−0.2015	−0.2288	−0.2507	−0.2661	−0.2843	−0.2896
	−0.0082	−0.0701	−0.1230	−0.1656	−0.2013	−0.2285	−0.2504	−0.2658	−0.2840	−0.2893
a/b	−0.0087	−0.0704	−0.1230	−0.1654	−0.2010	−0.2281	−0.2500	−0.2653	−0.2835	−0.2888
	−0.0092	−0.0706	−0.1230	−0.1652	−0.2007	−0.2277	−0.2495	−0.2648	−0.2830	−0.2883
	−0.0101	−0.0710	−0.1230	−0.1649	−0.2001	−0.2270	−0.2488	−0.2640	−0.2822	−0.2876
	−0.0110	−0.0714	−0.1230	−0.1644	−0.1994	−0.2261	−0.2477	−0.2630	−0.2811	−0.2865
	−0.0119	−0.0718	−0.1227	−0.1637	−0.1982	−0.2248	−0.2463	−0.2615	−0.2797	−0.2852
	−0.0147	−0.0724	−0.1222	−0.1623	−0.1963	−0.2225	−0.2439	−0.2591	−0.2774	−0.2829

Figure I.22: F2C: e=1b & d=3b

	c/b									
	−0.1067	−0.1492	−0.1847	−0.211	−0.2341	−0.2524	−0.2674	−0.2778	−0.2926	−0.2953
	−0.1068	−0.1492	−0.1847	−0.211	−0.234	−0.2523	−0.2672	−0.2777	−0.2924	−0.2952
	−0.1069	−0.1492	−0.1847	−0.2109	−0.2339	−0.2521	−0.2671	−0.2775	−0.2922	−0.295
	−0.107	−0.1492	−0.1846	−0.2107	−0.2337	−0.2519	−0.2668	−0.2772	−0.292	−0.2947
a/b	−0.1072	−0.1492	−0.1844	−0.2104	−0.2334	−0.2515	−0.2664	−0.2768	−0.2916	−0.2943
	−0.1073	−0.1491	−0.1842	−0.2101	−0.233	−0.2511	−0.266	−0.2764	−0.2911	−0.2939
	−0.1075	−0.149	−0.1839	−0.2096	−0.2324	−0.2504	−0.2653	−0.2757	−0.2904	−0.2932
	−0.1077	−0.1488	−0.1834	−0.2089	−0.2316	−0.2495	−0.2643	−0.2748	−0.2895	−0.2924
	−0.1077	−0.1483	−0.1826	−0.2079	−0.2304	−0.2483	−0.2631	−0.2735	−0.2883	−0.2912
	−0.1076	−0.1474	−0.1811	−0.2061	−0.2284	−0.2462	−0.261	−0.2715	−0.2863	−0.2893

Figure I.22: F2C: e=1b & d=3.5b

	c/b									
	−0.1763	−0.2028	−0.2256	−0.2417	−0.2569	−0.2695	−0.2799	−0.2872	−0.2994	−0.3003
	−0.1763	−0.2027	−0.2255	−0.2416	−0.2568	−0.2693	−0.2798	−0.287	−0.2993	−0.3002
	−0.1763	−0.2026	−0.2254	−0.2415	−0.2567	−0.2692	−0.2797	−0.2869	−0.2991	−0.3001
	−0.1762	−0.2025	−0.2252	−0.2413	−0.2565	−0.2689	−0.2794	−0.2866	−0.2989	−0.2998
a/b	−0.1761	−0.2024	−0.225	−0.241	−0.2561	−0.2686	−0.2791	−0.2863	−0.2985	−0.2995
	−0.176	−0.2021	−0.2247	−0.2407	−0.2558	−0.2682	−0.2787	−0.2859	−0.2982	−0.2991
	−0.1758	−0.2017	−0.2242	−0.2401	−0.2552	−0.2676	−0.278	−0.2853	−0.2976	−0.2985
	−0.1754	−0.2012	−0.2235	−0.2393	−0.2544	−0.2668	−0.2772	−0.2845	−0.2968	−0.2978
	−0.1747	−0.2003	−0.2225	−0.2382	−0.2532	−0.2656	−0.2761	−0.2834	−0.2957	−0.2968
	−0.1734	−0.1987	−0.2207	−0.2364	−0.2513	−0.2637	−0.2742	−0.2816	−0.294	−0.2952

Figure I.22: F2C: e=1b & d=4b

	c/b									
	−0.2211	−0.238	−0.2532	−0.2632	−0.2736	−0.2824	−0.2899	−0.2949	−0.3054	−0.305
	−0.2211	−0.238	−0.2531	−0.2631	−0.2735	−0.2823	−0.2898	−0.2948	−0.3053	−0.3049
	−0.221	−0.2379	−0.253	−0.263	−0.2733	−0.2822	−0.2897	−0.2947	−0.3052	−0.3047
	−0.2209	−0.2377	−0.2528	−0.2628	−0.2731	−0.2819	−0.2895	−0.2945	−0.3049	−0.3045
a/b	−0.2207	−0.2374	−0.2525	−0.2625	−0.2728	−0.2816	−0.2891	−0.2941	−0.3046	−0.3042
	−0.2204	−0.2371	−0.2521	−0.2621	−0.2724	−0.2813	−0.2888	−0.2938	−0.3043	−0.3039
	−0.22	−0.2366	−0.2516	−0.2616	−0.2719	−0.2807	−0.2882	−0.2932	−0.3038	−0.3034
	−0.2193	−0.236	−0.2509	−0.2608	−0.2711	−0.2799	−0.2875	−0.2926	−0.3031	−0.3027
	−0.2184	−0.2349	−0.2498	−0.2598	−0.2701	−0.2789	−0.2865	−0.2916	−0.3022	−0.3019
	−0.2167	−0.2331	−0.248	−0.258	−0.2683	−0.2772	−0.2848	−0.29	−0.3007	−0.3005

Figure I.22: F2C: e=1.5b & d=0.5b

	c/b									
a/b	0.0219	0.0166	0.0167	0.0023	−0.0108	−0.0247	−0.0359	−0.0390	−0.1772	−0.2621
	0.0219	0.0166	0.0166	0.0033	−0.0112	−0.0247	−0.0358	−0.0388	−0.1768	−0.2615
	0.0219	0.0166	0.0166	0.0023	−0.0112	−0.0245	−0.0356	−0.0382	−0.1763	−0.2607
	0.0216	0.0164	0.0165	0.0022	−0.0110	−0.0244	−0.0354	−0.0380	−0.1755	−0.2595
	0.0214	0.0162	0.0163	0.0022	−0.0110	−0.0242	−0.0350	−0.0376	−0.1744	−0.2580
	0.0213	0.0162	0.0163	0.0022	−0.0109	−0.0239	−0.0346	−0.0372	−0.1732	−0.2562
	0.0214	0.0162	0.0164	0.0023	−0.0107	−0.0235	−0.0339	−0.0366	−0.1715	−0.2536
	0.0214	0.0162	0.0164	0.0023	−0.0106	−0.0229	−0.0333	−0.0358	−0.1688	−0.2503
	0.0215	0.0163	0.0165	0.0024	−0.0103	−0.0226	−0.0321	−0.0349	−0.1663	−0.2462
	0.0213	0.0162	0.0164	0.0025	−0.0099	−0.0218	−0.0306	−0.0336	−0.1617	−0.2398

Figure I.22: F2C: e=1.5b & d=1b

	c/b									
a/b	0.0155	0.0121	0.0132	0.0054	0.0069	−0.0116	−0.0942	−0.1783	−0.2375	−0.2703
	0.0155	0.0121	0.0132	0.0054	0.0069	−0.0117	−0.0948	−0.1780	−0.2372	−0.2700
	0.0155	0.0121	0.0132	0.0054	0.0069	−0.0117	−0.0948	−0.1776	−0.2366	−0.2694
	0.0153	0.0119	0.0131	0.0054	0.0068	−0.0118	−0.0946	−0.1771	−0.2359	−0.2685
	0.0152	0.0119	0.0134	0.0054	0.0066	−0.0119	−0.0944	−0.1764	−0.2349	−0.2673
	0.0152	0.0118	0.0134	0.0054	0.0066	−0.0120	−0.0941	−0.1756	−0.2338	−0.2661
	0.0152	0.0119	0.0135	0.0055	0.0065	−0.0121	−0.0934	−0.1744	−0.2321	−0.2642
	0.0152	0.0119	0.0135	0.0056	0.0064	−0.0122	−0.0925	−0.1729	−0.2300	−0.2619
	0.0153	0.0119	0.0114	0.0057	0.0062	−0.0123	−0.0917	−0.1709	−0.2273	−0.2590
	0.0152	0.0119	0.0115	0.0058	0.0059	−0.0125	−0.0906	−0.1678	−0.2232	−0.2546

Figure I.22: F2C: e=1.5b & d=1.5b

	c/b									
a/b	0.0583	0.0654	0.0627	0.0174	−0.0589	−0.1267	−0.1869	−0.2275	−0.2615	−0.2777
	0.0582	0.0653	0.0625	0.0172	−0.0589	−0.1267	−0.1867	−0.2272	−0.2612	−0.2774
	0.0580	0.0650	0.0622	0.0169	−0.0590	−0.1265	−0.1864	−0.2268	−0.2608	−0.2770
	0.0576	0.0646	0.0616	0.0164	−0.0592	−0.1264	−0.1860	−0.2263	−0.2601	−0.2763
	0.0572	0.0640	0.0609	0.0158	−0.0595	−0.1262	−0.1854	−0.2255	−0.2593	−0.2754
	0.0567	0.0635	0.0602	0.0152	−0.0597	−0.1259	−0.1848	−0.2247	−0.2583	−0.2744
	0.0561	0.0627	0.0593	0.0144	−0.0599	−0.1255	−0.1839	−0.2234	−0.2569	−0.2730
	0.0554	0.0617	0.0580	0.0133	−0.0602	−0.1249	−0.1826	−0.2218	−0.2551	−0.2712
	0.0546	0.0606	0.0566	0.0122	−0.0605	−0.1240	−0.1810	−0.2198	−0.2529	−0.2689
	0.0532	0.0586	0.0541	0.0103	−0.0609	−0.1228	−0.1785	−0.2166	−0.2495	−0.2655

Figure I.22: F2C: e=1.5b & d=2b

	c/b									
a/b	0.0954	0.0399	−0.0300	−0.0947	−0.1505	−0.1932	−0.2276	−0.2512	−0.2750	−0.2843
	0.0951	0.0396	−0.0302	−0.0947	−0.1504	−0.1931	−0.2274	−0.2510	−0.2747	−0.2840
	0.0946	0.0392	−0.0304	−0.0947	−0.1503	−0.1928	−0.2271	−0.2506	−0.2743	−0.2836
	0.0937	0.0384	−0.0308	−0.0948	−0.1501	−0.1925	−0.2266	−0.2501	−0.2738	−0.2830
	0.0927	0.0375	−0.0313	−0.0948	−0.1499	−0.1920	−0.2260	−0.2494	−0.2731	−0.2823
	0.0916	0.0366	−0.0318	−0.0948	−0.1496	−0.1915	−0.2253	−0.2487	−0.2723	−0.2815
	0.0901	0.0353	−0.0324	−0.0948	−0.1491	−0.1907	−0.2243	−0.2475	−0.2711	−0.2803
	0.0881	0.0337	−0.0332	−0.0947	−0.1485	−0.1897	−0.2230	−0.2461	−0.2696	−0.2788
	0.0858	0.0318	−0.0340	−0.0945	−0.1476	−0.1883	−0.2214	−0.2443	−0.2678	−0.2770
	0.0821	0.0288	−0.0353	−0.0942	−0.1462	−0.1862	−0.2188	−0.2415	−0.2649	−0.2743

Figure I.22: F2C: e=1.5b & d=2.5b

	c/b									
a/b	−0.0073	−0.0696	−0.1229	−0.1657	−0.2016	−0.2290	−0.2511	−0.2665	−0.2847	−0.2900
	−0.0075	−0.0697	−0.1229	−0.1657	−0.2015	−0.2288	−0.2509	−0.2662	−0.2845	−0.2898
	−0.0078	−0.0698	−0.1229	−0.1655	−0.2013	−0.2286	−0.2506	−0.2659	−0.2841	−0.2895
	−0.0083	−0.0701	−0.1229	−0.1654	−0.2010	−0.2282	−0.2501	−0.2655	−0.2837	−0.2890
	−0.0089	−0.0703	−0.1229	−0.1652	−0.2006	−0.2277	−0.2496	−0.2649	−0.2830	−0.2884
	−0.0095	−0.0706	−0.1228	−0.1649	−0.2002	−0.2271	−0.2489	−0.2642	−0.2824	−0.2877
	−0.0102	−0.0709	−0.1227	−0.1644	−0.1995	−0.2263	−0.2480	−0.2632	−0.2814	−0.2867
	−0.0110	−0.0712	−0.1225	−0.1638	−0.1986	−0.2252	−0.2468	−0.2619	−0.2801	−0.2855
	−0.0118	−0.0715	−0.1221	−0.1629	−0.1973	−0.2237	−0.2452	−0.2604	−0.2786	−0.2840
	−0.0142	−0.0719	−0.1215	−0.1615	−0.1954	−0.2215	−0.2429	−0.2580	−0.2762	−0.2817

Figure I.22: F2C: e=1.5b & d=3b

	c/b									
a/b	−0.1067	−0.1492	−0.1847	−0.211	−0.2341	−0.2524	−0.2673	−0.2778	−0.2926	−0.2953
	−0.1068	−0.1491	−0.1847	−0.2109	−0.234	−0.2522	−0.2672	−0.2776	−0.2924	−0.2951
	−0.1068	−0.1491	−0.1845	−0.2107	−0.2337	−0.2519	−0.2669	−0.2774	−0.2921	−0.2948
	−0.107	−0.1491	−0.1844	−0.2104	−0.2334	−0.2516	−0.2665	−0.2769	−0.2917	−0.2944
	−0.1071	−0.149	−0.1841	−0.2101	−0.233	−0.2511	−0.266	−0.2764	−0.2911	−0.2939
	−0.1072	−0.1489	−0.1838	−0.2097	−0.2325	−0.2505	−0.2654	−0.2758	−0.2905	−0.2933
	−0.1073	−0.1486	−0.1834	−0.209	−0.2317	−0.2497	−0.2645	−0.2749	−0.2897	−0.2925
	−0.1074	−0.1483	−0.1827	−0.2082	−0.2307	−0.2486	−0.2634	−0.2738	−0.2886	−0.2914
	−0.1073	−0.1477	−0.1818	−0.207	−0.2295	−0.2473	−0.262	−0.2725	−0.2873	−0.2902
	−0.1071	−0.1468	−0.1804	−0.2053	−0.2275	−0.2452	−0.2599	−0.2704	−0.2852	−0.2882

Figure I.22: F2C: e=1.5b & d=3.5b

	c/b									
a/b	−0.1763	−0.2027	−0.2255	−0.2417	−0.2569	−0.2694	−0.2799	−0.2872	−0.2994	−0.3003
	−0.1762	−0.2027	−0.2254	−0.2416	−0.2568	−0.2693	−0.2798	−0.287	−0.2992	−0.3002
	−0.1762	−0.2025	−0.2252	−0.2414	−0.2565	−0.269	−0.2795	−0.2867	−0.299	−0.2999
	−0.1761	−0.2023	−0.225	−0.2411	−0.2562	−0.2687	−0.2791	−0.2864	−0.2986	−0.2996
	−0.1759	−0.2021	−0.2246	−0.2406	−0.2558	−0.2682	−0.2787	−0.2859	−0.2982	−0.2991
	−0.1757	−0.2017	−0.2242	−0.2402	−0.2553	−0.2677	−0.2781	−0.2854	−0.2976	−0.2986
	−0.1753	−0.2012	−0.2236	−0.2395	−0.2545	−0.2669	−0.2774	−0.2846	−0.2969	−0.2979
	−0.1748	−0.2005	−0.2228	−0.2386	−0.2535	−0.2659	−0.2764	−0.2836	−0.2959	−0.297
	−0.174	−0.1995	−0.2217	−0.2374	−0.2523	−0.2647	−0.2751	−0.2824	−0.2948	−0.2959
	−0.1728	−0.198	−0.2199	−0.2355	−0.2504	−0.2628	−0.2733	−0.2806	−0.293	−0.2942

Figure I.22: F2C: e=1.5b & d=4b

	c/b									
a/b	−0.2211	−0.238	−0.2531	−0.2632	−0.2736	−0.2824	−0.2899	−0.2949	−0.3054	−0.305
	−0.221	−0.2379	−0.253	−0.2631	−0.2734	−0.2823	−0.2898	−0.2948	−0.3053	−0.3048
	−0.2209	−0.2377	−0.2528	−0.2629	−0.2732	−0.282	−0.2895	−0.2945	−0.305	−0.3046
	−0.2207	−0.2375	−0.2525	−0.2625	−0.2729	−0.2817	−0.2892	−0.2942	−0.3047	−0.3043
	−0.2203	−0.2371	−0.2521	−0.2621	−0.2724	−0.2813	−0.2888	−0.2938	−0.3043	−0.3039
	−0.22	−0.2367	−0.2517	−0.2617	−0.2719	−0.2808	−0.2883	−0.2933	−0.3038	−0.3034
	−0.2194	−0.2361	−0.251	−0.2609	−0.2712	−0.2801	−0.2876	−0.2926	−0.3032	−0.3028
	−0.2186	−0.2352	−0.2501	−0.26	−0.2703	−0.2791	−0.2867	−0.2918	−0.3023	−0.302
	−0.2176	−0.2341	−0.249	−0.2589	−0.2692	−0.278	−0.2856	−0.2907	−0.3013	−0.301
	−0.216	−0.2324	−0.2472	−0.2571	−0.2674	−0.2763	−0.2839	−0.2891	−0.2998	−0.2996

Figure I.22: F2C: e=2b & d=0.5b

	c/b									
	0.0219	0.0166	0.0167	0.0023	−0.0104	−0.0247	−0.0359	−0.0390	−0.1772	−0.2621
	0.0219	0.0166	0.0166	0.0023	−0.0112	−0.0247	−0.0358	−0.0388	−0.1768	−0.2615
	0.0219	0.0166	0.0166	0.0026	−0.0112	−0.0245	−0.0358	−0.0382	−0.1762	−0.2606
	0.0218	0.0165	0.0166	0.0023	−0.0120	−0.0243	−0.0354	−0.0379	−0.1753	−0.2595
a/b	0.0217	0.0164	0.0165	0.0023	−0.0119	−0.0241	−0.0350	−0.0375	−0.1741	−0.2576
	0.0215	0.0163	0.0164	0.0023	−0.0108	−0.0238	−0.0345	−0.0371	−0.1728	−0.2557
	0.0213	0.0161	0.0163	0.0022	−0.0106	−0.0235	−0.0339	−0.0365	−0.1711	−0.2530
	0.0212	0.0161	0.0163	0.0023	−0.0105	−0.0230	−0.0333	−0.0358	−0.1689	−0.2498
	0.0212	0.0161	0.0163	0.0023	−0.0104	−0.0224	−0.0323	−0.0350	−0.1662	−0.2460
	0.0212	0.0161	0.0163	0.0024	−0.0098	−0.0221	−0.0310	−0.0338	−0.1622	−0.2404

Figure I.22: F2C: e=2b & d=1b

	c/b									
	0.0155	0.0121	0.0132	0.0054	0.0069	−0.0116	−0.0942	−0.1783	−0.2375	−0.2703
	0.0155	0.0121	0.0132	0.0054	0.0069	−0.0116	−0.0948	−0.1780	−0.2371	−0.2699
	0.0155	0.0121	0.0133	0.0054	0.0069	−0.0117	−0.0947	−0.1775	−0.2365	−0.2693
	0.0155	0.0120	0.0132	0.0054	0.0068	−0.0117	−0.0945	−0.1769	−0.2357	−0.2683
a/b	0.0154	0.0120	0.0132	0.0055	0.0067	−0.0118	−0.0941	−0.1761	−0.2345	−0.2670
	0.0153	0.0119	0.0135	0.0054	0.0066	−0.0119	−0.0939	−0.1752	−0.2333	−0.2656
	0.0152	0.0118	0.0134	0.0055	0.0065	−0.0120	−0.0931	−0.1740	−0.2315	−0.2636
	0.0151	0.0118	0.0134	0.0055	0.0064	−0.0121	−0.0921	−0.1724	−0.2294	−0.2612
	0.0151	0.0118	0.0113	0.0056	0.0062	−0.0121	−0.0914	−0.1705	−0.2268	−0.2584
	0.0151	0.0118	0.0114	0.0057	0.0060	−0.0122	−0.0903	−0.1677	−0.2231	−0.2545

Figure I.22: F2C: e=2b & d=1.5b

	c/b									
	0.0583	0.0655	0.0627	0.0174	−0.0588	−0.1267	−0.1869	−0.2275	−0.2615	−0.2777
	0.0582	0.0653	0.0625	0.0172	−0.0589	−0.1266	−0.1866	−0.2272	−0.2612	−0.2774
	0.0580	0.0651	0.0622	0.0170	−0.0590	−0.1265	−0.1863	−0.2268	−0.2607	−0.2769
	0.0577	0.0646	0.0617	0.0165	−0.0591	−0.1262	−0.1858	−0.2261	−0.2599	−0.2761
a/b	0.0573	0.0641	0.0610	0.0159	−0.0593	−0.1259	−0.1851	−0.2252	−0.2589	−0.2750
	0.0567	0.0635	0.0603	0.0153	−0.0595	−0.1256	−0.1844	−0.2242	−0.2578	−0.2739
	0.0560	0.0626	0.0592	0.0145	−0.0597	−0.1251	−0.1834	−0.2229	−0.2563	−0.2724
	0.0553	0.0617	0.0581	0.0135	−0.0599	−0.1245	−0.1821	−0.2213	−0.2545	−0.2705
	0.0545	0.0606	0.0567	0.0125	−0.0601	−0.1236	−0.1806	−0.2193	−0.2523	−0.2683
	0.0534	0.0590	0.0547	0.0110	−0.0603	−0.1224	−0.1783	−0.2164	−0.2491	−0.2651

Figure I.22: F2C: e=2b & d=2b

	c/b									
	0.0954	0.0399	−0.0300	−0.0947	−0.1505	−0.1932	−0.2276	−0.2512	−0.2750	−0.2842
	0.0951	0.0396	−0.0301	−0.0947	−0.1504	−0.1930	−0.2274	−0.2510	−0.2747	−0.2839
	0.0946	0.0392	−0.0303	−0.0946	−0.1502	−0.1927	−0.2270	−0.2506	−0.2742	−0.2835
	0.0938	0.0385	−0.0307	−0.0946	−0.1500	−0.1923	−0.2264	−0.2499	−0.2736	−0.2828
a/b	0.0928	0.0376	−0.0311	−0.0946	−0.1496	−0.1918	−0.2257	−0.2491	−0.2727	−0.2819
	0.0916	0.0367	−0.0316	−0.0946	−0.1493	−0.1911	−0.2249	−0.2482	−0.2718	−0.2810
	0.0900	0.0354	−0.0322	−0.0945	−0.1488	−0.1903	−0.2238	−0.2470	−0.2705	−0.2797
	0.0882	0.0339	−0.0329	−0.0944	−0.1481	−0.1892	−0.2225	−0.2455	−0.2690	−0.2782
	0.0861	0.0322	−0.0336	−0.0941	−0.1472	−0.1878	−0.2208	−0.2437	−0.2671	−0.2764
	0.0831	0.0298	−0.0346	−0.0938	−0.1459	−0.1858	−0.2184	−0.2411	−0.2645	−0.2737

Figure I.22: F2C: e=2b & d=2.5b

	c/b									
	−0.0073	−0.0696	−0.1229	−0.1657	−0.2016	−0.2290	−0.2511	−0.2664	−0.2847	−0.2900
	−0.0074	−0.0697	−0.1228	−0.1656	−0.2015	−0.2288	−0.2508	−0.2662	−0.2844	−0.2898
	−0.0077	−0.0698	−0.1228	−0.1655	−0.2012	−0.2285	−0.2505	−0.2658	−0.2841	−0.2894
	−0.0081	−0.0699	−0.1227	−0.1652	−0.2008	−0.2280	−0.2500	−0.2653	−0.2835	−0.2888
a/b	−0.0087	−0.0702	−0.1227	−0.1649	−0.2004	−0.2274	−0.2493	−0.2646	−0.2827	−0.2881
	−0.0093	−0.0704	−0.1226	−0.1646	−0.1998	−0.2267	−0.2485	−0.2638	−0.2820	−0.2873
	−0.0101	−0.0707	−0.1224	−0.1640	−0.1990	−0.2258	−0.2475	−0.2627	−0.2808	−0.2862
	−0.0108	−0.0710	−0.1221	−0.1634	−0.1981	−0.2246	−0.2462	−0.2614	−0.2795	−0.2849
	−0.0115	−0.0711	−0.1217	−0.1625	−0.1969	−0.2232	−0.2447	−0.2598	−0.2779	−0.2834
	−0.0135	−0.0714	−0.1211	−0.1612	−0.1951	−0.2211	−0.2424	−0.2575	−0.2757	−0.2811

Figure I.22: F2C: e=2b & d=3b

	c/b									
	−0.1067	−0.1491	−0.1847	−0.211	−0.2341	−0.2524	−0.2673	−0.2778	−0.2925	−0.2953
	−0.1067	−0.1491	−0.1846	−0.2109	−0.2339	−0.2522	−0.2671	−0.2776	−0.2923	−0.2951
	−0.1067	−0.149	−0.1845	−0.2106	−0.2337	−0.2519	−0.2668	−0.2773	−0.292	−0.2948
	−0.1068	−0.1489	−0.1842	−0.2103	−0.2332	−0.2514	−0.2663	−0.2768	−0.2915	−0.2943
a/b	−0.1069	−0.1487	−0.1839	−0.2098	−0.2327	−0.2508	−0.2657	−0.2761	−0.2909	−0.2936
	−0.107	−0.1486	−0.1835	−0.2093	−0.2321	−0.2501	−0.265	−0.2754	−0.2902	−0.2929
	−0.107	−0.1483	−0.183	−0.2086	−0.2313	−0.2492	−0.264	−0.2745	−0.2892	−0.292
	−0.107	−0.1479	−0.1823	−0.2077	−0.2302	−0.2481	−0.2629	−0.2733	−0.288	−0.2909
	−0.1069	−0.1473	−0.1814	−0.2066	−0.2289	−0.2467	−0.2615	−0.2719	−0.2867	−0.2897
	−0.1067	−0.1464	−0.18	−0.2049	−0.2271	−0.2448	−0.2595	−0.2699	−0.2847	−0.2877

Figure I.22: F2C: e=2b & d=3.5b

	c/b									
	−0.1763	−0.2027	−0.2255	−0.2417	−0.2569	−0.2694	−0.2799	−0.2871	−0.2994	−0.3003
	−0.1762	−0.2026	−0.2254	−0.2415	−0.2567	−0.2693	−0.2797	−0.287	−0.2992	−0.3001
	−0.1761	−0.2024	−0.2252	−0.2413	−0.2565	−0.269	−0.2794	−0.2867	−0.2989	−0.2998
	−0.1759	−0.2022	−0.2248	−0.2409	−0.256	−0.2685	−0.279	−0.2862	−0.2985	−0.2994
a/b	−0.1757	−0.2018	−0.2244	−0.2404	−0.2555	−0.268	−0.2784	−0.2856	−0.2979	−0.2988
	−0.1754	−0.2014	−0.2239	−0.2398	−0.2549	−0.2673	−0.2778	−0.285	−0.2973	−0.2982
	−0.175	−0.2008	−0.2232	−0.239	−0.2541	−0.2665	−0.2769	−0.2841	−0.2964	−0.2974
	−0.1744	−0.2001	−0.2223	−0.2381	−0.253	−0.2654	−0.2759	−0.2831	−0.2954	−0.2964
	−0.1736	−0.1991	−0.2212	−0.2369	−0.2518	−0.2641	−0.2746	−0.2819	−0.2942	−0.2953
	−0.1725	−0.1977	−0.2196	−0.2351	−0.25	−0.2623	−0.2728	−0.2801	−0.2925	−0.2936

Figure I.22: F2C: e=2b & d=4b

	c/b									
	−0.2211	−0.238	−0.2531	−0.2632	−0.2736	−0.2824	−0.2899	−0.2949	−0.3054	−0.305
	−0.221	−0.2379	−0.253	−0.263	−0.2734	−0.2822	−0.2897	−0.2948	−0.3052	−0.3048
	−0.2208	−0.2376	−0.2527	−0.2628	−0.2731	−0.282	−0.2895	−0.2945	−0.305	−0.3045
	−0.2205	−0.2373	−0.2524	−0.2624	−0.2727	−0.2815	−0.2891	−0.2941	−0.3046	−0.3042
a/b	−0.2201	−0.2369	−0.2519	−0.2619	−0.2722	−0.281	−0.2885	−0.2936	−0.3041	−0.3037
	−0.2197	−0.2364	−0.2513	−0.2613	−0.2716	−0.2804	−0.288	−0.293	−0.3035	−0.3031
	−0.219	−0.2357	−0.2506	−0.2605	−0.2708	−0.2796	−0.2872	−0.2922	−0.3027	−0.3024
	−0.2182	−0.2348	−0.2496	−0.2596	−0.2698	−0.2787	−0.2862	−0.2913	−0.3018	−0.3015
	−0.2171	−0.2336	−0.2485	−0.2584	−0.2686	−0.2775	−0.2851	−0.2902	−0.3008	−0.3005
	−0.2156	−0.232	−0.2468	−0.2566	−0.2669	−0.2758	−0.2834	−0.2886	−0.2992	−0.299

Figure I.22: F2C: e=2.5b & d=0.5b

	c/b									
a/b	0.0219	0.0166	0.0167	0.0023	−0.0111	−0.0247	−0.0360	−0.0390	−0.1772	−0.2621
	0.0219	0.0166	0.0166	0.0023	−0.0110	−0.0247	−0.0357	−0.0389	−0.1769	−0.2615
	0.0219	0.0166	0.0166	0.0023	−0.0111	−0.0245	−0.0357	−0.0383	−0.1763	−0.2607
	0.0218	0.0166	0.0166	0.0024	−0.0120	−0.0244	−0.0354	−0.0380	−0.1754	−0.2594
	0.0218	0.0165	0.0166	0.0023	−0.0119	−0.0241	−0.0350	−0.0376	−0.1742	−0.2576
	0.0217	0.0164	0.0165	0.0023	−0.0118	−0.0238	−0.0346	−0.0371	−0.1728	−0.2557
	0.0215	0.0163	0.0165	0.0024	−0.0107	−0.0235	−0.0340	−0.0366	−0.1711	−0.2531
	0.0214	0.0162	0.0164	0.0032	−0.0106	−0.0230	−0.0234	−0.0359	−0.1690	−0.2500
	0.0212	0.0161	0.0163	0.0023	−0.0104	−0.0225	−0.0326	−0.0351	−0.1665	−0.2464
	0.0211	0.0160	0.0162	0.0024	−0.0101	−0.0224	−0.0315	−0.0341	−0.1630	−0.2415

Figure I.22: F2C: e=2.5b & d=1b

	c/b									
a/b	0.0155	0.0121	0.0132	0.0054	0.0069	−0.0116	−0.0942	−0.1783	−0.2375	−0.2703
	0.0155	0.0121	0.0132	0.0054	0.0069	−0.0116	−0.0948	−0.1780	−0.2372	−0.2699
	0.0155	0.0121	0.0132	0.0054	0.0069	−0.0116	−0.0946	−0.1775	−0.2366	−0.2693
	0.0155	0.0121	0.0132	0.0054	0.0068	−0.0117	−0.0944	−0.1769	−0.2357	−0.2683
	0.0154	0.0120	0.0132	0.0055	0.0068	−0.0117	−0.0941	−0.1760	−0.2345	−0.2669
	0.0154	0.0120	0.0135	0.0055	0.0067	−0.0117	−0.0937	−0.1751	−0.2332	−0.2654
	0.0153	0.0119	0.0135	0.0055	0.0066	−0.0118	−0.0932	−0.1738	−0.2314	−0.2634
	0.0152	0.0119	0.0135	0.0055	0.0065	−0.0119	−0.0919	−0.1723	−0.2293	−0.2611
	0.0151	0.0118	0.0113	0.0056	0.0063	−0.0119	−0.0912	−0.1705	−0.2269	−0.2584
	0.0150	0.0117	0.0113	0.0056	0.0061	−0.0120	−0.0902	−0.1680	−0.2235	−0.2548

Figure I.22: F2C: e=2.5b & d=1.5b

	c/b									
a/b	0.0583	0.0655	0.0627	0.0174	−0.0588	−0.1267	−0.1869	−0.2275	−0.2615	−0.2777
	0.0582	0.0653	0.0626	0.0172	−0.0589	−0.1266	−0.1866	−0.2272	−0.2612	−0.2774
	0.0581	0.0651	0.0623	0.0170	−0.0589	−0.1264	−0.1863	−0.2267	−0.2606	−0.2769
	0.0578	0.0647	0.0618	0.0166	−0.0590	−0.1262	−0.1857	−0.2260	−0.2599	−0.2760
	0.0574	0.0642	0.0612	0.0161	−0.0591	−0.1258	−0.1850	−0.2251	−0.2588	−0.2749
	0.0568	0.0636	0.0605	0.0156	−0.0592	−0.1254	−0.1843	−0.2241	−0.2577	−0.2737
	0.0562	0.0628	0.0595	0.0148	−0.0594	−0.1248	−0.1832	−0.2227	−0.2561	−0.2721
	0.0555	0.0619	0.0584	0.0139	−0.0595	−0.1242	−0.1819	−0.2211	−0.2543	−0.2702
	0.0547	0.0609	0.0571	0.0130	−0.0597	−0.1234	−0.1804	−0.2191	−0.2522	−0.2681
	0.0537	0.0594	0.0554	0.0117	−0.0598	−0.1222	−0.1783	−0.2165	−0.2492	−0.2651

Figure I.22: F2C: e=2.5b & d=2b

	c/b									
a/b	0.0954	0.0399	−0.0300	−0.0947	−0.1505	−0.1932	−0.2276	−0.2512	−0.2750	−0.2842
	0.0951	0.0397	−0.0301	−0.0946	−0.1504	−0.1930	−0.2273	−0.2510	−0.2747	−0.2839
	0.0947	0.0393	−0.0303	−0.0946	−0.1502	−0.1927	−0.2270	−0.2505	−0.2742	−0.2835
	0.0940	0.0387	−0.0305	−0.0945	−0.1499	−0.1923	−0.2264	−0.2499	−0.2735	−0.2828
	0.0930	0.0379	−0.0309	−0.0944	−0.1495	−0.1916	−0.2256	−0.2490	−0.2726	−0.2818
	0.0919	0.0370	−0.0313	−0.0944	−0.1491	−0.1910	−0.2248	−0.2481	−0.2716	−0.2808
	0.0904	0.0358	−0.0319	−0.0942	−0.1485	−0.1900	−0.2236	−0.2468	−0.2703	−0.2795
	0.0887	0.0344	−0.0325	−0.0941	−0.1478	−0.1889	−0.2222	−0.2453	−0.2687	−0.2779
	0.0867	0.0329	−0.0331	−0.0938	−0.1469	−0.1876	−0.2206	−0.2435	−0.2669	−0.2761
	0.0841	0.0308	−0.0339	−0.0934	−0.1457	−0.1858	−0.2184	−0.2411	−0.2644	−0.2736

Figure I.22: F2C: e=2.5b & d=2.5b

	c/b									
a/b	−0.0072	−0.0696	−0.1229	−0.1657	−0.2016	−0.2290	−0.2511	−0.2664	−0.2847	−0.2900
	−0.0074	−0.0696	−0.1228	−0.1656	−0.2015	−0.2288	−0.2508	−0.2662	−0.2844	−0.2898
	−0.0076	−0.0697	−0.1227	−0.1654	−0.2012	−0.2285	−0.2505	−0.2658	−0.2840	−0.2894
	−0.0080	−0.0698	−0.1226	−0.1651	−0.2008	−0.2280	−0.2499	−0.2652	−0.2834	−0.2888
	−0.0085	−0.0700	−0.1225	−0.1648	−0.2002	−0.2273	−0.2492	−0.2644	−0.2826	−0.2880
	−0.0091	−0.0701	−0.1223	−0.1644	−0.1996	−0.2266	−0.2483	−0.2636	−0.2818	−0.2871
	−0.0098	−0.0703	−0.1221	−0.1638	−0.1988	−0.2256	−0.2472	−0.2624	−0.2806	−0.2859
	−0.0105	−0.0706	−0.1218	−0.1631	−0.1978	−0.2244	−0.2460	−0.2611	−0.2792	−0.2846
	−0.0111	−0.0707	−0.1214	−0.1622	−0.1966	−0.2230	−0.2444	−0.2595	−0.2777	−0.2831
	−0.0128	−0.0709	−0.1208	−0.1610	−0.1950	−0.2210	−0.2423	−0.2573	−0.2755	−0.2809

Figure I.22: F2C: e=2.5b & d=3b

	c/b									
a/b	−0.1067	−0.1491	−0.1847	−0.211	−0.2341	−0.2524	−0.2673	−0.2778	−0.2925	−0.2953
	−0.1067	−0.1491	−0.1846	−0.2108	−0.2339	−0.2522	−0.2671	−0.2776	−0.2923	−0.2951
	−0.1067	−0.149	−0.1844	−0.2106	−0.2336	−0.2518	−0.2668	−0.2773	−0.292	−0.2947
	−0.1067	−0.1488	−0.1841	−0.2102	−0.2332	−0.2513	−0.2663	−0.2767	−0.2914	−0.2942
	−0.1067	−0.1486	−0.1837	−0.2097	−0.2326	−0.2507	−0.2656	−0.276	−0.2907	−0.2935
	−0.1067	−0.1483	−0.1833	−0.2091	−0.2319	−0.25	−0.2648	−0.2753	−0.29	−0.2928
	−0.1067	−0.148	−0.1827	−0.2084	−0.231	−0.249	−0.2638	−0.2742	−0.2889	−0.2918
	−0.1067	−0.1475	−0.182	−0.2074	−0.23	−0.2478	−0.2626	−0.273	−0.2877	−0.2906
	−0.1065	−0.147	−0.1811	−0.2063	−0.2287	−0.2465	−0.2612	−0.2716	−0.2864	−0.2893
	−0.1063	−0.1462	−0.1799	−0.2048	−0.2269	−0.2446	−0.2593	−0.2697	−0.2845	−0.2874

Figure I.22: F2C: e=2.5b & d=3.5b

	c/b									
a/b	−0.1763	−0.2027	−0.2255	−0.2417	−0.2569	−0.2694	−0.2799	−0.2871	−0.2994	−0.3003
	−0.1762	−0.2026	−0.2254	−0.2415	−0.2567	−0.2692	−0.2797	−0.2869	−0.2992	−0.3001
	−0.176	−0.2024	−0.2251	−0.2412	−0.2564	−0.2689	−0.2794	−0.2866	−0.2989	−0.2998
	−0.1758	−0.2021	−0.2248	−0.2408	−0.256	−0.2685	−0.2789	−0.2861	−0.2984	−0.2993
	−0.1755	−0.2017	−0.2243	−0.2403	−0.2554	−0.2678	−0.2783	−0.2855	−0.2978	−0.2987
	−0.1752	−0.2012	−0.2237	−0.2396	−0.2547	−0.2672	−0.2776	−0.2848	−0.2971	−0.2981
	−0.1747	−0.2006	−0.2229	−0.2388	−0.2538	−0.2662	−0.2767	−0.2839	−0.2962	−0.2972
	−0.1741	−0.1998	−0.222	−0.2378	−0.2528	−0.2651	−0.2756	−0.2828	−0.2951	−0.2962
	−0.1733	−0.1988	−0.2209	−0.2366	−0.2515	−0.2639	−0.2743	−0.2816	−0.2939	−0.295
	−0.1723	−0.1975	−0.2194	−0.2349	−0.2498	−0.2621	−0.2726	−0.2798	−0.2922	−0.2934

Figure I.22: F2C: e=2.5b & d=4b

	c/b									
a/b	−0.2211	−0.238	−0.2531	−0.2632	−0.2736	−0.2824	−0.2899	−0.2949	−0.3054	−0.305
	−0.221	−0.2379	−0.253	−0.263	−0.2734	−0.2822	−0.2897	−0.2947	−0.3052	−0.3048
	−0.2207	−0.2376	−0.2527	−0.2627	−0.2731	−0.2819	−0.2894	−0.2945	−0.3049	−0.3045
	−0.2204	−0.2372	−0.2523	−0.2623	−0.2726	−0.2815	−0.289	−0.294	−0.3045	−0.3041
	−0.22	−0.2367	−0.2518	−0.2618	−0.2721	−0.2809	−0.2884	−0.2934	−0.3039	−0.3035
	−0.2195	−0.2362	−0.2512	−0.2611	−0.2714	−0.2803	−0.2878	−0.2928	−0.3033	−0.303
	−0.2188	−0.2354	−0.2503	−0.2603	−0.2706	−0.2794	−0.2869	−0.292	−0.3025	−0.3022
	−0.2179	−0.2345	−0.2494	−0.2593	−0.2696	−0.2784	−0.2859	−0.291	−0.3016	−0.3012
	−0.2169	−0.2334	−0.2482	−0.2581	−0.2684	−0.2772	−0.2848	−0.2899	−0.3005	−0.3002
	−0.2154	−0.2318	−0.2466	−0.2565	−0.2667	−0.2756	−0.2832	−0.2883	−0.299	−0.2988

Figure I.22: F2C: e=3b & d=0.5b

	c/b									
	0.0219	0.0166	0.0167	0.0023	−0.0112	−0.0248	−0.0358	−0.0390	−0.1772	−0.2621
	0.0219	0.0166	0.0166	0.0023	−0.0118	−0.0247	−0.0359	−0.0389	−0.1769	−0.2616
	0.0219	0.0166	0.0167	0.0023	−0.0112	−0.0246	−0.0357	−0.0387	−0.1763	−0.2608
	0.0219	0.0166	0.0166	0.0023	−0.0119	−0.0244	−0.0355	−0.0380	−0.1755	−0.2596
a/b	0.0218	0.0165	0.0166	0.0023	−0.0128	−0.0232	−0.0351	−0.0377	−0.1744	−0.2579
	0.0217	0.0165	0.0166	0.0024	−0.0118	−0.0239	−0.0347	−0.0372	−0.1731	−0.2561
	0.0216	0.0164	0.0165	0.0024	−0.0117	−0.0235	−0.0341	−0.0367	−0.1714	−0.2536
	0.0215	0.0163	0.0165	0.0023	−0.0106	−0.0231	−0.0335	−0.0361	−0.1694	−0.2506
	0.0214	0.0162	0.0164	0.0024	−0.0105	−0.0227	−0.0329	−0.0354	−0.1671	−0.2473
	0.0213	0.0161	0.0163	0.0024	−0.0102	−0.0224	−0.0319	−0.0344	−0.1640	−0.2428

Figure I.22: F2C: e=3b & d=1b

	c/b									
	0.0155	0.0121	0.0132	0.0054	0.0069	−0.0116	−0.0942	−0.1783	−0.2375	−0.2704
	0.0155	0.0121	0.0132	0.0054	0.0069	−0.0116	−0.0948	−0.1780	−0.2372	−0.2700
	0.0155	0.0121	0.0132	0.0054	0.0069	−0.0116	−0.0946	−0.1776	−0.2366	−0.2693
	0.0155	0.0121	0.0132	0.0054	0.0068	−0.0116	−0.0944	−0.1769	−0.2358	−0.2684
a/b	0.0155	0.0120	0.0132	0.0055	0.0068	−0.0116	−0.0941	−0.1761	−0.2346	−0.2671
	0.0154	0.0120	0.0132	0.0055	0.0067	−0.0117	−0.0936	−0.1751	−0.2333	−0.2656
	0.0154	0.0120	0.0136	0.0055	0.0066	−0.0117	−0.0931	−0.1739	−0.2316	−0.2636
	0.0153	0.0119	0.0135	0.0056	0.0065	−0.0117	−0.0922	−0.1724	−0.2295	−0.2614
	0.0152	0.0119	0.0113	0.0056	0.0064	−0.0118	−0.0911	−0.1707	−0.2272	−0.2588
	0.0151	0.0118	0.0113	0.0056	0.0062	−0.0118	−0.0902	−0.1684	−0.2241	−0.2564

Figure I.22: F2C: e=3b & d=1.5b

	c/b									
	0.0583	0.0655	0.0628	0.0174	−0.0588	−0.1267	−0.1869	−0.2275	−0.2615	−0.2777
	0.0582	0.0653	0.0626	0.0173	−0.0588	−0.1266	−0.1866	−0.2272	−0.2612	−0.2774
	0.0581	0.0651	0.0623	0.0171	−0.0589	−0.1264	−0.1863	−0.2268	−0.2607	−0.2769
	0.0578	0.0648	0.0619	0.0168	−0.0589	−0.1261	−0.1858	−0.2261	−0.2599	−0.2761
a/b	0.0575	0.0643	0.0614	0.0163	−0.0589	−0.1257	−0.1851	−0.2252	−0.2589	−0.2750
	0.0569	0.0638	0.0607	0.0159	−0.0590	−0.1253	−0.1843	−0.2241	−0.2577	−0.2738
	0.0564	0.0631	0.0599	0.0152	−0.0591	−0.1247	−0.1832	−0.2228	−0.2562	−0.2722
	0.0557	0.0622	0.0589	0.0144	−0.0592	−0.1241	−0.1819	−0.2211	−0.2544	−0.2703
	0.0550	0.0613	0.0577	0.0136	−0.0593	−0.1232	−0.1805	−0.2193	−0.2523	−0.2682
	0.0541	0.0600	0.0562	0.0125	−0.0593	−0.1222	−0.1785	−0.2167	−0.2496	−0.2654

Figure I.22: F2C: e=3b & d=2b

	c/b									
	0.0954	0.0399	−0.0300	−0.0947	−0.1505	−0.1932	−0.2276	−0.2512	−0.2750	−0.2842
	0.0952	0.0397	−0.0301	−0.0946	−0.1504	−0.1930	−0.2274	−0.2510	−0.2747	−0.2839
	0.0948	0.0394	−0.0302	−0.0945	−0.1502	−0.1927	−0.2270	−0.2506	−0.2743	−0.2835
	0.0941	0.0389	−0.0304	−0.0945	−0.1499	−0.1923	−0.2264	−0.2499	−0.2736	−0.2828
a/b	0.0933	0.0382	−0.0307	−0.0943	−0.1494	−0.1916	−0.2256	−0.2491	−0.2727	−0.2819
	0.0923	0.0374	−0.0310	−0.0942	−0.1490	−0.1909	−0.2248	−0.2481	−0.2717	−0.2809
	0.0909	0.0363	−0.0315	−0.0940	−0.1484	−0.1900	−0.2236	−0.2468	−0.2703	−0.2795
	0.0893	0.0351	−0.0320	−0.0938	−0.1477	−0.1889	−0.2222	−0.2453	−0.2687	−0.2779
	0.0876	0.0337	−0.0325	−0.0935	−0.1468	−0.1876	−0.2207	−0.2436	−0.2670	−0.2761
	0.0852	0.0319	−0.0332	−0.0931	−0.1457	−0.1859	−0.2186	−0.2413	−0.2646	−0.2738

Figure I.22: F2C: e=3b & d=2.5b

	c/b									
	−0.0072	−0.0696	−0.1229	−0.1657	−0.2016	−0.2290	−0.2511	−0.2665	−0.2847	−0.2900
	−0.0073	−0.0696	−0.1228	−0.1656	−0.2015	−0.2288	−0.2508	−0.2662	−0.2844	−0.2898
	−0.0075	−0.0697	−0.1227	−0.1654	−0.2012	−0.2285	−0.2505	−0.2658	−0.2840	−0.2894
	−0.0079	−0.0697	−0.1226	−0.1651	−0.2008	−0.2280	−0.2499	−0.2652	−0.2834	−0.2888
a/b	−0.0083	−0.0698	−0.1223	−0.1647	−0.2002	−0.2273	−0.2492	−0.2645	−0.2827	−0.2880
	−0.0088	−0.0699	−0.1222	−0.1643	−0.1996	−0.2265	−0.2483	−0.2636	−0.2818	−0.2871
	−0.0094	−0.0700	−0.1219	−0.1636	−0.1987	−0.2255	−0.2472	−0.2624	−0.2806	−0.2859
	−0.0101	−0.0702	−0.1216	−0.1629	−0.1977	−0.2243	−0.2459	−0.2611	−0.2792	−0.2845
	−0.0107	−0.0703	−0.1211	−0.1621	−0.1966	−0.2230	−0.2444	−0.2595	−0.2776	−0.2830
	−0.0113	−0.0704	−0.1206	−0.1609	−0.1950	−0.2211	−0.2424	−0.2575	−0.2756	−0.2810

Figure I.22: F2C: e=3b & d=3b

	c/b									
	−0.1067	−0.1491	−0.1847	−0.211	−0.2341	−0.2524	−0.2673	−0.2778	−0.2925	−0.2953
	−0.1067	−0.1491	−0.1846	−0.2108	−0.2339	−0.2522	−0.2671	−0.2776	−0.2923	−0.2951
	−0.1066	−0.1489	−0.1844	−0.2106	−0.2336	−0.2518	−0.2668	−0.2773	−0.292	−0.2947
	−0.1066	−0.1487	−0.1841	−0.2102	−0.2332	−0.2513	−0.2663	−0.2767	−0.2914	−0.2942
a/b	−0.1066	−0.1485	−0.1837	−0.2097	−0.2326	−0.2507	−0.2656	−0.276	−0.2907	−0.2935
	−0.1065	−0.1482	−0.1832	−0.2091	−0.2319	−0.2499	−0.2648	−0.2752	−0.2899	−0.2927
	−0.1064	−0.1478	−0.1826	−0.2083	−0.231	−0.2489	−0.2638	−0.2742	−0.2889	−0.2917
	−0.1063	−0.1474	−0.1818	−0.2073	−0.2299	−0.2478	−0.2625	−0.2729	−0.2877	−0.2905
	−0.1062	−0.1468	−0.181	−0.2062	−0.2286	−0.2464	−0.2612	−0.2716	−0.2863	−0.2892
	−0.1059	−0.146	−0.1798	−0.2048	−0.227	−0.2447	−0.2593	−0.2697	−0.2845	−0.2874

Figure I.22: F2C: e=3b & d=3.5b

	c/b									
	−0.1763	−0.2027	−0.2255	−0.2417	−0.2569	−0.2694	−0.2799	−0.2871	−0.2994	−0.3003
	−0.1762	−0.2026	−0.2254	−0.2415	−0.2567	−0.2692	−0.2797	−0.287	−0.2992	−0.3001
	−0.176	−0.2024	−0.2251	−0.2412	−0.2564	−0.2689	−0.2794	−0.2866	−0.2989	−0.2998
	−0.1758	−0.2021	−0.2247	−0.2408	−0.256	−0.2685	−0.2789	−0.2861	−0.2984	−0.2993
a/b	−0.1754	−0.2016	−0.2242	−0.2402	−0.2554	−0.2678	−0.2783	−0.2855	−0.2978	−0.2987
	−0.175	−0.2011	−0.2236	−0.2396	−0.2547	−0.2671	−0.2776	−0.2848	−0.2971	−0.298
	−0.1745	−0.2004	−0.2228	−0.2387	−0.2538	−0.2662	−0.2766	−0.2838	−0.2961	−0.2971
	−0.1739	−0.1997	−0.2219	−0.2377	−0.2527	−0.2651	−0.2755	−0.2827	−0.295	−0.2961
	−0.1732	−0.1987	−0.2208	−0.2365	−0.2515	−0.2638	−0.2742	−0.2815	−0.2938	−0.2949
	−0.1722	−0.1974	−0.2194	−0.235	−0.2498	−0.2621	−0.2726	−0.2798	−0.2922	−0.2933

Figure I.22: F2C: e=3b & d=4b

	c/b									
	−0.2211	−0.238	−0.2531	−0.2632	−0.2736	−0.2824	−0.2899	−0.2949	−0.3054	−0.305
	−0.221	−0.2379	−0.253	−0.263	−0.2734	−0.2822	−0.2897	−0.2947	−0.3052	−0.3048
	−0.2207	−0.2376	−0.2527	−0.2627	−0.2731	−0.2819	−0.2894	−0.2945	−0.3049	−0.3045
	−0.2204	−0.2372	−0.2523	−0.2623	−0.2726	−0.2815	−0.289	−0.294	−0.3045	−0.3041
a/b	−0.2199	−0.2367	−0.2517	−0.2617	−0.272	−0.2809	−0.2884	−0.2934	−0.3039	−0.3035
	−0.2194	−0.2361	−0.2511	−0.2611	−0.2714	−0.2802	−0.2877	−0.2928	−0.3033	−0.3029
	−0.2186	−0.2353	−0.2503	−0.2602	−0.2705	−0.2793	−0.2869	−0.2919	−0.3024	−0.3021
	−0.2178	−0.2344	−0.2493	−0.2592	−0.2695	−0.2783	−0.2858	−0.2909	−0.3015	−0.3011
	−0.2168	−0.2333	−0.2481	−0.258	−0.2683	−0.2771	−0.2847	−0.2898	−0.3004	−0.3001
	−0.2154	−0.2318	−0.2466	−0.2565	−0.2667	−0.2756	−0.2832	−0.2883	−0.2989	−0.2987

Figure I.22: F2C: e=3.5b & d=0.5b

	c/b									
	0.0219	0.0166	0.0167	0.0023	−0.0112	−0.0248	−0.0359	−0.0386	−0.1772	−0.2621
	0.0219	0.0166	0.0167	0.0023	−0.0112	−0.0247	−0.0359	−0.0389	−0.1769	−0.2617
	0.0219	0.0166	0.0167	0.0023	−0.0112	−0.0246	−0.0357	−0.0388	−0.1764	−0.2609
	0.0219	0.0166	0.0166	0.0023	−0.0111	−0.0244	−0.0355	−0.0381	−0.1757	−0.2598
a/b	0.0218	0.0166	0.0166	0.0023	−0.0119	−0.0242	−0.0352	−0.0378	−0.1746	−0.2583
	0.0218	0.0165	0.0166	0.0024	−0.0118	−0.0240	−0.0349	−0.0374	−0.1735	−0.2566
	0.0217	0.0165	0.0166	0.0024	−0.0117	−0.0237	−0.0344	−0.0369	−0.1719	−0.2542
	0.0216	0.0164	0.0165	0.0024	−0.0115	−0.0233	−0.0338	−0.0363	−0.1700	−0.2515
	0.0215	0.0163	0.0165	0.0024	−0.0104	−0.0229	−0.0332	−0.0357	−0.1679	−0.2485
	0.0214	0.0162	0.0164	0.0024	−0.0102	−0.0226	−0.0323	−0.0348	−0.1651	−0.2444

Figure I.22: F2C: e=3.5b & d=1b

	c/b									
	0.0155	0.0121	0.0132	0.0054	0.0069	−0.0116	−0.0942	−0.1783	−0.2375	−0.2704
	0.0155	0.0121	0.0132	0.0054	0.0069	−0.0116	−0.0941	−0.1780	−0.2385	−0.2700
	0.0155	0.0121	0.0132	0.0054	0.0069	−0.0116	−0.0946	−0.1776	−0.2368	−0.2694
	0.0155	0.0121	0.0132	0.0054	0.0069	−0.0116	−0.0944	−0.1770	−0.2359	−0.2685
a/b	0.0155	0.0121	0.0132	0.0055	0.0068	−0.0116	−0.0941	−0.1762	−0.2348	−0.2673
	0.0155	0.0120	0.0132	0.0055	0.0067	−0.0116	−0.0937	−0.1753	−0.2336	−0.2659
	0.0154	0.0120	0.0136	0.0055	0.0067	−0.0116	−0.0931	−0.1741	−0.2319	−0.2641
	0.0154	0.0120	0.0136	0.0055	0.0066	−0.0116	−0.0925	−0.1727	−0.2300	−0.2619
	0.0153	0.0119	0.0113	0.0056	0.0065	−0.0116	−0.0914	−0.1711	−0.2278	−0.2595
	0.0152	0.0119	0.0113	0.0056	0.0063	−0.0116	−0.0902	−0.1689	−0.2259	−0.2563

Figure I.22: F2C: e=3.5b & d=1.5b

	c/b									
	0.0583	0.0655	0.0628	0.0174	−0.0588	−0.1267	−0.1869	−0.2275	−0.2615	−0.2778
	0.0583	0.0654	0.0626	0.0173	−0.0588	−0.1266	−0.1867	−0.2273	−0.2612	−0.2775
	0.0581	0.0652	0.0624	0.0171	−0.0588	−0.1264	−0.1863	−0.2268	−0.2607	−0.2770
	0.0579	0.0649	0.0620	0.0169	−0.0588	−0.1261	−0.1858	−0.2262	−0.2600	−0.2762
a/b	0.0576	0.0645	0.0616	0.0165	−0.0588	−0.1258	−0.1851	−0.2253	−0.2590	−0.2752
	0.0571	0.0640	0.0610	0.0161	−0.0589	−0.1253	−0.1844	−0.2243	−0.2579	−0.2740
	0.0566	0.0633	0.0602	0.0155	−0.0589	−0.1247	−0.1833	−0.2230	−0.2564	−0.2725
	0.0560	0.0626	0.0593	0.0149	−0.0589	−0.1241	−0.1821	−0.2214	−0.2547	−0.2707
	0.0553	0.0617	0.0583	0.0141	−0.0589	−0.1233	−0.1807	−0.2197	−0.2528	−0.2687
	0.0546	0.0606	0.0570	0.0132	−0.0590	−0.1222	−0.1789	−0.2174	−0.2502	−0.2660

Figure I.22: F2C: e=3.5b & d=2b

	c/b									
	0.0954	0.0399	−0.0300	−0.0947	−0.1505	−0.1932	−0.2276	−0.2512	−0.2750	−0.2842
	0.0952	0.0398	−0.0301	−0.0946	−0.1504	−0.1930	−0.2274	−0.2510	−0.2747	−0.2840
	0.0949	0.0395	−0.0302	−0.0945	−0.1502	−0.1927	−0.2270	−0.2506	−0.2743	−0.2835
	0.0943	0.0391	−0.0303	−0.0944	−0.1499	−0.1923	−0.2265	−0.2500	−0.2737	−0.2829
a/b	0.0935	0.0385	−0.0305	−0.0943	−0.1495	−0.1917	−0.2257	−0.2492	−0.2728	−0.2820
	0.0927	0.0378	−0.0308	−0.0941	−0.1490	−0.1910	−0.2249	−0.2482	−0.2718	−0.2810
	0.0915	0.0368	−0.0312	−0.0939	−0.1484	−0.1901	−0.2237	−0.2470	−0.2705	−0.2797
	0.0901	0.0357	−0.0316	−0.0936	−0.1477	−0.1890	−0.2224	−0.2455	−0.2690	−0.2781
	0.0885	0.0345	−0.0320	−0.0933	−0.1468	−0.1878	−0.2209	−0.2439	−0.2672	−0.2764
	0.0864	0.0329	−0.0326	−0.0929	−0.1457	−0.1861	−0.2190	−0.2417	−0.2650	−0.2741

Figure I.22: F2C: e=3.5b & d=2.5b

	c/b									
	−0.0072	−0.0696	−0.1229	−0.1657	−0.2016	−0.2290	−0.2511	−0.2665	−0.2847	−0.2900
	−0.0073	−0.0696	−0.1228	−0.1656	−0.2015	−0.2288	−0.2509	−0.2662	−0.2845	−0.2898
	−0.0075	−0.0696	−0.1227	−0.1654	−0.2012	−0.2285	−0.2505	−0.2659	−0.2841	−0.2894
	−0.0077	−0.0697	−0.1225	−0.1651	−0.2008	−0.2280	−0.2500	−0.2653	−0.2835	−0.2888
a/b	−0.0081	−0.0697	−0.1223	−0.1647	−0.2002	−0.2274	−0.2492	−0.2645	−0.2827	−0.2880
	−0.0085	−0.0697	−0.1221	−0.1643	−0.1996	−0.2266	−0.2484	−0.2637	−0.2819	−0.2872
	−0.0090	−0.0698	−0.1218	−0.1636	−0.1988	−0.2256	−0.2473	−0.2625	−0.2807	−0.2860
	−0.0096	−0.0699	−0.1214	−0.1629	−0.1978	−0.2245	−0.2461	−0.2612	−0.2793	−0.2847
	−0.0102	−0.0700	−0.1210	−0.1621	−0.1967	−0.2231	−0.2446	−0.2597	−0.2778	−0.2832
	−0.0109	−0.0700	−0.1204	−0.1610	−0.1952	−0.2214	−0.2427	−0.2577	−0.2758	−0.2812

Figure I.22: F2C: e=3.5b & d=3b

	c/b									
	−0.1067	−0.1491	−0.1847	−0.211	−0.2341	−0.2524	−0.2673	−0.2778	−0.2926	−0.2953
	−0.1067	−0.1491	−0.1846	−0.2109	−0.2339	−0.2522	−0.2671	−0.2776	−0.2923	−0.2951
	−0.1066	−0.1489	−0.1844	−0.2106	−0.2336	−0.2519	−0.2668	−0.2773	−0.292	−0.2948
	−0.1065	−0.1487	−0.1841	−0.2102	−0.2332	−0.2514	−0.2663	−0.2768	−0.2915	−0.2942
a/b	−0.1065	−0.1484	−0.1837	−0.2097	−0.2326	−0.2507	−0.2656	−0.2761	−0.2908	−0.2936
	−0.1064	−0.1481	−0.1832	−0.2091	−0.2319	−0.25	−0.2649	−0.2753	−0.29	−0.2928
	−0.1063	−0.1477	−0.1826	−0.2083	−0.231	−0.249	−0.2638	−0.2743	−0.289	−0.2918
	−0.1061	−0.1472	−0.1818	−0.2074	−0.23	−0.2479	−0.2627	−0.2731	−0.2878	−0.2906
	−0.1059	−0.1467	−0.181	−0.2063	−0.2288	−0.2466	−0.2613	−0.2717	−0.2864	−0.2893
	−0.1056	−0.1459	−0.1798	−0.2049	−0.2272	−0.2449	−0.2596	−0.2699	−0.2847	−0.2857

Figure I.22: F2C: e=3.5b & d=3.5b

	c/b									
	−0.1763	−0.2027	−0.2255	−0.2417	−0.2569	−0.2694	−0.2799	−0.2872	−0.2994	−0.3003
	−0.1762	−0.2026	−0.2254	−0.2415	−0.2567	−0.2693	−0.2797	−0.287	−0.2992	−0.3001
	−0.176	−0.2024	−0.2251	−0.2413	−0.2564	−0.269	−0.2794	−0.2867	−0.2989	−0.2998
	−0.1757	−0.2021	−0.2247	−0.2408	−0.256	−0.2685	−0.279	−0.2862	−0.2984	−0.2994
a/b	−0.1754	−0.2016	−0.2242	−0.2403	−0.2554	−0.2679	−0.2783	−0.2856	−0.2978	−0.2988
	−0.175	−0.2011	−0.2236	−0.2396	−0.2547	−0.2672	−0.2776	−0.2848	−0.2971	−0.2981
	−0.1745	−0.2004	−0.2229	−0.2388	−0.2538	−0.2662	−0.2767	−0.2839	−0.2962	−0.2972
	−0.1738	−0.1996	−0.2219	−0.2378	−0.2528	−0.2651	−0.2756	−0.2828	−0.2951	−0.2961
	−0.1731	−0.1987	−0.2209	−0.2366	−0.2516	−0.2639	−0.2743	−0.2816	−0.2939	−0.295
	−0.1721	−0.1975	−0.2195	−0.2351	−0.25	−0.2623	−0.2727	−0.28	−0.2923	−0.2934

Figure I.22: F2C: e=3.5b & d=4b

	c/b									
	−0.2211	−0.238	−0.2531	−0.2632	−0.2736	−0.2824	−0.2899	−0.2949	−0.3054	−0.305
	−0.221	−0.2379	−0.253	−0.263	−0.2734	−0.2822	−0.2898	−0.2948	−0.3052	−0.3048
	−0.2207	−0.2376	−0.2527	−0.2628	−0.2731	−0.2819	−0.2895	−0.2945	−0.305	−0.3045
	−0.2204	−0.2372	−0.2523	−0.2623	−0.2727	−0.2815	−0.289	−0.294	−0.3045	−0.3041
a/b	−0.2199	−0.2367	−0.2518	−0.2618	−0.2721	−0.2809	−0.2884	−0.2935	−0.304	−0.3036
	−0.2194	−0.2361	−0.2511	−0.2611	−0.2714	−0.2803	−0.2878	−0.2928	−0.3033	−0.3029
	−0.2187	−0.2353	−0.2503	−0.2603	−0.2705	−0.2794	−0.2869	−0.292	−0.3025	−0.3021
	−0.2178	−0.2344	−0.2493	−0.2593	−0.2695	−0.2784	−0.2859	−0.291	−0.3015	−0.3012
	−0.2168	−0.2334	−0.2482	−0.2581	−0.2684	−0.2772	−0.2848	−0.2898	−0.3004	−0.3001
	−0.2155	−0.232	−0.2468	−0.2566	−0.2669	−0.2757	−0.2833	−0.2884	−0.299	−0.2988

Figure I.22: F2C: e=4b & d=0.5b

	c/b									
	0.0219	0.0166	0.0167	0.0023	−0.0112	−0.0248	−0.0360	−0.0390	−0.1772	−0.2621
	0.0219	0.0166	0.0167	0.0023	−0.0113	−0.0247	−0.0359	−0.0385	−0.1770	−0.2617
	0.0219	0.0166	0.0167	0.0023	−0.0111	−0.0246	−0.0358	−0.0384	−0.1765	−0.2618
	0.0219	0.0166	0.0166	0.0023	−0.0100	−0.0245	−0.0356	−0.0381	−0.1758	−0.2597
a/b	0.0218	0.0166	0.0166	0.0042	−0.0120	−0.0243	−0.0353	−0.0379	−0.1749	−0.2587
	0.0218	0.0165	0.0166	0.0024	−0.0118	−0.0241	−0.0350	−0.0375	−0.1738	−0.2571
	0.0218	0.0165	0.0166	0.0024	−0.0117	−0.0238	−0.0346	−0.0371	−0.1724	−0.2550
	0.0217	0.0165	0.0166	0.0024	−0.0116	−0.0234	−0.0338	−0.0366	−0.1707	−0.2525
	0.0216	0.0164	0.0165	0.0020	−0.0105	−0.0231	−0.0335	−0.0360	−0.1688	−0.2497
	0.0215	0.0163	0.0165	0.0024	−0.0104	−0.0231	−0.0328	−0.0352	−0.1662	−0.2460

Figure I.22: F2C: e=4b & d=1b

	c/b									
	0.0155	0.0121	0.0132	0.0054	0.0069	−0.0116	−0.0942	−0.1783	−0.2375	−0.2704
	0.0155	0.0121	0.0132	0.0054	0.0069	−0.0116	−0.0941	−0.1781	−0.2373	−0.2701
	0.0155	0.0121	0.0132	0.0054	0.0069	−0.0116	−0.0947	−0.1777	−0.2367	−0.2695
	0.0155	0.0121	0.0132	0.0054	0.0069	−0.0116	−0.0944	−0.1771	−0.2360	−0.2687
a/b	0.0155	0.0121	0.0132	0.0054	0.0068	−0.0116	−0.0941	−0.1764	−0.2350	−0.2676
	0.0155	0.0121	0.0132	0.0055	0.0068	−0.0116	−0.0938	−0.1756	−0.2339	−0.2663
	0.0154	0.0120	0.0136	0.0055	0.0067	−0.0116	−0.0932	−0.1744	−0.2324	−0.2646
	0.0154	0.0120	0.0136	0.0055	0.0066	−0.0115	−0.0927	−0.1731	−0.2295	−0.2626
	0.0153	0.0120	0.0113	0.0056	0.0066	−0.0115	−0.0916	−0.1716	−0.2286	−0.2603
	0.0153	0.0119	0.0113	0.0056	0.0064	−0.0115	−0.0904	−0.1696	−0.2259	−0.2573

Figure I.22: F2C: e=4b & d=1.5b

	c/b									
	0.0583	0.0655	0.0628	0.0174	−0.0588	−0.1267	−0.1869	−0.2275	−0.2615	−0.2778
	0.0583	0.0654	0.0627	0.0173	−0.0588	−0.1266	−0.1867	−0.2273	−0.2613	−0.2775
	0.0581	0.0652	0.0625	0.0172	−0.0588	−0.1264	−0.1864	−0.2269	−0.2608	−0.2770
	0.0579	0.0649	0.0621	0.0170	−0.0588	−0.1262	−0.1859	−0.2263	−0.2601	−0.2763
a/b	0.0577	0.0646	0.0617	0.0167	−0.0588	−0.1258	−0.1853	−0.2255	−0.2592	−0.2754
	0.0572	0.0642	0.0612	0.0163	−0.0588	−0.1254	−0.1845	−0.2245	−0.2582	−0.2743
	0.0568	0.0636	0.0606	0.0158	−0.0587	−0.1248	−0.1836	−0.2233	−0.2568	−0.2728
	0.0562	0.0629	0.0598	0.0153	−0.0587	−0.1241	−0.1824	−0.2218	−0.2551	−0.2711
	0.0557	0.0622	0.0589	0.0147	−0.0587	−0.1234	−0.1811	−0.2202	−0.2533	−0.2692
	0.0549	0.0612	0.0577	0.0138	−0.0587	−0.1224	−0.1794	−0.2180	−0.2509	−0.2667

Figure I.22: F2C: e=4b & d=2b

	c/b									
	0.0955	0.0399	−0.0300	−0.0947	−0.1505	−0.1932	−0.2276	−0.2513	−0.2750	−0.2842
	0.0953	0.0398	−0.0300	−0.0946	−0.1504	−0.1931	−0.2274	−0.2510	−0.2748	−0.2840
	0.0950	0.0396	−0.0301	−0.0945	−0.1502	−0.1928	−0.2271	−0.2507	−0.2744	−0.2836
	0.0945	0.0392	−0.0302	−0.0944	−0.1499	−0.1924	−0.2265	−0.2501	−0.2737	−0.2830
a/b	0.0938	0.0387	−0.0304	−0.0943	−0.1495	−0.1918	−0.2258	−0.2493	−0.2729	−0.2821
	0.0930	0.0381	−0.0306	−0.0941	−0.1490	−0.1911	−0.2250	−0.2484	−0.2720	−0.2812
	0.0920	0.0373	−0.0309	−0.0938	−0.1484	−0.1902	−0.2240	−0.2472	−0.2708	−0.2799
	0.0907	0.0364	−0.0312	−0.0936	−0.1477	−0.1892	−0.2227	−0.2458	−0.2693	−0.2785
	0.0893	0.0353	−0.0316	−0.0932	−0.1469	−0.1880	−0.2213	−0.2443	−0.2677	−0.2768
	0.0875	0.0339	−0.0320	−0.0928	−0.1459	−0.1865	−0.2195	−0.2423	−0.2656	−0.2747

Figure I.22: F2C: e=4b & d=2.5b

	c/b									
	−0.0072	−0.0696	−0.1229	−0.1657	−0.2016	−0.2290	−0.2511	−0.2665	−0.2847	−0.2900
	−0.0073	−0.0696	−0.1228	−0.1656	−0.2015	−0.2288	−0.2509	−0.2663	−0.2845	−0.2898
	−0.0074	−0.0696	−0.1227	−0.1654	−0.2012	−0.2285	−0.2505	−0.2659	−0.2841	−0.2894
	−0.0076	−0.0696	−0.1225	−0.1651	−0.2008	−0.2281	−0.2500	−0.2654	−0.2836	−0.2889
a/b	−0.0079	−0.0696	−0.1223	−0.1647	−0.2003	−0.2275	−0.2493	−0.2647	−0.2828	−0.2882
	−0.0082	−0.0696	−0.1221	−0.1643	−0.1997	−0.2267	−0.2486	−0.2638	−0.2820	−0.2873
	−0.0087	−0.0696	−0.1217	−0.1637	−0.1989	−0.2258	−0.2475	−0.2627	−0.2809	−0.2862
	−0.0092	−0.0697	−0.1214	−0.1630	−0.1979	−0.2247	−0.2463	−0.2615	−0.2796	−0.2849
	−0.0097	−0.0697	−0.1209	−0.1622	−0.1969	−0.2234	−0.2450	−0.2601	−0.2782	−0.2835
	−0.0104	−0.0697	−0.1203	−0.1611	−0.1955	−0.2218	−0.2432	−0.2582	−0.2763	−0.2816

Figure I.22: F2C: e=4b & d=3b

	c/b									
	−0.1067	−0.1491	−0.1847	−0.211	−0.2341	−0.2524	−0.2674	−0.2778	−0.2926	−0.2953
	−0.1066	−0.1491	−0.1846	−0.2109	−0.234	−0.2522	−0.2672	−0.2776	−0.2924	−0.2951
	−0.1066	−0.1489	−0.1844	−0.2106	−0.2337	−0.2519	−0.2669	−0.2773	−0.292	−0.2948
	−0.1065	−0.1487	−0.1841	−0.2102	−0.2333	−0.2514	−0.2664	−0.2768	−0.2915	−0.2943
a/b	−0.1064	−0.1484	−0.1837	−0.2097	−0.2327	−0.2508	−0.2657	−0.2762	−0.2909	−0.2937
	−0.1063	−0.1481	−0.1832	−0.2092	−0.232	−0.2501	−0.265	−0.2754	−0.2901	−0.2929
	−0.1061	−0.1477	−0.1826	−0.2084	−0.2312	−0.2492	−0.264	−0.2744	−0.2891	−0.2919
	−0.1059	−0.1472	−0.1819	−0.2075	−0.2301	−0.2481	−0.2629	−0.2733	−0.288	−0.2908
	−0.1057	−0.1466	−0.1811	−0.2065	−0.229	−0.2468	−0.2616	−0.272	−0.2867	−0.2895
	−0.1054	−0.1459	−0.18	−0.2051	−0.2275	−0.2452	−0.2599	−0.2703	−0.285	−0.2879

Figure I.22: F2C: e=4b & d=3.5b

	c/b									
	−0.1763	−0.2027	−0.2255	−0.2417	−0.2569	−0.2694	−0.2799	−0.2872	−0.2994	−0.3003
	−0.1762	−0.2026	−0.2254	−0.2415	−0.2568	−0.2693	−0.2798	−0.287	−0.2992	−0.3001
	−0.176	−0.2024	−0.2252	−0.2413	−0.2565	−0.269	−0.2795	−0.2867	−0.2989	−0.2999
	−0.1757	−0.2021	−0.2248	−0.2409	−0.256	−0.2685	−0.279	−0.2862	−0.2985	−0.2994
a/b	−0.1754	−0.2016	−0.2243	−0.2403	−0.2555	−0.2679	−0.2784	−0.2856	−0.2979	−0.2988
	−0.175	−0.2012	−0.2237	−0.2397	−0.2548	−0.2673	−0.2777	−0.2849	−0.2972	−0.2982
	−0.1745	−0.2005	−0.223	−0.2389	−0.2539	−0.2664	−0.2768	−0.284	−0.2963	−0.2973
	−0.1739	−0.1997	−0.2221	−0.2379	−0.2529	−0.2653	−0.2758	−0.283	−0.2953	−0.2963
	−0.1731	−0.1988	−0.2211	−0.2368	−0.2518	−0.2641	−0.2746	−0.2818	−0.2941	−0.2951
	−0.1722	−0.1977	−0.2197	−0.2354	−0.2503	−0.2626	−0.273	−0.2803	−0.2926	−0.2937

Figure I.22: F2C: e=4b & d=4b

	c/b									
	−0.2211	−0.238	−0.2531	−0.2632	−0.2736	−0.2824	−0.2899	−0.2949	−0.3054	−0.305
	−0.221	−0.2379	−0.253	−0.2631	−0.2734	−0.2822	−0.2898	−0.2948	−0.3052	−0.3048
	−0.2208	−0.2376	−0.2527	−0.2628	−0.2731	−0.282	−0.2895	−0.2945	−0.305	−0.3046
	−0.2204	−0.2373	−0.2523	−0.2624	−0.2727	−0.2816	−0.2891	−0.2941	−0.3046	−0.3042
a/b	−0.22	−0.2368	−0.2518	−0.2618	−0.2721	−0.281	−0.2885	−0.2935	−0.304	−0.3036
	−0.2194	−0.2362	−0.2512	−0.2612	−0.2715	−0.2804	−0.2879	−0.2929	−0.3034	−0.303
	−0.2187	−0.2354	−0.2504	−0.2604	−0.2707	−0.2795	−0.287	−0.2921	−0.3026	−0.3022
	−0.2179	−0.2345	−0.2495	−0.2594	−0.2697	−0.2785	−0.2861	−0.2911	−0.3016	−0.3013
	−0.2169	−0.2335	−0.2484	−0.2583	−0.2686	−0.2774	−0.285	−0.29	−0.3006	−0.3003
	−0.2157	−0.2322	−0.247	−0.2569	−0.2671	−0.276	−0.2835	−0.2886	−0.2992	−0.2989

Figure I.23: F1C: e=0.5a & d=0.5a

	c/a									
b/a	0.0030	0.0002	0.0003	0.0001	0.0273	0.1322	0.2566	0.3472	0.3947	0.4269
	0.0029	0.0002	0.0002	0.0003	0.0273	0.1322	0.2566	0.3471	0.3947	0.4269
	0.0031	0.0001	0.0000	−0.0002	0.0273	0.1321	0.2566	0.3472	0.3948	0.4269
	0.0012	0.0002	0.0002	−0.0002	0.0272	0.1319	0.2567	0.3471	0.3950	0.4269
	0.0051	0.0002	0.0001	0.0002	0.0274	0.1320	0.2565	0.3472	0.3958	0.4269
	0.0050	0.0001	0.0000	0.0003	0.0266	0.1314	0.2574	0.3486	0.3963	0.4268
	0.0022	0.0003	0.0002	0.0004	0.0050	0.1044	0.2551	0.3501	0.3977	0.4268
	0.0064	0.0049	0.0017	0.0019	0.0002	0.0001	0.0033	0.1559	0.3492	0.4136

Figure I.23: F1C: e=0.5a & d=1a

	c/a									
b/a	0.0007	0.0003	0.0136	0.0840	0.1800	0.2688	0.3399	0.3830	0.4023	0.4275
	0.0003	0.0002	0.0136	0.0840	0.1800	0.2688	0.3399	0.3830	0.4023	0.4275
	0.0007	0.0004	0.0136	0.0840	0.1800	0.2688	0.3399	0.3830	0.4023	0.4275
	0.0007	0.0003	0.0136	0.0840	0.1800	0.2688	0.3399	0.3830	0.4023	0.4275
	0.0007	0.0003	0.0136	0.0840	0.1800	0.2688	0.3399	0.3830	0.4023	0.4275
	0.0007	0.0003	0.0135	0.0838	0.1799	0.2689	0.3399	0.3830	0.4023	0.4275
	0.0002	0.0004	0.0071	0.0730	0.1733	0.2668	0.3391	0.3826	0.4024	0.4274
	0.0029	0.0002	0.0001	0.0004	0.0292	0.1290	0.2483	0.3369	0.3828	0.4167

Figure I.23: F1C: e=0.5a & d=1.5a

	c/a									
b/a	0.0013	0.0277	0.1098	0.2082	0.2882	0.3331	0.3725	0.3980	0.4086	0.4290
	0.0005	0.0277	0.1098	0.2082	0.2882	0.3330	0.3725	0.3980	0.4086	0.4290
	0.0013	0.0277	0.1098	0.2082	0.2882	0.3330	0.3725	0.3980	0.4086	0.4290
	0.0013	0.0277	0.1098	0.2082	0.2882	0.3331	0.3725	0.3980	0.4087	0.4290
	0.0013	0.0277	0.1098	0.2082	0.2882	0.3331	0.3725	0.3980	0.4086	0.4290
	0.0013	0.0276	0.1097	0.2081	0.2882	0.3330	0.3725	0.3980	0.4086	0.4290
	0.0011	0.0244	0.1047	0.2045	0.2862	0.3319	0.3719	0.3976	0.4084	0.4289
	0.0006	0.0002	0.0154	0.0835	0.1774	0.2632	0.3316	0.3739	0.3937	0.4198

Figure I.23: F1C: e=0.5a & d=2a

	c/a									
b/a	0.04844	0.1479	0.2226	0.2902	0.3392	0.3635	0.3897	0.4074	0.4136	0.4313
	0.04843	0.1479	0.2226	0.2902	0.3392	0.3635	0.3897	0.4074	0.4136	0.4313
	0.0484	0.1479	0.2226	0.2902	0.3392	0.3635	0.3896	0.4074	0.4136	0.4313
	0.04844	0.1479	0.2226	0.2902	0.3392	0.3635	0.3897	0.4074	0.4136	0.4313
	0.04845	0.1479	0.2226	0.2902	0.3392	0.3635	0.3897	0.4074	0.4136	0.4313
	0.0485	0.1479	0.2226	0.2902	0.3392	0.3635	0.3896	0.4073	0.4136	0.4313
	0.04577	0.1448	0.2202	0.2884	0.3382	0.3628	0.3892	0.407	0.4134	0.4311
	0.0011	0.03041	0.1115	0.2066	0.2831	0.326	0.3649	0.3907	0.402	0.4232

Figure I.23: F1C: e=0.5a & d=2.5a

	c/a									
b/a	0.1811	0.2463	0.2902	0.3355	0.3683	0.3822	0.4013	0.4144	0.4179	0.4336
	0.1811	0.2463	0.2902	0.3355	0.3683	0.3822	0.4013	0.4144	0.4179	0.4336
	0.1811	0.2463	0.2902	0.3355	0.3683	0.3822	0.4013	0.4144	0.4179	0.4336
	0.1811	0.2463	0.2902	0.3355	0.3683	0.3822	0.4013	0.4144	0.4179	0.4336
	0.1811	0.2463	0.2902	0.3355	0.3683	0.3822	0.4013	0.4144	0.4179	0.4336
	0.1811	0.2463	0.2902	0.3355	0.3683	0.3822	0.4012	0.4144	0.4179	0.4336
	0.1782	0.2442	0.2887	0.3345	0.3676	0.3817	0.4009	0.4142	0.4177	0.4335
	0.0565	0.1499	0.2202	0.2853	0.333	0.357	0.3833	0.4014	0.4082	0.4264

Figure I.23: F1C: e=0.5a & d=3a

	c/a									
b/a	0.2685	0.3081	0.3333	0.3649	0.3882	0.3958	0.4104	0.4205	0.422	0.4362
	0.2685	0.3081	0.3333	0.3649	0.3882	0.3958	0.4104	0.4205	0.422	0.4362
	0.2685	0.3081	0.3333	0.3649	0.3882	0.3958	0.4104	0.4205	0.422	0.4362
	0.2685	0.3081	0.3333	0.3649	0.3882	0.3958	0.4104	0.4205	0.422	0.4362
	0.2685	0.3081	0.3333	0.3649	0.3882	0.3958	0.4104	0.4205	0.422	0.4362
	0.2685	0.3081	0.3332	0.3649	0.3882	0.3958	0.4104	0.4205	0.422	0.4362
	0.2665	0.3067	0.3322	0.3642	0.3877	0.3954	0.4101	0.4203	0.4218	0.436
	0.1816	0.2437	0.2858	0.33	0.3625	0.3766	0.3959	0.4095	0.4132	0.4295

Figure I.23: F1C: e=0.5a & d=3.5a

	c/a									
b/a	0.324	0.3482	0.3622	0.3856	0.4029	0.4065	0.4179	0.4259	0.4259	0.4389
	0.324	0.3482	0.3622	0.3856	0.4029	0.4065	0.4179	0.4259	0.4259	0.4389
	0.324	0.3482	0.3622	0.3856	0.4029	0.4065	0.4179	0.4259	0.4259	0.4389
	0.324	0.3482	0.3622	0.3856	0.4029	0.4065	0.4179	0.4259	0.4259	0.4389
	0.324	0.3482	0.3622	0.3856	0.4029	0.4065	0.4179	0.4259	0.4259	0.4389
	0.324	0.3482	0.3622	0.3855	0.4029	0.4064	0.4179	0.4259	0.4259	0.4389
	0.3227	0.3472	0.3615	0.385	0.4025	0.4061	0.4177	0.4257	0.4257	0.4387
	0.2653	0.3037	0.3283	0.3597	0.383	0.391	0.4058	0.4163	0.4182	0.4327

Figure I.23: F1C: e=0.5a & d=4a

	c/a									
b/a	0.3602	0.3753	0.3826	0.4007	0.4142	0.4149	0.4243	0.4306	0.4295	0.4415
	0.3602	0.3753	0.3826	0.4007	0.4142	0.4149	0.4243	0.4306	0.4295	0.4415
	0.3601	0.3753	0.3826	0.4007	0.4142	0.4149	0.4243	0.4306	0.4295	0.4415
	0.3602	0.3753	0.3826	0.4007	0.4142	0.4149	0.4243	0.4306	0.4295	0.4415
	0.3601	0.3753	0.3826	0.4007	0.4142	0.4149	0.4243	0.4306	0.4295	0.4415
	0.3601	0.3753	0.3826	0.4006	0.4142	0.4149	0.4243	0.4306	0.4295	0.4415
	0.3592	0.3746	0.382	0.4002	0.4138	0.4147	0.4241	0.4304	0.4294	0.4414
	0.3195	0.3434	0.3574	0.3808	0.3983	0.4022	0.414	0.4223	0.4226	0.4359

Figure I.23: F1C: e=1a & d=0.5a

	c/a									
b/a	0.0007	0.0002	0.0136	0.0840	0.1800	0.2688	0.3399	0.3829	0.4022	0.4275
	0.0007	0.0003	0.0136	0.0840	0.1800	0.2688	0.3399	0.3829	0.4022	0.4275
	0.0003	0.0003	0.0135	0.0839	0.1800	0.2688	0.3399	0.3829	0.4022	0.4275
	0.0003	0.0004	0.0133	0.0836	0.1802	0.2689	0.3398	0.3829	0.4023	0.4257
	0.0007	0.0003	0.0149	0.0859	0.1815	0.2699	0.3396	0.3828	0.4031	0.4274
	0.0008	0.0003	0.0023	0.0733	0.1834	0.2702	0.3392	0.3825	0.4025	0.4273
	0.0035	0.0000	0.0000	0.0002	0.0042	0.1341	0.3074	0.3752	0.4020	0.4263
	0.0064	0.0050	0.0017	0.0018	0.0002	−0.0006	0.0032	0.1545	0.3451	0.4091

Figure I.23: F1C: e=1a & d=1a

	c/a									
b/a	0.0013	0.0277	0.1098	0.2082	0.2885	0.3330	0.3724	0.3980	0.4085	0.4292
	0.0005	0.0277	0.1098	0.2082	0.2885	0.3330	0.3724	0.3980	0.4085	0.4292
	0.0013	0.0276	0.1097	0.2081	0.2885	0.3330	0.3724	0.3980	0.4085	0.4292
	0.0013	0.0277	0.1098	0.2081	0.2885	0.3330	0.3724	0.3980	0.4085	0.4292
	0.0004	0.0278	0.1099	0.2081	0.2885	0.3330	0.3724	0.3980	0.4085	0.4292
	0.0013	0.0227	0.1051	0.2047	0.2873	0.3324	0.3722	0.3978	0.4084	0.4291
	0.0000	0.0001	0.0140	0.0977	0.2200	0.3026	0.3589	0.3914	0.4049	0.4271
	0.0031	0.0002	0.0001	0.0000	0.0290	0.1282	0.2465	0.3339	0.3791	0.4127

Figure I.23: F1C: e=1a & d=1.5a

	c/a									
b/a	0.0485	0.1480	0.2226	0.2902	0.3389	0.3634	0.3896	0.4073	0.4135	0.4311
	0.0485	0.1479	0.2226	0.2902	0.3389	0.3634	0.3896	0.4073	0.4135	0.4311
	0.0484	0.1479	0.2225	0.2902	0.3389	0.3634	0.3896	0.4073	0.4135	0.4311
	0.0485	0.1479	0.2225	0.2902	0.3389	0.3634	0.3896	0.4073	0.4135	0.4311
	0.0480	0.1478	0.2225	0.2902	0.3389	0.3634	0.3896	0.4073	0.4135	0.4311
	0.0381	0.1420	0.2197	0.2888	0.3382	0.3630	0.3894	0.4072	0.4134	0.4310
	0.0002	0.0437	0.1410	0.2412	0.3117	0.3477	0.3809	0.4015	0.4098	0.4287
	0.0006	0.0004	0.0154	0.0831	0.1764	0.2612	0.3288	0.3707	0.3903	0.4164

Figure I.23: F1C: e=1a & d=2a

	c/a									
b/a	0.1812	0.2464	0.2901	0.3355	0.3683	0.3821	0.4012	0.4144	0.4178	0.4336
	0.1812	0.2464	0.2901	0.3355	0.3683	0.3821	0.4012	0.4144	0.4178	0.4336
	0.1811	0.2463	0.2901	0.3355	0.3683	0.3821	0.4012	0.4144	0.4178	0.4336
	0.1811	0.2463	0.2901	0.3355	0.3683	0.3821	0.4012	0.4144	0.4178	0.4336
	0.1810	0.2463	0.2901	0.3355	0.3683	0.3821	0.4012	0.4144	0.4178	0.4336
	0.1761	0.2435	0.2885	0.3346	0.3678	0.3818	0.4010	0.4143	0.4177	0.4335
	0.0848	0.1808	0.2483	0.3092	0.3517	0.3712	0.3940	0.4095	0.4143	0.4311
	0.0003	0.0305	0.1112	0.2054	0.2812	0.3234	0.3620	0.3877	0.3990	0.4203

Figure I.23: F1C: e=1a & d=2.5a

	c/a									
b/a	0.2686	0.3081	0.3332	0.3649	0.3882	0.3957	0.4103	0.4205	0.4219	0.4361
	0.2686	0.3081	0.3332	0.3649	0.3882	0.3957	0.4103	0.4205	0.4219	0.4361
	0.2686	0.3081	0.3331	0.3649	0.3882	0.3957	0.4103	0.4205	0.4219	0.4361
	0.2686	0.3081	0.3331	0.3649	0.3882	0.3957	0.4103	0.4205	0.4219	0.4361
	0.2685	0.3081	0.3331	0.3649	0.3882	0.3957	0.4103	0.4205	0.4219	0.4361
	0.266	0.3065	0.3321	0.3642	0.3878	0.3954	0.4101	0.4203	0.4218	0.436
	0.2102	0.2688	0.3067	0.347	0.3759	0.3871	0.4041	0.416	0.4185	0.4336
	0.05693	0.1494	0.2189	0.2834	0.3306	0.3544	0.3806	0.3987	0.4056	0.4239

Figure I.23: F1C: e=1a & d=3a

	c/a									
b/a	0.3241	0.3483	0.3621	0.3855	0.4029	0.4064	0.4179	0.4258	0.4257	0.4388
	0.3241	0.3482	0.3621	0.3855	0.4029	0.4064	0.4179	0.4258	0.4257	0.4388
	0.3241	0.3482	0.3621	0.3855	0.4029	0.4064	0.4179	0.4258	0.4257	0.4388
	0.3241	0.3482	0.3621	0.3855	0.4029	0.4064	0.4179	0.4258	0.4257	0.4388
	0.3241	0.3482	0.3621	0.3855	0.4029	0.4064	0.4179	0.4258	0.4257	0.4388
	0.3226	0.3472	0.3614	0.385	0.4026	0.4061	0.4177	0.4257	0.4256	0.4387
	0.2884	0.3228	0.3439	0.3724	0.3933	0.3992	0.4125	0.4217	0.4226	0.4363
	0.181	0.2423	0.2839	0.3278	0.3601	0.3741	0.3934	0.4071	0.4112	0.4274

Figure I.23: F1C: e=1a & d=3.5a

	c/a									
b/a	0.3602	0.3753	0.3825	0.4006	0.4142	0.4149	0.4242	0.4305	0.4294	0.4414
	0.3602	0.3753	0.3825	0.4006	0.4142	0.4149	0.4242	0.4305	0.4294	0.4414
	0.3602	0.3753	0.3825	0.4006	0.4142	0.4148	0.4242	0.4305	0.4294	0.4414
	0.3602	0.3753	0.3825	0.4006	0.4142	0.4148	0.4242	0.4305	0.4294	0.4414
	0.3602	0.3753	0.3825	0.4006	0.4142	0.4148	0.4242	0.4305	0.4294	0.4414
	0.3593	0.3746	0.382	0.4003	0.4139	0.4146	0.424	0.4304	0.4293	0.4414
	0.3371	0.3579	0.3693	0.3906	0.4065	0.4089	0.4195	0.4268	0.4264	0.4391
	0.2639	0.3018	0.3262	0.3574	0.3807	0.3887	0.4036	0.4142	0.4162	0.4308

Figure I.23: F1C: e=1a & d=4a

	c/a									
b/a	0.3846	0.3942	0.3972	0.4119	0.4229	0.4217	0.4295	0.4346	0.4326	0.4439
	0.3846	0.3942	0.3972	0.4119	0.4229	0.4217	0.4295	0.4346	0.4326	0.4439
	0.3846	0.3942	0.3972	0.4119	0.4229	0.4217	0.4295	0.4346	0.4326	0.4439
	0.3846	0.3942	0.3972	0.4119	0.4229	0.4217	0.4295	0.4346	0.4326	0.4439
	0.3846	0.3942	0.3972	0.4119	0.4229	0.4217	0.4295	0.4346	0.4326	0.4439
	0.384	0.3937	0.3968	0.4116	0.4227	0.4215	0.4294	0.4345	0.4325	0.4439
	0.3688	0.3818	0.3874	0.4042	0.4167	0.4167	0.4255	0.4314	0.4299	0.4417
	0.3176	0.3413	0.3553	0.3786	0.3962	0.4001	0.412	0.4204	0.4209	0.4342

Figure I.23: F1C: e=1.5a & d=0.5a

	c/a									
	0.0005	0.0276	0.1097	0.2081	0.2885	0.3329	0.3724	0.3980	0.4085	0.4291
	0.0012	0.0272	0.1092	0.2079	0.2883	0.3328	0.3723	0.3979	0.4084	0.4291
	0.0011	0.0274	0.1095	0.2077	0.2880	0.3325	0.3721	0.3978	0.4083	0.4290
b/a	0.0009	0.0284	0.1121	0.2081	0.2880	0.3323	0.3719	0.3976	0.4082	0.4290
	0.0005	0.0001	0.0732	0.1979	0.2866	0.3321	0.3718	0.3976	0.4082	0.4289
	0.0093	−0.0001	0.0011	0.1022	0.2647	0.3275	0.3705	0.3971	0.4079	0.4288
	0.0037	0.0001	0.0000	−0.0001	0.0019	0.1391	0.3200	0.3834	0.4055	0.4266
	0.0062	0.0049	0.0017	0.0018	0.0002	−0.0001	0.0030	0.1536	0.3451	0.4074

Figure I.23: F1C: e=1.5a & d=1a

	c/a									
	0.0486	0.1479	0.2225	0.2902	0.3392	0.3633	0.3895	0.4073	0.4134	0.4312
	0.0490	0.1479	0.2224	0.2901	0.3391	0.3633	0.3895	0.4073	0.4134	0.4312
	0.0506	0.1485	0.2224	0.2900	0.3390	0.3632	0.3894	0.4072	0.4133	0.4311
b/a	0.0462	0.1473	0.2222	0.2899	0.3389	0.3631	0.3893	0.4071	0.4132	0.4311
	0.0157	0.1250	0.2136	0.2865	0.3376	0.3625	0.3890	0.4069	0.4131	0.4310
	0.0002	0.0553	0.1717	0.2686	0.3302	0.3589	0.3872	0.4060	0.4125	0.4307
	0.0001	0.0003	0.0137	0.1015	0.2268	0.3098	0.3647	0.3946	0.4061	0.4270
	0.0032	0.0002	0.0001	0.0000	0.0287	0.1277	0.2457	0.3327	0.3777	0.4109

Figure I.23: F1C: e=1.5a & d=1.5a

	c/a									
	0.1812	0.2463	0.2900	0.3355	0.3680	0.3821	0.4011	0.4144	0.4177	0.4334
	0.1812	0.2463	0.2899	0.3354	0.3680	0.3820	0.4011	0.4143	0.4177	0.4333
	0.1816	0.2464	0.2899	0.3353	0.3679	0.3819	0.4010	0.4143	0.4176	0.4333
b/a	0.1802	0.2458	0.2896	0.3352	0.3678	0.3819	0.4010	0.4142	0.4176	0.4333
	0.1631	0.2374	0.2855	0.3331	0.3667	0.3812	0.4006	0.4140	0.4174	0.4332
	0.1093	0.2066	0.2688	0.3243	0.3619	0.3784	0.3989	0.4129	0.4167	0.4327
	0.0007	0.0441	0.1444	0.2471	0.3176	0.3520	0.3832	0.4031	0.4103	0.4285
	0.0006	0.0003	0.0152	0.0827	0.1757	0.2603	0.3276	0.3692	0.3887	0.4147

Figure I.23: F1C: e=1.5a & d=2a

	c/a									
	0.2686	0.3081	0.3330	0.3649	0.3882	0.3957	0.4102	0.4204	0.4217	0.4361
	0.2685	0.3081	0.3330	0.3648	0.3882	0.3956	0.4102	0.4204	0.4217	0.4360
	0.2686	0.3080	0.3329	0.3648	0.3881	0.3956	0.4102	0.4203	0.4217	0.4360
b/a	0.2679	0.3077	0.3327	0.3646	0.3880	0.3955	0.4101	0.4203	0.4217	0.4360
	0.2600	0.3031	0.3300	0.3630	0.3870	0.3949	0.4097	0.4200	0.4215	0.4359
	0.2323	0.2865	0.3201	0.3569	0.3832	0.3923	0.4080	0.4188	0.4206	0.4352
	0.0851	0.1844	0.2528	0.3135	0.3551	0.3736	0.3954	0.4101	0.4144	0.4308
	0.0011	0.0302	0.1105	0.2046	0.2802	0.3223	0.3607	0.3862	0.3975	0.4188

Figure I.23: F1C: e=1.5a & d=2.5a

	c/a									
	0.3241	0.3483	0.362	0.3855	0.4029	0.4063	0.4178	0.4258	0.4256	0.4387
	0.3241	0.3482	0.362	0.3855	0.4029	0.4063	0.4178	0.4258	0.4256	0.4387
	0.324	0.3481	0.3619	0.3854	0.4028	0.4062	0.4177	0.4257	0.4256	0.4387
b/a	0.3237	0.3479	0.3618	0.3853	0.4028	0.4062	0.4177	0.4257	0.4255	0.4387
	0.3194	0.3451	0.3599	0.3841	0.4019	0.4056	0.4173	0.4254	0.4253	0.4385
	0.3042	0.335	0.3532	0.3795	0.3988	0.4033	0.4156	0.4242	0.4244	0.4378
	0.2139	0.2727	0.3101	0.3496	0.3778	0.3883	0.4048	0.4162	0.4184	0.4333
	0.05631	0.1488	0.2181	0.2824	0.3295	0.3531	0.3792	0.3973	0.4042	0.4225

Figure I.23: F1C: e=1.5a & d=3a

	c/a									
	0.3603	0.3753	0.3824	0.4006	0.4142	0.4148	0.4241	0.4305	0.4292	0.4414
	0.3602	0.3753	0.3823	0.4006	0.4141	0.4147	0.4241	0.4305	0.4292	0.4413
	0.3602	0.3752	0.3823	0.4005	0.4141	0.4147	0.4241	0.4304	0.4292	0.4413
b/a	0.3599	0.375	0.3821	0.4004	0.414	0.4146	0.424	0.4304	0.4292	0.4413
	0.3574	0.3732	0.3808	0.3995	0.4133	0.4141	0.4236	0.4301	0.4289	0.4411
	0.3482	0.3666	0.376	0.396	0.4108	0.4122	0.4222	0.429	0.428	0.4404
	0.2919	0.3257	0.3461	0.374	0.3944	0.3998	0.4127	0.4217	0.4223	0.4359
	0.1803	0.2415	0.2829	0.3267	0.3589	0.3728	0.3921	0.4058	0.4099	0.4261

Figure I.23: F1C: e=1.5a & d=3.5a

	c/a									
	0.3846	0.3942	0.3971	0.4119	0.4229	0.4216	0.4294	0.4346	0.4325	0.4439
	0.3846	0.3942	0.397	0.4119	0.4229	0.4216	0.4294	0.4346	0.4325	0.4438
	0.3845	0.3941	0.397	0.4118	0.4228	0.4215	0.4294	0.4345	0.4324	0.4438
b/a	0.3844	0.394	0.3969	0.4118	0.4228	0.4215	0.4293	0.4345	0.4324	0.4438
	0.3828	0.3928	0.396	0.4111	0.4222	0.4211	0.429	0.4342	0.4322	0.4436
	0.3768	0.3882	0.3925	0.4084	0.4201	0.4194	0.4277	0.4332	0.4314	0.443
	0.3398	0.3599	0.3708	0.3916	0.4071	0.4091	0.4195	0.4267	0.4261	0.4387
	0.263	0.3009	0.3251	0.3562	0.3795	0.3874	0.4024	0.413	0.415	0.4297

Figure I.23: F1C: e=1.5a & d=4a

	c/a									
	0.4017	0.4078	0.408	0.4205	0.4298	0.4271	0.4338	0.4381	0.4354	0.4461
	0.4016	0.4078	0.408	0.4205	0.4297	0.4271	0.4338	0.4381	0.4354	0.4461
	0.4016	0.4077	0.4079	0.4205	0.4297	0.4271	0.4338	0.4381	0.4354	0.4461
b/a	0.4015	0.4076	0.4079	0.4204	0.4296	0.427	0.4338	0.438	0.4353	0.4461
	0.4004	0.4067	0.4072	0.4199	0.4292	0.4267	0.4335	0.4378	0.4351	0.4459
	0.3962	0.4035	0.4045	0.4178	0.4275	0.4253	0.4324	0.4369	0.4344	0.4453
	0.3706	0.3831	0.3883	0.4047	0.417	0.4168	0.4254	0.4311	0.4296	0.4413
	0.3166	0.3402	0.3542	0.3774	0.395	0.399	0.4109	0.4192	0.4198	0.4332

Figure I.23: F1C: e=2a & d=0.5a

	c/a									
b/a	0.0506	0.1485	0.2225	0.2902	0.3392	0.3632	0.3895	0.4072	0.4133	0.4312
	0.0562	0.1503	0.2229	0.2902	0.3391	0.3631	0.3893	0.4071	0.4132	0.4311
	0.0297	0.1457	0.2230	0.2904	0.3392	0.3631	0.3893	0.4071	0.4132	0.4311
	0.0001	0.0646	0.2037	0.2872	0.3385	0.3629	0.3893	0.4071	0.4132	0.4311
	0.0009	0.0000	0.0984	0.2540	0.3317	0.3606	0.3885	0.4068	0.4130	0.4310
	0.0182	0.0004	−0.0003	0.1131	0.2960	0.3514	0.3855	0.4055	0.4124	0.4307
	0.0039	0.0001	0.0001	0.0001	0.0018	0.1408	0.3258	0.3881	0.4081	0.4276
	0.0062	0.0050	0.0017	0.0019	0.0001	−0.0004	0.0028	0.1530	0.3450	0.4072

Figure I.23: F1C: e=2a & d=1a

	c/a									
b/a	0.1817	0.2465	0.2899	0.3355	0.3683	0.3820	0.4010	0.4143	0.4176	0.4335
	0.1832	0.2472	0.2902	0.3356	0.3683	0.3819	0.4010	0.4143	0.4175	0.4334
	0.1776	0.2457	0.2898	0.3355	0.3683	0.3819	0.4010	0.4143	0.4175	0.4334
	0.1309	0.2279	0.2831	0.3329	0.3673	0.3814	0.4008	0.4141	0.4174	0.4334
	0.0256	0.1627	0.2551	0.3209	0.3620	0.3787	0.3994	0.4133	0.4170	0.4331
	0.0000	0.0609	0.1884	0.2903	0.3485	0.3719	0.3959	0.4114	0.4157	0.4324
	0.0001	0.0001	0.0132	0.1028	0.2290	0.3135	0.3679	0.3967	0.4072	0.4274
	0.0031	0.0002	0.0001	0.0001	0.0283	0.1275	0.2455	0.3324	0.3773	0.4101

Figure I.23: F1C: e=2a & d=1.5a

	c/a									
b/a	0.2688	0.3082	0.3330	0.3649	0.3879	0.3956	0.4102	0.4204	0.4216	0.4359
	0.2693	0.3084	0.3331	0.3649	0.3880	0.3956	0.4102	0.4203	0.4216	0.4358
	0.2671	0.3075	0.3327	0.3647	0.3879	0.3955	0.4101	0.4203	0.4216	0.4358
	0.2492	0.2986	0.3281	0.3624	0.3866	0.3948	0.4097	0.4200	0.4214	0.4357
	0.1985	0.2716	0.3135	0.3543	0.3820	0.3920	0.4079	0.4189	0.4207	0.4352
	0.1182	0.2225	0.2855	0.3387	0.3731	0.3864	0.4045	0.4167	0.4191	0.4342
	0.0008	0.0437	0.1450	0.2491	0.3203	0.3543	0.3849	0.4042	0.4107	0.4285
	0.0006	0.0002	0.0150	0.0825	0.1753	0.2599	0.3272	0.3687	0.3881	0.4139

Figure I.23: F1C: e=2a & d=2a

	c/a									
b/a	0.3243	0.3483	0.3619	0.3855	0.4029	0.4062	0.4177	0.4257	0.4255	0.4387
	0.3244	0.3484	0.3620	0.3855	0.4029	0.4062	0.4177	0.4257	0.4255	0.4387
	0.3234	0.3478	0.3616	0.3853	0.4028	0.4061	0.4177	0.4257	0.4255	0.4386
	0.3148	0.3426	0.3585	0.3834	0.4016	0.4053	0.4171	0.4253	0.4252	0.4384
	0.2901	0.3274	0.3489	0.3773	0.3976	0.4026	0.4153	0.4240	0.4243	0.4378
	0.2472	0.3006	0.3320	0.3665	0.3905	0.3978	0.4120	0.4216	0.4226	0.4365
	0.0840	0.1855	0.2548	0.3156	0.3570	0.3749	0.3963	0.4106	0.4146	0.4307
	0.0011	0.0298	0.1100	0.2041	0.2798	0.3218	0.3602	0.3856	0.3968	0.4180

Figure I.23: F1C: e=2a & d=2.5a

	c/a									
b/a	0.3604	0.3753	0.3823	0.4006	0.4142	0.4147	0.424	0.4304	0.4291	0.4413
	0.3604	0.3754	0.3823	0.4006	0.4142	0.4147	0.424	0.4304	0.4291	0.4413
	0.3598	0.375	0.382	0.4004	0.414	0.4146	0.424	0.4304	0.4291	0.4413
	0.3551	0.3718	0.3798	0.3989	0.413	0.4138	0.4234	0.43	0.4287	0.441
	0.3414	0.3624	0.3733	0.3943	0.4097	0.4114	0.4217	0.4287	0.4278	0.4403
	0.317	0.3457	0.3617	0.3862	0.404	0.4073	0.4186	0.4263	0.426	0.4389
	0.2152	0.2744	0.3118	0.3511	0.3789	0.389	0.4052	0.4163	0.4184	0.4331
	0.05543	0.1482	0.2177	0.2819	0.329	0.3526	0.3786	0.3966	0.4035	0.4218

Figure I.23: F1C: e=2a & d=3a

	c/a									
b/a	0.3847	0.3942	0.397	0.4119	0.4229	0.4215	0.4293	0.4345	0.4323	0.4438
	0.3847	0.3942	0.397	0.4119	0.4229	0.4215	0.4293	0.4345	0.4323	0.4438
	0.3844	0.394	0.3968	0.4118	0.4228	0.4214	0.4293	0.4345	0.4323	0.4437
	0.3815	0.3918	0.3952	0.4106	0.4219	0.4208	0.4288	0.4341	0.432	0.4435
	0.373	0.3856	0.3906	0.4071	0.4193	0.4187	0.4272	0.4328	0.431	0.4427
	0.358	0.3745	0.3824	0.401	0.4146	0.4152	0.4244	0.4307	0.4293	0.4414
	0.2936	0.3273	0.3474	0.3749	0.395	0.4002	0.4129	0.4217	0.4222	0.4357
	0.1798	0.241	0.2825	0.3262	0.3583	0.3722	0.3915	0.4051	0.4092	0.4254

Figure I.23: F1C: e=2a & d=3.5a

	c/a									
b/a	0.4017	0.4078	0.4079	0.4205	0.4297	0.427	0.4338	0.438	0.4352	0.446
	0.4017	0.4078	0.4079	0.4205	0.4297	0.427	0.4337	0.438	0.4352	0.446
	0.4015	0.4076	0.4077	0.4204	0.4296	0.427	0.4337	0.438	0.4352	0.446
	0.3996	0.4061	0.4066	0.4195	0.4289	0.4264	0.4332	0.4376	0.4349	0.4458
	0.394	0.4018	0.4032	0.4168	0.4268	0.4247	0.4319	0.4365	0.434	0.4451
	0.384	0.394	0.3971	0.4121	0.4231	0.4217	0.4295	0.4346	0.4324	0.4438
	0.3412	0.3611	0.3716	0.3922	0.4075	0.4093	0.4196	0.4266	0.4259	0.4384
	0.2626	0.3004	0.3246	0.3557	0.3789	0.3868	0.4017	0.4123	0.4144	0.429

Figure I.23: F1C: e=2a & d=4a

	c/a									
b/a	0.414	0.4179	0.4162	0.4272	0.4352	0.4316	0.4375	0.4411	0.4378	0.4481
	0.414	0.4179	0.4162	0.4272	0.4352	0.4316	0.4375	0.4411	0.4378	0.4481
	0.4139	0.4177	0.4161	0.4271	0.4351	0.4315	0.4374	0.441	0.4378	0.4481
	0.4125	0.4166	0.4152	0.4264	0.4345	0.431	0.437	0.4407	0.4375	0.4479
	0.4086	0.4135	0.4126	0.4243	0.4328	0.4296	0.4359	0.4397	0.4367	0.4472
	0.4016	0.4078	0.4081	0.4206	0.4298	0.4271	0.4338	0.438	0.4353	0.446
	0.3716	0.3838	0.3888	0.4051	0.4172	0.4168	0.4253	0.431	0.4294	0.4411
	0.3161	0.3397	0.3536	0.3768	0.3944	0.3983	0.4102	0.4186	0.4191	0.4326

Figure I.23: F1C: e=2.5a & d=0.5a

	c/a									
b/a	0.1816	0.2467	0.2900	0.3356	0.3684	0.3820	0.4010	0.4143	0.4175	0.4335
	0.1624	0.2437	0.2894	0.3355	0.3684	0.3820	0.4011	0.4143	0.4175	0.4334
	0.0490	0.2166	0.2834	0.3341	0.3680	0.3818	0.4010	0.4143	0.4175	0.4334
	0.0001	0.0803	0.2453	0.3249	0.3653	0.3806	0.4005	0.4141	0.4173	0.4334
	0.0006	0.0002	0.1083	0.2782	0.3538	0.3762	0.3987	0.4132	0.4168	0.4331
	0.0180	−0.0002	−0.0002	0.1187	0.3106	0.3645	0.3947	0.4114	0.4159	0.4326
	0.0040	0.0001	0.0000	−0.0001	0.0006	0.1417	0.3295	0.3917	0.4106	0.4289
	0.0064	0.0051	0.0018	0.0018	0.0002	0.0001	0.0026	0.1527	0.3455	0.4076

Figure I.23: F1C: e=2.5a & d=1a

	c/a									
b/a	0.2688	0.3082	0.3329	0.3649	0.3883	0.3956	0.4101	0.4204	0.4216	0.4360
	0.2628	0.3059	0.3320	0.3645	0.3881	0.3955	0.4101	0.4204	0.4215	0.4360
	0.2353	0.2951	0.3273	0.3624	0.3871	0.3949	0.4098	0.4202	0.4214	0.4359
	0.1539	0.2601	0.3120	0.3554	0.3837	0.3929	0.4087	0.4195	0.4210	0.4357
	0.0259	0.1754	0.2732	0.3376	0.3751	0.3882	0.4061	0.4179	0.4200	0.4350
	0.0000	0.0624	0.1952	0.3005	0.3581	0.3795	0.4014	0.4152	0.4183	0.4339
	−0.0001	0.0001	0.0128	0.1035	0.2303	0.3160	0.3704	0.3986	0.4085	0.4281
	0.0029	0.0001	0.0001	0.0002	0.0280	0.1274	0.2456	0.3325	0.3775	0.4101

Figure I.23: F1C: e=2.5a & d=1.5a

	c/a									
b/a	0.3243	0.3483	0.3619	0.3856	0.4027	0.4062	0.4177	0.4257	0.4254	0.4385
	0.3218	0.3469	0.3611	0.3851	0.4025	0.4060	0.4176	0.4257	0.4254	0.4385
	0.3104	0.3408	0.3576	0.3831	0.4013	0.4053	0.4171	0.4253	0.4252	0.4383
	0.2775	0.3230	0.3476	0.3773	0.3977	0.4030	0.4156	0.4243	0.4245	0.4378
	0.2117	0.2866	0.3271	0.3654	0.3906	0.3984	0.4127	0.4223	0.4230	0.4368
	0.1201	0.2294	0.2937	0.3463	0.3794	0.3914	0.4082	0.4193	0.4210	0.4354
	0.0003	0.0433	0.1453	0.2505	0.3222	0.3562	0.3864	0.4053	0.4115	0.4289
	0.0006	0.0004	0.0147	0.0823	0.1750	0.2597	0.3272	0.3687	0.3880	0.4137

Figure I.23: F1C: e=2.5a & d=2a

	c/a									
b/a	0.3604	0.3754	0.3822	0.4006	0.4142	0.4146	0.4240	0.4304	0.4290	0.4412
	0.3591	0.3745	0.3816	0.4003	0.4140	0.4145	0.4239	0.4303	0.4289	0.4412
	0.3534	0.3708	0.3792	0.3986	0.4129	0.4137	0.4234	0.4299	0.4287	0.4410
	0.3369	0.3603	0.3723	0.3941	0.4098	0.4115	0.4218	0.4288	0.4278	0.4404
	0.3038	0.3394	0.3588	0.3852	0.4037	0.4073	0.4188	0.4266	0.4262	0.4392
	0.2538	0.3077	0.3384	0.3719	0.3949	0.4012	0.4146	0.4236	0.4240	0.4375
	0.0829	0.1859	0.2561	0.3171	0.3584	0.3761	0.3972	0.4112	0.4150	0.4309
	0.0011	0.0294	0.1095	0.2038	0.2796	0.3217	0.3601	0.3854	0.3965	0.4177

Figure I.23: F1C: e=2.5a & d=2.5a

	c/a									
b/a	0.3848	0.3942	0.3969	0.4119	0.4229	0.4214	0.4293	0.4345	0.4322	0.4437
	0.384	0.3937	0.3965	0.4116	0.4227	0.4213	0.4292	0.4344	0.4322	0.4437
	0.3807	0.3913	0.3948	0.4104	0.4218	0.4206	0.4287	0.434	0.4319	0.4434
	0.3712	0.3846	0.39	0.4069	0.4192	0.4187	0.4272	0.4329	0.431	0.4428
	0.3523	0.3714	0.3806	0.4002	0.4143	0.415	0.4245	0.4308	0.4294	0.4415
	0.3236	0.3515	0.3667	0.3903	0.4072	0.4098	0.4205	0.4278	0.4271	0.4397
	0.2158	0.2756	0.3131	0.3523	0.38	0.3898	0.4058	0.4167	0.4186	0.4332
	0.05451	0.1476	0.2174	0.2818	0.3289	0.3524	0.3784	0.3963	0.4032	0.4214

Figure I.23: F1C: e=2.5a & d=3a

	c/a									
b/a	0.4018	0.4078	0.4078	0.4205	0.4298	0.427	0.4337	0.438	0.4351	0.446
	0.4013	0.4075	0.4075	0.4203	0.4296	0.4268	0.4336	0.4379	0.4351	0.4459
	0.3992	0.4058	0.4063	0.4193	0.4288	0.4263	0.4331	0.4375	0.4348	0.4457
	0.3932	0.4013	0.4028	0.4167	0.4268	0.4247	0.4319	0.4365	0.434	0.445
	0.3813	0.3924	0.3961	0.4115	0.4228	0.4216	0.4294	0.4346	0.4324	0.4438
	0.3633	0.379	0.3861	0.404	0.4171	0.4171	0.426	0.4319	0.4302	0.442
	0.2947	0.3284	0.3484	0.3758	0.3957	0.4007	0.4133	0.4219	0.4223	0.4357
	0.1793	0.2407	0.2823	0.326	0.3581	0.372	0.3912	0.4048	0.4088	0.4251

Figure I.23: F1C: e=2.5a & d=3.5a

	c/a									
b/a	0.4141	0.4179	0.4161	0.4272	0.4352	0.4315	0.4374	0.4410	0.4377	0.4480
	0.4138	0.4176	0.4159	0.4271	0.4351	0.4314	0.4373	0.4409	0.4376	0.4480
	0.4123	0.4165	0.4150	0.4263	0.4345	0.4309	0.4369	0.4406	0.4373	0.4478
	0.4082	0.4132	0.4124	0.4242	0.4328	0.4296	0.4358	0.4397	0.4366	0.4471
	0.4002	0.4069	0.4074	0.4203	0.4296	0.4270	0.4337	0.4380	0.4352	0.4460
	0.3881	0.3975	0.4000	0.4144	0.4250	0.4233	0.4307	0.4355	0.4332	0.4443
	0.3422	0.3620	0.3724	0.3928	0.4079	0.4097	0.4198	0.4267	0.4260	0.4384
	0.2623	0.3002	0.3244	0.3555	0.3787	0.3865	0.4014	0.4120	0.4140	0.4287

Figure I.23: F1C: e=2.5a & d=4a

	c/a									
b/a	0.4232	0.4255	0.4226	0.4325	0.4396	0.4352	0.4405	0.4436	0.4399	0.4499
	0.423	0.4253	0.4224	0.4324	0.4395	0.4351	0.4404	0.4435	0.4399	0.4498
	0.4219	0.4245	0.4217	0.4318	0.439	0.4347	0.4401	0.4432	0.4396	0.4496
	0.419	0.422	0.4197	0.4302	0.4376	0.4336	0.4391	0.4425	0.439	0.4491
	0.4133	0.4174	0.4159	0.427	0.435	0.4315	0.4374	0.4409	0.4377	0.448
	0.4047	0.4105	0.4103	0.4224	0.4313	0.422	0.4348	0.4388	0.4359	0.4465
	0.3725	0.3846	0.3894	0.4055	0.4175	0.4171	0.4255	0.4311	0.4294	0.441
	0.3159	0.3395	0.3534	0.3766	0.3941	0.398	0.4099	0.4183	0.4188	0.4322

Figure I.23: F1C: e=3a & d=0.5a

	c/a									
b/a	0.2626	0.3066	0.3322	0.3647	0.3882	0.3954	0.4101	0.4203	0.4215	0.4360
	0.2170	0.2965	0.3291	0.3636	0.3878	0.3952	0.4100	0.4203	0.4214	0.4359
	0.0538	0.2527	0.3179	0.3602	0.3865	0.3945	0.4097	0.4201	0.4213	0.4359
	0.0001	0.0879	0.2678	0.3469	0.3821	0.3924	0.4086	0.4195	0.4210	0.4357
	0.0005	0.0003	0.1136	0.2923	0.3677	0.3868	0.4061	0.4182	0.4202	0.4352
	0.0177	0.0000	−0.0001	0.1220	0.3196	0.3732	0.4014	0.4161	0.4190	0.4346
	0.0039	0.0001	−0.0001	−0.0001	0.0015	0.1425	0.3326	0.3948	0.4129	0.4305
	0.0064	0.0050	0.0017	0.0019	0.0002	−0.0006	0.0040	0.1526	0.3464	0.4083

Figure I.23: F1C: e=3a & d=1a

	c/a									
b/a	0.3221	0.3472	0.3612	0.3852	0.4028	0.4060	0.4176	0.4256	0.4253	0.4386
	0.3073	0.3406	0.3579	0.3835	0.4019	0.4054	0.4172	0.4254	0.4251	0.4385
	0.2649	0.3227	0.3495	0.3793	0.3996	0.4041	0.4164	0.4249	0.4248	0.4382
	0.1644	0.2778	0.3290	0.3694	0.3945	0.4010	0.4146	0.4237	0.4240	0.4377
	0.0257	0.1818	0.2838	0.3481	0.3838	0.3950	0.4111	0.4215	0.4226	0.4368
	0.0001	0.0629	0.1989	0.3069	0.3647	0.3849	0.4057	0.4183	0.4205	0.4355
	0.0000	0.0003	0.0125	0.1040	0.2313	0.3181	0.3726	0.4005	0.4099	0.4291
	0.0032	0.0002	0.0003	0.0001	0.0278	0.1274	0.2459	0.3329	0.3780	0.4109

Figure I.23: F1C: e=3a & d=1.5a

	c/a									
b/a	0.3594	0.3747	0.3817	0.4003	0.4138	0.4144	0.4239	0.4303	0.4289	0.4410
	0.3528	0.3708	0.3793	0.3988	0.4128	0.4138	0.4234	0.4300	0.4286	0.4409
	0.3348	0.3605	0.3732	0.3951	0.4104	0.4122	0.4224	0.4293	0.4281	0.4405
	0.2930	0.3374	0.3597	0.3870	0.4054	0.4089	0.4201	0.4277	0.4270	0.4396
	0.2187	0.2955	0.3357	0.3728	0.3967	0.4032	0.4163	0.4251	0.4251	0.4383
	0.1205	0.2334	0.2990	0.3515	0.3839	0.3951	0.4111	0.4216	0.4227	0.4366
	0.0008	0.0429	0.1454	0.2516	0.3239	0.3579	0.3879	0.4064	0.4123	0.4295
	0.0006	0.0002	0.0145	0.0821	0.1749	0.2598	0.3275	0.3689	0.3882	0.4138

Figure I.23: F1C: e=3a & d=2a

	c/a									
b/a	0.3843	0.3939	0.3965	0.4117	0.4228	0.4213	0.4291	0.4344	0.4321	0.4436
	0.3807	0.3914	0.3948	0.4105	0.4219	0.4206	0.4287	0.4340	0.4318	0.4434
	0.3713	0.3851	0.3905	0.4076	0.4199	0.4192	0.4276	0.4332	0.4312	0.4430
	0.3500	0.3713	0.3813	0.4013	0.4155	0.4160	0.4253	0.4315	0.4299	0.4420
	0.3120	0.3470	0.3654	0.3906	0.4082	0.4108	0.4216	0.4288	0.4279	0.4404
	0.2578	0.3123	0.3429	0.3759	0.3982	0.4039	0.4167	0.4253	0.4252	0.4385
	0.0817	0.1861	0.2571	0.3185	0.3598	0.3774	0.3982	0.4120	0.4155	0.4313
	0.0011	0.0291	0.1091	0.2035	0.2796	0.3219	0.3602	0.3855	0.3966	0.4177

Figure I.23: F1C: e=3a & d=2.5a

	c/a									
b/a	0.4015	0.4076	0.4075	0.4204	0.4296	0.4268	0.4336	0.4379	0.435	0.4459
	0.3994	0.406	0.4063	0.4194	0.4289	0.4263	0.4331	0.4376	0.4347	0.4457
	0.3937	0.4018	0.4033	0.4172	0.4272	0.425	0.4321	0.4368	0.4341	0.4452
	0.3812	0.3929	0.3967	0.4124	0.4237	0.4223	0.43	0.4352	0.4328	0.4442
	0.3593	0.3774	0.3856	0.4043	0.4177	0.4178	0.4266	0.4325	0.4307	0.4425
	0.3279	0.3555	0.3702	0.3933	0.4097	0.4118	0.4222	0.4291	0.4281	0.4405
	0.2162	0.2765	0.3142	0.3534	0.381	0.3907	0.4065	0.4173	0.419	0.4334
	0.05354	0.1471	0.2172	0.2818	0.329	0.3525	0.3785	0.3964	0.4031	0.4214

Figure I.23: F1C: e=3a & d=3a

	c/a									
b/a	0.4140	0.4177	0.4159	0.4271	0.4351	0.4313	0.4373	0.4409	0.4375	0.4479
	0.4125	0.4166	0.4150	0.4264	0.4345	0.4309	0.4369	0.4406	0.4373	0.4477
	0.4088	0.4137	0.4127	0.4246	0.4332	0.4298	0.4360	0.4399	0.4367	0.4472
	0.4008	0.4076	0.4080	0.4209	0.4303	0.4275	0.4342	0.4384	0.4355	0.4463
	0.3868	0.3970	0.4000	0.4148	0.4255	0.4237	0.4312	0.4360	0.4335	0.4447
	0.3670	0.3823	0.3889	0.4064	0.4190	0.4187	0.4273	0.4329	0.4310	0.4427
	0.2957	0.3294	0.3494	0.3767	0.3965	0.4013	0.4138	0.4223	0.4226	0.4359
	0.1789	0.2406	0.2822	0.3261	0.3582	0.3720	0.3912	0.4047	0.4087	0.4249

Figure I.23: F1C: e=3a & d=3.5a

	c/a									
b/a	0.4231	0.4254	0.4224	0.4324	0.4395	0.4351	0.4404	0.4435	0.4397	0.4497
	0.4221	0.4246	0.4217	0.4319	0.4391	0.4347	0.4401	0.4432	0.4395	0.4496
	0.4195	0.4225	0.42	0.4305	0.4379	0.4338	0.4393	0.4426	0.439	0.4491
	0.414	0.4181	0.4164	0.4276	0.4356	0.4319	0.4377	0.4413	0.4379	0.4482
	0.4045	0.4105	0.4104	0.4228	0.4317	0.4287	0.4351	0.4392	0.4361	0.4467
	0.3912	0.4001	0.4022	0.4163	0.4265	0.4245	0.4317	0.4364	0.4338	0.4448
	0.3432	0.3629	0.3732	0.3935	0.4085	0.4101	0.4202	0.427	0.4262	0.4385
	0.2622	0.3001	0.3244	0.3555	0.3787	0.3865	0.4014	0.4119	0.4139	0.4285

Figure I.23: F1C: e=3a & d=4a

	c/a									
b/a	0.4301	0.4313	0.4275	0.4367	0.4431	0.4382	0.443	0.4457	0.4417	0.4514
	0.4294	0.4307	0.427	0.4362	0.4427	0.4379	0.4427	0.4455	0.4415	0.4512
	0.4275	0.4291	0.4256	0.4351	0.4418	0.4371	0.4421	0.4449	0.441	0.4508
	0.4235	0.4258	0.4229	0.4328	0.4399	0.4355	0.4407	0.4438	0.4401	0.45
	0.4166	0.4202	0.4183	0.429	0.4367	0.4329	0.4385	0.4419	0.4385	0.4486
	0.4071	0.4125	0.412	0.4239	0.4325	0.4294	0.4356	0.4395	0.4364	0.4469
	0.3733	0.3853	0.39	0.406	0.4179	0.4174	0.4257	0.4313	0.4296	0.4411
	0.3159	0.3395	0.3534	0.3766	0.3941	0.398	0.4098	0.4182	0.4187	0.4321

Figure I.23: F1C: e=3.5a & d=0.5a

	c/a									
b/a	0.3133	0.3450	0.3604	0.3850	0.4027	0.4059	0.4175	0.4256	0.4252	0.4385
	0.2500	0.3299	0.3553	0.3829	0.4018	0.4053	0.4172	0.4254	0.4251	0.4385
	0.0564	0.2748	0.3406	0.3781	0.3999	0.4043	0.4167	0.4251	0.4249	0.4384
	0.0003	0.0926	0.2825	0.3621	0.3942	0.4015	0.4153	0.4243	0.4243	0.4381
	0.0004	0.0004	0.1171	0.3020	0.3778	0.3949	0.4123	0.4227	0.4233	0.4374
	0.0175	−0.0003	−0.0001	0.1244	0.3262	0.3801	0.4069	0.4203	0.4220	0.4367
	0.0038	0.0000	0.0000	0.0001	0.0017	0.1431	0.3354	0.3978	0.4154	0.4322
	0.0064	0.0050	0.0017	0.0018	0.0002	−0.0002	0.0039	0.1526	0.3474	0.4094

Figure I.23: F1C: e=3.5a & d=1a

	c/a									
b/a	0.3563	0.3732	0.3808	0.3999	0.4138	0.4142	0.4237	0.4302	0.4287	0.4411
	0.3355	0.3634	0.3757	0.3971	0.4122	0.4132	0.4231	0.4298	0.4284	0.4409
	0.2832	0.3407	0.3648	0.3915	0.4090	0.4112	0.4218	0.4290	0.4278	0.4405
	0.1707	0.2895	0.3409	0.3796	0.4027	0.4074	0.4195	0.4274	0.4268	0.4398
	0.0255	0.1859	0.2913	0.3559	0.3906	0.4005	0.4154	0.4248	0.4250	0.4386
	0.0001	0.0632	0.2016	0.3119	0.3699	0.3895	0.4094	0.4212	0.4227	0.4371
	0.0000	0.0001	0.0122	0.1044	0.2323	0.3201	0.3748	0.4024	0.4114	0.4303
	0.0032	0.0002	0.0002	0.0000	0.0276	0.1276	0.2464	0.3335	0.3769	0.4112

Figure I.23: F1C: e=3.5a & d=1.5a

	c/a									
b/a	0.3829	0.3930	0.3958	0.4113	0.4223	0.4210	0.4290	0.4343	0.4319	0.4434
	0.3734	0.3871	0.3921	0.4089	0.4207	0.4199	0.4282	0.4337	0.4315	0.4431
	0.3508	0.3741	0.3842	0.4040	0.4174	0.4177	0.4267	0.4326	0.4307	0.4425
	0.3034	0.3474	0.3685	0.3944	0.4113	0.4136	0.4238	0.4306	0.4292	0.4414
	0.2234	0.3019	0.3421	0.3786	0.4015	0.4071	0.4195	0.4276	0.4270	0.4398
	0.1205	0.2363	0.3031	0.3558	0.3878	0.3984	0.4138	0.4237	0.4243	0.4379
	0.0009	0.0425	0.1455	0.2526	0.3255	0.3596	0.3895	0.4078	0.4134	0.4304
	0.0006	0.0004	0.0143	0.0820	0.1749	0.2600	0.3279	0.3696	0.3888	0.4143

Figure I.23: F1C: e=3.5a & d=2a

	c/a									
b/a	0.4008	0.4070	0.4070	0.4201	0.4294	0.4266	0.4334	0.4378	0.4348	0.4458
	0.3955	0.4034	0.4044	0.4182	0.4281	0.4256	0.4326	0.4372	0.4343	0.4454
	0.3835	0.3953	0.3988	0.4143	0.4253	0.4235	0.4311	0.4360	0.4334	0.4447
	0.3591	0.3792	0.3880	0.4068	0.4200	0.4197	0.4283	0.4339	0.4318	0.4435
	0.3178	0.3526	0.3705	0.3950	0.4118	0.4139	0.4241	0.4308	0.4294	0.4417
	0.2608	0.3158	0.3465	0.3792	0.4011	0.4064	0.4187	0.4269	0.4266	0.4395
	0.0806	0.1863	0.2581	0.3198	0.3612	0.3787	0.3994	0.4130	0.4163	0.4319
	0.0003	0.0287	0.1087	0.2034	0.2798	0.3223	0.3607	0.3859	0.3969	0.4180

Figure I.23: F1C: e=3.5a & d=2.5a

	c/a									
b/a	0.4135	0.4174	0.4155	0.4269	0.4349	0.4311	0.4371	0.4408	0.4373	0.4478
	0.4102	0.4149	0.4136	0.4254	0.4338	0.4303	0.4364	0.4402	0.4369	0.4474
	0.403	0.4095	0.4096	0.4224	0.4315	0.4285	0.435	0.4391	0.436	0.4467
	0.3885	0.3991	0.4019	0.4167	0.4272	0.4252	0.4325	0.4371	0.4344	0.4455
	0.3645	0.382	0.3896	0.4077	0.4206	0.4201	0.4286	0.4341	0.432	0.4436
	0.3312	0.3588	0.3731	0.3959	0.4119	0.4137	0.4238	0.4304	0.4292	0.4413
	0.2166	0.2774	0.3153	0.3546	0.3821	0.3917	0.4074	0.418	0.4196	0.4339
	0.05261	0.1467	0.2172	0.2819	0.3292	0.3529	0.3788	0.3966	0.4034	0.4215

Figure I.23: F1C: e=3.5a & d=3a

	c/a									
b/a	0.4229	0.4252	0.422	0.4322	0.4394	0.4349	0.4402	0.4434	0.4395	0.4496
	0.4207	0.4234	0.4206	0.4311	0.4385	0.4342	0.4396	0.4429	0.4391	0.4493
	0.4159	0.4196	0.4177	0.4288	0.4366	0.4327	0.4384	0.4419	0.4383	0.4486
	0.4065	0.4124	0.4121	0.4244	0.4331	0.4299	0.4362	0.4401	0.4369	0.4474
	0.3911	0.4008	0.4032	0.4175	0.4278	0.4256	0.4328	0.4373	0.4346	0.4456
	0.3701	0.385	0.3913	0.4084	0.4208	0.4202	0.4285	0.434	0.4319	0.4434
	0.2966	0.3305	0.3505	0.3777	0.3974	0.4021	0.4144	0.4228	0.423	0.4362
	0.1786	0.2406	0.2824	0.3263	0.3584	0.3723	0.3914	0.4049	0.4089	0.4271

Figure I.23: F1C: e=3.5a & d=3.5a

	c/a									
b/a	0.4299	0.4312	0.4272	0.4365	0.443	0.438	0.4428	0.4456	0.4415	0.4512
	0.4284	0.4299	0.4261	0.4356	0.4423	0.4374	0.4423	0.4451	0.4411	0.4509
	0.425	0.4271	0.4239	0.4338	0.4407	0.4361	0.4413	0.4443	0.4404	0.4503
	0.4185	0.4219	0.4197	0.4303	0.4379	0.4338	0.4394	0.4427	0.4391	0.4492
	0.4079	0.4135	0.413	0.425	0.4336	0.4303	0.4365	0.4403	0.4371	0.4475
	0.3937	0.4023	0.4041	0.4179	0.4279	0.4257	0.4328	0.4372	0.4346	0.4454
	0.3442	0.3639	0.3741	0.3943	0.4092	0.4107	0.4207	0.4274	0.4265	0.4388
	0.2622	0.3003	0.3246	0.3557	0.3789	0.3867	0.4015	0.412	0.414	0.4286

Figure I.23: F1C: e=3.5a & d=4a

	c/a									
b/a	0.4354	0.4359	0.4314	0.44	0.446	0.4406	0.4451	0.4475	0.4432	0.4527
	0.4342	0.4349	0.4305	0.4393	0.4454	0.4401	0.4447	0.4471	0.4429	0.4524
	0.4317	0.4328	0.4288	0.4378	0.4441	0.4391	0.4438	0.4464	0.4423	0.4519
	0.427	0.4288	0.4255	0.4351	0.4418	0.4371	0.4421	0.445	0.4411	0.4508
	0.4194	0.4226	0.4203	0.4308	0.4382	0.4342	0.4396	0.4429	0.4393	0.4493
	0.4092	0.4143	0.4136	0.4252	0.4337	0.4304	0.4365	0.4402	0.437	0.4474
	0.3742	0.3861	0.3908	0.4067	0.4185	0.4179	0.4261	0.4316	0.4298	0.4413
	0.3161	0.3397	0.3535	0.3767	0.3942	0.3981	0.4099	0.4182	0.4187	0.4321

Figure I.23: F1C: e=4a & d=0.5a

	c/a									
	0.3463	0.3710	0.3801	0.3998	0.4138	0.4142	0.4237	0.4302	0.4286	0.4411
	0.2715	0.3526	0.3737	0.3971	0.4125	0.4134	0.4232	0.4299	0.4284	0.4410
	0.0582	0.2899	0.3566	0.3912	0.4101	0.4120	0.4225	0.4295	0.4282	0.4408
b/a	0.0001	0.0959	0.2931	0.3734	0.4036	0.4089	0.4209	0.4285	0.4275	0.4404
	0.0002	0.0005	0.1198	0.3095	0.3859	0.4016	0.4175	0.4267	0.4264	0.4397
	0.0174	−0.0001	−0.0001	0.1263	0.3313	0.3858	0.4117	0.4241	0.4249	0.4389
	0.0037	0.0000	0.0000	−0.0001	0.0004	0.1438	0.3380	0.4006	0.4178	0.4341
	0.0064	0.0048	0.0017	0.0018	0.0001	−0.0001	0.0037	0.1528	0.3486	0.4108

Figure I.23: F1C: e=4a & d=1a

	c/a									
	0.3795	0.3914	0.3949	0.4109	0.4223	0.4208	0.4288	0.4342	0.4318	0.4435
	0.3547	0.3795	0.3887	0.4074	0.4202	0.4195	0.4279	0.4336	0.4313	0.4432
	0.2959	0.3536	0.3760	0.4007	0.4164	0.4171	0.4264	0.4325	0.4306	0.4426
b/a	0.1751	0.2980	0.3498	0.3875	0.4092	0.4127	0.4237	0.4307	0.4294	0.4418
	0.0253	0.1890	0.2972	0.3621	0.3962	0.4052	0.4192	0.4278	0.4274	0.4404
	0.0000	0.0635	0.2038	0.3160	0.3743	0.3935	0.4127	0.4240	0.4249	0.4388
	0.0001	0.0001	0.0120	0.1049	0.2333	0.3221	0.3769	0.4043	0.4131	0.4316
	0.0032	0.0001	0.0002	0.0001	0.0274	0.1278	0.2470	0.3343	0.3799	0.4121

Figure I.23: F1C: e=4a & d=1.5a

	c/a									
	0.3993	0.4061	0.4063	0.4197	0.4290	0.4264	0.4332	0.4377	0.4346	0.4455
	0.3879	0.3990	0.4018	0.4167	0.4269	0.4249	0.4322	0.4369	0.4340	0.4451
	0.3622	0.3840	0.3926	0.4109	0.4231	0.4223	0.4303	0.4356	0.4331	0.4444
b/a	0.3110	0.3550	0.3754	0.4003	0.4162	0.4176	0.4271	0.4333	0.4314	0.4431
	0.2269	0.3069	0.3473	0.3834	0.4057	0.4106	0.4224	0.4299	0.4289	0.4413
	0.1205	0.2387	0.3065	0.3594	0.3911	0.4013	0.4163	0.4258	0.4260	0.4392
	0.0003	0.0423	0.1457	0.2536	0.3271	0.3613	0.3911	0.4092	0.4146	0.4314
	0.0003	0.0002	0.0141	0.0820	0.1750	0.2604	0.3286	0.3703	0.3895	0.4149

Figure I.23: F1C: e=4a & d=2a

	c/a									
	0.4128	0.4168	0.4150	0.4266	0.4348	0.4309	0.4369	0.4406	0.4371	0.4477
	0.4064	0.4123	0.4118	0.4242	0.4330	0.4296	0.4359	0.4399	0.4365	0.4472
	0.3926	0.4030	0.4053	0.4197	0.4297	0.4272	0.4341	0.4385	0.4355	0.4464
b/a	0.3661	0.3854	0.3934	0.4114	0.4239	0.4229	0.4309	0.4361	0.4336	0.4449
	0.3225	0.3572	0.3747	0.3987	0.4150	0.4166	0.4263	0.4327	0.4310	0.4429
	0.2632	0.3189	0.3496	0.3821	0.4037	0.4086	0.4207	0.4285	0.4279	0.4406
	0.0798	0.1866	0.2591	0.3211	0.3626	0.3800	0.4006	0.4141	0.4172	0.4327
	0.0004	0.0285	0.1084	0.2034	0.2802	0.3228	0.3613	0.3865	0.3975	0.4184

Figure I.23: F1C: e=4a & d=2.5a

	c/a									
	0.4225	0.4248	0.4217	0.432	0.4392	0.4347	0.44	0.4432	0.4394	0.4495
	0.4184	0.4217	0.4193	0.4302	0.4378	0.4336	0.4392	0.4425	0.4388	0.449
	0.41	0.4155	0.4147	0.4267	0.4351	0.4315	0.4375	0.4412	0.4377	0.4482
b/a	0.3943	0.404	0.4062	0.4203	0.4303	0.4278	0.4346	0.439	0.4359	0.4467
	0.3688	0.3859	0.3931	0.4107	0.4231	0.4223	0.4304	0.4357	0.4333	0.4447
	0.3341	0.3616	0.3758	0.3983	0.414	0.4155	0.4253	0.4317	0.4303	0.4422
	0.2171	0.2784	0.3165	0.3559	0.3833	0.3928	0.4083	0.4188	0.4203	0.4345
	0.05177	0.1464	0.2173	0.2823	0.3297	0.3534	0.3793	0.3971	0.4038	0.4219

Figure I.23: F1C: e=4a & d=3a

	c/a									
	0.4297	0.4309	0.4269	0.4363	0.4429	0.4378	0.4427	0.4455	0.4413	0.4511
	0.4269	0.4287	0.4252	0.4349	0.4417	0.4369	0.4419	0.4448	0.4408	0.4507
	0.4214	0.4244	0.4217	0.4322	0.4395	0.4351	0.4405	0.4436	0.4398	0.4499
b/a	0.4111	0.4164	0.4155	0.4273	0.4356	0.432	0.438	0.4416	0.4381	0.4485
	0.3947	0.4039	0.4059	0.4199	0.4298	0.4274	0.4343	0.4386	0.4357	0.4465
	0.3727	0.3875	0.3935	0.4104	0.4225	0.4217	0.4298	0.435	0.4328	0.4441
	0.2975	0.3315	0.3516	0.3788	0.3984	0.403	0.4152	0.4235	0.4236	0.4367
	0.1784	0.2407	0.2827	0.3267	0.3589	0.3727	0.3918	0.4053	0.4092	0.4253

Figure I.23: F1C: e=4a & d=3.5a

	c/a									
	0.4353	0.4357	0.4311	0.4399	0.4459	0.4405	0.445	0.4474	0.4431	0.4526
	0.4333	0.4341	0.4298	0.4387	0.4449	0.4397	0.4443	0.4468	0.4426	0.4522
	0.4293	0.4309	0.4271	0.4366	0.4431	0.4382	0.4431	0.4458	0.4417	0.4514
b/a	0.4221	0.425	0.4224	0.4327	0.44	0.4356	0.4409	0.444	0.4402	0.4501
	0.4109	0.4161	0.4152	0.4269	0.4353	0.4317	0.4377	0.4414	0.438	0.4483
	0.396	0.4044	0.406	0.4195	0.4293	0.427	0.4338	0.4381	0.4353	0.4461
	0.3452	0.3649	0.3751	0.3952	0.41	0.4115	0.4213	0.428	0.427	0.4392
	0.2624	0.3005	0.325	0.3561	0.3792	0.387	0.4018	0.4123	0.4142	0.4288

Figure I.23: F1C: e=4a & d=4a

	c/a									
	0.4396	0.4395	0.4345	0.4427	0.4483	0.4427	0.4469	0.449	0.4446	0.4539
	0.4381	0.4383	0.4335	0.4418	0.4476	0.442	0.4463	0.4486	0.4442	0.4535
	0.4352	0.4358	0.4314	0.4401	0.4461	0.4408	0.4453	0.4477	0.4434	0.4528
b/a	0.4299	0.4314	0.4277	0.437	0.4435	0.4386	0.4434	0.4461	0.442	0.4517
	0.4218	0.4247	0.4222	0.4324	0.4397	0.4354	0.4407	0.4438	0.4401	0.45
	0.4111	0.416	0.4151	0.4266	0.4348	0.4314	0.4373	0.441	0.4377	0.448
	0.3752	0.3871	0.3916	0.4075	0.4192	0.4185	0.4267	0.4321	0.4302	0.4417
	0.3163	0.34	0.3539	0.3771	0.3945	0.3984	0.4102	0.4184	0.4189	0.4322

Figure I.24: F2C: e=0.5a & d=0.5a

	c/a									
b/a	0.0157	0.0122	0.0133	0.0054	0.0069	−0.0116	−0.0950	−0.1783	−0.2376	−0.2705
	0.0161	0.0122	0.0113	0.0055	0.0070	−0.0116	−0.0950	−0.1783	−0.2376	−0.2705
	0.0207	0.0128	0.0115	0.0055	0.0070	−0.0122	−0.0950	−0.1783	−0.2376	−0.2705
	0.0254	0.0162	0.0107	0.0056	0.0069	−0.0092	−0.0942	−0.1782	−0.2375	−0.2705
	0.0214	0.0158	0.0099	0.0057	0.0072	−0.0113	−0.0942	−0.1783	−0.2373	−0.2705
	0.0268	0.0183	0.0112	0.0037	0.0072	−0.0055	−0.0943	−0.1781	−0.2370	−0.2704
	0.0287	0.0220	0.0176	0.0026	−0.0054	−0.0036	−0.0920	−0.1774	−0.2363	−0.2704
	0.0214	0.0162	0.0164	0.0025	−0.0100	−0.0218	−0.0306	−0.0351	−0.1644	−0.2444

Figure I.24: F2C: e=0.5a & d=1a

	c/a									
b/a	0.0584	0.0655	0.0629	0.0175	−0.0589	−0.1267	−0.1869	−0.2276	−0.2616	−0.2778
	0.0585	0.0656	0.0629	0.0175	−0.0589	−0.1267	−0.1869	−0.2276	−0.2616	−0.2778
	0.0587	0.0656	0.0629	0.0175	−0.0589	−0.1267	−0.1869	−0.2275	−0.2616	−0.2778
	0.0596	0.0658	0.0629	0.0175	−0.0589	−0.1267	−0.1869	−0.2276	−0.2616	−0.2778
	0.0580	0.0654	0.0628	0.0174	−0.0589	−0.1267	−0.1869	−0.2276	−0.2616	−0.2778
	0.0560	0.0644	0.0626	0.0174	−0.0589	−0.1267	−0.1869	−0.2276	−0.2616	−0.2778
	0.0448	0.0463	0.0501	0.0167	−0.0554	−0.1241	−0.1858	−0.2270	−0.2612	−0.2776
	0.0152	0.0119	0.0115	0.0058	0.0054	−0.0137	−0.0927	−0.1709	−0.2273	−0.2595

Figure I.24: F2C: e=0.5a & d=1.5a

	c/a									
b/a	0.0955	0.0400	−0.0299	−0.0946	−0.1506	−0.1933	−0.2277	−0.2513	−0.2751	−0.2843
	0.0956	0.0400	−0.0299	−0.0946	−0.1506	−0.1933	−0.2277	−0.2513	−0.2751	−0.2843
	0.0956	0.0401	−0.0299	−0.0946	−0.1506	−0.1932	−0.2276	−0.2513	−0.2751	−0.2843
	0.0956	0.0400	−0.0299	−0.0946	−0.1506	−0.1933	−0.2277	−0.2513	−0.2751	−0.2843
	0.0954	0.0400	−0.0300	−0.0946	−0.1506	−0.1933	−0.2277	−0.2513	−0.2751	−0.2843
	0.0945	0.0395	−0.0300	−0.0946	−0.1506	−0.1932	−0.2276	−0.2513	−0.2751	−0.2843
	0.0813	0.0372	−0.0281	−0.0925	−0.1491	−0.1922	−0.2270	−0.2508	−0.2747	−0.2841
	0.0533	0.0586	0.0538	0.0097	−0.0623	−0.1249	−0.1814	−0.2202	−0.2536	−0.2700

Figure I.24: F2C: e=0.5a & d=2a

	c/a									
b/a	−0.0071	−0.0695	−0.1228	−0.1657	−0.2017	−0.2291	−0.2511	−0.2665	−0.2848	−0.2900
	−0.0071	−0.0695	−0.1228	−0.1657	−0.2017	−0.2291	−0.2511	−0.2665	−0.2848	−0.2900
	−0.0071	−0.0695	−0.1228	−0.1657	−0.2017	−0.2291	−0.2511	−0.2665	−0.2848	−0.2900
	−0.0071	−0.0695	−0.1228	−0.1657	−0.2017	−0.2291	−0.2511	−0.2665	−0.2848	−0.2900
	−0.0071	−0.0696	−0.1228	−0.1657	−0.2017	−0.2291	−0.2511	−0.2665	−0.2848	−0.2900
	−0.0072	−0.0696	−0.1228	−0.1657	−0.2017	−0.2290	−0.2511	−0.2665	−0.2848	−0.2900
	−0.0063	−0.0680	−0.1213	−0.1643	−0.2008	−0.2284	−0.2506	−0.2661	−0.2845	−0.2898
	0.0823	0.0286	−0.0360	−0.0956	−0.1482	−0.1888	−0.2219	−0.2451	−0.2688	−0.2782

Figure I.24: F2C: e=0.5a & d=2.5a

	c/a									
b/a	−0.1066	−0.1491	−0.1848	−0.2110	−0.2341	−0.2524	−0.2674	−0.2779	−0.2926	−0.2953
	−0.1066	−0.1491	−0.1848	−0.2110	−0.2341	−0.2524	−0.2674	−0.2779	−0.2926	−0.2953
	−0.1066	−0.1491	−0.1848	−0.2110	−0.2341	−0.2524	−0.2674	−0.2778	−0.2926	−0.2953
	−0.1066	−0.1491	−0.1848	−0.2110	−0.2341	−0.2524	−0.2674	−0.2779	−0.2926	−0.2953
	−0.1066	−0.1491	−0.1848	−0.2110	−0.2341	−0.2524	−0.2674	−0.2779	−0.2926	−0.2953
	−0.1066	−0.1491	−0.1847	−0.2110	−0.2341	−0.2524	−0.2674	−0.2778	−0.2926	−0.2953
	−0.1045	−0.1475	−0.1835	−0.2101	−0.2335	−0.2519	−0.2670	−0.2776	−0.2924	−0.2951
	−0.0143	−0.0727	−0.1229	−0.1635	−0.1979	−0.2244	−0.2460	−0.2613	−0.2796	−0.2852

Figure I.24: F2C: e=0.5a & d=3a

	c/a									
b/a	−0.1762	−0.2027	−0.2256	−0.2417	−0.2569	−0.2695	−0.28	−0.2872	−0.2995	−0.3003
	−0.1762	−0.2027	−0.2256	−0.2417	−0.2569	−0.2695	−0.28	−0.2872	−0.2995	−0.3003
	−0.1762	−0.2027	−0.2256	−0.2417	−0.2569	−0.2695	−0.28	−0.2872	−0.2995	−0.3003
	−0.1762	−0.2027	−0.2256	−0.2417	−0.2569	−0.2695	−0.28	−0.2872	−0.2995	−0.3003
	−0.1762	−0.2027	−0.2256	−0.2417	−0.2569	−0.2695	−0.28	−0.2872	−0.2995	−0.3003
	−0.1762	−0.2027	−0.2256	−0.2417	−0.2569	−0.2695	−0.28	−0.2872	−0.2995	−0.3003
	−0.1746	−0.2015	−0.2246	−0.241	−0.2564	−0.269	−0.2796	−0.2869	−0.2992	−0.3001
	−0.108	−0.1483	−0.1823	−0.2076	−0.2301	−0.2481	−0.2629	−0.2735	−0.2885	−0.2913

Figure I.24: F2C: e=0.5a & d=3.5a

	c/a									
b/a	−0.2211	−0.2380	−0.2532	−0.2632	−0.2736	−0.2824	−0.2900	−0.2949	−0.3054	−0.3050
	−0.2211	−0.2380	−0.2532	−0.2632	−0.2736	−0.2824	−0.2900	−0.2949	−0.3054	−0.3050
	−0.2211	−0.2380	−0.2532	−0.2632	−0.2736	−0.2824	−0.2900	−0.2949	−0.3054	−0.3050
	−0.2211	−0.2380	−0.2532	−0.2632	−0.2736	−0.2824	−0.2900	−0.2949	−0.3054	−0.3050
	−0.2211	−0.2380	−0.2532	−0.2632	−0.2736	−0.2824	−0.2900	−0.2949	−0.3054	−0.3050
	−0.2210	−0.2380	−0.2532	−0.2632	−0.2736	−0.2824	−0.2900	−0.2949	−0.3054	−0.3049
	−0.2200	−0.2372	−0.2525	−0.2627	−0.2731	−0.2821	−0.2897	−0.2947	−0.3052	−0.3048
	−0.1744	−0.2000	−0.2222	−0.2380	−0.2530	−0.2655	−0.2761	−0.2834	−0.2958	−0.2969

Figure I.24: F2C: e=0.5a & d=4a

	c/a									
b/a	−0.2503	−0.2617	−0.2723	−0.2786	−0.2859	−0.2924	−0.2979	−0.3014	−0.3106	−0.3091
	−0.2503	−0.2617	−0.2723	−0.2786	−0.2859	−0.2924	−0.2979	−0.3014	−0.3106	−0.3091
	−0.2503	−0.2617	−0.2723	−0.2786	−0.2859	−0.2924	−0.2979	−0.3014	−0.3106	−0.3091
	−0.2503	−0.2617	−0.2723	−0.2786	−0.2859	−0.2924	−0.2979	−0.3014	−0.3106	−0.3091
	−0.2503	−0.2617	−0.2723	−0.2786	−0.2859	−0.2924	−0.2979	−0.3014	−0.3106	−0.3091
	−0.2502	−0.2617	−0.2723	−0.2786	−0.2859	−0.2924	−0.2979	−0.3013	−0.3106	−0.3091
	−0.2495	−0.2611	−0.2718	−0.2782	−0.2856	−0.2921	−0.2977	−0.3011	−0.3104	−0.3089
	−0.218	−0.2346	−0.2496	−0.2596	−0.27	−0.2789	−0.2865	−0.2917	−0.3023	−0.302

Figure I.24: F2C: e=1a & d=0.5a

	c/a									
b/a	0.0585	0.0656	0.0629	0.0175	−0.0589	−0.1267	−0.1869	−0.2275	−0.2616	−0.2777
	0.0579	0.0655	0.0629	0.0175	−0.0589	−0.1267	−0.1869	−0.2275	−0.2616	−0.2777
	0.0587	0.0647	0.0627	0.0175	−0.0588	−0.1266	−0.1869	−0.2275	−0.2616	−0.2777
	0.0598	0.0661	0.0626	0.0175	−0.0588	−0.1265	−0.1868	−0.2275	−0.2615	−0.2796
	0.0597	0.0665	0.0639	0.0171	−0.0589	−0.1263	−0.1868	−0.2274	−0.2610	−0.2777
	0.0649	0.0574	0.0484	0.0230	−0.0566	−0.1265	−0.1870	−0.2274	−0.2610	−0.2776
	0.0085	0.0036	−0.0004	−0.0091	−0.0199	−0.0266	−0.1417	−0.2135	−0.2542	−0.2751
	0.0214	0.0162	0.0164	0.0025	−0.0099	−0.0216	−0.0303	−0.0337	−0.1615	−0.2405

Figure I.24: F2C: e=1a & d=1a

	c/a									
b/a	0.0956	0.0401	−0.0299	−0.0946	−0.1505	−0.1932	−0.2276	−0.2513	−0.2751	−0.2842
	0.0956	0.0401	−0.0299	−0.0946	−0.1505	−0.1932	−0.2276	−0.2513	−0.2751	−0.2842
	0.0955	0.0401	−0.0298	−0.0946	−0.1505	−0.1932	−0.2276	−0.2512	−0.2751	−0.2842
	0.0958	0.0401	−0.0298	−0.0946	−0.1505	−0.1932	−0.2276	−0.2512	−0.2751	−0.2842
	0.0971	0.0412	−0.0294	−0.0945	−0.1505	−0.1932	−0.2276	−0.2512	−0.2751	−0.2842
	0.0942	0.0507	−0.0193	−0.0909	−0.1488	−0.1924	−0.2272	−0.2510	−0.2749	−0.2841
	0.0176	0.0208	0.0265	−0.0110	−0.0902	−0.1574	−0.2086	−0.2406	−0.2685	−0.2803
	0.0152	0.0118	0.0115	0.0059	0.0057	−0.0130	−0.0913	−0.1686	−0.2242	−0.2559

Figure I.24: F2C: e=1a & d=1.5a

	c/a									
b/a	−0.0070	−0.0695	−0.1228	−0.1657	−0.2018	−0.2290	−0.2511	−0.2665	−0.2848	−0.2901
	−0.0070	−0.0695	−0.1228	−0.1657	−0.2018	−0.2290	−0.2511	−0.2665	−0.2848	−0.2901
	−0.0070	−0.0695	−0.1227	−0.1657	−0.2017	−0.2290	−0.2511	−0.2664	−0.2848	−0.2901
	−0.0070	−0.0695	−0.1227	−0.1657	−0.2017	−0.2290	−0.2511	−0.2664	−0.2848	−0.2901
	−0.0067	−0.0693	−0.1227	−0.1657	−0.2017	−0.2290	−0.2511	−0.2664	−0.2848	−0.2901
	0.0016	−0.0641	−0.1195	−0.1639	−0.2008	−0.2284	−0.2507	−0.2662	−0.2846	−0.2900
	0.0612	0.0091	−0.0570	−0.1204	−0.1723	−0.2095	−0.2390	−0.2576	−0.2788	−0.2860
	0.0530	0.0583	0.0535	0.0097	−0.0616	−0.1235	−0.1794	−0.2177	−0.2507	−0.2669

Figure I.24: F2C: e=1a & d=2a

	c/a									
b/a	−0.1065	−0.1491	−0.1848	−0.2110	−0.2341	−0.2524	−0.2674	−0.2778	−0.2926	−0.2953
	−0.1065	−0.1490	−0.1848	−0.2110	−0.2341	−0.2524	−0.2674	−0.2778	−0.2926	−0.2953
	−0.1065	−0.1490	−0.1847	−0.2110	−0.2341	−0.2524	−0.2674	−0.2778	−0.2926	−0.2953
	−0.1065	−0.1490	−0.1847	−0.2110	−0.2341	−0.2524	−0.2674	−0.2778	−0.2926	−0.2953
	−0.1064	−0.1490	−0.1847	−0.2110	−0.2341	−0.2524	−0.2674	−0.2778	−0.2926	−0.2953
	−0.1022	−0.1463	−0.1830	−0.2099	−0.2334	−0.2519	−0.2671	−0.2776	−0.2924	−0.2952
	−0.0335	−0.0942	−0.1451	−0.1835	−0.2152	−0.2388	−0.2578	−0.2708	−0.2874	−0.2914
	0.0815	0.0281	−0.0359	−0.0949	−0.1470	−0.1870	−0.2198	−0.2426	−0.2662	−0.2756

Figure I.24: F2C: e=1a & d=2.5a

	c/a									
b/a	−0.1761	−0.2027	−0.2256	−0.2417	−0.2569	−0.2695	−0.2800	−0.2871	−0.2995	−0.3003
	−0.1761	−0.2027	−0.2256	−0.2417	−0.2569	−0.2695	−0.2800	−0.2871	−0.2995	−0.3003
	−0.1761	−0.2027	−0.2256	−0.2417	−0.2569	−0.2695	−0.2799	−0.2871	−0.2994	−0.3003
	−0.1761	−0.2027	−0.2256	−0.2417	−0.2569	−0.2695	−0.2799	−0.2871	−0.2994	−0.3003
	−0.1761	−0.2026	−0.2255	−0.2417	−0.2569	−0.2695	−0.2799	−0.2871	−0.2994	−0.3003
	−0.1739	−0.2011	−0.2245	−0.2409	−0.2564	−0.2691	−0.2797	−0.2869	−0.2993	−0.3001
	−0.1289	−0.1677	−0.1998	−0.2227	−0.2429	−0.2589	−0.2720	−0.2810	−0.2946	−0.2965
	−0.0147	−0.0724	−0.1222	−0.1623	−0.1963	−0.2225	−0.2439	−0.2591	−0.2774	−0.2829

Figure I.24: F2C: e=1a & d=3a

	c/a									
b/a	−0.221	−0.238	−0.2532	−0.2632	−0.2735	−0.2824	−0.2899	−0.2949	−0.3054	−0.3049
	−0.221	−0.238	−0.2532	−0.2632	−0.2735	−0.2824	−0.2899	−0.2949	−0.3054	−0.3049
	−0.221	−0.238	−0.2532	−0.2632	−0.2735	−0.2824	−0.2899	−0.2949	−0.3054	−0.3049
	−0.221	−0.238	−0.2532	−0.2632	−0.2735	−0.2824	−0.2899	−0.2949	−0.3054	−0.3049
	−0.2209	−0.2379	−0.2532	−0.2632	−0.2735	−0.2824	−0.2899	−0.2949	−0.3054	−0.3049
	−0.2198	−0.237	−0.2525	−0.2626	−0.2731	−0.2821	−0.2897	−0.2947	−0.3053	−0.3048
	−0.1919	−0.2154	−0.2356	−0.2495	−0.2629	−0.274	−0.2833	−0.2895	−0.3011	−0.3014
	−0.1076	−0.1474	−0.1811	−0.2061	−0.2284	−0.2462	−0.261	−0.2715	−0.2863	−0.2893

Figure I.24: F2C: e=1a & d=3.5a

	c/a									
b/a	−0.2502	−0.2616	−0.2723	−0.2786	−0.2859	−0.2924	−0.2979	−0.3013	−0.3106	−0.309
	−0.2502	−0.2616	−0.2723	−0.2786	−0.2859	−0.2924	−0.2979	−0.3013	−0.3106	−0.309
	−0.2502	−0.2616	−0.2723	−0.2786	−0.2859	−0.2924	−0.2979	−0.3013	−0.3106	−0.309
	−0.2502	−0.2616	−0.2723	−0.2786	−0.2859	−0.2924	−0.2979	−0.3013	−0.3106	−0.309
	−0.2502	−0.2616	−0.2723	−0.2786	−0.2859	−0.2923	−0.2979	−0.3013	−0.3106	−0.309
	−0.2494	−0.261	−0.2718	−0.2782	−0.2856	−0.2921	−0.2977	−0.3011	−0.3104	−0.3089
	−0.2315	−0.2465	−0.2599	−0.2686	−0.2777	−0.2856	−0.2924	−0.2967	−0.3067	−0.3058
	−0.1734	−0.1987	−0.2207	−0.2364	−0.2513	−0.2637	−0.2742	−0.2816	−0.294	−0.2952

Figure I.24: F2C: e=1a & d=4a

	c/a									
b/a	−0.2698	−0.278	−0.2858	−0.2898	−0.2952	−0.3001	−0.3042	−0.3066	−0.3149	−0.3127
	−0.2698	−0.278	−0.2858	−0.2898	−0.2952	−0.3001	−0.3042	−0.3066	−0.3149	−0.3127
	−0.2698	−0.278	−0.2858	−0.2898	−0.2952	−0.3	−0.3042	−0.3066	−0.3149	−0.3126
	−0.2698	−0.278	−0.2858	−0.2898	−0.2952	−0.3001	−0.3042	−0.3066	−0.3149	−0.3126
	−0.2698	−0.278	−0.2858	−0.2898	−0.2952	−0.3	−0.3042	−0.3066	−0.3149	−0.3126
	−0.2693	−0.2776	−0.2855	−0.2895	−0.2949	−0.2998	−0.3041	−0.3064	−0.3148	−0.3125
	−0.2572	−0.2674	−0.2769	−0.2823	−0.2888	−0.2947	−0.2997	−0.3027	−0.3116	−0.3098
	−0.2167	−0.2331	−0.248	−0.258	−0.2683	−0.2772	−0.2848	−0.29	−0.3007	−0.3005

Figure I.24: F2C: e=1.5a & d=0.5a

	c/a									
b/a	0.0947	0.0399	−0.0299	−0.0945	−0.1504	−0.1932	−0.2276	−0.2512	−0.2751	−0.2842
	0.0895	0.0380	−0.0304	−0.0946	−0.1504	−0.1931	−0.2276	−0.2512	−0.2751	−0.2842
	0.0894	0.0320	−0.0327	−0.0953	−0.1506	−0.1931	−0.2275	−0.2511	−0.2750	−0.2841
	0.0789	0.0363	−0.0330	−0.0969	−0.1514	−0.1935	−0.2276	−0.2511	−0.2749	−0.2841
	0.0328	0.0214	0.0066	−0.0829	−0.1490	−0.1926	−0.2275	−0.2511	−0.2749	−0.2841
	0.0004	−0.0062	−0.0034	−0.0239	−0.1225	−0.1850	−0.2249	−0.2500	−0.2744	−0.2838
	0.0084	0.0035	−0.0011	−0.0100	−0.0268	−0.0274	−0.1508	−0.2233	−0.2603	−0.2782
	0.0213	0.0162	0.0164	0.0025	−0.0099	−0.0218	−0.0306	−0.0336	−0.1617	−0.2398

Figure I.24: F2C: e=1.5a & d=1a

	c/a									
b/a	−0.0070	−0.0694	−0.1227	−0.1656	−0.2016	−0.2290	−0.2511	−0.2664	−0.2848	−0.2900
	−0.0076	−0.0696	−0.1227	−0.1656	−0.2016	−0.2290	−0.2510	−0.2664	−0.2847	−0.2899
	−0.0092	−0.0705	−0.1232	−0.1658	−0.2016	−0.2289	−0.2510	−0.2663	−0.2847	−0.2899
	−0.0051	−0.0692	−0.1229	−0.1658	−0.2017	−0.2290	−0.2510	−0.2663	−0.2847	−0.2899
	0.0202	−0.0515	−0.1130	−0.1615	−0.1997	−0.2279	−0.2505	−0.2660	−0.2845	−0.2898
	0.0375	−0.0051	−0.0772	−0.1425	−0.1901	−0.2226	−0.2475	−0.2642	−0.2833	−0.2890
	0.0184	0.0221	0.0297	−0.0085	−0.0931	−0.1627	−0.2149	−0.2454	−0.2715	−0.2820
	0.0152	0.0119	0.0115	0.0058	0.0059	−0.0125	−0.0906	−0.1678	−0.2232	−0.2546

Figure I.24: F2C: e=1.5a & d=1.5a

	c/a									
b/a	−0.1064	−0.1490	−0.1847	−0.2109	−0.2342	−0.2524	−0.2674	−0.2778	−0.2926	−0.2953
	−0.1064	−0.1490	−0.1847	−0.2109	−0.2342	−0.2523	−0.2673	−0.2777	−0.2926	−0.2953
	−0.1068	−0.1492	−0.1848	−0.2109	−0.2342	−0.2523	−0.2673	−0.2777	−0.2926	−0.2953
	−0.1056	−0.1486	−0.1845	−0.2108	−0.2341	−0.2523	−0.2673	−0.2777	−0.2925	−0.2952
	−0.0911	−0.1402	−0.1797	−0.2081	−0.2326	−0.2513	−0.2667	−0.2773	−0.2923	−0.2951
	−0.0498	−0.1129	−0.1626	−0.1978	−0.2263	−0.2472	−0.2640	−0.2755	−0.2910	−0.2942
	0.0676	0.0133	−0.0577	−0.1235	−0.1769	−0.2138	−0.2421	−0.2606	−0.2805	−0.2869
	0.0532	0.0586	0.0541	0.0103	−0.0609	−0.1228	−0.1785	−0.2166	−0.2495	−0.2655

Figure I.24: F2C: e=1.5a & d=2a

	c/a									
b/a	−0.1760	−0.2026	−0.2256	−0.2416	−0.2569	−0.2694	−0.2799	−0.2871	−0.2994	−0.3002
	−0.1760	−0.2025	−0.2255	−0.2416	−0.2569	−0.2694	−0.2799	−0.2870	−0.2994	−0.3002
	−0.1760	−0.2026	−0.2255	−0.2416	−0.2568	−0.2694	−0.2799	−0.2870	−0.2994	−0.3002
	−0.1755	−0.2022	−0.2253	−0.2414	−0.2567	−0.2693	−0.2798	−0.2870	−0.2994	−0.3002
	−0.1686	−0.1977	−0.2223	−0.2395	−0.2554	−0.2684	−0.2792	−0.2865	−0.2990	−0.2999
	−0.1455	−0.1820	−0.2118	−0.2324	−0.2506	−0.2650	−0.2767	−0.2847	−0.2977	−0.2989
	−0.0326	−0.0957	−0.1478	−0.1868	−0.2184	−0.2414	−0.2598	−0.2722	−0.2882	−0.2918
	0.0821	0.0288	−0.0353	−0.0942	−0.1462	−0.1862	−0.2188	−0.2415	−0.2649	−0.2743

Figure I.24: F2C: e=1.5a & d=2.5a

	c/a									
b/a	−0.2209	−0.2379	−0.2532	−0.2631	−0.2735	−0.2824	−0.2899	−0.2948	−0.3054	−0.3048
	−0.2208	−0.2378	−0.2531	−0.2631	−0.2735	−0.2824	−0.2899	−0.2948	−0.3054	−0.3048
	−0.2208	−0.2378	−0.2531	−0.2631	−0.2735	−0.2823	−0.2899	−0.2948	−0.3054	−0.3048
	−0.2205	−0.2376	−0.2529	−0.2629	−0.2734	−0.2823	−0.2898	−0.2947	−0.3053	−0.3048
	−0.2169	−0.2350	−0.2510	−0.2616	−0.2723	−0.2815	−0.2892	−0.2943	−0.3050	−0.3045
	−0.2042	−0.2256	−0.2442	−0.2565	−0.2686	−0.2786	−0.2871	−0.2926	−0.3037	−0.3035
	−0.1313	−0.1703	−0.2023	−0.2250	−0.2449	−0.2604	−0.2731	−0.2817	−0.2950	−0.2966
	−0.0142	−0.0719	−0.1215	−0.1615	−0.1954	−0.2215	−0.2429	−0.2580	−0.2762	−0.2817

Figure I.24: F2C: e=1.5a & d=3a

	c/a									
b/a	−0.2501	−0.2616	−0.2723	−0.2785	−0.2858	−0.2923	−0.2979	−0.3012	−0.3105	−0.309
	−0.25	−0.2615	−0.2722	−0.2785	−0.2858	−0.2923	−0.2979	−0.3012	−0.3105	−0.309
	−0.25	−0.2615	−0.2722	−0.2785	−0.2858	−0.2923	−0.2978	−0.3012	−0.3105	−0.3089
	−0.2498	−0.2613	−0.2721	−0.2784	−0.2857	−0.2922	−0.2978	−0.3012	−0.3105	−0.3089
	−0.2477	−0.2597	−0.2708	−0.2774	−0.2849	−0.2916	−0.2973	−0.3008	−0.3101	−0.3086
	−0.2402	−0.2538	−0.2661	−0.2737	−0.2821	−0.2893	−0.2954	−0.2993	−0.3089	−0.3076
	−0.1946	−0.2177	−0.2376	−0.2511	−0.2641	−0.2749	−0.2838	−0.2899	−0.3012	−0.3013
	−0.1071	−0.1468	−0.1804	−0.2053	−0.2275	−0.2452	−0.2599	−0.2704	−0.2852	−0.2882

Figure I.24: F2C: e=1.5a & d=3.5a

	c/a									
b/a	−0.2697	−0.2779	−0.2858	−0.2898	−0.2951	−0.3	−0.3042	−0.3065	−0.3149	−0.3126
	−0.2697	−0.2779	−0.2858	−0.2898	−0.2951	−0.3	−0.3042	−0.3065	−0.3149	−0.3126
	−0.2696	−0.2778	−0.2858	−0.2897	−0.2951	−0.3	−0.3042	−0.3065	−0.3148	−0.3126
	−0.2695	−0.2777	−0.2857	−0.2897	−0.295	−0.2999	−0.3041	−0.3064	−0.3148	−0.3125
	−0.2682	−0.2767	−0.2848	−0.2889	−0.2944	−0.2994	−0.3037	−0.3061	−0.3145	−0.3123
	−0.2634	−0.2727	−0.2815	−0.2862	−0.2922	−0.2976	−0.3022	−0.3048	−0.3134	−0.3114
	−0.2336	−0.2481	−0.2613	−0.2696	−0.2785	−0.2861	−0.2927	−0.2968	−0.3067	−0.3057
	−0.1728	−0.198	−0.2199	−0.2355	−0.2504	−0.2628	−0.2733	−0.2806	−0.293	−0.2942

Figure I.24: F2C: e=1.5a & d=4a

	c/a									
b/a	−0.2834	−0.2896	−0.2957	−0.2982	−0.3022	−0.306	−0.3093	−0.3108	−0.3185	−0.3157
	−0.2833	−0.2895	−0.2957	−0.2982	−0.3022	−0.306	−0.3093	−0.3108	−0.3185	−0.3157
	−0.2833	−0.2895	−0.2956	−0.2981	−0.3022	−0.306	−0.3093	−0.3108	−0.3185	−0.3157
	−0.2832	−0.2894	−0.2956	−0.2981	−0.3021	−0.306	−0.3092	−0.3108	−0.3184	−0.3156
	−0.2823	−0.2887	−0.2949	−0.2975	−0.3017	−0.3056	−0.3089	−0.3105	−0.3182	−0.3154
	−0.279	−0.2859	−0.2925	−0.2955	−0.2999	−0.3041	−0.3076	−0.3094	−0.3173	−0.3146
	−0.2586	−0.2685	−0.2777	−0.2829	−0.2893	−0.295	−0.2998	−0.3027	−0.3115	−0.3096
	−0.216	−0.2324	−0.2472	−0.2571	−0.2674	−0.2763	−0.2839	−0.2891	−0.2998	−0.2996

Figure I.24: F2C: e=2a & d=0.5a

	c/a									
b/a	−0.0094	−0.0703	−0.1231	−0.1658	−0.2017	−0.2290	−0.2511	−0.2664	−0.2848	−0.2899
	−0.0153	−0.0733	−0.1245	−0.1664	−0.2020	−0.2291	−0.2511	−0.2664	−0.2848	−0.2899
	0.0036	−0.0684	−0.1242	−0.1671	−0.2025	−0.2294	−0.2513	−0.2665	−0.2848	−0.2899
	0.0170	−0.0070	−0.0987	−0.1616	−0.2010	−0.2288	−0.2511	−0.2664	−0.2848	−0.2899
	0.0213	0.0156	−0.0002	−0.1173	−0.1889	−0.2230	−0.2489	−0.2653	−0.2840	−0.2896
	−0.0061	−0.0078	−0.0070	−0.0280	−0.1461	−0.2071	−0.2429	−0.2626	−0.2825	−0.2888
	0.0082	0.0034	−0.0015	−0.0108	−0.0276	−0.0279	−0.1555	−0.2288	−0.2646	−0.2811
	0.0212	0.0161	0.0163	0.0024	−0.0098	−0.0221	−0.0310	−0.0338	−0.1622	−0.2404

Figure I.24: F2C: e=2a & d=1a

	c/a									
b/a	−0.1068	−0.1492	−0.1849	−0.2110	−0.2341	−0.2524	−0.2674	−0.2777	−0.2926	−0.2952
	−0.1083	−0.1501	−0.1854	−0.2113	−0.2343	−0.2525	−0.2674	−0.2778	−0.2926	−0.2952
	−0.1029	−0.1483	−0.1849	−0.2113	−0.2344	−0.2526	−0.2675	−0.2778	−0.2927	−0.2952
	−0.0629	−0.1293	−0.1762	−0.2074	−0.2326	−0.2515	−0.2670	−0.2775	−0.2925	−0.2951
	0.0177	−0.0720	−0.1433	−0.1911	−0.2244	−0.2466	−0.2642	−0.2758	−0.2913	−0.2944
	0.0445	−0.0011	−0.0849	−0.1578	−0.2069	−0.2364	−0.2583	−0.2722	−0.2890	−0.2929
	0.0188	0.0230	0.0313	−0.0049	−0.0936	−0.1652	−0.2179	−0.2481	−0.2734	−0.2833
	0.0151	0.0118	0.0114	0.0057	0.0060	−0.0122	−0.0903	−0.1677	−0.2231	−0.2545

Figure I.24: F2C: e=2a & d=1.5a

	c/a									
b/a	−0.1761	−0.2026	−0.2256	−0.2416	−0.2570	−0.2694	−0.2799	−0.2870	−0.2995	−0.3003
	−0.1765	−0.2029	−0.2258	−0.2418	−0.2571	−0.2695	−0.2800	−0.2871	−0.2995	−0.3003
	−0.1745	−0.2019	−0.2253	−0.2415	−0.2570	−0.2694	−0.2800	−0.2871	−0.2995	−0.3003
	−0.1586	−0.1926	−0.2198	−0.2383	−0.2551	−0.2682	−0.2792	−0.2865	−0.2991	−0.3000
	−0.1152	−0.1656	−0.2031	−0.2280	−0.2486	−0.2638	−0.2763	−0.2845	−0.2977	−0.2990
	−0.0538	−0.1224	−0.1746	−0.2099	−0.2372	−0.2561	−0.2711	−0.2809	−0.2950	−0.2972
	0.0713	0.0162	−0.0571	−0.1242	−0.1787	−0.2158	−0.2439	−0.2620	−0.2815	−0.2875
	0.0534	0.0590	0.0547	0.0110	−0.0603	−0.1224	−0.1783	−0.2164	−0.2491	−0.2651

Figure I.24: F2C: e=2a & d=2a

	c/a									
b/a	−0.2208	−0.2379	−0.2532	−0.2631	−0.2735	−0.2824	−0.2899	−0.2948	−0.3054	−0.3048
	−0.2210	−0.2380	−0.2533	−0.2632	−0.2735	−0.2824	−0.2899	−0.2948	−0.3054	−0.3048
	−0.2201	−0.2374	−0.2529	−0.2629	−0.2734	−0.2823	−0.2899	−0.2948	−0.3054	−0.3048
	−0.2127	−0.2323	−0.2494	−0.2605	−0.2717	−0.2811	−0.2890	−0.2941	−0.3049	−0.3044
	−0.1915	−0.2176	−0.2391	−0.2533	−0.2666	−0.2773	−0.2863	−0.2921	−0.3033	−0.3032
	−0.1559	−0.1926	−0.2216	−0.2410	−0.2579	−0.2710	−0.2816	−0.2886	−0.3007	−0.3012
	−0.0314	−0.0958	−0.1488	−0.1882	−0.2198	−0.2428	−0.2609	−0.2730	−0.2888	−0.2921
	0.0831	0.0298	−0.0346	−0.0938	−0.1459	−0.1858	−0.2184	−0.2411	−0.2645	−0.2737

Figure I.24: F2C: e=2a & d=2.5a

	c/a									
b/a	−0.2500	−0.2615	−0.2723	−0.2785	−0.2858	−0.2923	−0.2979	−0.3012	−0.3105	−0.3089
	−0.2501	−0.2616	−0.2723	−0.2785	−0.2858	−0.2923	−0.2979	−0.3012	−0.3105	−0.3089
	−0.2496	−0.2612	−0.2720	−0.2783	−0.2857	−0.2922	−0.2978	−0.3011	−0.3105	−0.3089
	−0.2456	−0.2582	−0.2697	−0.2766	−0.2844	−0.2912	−0.2970	−0.3005	−0.3100	−0.3085
	−0.2341	−0.2494	−0.2631	−0.2715	−0.2805	−0.2882	−0.2946	−0.2987	−0.3085	−0.3073
	−0.2140	−0.2342	−0.2516	−0.2628	−0.2739	−0.2830	−0.2906	−0.2955	−0.3060	−0.3053
	−0.1319	−0.1714	−0.2035	−0.2262	−0.2459	−0.2612	−0.2737	−0.2821	−0.2953	−0.2967
	−0.0135	−0.0714	−0.1211	−0.1612	−0.1951	−0.2211	−0.2424	−0.2575	−0.2757	−0.2811

Figure I.24: F2C: e=2a & d=3a

	c/a									
b/a	−0.2696	−0.2779	−0.2858	−0.2897	−0.2951	−0.3	−0.3042	−0.3065	−0.3149	−0.3125
	−0.2696	−0.2779	−0.2858	−0.2898	−0.2951	−0.3	−0.3042	−0.3065	−0.3149	−0.3125
	−0.2693	−0.2776	−0.2856	−0.2896	−0.295	−0.2999	−0.3041	−0.3064	−0.3148	−0.3125
	−0.267	−0.2757	−0.2841	−0.2884	−0.294	−0.2991	−0.3035	−0.3059	−0.3144	−0.3121
	−0.26	−0.2701	−0.2796	−0.2847	−0.2911	−0.2967	−0.3015	−0.3043	−0.313	−0.311
	−0.2478	−0.2603	−0.2717	−0.2784	−0.286	−0.2926	−0.2981	−0.3015	−0.3107	−0.3091
	−0.1958	−0.2188	−0.2386	−0.252	−0.2648	−0.2754	−0.2842	−0.2901	−0.3013	−0.3013
	−0.1067	−0.1464	−0.18	−0.2049	−0.2271	−0.2448	−0.2595	−0.2699	−0.2847	−0.2877

Figure I.24: F2C: e=2a & d=3.5a

	c/a									
b/a	−0.2833	−0.2895	−0.2957	−0.2981	−0.3022	−0.306	−0.3093	−0.3108	−0.3185	−0.3156
	−0.2833	−0.2895	−0.2957	−0.2981	−0.3022	−0.306	−0.3093	−0.3108	−0.3185	−0.3156
	−0.2831	−0.2893	−0.2955	−0.298	−0.3021	−0.3059	−0.3092	−0.3107	−0.3184	−0.3156
	−0.2816	−0.288	−0.2944	−0.2971	−0.3013	−0.3053	−0.3087	−0.3103	−0.318	−0.3153
	−0.277	−0.2842	−0.2913	−0.2944	−0.2991	−0.3034	−0.3071	−0.3089	−0.3169	−0.3143
	−0.269	−0.2775	−0.2856	−0.2898	−0.2952	−0.3001	−0.3043	−0.3066	−0.3149	−0.3126
	−0.2347	−0.2491	−0.262	−0.2702	−0.2789	−0.2865	−0.2929	−0.297	−0.3067	−0.3057
	−0.1725	−0.1977	−0.2196	−0.2351	−0.25	−0.2623	−0.2728	−0.2801	−0.2925	−0.2936

Figure I.24: F2C: e=2a & d=4a

	c/a									
b/a	−0.2931	−0.298	−0.303	−0.3045	−0.3077	−0.3108	−0.3134	−0.3143	−0.3215	−0.3183
	−0.2931	−0.298	−0.303	−0.3045	−0.3077	−0.3108	−0.3134	−0.3143	−0.3215	−0.3183
	−0.293	−0.2979	−0.3029	−0.3044	−0.3076	−0.3107	−0.3133	−0.3143	−0.3215	−0.3182
	−0.2919	−0.297	−0.3021	−0.3038	−0.307	−0.3102	−0.3129	−0.3139	−0.3211	−0.318
	−0.2888	−0.2943	−0.2998	−0.3017	−0.3053	−0.3087	−0.3116	−0.3128	−0.3202	−0.3171
	−0.2832	−0.2895	−0.2956	−0.2982	−0.3022	−0.306	−0.3093	−0.3108	−0.3184	−0.3156
	−0.2594	−0.2691	−0.2783	−0.2834	−0.2896	−0.2951	−0.2999	−0.3027	−0.3114	−0.3096
	−0.2156	−0.232	−0.2468	−0.2566	−0.2669	−0.2758	−0.2834	−0.2886	−0.2992	−0.299

Figure I.24: F2C: e=2.5a & d=0.5a

	c/a									
b/a	−0.1065	−0.1494	−0.1851	−0.2111	−0.2342	−0.2524	−0.2674	−0.2777	−0.2927	−0.2952
	−0.0856	−0.1449	−0.1840	−0.2110	−0.2343	−0.2525	−0.2675	−0.2778	−0.2927	−0.2952
	−0.0071	−0.1137	−0.1744	−0.2083	−0.2334	−0.2520	−0.2673	−0.2777	−0.2927	−0.2952
	0.0209	−0.0047	−0.1233	−0.1927	−0.2281	−0.2491	−0.2660	−0.2770	−0.2922	−0.2950
	0.0214	0.0151	−0.0008	−0.1321	−0.2081	−0.2396	−0.2616	−0.2746	−0.2906	−0.2942
	−0.0062	−0.0075	−0.0068	−0.0280	−0.1570	−0.2199	−0.2537	−0.2709	−0.2884	−0.2930
	0.0081	0.0034	−0.0018	−0.0112	−0.0281	−0.0284	−0.1586	−0.2330	−0.2683	−0.2839
	0.0211	0.0160	0.0162	0.0024	−0.0101	−0.0224	−0.0315	−0.0341	−0.1630	−0.2415

Figure I.24: F2C: e=2.5a & d=1a

	c/a									
b/a	−0.1759	−0.2026	−0.2257	−0.2417	−0.2569	−0.2695	−0.2800	−0.2870	−0.2995	−0.3002
	−0.1700	−0.1998	−0.2243	−0.2410	−0.2567	−0.2693	−0.2799	−0.2870	−0.2995	−0.3002
	−0.1440	−0.1873	−0.2180	−0.2378	−0.2549	−0.2683	−0.2793	−0.2866	−0.2992	−0.3000
	−0.0749	−0.1506	−0.1988	−0.2277	−0.2494	−0.2648	−0.2772	−0.2852	−0.2983	−0.2994
	0.0233	−0.0775	−0.1552	−0.2044	−0.2366	−0.2568	−0.2723	−0.2820	−0.2961	−0.2979
	0.0501	0.0027	−0.0874	−0.1645	−0.2148	−0.2439	−0.2647	−0.2773	−0.2928	−0.2958
	0.0190	0.0235	0.0324	−0.0043	−0.0940	−0.1670	−0.2203	−0.2503	−0.2753	−0.2847
	0.0150	0.0117	0.0113	0.0056	0.0061	−0.0120	−0.0902	−0.1680	−0.2235	−0.2548

Figure I.24: F2C: e=2.5a & d=1.5a

	c/a									
b/a	−0.2207	−0.2378	−0.2532	−0.2631	−0.2736	−0.2824	−0.2899	−0.2948	−0.3054	−0.3049
	−0.2184	−0.2363	−0.2523	−0.2625	−0.2733	−0.2821	−0.2898	−0.2947	−0.3054	−0.3048
	−0.2082	−0.2299	−0.2481	−0.2598	−0.2715	−0.2809	−0.2889	−0.2941	−0.3049	−0.3045
	−0.1792	−0.2117	−0.2365	−0.2524	−0.2666	−0.2775	−0.2866	−0.2924	−0.3037	−0.3036
	−0.1235	−0.1761	−0.2137	−0.2377	−0.2569	−0.2708	−0.2819	−0.2890	−0.3012	−0.3017
	−0.0539	−0.1261	−0.1801	−0.2159	−0.2428	−0.2611	−0.2753	−0.2843	−0.2978	−0.2992
	0.0741	0.0185	−0.0564	−0.1247	−0.1800	−0.2174	−0.2455	−0.2634	−0.2826	−0.2884
	0.0537	0.0594	0.0554	0.0117	−0.0598	−0.1222	−0.1783	−0.2165	−0.2492	−0.2651

Figure I.24: F2C: e=2.5a & d=2a

	c/a									
b/a	−0.2499	−0.2615	−0.2723	−0.2785	−0.2858	−0.2923	−0.2979	−0.3012	−0.3106	−0.3089
	−0.2488	−0.2606	−0.2717	−0.2780	−0.2855	−0.2921	−0.2977	−0.3010	−0.3105	−0.3088
	−0.2438	−0.2570	−0.2690	−0.2761	−0.2841	−0.2910	−0.2969	−0.3004	−0.3100	−0.3084
	−0.2298	−0.2469	−0.2617	−0.2708	−0.2802	−0.2881	−0.2947	−0.2987	−0.3086	−0.3074
	−0.2017	−0.2269	−0.2474	−0.2605	−0.2727	−0.2824	−0.2904	−0.2955	−0.3061	−0.3054
	−0.1604	−0.1976	−0.2266	−0.2457	−0.2621	−0.2745	−0.2846	−0.2910	−0.3027	−0.3028
	−0.0302	−0.0957	−0.1494	−0.1892	−0.2210	−0.2439	−0.2619	−0.2739	−0.2894	−0.2926
	0.0841	0.0308	−0.0339	−0.0934	−0.1457	−0.1858	−0.2184	−0.2411	−0.2644	−0.2736

Figure I.24: F2C: e=2.5a & d=2.5a

	c/a									
b/a	−0.2695	−0.2778	−0.2858	−0.2897	−0.2951	−0.3000	−0.3042	−0.3064	−0.3149	−0.3125
	−0.2689	−0.2773	−0.2854	−0.2894	−0.2949	−0.2998	−0.3040	−0.3063	−0.3148	−0.3124
	−0.2661	−0.2751	−0.2837	−0.2880	−0.2938	−0.2989	−0.3034	−0.3058	−0.3143	−0.3120
	−0.2582	−0.2689	−0.2789	−0.2843	−0.2908	−0.2966	−0.3015	−0.3042	−0.3131	−0.3110
	−0.2426	−0.2568	−0.2695	−0.2770	−0.2851	−0.2921	−0.2979	−0.3013	−0.3107	−0.3091
	−0.2188	−0.2387	−0.2557	−0.2664	−0.2770	−0.2857	−0.2929	−0.2973	−0.3075	−0.3065
	−0.1322	−0.1721	−0.2044	−0.2272	−0.2468	−0.2620	−0.2744	−0.2827	−0.2957	−0.2970
	−0.0128	−0.0709	−0.1208	−0.1610	−0.1950	−0.2210	−0.2423	−0.2573	−0.2755	−0.2809

Figure I.24: F2C: e=2.5a & d=3a

	c/a									
b/a	−0.2832	−0.2895	−0.2957	−0.2981	−0.3022	−0.306	−0.3093	−0.3107	−0.3185	−0.3156
	−0.2828	−0.2891	−0.2954	−0.2979	−0.302	−0.3058	−0.3091	−0.3106	−0.3184	−0.3155
	−0.2811	−0.2877	−0.2942	−0.2969	−0.3012	−0.3052	−0.3086	−0.3102	−0.318	−0.3152
	−0.2762	−0.2836	−0.2909	−0.2942	−0.2989	−0.3033	−0.307	−0.3089	−0.3169	−0.3142
	−0.2665	−0.2757	−0.2844	−0.2889	−0.2946	−0.2997	−0.3041	−0.3064	−0.3148	−0.3125
	−0.2519	−0.2639	−0.2749	−0.2812	−0.2884	−0.2946	−0.2999	−0.3029	−0.312	−0.3101
	−0.1966	−0.2197	−0.2394	−0.2527	−0.2655	−0.276	−0.2847	−0.2905	−0.3016	−0.3015
	−0.1063	−0.1462	−0.1799	−0.2048	−0.2269	−0.2446	−0.2593	−0.2697	−0.2845	−0.2874

Figure I.24: F2C: e=2.5a & d=3.5a

	c/a									
b/a	−0.2931	−0.298	−0.303	−0.3045	−0.3077	−0.3107	−0.3133	−0.3143	−0.3215	−0.3182
	−0.2928	−0.2978	−0.3028	−0.3043	−0.3075	−0.3106	−0.3132	−0.3142	−0.3214	−0.3182
	−0.2916	−0.2967	−0.302	−0.3036	−0.3069	−0.3101	−0.3128	−0.3138	−0.3211	−0.3179
	−0.2883	−0.2939	−0.2996	−0.3016	−0.3052	−0.3086	−0.3115	−0.3127	−0.3202	−0.3171
	−0.2819	−0.2885	−0.295	−0.2976	−0.3019	−0.3058	−0.3091	−0.3107	−0.3184	−0.3155
	−0.2722	−0.2804	−0.2881	−0.2919	−0.2971	−0.3017	−0.3057	−0.3077	−0.3159	−0.3134
	−0.2355	−0.2498	−0.2627	−0.2708	−0.2794	−0.2869	−0.2932	−0.2972	−0.3069	−0.3058
	−0.1723	−0.1975	−0.2194	−0.2349	−0.2498	−0.2621	−0.2726	−0.2798	−0.2922	−0.2934

Figure I.24: F2C: e=2.5a & d=4a

	c/a									
b/a	−0.3004	−0.3044	−0.3086	−0.3095	−0.312	−0.3145	−0.3167	−0.3172	−0.324	−0.3205
	−0.3002	−0.3042	−0.3085	−0.3093	−0.3119	−0.3144	−0.3166	−0.3172	−0.324	−0.3204
	−0.2993	−0.3035	−0.3078	−0.3088	−0.3114	−0.314	−0.3162	−0.3168	−0.3237	−0.3202
	−0.297	−0.3015	−0.3061	−0.3072	−0.31	−0.3128	−0.3152	−0.3159	−0.3229	−0.3195
	−0.2925	−0.2975	−0.3026	−0.3042	−0.3075	−0.3106	−0.3132	−0.3142	−0.3214	−0.3181
	−0.2857	−0.2917	−0.2976	−0.2999	−0.3037	−0.3108	−0.3104	−0.3117	−0.3192	−0.3163
	−0.2601	−0.2697	−0.2788	−0.2838	−0.2899	−0.2954	−0.3001	−0.3029	−0.3115	−0.3096
	−0.2154	−0.2318	−0.2466	−0.2565	−0.2667	−0.2756	−0.2832	−0.2883	−0.299	−0.2988

Figure I.24: F2C: e=3a & d=0.5a

	c/a									
b/a	−0.1687	−0.2001	−0.2246	−0.2412	−0.2567	−0.2693	−0.2799	−0.2870	−0.2995	−0.3001
	−0.1201	−0.1859	−0.2193	−0.2390	−0.2558	−0.2688	−0.2796	−0.2868	−0.2994	−0.3001
	−0.0025	−0.1361	−0.2022	−0.2328	−0.2532	−0.2672	−0.2788	−0.2863	−0.2991	−0.2999
	0.0233	−0.0001	−0.1370	−0.2111	−0.2448	−0.2626	−0.2764	−0.2849	−0.2981	−0.2994
	0.0216	0.0147	−0.0009	−0.1408	−0.2203	−0.2508	−0.2707	−0.2816	−0.2959	−0.2981
	−0.0061	−0.0071	−0.0033	−0.0278	−0.1637	−0.2283	−0.2614	−0.2772	−0.2932	−0.2966
	0.0082	0.0034	−0.0019	−0.0115	−0.0284	−0.0288	−0.1610	−0.2365	−0.2715	−0.2866
	0.0213	0.0161	0.0163	0.0024	−0.0102	−0.0224	−0.0319	−0.0344	−0.1640	−0.2428

Figure I.24: F2C: e=3a & d=1a

	c/a									
b/a	−0.2184	−0.2365	−0.2524	−0.2626	−0.2732	−0.2822	−0.2898	−0.2946	−0.3054	−0.3047
	−0.2043	−0.2288	−0.2481	−0.2600	−0.2717	−0.2812	−0.2891	−0.2942	−0.3051	−0.3045
	−0.1646	−0.2087	−0.2372	−0.2540	−0.2681	−0.2788	−0.2876	−0.2932	−0.3044	−0.3040
	−0.0799	−0.1621	−0.2120	−0.2401	−0.2601	−0.2737	−0.2843	−0.2909	−0.3028	−0.3029
	0.0283	−0.0801	−0.1621	−0.2127	−0.2446	−0.2639	−0.2782	−0.2868	−0.2998	−0.3008
	0.0540	0.0041	−0.0887	−0.1687	−0.2202	−0.2491	−0.2694	−0.2812	−0.2960	−0.2984
	0.0193	0.0240	0.0334	0.0002	−0.0943	−0.1685	−0.2223	−0.2524	−0.2772	−0.2863
	0.0151	0.0118	0.0113	0.0056	0.0062	−0.0118	−0.0902	−0.1684	−0.2241	−0.2564

Figure I.24: F2C: e=3a & d=1.5a

	c/a									
b/a	−0.2489	−0.2607	−0.2718	−0.2781	−0.2857	−0.2921	−0.2977	−0.3010	−0.3105	−0.3089
	−0.2430	−0.2567	−0.2690	−0.2762	−0.2843	−0.2911	−0.2970	−0.3005	−0.3101	−0.3086
	−0.2270	−0.2462	−0.2620	−0.2714	−0.2811	−0.2888	−0.2953	−0.2992	−0.3091	−0.3078
	−0.1904	−0.2228	−0.2468	−0.2613	−0.2742	−0.2839	−0.2918	−0.2967	−0.3072	−0.3064
	−0.1277	−0.1822	−0.2203	−0.2440	−0.2627	−0.2757	−0.2861	−0.2924	−0.3040	−0.3040
	−0.0533	−0.1281	−0.1836	−0.2200	−0.2468	−0.2648	−0.2785	−0.2870	−0.3000	−0.3011
	0.0764	0.0204	−0.0558	−0.1252	−0.1811	−0.2188	−0.2470	−0.2647	−0.2838	−0.2893
	0.0541	0.0600	0.0562	0.0125	−0.0593	−0.1222	−0.1785	−0.2167	−0.2496	−0.2654

Figure I.24: F2C: e=3a & d=2a

	c/a									
b/a	−0.2690	−0.2774	−0.2855	−0.2894	−0.2949	−0.2998	−0.3041	−0.3063	−0.3148	−0.3124
	−0.2659	−0.2751	−0.2837	−0.2881	−0.2938	−0.2990	−0.3034	−0.3058	−0.3144	−0.3120
	−0.2579	−0.2690	−0.2792	−0.2847	−0.2913	−0.2970	−0.3019	−0.3046	−0.3134	−0.3113
	−0.2398	−0.2558	−0.2695	−0.2775	−0.2859	−0.2929	−0.2987	−0.3021	−0.3115	−0.3097
	−0.2076	−0.2328	−0.2528	−0.2654	−0.2770	−0.2861	−0.2936	−0.2981	−0.3083	−0.3072
	−0.1630	−0.2008	−0.2300	−0.2490	−0.2651	−0.2773	−0.2869	−0.2930	−0.3043	−0.3041
	−0.0291	−0.0955	−0.1499	−0.1901	−0.2220	−0.2450	−0.2629	−0.2748	−0.2902	−0.2933
	0.0852	0.0319	−0.0332	−0.0931	−0.1457	−0.1859	−0.2186	−0.2413	−0.2646	−0.2738

Figure I.24: F2C: e=3a & d=2.5a

	c/a									
b/a	−0.2828	−0.2892	−0.2955	−0.2979	−0.3020	−0.3059	−0.3092	−0.3106	−0.3184	−0.3155
	−0.2810	−0.2877	−0.2943	−0.2969	−0.3012	−0.3052	−0.3086	−0.3102	−0.3180	−0.3152
	−0.2764	−0.2839	−0.2913	−0.2945	−0.2993	−0.3036	−0.3073	−0.3091	−0.3172	−0.3144
	−0.2660	−0.2758	−0.2848	−0.2894	−0.2952	−0.3003	−0.3047	−0.3069	−0.3154	−0.3130
	−0.2479	−0.2616	−0.2738	−0.2808	−0.2884	−0.2949	−0.3003	−0.3034	−0.3125	−0.3106
	−0.2220	−0.2418	−0.2586	−0.2690	−0.2793	−0.2877	−0.2946	−0.2989	−0.3088	−0.3076
	−0.1324	−0.1726	−0.2052	−0.2280	−0.2477	−0.2629	−0.2751	−0.2833	−0.2963	−0.2975
	−0.0113	−0.0704	−0.1206	−0.1609	−0.1950	−0.2211	−0.2424	−0.2575	−0.2756	−0.2810

Figure I.24: F2C: e=3a & d=3a

	c/a									
b/a	−0.2928	−0.2978	−0.3029	−0.3043	−0.3075	−0.3106	−0.3132	−0.3142	−0.3214	−0.3181
	−0.2916	−0.2968	−0.302	−0.3036	−0.3069	−0.3101	−0.3128	−0.3138	−0.3211	−0.3178
	−0.2886	−0.2943	−0.2999	−0.3019	−0.3055	−0.3089	−0.3118	−0.3129	−0.3204	−0.3172
	−0.2821	−0.2888	−0.2954	−0.2981	−0.3024	−0.3063	−0.3096	−0.3111	−0.3188	−0.3159
	−0.2708	−0.2795	−0.2878	−0.2918	−0.2972	−0.302	−0.306	−0.3081	−0.3163	−0.3137
	−0.2547	−0.2665	−0.2772	−0.2833	−0.2902	−0.2962	−0.3013	−0.3042	−0.313	−0.311
	−0.1972	−0.2204	−0.2402	−0.2535	−0.2662	−0.2766	−0.2852	−0.2909	−0.302	−0.3018
	−0.1059	−0.146	−0.1798	−0.2048	−0.227	−0.2447	−0.2593	−0.2697	−0.2845	−0.2874

Figure I.24: F2C: e=3a & d=3.5a

	c/a									
b/a	−0.3001	−0.3042	−0.3085	−0.3093	−0.3119	−0.3145	−0.3166	−0.3171	−0.324	−0.3204
	−0.2993	−0.3035	−0.3079	−0.3088	−0.3114	−0.3141	−0.3162	−0.3168	−0.3237	−0.3201
	−0.2973	−0.3017	−0.3064	−0.3075	−0.3103	−0.3131	−0.3154	−0.3161	−0.3231	−0.3196
	−0.2928	−0.2979	−0.3031	−0.3047	−0.3079	−0.311	−0.3136	−0.3145	−0.3217	−0.3184
	−0.2852	−0.2914	−0.2976	−0.3	−0.3039	−0.3076	−0.3107	−0.312	−0.3195	−0.3165
	−0.2745	−0.2824	−0.29	−0.2936	−0.2985	−0.303	−0.3068	−0.3087	−0.3167	−0.3141
	−0.2362	−0.2505	−0.2634	−0.2714	−0.28	−0.2874	−0.2936	−0.2975	−0.3072	−0.306
	−0.1722	−0.1974	−0.2194	−0.235	−0.2498	−0.2621	−0.2726	−0.2798	−0.2922	−0.2933

Figure I.24: F2C: e=3a & d=4a

	c/a									
b/a	−0.3057	−0.3092	−0.3129	−0.3133	−0.3154	−0.3175	−0.3193	−0.3196	−0.3261	−0.3223
	−0.3051	−0.3087	−0.3124	−0.3128	−0.315	−0.3172	−0.319	−0.3193	−0.3259	−0.3221
	−0.3036	−0.3074	−0.3113	−0.3118	−0.3141	−0.3164	−0.3183	−0.3187	−0.3253	−0.3216
	−0.3005	−0.3046	−0.3088	−0.3097	−0.3122	−0.3148	−0.3169	−0.3174	−0.3242	−0.3206
	−0.2951	−0.2998	−0.3047	−0.3061	−0.3091	−0.312	−0.3144	−0.3153	−0.3223	−0.319
	−0.2875	−0.2933	−0.299	−0.3012	−0.3049	−0.3083	−0.3113	−0.3125	−0.3199	−0.3169
	−0.2607	−0.2703	−0.2793	−0.2843	−0.2903	−0.2958	−0.3004	−0.3031	−0.3118	−0.3098
	−0.2154	−0.2318	−0.2466	−0.2565	−0.2667	−0.2756	−0.2832	−0.2883	−0.2989	−0.2987

Figure I.24: F2C: e=3.5a & d=0.5a

	c/a									
b/a	−0.2080	−0.2330	−0.2511	−0.2620	−0.2729	−0.2820	−0.2897	−0.2946	−0.3054	−0.3047
	−0.1410	−0.2121	−0.2427	−0.2583	−0.2711	−0.2809	−0.2891	−0.2941	−0.3051	−0.3045
	0.0003	−0.1498	−0.2206	−0.2496	−0.2672	−0.2785	−0.2877	−0.2933	−0.3045	−0.3041
	0.0249	0.0035	−0.1461	−0.2239	−0.2568	−0.2727	−0.2846	−0.2914	−0.3032	−0.3033
	0.0219	0.0144	0.0015	−0.1471	−0.2293	−0.2594	−0.2780	−0.2876	−0.3007	−0.3018
	−0.0061	−0.0068	−0.0064	−0.0277	−0.1686	−0.2347	−0.2674	−0.2825	−0.2976	−0.3001
	0.0084	0.0036	−0.0019	−0.0114	−0.0286	−0.0297	−0.1632	−0.2397	−0.2747	−0.2894
	0.0214	0.0162	0.0164	0.0024	−0.0102	−0.0226	−0.0323	−0.0348	−0.1651	−0.2444

Figure I.24: F2C: e=3.5a & d=1a

	c/a									
b/a	−0.2458	−0.2589	−0.2707	−0.2774	−0.2851	−0.2918	−0.2975	−0.3009	−0.3104	−0.3087
	−0.2260	−0.2478	−0.2642	−0.2734	−0.2826	−0.2901	−0.2963	−0.3000	−0.3098	−0.3082
	−0.1773	−0.2225	−0.2502	−0.2654	−0.2777	−0.2868	−0.2942	−0.2985	−0.3087	−0.3075
	−0.0828	−0.1697	−0.2212	−0.2491	−0.2681	−0.2805	−0.2901	−0.2957	−0.3066	−0.3060
	0.0322	−0.0817	−0.1670	−0.2189	−0.2508	−0.2695	−0.2830	−0.2909	−0.3032	−0.3036
	0.0570	0.0062	−0.0897	−0.1720	−0.2244	−0.2535	−0.2734	−0.2847	−0.2990	−0.3008
	0.0196	0.0244	0.0342	0.0045	−0.0946	−0.1699	−0.2243	−0.2545	−0.2791	−0.2880
	0.0152	0.0119	0.0113	0.0056	0.0063	−0.0116	−0.0902	−0.1689	−0.2259	−0.2563

Figure I.24: F2C: e=3.5a & d=1.5a

	c/a									
b/a	−0.2676	−0.2764	−0.2849	−0.2889	−0.2947	−0.2996	−0.3039	−0.3061	−0.3147	−0.3123
	−0.2592	−0.2705	−0.2807	−0.2860	−0.2925	−0.2980	−0.3027	−0.3052	−0.3140	−0.3118
	−0.2392	−0.2572	−0.2717	−0.2798	−0.2882	−0.2948	−0.3003	−0.3034	−0.3126	−0.3107
	−0.1978	−0.2305	−0.2541	−0.2680	−0.2800	−0.2889	−0.2961	−0.3002	−0.3102	−0.3089
	−0.1305	−0.1865	−0.2252	−0.2489	−0.2672	−0.2798	−0.2896	−0.2954	−0.3065	−0.3061
	−0.0528	−0.1296	−0.1863	−0.2232	−0.2501	−0.2679	−0.2813	−0.2895	−0.3021	−0.3029
	0.0784	0.0221	−0.0553	−0.1257	−0.1822	−0.2202	−0.2484	−0.2662	−0.2851	−0.2905
	0.0546	0.0606	0.0570	0.0132	−0.0590	−0.1222	−0.1789	−0.2174	−0.2502	−0.2660

Figure I.24: F2C: e=3.5a & d=2a

	c/a									
b/a	−0.2821	−0.2886	−0.2951	−0.2975	−0.3017	−0.3057	−0.3090	−0.3104	−0.3183	−0.3153
	−0.2776	−0.2851	−0.2924	−0.2955	−0.3001	−0.3043	−0.3079	−0.3096	−0.3176	−0.3148
	−0.2674	−0.2774	−0.2866	−0.2910	−0.2967	−0.3017	−0.3059	−0.3080	−0.3163	−0.3137
	−0.2467	−0.2622	−0.2753	−0.2826	−0.2904	−0.2968	−0.3020	−0.3049	−0.3139	−0.3118
	−0.2119	−0.2371	−0.2570	−0.2692	−0.2804	−0.2892	−0.2962	−0.3004	−0.3103	−0.3089
	−0.1649	−0.2033	−0.2327	−0.2517	−0.2677	−0.2796	−0.2891	−0.2949	−0.3060	−0.3055
	−0.0282	−0.0954	−0.1504	−0.1909	−0.2231	−0.2461	−0.2640	−0.2758	−0.2912	−0.2941
	0.0864	0.0329	−0.0326	−0.0929	−0.1457	−0.1861	−0.2190	−0.2417	−0.2650	−0.2741

Figure I.24: F2C: e=3.5a & d=2.5a

	c/a									
b/a	−0.2923	−0.2974	−0.3026	−0.3041	−0.3073	−0.3105	−0.3131	−0.3140	−0.3213	−0.3180
	−0.2896	−0.2952	−0.3008	−0.3026	−0.3061	−0.3094	−0.3123	−0.3133	−0.3207	−0.3175
	−0.2836	−0.2903	−0.2969	−0.2994	−0.3035	−0.3073	−0.3105	−0.3119	−0.3195	−0.3165
	−0.2717	−0.2808	−0.2893	−0.2934	−0.2987	−0.3034	−0.3073	−0.3092	−0.3174	−0.3147
	−0.2518	−0.2653	−0.2772	−0.2838	−0.2911	−0.2973	−0.3024	−0.3052	−0.3141	−0.3119
	−0.2245	−0.2443	−0.2609	−0.2713	−0.2814	−0.2896	−0.2963	−0.3003	−0.3101	−0.3087
	−0.1325	−0.1731	−0.2059	−0.2289	−0.2486	−0.2638	−0.2760	−0.2841	−0.2970	−0.2981
	−0.0109	−0.0700	−0.1204	−0.1610	−0.1952	−0.2214	−0.2427	−0.2577	−0.2758	−0.2812

Figure I.24: F2C: e=3.5a & d=3a

	c/a									
b/a	−0.2998	−0.304	−0.3083	−0.3091	−0.3117	−0.3143	−0.3165	−0.317	−0.3239	−0.3203
	−0.298	−0.3024	−0.307	−0.308	−0.3108	−0.3135	−0.3158	−0.3164	−0.3234	−0.3198
	−0.2941	−0.2991	−0.3042	−0.3057	−0.3088	−0.3118	−0.3143	−0.3152	−0.3223	−0.3189
	−0.2865	−0.2928	−0.299	−0.3013	−0.3051	−0.3087	−0.3117	−0.3129	−0.3204	−0.3173
	−0.2741	−0.2825	−0.2905	−0.2943	−0.2994	−0.3039	−0.3077	−0.3096	−0.3176	−0.3149
	−0.257	−0.2687	−0.2792	−0.2851	−0.2919	−0.2977	−0.3026	−0.3053	−0.314	−0.3119
	−0.1978	−0.2211	−0.2409	−0.2543	−0.267	−0.2773	−0.2859	−0.2915	−0.3025	−0.3023
	−0.1056	−0.1459	−0.1798	−0.2049	−0.2272	−0.2449	−0.2596	−0.2699	−0.2847	−0.2857

Figure I.24: F2C: e=3.5a & d=3.5a

	c/a									
b/a	−0.3055	−0.309	−0.3128	−0.3131	−0.3152	−0.3174	−0.3192	−0.3194	−0.326	−0.3222
	−0.3042	−0.3079	−0.3118	−0.3122	−0.3145	−0.3168	−0.3186	−0.3189	−0.3256	−0.3218
	−0.3015	−0.3055	−0.3097	−0.3105	−0.313	−0.3154	−0.3175	−0.3179	−0.3247	−0.321
	−0.2963	−0.301	−0.3059	−0.3071	−0.3101	−0.313	−0.3153	−0.3161	−0.3231	−0.3196
	−0.2879	−0.2939	−0.2998	−0.3019	−0.3056	−0.3091	−0.312	−0.3132	−0.3206	−0.3175
	−0.2765	−0.2842	−0.2916	−0.2951	−0.2999	−0.3042	−0.3079	−0.3097	−0.3176	−0.3148
	−0.2369	−0.2512	−0.2641	−0.2721	−0.2806	−0.288	−0.2942	−0.298	−0.3076	−0.3063
	−0.1721	−0.1975	−0.2195	−0.2351	−0.25	−0.2623	−0.2727	−0.28	−0.2923	−0.2934

Figure I.24: F2C: e=3.5a & d=4a

	c/a									
b/a	−0.3098	−0.3129	−0.3163	−0.3163	−0.3181	−0.32	−0.3215	−0.3215	−0.3279	−0.3239
	−0.3089	−0.3121	−0.3155	−0.3156	−0.3175	−0.3194	−0.321	−0.3211	−0.3275	−0.3235
	−0.3069	−0.3103	−0.314	−0.3142	−0.3163	−0.3184	−0.3201	−0.3202	−0.3267	−0.3229
	−0.3032	−0.307	−0.311	−0.3117	−0.314	−0.3164	−0.3183	−0.3187	−0.3254	−0.3216
	−0.2972	−0.3018	−0.3064	−0.3076	−0.3105	−0.3133	−0.3156	−0.3163	−0.3232	−0.3198
	−0.2891	−0.2948	−0.3004	−0.3024	−0.3059	−0.3093	−0.3121	−0.3133	−0.3206	−0.3175
	−0.2614	−0.271	−0.2799	−0.2848	−0.2909	−0.2963	−0.3009	−0.3035	−0.3121	−0.3101
	−0.2155	−0.232	−0.2468	−0.2566	−0.2669	−0.2757	−0.2833	−0.2884	−0.299	−0.2988

Figure I.24: F2C: e=4a & d=0.5a

	c/a									
b/a	−0.2336	−0.2551	−0.2694	−0.2769	−0.2849	−0.2918	−0.2975	−0.3009	−0.3104	−0.3087
	−0.1547	−0.2298	−0.2590	−0.2721	−0.2825	−0.2902	−0.2966	−0.3002	−0.3100	−0.3084
	0.0022	−0.1591	−0.2336	−0.2619	−0.2778	−0.2873	−0.2949	−0.2991	−0.3092	−0.3079
	0.0261	0.0030	−0.1527	−0.2334	−0.2659	−0.2807	−0.2913	−0.2969	−0.3077	−0.3070
	0.0221	0.0143	0.0015	−0.1519	−0.2363	−0.2663	−0.2840	−0.2926	−0.3048	−0.3052
	−0.0060	−0.0066	−0.0031	−0.0276	−0.1720	−0.2400	−0.2726	−0.2872	−0.3015	−0.3033
	0.0085	0.0036	−0.0005	−0.0116	−0.0289	−0.0301	−0.1652	−0.2427	−0.2776	−0.2920
	0.0215	0.0163	0.0165	0.0024	−0.0104	−0.0231	−0.0328	−0.0352	−0.1662	−0.2460

Figure I.24: F2C: e=4a & d=1a

	c/a									
b/a	−0.2641	−0.2744	−0.2838	−0.2883	−0.2941	−0.2993	−0.3037	−0.3060	−0.3146	−0.3122
	−0.2406	−0.2611	−0.2758	−0.2833	−0.2909	−0.2971	−0.3021	−0.3048	−0.3138	−0.3115
	−0.1860	−0.2323	−0.2597	−0.2739	−0.2851	−0.2932	−0.2995	−0.3030	−0.3124	−0.3105
	−0.0849	−0.1753	−0.2280	−0.2559	−0.2744	−0.2861	−0.2948	−0.2997	−0.3100	−0.3088
	0.0351	−0.0830	−0.1708	−0.2238	−0.2558	−0.2741	−0.2872	−0.2945	−0.3063	−0.3062
	0.0593	0.0080	−0.0905	−0.1747	−0.2280	−0.2572	−0.2769	−0.2878	−0.3017	−0.3031
	0.0198	0.0248	0.0349	0.0041	−0.0949	−0.1713	−0.2262	−0.2565	−0.2810	−0.2897
	0.0153	0.0119	0.0113	0.0056	0.0064	−0.0115	−0.0904	−0.1696	−0.2259	−0.2573

Figure I.24: F2C: e=4a & d=1.5a

	c/a									
b/a	−0.2806	−0.2876	−0.2944	−0.2970	−0.3015	−0.3054	−0.3088	−0.3103	−0.3182	−0.3153
	−0.2705	−0.2805	−0.2893	−0.2934	−0.2988	−0.3034	−0.3072	−0.3091	−0.3173	−0.3146
	−0.2479	−0.2653	−0.2789	−0.2862	−0.2937	−0.2996	−0.3045	−0.3069	−0.3156	−0.3133
	−0.2033	−0.2363	−0.2597	−0.2732	−0.2847	−0.2931	−0.2997	−0.3034	−0.3129	−0.3112
	−0.1326	−0.1899	−0.2291	−0.2529	−0.2709	−0.2832	−0.2926	−0.2981	−0.3089	−0.3081
	−0.0523	−0.1308	−0.1886	−0.2260	−0.2530	−0.2707	−0.2839	−0.2918	−0.3042	−0.3046
	0.0801	0.0235	−0.0550	−0.1262	−0.1833	−0.2215	−0.2499	−0.2676	−0.2864	−0.2917
	0.0549	0.0612	0.0577	0.0138	−0.0587	−0.1224	−0.1794	−0.2180	−0.2509	−0.2667

Figure I.24: F2C: e=4a & d=2a

	c/a									
b/a	−0.2915	−0.2968	−0.3022	−0.3037	−0.3071	−0.3103	−0.3129	−0.3139	−0.3213	−0.3179
	−0.2861	−0.2926	−0.2989	−0.3011	−0.3050	−0.3086	−0.3116	−0.3128	−0.3204	−0.3171
	−0.2745	−0.2838	−0.2922	−0.2960	−0.3010	−0.3055	−0.3092	−0.3108	−0.3188	−0.3158
	−0.2520	−0.2672	−0.2798	−0.2867	−0.2940	−0.3000	−0.3049	−0.3074	−0.3160	−0.3136
	−0.2153	−0.2406	−0.2604	−0.2724	−0.2834	−0.2919	−0.2986	−0.3025	−0.3121	−0.3105
	−0.1665	−0.2054	−0.2351	−0.2541	−0.2700	−0.2818	−0.2910	−0.2966	−0.3075	−0.3069
	−0.0274	−0.0953	−0.1509	−0.1918	−0.2242	−0.2473	−0.2652	−0.2769	−0.2922	−0.2950
	0.0875	0.0339	−0.0320	−0.0928	−0.1459	−0.1865	−0.2195	−0.2423	−0.2656	−0.2747

Figure I.24: F2C: e=4a & d=2.5a

	c/a									
b/a	−0.2993	−0.3036	−0.3081	−0.3089	−0.3115	−0.3141	−0.3163	−0.3168	−0.3238	−0.3201
	−0.2960	−0.3008	−0.3058	−0.3070	−0.3100	−0.3128	−0.3152	−0.3159	−0.3230	−0.3195
	−0.2891	−0.2952	−0.3012	−0.3033	−0.3070	−0.3104	−0.3132	−0.3142	−0.3216	−0.3183
	−0.2761	−0.2848	−0.2929	−0.2966	−0.3016	−0.3060	−0.3096	−0.3113	−0.3191	−0.3162
	−0.2551	−0.2684	−0.2800	−0.2864	−0.2935	−0.2994	−0.3043	−0.3069	−0.3156	−0.3133
	−0.2266	−0.2464	−0.2630	−0.2733	−0.2833	−0.2913	−0.2979	−0.3017	−0.3113	−0.3098
	−0.1327	−0.1737	−0.2067	−0.2298	−0.2496	−0.2647	−0.2769	−0.2850	−0.2978	−0.2988
	−0.0104	−0.0697	−0.1203	−0.1611	−0.1955	−0.2218	−0.2432	−0.2582	−0.2763	−0.2816

Figure I.24: F2C: e=4a & d=3a

	c/a									
b/a	−0.3051	−0.3087	−0.3126	−0.3129	−0.3151	−0.3173	−0.3191	−0.3193	−0.326	−0.3221
	−0.3029	−0.3068	−0.3109	−0.3115	−0.3139	−0.3163	−0.3182	−0.3185	−0.3253	−0.3215
	−0.2984	−0.303	−0.3077	−0.3088	−0.3116	−0.3143	−0.3165	−0.3171	−0.3241	−0.3204
	−0.2901	−0.296	−0.3019	−0.3039	−0.3075	−0.3108	−0.3136	−0.3146	−0.3219	−0.3186
	−0.2768	−0.2851	−0.2928	−0.2964	−0.3013	−0.3056	−0.3093	−0.3109	−0.3188	−0.316
	−0.259	−0.2706	−0.281	−0.2868	−0.2934	−0.2991	−0.3039	−0.3065	−0.315	−0.3128
	−0.1985	−0.2219	−0.2418	−0.2551	−0.2678	−0.2781	−0.2867	−0.2922	−0.3032	−0.3029
	−0.1054	−0.1459	−0.18	−0.2051	−0.2275	−0.2452	−0.2599	−0.2703	−0.285	−0.2879

Figure I.24: F2C: e=4a & d=3.5a

	c/a									
b/a	−0.3096	−0.3127	−0.3161	−0.3161	−0.3179	−0.3198	−0.3214	−0.3214	−0.3278	−0.3238
	−0.308	−0.3113	−0.3149	−0.315	−0.317	−0.319	−0.3207	−0.3208	−0.3272	−0.3233
	−0.3049	−0.3086	−0.3125	−0.313	−0.3152	−0.3174	−0.3193	−0.3195	−0.3262	−0.3223
	−0.2991	−0.3036	−0.3082	−0.3093	−0.312	−0.3147	−0.3169	−0.3175	−0.3243	−0.3207
	−0.2902	−0.2959	−0.3017	−0.3037	−0.3072	−0.3105	−0.3133	−0.3144	−0.3217	−0.3184
	−0.2782	−0.2859	−0.2931	−0.2965	−0.3011	−0.3054	−0.3089	−0.3106	−0.3184	−0.3156
	−0.2377	−0.252	−0.2649	−0.2728	−0.2813	−0.2886	−0.2948	−0.2986	−0.3081	−0.3068
	−0.1722	−0.1977	−0.2197	−0.2354	−0.2503	−0.2626	−0.273	−0.2803	−0.2926	−0.2937

Figure I.24: F2C: e=4a & d=4a

	c/a									
b/a	−0.3131	−0.3159	−0.319	−0.3187	−0.3203	−0.322	−0.3233	−0.3231	−0.3293	−0.3252
	−0.3119	−0.3148	−0.318	−0.3179	−0.3195	−0.3213	−0.3227	−0.3226	−0.3289	−0.3248
	−0.3096	−0.3128	−0.3162	−0.3162	−0.3181	−0.32	−0.3216	−0.3216	−0.328	−0.324
	−0.3055	−0.3091	−0.3129	−0.3134	−0.3156	−0.3178	−0.3196	−0.3199	−0.3264	−0.3226
	−0.299	−0.3035	−0.308	−0.3091	−0.3118	−0.3145	−0.3167	−0.3173	−0.3241	−0.3206
	−0.2906	−0.2961	−0.3016	−0.3035	−0.307	−0.3103	−0.313	−0.3141	−0.3213	−0.3181
	−0.2621	−0.2717	−0.2806	−0.2855	−0.2915	−0.2968	−0.3014	−0.304	−0.3125	−0.3104
	−0.2157	−0.2322	−0.247	−0.2569	−0.2671	−0.276	−0.2835	−0.2886	−0.2992	−0.2989